

# **Chelation-Assisted C–H Activation by Ruthenium and Osmium Catalysts and Recyclable Hybrid Catalysts**

Dissertation  
for the award of the degree  
“Doctor rerum naturalium”  
of the Georg-August-Universität Göttingen

within the doctoral program of chemistry  
of the Georg-August-Universität School of Science (GAUSS)

Submitted by  
Isaac Choi  
From Seoul (Republic of Korea)



Göttingen, 2021

## **Thesis Committee**

Prof. Dr. Lutz Ackermann, Institute of Organic and Biomolecular Chemistry

Prof. Dr. Shoubhik Das, Department of Chemistry, University of Antwerp

## **Members of the Examination Board**

Reviewer: Prof. Dr. Lutz Ackermann, Institute of Organic and Biomolecular Chemistry

Second Reviewer: Prof. Dr. Shoubhik Das, Department of Chemistry, University of Antwerp

## **Further members of the Examination Board**

Prof. Dr. Manuel Alcarazo, Institute of Organic and Biomolecular Chemistry

Jun.-Prof. Dr. Johannes C. L. Walker, Institute of Organic and Biomolecular Chemistry

Dr. Michael John, Institute of Organic and Biomolecular Chemistry

Dr. Daniel Janßen-Müller, Institute of Organic and Biomolecular Chemistry

Date of the oral examination: 24. 09. 2021



**Contents**

|                                                                               |           |
|-------------------------------------------------------------------------------|-----------|
| <b>1. Introduction.....</b>                                                   | <b>1</b>  |
| 1.1 Homogeneous Metal-Catalyzed C–H Functionalization.....                    | 2         |
| 1.2 Ruthenium-Catalyzed C–H Activation .....                                  | 5         |
| 1.2.1 Ruthenium-Catalyzed C–N Formation .....                                 | 7         |
| 1.2.2 Ruthenium-Catalyzed Distal C–H Functionalization .....                  | 23        |
| 1.3 Osmium-Catalyzed C–H Activation .....                                     | 34        |
| 1.3.1 Osmium-Mediated C–H Functionalizations .....                            | 36        |
| 1.3.2 Osmium-Catalyzed C–H Functionalizations .....                           | 37        |
| 1.4 Manganese-Catalyzed C–H Activation.....                                   | 40        |
| 1.4.1 Manganese-Catalyzed C–H Arylations .....                                | 50        |
| 1.5 Copper-Catalyzed C–H Activation .....                                     | 52        |
| 1.5.1 Copper-Catalyzed C–H Arylations.....                                    | 53        |
| 1.6 Hybrid-Metal-Catalyzed C–H Activation .....                               | 65        |
| <b>2. Objectives.....</b>                                                     | <b>70</b> |
| <b>3. Results and Discussion.....</b>                                         | <b>74</b> |
| 3.1 Ruthenium(II)-Catalyzed C7–H Amidations and Alkenylations of Indoles..... | 74        |
| 3.1.1 Optimization Studies .....                                              | 75        |
| 3.1.2 Substrate Scope.....                                                    | 78        |
| 3.1.3 Investigations of Practical Utility .....                               | 80        |
| 3.1.4 Mechanistic Studies .....                                               | 82        |
| 3.1.5 Proposed Catalytic Cycle.....                                           | 86        |

|                                                                                |     |
|--------------------------------------------------------------------------------|-----|
| 3.2 Ruthenium(II)-Catalyzed C4/C6–H Dual Alkylations of Indoles.....           | 87  |
| 3.2.1 Optimization Studies .....                                               | 88  |
| 3.2.2 Substrate Scope.....                                                     | 91  |
| 3.2.3 Mechanistic Studies.....                                                 | 93  |
| 3.3 Osmium-Catalyzed Electrooxidative C–H Annulations .....                    | 94  |
| 3.3.1 Optimization Studies .....                                               | 95  |
| 3.3.2 Substrate Scope.....                                                     | 98  |
| 3.1.3 Site-Selectivity Studies.....                                            | 100 |
| 3.3.4 Mechanistic Studies .....                                                | 102 |
| 3.4 Photo-Induced C–H Arylation by Reusable Heterogeneous Copper Catalyst..... | 111 |
| 3.4.1 Preparation of Hybrid Copper Catalyst .....                              | 112 |
| 3.4.2 Optimization Studies .....                                               | 113 |
| 3.4.3 Substrate Scope.....                                                     | 116 |
| 3.4.4 Mechanistic Studies.....                                                 | 119 |
| 3.4.5 Heterogeneity Studies.....                                               | 121 |
| 3.4.6 Characterization of Hybrid Copper Catalyst .....                         | 123 |
| 3.4.7 Proposed Mechanism.....                                                  | 125 |
| 3.5 Distal C–H Activation by Reusable Heterogeneous Ruthenium Catalyst .....   | 126 |
| 3.5.1 Optimization Studies .....                                               | 127 |
| 3.5.2 Substrate Scope.....                                                     | 129 |
| 3.5.3 Mechanistic Studies.....                                                 | 130 |
| 3.5.4 Heterogeneity Studies.....                                               | 132 |
| 3.5.5 Characterizations of Hybrid Ruthenium Catalyst.....                      | 134 |
| 3.5.6 Proposed Mechanism.....                                                  | 137 |

|                                                                                           |            |
|-------------------------------------------------------------------------------------------|------------|
| 3.6 C–H Arylations and Alkylations by Reusable Heterogeneous Manganese Catalyst .....     | 138        |
| 3.6.1 Preparation of Hybrid Manganese Catalyst .....                                      | 139        |
| 3.6.2 Optimization Studies .....                                                          | 140        |
| 3.6.3 Substrate Scope .....                                                               | 142        |
| 3.6.4 Heterogeneity Studies .....                                                         | 144        |
| 3.6.5 Characterizations of Heterogeneous Catalyst .....                                   | 146        |
| <b>4. Summary and Outlook .....</b>                                                       | <b>147</b> |
| <b>5. Experimental Data .....</b>                                                         | <b>151</b> |
| 5.1 General Remarks .....                                                                 | 151        |
| 5.2 General Procedures .....                                                              | 155        |
| 5.2.1 General Procedure A: Ruthenium-Catalyzed C7–H Indole Amidations .....               | 155        |
| 5.2.2 General Procedure B: Ruthenium-Catalyzed C7–H Indole Alkenylations .....            | 155        |
| 5.2.3 General Procedure C: Ruthenium-Catalyzed C4–H/C6–H Indole Dual Alkylations .....    | 155        |
| 5.2.4 General Procedure D: Osmium-Catalyzed Electrooxidative [4+1] C–H annulations .....  | 155        |
| 5.2.5 General Procedure E: Osmium-Catalyzed Electrooxidative [4+2] C–H annulations .....  | 156        |
| 5.2.6 General Procedure F: Photo-Induced Hybrid Copper-Catalyzed C–H Arylations (1) ..... | 156        |
| 5.2.7 General Procedure G: Photo-Induced Hybrid Copper-Catalyzed C–H Arylations (2) ..... | 156        |
| 5.2.8 General Procedure H: Photo-Induced Hybrid Copper-Catalyzed C–H Arylations (3) ..... | 157        |
| 5.2.9 General Procedure I: Hybrid Ruthenium-Catalyzed <i>meta</i> -C–H Alkylation .....   | 157        |
| 5.2.10 General Procedure J: Hybrid Manganese-Catalyzed C–H Arylations .....               | 157        |
| 5.2.11 General Procedure K: Hybrid Manganese-Catalyzed C–H Alkylations .....              | 157        |
| 5.3 Ruthenium(II)-Catalyzed C7–H Amidations and Alkenylations of Indoles .....            | 159        |
| 5.3.1 Characterization Data .....                                                         | 159        |
| 5.3.2 Various Attempted C7–H Activations .....                                            | 179        |

---

|                                                                                |     |
|--------------------------------------------------------------------------------|-----|
| 5.3.3 Flow Reaction Setup.....                                                 | 182 |
| 5.3.4 Competition Experiment.....                                              | 182 |
| 5.3.5 Removal of Pivaloyl Directing Group.....                                 | 183 |
| 5.3.6 Hammett Correlation .....                                                | 186 |
| 5.3.7 H/D Exchange Study .....                                                 | 187 |
| 5.3.8 KIE Study .....                                                          | 190 |
| 5.3.9 Kinetic Analysis .....                                                   | 191 |
| 5.4 Ruthenium(II)-Catalyzed C4/C6–H Dual Alkylations of Indoles.....           | 194 |
| 5.4.1 Characterization Data .....                                              | 194 |
| 5.4.2 Mechanistic Investigation.....                                           | 207 |
| 5.5 Osmium-Catalyzed Electrooxidative C–H Annulations .....                    | 209 |
| 5.5.1 Characterization Data .....                                              | 209 |
| 5.5.2 Reaction Comparison with External Oxidant.....                           | 229 |
| 5.5.3 Selectivity Comparison with Different Catalysis (1) .....                | 230 |
| 5.5.4 Selectivity Comparison with Different Catalysis (2) .....                | 232 |
| 5.5.5 Synthesis of Osmium Complex .....                                        | 236 |
| 5.5.6 Reactions with Osmium Complex.....                                       | 240 |
| 5.5.7 <i>In-Operando</i> NMR and HR-ESI-MS Studies.....                        | 243 |
| 5.5.8 Competition Experiment.....                                              | 245 |
| 5.5.9 Hammett Correlation .....                                                | 247 |
| 5.5.10 KIE Study .....                                                         | 248 |
| 5.5.11 Crystallographic Information .....                                      | 251 |
| 5.6 Photo-Induced C–H Arylation by Reusable Heterogeneous Copper Catalyst..... | 256 |
| 5.6.1 Characterization Data .....                                              | 256 |

|                                                                                      |            |
|--------------------------------------------------------------------------------------|------------|
| 5.6.2 Synthesis of Hybrid Copper Catalyst .....                                      | 289        |
| 5.6.3 Determination of Catalyst Loading .....                                        | 291        |
| 5.6.4 Competition Experiment.....                                                    | 292        |
| 5.6.5 Radical Experiment .....                                                       | 292        |
| 5.6.7 On-Off Light Test.....                                                         | 293        |
| 5.6.8 Heterogeneity Test.....                                                        | 294        |
| 5.7 Distal C–H Activation by Reusable Heterogeneous Ruthenium Catalysis.....         | 296        |
| 5.7.1 Characterization Data .....                                                    | 296        |
| 5.7.2 Preparation of Hybrid Ruthenium Catalyst .....                                 | 310        |
| 5.7.3 Determination of Catalyst Loading .....                                        | 310        |
| 5.7.4 Competition Experiment.....                                                    | 311        |
| 5.7.5 H/D Exchange Study .....                                                       | 312        |
| 5.7.6 KIE Study .....                                                                | 314        |
| 5.7.7 Heterogeneity test .....                                                       | 316        |
| 5.8 C–H Arylations and Alkylations by Reusable Heterogeneous Manganese Catalyst..... | 320        |
| 5.8.1 Characterization Data .....                                                    | 320        |
| 5.8.2 Synthesis of Hybrid Manganese Catalyst.....                                    | 343        |
| 5.8.3 Determination of Catalyst Loading .....                                        | 345        |
| 5.8.4 Heterogeneity Test.....                                                        | 346        |
| <b>6. References .....</b>                                                           | <b>349</b> |
| <b>7. Appendix: NMR Spectra .....</b>                                                | <b>377</b> |

**List of Abbreviations**

|             |                                                   |
|-------------|---------------------------------------------------|
| Ac          | acetyl                                            |
| acac        | acetyl acetonate                                  |
| Alk         | alkyl                                             |
| AMLA        | ambiphilic metal-ligand activation                |
| aq.         | aqueous                                           |
| Ar          | aryl                                              |
| atm         | atmospheric pressure                              |
| BHT         | 2,6- <i>di-tert</i> -butyl-4-methylphenol         |
| BIES        | base-assisted internal electrophilic substitution |
| Bn          | benzyl                                            |
| Boc         | <i>tert</i> -butyloxycarbonyl                     |
| Bu          | butyl                                             |
| Bz          | benzoyl                                           |
| calc.       | calculated                                        |
| <i>cat.</i> | catalytic                                         |
| CMD         | concerted metalation deprotonation                |
| conv.       | conversion                                        |
| Cp*         | cyclopentadienyl                                  |
| Cy          | cyclohexyl                                        |
| $\delta$    | chemical shift                                    |
| d           | doublet                                           |
| DCB         | dichlorobutane                                    |
| DCE         | 1,2-dichloroethane                                |
| DCM         | dichloromethane                                   |

## List of Abbreviations

---

|          |                                                             |
|----------|-------------------------------------------------------------|
| dd       | doublet of doublet                                          |
| DFT      | density functional theory                                   |
| DG       | directing group                                             |
| DME      | dimethoxyethane                                             |
| DMF      | <i>N,N</i> -dimethylformamide                               |
| DMSO     | dimethyl sulfoxide                                          |
| DMPU     | 1,3-dimethyl-3,4,5,6-tetrahydro-2(1 <i>H</i> )-pyrimidinone |
| dt       | doublet of triplet                                          |
| EI       | electron ionization                                         |
| equiv    | equivalent                                                  |
| ES       | electrophilic substitution                                  |
| ESI      | electrospray ionization                                     |
| Et       | ethyl                                                       |
| FG       | functional group                                            |
| g        | gram                                                        |
| GC       | gas chromatography                                          |
| h        | hour                                                        |
| Hal      | halogen                                                     |
| Het      | hetero atom                                                 |
| Hept     | heptyl                                                      |
| Hex      | hexyl                                                       |
| HPLC     | high performance liquid chromatography                      |
| HR-MS    | high resolution mass spectrometry                           |
| Hz       | Hertz                                                       |
| <i>i</i> | <i>iso</i>                                                  |
| IR       | infrared spectroscopy                                       |
| IES      | internal electrophilic substitution                         |
| <i>J</i> | coupling constant                                           |

## List of Abbreviations

---

|                  |                                                                            |
|------------------|----------------------------------------------------------------------------|
| KIE              | kinetic isotope effect                                                     |
| L                | ligand                                                                     |
| <i>m</i>         | <i>meta</i>                                                                |
| m                | multiplet                                                                  |
| M                | molar                                                                      |
| [M] <sup>+</sup> | molecular ion peak                                                         |
| Me               | methyl                                                                     |
| Mes              | mesityl                                                                    |
| mg               | milligram                                                                  |
| MHz              | megahertz                                                                  |
| min              | minute                                                                     |
| mL               | milliliter                                                                 |
| mmol             | millimol                                                                   |
| M. p.            | melting point                                                              |
| MS               | mass spectrometry                                                          |
| <i>m/z</i>       | mass-to-charge ratio                                                       |
| NCTS             | <i>N</i> -cyano-4-methyl- <i>N</i> -phenyl benzenesulfonamide              |
| NMTS             | <i>N</i> -cyano- <i>N</i> -(4-methoxy)phenyl- <i>p</i> -toluenesulfonamide |
| NMP              | <i>N</i> -methylpyrrolidinone                                              |
| NMR              | nuclear magnetic resonance                                                 |
| <i>o</i>         | <i>ortho</i>                                                               |
| OA               | oxidative addition                                                         |
| OPV              | oil pump vacuum                                                            |
| <i>p</i>         | <i>para</i>                                                                |
| Ph               | phenyl                                                                     |
| PMP              | <i>para</i> -methoxyphenyl                                                 |
| Piv              | pivaloyl                                                                   |
| ppm              | parts per million                                                          |



## List of Abbreviations

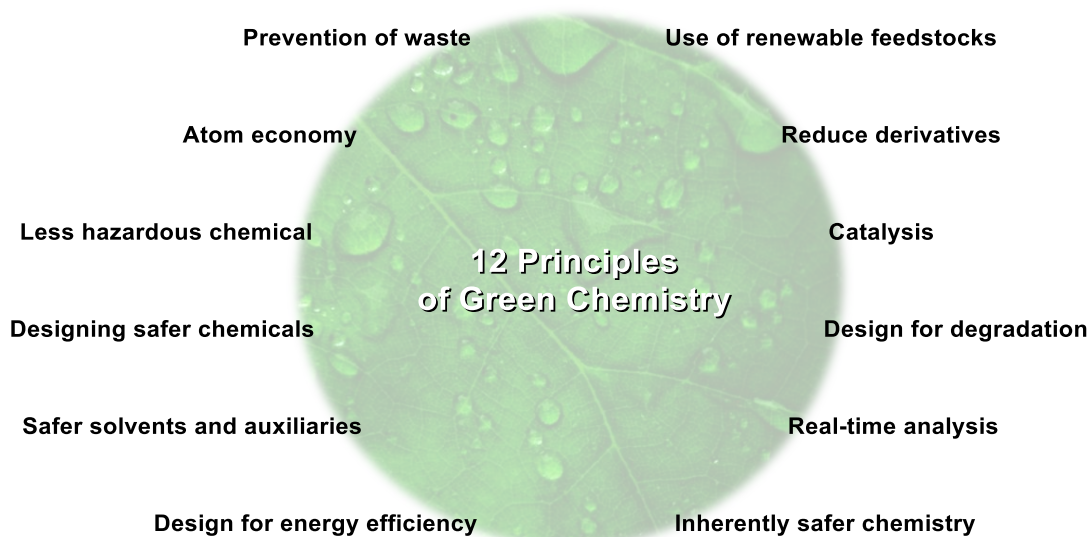
---

|            |                                |
|------------|--------------------------------|
| Pr         | propyl                         |
| PTSA       | <i>p</i> -Toluenesulfonic acid |
| py         | pyridyl                        |
| pym        | pyrimidine                     |
| pyr        | pyrazol                        |
| q          | quartet                        |
| RT         | room temperature               |
| s          | singlet                        |
| sat.       | saturated                      |
| SPS        | solvent purification system    |
| <i>t</i>   | <i>tert</i>                    |
| t          | triplet                        |
| T          | temperature                    |
| THF        | tetrahydrofuran                |
| TLC        | thin layer chromatography      |
| TM         | transition metal               |
| TMEDA      | tetramethylethylenediamine     |
| TMP        | 2,2,6,6-tetramethylpiperidine  |
| TMS        | trimethylsilyl                 |
| Ts         | <i>para</i> -toluenesulfonyl   |
| TS         | transition state               |
| <i>wt%</i> | weight by volume               |

## 1. Introduction

During the last century, tremendous advances in organic synthesis have been accomplished, allowing our life to be fertile, convenient, and efficient. For instance, crop protection products enable an unprecedented increase in the agricultural production output, while the development of pharmaceuticals saves many people's lives. In addition, petroleum becomes an inevitable part of our daily life, while materials are found everywhere around us. These enormous progress in organic chemistry, however, have brought about a series of problems related to environmental pollution and resource depletion by generating toxic materials and consuming a huge amount of energy.

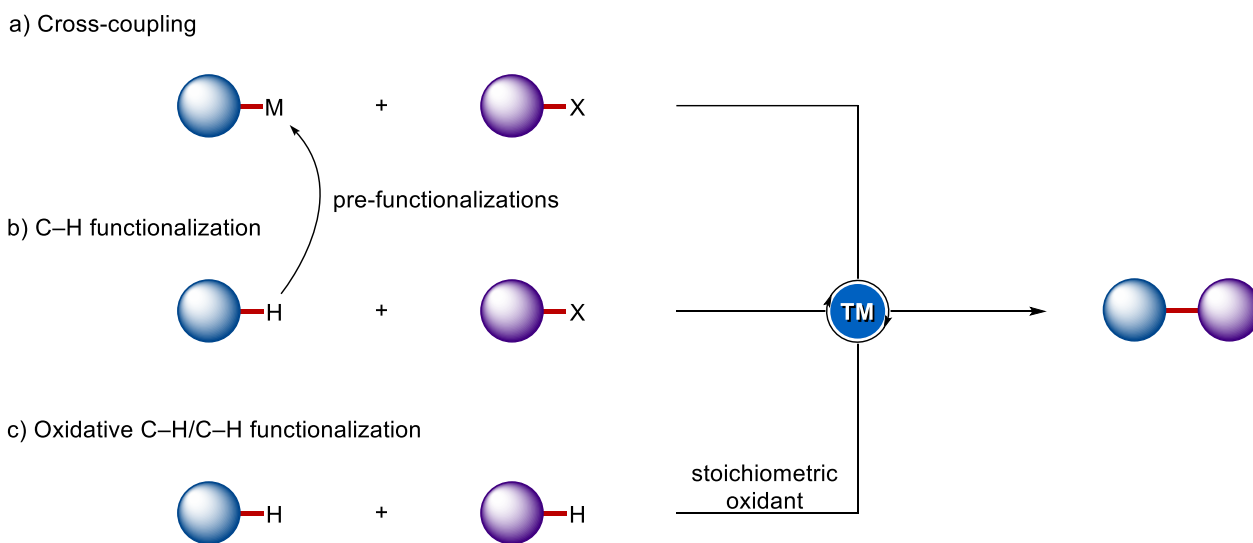
In order to alleviate the dark side of the chemical reactions, a new approach toward resource-,<sup>[1]</sup> step- and atom-economical<sup>[2]</sup> synthetic methodologies are in high demand. In 1998, Anastas and Warner proposed the "12 Principles of Green Chemistry",<sup>[3]</sup> which provides chemists with a general guideline for sustainable chemistry, which advises synthetic chemists to pursue environmentally benign chemical processes (Scheme 1.1.1). In this regard, catalysis helps to operate the chemical reactions with a reduced amount of chemicals in lieu of its excess uses, thus setting the stage for resource economical synthesis. Furthermore, direct utilization of easily accessible chemicals without pre-functionalization assists to achieve step- and atom-efficiency in the chemistry process. Additionally, mild reaction conditions and less toxic chemicals are expected to provide safer chemical processes.<sup>[4]</sup>



**Scheme 1.1.1** The 12 Principles of Green Chemistry.

## 1.1 Homogeneous Metal-Catalyzed C–H Functionalization

Since hydrocarbons are omnipresent structural units in organic compounds, the utilization of C–H bonds of hydrocarbons has great potential. Thereby, organic chemists have had utmost interests in the transformation of hydrocarbons to useful and high-valued compounds by straightforward and sustainable methods. Previously, a significant achievement of catalysis for C–C bond and C–Het bond formations has been made by transition metals (Scheme 1.1.2a),<sup>[5]</sup> leading to the development of numerous name reactions, such as the Suzuki–Miyaura,<sup>[6]</sup> Negishi,<sup>[7]</sup> Mizoroki–Heck,<sup>[8]</sup> Kumada–Corriu,<sup>[9]</sup> Hiyama,<sup>[10]</sup> Stille,<sup>[11]</sup> and Sonogashira–Hagihara<sup>[12]</sup> cross-couplings as well as the Tsuji–Trost reaction,<sup>[13]</sup> the Goldberg–Ullmann amination,<sup>[14]</sup> and the related Buchwald–Hartwig reaction.<sup>[15]</sup> The importance of the palladium-catalyzed chemical transformations was recognized by the Nobel Prize in Chemistry awarded collectively to Heck, Negishi, and Suzuki in 2010.<sup>[16]</sup>

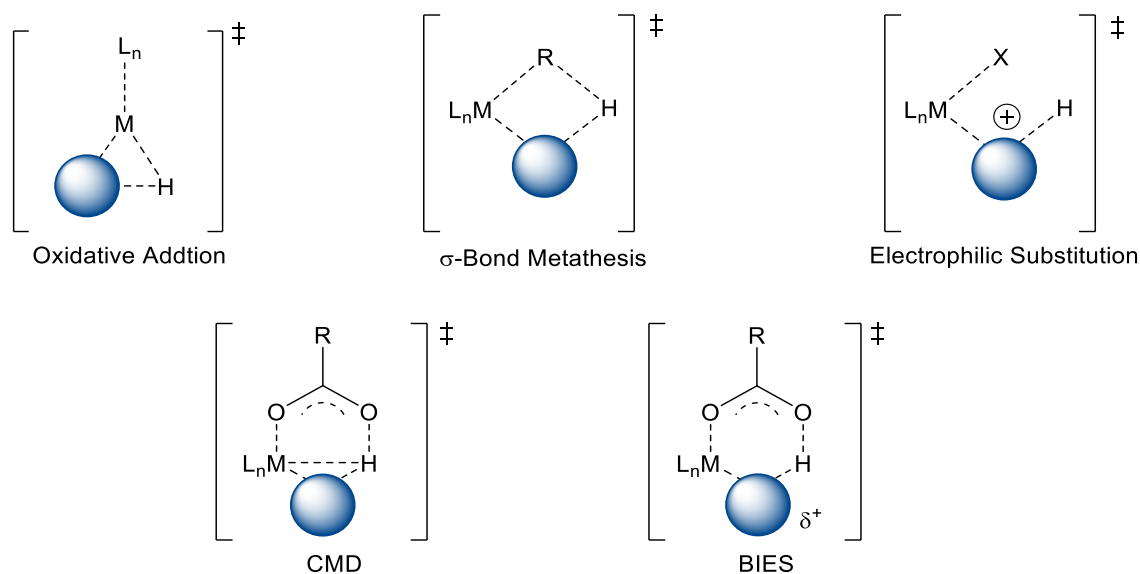


**Scheme 1.1.2** Metal-catalyzed cross-coupling versus C–H functionalization.

Although these palladium catalyses enabled to change paradigm of C–C bond formation reactions (Scheme 1.1.2a), there still existed a drawback where pre-functionalization should be involved, which impedes fulfilling atom- and step-economy as well as user-friendly access. For instance, organostannane reagents used in the Stille coupling are highly toxic, while organomagnesium reagents in the Kumada–Corriu cross-coupling or organozinc reagents in the Negishi cross-coupling are air- and moisture-sensitive. Additionally, the preparation and the use of the organometallic reagents generate

stoichiometric byproducts. In order to obviate such disadvantages of classical cross-coupling reactions, a new approach, namely C–H functionalization, was introduced to the synthetic community.<sup>[17]</sup> With this strategy, the organometallic nucleophile is directly replaced by an inert C–H bond, thereby forming a new C–C bond (Scheme 1.1.2b).<sup>[18]</sup> Additionally, oxidative C–H/C–H functionalization allowed for another scenario for C–C bond formation in the presence of a stoichiometric oxidant (Scheme 1.1.2c).<sup>[19]</sup>

Since C–H functionalization methods provide a sustainable approach for chemical transformation, synthetic chemists became interested in its detailed mechanistic understandings. Except metalloradical or metal carbene/nitrene outer-sphere mechanisms, the organometallic C–H cleavage is proposed to proceed *via* five different possible pathways: (i) oxidative addition; (ii)  $\sigma$ -bond metathesis; (iii) electrophilic substitution; (iv) concerted metallation deprotonation (CMD); (v) base-assisted internal electrophilic substitution (BIES) (Scheme 1.1.3).<sup>[20]</sup>

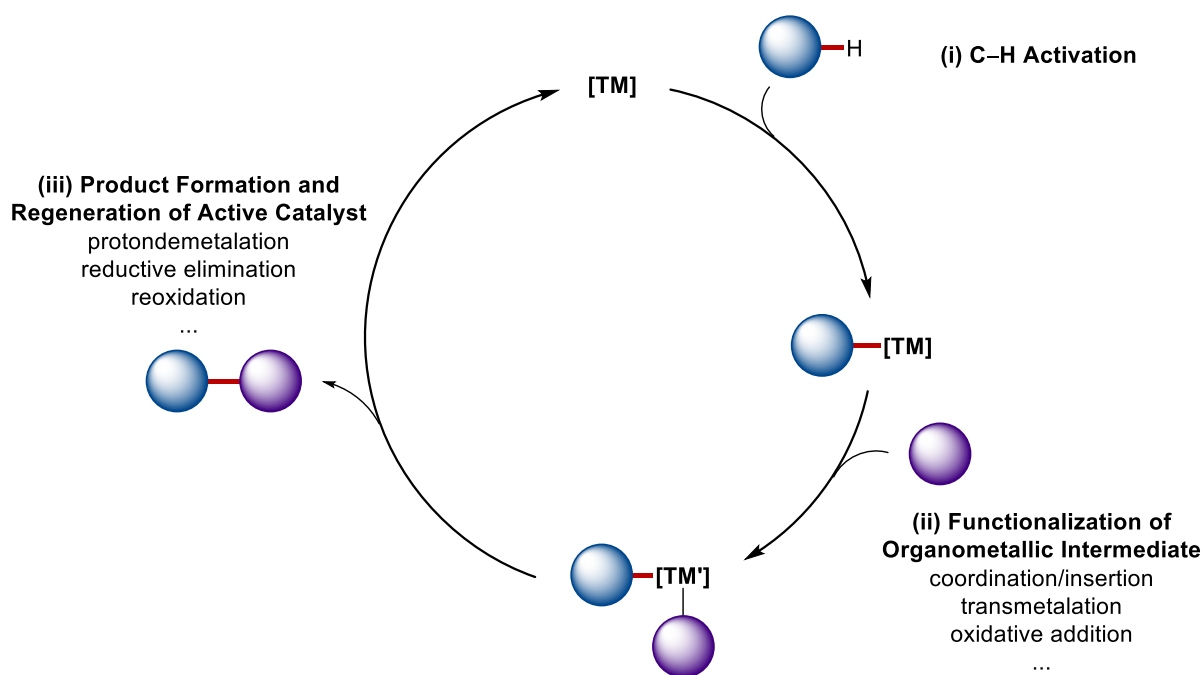


**Scheme 1.1.3** Five different modes of C–H bond cleavage process.

Among these plausible C–H scission pathways, base-assisted metallation models have been most generally accepted for transition metal-catalyzed C–H activation reactions. In this regard, transition state structure and partial charge accumulation are key criteria to subcategorize the base-assisted metallation manifold. Fagnou and Gorelsky proposed a concerted metallation deprotonation (CMD)

pathway, in which the formation of a deprotonative transition state is suggested in the case where C–H bond cleavage step is proposed to be a rate-determining step.<sup>[21]</sup> In a similar way, Macgregor and Davies proposed ambiphilic metal ligand activation (AMLA) pathway where agostic interaction occurs between the metal center and the C–H bond.<sup>[22]</sup> In sharp contrast, Ackermann proposed base-assisted internal electrophilic substitution (BIES), featuring that competition experiments between electronically differentiated substrates show the preferred functionalization of the more electron-rich substrate.<sup>[23]</sup> Notably, this finding cannot be explained by the deprotonative pathway through kinetic C–H acidity.<sup>[24]</sup>

Based on these proposals, general catalytic cycles for the transition metal-catalyzed C–H functionalization can be envisaged, while the mechanistic details can vary reactions (Scheme 1.1.4).

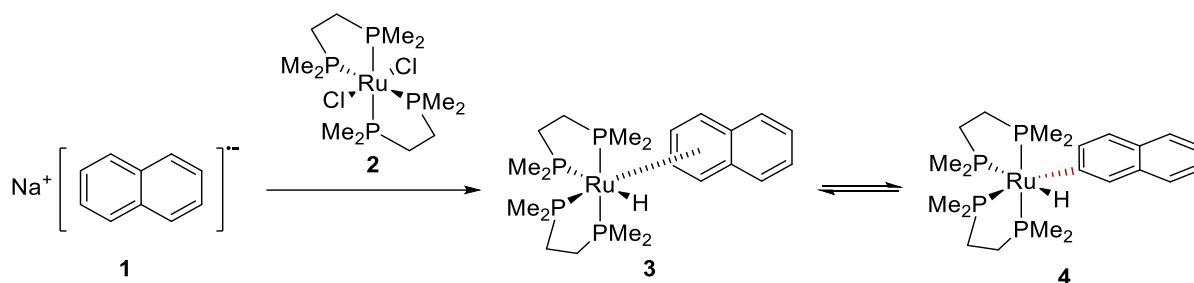


**Scheme 1.1.4** General catalytic pathways for transition metal-catalyzed C–H activation reactions.

In the following chapters, C–H activation reactions using representative metals, including ruthenium, osmium, manganese, and copper are described. Beyond homogeneous realm, recyclable hybrid metal-catalyzed C–H activation approach will be presented.

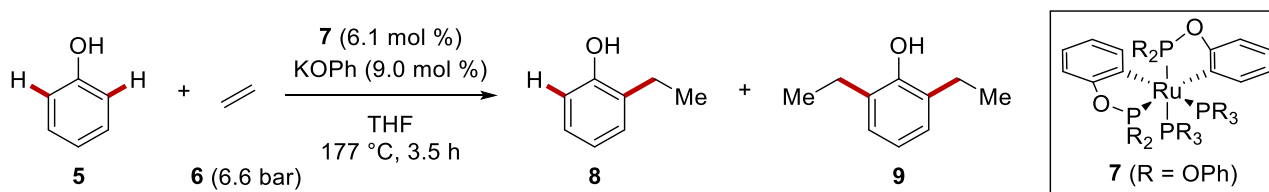
## 1.2 Ruthenium-Catalyzed C–H Activation

Transition metal-catalyzed C–H functionalization has gained enormous attention with precious 4d and 5d metal catalysis, such as rhodium,<sup>[25]</sup> palladium,<sup>[26]</sup> and iridium,<sup>[27]</sup> providing the direct transformation from omnipresent C–H bonds to new C–C or C–Het bonds. In sharp contrast, ruthenium has recently come into the spotlight due to its cost-effectiveness and unique selectivities and reactivities.<sup>[28]</sup> The first example of the stoichiometric C–H activation with ruthenium complex was reported by Chatt and Davidson, with sodium naphthalene salts by *in-situ* generated ruthenium(0) complex, which was in equilibrium between **3** and **4** (Scheme 1.2.1).<sup>[29]</sup>



**Scheme 1.2.1** Ruthenium-mediated C–H functionalization.

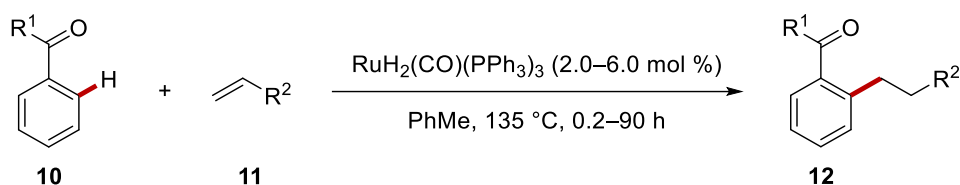
The first ruthenium-catalyzed C–H activation was arguably reported by Lewis and Smith in 1986 (Scheme 1.2.2).<sup>[30]</sup> In this study, the *ortho*-position of phenol **5** was functionalized with ethylene gas **6**, affording mono-alkylated **8** and di-alkylated phenol **9** with the aid of phosphites as transient directing group.



**Scheme 1.2.2** The first catalytic C–H activation with the ruthenium complex.

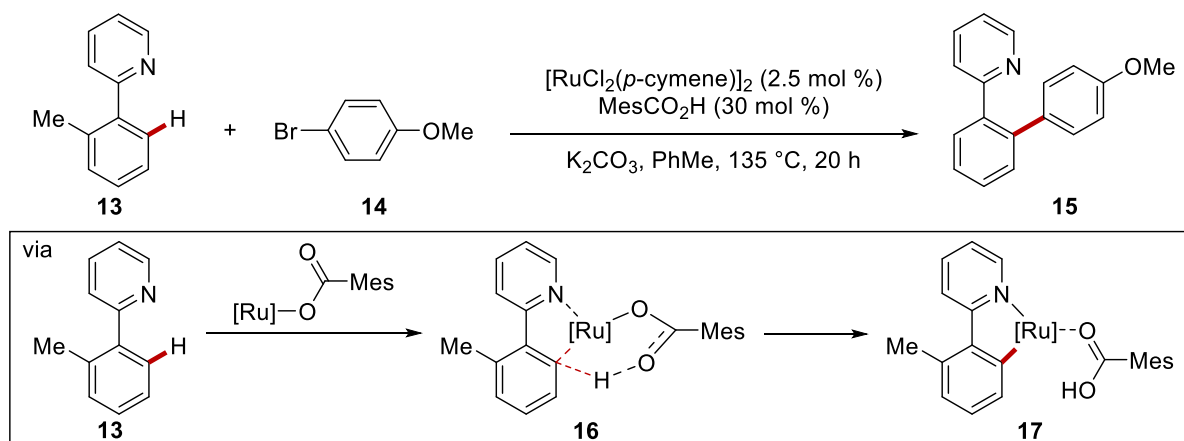
In 1993, Kakiuchi and Murai showed ruthenium-catalyzed C–H hydroarylations with aromatic ketones **10** and alkenes **11** (Scheme 1.2.3).<sup>[31]</sup> With the aid of weak *O*-coordination,<sup>[31]</sup> the C–H bond cleavage

occurred *via* a five-membered ruthenacycle formation, which was later rationalized by DFT studies from the Morokuma group.<sup>[32]</sup> This achievement was key to enable other researchers to develop related ruthenium-catalyzed C–H activations.



**Scheme 1.2.3** Ruthenium-catalyzed direct C–H hydroarylation.

Inspired by base-assisted metalation manifold by Shaw<sup>[33]</sup> and Davies,<sup>[34]</sup> Ackermann<sup>[23, 20a]</sup> demonstrated a significant advance in ruthenium catalysis, in which carboxylate assistance played the key role in the C–H activation process (Scheme 1.2.4).<sup>[35]</sup> Importantly, the mechanistic rationale of the carboxylate-assisted ruthenium-catalyzed C–H activation was suggested to proceed *via* a six-membered transition state.<sup>[36a, 21b, 36b]</sup>

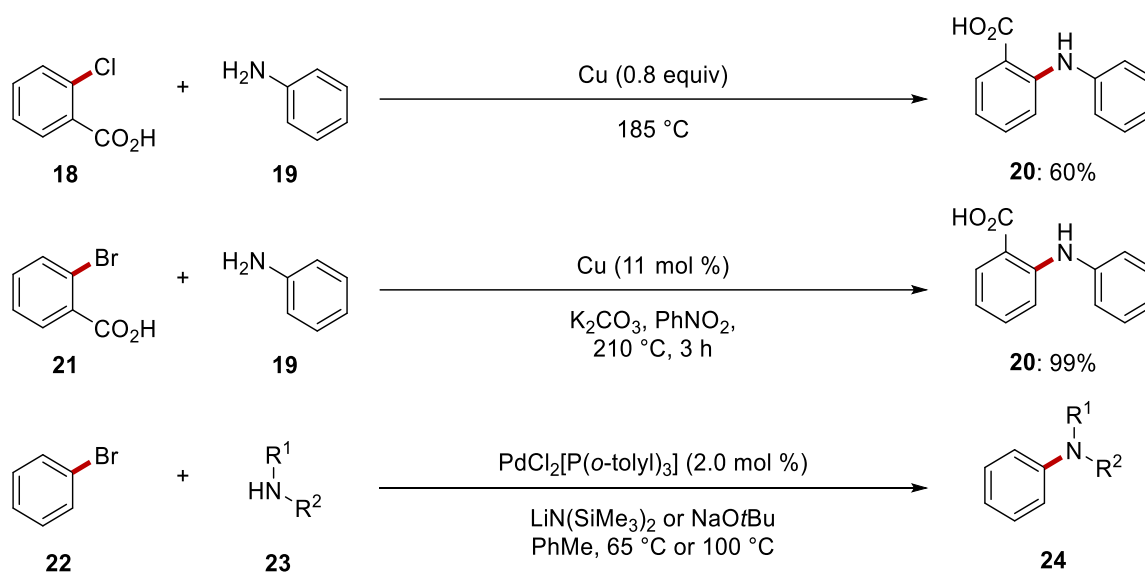


**Scheme 1.2.4** Base-assisted ruthenium-catalyzed C–H activation.

While the thus established ruthenium(II)-catalysis has enabled various types of C–H activation reactions,<sup>[17]</sup> C–N formation and distal C–C formation reactions are to be covered in the following chapters.

### 1.2.1 Ruthenium-Catalyzed C–N Formation

Carbon–nitrogen bonds are prevalent in a plethora of pharmaceuticals, natural products, and biologically active compounds.<sup>[37]</sup> For this reason, there is a strong demand to achieve sustainable and selective C–N bond formation reactions. Among the conventional approaches toward C–N bond formations, copper-catalyzed Goldberg–Ullmann amination reactions<sup>[14a, 38a, 14b, 38b]</sup> and palladium-catalyzed Buchwald–Hartwig amination reactions<sup>[39]</sup> have been utilized, giving synthetic chemists a facile method for a broad range of aryl amines (Scheme 1.2.5).



**Scheme 1.2.5** Copper and palladium-catalyzed aminations.

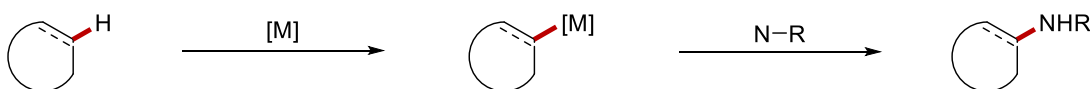
Although these aminations provided easy access to C–N bond formations, such approaches have highly relied on the pre-functionalization of substrates, producing inherently stoichiometric amounts of byproducts. In stark contrast, the transition metal-catalyzed C–H activation approach was able to overcome the limitation, thereby offering synthetic and economic efficiency. The initial contributions for C–H aminations had mainly been achieved by precious metals, such as rhodium,<sup>[40]</sup> palladium,<sup>[41]</sup> and iridium.<sup>[42]</sup> Thereby, the motivation of the search for inexpensive, but active metal catalysts to utilizing ruthenium complexes for C–N bond formations.

Ruthenium-catalyzed C–H amination reactions can be categorized by three realms (Scheme 1.2.6). The inner-sphere mechanism is generally involved in the formation of organometallic intermediate

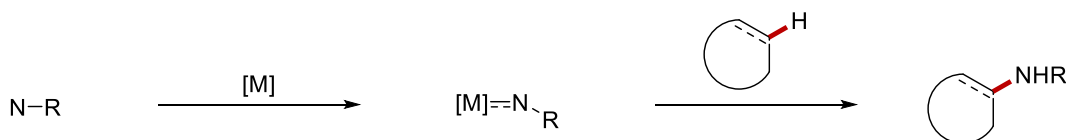


including Metal–C bond and thus generated ruthenacycle complexes is subsequently engaged in C–N bond forming process. The outer-sphere mechanism<sup>[43]</sup> commonly represents C–H insertion catalysis, in which ruthenium–nitrenoid species react with a coupling partner, resulting in C–H aminations. The third approach is to utilize ruthenium-based photoredox catalysis *via* a single electron transfer process, in which the organoradical species indirectly generated upon irradiation interacts with a substrate, thus giving amidated products.

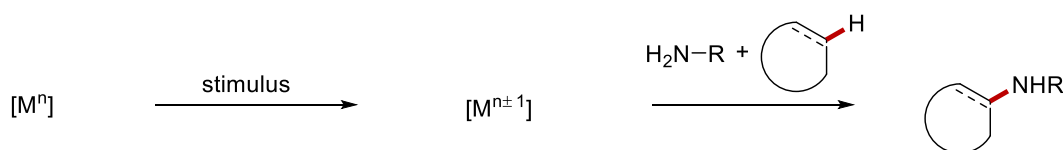
a) Inner-sphere C–H activation



b) Outer-sphere C–H functionalization



c) Single electron transfer mechanism

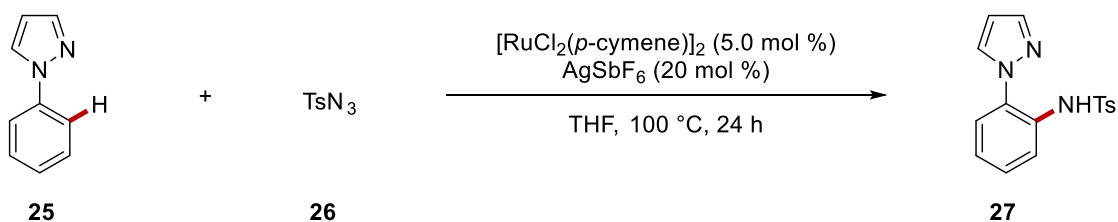


**Scheme 1.2.6** Different modes of C–N formations.

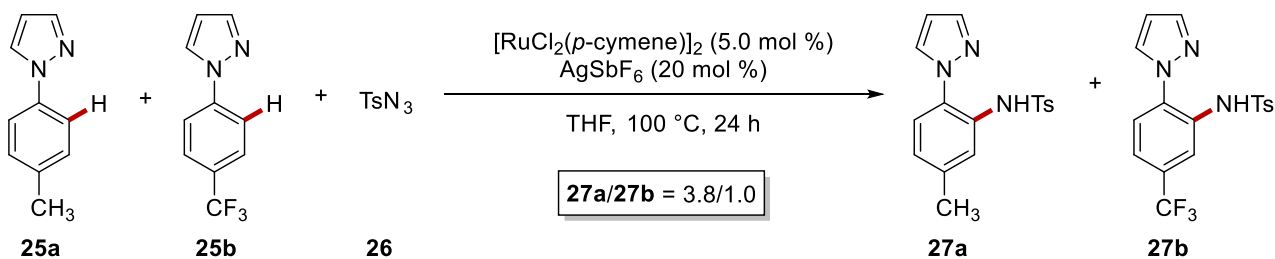
Notably, in a general scenario of amination reactions, C(sp<sup>2</sup>)–H (~113 kcal/mol) and N–H (~108 kcal/mol) bonds are transformed to new C–N (~103 kcal/mol) and H–H (~104 kcal/mol) bonds, which is thermodynamically uphill process.<sup>[44]</sup> Therefore, a selection of reaction components is the key to success for the amination reactions.

In 2013, Ackermann and co-workers successfully showed C–H amidations of arenes with tosyl azide **26** as an amidating reagent (Scheme 1.2.7).<sup>[45]</sup> With the aid of pyrazole directing groups, *ortho* C–H bonds of arenes **25** could be selectively functionalized. Detailed mechanistic studies revealed that electrophilic-type ruthenation was likely operative and the C–H scission process was reversible. Based on their mechanistic studies, the catalytic cycle was proposed. Thus, ruthenium cation species **30** is *in-situ* generated, which enables to form five-membered ruthenacycle **31**. Thereafter, tosyl azide **26** is

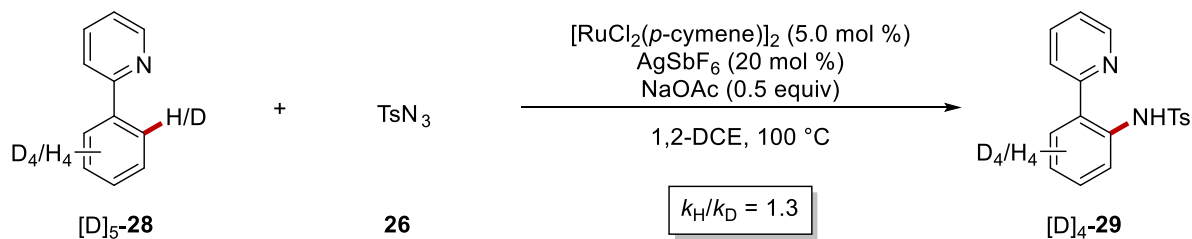
coordinated to the ruthenium center. Insertion followed by protodemetalation affords the amidated product **27** and regenerates the active catalyst **30**.



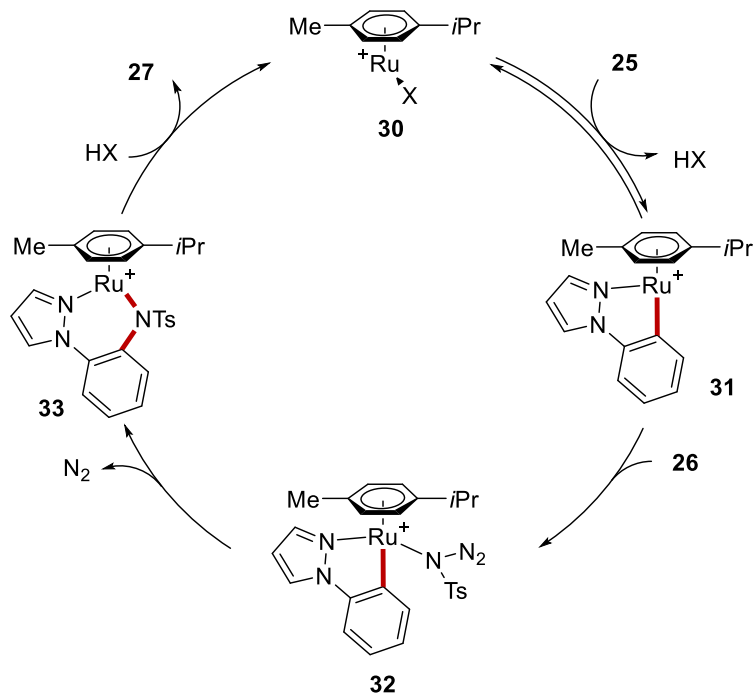
a) competition experiment



b) KIE experiment

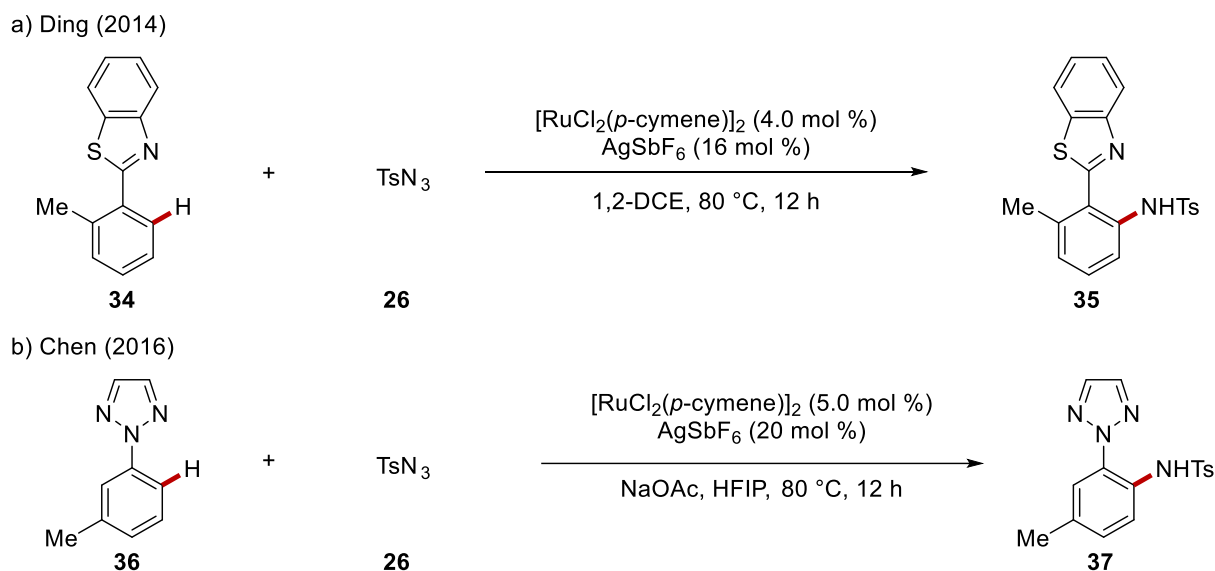


c) Proposed mechanism



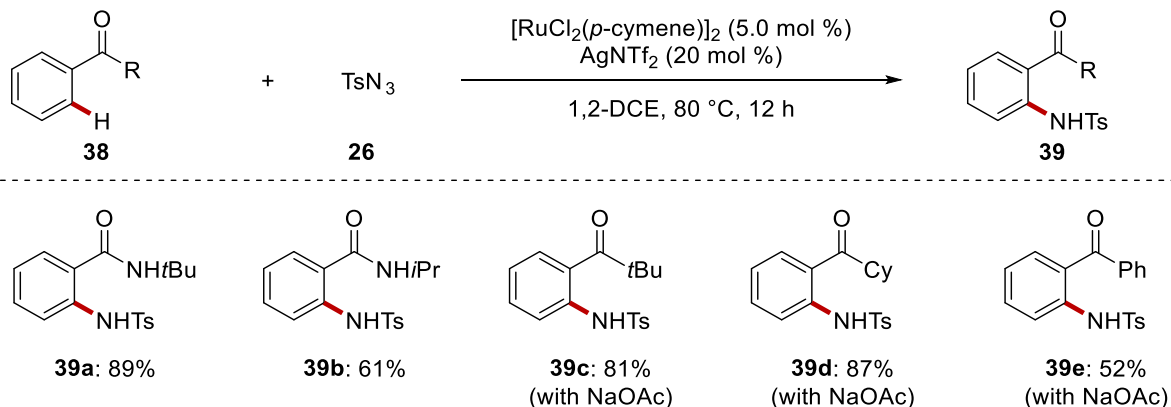
**Scheme 1.2.7** C–H amidation of arenes **25** with tosyl azide **26**.

Using a strong directing group strategy, Ding<sup>[46]</sup> and Chen<sup>[47]</sup> independently reported C–H amidation, in which benzothiazoles and triazole directing groups were employed although one *ortho*- or *meta*-position was required to be sterically blocked to inhibit difunctionalizations of the arenes **34** or **36** (Scheme 1.2.8).



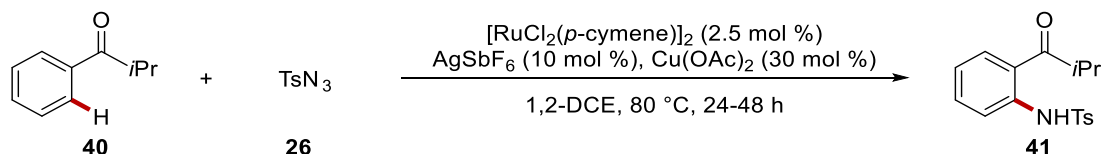
**Scheme 1.2.8** C–N bond formation using strong *N*-directing groups.

Instead of strongly coordinating directing groups, weak coordination also allowed for efficient C–H amination reactions. In 2013, Chang and co-workers showed that amide or ketone based substrates were effective for the C(sp<sup>2</sup>)–H amidations (Scheme 1.2.9).<sup>[48]</sup>



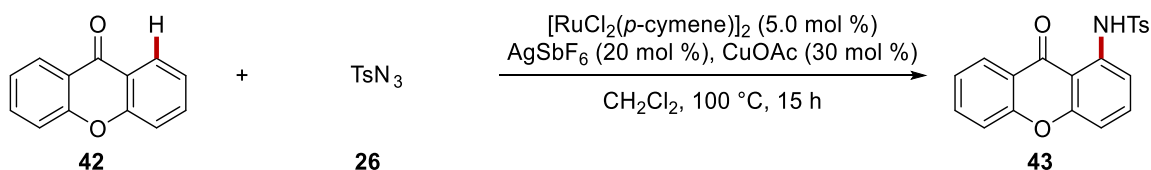
**Scheme 1.2.9** C–H amidations by weak *O*-coordination.

Similar to the approach presented by Chang, Jiao also reported C–H amidations of the aromatic ketone **40**, in which a catalytic amount of copper acetate was used as addition to *in-situ* form a ruthenium(II)-carboxylate complex (Scheme 1.2.10).<sup>[49]</sup>



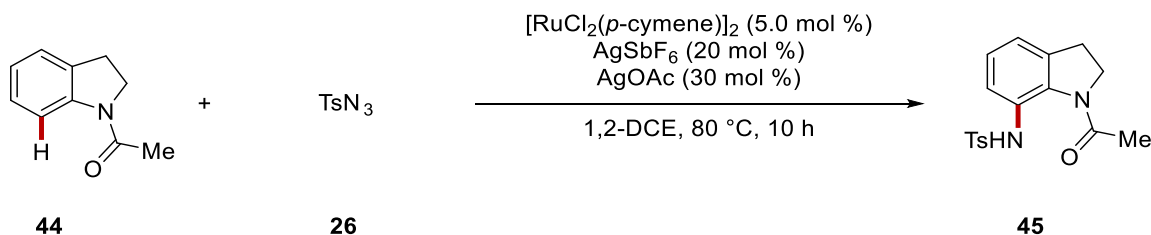
**Scheme 1.2.10** Ketones as a directing group for ruthenium-catalyzed C–N bond formation.

In 2014, Kim disclosed ruthenium-catalyzed C–H amidations of xanthenes **42**, which enabled to access mono-amidated xanthenes **43** as a sole product (Scheme 1.2.11).<sup>[50]</sup> Notably, the thus synthesized nitrogenated products were screened for growth inhibition activity against human breast cancer MCF-7 cells.



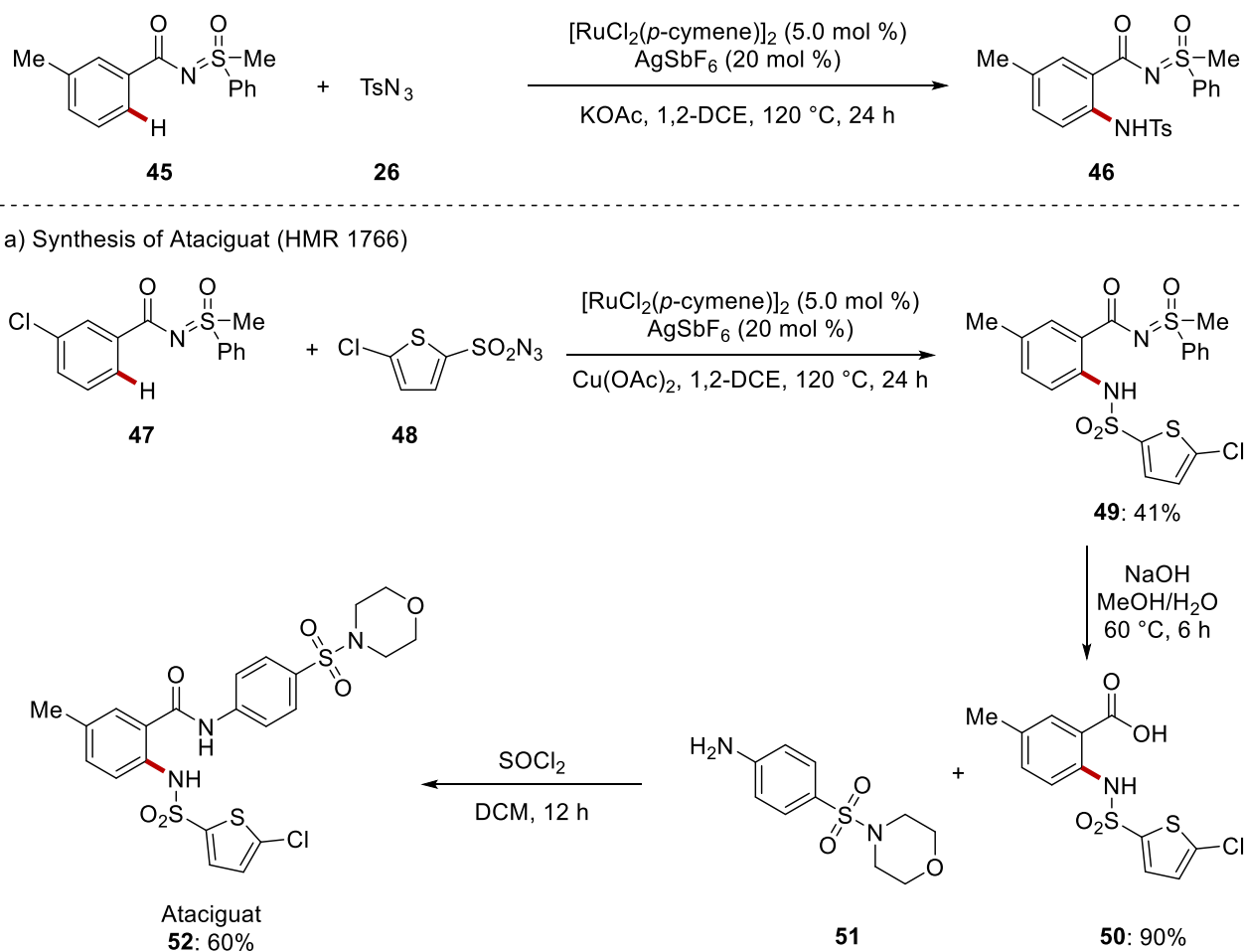
**Scheme 1.2.11** Ruthenium-catalyzed C–H amidation of xanthenes **42**.

At the same time, Zhu reported ruthenium-catalyzed C7–H amidation of indolines **44** through the installation of a ketone directing group (Scheme 1.2.12).<sup>[51]</sup> Here, six-membered metallacycles were presumably formed, enabling direct access toward C7 indoline functionalizations.



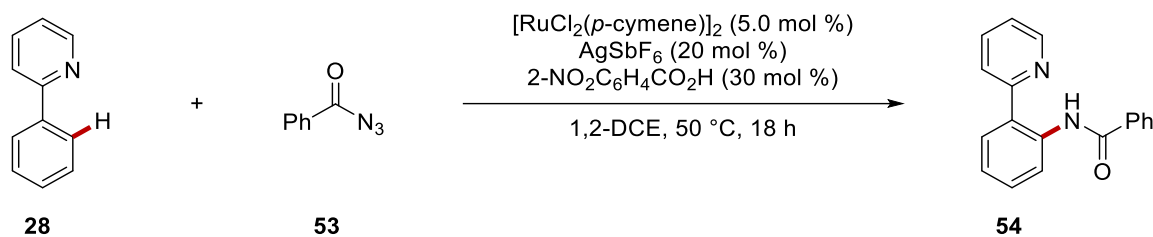
**Scheme 1.2.12** Ruthenium-catalyzed C7–N bond formation of indoline **44**.

Interestingly, Sahoo used sulfoximine directing group strategy which had been commonly used for rhodium catalysis (Scheme 1.2.13).<sup>[52]</sup> Particularly, the reported method was used for the synthesis of a potent medication, namely Ataciguat, which had been studied for calcific aortic valve stenosis.<sup>[53]</sup>



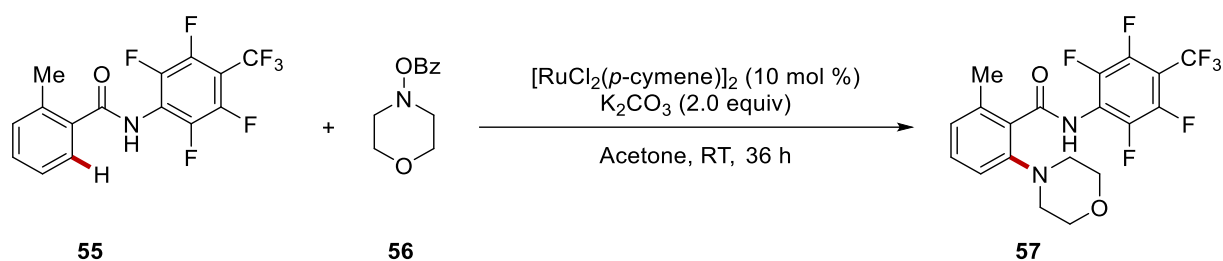
**Scheme 1.2.13** Sulfoximine directing group approach for C–H amidation and its use for natural product synthesis.

Other organic azides and hydroxylamines were also viable for ruthenium-catalyzed amidations. Chang thus showed the use of acyl azides **53** as an aminating reagent for ruthenium-catalyzed amidation reactions (Scheme 1.2.14).<sup>[54]</sup> Although benzoyl azides **53** are prone to undergo Curtius rearrangement, mechanistic studies revealed that facile C–H ruthenations enabled the direct amidation.



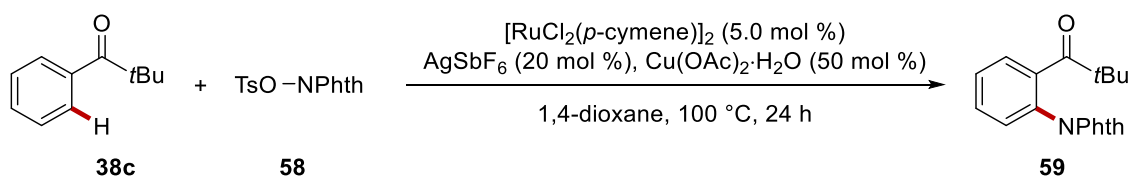
**Scheme 1.2.14** C–H amidations with acyl azides **53**.

Additionally, the Yu group used *O*-benzoylhydroxylamines **56** as an amine source, providing *ortho*-C–H aminations of benzamides **55** under mild conditions at room temperature (Scheme 1.2.15).<sup>[55]</sup>

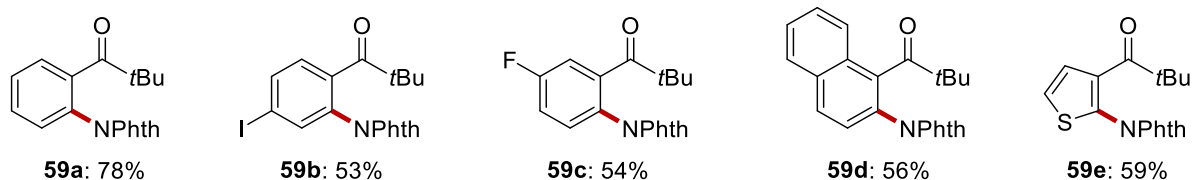
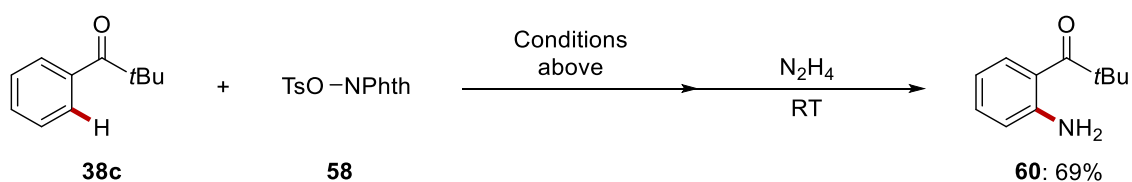


**Scheme 1.2.15** C–H amidations through N–O bond cleavage.

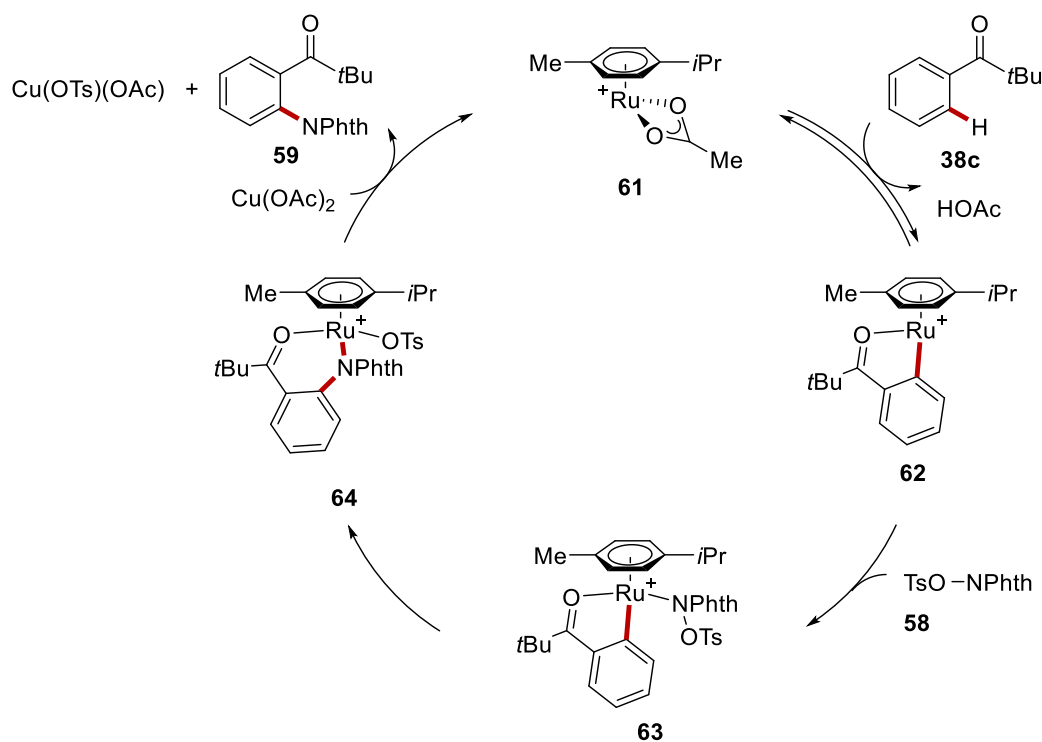
Ackermann showed ruthenium(II)carboxylate-catalyzed C–H imidations with (*N*-OTs)phthalimide **58** as the amination source (Scheme 1.2.16).<sup>[56]</sup> Notable, a wide range of substrates was presented. A simple additional step allowed for easy access to aminophenones **60**. The catalytic cycle has been also proposed, in which an *in-situ* generated the cationic ruthenium(II)carboxylate catalyst **61** forms cyclometalated intermediate **62**. The subsequent imidating reagent coordinates followed by the N–O cleavage to deliver the cationic complex **64**. Lastly, the active ruthenium catalyst **61** is regenerated while liberating the desired product **59**.



## a) Selected examples

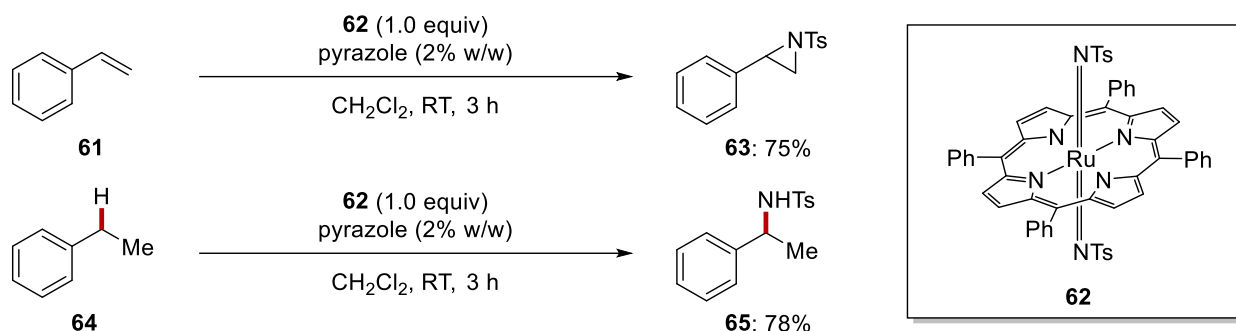
b) Facile access to primary aminophenones **60**

## c) Proposed mechanism



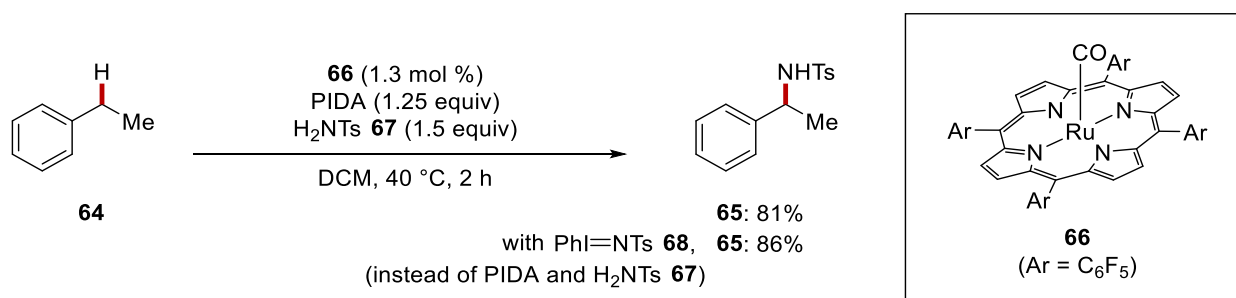
**Scheme 1.2.16** Ruthenium-catalyzed C–H amidation of arenes **38c** with (*N*-OTs)phthalimide **58**.

As the second manifold of C–H amination, various ruthenium-nitrenoid formation strategies were employed. In 1997, Che<sup>[57]</sup> and co-workers showed that stoichiometric use of bis(tosyl)imidoruthenium(VI) porphyrin complex **62** enabled amino group transfer, which was later highlighted by detailed mechanistic studies as well as by the scope of aziridinations and C–H amidations (Scheme 1.2.17).<sup>[58]</sup>



**Scheme 1.2.17** Stoichiometric C–N bond formation with ruthenium-porphyrin complex **62**.

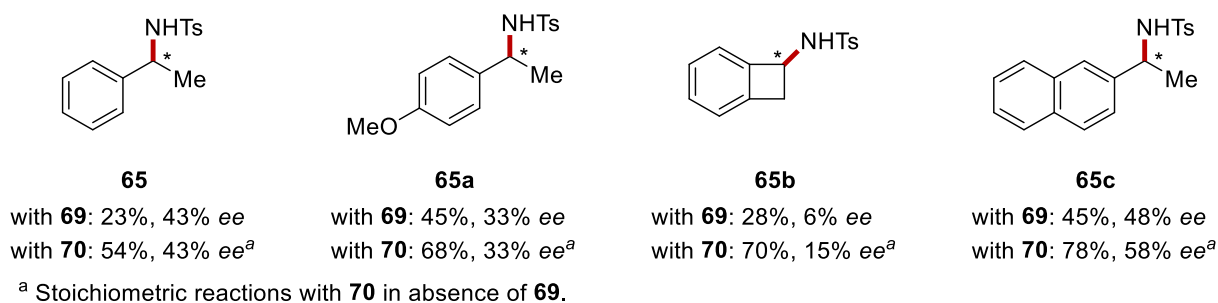
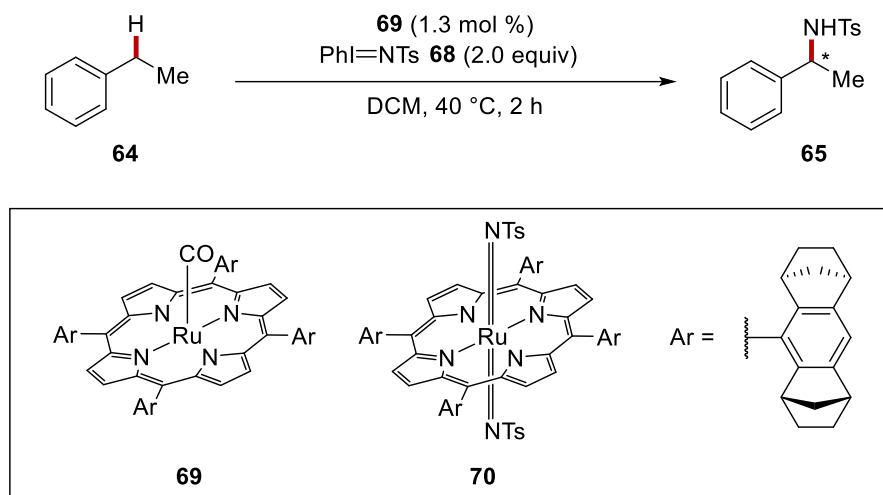
Two years later, Che reported the ruthenium(II) porphyrin-catalyzed C–H amidations with exceptionally high turnovers (Scheme 1.2.18).<sup>[59]</sup> The combination of PIDA and tosylamide **67** or the direct use of *N*-tosyliminobenzylidene **68** enabled a broad range of C–H bond formations.



**Scheme 1.2.18** Ruthenium-catalyzed C–N bond formation.

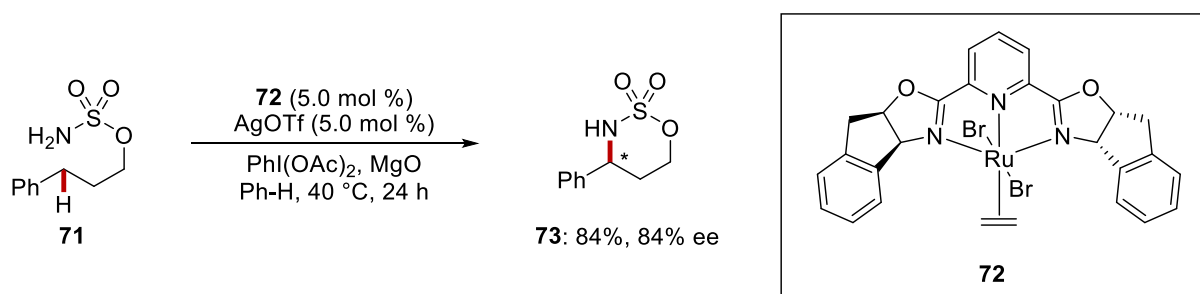
Around the same time, the same research group disclosed asymmetric C–N bond formations catalyzed by chiral ruthenium complex **69** (Scheme 1.2.19).<sup>[60]</sup> While the dimethanoanthracene-based porphyrin macrocycle induced relatively low enantioselectivity (6% *ee* to 48 % *ee*), the stoichiometric use of bis(tosyl)imidoruthenium species enabled slightly increased yield and enantiomeric excess.





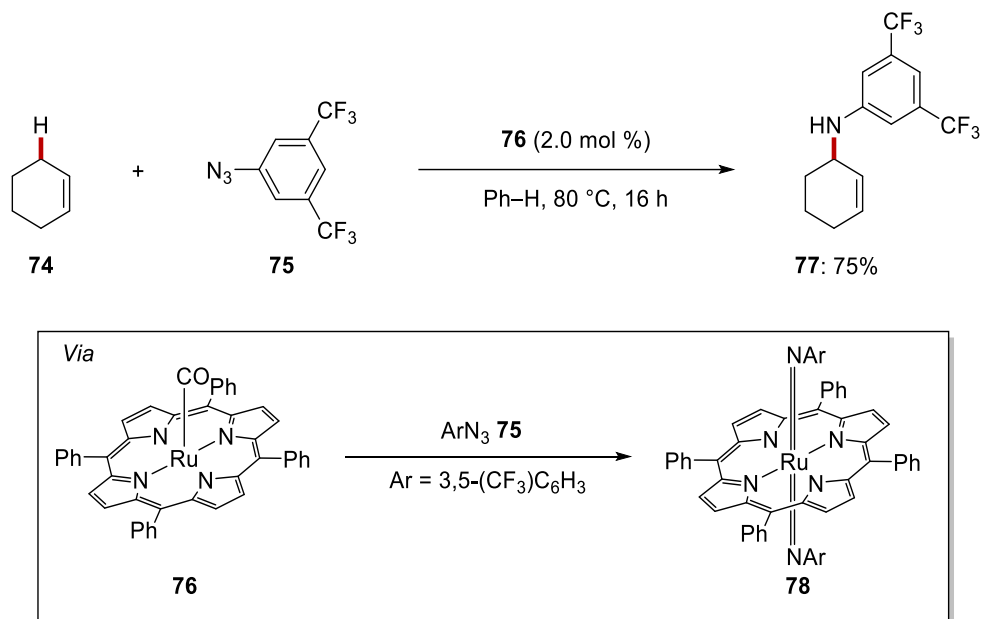
### Scheme 1.2.19 Enantioselective ruthenium-catalyzed C–H amidation.

In 2008, Group of Blakey reported enantioselective ruthenium-catalyzed C–H amidations, in which the chiral pybox ligand was employed to construct cyclosulfamates under mild conditions (Scheme 1.2.20).<sup>[61]</sup> In the presence of hypervalent iodine oxidant, the benzylic C–H bond was selectively transformed to a new C–N bond, while a five-membered sulfamate was not observed.



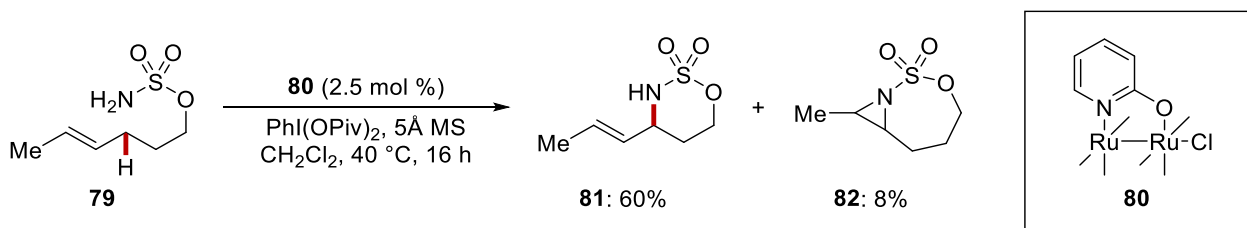
### Scheme 1.2.20 Enantioselective cyclosulfamate synthesis by ruthenium-pybox catalyst **72**.

The next year, Gallo and co-workers revealed C(sp<sup>3</sup>)-H amidations at the vinyl position with aryl azides **75** (Scheme 1.2.21).<sup>[62]</sup> Notably, the isolated stable ruthenium(IV) intermediate **78** allowed for detailed mechanistic investigation by means of spectrometric analyses. Later, independent DFT studies showed two possible mechanisms, in which a pathway through monoimido Ru(IV) species formation cannot be ruled out.<sup>[63]</sup>



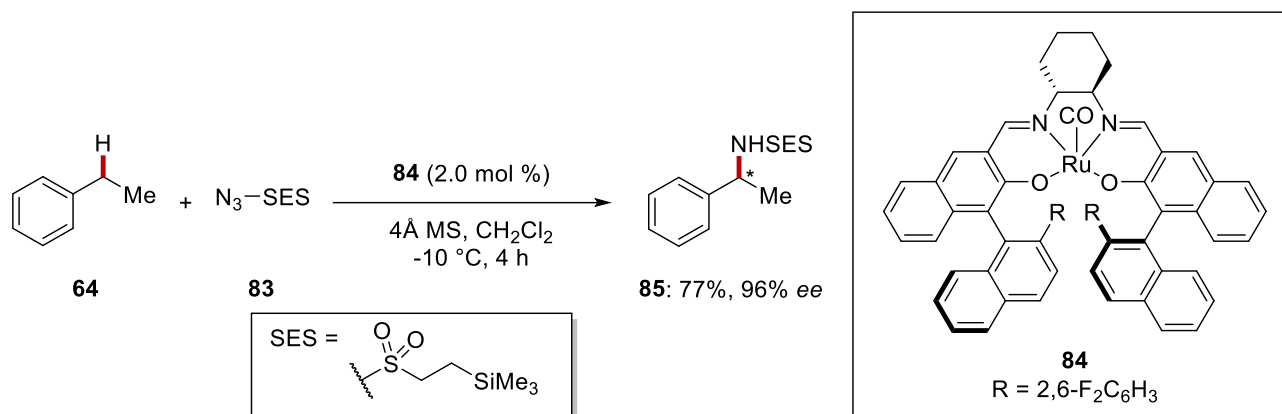
**Scheme 1.2.21** Ruthenium-catalyzed C(sp<sup>3</sup>)-H amination.

In 2011, Du Bois disclosed diruthenium(II/III)-catalyzed ring-closing allylic C-H aminations (Scheme 1.2.22).<sup>[64]</sup> Taking advantage of the mixed valent ruthenium complex **80**, a one-electron oxidation could be achieved by catalytic atom-transfer process. Additionally, the selectivity toward C-H insertion process over aziridination was analyzed by computational studies.

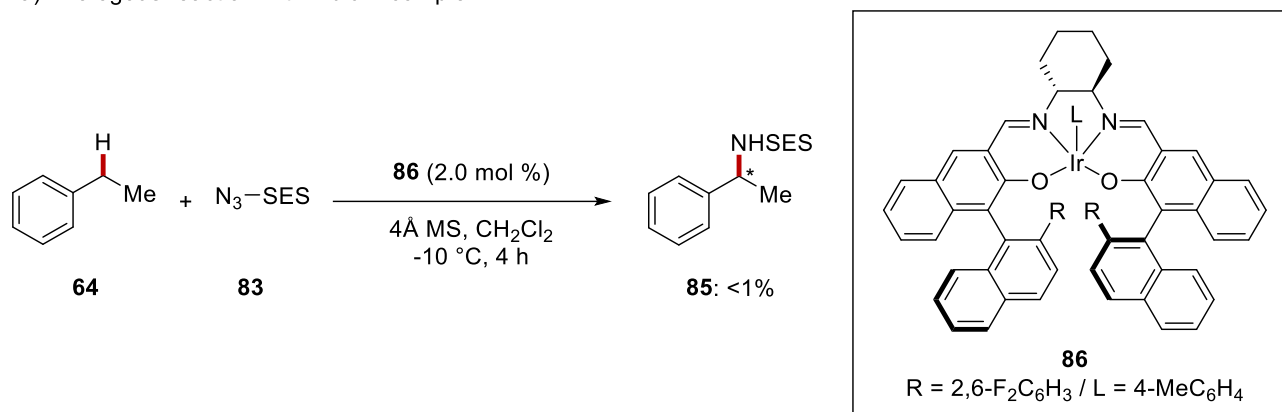


**Scheme 1.2.22** Diruthenium complex-catalyzed intramolecular C-H amidation.

In 2013, Katsuki reported enantioselective intermolecular benzylic amidation using the salen-based chiral ruthenium(II) complex **84** (Scheme 1.2.23).<sup>[65]</sup> Interestingly, an analogous iridium catalyst fell short in delivering the desired product.

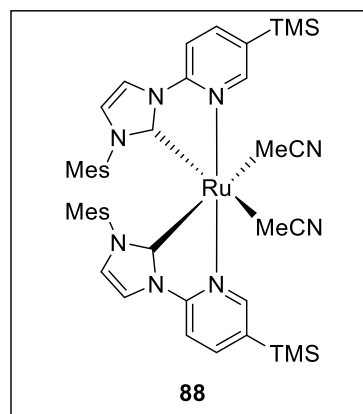
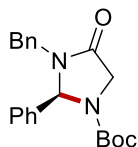
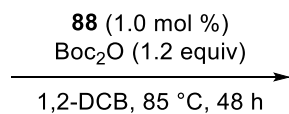
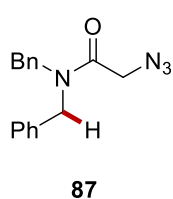


a) Analogous reaction with iridium complex **xxx**

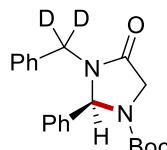
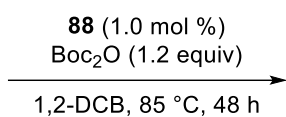
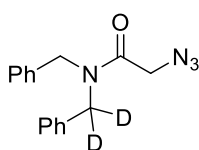


**Scheme 1.2.23** Enantioselective C–H amidation with salen complexes **84** and **86**.

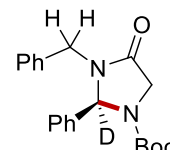
Recently, Meggers showed asymmetric intramolecular C–H amination by a chiral-at-metal ruthenium complex, affording five-membered heterocycles with high enantioselectivity (Scheme 1.2.24).<sup>[66]</sup> Notably, high catalytic efficiency (TON = 740) was also accomplished. Detailed mechanistic studies revealed that the concerted singlet ruthenium-nitrenoid insertion process is likely to be operative.



a) KIE study



+



[D]<sub>n</sub>-**87**

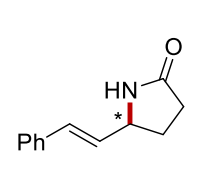
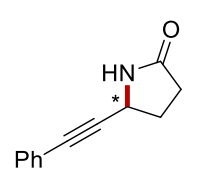
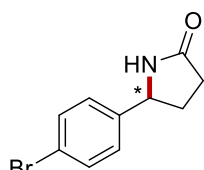
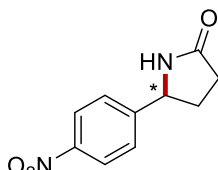
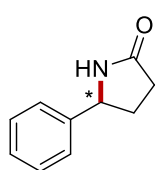
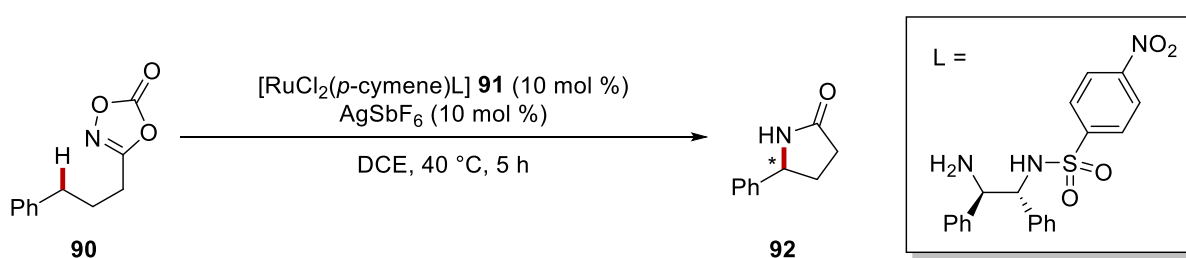
[D]<sub>n</sub>-**89a**: [D]<sub>n</sub>-**89b** = 1.5:1

[D]<sub>n</sub>-**89a**

[D]<sub>n</sub>-**89b**

**Scheme 1.2.24** Enantioselective intramolecular C–N bond formation.

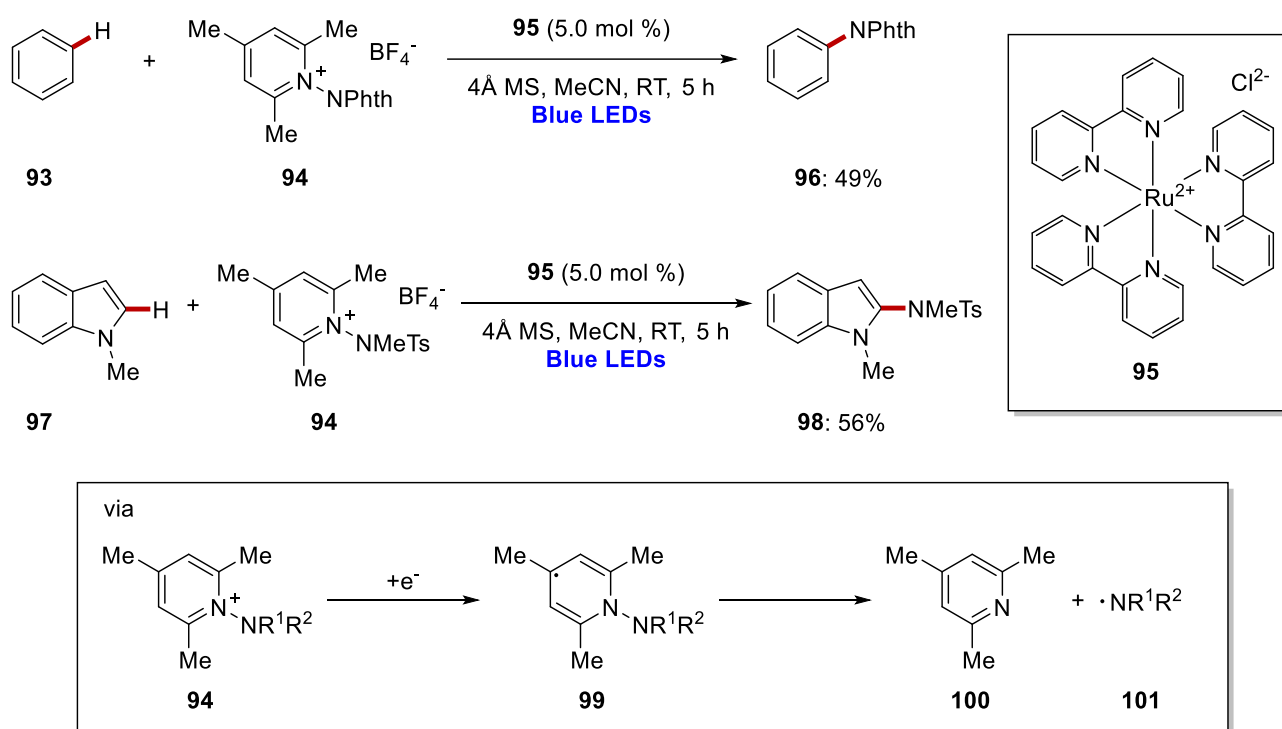
Very recently, Yu and co-workers reported ruthenium-catalyzed enantioselective  $\gamma$ -lactam formation *via* intramolecular C–N bond formation (Scheme 1.2.25).<sup>[67]</sup> The nitrene C–H insertion process was enabled by a chiral diphenylethylene diamine-based ligands, which bear an electron-withdrawing arylsulfonyl substituent. Similar to Chang's report,<sup>[54]</sup> the competing Curtius-type rearrangement was not observed.



**Scheme 1.2.25** Ruthenium-catalyzed enantioselective  $\gamma$ -lactam synthesis.

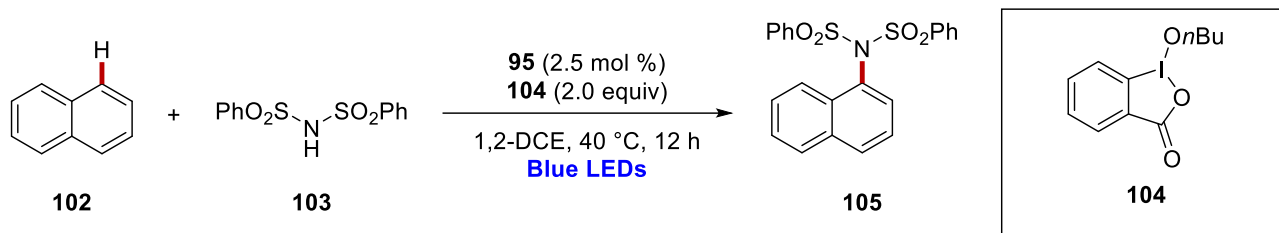
As the last approach toward C–N bond formation, single electron transfer manifold through photoredox catalysis has recently gained major attention due to its sustainability, even though it has been scarcely reported for amidation reactions.

In 2015, Studer showed visible-light-induced C–H amidation and imidation by using ruthenium-based photocatalyst **95** (Scheme 1.2.26).<sup>[68]</sup> *N*-aminopyridinium salts were employed as an amidyl radical source **101** through a deaminative process, allowing divergent C–N bond formations.

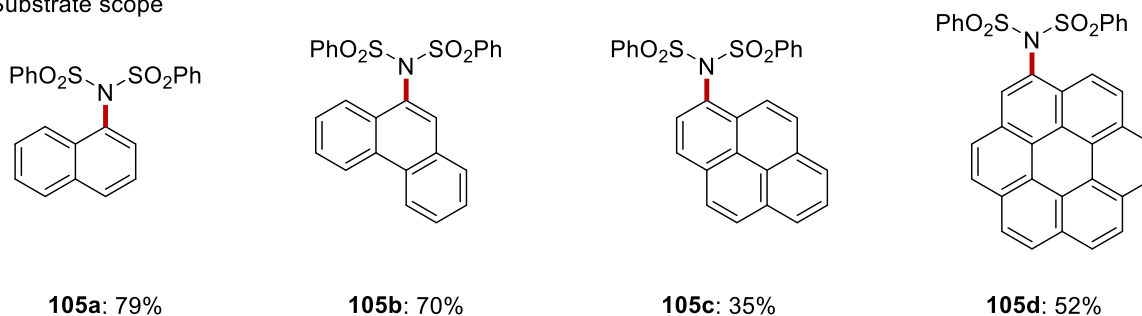


**Scheme 1.2.26** Visible-light-induced deaminative C–H amidation.

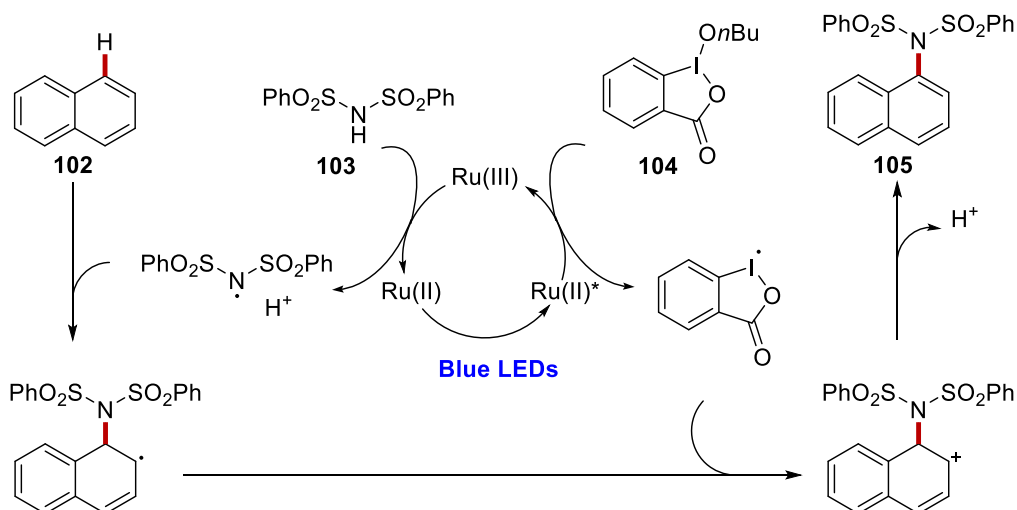
In 2017, Itami and Murakami reported photoredox ruthenium-catalyzed C–H/N–H coupling by blue-light irradiation (Scheme 1.2.27).<sup>[69]</sup> Thus, a wide range of polycyclic aromatic hydrocarbons was transformed to aryl amines through the oxidation of sulfonimides by the photoredox catalyst **95**. Additionally, catalytic cycle was proposed based on the detailed mechanistic studies by means of cyclovoltametric analyses.



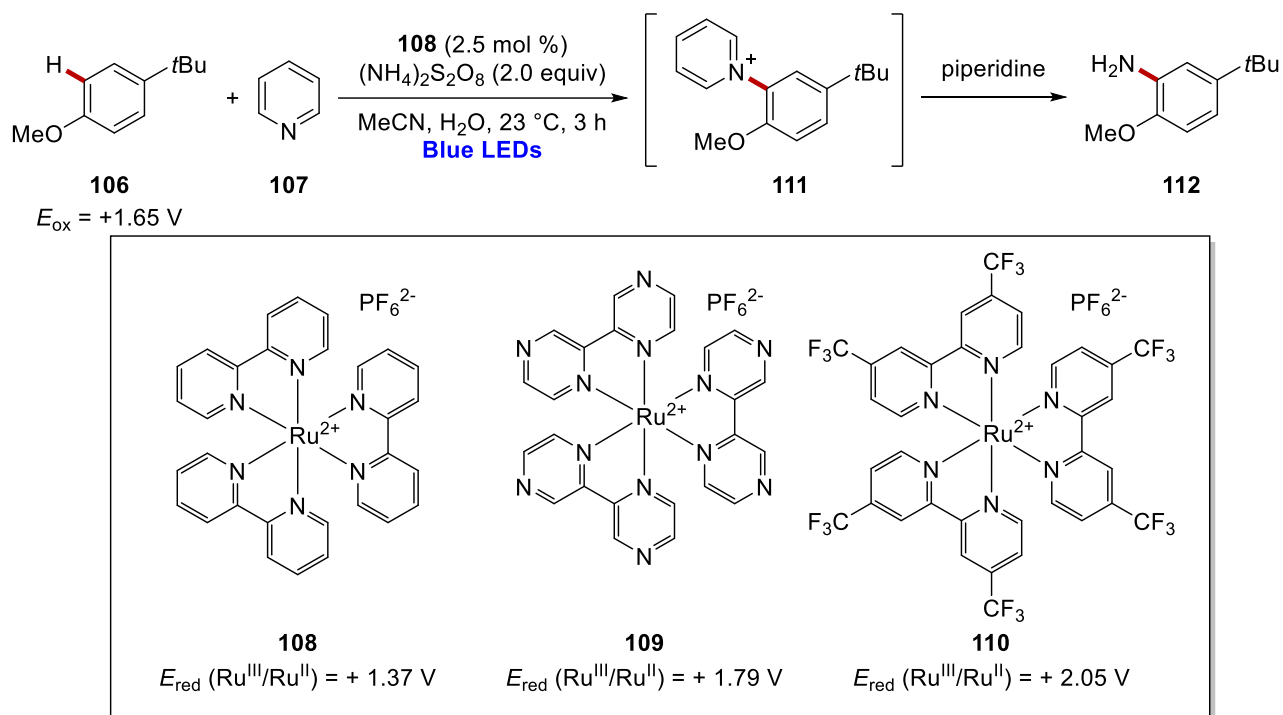
a) Substrate scope



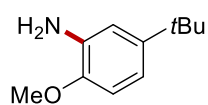
b) Proposed mechanism

**Scheme 1.2.27** Photo-induced C–H/N–H coupling by ruthenium-based photocatalyst **95**.

Inspired by cation pool methods of Yoshida,<sup>[70]</sup> Morofuki and Kano very recently disclosed photocatalytic C–H aminations of aromatic compounds **106** (Scheme 1.2.28).<sup>[71]</sup> Taking advantage of substrates with higher oxidation potentials than the reduction potential of the oxidation state of the ruthenium-based photocatalyst **108** among other photocatalysts, **109** and **110**, a variety of functional group tolerance was described, while featuring high regioselectivity in C–H aminations.



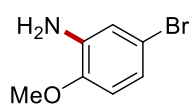
## a) Substrate scope



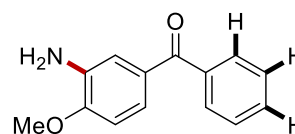
with **108**, **112**: 97%  
with **109**, **112**: 40%  
with **110**, **112**: 47%



with **108**, **112a**: 73%



with **108**, **112b**: 46%

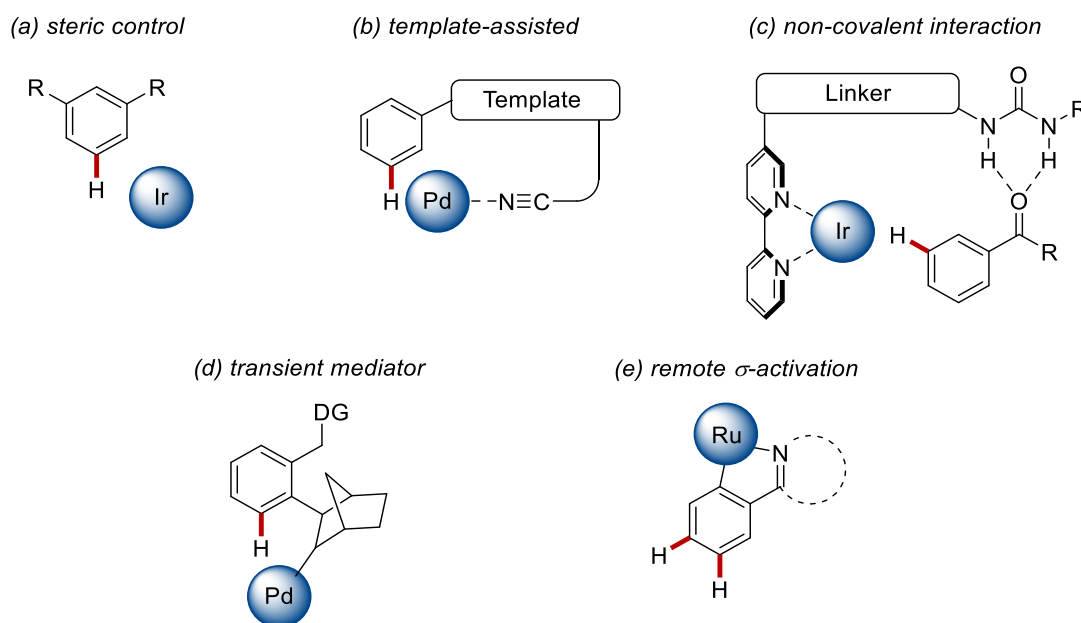


with **108**, **112c**: 91%  
Gram scale: 92% (1.15 g)

**Scheme 1.2.28** Oxidative C–H amination by the ruthenium photocatalyst **108** under visible-light-induced conditions.

### 1.2.2 Ruthenium-Catalyzed Distal C–H Functionalization

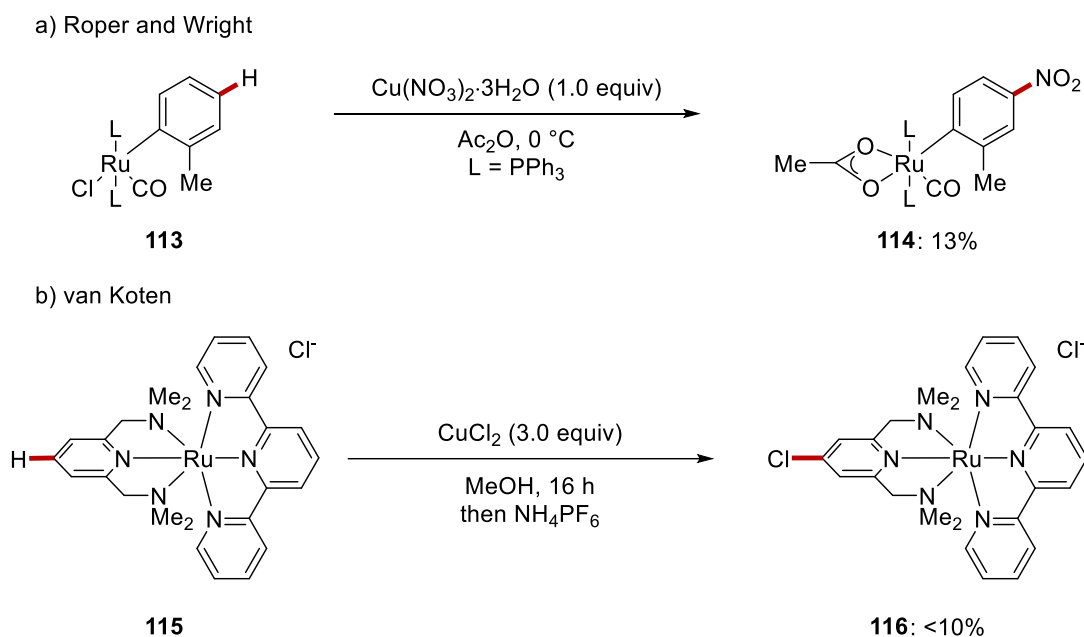
Ruthenium-catalyzed C–H activation has generally provided robust methods for *ortho*-selective C–H functionalization for new C–C bond or C–Het bond formations *via* a proximity-induced approach. In sharp contrast, C–H functionalizations at distal positions of arenes have been considerably less investigated (Scheme 1.2.29).<sup>[72a-e, 26e, 72f]</sup> In most methods, either the intrinsic electronic properties of substrates<sup>[73]</sup> or less atom-economical templates<sup>[74]</sup> and ligands<sup>[75, 26f]</sup> have been utilized to guide selectivity. Also, such reactions required cost-intensive metals, such as iridium and palladium catalysts. In stark contrast, ruthenium complexes have recently gained major attention for distal C–H functionalizations, in which C–H ruthenation results in remote *meta*-functionalizations.<sup>[76, 72d]</sup>



**Scheme 1.2.29** Strategies for distal C–H functionalizations.

Early examples of distal functionalization were reported by Roper and Wright in a stoichiometric manner (Scheme 1.2.30a).<sup>[77]</sup> Thereafter, van Koten employed a similar stoichiometric approach for halogenations of cyclometalated ruthenium complexes (Scheme 1.2.30b).<sup>[78]</sup>

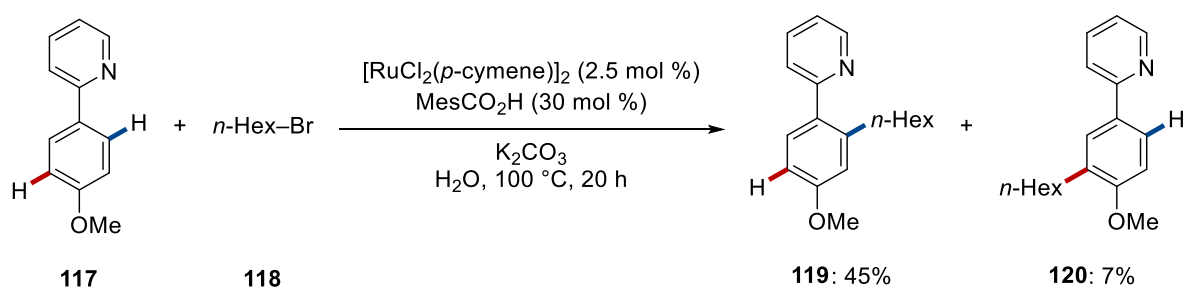




**Scheme 1.2.30** Stoichiometric distal C–H functionalization of ruthenium complexes.

Thereafter, the groups of Coudret,<sup>[79]</sup> Roper/Wright,<sup>[80]</sup> and van Koten<sup>[78]</sup> extended this method towards oxidative transformations of cyclometalated ruthenium complexes.

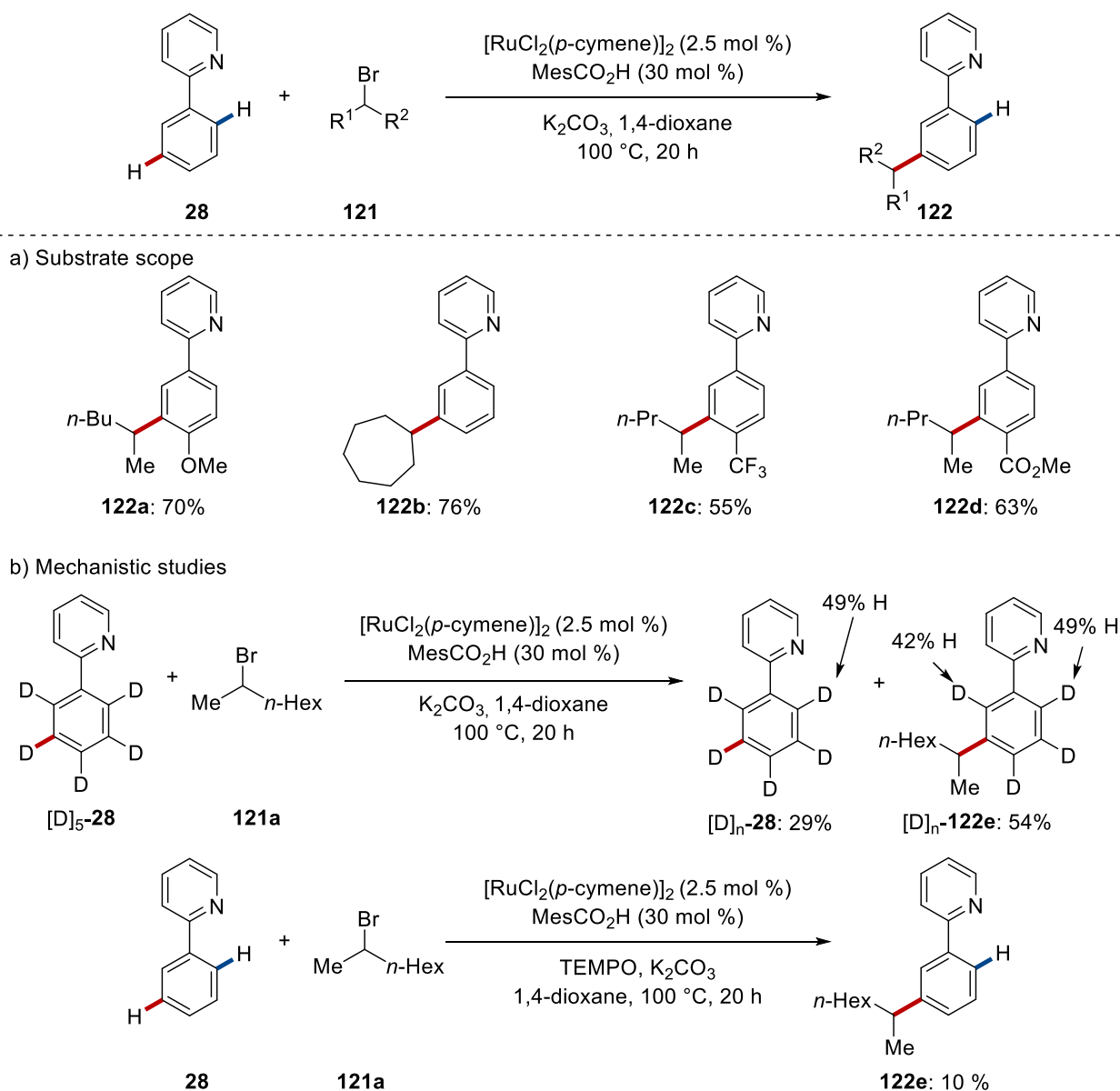
In 2011, Ackermann observed the first catalytic *meta*-C–H functionalization by C–H ruthenation (Scheme 1.2.31).<sup>[35e]</sup> Albeit in low yield, the result became a milestone for the further developments of ruthenium-catalyzed distal functionalizations.



**Scheme 1.2.31** The first observation of ruthenium-catalyzed *meta*-C–H alkylation.

At the same time, Li showed the *para*-selective, oxidative C–H/C–H alkylation of arenes **28**, albeit with limited selectivity.<sup>[81]</sup> In contrast, Ackermann disclosed a general strategy for *meta*-C–H alkylations *via* carboxylate-assisted *ortho*-ruthenation, featuring excellent levels of unusual *meta*-position-selectivity of arenes **28** (Scheme 1.2.32).<sup>[82]</sup> Mechanistic investigations revealed that the

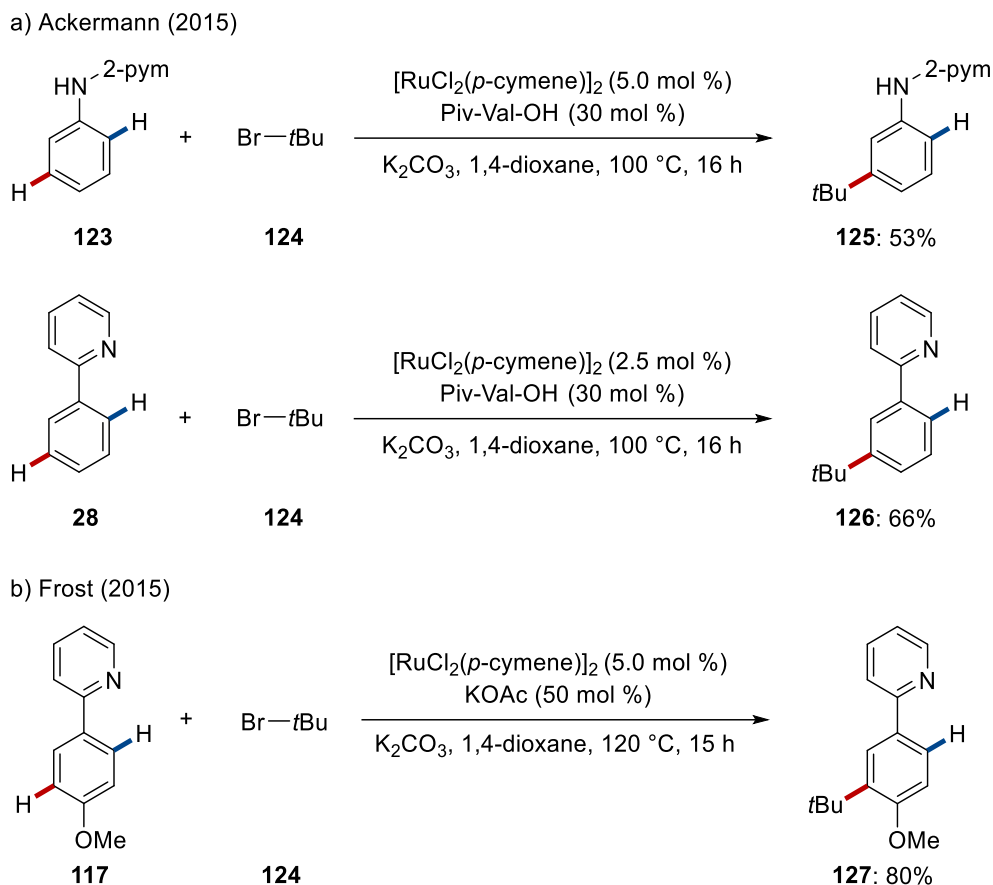
transformation occurred via reversible C–H ruthenation, while the use of typical radical scavenger TEMPO inhibited the *meta*-C–H alkylation. Notably, direct *meta*-alkylation with enantiomerically enriched substrate showed that a racemization of the chiral organic electrophile occurred under the reaction conditions.



**Scheme 1.2.32** Ruthenium-catalyzed *meta*-C–H alkylations with secondary alkyl bromide **121a**.

Distal C–C bond formation was not limited to secondary alkylation, but tertiary alkyl halides also were viable reaction partners. In 2015, Ackermann<sup>[83]</sup> and then Frost<sup>[84]</sup> independently showed the ruthenium-catalyzed *meta*-C–H alkylations with tertiary alkyl bromides **124** (Scheme 1.2.33). Notably,

Ackermann firstly used monoprotected amino acids (MPAA), illustrating the importance of carboxylate assistance.

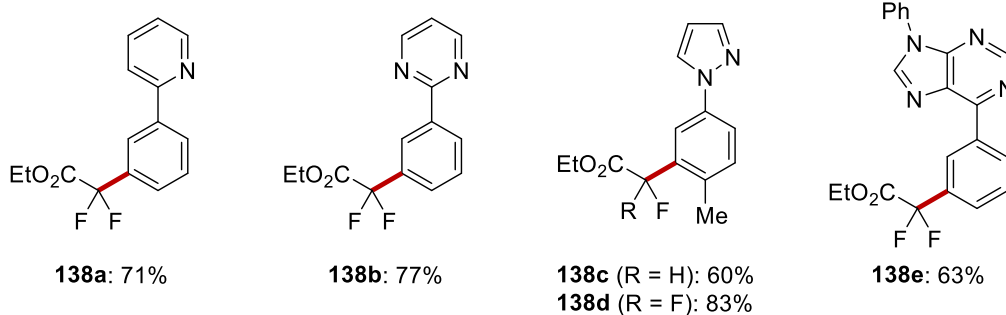
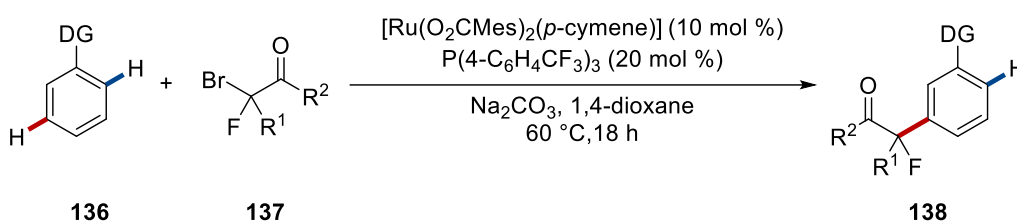


**Scheme 1.2.33** Ruthenium-catalyzed *meta*-C–H alkylations with tertiary bromides **124**.

Two years later, Ackermann and co-workers reported *meta*-C–H functionalizations of ketimines **128** (Scheme 1.2.34).<sup>[85]</sup> It was not until then that the majority of the ruthenium-catalyzed *meta*-C–C bond formation reaction had highly relied on *N*-containing strong directing groups, which were not readily modified under mild conditions. However, this reaction allowed for the access to *meta*-functionalized aryl ketones **130** from imines through acidic work-up. Moreover, various alkyl halides including tertiary and secondary bromides **129** were found to be viable alkylating reagents.

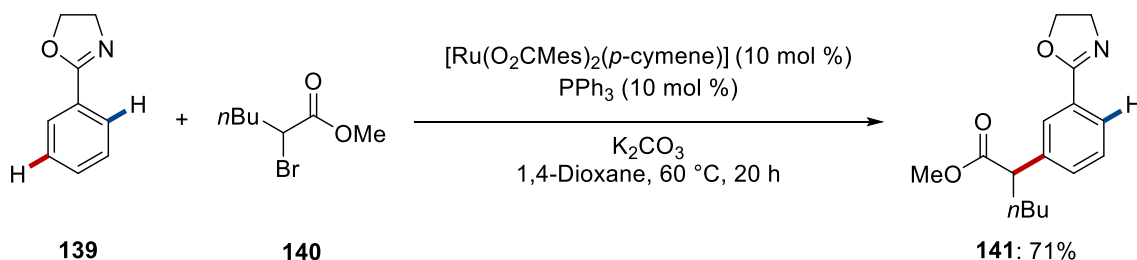


In 2017, the group of Ackermann accomplished the first remote C–H mono- and difluoromethylation through the combination of ruthenium(II) carboxylate and a phosphine ligand (Scheme 1.2.36).<sup>[88]</sup> Various directing groups, such as pyridines, pyrimidines, pyrazoles, and purine, efficiently afforded *meta*-decorated fluoromethylated products. It is noteworthy that the difluoromethylations did not occur at the kinetically more acidic C8–H positions of the purine motif. Around the same time, Wang group showed a similar approach for ruthenium-catalyzed remote mono- and difluoromethylations, utilizing a ruthenium and palladium bimetallic catalysis.<sup>[89]</sup>

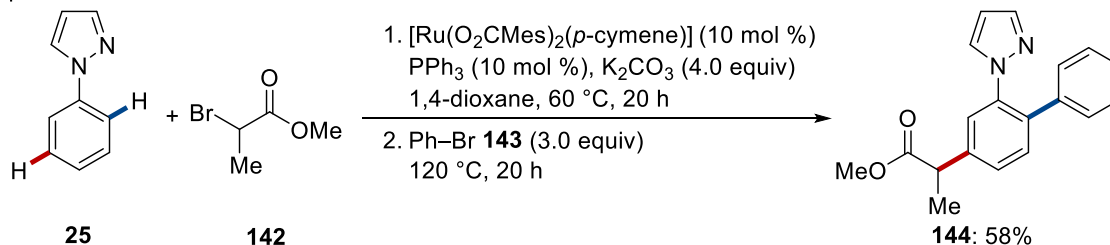


**Scheme 1.2.36** Ruthenium-catalyzed *meta*-C–H difluoroalkylations.

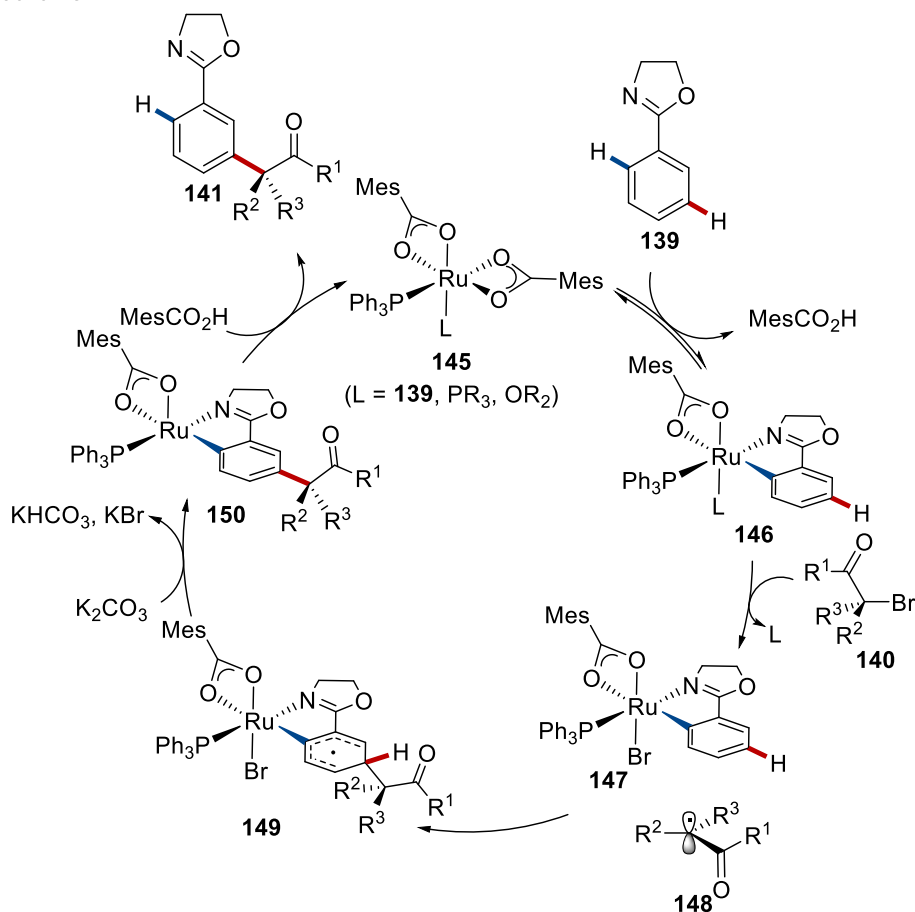
Ackermann and co-workers disclosed sequential *meta*-/*ortho*-C–H difunctionalizations in 2018 (Scheme 1.2.37).<sup>[90]</sup> Thus, the double C–H activation proved viable in a one-pot fashion, providing operationally simple twofold C–H functionalizations. In addition, detailed mechanistic studies provided strong support for homolytic C–X bond cleavage and facile C–H ruthenation, while a radical Fukui indices based on computational density functional theory (DFT) analysis supported a radical pathway.



a) Sequential reaction



b) Proposed mechanism

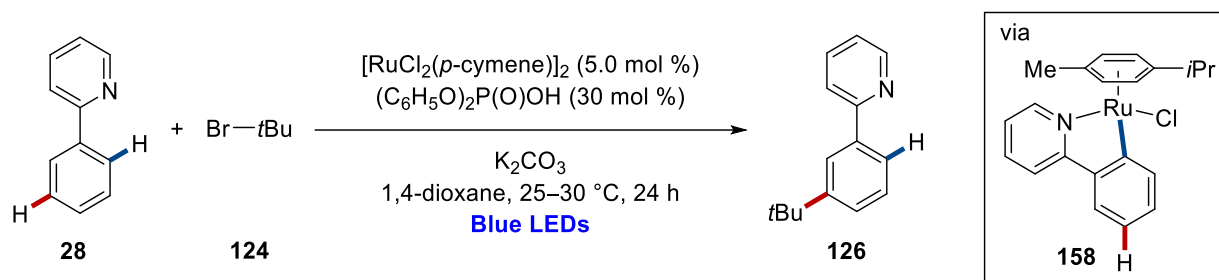


**Scheme 1.2.37** Distal C–H alkylation *via* ruthenium (II/III) catalysis and sequential strategy for dual functionalizations

The established cooperative use of phosphine and carboxylate ligands in ruthenium catalysis was further extended to three-component *meta*-C–H functionalizations (Scheme 1.2.38).<sup>[91]</sup>

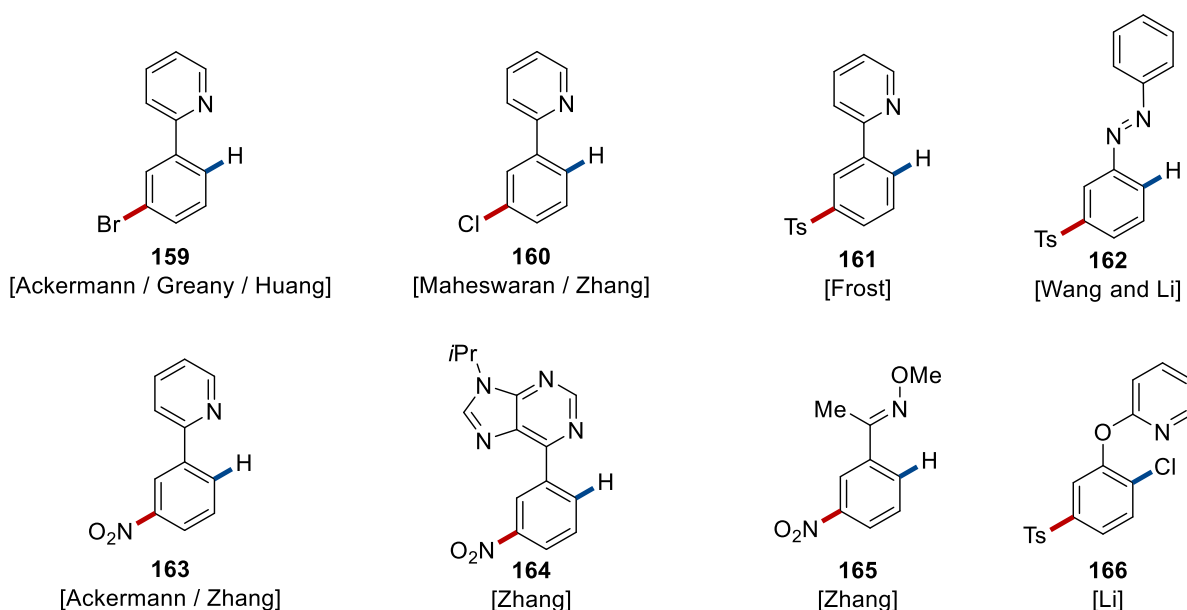


Very recently, the group of Ackermann reported on visible-light-induced ruthenium-catalyzed *meta*-C–H alkylation at ambient temperature (Scheme 1.2.41).<sup>[94]</sup> Notably, the photocatalytic reactions were performed under exceedingly mild reaction conditions at ambient temperature and without any additional exogenous photocatalysts. Around the same time, Greaney also reported similar remote C–H alkylations with alkyl iodide under visible-light induced conditions.<sup>[95]</sup>



**Scheme 1.2.41** Visible-light-induced ruthenium-catalyzed *meta*-C–H alkylation.

In addition to the aforementioned site-selective distal C–C bond formation, ruthenium catalysis enabled other *meta*-functionalizations, such as sulfonylations,<sup>[96]</sup> halogenations,<sup>[97]</sup> and nitrations (Scheme 1.2.42).<sup>[98]</sup>

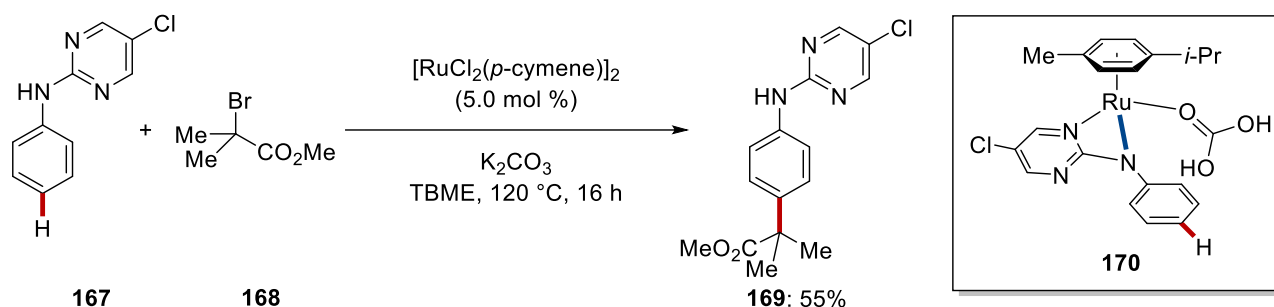


**Scheme 1.2.42** Ruthenium-catalyzed distal C–H functionalizations, halogenations, sulfonylations, and nitrations.

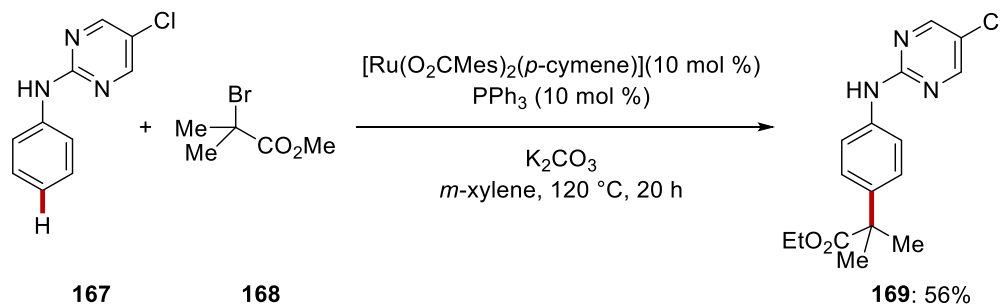


In contrast to the indisputable progress in *meta*-selective C–H functionalizations, general procedures for ruthenium-catalyzed *para*-C–H functionalization are under developed. Frost<sup>[99]</sup> and Ackermann<sup>[90]</sup> independently reported on ruthenium-catalyzed *para*-C–H alkylations of pyrimidylanilines **167** with  $\alpha$ -halo carbonyl compound **168** (Scheme 1.2.43). Notably, Frost suggested that the formation of four-membered ruthenacycle **170** is the key intermediate.

a) Frost (2017)



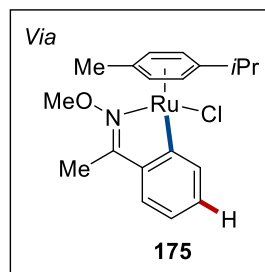
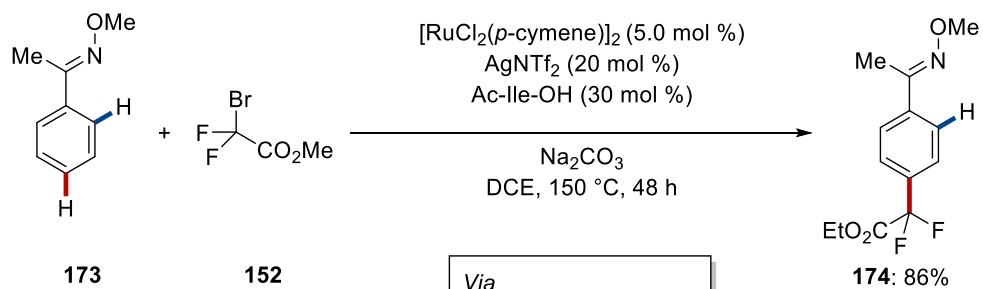
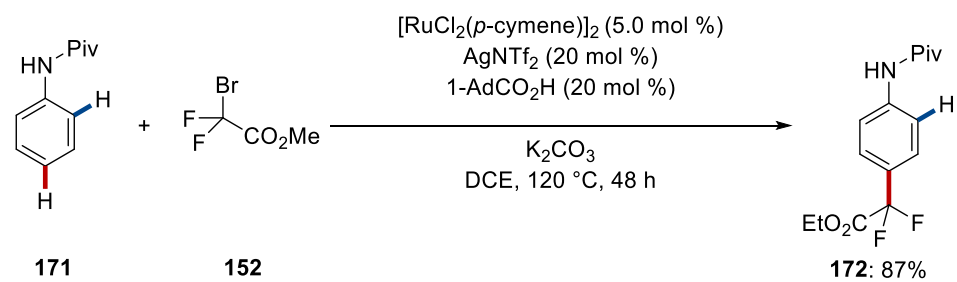
b) Ackermann (2018)



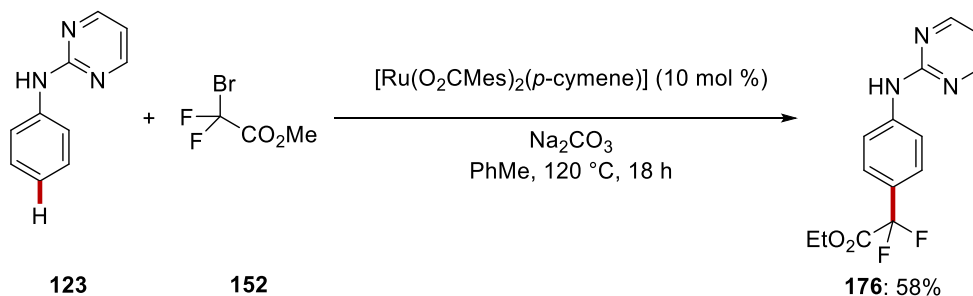
**Scheme 1.2.43** Ruthenium-catalyzed *para*-C–H alkylations.

Later, Zhao/Lan and Liang utilized a similar ruthenium-catalyzed *para*-C–H functionalization method to achieve mono- and difluoroalkylations (Scheme 1.2.44).<sup>[100]</sup> Unlike the mechanistic hypothesis offered by Frost, Zhao/Lan proposed that *ortho*-C–H ruthenation enabled the *para*-selectivity, although detailed experimental support was not provided.

a) Zhao/Lan



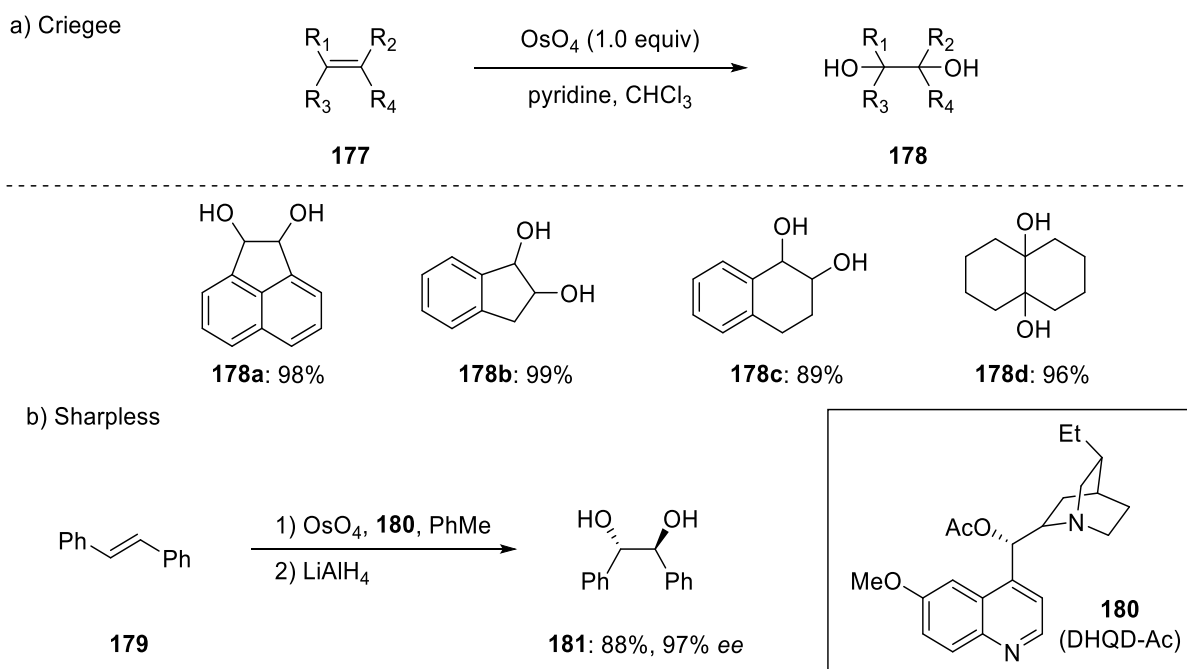
b) Liang

Scheme 1.2.44 Ruthenium-catalyzed *para*-C–H difluoromethylations.

### 1.3 Osmium-Catalyzed C–H Activation

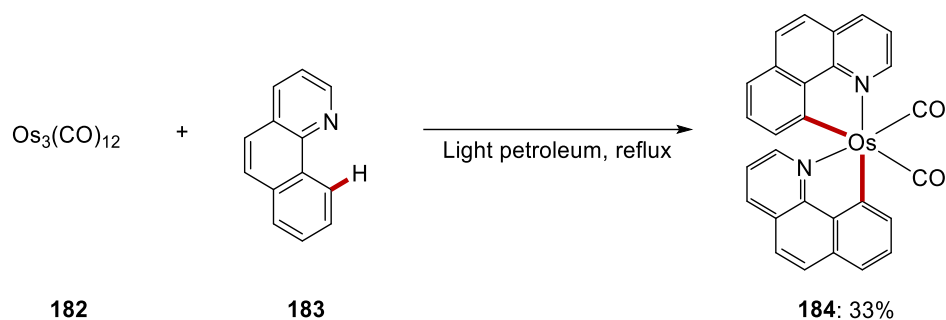
Osmium is the heaviest and rarest element in the earth's crust, with a concentration of approximately 0.05 parts per billion.<sup>[101]</sup> Osmium complexes – for instance, osmium tetroxide – are often considered toxic. In addition, osmium forms relatively strong Os–C bonds due to the stability in its higher oxidation state. For these reasons, osmium is a less attractive metal for catalysis compared to other group 8 metals<sup>[102]</sup>

Interestingly, osmium complexes have been introduced for useful chemical transformations.<sup>[103]</sup> As a major example, inspired by the pioneering work by Criegee,<sup>[104]</sup> Sharpless significantly expanded this realm to osmium-catalyzed enantioselective dihydroxylations (Scheme 1.3.1).<sup>[105]</sup>



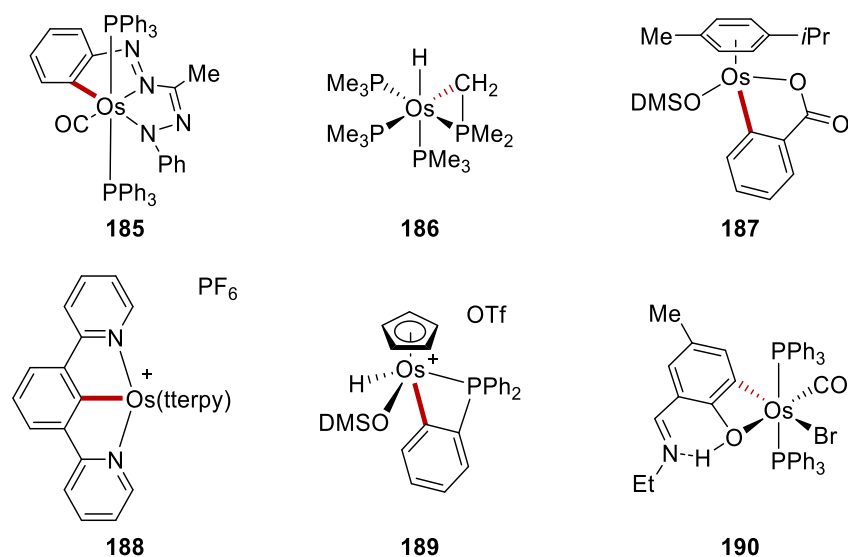
**Scheme 1.3.1** Representative examples of chemical transformation with osmium tetroxide.

C–H functionalizations by osmium complexes have also emerged as a powerful toolbox for chemical transformations. In 1973, Bruce disclosed the formation of osmacycle complex through C–H bond cleavage of benzo[*h*]quinolone **183** (Scheme 1.3.2).<sup>[106]</sup>



**Scheme 1.3.2** Synthesis of osmacycle complex **184**.

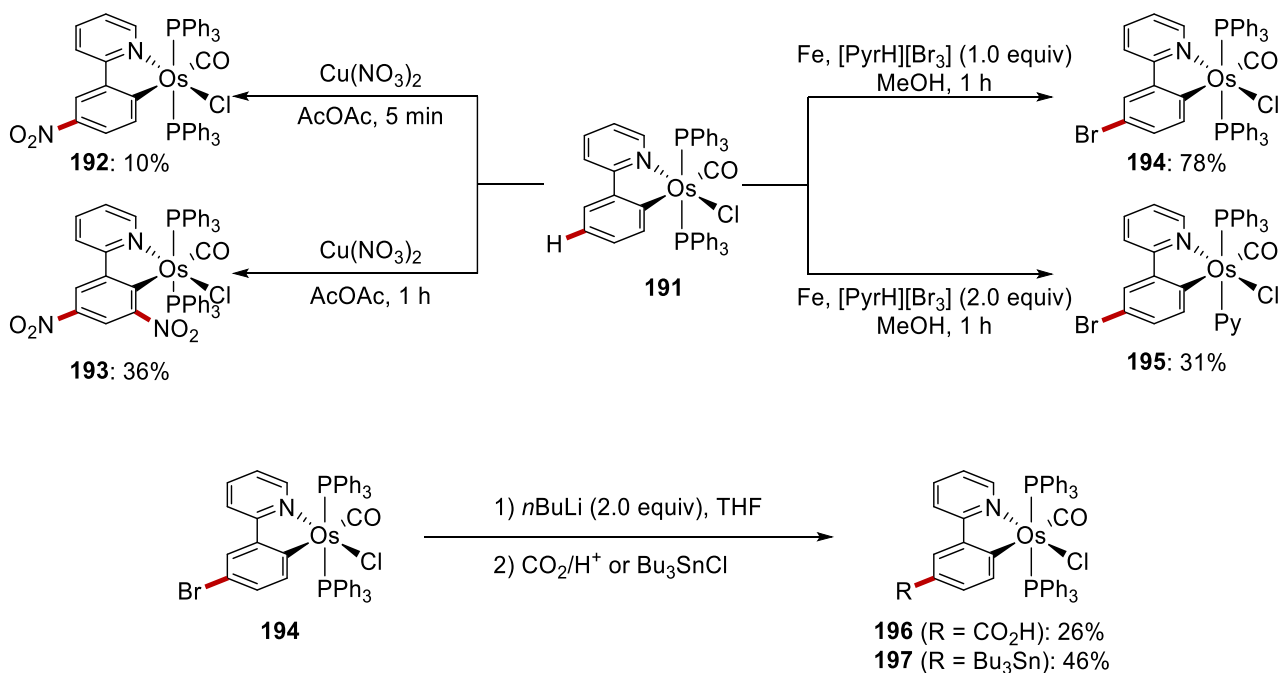
On the basis of this work, well-defined osmacycles were successfully isolated in a stoichiometric fashion (Scheme 1.3.3).<sup>[107]</sup> Thus, *N*-, *P*- and *O*-directing groups are coordinated to the osmium center, leading to C–H cleavage, resulting in the formation of osmacycle **185–190**.



**Scheme 1.3.3** Osmacycles **185–190**.

### 1.3.1 Osmium-Mediated C–H Functionalizations

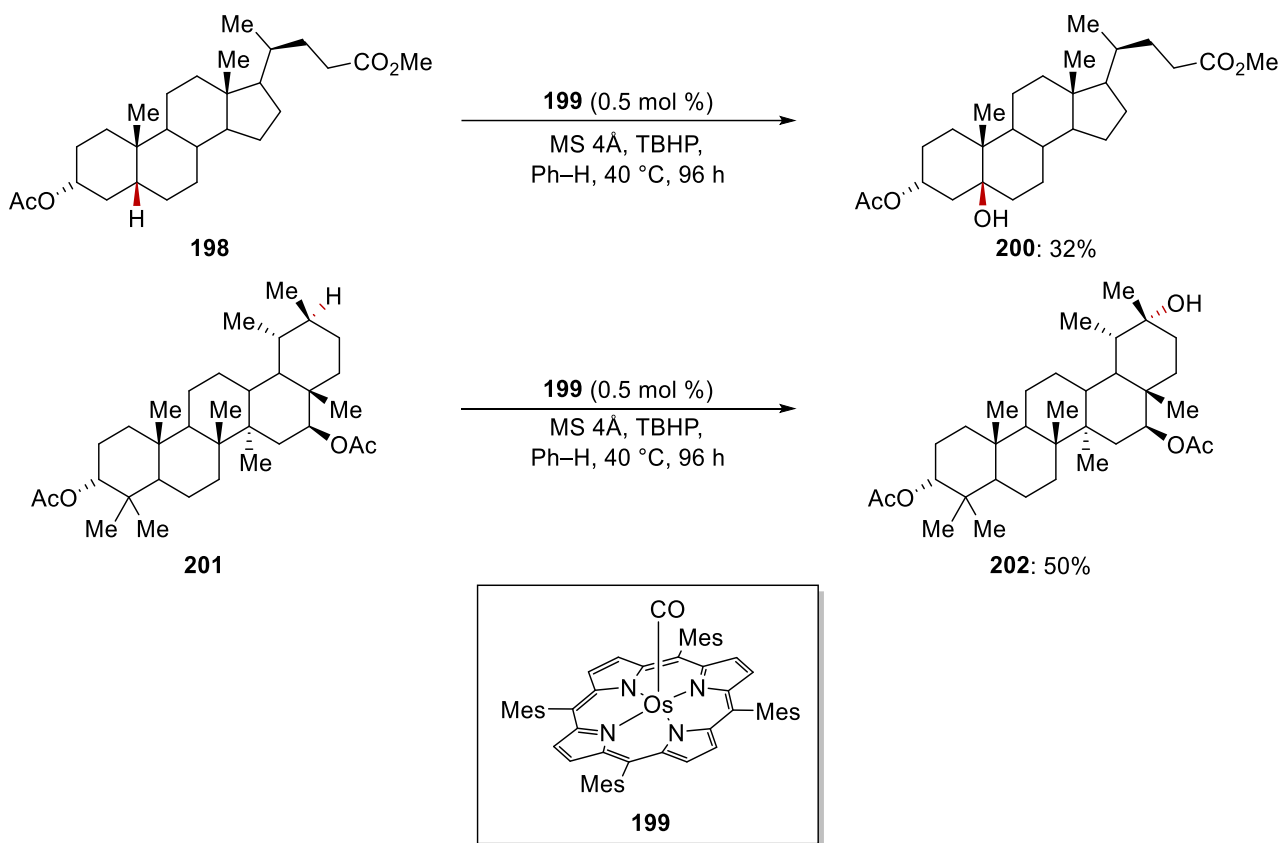
With this progress in the stoichiometric formation of osmacycles, such complexes were subjected to subsequent C–H functionalizations. In 1999, Roper and Wright disclosed an electrophilic substitution-type C–H bromination and nitration of 2-(2'-pyridyl)phenyl osmium complex **191** (Scheme 1.3.4).<sup>[80a]</sup> The C–H functionalizations of osmium complex **191** selectively occurred at the position *para*-to-the-osmium center. Interestingly, while the excess use of bromination source provided a ligand exchange from phosphine to pyridine, the prolonged reaction time in the nitration afforded dual C–H functionalized product **193**. With brominated osmium complex **194**, further diversifications were also presented, thus generating carboxylated **196** or stannylated osmium complex **197**.



**Scheme 1.3.4** *meta*-C–H functionalizations from osmacycle complex **191**.

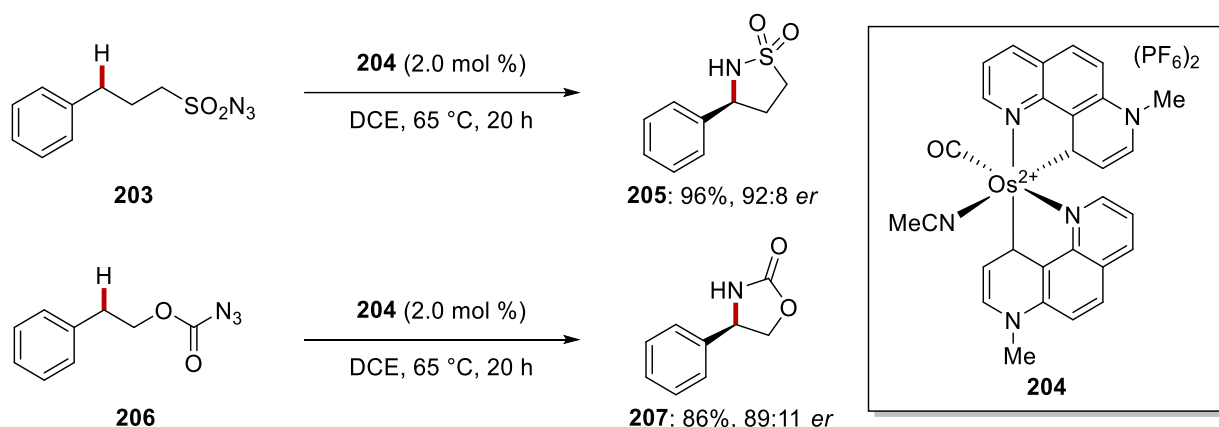
### 1.3.2 Osmium-Catalyzed C–H Functionalizations

Despite the aforementioned advances in stoichiometric osmacycle synthesis and its reactions, osmium complexes have rarely been used for catalytic C–H functionalization. In 2007, Iida disclosed osmium(II) porphyrin complex-catalyzed oxidative C–H oxygenation of steroid **198** (Scheme 1.3.5).<sup>[108]</sup> In this study, the least hindered tertiary C–H bond was selectively transformed, albeit with low efficiency. Additional reports also showed that pentacyclic triterpenoids **201** were converted to oxygenated product **202**.<sup>[109]</sup>



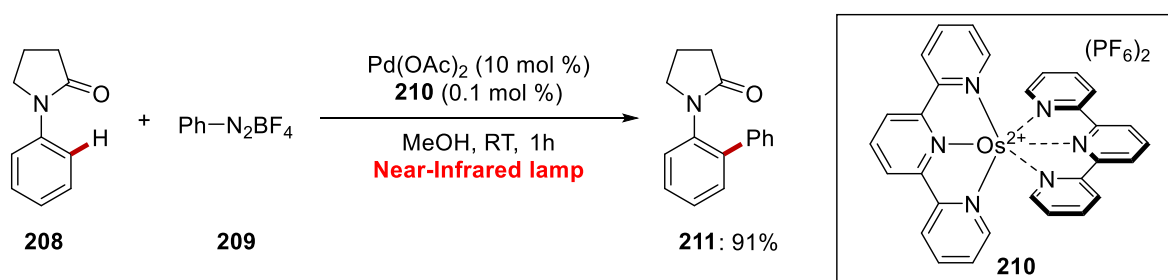
**Scheme 1.3.5** Osmium porphyrin-catalyzed C–H oxygenations.

In 2020, Meggers and co-workers disclosed osmium-catalyzed enantioselective C–H amidation (Scheme 1.3.6).<sup>[110]</sup> As an extension of their previous studies, newly synthesized non-C2-symmetric chiral-at-osmium complex **204** provided amidated products **205** and **207**.



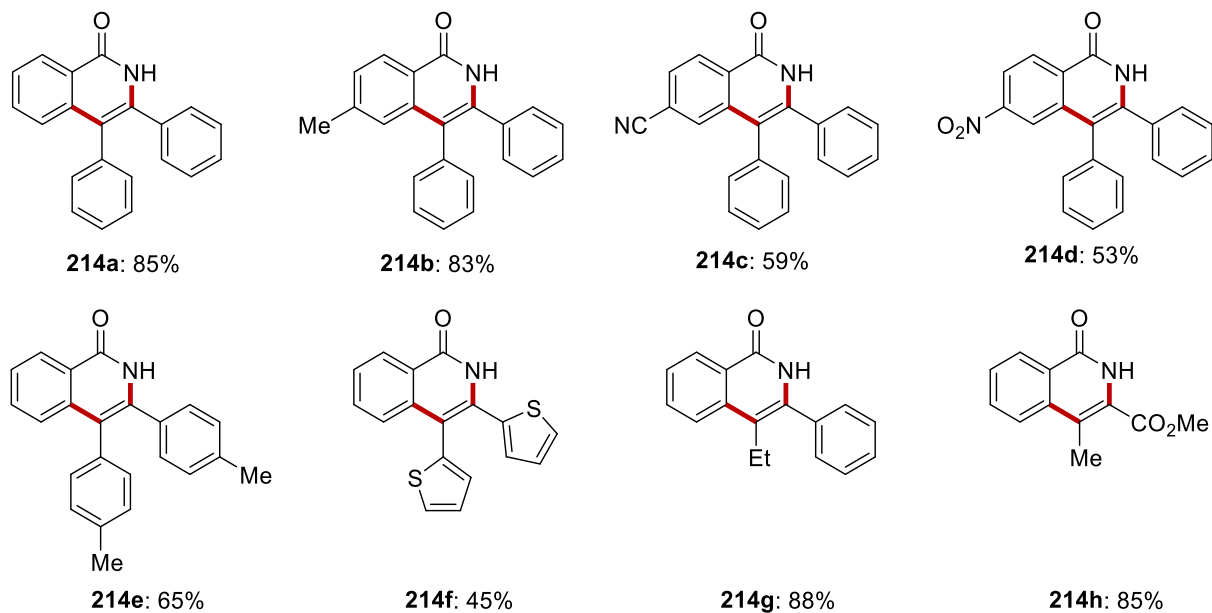
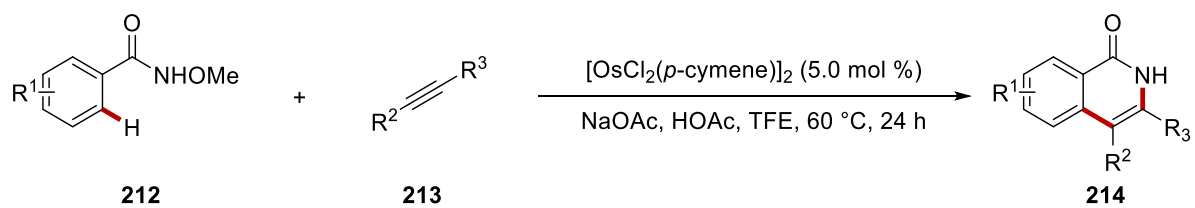
**Scheme 1.3.6** Enantioselective C–H amidations with chiral-at-osmium catalyst **204**.

In 2020, the Rovis group showcased near-infrared-induced photocatalysis regime utilizing an osmium-based photocatalyst **210** (Scheme 1.3.7).<sup>[111]</sup> Unlike ruthenium-based polypyridyl photocatalysts, osmium analogous featured a spin-forbidden  $S_0 \rightarrow T_1$  excitation in the near-infrared region, thereby increasing light penetration into the reaction medium.



**Scheme 1.3.7** Near-infrared photo-catalyzed C–H arylations with osmium-based photocatalyst **210**.

Recently, Yi and co-workers reported on unprecedented osmium(II)-catalyzed C–H activation (Scheme 1.3.8).<sup>[112]</sup> While transition metal-catalyzed C–H annulation has been well established,<sup>[113]</sup> the osmium complex was firstly employed in this study. Notably, the use of internal oxidant brought about less atom efficiency in this reaction, while a wide range of substrates was amenable. Additionally, experimental mechanistic studies revealed that the C–H bond scission process is irreversible, while osmium(II) carboxylate-assisted C–H activation was studied by computational DFT analysis.



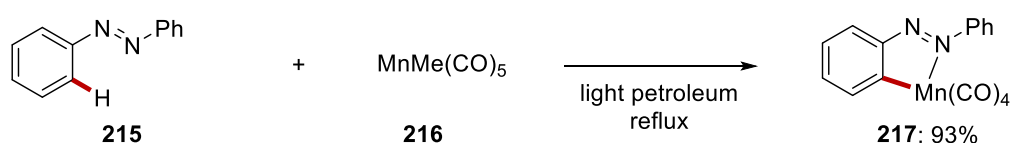
**Scheme 1.3.8** Osmium-catalyzed alkyne annulations.



### 1.4 Manganese-Catalyzed C–H Activation

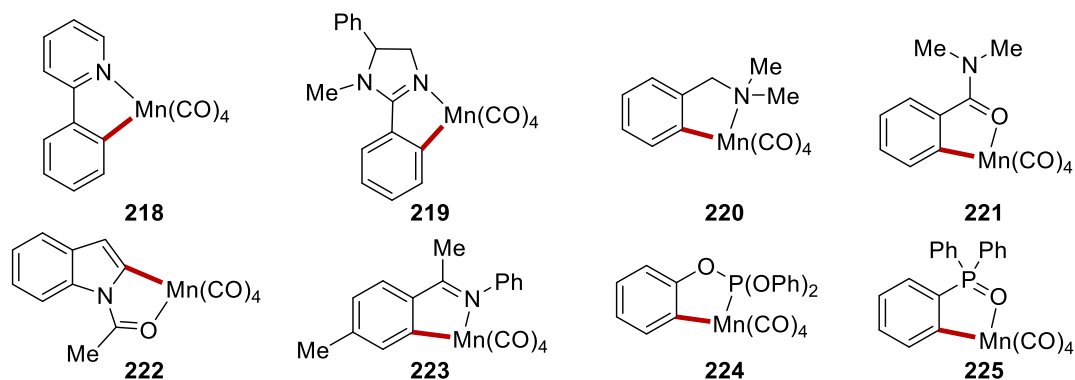
As the twelfth most abundant element in the earth's crust, manganese has a huge potential for sustainable, low toxic and cost-effective C–H activation.<sup>[114]</sup> In addition, a wide range of oxidation states of manganese from –3 to +7 enables various coordination geometries.<sup>[115]</sup> Notably, manganese complexes have been widely used in epoxidation reactions<sup>[116]</sup> and radical-type C–H functionalizations,<sup>[117]</sup> but limitedly employed in cross-coupling,<sup>[118]</sup> Together with these indisputable advances, organometallic C–H functionalizations have recently emerged as a powerful toolbox for chemical transformations.

In 1970, Stone and Bruce reported the stoichiometric manganese-mediated C–H activation of azobenzene (Scheme 1.4.1).<sup>[119]</sup> Thus, manganacycle **217** was synthesized in 93% yield from  $\text{MnMe}(\text{CO})_5$  (**216**).



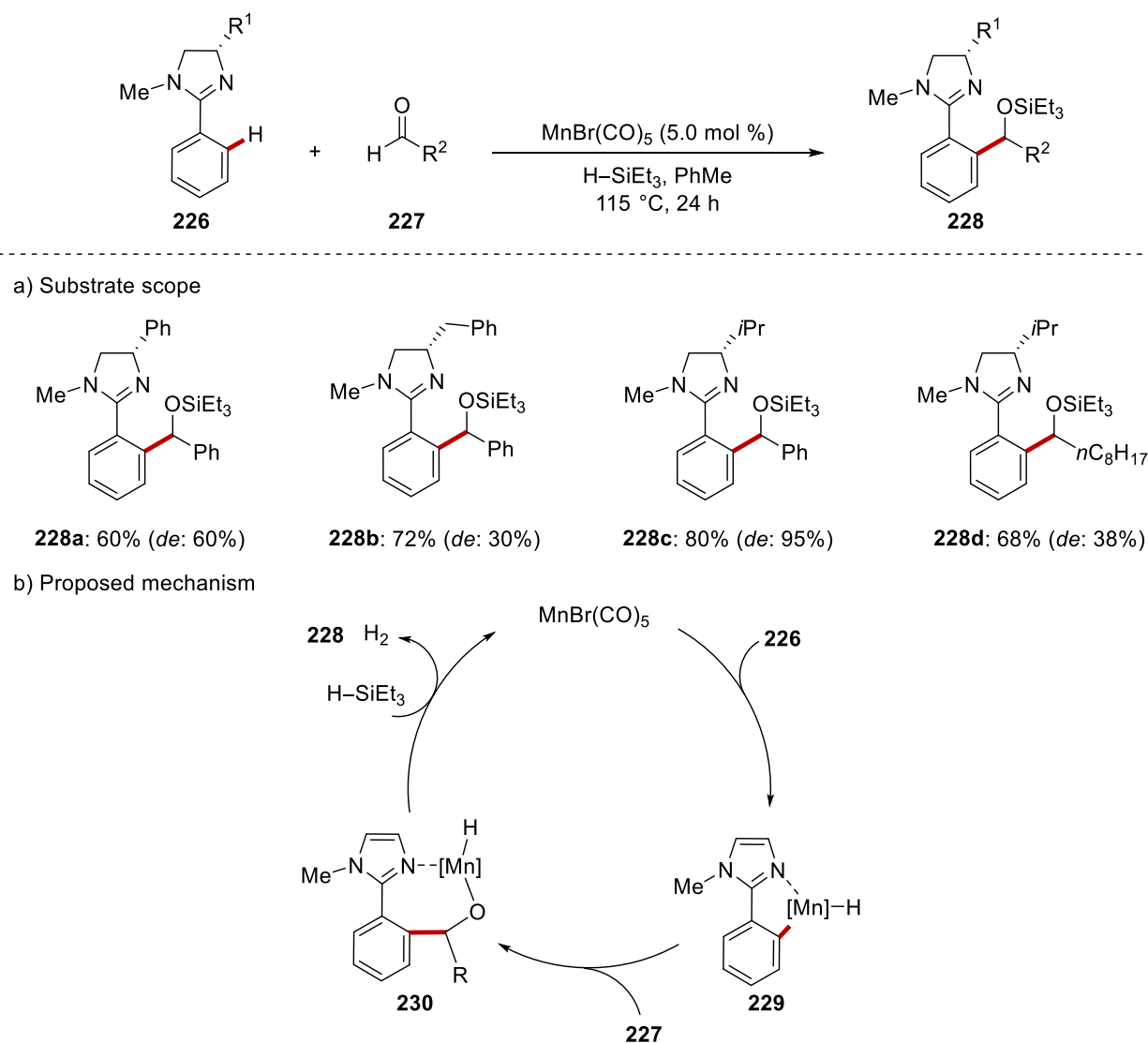
**Scheme 1.4.1** Stoichiometric C–H activation with manganese.

On the basis of this work, a plethora of well-defined manganacycles was successfully prepared in a stoichiometric fashion (Scheme 1.4.2).<sup>[120]</sup> Thus, the directing groups are coordinated to the manganese center, leading to C–H cleavage followed by manganacycle formations.



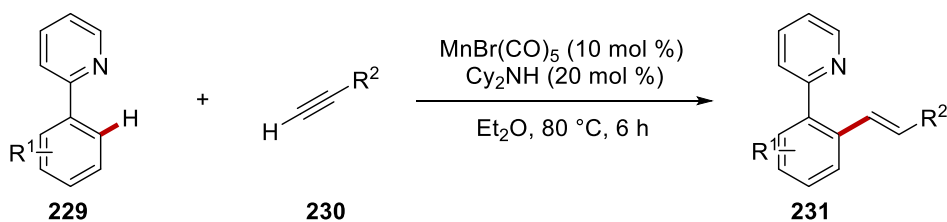
**Scheme 1.4.2** Well-defined manganacycles.

Despite the indisputable progress, manganese-catalyzed C–H activation had been put in the shade before Kuninobu and Takai disclosed a seminal study in 2007.<sup>[121]</sup> Thereby, a manganese(I) complex catalytically enabled C–H activation of arenes **226** with aldehydes **227** and Et<sub>3</sub>SiH, affording silylated alcohols **228**. Additionally, the catalytic cycle was proposed, in which Mn–C bond was suggested as a manganese(III)-hydride species **229** is formed *via* an oxidative addition. The exact structure of the active catalyst has thus far remained elusive, while recent manganese-catalyzed hydroarylation reactions are generally proposed to undergo redox-neutral isohypsic pathway. Thereafter, a migratory insertion followed by reductive eliminations afforded the desired product **228**.

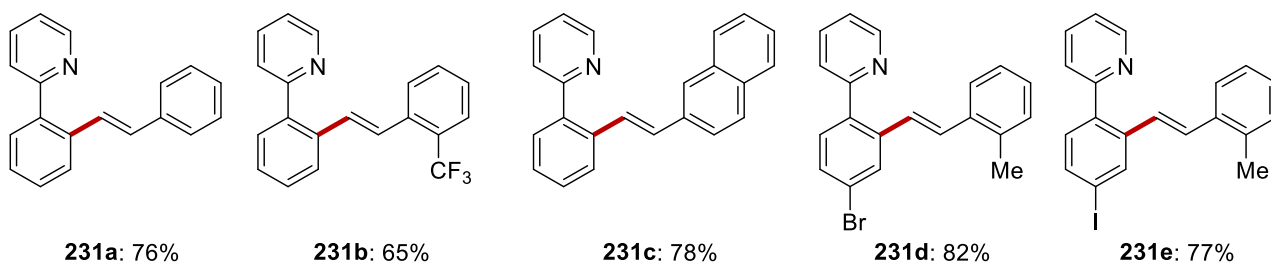


**Scheme 1.4.3** Manganese-catalyzed C–H addition to aldehydes **227** and proposed mechanism.

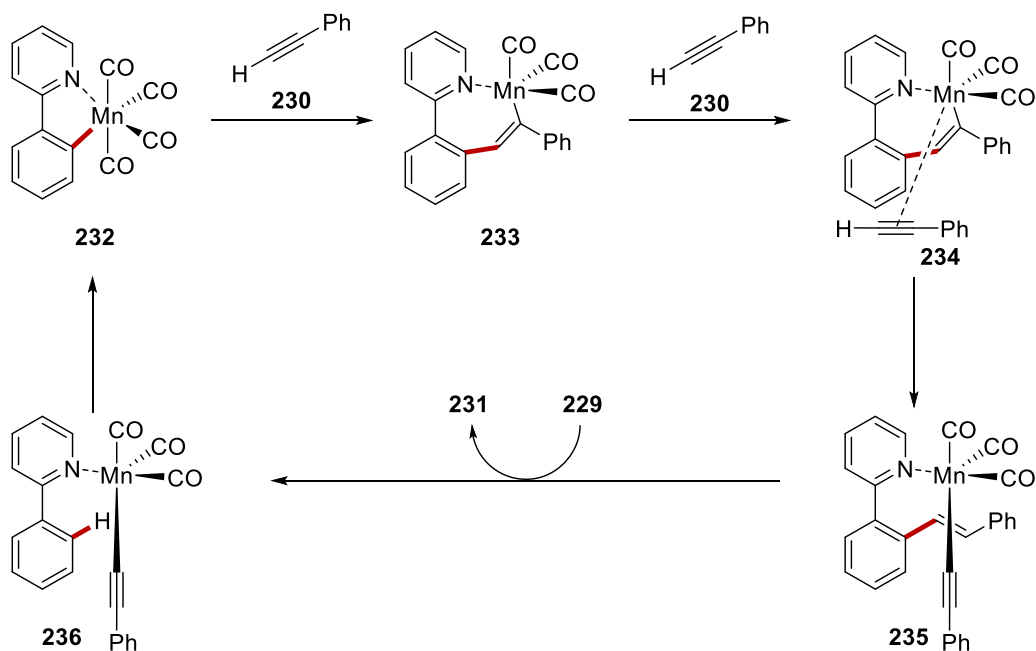
In 2013, Wang showcased manganese-catalyzed C–H alkenylation of arenes **229** with terminal alkynes **230** (Scheme 1.4.4).<sup>[122]</sup> The hydroarylation manifold was functional group tolerate. Detailed experimental mechanistic studies along with computational DFT studies suggested that the reaction proceeds through the formation of five-membered manganacycle **232** followed by seven-membered intermediate **233** construction.<sup>[123]</sup>



## a) Substrate scope

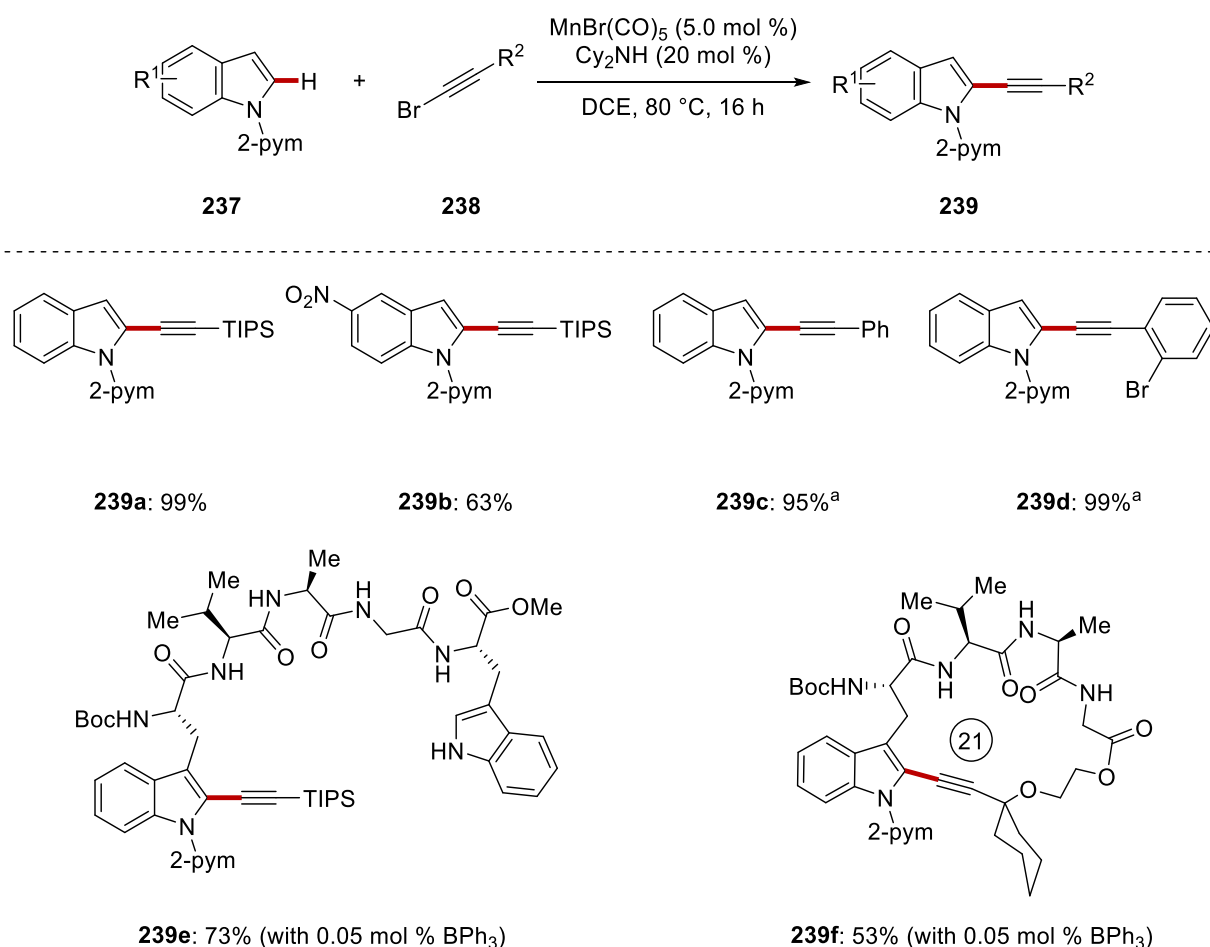


## b) Proposed mechanism



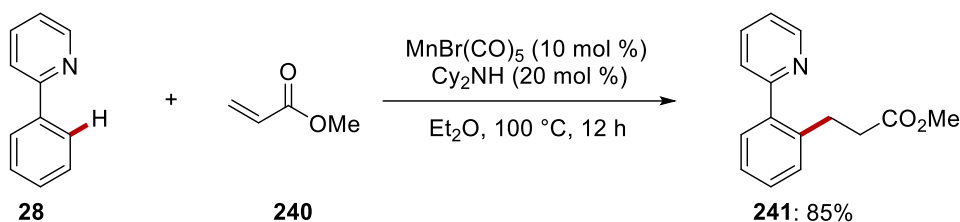
**Scheme 1.4.4** Manganese-catalyzed C–H alkenylations of arenes **229**.

Then, researchers utilized different combinations of arenes and alkynes, providing synthetically useful products. For instance, while manganese-catalyzed annulation reactions with various types of alkynes were reported by Ackermann,<sup>[124]</sup> Wang<sup>[125]</sup> among others,<sup>[126]</sup> Glorius showed the manganese-catalyzed C–H allenylation of indoles by using propargylic carbonate.<sup>[127]</sup> Recently, Ackermann and coworkers employed bromo alkynes **238**, for the first time, delivering alkynylated heteroarenes **239** by manganese catalysis (Scheme 1.4.5).<sup>[128]</sup> Notably, this reaction manifold was extended to feature peptide modification, thus providing acyclic and cyclic alkynylated peptides under epimerization-free reaction conditions. Based on detailed mechanistic studies, they proposed a plausible catalytic cycle, in which the substrate **237** undergoes facile and reversible C–H manganeseation, followed by alkyne migratory insertion and  $\beta$ -Br-elimination.



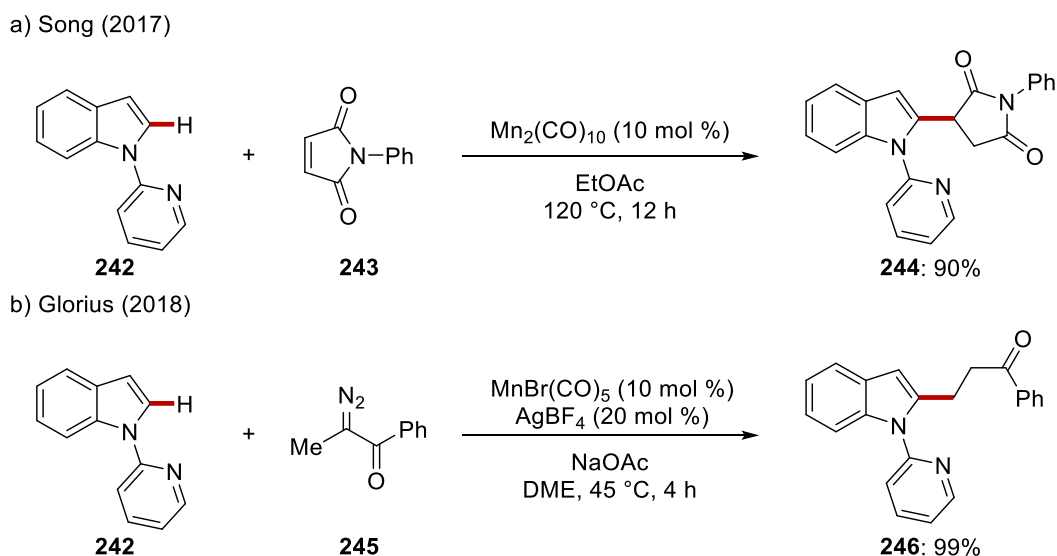
**Scheme 1.4.5** Manganese-catalyzed C–H alkynylations with alkynyl bromides **238**.

The manganese(I) catalysis was not limited to reactions with alkynes. Indeed, the manganese-catalyzed hydroarylation process was also applied to feature alkenes as coupling partners. In 2014, Wang and co-workers developed the manganese-catalyzed direct aromatic C–H conjugate addition to  $\alpha,\beta$ -unsaturated carbonyls (Scheme 1.4.6).<sup>[129]</sup>



**Scheme 1.4.6** Manganese-catalyzed C–H alkylation with acrylates **240**.

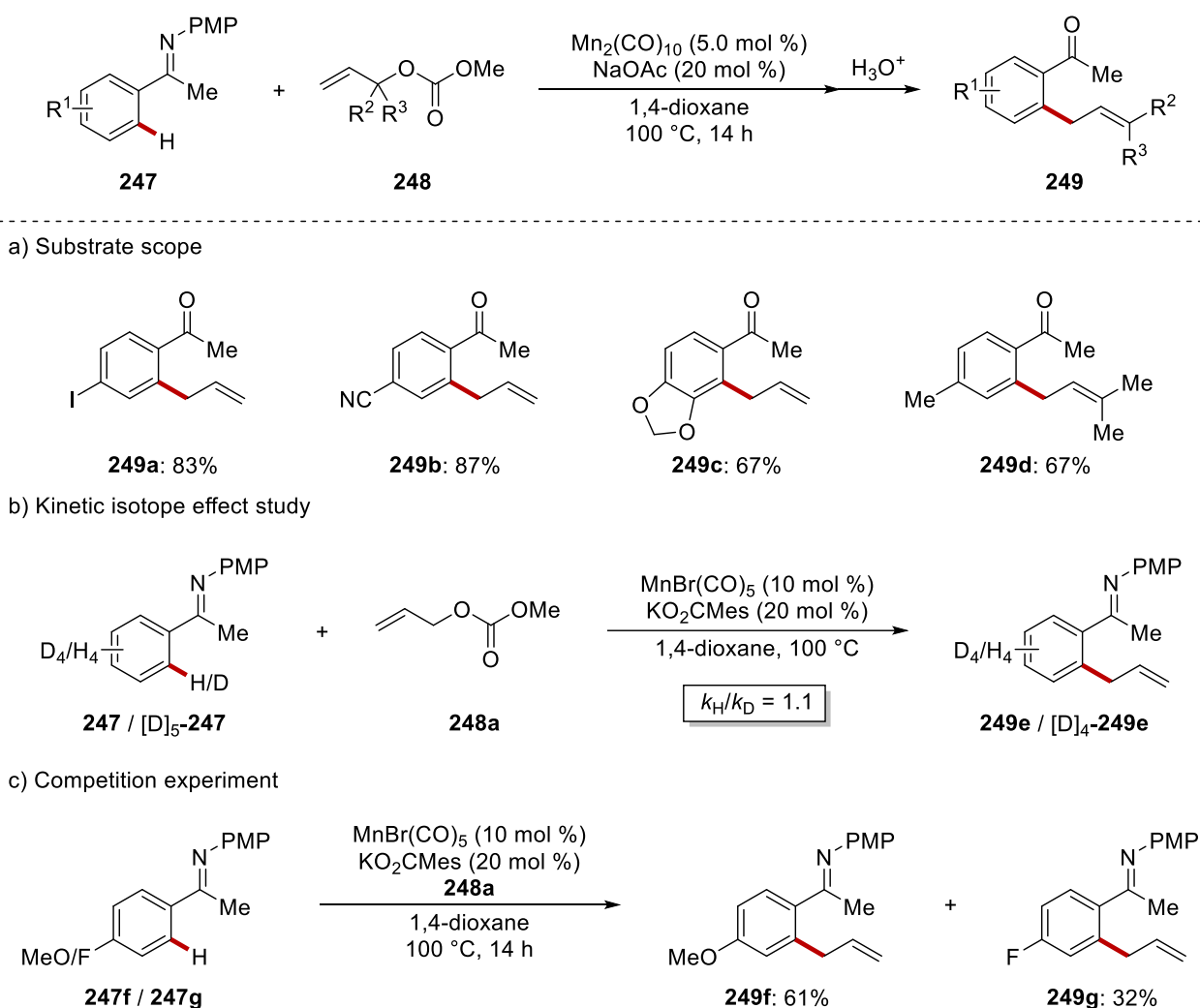
As an extension of this approach, in 2017, Song reported manganese-catalyzed hydroarylations of indoles **242** with maleimides **243** (Scheme 1.4.7a).<sup>[130]</sup> Later, Glorius employed *in-situ* generated  $\alpha,\beta$ -unsaturated carbonyls from  $\alpha$ -diazoketones **245** with the aid of silver additives (Scheme 1.4.7b).<sup>[131]</sup>



**Scheme 1.4.7** C–H alkylations of arenes **242** via manganese-catalyzed hydroarylation manifold.

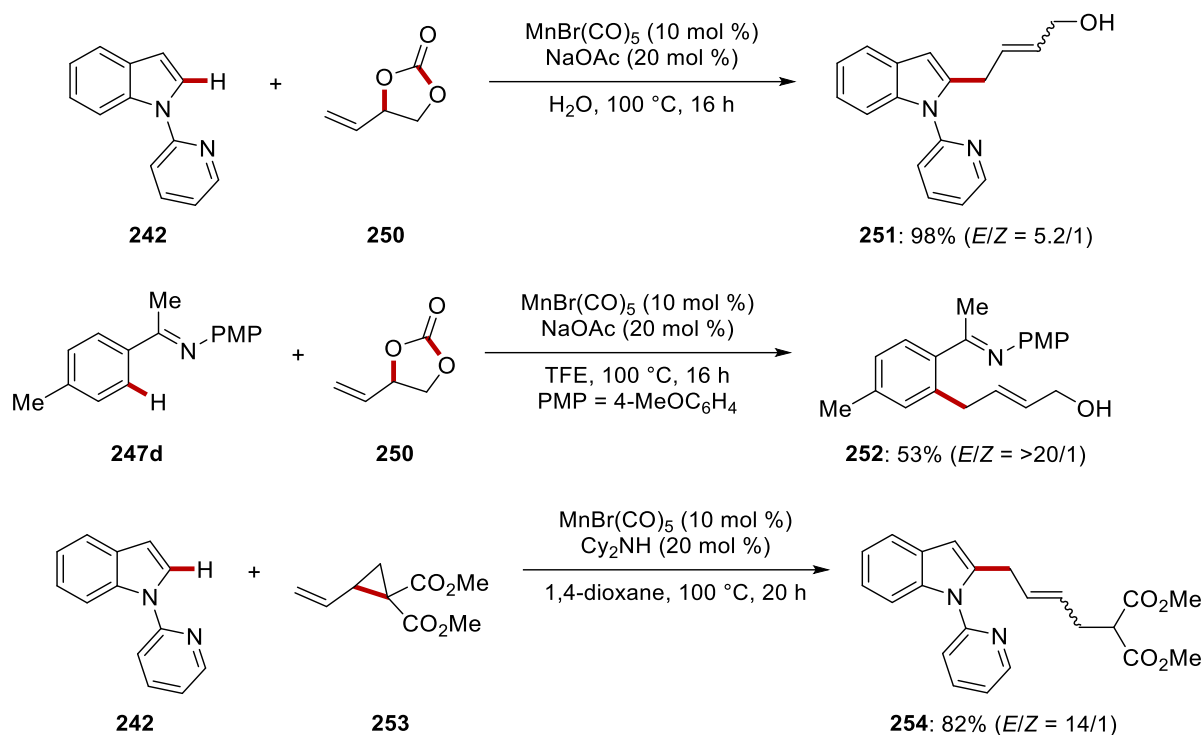
In 2016, Ackermann and co-workers disclosed manganese-catalyzed C–H allylations of arenes **247** with allyl carbonates **248** (Scheme 1.4.8).<sup>[132]</sup> While valuable functional groups, including halides, cyano, and carbonyls were tolerated, secondary interaction with a *meta*-substituent enabled the

synthesis of 1,2,3-substituted arene **249c**. While mechanistic investigation showed that C–H the manganese process is not involved in the rate-determining step, a base-assisted intramolecular electrophilic-type substitution (BIES) regime for manganese-catalyzed C–H allylation was proposed by among other competition experiments.



**Scheme 1.4.8** Manganese-catalyzed C–H allylations.

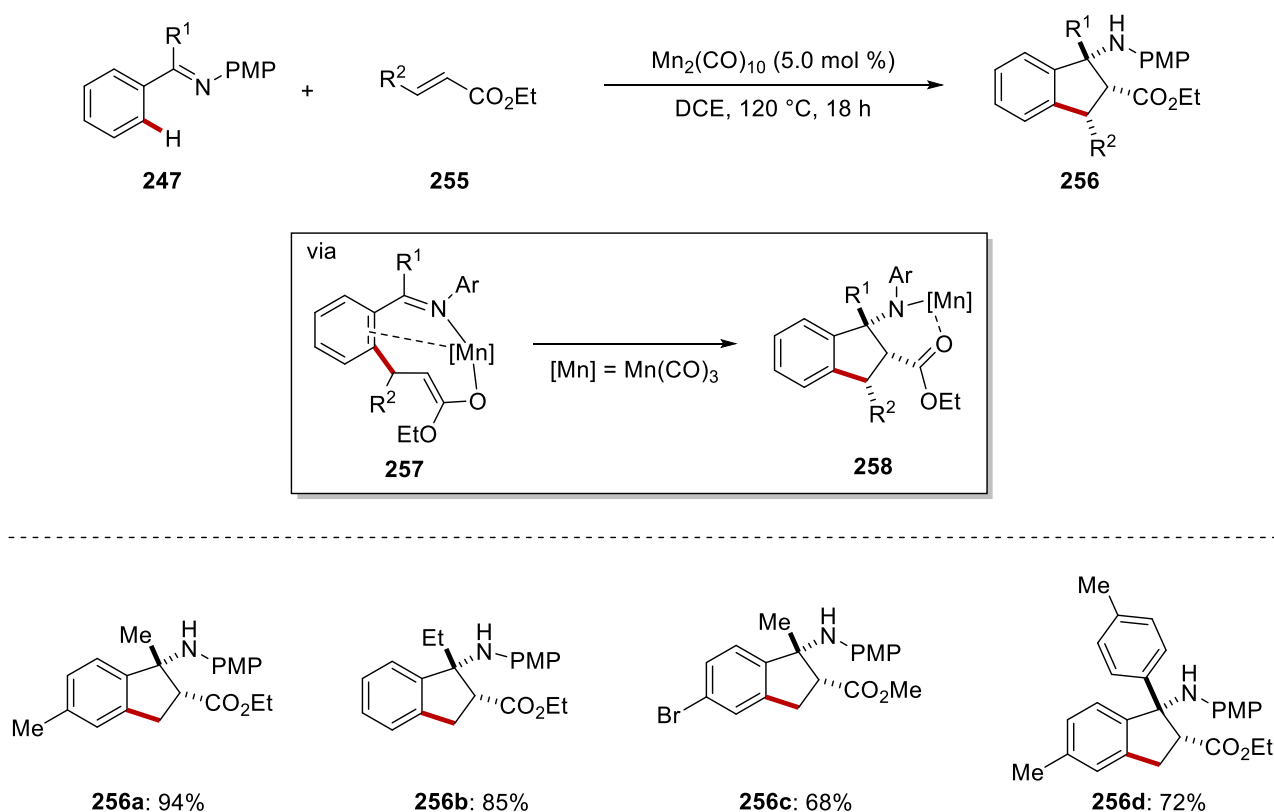
In 2017, the same group reported manganese-catalyzed decarboxylative C–H allylations of heteroarenes **242** and arenes **247d** with dioxolanones **250** (Scheme 1.4.9).<sup>[133]</sup> Thus, C–H/C–O bond cleavages with concomitant formation of CO<sub>2</sub> delivered the desired allyl alcohols **251** or **252** with high levels of the site- and chemo-selectivity. Later, this manganese catalysis manifold was further extended to include C–H/C–C activation, affording allylated heteroarenes **254** (Scheme 1.4.9).<sup>[134]</sup>



**Scheme 1.4.9** Manganese-catalyzed C–H allylation *via* C–H/C–O or C–H/C–C cleavage.

Thereafter, Glorius reported a similar manganese-catalyzed C–H allylation.<sup>[135]</sup> Along the same lines, Wang<sup>[136]</sup> and Zhang<sup>[137]</sup> independently reported manganese-catalyzed C–H allylation reactions with allenes and perfluoroallyl bromides as coupling partners respectively.

Manganese-catalyzed C–H functionalizations with substrates including C–C double bonds are not limited to allylations. Indeed, Ackermann and coworkers developed manganese-catalyzed C–H annulation<sup>[138]</sup> of arenes **247** with acrylates **255**, affording *cis*- $\beta$ -amino acid esters **256** (Scheme 1.4.10).<sup>[139]</sup> This interesting transformation involved the formation of a nucleophilic manganese intermediate, followed by intramolecular nucleophilic addition to the iminyl carbon. The operationally simple transformation featured high catalytic efficacy, good functional group tolerance, and an excellent *cis* stereoselectivity.

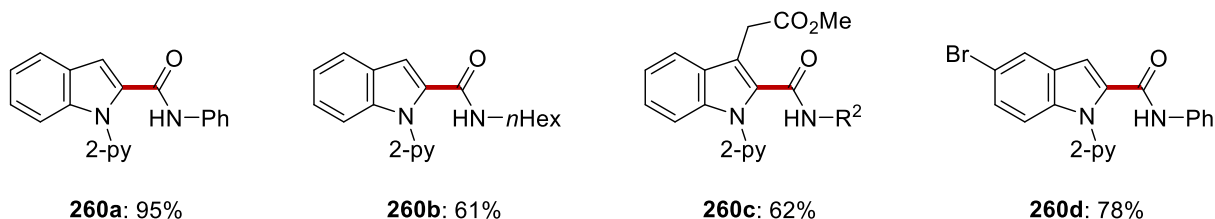
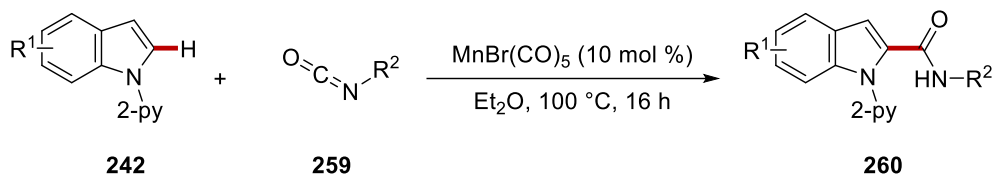


**Scheme 1.4.10** Manganese-catalyzed alkene annulations.

Allenes are a class of unique compounds with two  $\pi$ -orbitals perpendicular to each other at the centered carbon. These unique features of allenes have been also introduced into manganese-catalyzed C–H activation reactions, thereby producing interesting and useful chemical transformations. While Glorius reported manganese-catalyzed C–H propargylation with bromoallenes with the aid of a borane-based Lewis acid,<sup>[140]</sup> Wang<sup>[141]</sup> and Rueping,<sup>[142]</sup> among others,<sup>[143]</sup> showcased C–H annulations of heteroarenes with allene moieties *via* Smiles rearrangement.

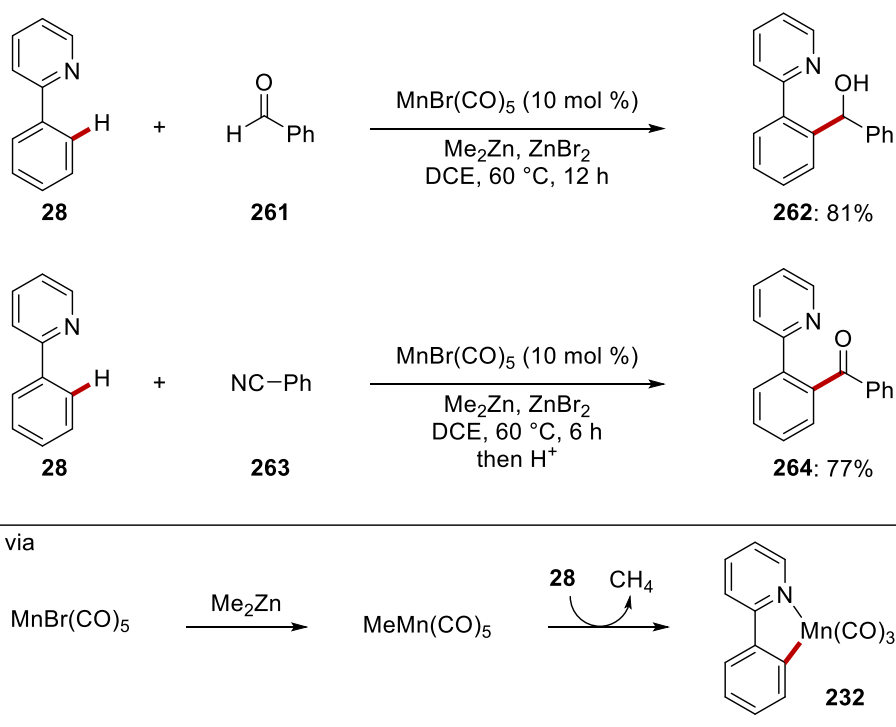
Apart from C–C multiple bonds, electrophilic C–Het multiple bonds were also found to be viable reaction partners.<sup>[144]</sup> Thus, aldehydes, imines, or nitrile-containing substrates were introduced to the manganese-catalyzed hydroarylation reactions. In 2015, Ackermann and coworkers reported manganese-catalyzed C–H aminocarbonylation of heteroarenes **242** with isocyanates **259**, featuring a broad range of functional groups (Scheme 1.4.11).<sup>[145]</sup> In addition, traceless removal of the pyridyl directing group was achieved, enabling expedient access to C2–H functionalized indoles **260**.





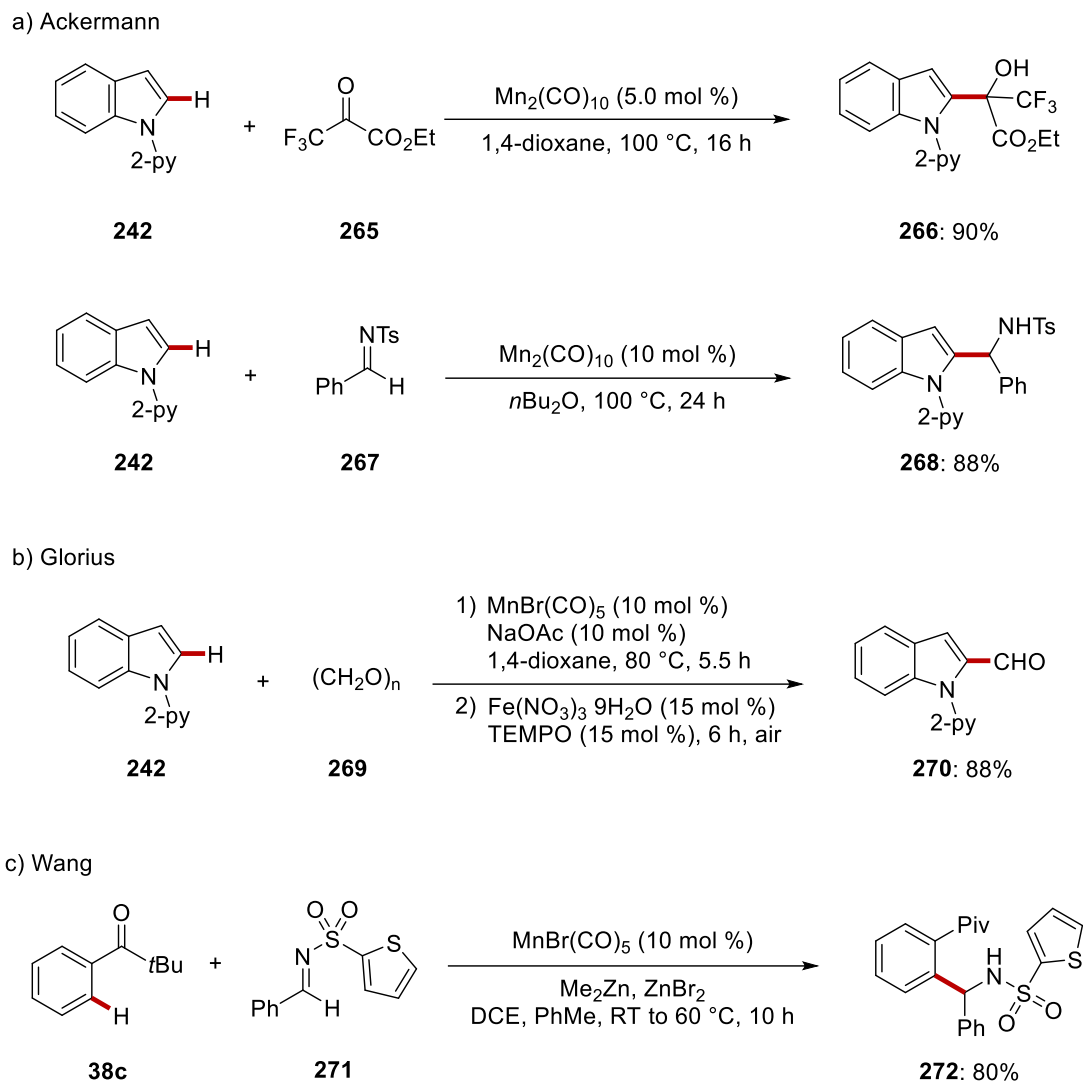
**Scheme 1.4.11** Manganese-catalyzed C–H aminocarbonylations.

Around the same time, the Wang group showed the manganese-catalyzed Grignard-type nucleophilic addition to aldehydes **261** or nitriles **263**, providing benzylic alcohols **262** or ketones **264**, respectively (Scheme 1.4.12).<sup>[146]</sup>



**Scheme 1.4.12** Manganese-catalyzed C–H addition of arenes **28** to aldehydes **261** or nitriles **263**.

Ackermann<sup>[147]</sup> and others<sup>[148]</sup> additionally reported manganese-catalyzed hydroarylations with substrates having electrophilic C–Het multiple bonds (Scheme 1.4.13).

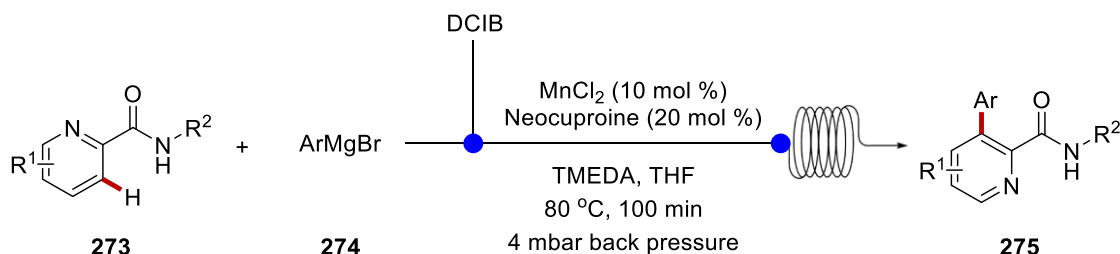


**Scheme 1.4.13** Manganese-catalyzed hydroarylation with carbonyl groups **265**, **269** or imines **267**, **271**.

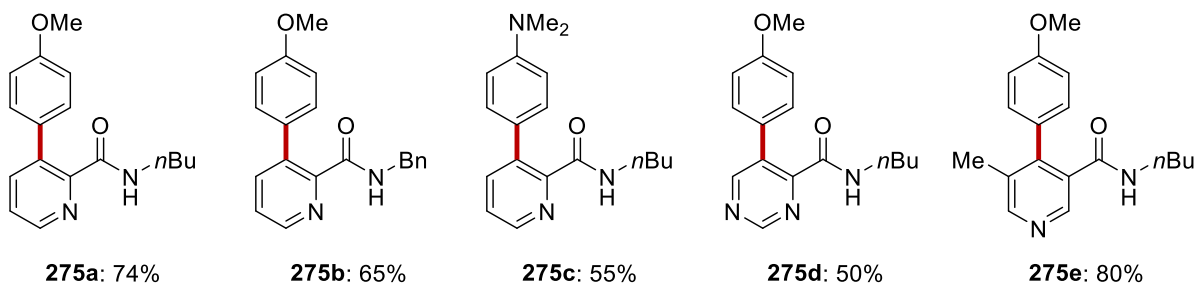
### 1.4.1 Manganese-Catalyzed C–H Arylations

Manganese(I)-catalyzed C–H activation of arenes has been generally governed by isohypsic mechanisms, which often impedes redox active catalysis. For this reason, manganese-catalyzed C–H arylation reaction requires a different approach.

Ackermann and coworkers disclosed a manganese-catalyzed C–H arylation by using a user-friendly and scalable flow technique (Scheme 1.4.14).<sup>[149]</sup> The combination of the manganese salts  $\text{MnCl}_2$  and neocuproine allowed for expedient C–H arylations of azines **273** with a broad substrate scope. On the basis of detailed experimental and computational studies, a Mn(II/III/I) manifold was proposed to be operative. Interestingly, the same group, later, reported electrochemical manganese-catalyzed C–H arylations, in which electricity could replace the external oxidant DCIB.<sup>[150]</sup>

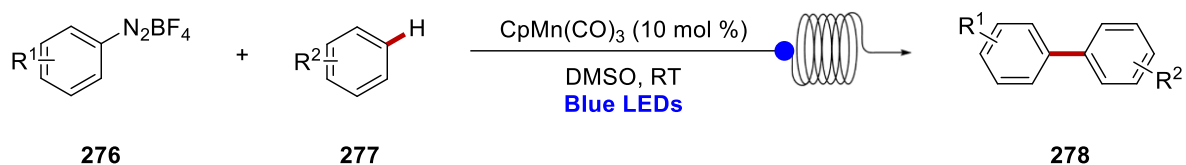


a) Substrate scope

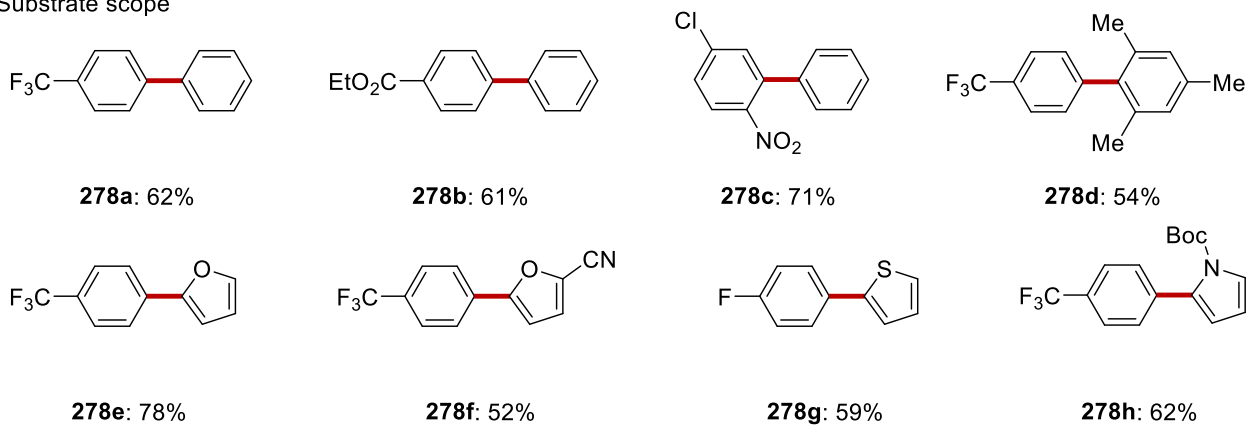


**Scheme 1.4.14** Manganese-catalyzed C–H arylations using flow technique.

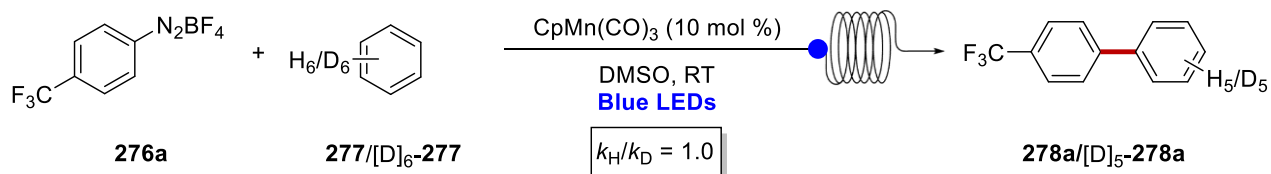
More recently, Ackermann developed photo-induced manganese-catalyzed C–H arylations by flow-chemistry (Scheme 1.4.15).<sup>[151]</sup> Thus, a plethora of aryldiazonium salts **276** was transformed to biaryls **278** under the optimized conditions. The robustness of the manganese-catalyzed C–H arylation in continuous photoflow was extended to feature heteroarenes (**278e–278h**) with high functional group tolerance. Interestingly, an intermolecular kinetic isotope effect was not observed, indicating a non-kinetically relevant C–H cleavage.



## a) Substrate scope



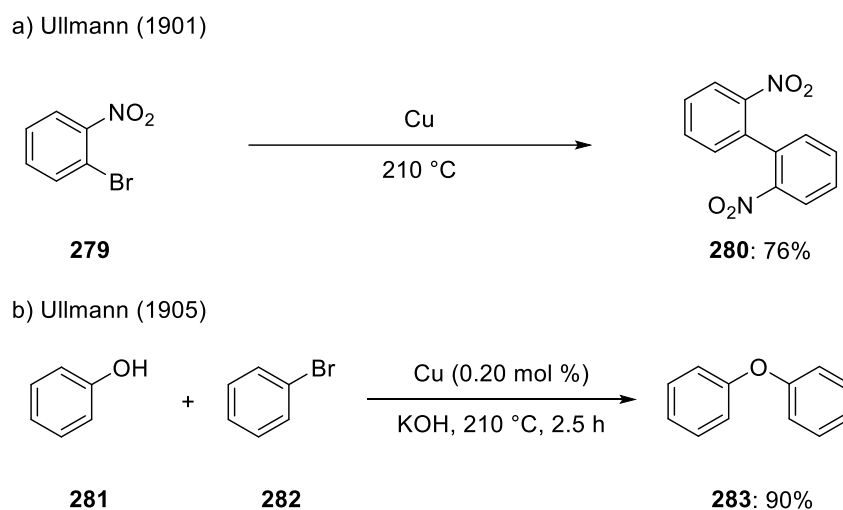
## b) Kinetic study



Scheme 1.4.15 Visible-light-induced manganese-catalyzed C–H arylation in flow.

## 1.5 Copper-Catalyzed C–H Activation

Similar to manganese, copper is an inexpensive and environmentally benign element. In addition, its readily accessible oxidation states from 0 to +3 provide new bond formation processes through radical or one- and two-electron transfer processes.<sup>[152]</sup> With these inherent benefits, copper catalysis has emerged as an important tool for organic reactions with a long history. Starting from the Glaser coupling,<sup>[153]</sup> copper-mediated reaction enabled a plethora of chemical transformations. Hence, copper has played a significant role in catalysis. Inspired by the pioneering work of Ullmann and Goldberg from 1901 to 1906 (Scheme 1.5.1),<sup>[154]</sup> a variety of transformation by copper catalysis have been achieved.<sup>[155]</sup>



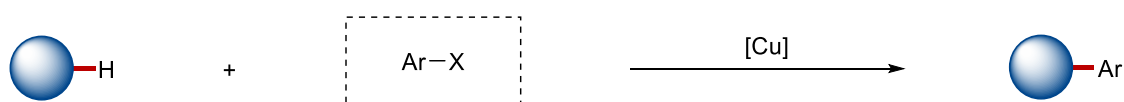
**Scheme 1.5.1** Ullmann's seminal work on arylation reactions.

### 1.5.1 Copper-Catalyzed C–H Arylations

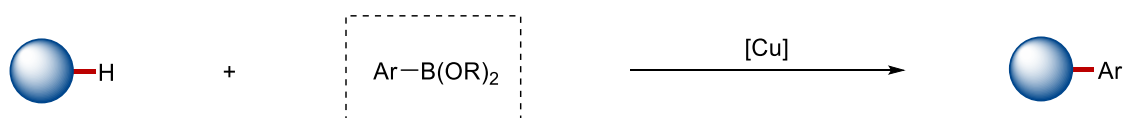
In 1901, Ullmann disclosed the first arylation using a stoichiometric amount of copper *via* reductive coupling.<sup>[38b]</sup> Thereafter, Ullmann reported copper-catalyzed N–H arylations of anilines as well as O–H arylations of phenol.<sup>[38a, 14b]</sup> In 1906, Goldberg additionally revealed copper-catalyzed aminations with anilines or amides.<sup>[14a]</sup> With these pioneering reports, copper enabled C–C, C–N, and C–O bond formations, which became a milestone for the development of copper-catalyzed C–H arylations.

Copper-catalyzed C–H arylation can be categorized by four different approaches, including (i) the use of electrophilic reagents, (ii) the use of nucleophilic reagents, (iii) the use of carboxylic acids for decarboxylations, and (iv) cross-dehydrogenative couplings.

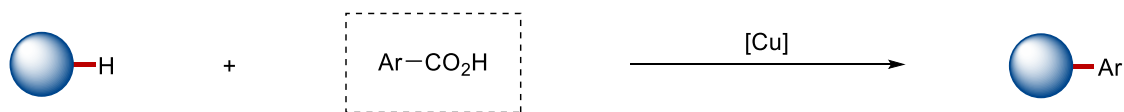
a) Electrophilic coupling partners



b) Arylations with nucleophilic coupling partners



c) Decarboxylative arylations



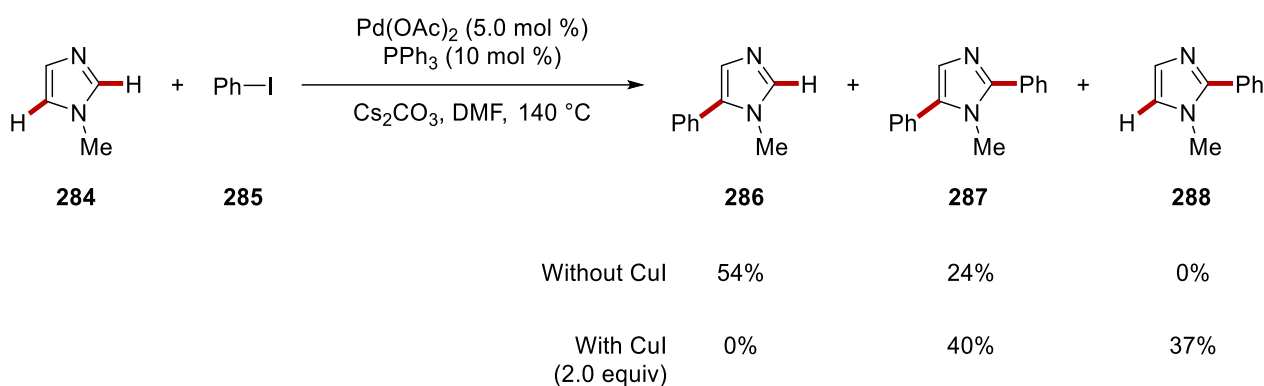
d) Cross-dehydrogenative arylations



**Scheme 1.5.2** Strategies for copper-catalyzed C–H arylations.

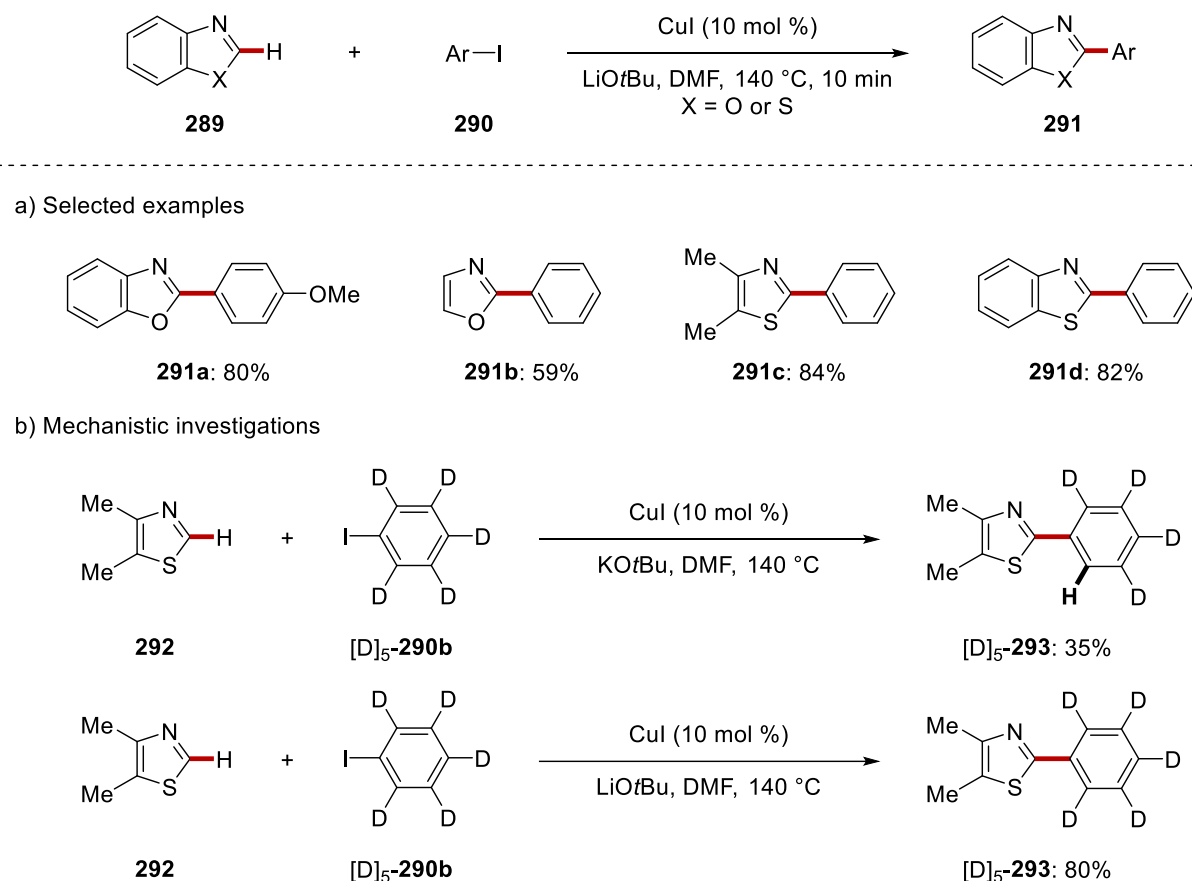
Nilsson<sup>[156]</sup> and Wahren<sup>[157]</sup> reported an early C–H arylation with copper complexes in 1968 and in 1973 respectively. Although the stoichiometric use of copper complex was required in presence of the palladium(II) catalyst, Miura clearly showed that copper enabled a switch in the site-selectivity of C–

H arylations (Scheme 1.5.3).<sup>[158]</sup> Notably, since C5–H arylation of *N*-methylimidazole **284** occurs *via* an electrophilic palladation, the copper complex plays a significant role in the C2–H arylations.<sup>[159]</sup> Interestingly, *N*-methylbenzimidazole only showed C2–H arylation with stoichiometric use of copper iodide in absence of the palladium(II) catalyst.



**Scheme 1.5.3** The effect of copper additives in palladium-catalyzed C–H arylation.

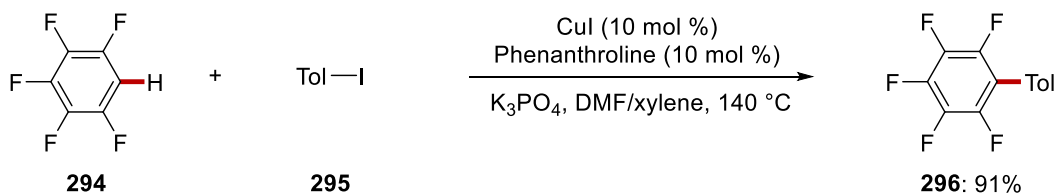
These findings allowed researchers to envisage the involvement of catalytic organocopper intermediates in the C–H arylation reactions. Inspired by these studies, Daugulis disclosed copper-catalyzed C–H arylation of electron-rich heterocycles, including oxazoles, benzoxazoles, thiazoles, and benzothiazoles (Scheme 1.5.4).<sup>[160]</sup> The combination of lithium alkoxide bases and aryl iodides enabled sustainable C–H arylations, while other aryl halides or tosylates fell short in delivering the desired arylated product. In their mechanistic proposal, deprotonation followed by lithium-copper transmetallation affords organocopper species, while the involvement of arynes intermediates could be ruled out through mechanistic investigations.



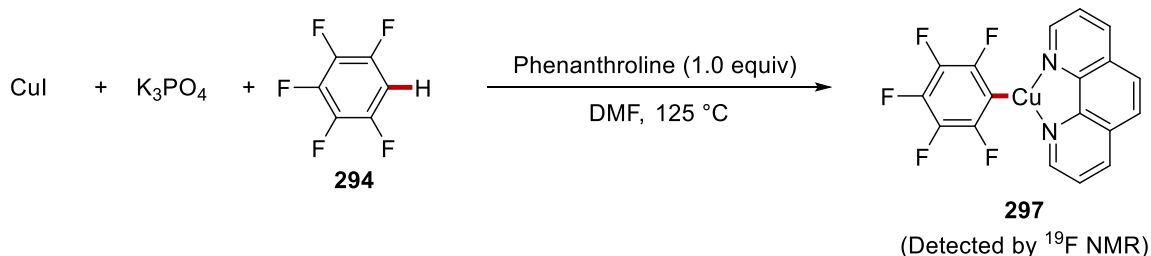
**Scheme 1.5.4** Copper-catalyzed C–H arylations.

Then, the same group reported copper-catalyzed C–H arylations of electron-deficient as well as polyfluorinated arenes,<sup>[161]</sup> which was further extended to the new methods where both electron-rich and electron-poor heterocycles could be employed as viable substrates (Scheme 1.5.5).<sup>[162]</sup> Pentafluorophenyl copper intermediate **297** was separately prepared with the aid of phenanthroline ligand. The copper complex **297** was transformed to the biaryl product in a stoichiometric fashion, which showed to conclude that C–H cuperation is the key to the success of the copper-catalyzed C–H arylations. Notably, while the early example of copper-catalyzed C–H activation was proposed to proceed *via* SET mechanisms, this study proposed organometallic C–Cu intermediates.





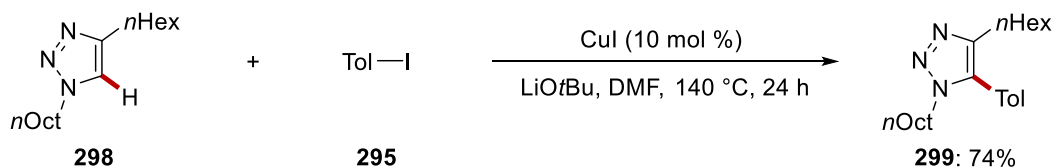
a) Mechanistic studies



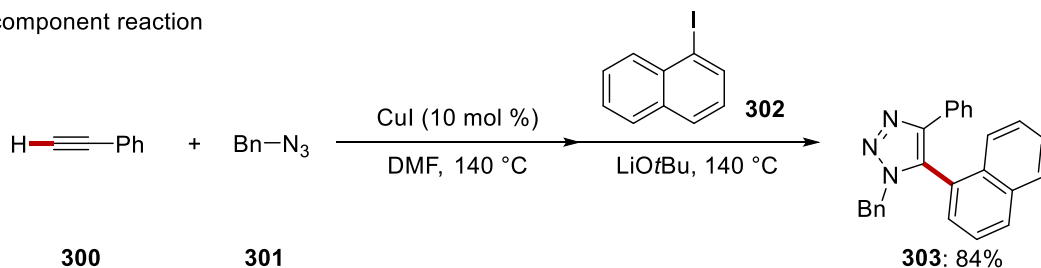
**Scheme 1.5.5** Copper-catalyzed C–H arylation of perfluoroarene **294**.

Concurrently, Ackermann disclosed the copper-catalyzed C–H arylation of triazoles **298** (Scheme 1.5.6).<sup>[163]</sup> The 1,2,3-triazoles **298** were readily obtained by copper-catalyzed click reaction followed by C–H arylation, establishing multicomponent protocols to synthesized a variety of fully substituted triazoles.

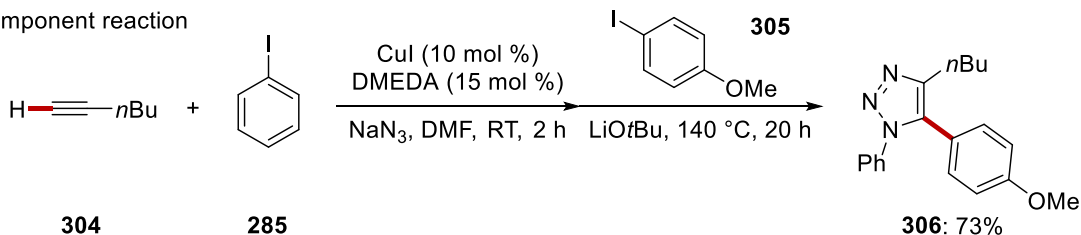
a) Two-components reaction



b) Three-component reaction



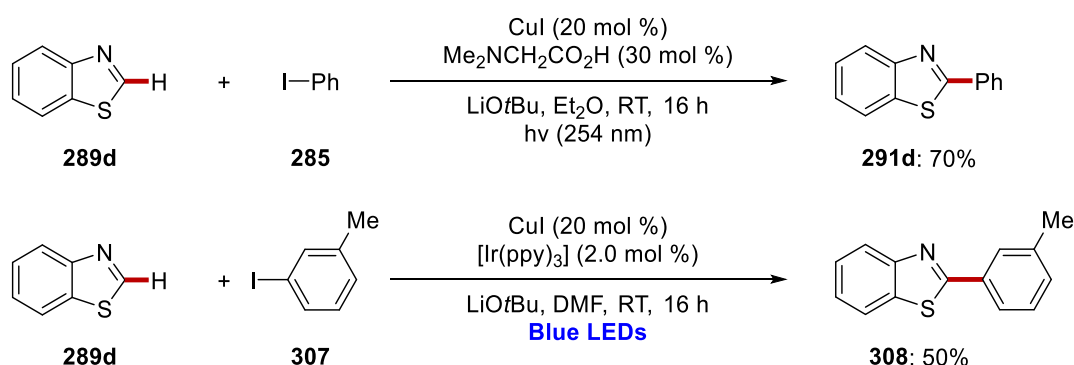
c) Four-component reaction



**Scheme 1.5.6** Multi-component copper-catalyzed C–H arylation.

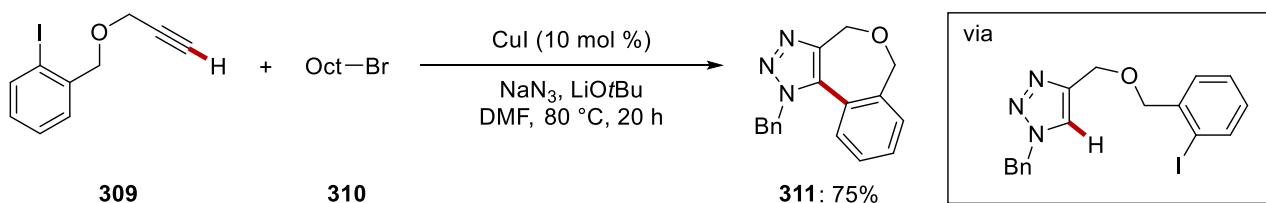
Inspired by these studies by Daugulis, Miura, and Ackermann, a plethora of C–H arylation studies was reported with various heterocycles, including azoles,<sup>[164]</sup> benzotriazepines,<sup>[165]</sup> caffeine,<sup>[166]</sup> uracil,<sup>[167]</sup> among others.<sup>[168]</sup>

In 2016, Ackermann and coworkers reported unprecedented photo-induced copper-catalyzed C–H arylation under exceedingly mild conditions at room temperature (Scheme 1.5.7).<sup>[169]</sup> Additionally, this manifold was further extended to the reaction under visible light conditions with a iridium photocatalyst.



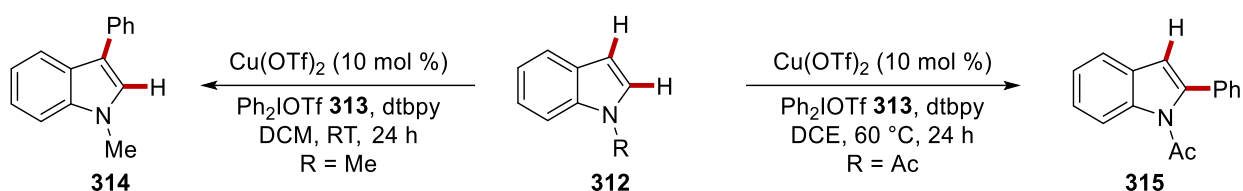
**Scheme 1.5.7** Photo-induced copper-catalyzed C–H arylations.

With these aforementioned established studies, intramolecular approaches of copper-catalyzed C–H arylations were also developed. Namely, Ackermann showed the intramolecular C–H/C–X activation, in which the construction of fully substituted cyclic 1,2,3-triazoles **311** was successfully achieved through [3+2] azide–alkyne cycloadditions followed by C–H activation (Scheme 1.5.8).<sup>[170]</sup>



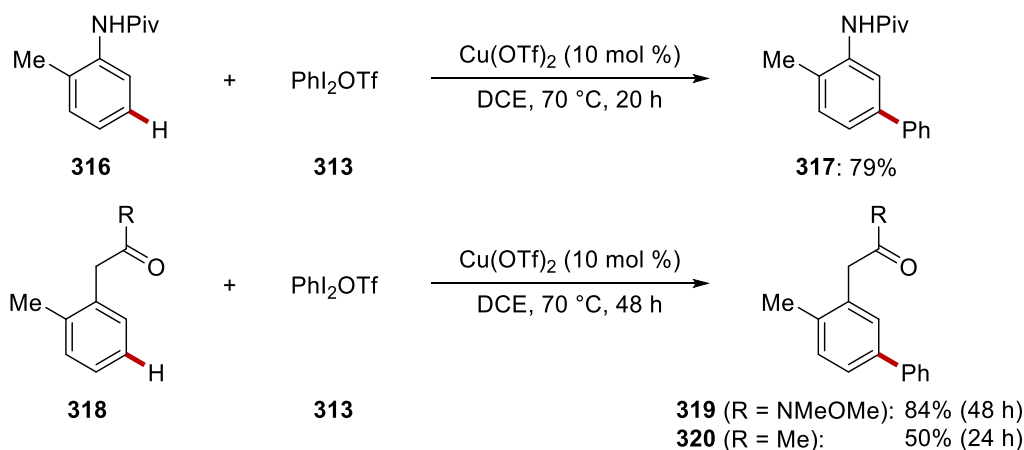
**Scheme 1.5.8** Three-component intramolecular copper-catalyzed C–H arylation.

The use of electrophilic reagents was not limited to aryl halides, but was extended to include diaryliodonium salts. In 2008, Gaunt disclosed a copper-catalyzed divergent C–H arylation of indoles **312** with diphenyliodonium salt **313** (Scheme 1.5.9).<sup>[171]</sup> Thus, C2–H and C3–H of indoles could be independently functionalized under slightly different conditions. They also proposed possible reaction mechanisms for each functionalization, starting from the key aryl–copper(III) intermediate. Notably, the established method was further applied to the synthesis of alkaloid dictyodendrin B.<sup>[172]</sup>



**Scheme 1.5.9** Divergent copper-catalyzed C–H arylations of indole **312** with diaryliodonium salt **313**.

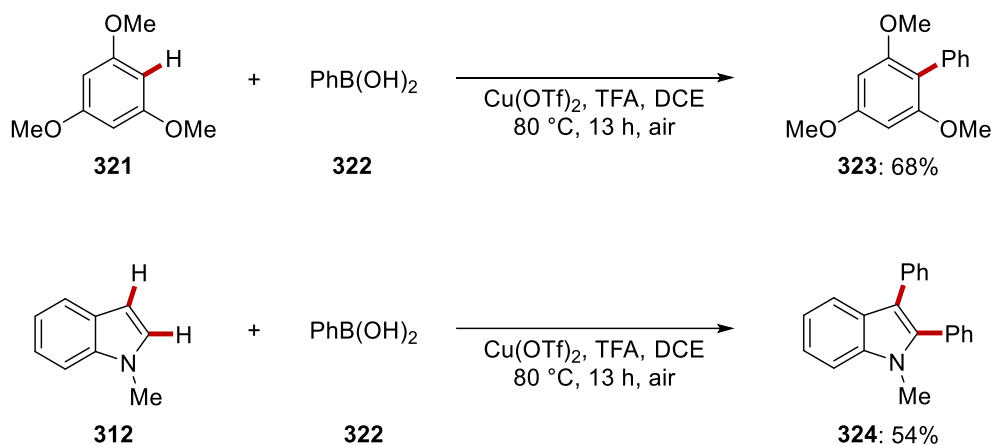
Gaunt also expanded the copper catalysis using diaryliodonium salts to C–H arylation, particularly providing *meta*-C–H functionalizations of arenes (Scheme 1.5.10).<sup>[173, 73c]</sup> The catalytic cycle was proposed as two different pathways; oxycuperation mechanism and Mizoroki-Heck-type mechanism.<sup>[174]</sup>



**Scheme 1.5.10** Copper-catalyzed C–H arylations with diphenyliodonium salt **313**.

Later, Gaunt reported *para*-C–H arylations of anisole and anilines using copper catalysis with diphenyliodonium salts **313**.<sup>[175]</sup>

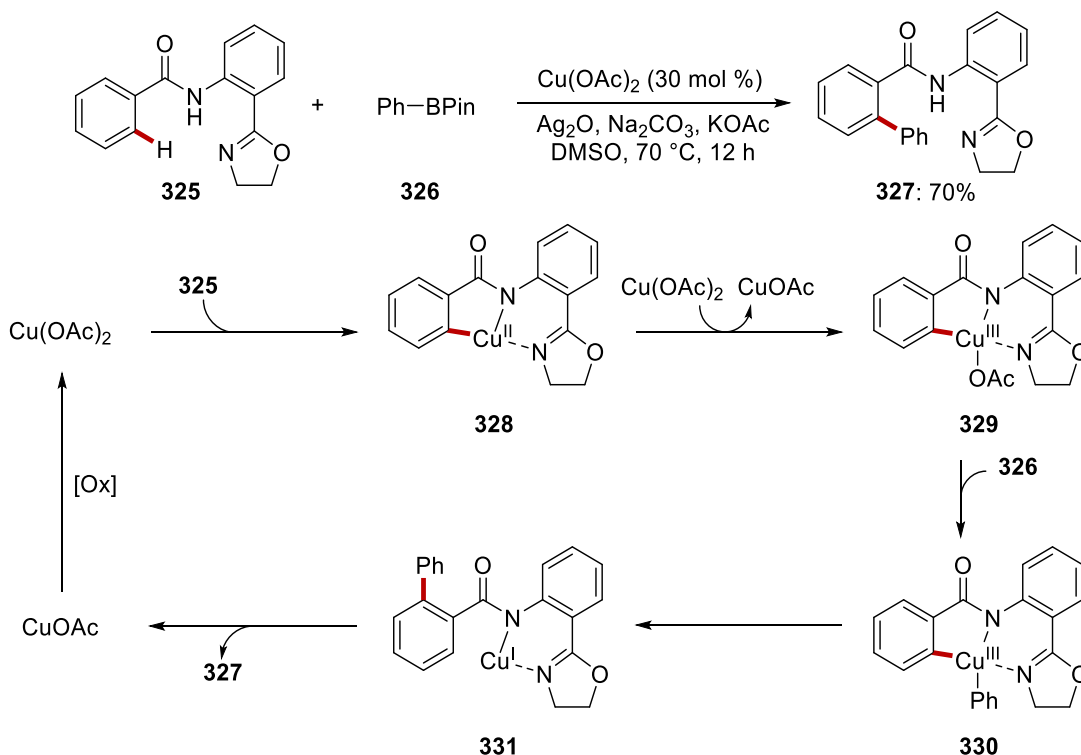
As the use of nucleophile organometallic reagents, in 2008, Itami showed the copper-mediated C–H arylation of arenes **321** and heteroarenes **312** with aryl boronic acids **322** (Scheme 1.5.11).<sup>[176]</sup> Afterwards, this reaction manifold was extended for the arylation of various heteroarene with aryl boronic esters as well as aryl Grignard reagents.<sup>[177]</sup>



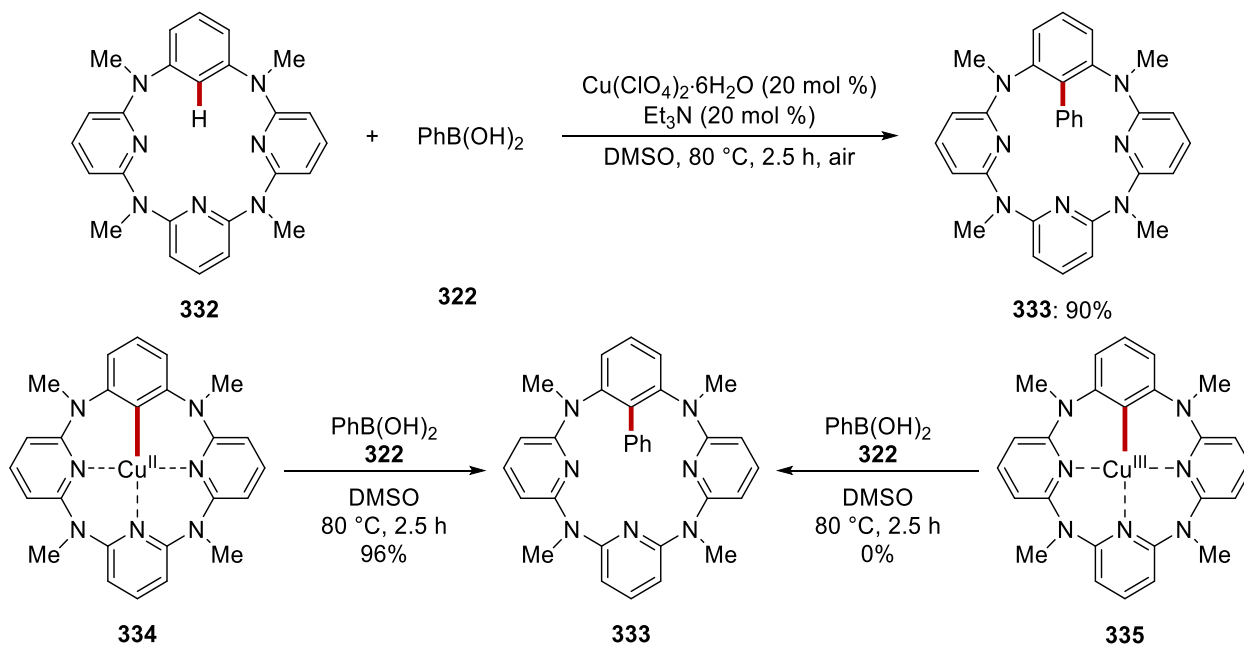
**Scheme 1.5.11** Copper-mediated C–H arylations with aryl boronic acid **322**.

In 2014, Dai and Yu group disclosed oxidative C–H arylations with organoboron reagents with the aid of a bidentate directing group (Scheme 1.5.12a).<sup>[178]</sup> Thereafter, Wang reported the copper-catalyzed C–H arylation of azacalix[1]arene[3]-pyridines **332** with aryl boronic acids **322** (Scheme 1.5.12b).<sup>[179]</sup> Interestingly, these two studies proposed slightly different catalytic mechanisms. In Yu's study, the reaction was proposed to proceed through aryl copper(III) intermediates followed by reductive elimination and oxidation, regenerating the active copper(II) species. However, Wang performed stoichiometric reactions with independently prepared well-defined copper(II) and copper(III) intermediates, but interestingly, only the reaction with the copper(II) compound **334** afforded the arylated product **333**.

a) Yu's work and their proposed mechanism

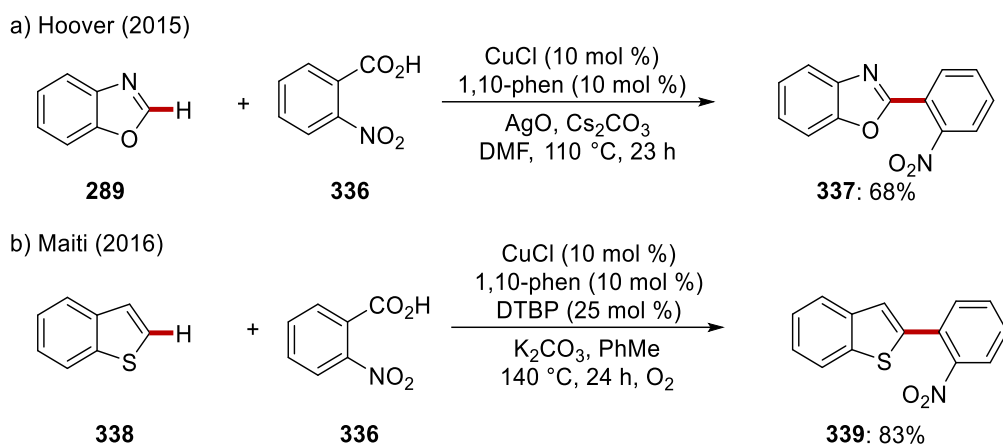


b) Wang's work and their proposed mechanism



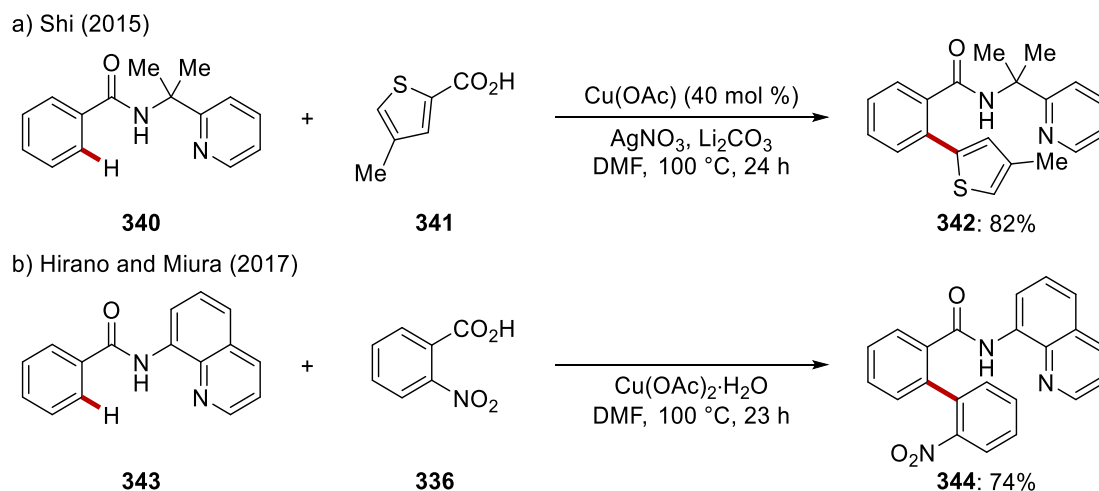
Scheme 1.5.12 Copper-catalyzed and mediated C–H arylations.

For the third type of copper-catalyzed C–H arylations, decarboxylation of aryl carboxylic acid has also emerged as a viable arylating method.<sup>[180]</sup> Hoover and coworkers reported decarboxylative arylations by copper catalysis in 2015 (Scheme 1.5.13a).<sup>[181]</sup> In the next year, Maiti reported a similar copper-catalyzed C–H arylation *via* decarboxylation (Scheme 1.5.13b).<sup>[182]</sup>



**Scheme 1.5.13** Decarboxylative copper-catalyzed C–H arylations.

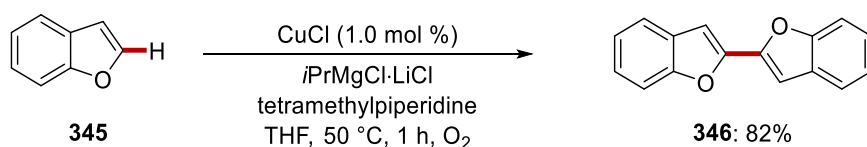
This arylation could be extended to arenes with bidentate directing group. Shi reported decarboxylative copper-catalyzed C–H arylation enabled by the (pyridin-2-yl)isopropyl amine (PIP-amine) directing group (Scheme 1.5.14a).<sup>[183]</sup> Hirano and Miura also reported a similar reactivity with the 8-aminoquinoline-based bidentate auxiliary (Scheme 1.5.14b).<sup>[184]</sup>



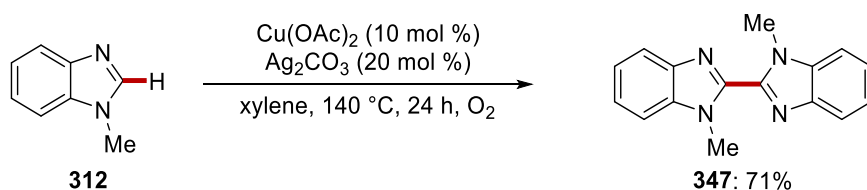
**Scheme 1.5.14** Bidentate directing group enabling decarboxylative C–H arylations.

The fourth method for copper-catalyzed C–H arylations are dehydrogenative C–H/C–H arylation. Although this approach does not require prefunctionalization of substrates, the achievement of selectivity control is the key challenging issue.<sup>[185]</sup> In this regard, while copper-catalyzed oxidative C–H/C–H arylations for homo-couplings could be readily achieved,<sup>[186]</sup> unsymmetric biaryl formation commonly required electronic bias of two starting materials<sup>[187]</sup> or intramolecular settings (Scheme 1.5.15).<sup>[188]</sup>

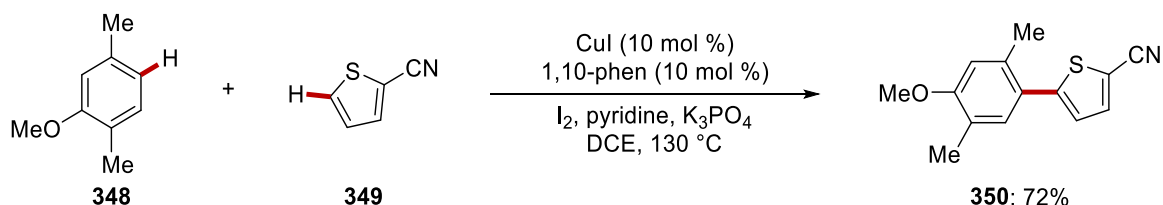
a) Daugulis (2009)



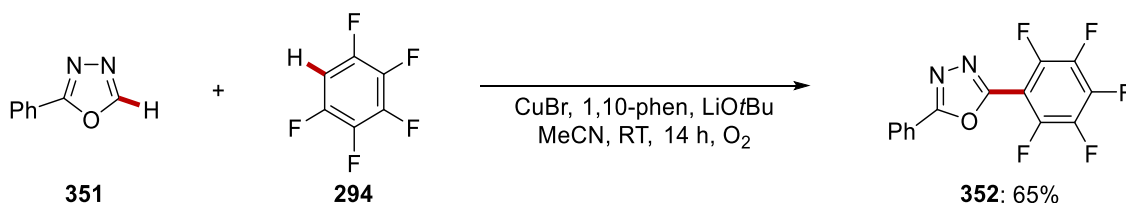
b) Mori (2010)



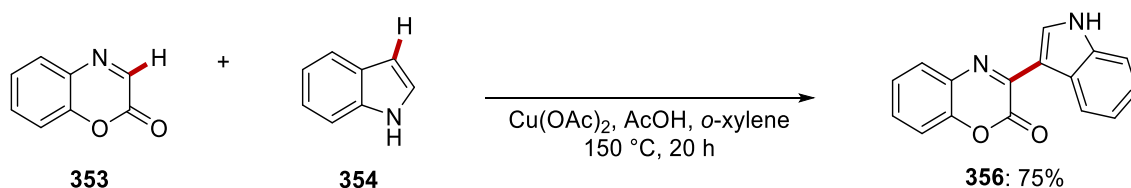
c) Daugulis (2011)



d) Bolm (2013)



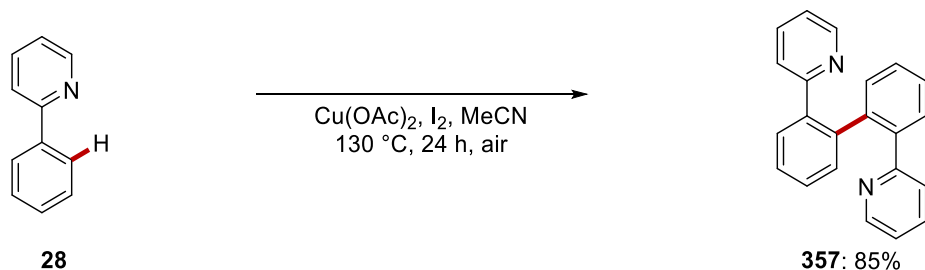
e) Lee (2017)



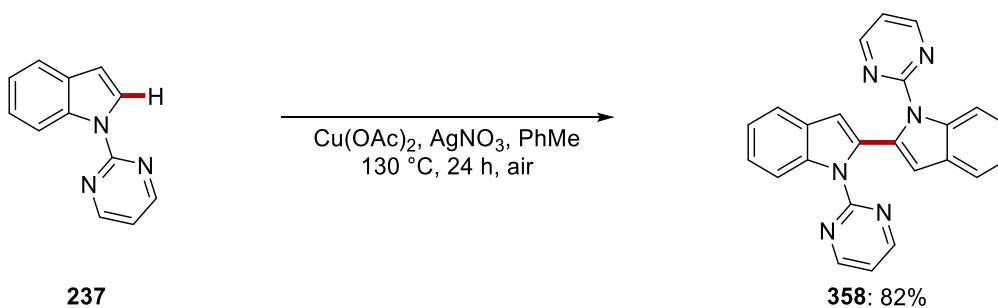
**Scheme 1.5.15** Dehydrogenative copper-mediated C–H arylations.

This arylation manifold could also be extended to arenes using suitable directing groups (Scheme 1.5.16).<sup>[189]</sup>

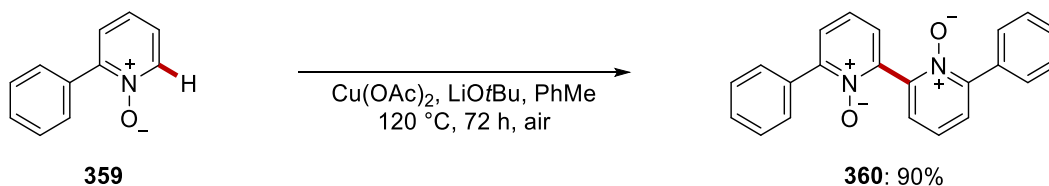
a) Yu (2006)



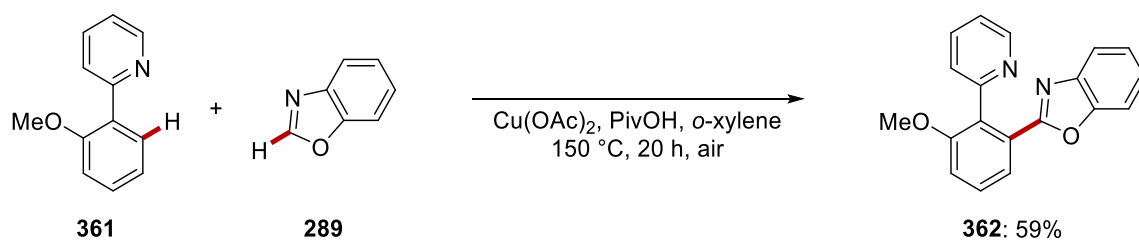
b) Jiang (2016)



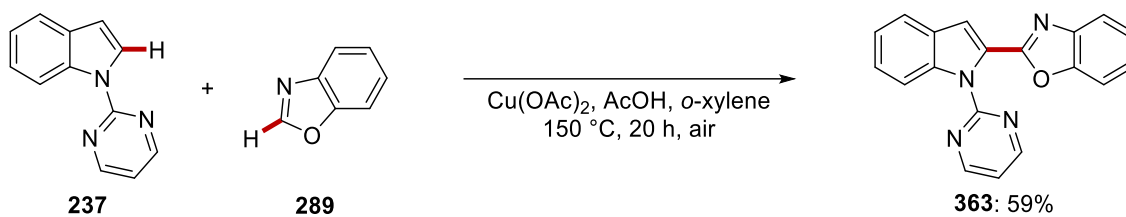
c) Jain (2017)



d) Hirano and Miura (2011)



e) Hirano and Miura (2012)

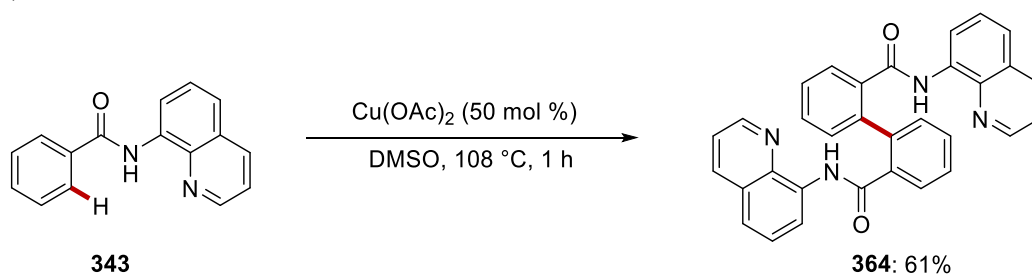


**Scheme 1.5.16** Dehydrogenative copper-mediated C–H/C–H arylations.

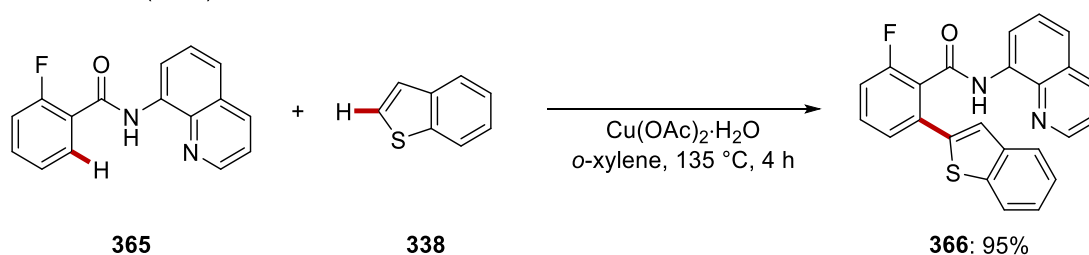


Furthermore, the bidentate directing group enabled various C–H/C–H cleavage (Scheme 1.5.17).<sup>[190]</sup>

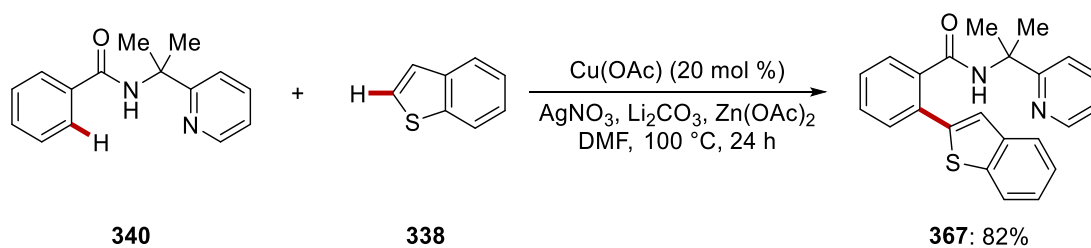
a) Sun (2013)



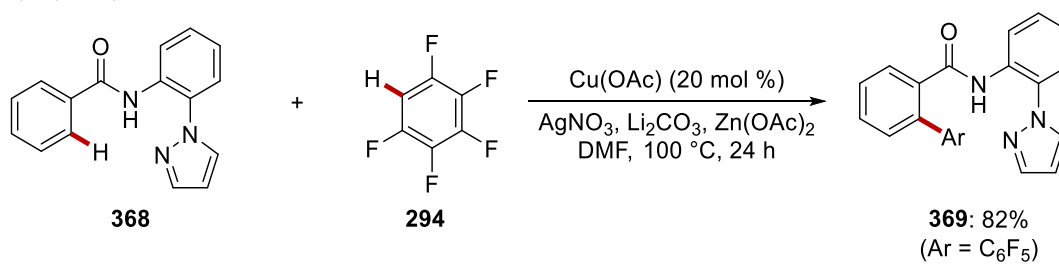
a) Hirano and Miura (2013)



a) Shi (2015)



a) Baidya (2018)



**Scheme 1.5.17** Copper-catalyzed cross-dehydrogenative C–H arylations.

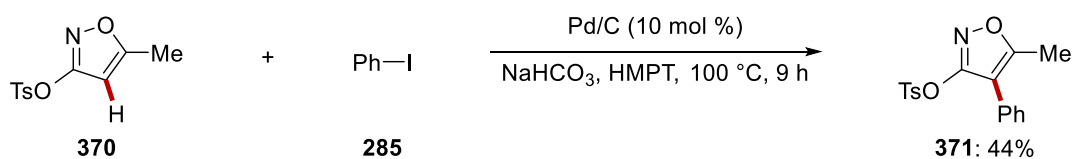
## 1.6 Hybrid-Metal-Catalyzed C–H Activation

While there are indisputable and considerable advances in homogeneous metal-catalyzed C–H functionalization, the homogeneous catalytic process possessed inherent disadvantages of difficult catalyst reusability, which can be directly connected to environmental issues as well as economical concerns in the industries.<sup>[191]</sup> In sharp contrast, the advent of heterogeneous catalysts enabled a shift of paradigm. The heterogeneous catalyst basically consisted of different phases<sup>[192]</sup> which are exposed to the reacting chemicals, allowing the recovery of the catalyst.<sup>[193]</sup> Thereby, heterogeneous catalysis often provides sustainable pathways toward molecular syntheses.<sup>[194]</sup>

In 1817, the first heterogeneous catalysis was discovered by the Cornish chemist Humphry Davy who identified that gas burning could occur without a flame in presence of platinum wire in his research on miner's safety lamps.<sup>[195]</sup> A few years later, Döbereiner discovered the reaction of hydrogen gas with a platinum sponge could produce a flame at room temperature.<sup>[196]</sup> At the end of the 1990s, the Deacon process was developed, which generated chlorine from hydrochloric acid with the copper salt  $\text{CuCl}_2$  as a catalyst.<sup>[197]</sup> This discovery provided a catalytic approach as well as a sustainable replacement of the previous process using stoichiometric  $\text{MnO}_2$ . At the beginning of the twentieth century, the Haber-Bosch process was developed, in which iron oxide carriers accompanied with promoters could catalyze the ammonia production.<sup>[198]</sup>

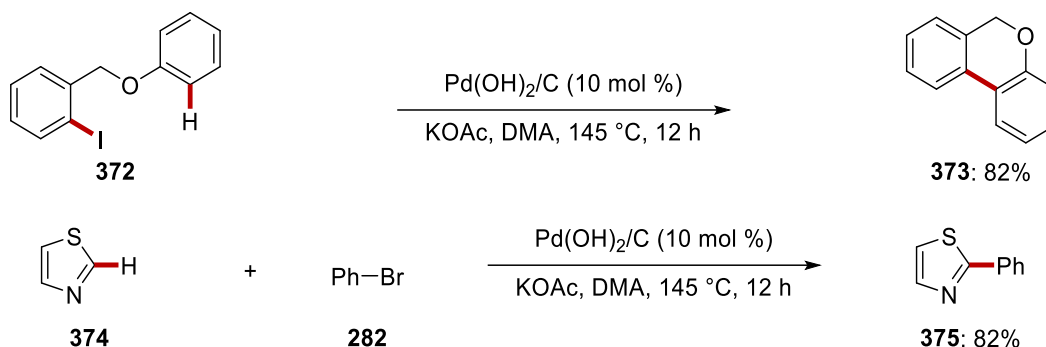
Thereafter, a number of recyclable and reusable heterogeneous catalysts have been developed, which could also recently be used for C–H activation chemistry.<sup>[199]</sup>

The first example of heterogeneous metal-catalyzed C–H activation was disclosed by Nakamura in 1982 (Scheme 1.6.1).<sup>[200]</sup> In this report, palladium on charcoal catalyzed C–H arylations of heteroarenes **370** with aryl iodides **285**, while recyclability and heterogeneity of the catalyst were not studied.



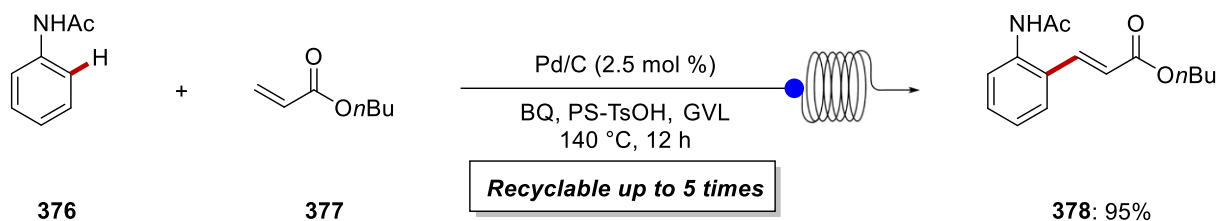
**Scheme 1.6.1** The first heterogeneous palladium-catalyzed C–H arylation.

In 2005, Fagnou extended heterogeneous palladium catalysis to intra- and intermolecular C–H arylations (Scheme 1.6.2).<sup>[201]</sup> Here, a wide range of substrate scopes was presented with Pearlman's catalyst, while a three-phase test revealed that a homogeneous process is likely operative.



**Scheme 1.6.2** The seminal example of recyclable heterogeneous palladium-catalyzed C–H arylation.

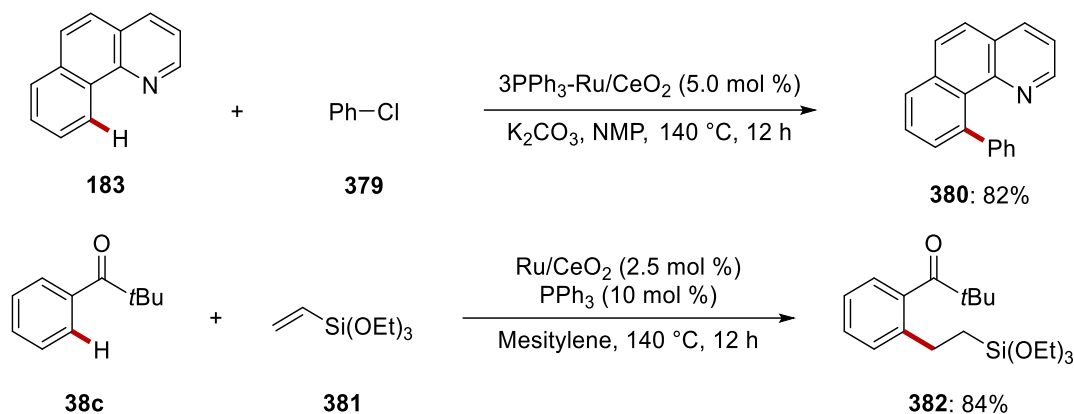
In 2017, Ackermann and Vaccaro reported heterogeneous palladium-catalyzed Fujiwara-Moritani reaction in continuous flow (Scheme 1.6.3). Thus, a tailor-made flow reactor set the stage to not only reuse the catalyst but also scale the reaction, while detailed ICP-OES analysis of the reaction medium only showed less than 5 ppm of palladium leaching. In addition, various heterogeneity tests, such as hot-filtration and Hg(0) poisoning, provide a strong support for the heterogeneous nature of the developed catalysis.



**Scheme 1.6.3** Heterogeneous palladium-catalyzed Fujiwara-Moritani reaction in flow.

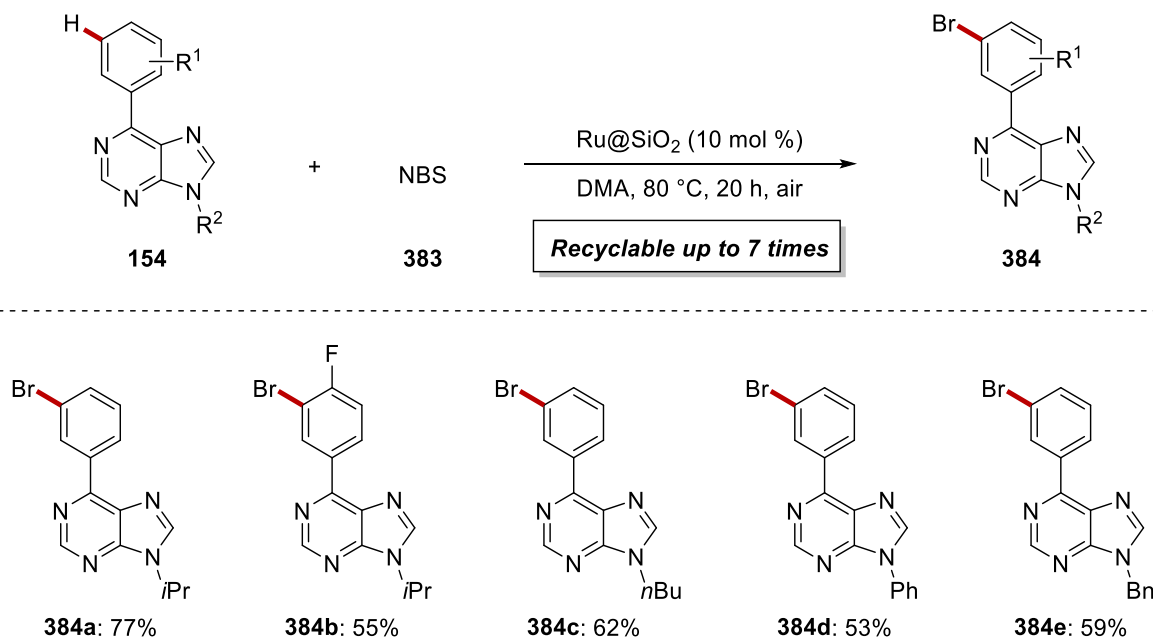
Inspired by these early examples, the heterogeneous catalysis realm in C–H activation was expanded to feature not only palladium catalysis but also other transition metal catalysis. In 2010, Wada and Inoue disclosed heterogeneous ruthenium-catalyzed C–H arylation, in which they utilized cerium(IV)

oxide support to immobilize the ruthenium catalyst (Scheme 1.6.4).<sup>[202]</sup> Although the developed heterogeneous ruthenium catalyst was required to perform reactivation for the reuse, later, this reaction manifold could be efficiently introduced to C–H hydroarylation reactions.<sup>[203]</sup>



**Scheme 1.6.4** Heterogeneous ruthenium-catalyzed C–H activations.

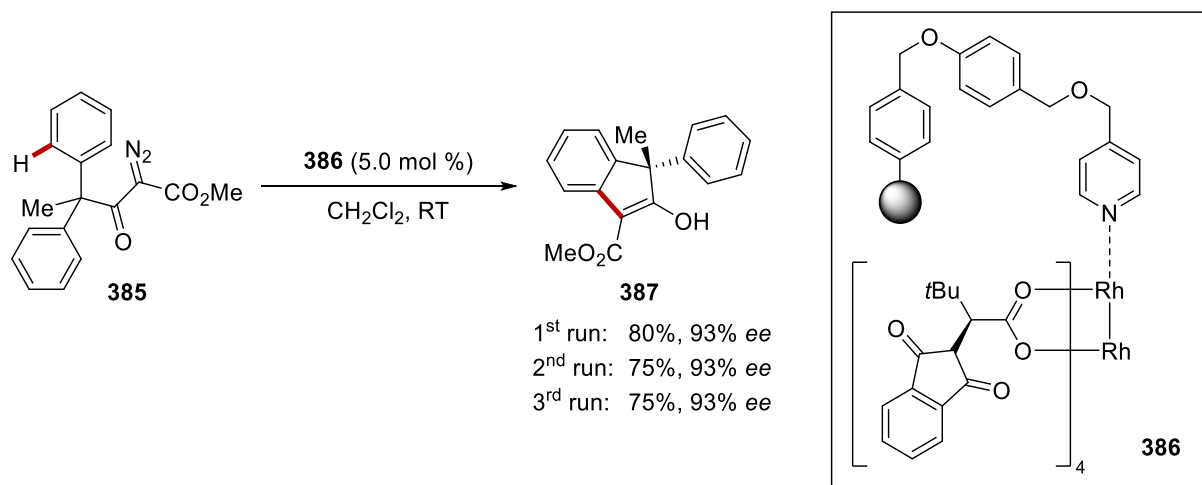
In 2017, Ackermann developed heterogeneous ruthenium-catalyzed *meta*-C–H bromination of purines **154** (Scheme 1.6.5).<sup>[98c]</sup> In this study, the silica-based heterogeneous ruthenium catalyst was highly recyclable without a significant loss of reactivity and selectivity, while a broad range of functional groups was tolerated, which set the stage of direct fluorescent labeling of purines.



**Scheme 1.6.5** Heterogeneous ruthenium-catalyzed *meta*-C–H brominations.

Despite indisputable advances in heterogeneous catalysis for C–H activation, it remains a critical concern that such catalysis is restricted by the surface area of the supported catalyst due to the physical limitation of active site. To overcome this disadvantage, researchers devised a new concept – hybrid catalysts cooperating inorganic materials and homogeneous catalysts – expecting to have a designable and tailorable heterogeneous catalyst while being recyclable and reusable.<sup>[204]</sup>

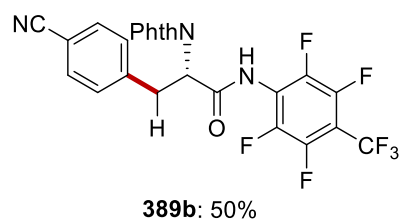
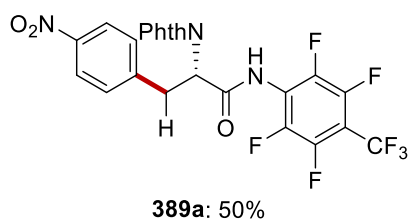
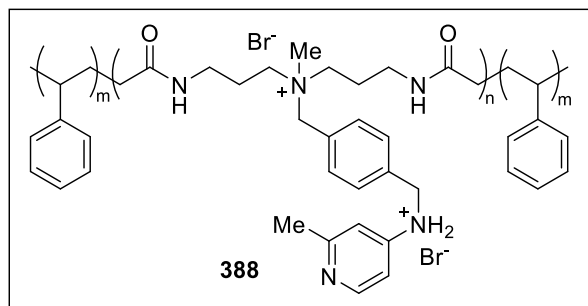
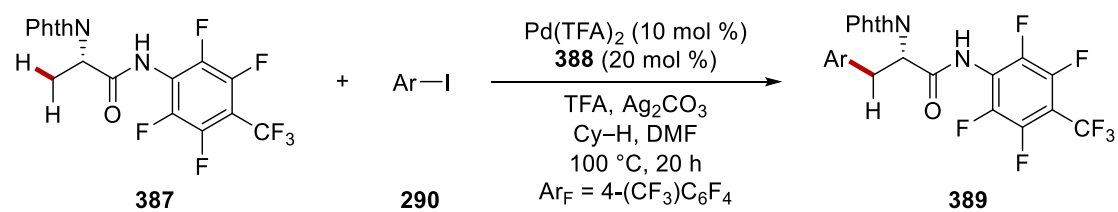
In 2005, Davies reported a strategy for the immobilization of chiral dirhodium(II) catalysts (Scheme 1.6.6).<sup>[205]</sup> In this study, various dirhodium catalysts were anchored to pyridine-containing resin by a simple preparation, which was directly employed for C–H arylation reactions in a reusable manner.



**Scheme 1.6.6** Hybrid rhodium catalyst for enantioselective C–H arylation.

Thereafter, Jones and Davies developed silica-based hybrid dirhodium(II) catalyst for  $\text{C}(\text{sp}^3)\text{--H}$  functionalizations.<sup>[206]</sup> In contrast to the previous report,<sup>[207]</sup> this study described covalent anchoring approach, enabling to have a more stable hybrid rhodium catalyst. Later, this reaction manifold was further extended to introduce a continuous flow technique, in which the dirhodium complexes were immobilized inside of a hollow fiber flow reactor, thus providing potential scalability and sustainability.<sup>[208]</sup>

In 2016, Jones and Yu reported polymer-supported hybrid palladium catalyst for  $\text{C}(\text{sp}^3)\text{--H}$  arylations (Scheme 1.6.7).<sup>[209]</sup> While ample substrates scope with a wide range of functional group tolerance was described, the hybrid palladium catalyst was efficiently reusable only up to the two times.

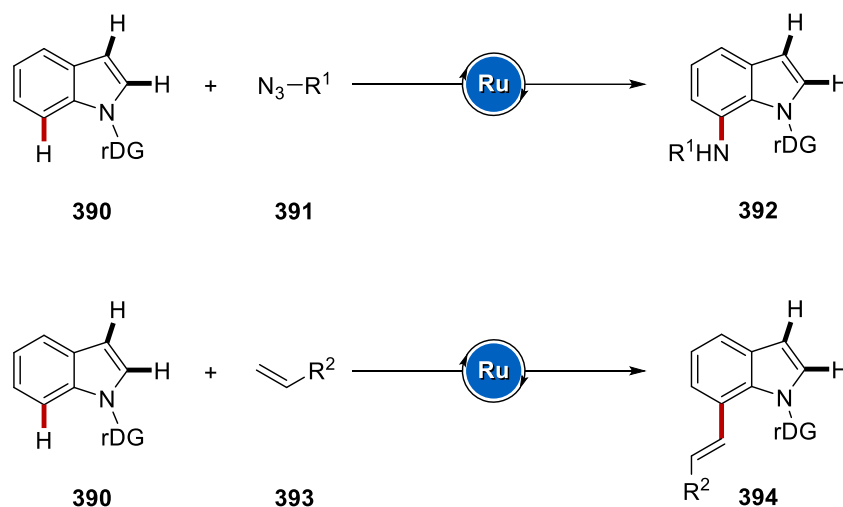


**Scheme 1.6.7** Hybrid palladium-catalyzed C(sp<sup>3</sup>)-H arylation.

## 2. Objectives

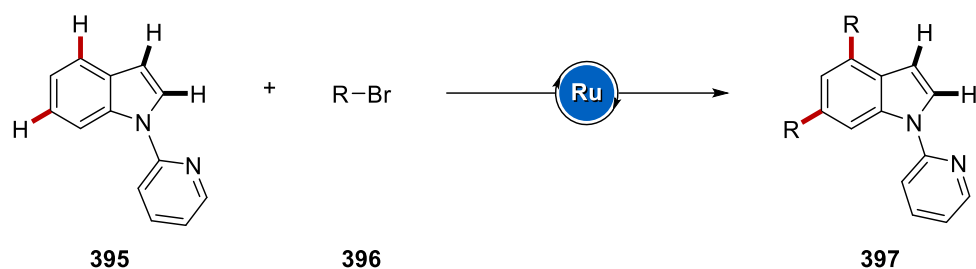
Transition metal-catalyzed C–H activations have emerged as a robust toolbox for synthetic chemistry.<sup>[18b, 18i, 18j]</sup> The development of new synthetic pathways and approaches is in high demand. In this regard, Ackermann and coworkers have presented remarkable achievements during the last two decades,<sup>[210a, 72d, 113c, 20a, 210b, 210c]</sup> which have focused on the development of new and sustainable catalysis in a wide range of metals. Thus, the objective of this thesis was to aim at the development of cost-effective and environmentally-sound homogeneous and recyclable hybrid metal-catalyzed C–H activations, along with mechanistic understandings and characterizations.

Indole benzenoid functionalizations have recently gained major attention from organic chemists, since such methods enable access biologically active molecules. For this reason, we became interested in exploring ruthenium-catalyzed C7–H indole amidations and alkenylations with the aid of a removable directing group under mild reaction conditions (Scheme 2.1.1).<sup>[211]</sup>



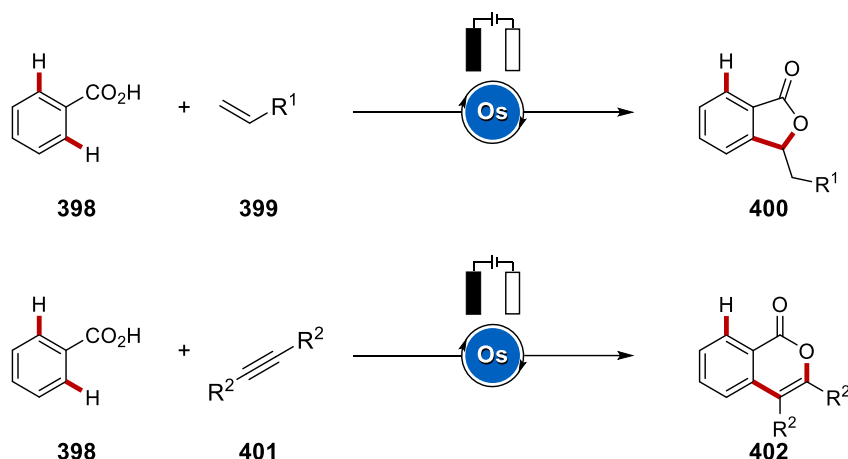
**Scheme 2.1.1** Ruthenium-catalyzed C7–H indole amidation and alkenylation.

Beyond thus developed C7–H indole activations, we also sought for a general synthetic pathway to functionalize other bonds of the indole motif. Thus, inspired by great progress in ruthenium-catalyzed distal C–H functionalization by Ackermann and coworkers, we developed site-selective dual C4–H/C6–H alkylations of indoles (Scheme 2.1.2).<sup>[212]</sup>



**Scheme 2.1.2** Ruthenium-catalyzed C4-H/C6-H dual alkylations.

While ruthenium and iron among group 8 metals have been extensively studied for C-H activation, osmium-catalyzed C-H activation is under developed. Motivated by the recent trend of electrochemical methods for C-H activation, which has been mainly developed by Ackermann and coworkers, we became interested in electrochemical osmium-catalyzed C-H activation (Scheme 2.1.3). Thereby, osmium catalyst enabled [4+1] and [4+2] annulations under electrooxidative conditions.

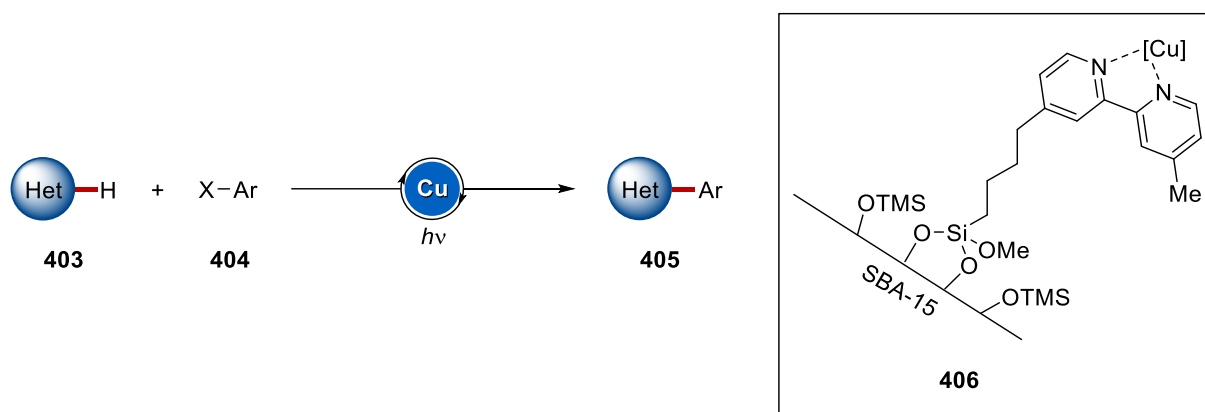


**Scheme 2.1.3** Osmium-catalyzed electrooxidative C-H activation.

Despite enormous advances in homogeneous catalysis for C-H activation, recyclable heterogeneous catalysis has emerged as a powerful tool to improve sustainability. Particularly, the combination of organic ligands immobilized onto inorganic support, namely hybrid catalyst, enabled to tune the heterogeneous catalyst and simultaneously provide recyclability. In this regard, we became intrigued to develop hybrid metal-catalyzed C-H activation.

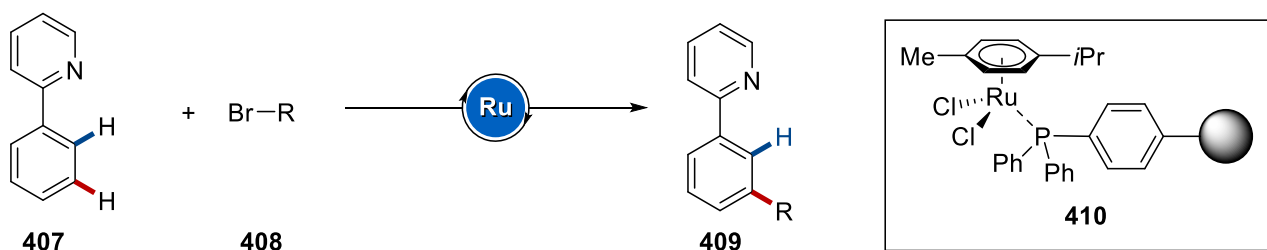


On the basis of Ackermann's report in 2016,<sup>[169]</sup> we developed recyclable hybrid copper catalyst for photo-induced C–H arylation (Scheme 2.1.4).<sup>[213]</sup> The SBA-15 silica-based hybrid copper catalyst enabled a wide range of arylations of heterocycles under exceedingly mild conditions at room temperature and was reusable at least up to five times.



**Scheme 2.1.4** Recyclable hybrid copper-catalyzed C–H arylation.

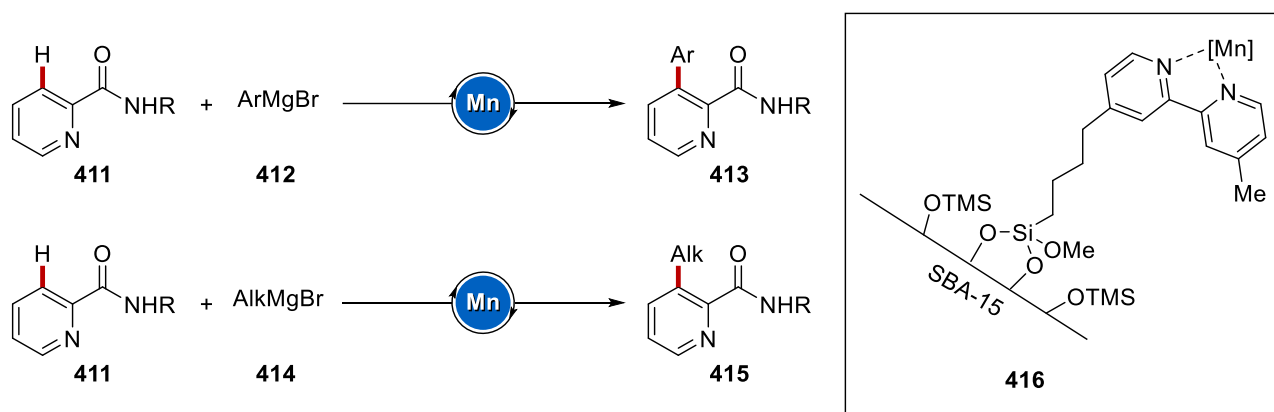
Based on the concept of hybrid catalysis, we envisaged site-selective C–H activation with hybrid metal catalysts. Especially, Ackermann and coworkers have recently presented numerous studies about ruthenium-catalyzed *meta*-C–H functionalization with the aid of phosphine ligand as a key component for the reaction. Thus, we introduced phosphine-based polymers to immobilize ruthenium(II) catalyst, enabling distal C–H functionalizations (Scheme 2.1.5).<sup>[214]</sup>



**Scheme 2.1.5** Recyclable ruthenium-catalyzed *meta*-C–H alkylation.

During the past decades, the activation of inert C–H bonds has been predominantly made with the aid of noble 4d and 5d transition metals.<sup>[215a-c, 210b, 215d]</sup> In sharp contrast, the introduction of Earth-abundant 3d metal catalysts, particularly manganese, allows for sustainable and cost-effective C–H

activations.<sup>[216]</sup> Here, we envisioned adding the value of heterogeneity to manganese catalysis. Thus, we developed a hybrid manganese catalyst, providing C–H arylation and C–H alkylation in a reusable manner (Scheme 2.1.6).

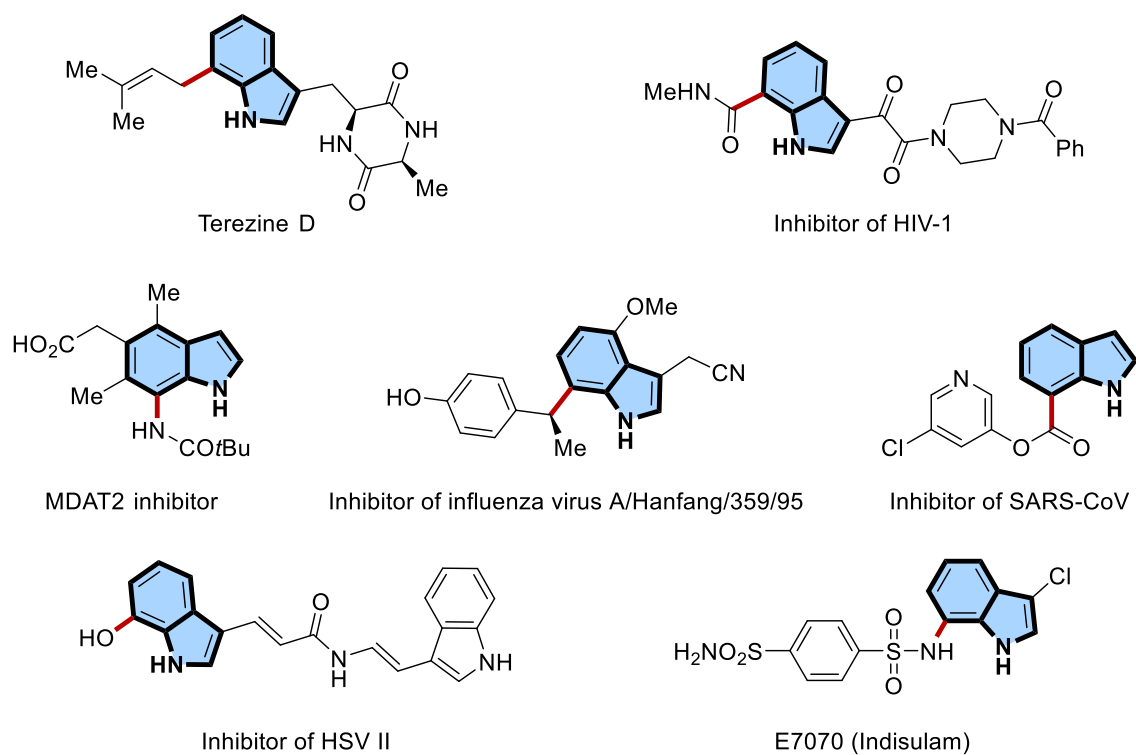


**Scheme 2.1.6** Hybrid manganese-catalyzed C–H arylation and alkylation.

### 3. Results and Discussion

#### 3.1 Ruthenium(II)-Catalyzed C7-H Amidations and Alkenylations of Indoles

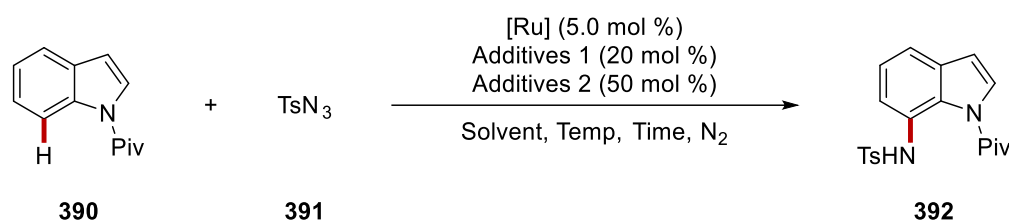
Substituted indoles<sup>[217]</sup> are a key structural motif in a plethora of important bio-relevant compounds, drugs, and pharmaceuticals (Scheme 3.1.1).<sup>[218]</sup> Since the precise synthesis of structural complex indoles having substituent groups in a specific position is often challenging, various researches have tested site-selective indole functionalizations. While C2- or C3-selective functionalizations have been widely established,<sup>[219]</sup> C7-manifolds,<sup>[220]</sup> particularly by ruthenium catalysis, have thus far remained elusive.



**Scheme 3.1.1** Bioactive C7-functionalized indoles.

### 3.1.1 Optimization Studies

The C7–H functionalization of indole **392** was envisaged with the aid of pivaloyl directing group (Table 3.1.1). In this context, organic azide **391** was used as the amidating reagent for ruthenium(II) catalysis. Particularly, the use of a ruthenium catalyst together with metal acetate and silver salts was expected to *in-situ* generate a cationic ruthenium(II)-carboxylate. Also, *N*-pivaloyl orienting group was expected to enable the formation of a six-membered ruthenacycle. The optimization studies were commenced by testing solvents. While various reaction mediums, including ethereal (entries 1–2) and alcoholic solvents (entries 3–4) as well as other solvents (entries 5–12) were attempted. Unfortunately, the desired product was not detected. Only when DCE, DCM, or TFE were used as the solvent, the C7–H amidated product **392** was formed (entries 13–15). It is noteworthy that the nitrogenated product was selectively formed at the C7–H position as the sole product, while the C2–H bond remained unmodified. Next, the effect of the reaction temperature was explored. Interestingly, while the decrease in the temperature to 40 °C provided an increase in the yield, temperature lower than 40 °C were not beneficial (entries 16–19). Bases fell short in providing the desired product in a high yield (entries 20–22). Although the use of AgNTf<sub>2</sub> showed comparable results (entry 23), AgSbF<sub>6</sub> was chosen for the issue of cost. The employment of Ru(OAc)<sub>2</sub>(*p*-cymene)<sub>2</sub> allowed to avoid additional acetate sources (entry 24), not only highlighting the importance of the ruthenium(II)biscarboxylate catalysis regime. While prolonged reaction time provided increased C7–H amidated indole production (entry 25), elevated temperature gave unsatisfactory results (entry 26).

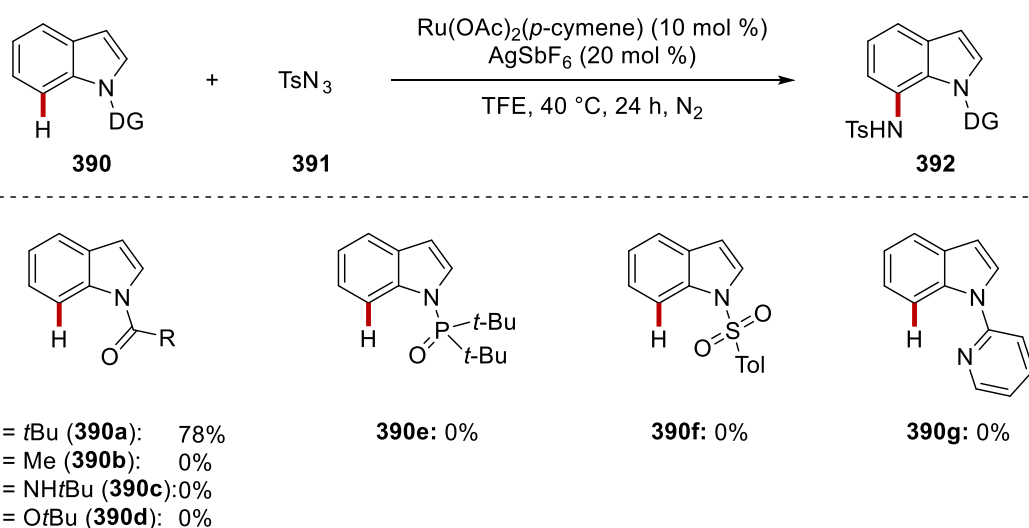
**Table 3.1.1** Optimization of the ruthenium(II)-catalyzed C7–H amidation<sup>[a]</sup>

| Entry | [Ru]                                                 | Additive<br>1      | Additive<br>2 | Solvent           | Temp<br>(°C) | Time<br>(h) | Yield<br>(%) |
|-------|------------------------------------------------------|--------------------|---------------|-------------------|--------------|-------------|--------------|
| 1     | [RuCl <sub>2</sub> ( <i>p</i> -cymene)] <sub>2</sub> | AgSbF <sub>6</sub> | AgOAc         | 1,4-dioxane       | 60           | 16          | NR           |
| 2     | [RuCl <sub>2</sub> ( <i>p</i> -cymene)] <sub>2</sub> | AgSbF <sub>6</sub> | AgOAc         | DME               | 60           | 16          | NR           |
| 3     | [RuCl <sub>2</sub> ( <i>p</i> -cymene)] <sub>2</sub> | AgSbF <sub>6</sub> | AgOAc         | MeOH              | 60           | 16          | NR           |
| 4     | [RuCl <sub>2</sub> ( <i>p</i> -cymene)] <sub>2</sub> | AgSbF <sub>6</sub> | AgOAc         | <i>t</i> AmOH     | 60           | 16          | NR           |
| 5     | [RuCl <sub>2</sub> ( <i>p</i> -cymene)] <sub>2</sub> | AgSbF <sub>6</sub> | AgOAc         | <i>o</i> -xylene  | 60           | 16          | NR           |
| 6     | [RuCl <sub>2</sub> ( <i>p</i> -cymene)] <sub>2</sub> | AgSbF <sub>6</sub> | AgOAc         | NMP               | 60           | 16          | NR           |
| 7     | [RuCl <sub>2</sub> ( <i>p</i> -cymene)] <sub>2</sub> | AgSbF <sub>6</sub> | AgOAc         | DMA               | 60           | 16          | NR           |
| 8     | [RuCl <sub>2</sub> ( <i>p</i> -cymene)] <sub>2</sub> | AgSbF <sub>6</sub> | AgOAc         | DMF               | 60           | 16          | NR           |
| 9     | [RuCl <sub>2</sub> ( <i>p</i> -cymene)] <sub>2</sub> | AgSbF <sub>6</sub> | AgOAc         | DMSO              | 60           | 16          | NR           |
| 10    | [RuCl <sub>2</sub> ( <i>p</i> -cymene)] <sub>2</sub> | AgSbF <sub>6</sub> | AgOAc         | MeCN              | 60           | 16          | NR           |
| 11    | [RuCl <sub>2</sub> ( <i>p</i> -cymene)] <sub>2</sub> | AgSbF <sub>6</sub> | AgOAc         | CHCl <sub>3</sub> | 60           | 16          | NR           |
| 12    | [RuCl <sub>2</sub> ( <i>p</i> -cymene)] <sub>2</sub> | AgSbF <sub>6</sub> | AgOAc         | CCl <sub>4</sub>  | 60           | 16          | NR           |
| 13    | [RuCl <sub>2</sub> ( <i>p</i> -cymene)] <sub>2</sub> | AgSbF <sub>6</sub> | AgOAc         | DCE               | 60           | 16          | 25           |
| 14    | [RuCl <sub>2</sub> ( <i>p</i> -cymene)] <sub>2</sub> | AgSbF <sub>6</sub> | AgOAc         | DCM               | 60           | 16          | 42           |
| 15    | [RuCl <sub>2</sub> ( <i>p</i> -cymene)] <sub>2</sub> | AgSbF <sub>6</sub> | AgOAc         | TFE               | 60           | 16          | 41           |
| 16    | [RuCl <sub>2</sub> ( <i>p</i> -cymene)] <sub>2</sub> | AgSbF <sub>6</sub> | AgOAc         | TFE               | 50           | 16          | 52           |
| 17    | [RuCl <sub>2</sub> ( <i>p</i> -cymene)] <sub>2</sub> | AgSbF <sub>6</sub> | AgOAc         | TFE               | 40           | 16          | 60           |
| 18    | [RuCl <sub>2</sub> ( <i>p</i> -cymene)] <sub>2</sub> | AgSbF <sub>6</sub> | AgOAc         | TFE               | 30           | 16          | 54           |
| 19    | [RuCl <sub>2</sub> ( <i>p</i> -cymene)] <sub>2</sub> | AgSbF <sub>6</sub> | AgOAc         | TFE               | 25           | 16          | 32           |
| 20    | [RuCl <sub>2</sub> ( <i>p</i> -cymene)] <sub>2</sub> | AgSbF <sub>6</sub> | CsOAc         | TFE               | 40           | 16          | trace        |
| 21    | [RuCl <sub>2</sub> ( <i>p</i> -cymene)] <sub>2</sub> | AgSbF <sub>6</sub> | LiOAc         | TFE               | 40           | 16          | 32           |

|                         |                                                      |                                   |           |            |           |           |           |
|-------------------------|------------------------------------------------------|-----------------------------------|-----------|------------|-----------|-----------|-----------|
| 22                      | [RuCl <sub>2</sub> ( <i>p</i> -cymene)] <sub>2</sub> | AgSbF <sub>6</sub>                | AgOTFA    | TFE        | 40        | 16        | NR        |
| 23                      | [RuCl <sub>2</sub> ( <i>p</i> -cymene)] <sub>2</sub> | AgNTf <sub>2</sub> <sup>[c]</sup> | AgOAc     | TFE        | 40        | 16        | 63        |
| 24 <sup>[b]</sup>       | Ru(OAc) <sub>2</sub> ( <i>p</i> -cymene)             | AgSbF <sub>6</sub>                | --        | TFE        | 40        | 16        | 64        |
| <b>25<sup>[b]</sup></b> | <b>Ru(OAc)<sub>2</sub>(<i>p</i>-cymene)</b>          | <b>AgSbF<sub>6</sub></b>          | <b>--</b> | <b>TFE</b> | <b>40</b> | <b>24</b> | <b>78</b> |
| 26 <sup>[b]</sup>       | Ru(OAc) <sub>2</sub> ( <i>p</i> -cymene)             | AgSbF <sub>6</sub>                | --        | TFE        | 60        | 24        | 48        |

<sup>[a]</sup> Reaction condition: **390** (0.25 mmol), **391** (0.75 mmol), [Ru] (5.0 mol %), additive 1 (20 mol %), additive 2 (50 mol %), solvent (1.0 mL), isolated yield. <sup>[b]</sup> [Ru] (10 mol %). <sup>[c]</sup> Price comparison (in Sigma-Aldrich): AgSbF<sub>6</sub>: \$60.10/5g, AgNTf<sub>2</sub>: \$476.00/5g.

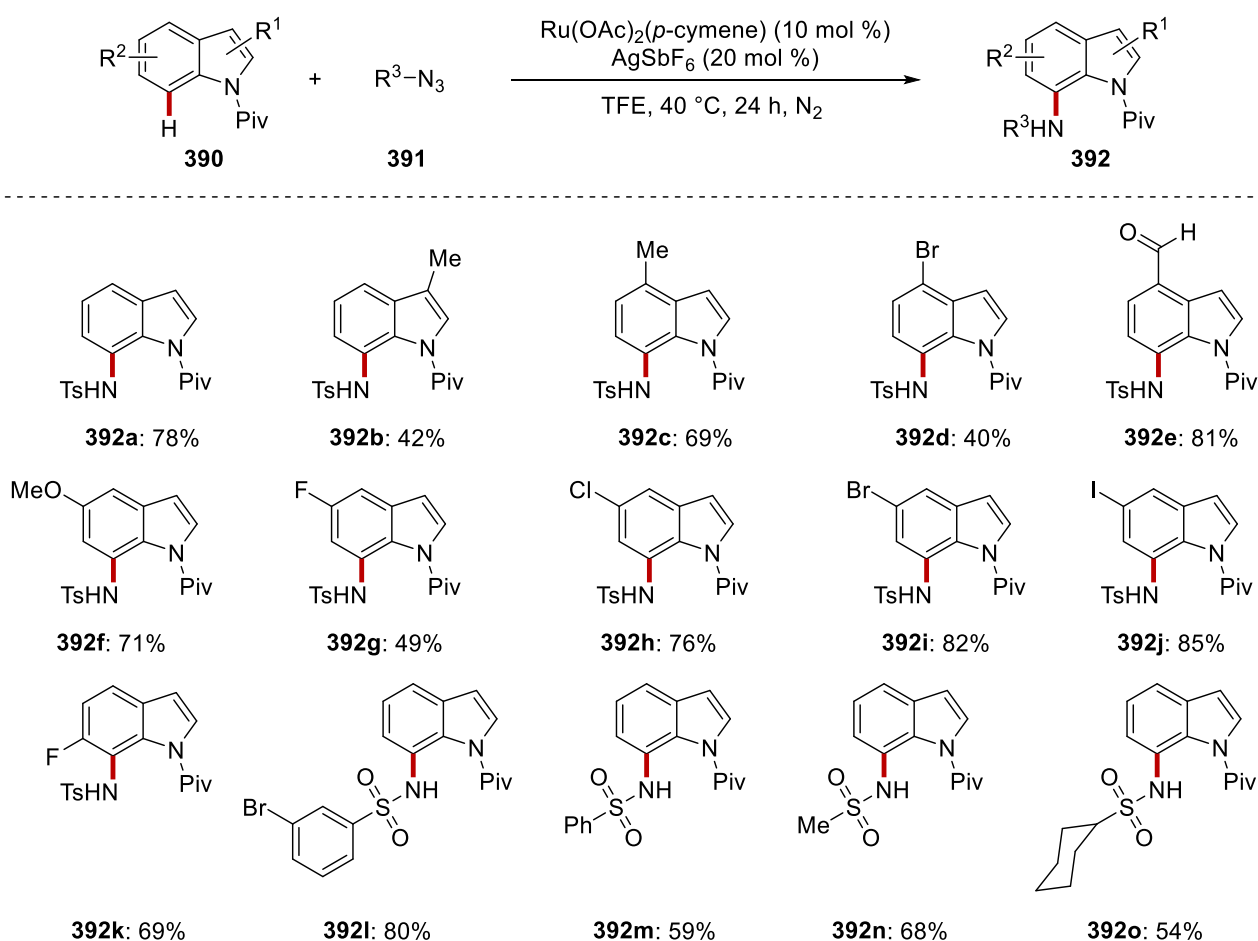
Thereafter, the indole *N*-substituent pattern was examined, and a variety of ketones, amide, ester, phosphine oxide, sulfone, and pyridine were explored (Scheme 3.1.2). Interestingly, only the *N*-pivaloyl indole **390** provided the C7–H amidation product, illustrating the importance of steric and electronic effects of the *N*-substituent for enabling the indole C7–H activation.



**Scheme 3.1.2** Examination of *N*-substitution pattern.

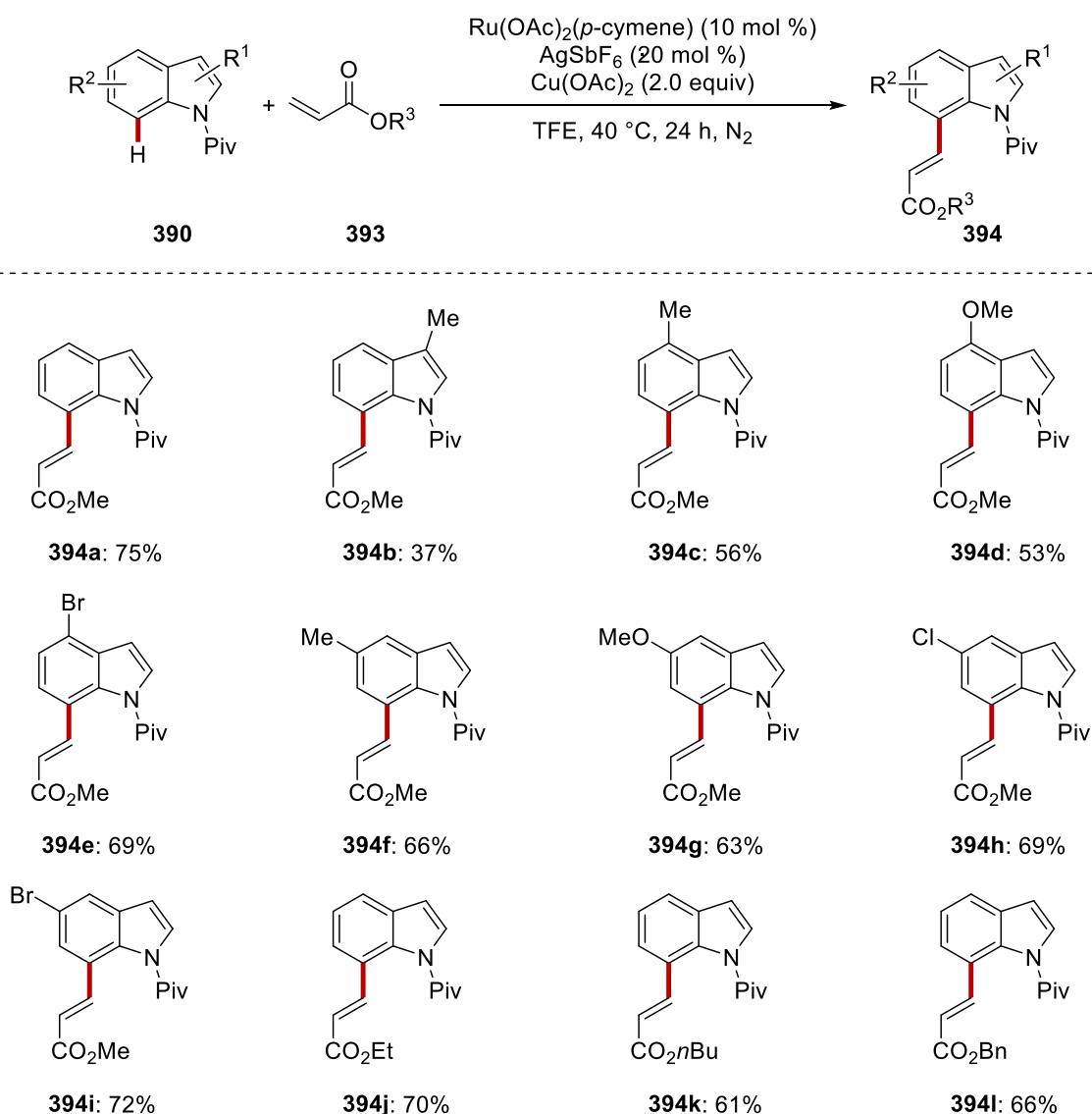
### 3.1.2 Substrate Scope

With the optimized reaction conditions in hand, the scope of the C7–H functionalization was explored with various indoles **390** and organic azides **391** (Scheme 3.1.3). Differently substituted indoles **390** bearing alkyl and alkoxy groups at the C3-, C4-, C5-, and C6-position were site-selectively transformed into the desired C7–H nitrogenated products. It is noteworthy that indole **390e** having labile aldehyde group was efficiently transformed to the desired product **392e** and synthetically valuable halogen functional groups were tolerated under the optimized reaction conditions (**392d**, **392g–392k**). The ruthenium(II)biscarboxylate-catalyzed C7–H activation also tolerated various azides bearing arenesulfonyl (**392l–392m**) and alkanesulfonyl groups (**392n–392o**).



**Scheme 3.1.3** Scope of ruthenium-catalyzed C7–N formation of indoles **390**.

The robustness of the ruthenium(II)-catalyzed C7–H activation was further reflected by the C7–H alkenylation of *N*-pivaloyl indoles **390** with acrylates **393** through a redox process (Scheme 3.1.4). Thus, the site-selective alkenylated products **394** were efficiently obtained under slightly modified reaction conditions using copper(II) acetate as the oxidant. A variety of substituted indoles **390** bearing alkyl or halogen groups and different acrylates **393** were fully tolerated, thus efficiently giving into the desired indole-7-alkenyl derivatives **394** with excellent site-selectivity.

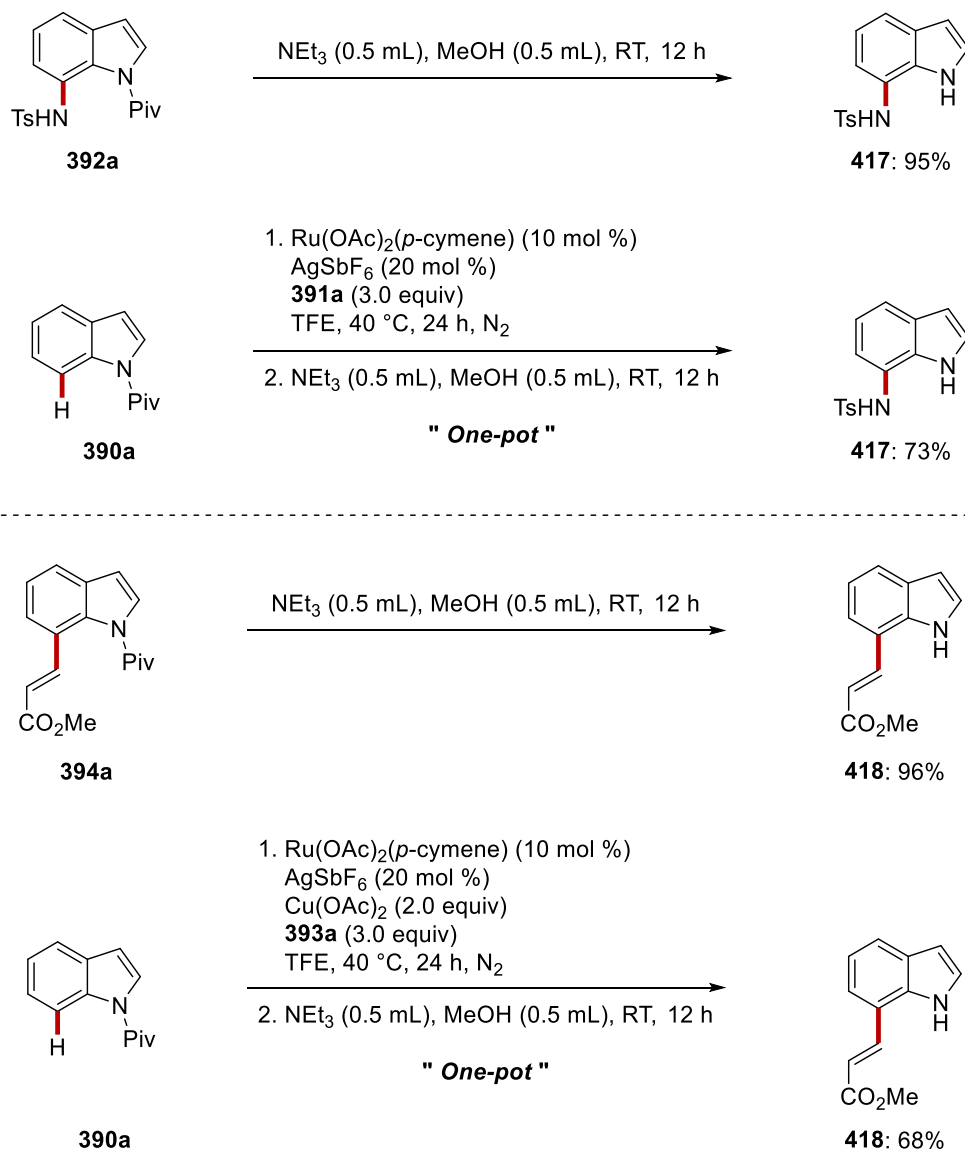


**Scheme 3.1.4** Scope of ruthenium-catalyzed C7–C bond formation of indoles **390**.



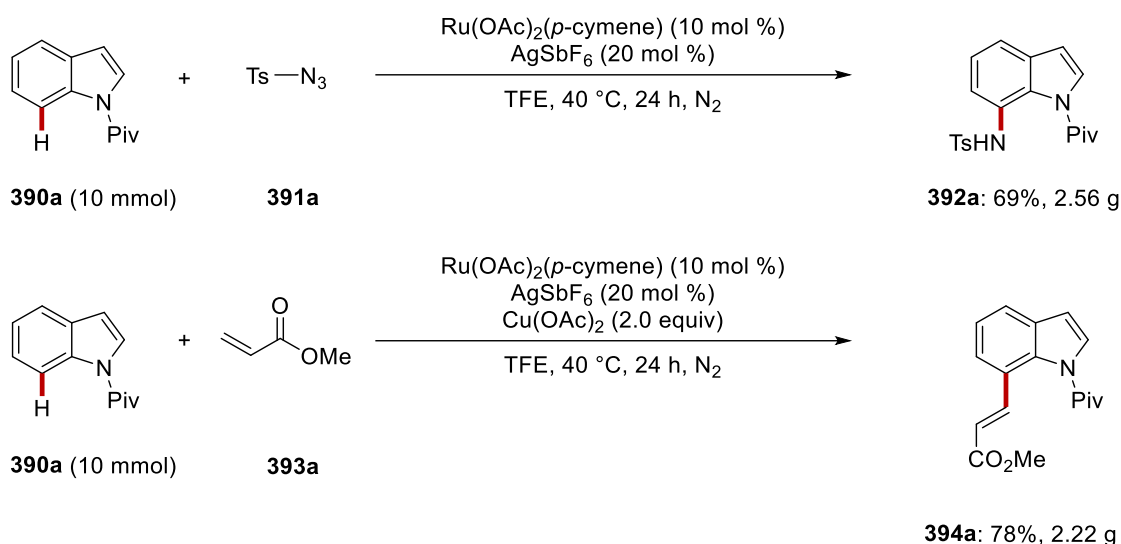
### 3.1.3 Investigations of Practical Utility

The traceless removal of the *N*-pivaloyl motif was performed to showcase the practical utility into the established carboxylate-assisted ruthenium(II)-catalyzed C7–H activation (Scheme 3.1.5). Thus, the pivaloyl orienting group was readily removed at room temperature. It is noteworthy that the traceless removal of *N*-pivaloyl directing group could also sequentially be carried out in a one-pot strategy.



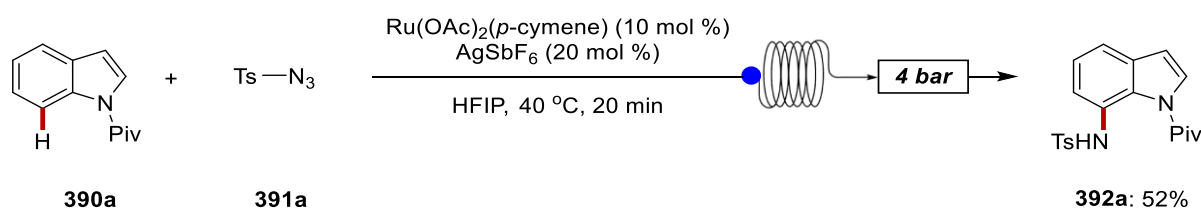
**Scheme 3.1.5** The traceless removal of *N*-pivaloyl orienting group and a one-pot process.

Additionally, the ruthenium(II)-catalyzed C7–H amidation and alkenylation could be easily conducted on a gram scale without significant loss of catalytic efficacy, thereby highlighting the robustness of the ruthenium(II)biscarboxylate catalysis (Scheme 3.1.6).



**Scheme 3.1.6** Gram-scale C7–H indole activations.

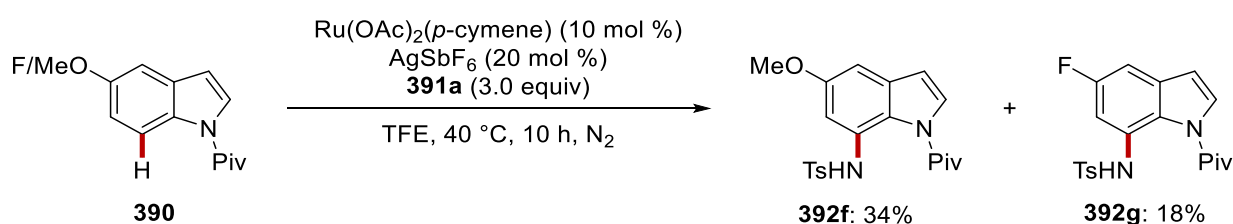
Flow technology provides organic chemists with tremendous benefits, including an improved heat and mass transfer, reaction safeness, and scalability.<sup>[221]</sup> The C7–H activation of indoles was indeed demonstrated in a flow set-up, giving the desired amidated product **392** without loss of efficiency and selectivity at shortened reaction time (Scheme 3.1.7).



**Scheme 3.1.7** Scalable flow reaction for C7–H amidation of indole.

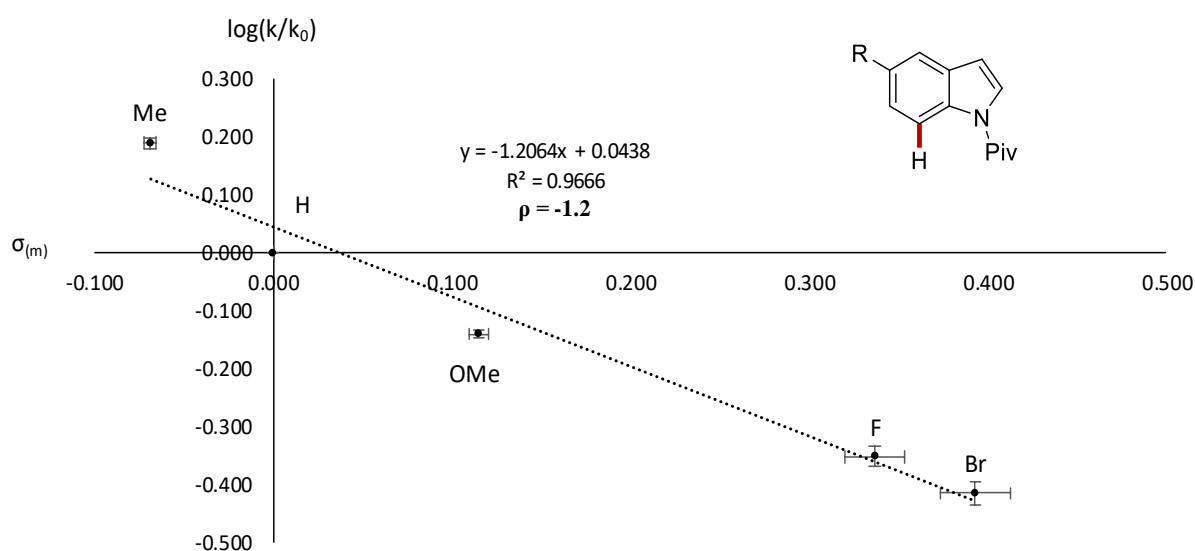
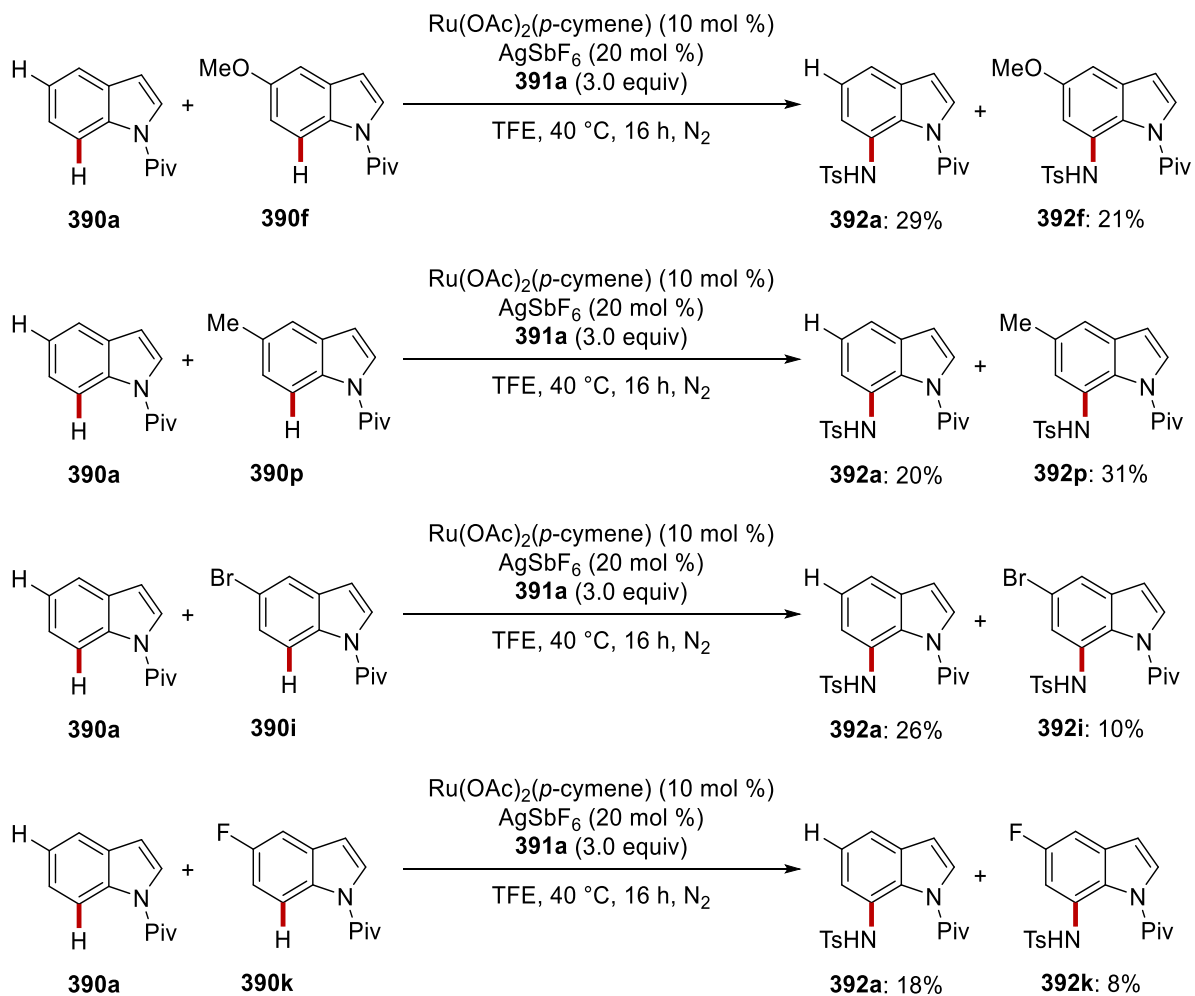
### 3.1.4 Mechanistic Studies

Given the unique robustness, broad applicability, and synthetic utility of the unprecedented carboxylate-assisted ruthenium(II)-catalyzed C7–H activation, we became interested in delineating its mode of action. To this end, intermolecular competition experiments with differently substituted *N*-pivaloyl indoles **390** were conducted (Scheme 3.1.8). Thus, electron-rich substrate possessed an inherent higher reactivity, proposing that a concerted metalation deprotonation (CMD) less likely, while providing support for a base-assisted internal electrophile-type substitution (BIES) manifold.<sup>[23]</sup>



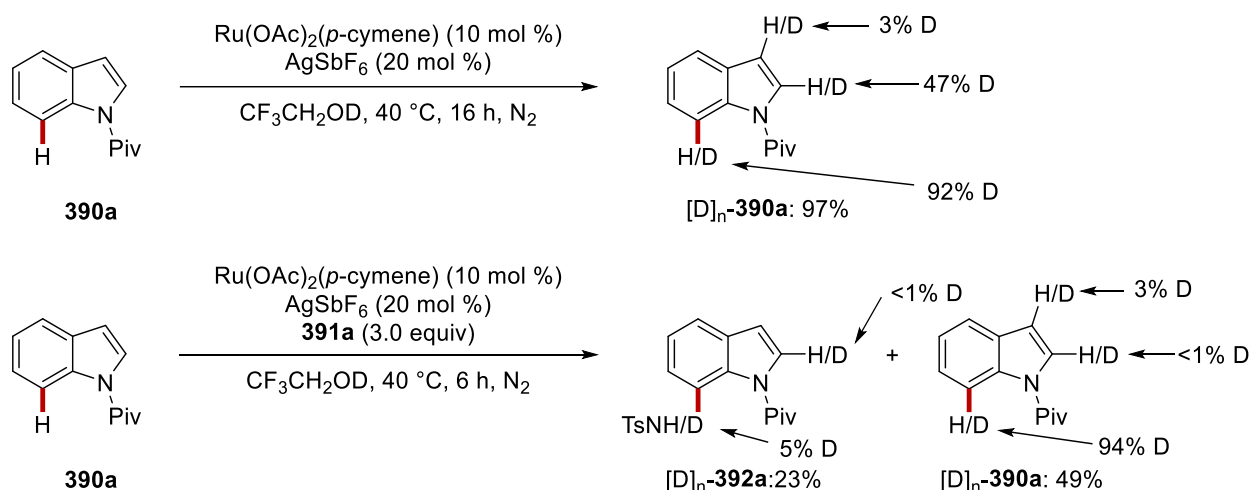
**Scheme 3.1.8** Competition experiment.

The Hammett equation exhibits a linear free-energy relationship between two reactions that only differ in the substituents. Thus, a substituent constant and the reaction constant become the parameter of the x and the y axis, respectively, which enables to derive the  $\rho$  value. Here, a Hammett correlation was found in electronically different substrates which have a substituent in *meta*-position to the reaction center where C–H bond cleavage occurs, showing that electrophilic mechanism might occur in the C–H scission step (Scheme 3.1.9).



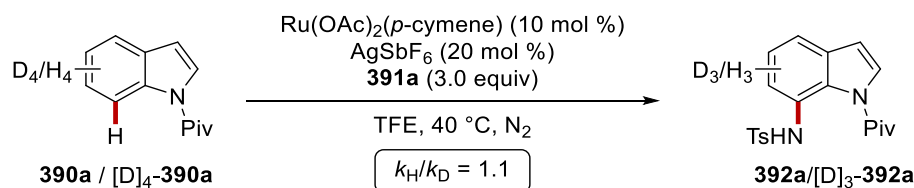
Scheme 3.1.9 Independent reactions for Hammett plot analysis.

Furthermore, we performed the C7–H activation in the presence of isotopically labeled TFE (Scheme 3.1.10). H/D-scrambling in the C7- and C2-position was observed in the absence of substrate **391a**, indicating the reversible nature of the C–H bond cleavage event. Also, a H/D exchange experiment in the presence of **391a** provided evidence for a facile C–H cleavage.



**Scheme 3.1.10** H/D exchange studies.

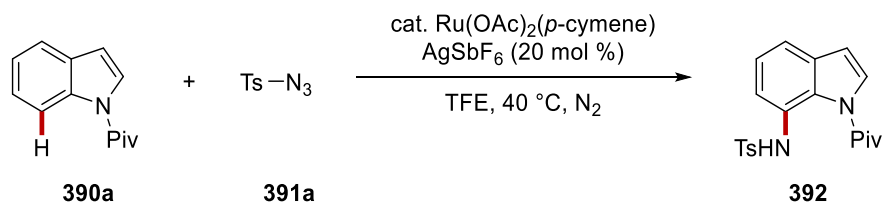
Subsequently, independent reactions performed with substrate **390a** and isotopically labeled compound **[D]<sub>4</sub>-390a** showed a primary kinetic isotope effect (KIE) of  $k_{\text{H}}/k_{\text{D}} \approx 1.1$ , giving a support for a fast C7–H scission (Scheme 3.1.11).



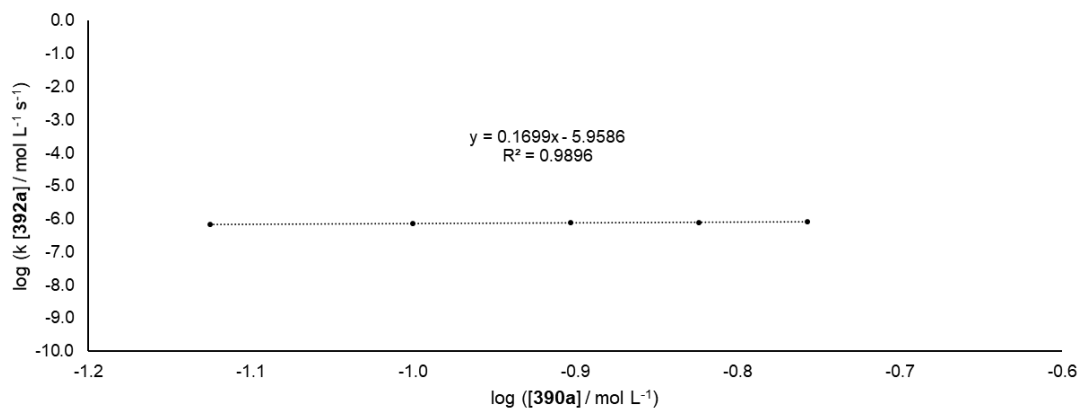
**Scheme 3.1.11** KIE study.

In good agreement with this finding, detailed kinetic experiments unraveled a zero-order dependence of the reaction rate on the *N*-pivaloyl indole **390a**, while a first-order dependence was observed for the concentration of the tosyl azide **391a** as well as the catalyst  $\text{Ru(OAc)}_2(\textit{p}\text{-cymene)}$  (Scheme 3.1.12).

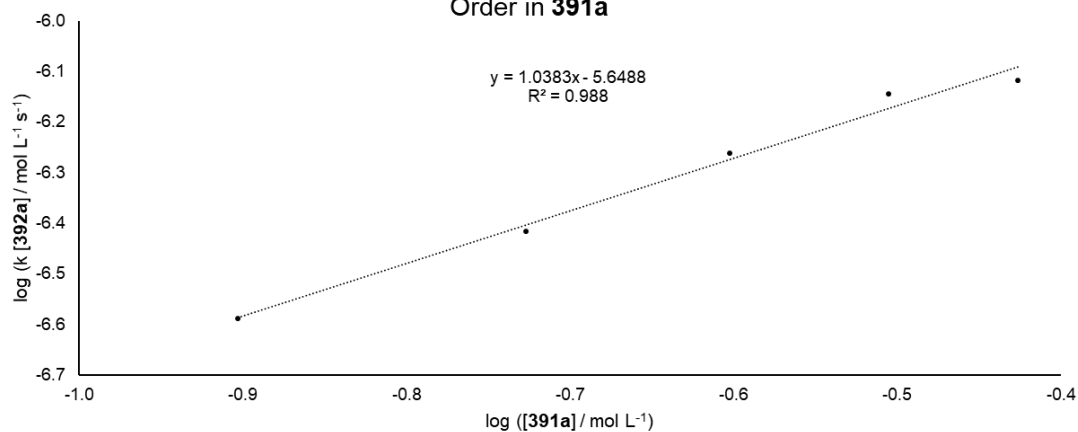
## Results and Discussion



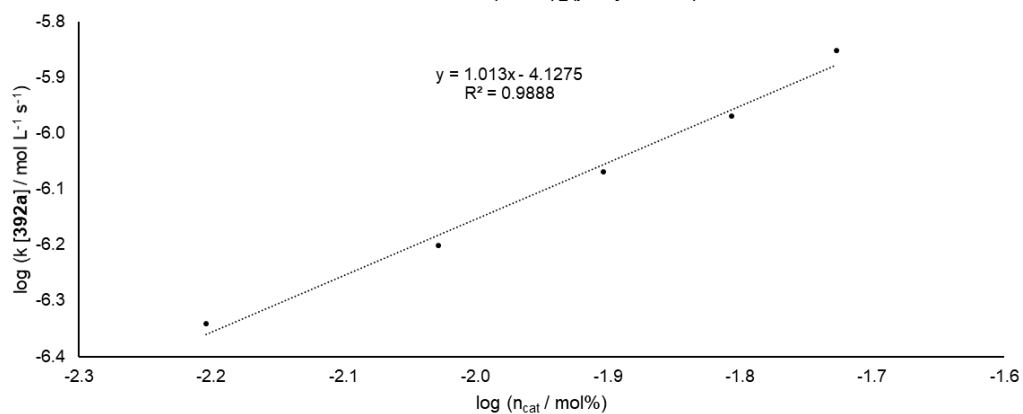
Order in **390a**



Order in **391a**



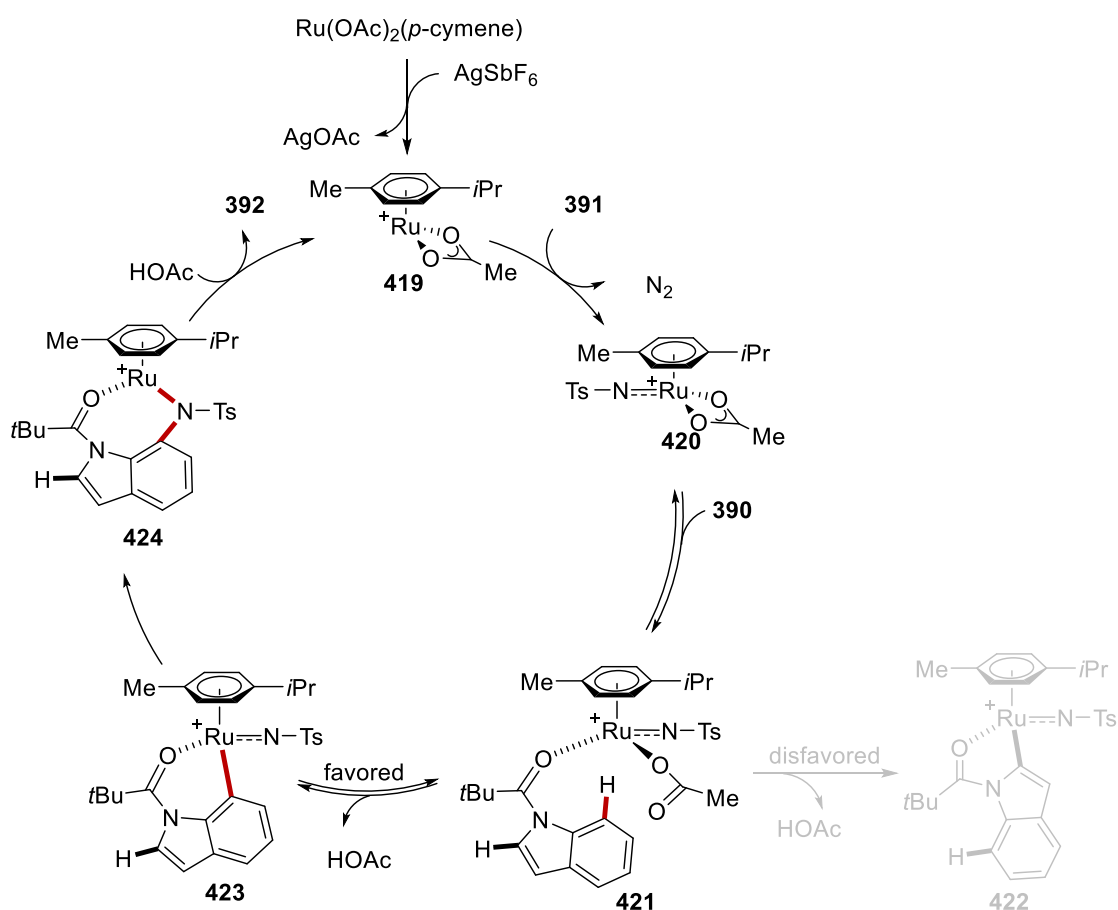
Order in  $\text{Ru(OAc)}_2(\textit{p-cymene})$



**Scheme 3.1.12** Detailed kinetic experiments.

### 3.1.5 Proposed Catalytic Cycle

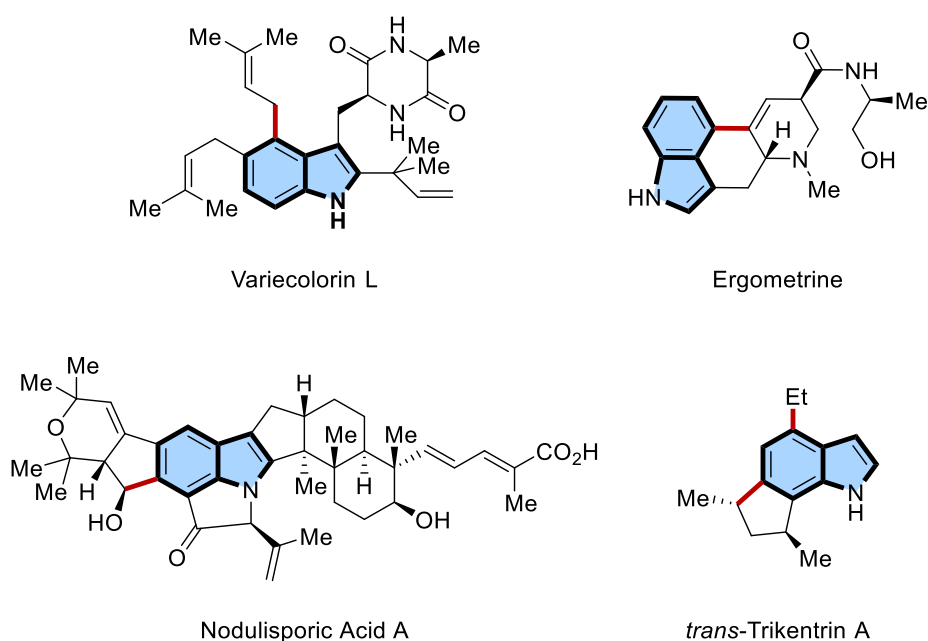
On the basis of our detailed experimental mechanistic studies, a plausible catalytic cycle for the carboxylate-assisted ruthenium(II)-catalyzed C7–H indole activation is proposed in Scheme 3.1.13. The mechanism rationale commences with the coordination of substrate **391a** to the active ruthenium catalyst **419** to form ruthenium amide intermediate **420**, which previously has been often described as the latter step after C–H activation. C–H activation occurs through a BIES mechanism, preferentially leading to ruthenium(II) species **423** rather than **422**. The intermediate **423** is transformed to ruthenium(II) amido intermediate **424** via amido insertion. Finally, a proto-demetalation affords product **392** and regenerates the active catalyst **419**.



**Scheme 3.1.13** Proposed catalytic cycle.

### 3.2 Ruthenium(II)-Catalyzed C4/C6–H Dual Alkylations of Indoles

The C2–H and C3–H bonds of indoles has been widely modified by both direct and directed C–H functionalization methods.<sup>[222, 219]</sup> In sharp contrast, site-selective C–H functionalization on the benzenoid ring has remained challenging. Particularly, C4–H or C6–H functionalized indole scaffolds exhibit noteworthy medical or agrochemical properties (Scheme 3.2.1).<sup>[223]</sup> As a consequence, there is a continued interest for general strategies providing easy access to C4/C6-substituted indoles in a sustainable fashion.



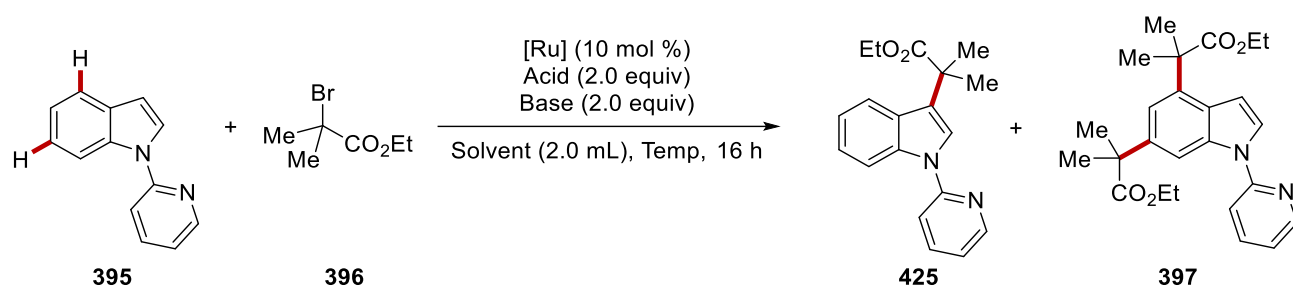
**Scheme 3.2.1** Bioactive compounds with C4/C6 functionalized indoles.

While different methods have provided access to C4 and C6-functionalized indoles by Prabhu,<sup>[224]</sup> Shi,<sup>[225]</sup> Yu,<sup>[226]</sup> and Baran<sup>[227]</sup> among others,<sup>[228]</sup> challenging dual functionalizations of C4– and C6–H bonds of indoles have thus far remained elusive.



### 3.2.1 Optimization Studies

At the outset, various reaction conditions were probed for the envisioned ruthenium(II)-catalyzed C4/C6-H alkylations of indole **395** with ethyl 2-bromoisobutyrate (**396**) (Table 3.2.1). In the initial studies with  $\text{RuCl}_2(\text{PPh}_3)(p\text{-cymene})$  as the catalyst, the C3-alkylated product **425** was formed as a by-product, likely obtained *via* electrophilic substitution (entry 1). While KOAc as the base was crucial to obtain a good conversion in the absence of acetic acid (entries 2–3), C3-alkylated product **425** was still observed. Thus, we focused our optimization towards reducing the formation of the C3-functionalized product **425**, while increasing the desired C4/C6-H alkylated product **397**. Although arene-ligand-free ruthenium complex  $\text{RuCl}_2(\text{PPh}_3)_3$  with different bases showed a poor reactivity (entries 4–6),  $\text{Ru}(\text{OAc})_2(\text{PPh}_3)_2$  demonstrated effective conversion to the desired product **397** (entry 7). Among various bases, such as acetates (entries 7–10), carbonate (entry 11), and phosphate (entry 12), NaOAc gave the most effective reactivity while reducing the formation of by-product **425** (entry 8). Furthermore, among a variety of solvents, DCE proved to be the most efficient for C4/C6-H alkylation (entries 13–16). Interestingly, as the reaction temperature was decreased, both the reactivity and the selectivity were significantly improved (entries 16–20). Although the arene-containing ruthenium catalyst was again probed under the optimized conditions, it afforded a less satisfactory result, highlighting the unique feature of arene-ligand-free ruthenium catalysis (entry 21).

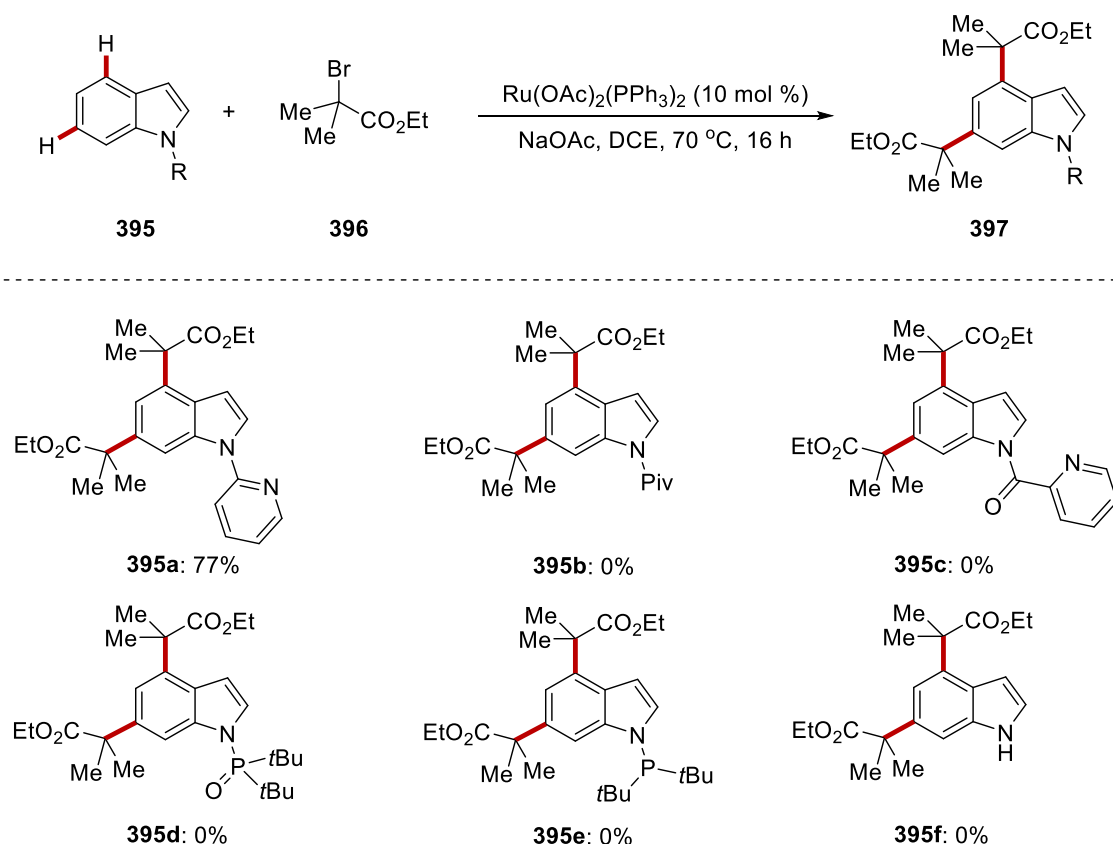
**Table 3.2.1** Optimization of the ruthenium(II)-catalyzed dual alkylation<sup>[a]</sup>

| Entry     | [Ru]                                                    | Acid | Base                           | Solvent           | Temp<br>(°C) | Yield (%)  |            |                |
|-----------|---------------------------------------------------------|------|--------------------------------|-------------------|--------------|------------|------------|----------------|
|           |                                                         |      |                                |                   |              | <b>395</b> | <b>425</b> | <b>397</b>     |
| 1         | RuCl <sub>2</sub> PPh <sub>3</sub> ( <i>p</i> -cymene)  | HOAc | KOAc                           | THF               | 120          | trace      | 19         | 58             |
| 2         | RuCl <sub>2</sub> PPh <sub>3</sub> ( <i>p</i> -cymene)  | --   | KOAc                           | THF               | 120          | 4          | 23         | 58             |
| 3         | RuCl <sub>2</sub> PPh <sub>3</sub> ( <i>p</i> -cymene)  | HOAc | --                             | THF               | 120          | 94         | 0          | 0              |
| 4         | RuCl <sub>2</sub> (PPh <sub>3</sub> ) <sub>3</sub>      | --   | KOAc                           | THF               | 120          | 82         | trace      | 5              |
| 5         | RuCl <sub>2</sub> (PPh <sub>3</sub> ) <sub>3</sub>      | --   | K <sub>2</sub> CO <sub>3</sub> | THF               | 120          | 76         | 2          | 14             |
| 6         | RuCl <sub>2</sub> (PPh <sub>3</sub> ) <sub>3</sub>      | --   | K <sub>3</sub> PO <sub>4</sub> | THF               | 120          | 70         | 3          | 15             |
| 7         | Ru(OAc) <sub>2</sub> (PPh <sub>3</sub> ) <sub>2</sub>   | --   | KOAc                           | THF               | 120          | 26         | 13         | 43             |
| 8         | Ru(OAc) <sub>2</sub> (PPh <sub>3</sub> ) <sub>2</sub>   | --   | NaOAc                          | THF               | 120          | 32         | 4          | 46             |
| 9         | Ru(OAc) <sub>2</sub> (PPh <sub>3</sub> ) <sub>2</sub>   | --   | LiOAc                          | THF               | 120          | 80         | trace      | 16             |
| 10        | Ru(OAc) <sub>2</sub> (PPh <sub>3</sub> ) <sub>2</sub>   | --   | CsOAc                          | THF               | 120          | 84         | 4          | 10             |
| 11        | Ru(OAc) <sub>2</sub> (PPh <sub>3</sub> ) <sub>2</sub>   | --   | K <sub>2</sub> CO <sub>3</sub> | THF               | 120          | 85         | 3          | trace          |
| 12        | Ru(OAc) <sub>2</sub> (PPh <sub>3</sub> ) <sub>2</sub>   | --   | K <sub>3</sub> PO <sub>4</sub> | THF               | 120          | 86         | trace      | trace          |
| 13        | Ru(OAc) <sub>2</sub> (PPh <sub>3</sub> ) <sub>2</sub>   | --   | NaOAc                          | 1,4-dioxane       | 120          | 8          | 33         | 53             |
| 14        | Ru(OAc) <sub>2</sub> (PPh <sub>3</sub> ) <sub>2</sub>   | --   | NaOAc                          | PhMe              | 120          | 0          | 23         | 50             |
| 15        | Ru(OAc) <sub>2</sub> (PPh <sub>3</sub> ) <sub>2</sub>   | --   | NaOAc                          | PhCF <sub>3</sub> | 120          | 0          | 21         | 59             |
| 16        | Ru(OAc) <sub>2</sub> (PPh <sub>3</sub> ) <sub>2</sub>   | --   | NaOAc                          | DCE               | 120          | 0          | 8          | 63             |
| 17        | Ru(OAc) <sub>2</sub> (PPh <sub>3</sub> ) <sub>2</sub>   | --   | NaOAc                          | DCE               | 100          | 0          | 12         | 65             |
| 18        | Ru(OAc) <sub>2</sub> (PPh <sub>3</sub> ) <sub>2</sub>   | --   | NaOAc                          | DCE               | 80           | 0          | 11         | 72             |
| <b>19</b> | <b>Ru(OAc)<sub>2</sub>(PPh<sub>3</sub>)<sub>2</sub></b> | --   | <b>NaOAc</b>                   | <b>DCE</b>        | <b>70</b>    | <b>0</b>   | <b>4</b>   | <b>80 (77)</b> |

|    |                                                        |    |       |     |    |    |    |    |
|----|--------------------------------------------------------|----|-------|-----|----|----|----|----|
| 20 | Ru(OAc) <sub>2</sub> (PPh <sub>3</sub> ) <sub>2</sub>  | -- | NaOAc | DCE | 60 | 58 | 10 | 24 |
| 21 | RuCl <sub>2</sub> PPh <sub>3</sub> ( <i>p</i> -cymene) | -- | NaOAc | DCE | 70 | 64 | 5  | 4  |

<sup>[a]</sup> Reaction condition: **395** (0.25 mmol), **396** (1.25 mmol), [Ru] (10 mol %). Yields were determined by <sup>1</sup>H NMR with CH<sub>2</sub>Br<sub>2</sub> as an internal standard. Isolated yield in the parenthesis.

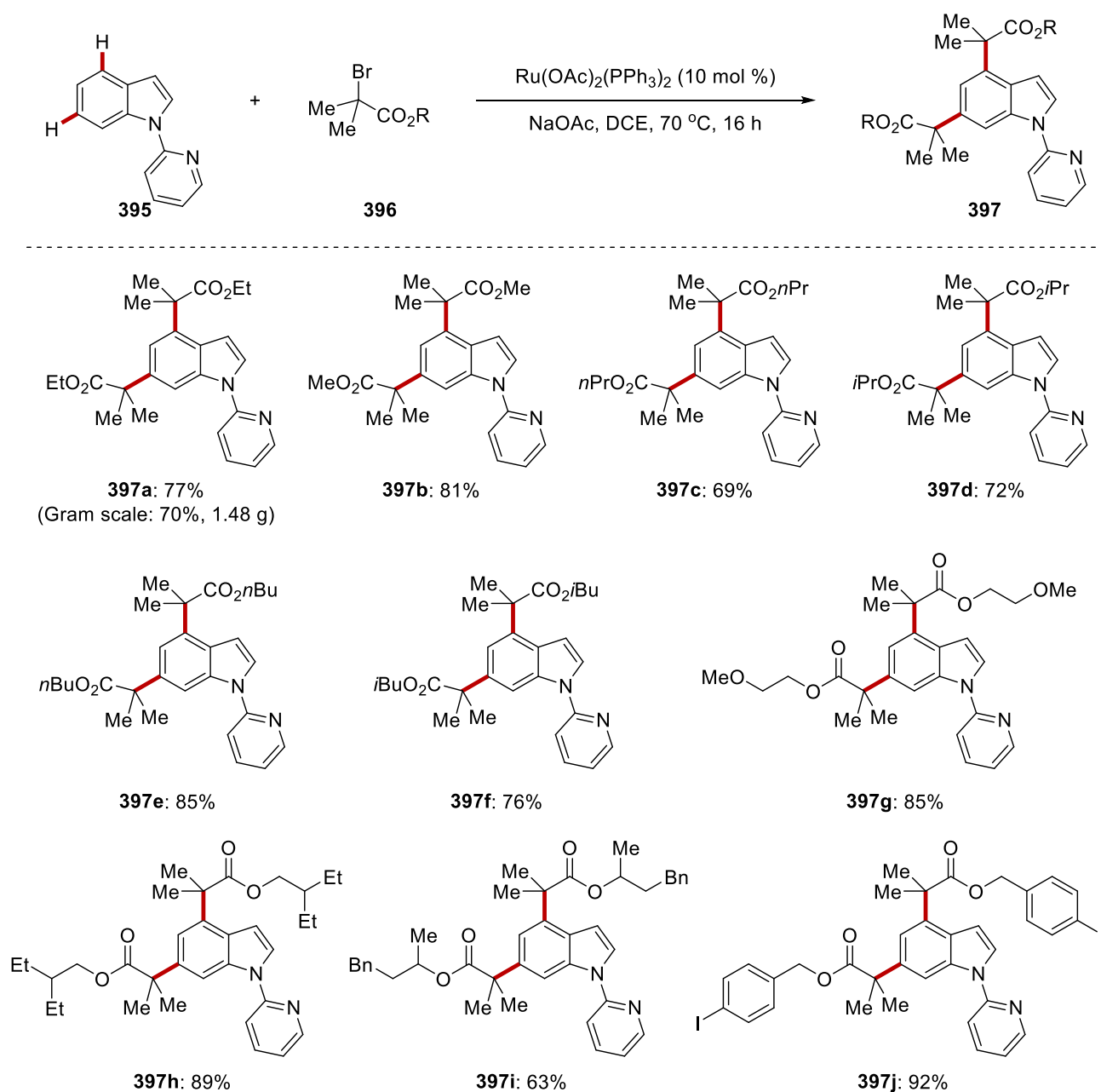
Thereafter, we examined the effect of the *N*-substituent pattern in indoles **395** on the outcome of the reaction (Scheme 3.2.2). Hence, indoles **395** with a variety of orienting groups, such as pyridine (**395a**) amides (**395b**) and (**395c**), phosphine oxide (**395d**), and phosphine (**395e**), as well as free-indole (**395f**) were subjected to the established reaction conditions for the C4/C6–H distal functionalizations of the heterocycle. Interestingly, only the pyridine group afforded the desired C4/C6–H alkylation product **397**, clearly demonstrating the unique ability of the pyridine directing group in this transformation. These results illustrated the importance of the five-membered ruthenacycles formation by the *N*(sp<sup>2</sup>)-group for allowing for C4/C6–H double functionalizations.



**Scheme 3.2.2** Examination of *N*-substitution pattern.

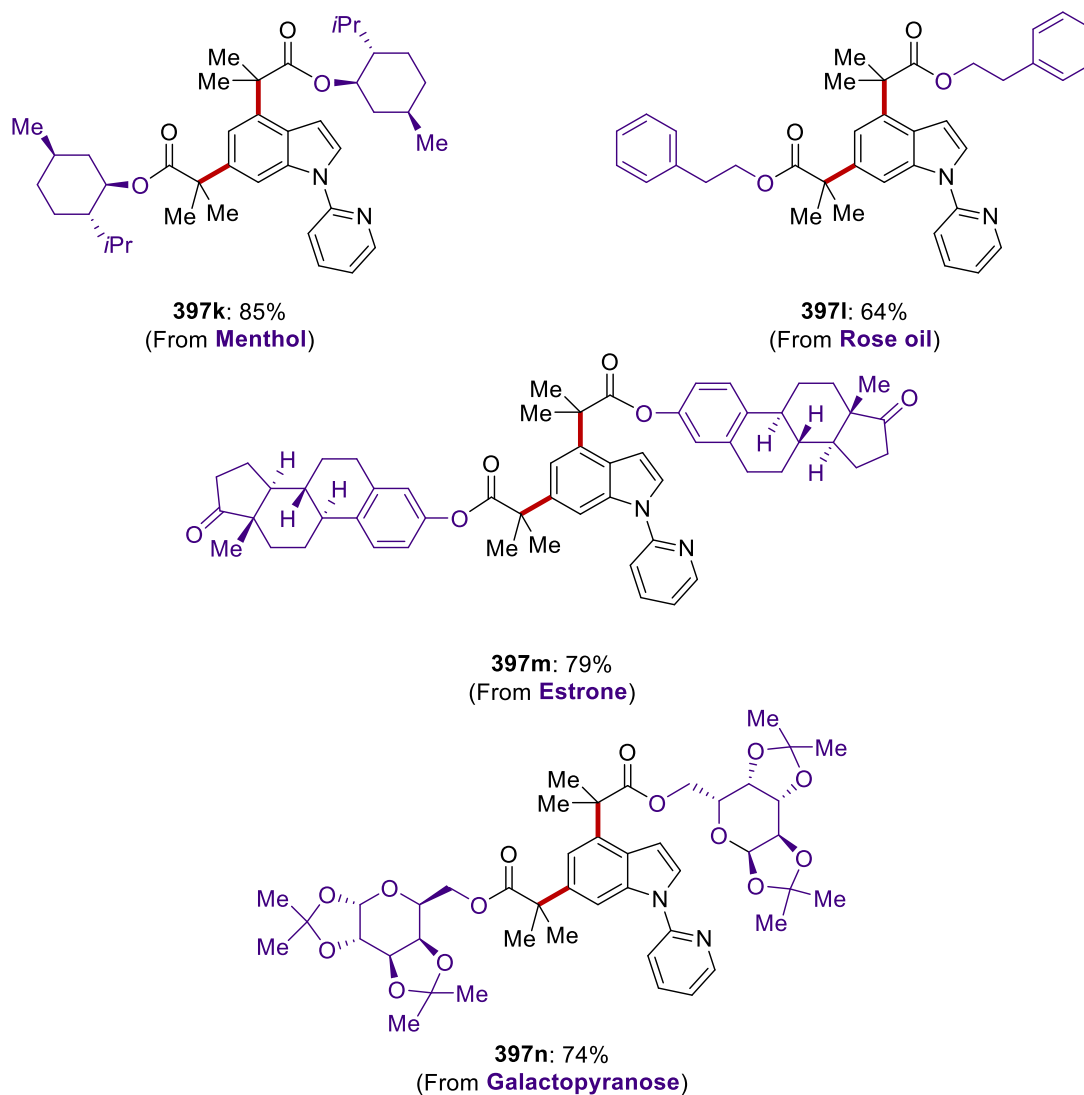
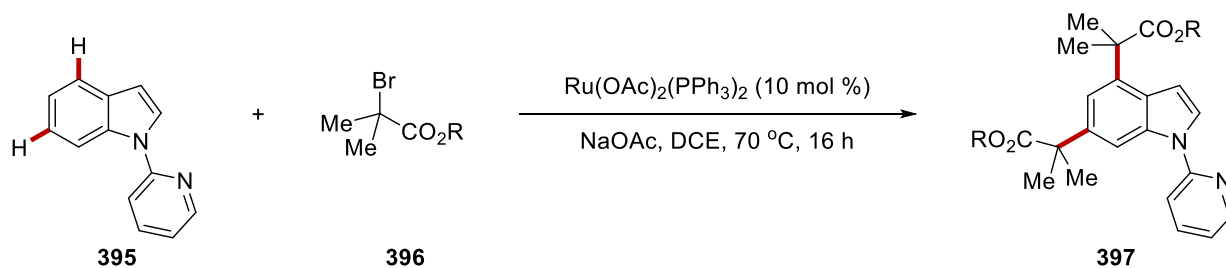
### 3.2.2 Substrate Scope

With the optimal reaction conditions in hand, we next explored the versatility of the C4/C6–H functionalization with a set of representative indoles **395** and alkyl bromides **396** (Scheme 3.2.3). Indeed, alkyl bromides **396** having different types of alkyl groups were selectively transformed into the desired C4/C6–H double alkylated products **397**. Notably, a synthetically valuable aryl iodide was fully tolerated under the reaction conditions. It is noteworthy that the reaction could be easily conducted on a gram scale without significant loss of catalytic efficacy.



**Scheme 3.2.3** C4–H/C6–H alkylations with differently substituted alkyl bromides **396**.

This reaction manifold was further extended to exploit natural product-derived alkyl bromides, including menthol **396k**, rose oil **396l**, estrone **396m**, and galactopyranose **396n**, providing selectively C4–H and C6–H dual functionalized indoles **397k–397n** without racemization (Scheme 3.2.4).

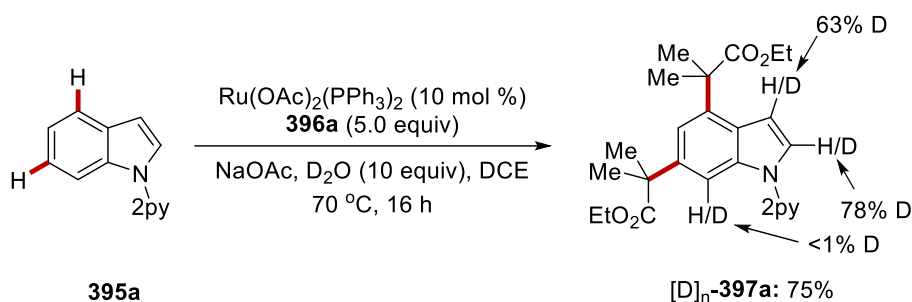


**Scheme 3.2.4** Dual C–H alkylations of indoles **395** with natural product motifs.

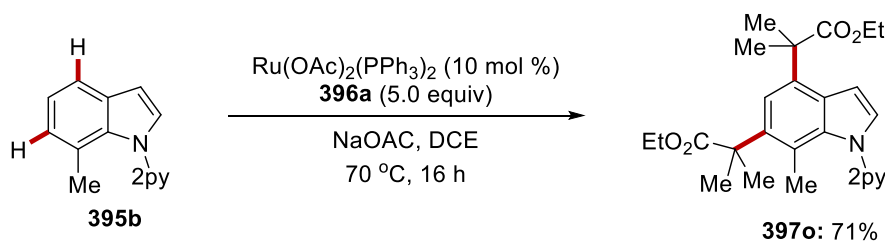
### 3.2.3 Mechanistic Studies

Given the unique features of the unprecedented arene-ligand-free ruthenium-catalyzed dual C4/C6–H alkylations, we became interested in deciphering its mode of action (Scheme 3.2.4). To this end, we performed the C4/C6–H alkylation in the presence of isotopically labeled D<sub>2</sub>O under the optimized reaction conditions (Scheme 3.2.5a). Hence, H/D-scrambling was only observed in the C2– and C3–H positions, while the C7–H position was not deuterated. This finding clearly proved that C2–H bond scission occurs in a reversible fashion and indicates that C4/C6–H double alkylations were presumably governed by the C2–ruthenation event. Further experiments showed that the C7–H blocked substrate **395b** efficiently underwent the C4/C6–H alkylation process, showing a C7–metallation-initiated distal-functionalization unlikely to be operative (Scheme 3.2.5b).

(a) H/D exchange study



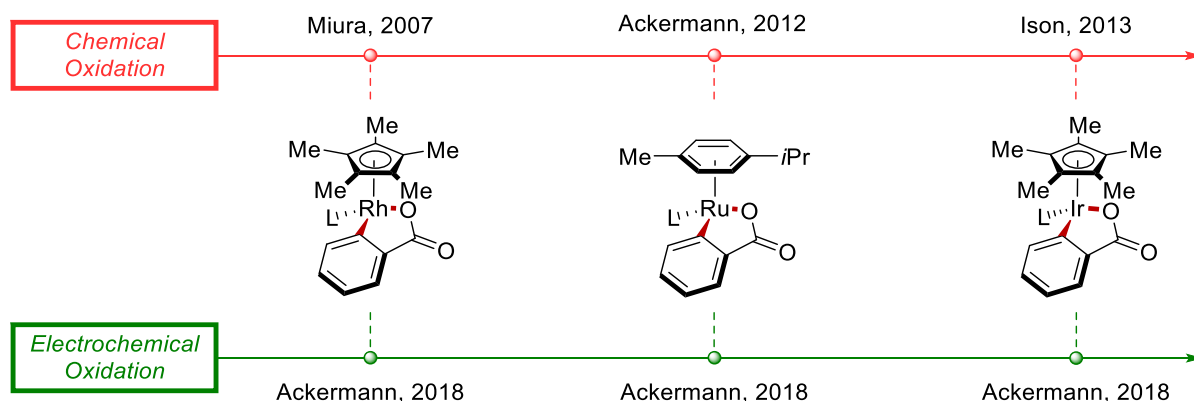
(b) Experiment with C7-blocked substrate **395b**



**Scheme 3.2.5** Mechanistic investigations for C4/C6–H functionalizations.

### 3.3 Osmium-Catalyzed Electrooxidative C–H Annulations

Carboxylate-assisted<sup>[20a]</sup> oxidative C–H annulations by weak *O*-coordination have been realized by consecutive C–H and O–H bond scission of aromatic carboxylic acids. With pioneering contributions in rhodium, ruthenium, and iridium catalysis by Miura/Satoh,<sup>[229]</sup> Ackermann,<sup>[230]</sup> and Ison<sup>[231]</sup> among others,<sup>[232]</sup> the modular assembly of five- or six-membered heterocycles has been established.<sup>[233, 215d]</sup> However, these reactions require the additional use of stoichiometric chemical oxidants, such as copper(II) or silver(I) salts, to facilitate the redox processes. To overcome this disadvantage, metallaecatalysis has recently emerged as a sustainable platform.<sup>[234a-d, 1a, 234e-n]</sup> Specifically, C–H activations enabled by electricity, facilitating the crucial catalysts reoxidation by an anodic event, allowed for a variety of oxidative chemical transformations, thus avoiding cost-intensive or toxic chemical oxidants.<sup>[235]</sup> Recently, Ackermann<sup>[236]</sup> and others<sup>[237]</sup> have developed electrooxidative C–H annulations by ruthenium, rhodium, and iridium catalysts (Scheme 3.3.1).



**Scheme 3.3.1** Timeline of C–H annulations by rhodium(III), ruthenium(II), and iridium(III) catalysis: chemical oxidants versus electrocatalysis.



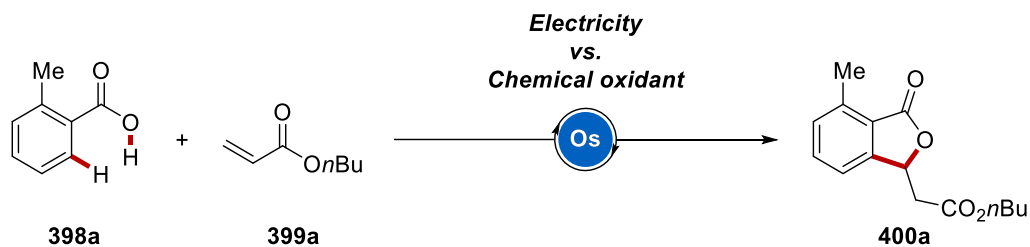


|    |                   |                             |                             |     |                   |
|----|-------------------|-----------------------------|-----------------------------|-----|-------------------|
| 6  | KOAc              | KPF <sub>6</sub>            | HFIP/H <sub>2</sub> O (1/1) | 100 | 38                |
| 7  | KOAc              | KSbF <sub>6</sub>           | HFIP/H <sub>2</sub> O (1/1) | 100 | 54                |
| 8  | KOAc              | NaSbF <sub>6</sub>          | HFIP/H <sub>2</sub> O (1/1) | 100 | 60                |
| 9  | KOAc              | <i>n</i> BuN <sub>4</sub> I | HFIP/H <sub>2</sub> O (1/1) | 100 | 20                |
| 10 | KOAc              | I <sub>2</sub>              | HFIP/H <sub>2</sub> O (1/1) | 100 | 23                |
| 11 | KOAc              | KI                          | HFIP/H <sub>2</sub> O (1/1) | 100 | 76 <sup>[b]</sup> |
| 12 | NOAc              | KI                          | HFIP/H <sub>2</sub> O (1/1) | 100 | 36                |
| 13 | NO <sub>Piv</sub> | KI                          | HFIP/H <sub>2</sub> O (1/1) | 100 | 38                |
| 14 | KOAc              | KI                          | HFIP/H <sub>2</sub> O (1/1) | 60  | 35                |
| 15 | KOAc              | KI                          | HFIP/H <sub>2</sub> O (1/1) | 25  | 0                 |
| 16 | KOAc              | KI                          | HFIP/H <sub>2</sub> O (3/1) | 100 | 76                |
| 17 | KOAc              | KI                          | HFIP/H <sub>2</sub> O (1/1) | 100 | 7 <sup>[c]</sup>  |
| 18 | KOAc              | KI                          | HFIP/H <sub>2</sub> O (1/1) | 100 | 16 <sup>[d]</sup> |
| 19 | KOAc              | KI                          | HFIP/H <sub>2</sub> O (1/1) | 100 | 90 <sup>[e]</sup> |
| 20 | KOAc              | KI                          | HFIP/H <sub>2</sub> O (1/1) | 100 | 0 <sup>[f]</sup>  |
| 21 | KOAc              | KI                          | HFIP/H <sub>2</sub> O (1/1) | 100 | 6 <sup>[g]</sup>  |
| 22 | KOAc              | --                          | HFIP/H <sub>2</sub> O (1/1) | 100 | 11                |

[a] Reaction conditions: **398** (0.20 mmol), **399** (0.60 mmol), [OsCl<sub>2</sub>(*p*-cymene)]<sub>2</sub> (5.0 mol %), base (2.0 equiv), additive (2.0 equiv), solvent mixture (4.0 mL), 100 °C, 16 h. Yield was determined by <sup>1</sup>H NMR with CH<sub>2</sub>Br<sub>2</sub> as the internal standard. Yield in the parenthesis is isolated yield. [b] KI (4.0 equiv) was used. [c] [Cp\**Rh*Cl<sub>2</sub>]<sub>2</sub> (2.5 mol %) was used. [d] [Cp\**Ir*Cl<sub>2</sub>]<sub>2</sub> (2.5 mol %) was used. [e] [RuCl<sub>2</sub>(*p*-cymene)]<sub>2</sub> (5.0 mol %) was used. [f] Without catalyst. [g] Without electricity. The reaction was equipped with electrodes, but no electricity. GF = Graphite Felt. HFIP = Hexafluoroisopropyl alcohol. BQ = Benzoquinone. Fc = Ferrocene. HOBt = Hydroxybenzotriazole.

To highlight the advantages of the electrochemical approach, a set of experiments were carried out under air or with commonly employed chemical oxidants, such as AgOAc, Cu(OAc)<sub>2</sub>, Mn(OAc)<sub>3</sub>, PhI(OAc)<sub>2</sub>, or K<sub>2</sub>S<sub>2</sub>O<sub>8</sub> (Scheme 3.3.2). All of the attempts met with unsatisfactory results, showing

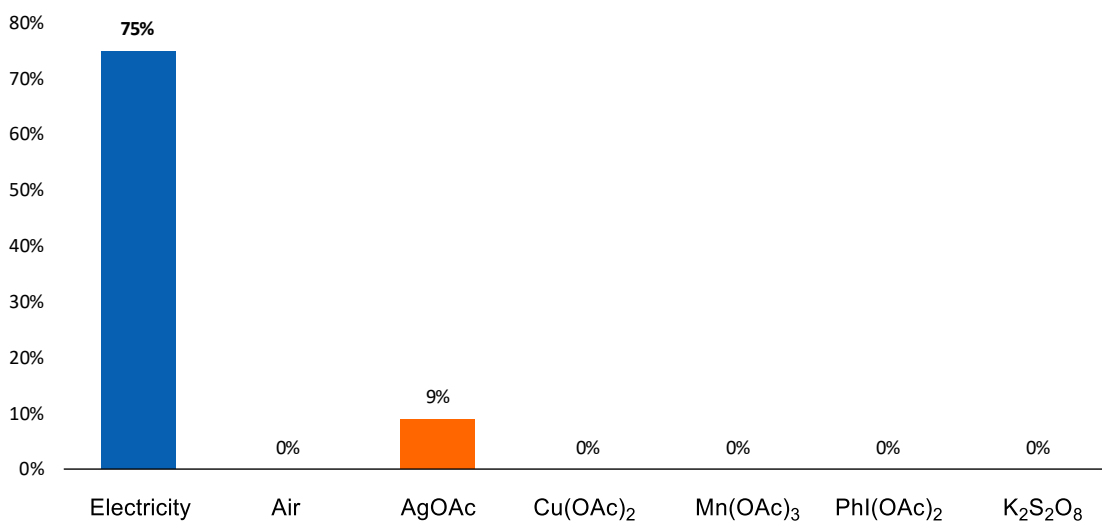
that electricity not only played a crucial role in sustainable oxidation, but also gave optimal and unique efficiency for the osmium-catalyzed oxidative C–H annulation.



[Reaction conditions]

Electricity:  $[\text{OsCl}_2(p\text{-cymene})]_2$  (5.0 mol %), KI, KOAc, HFIP/ $\text{H}_2\text{O}$ , 100 °C, 16 h,  $\text{N}_2$ , CCE at 4.0 mA

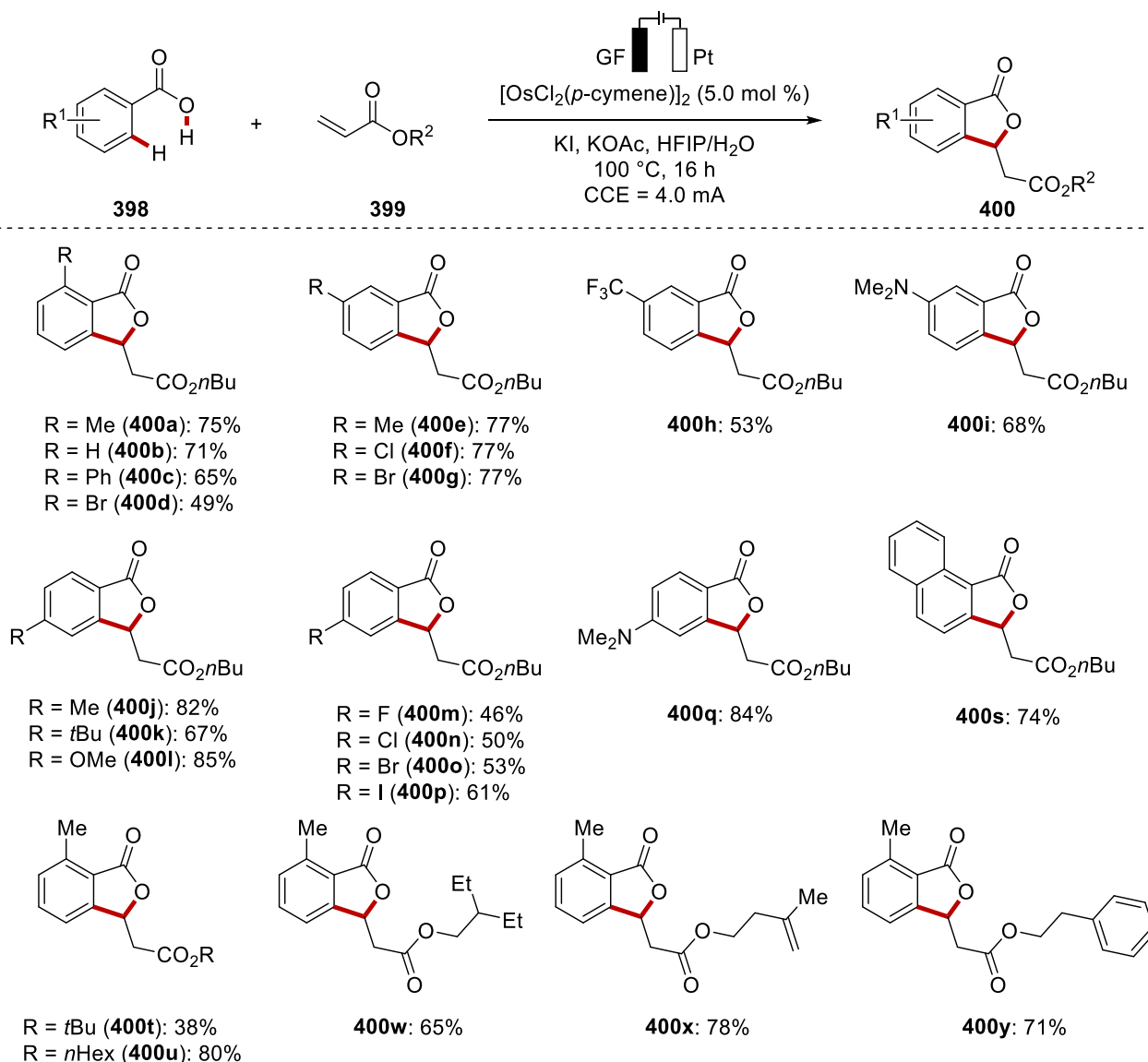
Chemical oxidant:  $[\text{OsCl}_2(p\text{-cymene})]_2$  (5.0 mol %), oxidant, KOAc, HFIP/ $\text{H}_2\text{O}$ , 100 °C, 16 h,  $\text{N}_2$



**Scheme 3.3.2** Comparison between electricity and representative chemical oxidants.

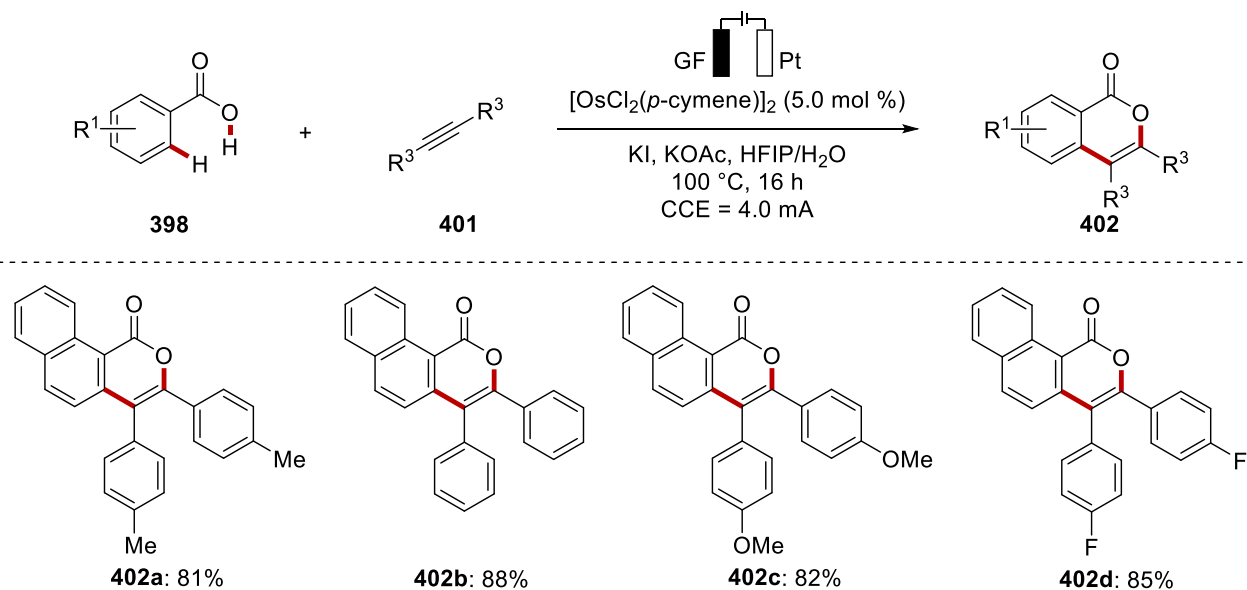
### 3.3.2 Substrate Scope

Next, we explored the viable substrate scope of the electrochemical osmium-catalyzed [4+1] and [4+2] C–H/O–H annulations of benzoic acids **398** with alkenes **399** and alkynes **400** (Scheme 3.3.3). A wide range of benzoic acids gave the desired heterocycles, fully tolerating valuable functional groups, such as halides (**400d**, **400f**, **400g**, **400m**, **400n**, **400o**, and **400p**) or basic amines (**400i** and **400q**). Notably, the C–H activation with the substrate having two competing olefins selectively afforded a single annulated product **400x**.



**Scheme 3.3.3** Substrate scope for electrooxidative osmium-catalyzed [4+1] annulations.

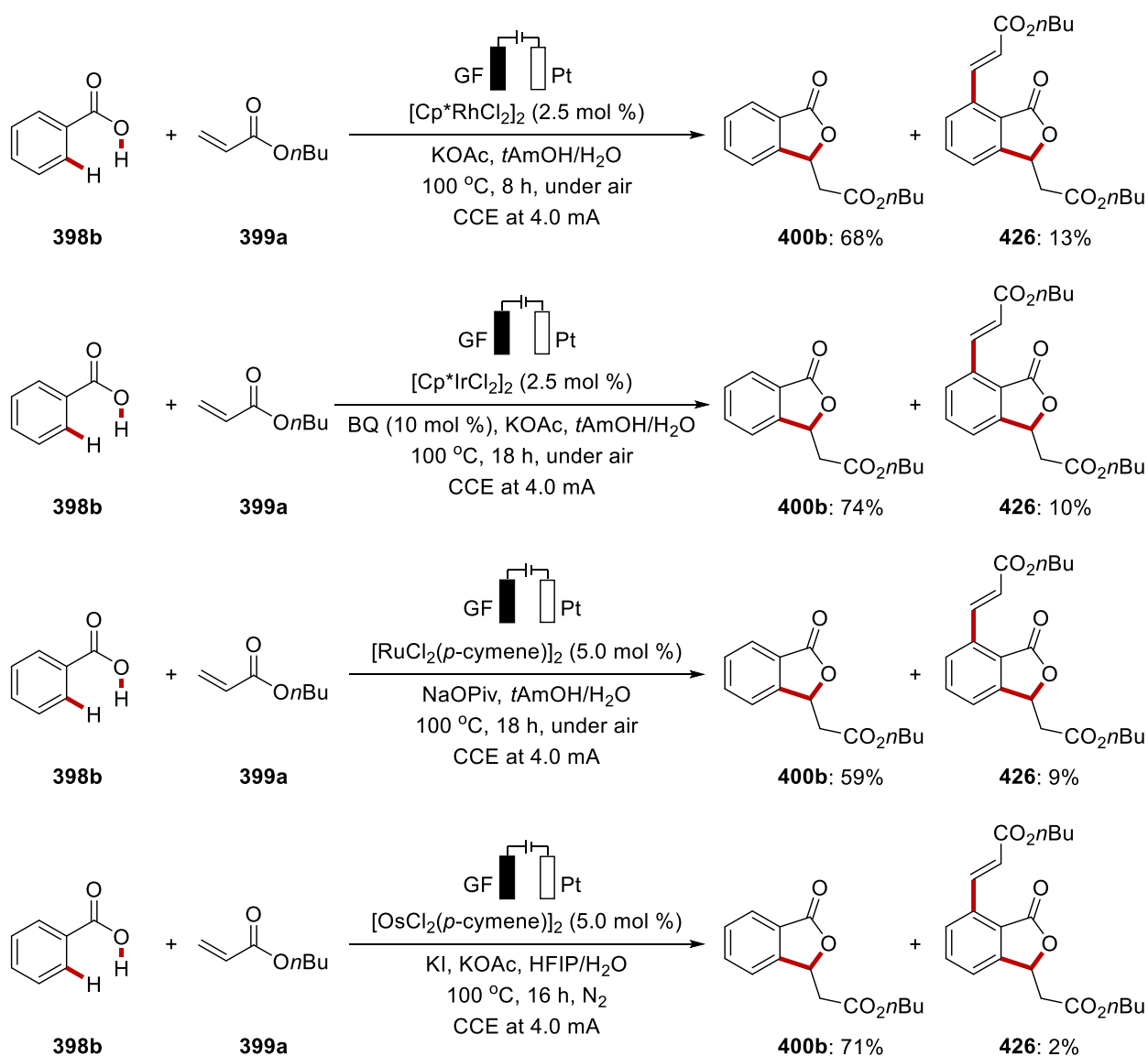
The annulation manifold was not limited to the assembly of five-membered rings, but six-membered heterocycle assembly with differently-substituted alkynes **401** was also found to be viable, thus providing the extension of conjugated  $\pi$ -system. Thereby, differently substituted alkynes **401** having alkyl (**402a**), methoxy (**402c**) or halides (**402d**) groups were fully acceptable by the optimized osmium catalysis (Scheme 3.3.4).



**Scheme 3.3.4** Substrate scope for electrooxidative osmium-catalyzed [4+2] annulations.

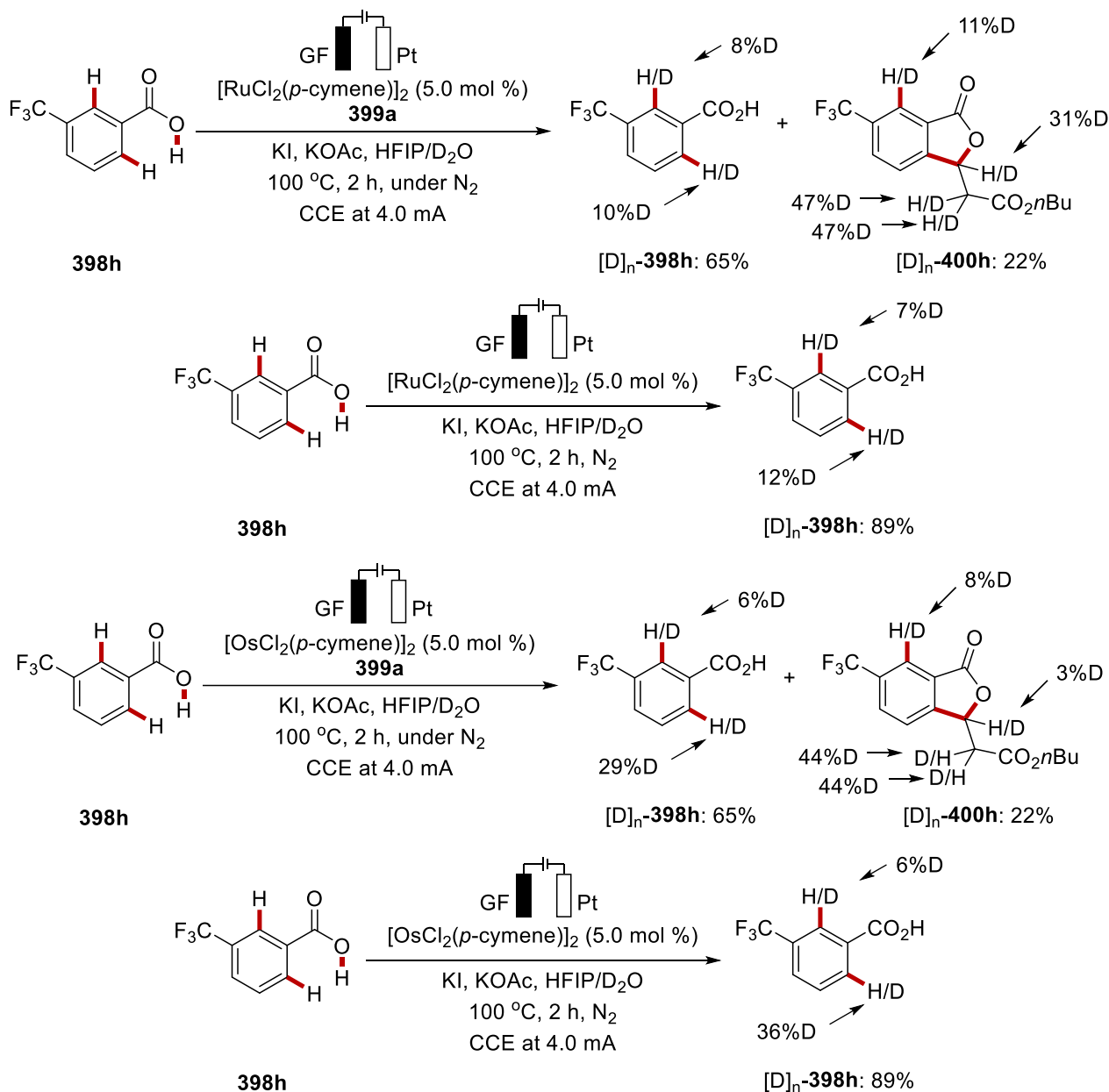
## 3.1.3 Site-Selectivity Studies

Inspired by the unprecedented reactivity, we were interested to interrogate the selectivity feature (Figure 3.3.5). To this end, we performed a series of metallaelectro-catalyzed reactions with benzoic acid **398b** possessing two accessible *ortho*-C–H bonds. First, we assessed the catalysts that were already used for the electrooxidative C–H annulation reactions. Thus, the rhodium, iridium, and ruthenium catalysts were examined, giving 68%/13% (5.2:1), 74%/10% (7.4:1), and 59%/9% (6.3:1) of mono- and difunctionalized product **400b** and **426**, respectively. In sharp contrast, the use of the osmium electrocatalysis showed a significantly improved mono-selectivity.



Scheme 3.3.5 Selectivity comparisons by different catalysis.

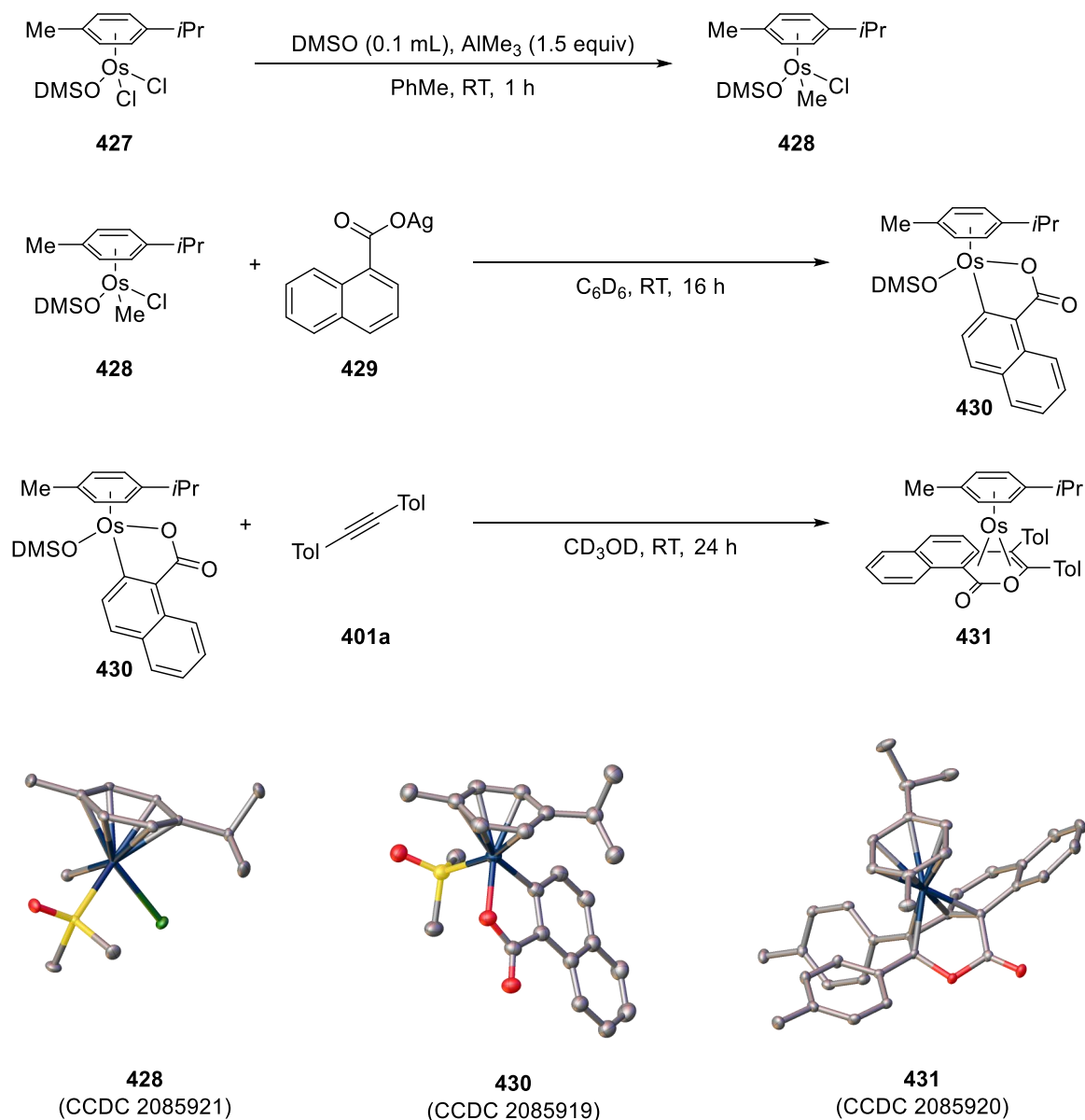
The excellent chemo-selectivity was also observed in the H/D scrambling experiments in the presence of an isotopically labelled solvent (Scheme 3.3.6). Ruthenium dimer  $[\text{RuCl}_2(\textit{p}\text{-cymene})]_2$  showed comparable deuterations on C2–H and C6–H of 3-trifluoromethyl benzoic acid (**398h**) with and without *n*-butyl acrylate (**399a**). However, the osmium-electrocatalysis provided significantly increased deuteration at the C6–H position as compared to sterically hindered C2–H position.



**Scheme 3.3.6** Reaction comparisons for H/D exchange experiments.

### 3.3.4 Mechanistic Studies

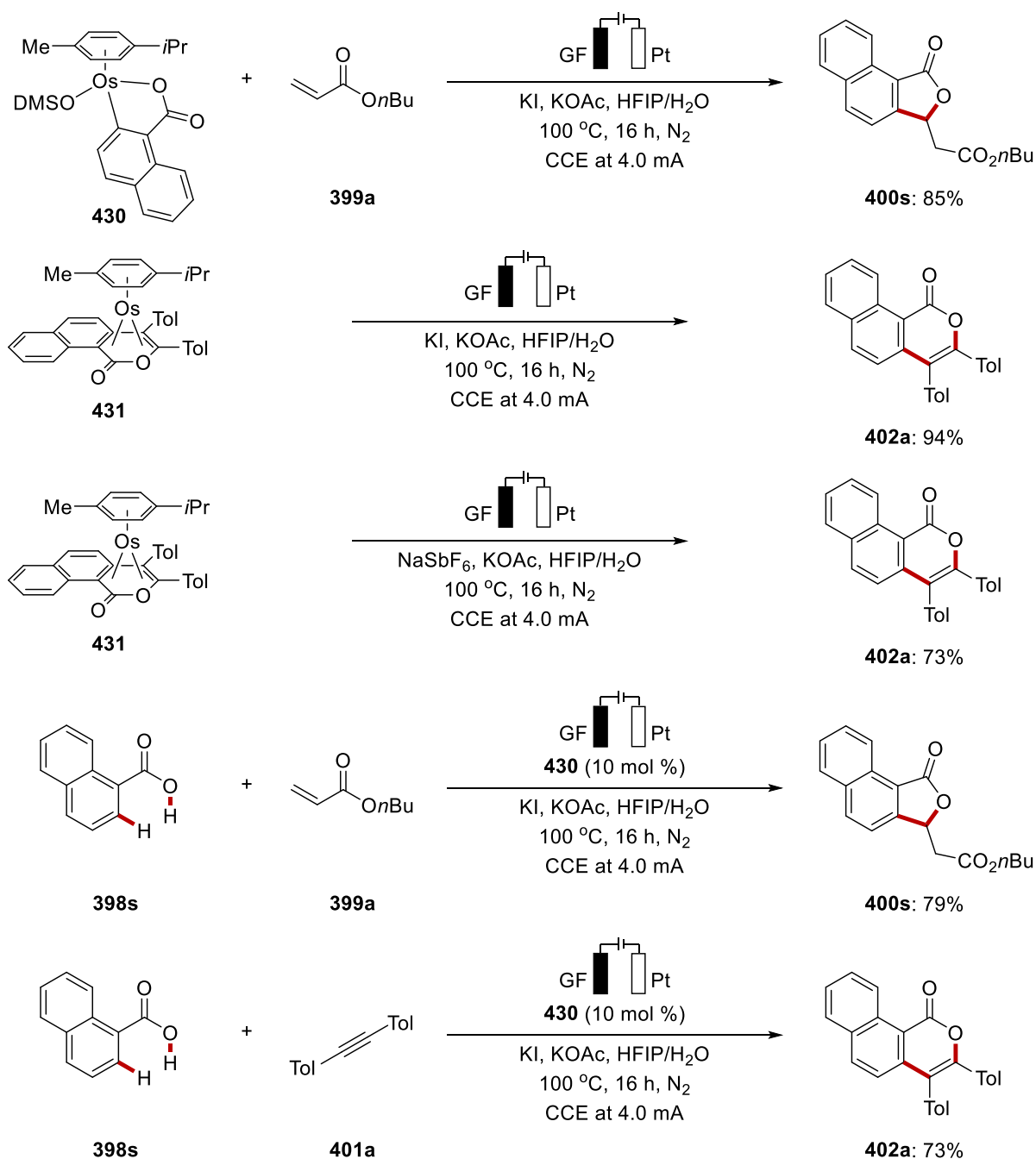
Subsequently, we set out to study the working mode of the electrooxidative osmium-catalyzed C–H activation. To this end, novel key intermediates, **430** and **431**, were independently prepared (Scheme 3.3.7). It is noteworthy that these osmium complexes have not been obtained earlier and the structures were characterized by X-ray crystallographic analyses.



**Scheme 3.3.7** Synthesis of osmacomplexes and their X-ray structures.

The thus synthesized osmium complexes were found to be competent to afford the desired products **400s** and **402a** in both stoichiometric and catalytic reactions (Scheme 3.3.8). The five-membered

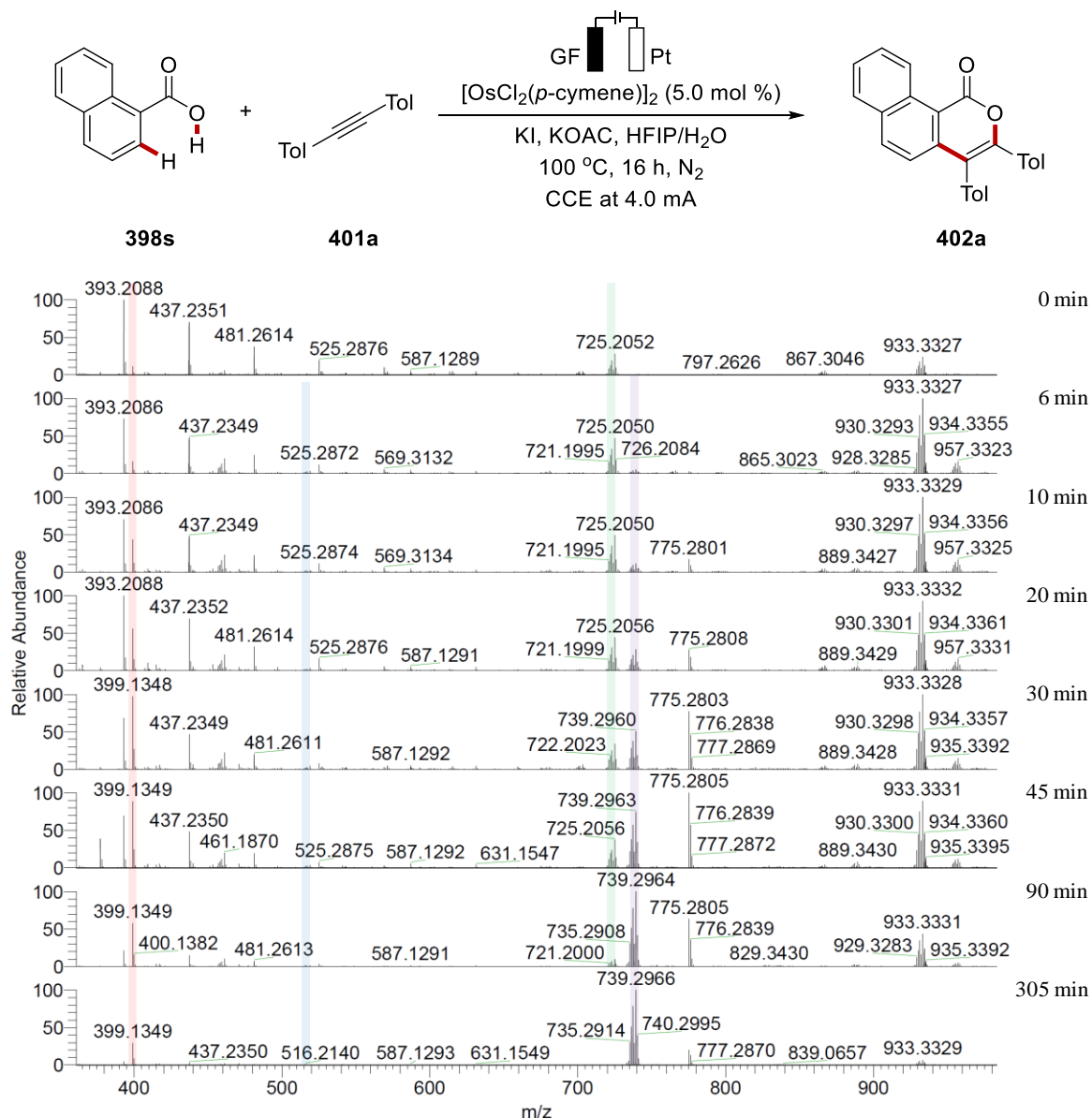
osmium complex **430** was transformed to the desired product under the optimized conditions, while osmium(0) sandwich complex was converted to the annulated product in the presence of KI or NaSbF<sub>6</sub>. The synthesized osmium complex **430** was also used as a catalyst, providing the [4+1] or [4+2] cycloadditions product under the optimized conditions.



**Scheme 3.3.8** Stoichiometric and catalytic reactions with the synthesized osmium complexes **430–431**.

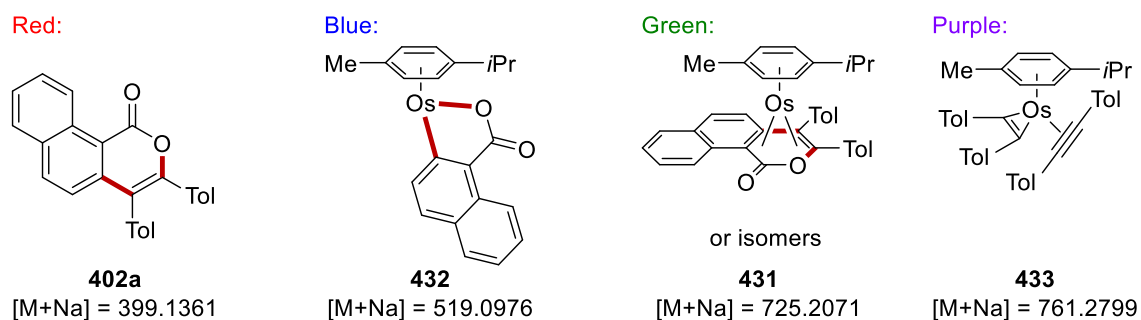


Furthermore, with the assistance of Dr. Antonis M. Messinis of the Ackermann group, high resolution-electrospray ionization-mass spectrometric (HR-ESI-MS) analysis was performed, demonstrating the successive formation and consumption of key reaction species (Scheme 3.3.9).



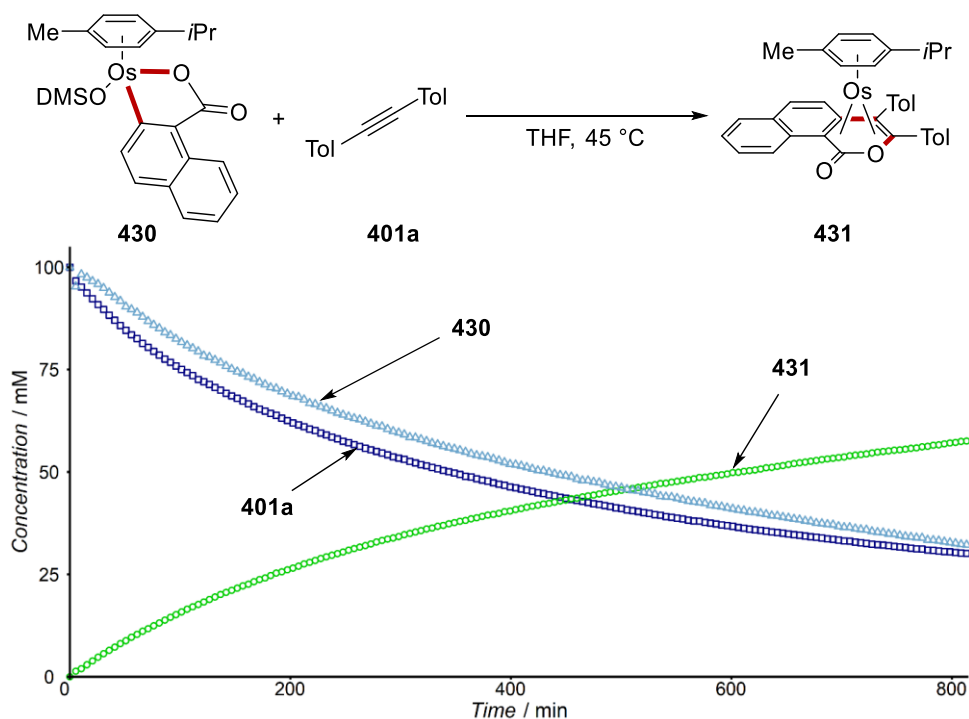
**Scheme 3.3.9** HR-ESI-MS study of electrooxidative osmium-catalyzed C–H annulation.

By detailed investigation of the isotopic patterns, we could analyze each component, in which red, blue, green, and purple bars correspond to the annulation product **402a**, the cyclometalated osmium intermediate **432**, the sandwich osmium(0) intermediate **431** with its possible isomers, and alkyne-coordinated osmium intermediate **433**, respectively (Scheme 3.3.10).



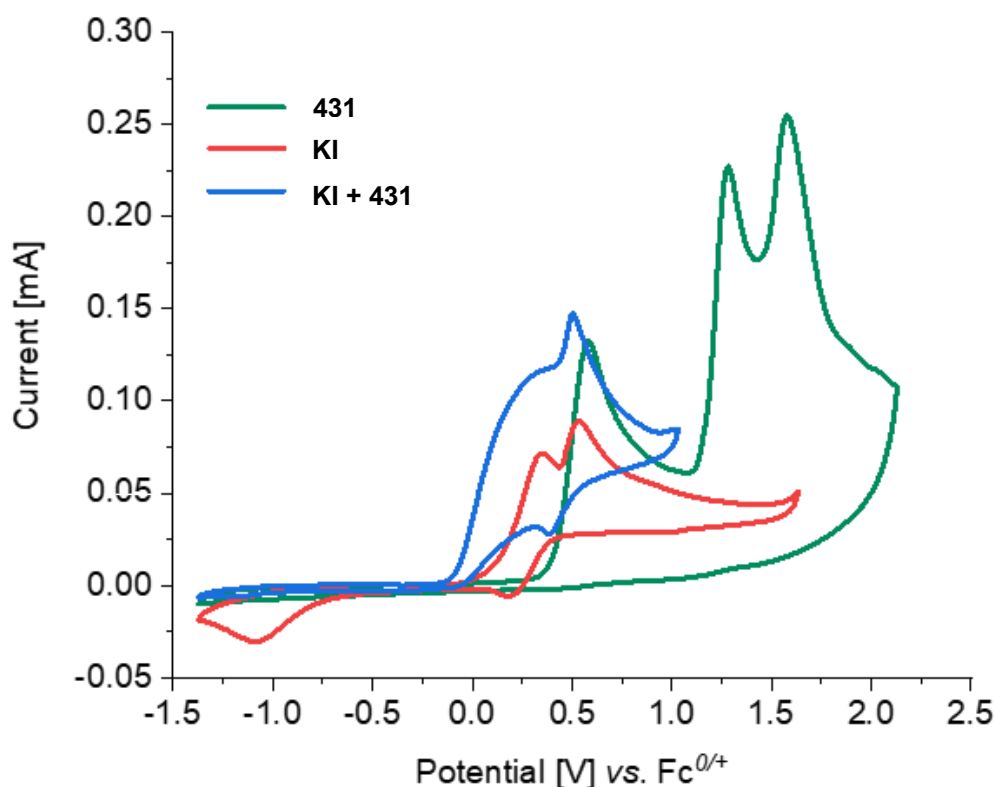
**Scheme 3.3.10** Investigation of the isotopic patterns from HR-ESI-MS study.

Additionally, Dr. Antonis M. Messinis of the Ackermann group performed *in-operando* NMR studies with the isolated osmium complex **430** and alkyne **401a**, which highlighted the formation of the osmium(0) sandwich complex, along with the consumption of complex **430** and alkyne **401a** (Scheme 3.3.11). Here, we were not able to observe an induction period and the seven-membered intermediate formed by the migratory insertion of alkyne **401a** was hardly observed. These results presumably suggest the facile formation of the osmium(0) complex **431** after the insertion step.



**Scheme 3.3.11** *In-operando* NMR study with osmium complex **430** and alkyne **401a**.

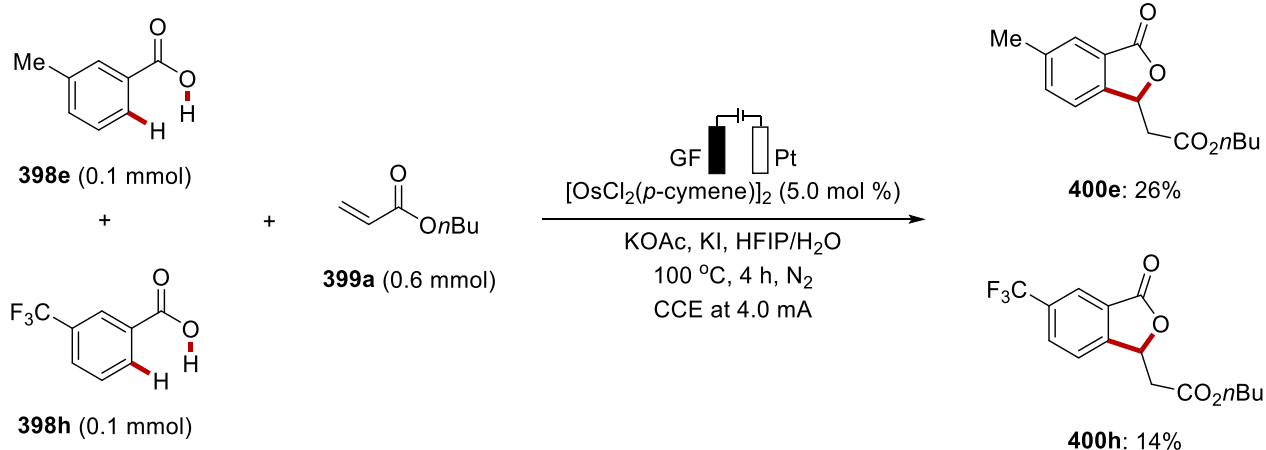
Thereafter, Xiaoyan Hou of the Ackermann group performed cyclic voltammetric analysis for the oxidation potential of the osmium(0) sandwich complex **431**, showing that the oxidation event occurred at  $E = 0.58$  V vs. Fc/Fc<sup>+</sup> (Scheme 3.3.12). This oxidation potential is slightly lower than the ruthenium(0) to ruthenium(II) oxidation potential of the previously reported ruthenaelectro-catalyzed C–H annulation.<sup>[236f]</sup>



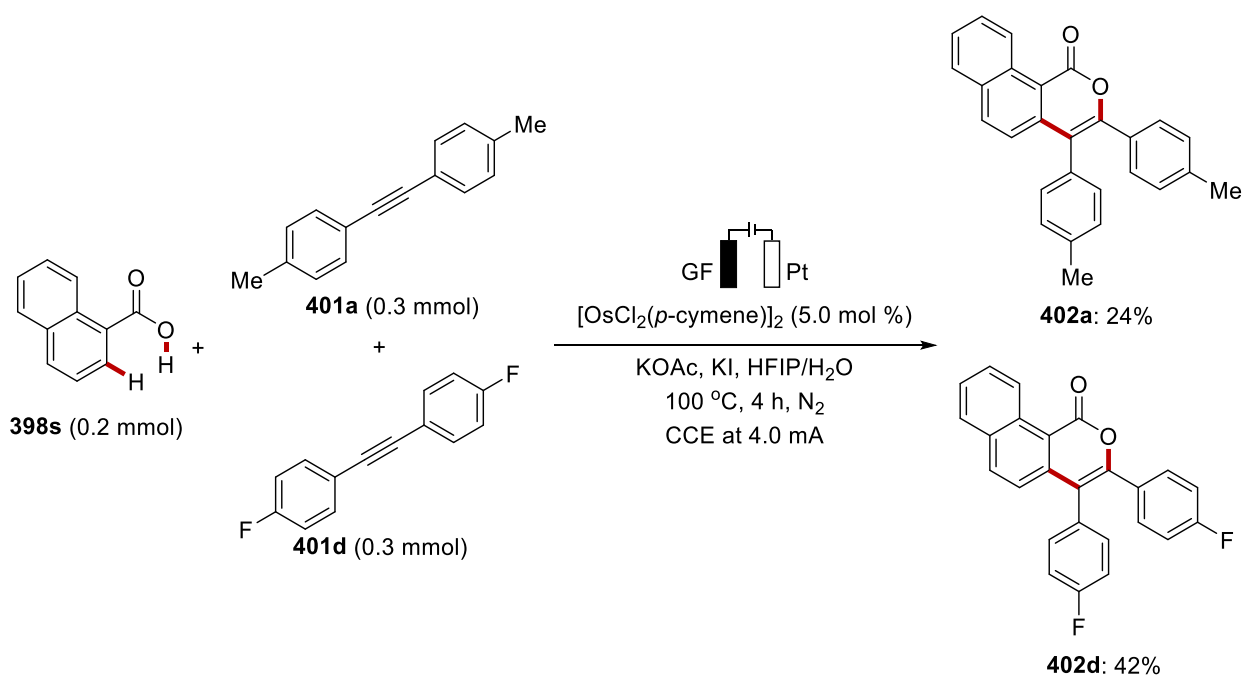
**Scheme 3.3.12** Cyclic voltammetry measurement.

Next, an intermolecular competition experiment with differently substituted benzoic acids (**398e** and **398h**) was carried out (Scheme 3.3.13a). The competition experiment showed that electron-donating groups on the benzoic acid **398e** resulted in a higher reactivity, suggesting a BIES mechanism.<sup>[238a, 238b, 24a, 238c]</sup> Additionally, an intermolecular competition experiment with differently substituted alkynes **401a** and **401d** was also performed (Scheme 3.3.13b), in which an alkyne **401a** having electron-donating groups afforded less product.

## a) Competition experiment between different benzoic acids

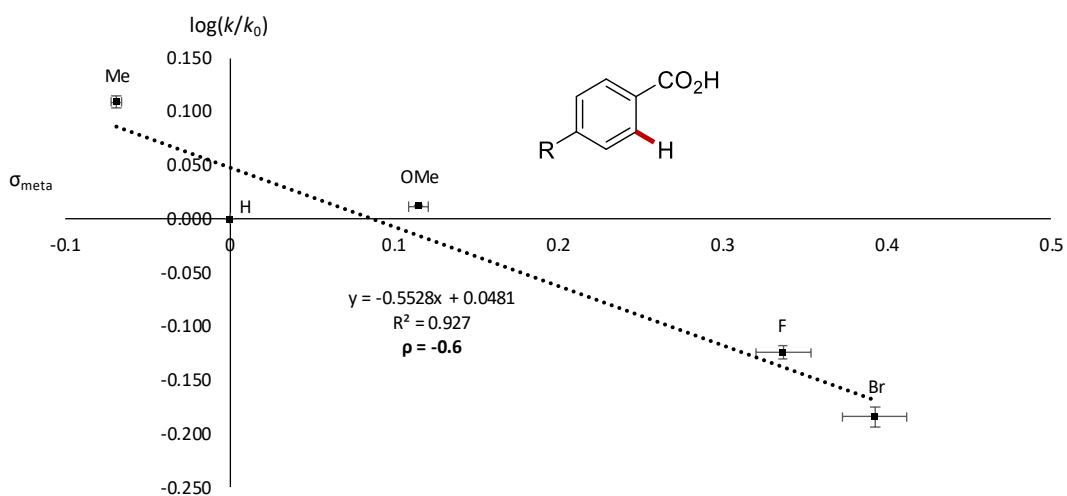
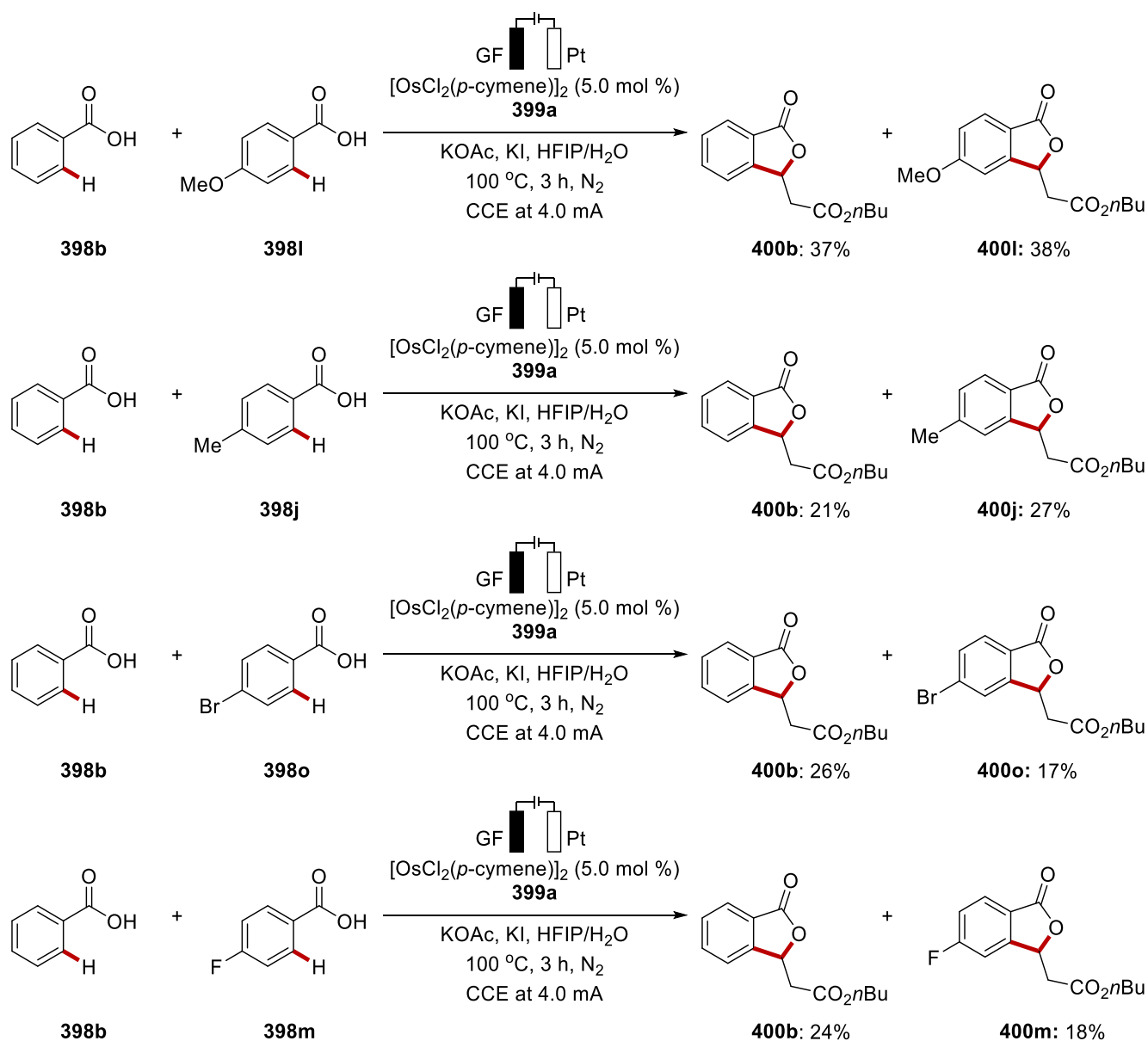


## b) Competition experiment between different alkynes



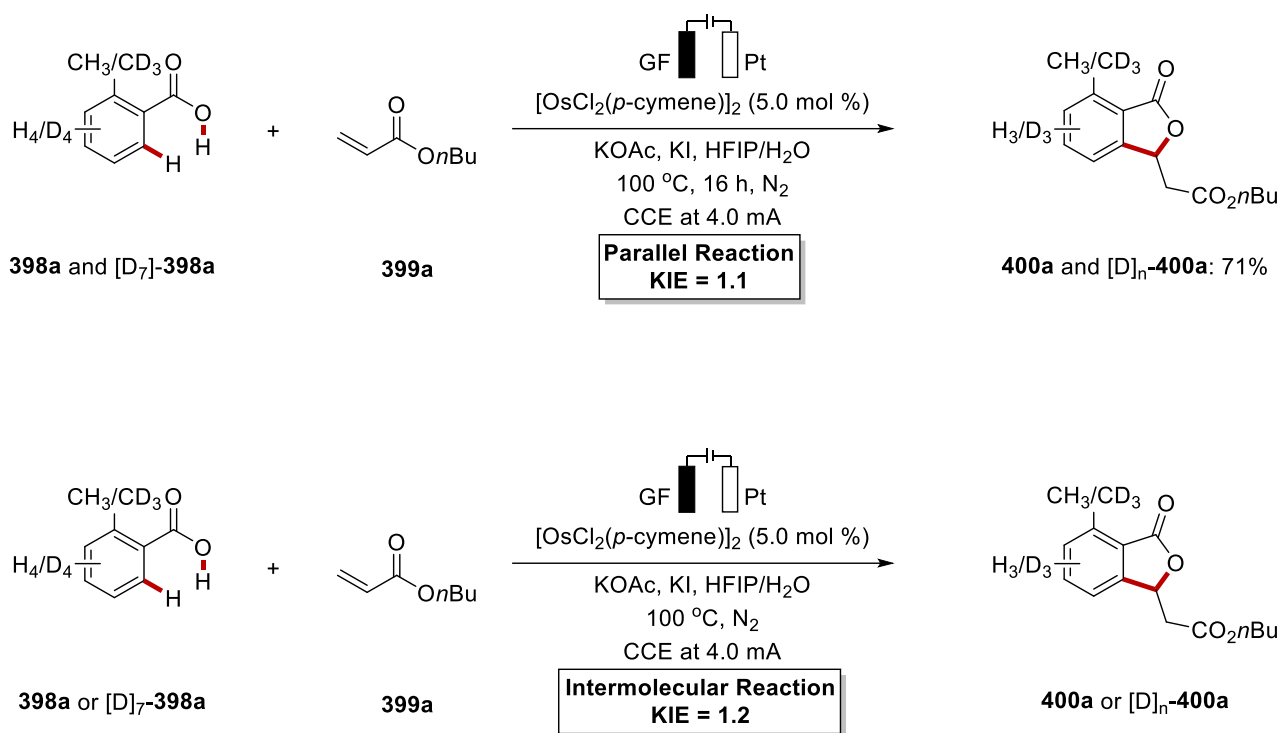
Scheme 3.3.13 Competition experiments.

A series of reactions with differently decorated benzoic acids in the *meta*-position to the C–H bond to be cleaved provided a linear Hammett correlation with a negative  $\rho$  value (Scheme 3.3.14). This result indicates that an electrophilic mechanism is likely operative in the C–H cleavage.



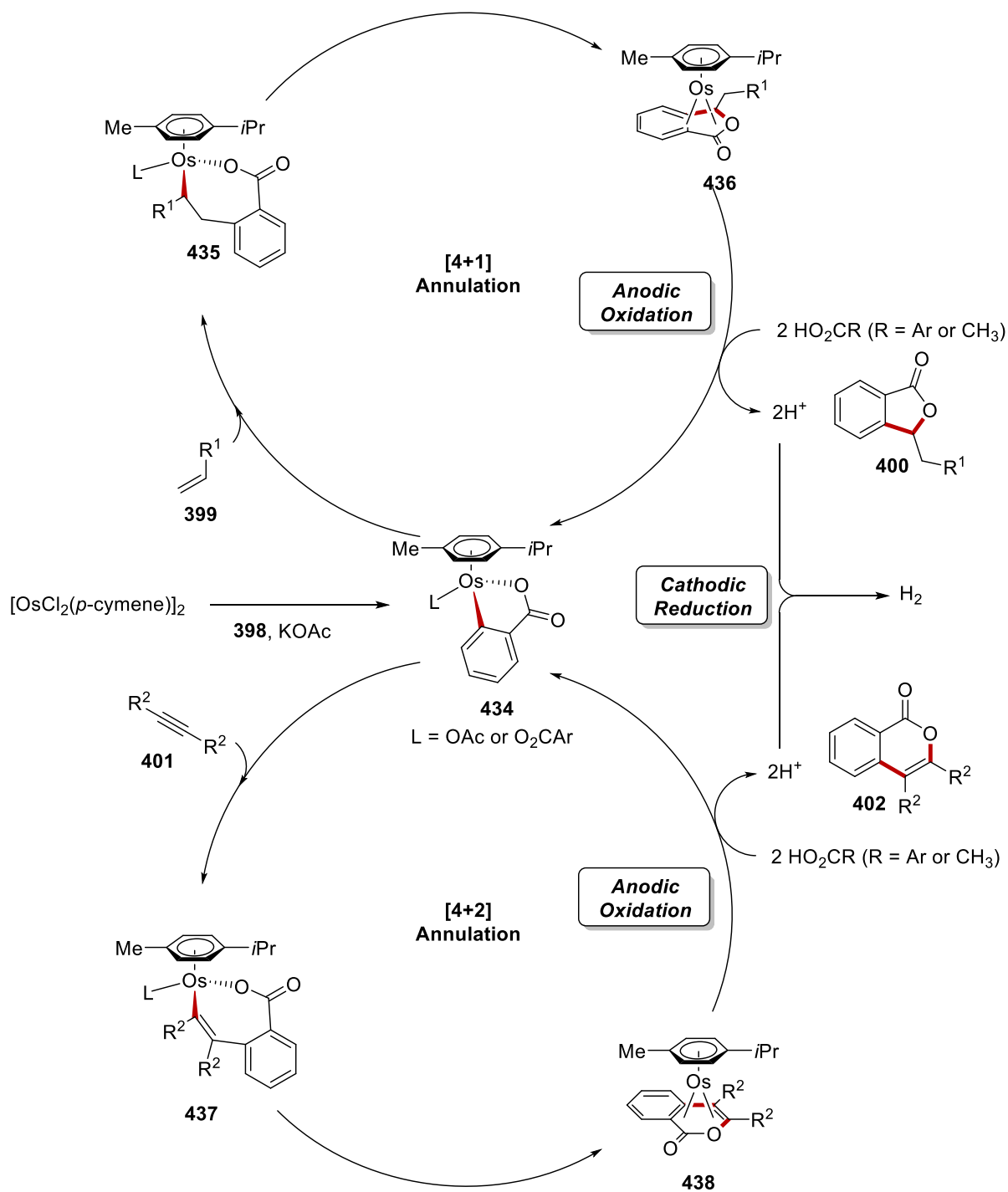
Scheme 3.3.14 Hammett correlation.

Subsequently, an intermolecular competition experiment and a pair of parallel reactions were performed with *o*-toluic acid **398a** and the isotopically labelled compound [D]<sub>7</sub>-**398a** to determine the kinetic isotope effect (Scheme 3.3.15). In both cases, a negligible KIE of  $k_H/k_D \approx 1.1$  and 1.2 were observed, suggesting a facile C–H scission.



**Scheme 3.3.15** Experiments for kinetic isotope effect.

On the basis of our mechanistic findings, a plausible catalytic cycle for the osmaelectro-catalyzed C–H activation is depicted in Scheme 3.3.16. The mechanistic rationale commences with a facile C–H bond cleavage, which gives osmacycle **434**. Thereafter, migratory insertion of alkenes **399** or alkynes **401** occurs, which enables the formation of intermediate **435** or **437**, respectively. Next, reductive elimination delivers osmium(0) sandwich complex **436** or **438**. Finally, the key anodic oxidation regenerates the catalytically active complex **434**, while liberating the desired product **400** or **402**.



Scheme 3.3.16 Proposed catalytic cycle.

### 3.4 Photo-Induced C–H Arylation by Reusable Heterogeneous Copper Catalyst

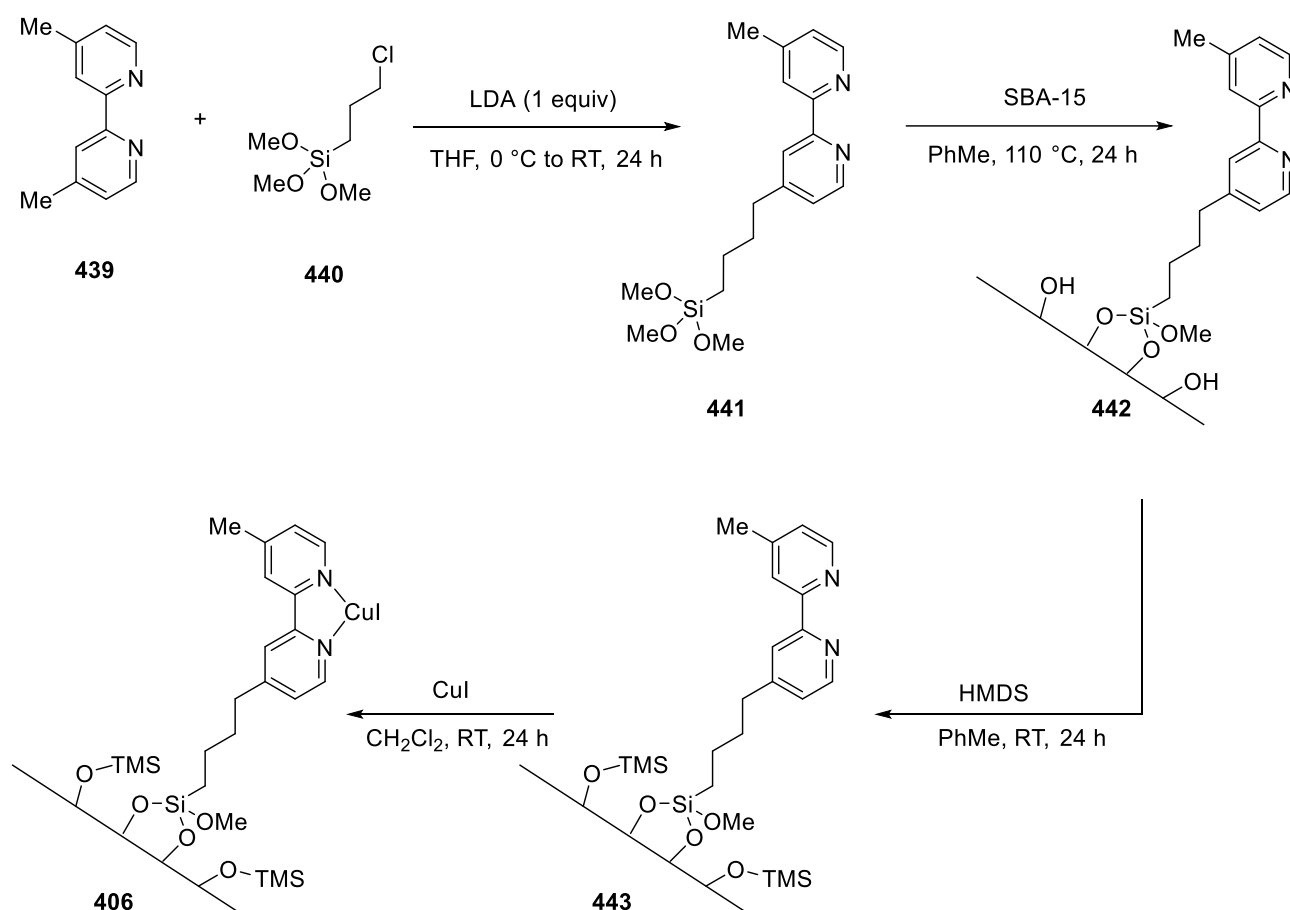
Recently, significant progress was realized in C–H activation chemistry with the aid of Earth-abundant, cost-effective 3d metal catalysts.<sup>[216]</sup> Among the 3d metals, copper has emerged as a viable metal for C–H activation.<sup>[152b, 155c, 189g, 239]</sup> Particularly, copper-catalyzed C–H arylations have been extensively investigated with notable contributions by Daugulis,<sup>[160, 161, 162]</sup> Miura<sup>[240]</sup> and Ackermann,<sup>[163]</sup> among others. Despite these major advances, copper-catalyzed C–H activation with aryl halides has been severely restricted by their harsh reaction conditions with reaction temperatures commonly ranging from 120 to 160 °C.

In recent years, photocatalysis<sup>[241]</sup> has been identified as an increasingly powerful approach towards various sustainable organic syntheses,<sup>[242]</sup> such as C–N bond formations, immensely elaborated by Fu,<sup>[243]</sup> MacMillan,<sup>[244]</sup> and Kobayashi.<sup>[245]</sup> Thus, Photoredox-catalyzed C–H functionalizations proved viable, albeit predominantly relying on precious transition metals, such as rhodium, palladium, and ruthenium complexes.<sup>[94, 246]</sup> In contrast, the Ackermann group has very recently devised photo-induced C–H arylations and chalcogenations by less toxic base metal catalysts.<sup>[247, 169]</sup> In spite of notable progress, photo-induced organometallic C–H activations were thus far limited to homogeneous catalysis, often leading to undesired trace metal impurities in the target products, and, more importantly, inherently preventing the catalysts from their reuse. While selected silica-supported catalysts<sup>[204a, 248a-c, 192h, 248d-f, 204b, 193b, 193m, 248g, 248h]</sup> were developed by Jones/Davies<sup>[208, 249, 206]</sup> and Sawamura<sup>[250]</sup> with non-excited-state reactivity, heterogeneous catalysis for photo-induced C–H activation has thus far unfortunately proven elusive.



### 3.4.1 Preparation of Hybrid Copper Catalyst

The hybrid copper catalyst **406** was synthesized by a modified procedure from Christopher's study (Scheme 3.4.1).<sup>[249a]</sup> To construct a linker, LDA deprotonated a C–H bond of a methyl group of 4,4'-dimethyl-2,2'-dipyridyl (**439**), which underwent a substitution reaction with (3-chloropropyl)trimethoxysilane (**440**). The thus synthesized linker **441** was grafted on SBA-15 in toluene by heating, giving the tethered linker **442**. Since the covalently anchored linker **442** contains hydroxyl groups on the surface, the end-capping procedure was subsequently carried out with hexamethyldisilazane, providing the globally protected hydroxyl groups. Lastly, CuI was used as a catalyst precursor for the metallation step, thus generating hybrid copper catalyst **406**.



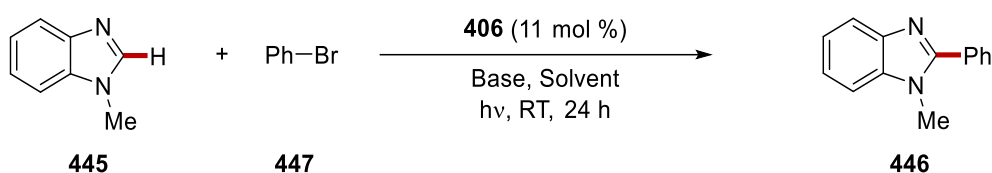
Scheme 3.4.1 Preparation of hybrid copper catalyst.





Additionally, the photo-induced heterogeneous C–H arylation manifold could be extended to the use of more cost-effective aryl bromides **447** (Table 3.4.3). Among various attempts employing different bases, Cs<sub>2</sub>CO<sub>3</sub> proved most efficient, affording 59% of C–H arylated product **446** under photo-induced conditions, and a subsequent reaction with the re-isolated hybrid copper catalyst **406** provided only a slightly lower yield. The use of relatively weak carbonate bases should prove instrumental for applications to substrates with sensitive functional groups.

**Table 3.4.3** Optimization of photo-induced C–H arylation with aryl bromide **447**<sup>[a]</sup>

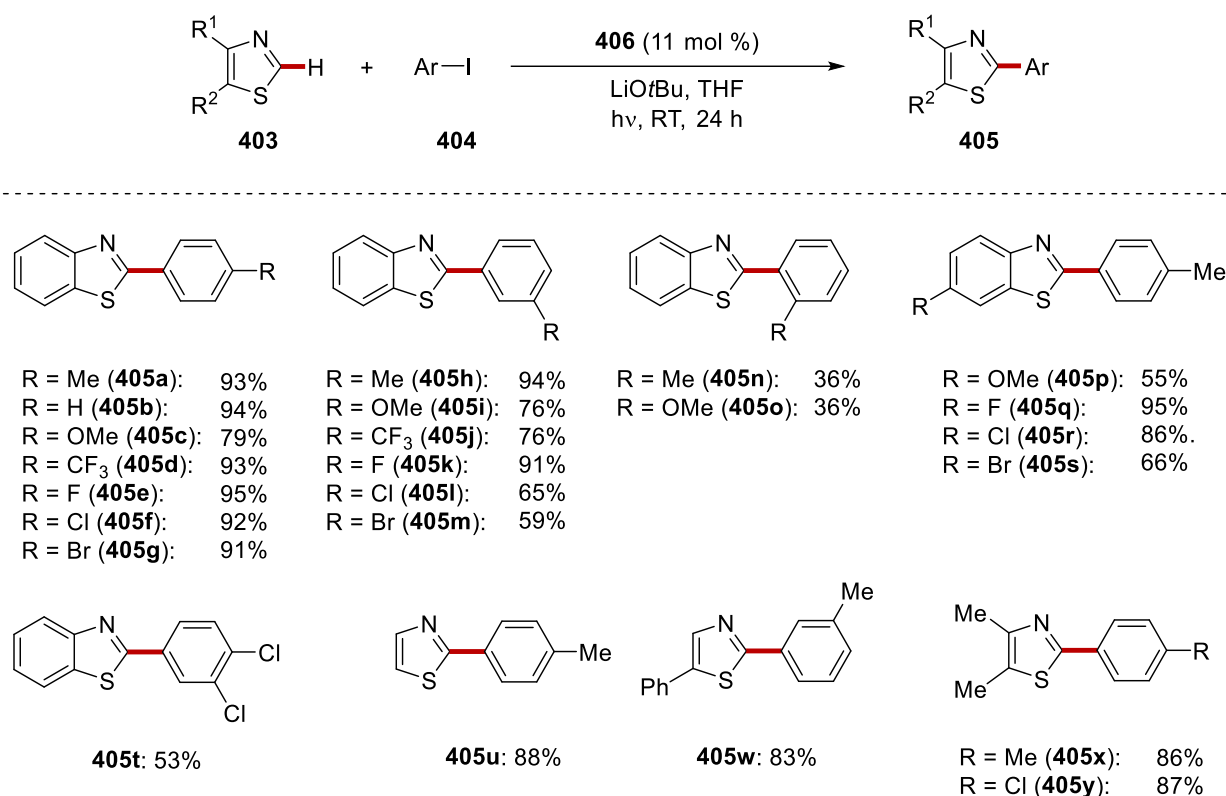


| Entry | Base                            | Solvent           | Yield (%)         |
|-------|---------------------------------|-------------------|-------------------|
| 1     | LiOtBu                          | Et <sub>2</sub> O | 0                 |
| 2     | KOtBu                           | Et <sub>2</sub> O | 0                 |
| 3     | Li <sub>2</sub> CO <sub>3</sub> | Et <sub>2</sub> O | trace             |
| 4     | Na <sub>2</sub> CO <sub>3</sub> | Et <sub>2</sub> O | trace             |
| 5     | K <sub>2</sub> CO <sub>3</sub>  | Et <sub>2</sub> O | 21                |
| 6     | Cs <sub>2</sub> CO <sub>3</sub> | Et <sub>2</sub> O | 59 <sup>[b]</sup> |
| 7     | Cs <sub>2</sub> CO <sub>3</sub> | Et <sub>2</sub> O | 47 <sup>[c]</sup> |

<sup>[a]</sup> Reaction conditions: **445** (0.25 mmol), **447** (1.25 mmol), **406** (11 mol %), base (0.75 mmol), solvent (1.0 mL), 254 nm, RT, 24 h, isolated yield. <sup>[b]</sup> Average yield over two runs. <sup>[c]</sup> With the reused **406**.

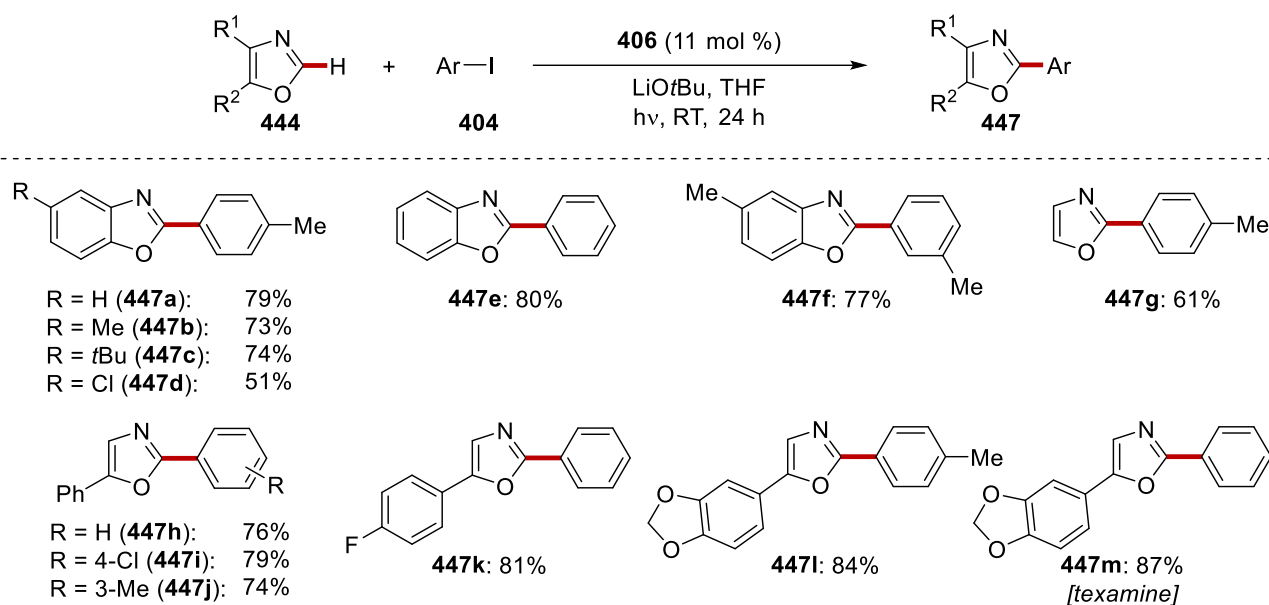
### 3.4.3 Substrate Scope

We explored the versatility of the hybrid copper catalysis for the photo-induced C–H arylation of thiazoles **403** with diversely substituted aryl iodides **404** (Scheme 3.4.2). Thus, we gladly observed high functional group tolerance, including both electron-rich and electron-deficient aryl halides. Particularly, valuable halide functional groups, such as bromo or chloro arenes, remained unreacted, thereby providing high chemoselectivity for C–H arylations.



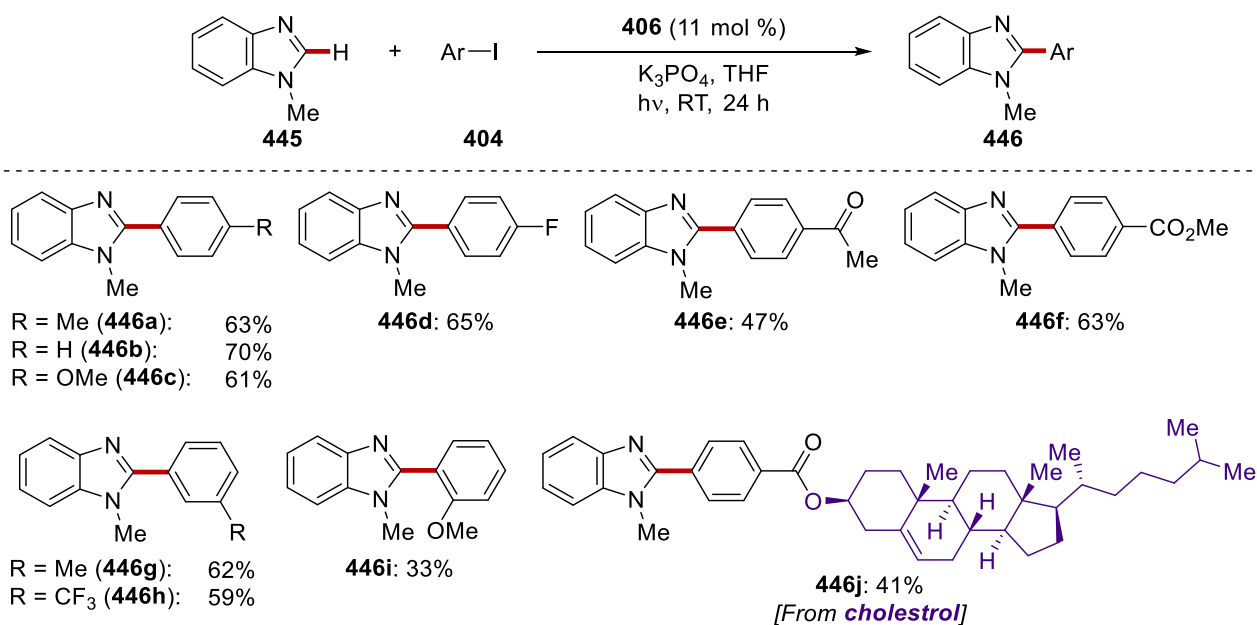
**Scheme 3.4.2** Scope of hybrid copper-catalyzed C–H arylation of (benzo)thiazoles **403** with aryl iodide **404**.

The hybrid copper catalysis manifold was also demonstrated with (benz)oxazoles **444** under photo-induced conditions (Scheme 3.4.3). Likewise, a wide range of functional groups tolerance was depicted with a set of diversely decorated aryl iodides **404**. Notably, with this approach, facile and sustainable access to the alkaloid natural product texamine **447m** was realized.



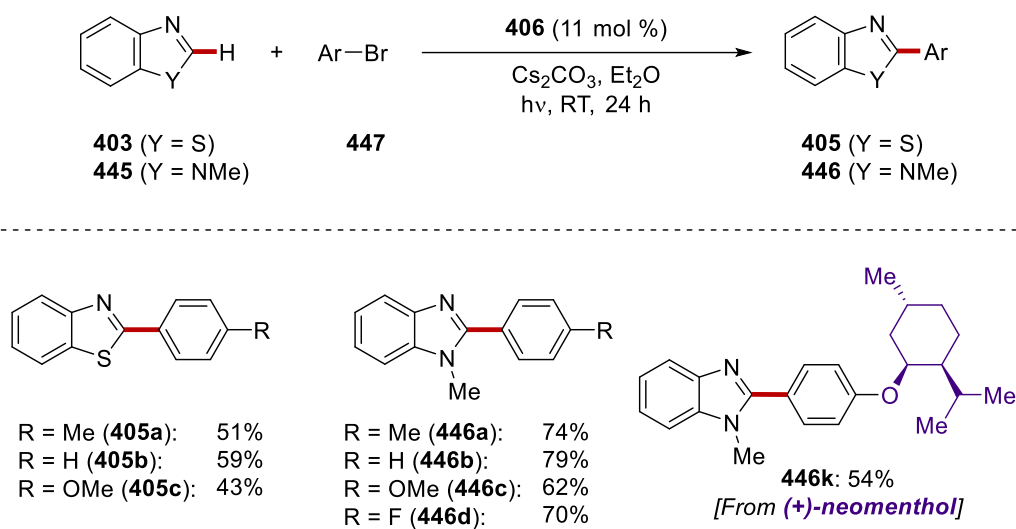
**Scheme 3.4.3** Substrate scope for heterogeneous photo-induced C–H arylation of (benz)oxazole **444**.

The heterogeneous photocatalysis for C–H arylation of *N*-methyl benzimidazoles **445** efficiently provided the C2–H arylated products **446** with a variety of aryl iodides **404** (Scheme 3.4.4). Besides valuable halides groups, this catalytic system tolerated sensitive functional groups, such as ketones **446e** and ester **446f**, by the use of the weak base  $K_3PO_4$  instead of  $LiOtBu$ . Additionally, a steroid derivative was converted to the arylated product **446j** by the photo-induced hybrid copper catalysis.



**Scheme 3.4.4** Hybrid copper-catalyzed C–H arylations of *N*-methyl benzimidazole **445**.

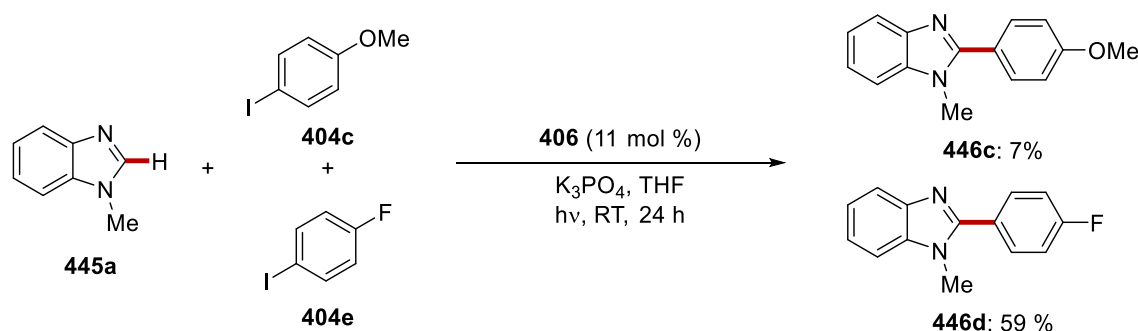
Under the slightly modified condition, aryl bromides **447** were fully acceptable for the direct arylation by the heterogeneous photocatalysis (Scheme 3.4.5). Interestingly, benzothiazole **403** and *N*-methyl benzimidazoles **445** were transformed to the arylated products **405** and **446**, respectively. Consequently, the robustness of the photo-induced C–H arylation by hybrid-copper catalyst was shown by mild and sustainable catalysis along with ample substrate scope.



**Scheme 3.4.5** Photo-induced hybrid copper-catalyzed C–H arylations with aryl bromides **447**.

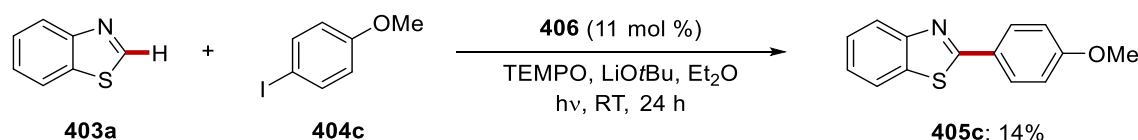
### 3.4.4 Mechanistic Studies

To gain mechanistic insights, an intermolecular competition experiment was performed with differently substituted aryl iodides **404c** and **404e** (Scheme 3.4.6). Here, it was found that the electron-deficient aryl iodide **404e** underwent faster direct arylation. This result suggests the oxidative addition of the aryl halide onto the copper(I) intermediate to be rate-determining.



**Scheme 3.4.6** Intermolecular competition experiment.

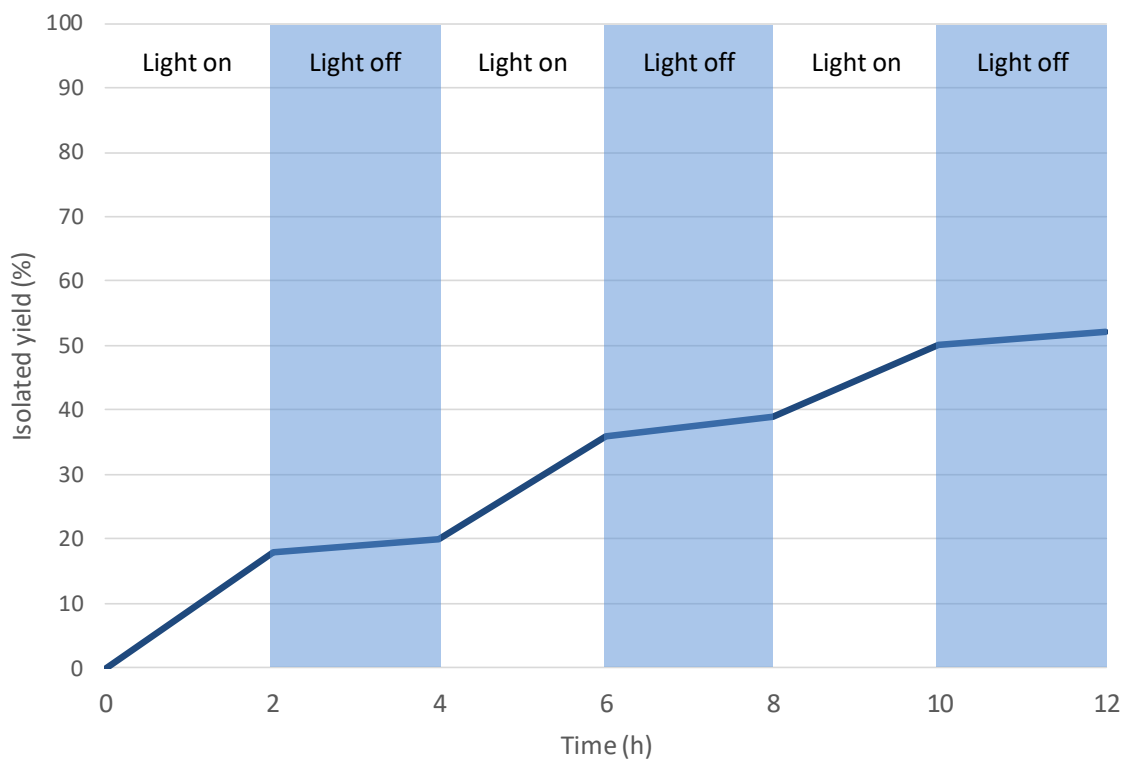
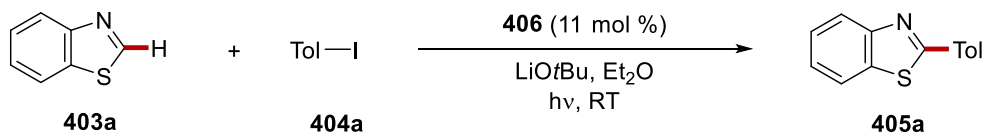
Furthermore, the reaction in the presence of representative radical scavenger TEMPO probed a SET-type regime by resulting in significant inhibition of the photo-induced hybrid-copper catalysis for C–H arylation (Scheme 3.4.7).



**Scheme 3.4.7** Radical experiment.

Finally, we probed the photo-induced C–H arylation by an on-off experiment, in which the light source was turned off every two hours. This study highlighted that the hybrid-copper-catalyzed C–H arylation was fully suppressed in the absence of light, and simultaneously showed that constant irradiation is required for effective product formation (Scheme 3.4.8).

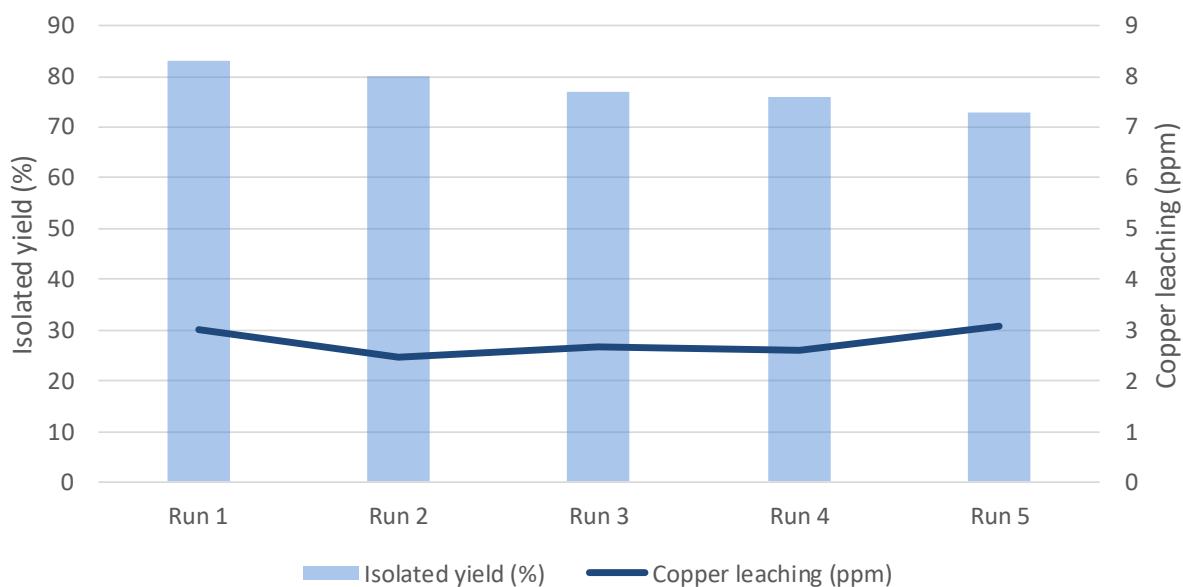
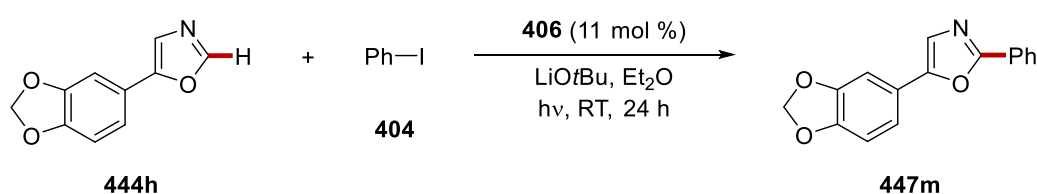




**Scheme 3.4.8** On-off light experiments for photo-induced hybrid-copper-catalyzed C–H arylation.

### 3.4.5 Heterogeneity Studies

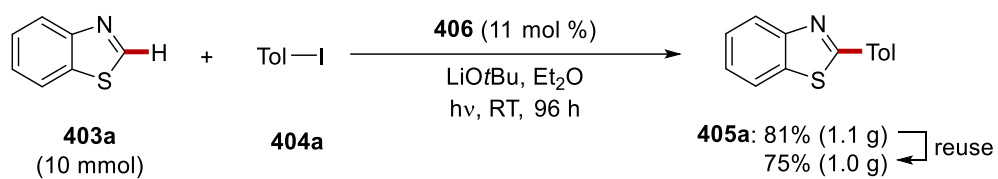
Next, we became intrigued to probing potential reusable nature. We were delighted to observe that the hybrid copper catalyst **406** could be recycled without a significant loss of catalytic efficacy over the five runs of the reaction (Scheme 3.4.9). Especially, this approach enabled us to construct the natural product **447m** in a sustainable fashion. Within a collaboration with Dr. Volker Karius, a ICP-OES analysis of the reaction mixture was performed, thus revealing that less than 4 ppm of copper was detected in the solution.



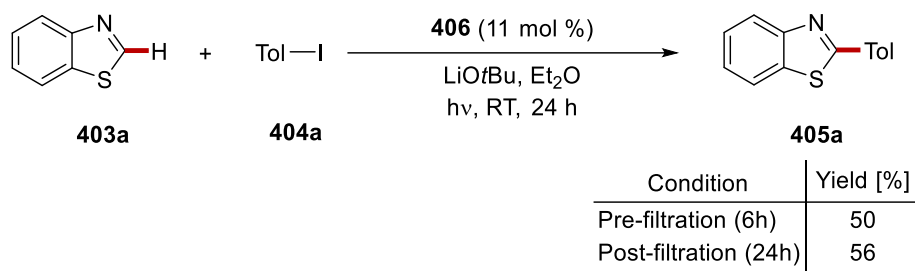
**Scheme 3.4.9** Reuse test for the hybrid-copper catalyzed photo-induced C–H arylation.

Additionally, the reusability was also demonstrated in a gram-scale reaction (Scheme 3.4.10a). The classical heterogeneity experiment, a filtration test (Scheme 3.4.10b), was performed, reflecting homogeneous catalysis not to be operative.

a) Scaled reuse test



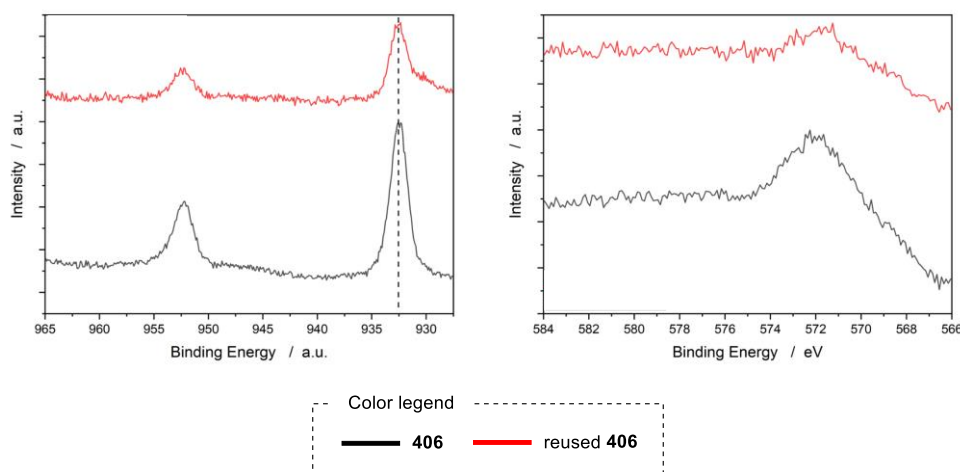
b) Filtration test



Scheme 3.4.10 Reuse test and filtration test.

### 3.4.6 Characterization of Hybrid Copper Catalyst

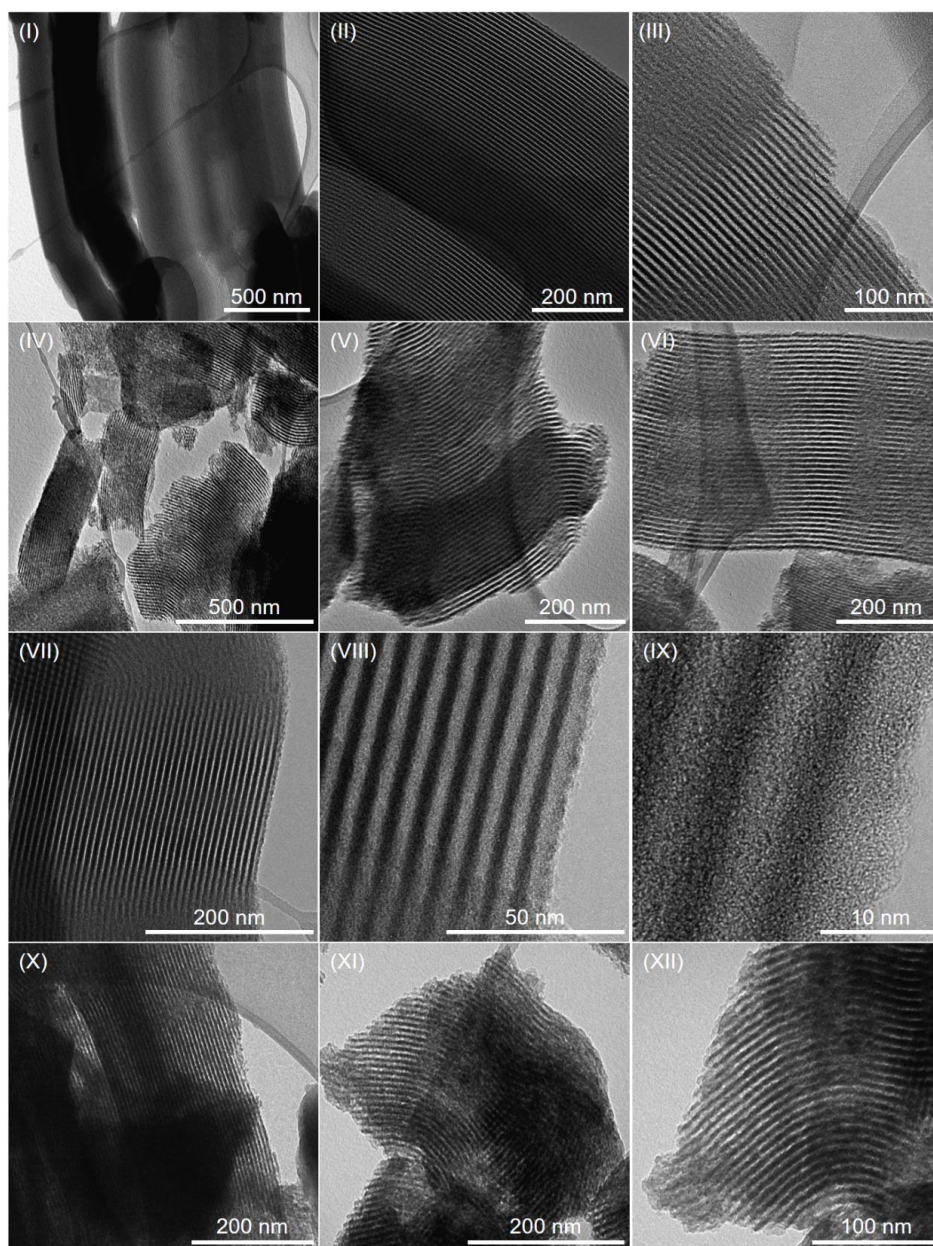
In a collaboration with Prof. Dr. Wolfgang Viöl and Dr. Robert Köhler, X-ray photoelectron spectroscopic analysis was performed (Scheme 3.4.11). In this study, the Cu  $2p_{3/2}$  peak was investigated for the determination of the oxidation state of copper. The peaks of the hybrid copper catalyst **406** and the reused hybrid copper catalyst were located at 932.6 eV, indicating the presence of either Cu(0) or Cu(I). For the differentiation of Cu(0) and Cu(I), the Cu LMM-Auger peak was additionally analyzed. The measured Cu LMM peaks were compared with the reported results, which clearly revealed Cu(I) of the oxidation state of hybrid copper catalyst **406** as well as the reused hybrid copper catalyst. These results showed that the oxidation state of the hybrid catalyst was not changed after the photo-induced C–H arylation reaction.



**Scheme 3.4.11** X-ray photoelectron spectroscopic (XPS) analysis of **406** and reused **406**.

In a collaboration with Prof. Dr. Christian Jooss and Gaurav Lole, detailed transmission electron microscopic studies were performed (Scheme 3.4.12). Thereby, SBA-15, **443**, the hybrid copper catalyst **406**, and the reused hybrid copper catalyst were subjected to the microscopic analyses. TEM images of the SBA-15 and **406** showed homogeneously ordered one-dimensional mesoporous channels with homogeneous morphology, which was observed by the striped contrast with the average distance of 10.2 nm between the centers of the one-dimensional mesoporous channel and its adjacent channel (Scheme 3.4.12I–VI). TEM images of the hybrid copper catalyst **406** revealed that the highly ordered

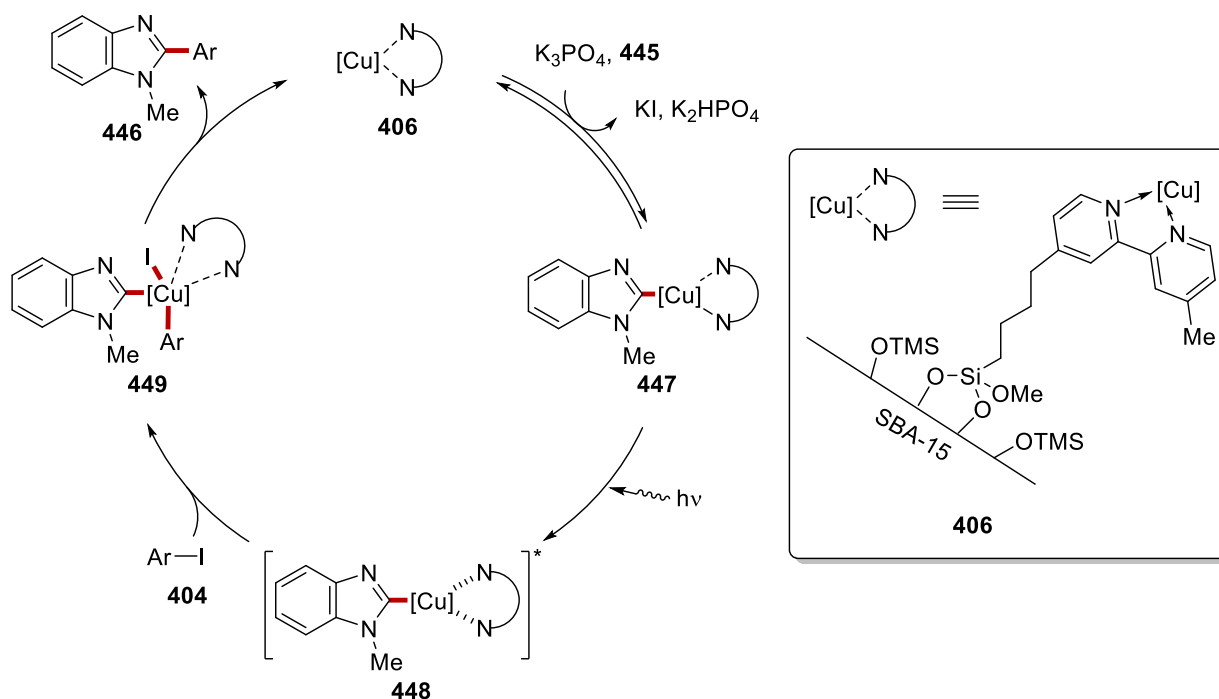
structure of SBA-15 was preserved and a tendency of aggregation was not observed (Scheme 3.4.12VII–XII). TEM analysis of the reused hybrid copper catalyst also showed that there were no copper nanoparticles formed by agglomeration while ordered striped contrast remained unchanged in the one-dimensional mesoporous channels (Figure 3.4.12). These results highlighted the outstanding reusability and stability during the preparation of the hybrid copper catalyst **406** as well as the course of the photo-induced C–H arylations.



**Scheme 3.4.12** Transmission electron microscopic (TEM) studies of hybrid copper catalysts **406**.

### 3.4.7 Proposed Mechanism

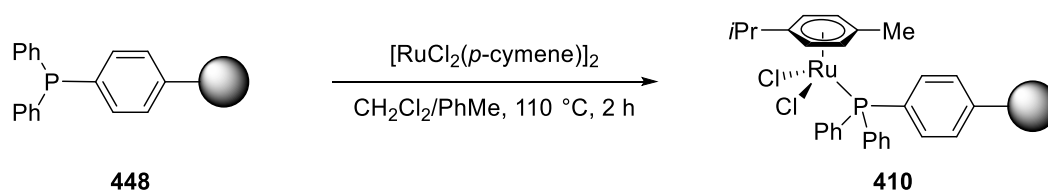
On the basis of our detailed mechanistic studies and the characterization of the hybrid copper catalyst, a plausible catalytic cycle for the photo-induced heterogeneous C–H arylation is proposed in Scheme 3.4.13. The mechanistic rationale commences with hybrid copper(I) catalyst **406** and *N*-Methyl benzimidazole **445**, forming copper complex **447** with the aid of a base. Irradiation of the copper complex **447** leads to a photo-excited state **448**, followed by a SET process involving aryl iodides **404** generating intermediate **449**. Finally, subsequent reductive elimination affords arylated product **446**, while simultaneously regenerating the hybrid copper(I) catalyst.



**Scheme 3.4.13** Proposed catalytic cycle of photo-induced hybrid copper-catalyzed C–H arylation.

### 3.5 Distal C–H Activation by Reusable Heterogeneous Ruthenium Catalyst

A plethora of *ortho*-selective aromatic C–H functionalizations has been accomplished by proximity-induced C–H activation through chelation assistance.<sup>[20a]</sup> In sharp contrast, distal C–H functionalizations continue to be challenging with considerable momentum gained by steric control, template assistance, weak hydrogen bonding, or transient mediator as described in the Chapter 1.2.2. Recently, Ackermann,<sup>[82, 83, 85, 88, 90, 92, 251]</sup> Greaney,<sup>[252]</sup> and Frost<sup>[72f, 96d]</sup> among others<sup>[253]</sup> developed site-selective C–H functionalization *via* ruthenium-catalyzed  $\sigma$ -activation, allowing *meta*- and *para*-functionalization of arenes.<sup>[72c, 72d]</sup> In spite of recent notable progress, the realm of C–H functionalizations was thus far considerably limited to homogeneous catalysis. Taking advantage of the use of phosphine ligands in the ruthenium-catalyzed distal functionalizations,<sup>[88, 251]</sup> we envisaged using phosphine-based polymer support to immobilize the ruthenium catalyst (Scheme 3.5.1).

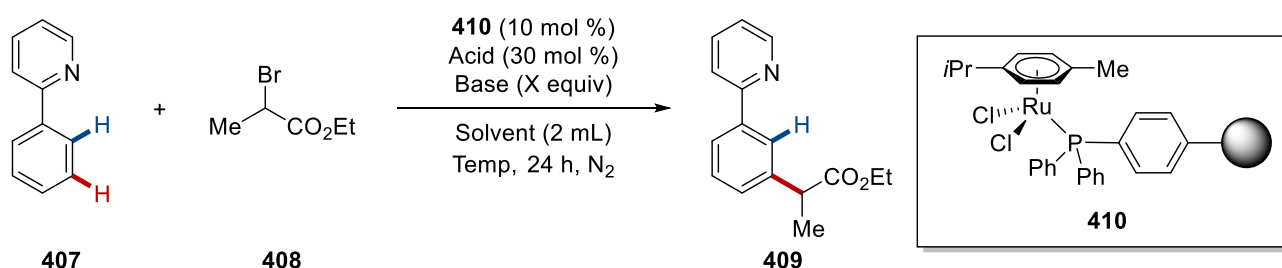


**Scheme 3.5.1** Preparation of the hybrid ruthenium catalyst.

### 3.5.1 Optimization Studies

We initiated our studies by probing various reaction conditions with the thus synthesized polymer-based hybrid ruthenium catalyst for the *meta*-C–H alkylation of arene **407** (Table 3.5.1). First, we explored different types of bases in 1,4-dioxane as the solvent at 100 °C (entries 1–5). However, it was found that the addition of acid was not necessary for the ruthenium-catalyzed *meta*-C–H alkylation, while KOAc provided better conversion among various bases (entries 6–10). After a considerable testing of solvents and reaction temperatures, we were delighted to obtain the optimized conditions where the use of 2-MeTHF as the solvent and 60 °C of reaction temperature could provide 70% of isolated yield (entries 11–15). Notably, biomass-derived 2-MeTHF is considered as a green alternative to THF, and can be produced from renewable resources.<sup>[254]</sup> A control experiment confirmed the essential role of the recyclable hybrid-ruthenium catalyst (entry 16), while the recyclability of the hybrid ruthenium catalyst **410** was proved (entry 17).

**Table 3.5.1** Optimization studies for hybrid-ruthenium-catalyzed *meta*-C–H alkylation.<sup>[a]</sup>



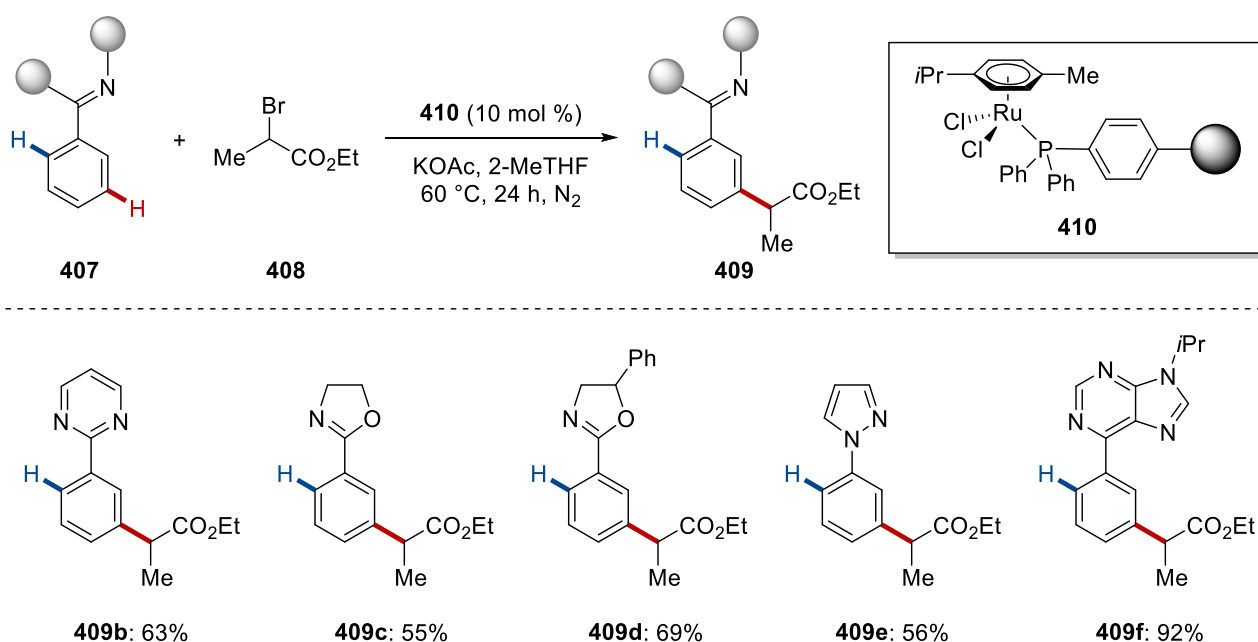
| Entry | Acid                 | Base (X equiv)                        | Solvent     | Temp (°C) | Yield (%) <sup>a</sup> |
|-------|----------------------|---------------------------------------|-------------|-----------|------------------------|
| 1     | MesCO <sub>2</sub> H | Na <sub>2</sub> CO <sub>3</sub> (1.0) | 1,4-Dioxane | 100       | 31                     |
| 2     | MesCO <sub>2</sub> H | K <sub>2</sub> CO <sub>3</sub> (1.0)  | 1,4-Dioxane | 100       | 32                     |
| 3     | MesCO <sub>2</sub> H | K <sub>3</sub> PO <sub>4</sub> (1.0)  | 1,4-Dioxane | 100       | 40                     |
| 4     | MesCO <sub>2</sub> H | NaOAc (1.0)                           | 1,4-Dioxane | 100       | 25                     |
| 5     | MesCO <sub>2</sub> H | KOAc (1.0)                            | 1,4-Dioxane | 100       | 11                     |
| 6     | --                   | K <sub>2</sub> CO <sub>3</sub> (1.0)  | 1,4-Dioxane | 100       | trace                  |
| 7     | --                   | Na <sub>2</sub> CO <sub>3</sub> (1.0) | 1,4-Dioxane | 100       | 21                     |



|    |    |                                      |                    |     |                   |
|----|----|--------------------------------------|--------------------|-----|-------------------|
| 8  | -- | K <sub>3</sub> PO <sub>4</sub> (1.0) | 1,4-Dioxane        | 100 | 31                |
| 9  | -- | KOAc (1.0)                           | 1,4-Dioxane        | 100 | 33                |
| 10 | -- | KOAc (1.0)                           | 1,4-Dioxane        | 80  | 40                |
| 11 | -- | KOAc (1.0)                           | PhCMe <sub>3</sub> | 80  | 25                |
| 12 | -- | KOAc (1.0)                           | 2-MeTHF            | 80  | 44                |
| 13 | -- | KOAc (2.0)                           | 2-MeTHF            | 80  | 61                |
| 14 | -- | KOAc (2.0)                           | 2-MeTHF            | 60  | 70                |
| 15 | -- | KOAc (2.0)                           | 2-MeTHF            | 40  | 53                |
| 16 | -- | KOAc (2.0)                           | 2-MeTHF            | 60  | 0 <sup>[b]</sup>  |
| 17 | -- | KOAc (2.0)                           | 2-MeTHF            | 60  | 69 <sup>[c]</sup> |

<sup>[a]</sup> Reaction conditions: **407** (0.25 mmol), **408** (0.75 mmol), **410** (10 mol %), solvent (1.0 mL), 24 h, isolated yield. <sup>[b]</sup> Without **410**. <sup>[c]</sup> With the reused **410**.

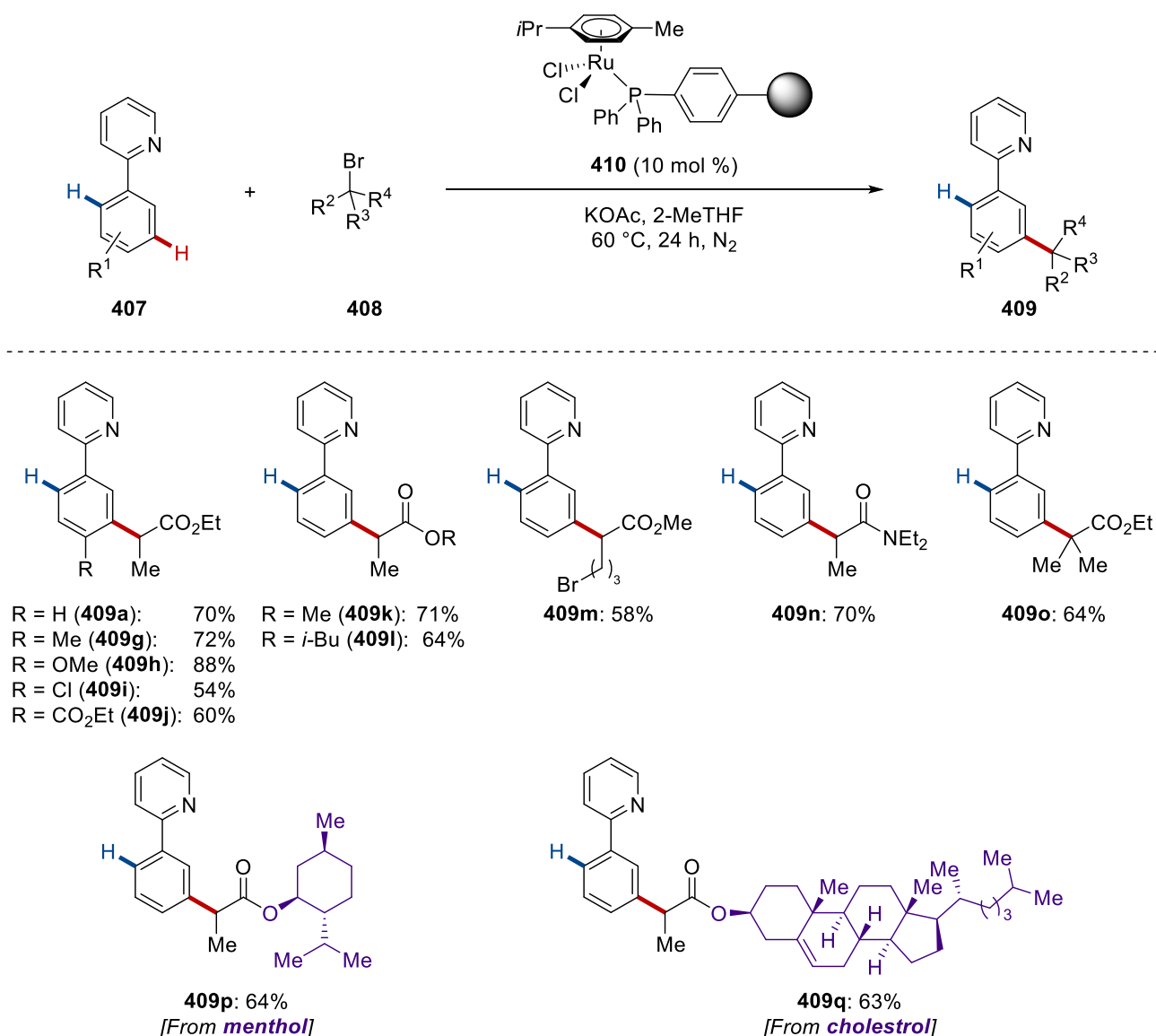
The optimized heterogeneous catalyst was not limited to substrates bearing the pyridine directing group. Indeed, other directing groups, such as pyrimidines, oxazolines, pyrazoles, and purines were acceptable for the hybrid ruthenium-catalyzed *meta*-C–H alkylation (Scheme 3.5.2).



**Scheme 3.5.2** Different directing groups for hybrid ruthenium-catalyzed *meta*-C–H alkylation.

### 3.5.2 Substrate Scope

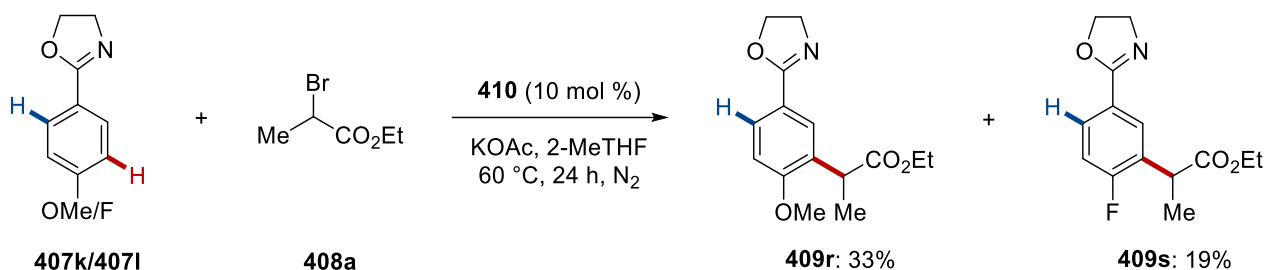
We commenced exploring the versatility of the hybrid-ruthenium-catalyzed *meta*-C–H functionalization with a set of representative arenes **407** (Scheme 3.5.3). Differently substituted arenes **407** bearing electron-deficient and electron-rich functional groups were position-selectively transformed to the desired *meta*-functionalized products **408**. Distal *meta*-C–H alkylation by the hybrid ruthenium catalyst **410** tolerated various alkyl bromides **408**, including valuable functional groups, featuring halides, ethers, esters, and amides, while natural product derivatives **409p** and **409q** were selectively converted.



**Scheme 3.5.3** Substrate scope for hybrid ruthenium-catalyzed *meta*-C–H alkylations.

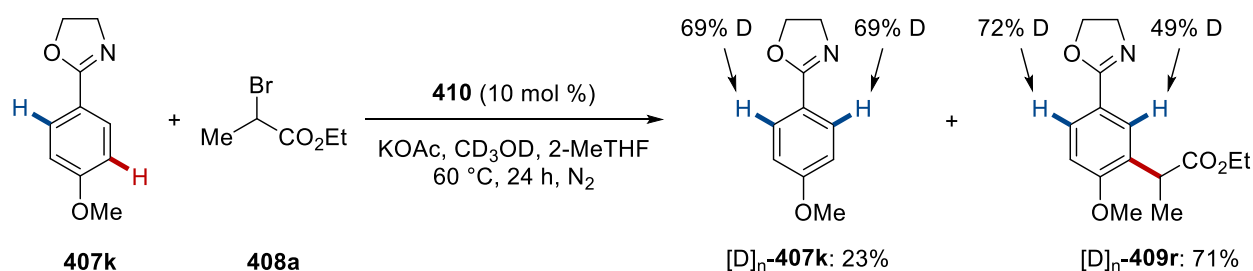
### 3.5.3 Mechanistic Studies

Furthermore, we performed detailed mechanistic studies to elucidate the hybrid ruthenium catalyst's mode of action. To this end, an intermolecular competition experiment was carried out, revealing that the electron-rich arene **407k** was preferentially reacted (Scheme 3.5.4). This result suggests that a BIES-type C–H metalation pathway is involved in the hybrid ruthenium-catalyzed *meta*-C–H alkylation.



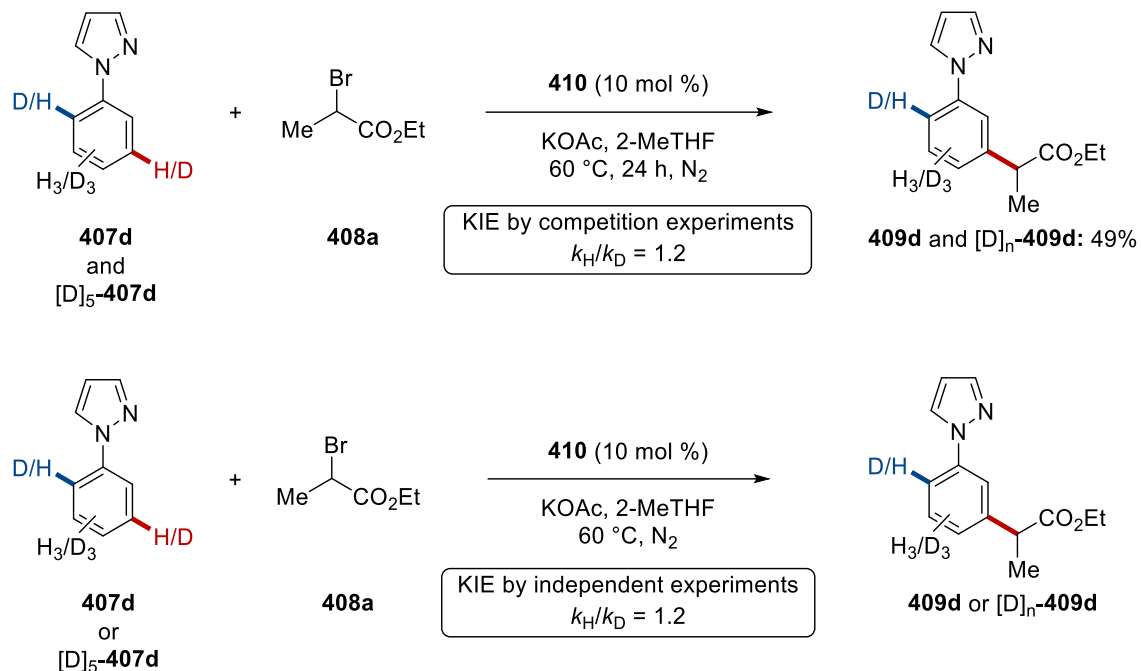
**Scheme 3.5.4** Competition experiment between arenes **407k** and **407l**.

Additionally, the reaction in the presence of isotopically labelled CD<sub>3</sub>OD afforded 69% of deuteration in the reisolated substrate [D]<sub>n</sub>-**407k** and 72% and 49% of deuteration in the *ortho*-positions of the desired product **409r** (Scheme 3.5.5). These experimental results provided a strong support for a reversible C–H activation.



**Scheme 3.5.5** H/D exchange study.

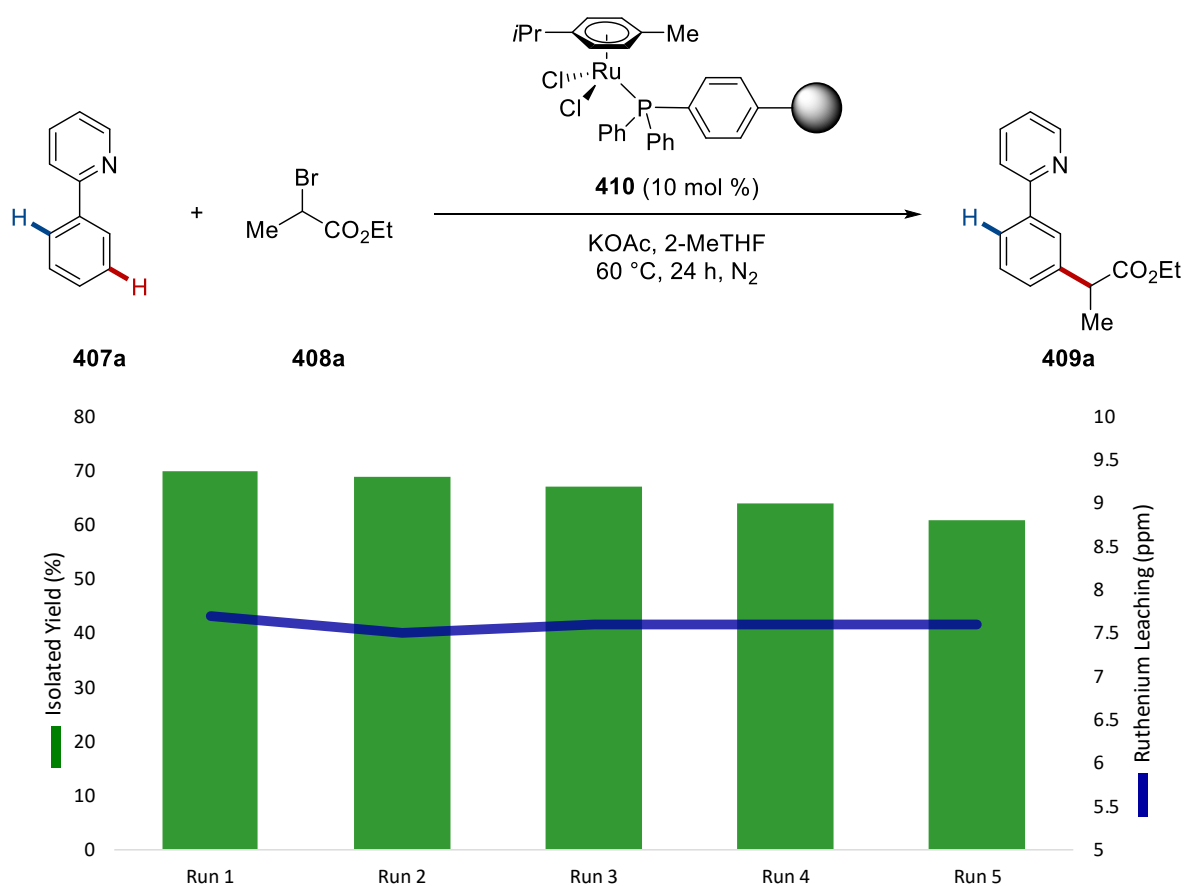
In addition, the KIE was studied, indicating a primary isotope effect in both competition and independent experiments (Scheme 3.5.6). This study clearly revealed that C–H cleavages at the *ortho* and *meta* positions are not kinetically relevant.



**Scheme 3.5.6** Kinetic isotope effect studies.

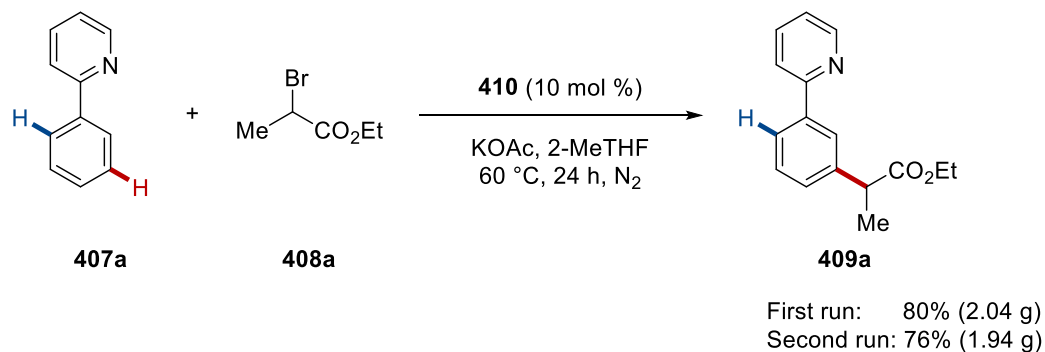
### 3.5.4 Heterogeneity Studies

To probe the heterogeneity of the hybrid-ruthenium-catalyst, a variety of experiments were conducted. We were hence delighted to observe that the hybrid-ruthenium featured an excellent reusability, enabling practical access to *meta*-C–H alkylated arenes (Scheme 3.5.7). Industries and pharma companies performing large-scale reactions or flow applications in homogeneous catalysis mainly are concerned with the removal of metal impurities, which are detrimental to synthetic and economic efficiency, while the well-designed heterogeneous catalysts could avoid the additional processes by a simple separation. Within a collaboration with Dr. Volker Karius, less than 8 ppm of ruthenium was detected by ICP-OES studies of the reaction mixture, reflecting a negligible leaching of the transition metal.



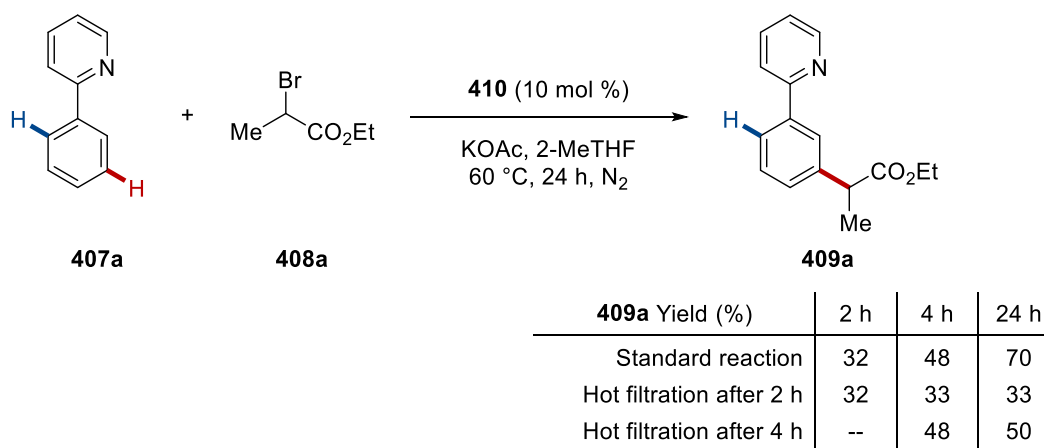
**Scheme 3.5.7** Reuse test for hybrid ruthenium-catalyzed *meta*-C–H alkylation and the determination of ruthenium leaching.

The sustainable feature of the hybrid-ruthenium catalysis was also mirrored by a gram-scale reaction, maintaining a high efficiency with position-selectivity and reusability of the hybrid-ruthenium catalyst (Scheme 3.5.8).



**Scheme 3.5.8** Scaled reuse test.

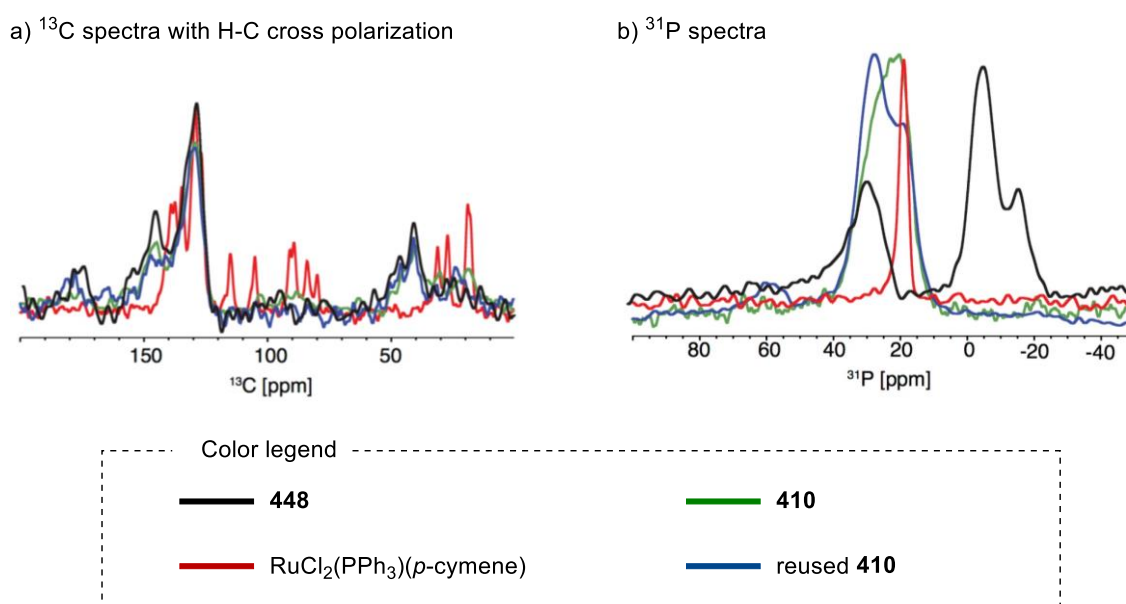
Additionally, a hot-filtration test demonstrated that the physical removal of the hybrid-ruthenium catalyst completely inhibited the hybrid catalysis for *meta*-C–H alkylation (Scheme 3.5.9).



**Scheme 3.5.9** Hot filtration test.

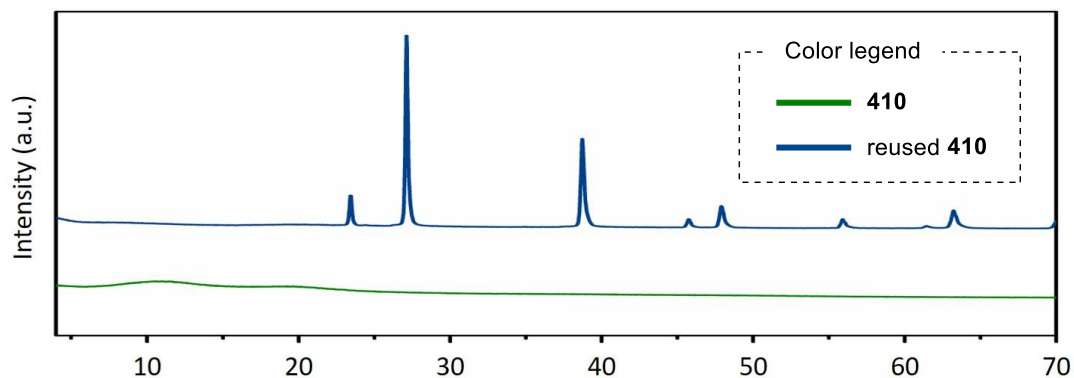
### 3.5.5 Characterizations of Hybrid Ruthenium Catalyst

Given the unique features of recyclable and reusable hybrid ruthenium catalyst **410**, we sought to determine its chemical and physical properties. Within a collaboration with the Loren group, we conducted detailed solid-state NMR spectroscopic studies of the **448**,  $\text{RuCl}_2\text{PPh}_3(p\text{-cymene})$ , **410**, and reused **410** (Scheme 3.5.10). Interestingly,  $^{13}\text{C}$  and  $^{31}\text{P}$  NMR spectra showed similar chemical shifts among  $\text{RuCl}_2\text{PPh}_3(p\text{-cymene})$ , **410**, and the reused **410**, providing a strong evidence that the coordination of ruthenium by phosphorus remained stable during the course of the hybrid-ruthenium catalysis.



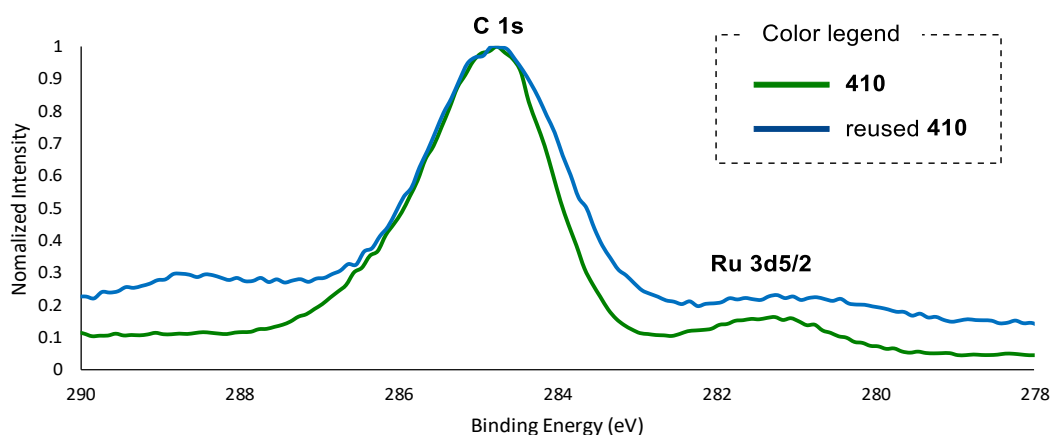
**Scheme 3.5.10** Solid-state NMR analysis

Furthermore, with the assistance of the Alauzun group, the powder X-ray diffraction (PXRD) patterns of the **410** identified two very wide peaks around  $10^\circ$  and  $20^\circ$  showing the amorphous support, whereas the formation of crystalline ruthenium compounds, for example, ruthenium oxide, was not detected (Scheme 3.5.11). The PXRD patterns from the reused **410** confirmed crystalline KBr (JCPDS 730381) as an insoluble byproduct in 2-MeTHF, while the residue was proven to be innocuous to the reusability of the hybrid-ruthenium catalyst.



**Scheme 3.5.11** Powder X-ray diffraction studies.

Dr. Alauzun and Dr. Wang also performed X-ray photoelectron spectroscopy to determine the oxidation state of ruthenium from **410** and the reused **410** (Scheme 3.5.12). In this analysis, the peak of Ru 3d5/2 at 281.1 eV from the surface of both catalysts was observed, which corresponds to ruthenium(II) species.



**Scheme 3.5.12** X-ray photoelectron spectroscopic analysis.

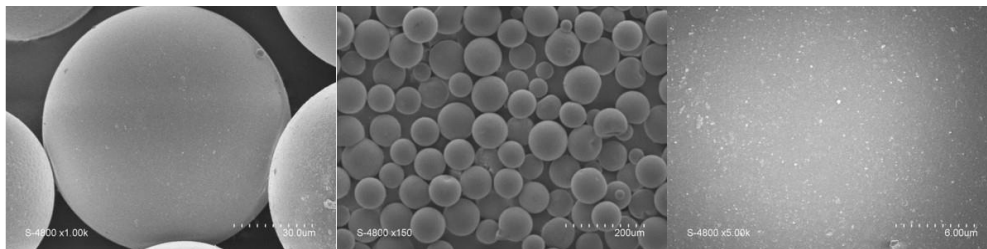
Additionally, the Alauzun group performed detailed microscopic studies, including scanning electron microscopy (SEM), transmission electron microscopy (TEM), and transmission electron microscopy energy-dispersive X-ray spectroscopy (TEM-EDX) studies of the hybrid catalyst **410** and the reused catalyst **410** (Scheme 3.5.13). SEM analysis of the **410** revealed non-aggregated spheres up to 100  $\mu\text{m}$  in diameter with a relatively smooth surface. The reused **410** in SEM studies showed innocent KBr on



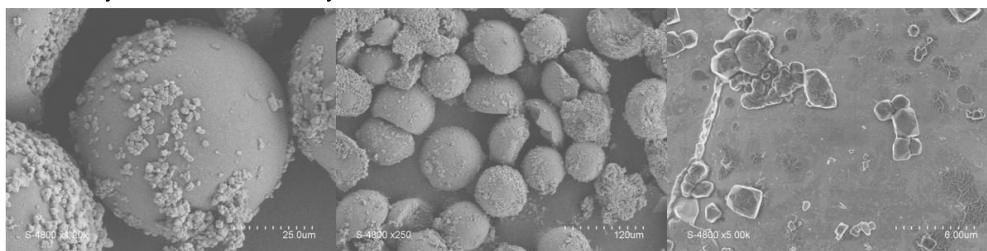
the surface previously detected by PXRD. TEM analysis of the **410** and the reused **410** revealed that both hybrid catalysts have homogeneous non-porous amorphous morphology.

a) Scanning electron microscopy analysis

i) Hybrid ruthenium catalyst **410**

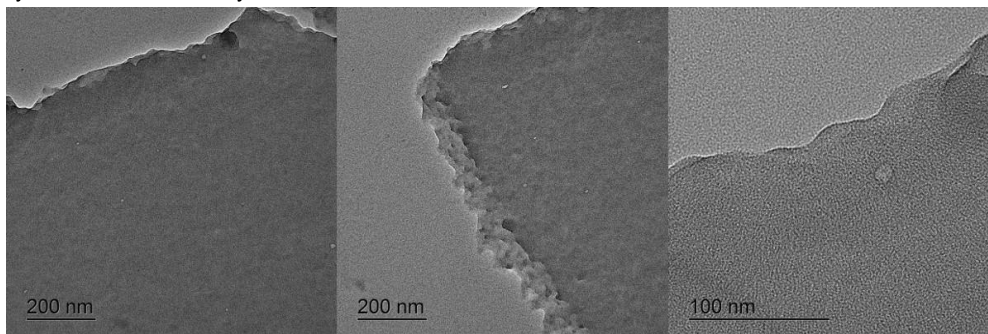


ii) Reused hybrid ruthenium catalyst **410**

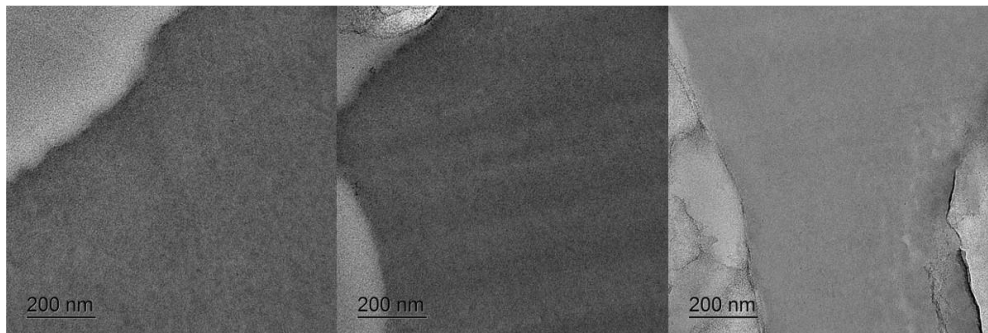


b) Transmission electron microscopy analysis

i) Hybrid ruthenium catalyst **410**



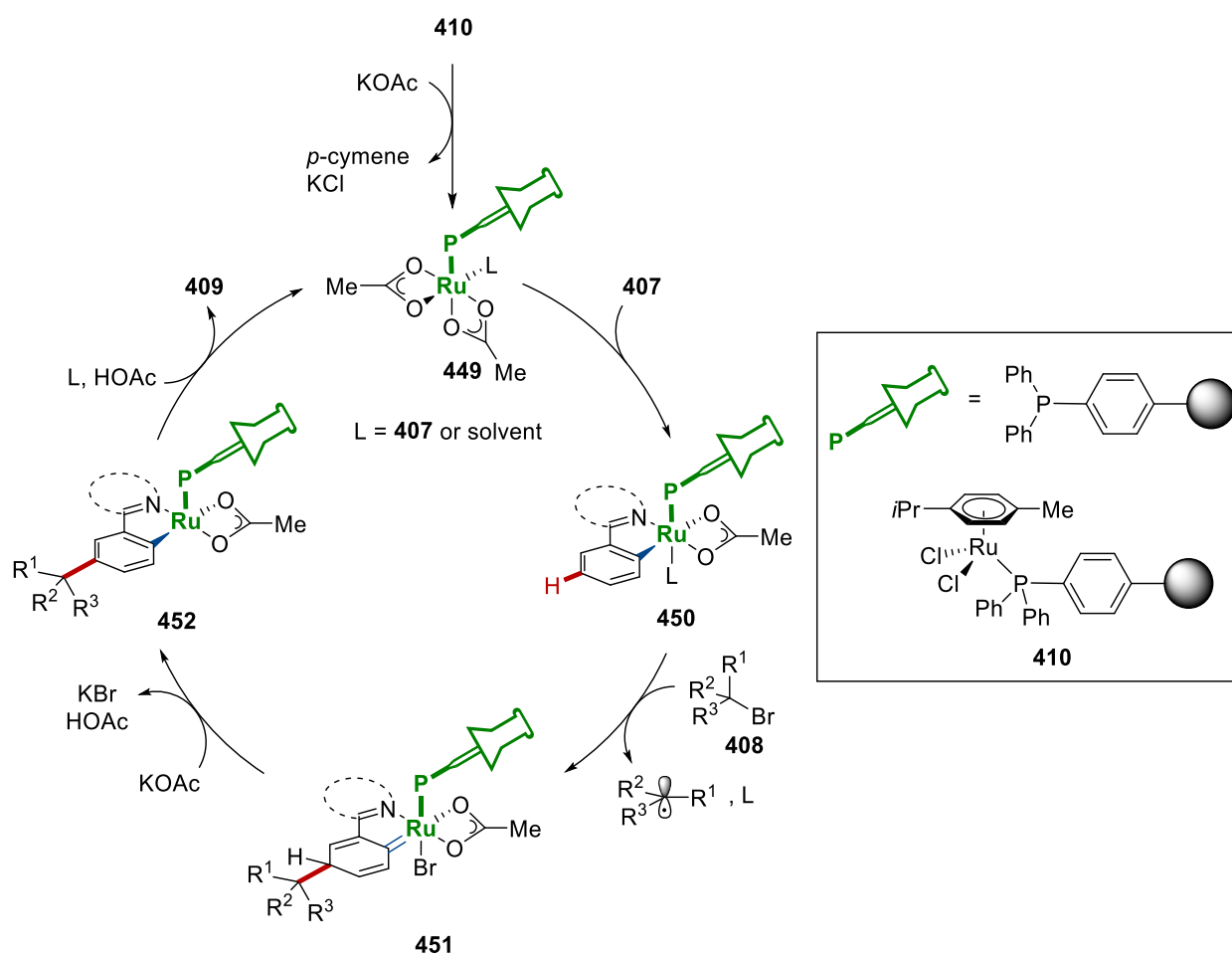
ii) Reused hybrid ruthenium catalyst **410**



**Scheme 3.5.12** X-ray photoelectron spectroscopic analysis.

### 3.5.6 Proposed Mechanism

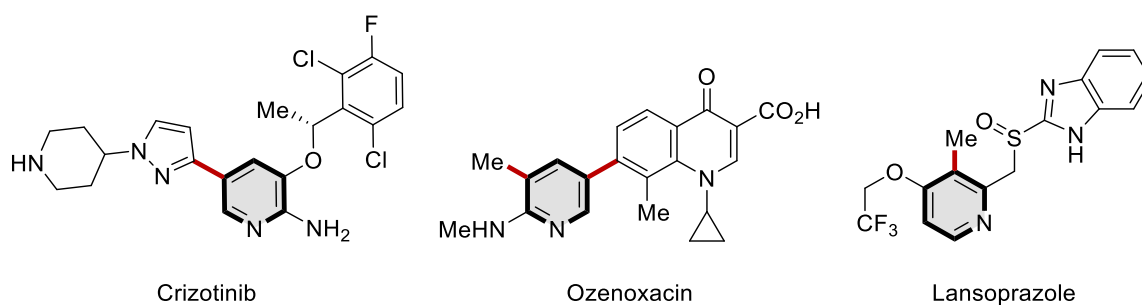
On the basis of our detailed experimental mechanistic studies along with the spectroscopic and microscopic characterization of the hybrid-ruthenium catalyst, a plausible catalytic cycle for the heterogeneous *meta*-C–H alkylation is proposed in Scheme 3.5.13. The mechanistic rationale commences by a carboxylate-assisted, BIES-C–H ruthenation. Subsequently, ruthenium(III) intermediate is generated *via* a single electron transfer from the ruthenium(II) complex **449** to the alkyl halide **408**. The alkyl radical attacks the aromatic moiety at the *para*-position to ruthenium, giving intermediate **451**. Thereafter, aromatization followed by protodemetalation delivers the desired *meta*-alkylated product **409** and regenerates the catalytically active ruthenium hybrid catalyst **449**.



**Scheme 3.5.13** Proposed mechanism of hybrid ruthenium-catalyzed *meta*-C–H alkylation.

### 3.6 C–H Arylations and Alkylations by Reusable Heterogeneous Manganese Catalyst

Azines are key structural motifs in a plethora of bio-relevant, pharmaceuticals, and drugs.<sup>[217, 255]</sup> Particularly, C3–H functionalized pyridine scaffolds broadly exhibit numerous biological activities (Scheme 3.6.1).<sup>[256]</sup> Consequently, there is a continued strong demand for efficient C–H functionalizations of pyridines in a sustainable manner.<sup>[257]</sup>

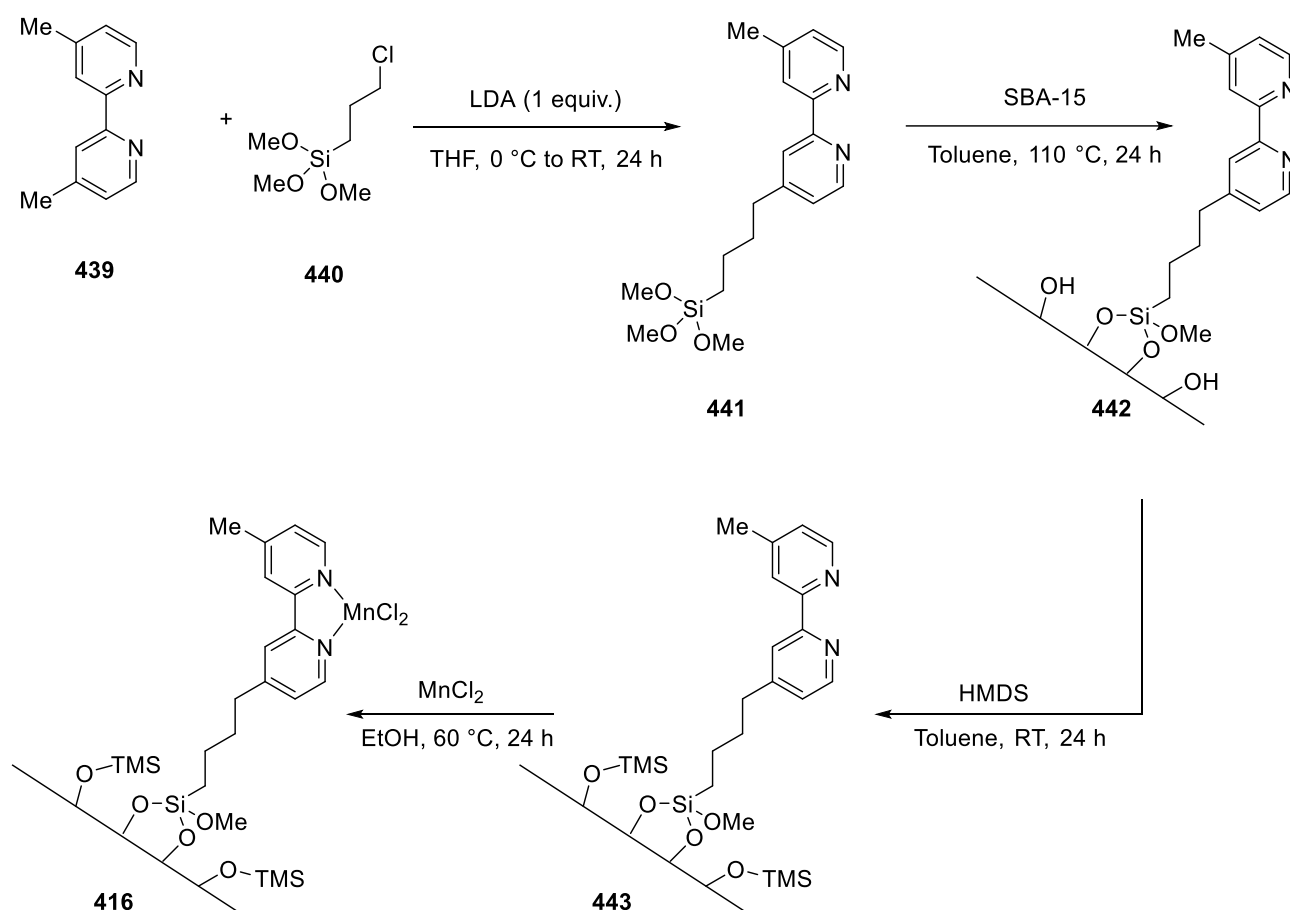


**Scheme 3.6.1** Selected bio-active drugs containing C3–H functionalized pyridine motifs.

Earth-abundant 3d metal catalysts provide prospect for less toxic metals in C–H activations<sup>[216]</sup> with notable advances in manganese-catalyzed C–H activation<sup>[258, 168c]</sup> by Kuninobu/Takai,<sup>[259]</sup> Wang,<sup>[260, 122]</sup> and Ackermann,<sup>[261, 128, 132, 147b, 186b]</sup> among others.<sup>[140, 262, 127]</sup> Despite the indisputable progress, manganese-catalyzed-C–H functionalizations continue to be largely limited to homogeneous catalysis.

### 3.6.1 Preparation of Hybrid Manganese Catalyst

The hybrid manganese catalyst **416** was synthesized under a modified protocol from Christopher (Scheme 3.6.2).<sup>[249a]</sup> To construct the linker, LDA deprotonated a C–H bond of a methyl group of 4,4'-dimethyl-2,2'-dipyridyl (**439**), which underwent a substitution reaction with (3-chloropropyl)trimethoxysilane (**440**). The thus obtained linker **441** was grafted on SBA-15 in toluene under the reflux conditions, giving the tethered linker **442**. Since the covalently anchored ligand **442** contains hydroxyl groups on the surface, the end-capping procedure was subsequently carried out with HMDS. Lastly,  $\text{MnCl}_2$  was used as a catalyst precursor for the metallation step, thus giving the hybrid manganese catalyst **416**.

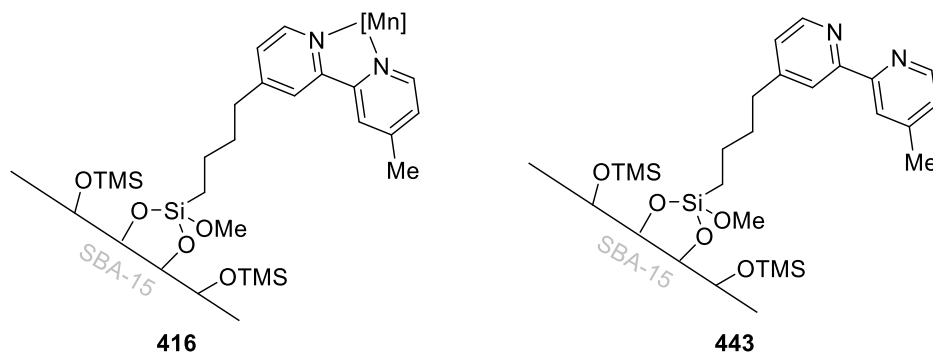
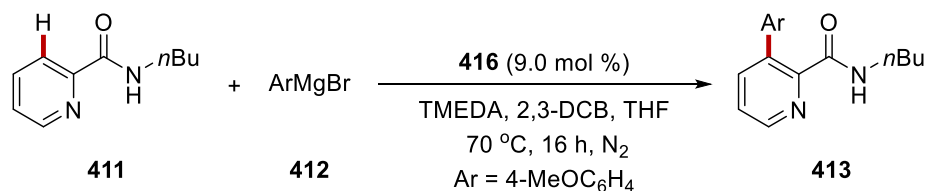


Scheme 3.6.2 Preparation of hybrid manganese catalyst.

### 3.6.2 Optimization Studies

Next, we probed various reaction conditions for the envisioned C–H arylation of pyridines **411** with the synthesized hybrid-manganese catalyst **416** (Table 3.6.1). We were pleased to observe that the desired arylated product **413** was obtained (entry 1). It is noteworthy that the hybrid catalyst could be successfully recycled and reused (entry 2). In contrast, the use of simple MnCl<sub>2</sub> provided unsatisfactory results (entry 3). Control experiments verified the essential role of the hybrid-manganese catalyst, the ligand, and the DCB oxidant for C–H arylations (entries 4–7).

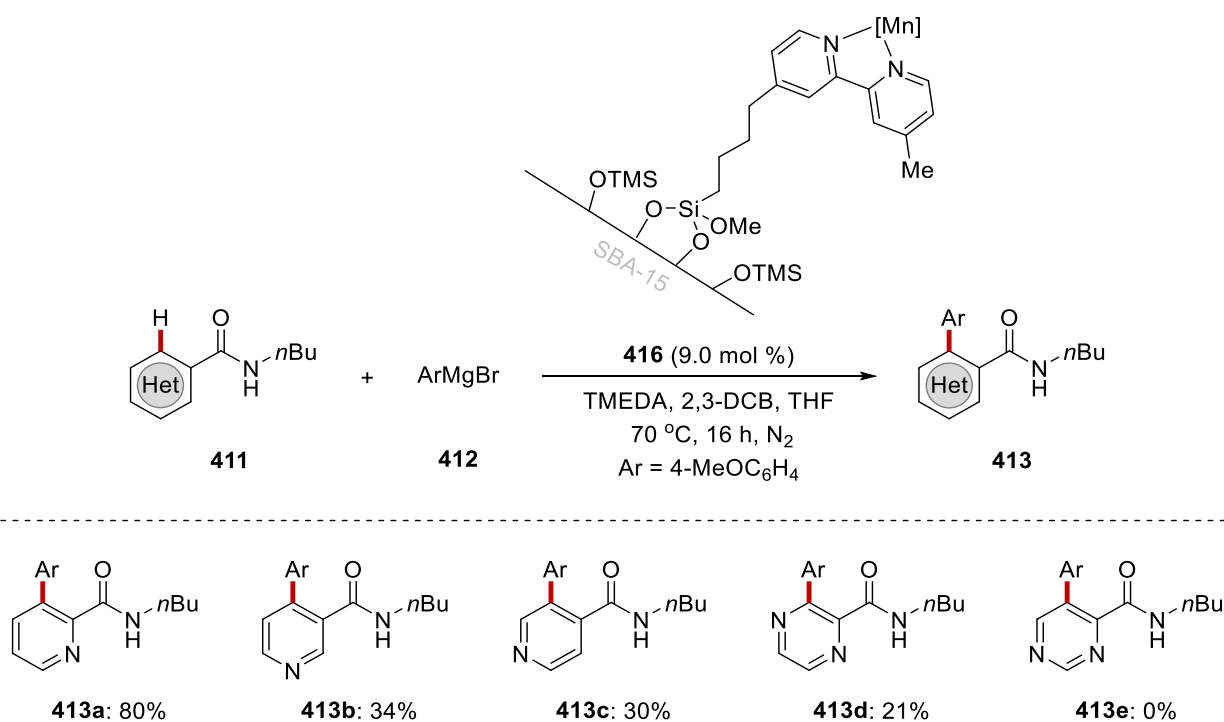
**Table 3.6.1** Establishing C–H arylation by hybrid-manganese catalyst.



| Entry | Deviation from standard condition                   | Yield (%) |
|-------|-----------------------------------------------------|-----------|
| 1     | Standard conditions                                 | 80        |
| 2     | Second run with the reused <b>416</b>               | 75        |
| 3     | MnCl <sub>2</sub> as catalyst                       | 17        |
| 4     | Immobilized ligand <b>443</b> instead of <b>416</b> | NR        |
| 5     | Without <b>416</b>                                  | NR        |
| 6     | Without TMEDA                                       | 43        |

[a] Reaction conditions: **411** (0.25 mmol), **412** (1.00 mmol, 1.0 M in THF), **416** (9.0 mol %), TMEDA (0.50 mmol), 2,3-DCB (0.75 mmol), 70 °C, 16 h, under N<sub>2</sub> atmosphere, isolated yields. TMEDA = Tetramethylethylenediamine. 2,3-DCB = 2,3-Dichlorobutane. NR = No Reaction.

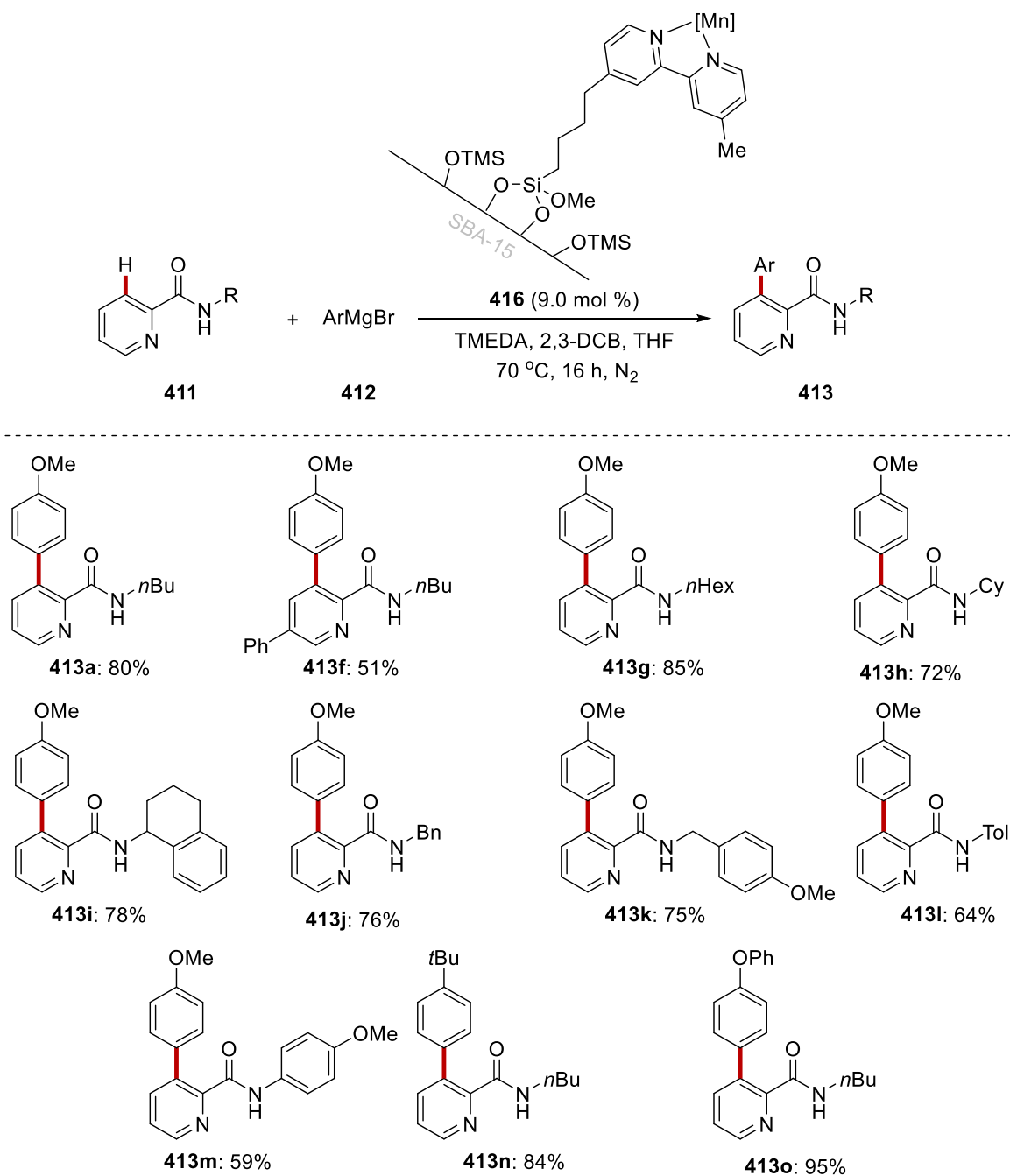
Thereafter, we probed the effect exerted by changing the substitution pattern on the azines **411** (Scheme 3.6.3). Differently decorated heteroarenes, such as structural isomeric azines (**411a**, **411b**, and **411c**) or diazines (**411d** and **411e**), were thus subjected to the optimized reaction conditions for the C–H arylation. While the picolinic amide **411a** gave an effective transformation, other heteroarenes afforded lower conversion.



**Scheme 3.6.3** Examination of heteroarenes effect.

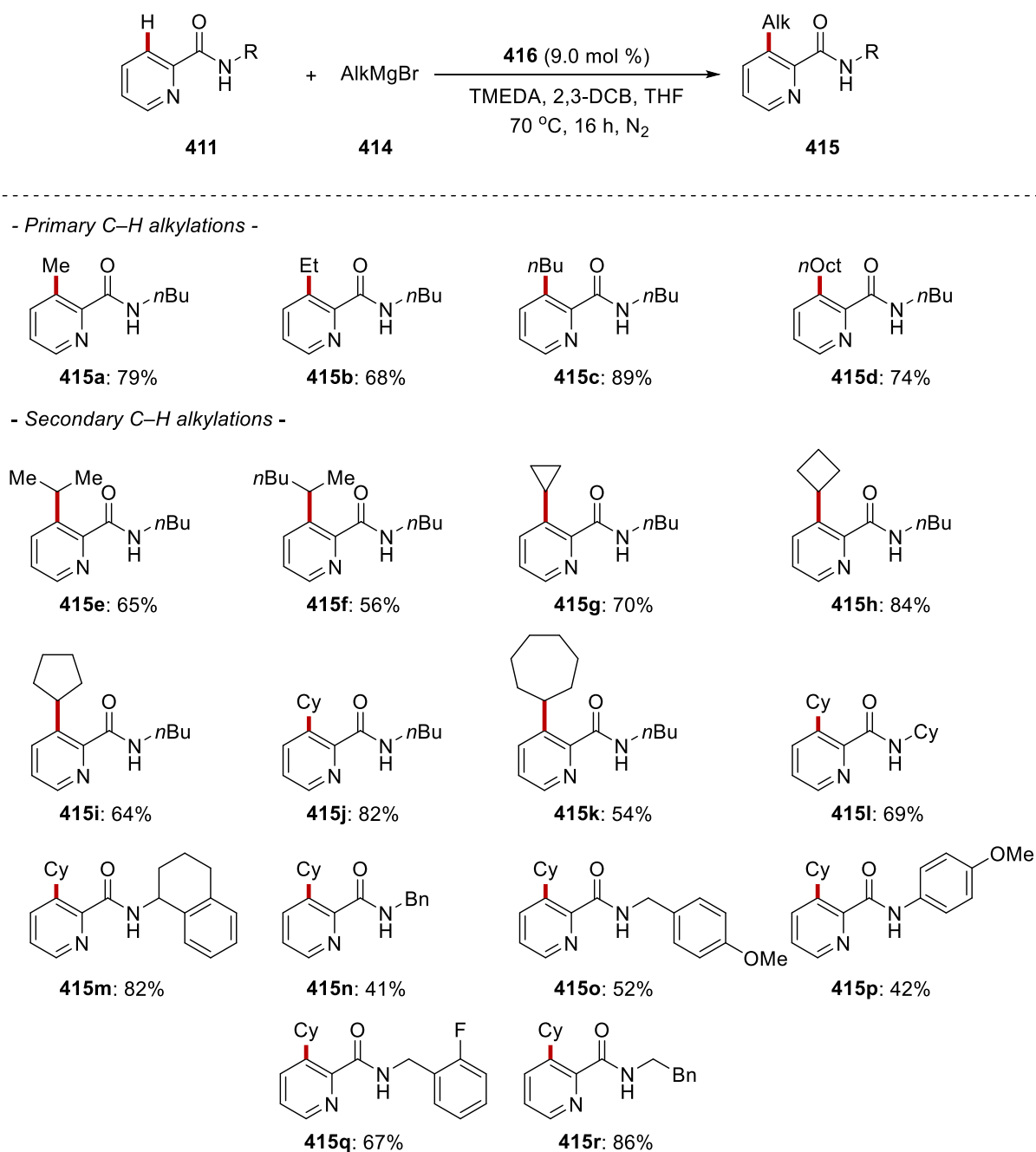
### 3.6.3 Substrate Scope

With the optimized reaction conditions in hand, we set out to explore the catalytic performance in the C3–H arylations of azines **411** (Scheme 3.6.4). Various pyridines **411** were efficiently converted to the desired C3-arylated product **413** by weak amide-chelation assistance, while alkyl, benzyl, and aryl substituted amides were fully tolerated.



**Scheme 3.6.4** Substrate scope of hybrid manganese-catalyzed C–H arylation.

Additionally, the versatility of the hybrid-manganese catalysis was highlighted by C–H alkylations, providing a broadly applicable strategy (Scheme 3.6.5). Therefore, the robust hybrid-manganese-catalyzed C–H functionalization enabled direct primary alkylations. It is noteworthy that the hybrid-manganese catalysis also enabled the installation of the methyl group<sup>[263]</sup> onto azines **411**. Furthermore, challenging secondary alkylations proved viable, including cyclopropylation **415g** and cyclobutylation **415h**, while isomerizations were not observed.



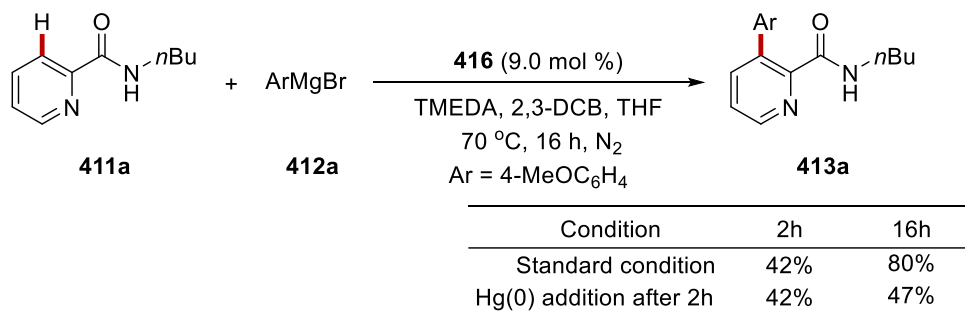
**Scheme 3.6.5** Substrate scope of hybrid manganese-catalyzed C–H alkylation.



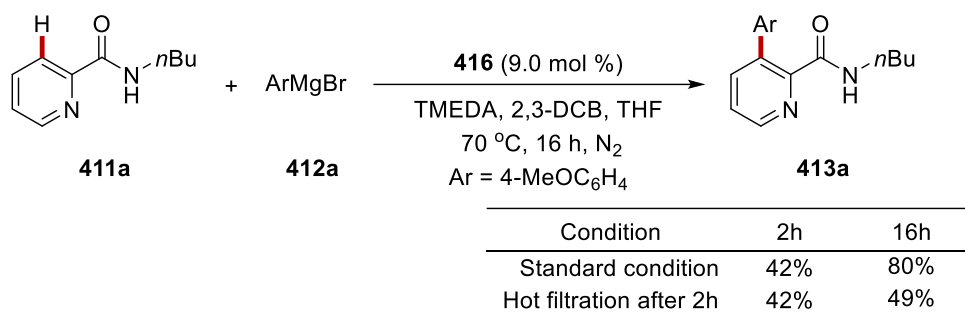


The addition of mercury and a hot-filtration test were subsequently probed, showing that the hybrid-manganese-catalyzed C–H arylation was operating by heterogeneous catalysis (Scheme 3.6.7).

a) Mercury test



b) Hot-filtration test

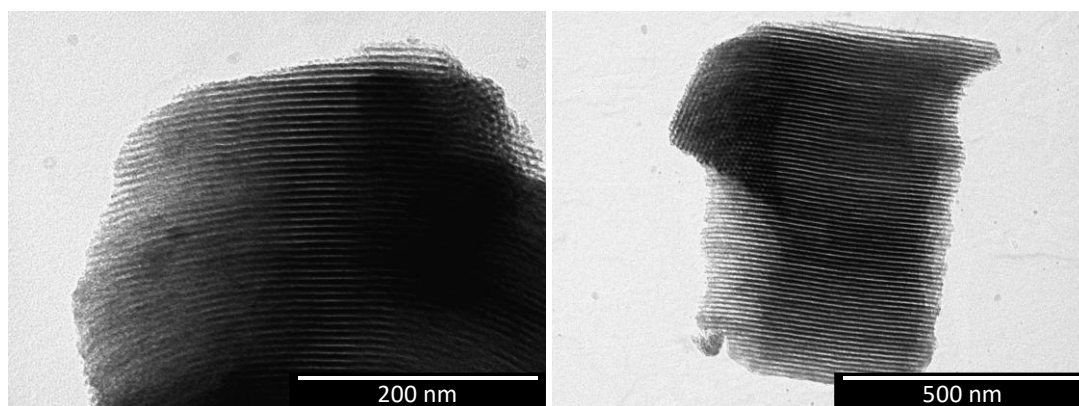


Scheme 3.6.7 Various heterogeneity tests.

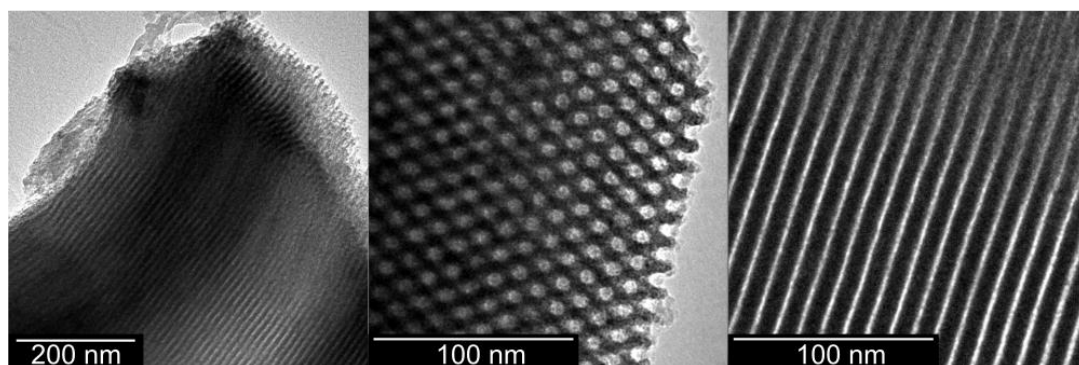
### 3.6.5 Characterizations of Heterogeneous Catalyst

Thereafter, the pristine ligand-support **443**, the hybrid-manganese catalyst **416**, and reused **416** were characterized in detail by TEM techniques to determine the morphological properties (Scheme 3.6.8). Thereby, we observed highly ordered one-dimensional mesoporous channels without morphological agglomeration or disorder during the process of end-capping or the binding of the manganese.

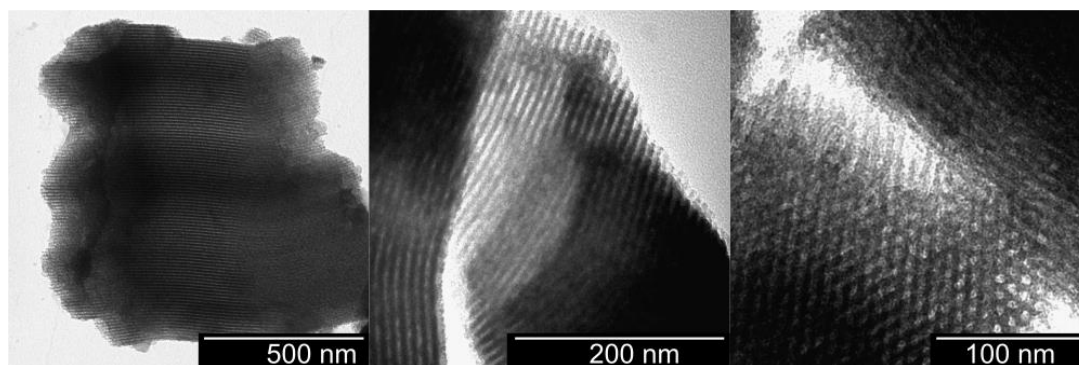
a) TEM analysis of **443**



b) TEM analysis of **416**



c) TEM analysis of reused **416**

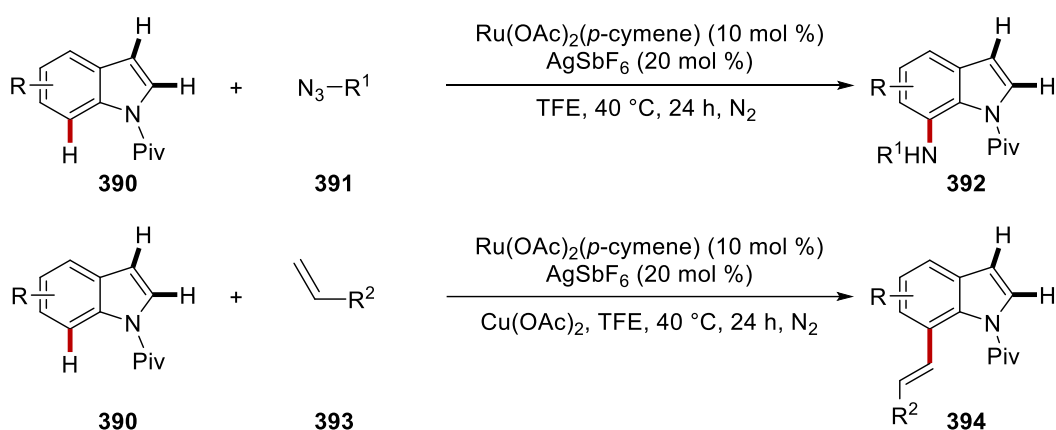


**Scheme 3.6.8** Microscopic analysis of hybrid manganese catalysts.

## 4. Summary and Outlook

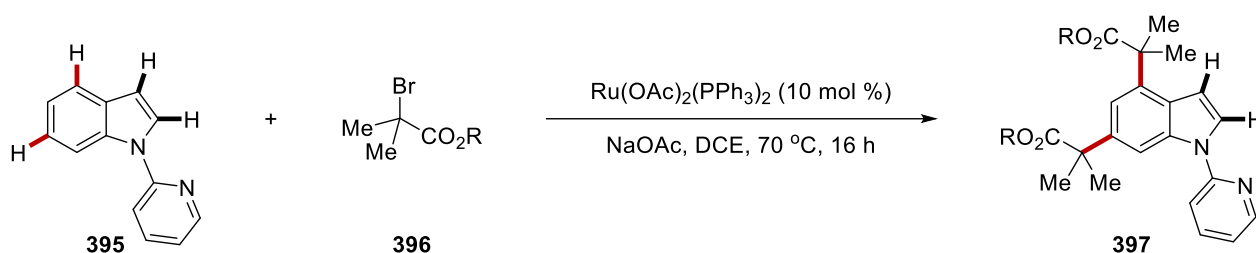
Classical C–C or C–Het bond formation reactions have been considered to be user-friendly methods, while pre-functionalizations are generally accompanied for desired reactivities and selectivities. In stark contrast, metal-catalyzed C–H activation enabled direct C–C or C–Het bond formation in an atom- and step-economical fashion. In addition to this emerging synthesis tool, photochemistry and electrochemistry have recently added a great value to the C–H activation manifold. Furthermore, hybrid catalysis allows for recyclability and reusability of the catalyst, resulting in the accomplishment of environmentally-sound syntheses.

In the first project, ruthenium(II)carboxylate-catalyzed C7–H indole functionalization was achieved via challenging six-membered ruthenacycles (Scheme 4.1.1). Notable features of this development were a wide substrate scope, including C–C and C–N bond formation at C7 position of indoles with a tolerance of various functional groups under mild conditions. The detailed kinetic study by spectroscopic and spectrometric analyses highlighted the importance of ruthenium nitrenoid intermediate for the unique C7–H amidation. Additionally, the traceless removal of the pivaloyl group, utilization of flow technique, and gram-scale reaction clearly showed the robustness and versatility of the ruthenium-catalyzed C7–H activations.



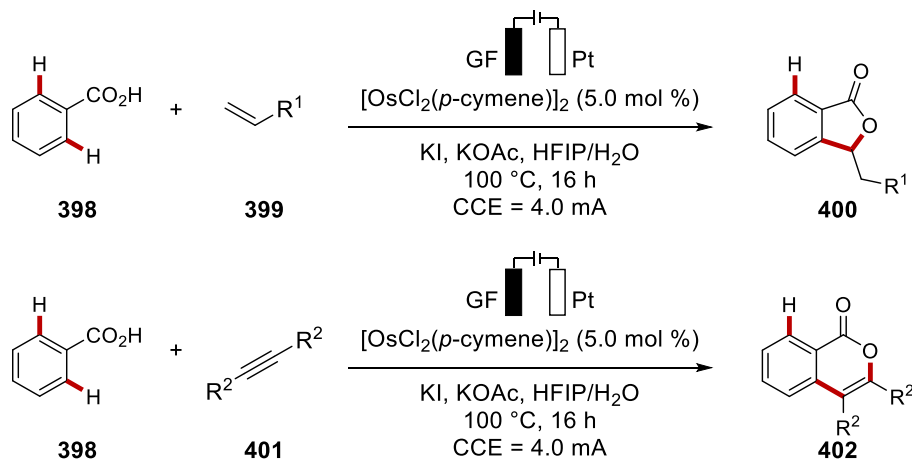
**Scheme 4.1.1** Ruthenium(II)-catalyzed C7–H indole amidation and alkenylation.

In the second project, arene-ligand-free ruthenium(II)-catalyzed remote C4/C6–H functionalization of indoles benzenoid was developed (Scheme 4.1.2). The unique ruthenium catalysis enabled double C–C bond formation with excellent levels of site-selectivity. The versatility and robustness of the ruthenium catalysis were demonstrated by ample substrate scope and a gram-scale reaction. Additionally, the mechanistic investigation highlighted the key importance of C2-ruthenation, affording unique C4/C6–H double indole alkylations.



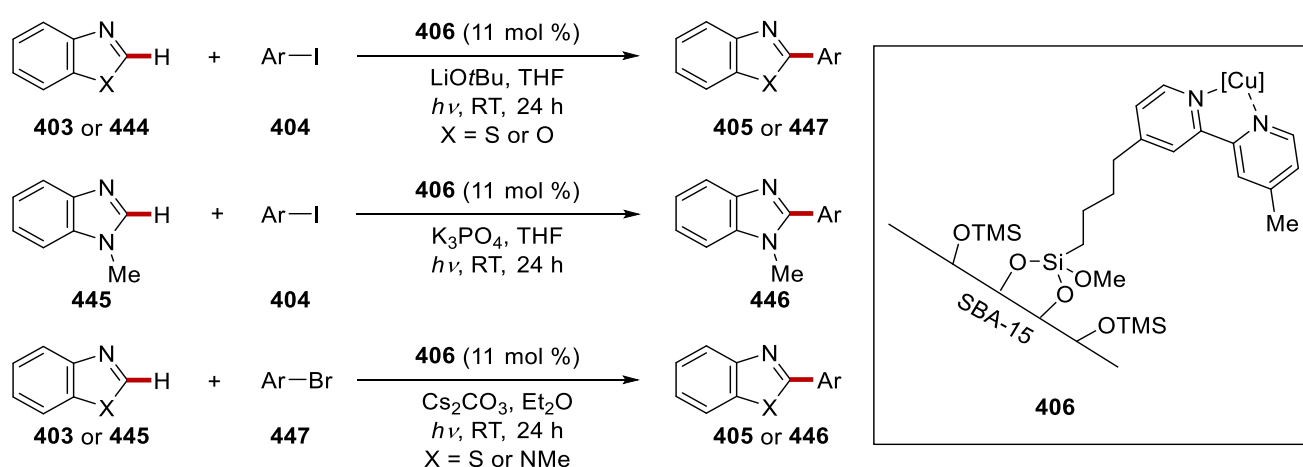
**Scheme 4.1.2** Ruthenium(II)-catalyzed C4–H/C6–H dual indole alkylations.

In the third project, electrochemical osmium(II)-catalyzed C–H annulations were accomplished (Scheme 4.1.3). Weak *O*-coordination enabled to provide ample substrate scope for [4+1] and [4+2] annulations under osmaelectrooxidative C–H activation. Notably, detailed reaction comparison with other transition metal catalytic systems highlighted advantageous characteristics of the osmium catalysis. Also, spectrometric, spectroscopic, and kinetic studies revealed the electrocatalytic mode of action.



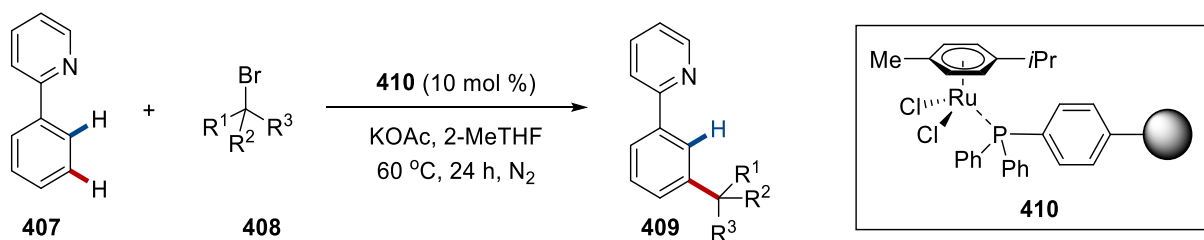
**Scheme 4.1.3** Electrooxidative osmium-catalyzed C–H annulation.

In the fourth project, a photo-induced C–H arylation by hybrid copper catalysis was achieved under exceedingly mild reaction conditions at room temperature (Scheme 4.1.4). The hybrid copper catalyst enabled site-selective C–H arylations with ample scope, including a wide range of functional group tolerance. Also, the hybrid copper catalyst was reusable without significant loss of catalytic efficacy, the heterogeneity of which was experimentally proved. Detailed microscopic and spectroscopic analyses showed the physical and chemical stability of the hybrid copper catalyst for photoinduced C–H arylation.



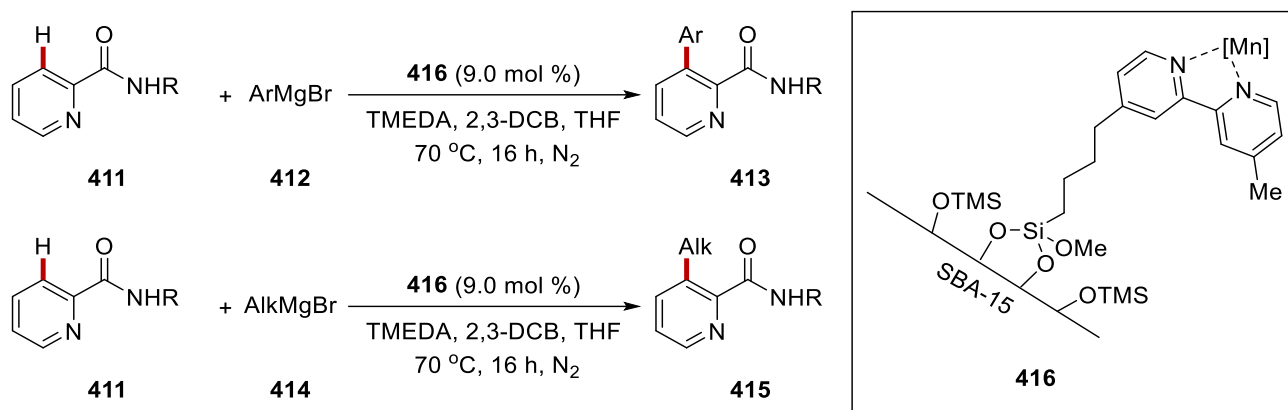
**Scheme 4.1.4** Photo-induced copper-catalyzed heterogeneous C–H arylation.

In the fifth project, a recyclable ruthenium hybrid catalyst was developed for remote C–H functionalizations (Scheme 4.1.5). The hybrid ruthenium catalyst featured remarkable robustness towards *meta*-C–H alkylations, while the catalyst was highly recyclable. Microscopic and spectroscopic analyses together with mechanistic studies delineated the excellent physical and chemical properties of the hybrid ruthenium catalyst for position-selective C–H functionalization.



**Scheme 4.1.5** Hybrid ruthenium(II)-catalyzed *meta*-C–H alkylation.

In the last project, a recyclable hybrid manganese catalyst was described for C–H arylation and alkylation of azines (Scheme 4.1.6). The hybrid manganese catalyst showed a remarkable catalytic performance towards site-selective C3–H arylations and C3–H alkylations of azines by weak amide-chelation assistance in a reusable fashion. Detailed heterogeneity investigations and characterizations of the hybrid-manganese catalyst reflected its stability during the course of azine C–H activation.



**Scheme 4.1.6** Hybrid manganese-catalyzed C–H arylation and alkylation.

## 5. Experimental Data

### 5.1 General Remarks

Reactions involving air- or moisture-sensitive compounds were conducted under an atmosphere of nitrogen using pre-dried glassware and standard Schlenk or glovebox techniques. If not otherwise noted, yields refer to isolated compounds, estimated to be >95% pure by GC and NMR.

#### Vacuum

The following average pressure was measured on the used rotary vane pump RD4 from Vacuubrand®:  $0.8 \times 10^{-1}$  mbar (uncorrected value).

#### Melting points

Melting points were measured on a Stuart® Melting Point Apparatus SMP3 from Barloworld Scientific. All values are uncorrected.

#### Liquid Chromatography

Analytical thin layer chromatography (TLC) was performed on TLC Silica gel 60 F254 from Merck with detection at 254 nm or 360 nm or developed by treatment with a  $\text{KMnO}_4$  solution followed by careful warming. Preparative chromatographic separations were carried out on Merck Geduran® SI 60 (40–63  $\mu\text{m}$ , 70–230 mesh ASTM) silica gel.

#### Gas Chromatography

Gas chromatographic analysis (GC) was performed on an Agilent 7890A or 7890B GC System equipped with an Agilent HP-5 column (30 m, 0.320 mm diameter, 0.25  $\mu\text{m}$  film thickness) and a flame-ionization detector (FID) using hydrogen as the carrier gas. Gas chromatography coupled with mass spectrometry (GC-MS) was performed on the same instrument equipped with an Agilent 5875C Triple-Axis-Detector or an Agilent 5977B MSD. Mass spectra were obtained with electron-ionization (EI) at 70 eV in positive ion mode.



## Mass Spectrometry

Electron-ionization (EI) mass spectra were recorded on a time-of flight mass spectrometer AccuTOF™ from Jeol at 70 eV. Electrospray-ionization (ESI) mass spectra were recorded on a quadrupole time-of-flight maXis or on a time-of-flight mass spectrometer microTOF, both from Bruker Daltonic. The ratios of mass to charge ( $m/z$ ) are reported and the intensity relative to the base peak ( $I = 100$ ) is given in parenthesis.

## Infrared Spectroscopy

Infrared (IR) spectra of were measured on a Bruker Alpha-P FT-IR spectrometer with a diamond ATR probe in the range of 4000–400  $\text{cm}^{-1}$ . *In-situ* IR measurements were performed with a Mettler-Toledo ReactIR 15 spectrometer equipped with a diamond ATR probe and an MCT detector. Spectra were acquired using Mettler-Toledo iC IR software version 7.0.297 in the range of 650–2200  $\text{cm}^{-1}$  with a 4  $\text{cm}^{-1}$  resolution. A Pearson's Correction was used as baseline correction in all measurements.

## Nuclear Magnetic Resonance Spectroscopy

Nuclear magnetic resonance (NMR) spectra were recorded on Varian MercuryPlus™ 300, Bruker Avance™ III 300, Avance III HD 300, Avance III 400, Avance III HD 400, Avance Neo 400, Avance III HD 500 and Bruker Avance Neo 600 spectrometer. Unless stated otherwise, all measurements were performed at 298 K. Chemical shifts ( $\delta$ ) are reported relative to tetramethylsilane and are referenced using the residual proton or carbon solvent signal.<sup>[264]</sup>

**Table 5.1.1** Chemical shifts of common deuterated solvents.

| Solvent                 | <sup>1</sup> H NMR | <sup>13</sup> C NMR |
|-------------------------|--------------------|---------------------|
| CDCl <sub>3</sub>       | 7.26 ppm           | 77.16 ppm           |
| DMSO-d <sub>6</sub>     | 2.50 ppm           | 39.52 ppm           |
| Acetone-d <sub>6</sub>  | 2.05 ppm           | 206.7, 29.92 ppm    |
| Methanol-d <sub>4</sub> | 4.78, 3.31 ppm     | 49.15 ppm           |
| THF-d <sub>8</sub>      | 3.58, 1.73 ppm     | 67.57, 25.37 ppm    |

## Data Analysis and Plots

Data analysis and plotting were performed using Microsoft Excel 2016 software.

## Solvents

All solvents used for work-up and purification were distilled prior to use. Solvents used in reactions involving air- or moisture-sensitive compounds were dried and stored under an inert atmosphere of nitrogen or argon according to the following standard procedures: Solvents purified by solvent purification system (SPS-800) from M. Braun: Toluene, tetrahydrofuran, diethylether, dichloromethane and *N,N*-dimethylformamide. Solvents dried and distilled over CaH<sub>2</sub>: 1,2-dichloroethane, *N,N*-dimethylacetamide and *N*-methyl-2-pyrrolidone. Solvents dried over 4Å molecular sieves and degassed using multiple cycles of freeze-pump-thaw: *t*-Amyl alcohol, *o*-, *m*-, *p*-xylene, 1,4-dioxane, 1,2-dimethoxyethane, *n*-butyl ether, methanol, trifluoroethanol, and hexafluoroisopropanol, 2-methyltetrahydrofuran, *n*-hexane, toluene-d<sub>8</sub>, and THF-d<sub>8</sub>. Water was degassed before its use applying repeated freeze-pump-thaw cycles.

## Electrochemistry

Platinum electrodes (10 mm × 25 mm × 0.125 mm, 99.9%; obtained from ChemPur® Karlsruhe, Germany) and CF electrodes (10 mm × 25 mm × 6 mm, SIGRACELL®GFA 6 EA, obtained from SGL Carbon, Wiesbaden, Germany) were connected using stainless steel adapters. Electrolysis was conducted using an AXIOMET AX-3003P potentiostat in constant current mode, CV studies were performed using a Metrohm Autolab PGSTAT204 workstation and Nova 2.0 software.

## Reagents

Reagents obtained from commercial sources with a purity >95% were used without further purification unless stated otherwise. The following compounds were synthesized according to previously reported procedures: **390**,<sup>[265,266]</sup> **391**,<sup>[265,266]</sup> **412**,<sup>[267]</sup> and **414**<sup>[267]</sup>

The following compounds were kindly synthesized and/or provided by the persons listed below:

Karsten Rauch:  $[\text{RuCl}_2(p\text{-cymene})]_2$  and  $[\text{Ru}(\text{OAc})_2p\text{-cymene}]$

Dr. Uttam Dhawa: **399**

Dr. Nikolaos Kaplaneris: **395, 396, 402, and 407**

Dr. Julian Koeller: **404 and 444**

Dr. Valentin Mueller: **407**

Dr. Cuiju Zhu: **411 and 413**

## 5.2 General Procedures

### 5.2.1 General Procedure A: Ruthenium-Catalyzed C7–H Indole Amidations

A suspension of *N*-pivaloyl indoles **390** (0.25 mmol, 1.0 equiv), organic azides **391** (0.75 mmol, 3.0 equiv), Ru(OAc)<sub>2</sub>(*p*-cymene) (10 mol %), AgSbF<sub>6</sub> (20 mol %), in TFE (1.0 mL) was stirred at 40 °C for 24 h under N<sub>2</sub>. After cooling to ambient temperature, the mixture was concentrated *in vacuo*. Purification by column chromatography on silica gel afforded the desired products **392**.

### 5.2.2 General Procedure B: Ruthenium-Catalyzed C7–H Indole Alkenylations

A suspension of *N*-pivaloyl indoles **390** (0.25 mmol, 1.0 equiv), acrylates **393** (0.75 mmol, 3.0 equiv), Ru(OAc)<sub>2</sub>(*p*-cymene) (10 mol %), AgSbF<sub>6</sub> (20 mol %), and Cu(OAc)<sub>2</sub> (0.50 mmol, 2.0 equiv) in TFE (1.0 mL) was stirred at 40 °C for 24 h under N<sub>2</sub>. After cooling to ambient temperature, the mixture was concentrated *in vacuo*. Purification by column chromatography on silica gel afforded the desired products **394**.

### 5.2.3 General Procedure C: Ruthenium-Catalyzed C4–H/C6–H Indole Dual Alkylations

A suspension of 1-(pyridin-2-yl)-1*H*-indoles (**395**) (0.25 mmol, 1.0 equiv), alkyl bromides **396** (1.25 mmol, 5 equiv), Ru(OAc)<sub>2</sub>(PPh<sub>3</sub>)<sub>2</sub> (10 mol %), and NaOAc (0.50 mmol, 2.0 equiv) in DCE (2.0 mL) was stirred at 70 °C for 16 h under N<sub>2</sub>. After cooling to room temperature, the mixture was concentrated *in vacuo*. Purification by column chromatography on silica gel afforded the desired products **397**.

### 5.2.4 General Procedure D: Osmium-Catalyzed Electrooxidative [4+1] C–H annulations

A suspension of benzoic acids **398** (0.20 mmol), olefins **399** (3.0 equiv), [OsCl<sub>2</sub>(*p*-cymene)]<sub>2</sub> (5.0 mol %), KI (0.40 mmol, 2.0 equiv), and KOAc (0.40 mmol, 2.0 equiv) in HFIP (2.0 mL) and H<sub>2</sub>O (2.0 mL) was stirred at 100 °C for 16 h at 4.0 mA of a constant current under N<sub>2</sub>. After cooling to ambient temperature, the electrodes were washed with ethyl acetate (3 × 10 mL). The reaction mixtures were extracted with brine (20 mL), dried over Na<sub>2</sub>SO<sub>4</sub>, and concentrated under reduced pressure. Purification by column chromatography on silica gel afforded the desired products **400**.

**5.2.5 General Procedure E: Osmium-Catalyzed Electrooxidative [4+2] C–H annulations**

A suspension of benzoic acids **398** (0.20 mmol), alkynes **401** (3.0 equiv),  $[\text{OsCl}_2(p\text{-cymene})]_2$  (5.0 mol %), KI (0.40 mmol, 2.0 equiv), and KOAc (0.40 mmol, 2.0 equiv) in HFIP (2.0 mL) and H<sub>2</sub>O (2.0 mL) was stirred at 100 °C for 16 h at 4.0 mA of a constant current under N<sub>2</sub>. After cooling to ambient temperature, the electrodes were washed with ethyl acetate (3 × 10 mL). The reaction mixtures were extracted with brine (20 mL), dried over Na<sub>2</sub>SO<sub>4</sub>, and concentrated under reduced pressure. Purification by column chromatography on silica gel afforded the desired products **402**.

**5.2.6 General Procedure F: Photo-Induced Hybrid Copper-Catalyzed C–H Arylations (1)**

To a pre-dried 10 mL quartz tube was added azoles **403** (0.25 mmol, 1.0 equiv), aryl iodide **404** (1.25 mmol, 5.0 equiv), **406** (30 mg, 11 mol %), LiOtBu (0.75 mmol, 3.0 equiv), and Et<sub>2</sub>O (0.5 mL) under N<sub>2</sub> atmosphere. The tube was sealed and stirred under 254 nm irradiation in a Luzchem LZC-ICH2 photoreactor at ambient temperature for 24 h. The temperature was determined to be 30 °C in the reaction mixture. Afterwards, the solvent was removed under reduced pressure. Purification by column chromatography on silica gel afforded the desired products **405**.

**5.2.7 General Procedure G: Photo-Induced Hybrid Copper-Catalyzed C–H Arylations (2)**

To a pre-dried 10 mL quartz tube was added *N*-methyl benzimidazole (**445**) (0.25 mmol), aryl iodide **404** (1.25 mmol), **406** (30 mg, 11 mol %), K<sub>3</sub>PO<sub>4</sub> (0.75 mmol, 3.0 equiv), and THF (0.5 mL) under N<sub>2</sub> atmosphere. The tube was sealed and stirred under 254 nm irradiation in a Luzchem LZC-ICH2 photoreactor at ambient temperature for 24 h. The temperature was determined to be 30 °C in the reaction mixture. Afterwards, the solvent was removed under reduced pressure. Purification by column chromatography on silica gel afforded the desired products **446**.

**5.2.8 General Procedure H: Photo-Induced Hybrid Copper-Catalyzed C–H Arylations (3)**

To a pre-dried 10 mL quartz tube was added heterocycles **403** or **445** (0.25 mmol, 1.0 equiv), aryl bromide **447** (1.25 mmol, 5.0 equiv), **406** (30 mg, 11 mol %), Cs<sub>2</sub>CO<sub>3</sub> (0.75 mmol, 3.0 equiv), and Et<sub>2</sub>O (0.5 mL) under N<sub>2</sub> atmosphere. The tube was sealed and stirred under 254 nm irradiation in a Luzchem LZC-ICH2 photoreactor at ambient temperature for 24 h. The temperature was determined to be 30 °C in the reaction mixture. Afterwards, the solvent was removed under reduced pressure. Purification by column chromatography on silica gel afforded the desired products **405** or **446**.

**5.2.9 General Procedure I: Hybrid Ruthenium-Catalyzed *meta*-C–H Alkylation**

A suspension of arenes **407** (0.25 mmol, 1.0 equiv), alkyl halides **408** (0.75 mmol, 3.0 equiv), **410** (30.0 mg, 10 mol %) and KOAc (0.50 mmol, 2.0 equiv) in 2-MeTHF (2.0 mL) was stirred at 60 °C for 24 h under N<sub>2</sub>. After cooling to ambient temperature, the mixture was concentrated *in vacuo*. Purification by column chromatography on silica gel afforded the desired products **409**.

**5.2.10 General Procedure J: Hybrid Manganese-Catalyzed C–H Arylations**

A suspension of picolinamides **411** (0.25 mmol, 1.0 equiv), aryl Grignards **412** (4 equiv, 1.0 mL, 1.0 M in THF) was added to a pre-dried Schlenk tube at room temperature under N<sub>2</sub>. After stirring for 10 min, **416** (30 mg, 9.0 mol %), TMEDA (0.50 mmol, 2.0 equiv) and 2,3-DCB (0.75 mmol, 3.0 equiv) were added to the suspension under N<sub>2</sub>. The Schlenk tube was transferred to pre-heated oil bath (70 °C) and stirred for 16 h. After cooling to ambient temperature, saturated aqueous NH<sub>4</sub>Cl (15 mL) was added and the reaction mixture was extracted with EtOAc (3 × 15 mL). The combined organic layers were dried over Na<sub>2</sub>SO<sub>4</sub>, filtered, and concentrated *in vacuo*. Purification by column chromatography on silica gel afforded the desired products **415**.

**5.2.11 General Procedure K: Hybrid Manganese-Catalyzed C–H Alkylations**

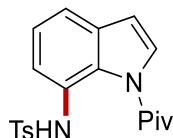
A suspension of picolinamides **411** (0.25 mmol, 1.0 equiv), alkyl Grignards **414** (4 equiv, 1.0 mL, 1.0 M in THF) was added to a pre-dried Schlenk tube at room temperature under N<sub>2</sub>. After stirring for 10 min, **416** (30 mg, 9.0 mol %), TMEDA (0.50 mmol, 2.0 equiv) and 2,3-DCB (0.75 mmol, 3.0 equiv)

were added to the suspension under N<sub>2</sub>. The Schlenk tube was transferred to pre-heated oil bath (70 °C) and stirred for 16 h. After cooling to ambient temperature, saturated aqueous NH<sub>4</sub>Cl (15 mL) was added and the reaction mixture was extracted with EtOAc (3 × 15 mL). The combined organic layers were dried over Na<sub>2</sub>SO<sub>4</sub>, filtered, and concentrated *in vacuo*. Purification by column chromatography on silica gel afforded the desired products **415**.

### 5.3 Ruthenium(II)-Catalyzed C7-H Amidations and Alkenylations of Indoles

#### 5.3.1 Characterization Data

##### 4-Methyl-*N*-(1-pivaloyl-1*H*-indol-7-yl)benzenesulfonamide (**392a**)



The **General Procedure A** was followed using *N*-pivaloyl indole **390a** (50.3 mg, 0.25 mmol), tosyl azide **391a** (148 mg, 0.75 mmol), Ru(OAc)<sub>2</sub>(*p*-cymene) (8.8 mg, 10 mol %) and AgSbF<sub>6</sub> (17.2 mg, 20 mol %) in TFE (1.0 mL). Purification by column chromatography on silica gel (*n*-hexane/EtOAc: 4/1) yielded **392a** (72.2 mg, 78%) as a light brown solid.

**M. p.** 120 °C.

<sup>1</sup>H NMR (400 MHz, CDCl<sub>3</sub>) δ 9.21 (s, 1H), 7.51 (dd, *J* = 7.8, 1.2 Hz, 1H), 7.49 (d, *J* = 4.0 Hz, 1H), 7.38 (ddd, *J* = 8.3, 4.0, 2.2 Hz, 2H), 7.35 (dd, *J* = 7.8, 1.2 Hz, 1H), 7.28 (t, *J* = 7.8 Hz, 1H), 7.08 – 7.03 (m, 2H), 6.55 (d, *J* = 4.0 Hz, 1H), 2.27 (s, 3H), 1.35 (s, 9H).

<sup>13</sup>C NMR (100 MHz, CDCl<sub>3</sub>) δ 179.2 (C<sub>q</sub>), 143.1 (C<sub>q</sub>), 137.4 (C<sub>q</sub>), 132.2 (C<sub>q</sub>), 129.3 (C<sub>q</sub>), 129.3 (CH), 126.7 (CH), 126.4 (CH), 125.1 (CH), 125.1 (C<sub>q</sub>), 122.8 (CH), 118.7 (CH), 109.2 (CH), 41.6 (C<sub>q</sub>), 28.9 (CH<sub>3</sub>), 21.3 (CH<sub>3</sub>).

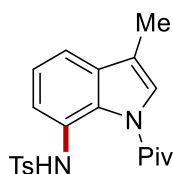
**IR** (ATR): 3174, 2991, 1745, 1570, 1322, 1164, 1099, 901, 818, 712 cm<sup>-1</sup>.

**MS** (ESI) *m/z* (relative intensity): 371 (34) [M+H]<sup>+</sup>, 393 (60) [M+Na]<sup>+</sup>.

**HR-MS** (ESI) C<sub>20</sub>H<sub>23</sub>N<sub>2</sub>O<sub>3</sub>S [M+H]<sup>+</sup>: 371.1427, found: 371.1424.

The spectral data were in accordance with those reported in the literature.<sup>[42g]</sup>

##### 4-Methyl-*N*-(3-methyl-1-pivaloyl-1*H*-indol-7-yl)benzenesulfonamide (**392b**)



The **General Procedure A** was followed using 2,2-dimethyl-1-(3-methyl-1*H*-indol-1-yl)propan-1-one **390b** (53.8 mg, 0.25 mmol), tosyl azide **391a** (148 mg, 0.75 mmol), Ru(OAc)<sub>2</sub>(*p*-cymene) (8.8 mg, 10



mol %) and AgSbF<sub>6</sub> (17.2 mg, 20 mol %) in TFE (1.0 mL). Purification by column chromatography on silica gel (*n*-hexane/EtOAc: 4/1) yielded **392b** (40.4 mg, 42%) as a light yellow solid.

**M. p.** 135 °C.

**<sup>1</sup>H NMR** (400 MHz, CDCl<sub>3</sub>) δ 9.43 (s, 1H), 7.52 (dd, *J* = 7.1, 1.9 Hz, 1H), 7.40 (ddd, *J* = 8.0, 1.9, 1.7 Hz, 2H), 7.30 – 7.23 (m, 3H), 7.06 (dd, *J* = 8.0, 1.7 Hz, 2H), 2.28 (s, 3H), 2.19 (s, 3H), 1.34 (s, 9H).

**<sup>13</sup>C NMR** (100 MHz, CDCl<sub>3</sub>) δ 178.8 (C<sub>q</sub>), 143.0 (C<sub>q</sub>), 137.5 (C<sub>q</sub>), 133.2 (C<sub>q</sub>), 129.6 (C<sub>q</sub>), 129.3 (CH), 126.8 (CH), 125.2 (C<sub>q</sub>), 124.9 (CH), 123.3 (CH), 122.6 (CH), 118.1 (C<sub>q</sub>), 116.4 (CH), 41.4 (C<sub>q</sub>), 28.9 (CH<sub>3</sub>), 21.4 (CH<sub>3</sub>), 9.7 (CH<sub>3</sub>).

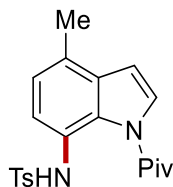
**IR** (ATR): 2975, 1665, 1440, 1342, 1162, 1091, 968, 909, 766, 554 cm<sup>-1</sup>.

**MS** (ESI) *m/z* (relative intensity): 385 (34) [M+H]<sup>+</sup>, 407 (66) [M+Na]<sup>+</sup>.

**HR-MS** (ESI) C<sub>21</sub>H<sub>25</sub>N<sub>2</sub>O<sub>3</sub>S [M+H]<sup>+</sup>: 385.1582, found: 385.1580.

The spectral data were in accordance with those reported in the literature.<sup>[42g]</sup>

#### 4-Methyl-*N*-(4-methyl-1-pivaloyl-1*H*-indol-7-yl)benzenesulfonamide (**392c**)



The **General Procedure A** was followed using 2,2-dimethyl-1-(4-methyl-1*H*-indol-1-yl)propan-1-one **390c** (53.8 mg, 0.25 mmol), tosyl azide **391a** (148 mg, 0.75 mmol), Ru(OAc)<sub>2</sub>(*p*-cymene) (8.8 mg, 10 mol %) and AgSbF<sub>6</sub> (17.2 mg, 20 mol %) in TFE (1.0 mL). Purification by column chromatography on silica gel (*n*-hexane/EtOAc: 4/1) yielded **392c** (66.3 mg, 69%) as a light yellow solid.

**M. p.** 165 °C.

**<sup>1</sup>H NMR** (400 MHz, CDCl<sub>3</sub>) δ 8.95 (s, 1H), 7.47 (d, *J* = 4.0 Hz, 1H), 7.39 (d, *J* = 8.2 Hz, 1H), 7.36 (dd, *J* = 8.2, 1.8 Hz, 2H), 7.08 (d, *J* = 8.2 Hz, 1H), 7.07 – 7.03 (m, 2H), 6.58 (d, *J* = 4.0 Hz, 1H), 2.45 (s, 3H), 2.28 (s, 3H), 1.33 (s, 9H).

**<sup>13</sup>C NMR** (100 MHz, CDCl<sub>3</sub>) δ 179.20 (C<sub>q</sub>), 142.95 (C<sub>q</sub>), 137.57 (C<sub>q</sub>), 131.37 (C<sub>q</sub>), 129.37 (C<sub>q</sub>), 129.24 (CH), 128.31 (C<sub>q</sub>), 126.77 (CH), 125.81 (CH), 125.56 (CH), 123.42 (CH), 122.61 (C<sub>q</sub>), 107.48 (CH),

41.58 (C<sub>q</sub>), 28.92 (CH<sub>3</sub>), 21.33 (CH<sub>3</sub>), 18.11 (CH<sub>3</sub>).

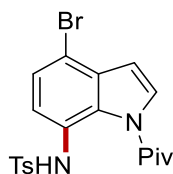
**IR** (ATR): 3193, 2977, 1671, 1498, 1329, 1164, 1091, 899, 814, 721 cm<sup>-1</sup>.

**MS** (ESI) *m/z* (relative intensity): 385 (66) [M+H]<sup>+</sup>, 407 (34) [M+Na]<sup>+</sup>.

**HR-MS** (ESI) C<sub>21</sub>H<sub>25</sub>N<sub>2</sub>O<sub>3</sub>S [M+H]<sup>+</sup>: 385.1585, found: 385.1583.

The spectral data were in accordance with those reported in the literature.<sup>[42g]</sup>

### ***N*-(4-Bromo-1-pivaloyl-1*H*-indol-7-yl)-4-methylbenzenesulfonamide (392d)**



The **General Procedure A** was followed using 1-(4-bromo-1*H*-indol-1-yl)-2,2-dimethylpropan-1-one **390d** (70.0 mg, 0.25 mmol), tosyl azide **391a** (148 mg, 0.75 mmol), Ru(OAc)<sub>2</sub>(*p*-cymene) (8.8 mg, 10 mol %) and AgSbF<sub>6</sub> (17.2 mg, 20 mol %) in TFE (1.0 mL). Purification by column chromatography on silica gel (*n*-hexane/EtOAc: 4/1) yielded **392d** (44.9 mg, 40%) as a light yellow solid.

**M. p.** 143 °C.

**<sup>1</sup>H NMR** (400 MHz, CDCl<sub>3</sub>) δ 8.99 (s, 1H), 7.55 (d, *J* = 4.0 Hz, 1H), 7.44 – 7.40 (d, *J* = 8.6, 2H), 7.38 (d, *J* = 8.6, 2H), 7.14 – 7.05 (m, 2H), 6.65 (d, *J* = 4.0 Hz, 1H), 2.29 (s, 3H), 1.35 (s, 9H).

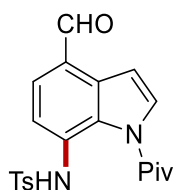
**<sup>13</sup>C NMR** (100 MHz, CDCl<sub>3</sub>) δ 179.5 (C<sub>q</sub>), 143.4 (C<sub>q</sub>), 137.2 (C<sub>q</sub>), 132.3 (C<sub>q</sub>), 129.7 (C<sub>q</sub>), 129.4 (CH), 127.9 (CH), 126.9 (CH), 126.7 (CH), 124.4 (C<sub>q</sub>), 123.6 (CH), 112.2 (C<sub>q</sub>), 109.1 (CH), 41.8 (C<sub>q</sub>), 28.8 (CH<sub>3</sub>), 21.3 (CH<sub>3</sub>).

**IR** (ATR): 3190, 2976, 1679, 1478, 1328, 1164, 1090, 910, 867, 670 cm<sup>-1</sup>.

**MS** (ESI) *m/z* (relative intensity): 449 (100) (<sup>79</sup>Br) [M+H]<sup>+</sup>, 451 (100) (<sup>81</sup>Br) [M+H]<sup>+</sup>.

**HR-MS** (ESI) C<sub>20</sub>H<sub>22</sub><sup>79</sup>BrN<sub>2</sub>O<sub>3</sub>S [M+H]<sup>+</sup>: 449.0534, found: 449.0529.

The spectral data were in accordance with those reported in the literature.<sup>[42g]</sup>

***N*-(4-Formyl-1-pivaloyl-1*H*-indol-7-yl)-4-methylbenzenesulfonamide (392e)**

The **General Procedure A** was followed using 1-pivaloyl-1*H*-indole-4-carbaldehyde **390e** (57.3 mg, 0.25 mmol), tosyl azide **391a** (148 mg, 0.75 mmol), Ru(OAc)<sub>2</sub>(*p*-cymene) (8.8 mg, 10 mol %) and AgSbF<sub>6</sub> (17.2 mg, 20 mol %) in TFE (1.0 mL). Purification by column chromatography on silica gel (*n*-hexane/EtOAc: 4/1) yielded **392e** (80.7 mg, 81%) as a light yellow solid.

**M. p.** 125 °C.

<sup>1</sup>H NMR (400 MHz, CDCl<sub>3</sub>) δ 10.28 (s, 1H), 9.78 (s, 1H), 8.81 (d, *J* = 8.2 Hz, 1H), 8.09 (m, 1H), 7.67 (dd, *J* = 7.5, 1.1 Hz, 1H), 7.64 (d, *J* = 8.2, 2.0 Hz, 2H), 7.44 (dd, *J* = 8.2, 7.5 Hz, 1H), 7.12 – 7.09 (m, 2H), 2.28 (s, 3H), 1.51 (s, 9H).

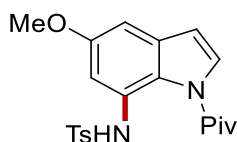
<sup>13</sup>C NMR (100 MHz, CDCl<sub>3</sub>) δ 195.7 (CH), 177.2 (C<sub>q</sub>), 143.6 (C<sub>q</sub>), 136.3 (C<sub>q</sub>), 136.0 (C<sub>q</sub>), 134.0 (CH), 129.4 (CH), 128.3 (C<sub>q</sub>), 127.1 (CH), 125.1 (CH), 124.6 (CH), 121.8 (C<sub>q</sub>), 120.1 (C<sub>q</sub>), 117.4 (CH), 41.6 (C<sub>q</sub>), 28.5 (CH<sub>3</sub>), 21.4 (CH<sub>3</sub>).

**IR** (ATR): 3180, 2742, 1670, 1303, 1264, 1164, 1091, 905, 732, 547 cm<sup>-1</sup>.

**MS** (ESI) *m/z* (relative intensity): 399 (30) [M+H]<sup>+</sup>, 421 (70) [M+Na]<sup>+</sup>.

**HR-MS** (ESI) C<sub>21</sub>H<sub>23</sub>N<sub>2</sub>O<sub>4</sub>S [M+H]<sup>+</sup>: 399.1372, found: 399.1373.

The spectral data were in accordance with those reported in the literature.<sup>[42g]</sup>

***N*-(5-Methoxy-1-pivaloyl-1*H*-indol-7-yl)-4-methylbenzenesulfonamide (392f)**

The **General Procedure A** was followed using 1-(5-methoxy-1*H*-indol-1-yl)-2,2-dimethylpropan-1-one **390f** (57.8 mg, 0.25 mmol), tosyl azide **391a** (148 mg, 0.75 mmol), Ru(OAc)<sub>2</sub>(*p*-cymene) (8.8 mg, 10 mol %) and AgSbF<sub>6</sub> (17.2 mg, 20 mol %) in TFE (1.0 mL). Purification by column chromatography on silica gel (*n*-hexane/EtOAc: 4/1) yielded **392f** (71.1 mg, 71%) as a light yellow solid.

**M. p.** 128 °C.

**<sup>1</sup>H NMR** (400 MHz, CDCl<sub>3</sub>) δ 9.62 (s, 1H), 7.47 (d, *J* = 3.9 Hz, 1H), 7.45 (ddd, *J* = 8.2, 3.9, 1.9 Hz, 2H), 7.14 (dd, *J* = 2.5, 0.5 Hz, 1H), 7.08 (dd, *J* = 8.2, 1.9 Hz, 2H), 6.79 (d, *J* = 2.5 Hz, 1H), 6.46 (d, *J* = 3.9 Hz, 1H), 3.82 (s, 3H), 2.28 (s, 3H), 1.35 (s, 9H).

**<sup>13</sup>C NMR** (100 MHz, CDCl<sub>3</sub>) δ 178.8 (C<sub>q</sub>), 157.4 (C<sub>q</sub>), 143.1 (C<sub>q</sub>), 137.4 (C<sub>q</sub>), 133.0 (C<sub>q</sub>), 129.3 (CH), 127.2 (CH), 126.9 (CH), 126.1 (C<sub>q</sub>), 123.6 (C<sub>q</sub>), 109.4 (CH), 109.3 (CH), 101.8 (CH), 55.7 (CH<sub>3</sub>), 41.5 (C<sub>q</sub>), 29.0 (CH<sub>3</sub>), 21.4 (CH<sub>3</sub>).

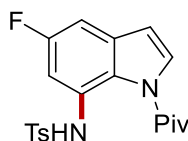
**IR** (ATR): 3182, 2976, 1663, 1614, 1287, 1160, 1090, 1041, 905, 739 cm<sup>-1</sup>.

**MS** (ESI) *m/z* (relative intensity): 401 (66) [M+H]<sup>+</sup>, 423 (34) [M+Na]<sup>+</sup>.

**HR-MS** (ESI) C<sub>21</sub>H<sub>25</sub>N<sub>2</sub>O<sub>4</sub>S [M+H]<sup>+</sup>: 401.1528, found: 401.1530.

The spectral data were in accordance with those reported in the literature.<sup>[42g]</sup>

#### ***N*-(5-Fluoro-1-*pivaloyl*-1*H*-indol-7-yl)-4-methylbenzenesulfonamide (392g)**



The **General Procedure A** was followed using 1-(5-fluoro-1*H*-indol-1-yl)-2,2-dimethylpropan-1-one **390g** (54.8 mg, 0.25 mmol), tosyl azide **391a** (148 mg, 0.75 mmol), Ru(OAc)<sub>2</sub>(*p*-cymene) (8.8 mg, 10 mol %) and AgSbF<sub>6</sub> (17.2 mg, 20 mol %) in TFE (1.0 mL). Purification by column chromatography on silica gel (*n*-hexane/EtOAc: 4/1) yielded **392g** (47.6 mg, 49%) as a light yellow solid.

**M. p.** 125 °C.

**<sup>1</sup>H NMR** (500 MHz, CDCl<sub>3</sub>) δ 9.55 (s, 1H), 7.56 (d, *J* = 3.9 Hz, 1H), 7.49 (ddd, *J* = 8.3, 3.9, 2.0 Hz, 2H), 7.28 (ddd, *J* = 10.5, 2.6, 0.5 Hz, 1H), 7.15 – 7.09 (m, 2H), 6.98 (dd, *J* = 7.5, 2.6 Hz, 1H), 6.51 (d, *J* = 3.9 Hz, 1H), 2.30 (s, 3H), 1.38 (s, 9H).

**<sup>13</sup>C NMR** (125 MHz, CDCl<sub>3</sub>) δ 179.2 (C<sub>q</sub>), 160.0 (d, *J*<sub>C-F</sub> = 242.2 Hz, C<sub>q</sub>), 143.4 (C<sub>q</sub>), 137.1 (C<sub>q</sub>), 132.9 (d, *J*<sub>C-F</sub> = 11.1 Hz, C<sub>q</sub>), 129.4 (CH), 128.0 (CH), 126.8 (CH), 126.5 (d, *J*<sub>C-F</sub> = 12.0 Hz, C<sub>q</sub>), 125.2 (d, *J*<sub>C-F</sub> = 2.0 Hz, C<sub>q</sub>), 109.2 (d, *J*<sub>C-F</sub> = 4.1 Hz, CH), 109.1 (d, *J*<sub>C-F</sub> = 28.2 Hz, CH), 103.7 (d, *J*<sub>C-F</sub> = 23.6 Hz, CH), 41.7 (C<sub>q</sub>), 29.0 (CH<sub>3</sub>), 21.4 (CH<sub>3</sub>).

**<sup>19</sup>F NMR** (471 MHz, CDCl<sub>3</sub>) δ -116.82 (dd, *J* = 10.8, 7.5 Hz).

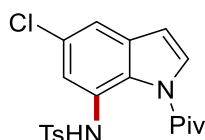
**IR** (ATR): 3179, 2997, 1622, 1609, 1310, 1089, 1090, 1053, 899, 817, 739  $\text{cm}^{-1}$ .

**MS** (ESI)  $m/z$  (relative intensity): 389 (33)  $[\text{M}+\text{H}]^+$ , 411 (66)  $[\text{M}+\text{Na}]^+$ .

**HR-MS** (ESI)  $\text{C}_{21}\text{H}_{25}\text{N}_2\text{O}_4\text{S}$   $[\text{M}+\text{H}]^+$ : 389.1329, found: 389.1330.

The spectral data were in accordance with those reported in the literature.<sup>[42g]</sup>

### ***N*-(5-Chloro-1-pivaloyl-1*H*-indol-7-yl)-4-methylbenzenesulfonamide (392h)**



The **General Procedure A** was followed using 1-(5-chloro-1*H*-indol-1-yl)-2,2-dimethylpropan-1-one **390h** (58.9 mg, 0.25 mmol), tosyl azide **391a** (148 mg, 0.75 mmol),  $\text{Ru}(\text{OAc})_2(p\text{-cymene})$  (8.8 mg, 10 mol %) and  $\text{AgSbF}_6$  (17.2 mg, 20 mol %) in TFE (1.0 mL). Purification by column chromatography on silica gel (*n*-hexane/EtOAc: 4/1) yielded **392h** (76.9 mg, 76%) as a light yellow solid.

**M. p.** 150 °C.

**$^1\text{H}$  NMR** (400 MHz,  $\text{CDCl}_3$ )  $\delta$  9.36 (s, 1H), 7.53 (dd,  $J = 3.9, 0.5$  Hz, 1H), 7.50 (dd,  $J = 2.1, 0.5$  Hz, 1H), 7.45 (ddd,  $J = 8.2, 3.9, 2.1$  Hz, 2H), 7.29 (d,  $J = 2.1$  Hz, 1H), 7.13 – 7.06 (m, 2H), 6.49 (d,  $J = 3.9$  Hz, 1H), 2.29 (s, 3H), 1.35 (s, 9H).

**$^{13}\text{C}$  NMR** (100 MHz,  $\text{CDCl}_3$ )  $\delta$  179.3 ( $\text{C}_q$ ), 143.5 ( $\text{C}_q$ ), 137.1 ( $\text{C}_q$ ), 133.1 ( $\text{C}_q$ ), 130.5 ( $\text{C}_q$ ), 129.4 (CH), 127.7 (CH), 127.6 ( $\text{C}_q$ ), 126.8 (CH), 126.1 ( $\text{C}_q$ ), 121.7 (CH), 117.9 (CH), 108.7 (CH), 41.7 ( $\text{C}_q$ ), 28.9 ( $\text{CH}_3$ ), 21.4 ( $\text{CH}_3$ ).

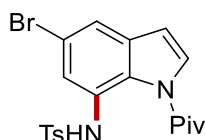
**IR** (ATR): 3210, 2980, 1674, 1581, 1404, 1332, 1163, 1091, 904, 792  $\text{cm}^{-1}$ .

**MS** (ESI)  $m/z$  (relative intensity): 405 (80)  $[\text{M}+\text{H}]^+$ , 809 (20)  $[2\text{M}+\text{H}]^+$ .

**HR-MS** (ESI)  $\text{C}_{20}\text{H}_{22}^{35}\text{ClN}_2\text{O}_3\text{S}$   $[\text{M}+\text{H}]^+$ : 405.1034, found: 405.1034.

The spectral data were in accordance with those reported in the literature.<sup>[42g]</sup>

### ***N*-(5-Bromo-1-pivaloyl-1*H*-indol-7-yl)-4-methylbenzenesulfonamide (392i)**



The **General Procedure A** was followed using 1-(5-bromo-1*H*-indol-1-yl)-2,2-dimethylpropan-1-one **390i** (70.0 mg, 0.25 mmol), tosyl azide **391a** (148 mg, 0.75 mmol), Ru(OAc)<sub>2</sub>(*p*-cymene) (8.8 mg, 10 mol %) and AgSbF<sub>6</sub> (17.2 mg, 20 mol %) in TFE (1.0 mL). Purification by column chromatography on silica gel (*n*-hexane/EtOAc: 4/1) yielded **392i** (92.1 mg, 82%) as a light yellow solid.

**M. p.** 160 °C.

<sup>1</sup>H NMR (400 MHz, CDCl<sub>3</sub>) δ 9.31 (s, 1H), 7.63 (d, *J* = 1.9 Hz, 1H), 7.51 (d, *J* = 3.9 Hz, 1H), 7.45 (dd, *J* = 7.1, 1.9 Hz, 3H), 7.09 (d, *J* = 7.8 Hz, 2H), 6.49 (d, *J* = 3.9 Hz, 1H), 2.29 (s, 3H), 1.35 (s, 9H).

<sup>13</sup>C NMR (100 MHz, CDCl<sub>3</sub>) δ 179.3 (C<sub>q</sub>), 143.5 (C<sub>q</sub>), 137.1 (C<sub>q</sub>), 133.5 (C<sub>q</sub>), 129.4 (CH), 128.0 (C<sub>q</sub>), 127.6 (CH), 126.8 (CH), 126.2 (C<sub>q</sub>), 124.4 (CH), 121.0 (CH), 118.0 (C<sub>q</sub>), 108.5 (CH), 41.7 (C<sub>q</sub>), 28.8 (CH<sub>3</sub>), 21.4 (CH<sub>3</sub>).

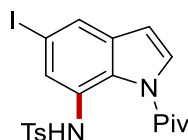
IR (ATR): 3180, 2978, 1637, 1579, 1330, 1299, 1160, 1089, 903, 852 cm<sup>-1</sup>.

MS (ESI) *m/z* (relative intensity): 449 (100) (<sup>79</sup>Br) [M+H]<sup>+</sup>, 451 (100) (<sup>81</sup>Br) [M+H]<sup>+</sup>.

HR-MS (ESI) C<sub>20</sub>H<sub>22</sub><sup>79</sup>BrN<sub>2</sub>O<sub>3</sub>S [M+H]<sup>+</sup>: 449.0531, found: 449.0529.

The spectral data were in accordance with those reported in the literature.<sup>[42g]</sup>

#### ***N*-(5-Iodo-1-pivaloyl-1*H*-indol-7-yl)-4-methylbenzenesulfonamide (392j)**



The **General Procedure A** was followed using 1-(5-iodo-1*H*-indol-1-yl)-2,2-dimethylpropan-1-one **390j** (81.8 mg, 0.25 mmol), tosyl azide **391a** (148 mg, 0.75 mmol), Ru(OAc)<sub>2</sub>(*p*-cymene) (8.8 mg, 10 mol %) and AgSbF<sub>6</sub> (17.2 mg, 20 mol %) in TFE (1.0 mL). Purification by column chromatography on silica gel (*n*-hexane/EtOAc: 4/1) yielded **392j** (105.4 mg, 85%) as a light yellow solid.

**M. p.** 160 °C.

<sup>1</sup>H NMR (400 MHz, CDCl<sub>3</sub>) δ 9.20 (s, 1H), 7.77 (dd, *J* = 1.6, 0.4 Hz, 1H), 7.67 (d, *J* = 1.6 Hz, 1H), 7.48 (d, *J* = 3.9 Hz, 1H), 7.45 (ddd, *J* = 8.3, 3.9, 1.6 Hz, 2H), 7.13 – 7.08 (m, 2H), 6.48 (d, *J* = 3.9 Hz, 1H), 2.30 (s, 3H), 1.36 (s, 9H).

<sup>13</sup>C NMR (100 MHz, CDCl<sub>3</sub>) δ 179.3 (C<sub>q</sub>), 143.4 (C<sub>q</sub>), 137.2 (C<sub>q</sub>), 133.9 (C<sub>q</sub>), 130.2 (CH), 129.4 (CH), 128.9 (C<sub>q</sub>), 127.3 (CH), 127.2 (CH), 126.9 (CH), 126.3 (C<sub>q</sub>), 108.2 (CH), 88.5 (C<sub>q</sub>), 41.8 (C<sub>q</sub>), 28.9

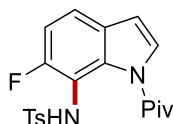
(CH<sub>3</sub>), 21.4 (CH<sub>3</sub>).

**IR** (ATR): 3187, 2977, 1674, 1575, 1331, 1164, 1090, 905, 812, 716 cm<sup>-1</sup>.

**MS** (ESI) *m/z* (relative intensity): 497 (70) [M+H]<sup>+</sup>, 519 (30) [M+Na]<sup>+</sup>.

**HR-MS** (ESI) C<sub>20</sub>H<sub>22</sub>IN<sub>2</sub>O<sub>3</sub>S [M+H]<sup>+</sup>: 497.0388, found: 497.0390.

***N*-(6-Fluoro-1-*pivaloyl*-1*H*-indol-7-yl)-4-methylbenzenesulfonamide (392k)**



The general procedure was followed using 1-(6-fluoro-1*H*-indol-1-yl)-2,2-dimethylpropan-1-one **390k** (54.8 mg, 0.25 mmol), tosyl azide **391a** (148 mg, 0.75 mmol), Ru(OAc)<sub>2</sub>(*p*-cymene) (8.8 mg, 10 mol %) and AgSbF<sub>6</sub> (17.2 mg, 20 mol %) in TFE (1.0 mL). Purification by column chromatography on silica gel (*n*-hexane/EtOAc: 4/1) yielded **392k** (67.0 mg, 69%) as a light yellow solid.

**M. p.** 125 °C.

**<sup>1</sup>H NMR** (400 MHz, CDCl<sub>3</sub>) δ 7.80 (s, 1H), 7.57 (ddd, *J* = 8.4, 3.8, 1.5 Hz, 2H), 7.54 (d, *J* = 3.8 Hz, 1H), 7.40 (dd, *J* = 8.4, 4.9 Hz, 1H), 7.20 – 7.16 (m, 2H), 7.11 (dd, *J* = 10.0, 8.5 Hz, 1H), 6.56 (d, *J* = 3.8 Hz, 1H), 2.36 (s, 3H), 1.41 (s, 9H).

**<sup>13</sup>C NMR** (100 MHz, CDCl<sub>3</sub>) δ 179.5 (C<sub>q</sub>), 157.7 (d, *J*<sub>C-F</sub> = 246.9 Hz, C<sub>q</sub>), 143.6 (C<sub>q</sub>), 137.7 (C<sub>q</sub>), 132.9 (d, *J*<sub>C-F</sub> = 3.7 Hz, C<sub>q</sub>), 129.5 (CH), 128.1 (d, *J*<sub>C-F</sub> = 1.9 Hz, C<sub>q</sub>), 127.4 (CH), 127.0 (d, *J*<sub>C-F</sub> = 3.8 Hz, CH), 120.4 (d, *J*<sub>C-F</sub> = 9.8 Hz, CH), 113.6 (d, *J*<sub>C-F</sub> = 24.1 Hz, CH), 113.4 (d, *J*<sub>C-F</sub> = 17.5 Hz, C<sub>q</sub>), 108.4 (d, *J*<sub>C-F</sub> = 1.6 Hz, CH), 41.8 (C<sub>q</sub>), 29.0 (CH<sub>3</sub>), 21.6 (CH<sub>3</sub>).

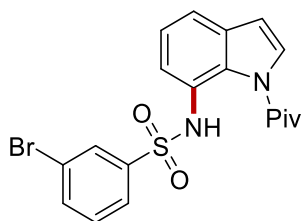
**<sup>19</sup>F NMR** (282 MHz, CDCl<sub>3</sub>) δ -121.9 (dd, *J* = 10.1, 4.9 Hz).

**IR** (ATR): 3181, 2978, 1675, 1406, 1305, 1164, 1091, 899, 813, 739 cm<sup>-1</sup>.

**MS** (ESI) *m/z* (relative intensity): 389 (30) [M+H]<sup>+</sup>, 411 (70) [M+Na]<sup>+</sup>.

**HR-MS** (ESI) C<sub>20</sub>H<sub>21</sub>FN<sub>2</sub>O<sub>3</sub>S [M+H]<sup>+</sup>: 389.1330, found: 389.1330.

The spectral data were in accordance with those reported in the literature.<sup>[42g]</sup>

**3-Bromo-*N*-(1-pivaloyl-1*H*-indol-7-yl)benzenesulfonamide (392l)**

The **General Procedure A** was followed using *N*-pivaloyl indole **390a** (50.3 mg, 0.25 mmol), 3-bromobenzenesulfonyl azide **391b** (197 mg, 0.75 mmol), Ru(OAc)<sub>2</sub>(*p*-cymene) (8.8 mg, 10 mol %) and AgSbF<sub>6</sub> (17.2 mg, 20 mol %) in TFE (1.0 mL). Purification by column chromatography on silica gel (*n*-hexane/EtOAc: 4/1) yielded **392l** (87.1 mg, 80%) as a dark yellow solid.

**M. p.** 105 °C.

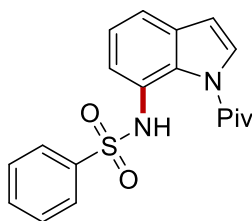
**<sup>1</sup>H NMR** (400 MHz, CDCl<sub>3</sub>) δ 9.42 (s, 1H), 7.68 (ddd, *J* = 1.9, 1.7, 0.4 Hz, 1H), 7.52 (ddd, *J* = 3.9, 1.9, 1.3 Hz, 3H), 7.40 (dd, *J* = 7.8, 1.3 Hz, 1H), 7.30 (t, *J* = 7.8 Hz, 1H), 7.28 (ddd, *J* = 7.8, 1.7, 1.0 Hz, 1H), 7.10 (t, *J* = 7.8 Hz, 1H), 6.57 (d, *J* = 3.9 Hz, 1H), 1.37 (s, 9H).

**<sup>13</sup>C NMR** (100 MHz, CDCl<sub>3</sub>) δ 179.3 (C<sub>q</sub>), 142.0 (C<sub>q</sub>), 135.4 (CH), 132.3 (C<sub>q</sub>), 130.1 (CH), 129.6 (CH), 129.4 (C<sub>q</sub>), 126.6 (CH), 125.3 (CH), 125.2 (CH), 124.5 (C<sub>q</sub>), 122.9 (CH), 122.7 (C<sub>q</sub>), 119.2 (CH), 109.4 (CH), 41.7 (C<sub>q</sub>), 29.0 (CH<sub>3</sub>).

**IR** (ATR): 3180, 2988, 1671, 1479, 1301, 1264, 1168, 1084, 731, 565 cm<sup>-1</sup>.

**MS** (ESI) *m/z* (relative intensity): 435 (100) (<sup>79</sup>Br) [M+H]<sup>+</sup>, 437 (100) (<sup>81</sup>Br) [M+H]<sup>+</sup>.

**HR-MS** (ESI) C<sub>19</sub>H<sub>20</sub><sup>79</sup>BrN<sub>2</sub>O<sub>3</sub>S [M+H]<sup>+</sup>: 435.0372, found: 435.0373.

***N*-(1-Pivaloyl-1*H*-indol-7-yl)benzenesulfonamide (392m)**

The **General Procedure A** was followed using *N*-pivaloyl indole **390a** (50.3 mg, 0.25 mmol), benzenesulfonyl azide **391c** (137 mg, 0.75 mmol), Ru(OAc)<sub>2</sub>(*p*-cymene) (8.8 mg, 10 mol %) and AgSbF<sub>6</sub> (17.2 mg, 20 mol %) in TFE (1.0 mL). Purification by column chromatography on silica gel



(*n*-hexane/EtOAc: 4/1) yielded **392m** (52.6 mg, 59%) as a light yellow solid.

**M. p.** 134 °C.

**<sup>1</sup>H NMR** (400 MHz, CDCl<sub>3</sub>)  $\delta$  9.27 (s, 1H), 7.53 (dd, *J* = 7.7, 1.3 Hz, 1H), 7.51 – 7.49 (m, 2H), 7.48 (d, *J* = 3.9 Hz, 1H), 7.39 (ddd, *J* = 7.7, 2.6, 1.3 Hz, 1H), 7.36 (dd, *J* = 7.7, 1.3 Hz, 1H), 7.28 (t, *J* = 7.7 Hz, 1H) 7.29 – 7.23 (m, 2H), 6.54 (d, *J* = 3.9 Hz, 1H), 1.35 (s, 9H).

**<sup>13</sup>C NMR** (100 MHz, CDCl<sub>3</sub>)  $\delta$  179.3 (C<sub>q</sub>), 140.30 (C<sub>q</sub>), 132.4 (CH), 132.2 (C<sub>q</sub>), 129.4 (C<sub>q</sub>), 128.7 (CH), 126.7 (CH), 126.5 (CH), 125.2 (CH), 125.0 (C<sub>q</sub>), 122.8 (CH), 118.9 (CH), 109.3 (CH), 41.6 (C<sub>q</sub>), 29.0 (CH<sub>3</sub>).

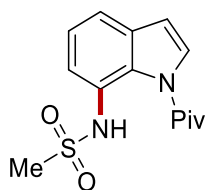
**IR** (ATR): 3174, 2976, 1667, 1446, 1326, 1299, 1160, 1090, 904, 716 cm<sup>-1</sup>.

**MS** (ESI) *m/z* (relative intensity): 357 (30) [M+H]<sup>+</sup>, 379 (70) [M+Na]<sup>+</sup>.

**HR-MS** (ESI) C<sub>19</sub>H<sub>21</sub>N<sub>2</sub>O<sub>3</sub>S [M+H]<sup>+</sup>: 357.1269, found: 357.1267.

The spectral data were in accordance with those reported in the literature.<sup>[42g]</sup>

#### *N*-(1-Pivaloyl-1*H*-indol-7-yl)methanesulfonamide (**392n**)



The **General Procedure A** was followed using *N*-pivaloyl indole **390a** (50.3 mg, 0.25 mmol), methanesulfonyl azide **391d** (90.8 mg, 0.75 mmol), Ru(OAc)<sub>2</sub>(*p*-cymene) (8.8 mg, 10 mol %) and AgSbF<sub>6</sub> (17.2 mg, 20 mol %) in TFE (1.0 mL). Purification by column chromatography on silica gel (*n*-hexane/EtOAc: 4/1) yielded **392n** (50.0 mg, 68%) as a light yellow liquid.

**<sup>1</sup>H NMR** (400 MHz, CDCl<sub>3</sub>)  $\delta$  9.01 (s, 1H), 7.71 (d, *J* = 3.9 Hz, 1H), 7.49 (dd, *J* = 7.8, 1.3 Hz, 1H), 7.40 (dd, *J* = 7.8, 1.3 Hz, 1H), 7.31 (t, *J* = 7.8 Hz, 1H), 6.67 (d, *J* = 3.9 Hz, 1H), 2.90 (s, 3H), 1.54 (s, 9H).

**<sup>13</sup>C NMR** (100 MHz, CDCl<sub>3</sub>)  $\delta$  179.9 (C<sub>q</sub>), 132.7 (C<sub>q</sub>), 128.9 (C<sub>q</sub>), 126.8 (CH), 125.5 (C<sub>q</sub>), 125.3 (CH), 120.6 (CH), 118.6 (CH), 109.4 (CH), 42.0 (C<sub>q</sub>), 39.8 (CH<sub>3</sub>), 29.2 (CH<sub>3</sub>).

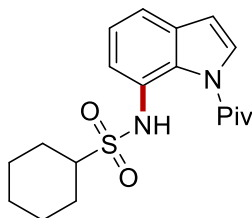
**IR** (ATR): 3196, 2976, 1670, 1590, 1359, 1317, 1153, 905, 755, 510 cm<sup>-1</sup>.

**MS** (ESI) *m/z* (relative intensity): 295 (10) [M+H]<sup>+</sup>, 317 (90) [M+Na]<sup>+</sup>.

**HR-MS** (ESI)  $C_{14}H_{19}N_2O_3S$   $[M+H]^+$ : 295.1111, found: 295.1111.

The spectral data were in accordance with those reported in the literature.<sup>[42g]</sup>

***N*-(1-Pivaloyl-1*H*-indol-7-yl)cyclohexanesulfonamide (392o)**



The **General Procedure A** was followed using *N*-pivaloyl indole **390a** (50.3 mg, 0.25 mmol), cyclohexanesulfonyl azide **391e** (142 mg, 0.75 mmol),  $Ru(OAc)_2(p\text{-cymene})$  (8.8 mg, 10 mol %) and  $AgSbF_6$  (17.2 mg, 20 mol %) in TFE (1.0 mL). Purification by column chromatography on silica gel (*n*-hexane/EtOAc: 4/1) yielded **392o** (48.9 mg, 54%) as a light yellow solid.

**M. p.** 113 °C.

**<sup>1</sup>H NMR** (400 MHz,  $CDCl_3$ )  $\delta$  8.72 (s, 1H), 7.69 (d,  $J = 3.9$  Hz, 1H), 7.53 (dd,  $J = 7.7, 1.3$  Hz, 1H), 7.35 (dd,  $J = 7.7, 1.3$  Hz, 1H), 7.27 (t,  $J = 7.3$  Hz, 1H), 6.65 (d,  $J = 3.9$  Hz, 1H), 2.88 (tt,  $J = 12.1, 3.5$  Hz, 1H), 2.18 – 2.03 (m, 2H), 1.86 – 1.77 (m, 2H), 1.67 – 1.54 (m, 2H), 1.53 (s, 9H), 1.49 – 1.52 (m, 2H), 1.19 – 1.10 (m, 2H).

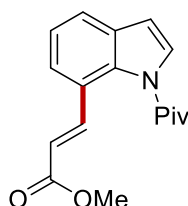
**<sup>13</sup>C NMR** (100 MHz,  $CDCl_3$ )  $\delta$  180.0 ( $C_q$ ), 132.5 ( $C_q$ ), 128.5 ( $C_q$ ), 126.6 (CH), 125.9 ( $C_q$ ), 125.3 (CH), 119.7 (CH), 117.9 (CH), 109.4 (CH), 60.7 (CH), 42.0 ( $C_q$ ), 29.2 ( $CH_3$ ), 26.3 ( $CH_2$ ), 25.1 ( $CH_2$ ), 25.1 ( $CH_2$ ).

**IR** (ATR): 3188, 2945, 1552, 1413, 1391, 1135, 909, 723, 405  $cm^{-1}$ .

**MS** (ESI)  $m/z$  (relative intensity): 363 (10)  $[M+H]^+$ , 385 (90)  $[M+Na]^+$ .

**HR-MS** (ESI)  $C_{19}H_{27}N_2O_3S$   $[M+H]^+$ : 363.1738, found: 363.1737.

**Methyl-3-(1-pivaloyl-1*H*-indol-7-yl)acrylate (394a)**



The **General Procedure B** was followed using *N*-pivaloyl indole **390a** (50.3 mg, 0.25 mmol), methyl acrylate **393a** (64.6 mg, 0.75 mmol), Ru(OAc)<sub>2</sub>(*p*-cymene) (8.8 mg, 10 mol %), AgSbF<sub>6</sub> (17.2 mg, 20 mol %) and Cu(OAc)<sub>2</sub> (90.8 mg, 2 equiv) in TFE (1.0 mL). Purification by column chromatography on silica gel (*n*-hexane/EtOAc: 10/1) yielded **394a** (53.5 mg, 75%) as a light yellow solid.

**M. p.** 121 °C.

<sup>1</sup>H NMR (400 MHz, CDCl<sub>3</sub>) δ 7.81 (d, *J* = 15.7 Hz, 1H), 7.58 (d, *J* = 7.6 Hz, 1H), 7.57 (d, *J* = 3.8 Hz, 1H), 7.44 (d, *J* = 7.6, 1H), 7.26 (t, *J* = 7.6 Hz, 1H), 6.62 (d, *J* = 3.8 Hz, 1H), 6.28 (d, *J* = 15.7 Hz, 1H), 3.79 (s, 3H), 1.54 (s, 9H).

<sup>13</sup>C NMR (100 MHz, CDCl<sub>3</sub>) δ 179.4 (C<sub>q</sub>), 167.4 (C<sub>q</sub>), 143.3 (CH), 134.8 (C<sub>q</sub>), 131.2 (C<sub>q</sub>), 126.5 (CH), 124.0 (CH), 123.5 (CH), 123.2 (C<sub>q</sub>), 122.4 (CH), 117.2 (CH), 107.5 (CH), 51.6 (CH<sub>3</sub>), 42.0 (C<sub>q</sub>), 29.0 (CH<sub>3</sub>).

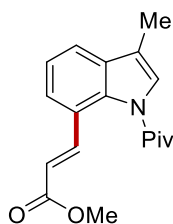
**IR** (ATR): 2958, 2156, 1704, 1636, 1312, 1309, 1167, 949, 753, 592 cm<sup>-1</sup>.

**MS** (ESI) *m/z* (relative intensity): 286 (10) [M+H]<sup>+</sup>, 308 (90) [M+Na]<sup>+</sup>.

**HR-MS** (ESI) C<sub>17</sub>H<sub>20</sub>NO<sub>3</sub> [M+H]<sup>+</sup>: 286.1437, found: 286.1438.

The spectral data were in accordance with those reported in the literature.<sup>[265]</sup>

### Methyl-3-(3-methyl-1-pivaloyl-1*H*-indol-7-yl)acrylate (**394b**)



The **General Procedure B** was followed using 2,2-dimethyl-1-(3-methyl-1*H*-indol-1-yl)propan-1-one **390b** (53.8 mg, 0.25 mmol), methyl acrylate **393a** (64.6 mg, 0.75 mmol), Ru(OAc)<sub>2</sub>(*p*-cymene) (8.8 mg, 10 mol %), AgSbF<sub>6</sub> (17.2 mg, 20 mol %) and Cu(OAc)<sub>2</sub> (90.8 mg, 2 equiv) in TFE (1.0 mL). Purification by column chromatography on silica gel (*n*-hexane/EtOAc: 10/1) yielded **394b** (27.7 mg, 37%) as a light yellow solid.

**M. p.** 107 °C.

<sup>1</sup>H NMR (400 MHz, CDCl<sub>3</sub>) δ 7.81 (d, *J* = 15.8 Hz, 1H), 7.50 (dd, *J* = 7.7, 1.2 Hz, 1H), 7.45 (d, *J* =

7.7 Hz, 1H), 7.35 (q,  $J = 1.2$  Hz, 1H), 7.28 (t,  $J = 7.7$  Hz, 1H), 6.26 (d,  $J = 15.8$  Hz, 1H), 3.78 (s, 3H), 2.27 (s, 3H), 1.52 (s, 9H).

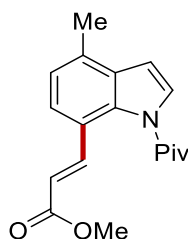
$^{13}\text{C}$  NMR (100 MHz,  $\text{CDCl}_3$ )  $\delta$  179.0 ( $\text{C}_q$ ), 167.5 ( $\text{C}_q$ ), 143.6 (CH), 135.4 ( $\text{C}_q$ ), 132.3 ( $\text{C}_q$ ), 124.1 (CH), 123.6 (CH), 123.4 ( $\text{C}_q$ ), 123.3 (CH), 120.3 (CH), 116.9 (CH), 116.6 ( $\text{C}_q$ ), 51.6 ( $\text{CH}_3$ ), 41.8 ( $\text{C}_q$ ), 29.0 ( $\text{CH}_3$ ), 9.7 ( $\text{CH}_3$ ).

IR (ATR): 2970, 2169, 1711, 1434, 1371, 1265, 1170, 1038, 906, 731  $\text{cm}^{-1}$ .

MS (ESI)  $m/z$  (relative intensity): 300 (10)  $[\text{M}+\text{H}]^+$ , 322 (34)  $[\text{M}+\text{Na}]^+$ .

HR-MS (ESI)  $\text{C}_{18}\text{H}_{22}\text{NO}_3$   $[\text{M}+\text{H}]^+$ : 300.1594, found: 300.1594.

### Methyl-3-(4-methyl-1-pivaloyl-1H-indol-7-yl)acrylate (**394c**)



The **General Procedure B** was followed using 2,2-dimethyl-1-(4-methyl-1H-indol-1-yl)propan-1-one **390c** (53.8 mg, 0.25 mmol), methyl acrylate **393a** (64.6 mg, 0.75 mmol),  $\text{Ru}(\text{OAc})_2(p\text{-cymene})$  (8.8 mg, 10 mol %),  $\text{AgSbF}_6$  (17.2 mg, 20 mol %) and  $\text{Cu}(\text{OAc})_2$  (90.8 mg, 2 equiv) in TFE (1.0 mL). Purification by column chromatography on silica gel (*n*-hexane/EtOAc: 10/1) yielded **394c** (41.9 mg, 56%) as a light yellow solid.

**M. p.** 113  $^\circ\text{C}$ .

$^1\text{H}$  NMR (400 MHz,  $\text{CDCl}_3$ )  $\delta$  7.73 (d,  $J = 15.7$  Hz, 1H), 7.51 (d,  $J = 3.8$  Hz, 1H), 7.32 (d,  $J = 7.9$  Hz, 1H), 7.02 (ddd,  $J = 7.9, 1.4, 0.7$  Hz, 1H), 6.59 (d,  $J = 3.8$  Hz, 1H), 6.20 (d,  $J = 15.7$  Hz, 1H), 3.73 (s, 3H), 2.47 (s, 3H), 1.49 (s, 9H).

$^{13}\text{C}$  NMR (100 MHz,  $\text{CDCl}_3$ )  $\delta$  179.7 ( $\text{C}_q$ ), 167.6 ( $\text{C}_q$ ), 143.3 (CH), 134.6 ( $\text{C}_q$ ), 132.5 ( $\text{C}_q$ ), 130.8 ( $\text{C}_q$ ), 125.9 (CH), 124.1 (CH), 124.0 (CH), 120.8 ( $\text{C}_q$ ), 116.3 (CH), 105.8 (CH), 51.5 ( $\text{CH}_3$ ), 42.1 ( $\text{C}_q$ ), 29.0 ( $\text{CH}_3$ ), 18.6 ( $\text{CH}_3$ ).

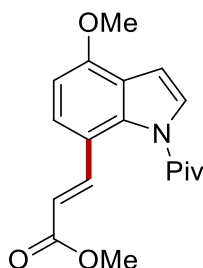
IR (ATR): 2969, 1706, 1633, 1264, 1159, 1080, 900, 730, 616, 444  $\text{cm}^{-1}$ .

MS (ESI)  $m/z$  (relative intensity): 300 (66)  $[\text{M}+\text{H}]^+$ , 322 (34)  $[\text{M}+\text{Na}]^+$ .

**HR-MS** (ESI)  $C_{18}H_{22}NO_3$   $[M+H]^+$ : 300.1598, found: 300.1596.

The spectral data were in accordance with those reported in the literature.<sup>[265]</sup>

**Methyl-3-(4-methoxy-1-pivaloyl-1*H*-indol-7-yl)acrylate (394d)**



The **General Procedure B** was followed using 1-(4-methoxy-1*H*-indol-1-yl)-2,2-dimethylpropan-1-one **390d** (57.8 mg, 0.25 mmol), methyl acrylate **393a** (64.6 mg, 0.75 mmol),  $Ru(OAc)_2(p\text{-cymene})$  (8.8 mg, 10 mol %),  $AgSbF_6$  (17.2 mg, 20 mol %) and  $Cu(OAc)_2$  (90.8 mg, 2 equiv) in TFE (1.0 mL). Purification by column chromatography on silica gel (*n*-hexane/EtOAc: 10/1) yielded **394d** (41.8 mg, 53%) as a light yellow solid.

**M. p.** 132 °C.

**$^1H$  NMR** (400 MHz,  $CDCl_3$ )  $\delta$  7.75 (d,  $J = 15.7$  Hz, 1H), 7.46 (d,  $J = 3.7$  Hz, 1H), 7.43 (d,  $J = 8.3$  Hz, 1H), 6.73 (d,  $J = 3.7$  Hz, 1H), 6.69 (d,  $J = 8.3$  Hz, 1H), 6.18 (d,  $J = 15.7$  Hz, 1H), 3.94 (s, 3H), 3.77 (s, 3H), 1.53 (s, 9H).

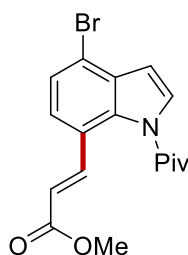
**$^{13}C$  NMR** (100 MHz,  $CDCl_3$ )  $\delta$  179.8 ( $C_q$ ), 167.7 ( $C_q$ ), 154.6 ( $C_q$ ), 142.9 (CH), 136.2 ( $C_q$ ), 125.6 (CH), 125.0 (CH), 121.3 ( $C_q$ ), 116.4 ( $C_q$ ), 115.1 (CH), 104.3 (CH), 103.8 (CH), 55.6 ( $CH_3$ ), 51.5 ( $CH_3$ ), 42.2 ( $C_q$ ), 28.9 ( $CH_3$ ).

**IR** (ATR): 2967, 1706, 1601, 1498, 1262, 1156, 1065, 901, 731, 584  $cm^{-1}$ .

**MS** (ESI)  $m/z$  (relative intensity): 316 (10)  $[M+H]^+$ , 338 (34)  $[M+Na]^+$ .

**HR-MS** (ESI)  $C_{18}H_{22}NO_4$   $[M+H]^+$ : 316.1539, found: 316.1540.

The spectral data were in accordance with those reported in the literature.<sup>[265]</sup>

**Methyl-3-(4-bromo-1-pivaloyl-1H-indol-7-yl)acrylate (394e)**

The **General Procedure B** was followed using 1-(4-bromo-1H-indol-1-yl)-2,2-dimethylpropan-1-one **390e** (70.0 mg, 0.25 mmol), methyl acrylate **393a** (64.6 mg, 0.75 mmol), Ru(OAc)<sub>2</sub>(*p*-cymene) (8.8 mg, 10 mol %), AgSbF<sub>6</sub> (17.2 mg, 20 mol %) and Cu(OAc)<sub>2</sub> (90.8 mg, 2 equiv) in TFE (1.0 mL). Purification by column chromatography on silica gel (*n*-hexane/EtOAc: 10/1) yielded **394e** (62.8 mg, 69%) as a light yellow solid.

**M. p.** 101 °C.

**<sup>1</sup>H NMR** (400 MHz, CDCl<sub>3</sub>) δ 7.70 (d, *J* = 15.7 Hz, 1H), 7.60 (dd, *J* = 3.7, 0.4 Hz, 1H), 7.42 (dd, *J* = 8.1, 0.4 Hz, 1H), 7.28 (ddd, *J* = 8.1, 1.1, 0.4 Hz, 1H), 6.70 (d, *J* = 3.7 Hz, 1H), 6.26 (d, *J* = 15.7 Hz, 1H), 3.78 (s, 3H), 1.50 (s, 9H).

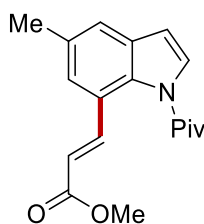
**<sup>13</sup>C NMR** (100 MHz, CDCl<sub>3</sub>) δ 179.5 (C<sub>q</sub>), 167.2 (C<sub>q</sub>), 142.2 (CH), 134.9 (C<sub>q</sub>), 131.7 (C<sub>q</sub>), 126.9 (CH), 126.4 (CH), 124.7 (CH), 122.3 (C<sub>q</sub>), 117.8 (CH), 116.5 (C<sub>q</sub>), 107.4 (CH), 51.7 (CH<sub>3</sub>), 42.2 (C<sub>q</sub>), 28.8 (CH<sub>3</sub>).

**IR** (ATR): 2968, 1041, 1714, 1475, 1263, 1170, 1009, 875, 703, 534 cm<sup>-1</sup>.

**MS** (ESI) *m/z* (relative intensity): 364 (10) (<sup>79</sup>Br) [M+H]<sup>+</sup>, 366 (10) (<sup>81</sup>Br) [M+H]<sup>+</sup>, 386 (90) (<sup>79</sup>Br) [M+Na]<sup>+</sup>, 388 (90) (<sup>81</sup>Br) [M+Na]<sup>+</sup>.

**HR-MS** (ESI) C<sub>17</sub>H<sub>19</sub><sup>79</sup>BrNO<sub>3</sub> [M+H]<sup>+</sup>: 364.0553, found: 364.0554.

The spectral data were in accordance with those reported in the literature.<sup>[265]</sup>

**Methyl-3-(5-methyl-1-pivaloyl-1H-indol-7-yl)acrylate (394f)**

The **General Procedure B** was followed using 1-(5-methyl-1*H*-indol-1-yl)-2,2-dimethylpropan-1-one **390f** (53.8 mg, 0.25 mmol), methyl acrylate **393a** (64.6 mg, 0.75 mmol), Ru(OAc)<sub>2</sub>(*p*-cymene) (8.8 mg, 10 mol %), AgSbF<sub>6</sub> (17.2 mg, 20 mol %) and Cu(OAc)<sub>2</sub> (90.8 mg, 2 equiv) in TFE (1.0 mL). Purification by column chromatography on silica gel (*n*-hexane/EtOAc: 10/1) yielded **394f** (49.4 mg, 66%) as a light yellow solid.

**M. p.** 121 °C.

<sup>1</sup>H NMR (400 MHz, CDCl<sub>3</sub>) δ 7.80 (d, *J* = 15.7 Hz, 1H), 7.54 (d, *J* = 3.7 Hz, 1H), 7.35 – 7.36 (m, 1H), 7.27 – 7.26 (m, 1H), 6.53 (d, *J* = 3.7 Hz, 1H), 6.25 (d, *J* = 15.7 Hz, 1H), 3.78 (s, 3H), 2.42 (s, 3H), 1.53 (s, 9H).

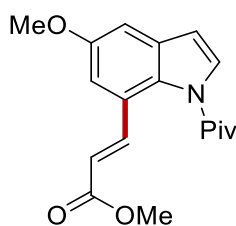
<sup>13</sup>C NMR (100 MHz, CDCl<sub>3</sub>) δ 179.2 (C<sub>q</sub>), 167.5 (C<sub>q</sub>), 143.5 (CH), 133.2 (C<sub>q</sub>), 133.1 (C<sub>q</sub>), 131.6 (C<sub>q</sub>), 126.6 (CH), 125.6 (CH), 122.9 (C<sub>q</sub>), 122.4 (CH), 117.0 (CH), 107.3 (CH), 51.6 (CH<sub>3</sub>), 41.9 (C<sub>q</sub>), 29.0 (CH<sub>3</sub>), 21.1 (CH<sub>3</sub>).

IR (ATR): 2973, 1709, 1612, 1495, 1301, 1257, 1168, 902, 713, 622 cm<sup>-1</sup>.

MS (ESI) *m/z* (relative intensity): 300 (10) [M+H]<sup>+</sup>, 322 (90) [M+Na]<sup>+</sup>.

HR-MS (ESI) C<sub>18</sub>H<sub>22</sub>NO<sub>3</sub> [M+H]<sup>+</sup>: 300.1599, found: 300.1597.

#### Methyl-3-(5-methoxy-1-pivaloyl-1*H*-indol-7-yl)acrylate (**394g**)



The **General Procedure B** was followed using 1-(5-methoxy-1*H*-indol-1-yl)-2,2-dimethylpropan-1-one **390g** (57.8 mg, 0.25 mmol), methyl acrylate **393a** (64.6 mg, 0.75 mmol), Ru(OAc)<sub>2</sub>(*p*-cymene) (8.8 mg, 10 mol %), AgSbF<sub>6</sub> (17.2 mg, 20 mol %) and Cu(OAc)<sub>2</sub> (90.8 mg, 2 equiv) in TFE (1.0 mL). Purification by column chromatography on silica gel (*n*-hexane/EtOAc: 10/1) yielded **394g** (49.7 mg, 63%) as a light yellow solid.

**M. p.** 102 °C.

<sup>1</sup>H NMR (400 MHz, CDCl<sub>3</sub>) δ 7.80 (d, *J* = 15.7 Hz, 1H), 7.56 (d, *J* = 3.7 Hz, 1H), 7.05 (m, 2H), 6.53

(d,  $J = 3.7$  Hz, 1H), 6.25 (d,  $J = 15.7$  Hz, 1H), 3.84 (s, 3H), 3.78 (s, 3H), 1.52 (s,  $J = 4.5$  Hz, 9H).

$^{13}\text{C}$  NMR (100 MHz,  $\text{CDCl}_3$ )  $\delta$  178.9 ( $\text{C}_q$ ), 167.3 ( $\text{C}_q$ ), 156.4 ( $\text{C}_q$ ), 143.2 (CH), 132.4 ( $\text{C}_q$ ), 129.8 ( $\text{C}_q$ ), 127.3 (CH), 124.1 ( $\text{C}_q$ ), 117.5 (CH), 112.3 (CH), 107.5 (CH), 105.2 (CH), 55.8 ( $\text{CH}_3$ ), 51.6 ( $\text{CH}_3$ ), 41.8 ( $\text{C}_q$ ), 29.0 ( $\text{CH}_3$ ).

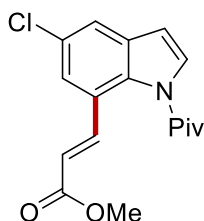
IR (ATR): 2970, 1713, 1620, 1487, 1315, 1260, 1043, 902, 722, 691  $\text{cm}^{-1}$ .

MS (ESI)  $m/z$  (relative intensity): 316 (20)  $[\text{M}+\text{H}]^+$ , 338 (80)  $[\text{M}+\text{Na}]^+$ .

HR-MS (ESI)  $\text{C}_{18}\text{H}_{22}\text{NO}_4$   $[\text{M}+\text{H}]^+$ : 316.1541, found: 316.1543.

The spectral data were in accordance with those reported in the literature.<sup>[265]</sup>

### Methyl-3-(5-chloro-1-pivaloyl-1H-indol-7-yl)acrylate (394h)



The **General Procedure B** was followed using 1-(5-chloro-1H-indol-1-yl)-2,2-dimethylpropan-1-one **390h** (58.9 mg, 0.25 mmol), methyl acrylate **393a** (64.6 mg, 0.75 mmol),  $\text{Ru}(\text{OAc})_2(p\text{-cymene})$  (8.8 mg, 10 mol %),  $\text{AgSbF}_6$  (17.2 mg, 20 mol %) and  $\text{Cu}(\text{OAc})_2$  (90.8 mg, 2 equiv) in TFE (1.0 mL). Purification by column chromatography on silica gel (*n*-hexane/EtOAc: 10/1) yielded **394h** (55.2 mg, 69%) as a light yellow solid.

**M. p.** 105 °C.

$^1\text{H}$  NMR (400 MHz,  $\text{CDCl}_3$ )  $\delta$  7.72 (d,  $J = 15.7$  Hz, 1H), 7.59 (dd,  $J = 3.7, 0.5$  Hz, 1H), 7.53 (d,  $J = 2.0$  Hz, 1H), 7.39 (dd,  $J = 2.0, 0.5$  Hz, 1H), 6.55 (d,  $J = 3.7$  Hz, 1H), 6.26 (d,  $J = 15.7$  Hz, 1H), 3.79 (s, 3H), 1.52 (s, 9H).

$^{13}\text{C}$  NMR (100 MHz,  $\text{CDCl}_3$ )  $\delta$  179.2 ( $\text{C}_q$ ), 167.0 ( $\text{C}_q$ ), 142.0 (CH), 133.2 ( $\text{C}_q$ ), 132.4 ( $\text{C}_q$ ), 129.1 ( $\text{C}_q$ ), 127.7 (CH), 124.4 ( $\text{C}_q$ ), 123.8 (CH), 121.6 (CH), 118.4 (CH), 106.8 (CH), 51.7 ( $\text{CH}_3$ ), 42.1 ( $\text{C}_q$ ), 28.9 ( $\text{CH}_3$ ).

IR (ATR): 2971, 1707, 1639, 1400, 1259, 1166, 1043, 905, 811, 714  $\text{cm}^{-1}$ .

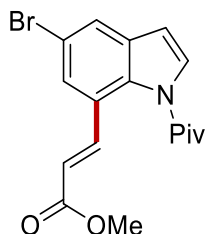
MS (ESI)  $m/z$  (relative intensity): 320 (10)  $[\text{M}+\text{H}]^+$ , 342 (90)  $[\text{M}+\text{Na}]^+$ .



**HR-MS** (ESI)  $C_{17}H_{19}^{35}ClNO_3$   $[M+H]^+$ : 320.1043, found: 320.1045.

The spectral data were in accordance with those reported in the literature.<sup>[265]</sup>

**Methyl-3-(5-bromo-1-pivaloyl-1*H*-indol-7-yl)acrylate (394i)**



The **General Procedure B** was followed using 1-(5-bromo-1*H*-indol-1-yl)-2,2-dimethylpropan-1-one **390i** (70.0 mg, 0.25 mmol), methyl acrylate **393a** (64.6 mg, 0.75 mmol),  $Ru(OAc)_2(p\text{-cymene})$  (8.8 mg, 10 mol %),  $AgSbF_6$  (17.2 mg, 20 mol %) and  $Cu(OAc)_2$  (90.8 mg, 2 equiv) in TFE (1.0 mL). Purification by column chromatography on silica gel (*n*-hexane/EtOAc: 10/1) yielded **394i** (65.6 mg, 72%) as a light yellow solid.

**M. p.** 97 °C.

**$^1H$  NMR** (400 MHz,  $CDCl_3$ )  $\delta$  7.71 (d,  $J = 15.7$  Hz, 1H), 7.69 (t,  $J = 1.9$  Hz, 1H), 7.57 (d,  $J = 3.8$  Hz, 1H), 7.52 (ddd,  $J = 1.9, 1.1, 0.6$  Hz, 1H), 6.56 (d,  $J = 3.8$  Hz, 1H), 6.26 (d,  $J = 15.7$  Hz, 1H), 3.79 (s, 3H), 1.51 (s, 9H).

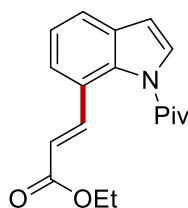
**$^{13}C$  NMR** (100 MHz,  $CDCl_3$ )  $\delta$  179.2 ( $C_q$ ), 167.0 ( $C_q$ ), 141.9 (CH), 133.6 ( $C_q$ ), 132.8 ( $C_q$ ), 127.6 (CH), 126.4 (CH), 124.7 ( $C_q$ ), 124.6 (CH), 118.5 (CH), 116.7 ( $C_q$ ), 106.8 (CH), 51.7 ( $CH_3$ ), 42.1 ( $C_q$ ), 28.9 ( $CH_3$ ).

**IR** (ATR): 2971, 1706, 1444, 1399, 1285, 1258, 1165, 1042, 904, 809  $cm^{-1}$ .

**MS** (ESI)  $m/z$  (relative intensity): 364 (10) ( $^{79}Br$ )  $[M+H]^+$ , 366 (10) ( $^{81}Br$ )  $[M+H]^+$ , 386 (90) ( $^{79}Br$ )  $[M+H]^+$ , 388 (90) ( $^{81}Br$ )  $[M+H]^+$

**HR-MS** (ESI)  $C_{17}H_{19}^{79}BrNO_3$   $[M+H]^+$ : 364.0547, found: 364.0544.

The spectral data were in accordance with those reported in the literature.<sup>[265]</sup>

**Ethyl-3-(1-pivaloyl-1*H*-indol-7-yl)acrylate (394j)**

The **General Procedure B** was followed using *N*-pivaloyl indole **390j** (50.3 mg, 0.25 mmol), ethyl acrylate **393b** (75.1 mg, 0.75 mmol), Ru(OAc)<sub>2</sub>(*p*-cymene) (8.8 mg, 10 mol %), AgSbF<sub>6</sub> (17.2 mg, 20 mol %) and Cu(OAc)<sub>2</sub> (90.8 mg, 2 equiv) in TFE (1.0 mL). Purification by column chromatography on silica gel (*n*-hexane/EtOAc: 10/1) yielded **394j** (52.4 mg, 70%) as a light yellow solid.

**M. p.** 76 °C.

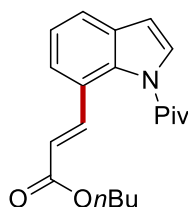
<sup>1</sup>H NMR (400 MHz, CDCl<sub>3</sub>) δ 7.79 (d, *J* = 15.8 Hz, 1H), 7.57 (dd, *J* = 7.7, 0.6 Hz, 1H) 7.56 (d, *J* = 3.8 Hz, 1H), 7.45 (ddd, *J* = 7.7, 1.4, 0.6 Hz, 1H), 7.25 (t, *J* = 7.7 Hz, 1H), 6.61 (d, *J* = 3.8 Hz, 1H), 6.27 (d, *J* = 15.8 Hz, 1H), 4.24 (q, *J* = 7.1 Hz, 2H), 1.54 (s, 9H), 1.32 (t, *J* = 7.1 Hz, 3H).

<sup>13</sup>C NMR (100 MHz, CDCl<sub>3</sub>) δ 179.5 (C<sub>q</sub>), 166.9 (C<sub>q</sub>), 142.9 (CH), 134.8 (C<sub>q</sub>), 131.2 (C<sub>q</sub>), 126.5 (CH), 123.9 (CH), 123.5 (CH), 123.3 (C<sub>q</sub>), 122.3 (CH), 117.7 (CH), 107.4 (CH), 60.3 (CH<sub>2</sub>), 42.1 (C<sub>q</sub>), 29.0 (CH<sub>3</sub>), 14.3 (CH<sub>3</sub>).

**IR** (ATR): 2975, 1703, 1635, 1477, 1413, 1286, 1268, 1164, 1038, 715 cm<sup>-1</sup>.

**MS** (ESI) *m/z* (relative intensity): 300 (34) [M+H]<sup>+</sup>, 322 (66) [M+Na]<sup>+</sup>.

**HR-MS** (ESI) C<sub>18</sub>H<sub>22</sub>NO<sub>3</sub> [M+H]<sup>+</sup>: 300.1595, found: 300.1594.

**Butyl-3-(1-pivaloyl-1*H*-indol-7-yl)acrylate (394k)**

The **General Procedure B** was followed using *N*-pivaloyl indole **390k** (50.3 mg, 0.25 mmol), butyl acrylate **393c** (96.1 mg, 0.75 mmol), Ru(OAc)<sub>2</sub>(*p*-cymene) (8.8 mg, 10 mol %), AgSbF<sub>6</sub> (17.2 mg, 20 mol %) and Cu(OAc)<sub>2</sub> (90.8 mg, 2 equiv) in TFE (1.0 mL). Purification by column chromatography on silica gel (*n*-hexane/EtOAc: 10/1) yielded **394k** (49.9 mg, 61%) as a light yellow liquid.

<sup>1</sup>H NMR (400 MHz, CDCl<sub>3</sub>) δ 7.79 (d, *J* = 15.7 Hz, 1H), 7.58 (d, *J* = 3.8 Hz, 1H), 7.57 (dd, *J* = 7.5,

1.1 Hz, 1H), 7.45 (ddd,  $J = 7.5, 1.1, 0.6$  Hz, 1H), 7.25 (dd,  $J = 7.5, 0.6$  Hz, 1H), 6.61 (d,  $J = 3.8$  Hz, 1H), 6.28 (d,  $J = 15.8$  Hz, 1H), 4.19 (t,  $J = 6.6$  Hz, 2H), 1.73 – 1.62 (m, 2H), 1.53 (s, 9H), 1.48 – 1.38 (m, 2H), 0.95 (t,  $J = 7.4$  Hz, 3H).

$^{13}\text{C}$  NMR (100 MHz,  $\text{CDCl}_3$ )  $\delta$  179.3 ( $\text{C}_q$ ), 167.0 ( $\text{C}_q$ ), 142.9 (CH), 134.8 ( $\text{C}_q$ ), 131.2 ( $\text{C}_q$ ), 126.5 (CH), 124.0 (CH), 123.5 (CH), 123.3 ( $\text{C}_q$ ), 122.3 (CH), 117.7 (CH), 107.5 (CH), 64.3 ( $\text{CH}_2$ ), 42.0 ( $\text{C}_q$ ), 30.8 ( $\text{CH}_2$ ), 29.0 ( $\text{CH}_3$ ), 19.2 ( $\text{CH}_2$ ), 13.7 ( $\text{CH}_3$ ).

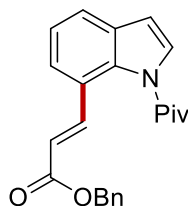
IR (ATR): 2959, 1704, 1636, 1413, 1284, 1165, 1075, 906, 714, 583  $\text{cm}^{-1}$ .

MS (ESI)  $m/z$  (relative intensity): 328 (45)  $[\text{M}+\text{H}]^+$ , 350 (55)  $[\text{M}+\text{Na}]^+$ .

HR-MS (ESI)  $\text{C}_{20}\text{H}_{26}\text{NO}_3$   $[\text{M}+\text{H}]^+$ : 328.1910, found: 328.1907.

The spectral data were in accordance with those reported in the literature.<sup>[265]</sup>

#### Benzyl-3-(1-pivaloyl-1*H*-indol-7-yl)acrylate (**394I**)



The **General Procedure B** was followed using *N*-pivaloyl indole **390I** (50.3 mg, 0.25 mmol), benzyl acrylate **393d** (121.6 mg, 0.75 mmol),  $\text{Ru}(\text{OAc})_2(p\text{-cymene})$  (8.8 mg, 10 mol %),  $\text{AgSbF}_6$  (17.2 mg, 20 mol %) and  $\text{Cu}(\text{OAc})_2$  (90.8 mg, 2 equiv) in TFE (1.0 mL). Purification by column chromatography on silica gel (*n*-hexane/EtOAc: 10/1) yielded **394I** (59.6 mg, 66%) as a light yellow liquid.

$^1\text{H}$  NMR (400 MHz,  $\text{CDCl}_3$ )  $\delta$  7.86 (d,  $J = 15.7$  Hz, 1H), 7.58 (dd,  $J = 7.6, 1.1$  Hz, 1H), 7.57 (d,  $J = 3.6$  Hz, 1H), 7.45 (ddd,  $J = 7.6, 1.1, 0.5$  Hz, 1H), 7.43 – 7.39 (m, 2H), 7.38 – 7.33 (m, 3H), 7.26 (dd,  $J = 7.6, 0.5$  Hz, 1H), 6.61 (d,  $J = 3.6$  Hz, 1H), 6.34 (d,  $J = 15.7$  Hz, 1H), 5.24 (s, 2H), 1.50 (s, 9H).

$^{13}\text{C}$  NMR (100 MHz,  $\text{CDCl}_3$ )  $\delta$  179.3 ( $\text{C}_q$ ), 166.7 ( $\text{C}_q$ ), 143.6 (CH), 136.1 ( $\text{C}_q$ ), 134.8 ( $\text{C}_q$ ), 131.2 ( $\text{C}_q$ ), 128.2 (CH), 128.2 (CH), 128.1 (CH), 126.5 (CH), 124.0 (CH), 123.5 (CH), 123.2 ( $\text{C}_q$ ), 122.4 (CH), 117.2 (CH), 107.5 (CH), 66.2 ( $\text{CH}_2$ ), 42.0 ( $\text{C}_q$ ), 28.9 ( $\text{CH}_3$ ).

IR (ATR): 2970, 1704, 1635, 1477, 1413, 1286, 1159, 1076, 980, 732  $\text{cm}^{-1}$ .

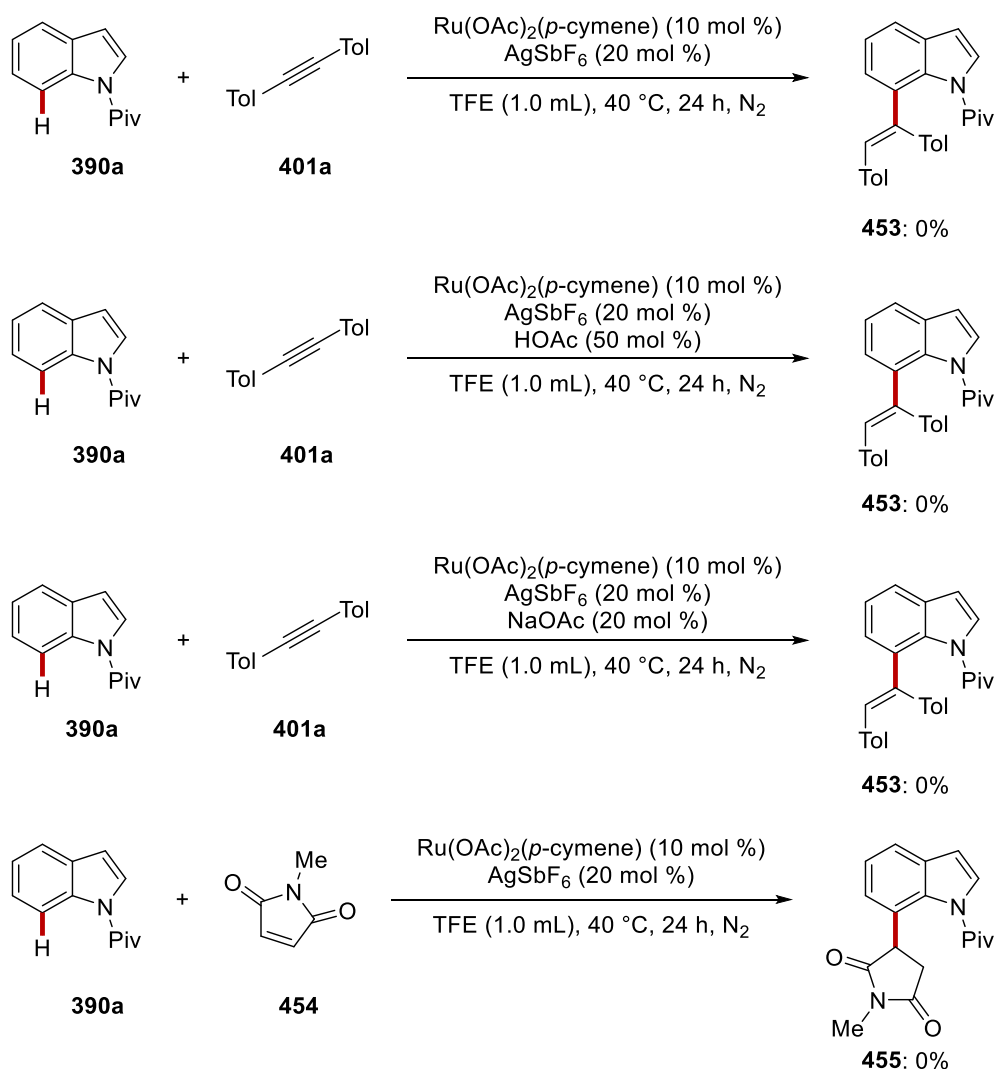
MS (ESI)  $m/z$  (relative intensity): 362 (55)  $[\text{M}+\text{H}]^+$ , 384 (45)  $[\text{M}+\text{Na}]^+$ .

HR-MS (ESI)  $\text{C}_{23}\text{H}_{24}\text{NO}_3$   $[\text{M}+\text{H}]^+$ : 362.1753, found: 362.1751.

### 5.3.2 Various Attempted C7–H Activations

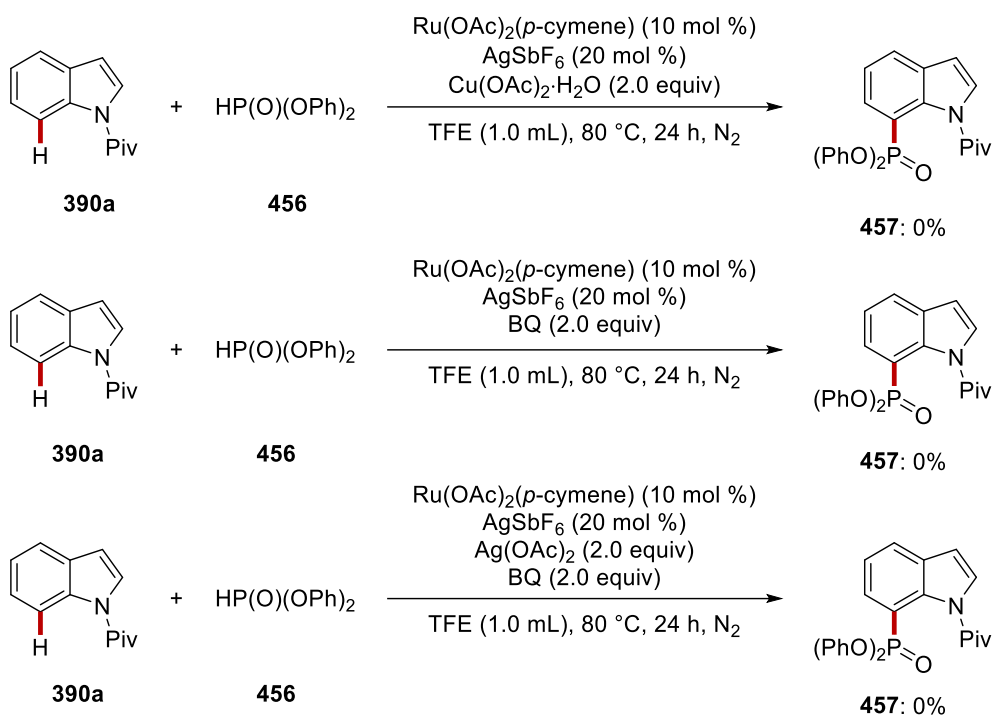
Not only were C7–H amidations and alkenylations tried, but also a variety of coupling partners was chosen to gain a wider perspective toward more broadly applicable ruthenium(II)-catalyzed C7–H activation. Although different types of reactions such as hydroarylations, phosphorylations, trifluoromethylations, arylations, and halogenations among others were additionally attempted, respective desired products were hardly observed, in which a part of the optimization study was displayed below (Scheme 5.3.1 – 5.3.5).

#### 1) Hydroarylation



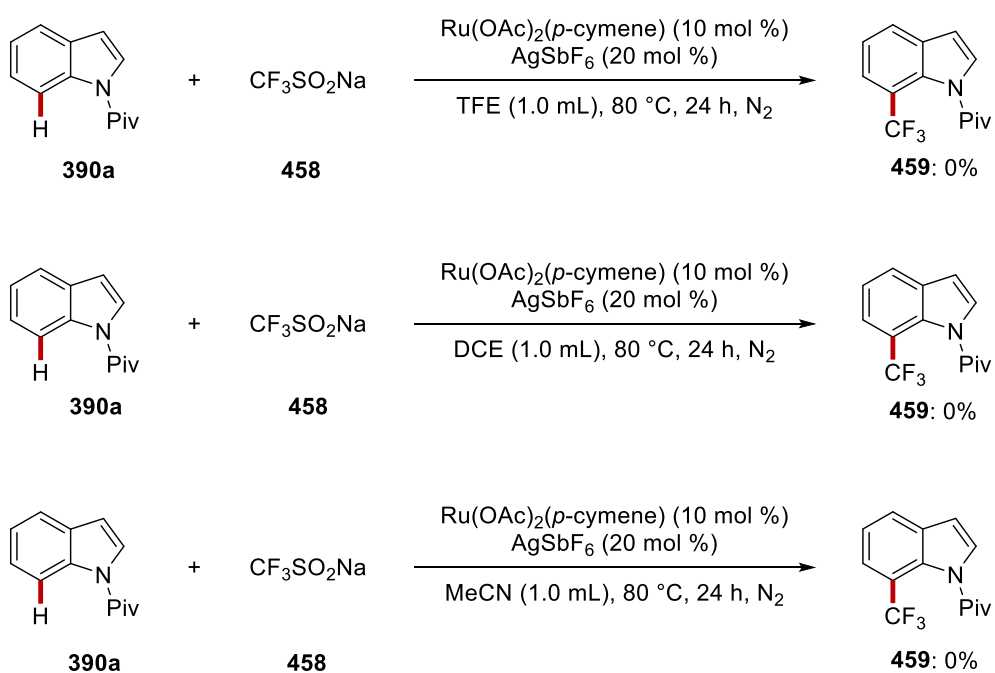
**Scheme 5.3.1** Attempted ruthenium-catalyzed C7–H hydroarylations.

## 2) Phosphorylation



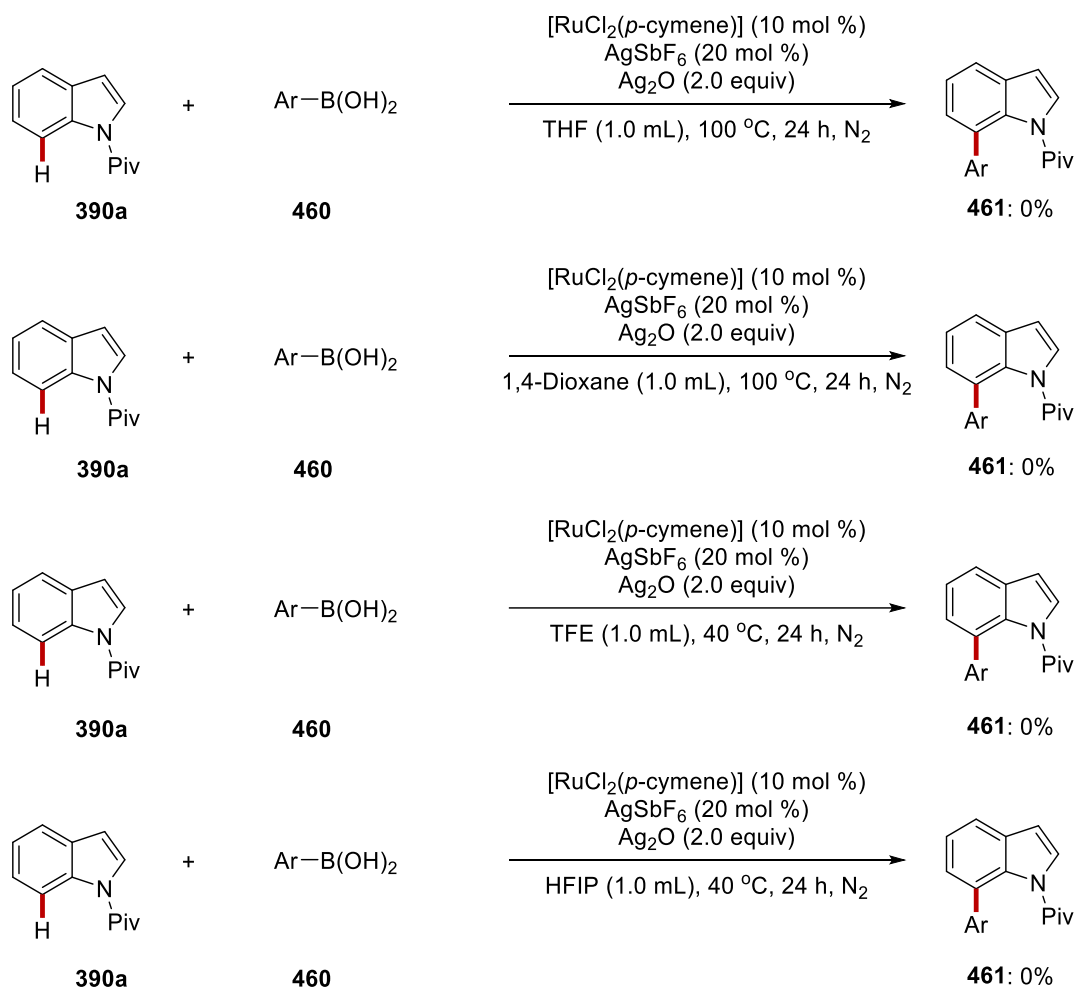
Scheme 5.3.2 Attempted ruthenium-catalyzed C7–H phosphorylations.

## 3) Trifluoromethylation



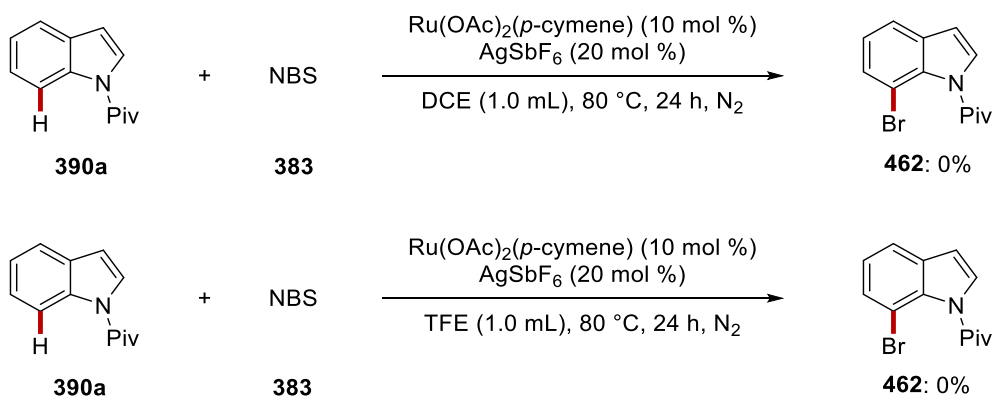
Scheme 5.3.3 Attempted ruthenium-catalyzed C7–H trifluoromethylations.

## 4) Arylation



Scheme 5.3.4 Attempted ruthenium-catalyzed C7–H arylations.

## 5) Halogenation



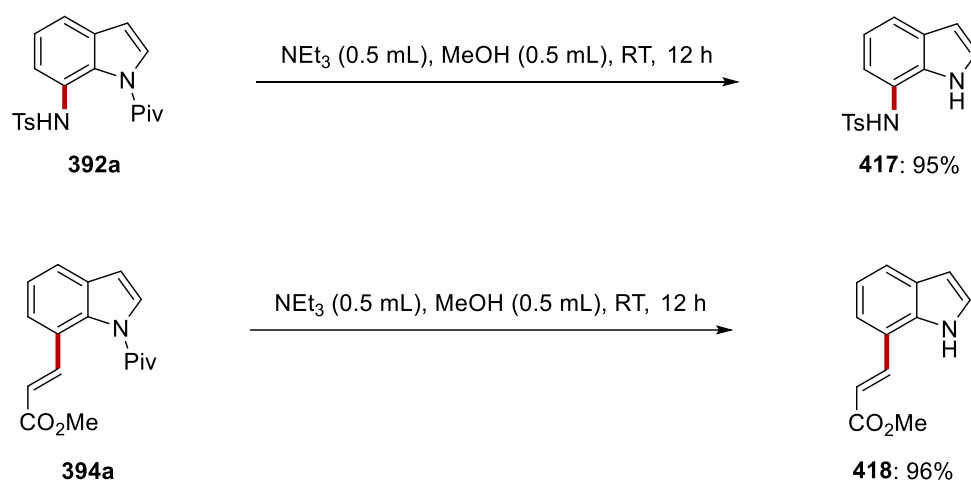
Scheme 5.3.5 Attempted ruthenium-catalyzed C7–H halogenations.



### 5.3.5 Removal of Pivaloyl Directing Group

#### 1) Procedure for the traceless removal of pivaloyl group

A suspension of 4-methyl-*N*-(1-pivaloyl-1*H*-indol-7-yl)benzenesulfonamide **392a** (0.25 mmol, 1.0 equiv) or methyl-3-(1-pivaloyl-1*H*-indol-7-yl)acrylate **394a** (0.25 mmol, 1.0 equiv) in NEt<sub>3</sub> (0.5 mL) and MeOH (0.5 mL) was stirred at room temperature for 12 h (Scheme 5.3.8). The mixture was concentrated *in vacuo*. Purification by column chromatography on silica gel afforded the desired products **417** and **418**, respectively.

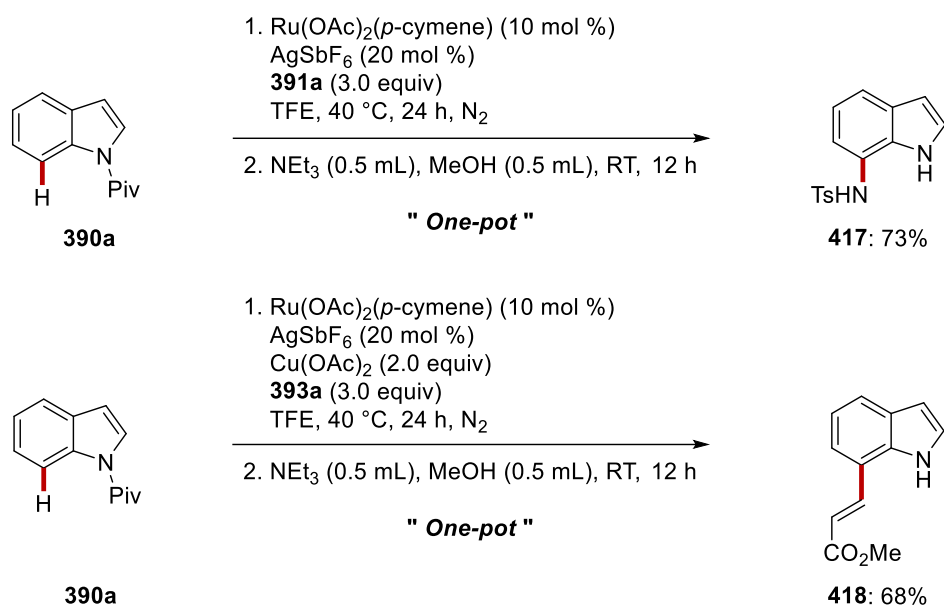


**Scheme 5.3.8** Competition experiments.

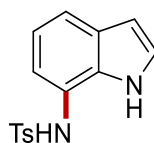
#### 2) Procedure for one-pot strategy of removal of pivaloyl group

Reactions were initially performed by using general procedure described in the general procedure. After cooling to ambient temperature, the solvent is removed by rotary evaporator. Triethylamine (0.5 mL) and MeOH (0.5 mL) were added and stirred at room temperature for 12 h (Scheme 5.3.9). The mixture was concentrated *in vacuo*. Purification by column chromatography on silica gel afforded the desired products **417** and **418** respectively.





Scheme 5.3.9 Competition experiments.

***N*-(1*H*-Indol-7-yl)-4-methylbenzenesulfonamide (417)**

A suspension of 4-Methyl-*N*-(1-pivaloyl-1*H*-indol-7-yl)benzenesulfonamide **390a** (92.6 mg, 0.25 mmol), triethylamine (0.5 mL) in MeOH (0.5 mL) was stirred at room temperature for 12 h. Purification by column chromatography on silica gel (*n*-hexane/EtOAc: 10/1) yielded **417** (68.0 mg, 95%) as a light yellow solid.

**M. p.** 152 °C.

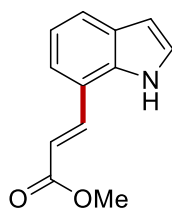
**<sup>1</sup>H NMR** (400 MHz, CDCl<sub>3</sub>) δ 9.27 (s, 1H), 7.53 (ddd, *J* = 8.2, 3.5, 2.1 Hz, 2H), 7.46 (ddd, *J* = 8.2, 2.1, 0.9 Hz, 1H), 7.24 (dd, *J* = 3.5, 2.1 Hz, 1H), 7.15 (ddd, *J* = 7.6, 2.1, 0.9 Hz, 2H), 6.83 (t, *J* = 7.6 Hz, 1H), 6.79 (s, 1H), 6.52 (dd, *J* = 3.5, 2.1 Hz, 1H), 6.42 (d, *J* = 7.6 Hz, 1H), 2.34 (s, 3H).

**<sup>13</sup>C NMR** (100 MHz, CDCl<sub>3</sub>) δ 144.04 (C<sub>q</sub>), 134.77 (C<sub>q</sub>), 131.8 (C<sub>q</sub>), 130.06 (C<sub>q</sub>), 129.55 (CH), 127.37 (CH), 125.25 (CH), 119.92 (C<sub>q</sub>), 119.78 (CH), 119.61 (CH), 117.87 (CH), 102.61 (CH), 21.53 (CH<sub>3</sub>).

**IR** (ATR): 3413, 3251, 2922, 1583, 1334, 1156, 1090, 1038, 730, 551 cm<sup>-1</sup>.

**MS** (ESI) *m/z* (relative intensity): 287 (10) [M+H]<sup>+</sup>, 309 (90) [M+Na]<sup>+</sup>.

**HR-MS** (ESI) C<sub>15</sub>H<sub>15</sub>N<sub>2</sub>O<sub>2</sub>S [M+H]<sup>+</sup>: 287.0847, found: 287.0847.

**Methyl-3-(1*H*-indol-7-yl)acrylate (418)**

A suspension of Methyl-3-(1-pivaloyl-1*H*-indol-7-yl)acrylate **394a** (71.3 mg, 0.25 mmol), triethylamine (0.5 mL) in MeOH (0.5 mL) was stirred at room temperature for 12 h. Purification by column chromatography on silica gel (*n*-hexane/EtOAc: 10/1) yielded **418** (48.3 mg, 96%) as a light yellow solid.

**M. p.** 101 °C.

**<sup>1</sup>H NMR** (400 MHz, CDCl<sub>3</sub>)  $\delta$  9.06 (s, 1H), 8.13 (d,  $J = 16.0$  Hz, 1H), 7.71 (d,  $J = 7.9$  Hz, 1H), 7.43 (d,  $J = 7.9$  Hz, 1H), 7.22 (dd,  $J = 3.2, 1.9$  Hz, 1H), 7.15 (t,  $J = 7.9$  Hz, 1H), 6.61 (dd,  $J = 3.2, 1.9$  Hz, 1H), 6.57 (d,  $J = 16.0$  Hz, 1H), 3.85 (s, 3H).

**<sup>13</sup>C NMR** (100 MHz, CDCl<sub>3</sub>)  $\delta$  168.0 (C<sub>q</sub>), 141.4 (CH), 134.3 (C<sub>q</sub>), 128.9 (C<sub>q</sub>), 124.9 (CH), 123.4 (CH), 121.9 (CH), 120.0 (CH), 118.1 (C<sub>q</sub>), 117.3 (CH), 103.1 (CH), 51.8 (CH<sub>3</sub>).

**IR** (ATR): 3431, 3339, 2949, 1691, 1308, 1264, 975, 796, 716, 429 cm<sup>-1</sup>.

**MS** (ESI)  $m/z$  (relative intensity): 202 (40) [M+H]<sup>+</sup>, 224 (60) [M+Na]<sup>+</sup>.

**HR-MS** (ESI) C<sub>12</sub>H<sub>12</sub>NO<sub>2</sub> [M+H]<sup>+</sup>: 202.0859, found: 202.0860.

## 5.3.6 Hammett Correlation

The **General Procedure A** was followed using electronically different substrates (Scheme 5.3.10).

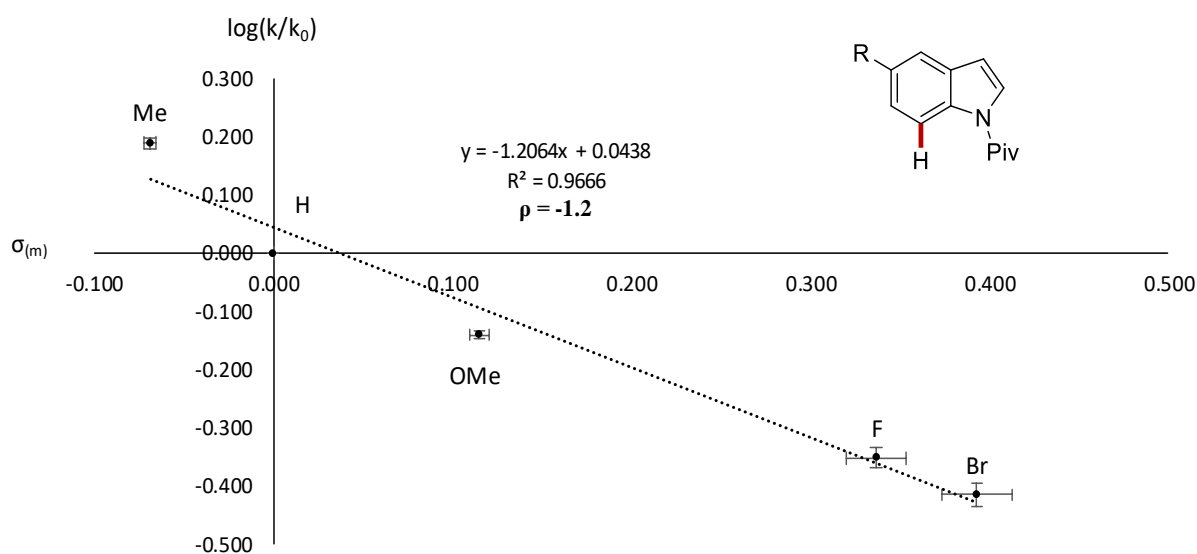
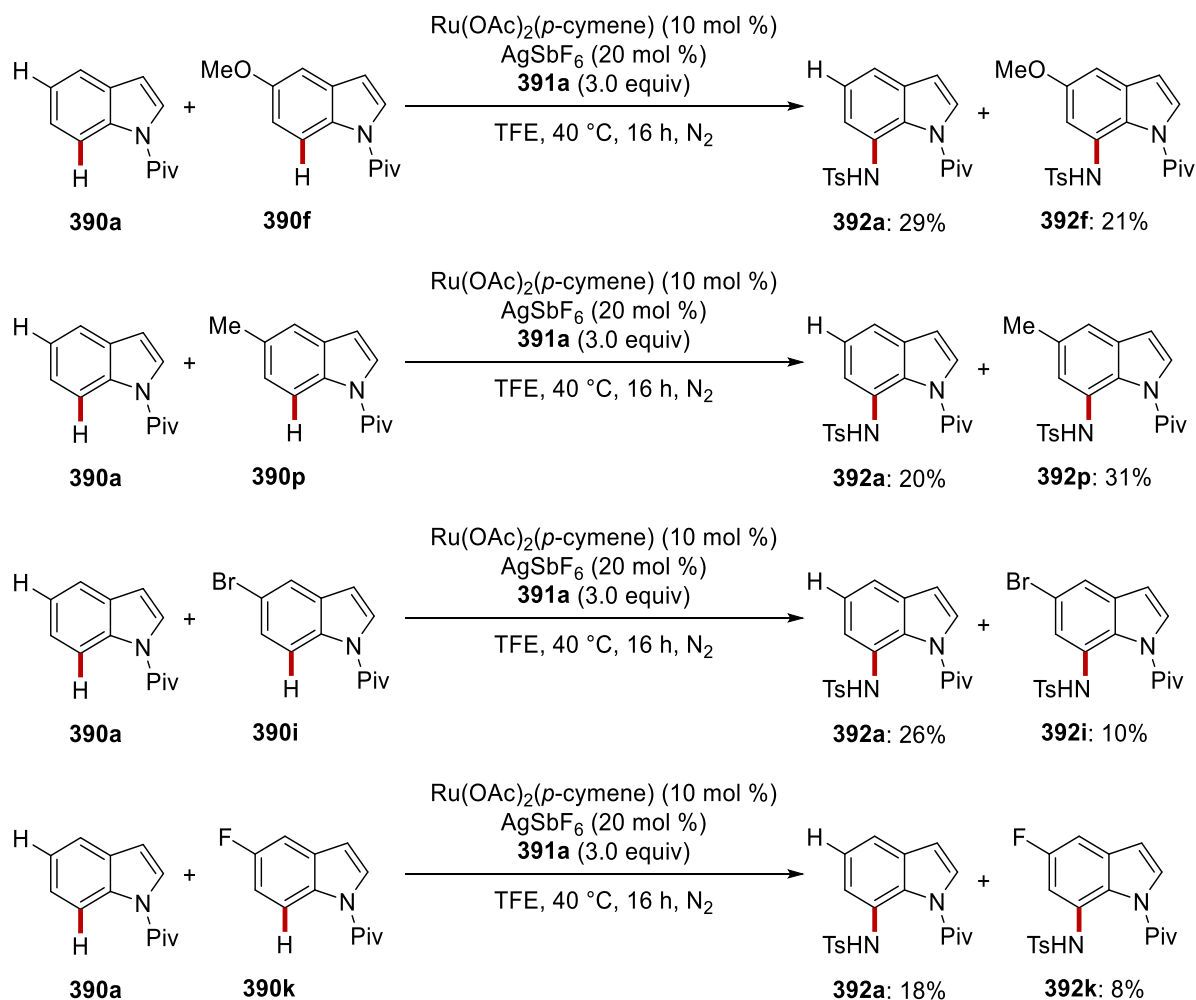
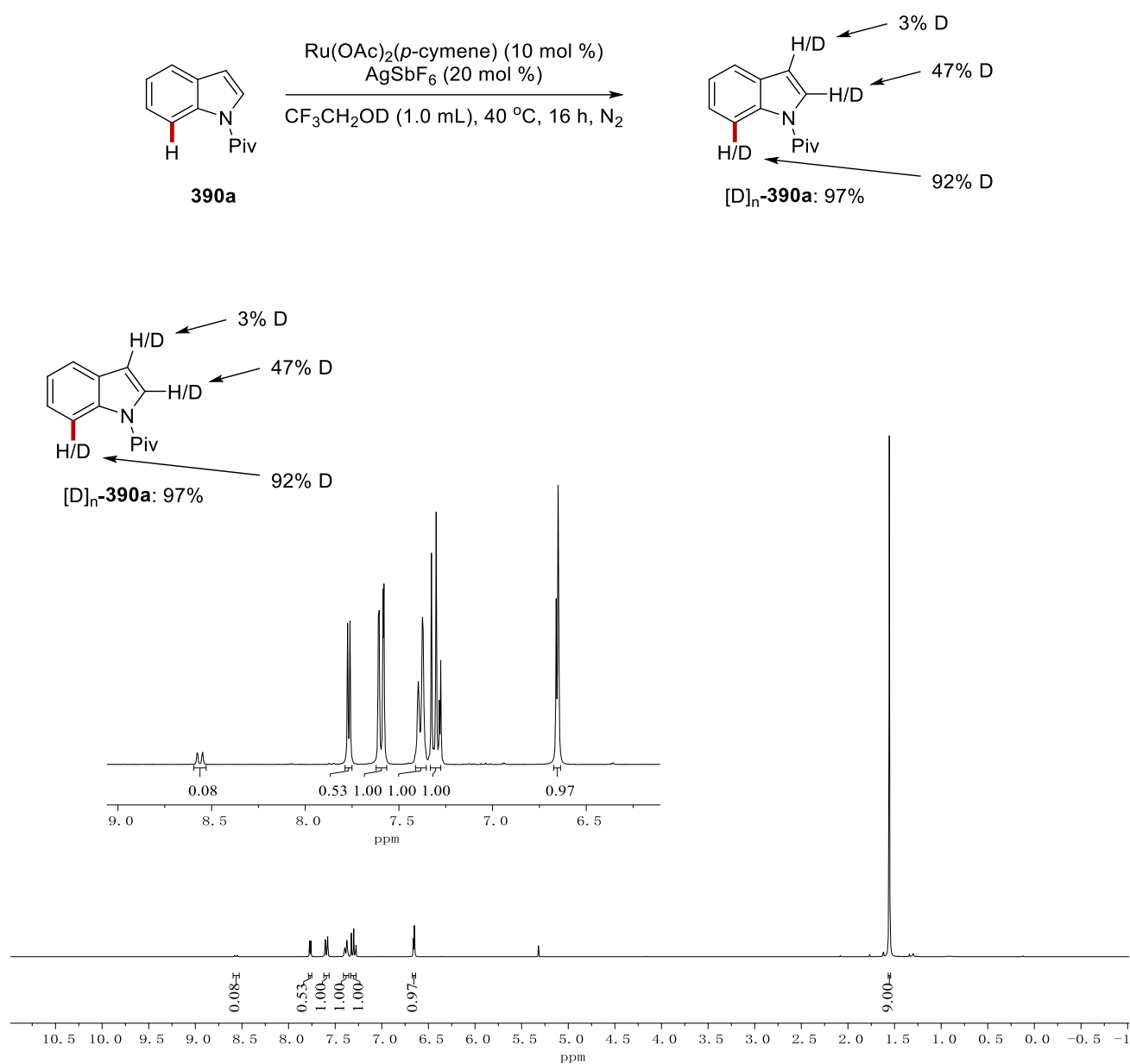


Figure 5.3.10 Hammett correlation plot.

### 5.3.7 H/D Exchange Study

#### 1) Procedure for H/D exchange experiment 1

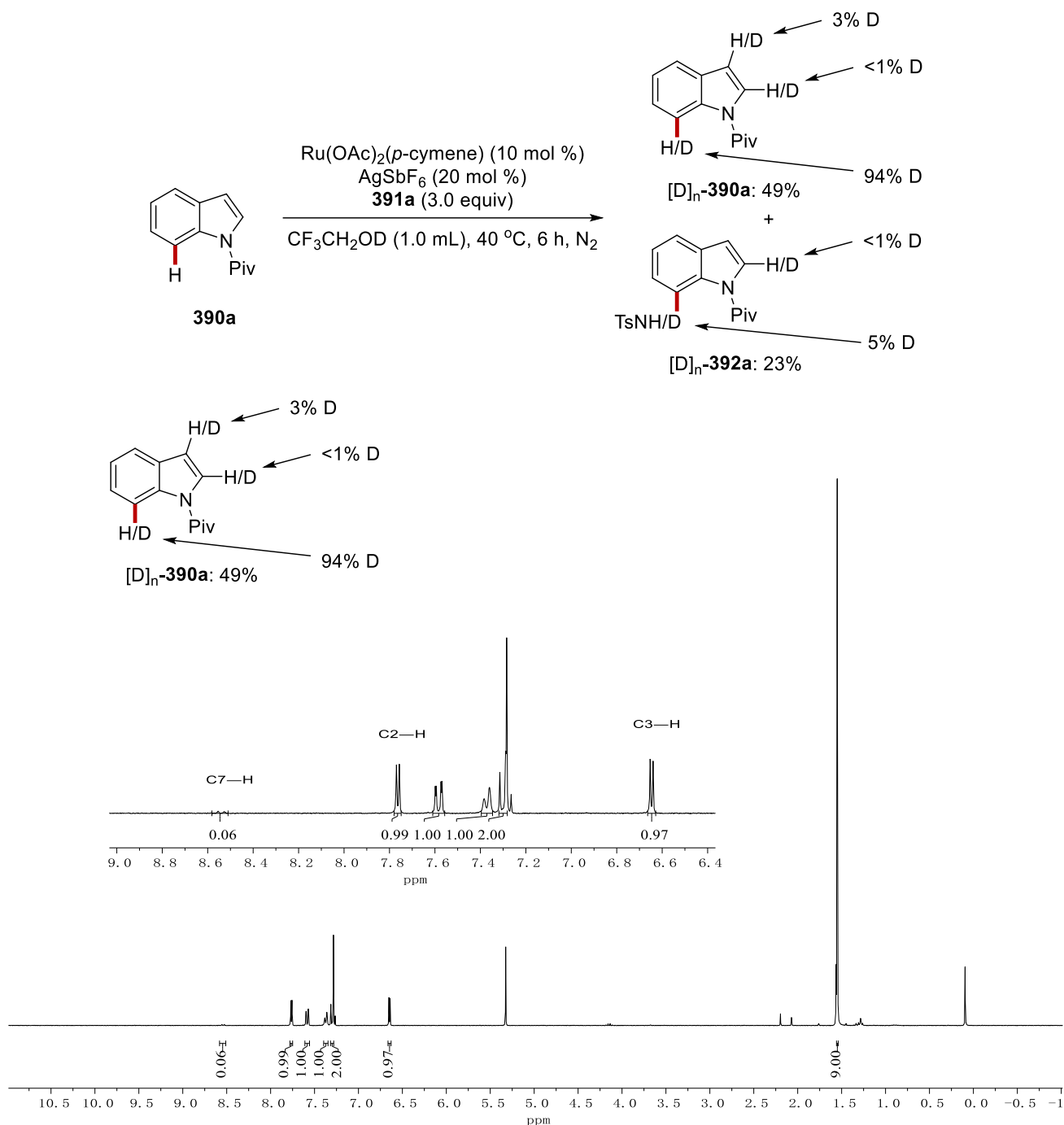
A suspension of *N*-pivaloyl indole **390a** (0.25 mmol, 1.0 equiv), Ru(OAc)<sub>2</sub>(*p*-cymene) (10 mol %), AgSbF<sub>6</sub> (20 mol %), in [D]<sub>1</sub>-TFE (CF<sub>3</sub>CH<sub>2</sub>OD, 1.0 mL) was stirred at 40 °C for 16 h under N<sub>2</sub> (Scheme 5.3.11). After cooling to ambient temperature, the mixture was concentrated *in vacuo*. Purification by column chromatography on silica gel afforded the desired products [D]<sub>n</sub>-**390a**.



Scheme 5.3.11 H/D exchange study 1.

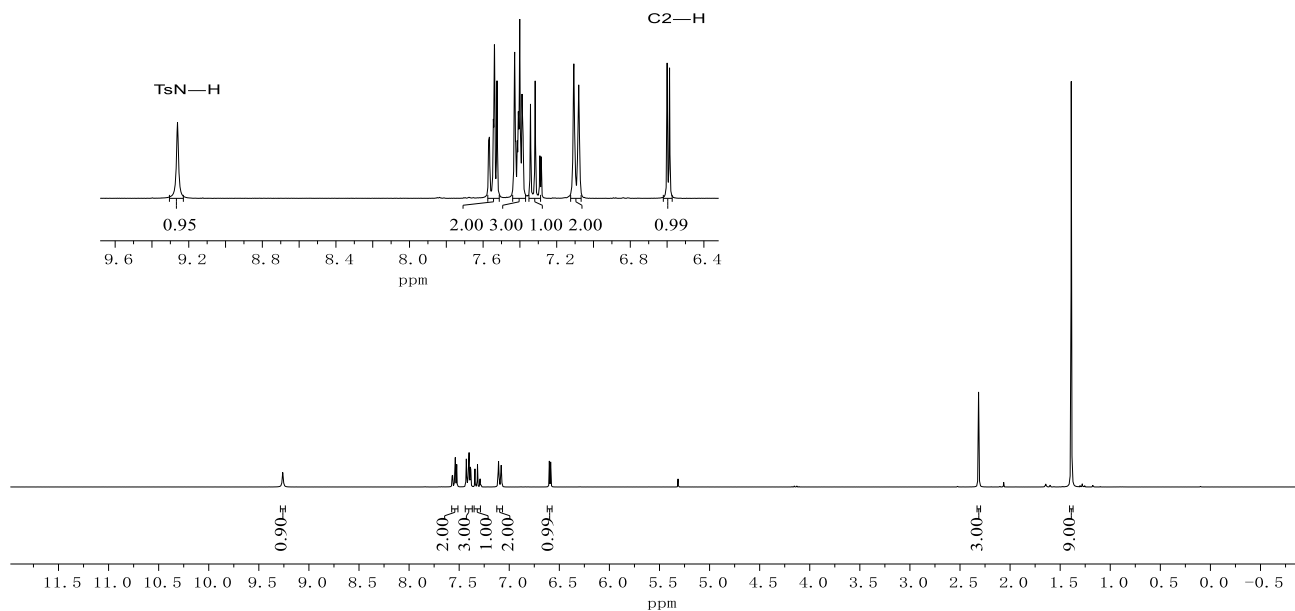
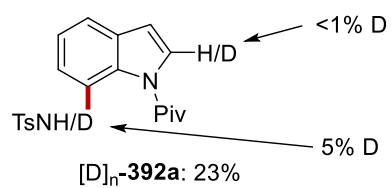
## 2) Procedure for H/D exchange experiment 2

A suspension of *N*-pivaloyl indole **390a** (0.25 mmol, 1.0 equiv), tosyl azide **391a** (0.75 mmol, 3.0 equiv), Ru(OAc)<sub>2</sub>(*p*-cymene) (10 mol %), AgSbF<sub>6</sub> (20 mol %), in [D]<sub>1</sub>-TFE (CF<sub>3</sub>CH<sub>2</sub>OD, 1.0 mL) was stirred at 40 °C for 6 h under N<sub>2</sub> (Scheme 5.3.12 and 5.3.13). After cooling to ambient temperature, the mixture is concentrated *in vacuo*. Purification by column chromatography on silica gel afforded the desired products [D]<sub>n</sub>-**390a** and [D]<sub>n</sub>-**392a**.



Scheme 5.3.12 H/D exchange study 2.

## Experimental Data



**Scheme 5.3.13** H/D exchange study 3.

### 5.3.8 KIE Study

Two independent reactions using substrate **390a** and  $[D]_4\text{-390a}$  were performed to determine the KIE by comparison of the initial rates (Scheme 5.3.14). The conversion was determined by  $^1\text{H}$  NMR spectroscopy using 1,3,5-trimethoxybenzene as the internal standard. Blue line is for **392a** and red line is for  $[D]_3\text{-392a}$ .

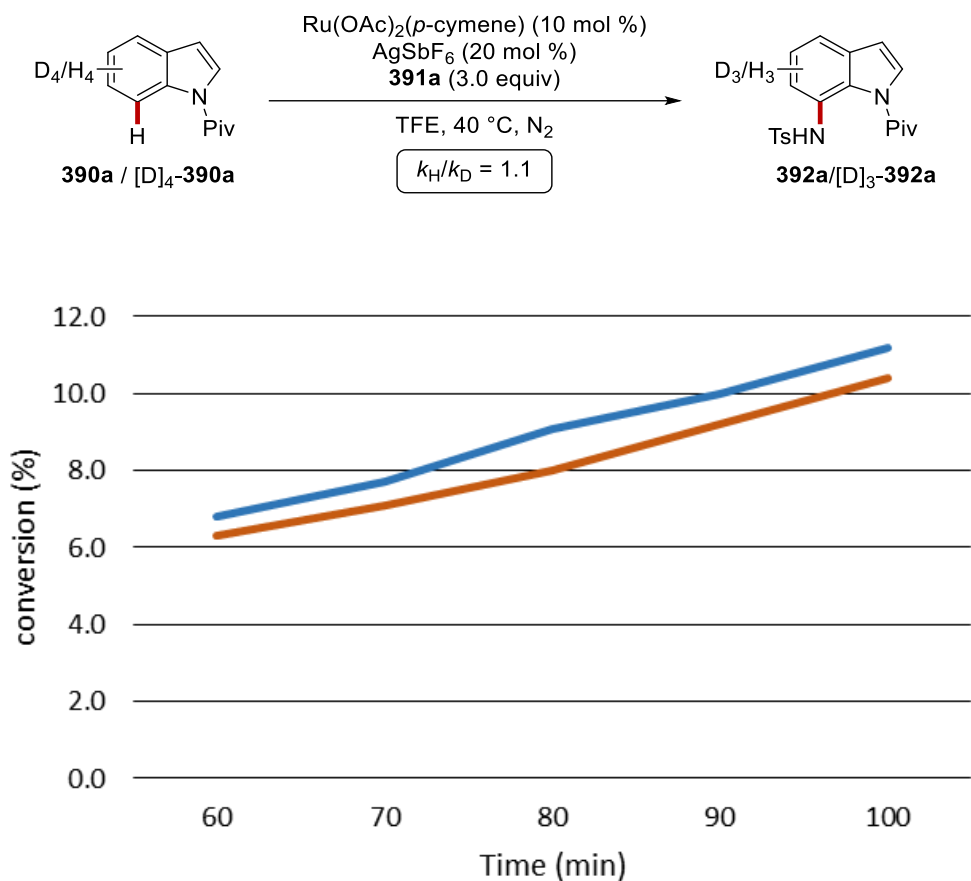


Figure 5.3.14 H/D exchange study.

### 5.3.9 Kinetic Analysis

#### 1) Reaction order with respect to **390a**

The reaction order with respect to **390a** was examined using the initial rate method. A Schlenk-tube was charged with *N*-pivaloyl indole **390a** (0.15, 0.20, 0.25, 0.30, 0.35 mmol), tosyl azide **391a** (0.75 mmol), Ru(OAc)<sub>2</sub>(*p*-cymene) (0.025 mmol) and 1,3,5-trimethoxybenzene (0.25 mmol) under N<sub>2</sub> condition (Table 5.3.1 and Scheme 5.3.15). TFE (2.0 mL) was added and the mixture was stirred at 40 °C. Aliquots up to ca. 10% conversion (25 μL; 30, 40, 50, 60, 70 min) were periodically removed by a syringe and directly analyzed by gas chromatography.

**Table 5.3.1** Kinetic analysis with respect to **390a**.

| Entry | $k / \text{mol L}^{-1} \text{s}^{-1} 10^{-6}$ | $\log(k / \text{mol L}^{-1} \text{s}^{-1} 10^{-6})$ | $c$   | $\log(c)$ |
|-------|-----------------------------------------------|-----------------------------------------------------|-------|-----------|
| 1     | 0.7118                                        | -6.1476                                             | 0.075 | -1.1249   |
| 2     | 0.7421                                        | -6.1295                                             | 0.1   | -1.0000   |
| 3     | 0.7659                                        | -6.1158                                             | 0.125 | -0.9031   |
| 4     | 0.7973                                        | -6.0984                                             | 0.15  | -0.8239   |
| 5     | 0.8226                                        | -6.0848                                             | 0.175 | -0.7570   |

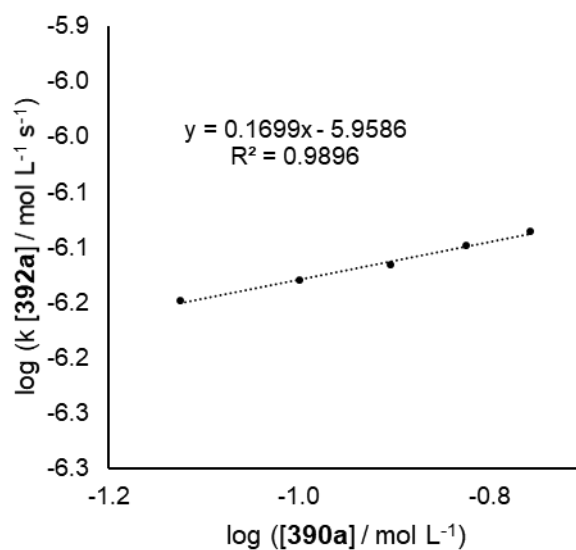


**Figure 5.3.15** Kinetic analysis with respect to **390a**.

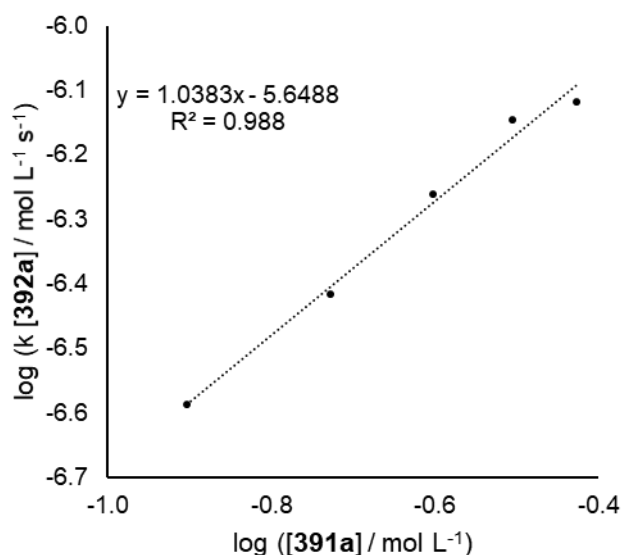


2) Reaction order with respect to **391a**

The reaction order with respect to **391a** was examined using the initial rate method. A Schlenk-tube was charged with *N*-pivaloyl indole **390a** (0.25 mmol), tosyl azide **391a** (0.25, 0.375, 0.50, 0.625, 0.75 mmol), Ru(OAc)<sub>2</sub>(*p*-cymene) (0.025 mmol) and 1,3,5-trimethoxybenzene (0.25 mmol) under N<sub>2</sub> condition (Table 5.3.2 and Scheme 5.3.16). TFE (2.0 mL) was added and the mixture was stirred at 40 °C. Aliquots up to ca. 10% conversion (25 μL; 30, 40, 50, 60, 70 min) were periodically removed by a syringe and directly analyzed by gas chromatography.

**Table 5.3.2** Kinetic analysis with respect to **391a**.

| Entry | $k / \text{mol L}^{-1} \text{s}^{-1} 10^{-6}$ | $\log(k / \text{mol L}^{-1} \text{s}^{-1} 10^{-6})$ | $c$    | $\log(c)$ |
|-------|-----------------------------------------------|-----------------------------------------------------|--------|-----------|
| 1     | 0.2584                                        | -6.5877                                             | 0.125  | -0.9031   |
| 2     | 0.3831                                        | -6.4167                                             | 0.1875 | -0.7270   |
| 3     | 0.5478                                        | -6.2614                                             | 0.25   | -0.6021   |
| 4     | 0.7163                                        | -6.1449                                             | 0.3125 | -0.5051   |
| 5     | 0.7621                                        | -6.1180                                             | 0.375  | -0.4260   |

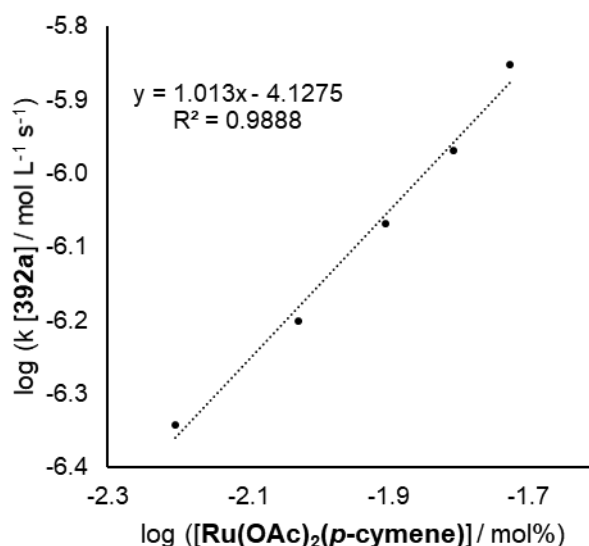
**Figure 5.3.16** Kinetic analysis with respect to **391a**.

3) Reaction order with respect to Ru(OAc)<sub>2</sub>(*p*-cymene)

The reaction order with respect to Ru(OAc)<sub>2</sub>(*p*-cymene) was examined using the initial rate method. A Schlenk-tube was charged with *N*-pivaloyl indole **390a** (0.25 mmol), tosyl azide **391a** (0.75 mmol), Ru(OAc)<sub>2</sub>(*p*-cymene) (0.01250, 0.01875, 0.02500, 0.03125, 0.03750 mmol) and 1,3,5-trimethoxybenzene (0.25 mmol) under N<sub>2</sub> condition (Table 5.3.3 and Scheme 5.3.17). TFE (2.0 mL) was added and the mixture was stirred at 40 °C. Aliquots up to ca. 10% conversion (25 μL; 30, 40, 50, 60, 70 min) were periodically removed by a syringe and directly analyzed by gas chromatography.

**Table 5.3.3** Kinetic analysis with respect to Ru(OAc)<sub>2</sub>(*p*-cymene).

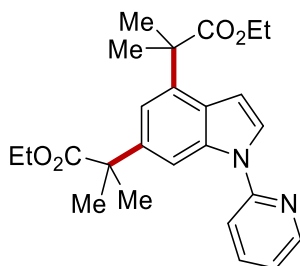
| Entry | $k / \text{mol L}^{-1} \text{s}^{-1} 10^{-6}$ | $\log(k / \text{mol L}^{-1} \text{s}^{-1} 10^{-6})$ | $c$  | $\log(c)$ |
|-------|-----------------------------------------------|-----------------------------------------------------|------|-----------|
| 1     | 0.4556                                        | -6.3414                                             | 5    | -2.2041   |
| 2     | 0.6298                                        | -6.2008                                             | 7.5  | -2.0280   |
| 3     | 0.8541                                        | -6.0685                                             | 10   | -1.9031   |
| 4     | 1.0745                                        | -5.9688                                             | 12.5 | -1.8062   |
| 5     | 1.4067                                        | -5.8518                                             | 15   | -1.7270   |

**Figure 5.3.17** Kinetic analysis with respect to Ru(OAc)<sub>2</sub>(*p*-cymene).

## 5.4 Ruthenium(II)-Catalyzed C4/C6-H Dual Alkylations of Indoles

### 5.4.1 Characterization Data

#### Diethyl 2,2'-[1-(pyridin-2-yl)-1*H*-indole-4,6-diyl]bis(2-methylpropanoate) (**397a**)



The **General Procedure C** was followed using 1-(pyridin-2-yl)-1*H*-indole **395a** (48.6 mg, 0.25 mmol), ethyl 2-bromo-2-methylpropanoate **396a** (243 mg, 1.25 mmol), Ru(OAc)<sub>2</sub>(PPh<sub>3</sub>)<sub>2</sub> (18.6 mg, 10 mol %), NaOAc (41.0 mg, 0.50 mmol) in DCE (2.0 mL). Purification by column chromatography on silica gel (*n*-hexane/EtOAc: 5/1) yielded **397a** (81.3 mg, 77%) as colorless oil.

**<sup>1</sup>H NMR** (400 MHz, CDCl<sub>3</sub>)  $\delta$  8.55 (ddd,  $J = 4.9, 2.0, 0.9$  Hz, 1H), 8.10 (dd,  $J = 1.6, 0.9$  Hz, 1H), 7.80 (ddd,  $J = 8.2, 7.4, 2.0$  Hz, 1H), 7.60 (d,  $J = 3.6$  Hz, 1H), 7.43 (dd,  $J = 8.2, 0.9$  Hz, 1H), 7.16 (ddd,  $J = 7.4, 4.9, 0.9$  Hz, 1H), 7.13 (d,  $J = 1.6$  Hz, 1H), 6.64 (dd,  $J = 3.6, 0.9$  Hz, 1H), 4.12 (q,  $J = 7.1$  Hz, 2H), 4.08 (q,  $J = 7.1$  Hz, 2H), 1.65 (s, 6H), 1.64 (s, 6H), 1.16 (t,  $J = 7.1$  Hz, 3H), 1.09 (t,  $J = 7.1$  Hz, 3H).

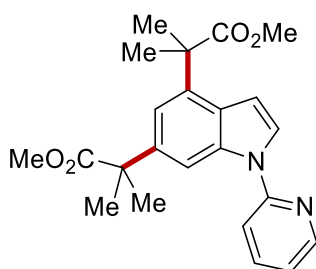
**<sup>13</sup>C NMR** (100 MHz, CDCl<sub>3</sub>)  $\delta$  177.7 (C<sub>q</sub>), 177.1 (C<sub>q</sub>), 152.4 (C<sub>q</sub>), 149.0 (CH), 139.7 (C<sub>q</sub>), 138.4 (CH), 136.9 (C<sub>q</sub>), 135.4 (C<sub>q</sub>), 126.7 (C<sub>q</sub>), 125.8 (CH), 120.2 (CH), 115.7 (CH), 115.1 (CH), 108.4 (CH), 104.2 (CH), 60.7 (CH<sub>2</sub>), 60.6 (CH<sub>2</sub>), 46.9 (C<sub>q</sub>), 46.5 (C<sub>q</sub>), 26.9 (CH<sub>3</sub>), 26.3 (CH<sub>3</sub>), 14.1 (CH<sub>3</sub>), 14.0 (CH<sub>3</sub>).

**IR** (ATR): 2979, 1721, 1468, 1439, 1249, 1134, 1024, 912, 772, 717 cm<sup>-1</sup>.

**MS** (ESI)  $m/z$  (relative intensity): 423 (70) [M+H]<sup>+</sup>, 440 (30) [M+NH<sub>4</sub>]<sup>+</sup>.

**HR-MS** (ESI) C<sub>25</sub>H<sub>31</sub>N<sub>2</sub>O<sub>4</sub> [M+H]<sup>+</sup>: 423.2278, found: 423.2282.

The spectral data were in accordance with those reported in the literature.<sup>[214]</sup>

**Dimethyl 2,2'-[1-(pyridin-2-yl)-1*H*-indole-4,6-diyl]bis(2-methylpropanoate) (397b)**

The **General Procedure C** was followed using 1-(pyridin-2-yl)-1*H*-indole **395a** (48.6 mg, 0.25 mmol), methyl 2-bromo-2-methylpropanoate **396b** (148 mg, 0.75 mmol), Ru(OAc)<sub>2</sub>(PPh<sub>3</sub>)<sub>2</sub> (18.6 mg, 10 mol %), NaOAc (41.0 mg, 0.50 mmol) in DCE (2.0 mL). Purification by column chromatography on silica gel (*n*-hexane/EtOAc: 5/1) yielded **397b** (79.8 mg, 81%) as colorless oil.

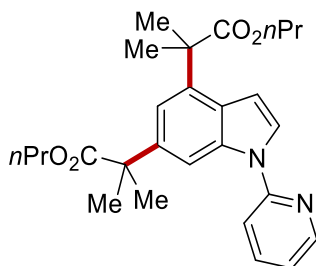
**<sup>1</sup>H NMR** (400 MHz, CDCl<sub>3</sub>)  $\delta$  8.55 (ddd,  $J = 4.9, 1.6, 0.9$  Hz, 1H), 8.09 (dd,  $J = 1.6, 0.9$  Hz, 1H), 7.81 (ddd,  $J = 8.2, 7.4, 1.6$  Hz, 1H), 7.61 (d,  $J = 3.6$  Hz, 1H), 7.43 (dd,  $J = 8.2, 0.9$  Hz, 1H), 7.16 (ddd,  $J = 7.4, 4.9, 0.9$  Hz, 1H), 7.13 (d,  $J = 1.6$  Hz, 1H), 6.60 (dd,  $J = 3.6, 0.9$  Hz, 1H), 3.64 (s, 3H), 3.59 (s, 3H), 1.67 (s, 6H), 1.65 (s, 6H).

**<sup>13</sup>C NMR** (100 MHz, CDCl<sub>3</sub>)  $\delta$  178.3 (C<sub>q</sub>), 177.6 (C<sub>q</sub>), 152.3 (C<sub>q</sub>), 149.0 (CH), 139.5 (C<sub>q</sub>), 138.4 (CH), 136.9 (C<sub>q</sub>), 135.3 (C<sub>q</sub>), 126.8 (C<sub>q</sub>), 126.1 (CH), 120.3 (CH), 115.4 (CH), 115.1 (CH), 108.6 (CH), 103.8 (CH), 52.2 (CH<sub>3</sub>), 52.1 (CH<sub>3</sub>), 46.9 (C<sub>q</sub>), 46.5 (C<sub>q</sub>), 26.9 (CH<sub>3</sub>), 26.3 (CH<sub>3</sub>).

**IR** (ATR): 2976, 2949, 1729, 1721, 1469, 1436, 1250, 1130, 730, 719 cm<sup>-1</sup>.

**MS** (ESI)  $m/z$  (relative intensity): 395 (80) [M+H]<sup>+</sup>, 412 (20) [M+NH<sub>4</sub>]<sup>+</sup>.

**HR-MS** (ESI) C<sub>23</sub>H<sub>27</sub>N<sub>2</sub>O<sub>4</sub> [M+H]<sup>+</sup>: 395.1965, found: 395.1967.

**Dipropyl 2,2'-[1-(pyridin-2-yl)-1*H*-indole-4,6-diyl]bis(2-methylpropanoate) (397c)**

The **General Procedure C** was followed using 1-(pyridin-2-yl)-1*H*-indole **395a** (48.6 mg, 0.25 mmol), propyl 2-bromo-2-methylpropanoate **396c** (261 mg, 1.25 mmol), Ru(OAc)<sub>2</sub>(PPh<sub>3</sub>)<sub>2</sub> (18.6 mg,

10 mol %), NaOAc (41.0 mg, 0.50 mmol) in DCE (2.0 mL). Purification by column chromatography on silica gel (*n*-hexane/EtOAc: 5/1) yielded **397c** (77.7 mg, 69%) as colorless oil.

**<sup>1</sup>H NMR** (400 MHz, CDCl<sub>3</sub>)  $\delta$  8.55 (ddd,  $J = 4.9, 2.0, 0.9$  Hz, 1H), 8.10 (dd,  $J = 1.6, 0.9$  Hz, 1H), 7.80 (ddd,  $J = 8.2, 7.4, 2.0$  Hz, 1H), 7.60 (d,  $J = 3.6$  Hz, 1H), 7.43 (dd,  $J = 8.2, 0.9$  Hz, 1H), 7.15 (ddd,  $J = 7.4, 4.9, 0.9$  Hz, 1H), 7.14 (d,  $J = 1.6$  Hz, 1H), 6.64 (dd,  $J = 3.6, 0.9$  Hz, 1H), 4.01 (t,  $J = 6.6$  Hz, 2H), 3.97 (t,  $J = 6.6$  Hz, 2H), 1.67 (s, 6H), 1.65 (s, 6H), 1.50 – 1.59 (m, 2H), 1.43 – 1.51 (m, 2H), 0.79 (t,  $J = 7.4$  Hz, 3H), 0.69 (t,  $J = 7.4$  Hz, 3H).

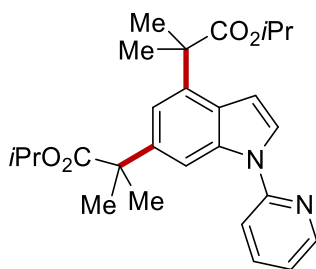
**<sup>13</sup>C NMR** (100 MHz, CDCl<sub>3</sub>)  $\delta$  177.7 (C<sub>q</sub>), 177.2 (C<sub>q</sub>), 152.4 (C<sub>q</sub>), 149.0 (CH), 139.7 (C<sub>q</sub>), 138.3 (CH), 137.0 (C<sub>q</sub>), 135.4 (C<sub>q</sub>), 126.7 (C<sub>q</sub>), 125.8 (CH), 120.2 (CH), 115.7 (CH), 115.1 (CH), 108.5 (CH), 104.2 (CH), 66.3 (CH<sub>2</sub>), 66.3 (CH<sub>2</sub>), 46.9 (C<sub>q</sub>), 46.6 (C<sub>q</sub>), 26.9 (CH<sub>3</sub>), 26.3 (CH<sub>3</sub>), 21.9 (CH<sub>2</sub>), 21.8 (CH<sub>2</sub>), 10.4 (CH<sub>3</sub>), 10.1 (CH<sub>3</sub>).

**IR** (ATR): 2971, 2933, 2880, 1722, 1467, 1439, 1247, 1131, 773, 727 cm<sup>-1</sup>.

**MS** (ESI)  $m/z$  (relative intensity): 451 (66) [M+H]<sup>+</sup>, 473 (34) [M+Na]<sup>+</sup>.

**HR-MS** (ESI) C<sub>27</sub>H<sub>35</sub>N<sub>2</sub>O<sub>4</sub> [M+H]<sup>+</sup>: 451.2595, found: 451.2591.

#### Diisopropyl 2,2'-[1-(pyridin-2-yl)-1*H*-indole-4,6-diyl]bis(2-methylpropanoate) (**397d**)



The **General Procedure C** was followed using 1-(pyridin-2-yl)-1*H*-indole **395a** (48.6 mg, 0.25 mmol), isopropyl 2-bromo-2-methylpropanoate **396d** (261 mg, 1.25 mmol), Ru(OAc)<sub>2</sub>(PPh<sub>3</sub>)<sub>2</sub> (18.6 mg, 10 mol %), NaOAc (41.0 mg, 0.50 mmol) in DCE (2.0 mL). Purification by column chromatography on silica gel (*n*-hexane/EtOAc: 5/1) yielded **397d** (81.1 mg, 72%) as colorless oil.

**<sup>1</sup>H NMR** (400 MHz, CDCl<sub>3</sub>)  $\delta$  8.54 (ddd,  $J = 4.9, 1.9, 0.9$  Hz, 1H), 8.09 (dd,  $J = 1.6, 0.9$  Hz, 1H), 7.79 (ddd,  $J = 8.3, 7.4, 2.0$  Hz, 1H), 7.59 (d,  $J = 3.6$  Hz, 1H), 7.43 (dd,  $J = 8.3, 0.9$  Hz, 1H), 7.14 (ddd,  $J = 7.4, 4.9, 0.9$  Hz, 1H), 7.10 (d,  $J = 1.6$  Hz, 1H), 6.65 (dd,  $J = 3.6, 0.9$  Hz, 1H), 4.94 – 5.05 (m, 2H), 1.65 (s, 6H), 1.63 (s, 6H), 1.14 (s, 3H), 1.12 (s, 3H), 1.03 (s, 3H), 1.03 (s, 3H).

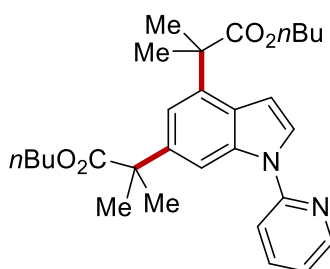
$^{13}\text{C}$  NMR (100 MHz,  $\text{CDCl}_3$ )  $\delta$  177.1 ( $\text{C}_q$ ), 176.6 ( $\text{C}_q$ ), 152.5 ( $\text{C}_q$ ), 148.9 (CH), 139.9 ( $\text{C}_q$ ), 138.3 (CH), 137.0 ( $\text{C}_q$ ), 135.4 ( $\text{C}_q$ ), 126.6 ( $\text{C}_q$ ), 125.5 (CH), 120.1 (CH), 115.9 (CH), 115.0 (CH), 108.2 (CH), 104.4 (CH), 67.9 (CH), 67.7 (CH), 46.9 ( $\text{C}_q$ ), 46.6 ( $\text{C}_q$ ), 26.8 ( $\text{CH}_3$ ), 26.3 ( $\text{CH}_3$ ), 21.5 ( $\text{CH}_3$ ), 21.5 ( $\text{CH}_3$ ).

IR (ATR): 2978, 2934, 1713, 1573, 1469, 1439, 1253, 1152, 1104, 906, 729, 718  $\text{cm}^{-1}$ .

MS (ESI)  $m/z$  (relative intensity): 451 (60)  $[\text{M}+\text{H}]^+$ , 473 (40)  $[\text{M}+\text{Na}]^+$ .

HR-MS (ESI)  $\text{C}_{27}\text{H}_{35}\text{N}_2\text{O}_4$   $[\text{M}+\text{H}]^+$ : 451.2592, found: 451.2591.

### Dibutyl 2,2'-[1-(pyridin-2-yl)-1*H*-indole-4,6-diyl]bis(2-methylpropanoate) (**397e**)



The **General Procedure C** was followed using 1-(pyridin-2-yl)-1*H*-indole **395a** (48.6 mg, 0.25 mmol), butyl 2-bromo-2-methylpropanoate **396e** (279 mg, 1.25 mmol),  $\text{Ru}(\text{OAc})_2(\text{PPh}_3)_2$  (18.6 mg, 10 mol %),  $\text{NaOAc}$  (41.0 mg, 0.50 mmol) in DCE (2.0 mL). Purification by column chromatography on silica gel (*n*-hexane/EtOAc: 5/1) yielded **397e** (101.7 mg, 85%) as colorless oil.

$^1\text{H}$  NMR (400 MHz,  $\text{CDCl}_3$ )  $\delta$  8.55 (ddd,  $J = 4.8, 2.0, 0.9$  Hz, 1H), 8.09 (dd,  $J = 1.6, 0.9$  Hz, 1H), 7.80 (ddd,  $J = 8.2, 7.3, 2.0$  Hz, 1H), 7.60 (d,  $J = 3.6$  Hz, 1H), 7.43 (dd,  $J = 8.2, 0.9$  Hz, 1H), 7.15 (ddd,  $J = 7.3, 4.8, 0.9$  Hz, 1H), 7.13 (d,  $J = 1.6$  Hz, 1H), 6.64 (dd,  $J = 3.6, 0.9$  Hz, 1H), 4.05 (d,  $J = 6.6$  Hz, 2H), 4.01 (d,  $J = 6.6$  Hz, 2H), 1.67 (s, 6H), 1.64 (s, 6H), 1.51 (dt,  $J = 14.4, 6.6$  Hz, 2H), 1.44 (dt,  $J = 14.4, 6.6$  Hz, 2H), 1.24 (dq,  $J = 14.4, 7.4$  Hz, 2H), 1.12 (dq,  $J = 14.4, 7.4$  Hz, 2H), 0.81 (t,  $J = 7.4$  Hz, 3H), 0.74 (t,  $J = 7.4$  Hz, 3H).

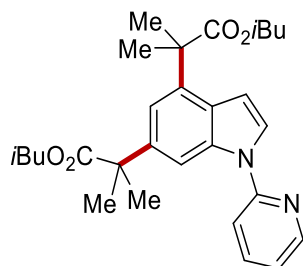
$^{13}\text{C}$  NMR (100 MHz,  $\text{CDCl}_3$ )  $\delta$  177.7 ( $\text{C}_q$ ), 177.2 ( $\text{C}_q$ ), 152.4 ( $\text{C}_q$ ), 149.0 (CH), 139.7 ( $\text{C}_q$ ), 138.3 (CH), 136.9 ( $\text{C}_q$ ), 135.4 ( $\text{C}_q$ ), 126.7 ( $\text{C}_q$ ), 125.8 (CH), 120.2 (CH), 115.7 (CH), 115.0 (CH), 108.5 (CH), 104.1 (CH), 64.6 ( $\text{CH}_2$ ), 64.5 ( $\text{CH}_2$ ), 46.9 ( $\text{C}_q$ ), 46.6 ( $\text{C}_q$ ), 30.6 ( $\text{CH}_2$ ), 30.4 ( $\text{CH}_2$ ), 26.9 ( $\text{CH}_3$ ), 26.2 ( $\text{CH}_3$ ), 19.0 ( $\text{CH}_2$ ), 18.9 ( $\text{CH}_2$ ), 13.6 ( $\text{CH}_3$ ), 13.5 ( $\text{CH}_3$ ).

IR (ATR): 2959, 2932, 2876, 1720, 1469, 1437, 1247, 1133, 730, 717  $\text{cm}^{-1}$ .

MS (ESI)  $m/z$  (relative intensity): 479 (70)  $[\text{M}+\text{H}]^+$ , 501 (30)  $[\text{M}+\text{Na}]^+$ .

**HR-MS** (ESI)  $C_{29}H_{39}N_2O_4$   $[M+H]^+$ : 479.2907, found: 479.2904.

**Diisobutyl 2,2'-[1-(pyridin-2-yl)-1*H*-indole-4,6-diyl]bis(2-methylpropanoate) (397f)**



The **General Procedure C** was followed using 1-(pyridin-2-yl)-1*H*-indole **395a** (48.6 mg, 0.25 mmol), isobutyl 2-bromo-2-methylpropanoate **396f** (243 mg, 1.25 mmol),  $Ru(OAc)_2(PPh_3)_2$  (18.6 mg, 10 mol %), NaOAc (41.0 mg, 0.50 mmol) in DCE (2.0 mL). Purification by column chromatography on silica gel (*n*-hexane/EtOAc: 5/1) yielded **397f** (90.9 mg, 76%) as colorless oil.

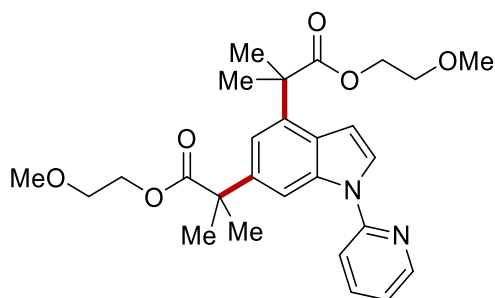
**$^1H$  NMR** (400 MHz,  $CDCl_3$ )  $\delta$  8.55 (ddd,  $J = 4.9, 2.0, 0.9$  Hz, 1H), 8.14 – 8.07 (m, 1H), 7.79 (ddd,  $J = 8.2, 7.3, 1.9$  Hz, 1H), 7.59 (d,  $J = 3.5$  Hz, 1H), 7.43 (dd,  $J = 8.2, 1.0$  Hz, 1H), 7.15 (ddd,  $J = 7.4, 4.9, 0.9$  Hz, 1H), 7.11 (d,  $J = 1.6$  Hz, 1H), 6.66 (dd,  $J = 3.6, 0.8$  Hz, 1H), 4.75 – 4.87 (m, 2H), 1.66 (s, 3H), 1.65 (s, 3H), 1.64 (s, 3H), 1.63 (s, 3H), 1.50 – 1.40 (m, 2H), 1.39 – 1.30 (m, 2H), 1.09 (dd,  $J = 6.3, 1.0$  Hz, 3H), 1.01 (dd,  $J = 6.3, 2.4$  Hz, 3H), 0.74 (td,  $J = 7.4, 1.2$  Hz, 3H), 0.61 (td,  $J = 7.4, 5.0$  Hz, 3H).

**$^{13}C$  NMR** (100 MHz,  $CDCl_3$ )  $\delta$  177.3 ( $C_q$ ), 176.8 ( $C_q$ ), 152.5 ( $C_q$ ), 149.0 (CH), 139.9 ( $C_q$ ), 138.3 (CH), 137.0 ( $C_q$ ), 135.4 ( $C_q$ ), 126.6 ( $C_q$ ), 125.5 (CH), 120.1 (CH), 115.9 (CH), 115.0 (CH), 108.2 (CH), 104.5 (CH), 72.5 (CH), 72.3 (CH), 47.0 ( $C_q$ ), 46.6 ( $C_q$ ), 28.7 ( $CH_2$ ), 28.6 ( $CH_2$ ), 26.9 ( $CH_3$ ), 26.2 ( $CH_3$ ), 19.2 ( $CH_3$ ), 19.1 ( $CH_3$ ), 9.72 ( $CH_3$ ), 9.42 ( $CH_3$ ).

**IR** (ATR): 2973, 2935, 2878, 1715, 1470, 1437, 1250, 1150, 1110, 733  $cm^{-1}$ .

**MS** (ESI)  $m/z$  (relative intensity): 479 (66)  $[M+H]^+$ , 501 (34)  $[M+Na]^+$ .

**HR-MS** (ESI)  $C_{29}H_{39}N_2O_4$   $[M+H]^+$ : 479.2905, found: 479.2904.

**Bis(2-methoxyethyl) 2,2'-[1-(pyridin-2-yl)-1H-indole-4,6-diyl]bis(2-methylpropanoate) (397g)**

The **General Procedure C** was followed using 1-(pyridin-2-yl)-1H-indole **395a** (48.6 mg, 0.25 mmol), 2-methoxyethyl 2-bromo-2-methylpropanoate **396g** (281 mg, 1.25 mmol), Ru(OAc)<sub>2</sub>(PPh<sub>3</sub>)<sub>2</sub> (18.6 mg, 10 mol %), NaOAc (41.0 mg, 0.50 mmol) in DCE (2.0 mL). Purification by column chromatography on silica gel (*n*-hexane/EtOAc: 5/1) yielded **397g** (103 mg, 85%) as colorless oil.

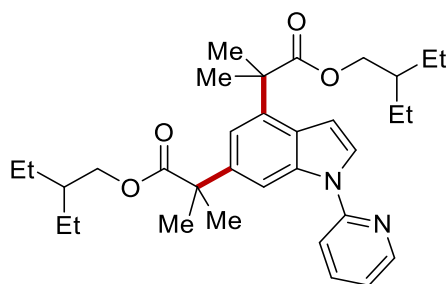
**<sup>1</sup>H NMR** (400 MHz, CDCl<sub>3</sub>) δ 8.55 (ddd, *J* = 4.8, 1.9, 0.8 Hz, 1H), 8.08 (dd, *J* = 1.6, 0.8 Hz, 1H), 7.81 (ddd, *J* = 8.2, 7.4, 1.9 Hz, 1H), 7.61 (d, *J* = 3.5 Hz, 1H), 7.44 (dd, *J* = 8.2, 0.9 Hz, 1H), 7.22 – 7.10 (m, 2H), 6.65 (dd, *J* = 3.5, 0.8 Hz, 1H), 4.28 – 4.06 (m, 4H), 3.55 – 3.47 (m, 2H), 3.47 – 3.37 (m, 2H), 3.21 (s, 3H), 3.14 (s, 3H), 1.69 (s, 6H), 1.66 (s, 6H).

**<sup>13</sup>C NMR** (100 MHz, CDCl<sub>3</sub>) δ 177.6 (C<sub>q</sub>), 177.0 (C<sub>q</sub>), 152.4 (C<sub>q</sub>), 149.1 (CH), 139.5 (C<sub>q</sub>), 138.4 (CH), 136.8 (C<sub>q</sub>), 135.4 (C<sub>q</sub>), 126.8 (C<sub>q</sub>), 126.0 (CH), 120.3 (CH), 115.7 (CH), 115.1 (CH), 108.7 (CH), 104.1 (CH), 70.3 (CH<sub>2</sub>), 70.3 (CH<sub>2</sub>), 64.0 (CH<sub>2</sub>), 63.8 (CH<sub>2</sub>), 58.8 (CH<sub>3</sub>), 58.8 (CH<sub>3</sub>), 46.9 (C<sub>q</sub>), 46.6 (C<sub>q</sub>), 26.9 (CH<sub>3</sub>), 26.2 (CH<sub>3</sub>).

**IR** (ATR): 2981, 2928, 1727, 1584, 1470, 1441, 1250, 1194, 1153, 1125 cm<sup>-1</sup>.

**MS** (ESI) *m/z* (relative intensity): 483 (70) [M+H]<sup>+</sup>, 500 (30) [M+NH<sub>4</sub>]<sup>+</sup>.

**HR-MS** (ESI) C<sub>27</sub>H<sub>35</sub>N<sub>2</sub>O<sub>6</sub> [M+H]<sup>+</sup>: 483.2491, found: 483.2490.

**Bis(2-ethylbutyl) 2,2'-[1-(pyridin-2-yl)-1H-indole-4,6-diyl]bis(2-methylpropanoate) (397h)**

The **General Procedure C** was followed using 1-(pyridin-2-yl)-1H-indole **395a** (48.6 mg, 0.25



mmol), 2-ethylbutyl 2-bromo-2-methylpropanoate **396h** (314 mg, 1.25 mmol), Ru(OAc)<sub>2</sub>(PPh<sub>3</sub>)<sub>2</sub> (18.6 mg, 10 mol %), NaOAc (41.0 mg, 0.50 mmol) in DCE (2.0 mL). Purification by column chromatography on silica gel (*n*-hexane/EtOAc: 5/1) yielded **397h** (119 mg, 89%) as colorless oil.

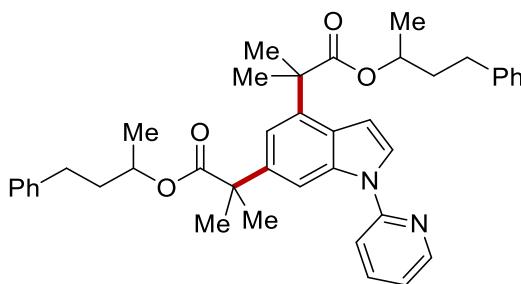
<sup>1</sup>H NMR (400 MHz, CDCl<sub>3</sub>) δ 8.55 (ddd, *J* = 4.9, 2.0, 0.9 Hz, 1H), 8.08 (dd, *J* = 1.6, 0.8 Hz, 1H), 7.79 (ddd, *J* = 8.2, 7.4, 2.0 Hz, 1H), 7.60 (d, *J* = 3.6 Hz, 1H), 7.42 (dd, *J* = 8.2, 1.0 Hz, 1H), 7.17 – 7.13 (ddd, *J* = 7.4, 4.9, 0.9 Hz, 1H), 7.16 (d, *J* = 1.6 Hz, 1H), 6.63 (dd, *J* = 3.6, 0.8 Hz, 1H), 3.96 (d, *J* = 5.7 Hz, 2H), 3.91 (d, *J* = 5.8 Hz, 2H), 1.67 (s, 6H), 1.64 (s, 6H), 1.45 – 1.39 (m, 1H), 1.35 – 1.29 (m, 1H), 1.24 – 1.17 (m, 4H), 1.13 – 0.98 (m, 4H), 0.75 (t, *J* = 7.5 Hz, 6H), 0.65 (t, *J* = 7.5 Hz, 6H).  
<sup>13</sup>C NMR (100 MHz, CDCl<sub>3</sub>) δ 177.8 (C<sub>q</sub>), 177.2 (C<sub>q</sub>), 152.4 (C<sub>q</sub>), 149.0 (CH), 139.7 (C<sub>q</sub>), 138.3 (CH), 136.9 (C<sub>q</sub>), 135.4 (C<sub>q</sub>), 126.8 (C<sub>q</sub>), 125.8 (CH), 120.2 (CH), 115.6 (CH), 115.0 (CH), 108.5 (CH), 104.1 (CH), 66.7 (CH<sub>2</sub>), 66.6 (CH<sub>2</sub>), 47.0 (C<sub>q</sub>), 46.6 (C<sub>q</sub>), 40.2 (CH), 40.0 (CH), 26.9 (CH<sub>3</sub>), 26.1 (CH<sub>3</sub>), 23.2 (CH<sub>2</sub>), 23.1 (CH<sub>2</sub>), 10.9 (CH<sub>3</sub>), 10.8 (CH<sub>3</sub>).

IR (ATR): 2964, 2930, 2870, 1724, 1466, 1438, 1249, 1130, 992, 774 cm<sup>-1</sup>.

MS (ESI) *m/z* (relative intensity): 535 (70) [M+H]<sup>+</sup>, 557 (30) [M+Na]<sup>+</sup>.

HR-MS (ESI) C<sub>33</sub>H<sub>47</sub>N<sub>2</sub>O<sub>4</sub> [M+H]<sup>+</sup>: 535.3533, found: 535.3530.

#### Bis(4-phenylbutan-2-yl) 2,2'-[1-(pyridin-2-yl)-1*H*-indole-4,6-diyl]bis(2-methylpropanoate) (**397i**)



The **General Procedure C** was followed using 1-(pyridin-2-yl)-1*H*-indole **395a** (48.6 mg, 0.25 mmol), 4-phenylbutan-2-yl 2-bromo-2-methylpropanoate **396i** (374 mg, 1.25 mmol), Ru(OAc)<sub>2</sub>(PPh<sub>3</sub>)<sub>2</sub> (18.6 mg, 10 mol %), NaOAc (41.0 mg, 0.50 mmol) in DCE (2.0 mL). Purification by column chromatography on silica gel (*n*-hexane/EtOAc: 5/1) yielded **397i** (99.4 mg, 63%) as colorless oil.

<sup>1</sup>H NMR (400 MHz, CDCl<sub>3</sub>) δ 8.54 (ddd, *J* = 4.9, 1.9, 0.7 Hz, 1H), 8.16 (d, *J* = 2.5 Hz, 1H), 7.80 – 7.70 (m, 1H), 7.60 (dd, *J* = 3.6, 1.7 Hz, 1H), 7.36 (dd, *J* = 8.2, 5.7 Hz, 1H), 7.22 – 7.18 (m, 1H), 7.18

– 7.15 (m, 2H), 7.15 – 7.07 (m, 5H), 7.00 – 6.96 (m, 2H), 6.90 – 6.84 (m, 2H), 6.71 (d,  $J = 3.7$  Hz, 1H), 4.98 – 4.80 (m, 2H), 2.53 – 2.38 (m, 2H), 2.32 – 2.15 (m, 2H), 1.86 – 1.71 (m, 2H), 1.70 (s, 3H), 1.69 (s, 3H), 1.68 (s, 3H), 1.67 (s, 3H), 1.65 – 1.53 (m, 2H), 1.13 (dd,  $J = 6.3, 1.8$  Hz, 3H), 1.05 (dd,  $J = 12.4, 6.2$  Hz, 3H).

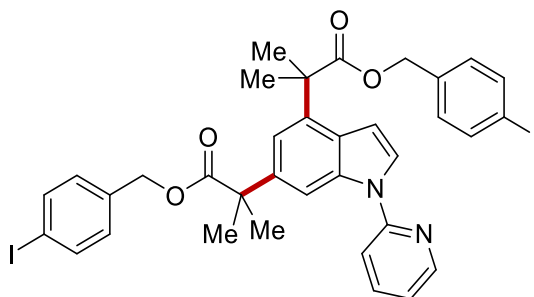
$^{13}\text{C}$  NMR (100 MHz,  $\text{CDCl}_3$ )  $\delta$  177.2 ( $\text{C}_q$ ), 176.7 ( $\text{C}_q$ ), 152.4 ( $\text{C}_q$ ), 149.0 (CH), 141.6 ( $\text{C}_q$ ), 141.5 ( $\text{C}_q$ ), 139.9 ( $\text{C}_q$ ), 138.3 (CH), 137.0 ( $\text{C}_q$ ), 135.5 ( $\text{C}_q$ ), 128.3 (CH), 128.3 (CH), 128.2 (CH), 128.2 (CH), 126.7 ( $\text{C}_q$ ), 125.8 (CH), 125.7 (CH), 125.6 (CH), 120.2 (CH), 115.8 (CH), 115.0 (CH), 108.6 (CH), 104.5 (CH), 70.6 (CH), 70.5 (CH), 47.0 ( $\text{C}_q$ ), 46.7 ( $\text{C}_q$ ), 37.6 ( $\text{CH}_2$ ), 37.4 ( $\text{CH}_2$ ), 31.7 ( $\text{CH}_2$ ), 31.2 ( $\text{CH}_2$ ), 26.9 ( $\text{CH}_3$ ), 26.2 ( $\text{CH}_3$ ), 19.8 ( $\text{CH}_3$ ), 19.7 ( $\text{CH}_3$ ).

IR (ATR): 2976, 2935, 1719, 1466, 1442, 1250, 1155, 1127, 741, 726  $\text{cm}^{-1}$ .

MS (ESI)  $m/z$  (relative intensity): 631 (66)  $[\text{M}+\text{H}]^+$ , 653 (34)  $[\text{M}+\text{Na}]^+$ .

HR-MS (ESI)  $\text{C}_{41}\text{H}_{47}\text{N}_2\text{O}_4$   $[\text{M}+\text{H}]^+$ : 631.3530, found: 631.3530.

### Bis(4-iodobenzyl) 2,2'-[1-(pyridin-2-yl)-1*H*-indole-4,6-diyl]bis(2-methylpropanoate) (**397j**)



The **General Procedure C** was followed using 1-(pyridin-2-yl)-1*H*-indole **395a** (48.6 mg, 0.25 mmol), 4-iodobenzyl 2-bromo-2-methylpropanoate **396j** (479 mg, 1.25 mmol),  $\text{Ru}(\text{OAc})_2(\text{PPh}_3)_2$  (18.6 mg, 10 mol %),  $\text{NaOAc}$  (41.0 mg, 0.50 mmol) in DCE (2.0 mL). Purification by column chromatography on silica gel (*n*-hexane/EtOAc: 5/1) yielded **397j** (184 mg, 92%) as colorless oil.

$^1\text{H}$  NMR (400 MHz,  $\text{CDCl}_3$ )  $\delta$  8.54 (ddd,  $J = 4.9, 2.0, 0.9$  Hz, 1H), 8.15 (dd,  $J = 1.4, 0.8$  Hz, 1H), 7.79 (ddd,  $J = 8.2, 7.4, 2.0$  Hz, 1H), 7.50 (d,  $J = 3.6$  Hz, 1H), 7.47 (d,  $J = 8.3$  Hz, 2H), 7.46 (d,  $J = 8.3$  Hz, 2H), 7.36 (d,  $J = 8.2$  Hz, 1H), 7.17 (ddd,  $J = 7.4, 4.9, 0.9$  Hz, 1H), 7.08 (d,  $J = 1.6$  Hz, 1H), 6.87 (d,  $J = 8.3$  Hz, 2H), 6.75 (d,  $J = 8.3$  Hz, 2H), 6.48 (dd,  $J = 3.6, 0.8$  Hz, 1H), 4.99 (s, 2H), 4.97 (s, 2H), 1.68 (s, 6H), 1.63 (s, 6H).

$^{13}\text{C}$  NMR (100 MHz,  $\text{CDCl}_3$ )  $\delta$  177.2 ( $\text{C}_q$ ), 176.7 ( $\text{C}_q$ ), 152.3 ( $\text{C}_q$ ), 149.0 (CH), 139.2 ( $\text{C}_q$ ), 138.4 (CH),

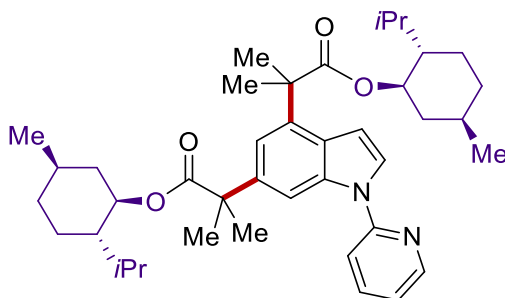
137.4 (CH), 137.2 (CH), 136.5 (C<sub>q</sub>), 135.8 (C<sub>q</sub>), 135.7 (C<sub>q</sub>), 135.4 (C<sub>q</sub>), 129.6 (CH), 129.5 (CH), 126.7 (C<sub>q</sub>), 125.9 (CH), 120.3 (CH), 115.5 (CH), 115.0 (CH), 109.0 (CH), 103.9 (CH), 93.5 (C<sub>q</sub>), 93.4 (C<sub>q</sub>), 65.6 (CH<sub>2</sub>), 65.5 (CH<sub>2</sub>), 46.9 (C<sub>q</sub>), 46.5 (C<sub>q</sub>), 26.8 (CH<sub>3</sub>), 26.0 (CH<sub>3</sub>).

**IR** (ATR): 2976, 1722, 1466, 1441, 1314, 1247, 1132, 742, 726, 696 cm<sup>-1</sup>.

**MS** (ESI) *m/z* (relative intensity): 799 (66) [M+H]<sup>+</sup>, 821 (34) [M+Na]<sup>+</sup>.

**HR-MS** (ESI) C<sub>35</sub>H<sub>33</sub>I<sub>2</sub>N<sub>2</sub>O<sub>4</sub> [M+H]<sup>+</sup>: 799.0526, found: 799.0524.

**Bis[(1*R*,2*S*,5*R*)-2-isopropyl-5-methylcyclohexyl] 2,2'-[1-(pyridin-2-yl)-1*H*-indole-4,6-diyl]bis(2-methylpropanoate) (**397k**)**



The **General Procedure C** was followed using 1-(pyridin-2-yl)-1*H*-indole **395a** (48.6 mg, 0.25 mmol), (1*R*,2*S*,5*R*)-2-isopropyl-5-methylcyclohexyl 2-bromo-2-methylpropanoate **396k** (382 mg, 1.25 mmol), Ru(OAc)<sub>2</sub>(PPh<sub>3</sub>)<sub>2</sub> (18.6 mg, 10 mol %), NaOAc (41.0 mg, 0.50 mmol) in DCE (2.0 mL). Purification by column chromatography on silica gel (*n*-hexane/EtOAc: 5/1) yielded **397k** (137 mg, 85%) as colorless oil.

**<sup>1</sup>H NMR** (400 MHz, CDCl<sub>3</sub>) δ 8.55 (ddd, *J* = 4.9, 2.0, 0.8 Hz, 1H), 8.06 (dd, *J* = 1.5, 0.8 Hz, 1H), 7.79 (ddd, *J* = 8.2, 7.3, 1.9 Hz, 1H), 7.58 (d, *J* = 3.6 Hz, 1H), 7.42 (d, *J* = 8.2 Hz, 1H), 7.14 (ddd, *J* = 7.4, 4.9, 0.9 Hz, 1H), 7.09 (d, *J* = 1.5 Hz, 1H), 6.68 (dd, *J* = 3.6, 0.8 Hz, 1H), 4.64 (td, *J* = 10.9, 4.3 Hz, 1H), 4.53 (td, *J* = 10.9, 4.3 Hz, 1H), 2.09 – 1.86 (m, 2H), 1.67 (s, 3H), 1.65 (s, 3H), 1.64 (s, 3H), 1.60 (s, 3H), 1.58 – 1.47 (m, 3H), 1.47 – 1.37 (m, 2H), 1.35 – 1.29 (m, 1H), 1.30 – 1.22 (m, 1H), 1.17 – 1.10 (m, 1H), 1.03 – 0.86 (m, 2H), 0.83 (d, *J* = 2.6 Hz, 3H), 0.81 (d, *J* = 2.6 Hz, 3H), 0.80 – 0.73 (m, 6H), 0.71 (d, *J* = 7.0 Hz, 3H), 0.61 (d, *J* = 7.0 Hz, 3H), 0.59 (d, *J* = 7.0 Hz, 3H), 0.46 (d, *J* = 7.0 Hz, 3H).

**<sup>13</sup>C NMR** (100 MHz, CDCl<sub>3</sub>) δ 177.0 (C<sub>q</sub>), 176.8 (C<sub>q</sub>), 152.5 (C<sub>q</sub>), 149.0 (CH), 140.0 (C<sub>q</sub>), 138.3 (CH), 136.8 (C<sub>q</sub>), 135.4 (C<sub>q</sub>), 126.7 (C<sub>q</sub>), 125.4 (CH), 120.1 (CH), 115.7 (CH), 115.0 (CH), 108.2 (CH), 104.7

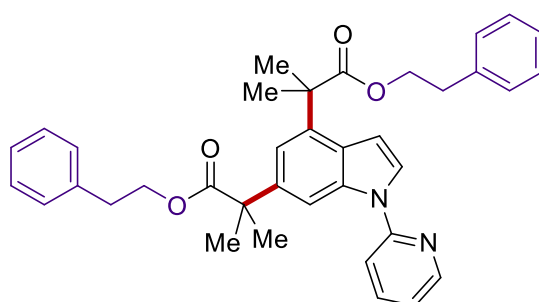
(CH), 74.6 (CH), 74.3 (CH), 47.1 (CH<sub>2</sub>), 47.1 (CH<sub>2</sub>), 46.8 (CH), 46.7 (CH), 40.5 (C<sub>q</sub>), 40.3 (C<sub>q</sub>), 34.2 (CH<sub>2</sub>), 47.1 (CH<sub>2</sub>), 31.3 (CH), 31.3 (CH), 27.2 (CH<sub>3</sub>), 26.8 (CH<sub>3</sub>), 26.2 (CH), 26.0 (CH), 25.8 (CH<sub>3</sub>), 23.1 (CH<sub>2</sub>), 23.1 (CH<sub>2</sub>), 22.0 (CH<sub>3</sub>), 20.7 (CH<sub>3</sub>), 15.9 (CH<sub>3</sub>).

**IR** (ATR): 2975, 1724, 1474, 1465, 1439, 1245, 1127, 909, 772, 727 cm<sup>-1</sup>.

**MS** (ESI) *m/z* (relative intensity): 643 (30) [M+H]<sup>+</sup>, 660 (70) [M+NH<sub>4</sub>]<sup>+</sup>.

**HR-MS** (ESI) C<sub>41</sub>H<sub>59</sub>N<sub>2</sub>O<sub>4</sub> [M+H]<sup>+</sup>: 643.4472, found: 643.4469.

### Diphenethyl 2,2'-[1-(pyridin-2-yl)-1*H*-indole-4,6-diyl]bis(2-methylpropanoate) (**397I**)



The **General Procedure C** was followed using 1-(pyridin-2-yl)-1*H*-indole **395a** (48.6 mg, 0.25 mmol), phenethyl 2-bromo-2-methylpropanoate **396I** (339 mg, 1.25 mmol), Ru(OAc)<sub>2</sub>(PPh<sub>3</sub>)<sub>2</sub> (18.6 mg, 10 mol%), NaOAc (41.0 mg, 0.50 mmol) in DCE (2.0 mL). Purification by column chromatography on silica gel (*n*-hexane/EtOAc: 5/1) yielded **397I** (92.0 mg, 64%) as colorless oil.

**<sup>1</sup>H NMR** (400 MHz, CDCl<sub>3</sub>)  $\delta$  8.56 (ddd, *J* = 4.9, 2.0, 0.9 Hz, 1H), 8.12 (dd, *J* = 1.5, 0.8 Hz, 1H), 7.80 (ddd, *J* = 8.3, 7.4, 2.0 Hz, 1H), 7.58 (d, *J* = 3.6 Hz, 1H), 7.39 (d, *J* = 8.3 Hz, 1H), 7.19 – 7.16 (m, 2H), 7.13 – 7.08 (m, 6H), 7.02 – 6.98 (m, 2H), 6.94 – 6.87 (m, 2H), 6.58 (dd, *J* = 3.6, 0.9 Hz, 1H), 4.25 (t, *J* = 7.0 Hz, 2H), 4.20 (t, *J* = 6.9 Hz, 2H), 2.81 (t, *J* = 7.0 Hz, 2H), 2.72 (t, *J* = 7.0 Hz, 2H), 1.66 (s, 6H), 1.65 (s, 6H).

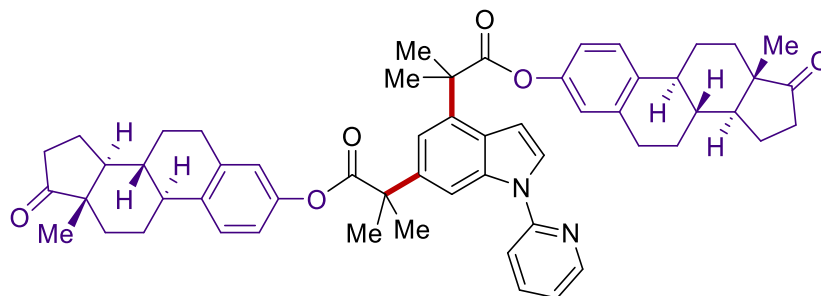
**<sup>13</sup>C NMR** (100 MHz, CDCl<sub>3</sub>)  $\delta$  177.6 (C<sub>q</sub>), 177.0 (C<sub>q</sub>), 152.4 (C<sub>q</sub>), 149.0 (CH), 139.5 (C<sub>q</sub>), 138.3 (CH), 137.8 (C<sub>q</sub>), 137.8 (C<sub>q</sub>), 136.8 (C<sub>q</sub>), 135.5 (C<sub>q</sub>), 128.9 (CH), 128.8 (CH), 128.2 (CH), 128.1 (CH), 126.8 (C<sub>q</sub>), 126.3 (CH), 126.2 (CH), 125.9 (CH), 120.2 (CH), 115.5 (CH), 115.0 (CH), 108.8 (CH), 104.0 (CH), 65.3 (CH<sub>2</sub>), 65.2 (CH<sub>2</sub>), 46.8 (C<sub>q</sub>), 46.5 (C<sub>q</sub>), 35.0 (CH<sub>2</sub>), 34.9 (CH<sub>2</sub>), 26.7 (CH<sub>3</sub>), 26.2 (CH<sub>3</sub>).

**IR** (ATR): 2954, 2927, 2869, 1710, 1470, 1437, 1251, 1139, 907, 731 cm<sup>-1</sup>.

**MS** (ESI) *m/z* (relative intensity): 575 (66) [M+H]<sup>+</sup>, 597 (34) [M+Na]<sup>+</sup>.

**HR-MS** (ESI) C<sub>37</sub>H<sub>39</sub>N<sub>2</sub>O<sub>4</sub> [M+H]<sup>+</sup>: 575.2908, found: 575.2904.

**Bis[(8*R*,9*S*,13*S*,14*S*)-13-methyl-17-oxo-7,8,9,11,12,13,14,15,16,17-decahydro-6*H*-cyclopenta[*a*]phenanthren-3-yl] 2,2'-[1-(pyridin-2-yl)-1*H*-indole-4,6-diyl]bis(2-methylpropanoate) (**397m**)**



The **General Procedure C** was followed using 1-(pyridin-2-yl)-1*H*-indole **395a** (48.6 mg, 0.25 mmol), (8*R*,9*S*,13*S*,14*S*)-13-methyl-17-oxo-7,8,9,11,12,13,14,15,16,17-decahydro-6*H*-cyclopenta[*a*]phenanthren-3-yl 2-bromo-2-methylpropanoate **396m** (524 mg, 1.25 mmol), Ru(OAc)<sub>2</sub>(PPh<sub>3</sub>)<sub>2</sub> (18.6 mg, 10 mol %), NaOAc (41.0 mg, 0.50 mmol) in DCE (2.0 mL). Purification by column chromatography on silica gel (*n*-hexane/EtOAc: 5/1) yielded **397m** (172.0 mg, 79%) as colorless oil.

<sup>1</sup>H NMR (400 MHz, CDCl<sub>3</sub>) δ 8.58 (ddd, *J* = 4.9, 2.0, 0.9 Hz, 1H), 8.33 – 8.25 (m, 1H), 7.82 (ddd, *J* = 8.2, 7.4, 2.0 Hz, 1H), 7.70 (d, *J* = 3.6 Hz, 1H), 7.48 (d, *J* = 8.2 Hz, 1H), 7.34 (d, *J* = 1.6 Hz, 1H), 7.19 (ddd, *J* = 8.2, 4.9, 0.9 Hz, 1H), 7.18 – 7.11 (m, 2H), 6.82 (dd, *J* = 3.6, 0.8 Hz, 1H), 6.72 (dd, *J* = 8.5, 2.6 Hz, 1H), 6.68 – 6.60 (m, 3H), 2.83 – 2.74 (m, 4H), 2.49 (d, *J* = 8.9 Hz, 1H), 2.44 (d, *J* = 8.6 Hz, 1H), 2.36 – 2.29 (m, 2H), 2.25 – 2.17 (m, 2H), 2.09 (dd, *J* = 18.9, 8.9 Hz, 2H), 2.04 – 1.98 (m, 2H), 1.98 – 1.89 (m, 5H), 1.84 (s, 6H), 1.80 (s, 6H), 1.65 – 1.28 (m, 11H), 0.86 (s, 3H), 0.86 (s, 3H).

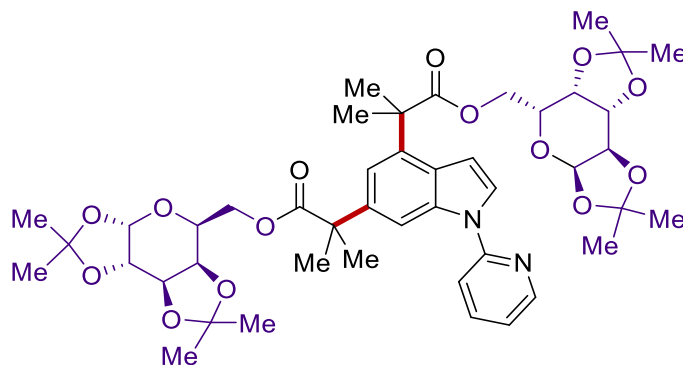
<sup>13</sup>C NMR (100 MHz, CDCl<sub>3</sub>) δ 220.6 (C<sub>q</sub>), 220.6 (C<sub>q</sub>), 176.6 (C<sub>q</sub>), 176.0 (C<sub>q</sub>), 152.4 (C<sub>q</sub>), 149.0 (CH), 149.0 (CH), 148.9 (C<sub>q</sub>), 148.9 (C<sub>q</sub>), 139.3 (C<sub>q</sub>), 138.5 (CH), 137.7 (C<sub>q</sub>), 137.7 (C<sub>q</sub>), 137.0 (C<sub>q</sub>), 137.0 (C<sub>q</sub>), 136.5 (C<sub>q</sub>), 135.6 (C<sub>q</sub>), 126.8 (C<sub>q</sub>), 126.1 (CH), 126.1 (CH), 121.4 (CH), 121.3 (CH), 120.3 (CH), 118.7 (CH), 118.5 (CH), 115.7 (CH), 115.1 (CH), 109.0 (CH), 104.1 (CH), 50.3 (CH), 50.3 (CH), 47.9 (C<sub>q</sub>), 47.9 (C<sub>q</sub>), 47.3 (C<sub>q</sub>), 46.8 (C<sub>q</sub>), 44.0 (CH), 44.0 (CH), 37.9 (CH), 37.9 (CH), 35.8 (CH<sub>2</sub>), 35.8 (CH<sub>2</sub>), 31.5 (CH<sub>2</sub>), 31.5 (CH<sub>2</sub>), 29.3 (CH<sub>2</sub>), 29.2 (CH<sub>2</sub>), 26.7 (CH<sub>3</sub>), 26.7 (CH<sub>3</sub>), 26.3 (CH<sub>2</sub>), 26.3 (CH<sub>2</sub>), 26.3 (CH<sub>3</sub>), 26.3 (CH<sub>3</sub>), 25.7 (CH<sub>2</sub>), 25.7 (CH<sub>2</sub>), 21.5 (CH<sub>2</sub>), 21.5 (CH<sub>2</sub>), 13.7 (CH<sub>3</sub>), 13.7 (CH<sub>3</sub>).

IR (ATR): 2976, 2931, 1734, 1437, 1207, 1150, 1118, 908, 734, 722 cm<sup>-1</sup>.

MS (ESI) *m/z* (relative intensity): 871 (50) [M+H]<sup>+</sup>, 888 (90) [M+NH<sub>4</sub>]<sup>+</sup>.

HR-MS (ESI) C<sub>57</sub>H<sub>63</sub>N<sub>2</sub>O<sub>6</sub> [M+H]<sup>+</sup>: 871.4665, found: 871.4681.

[(4*aS*,5*S*,5*aR*,8*aR*,8*bS*)-2,2,7,7-tetramethyltetrahydro-5*H*-bis([1,3]dioxolo)[4,5-*b*:4',5'-*d*]pyran-5-yl)methyl 2-methyl-2-(4-(2-methyl-1-oxo-1-((4*aR*,5*R*,5*aS*,8*aS*,8*bR*)-2,2,7,7-tetramethyltetrahydro-5*H*-bis([1,3]dioxolo)[4,5-*b*:4',5'-*d*]pyran-5-yl)methoxy)propan-2-yl)-1-(pyridin-2-yl)-1*H*-indol-6-yl)propanoate (**397n**)



The **General Procedure C** was followed using 1-(pyridin-2-yl)-1*H*-indole **395a** (48.6 mg, 0.25 mmol), ((3*aR*,5*R*,5*aS*,8*aS*,8*bR*)-2,2,7,7-tetramethyltetrahydro-5*H*-bis([1,3]dioxolo)[4,5-*b*:4',5'-*d*]pyran-5-yl) methyl 2-bromo-2-methylpropanoate **396n** (512 mg, 1.25 mmol), Ru(OAc)<sub>2</sub>(PPh<sub>3</sub>)<sub>2</sub> (18.6 mg, 10 mol %), NaOAc (41.0 mg, 0.50 mmol) in DCE (2.0 mL). Purification by column chromatography on silica gel (*n*-hexane/EtOAc: 5/1) yielded **397n** (157.4 mg, 74%) as colorless oil.

<sup>1</sup>H NMR (400 MHz, CDCl<sub>3</sub>) δ 8.54 (ddd, *J* = 4.9, 2.0, 0.9 Hz, 1H), 8.08 – 8.07 (m, 1H), 7.80 (ddd, *J* = 8.2, 7.4, 2.0 Hz, 1H), 7.59 (d, *J* = 3.6 Hz, 1H), 7.43 (d, *J* = 8.3 Hz, 1H), 7.17 (d, *J* = 1.3 Hz, 1H), 7.15 (ddd, *J* = 8.3, 4.9, 0.9 Hz, 1H), 6.62 (dd, *J* = 3.5, 0.9 Hz, 1H), 5.44 (t, *J* = 4.9 Hz, 2H), 4.49 (dd, *J* = 7.9, 2.4 Hz, 1H), 4.43 (dd, *J* = 7.9, 2.4 Hz, 1H), 4.26 – 4.20 (m, 4H), 4.19 – 4.13 (m, 2H), 4.01 (dd, *J* = 7.9, 1.8 Hz, 1H), 3.94 (ddd, *J* = 7.2, 5.1, 1.8 Hz, 1H), 3.89 (ddd, *J* = 7.2, 5.1, 1.8 Hz, 1H), 3.86 (dd, *J* = 7.9, 1.8 Hz, 1H), 1.70 (s, 3H), 1.67 (s, 3H), 1.67 (s, 3H), 1.64 (s, 3H), 1.42 (s, 3H), 1.37 (s, 3H), 1.36 (s, 3H), 1.35 (s, 3H), 1.27 (s, 3H), 1.25 (s, 3H), 1.19 (s, 3H), 1.19 (s, 3H).

<sup>13</sup>C NMR (100 MHz, CDCl<sub>3</sub>) δ 177.4 (C<sub>q</sub>), 176.8 (C<sub>q</sub>), 152.3 (C<sub>q</sub>), 149.1 (CH), 139.3 (C<sub>q</sub>), 138.4 (CH), 136.7 (C<sub>q</sub>), 135.3 (C<sub>q</sub>), 126.8 (C<sub>q</sub>), 126.0 (CH), 120.2 (CH), 115.5 (CH), 115.0 (CH), 109.4 (C<sub>q</sub>), 109.3 (C<sub>q</sub>), 108.9 (CH), 108.6 (C<sub>q</sub>), 108.6 (C<sub>q</sub>), 104.0 (CH), 96.2 (CH), 96.1 (CH), 70.8 (CH), 70.7 (CH), 70.5 (CH), 70.5 (CH), 65.8 (CH), 65.7 (CH), 63.4 (CH<sub>2</sub>), 63.3 (CH<sub>2</sub>), 46.8 (C<sub>q</sub>), 46.6 (C<sub>q</sub>), 27.1 (CH<sub>3</sub>), 26.6 (CH<sub>3</sub>), 26.4 (CH<sub>3</sub>), 26.1 (CH<sub>3</sub>), 26.0 (CH<sub>3</sub>), 25.8 (CH<sub>3</sub>), 25.0 (CH<sub>3</sub>), 24.2 (CH<sub>3</sub>).

IR (ATR): 2991, 2936, 1210, 1132, 1112, 1066, 1009, 998, 888, 727 cm<sup>-1</sup>.

## Experimental Data

---

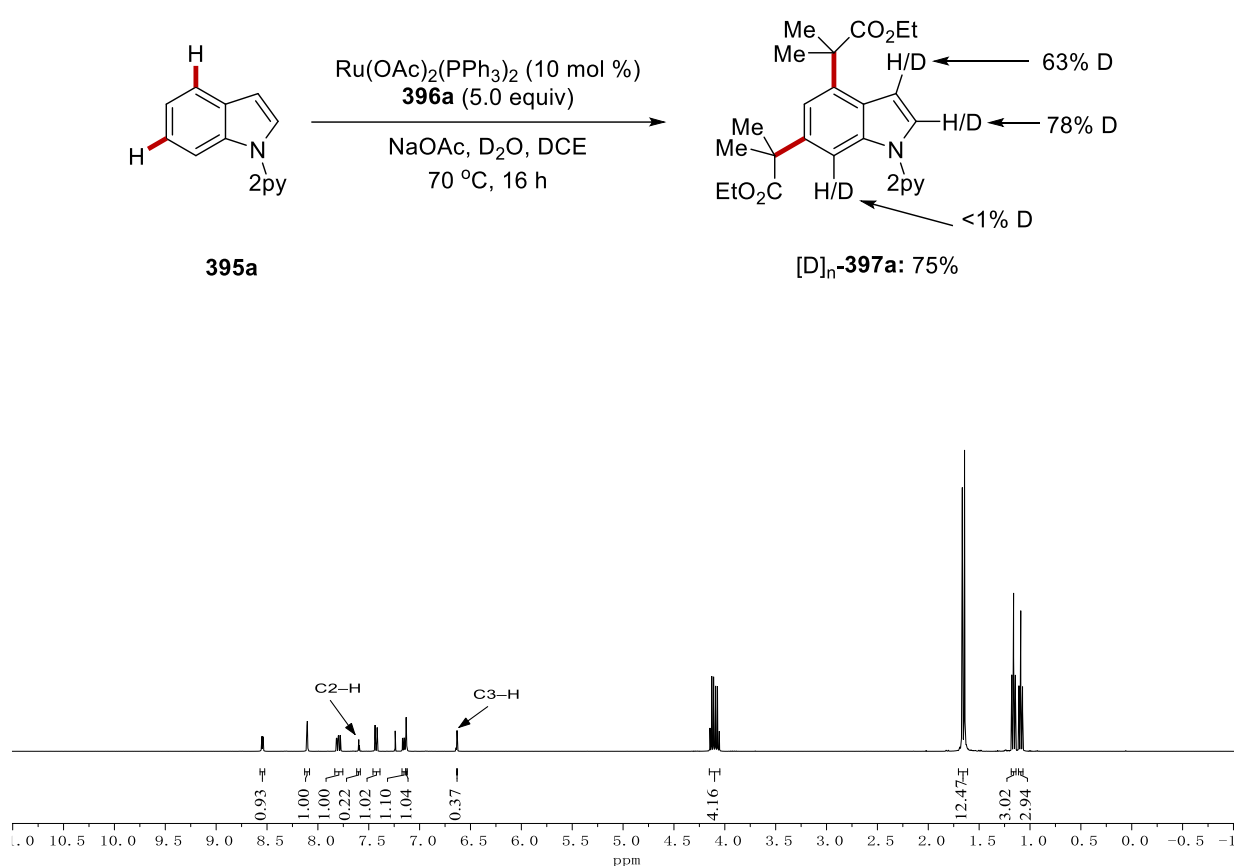
**MS** (ESI)  $m/z$  (relative intensity): 851 (30)  $[M+H]^+$ , 868 (70)  $[M+NH_4]^+$ .

**HR-MS** (ESI)  $C_{45}H_{59}N_2O_{14}$   $[M+H]^+$ : 851.3965, found: 851.3961.

### 5.4.2 Mechanistic Investigation

#### 1) Procedure for H/D exchange experiment

A suspension of 1-(pyridin-2-yl)-1*H*-indole **395a** (0.25 mmol, 1.0 equiv), ethyl  $\alpha$ -bromoisobutyrate **396a** (1.25 mmol, 5.0 equiv), Ru(OAc)<sub>2</sub>(PPh<sub>3</sub>)<sub>2</sub> (10 mol %), NaOAc (2 equiv), and D<sub>2</sub>O (10 equiv) in DCE (2.0 mL) was stirred at 70 °C for 16 h under N<sub>2</sub> (Scheme 5.4.1). After cooling to room temperature, the mixture was concentrated *in vacuo*. Purification by column chromatography on silica gel afforded the desired product [D]<sub>n</sub>-**397a**.



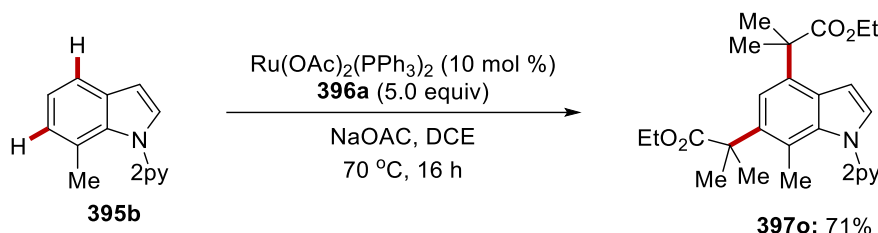
**Scheme 5.4.1** H/D exchange study for ruthenium-catalyzed C4/C6-H alkylations.

#### 2) Experiment with C7-blocked substrate

A suspension of 7-methyl-1-(pyridin-2-yl)-1*H*-indole **395b** (0.25 mmol, 1.0 equiv), ethyl  $\alpha$ -bromoisobutyrate **396a** (1.25 mmol, 5.0 equiv), Ru(OAc)<sub>2</sub>(PPh<sub>3</sub>)<sub>2</sub> (10 mol %), and NaOAc (0.50 mmol, 2 equiv) in DCE (2.0 mL) was stirred at 70 °C for 16 h under N<sub>2</sub> (Scheme 5.4.2). After cooling to room

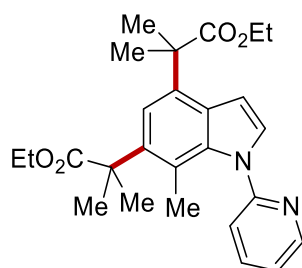


temperature, the mixture is concentrated *in vacuo*. Purification by column chromatography on silica gel afforded the desired product **397o**.



**Scheme 5.4.2** ruthenium-catalyzed C4/C6-H alkylations with **395b**.

#### Diethyl 2,2'-[7-methyl-1-(pyridin-2-yl)-1H-indole-4,6-diyl]bis(2-methylpropanoate) (**397o**)



The **General Procedure C** was followed using 7-methyl-1-(pyridin-2-yl)-1H-indole **395b** (52.1 mg, 0.25 mmol), Ethyl  $\alpha$ -bromoisobutyrate **396a** (243 mg, 1.25 mmol),  $\text{Ru(OAc)}_2(\text{PPh}_3)_2$  (18.6 mg, 10 mol %), NaOAc (41.0 mg, 0.50 mmol) in DCE (2.0 mL). Purification by column chromatography on silica gel (*n*-hexane/EtOAc: 5/1) yielded **397o** (84.0 mg, 71%) as colorless oil.

**$^1\text{H}$  NMR** (400 MHz,  $\text{CDCl}_3$ )  $\delta$  8.52 (ddd,  $J = 4.9, 2.0, 0.9$  Hz, 1H), 7.75 (ddd,  $J = 7.9, 7.6, 2.0$  Hz, 1H), 7.24 (ddd,  $J = 7.9, 4.9, 0.9$  Hz, 1H), 7.23 (dd,  $J = 4.9, 4.9$  Hz, 1H), 7.20 (s, 1H), 7.19 (ddd,  $J = 7.9, 0.9, 0.9$  Hz, 1H), 6.59 (d,  $J = 3.5$  Hz, 1H), 4.11 (q,  $J = 7.1$  Hz, 2H), 4.11 (q,  $J = 7.1$  Hz, 2H), 1.83 (s, 3H), 1.69 (s, 6H), 1.61 (s, 6H), 1.18 (t,  $J = 7.1$  Hz, 3H), 1.14 (t,  $J = 7.1$  Hz, 3H).

**$^{13}\text{C}$  NMR** (100 MHz,  $\text{CDCl}_3$ )  $\delta$  178.8 ( $\text{C}_q$ ), 178.0 ( $\text{C}_q$ ), 154.1 ( $\text{C}_q$ ), 148.7 (CH), 137.8 ( $\text{C}_q$ ), 137.7 (CH), 137.1 ( $\text{C}_q$ ), 134.1 ( $\text{C}_q$ ), 130.4 (CH), 127.2 ( $\text{C}_q$ ), 121.9 (CH), 120.5 (CH), 119.1 ( $\text{C}_q$ ), 115.2 (CH), 103.2 (CH), 60.7 ( $\text{CH}_2$ ), 60.7 ( $\text{CH}_2$ ), 46.9 ( $\text{C}_q$ ), 46.5 ( $\text{C}_q$ ), 27.9 ( $\text{CH}_3$ ), 26.4 ( $\text{CH}_3$ ), 17.4 ( $\text{CH}_3$ ), 14.1 ( $\text{CH}_3$ ).

**IR** (ATR): 2975, 2945, 1732, 1720, 1468, 1438, 1250, 1150, 731, 720  $\text{cm}^{-1}$ .

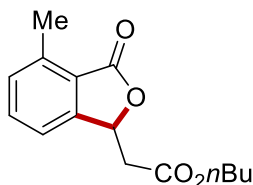
**MS** (ESI)  $m/z$  (relative intensity): 385 (34)  $[\text{M}+\text{H}]^+$ , 407 (66)  $[\text{M}+\text{Na}]^+$ .

**HR-MS** (ESI)  $\text{C}_{26}\text{H}_{33}\text{N}_2\text{O}_4$   $[\text{M}+\text{H}]^+$ : 385.1582, found: 385.1580.

## 5.5 Osmium-Catalyzed Electrooxidative C–H Annulations

### 5.5.1 Characterization Data

#### Butyl 2-(4-methyl-3-oxo-1,3-dihydroisobenzofuran-1-yl)acetate (**400a**)



The **General Procedure D** was followed using 2-methylbenzoic acid **398a** (27.2 mg, 0.20 mmol), *n*-butyl acrylate **399a** (76.9 mg, 0.60 mmol), [OsCl<sub>2</sub>(*p*-cymene)]<sub>2</sub> (7.9 mg, 5.0 mol %), KI (66.4 mg, 2.0 equiv), KOAc (39.3 mg, 2.0 equiv) in HFIP (2.0 mL) and H<sub>2</sub>O (2.0 mL). Purification by column chromatography on silica gel (*n*-hexane/EtOAc: 8/1) yielded **400a** (39.3 mg, 75%) as a colorless oil.

<sup>1</sup>H NMR (400 MHz, CDCl<sub>3</sub>) δ 7.49 (t, *J* = 7.6 Hz, 1H), 7.24 (ddd, *J* = 7.6, 3.8, 0.8 Hz, 2H), 5.77 (t, *J* = 6.5 Hz, 1H), 4.11 (t, *J* = 6.5 Hz, 2H), 2.83 (d, *J* = 6.5 Hz, 2H), 2.64 (s, 3H), 1.61 – 1.52 (m, 2H), 1.32 (dq, *J* = 14.6, 7.4 Hz, 2H), 0.88 (t, *J* = 7.4 Hz, 3H).

<sup>13</sup>C NMR (100 MHz, CDCl<sub>3</sub>) δ 170.0 (C<sub>q</sub>), 169.3 (C<sub>q</sub>), 149.2 (C<sub>q</sub>), 139.8 (C<sub>q</sub>), 133.9 (CH), 131.0 (CH), 123.3 (C<sub>q</sub>), 119.2 (CH), 76.0 (CH), 65.0 (CH<sub>2</sub>), 39.7 (CH<sub>2</sub>), 30.4 (CH<sub>2</sub>), 19.0 (CH<sub>2</sub>), 17.2 (CH<sub>3</sub>), 13.6 (CH<sub>3</sub>).

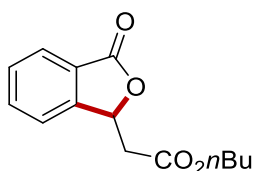
IR (ATR): 2960, 2927, 1745, 1711, 1519, 1371, 1321, 1065, 956, 608 cm<sup>-1</sup>.

MS (ESI) *m/z* (relative intensity): 263 (40) [M+H]<sup>+</sup>, 285 (60) [M+Na]<sup>+</sup>.

HR-MS (ESI) C<sub>15</sub>H<sub>19</sub>O<sub>4</sub> [M+H]<sup>+</sup>: 263.1279, found: 263.1281.

The spectral data were in accordance with those reported in the literature.<sup>[236h]</sup>

#### Butyl 2-(3-oxo-1,3-dihydroisobenzofuran-1-yl)acetate (**400b**)



The **General Procedure D** was followed using benzoic acid **398b** (24.4 mg, 0.20 mmol), *n*-butyl acrylate **399a** (76.9 mg, 0.60 mmol), [OsCl<sub>2</sub>(*p*-cymene)]<sub>2</sub> (7.9 mg, 5.0 mol %), KI (66.4 mg, 2.0 equiv), KOAc (39.3 mg, 2.0 equiv) in HFIP (2.0 mL) and H<sub>2</sub>O (2.0 mL). Purification by column

chromatography on silica gel (*n*-hexane/EtOAc: 8/1) yielded **400b** (35.3 mg, 71%) as a colorless oil.

$^1\text{H NMR}$  (400 MHz,  $\text{CDCl}_3$ )  $\delta$  7.90 (d,  $J = 7.7$  Hz, 1H), 7.66 (dd,  $J = 7.5, 1.1$  Hz, 1H), 7.54 (t,  $J = 7.5$  Hz, 1H), 7.48 (ddd,  $J = 7.7, 1.1, 0.8$  Hz, 1H), 5.87 (t,  $J = 6.6$  Hz, 1H), 4.14 (t,  $J = 6.6$  Hz, 2H), 2.98 – 2.80 (m, 2H), 1.69 – 1.54 (m, 2H), 1.35 (dq,  $J = 14.7, 7.4$  Hz, 2H), 0.91 (t,  $J = 7.4$  Hz, 3H).

$^{13}\text{C NMR}$  (100 MHz,  $\text{CDCl}_3$ )  $\delta$  169.8 ( $\text{C}_q$ ), 169.3 ( $\text{C}_q$ ), 148.8 ( $\text{C}_q$ ), 134.2 (CH), 129.5 (CH), 126.0 ( $\text{C}_q$ ), 125.8 (CH), 122.1 (CH), 77.0 (CH), 65.2 ( $\text{CH}_2$ ), 39.6 ( $\text{CH}_2$ ), 30.5 ( $\text{CH}_2$ ), 19.0 ( $\text{CH}_2$ ), 13.6 ( $\text{CH}_3$ ).

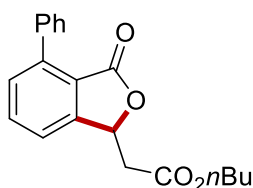
**IR** (ATR): 2959, 2933, 1759, 1599, 1466, 1288, 1172, 1059, 748, 571  $\text{cm}^{-1}$ .

**MS** (ESI)  $m/z$  (relative intensity): 249 (40)  $[\text{M}+\text{H}]^+$ , 271 (60)  $[\text{M}+\text{Na}]^+$ .

**HR-MS** (ESI)  $\text{C}_{14}\text{H}_{17}\text{O}_4$   $[\text{M}+\text{H}]^+$ : 249.1124, found: 249.1121.

The spectral data were in accordance with those reported in the literature.<sup>[236h]</sup>

#### Butyl 2-(3-oxo-4-phenyl-1,3-dihydroisobenzofuran-1-yl)acetate (**400c**)



The **General Procedure D** was followed using 2-phenyl benzoic acid **398c** (39.6 mg, 0.20 mmol), *n*-butyl acrylate **399a** (76.9 mg, 0.60 mmol),  $[\text{OsCl}_2(p\text{-cymene})]_2$  (7.9 mg, 5.0 mol %), KI (66.4 mg, 2.0 equiv), KOAc (39.3 mg, 2.0 equiv) in HFIP (2.0 mL) and  $\text{H}_2\text{O}$  (2.0 mL). Purification by column chromatography on silica gel (*n*-hexane/EtOAc: 8/1) yielded **400c** (42.2 mg, 65%) as a colorless oil.

$^1\text{H NMR}$  (400 MHz,  $\text{CDCl}_3$ )  $\delta$  7.72 (t,  $J = 7.6$  Hz, 1H), 7.59 – 7.43 (m, 7H), 5.89 (t,  $J = 6.5$  Hz, 1H), 4.20 (t,  $J = 6.5$  Hz, 2H), 2.96 (dd,  $J = 6.5, 1.5$  Hz, 2H), 1.71 – 1.55 (m, 2H), 1.47 – 1.32 (m, 2H), 0.96 (t,  $J = 7.3$  Hz, 3H).

$^{13}\text{C NMR}$  (100 MHz,  $\text{CDCl}_3$ )  $\delta$  169.4 ( $\text{C}_q$ ), 168.6 ( $\text{C}_q$ ), 150.1 ( $\text{C}_q$ ), 143.0 ( $\text{C}_q$ ), 136.2 ( $\text{C}_q$ ), 134.0 (CH), 131.3 (CH), 129.5 (CH), 128.4 (CH), 128.0 (CH), 121.9 ( $\text{C}_q$ ), 120.7 (CH), 75.6 (CH), 65.2 ( $\text{CH}_2$ ), 39.8 ( $\text{CH}_2$ ), 30.5 ( $\text{CH}_2$ ), 19.1 ( $\text{CH}_2$ ), 13.7 ( $\text{CH}_3$ ).

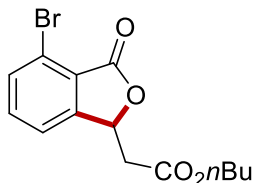
**IR** (ATR): 2959, 2931, 1760, 1575, 1308, 1236, 1199, 1015, 944, 697  $\text{cm}^{-1}$ .

**MS** (ESI)  $m/z$  (relative intensity): 325 (66)  $[\text{M}+\text{H}]^+$ , 347 (34)  $[\text{M}+\text{Na}]^+$ .

**HR-MS** (ESI)  $\text{C}_{20}\text{H}_{21}\text{O}_4$   $[\text{M}+\text{H}]^+$ : 325.1435, found: 325.1434.

The spectral data were in accordance with those reported in the literature.<sup>[236g]</sup>

#### Butyl 2-(4-bromo-3-oxo-1,3-dihydroisobenzofuran-1-yl)acetate (**400d**)



The **General Procedure D** was followed using 2-bromo benzoic acid **398d** (40.2 mg, 0.20 mmol), *n*-butyl acrylate **399a** (76.9 mg, 0.60 mmol), [OsCl<sub>2</sub>(*p*-cymene)]<sub>2</sub> (7.9 mg, 5.0 mol %), KI (66.4 mg, 2.0 equiv), KOAc (39.3 mg, 2.0 equiv) in HFIP (2.0 mL) and H<sub>2</sub>O (2.0 mL). Purification by column chromatography on silica gel (*n*-hexane/EtOAc: 8/1) yielded **400d** (32.1 mg, 49%) as a colorless oil.

<sup>1</sup>H NMR (400 MHz, CDCl<sub>3</sub>) δ 7.69 (d, *J* = 7.7 Hz, 1H), 7.49 (t, *J* = 7.7 Hz, 1H), 7.43 (d, *J* = 7.6 Hz, 1H), 5.79 (t, *J* = 6.5 Hz, 1H), 4.13 (t, *J* = 6.7 Hz, 2H), 2.99 – 2.81 (m, 2H), 1.64 – 1.52 (m, 2H), 1.34 (dq, *J* = 14.6, 7.4 Hz, 2H), 0.91 (t, *J* = 7.4 Hz, 3H).

<sup>13</sup>C NMR (100 MHz, CDCl<sub>3</sub>) δ 169.1 (C<sub>q</sub>), 167.1 (C<sub>q</sub>), 151.2 (C<sub>q</sub>), 135.1 (CH), 134.3 (CH), 124.4 (C<sub>q</sub>), 121.2 (C<sub>q</sub>), 121.1 (CH), 75.3 (CH), 65.3 (CH<sub>2</sub>), 39.4 (CH<sub>2</sub>), 30.5 (CH<sub>2</sub>), 19.0 (CH<sub>2</sub>), 13.6 (CH<sub>3</sub>).

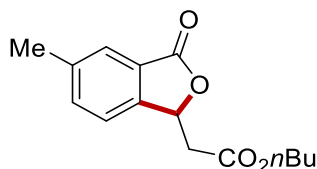
IR (ATR): 2959, 2932, 1763, 1722, 1582, 1343, 1207, 1173, 1011, 679 cm<sup>-1</sup>.

MS (ESI) *m/z* (relative intensity): 327 (66) (<sup>79</sup>Br) [M+H]<sup>+</sup>, 349 (34) (<sup>79</sup>Br) [M+Na]<sup>+</sup>.

HR-MS (ESI) C<sub>14</sub>H<sub>16</sub><sup>79</sup>BrO<sub>4</sub> [M+H]<sup>+</sup>: 327.0225, found: 327.0226.

The spectral data were in accordance with those reported in the literature.<sup>[266]</sup>

#### Butyl 2-(5-methyl-3-oxo-1,3-dihydroisobenzofuran-1-yl)acetate (**400e**)



The **General Procedure D** was followed using 3-methyl benzoic acid **398e** (27.2 mg, 0.20 mmol), *n*-butyl acrylate **399a** (76.9 mg, 0.60 mmol), [OsCl<sub>2</sub>(*p*-cymene)]<sub>2</sub> (7.9 mg, 5.0 mol %), KI (66.4 mg, 2.0 equiv), KOAc (39.3 mg, 2.0 equiv) in HFIP (2.0 mL) and H<sub>2</sub>O (2.0 mL). Purification by column chromatography on silica gel (*n*-hexane/EtOAc: 8/1) yielded **400e** (51.7 mg, 77%) as a colorless oil.

**<sup>1</sup>H NMR** (400 MHz, CDCl<sub>3</sub>)  $\delta$  7.68 (s, 1H), 7.46 (ddd,  $J$  = 7.8, 1.6, 0.8 Hz, 1H), 7.35 (d,  $J$  = 7.8 Hz, 1H), 5.82 (t,  $J$  = 6.6 Hz, 1H), 4.14 (t,  $J$  = 6.7 Hz, 2H), 2.94 – 2.76 (m, 2H), 2.44 (s, 3H), 1.64 – 1.55 (m, 2H), 1.40 – 1.29 (m, 2H), 0.91 (t,  $J$  = 7.4 Hz, 3H).

**<sup>13</sup>C NMR** (100 MHz, CDCl<sub>3</sub>)  $\delta$  170.0 (C<sub>q</sub>), 169.4 (C<sub>q</sub>), 146.2 (C<sub>q</sub>), 139.9 (C<sub>q</sub>), 135.4 (CH), 126.1 (C<sub>q</sub>), 125.8 (CH), 121.7 (CH), 76.9 (CH), 65.1 (CH<sub>2</sub>), 39.7 (CH<sub>2</sub>), 30.5 (CH<sub>2</sub>), 21.2 (CH<sub>3</sub>), 19.1 (CH<sub>2</sub>), 13.7 (CH<sub>3</sub>).

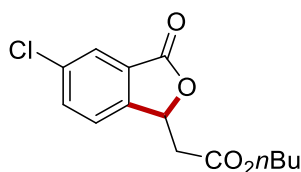
**IR** (ATR): 2960, 2929, 1771, 1733, 1495, 1290, 1154, 1009, 750, 557 cm<sup>-1</sup>.

**MS** (ESI)  $m/z$  (relative intensity): 263 (45) [M+H]<sup>+</sup>, 285 (55) [M+Na]<sup>+</sup>.

**HR-MS** (ESI) C<sub>15</sub>H<sub>19</sub>O<sub>4</sub> [M+H]<sup>+</sup>: 263.1281, found: 263.1278.

The spectral data were in accordance with those reported in the literature.<sup>[236h]</sup>

#### Butyl 2-(5-chloro-3-oxo-1,3-dihydroisobenzofuran-1-yl)acetate (**400f**)



The **General Procedure D** was followed using 3-chloro benzoic acid **398f** (31.4 mg, 0.20 mmol), *n*-butyl acrylate **399a** (76.9 mg, 0.60 mmol), [OsCl<sub>2</sub>(*p*-cymene)]<sub>2</sub> (7.9 mg, 5.0 mol %), KI (66.4 mg, 2.0 equiv), KOAc (39.3 mg, 2.0 equiv) in HFIP (2.0 mL) and H<sub>2</sub>O (2.0 mL). Purification by column chromatography on silica gel (*n*-hexane/EtOAc: 8/1) yielded **400f** (24.3 mg, 43%) as a colorless oil.

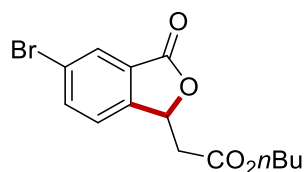
**<sup>1</sup>H NMR** (400 MHz, CDCl<sub>3</sub>)  $\delta$  8.02 (s, 1H), 7.77 (d,  $J$  = 8.1 Hz, 1H), 7.39 (d,  $J$  = 8.1 Hz, 1H), 5.81 (t,  $J$  = 6.5 Hz, 1H), 4.14 (t,  $J$  = 6.7 Hz, 2H), 3.00 – 2.78 (m, 2H), 1.59 (dt,  $J$  = 14.6, 6.7 Hz, 2H), 1.34 (dq,  $J$  = 14.6, 7.4 Hz, 2H), 0.91 (t,  $J$  = 7.4 Hz, 3H).

**<sup>13</sup>C NMR** (100 MHz, CDCl<sub>3</sub>)  $\delta$  169.1 (C<sub>q</sub>), 168.2 (C<sub>q</sub>), 147.4 (C<sub>q</sub>), 137.3 (CH), 128.8 (CH), 128.1 (C<sub>q</sub>), 123.8 (CH), 123.6 (C<sub>q</sub>), 76.9 (CH), 65.3 (CH<sub>2</sub>), 39.2 (CH<sub>2</sub>), 30.5 (CH<sub>2</sub>), 19.0 (CH<sub>2</sub>), 13.6 (CH<sub>3</sub>).

**IR** (ATR): 2959, 2932, 1654, 1710, 1418, 1287, 1174, 1071, 1006, 771 cm<sup>-1</sup>.

**MS** (ESI)  $m/z$  (relative intensity): 283 (45) [M+H]<sup>+</sup>, 305 (55) [M+Na]<sup>+</sup>.

**HR-MS** (ESI) C<sub>14</sub>H<sub>16</sub><sup>35</sup>ClO<sub>4</sub> [M+H]<sup>+</sup>: 283.0733, found: 283.0732.

**Butyl 2-(5-bromo-3-oxo-1,3-dihydroisobenzofuran-1-yl)acetate (400g)**

The **General Procedure D** was followed using 3-bromo benzoic acid **398g** (40.2 mg, 0.20 mmol), *n*-butyl acrylate **399a** (76.9 mg, 0.60 mmol), [OsCl<sub>2</sub>(*p*-cymene)]<sub>2</sub> (7.9 mg, 5.0 mol %), KI (66.4 mg, 2.0 equiv), KOAc (39.3 mg, 2.0 equiv) in HFIP (2.0 mL) and H<sub>2</sub>O (2.0 mL). Purification by column chromatography on silica gel (*n*-hexane/EtOAc: 8/1) yielded **400g** (34.0 mg, 52%) as a colorless oil.

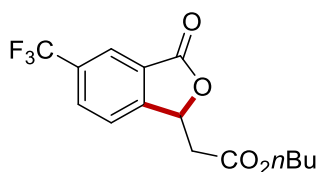
<sup>1</sup>H NMR (400 MHz, CDCl<sub>3</sub>) δ 7.86 (s, 1H), 7.62 (d, *J* = 8.2 Hz, 1H), 7.45 (d, *J* = 8.2 Hz, 1H), 5.84 (t, *J* = 6.6 Hz, 1H), 4.14 (t, *J* = 6.7 Hz, 2H), 3.00 – 2.78 (m, 2H), 1.60 (dt, *J* = 14.6, 6.7 Hz, 2H), 1.34 (dq, *J* = 14.6, 7.4 Hz, 2H), 0.91 (s, 3H).

<sup>13</sup>C NMR (100 MHz, CDCl<sub>3</sub>) δ 169.1 (C<sub>q</sub>), 168.4 (C<sub>q</sub>), 146.9 (C<sub>q</sub>), 135.9 (C<sub>q</sub>), 134.5 (CH), 127.9 (C<sub>q</sub>), 125.8 (CH), 123.5 (CH), 76.8 (CH), 65.3 (CH<sub>2</sub>), 39.3 (CH<sub>2</sub>), 30.5 (CH<sub>2</sub>), 19.0 (CH<sub>2</sub>), 13.6 (CH<sub>3</sub>).

IR (ATR): 2960, 2934, 1776, 1763, 1425, 1288, 1204, 1175, 1006, 832 cm<sup>-1</sup>.

MS (ESI) *m/z* (relative intensity): 327 (50) (<sup>79</sup>Br) [M+H]<sup>+</sup>, 349 (50) (<sup>79</sup>Br) [M+Na]<sup>+</sup>.

HR-MS (ESI) C<sub>14</sub>H<sub>16</sub><sup>79</sup>BrO<sub>4</sub> [M+H]<sup>+</sup>: 327.0229, found: 327.0226.

**Butyl 2-(3-oxo-5-(trifluoromethyl)-1,3-dihydroisobenzofuran-1-yl)acetate (400h)**

The **General Procedure D** was followed using 3-trifluoromethyl benzoic acid **398h** (38.0 mg, 0.20 mmol), *n*-butyl acrylate **399a** (76.9 mg, 0.60 mmol), [OsCl<sub>2</sub>(*p*-cymene)]<sub>2</sub> (7.9 mg, 5.0 mol %), KI (66.4 mg, 2.0 equiv), KOAc (39.3 mg, 2.0 equiv) in HFIP (2.0 mL) and H<sub>2</sub>O (2.0 mL). Purification by column chromatography on silica gel (*n*-hexane/EtOAc: 8/1) yielded **400h** (33.5 mg, 53%) as a white solid.

**M. p.** 94 °C

<sup>1</sup>H NMR (400 MHz, CDCl<sub>3</sub>) δ 8.16 (s, 1H), 7.95 – 7.90 (m, 1H), 7.69 – 7.65 (m, 1H), 5.91 (t, *J* = 6.5

Hz, 1H), 4.14 (t,  $J = 6.7$  Hz, 2H), 3.05 – 2.82 (m, 2H), 1.63 – 1.55 (m, 2H), 1.34 (dq,  $J = 14.7, 7.4$  Hz, 2H), 0.91 (t,  $J = 7.4$  Hz, 3H).

$^{13}\text{C}$  NMR (100 MHz,  $\text{CDCl}_3$ )  $\delta$  168.9 ( $\text{C}_q$ ), 168.3 ( $\text{C}_q$ ), 151.9 ( $\text{C}_q$ ), 132.6 (q,  $J_{\text{C-F}} = 33.5$  Hz,  $\text{C}_q$ ), 131.1 (q,  $J_{\text{C-F}} = 3.5$  Hz, CH), 127.0 ( $\text{C}_q$ ), 123.2 (CH), 123.2 (d,  $J_{\text{C-F}} = 272.8$  Hz,  $\text{C}_q$ ), 123.1 (q,  $J_{\text{C-F}} = 4.1$  Hz, CH), 77.0 (CH), 65.4 ( $\text{CH}_2$ ), 39.0 ( $\text{CH}_2$ ), 30.5 ( $\text{CH}_2$ ), 19.0 ( $\text{CH}_2$ ), 13.6 ( $\text{CH}_3$ ).

$^{19}\text{F}$  NMR (282 MHz,  $\text{CDCl}_3$ )  $\delta$  -62.6.

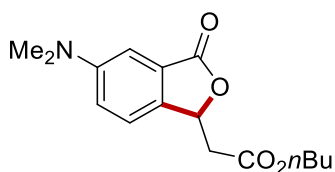
IR (ATR): 2962, 2935, 1779, 1734, 1398, 1329, 1168, 1126, 1007, 615  $\text{cm}^{-1}$ .

MS (ESI)  $m/z$  (relative intensity): 317 (30)  $[\text{M}+\text{H}]^+$ , 339 (70)  $[\text{M}+\text{Na}]^+$ .

HR-MS (ESI)  $\text{C}_{15}\text{H}_{16}\text{F}_3\text{O}_4$   $[\text{M}+\text{H}]^+$ : 317.0996, found: 317.0995.

The spectral data were in accordance with those reported in the literature.<sup>[236g]</sup>

#### Butyl 2-(5-(dimethylamino)-3-oxo-1,3-dihydroisobenzofuran-1-yl)acetate (400i)



The **General Procedure D** was followed using 3-(dimethylamino)benzoic acid **398i** (33.0 mg, 0.20 mmol), *n*-butyl acrylate **399a** (76.9 mg, 0.60 mmol),  $[\text{OsCl}_2(p\text{-cymene})]_2$  (7.9 mg, 5.0 mol %), KI (66.4 mg, 2.0 equiv), KOAc (39.3 mg, 2.0 equiv) in HFIP (2.0 mL) and  $\text{H}_2\text{O}$  (2.0 mL). Purification by column chromatography on silica gel (*n*-hexane/EtOAc: 8/1) yielded **400i** (39.6 mg, 68%) as a colorless oil.

$^1\text{H}$  NMR (400 MHz,  $\text{CDCl}_3$ )  $\delta$  7.27 (d,  $J = 8.5$  Hz, 1H), 7.08 (d,  $J = 2.4$  Hz, 1H), 6.98 (dd,  $J = 8.5, 2.4$  Hz, 1H), 5.77 (t,  $J = 6.6$  Hz, 1H), 4.14 (t,  $J = 6.7$  Hz, 2H), 3.00 (s, 6H), 2.91 – 2.72 (m, 2H), 1.65 – 1.55 (m, 2H), 1.35 (dq,  $J = 14.7, 7.4$  Hz, 2H), 0.91 (t,  $J = 7.4$  Hz, 3H).

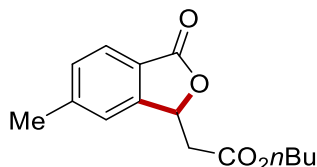
$^{13}\text{C}$  NMR (100 MHz,  $\text{CDCl}_3$ )  $\delta$  170.9 ( $\text{C}_q$ ), 169.6 ( $\text{C}_q$ ), 151.5 ( $\text{C}_q$ ), 136.2 ( $\text{C}_q$ ), 126.9 ( $\text{C}_q$ ), 122.3 (CH), 118.7 (CH), 106.9 (CH), 76.9 (CH), 65.0 ( $\text{CH}_2$ ), 40.6 ( $\text{CH}_3$ ), 40.1 ( $\text{CH}_2$ ), 30.5 ( $\text{CH}_2$ ), 19.1 ( $\text{CH}_2$ ), 13.7 ( $\text{CH}_3$ ).

IR (ATR): 2959, 2930, 1767, 1758, 1625, 1510, 1345, 1166, 776, 567  $\text{cm}^{-1}$ .

MS (ESI)  $m/z$  (relative intensity): 292 (70)  $[\text{M}+\text{H}]^+$ , 314 (30)  $[\text{M}+\text{Na}]^+$ .

**HR-MS** (ESI)  $C_{16}H_{22}NO_4$   $[M+H]^+$ : 292.1545, found: 292.1543.

**Butyl 2-(6-methyl-3-oxo-1,3-dihydroisobenzofuran-1-yl)acetate (400j)**



The **General Procedure D** was followed using 4-methyl benzoic acid **398j** (27.2 mg, 0.20 mmol), *n*-butyl acrylate **399a** (76.9 mg, 0.60 mmol),  $[OsCl_2(p\text{-cymene})]_2$  (7.9 mg, 5.0 mol %), KI (66.4 mg, 2.0 equiv), KOAc (39.3 mg, 2.0 equiv) in HFIP (2.0 mL) and  $H_2O$  (2.0 mL). Purification by column chromatography on silica gel (*n*-hexane/EtOAc: 8/1) yielded **400j** (43.0 mg, 82%) as a colorless oil.

**$^1H$  NMR** (400 MHz,  $CDCl_3$ )  $\delta$  7.76 (d,  $J = 7.8$  Hz, 1H), 7.33 (d,  $J = 7.8$  Hz, 1H), 7.28 – 7.22 (m, 1H), 5.80 (t,  $J = 6.6$  Hz, 1H), 4.14 (t,  $J = 6.7$  Hz, 2H), 2.93 – 2.77 (m, 2H), 2.46 (s, 3H), 1.64 – 1.56 (m, 2H), 1.35 (dq,  $J = 14.7, 7.4$  Hz, 2H), 0.91 (t,  $J = 7.4$  Hz, 3H).

**$^{13}C$  NMR** (100 MHz,  $CDCl_3$ )  $\delta$  169.9 ( $C_q$ ), 169.4 ( $C_q$ ), 149.4 ( $C_q$ ), 145.6 ( $C_q$ ), 130.7 (CH), 125.6 (CH), 123.4 ( $C_q$ ), 122.4 (CH), 76.7 (CH), 65.2 ( $CH_2$ ), 39.6 ( $CH_2$ ), 30.5 ( $CH_2$ ), 22.1 ( $CH_3$ ), 19.1 ( $CH_2$ ), 13.7 ( $CH_3$ ).

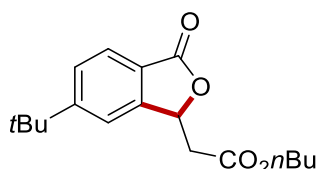
**IR** (ATR): 2960, 2932, 1768, 1758, 1617, 1314, 1279, 1166, 1012, 687  $cm^{-1}$ .

**MS** (ESI)  $m/z$  (relative intensity): 263 (60)  $[M+H]^+$ , 285 (40)  $[M+Na]^+$ .

**HR-MS** (ESI)  $C_{15}H_{19}O_4$   $[M+H]^+$ : 263.1278, found: 263.1278.

The spectral data were in accordance with those reported in the literature.<sup>[236h]</sup>

**Butyl 2-(6-(*tert*-butyl)-3-oxo-1,3-dihydroisobenzofuran-1-yl)acetate (400k)**



The **General Procedure D** was followed using 4-*tert*-butyl benzoic acid **398k** (35.6 mg, 0.20 mmol), *n*-butyl acrylate **399a** (76.9 mg, 0.60 mmol),  $[OsCl_2(p\text{-cymene})]_2$  (7.9 mg, 5.0 mol %), KI (66.4 mg, 2.0 equiv), KOAc (39.3 mg, 2.0 equiv) in HFIP (2.0 mL) and  $H_2O$  (2.0 mL). Purification by column



chromatography on silica gel (*n*-hexane/EtOAc: 8/1) yielded **400k** (40.8 mg, 67%) as a white solid.

**M. p.** 96 °C

**<sup>1</sup>H NMR** (400 MHz, CDCl<sub>3</sub>) δ 7.81 (d, *J* = 8.2 Hz, 1H), 7.57 (dd, *J* = 8.2, 1.6 Hz, 1H), 7.47 – 7.42 (m, 1H), 5.84 (t, *J* = 6.7 Hz, 1H), 4.15 (td, *J* = 6.7, 2.7 Hz, 2H), 2.96 – 2.80 (m, 2H), 1.61 (dt, *J* = 14.6, 6.7 Hz, 2H), 1.38 – 1.32 (m, 2H), 1.34 (s, 9H), 0.91 (t, *J* = 7.4 Hz, 3H).

**<sup>13</sup>C NMR** (100 MHz, CDCl<sub>3</sub>) δ 169.9 (C<sub>q</sub>), 169.5 (C<sub>q</sub>), 158.7 (C<sub>q</sub>), 149.2 (C<sub>q</sub>), 127.2 (CH), 125.4 (CH), 123.3 (C<sub>q</sub>), 118.5 (CH), 77.0 (CH), 65.1 (CH<sub>2</sub>), 39.8 (CH<sub>2</sub>), 35.6 (C<sub>q</sub>), 31.2 (CH<sub>3</sub>), 30.6 (CH<sub>2</sub>), 19.1 (CH<sub>2</sub>), 13.7 (CH<sub>3</sub>).

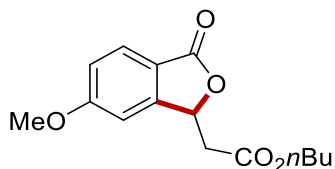
**IR** (ATR): 2967, 2935, 1771, 1750, 1697, 1315, 1280, 1005, 874, 666 cm<sup>-1</sup>.

**MS** (ESI) *m/z* (relative intensity): 305 (60) [M+H]<sup>+</sup>, 327 (40) [M+Na]<sup>+</sup>.

**HR-MS** (ESI) C<sub>18</sub>H<sub>25</sub>O<sub>4</sub> [M+H]<sup>+</sup>: 305.1749, found: 305.1747.

The spectral data were in accordance with those reported in the literature.<sup>[236g]</sup>

#### Butyl 2-(6-methoxy-3-oxo-1,3-dihydroisobenzofuran-1-yl)acetate (**400l**)



The **General Procedure D** was followed using 4-methoxybenzoic acid **398l** (30.4 mg, 0.20 mmol), *n*-butyl acrylate **399a** (76.9 mg, 0.60 mmol), [OsCl<sub>2</sub>(*p*-cymene)]<sub>2</sub> (7.9 mg, 5.0 mol %), KI (66.4 mg, 2.0 equiv), KOAc (39.3 mg, 2.0 equiv) in HFIP (2.0 mL) and H<sub>2</sub>O (2.0 mL). Purification by column chromatography on silica gel (*n*-hexane/EtOAc: 8/1) yielded **400l** (47.3 mg, 85%) as a colorless oil.

**<sup>1</sup>H NMR** (400 MHz, CDCl<sub>3</sub>) δ 7.79 (d, *J* = 8.6 Hz, 1H), 7.03 (dd, *J* = 8.6, 2.2 Hz, 1H), 6.91 (d, *J* = 2.2 Hz, 1H), 5.78 (t, *J* = 6.6 Hz, 1H), 4.15 (t, *J* = 6.7 Hz, 2H), 3.87 (s, 3H), 2.95 – 2.77 (m, 2H), 1.64 – 1.56 (m, 2H), 1.35 (dq, *J* = 14.6, 7.4 Hz, 2H), 0.91 (t, *J* = 7.4 Hz, 3H).

**<sup>13</sup>C NMR** (100 MHz, CDCl<sub>3</sub>) δ 169.6 (C<sub>q</sub>), 169.4 (C<sub>q</sub>), 164.8 (C<sub>q</sub>), 151.6 (C<sub>q</sub>), 127.3 (CH), 118.2 (C<sub>q</sub>), 116.7 (CH), 106.2 (CH), 76.2 (CH), 65.2 (CH<sub>2</sub>), 55.8 (CH<sub>3</sub>), 39.6 (CH<sub>2</sub>), 30.5 (CH<sub>2</sub>), 19.1 (CH<sub>2</sub>), 13.7 (CH<sub>3</sub>).

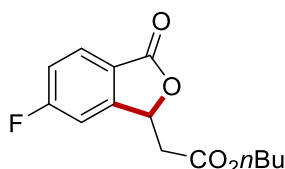
**IR** (ATR): 2960, 2935, 1759, 1731, 1605, 1460, 1359, 1281, 1253, 1007, 690 cm<sup>-1</sup>.

**MS** (ESI)  $m/z$  (relative intensity): 279 (60)  $[M+H]^+$ , 301 (40)  $[M+Na]^+$ .

**HR-MS** (ESI)  $C_{15}H_{19}O_5$   $[M+H]^+$ : 279.1229, found: 279.1227.

The spectral data were in accordance with those reported in the literature.<sup>[236g]</sup>

**Butyl 2-(6-fluoro-3-oxo-1,3-dihydroisobenzofuran-1-yl)acetate (400m)**



The **General Procedure D** was followed using 4-fluorobenzoic acid **398m** (28.0 mg, 0.20 mmol), *n*-butyl acrylate **399a** (76.9 mg, 0.60 mmol),  $[OsCl_2(p\text{-cymene})]_2$  (7.9 mg, 5.0 mol %), KI (66.4 mg, 2.0 equiv), KOAc (39.3 mg, 2.0 equiv) in HFIP (2.0 mL) and  $H_2O$  (2.0 mL). Purification by column chromatography on silica gel (*n*-hexane/EtOAc: 8/1) yielded **400m** (24.5 mg, 46%) as a colorless oil.

**$^1H$  NMR** (400 MHz,  $CDCl_3$ )  $\delta$  7.88 (dd,  $J = 8.4, 4.8$  Hz, 1H), 7.25 – 7.17 (m, 2H), 5.81 (t,  $J = 6.6$  Hz, 1H), 4.15 (t,  $J = 6.7$  Hz, 2H), 3.02 – 2.78 (m, 2H), 1.65 – 1.57 (m, 2H), 1.35 (dq,  $J = 14.7, 7.4$  Hz, 2H), 0.91 (t,  $J = 7.4$  Hz, 3H).

**$^{13}C$  NMR** (100 MHz,  $CDCl_3$ )  $\delta$  169.1 ( $C_q$ ), 168.2 (d,  $J = 75.8$  Hz,  $C_q$ ), 165.3 ( $C_q$ ), 151.6 (d,  $J_{C-F} = 10.3$  Hz,  $C_q$ ), 128.2 (d,  $J_{C-F} = 10.4$  Hz, CH), 122.0 (d,  $J_{C-F} = 2.0$  Hz,  $C_q$ ), 117.8 (d,  $J_{C-F} = 24.0$  Hz, CH), 109.8 (d,  $J_{C-F} = 24.9$  Hz, CH), 76.2 (d,  $J_{C-F} = 2.9$  Hz, CH), 65.3 ( $CH_2$ ), 39.2 ( $CH_2$ ), 30.5 ( $CH_2$ ), 19.0 ( $CH_2$ ), 13.6 ( $CH_3$ ).

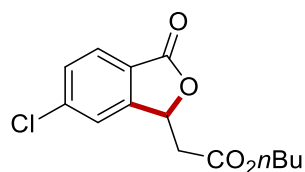
**$^{19}F$  NMR** (282 MHz,  $CDCl_3$ )  $\delta$  -102.13 (td,  $J = 8.4, 4.9$  Hz).

**IR** (ATR): 2961, 1934, 1761, 1723, 1604, 1243, 1008, 882, 742, 682  $cm^{-1}$ .

**MS** (ESI)  $m/z$  (relative intensity): 267 (30)  $[M+H]^+$ , 289 (70)  $[M+Na]^+$ .

**HR-MS** (ESI)  $C_{14}H_{16}FO_4$   $[M+H]^+$ : 267.1030, found: 267.1027.

The spectral data were in accordance with those reported in the literature.<sup>[236g]</sup>

**Butyl 2-(6-chloro-3-oxo-1,3-dihydroisobenzofuran-1-yl)acetate (400n)**

The **General Procedure D** was followed using 4-chlorobenzoic acid **398n** (31.3 mg, 0.20 mmol), *n*-butyl acrylate **399a** (76.9 mg, 0.60 mmol), [OsCl<sub>2</sub>(*p*-cymene)]<sub>2</sub> (7.9 mg, 5.0 mol %), KI (66.4 mg, 2.0 equiv), KOAc (39.3 mg, 2.0 equiv) in HFIP (2.0 mL) and H<sub>2</sub>O (2.0 mL). Purification by column chromatography on silica gel (*n*-hexane/EtOAc: 8/1) yielded **400n** (28.3 mg, 50%) as a colorless oil.

<sup>1</sup>H NMR (400 MHz, CDCl<sub>3</sub>) δ 7.81 (d, *J* = 8.6 Hz, 1H), 7.53 – 7.49 (m, 2H), 5.81 (t, *J* = 6.6 Hz, 1H), 4.14 (t, *J* = 6.7 Hz, 2H), 3.01 – 2.78 (m, 2H), 1.64 – 1.56 (m, 2H), 1.35 (dq, *J* = 14.7, 7.4 Hz, 2H), 0.91 (t, *J* = 7.4 Hz, 3H).

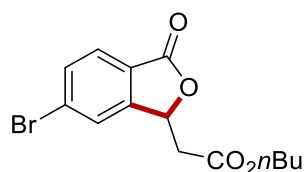
<sup>13</sup>C NMR (100 MHz, CDCl<sub>3</sub>) δ 169.1 (C<sub>q</sub>), 168.7 (C<sub>q</sub>), 150.4 (C<sub>q</sub>), 141.0 (C<sub>q</sub>), 130.3 (CH), 127.0 (CH), 124.5 (C<sub>q</sub>), 122.8 (CH), 76.4 (CH), 65.3 (CH<sub>2</sub>), 39.2 (CH<sub>2</sub>), 30.5 (CH<sub>2</sub>), 19.0 (CH<sub>2</sub>), 13.6 (CH<sub>3</sub>).

IR (ATR): 2960, 2932, 1768, 1722, 1617, 1314, 1166, 1012, 904, 687 cm<sup>-1</sup>.

MS (ESI) *m/z* (relative intensity): 283 (55) [M+H]<sup>+</sup>, 305 (45) [M+Na]<sup>+</sup>.

HR-MS (ESI) C<sub>14</sub>H<sub>16</sub>ClO<sub>4</sub> [M+H]<sup>+</sup>: 283.0733, found: 283.0732.

The spectral data were in accordance with those reported in the literature.<sup>[236g]</sup>

**Butyl 2-(6-bromo-3-oxo-1,3-dihydroisobenzofuran-1-yl)acetate (400o)**

The **General Procedure D** was followed using 4-bromobenzoic acid **398o** (40.2 mg, 0.20 mmol), *n*-butyl acrylate **399a** (76.9 mg, 0.60 mmol), [OsCl<sub>2</sub>(*p*-cymene)]<sub>2</sub> (7.9 mg, 5.0 mol %), KI (66.4 mg, 2.0 equiv), KOAc (39.3 mg, 2.0 equiv) in HFIP (2.0 mL) and H<sub>2</sub>O (2.0 mL). Purification by column chromatography on silica gel (*n*-hexane/EtOAc: 8/1) yielded **400o** (34.7 mg, 53%) as a colorless oil.

<sup>1</sup>H NMR (400 MHz, CDCl<sub>3</sub>) δ 7.74 (d, *J* = 8.7 Hz, 1H), 7.69 – 7.66 (m, 2H), 5.82 (t, *J* = 6.6 Hz, 1H), 4.15 (t, *J* = 6.8 Hz, 2H), 3.02 – 2.77 (m, 2H), 1.66 – 1.54 (m, 2H), 1.35 (dq, *J* = 14.7, 7.4 Hz, 2H), 0.92

(t,  $J = 7.4$  Hz, 3H).

$^{13}\text{C}$  NMR (100 MHz,  $\text{CDCl}_3$ )  $\delta$  169.1 ( $\text{C}_q$ ), 168.8 ( $\text{C}_q$ ), 150.5 ( $\text{C}_q$ ), 133.2 (CH), 129.5 ( $\text{C}_q$ ), 127.1 (CH), 125.8 (CH), 125.0 ( $\text{C}_q$ ), 76.3 (CH), 65.3 ( $\text{CH}_2$ ), 39.2 ( $\text{CH}_2$ ), 30.5 ( $\text{CH}_2$ ), 19.1 ( $\text{CH}_2$ ), 13.6 ( $\text{CH}_3$ ).

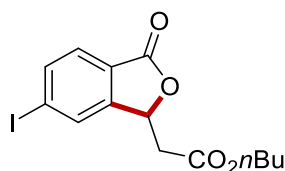
IR (ATR): 2959, 2933, 1761, 1722, 1588, 1395, 1263, 1210, 1062, 781  $\text{cm}^{-1}$ .

MS (ESI)  $m/z$  (relative intensity): 327 (50) ( $^{79}\text{Br}$ )  $[\text{M}+\text{H}]^+$ , 349 (50)  $[\text{M}+\text{Na}]^+$ .

HR-MS (ESI)  $\text{C}_{14}\text{H}_{16}^{79}\text{BrO}_4$   $[\text{M}+\text{H}]^+$ : 327.0231, found: 327.0226.

The spectral data were in accordance with those reported in the literature.<sup>[236g]</sup>

### Butyl 2-(6-iodo-3-oxo-1,3-dihydroisobenzofuran-1-yl)acetate (400p)



The **General Procedure D** was followed using 4-iodobenzoic acid **398p** (49.6 mg, 0.20 mmol), *n*-butyl acrylate **399a** (76.9 mg, 0.60 mmol),  $[\text{OsCl}_2(p\text{-cymene})]_2$  (7.9 mg, 5.0 mol %), KI (66.4 mg, 2.0 equiv), KOAc (39.3 mg, 2.0 equiv) in HFIP (2.0 mL) and  $\text{H}_2\text{O}$  (2.0 mL). Purification by column chromatography on silica gel (*n*-hexane/EtOAc: 8/1) yielded **400p** (45.6 mg, 61%) as a colorless oil.

$^1\text{H}$  NMR (400 MHz,  $\text{CDCl}_3$ )  $\delta$  7.90 – 7.87 (m, 2H), 7.62 – 7.59 (m, 1H), 5.80 (t,  $J = 6.6$  Hz, 1H), 4.15 (td,  $J = 6.7, 1.6$  Hz, 2H), 2.99 – 2.78 (m, 2H), 1.64 – 1.57 (m, 2H), 1.35 (dq,  $J = 14.8, 7.4$  Hz, 2H), 0.92 (t,  $J = 7.4$  Hz, 3H).

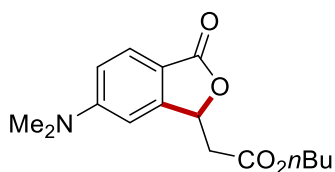
$^{13}\text{C}$  NMR (100 MHz,  $\text{CDCl}_3$ )  $\delta$  169.1 ( $\text{C}_q$ ), 169.1 ( $\text{C}_q$ ), 150.4 ( $\text{C}_q$ ), 139.0 (CH), 131.7 (CH), 127.0 (CH), 125.5 ( $\text{C}_q$ ), 102.1 ( $\text{C}_q$ ), 76.2 (CH), 65.3 ( $\text{CH}_2$ ), 39.2 ( $\text{CH}_2$ ), 30.5 ( $\text{CH}_2$ ), 19.1 ( $\text{CH}_2$ ), 13.7 ( $\text{CH}_3$ ).

IR (ATR): 2958, 2931, 1765, 1728, 1584, 1395, 1264, 1178, 1007, 678  $\text{cm}^{-1}$ .

MS (ESI)  $m/z$  (relative intensity): 375 (60)  $[\text{M}+\text{H}]^+$ , 397 (40)  $[\text{M}+\text{Na}]^+$ .

HR-MS (ESI)  $\text{C}_{14}\text{H}_{16}\text{IO}_4$   $[\text{M}+\text{H}]^+$ : 375.0088, found: 375.0089.  $\text{C}_{14}\text{H}_{15}\text{IO}_4\text{Na}$   $[\text{M}+\text{Na}]^+$ : 396.9909, found: 396.9907.

The spectral data were in accordance with those reported in the literature.<sup>[236g]</sup>

**Butyl 2-(6-(dimethylamino)-3-oxo-1,3-dihydroisobenzofuran-1-yl)acetate (400q)**

The **General Procedure D** was followed using 4-(dimethylamino)benzoic acid **398q** (33.0 mg, 0.20 mmol), *n*-butyl acrylate **399a** (76.9 mg, 0.60 mmol), [OsCl<sub>2</sub>(*p*-cymene)]<sub>2</sub> (7.9 mg, 5.0 mol %), KI (66.4 mg, 2.0 equiv), KOAc (39.3 mg, 2.0 equiv) in HFIP (2.0 mL) and H<sub>2</sub>O (2.0 mL). Purification by column chromatography on silica gel (*n*-hexane/EtOAc: 8/1) yielded **400q** (48.9 mg, 84%) as a colorless oil.

<sup>1</sup>H NMR (400 MHz, CDCl<sub>3</sub>) δ 7.65 (d, *J* = 8.7 Hz, 1H), 6.72 (dd, *J* = 8.7, 2.2 Hz, 1H), 6.51 (d, *J* = 2.2 Hz, 1H), 5.70 (t, *J* = 6.6 Hz, 1H), 4.12 (t, *J* = 6.7 Hz, 2H), 3.05 (s, 6H), 2.82 (dd, *J* = 6.6, 4.2 Hz, 2H), 1.63 – 1.54 (m, 2H), 1.34 (dq, *J* = 14.7, 7.4 Hz, 2H), 0.89 (t, *J* = 7.4 Hz, 3H).

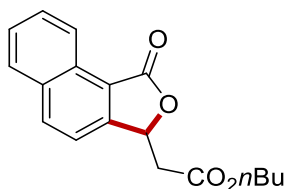
<sup>13</sup>C NMR (100 MHz, CDCl<sub>3</sub>) δ 170.4 (C<sub>q</sub>), 169.7 (C<sub>q</sub>), 154.4 (C<sub>q</sub>), 151.7 (C<sub>q</sub>), 126.7 (CH), 113.0 (CH), 112.3 (C<sub>q</sub>), 102.4 (CH), 76.2 (CH), 65.0 (CH<sub>2</sub>), 40.3 (CH<sub>3</sub>), 40.0 (CH<sub>2</sub>), 30.5 (CH<sub>2</sub>), 19.0 (CH<sub>2</sub>), 13.6 (CH<sub>3</sub>).

IR (ATR): 2958, 2931, 1723, 1605, 1519, 1351, 1116, 1005, 791, 692 cm<sup>-1</sup>.

MS (ESI) *m/z* (relative intensity): 292 (60) [M+H]<sup>+</sup>, 314 (40) [M+Na]<sup>+</sup>.

HR-MS (ESI) C<sub>16</sub>H<sub>22</sub>NO<sub>4</sub> [M+H]<sup>+</sup>: 292.1544, found: 292.1543.

The spectral data were in accordance with those reported in the literature.<sup>[266]</sup>

**Butyl 2-(1-oxo-1,3-dihydronaphtho[1,2-*c*]furan-3-yl)acetate (400s)**

The **General Procedure D** was followed using naphthoic acid **398s** (34.4 mg, 0.20 mmol), *n*-butyl acrylate **399a** (76.9 mg, 0.60 mmol), [OsCl<sub>2</sub>(*p*-cymene)]<sub>2</sub> (7.9 mg, 5.0 mol %), KI (66.4 mg, 2.0 equiv), KOAc (39.3 mg, 2.0 equiv) in HFIP (2.0 mL) and H<sub>2</sub>O (2.0 mL). Purification by column chromatography on silica gel (*n*-hexane/EtOAc: 8/1) yielded **400s** (35.2 mg, 74%) as a colorless oil.

**<sup>1</sup>H NMR** (400 MHz, CDCl<sub>3</sub>)  $\delta$  8.99 (d,  $J$  = 8.3 Hz, 1H), 8.13 (d,  $J$  = 8.3 Hz, 1H), 7.95 (d,  $J$  = 8.3 Hz, 1H), 7.72 (ddd,  $J$  = 8.3, 7.0, 1.3 Hz, 1H), 7.63 (ddd,  $J$  = 8.3, 7.0, 1.3 Hz, 1H), 7.51 (d,  $J$  = 8.3 Hz, 1H), 5.94 (t,  $J$  = 6.6 Hz, 1H), 4.16 (t,  $J$  = 6.7 Hz, 2H), 2.94 (d,  $J$  = 6.6 Hz, 2H), 1.64 – 1.56 (m, 2H), 1.34 (dq,  $J$  = 14.9, 7.4 Hz, 2H), 0.89 (t,  $J$  = 7.4 Hz, 3H).

**<sup>13</sup>C NMR** (100 MHz, CDCl<sub>3</sub>)  $\delta$  170.1 (C<sub>q</sub>), 169.4 (C<sub>q</sub>), 150.4 (C<sub>q</sub>), 135.7 (CH), 133.5 (C<sub>q</sub>), 129.2 (CH), 129.1 (C<sub>q</sub>), 128.4 (CH), 127.5 (CH), 123.6 (CH), 120.3 (C<sub>q</sub>), 118.4 (CH), 76.4 (CH), 65.2 (CH<sub>2</sub>), 39.4 (CH<sub>2</sub>), 30.5 (CH<sub>2</sub>), 19.1 (CH<sub>2</sub>), 13.6 (CH<sub>3</sub>).

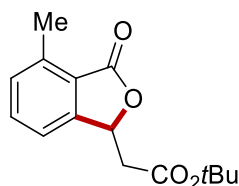
**IR** (ATR): 2961, 2933, 1760, 1734, 1610, 1699, 1340, 1291, 1154, 1009, 844, 596 cm<sup>-1</sup>.

**MS** (ESI)  $m/z$  (relative intensity): 299 (70) [M+H]<sup>+</sup>, 321 (30) [M+Na]<sup>+</sup>.

**HR-MS** (ESI) C<sub>18</sub>H<sub>19</sub>O<sub>4</sub> [M+H]<sup>+</sup>: 299.1278, found: 299.1278.

The spectral data were in accordance with those reported in the literature.<sup>[268]</sup>

#### ***tert*-Butyl 2-(4-methyl-3-oxo-1,3-dihydroisobenzofuran-1-yl)acetate (400t)**



The **General Procedure D** was followed using 2-methylbenzoic acid **398t** (27.2 mg, 0.20 mmol), *t*-butyl acrylate **399b** (76.9 mg, 0.60 mmol), [OsCl<sub>2</sub>(*p*-cymene)]<sub>2</sub> (7.9 mg, 5.0 mol %), KI (66.4 mg, 2.0 equiv), KOAc (39.3 mg, 2.0 equiv) in HFIP (2.0 mL) and H<sub>2</sub>O (2.0 mL). Purification by column chromatography on silica gel (*n*-hexane/EtOAc: 8/1) yielded **400t** (19.9 mg, 38%) as a colorless oil.

**<sup>1</sup>H NMR** (400 MHz, CDCl<sub>3</sub>)  $\delta$  7.50 (t,  $J$  = 7.6 Hz, 1H), 7.30 – 7.22 (m, 2H), 5.74 (t,  $J$  = 6.4 Hz, 1H), 2.79 (dd,  $J$  = 6.4, 2.7 Hz, 2H), 2.67 (s, 3H), 1.42 (s, 9H).

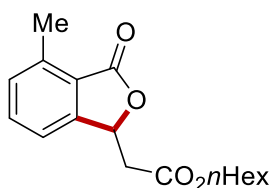
**<sup>13</sup>C NMR** (100 MHz, CDCl<sub>3</sub>)  $\delta$  170.2 (C<sub>q</sub>), 168.5 (C<sub>q</sub>), 149.5 (C<sub>q</sub>), 139.8 (C<sub>q</sub>), 133.8 (CH), 131.0 (CH), 123.6 (C<sub>q</sub>), 119.2 (CH), 81.9 (C<sub>q</sub>), 40.8 (CH), 29.7 (CH<sub>2</sub>), 28.0 (CH<sub>3</sub>), 17.3 (CH<sub>3</sub>).

**IR** (ATR): 2959, 2931, 1760, 1722, 1486, 1304, 1210, 1157, 1005, 627 cm<sup>-1</sup>.

**MS** (ESI)  $m/z$  (relative intensity): 263 (45) [M+H]<sup>+</sup>, 285 (55) [M+Na]<sup>+</sup>.

**HR-MS** (ESI) C<sub>15</sub>H<sub>19</sub>O<sub>4</sub> [M+H]<sup>+</sup>: 263.1278, found: 263.1278.

The spectral data were in accordance with those reported in the literature.<sup>[236g]</sup>

**Hexyl 2-(4-methyl-3-oxo-1,3-dihydroisobenzofuran-1-yl)acetate (400u)**

The **General Procedure D** was followed using 2-methylbenzoic acid **398u** (27.2 mg, 0.20 mmol), *n*-hexyl acrylate **399c** (93.7 mg, 0.60 mmol), [OsCl<sub>2</sub>(*p*-cymene)]<sub>2</sub> (7.9 mg, 5.0 mol %), KI (66.4 mg, 2.0 equiv), KOAc (39.3 mg, 2.0 equiv) in HFIP (2.0 mL) and H<sub>2</sub>O (2.0 mL). Purification by column chromatography on silica gel (*n*-hexane/EtOAc: 8/1) yielded **400u** (46.5 mg, 80%) as a colorless oil.

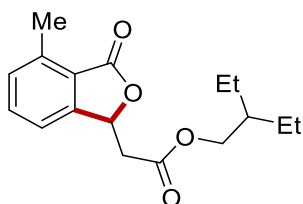
<sup>1</sup>H NMR (400 MHz, CDCl<sub>3</sub>) δ 7.50 (t, *J* = 7.6 Hz, 1H), 7.30 – 7.21 (m, 2H), 5.79 (t, *J* = 6.6 Hz, 1H), 4.12 (t, *J* = 6.8 Hz, 2H), 2.85 (d, *J* = 6.6 Hz, 2H), 2.66 (s, 3H), 1.66 – 1.54 (m, 2H), 1.37 – 1.22 (m, 6H), 0.86 (t, *J* = 6.9 Hz, 3H).

<sup>13</sup>C NMR (100 MHz, CDCl<sub>3</sub>) δ 170.0 (C<sub>q</sub>), 169.4 (C<sub>q</sub>), 149.3 (C<sub>q</sub>), 139.9 (C<sub>q</sub>), 133.9 (CH), 131.1 (CH), 123.4 (C<sub>q</sub>), 119.2 (CH), 76.0 (CH), 65.4 (CH<sub>2</sub>), 39.8 (CH<sub>2</sub>), 31.4 (CH<sub>2</sub>), 28.4 (CH<sub>2</sub>), 25.5 (CH<sub>2</sub>), 22.5 (CH<sub>2</sub>), 17.3 (CH<sub>3</sub>), 14.0 (CH<sub>3</sub>).

IR (ATR): 2960, 2935, 1763, 1739, 1601, 1448, 1328, 1175, 1057, 691 cm<sup>-1</sup>.

MS (ESI) *m/z* (relative intensity): 291 (70) [M+H]<sup>+</sup>, 313 (30) [M+Na]<sup>+</sup>.

HR-MS (ESI) C<sub>17</sub>H<sub>23</sub>O<sub>4</sub> [M+H]<sup>+</sup>: 291.1594, found: 291.1591.

**Pentan-3-yl 2-(4-methyl-3-oxo-1,3-dihydroisobenzofuran-1-yl)acetate (400w)**

The **General Procedure D** was followed using 2-methylbenzoic acid **398w** (27.2 mg, 0.20 mmol), pentan-3-yl acrylate **399d** (85.3 mg, 0.60 mmol), [OsCl<sub>2</sub>(*p*-cymene)]<sub>2</sub> (7.9 mg, 5.0 mol %), KI (66.4 mg, 2.0 equiv), KOAc (39.3 mg, 2.0 equiv) in HFIP (2.0 mL) and H<sub>2</sub>O (2.0 mL). Purification by column chromatography on silica gel (*n*-hexane/EtOAc: 8/1) yielded **400w** (35.9 mg, 65%) as a colorless oil.

<sup>1</sup>H NMR (400 MHz, CDCl<sub>3</sub>) δ 7.50 (d, *J* = 7.6 Hz, 1H), 7.30 – 7.23 (m, 2H), 5.79 (t, *J* = 6.6 Hz, 1H),

4.06 (dd,  $J = 5.8, 2.4$  Hz, 2H), 2.86 (d,  $J = 6.6$  Hz, 2H), 2.67 (s, 3H), 1.50 (dt,  $J = 12.6, 6.4$  Hz, 1H), 1.38 – 1.25 (m, 4H), 0.86 (t,  $J = 7.4$  Hz, 6H).

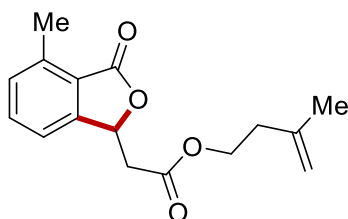
$^{13}\text{C}$  NMR (100 MHz,  $\text{CDCl}_3$ )  $\delta$  170.0 ( $\text{C}_q$ ), 169.5 ( $\text{C}_q$ ), 149.3 ( $\text{C}_q$ ), 139.9 ( $\text{C}_q$ ), 133.9 (CH), 131.1 (CH), 123.4 ( $\text{C}_q$ ), 119.2 (CH), 76.0 (CH), 67.3 ( $\text{CH}_2$ ), 40.2 (CH), 39.8 ( $\text{CH}_2$ ), 23.2 ( $\text{CH}_2$ ), 23.2 ( $\text{CH}_2$ ), 17.3 ( $\text{CH}_3$ ), 11.0 ( $\text{CH}_3$ ), 10.9 ( $\text{CH}_3$ ).

IR (ATR): 2960, 2933, 1758, 1730, 1495, 1453, 1310, 1277, 1005, 690  $\text{cm}^{-1}$ .

MS (ESI)  $m/z$  (relative intensity): 291 (60)  $[\text{M}+\text{H}]^+$ , 313 (40)  $[\text{M}+\text{Na}]^+$ .

HR-MS (ESI)  $\text{C}_{17}\text{H}_{23}\text{O}_4$   $[\text{M}+\text{H}]^+$ : 291.1595, found: 291.1591.

### 3-Methylbut-3-en-1-yl 2-(4-methyl-3-oxo-1,3-dihydroisobenzofuran-1-yl)acetate (400x)



The **General Procedure D** was followed using 2-methylbenzoic acid **398x** (27.2 mg, 0.20 mmol), 3-methylbut-3-en-1-yl acrylate **399e** (84.1 mg, 0.60 mmol),  $[\text{OsCl}_2(p\text{-cymene})]_2$  (7.9 mg, 5.0 mol %), KI (66.4 mg, 2.0 equiv), KOAc (39.3 mg, 2.0 equiv) in HFIP (2.0 mL) and  $\text{H}_2\text{O}$  (2.0 mL). Purification by column chromatography on silica gel ( $n\text{-hexane}/\text{EtOAc}$ : 8/1) yielded **400x** (42.8 mg, 78%) as a colorless oil.

$^1\text{H}$  NMR (400 MHz,  $\text{CDCl}_3$ )  $\delta$  7.51 (d,  $J = 7.6$  Hz, 1H), 7.30 – 7.23 (m, 2H), 5.79 (t,  $J = 6.6$  Hz, 1H), 4.82 – 4.76 (m, 1H), 4.75 – 4.68 (m, 1H), 4.26 (t,  $J = 6.9$  Hz, 2H), 2.85 (d,  $J = 6.6$  Hz, 2H), 2.67 (s, 3H), 2.34 (t,  $J = 6.9$  Hz, 2H), 1.74 (s, 3H).

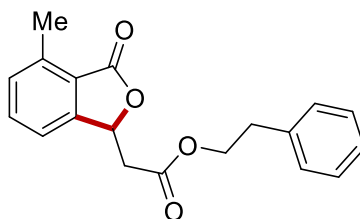
$^{13}\text{C}$  NMR (100 MHz,  $\text{CDCl}_3$ )  $\delta$  170.0 ( $\text{C}_q$ ), 169.3 ( $\text{C}_q$ ), 149.2 ( $\text{C}_q$ ), 141.3 ( $\text{C}_q$ ), 140.0 ( $\text{C}_q$ ), 133.9 (CH), 131.1 (CH), 123.4 ( $\text{C}_q$ ), 119.2 (CH), 112.5 ( $\text{CH}_2$ ), 76.0 (CH), 63.3 ( $\text{CH}_2$ ), 39.8 ( $\text{CH}_2$ ), 36.6 ( $\text{CH}_2$ ), 22.4 ( $\text{CH}_3$ ), 17.3 ( $\text{CH}_3$ ).

IR (ATR): 2959, 2933, 1760, 1735, 1599, 1467, 1345, 1170, 1005, 784, 698  $\text{cm}^{-1}$ .

MS (ESI)  $m/z$  (relative intensity): 275 (55)  $[\text{M}+\text{H}]^+$ , 297 (45)  $[\text{M}+\text{Na}]^+$ .

HR-MS (ESI)  $\text{C}_{16}\text{H}_{19}\text{O}_4$   $[\text{M}+\text{H}]^+$ : 275.1282, found: 275.1278.



**Phenethyl 2-(4-methyl-3-oxo-1,3-dihydroisobenzofuran-1-yl)acetate (400y)**

The **General Procedure D** was followed using 2-methylbenzoic acid **398y** (27.2 mg, 0.20 mmol), phenethyl acrylate **399f** (85.9 mg, 0.60 mmol),  $[\text{OsCl}_2(p\text{-cymene})]_2$  (7.9 mg, 5.0 mol %), KI (66.4 mg, 2.0 equiv), KOAc (39.3 mg, 2.0 equiv) in HFIP (2.0 mL) and  $\text{H}_2\text{O}$  (2.0 mL). Purification by column chromatography on silica gel (*n*-hexane/EtOAc: 8/1) yielded **400y** (44.1 mg, 71%) as a colorless oil.

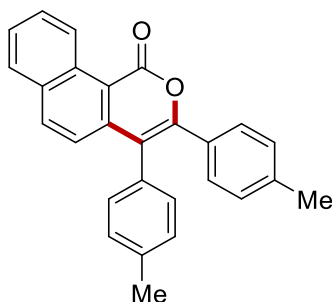
$^1\text{H NMR}$  (400 MHz,  $\text{CDCl}_3$ )  $\delta$  7.48 (d,  $J = 7.6$  Hz, 1H), 7.31 – 7.24 (m, 3H), 7.24 – 7.15 (m, 4H), 5.76 (t,  $J = 7.0$  Hz, 1H), 4.39 – 4.34 (m, 2H), 2.94 (d,  $J = 7.0$  Hz, 2H), 2.83 (dd,  $J = 6.6, 4.6$  Hz, 2H), 2.67 (s, 3H).

$^{13}\text{C NMR}$  (100 MHz,  $\text{CDCl}_3$ )  $\delta$  170.0 ( $\text{C}_q$ ), 169.2 ( $\text{C}_q$ ), 149.2 ( $\text{C}_q$ ), 140.0 ( $\text{C}_q$ ), 137.4 ( $\text{C}_q$ ), 133.9 (CH), 131.1 (CH), 128.8 (CH), 128.5 (CH), 126.6 (CH), 123.3 ( $\text{C}_q$ ), 119.2 (CH), 75.9 (CH), 65.6 ( $\text{CH}_2$ ), 39.8 ( $\text{CH}_2$ ), 34.9 ( $\text{CH}_2$ ), 17.3 ( $\text{CH}_3$ ).

**IR** (ATR): 2959, 2931, 1765, 1730, 1605, 1344, 1277, 1137, 1010, 905, 686  $\text{cm}^{-1}$ .

**MS** (ESI)  $m/z$  (relative intensity): 311 (30)  $[\text{M}+\text{H}]^+$ , 333 (70)  $[\text{M}+\text{Na}]^+$ .

**HR-MS** (ESI)  $\text{C}_{19}\text{H}_{19}\text{O}_4$   $[\text{M}+\text{H}]^+$ : 311.1280, found: 311.1278.

**3,4-Di-*p*-tolyl-1*H*-benzo[*h*]isochromen-1-one (402a)**

The **General Procedure E** was followed using naphthoic acid **398s** (34.4 mg, 0.20 mmol), 1,2-di-*p*-tolylethyne **401a** (123.8 mg, 0.60 mmol),  $[\text{OsCl}_2(p\text{-cymene})]_2$  (7.9 mg, 5.0 mol %), KI (66.4 mg, 2.0 equiv), KOAc (39.3 mg, 2.0 equiv) in HFIP (2.0 mL) and  $\text{H}_2\text{O}$  (2.0 mL). Purification by column chromatography on silica gel (*n*-hexane/EtOAc: 20/1) yielded **402a** (61.0 mg, 81%) as a yellow solid.

**M. p.** 197 °C

**<sup>1</sup>H NMR** (400 MHz, CDCl<sub>3</sub>) δ 9.84 (d, *J* = 8.7 Hz, 1H), 7.95 (d, *J* = 8.7 Hz, 1H), 7.84 (d, *J* = 8.0 Hz, 1H), 7.76 (ddd, *J* = 8.7, 6.9, 1.4 Hz, 1H), 7.59 (ddd, *J* = 8.0, 6.9, 1.1 Hz, 1H), 7.29 (d, *J* = 8.0 Hz, 2H), 7.25 (d, *J* = 6.9 Hz, 3H), 7.16 (d, *J* = 8.0 Hz, 2H), 7.01 (d, *J* = 8.0 Hz, 2H), 2.43 (s, 3H), 2.28 (s, 3H).

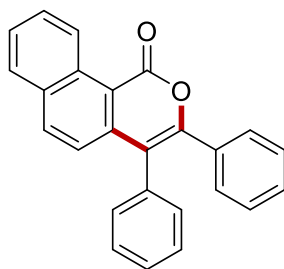
**<sup>13</sup>C NMR** (100 MHz, CDCl<sub>3</sub>) δ 161.5 (C<sub>q</sub>), 152.5 (C<sub>q</sub>), 141.4 (C<sub>q</sub>), 139.1 (C<sub>q</sub>), 137.8 (C<sub>q</sub>), 135.6 (CH), 132.5 (C<sub>q</sub>), 131.8 (C<sub>q</sub>), 131.5 (C<sub>q</sub>), 131.2 (CH), 130.0 (C<sub>q</sub>), 129.9 (CH), 129.3 (CH), 129.0 (CH), 128.6 (CH), 128.4 (CH), 130.0 (CH), 126.8 (CH), 122.7 (CH), 116.8 (C<sub>q</sub>), 113.7 (C<sub>q</sub>), 21.3 (CH<sub>3</sub>), 21.3 (CH<sub>3</sub>).

**IR** (ATR): 3057, 1712, 1591, 1508, 1216, 1105, 921, 753, 636, 503 cm<sup>-1</sup>.

**MS** (ESI) *m/z* (relative intensity): 377 (100) [M+H]<sup>+</sup>.

**HR-MS** (ESI) C<sub>27</sub>H<sub>21</sub>O<sub>2</sub> [M+H]<sup>+</sup>: 377.1535, found: 377.1536.

### 3,4-Diphenyl-1*H*-benzo[*h*]isochromen-1-one (402b)



The **General Procedure E** was followed using 2-methyl benzoic acid **398s** (34.4 mg, 0.20 mmol), 1,2-diphenylethyne **401b** (106.9 mg, 0.60 mmol), [OsCl<sub>2</sub>(*p*-cymene)]<sub>2</sub> (7.9 mg, 5.0 mol %), KI (66.4 mg, 2.0 equiv), KOAc (39.3 mg, 2.0 equiv) in HFIP (2.0 mL) and H<sub>2</sub>O (2.0 mL). Purification by column chromatography on silica gel (*n*-hexane/EtOAc: 20/1) yielded **402b** (61.3 mg, 88%) as a white solid.

**M. p.** 192 °C

**<sup>1</sup>H NMR** (400 MHz, CDCl<sub>3</sub>) δ 9.85 (d, *J* = 8.7 Hz, 1H), 7.99 (d, *J* = 8.7 Hz, 1H), 7.87 (d, *J* = 7.9 Hz, 1H), 7.78 (ddd, *J* = 8.6, 6.9, 1.4 Hz, 1H), 7.62 (ddd, *J* = 8.0, 7.0, 1.1 Hz, 1H), 7.47 – 7.41 (m, 3H), 7.40 – 7.34 (m, 2H), 7.31 – 7.27 (m, 2H), 7.26 – 7.17 (m, 4H).

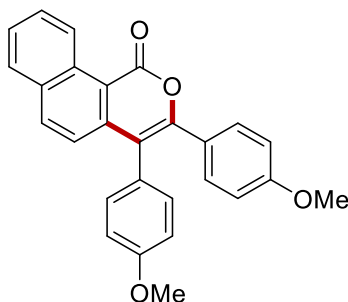
**<sup>13</sup>C NMR** (100 MHz, CDCl<sub>3</sub>) δ 161.4 (C<sub>q</sub>), 152.5 (C<sub>q</sub>), 141.0 (C<sub>q</sub>), 135.8 (CH), 134.8 (C<sub>q</sub>), 132.8 (C<sub>q</sub>), 132.6 (C<sub>q</sub>), 131.5 (C<sub>q</sub>), 131.5 (CH), 129.5 (CH), 129.2 (CH), 129.1 (CH), 129.1 (CH), 128.4 (CH), 128.2 (CH), 127.9 (CH), 127.1 (CH), 127.0 (CH), 122.7 (CH), 117.4 (C<sub>q</sub>), 114.0 (C<sub>q</sub>).

**IR** (ATR): 3026, 1702, 1590, 1510, 1430, 1215, 1105, 1019, 820, 503 cm<sup>-1</sup>.

**MS** (ESI)  $m/z$  (relative intensity): 349 (100)  $[M+H]^+$ .

**HR-MS** (ESI)  $C_{25}H_{17}O_2$   $[M+H]^+$ : 349.1225, found: 349.1223.

**3,4-Bis(4-methoxyphenyl)-1*H*-benzo[*h*]isochromen-1-one (402c)**



The **General Procedure E** was followed using 2-methyl benzoic acid **398s** (34.4 mg, 0.20 mmol), 1,2-bis(4-methoxyphenyl)ethyne **401c** (142.9 mg, 0.60 mmol),  $[OsCl_2(p\text{-cymene})]_2$  (7.9 mg, 5.0 mol %), KI (66.4 mg, 2.0 equiv), KOAc (39.3 mg, 2.0 equiv) in HFIP (2.0 mL) and  $H_2O$  (2.0 mL). Purification by column chromatography on silica gel (*n*-hexane/EtOAc: 20/1) yielded **402c** (67.0 mg, 82%) as an orange solid.

**M. p.** 217 °C

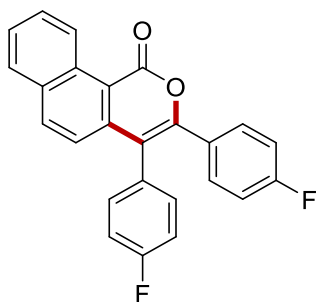
**$^1H$  NMR** (400 MHz,  $CDCl_3$ )  $\delta$  9.82 (d,  $J = 8.6$  Hz, 1H), 7.96 (d,  $J = 8.6$  Hz, 1H), 7.84 (d,  $J = 8.0$  Hz, 1H), 7.75 (ddd,  $J = 8.6, 6.9, 1.4$  Hz, 1H), 7.59 (ddd,  $J = 8.0, 6.9, 1.1$  Hz, 1H), 7.33 (d,  $J = 8.6$  Hz, 2H), 7.24 (d,  $J = 8.6$  Hz, 1H), 7.18 (d,  $J = 8.6$  Hz, 2H), 6.99 (d,  $J = 8.6$  Hz, 2H), 6.73 (d,  $J = 8.6$  Hz, 2H), 3.86 (s, 3H), 3.75 (s, 3H).

**$^{13}C$  NMR** (100 MHz,  $CDCl_3$ )  $\delta$  161.5 ( $C_q$ ), 160.0 ( $C_q$ ), 159.3 ( $C_q$ ), 152.5 ( $C_q$ ), 141.7 ( $C_q$ ), 135.7 (CH), 132.5 (CH), 132.4 ( $C_q$ ), 131.6 ( $C_q$ ), 130.6 (CH), 129.3 (CH), 128.4 (CH), 127.0 ( $C_q$ ), 126.9 (CH), 126.8 (CH), 125.3 ( $C_q$ ), 122.6 (CH), 115.8 ( $C_q$ ), 114.7 (CH), 113.5 ( $C_q$ ), 113.3 (CH), 55.3 ( $CH_3$ ), 55.2 ( $CH_3$ ).

**IR** (ATR): 3203, 1703, 1510, 1441, 1247, 1177, 1091, 831, 765, 570  $cm^{-1}$ .

**MS** (ESI)  $m/z$  (relative intensity): 409 (100)  $[M+H]^+$ .

**HR-MS** (ESI)  $C_{27}H_{21}O_4$   $[M+H]^+$ : 409.1435, found: 409.1434.

**3,4-Bis(4-fluorophenyl)-1*H*-benzo[*h*]isochromen-1-one (402d)**

The **General Procedure E** was followed using 2-methyl benzoic acid **398s** (34.4 mg, 0.20 mmol), 1,2-bis(4-fluorophenyl)ethyne **401D** (128.5 mg, 0.60 mmol), [OsCl<sub>2</sub>(*p*-cymene)]<sub>2</sub> (7.9 mg, 5.0 mol %), KI (66.4 mg, 2.0 equiv), KOAc (39.3 mg, 2.0 equiv) in HFIP (2.0 mL) and H<sub>2</sub>O (2.0 mL). Purification by column chromatography on silica gel (*n*-hexane/EtOAc: 20/1) yielded **402d** (65.3 mg, 85%) as a yellow solid.

**M. p.** 196 °C

**<sup>1</sup>H NMR** (400 MHz, CDCl<sub>3</sub>) δ 9.85 (dd, *J* = 8.7, 1.0 Hz, 1H), 8.05 (d, *J* = 8.7 Hz, 1H), 7.91 (d, *J* = 8.0 Hz, 1H), 7.82 (ddd, *J* = 8.7, 6.9, 1.4 Hz, 1H), 7.67 (ddd, *J* = 8.0, 6.9, 1.4 Hz, 1H), 7.38 (dd, *J* = 9.0, 5.3 Hz, 2H), 7.30 (dd, *J* = 9.0, 5.3 Hz, 2H), 7.23 (d, *J* = 8.7 Hz, 1H), 7.25 – 7.22 (m, 2H), 6.99 – 6.93 (m, 2H).

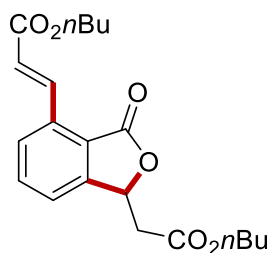
**<sup>13</sup>C NMR** (100 MHz, CDCl<sub>3</sub>) δ 163.6 (d, *J*<sub>C-F</sub> = 44.6 Hz, C<sub>q</sub>), 161.9 (d, *J*<sub>C-F</sub> = 42.2 Hz, C<sub>q</sub>), 161.0 (C<sub>q</sub>), 151.8 (C<sub>q</sub>), 140.7 (C<sub>q</sub>), 136.1 (CH), 133.2 (d, *J*<sub>C-F</sub> = 8.0 Hz, CH), 132.6 (C<sub>q</sub>), 131.5 (C<sub>q</sub>), 131.2 (d, *J*<sub>C-F</sub> = 8.5 Hz, CH), 130.5 (d, *J*<sub>C-F</sub> = 3.6 Hz, C<sub>q</sub>), 129.6 (CH), 128.8 (d, *J*<sub>C-F</sub> = 3.4 Hz, C<sub>q</sub>), 128.5 (CH), 127.2 (CH), 127.0 (CH), 122.3 (CH), 116.5 (d, *J*<sub>C-F</sub> = 21.5 Hz, CH), 116.3 (C<sub>q</sub>), 115.2 (d, *J*<sub>C-F</sub> = 21.8 Hz, CH), 113.9 (C<sub>q</sub>).

**<sup>19</sup>F NMR** (282 MHz, CDCl<sub>3</sub>) δ -110.52, -112.72.

**IR** (ATR): 3501, 1720, 1595, 1510, 1330, 1229, 1106, 833, 730, 530, cm<sup>-1</sup>.

**MS** (ESI) *m/z* (relative intensity): 385 (100) [M+H]<sup>+</sup>.

**HR-MS** (ESI) C<sub>25</sub>H<sub>15</sub>F<sub>2</sub>O<sub>2</sub> [M+H]<sup>+</sup>: 385.1037, found: 385.1035.

**Butyl (*E*)-3-(1-(2-butoxy-2-oxoethyl)-3-oxo-1,3-dihydroisobenzofuran-4-yl)acrylate (426)**

The **General Procedure D** was followed using benzoic acid **398b** (24.4 mg, 0.20 mmol), *n*-butyl acrylate **399a** (76.9 mg, 0.60 mmol), [OsCl<sub>2</sub>(*p*-cymene)]<sub>2</sub> (7.9 mg, 5.0 mol %), KI (66.4 mg, 2.0 equiv), KOAc (39.3 mg, 2.0 equiv) in HFIP (2.0 mL) and H<sub>2</sub>O (2.0 mL). Purification by column chromatography on silica gel (*n*-hexane/EtOAc: 4/1) yielded **426** (1.5 mg, 2%) as a colorless oil.

**<sup>1</sup>H NMR** (400 MHz, CDCl<sub>3</sub>)  $\delta$  8.65 (d, *J* = 16.3 Hz, 1H), 7.73 (d, *J* = 8.3 Hz, 1H), 7.63 (t, *J* = 7.6 Hz, 1H), 7.46 (d, *J* = 7.6 Hz, 1H), 6.55 (d, *J* = 16.3 Hz, 1H), 5.80 (t, *J* = 6.4 Hz, 1H), 4.17 (t, *J* = 6.7 Hz, 2H), 4.09 (t, *J* = 6.7 Hz, 2H), 2.87 (d, *J* = 6.4 Hz, 2H), 1.69 – 1.61 (m, 2H), 1.59 – 1.50 (m, 2H), 1.39 (dq, *J* = 15.2, 7.4 Hz, 2H), 1.29 (dq, *J* = 14.7, 7.4 Hz, 2H), 0.91 (t, *J* = 7.4 Hz, 3H), 0.86 (t, *J* = 7.4 Hz, 3H).

**<sup>13</sup>C NMR** (100 MHz, CDCl<sub>3</sub>)  $\delta$  169.1 (C<sub>q</sub>), 168.8 (C<sub>q</sub>), 166.1 (C<sub>q</sub>), 149.6 (C<sub>q</sub>), 137.2 (CH), 134.9 (C<sub>q</sub>), 134.2 (CH), 126.5 (CH), 123.1 (C<sub>q</sub>), 123.0 (CH), 122.9 (CH), 76.0 (CH), 65.1 (CH<sub>2</sub>), 64.6 (CH<sub>2</sub>), 39.3 (CH<sub>2</sub>), 30.6 (CH<sub>2</sub>), 30.4 (CH<sub>2</sub>), 19.1 (CH<sub>2</sub>), 18.9 (CH<sub>2</sub>), 13.6 (CH<sub>3</sub>), 13.5 (CH<sub>3</sub>).

**IR** (ATR): 2960, 2936, 1771, 1730, 1487, 1281, 1172, 1109, 1005, 747, 686 cm<sup>-1</sup>.

**MS** (ESI) *m/z* (relative intensity): 374 (60) [M+H]<sup>+</sup>, 396 (40) [M+Na]<sup>+</sup>.

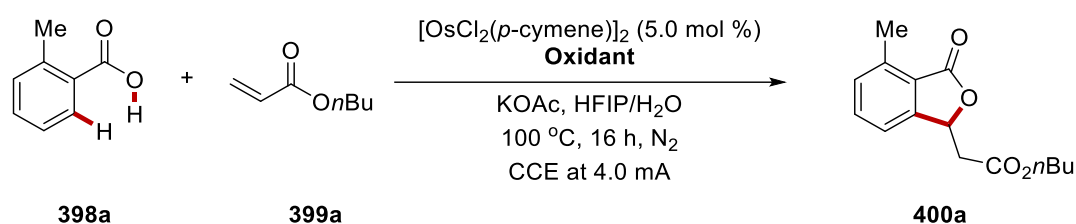
**HR-MS** (ESI) C<sub>21</sub>H<sub>27</sub>O<sub>6</sub> [M+H]<sup>+</sup>: 374.1729, found: 374.1731.

The spectral data were in accordance with those reported in the literature.<sup>[267]</sup>

### 5.5.2 Reaction Comparison with External Oxidant

A suspension of *o*-toluic acid **398a** (0.20 mmol, 1.0 equiv), *n*-butyl acrylate **399a** (0.60 mmol, 3.0 equiv), [OsCl<sub>2</sub>(*p*-cymene)]<sub>2</sub> (5.0 mol %), oxidant (0.40 mmol, 2.0 equiv), and KOAc (0.40 mmol, 2.0 equiv) in HFIP (2.0 mL) and H<sub>2</sub>O (2.0 mL) was stirred at 100 °C for 16 h under N<sub>2</sub> (Table 5.5.1). Chemical oxidants used were AgOAc, Cu(OAc)<sub>2</sub>, Mn(OAc)<sub>3</sub>, PhI(OAc)<sub>2</sub>, and K<sub>2</sub>S<sub>2</sub>O<sub>8</sub>. Additionally, the same reaction was performed under air as a terminal oxidant.

**Table 5.5.1** Osmium-catalyzed C–H annulations with external oxidants.

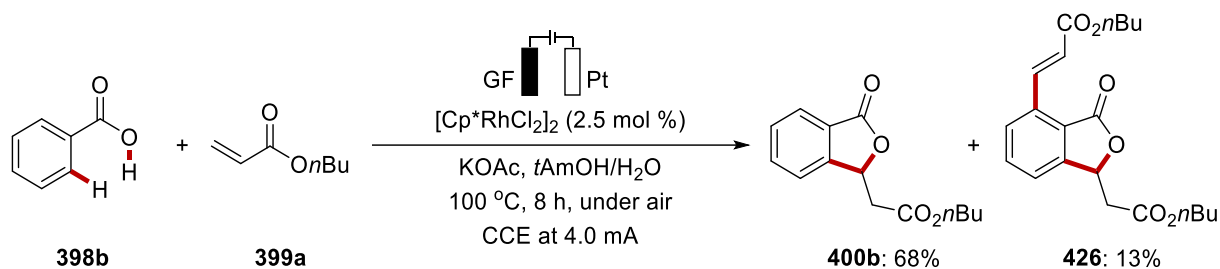


| Oxidant                                      | Isolated yield |
|----------------------------------------------|----------------|
| Air                                          | 0%             |
| AgOAc                                        | 9%             |
| Cu(OAc) <sub>2</sub>                         | 0%             |
| Mn(OAc) <sub>3</sub>                         | 0%             |
| PhI(OAc) <sub>2</sub>                        | 0%             |
| K <sub>2</sub> S <sub>2</sub> O <sub>8</sub> | 0%             |

### 5.5.3 Selectivity Comparison with Different Catalysis (1)

#### 1) Procedure for the reaction with $[\text{Cp}^*\text{RhCl}_2]_2$

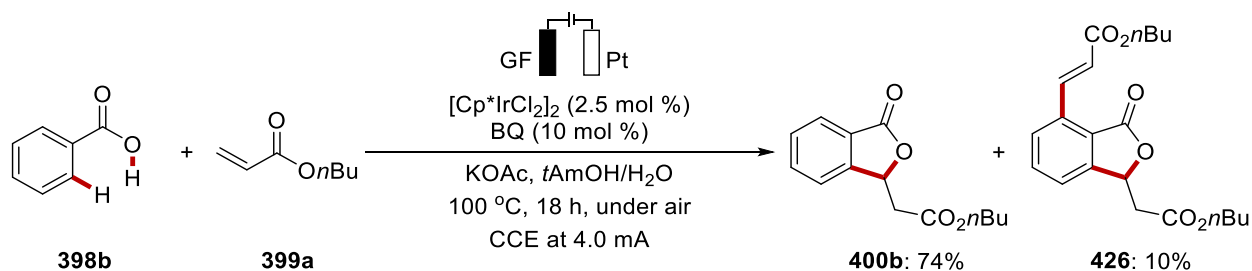
A suspension of benzoic acid **398b** (0.40 mmol, 2.0 equiv), *n*-butyl acrylate **399a** (0.20 mmol, 0.20 mmol),  $[\text{Cp}^*\text{RhCl}_2]_2$  (2.5 mol %), and KOAc (0.40 mmol, 2.0 equiv) in *t*AmOH (3.0 mL) and H<sub>2</sub>O (1.0 mL) was stirred at 100 °C for 8 h at 4.0 mA of constant current under air (Scheme 5.5.1).



**Scheme 5.5.1** Rhodium-catalyzed electrooxidative C–H annulation.

#### 2) Procedure for the reaction with $[\text{Cp}^*\text{IrCl}_2]_2$

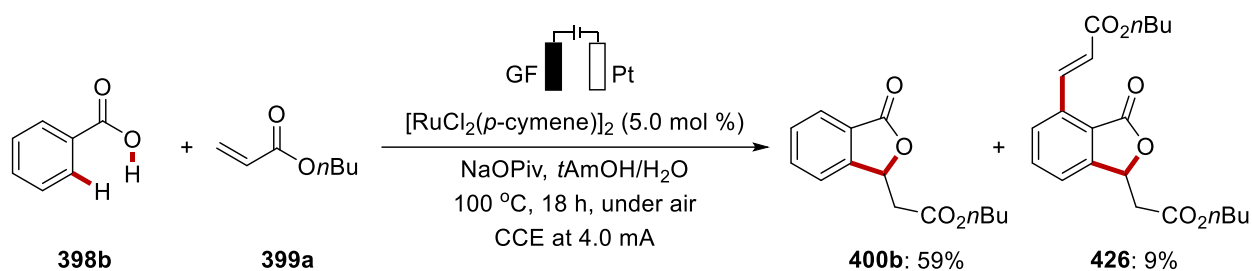
A suspension of benzoic acid **398b** (0.20 mmol, 1.0 equiv), *n*-butyl acrylate **399a** (0.40 mmol, 2.0 equiv),  $[\text{Cp}^*\text{IrCl}_2]_2$  (2.5 mol %), benzoquinone (10 mol %), KOAc (0.4 mmol, 2.0 equiv) in *t*AmOH (3.0 mL) and H<sub>2</sub>O (1.0 mL) was stirred at 100 °C for 18 h at 4.0 mA of constant current under air (Scheme 5.5.2).



**Scheme 5.5.2** Iridium-catalyzed electrooxidative C–H annulation.

3) Procedure for the reaction with  $[\text{RuCl}_2(p\text{-cymene})]_2$ 

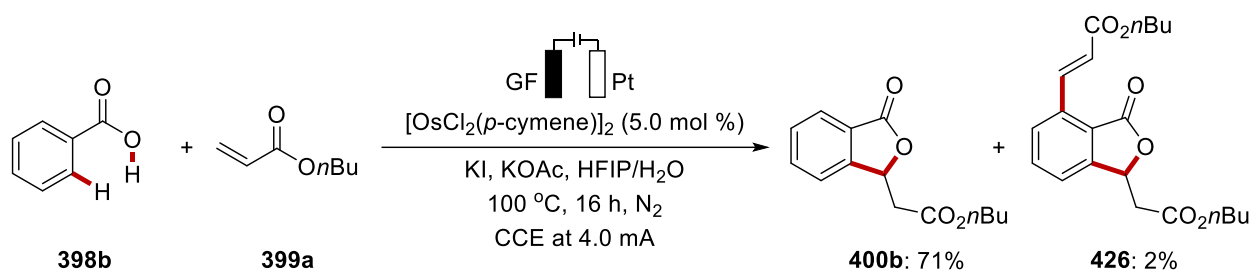
A suspension of benzoic acid **398b** (0.40 mmol, 2.0 equiv), *n*-butyl acrylate **399a** (0.20 mmol, 1.0 equiv),  $[\text{RuCl}_2(p\text{-cymene})]_2$  (5.0 mol %), and NaOPiv (0.40 mmol, 2.0 equiv) in *t*AmOH (3.0 mL) and H<sub>2</sub>O (1.0 mL) was stirred at 100 °C for 18 h at 4.0 mA of constant current under air (Scheme 5.5.3).



**Scheme 5.5.3** Ruthenium-catalyzed electrooxidative C–H annulation.

4) Procedure for the reaction with  $[\text{OsCl}_2(p\text{-cymene})]_2$ 

The **General Procedure D** was followed using benzoic acid **398b** (0.20 mmol, 1.0 equiv), *n*-butyl acrylate **399a** (0.60 mmol, 3.0 equiv),  $[\text{OsCl}_2(p\text{-cymene})]_2$  (5.0 mol %), KI (0.40 mmol, 2.0 equiv), KOAc (0.40 mmol, 2.0 equiv) in HFIP (2.0 mL) and H<sub>2</sub>O (2.0 mL) at 100 °C for 16 h at 4.0 mA of constant current under N<sub>2</sub> (Scheme 5.5.4).



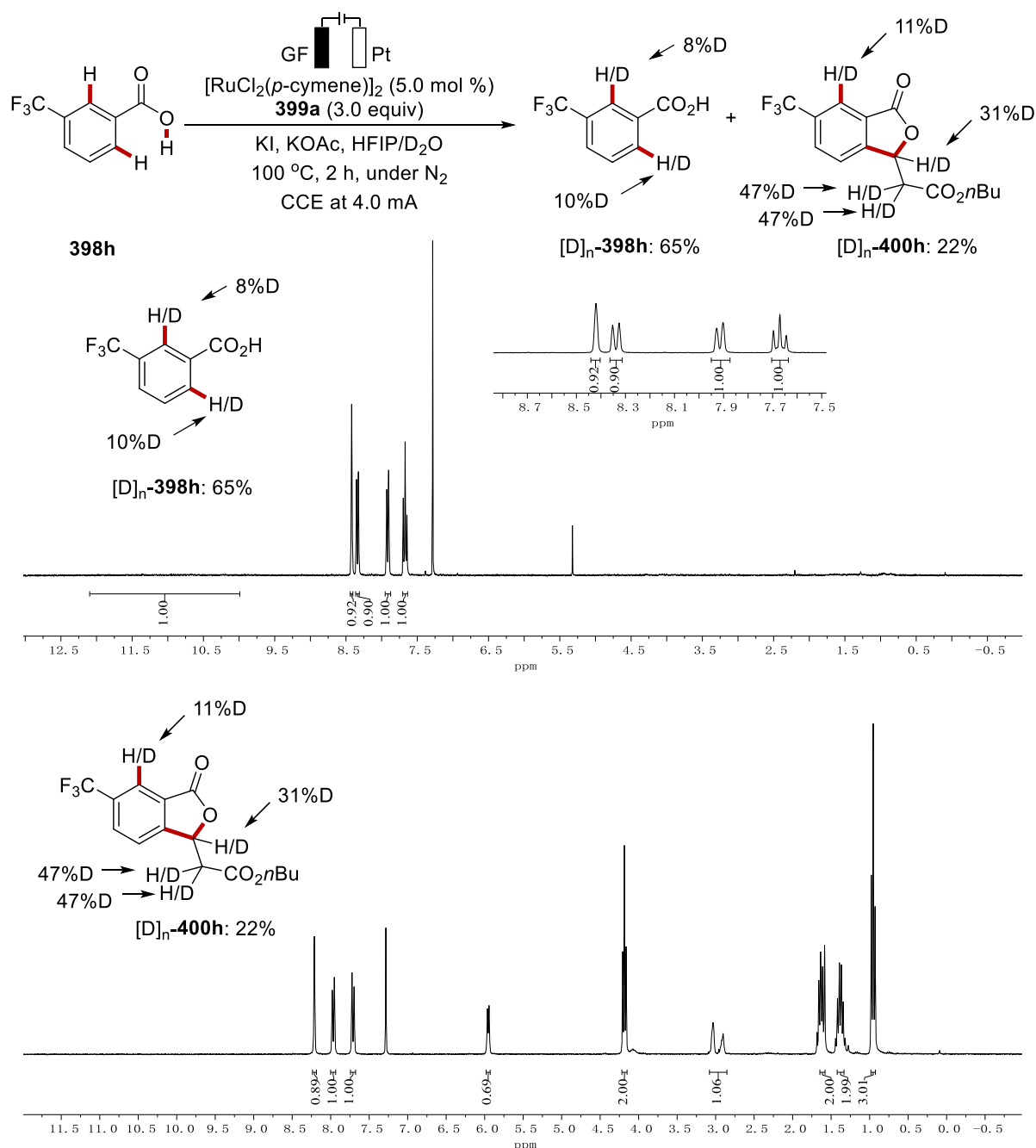
**Scheme 5.5.4** Osmium-catalyzed electrooxidative C–H annulation.



## 5.5.4 Selectivity Comparison with Different Catalysis (2)

## 1) Procedure for H/D exchange studies: Ruthenium catalysis (1)

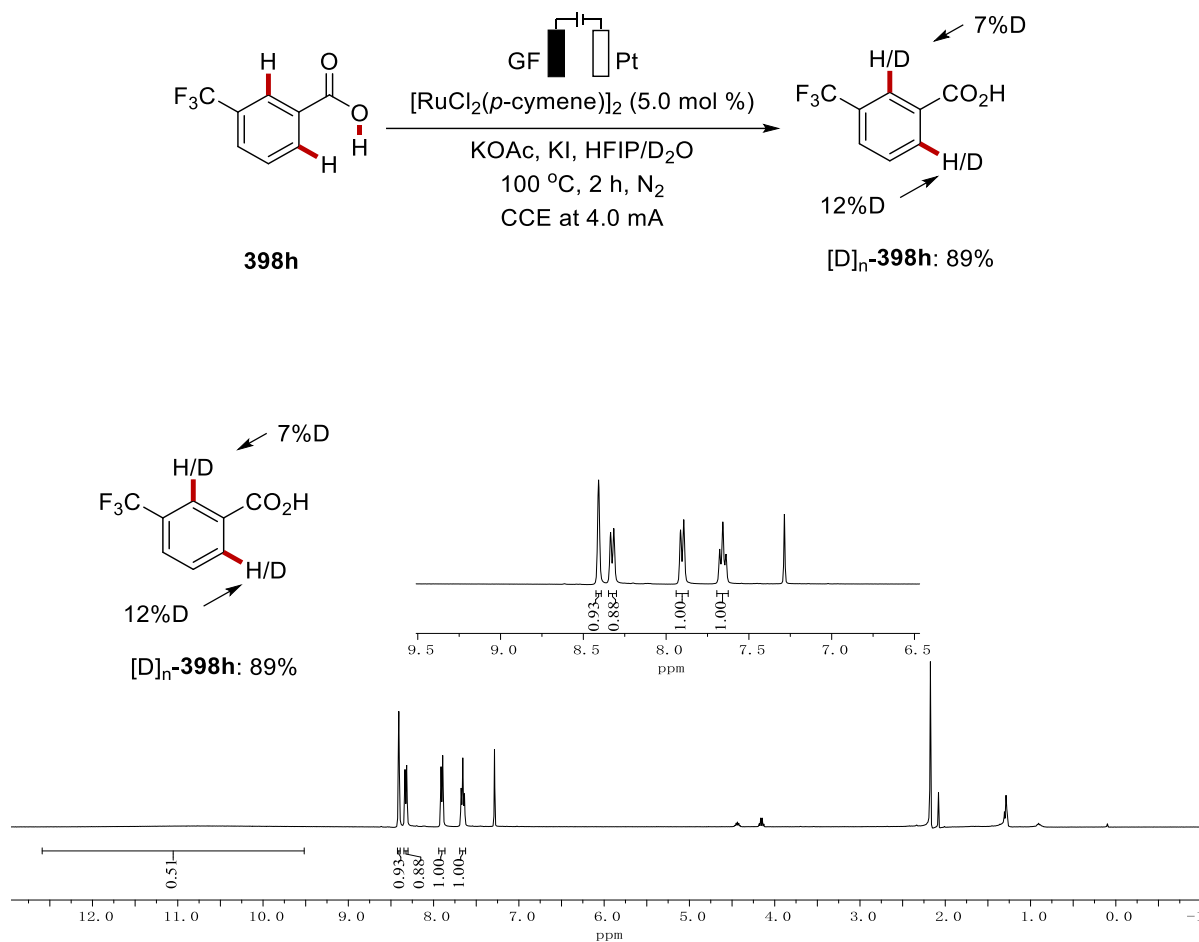
The **General Procedure D** was followed using 3-(trifluoromethyl)benzoic acid **398h** (0.20 mmol, 1.0 equiv), *n*-butyl acrylate **399a** (0.60 mmol, 3.0 equiv),  $[\text{RuCl}_2(p\text{-cymene})]_2$  (5.0 mol %), KI (0.40 mmol, 2.0 equiv), KOAc (0.40 mmol, 2.0 equiv) in HFIP (1.0 mL) and  $\text{D}_2\text{O}$  (3.0 mL) at 100 °C for 2 h at 4.0 mA of constant current under  $\text{N}_2$  (Scheme 5.5.5).



Scheme 5.5.5 H/D exchange study in electrochemical ruthenium catalysis 1.

## 2) Procedure for H/D exchange studies: Ruthenium catalysis (2)

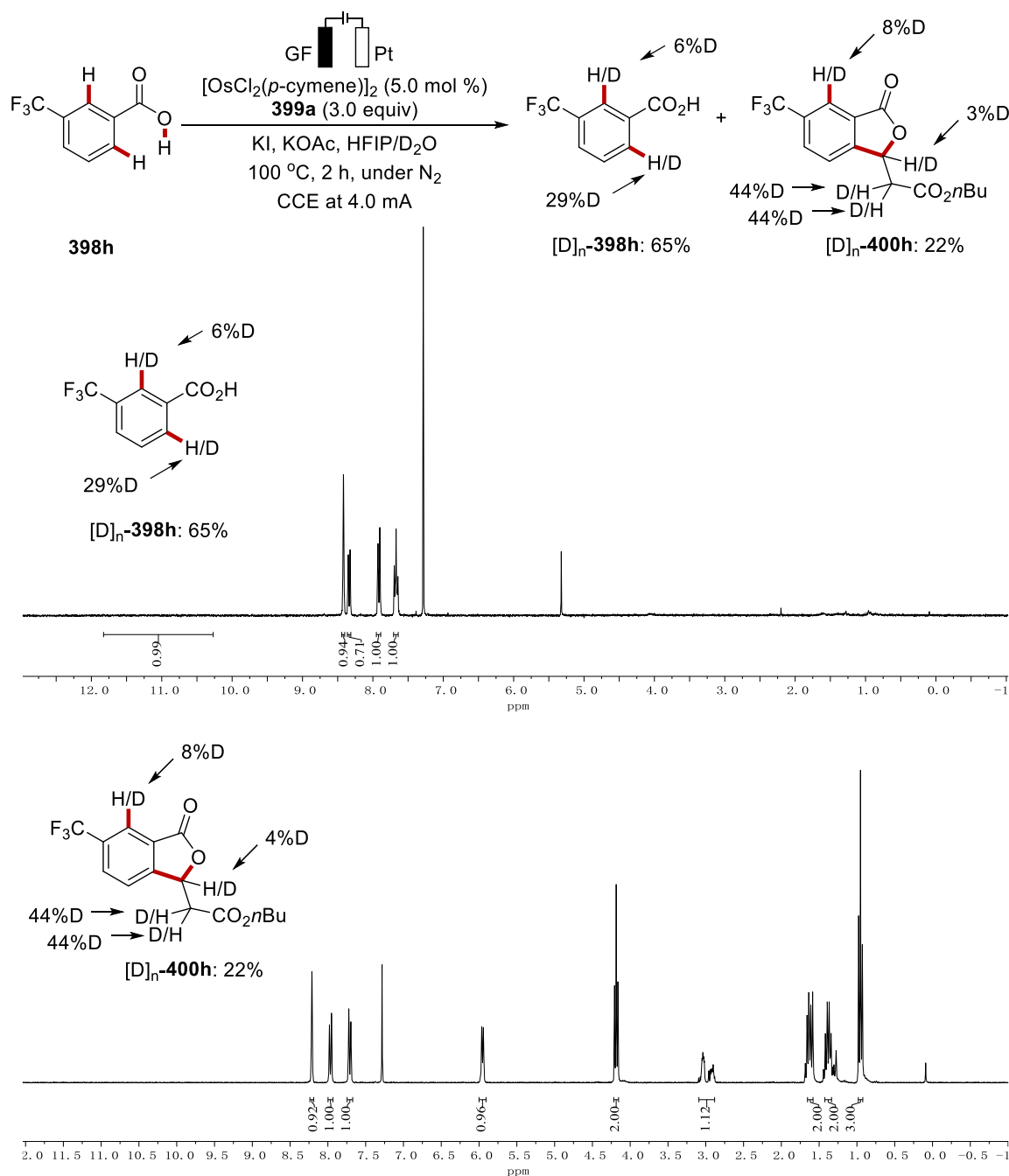
The **General Procedure D** was followed using 3-(trifluoromethyl)benzoic acid **398h** (0.20 mmol, 1.0 equiv),  $[\text{RuCl}_2(p\text{-cymene})]_2$  (5.0 mol %), KI (0.40 mmol, 2.0 equiv), KOAc (0.40 mmol, 2.0 equiv) in HFIP (1.0 mL) and  $\text{D}_2\text{O}$  (3.0 mL) at 100 °C for 2 h at 4.0 mA of constant current under  $\text{N}_2$  (Scheme 5.5.6).



**Scheme 5.5.6** H/D exchange study in electrochemical ruthenium catalysis 2.

## 3) Procedure for H/D exchange studies: Osmium catalysis (1)

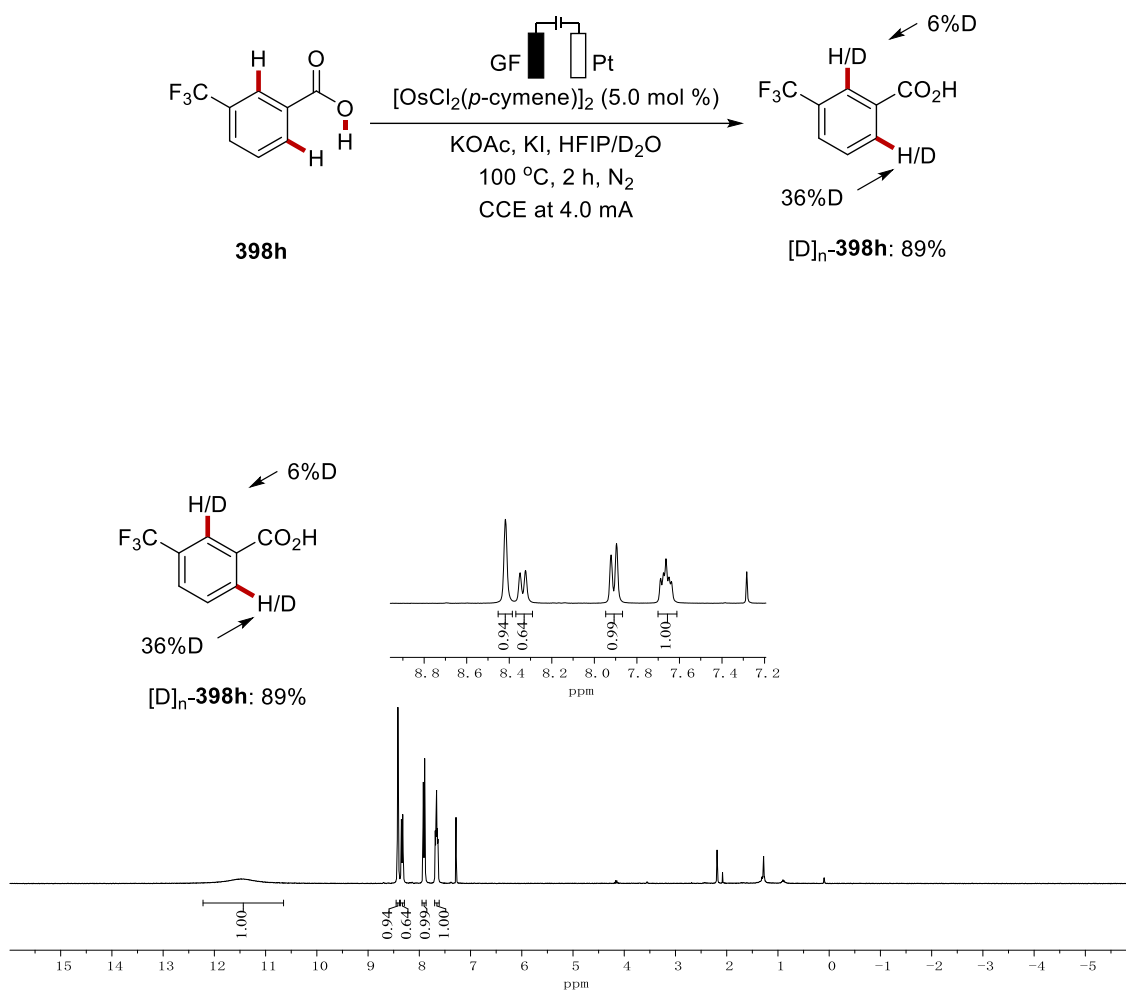
The **General Procedure D** was followed using 3-(trifluoromethyl)benzoic acid **398h** (0.20 mmol, 1.0 equiv), *n*-butyl acrylate **399a** (0.60 mmol, 3.0 equiv),  $[\text{OsCl}_2(p\text{-cymene})]_2$  (5.0 mol %), KI (0.40 mmol, 2.0 equiv), KOAc (0.40 mmol, 2.0 equiv) in HFIP (1.0 mL) and  $\text{D}_2\text{O}$  (3.0 mL) at 100 °C for 2 h at 4.0 mA of constant current under  $\text{N}_2$ .



**Scheme 5.5.7** H/D exchange study in electrochemical osmium catalysis 1.

## 4) Procedure for H/D exchange studies: Osmium catalysis (2)

The **General Procedure D** was followed using 3-(trifluoromethyl)benzoic acid **398h** (0.20 mmol, 1.0 equiv),  $[\text{OsCl}_2(p\text{-cymene})]_2$  (5.0 mol %), KI (0.40 mmol, 2.0 equiv), KOAc (0.40 mmol, 2.0 equiv) in HFIP (1.0 mL) and  $\text{D}_2\text{O}$  (3.0 mL) at 100 °C for 2 h at 4.0 mA of constant current under  $\text{N}_2$ .

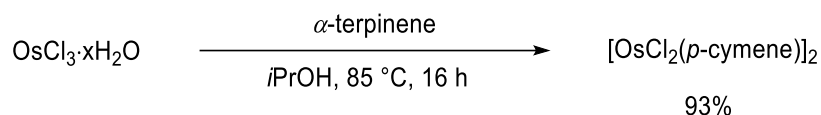


**Scheme 5.5.8** H/D exchange study in electrochemical osmium catalysis 2.

### 5.5.5 Synthesis of Osmium Complex

#### 1) Procedure for the synthesis of $[\text{OsCl}_2(p\text{-cymene})]_2$

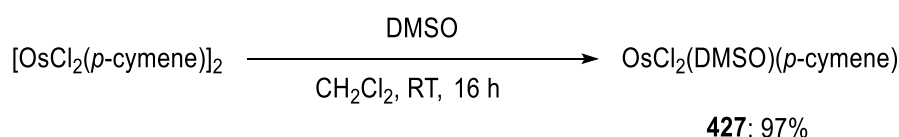
A suspension of  $\text{OsCl}_3 \cdot x\text{H}_2\text{O}$  (1.0 mmol, 1.0 equiv) and  $\alpha$ -terpinene (9.0 mmol, 9.0 equiv) in isopropanol (5.0 mL) was stirred at 85 °C for 16 h under  $\text{N}_2$ . Filtration (Por 3) with MeOH ( $3 \times 5$  mL) gave yellow solid, which was dried *in vacuo* for 6 h (Scheme 5.5.9).



**Scheme 5.5.9** Synthesis of  $[\text{OsCl}_2(p\text{-cymene})]_2$ .

#### 2) Procedure for the synthesis of $\text{OsCl}_2(\text{DMSO})(p\text{-cymene})$

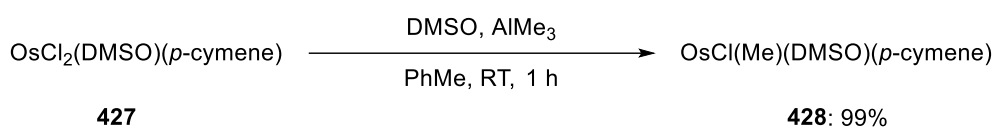
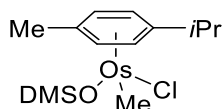
A suspension of dimethyl sulfoxide (0.5 mL) and  $[\text{OsCl}_2(p\text{-cymene})]_2$  (0.20 mmol) in dichloromethane (5.0 mL) was stirred at room temperature for 16 h under  $\text{N}_2$ . The reaction mixture was concentrated *in vacuo* for 24 h, giving reddish yellow solid (Scheme 5.5.10).



**Scheme 5.5.10** Synthesis of **427**.

#### 3) Procedure for the synthesis of **428**

To a solution of dimethyl sulfoxide (0.1 mL) and  $\text{OsCl}_2(\text{DMSO})(p\text{-cymene})$  (0.20 mmol) in PhMe was added dropwise  $\text{AlMe}_3$  (2.0 M solution in PhMe, 0.15 mL) in the glove box (Scheme 5.5.11). After stirring at room temperature for 30 min, reaction vessel was taken out from the glove box. While stirring at room temperature for additional 20 min, acetone (1.0 mL) and  $\text{H}_2\text{O}$  (0.05 mL) were added dropwise (Caution: This step generates gas). Afterwards, diethyl ether (2.0 mL) was added, then forming the white solid. A short  $\text{Na}_2\text{SO}_4$  packed filter followed by PTFE filter (Simplepure™, 0.22  $\mu\text{m}$ ) gave yellow solution which was vacuum evaporated for 16 h, giving yellow solid. (Caution: Do not use rotary evaporator to remove solvents, which can give a color change of solution to dark brown.)

Scheme 5.5.11 Synthesis of **428**.**OsCl(Me)(DMSO)(*p*-cymene) (428)**

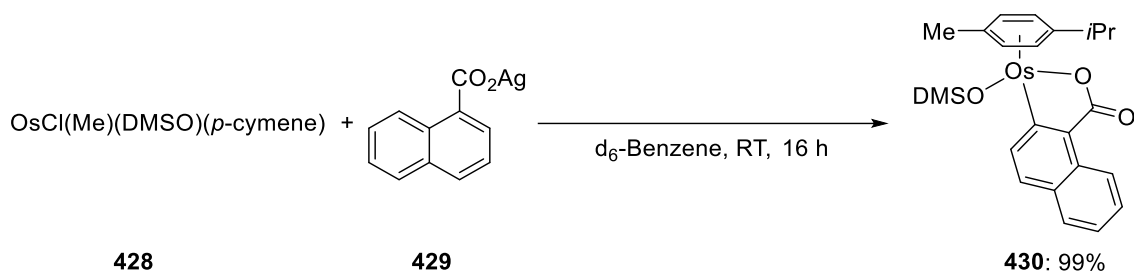
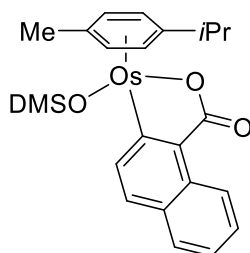
**$^1\text{H}$  NMR** (400 MHz, Benzene- $d_6$ )  $\delta$  5.06 (d,  $J = 5.5$  Hz, 1H), 4.88 (d,  $J = 5.5$  Hz, 1H), 4.84 (d,  $J = 5.5$  Hz, 1H), 4.67 (d,  $J = 5.5$  Hz, 1H), 3.01 (s, 3H), 2.66 – 2.59 (m, 1H), 2.56 (s, 3H), 1.86 (s, 3H), 1.43 (s, 3H), 1.05 (d,  $J = 7.0$  Hz, 3H), 1.02 (d,  $J = 7.0$  Hz, 3H).

**$^{13}\text{C}$  NMR** (100 MHz, Benzene- $d_6$ )  $\delta$  99.7 ( $\text{C}_q$ ), 92.9 ( $\text{C}_q$ ), 84.5 (CH), 83.5 (CH), 76.2 (CH), 74.9 (CH), 49.2 ( $\text{CH}_3$ ), 40.7 ( $\text{CH}_3$ ), 37.3 ( $\text{CH}_3$ ), 30.4 (CH), 23.2 ( $\text{CH}_3$ ), 21.9 ( $\text{CH}_3$ ), 17.7 ( $\text{CH}_3$ ), -16.0 ( $\text{CH}_3$ ).

**HR-MS** (ESI)  $\text{C}_{13}\text{H}_{23}\text{ClO}_2\text{S}$  [M]: 454.0755, found: 454.0764.

4) Procedure for the synthesis of **430**

A suspension of  $\text{OsCl}(\text{Me})(\text{DMSO})(p\text{-cymene})$  (0.20 mmol, 1.0 equiv) and ((1-naphthoyl)oxy)silver **429** (0.22 mmol, 1.1 equiv) in  $\text{C}_6\text{D}_6$  was stirred at room temperature for 16 h (Scheme 5.5.12). During the course of reaction, the aliquot was taken to monitor the reaction. When  $\text{OsCl}(\text{Me})(\text{DMSO})(p\text{-cymene})$  was fully consumed, the solution was filtered with benzene by PTFE filter (Simplepure<sup>TM</sup>, 0.22  $\mu\text{m}$ ) to remove  $\text{AgCl}$  (Caution: Benzene is highly toxic. Please use it under ventilated condition). The filtrate was vacuum evaporated for 16 h, giving yellow solid. (Caution: Do not use rotary evaporator to remove solvents, which may decompose the osmium complex.) The crystal structure of **Os-I** was obtained in THF in the glove box.

Scheme 5.5.12 Synthesis of **430**.Osmium complex **430**

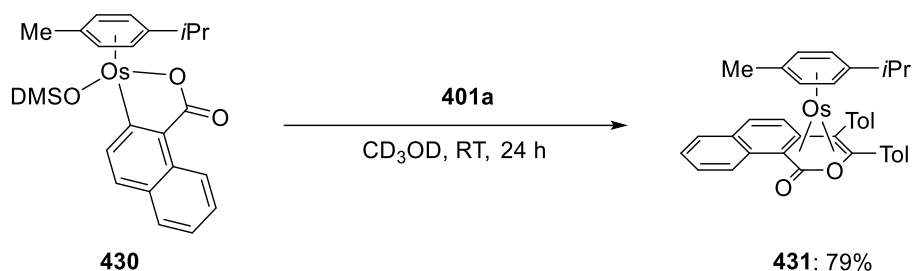
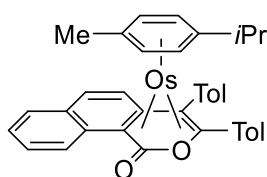
**$^1\text{H NMR}$**  (400 MHz,  $\text{CD}_2\text{Cl}_2$ )  $\delta$  9.45 (d,  $J = 8.2$  Hz, 1H), 7.92 (d,  $J = 8.2$  Hz, 1H), 7.76 (d,  $J = 8.2$  Hz, 1H), 7.67 (d,  $J = 8.2$  Hz, 1H), 7.53 – 7.44 (m, 1H), 7.39 – 7.30 (m, 1H), 5.67 – 5.57 (m, 3H), 5.51 (d,  $J = 5.7$  Hz, 1H), 2.88 – 2.80 (m, 1H), 2.82 (s, 3H), 2.41 (s, 3H), 2.30 (s, 3H), 1.23 (d,  $J = 6.9$  Hz, 3H), 1.12 (d,  $J = 6.9$  Hz, 3H).

**$^{13}\text{C NMR}$**  (100 MHz,  $\text{CD}_2\text{Cl}_2$ )  $\delta$  183.7 ( $\text{C}_q$ ), 160.1 ( $\text{C}_q$ ), 138.1 (CH), 133.3 ( $\text{C}_q$ ), 132.3 ( $\text{C}_q$ ), 131.2 (CH), 129.8 ( $\text{C}_q$ ), 128.1 (CH), 126.7 (CH), 124.2 (CH), 123.1 (CH), 108.3 ( $\text{C}_q$ ), 98.9 ( $\text{C}_q$ ), 81.7 (CH), 80.8(CH), 80.2(CH), 79.7(CH), 46.3 ( $\text{CH}_3$ ), 42.3 ( $\text{CH}_3$ ), 30.9 (CH), 22.6 ( $\text{CH}_3$ ), 22.5 ( $\text{CH}_3$ ), 18.5 ( $\text{CH}_3$ ).

**HR-MS** (ESI)  $\text{C}_{23}\text{H}_{27}\text{O}_3\text{OsS}$   $[\text{M}+\text{H}]^+$ : 575.1290, found: 575.1285.

5) Procedure for the synthesis of **431**

A suspension of **430** (0.20 mmol, 1.0 equiv) and 1,2-di-*p*-tolylethyne **401a** (0.22 mmol, 1.1 equiv) in  $\text{CD}_3\text{OD}$  was stirred at room temperature for 24 h (Scheme 5.5.13). During the course of reaction, the aliquot was taken to monitor the reaction. The solution was concentrated under reduced pressure. Purification by column chromatography on silica gel afforded the desired products **431** as a yellow solid. The crystal structure of **431** was obtained in DCM/hexane.

Scheme 5.5.13 Synthesis of **431**.Osmium complex **431**

**$^1\text{H}$  NMR** (400 MHz,  $\text{CDCl}_3$ )  $\delta$  8.12 (d,  $J = 7.9$  Hz, 1H), 7.52 – 7.40 (m, 2H), 7.36 (d,  $J = 7.9$  Hz, 1H), 7.29 (d,  $J = 7.0$  Hz, 1H), 7.24 – 7.15 (m, 1H), 7.09 (d,  $J = 7.0$  Hz, 1H), 7.01 (d,  $J = 6.2$  Hz, 1H), 7.02 – 6.98 (m, 2H), 6.93 (d,  $J = 8.2$  Hz, 2H), 6.84 (d,  $J = 8.2$  Hz, 2H), 5.45 (d,  $J = 5.4$  Hz, 1H), 5.39 (d,  $J = 5.4$  Hz, 1H), 3.91 (d,  $J = 5.4$  Hz, 1H), 3.40 (d,  $J = 5.4$  Hz, 1H), 2.37 (s, 3H), 2.20 (s, 3H), 1.67 – 1.59 (m, 1H), 1.64 (s, 3H), 1.13 (d,  $J = 6.8$  Hz, 3H), 0.95 (d,  $J = 6.8$  Hz, 3H).

**$^{13}\text{C}$  NMR** (100 MHz,  $\text{CDCl}_3$ )  $\delta$  175.1 ( $\text{C}_q$ ), 140.2 ( $\text{C}_q$ ), 138.8 ( $\text{C}_q$ ), 137.0 ( $\text{C}_q$ ), 133.4 ( $\text{C}_q$ ), 133.1 ( $\text{C}_q$ ), 132.6 (CH), 131.5 (CH), 129.5 (CH), 129.3 (CH), 129.1 ( $\text{C}_q$ ), 128.7 (CH), 128.7 (CH), 127.6 (CH), 127.6 (CH), 125.1 (CH), 125.0 (CH), 123.8 (CH), 110.0 ( $\text{C}_q$ ), 103.0 ( $\text{C}_q$ ), 92.2 ( $\text{C}_q$ ), 85.1 ( $\text{C}_q$ ), 79.0 (CH), 79.0 (CH), 76.3 ( $\text{C}_q$ ), 74.2 (CH), 51.9 ( $\text{C}_q$ ), 30.1 (CH), 24.8 ( $\text{CH}_3$ ), 21.6 ( $\text{CH}_3$ ), 21.3 ( $\text{CH}_3$ ), 20.9 ( $\text{CH}_3$ ), 17.5 ( $\text{CH}_3$ ).

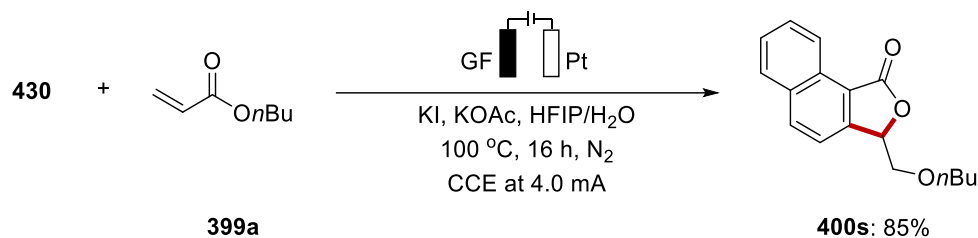
**HR-MS** (ESI)  $\text{C}_{37}\text{H}_{35}\text{O}_2\text{Os}$   $[\text{M}+\text{H}]^+$ : 703.2249, found: 703.2236.



### 5.5.6 Reactions with Osmium Complex

#### 1) Procedure for the stoichiometric reaction with **430**

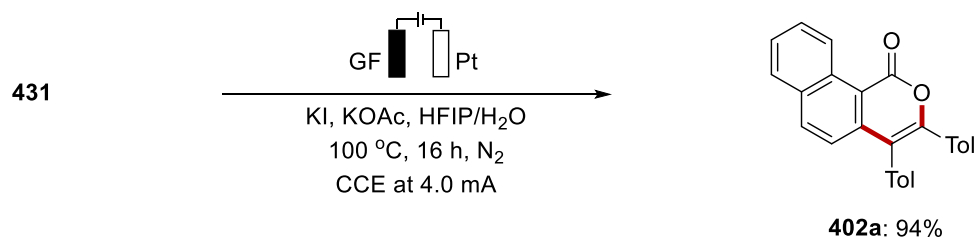
The **General Procedure D** was followed using **430** (0.1 mmol, 1.0 equiv), *n*-butyl acrylate **399a** (0.3 mmol, 3.0 equiv), KI (0.4 mmol, 2.0 equiv), KOAc (0.4 mmol, 2.0 equiv) in HFIP (2.0 mL) and H<sub>2</sub>O (2.0 mL) at 100 °C for 16 h at 4.0 mA of constant current under N<sub>2</sub> (Scheme 5.5.14).



**Scheme 5.5.14** Stoichiometric reaction with osmium complex **430**.

#### 2) Procedure for the stoichiometric reaction with **431**

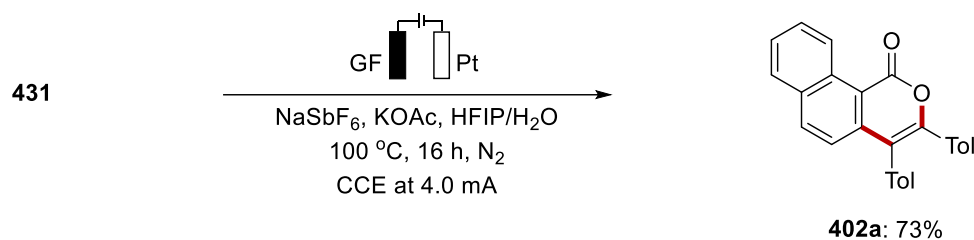
The **General Procedure E** was followed using **431** (0.1 mmol, 1.0 equiv), KI (0.2 mmol, 2.0 equiv), KOAc (0.2 mmol, 2.0 equiv) in HFIP (2.0 mL) and H<sub>2</sub>O (2.0 mL) was stirred at 100 °C for 16 h at 4.0 mA of constant current under N<sub>2</sub> (Scheme 5.5.15).



**Scheme 5.5.15** Stoichiometric reaction with osmium complex **431**.

3) Procedure for the stoichiometric reaction with **431**

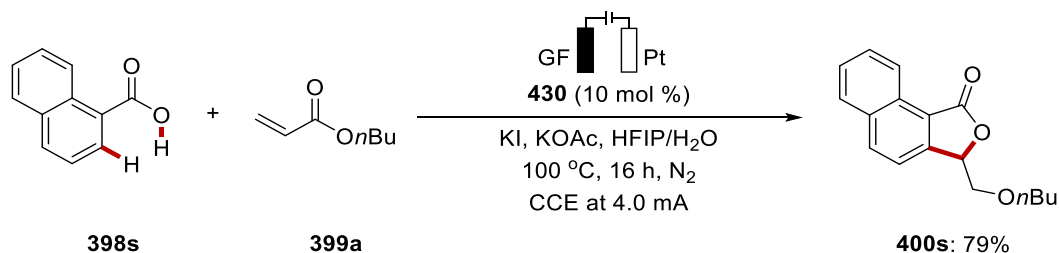
The **General Procedure E** was followed using **431** (0.1 mmol, 1.0 equiv), NaSbF<sub>6</sub> (0.2 mmol, 2.0 equiv), KOAc (0.2 mmol, 2.0 equiv) in HFIP (2.0 mL) and H<sub>2</sub>O (2.0 mL) was stirred at 100 °C for 16 h at 4.0 mA of constant current under N<sub>2</sub> (Scheme 5.5.16).



**Scheme 5.5.16** Stoichiometric reaction with osmium complex **431** with NaSbF<sub>6</sub>.

4) Procedure for the catalytic reaction with **430**

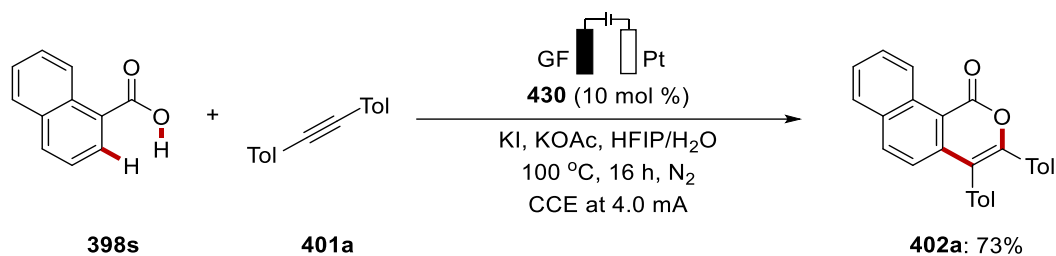
The **General Procedure D** was followed using naphthoic acid **398s** (0.1 mmol, 1.0 equiv), *n*-butyl acrylate **399a** (0.3 mmol, 3.0 equiv), **430** (10 mol %), KI (0.2 mmol, 2.0 equiv), KOAc (0.2 mmol, 2.0 equiv) in HFIP (2.0 mL) and H<sub>2</sub>O (2.0 mL) at 100 °C for 16 h at 4.0 mA of constant current under N<sub>2</sub> (Scheme 5.5.17).



**Scheme 5.5.17** Catalytic reaction with osmium complex **430**.

5) Procedure for the catalytic reaction with **430**

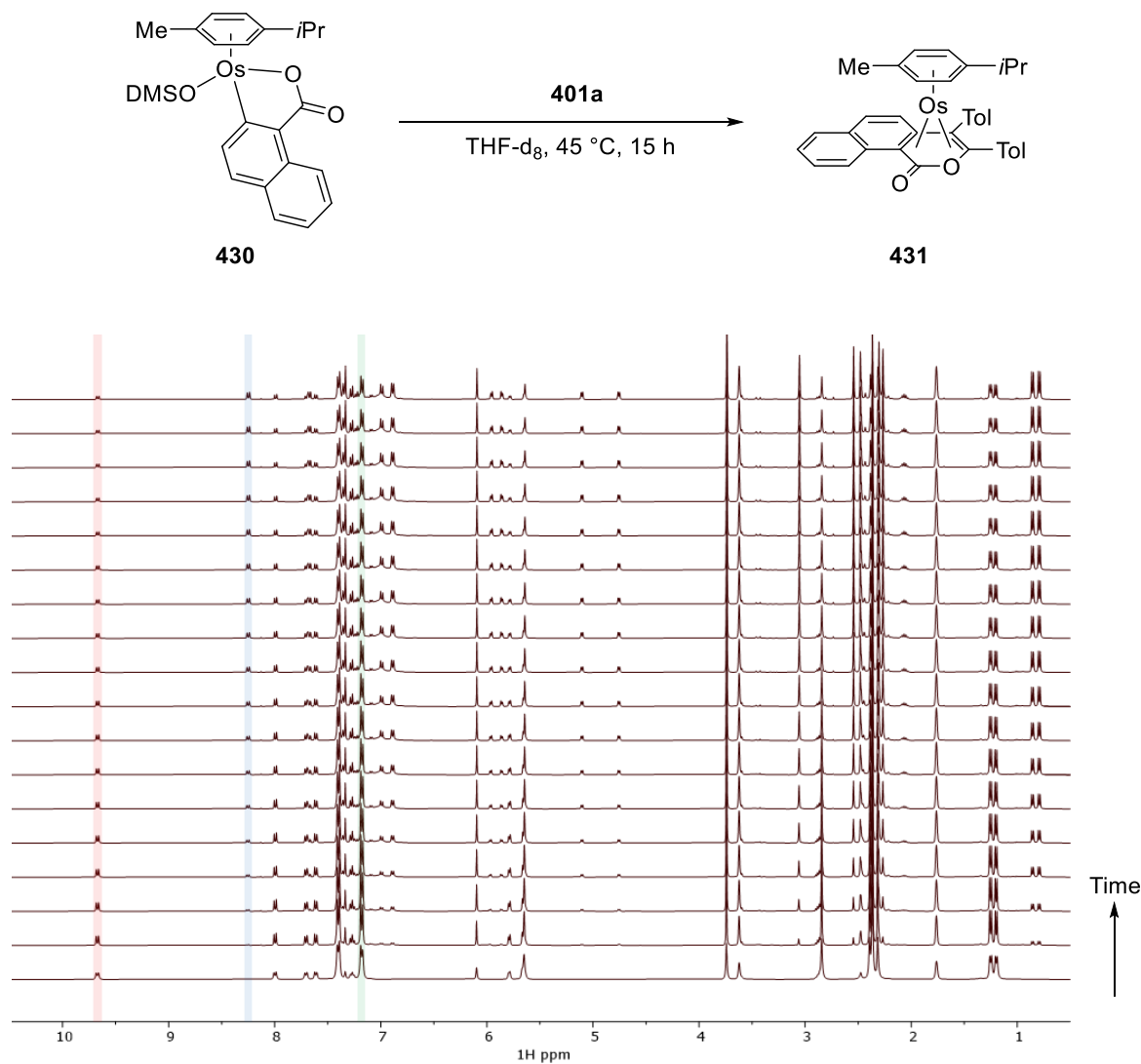
The **General Procedure E** was followed using naphthoic acid **430** (0.1 mmol, 1.0 equiv), 1,2-di-*p*-tolylethyne **401a** (0.3 mmol, 3.0 equiv), **430** (10 mol %), KI (0.2 mmol, 2.0 equiv), KOAc (0.2 mmol, 2.0 equiv) in HFIP (2.0 mL) and H<sub>2</sub>O (2.0 mL) at 100 °C for 16 h at 4.0 mA of constant current under N<sub>2</sub> (Scheme 5.5.18).



**Scheme 5.5.18** Catalytic reaction with osmium complex **430**.

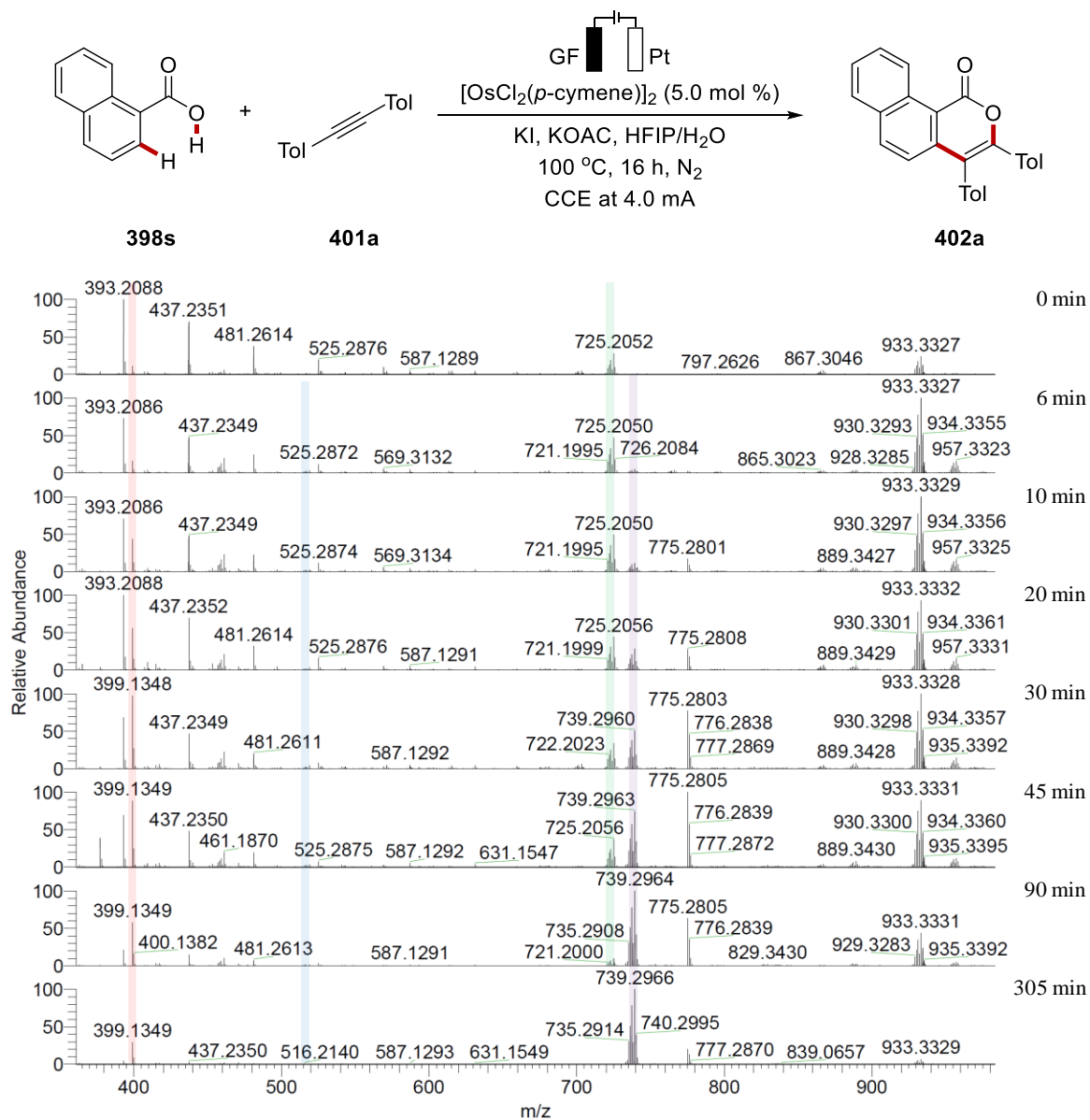
### 5.5.7 *In-Operando* NMR and HR-ESI-MS Studies

In a nitrogen filled glove box, a screw top NMR tube was loaded with **430** (0.050 mmol), **401a** (0.050 mmol), (1,3,5-trimethoxybenzene (500 mM stock solution in THF- $d_8$ , 0.0125 mmol), and THF- $d_8$  (475.0  $\mu$ L) (Scheme 5.5.19). An  $^1\text{H}$  NMR (400 MHz) spectrum of the resulted solution was then obtained. Subsequently, alkyne (0.050 mmol) was added and after homogenization, the progress of the reaction was monitored by  $^1\text{H}$  NMR (400 MHz) spectroscopy at 45  $^\circ\text{C}$  by collecting spectra every five minutes for a total period of 15 hours (18 data points out of the 180 collected spectra are only presented below for clarity, Color legend: Red = **430**, Blue = **431**, Green = **401a**).



Scheme 5.5.19 *In-operando* NMR study.

The **General Procedure E** was followed using naphthoic acid **398s** (0.1 mmol), 1,2-di-*p*-tolylethyne **401a** (3.0 equiv),  $[\text{OsCl}_2(p\text{-cymene})]_2$  (5.0 mol %), KI (66.4 mg, 2.0 equiv), KOAc (39.3 mg, 2.0 equiv) in HFIP (2.0 mL) and  $\text{H}_2\text{O}$  (2.0 mL) under  $\text{N}_2$  (Scheme 5.5.20). The reaction mixture was then left to stir at 100 °C for 1 minutes at which time a sample ( $t_0$ ) was collected and analyzed by HR-ESI-MS. Subsequently, the reaction was initiated by passing a constant current of 4.0 mA through the reaction mixture followed by sampling at time intervals for a total length of 425 min. Each aliquot collected ( $\sim 0.1$  mL) was passed through a pipette filled with  $\text{Na}_2\text{SO}_4$  and diluted with THF prior to analysis.

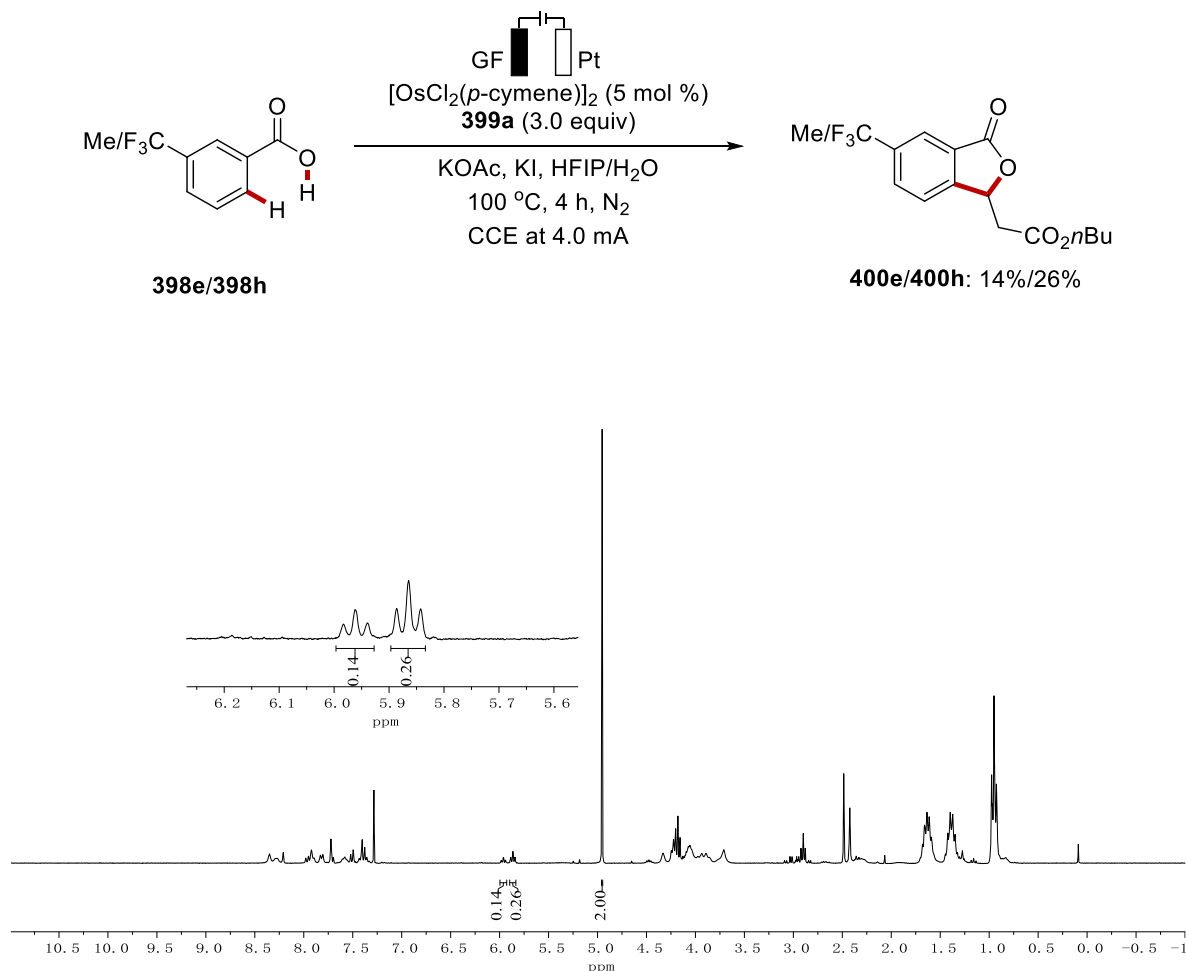


**Scheme 5.20** HR-ESI-MS study.

## 5.5.8 Competition Experiment

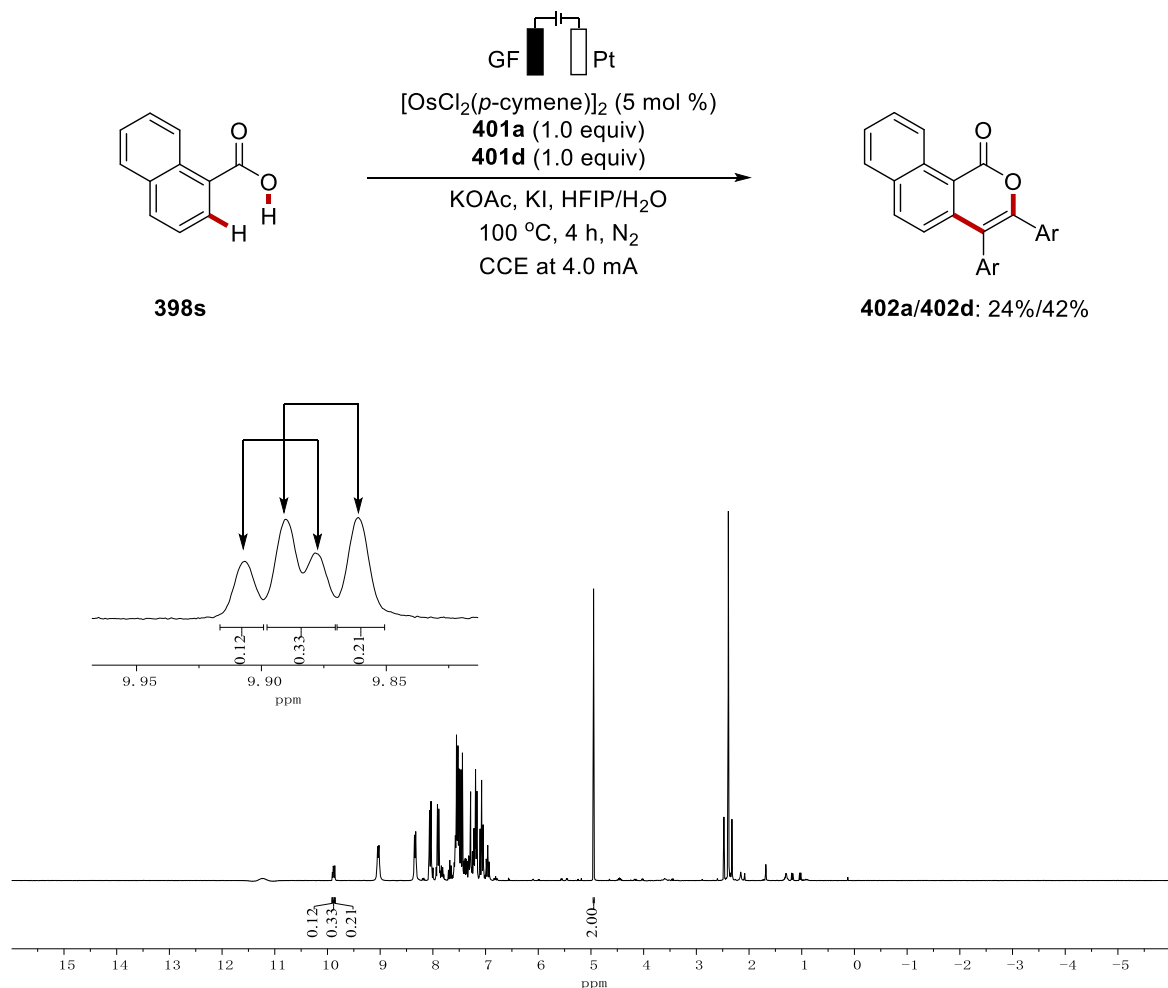
## 1) Procedure for competition experiment (1)

The **General Procedure D** was followed using 3-methyl benzoic acid **398e** (0.1 mmol, 1.0 equiv), 3-trifluoromethyl benzoic acid **398h** (0.1 mmol, 1.0 equiv), *n*-butyl acrylate **399a** (0.3 mmol, 3.0 equiv),  $[\text{OsCl}_2(p\text{-cymene})]_2$  (5.0 mol %), KI (0.2 mmol, 2.0 equiv), KOAc (0.2 mmol, 2.0 equiv) in HFIP (2.0 mL) and  $\text{H}_2\text{O}$  (2.0 mL) at 100 °C for 4 h at 4.0 mA of constant current under  $\text{N}_2$  (Scheme 5.5.21). After cooling to ambient temperature, the electrodes were washed with ethyl acetate ( $3 \times 10$  mL). The reaction mixtures were extracted with brine (20 mL), dried over  $\text{Na}_2\text{SO}_4$ , and concentrated under reduced pressure. The crude mixture was analyzed by  $^1\text{H}$  NMR with  $\text{CH}_2\text{Br}_2$  as the internal standard.

Scheme 5.5.21 Competition experiment with **398e** and **398h**.

## 2) Procedure for competition experiment (2)

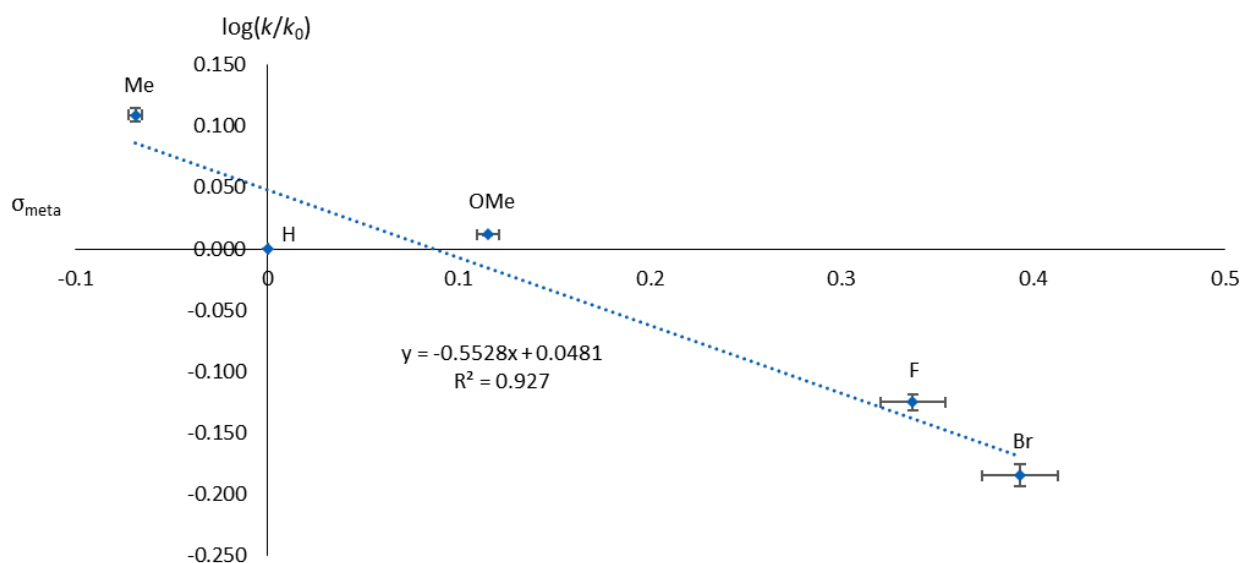
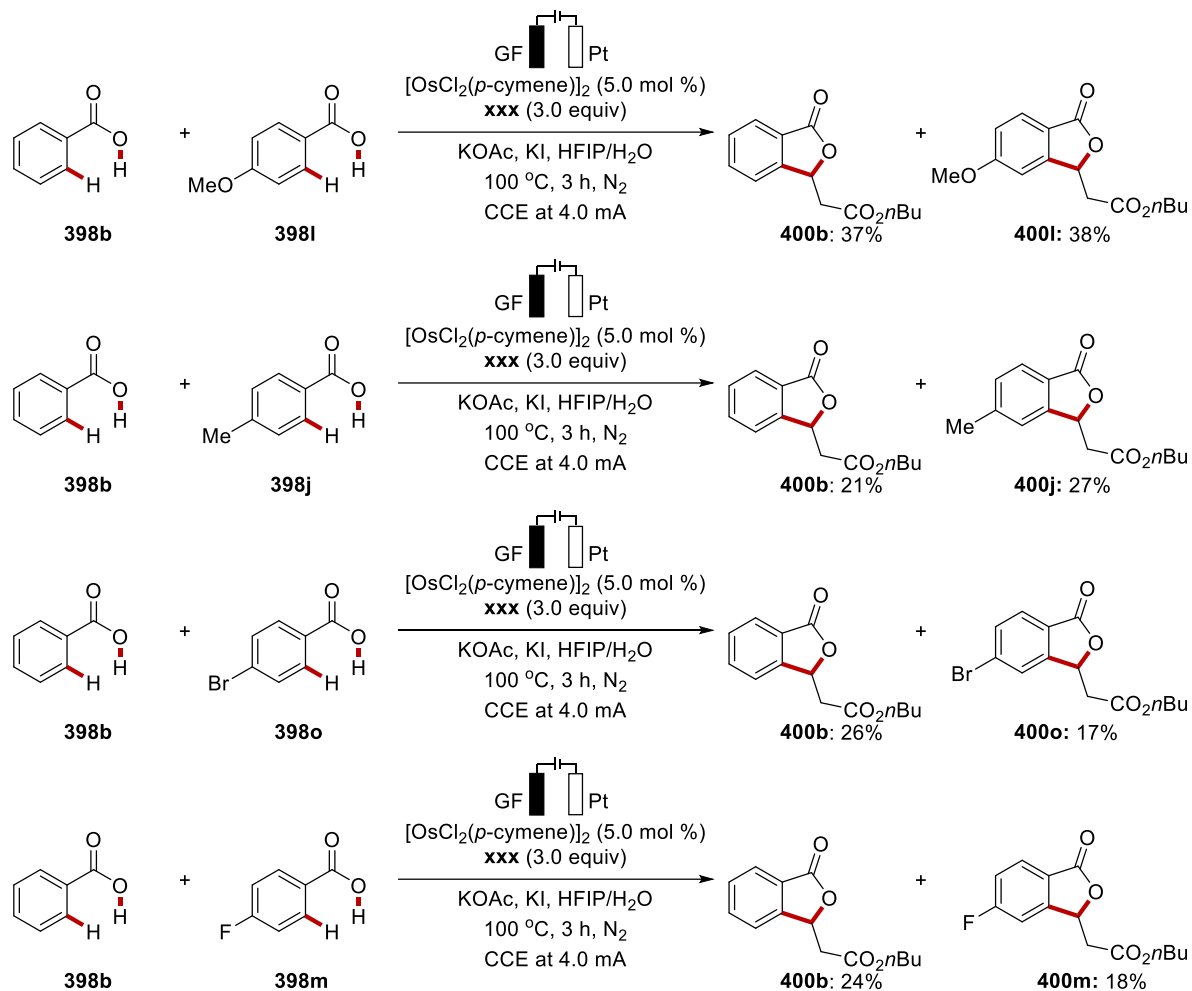
The **General Procedure E** was followed using naphthoic acid **398s** (0.20 mmol, 1.0 equiv), 1,2-di-*p*-tolylethyne **401a** (0.20 mmol, 1.0 equiv), 1,2-bis(4-fluorophenyl)ethyne **401d** (0.20 mmol, 1.0 equiv),  $[\text{OsCl}_2(p\text{-cymene})]_2$  (5.0 mol %), KI (0.40 mmol, 2.0 equiv), KOAc (0.40 mmol, 2.0 equiv) in HFIP (2.0 mL) and H<sub>2</sub>O (2.0 mL) at 100 °C for 4 h at 4.0 mA of constant current under N<sub>2</sub> (Scheme 5.5.22). After cooling to ambient temperature, the electrodes were washed with ethyl acetate (3 × 10 mL). The reaction mixture was extracted with brine (20 mL), dried over Na<sub>2</sub>SO<sub>4</sub>, and concentrated under reduced pressure. The crude mixture was analyzed by <sup>1</sup>H NMR with CH<sub>2</sub>Br<sub>2</sub> as the internal standard.



**Scheme 5.5.22** Competition experiment with **401a** and **401d**.

## 5.5.9 Hammett Correlation

A series of reactions were performed with different substrates under standard reaction conditions (Scheme 5.5.23).



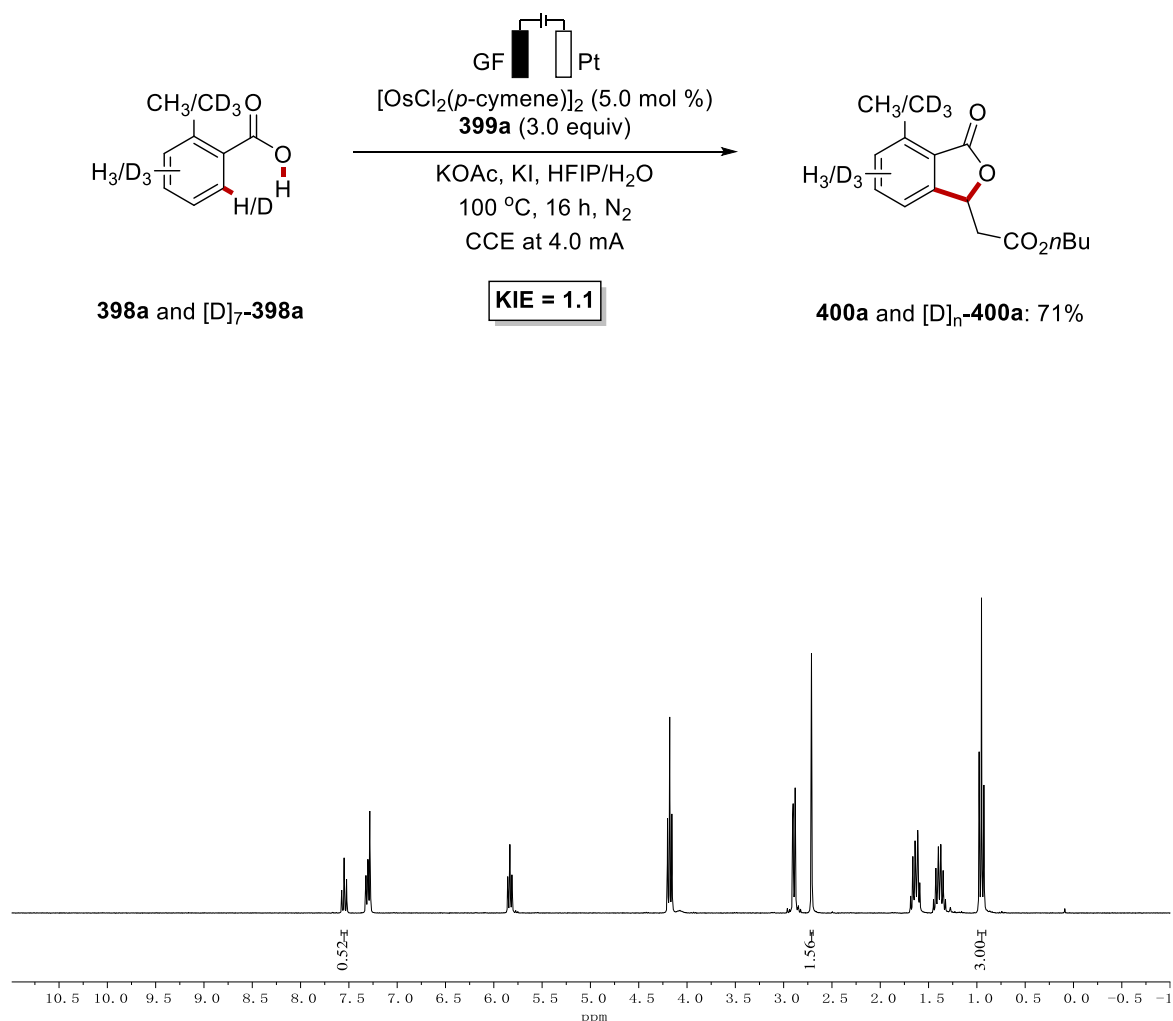
Scheme 5.5.23 Hammett correlation plot.



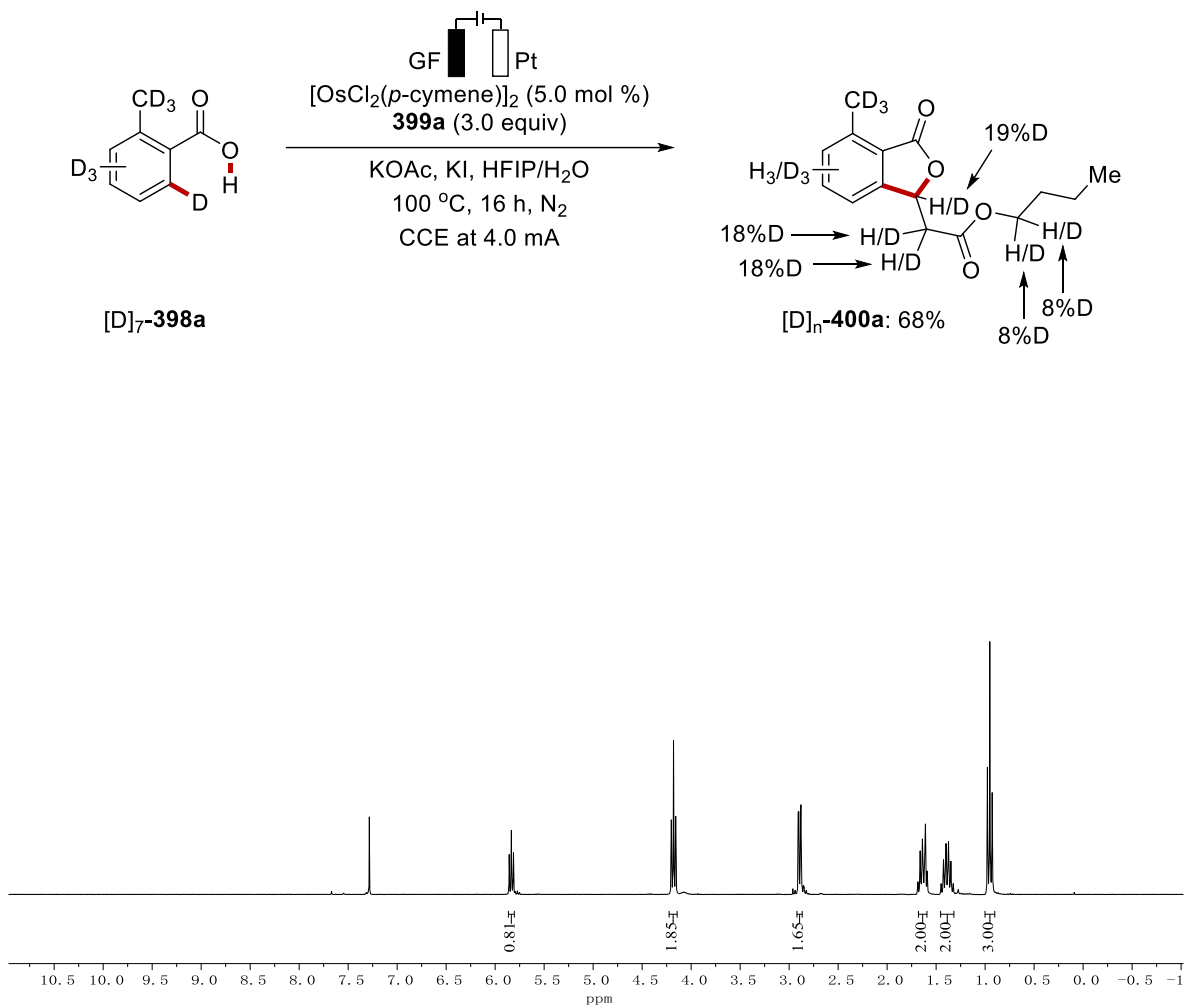
## 5.5.10 KIE Study

## 1) Procedure for KIE study (Intermolecular competition reaction)

The **General Procedure D** was followed using **398a** (0.1 mmol, 1.0 equiv), [D]<sub>7</sub>-**398a** (0.1 mmol, 1.0 equiv), *n*-butyl acrylate **399a** (0.3 mmol, 3.0 equiv), [OsCl<sub>2</sub>(*p*-cymene)]<sub>2</sub> (5.0 mol %), KI (0.2 mmol, 2.0 equiv), KOAc (39.3 mg, 2.0 equiv) in HFIP (2.0 mL) and H<sub>2</sub>O (2.0 mL) at 100 °C for 16 h at 4.0 mA of constant current under N<sub>2</sub> (Scheme 5.5.24).



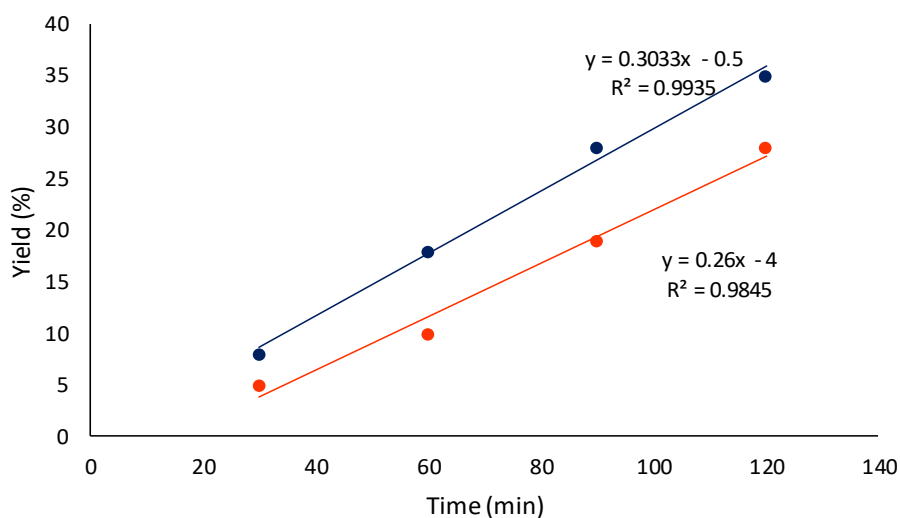
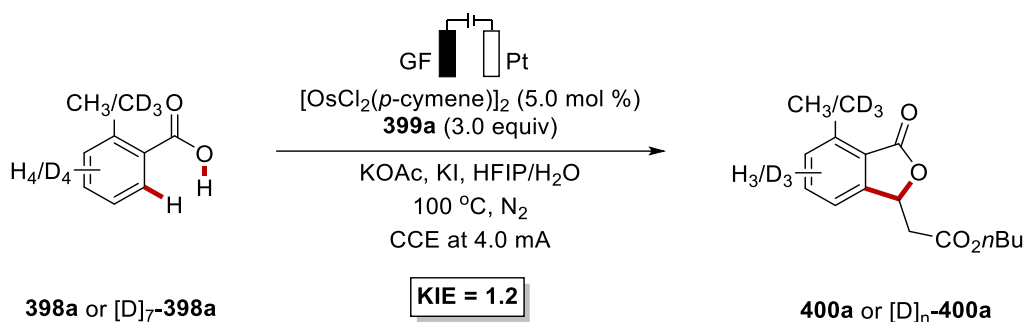
**Scheme 5.5.24** Intermolecular kinetic isotope exchange. Note: CH<sub>3</sub> of aromatic and CH<sub>3</sub> of butyl group should be compared. Other C–H bonds were isotopically labelled by post-catalysis H/D exchange (Scheme 5.5.25).



Scheme 5.5.25 H/D exchange study of [D]<sub>7</sub>-398a.

## 2) Procedure for KIE study (Two parallel reactions)

The **General Procedure D** was followed for four independent reactions using substrate **398a** (0.20 mmol) *n*-butyl acrylate **399a** (3.0 equiv), and another four independent reactions using substrate [D]<sub>7</sub>-**398a** (0.20 mmol) and *n*-butyl acrylate **399a** (3.0 equiv) for specified reaction time (30 min, 60 min, 90 min, and 120 min). The crude mixture was dried in vacuo for 6 h and analyzed by <sup>1</sup>H NMR with CH<sub>2</sub>Br<sub>2</sub> as the internal standard (Scheme 5.5.26). Blue line is for **400a** and red line is for [D]<sub>n</sub>-**400a**.

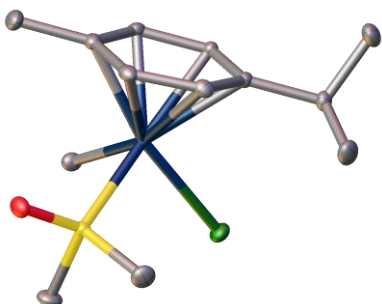


**Scheme 5.5.26** Parallel kinetic isotope exchange study.

### 5.5.11 Crystallographic Information

X-ray diffraction experiments for all of the compounds were carried out at 100(2) K on a Bruker D8 Venture four-circle-diffractometer from Bruker AXS GmbH equipped with a Photon II detector purchased from Bruker AXS GmbH and using microfocus I $\mu$ S Cu/Mo radiation from Incoatec GmbH with HELIOS mirror optics and single-hole collimator from Bruker AXS GmbH. Intensities were integrated and absorption corrections based on equivalent reflections were applied using SADABS. The structures were all solved using SHELXT<sup>[287]</sup> and refined against all F<sub>2</sub> in SHELXL using Olex 2. All of the non-hydrogen atoms were refined anisotropically while the carbon bond hydrogen atoms were located geometrically and refined using a riding model. Crystal structure and refinement data are given in Table 5.5.2, 5.5.3, and 5.5.4. Crystallographic data for the compounds have been deposited with the Cambridge Crystallographic Data Centre as supplementary publication CCDC 2085919, 2085920 and 2085921.

**Table 5.5.2** Crystal data and structure refinement for OsCl(Me)(DMSO)(*p*-cymene) (**428**).

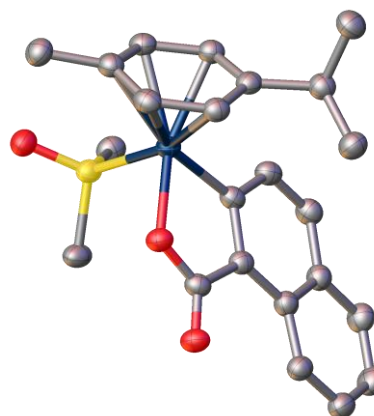
| Compound          | <br>OsCl(Me)(DMSO)( <i>p</i> -cymene) ( <b>428</b> ) |
|-------------------|------------------------------------------------------------------------------------------------------------------------------------------|
| Empirical formula | C <sub>13</sub> H <sub>23</sub> ClOOS                                                                                                    |
| Formula weight    | 453.02                                                                                                                                   |
| Temperature/K     | 100                                                                                                                                      |
| Crystal system    | monoclinic                                                                                                                               |
| Space group       | Cc                                                                                                                                       |
| <i>a</i> /Å       | 11.2960(8)                                                                                                                               |
| <i>b</i> /Å       | 15.1437(12)                                                                                                                              |
| <i>c</i> /Å       | 9.2214(8)                                                                                                                                |

Experimental Data

---

|                                               |                                                               |
|-----------------------------------------------|---------------------------------------------------------------|
| $\alpha/^\circ$                               | 90                                                            |
| $\beta/^\circ$                                | 106.298(3)                                                    |
| $\gamma/^\circ$                               | 90                                                            |
| Volume/ $\text{\AA}^3$                        | 1514.1(2)                                                     |
| Z                                             | 4                                                             |
| $\rho_{\text{calc}}/\text{g}/\text{cm}^3$     | 1.987                                                         |
| $\mu/\text{mm}^{-1}$                          | 4.684                                                         |
| F(000)                                        | 872                                                           |
| Crystal size/ $\text{mm}^3$                   | $0.151 \times 0.113 \times 0.1$                               |
| Radiation                                     | AgK $\alpha$ ( $\lambda = 0.56086$ )                          |
| $2\Theta$ range for data collection/ $^\circ$ | 4.244 to 57.874                                               |
| Index ranges                                  | $-19 \leq h \leq 19, -25 \leq k \leq 26, -15 \leq l \leq 15$  |
| Reflections collected                         | 39100                                                         |
| Independent reflections                       | 7428 [ $R_{\text{int}} = 0.0237, R_{\text{sigma}} = 0.0182$ ] |
| Data/restraints/parameters                    | 7428/71/160                                                   |
| Goodness-of-fit on $F^2$                      | 1.116                                                         |
| Final R indexes [ $I \geq 2\sigma(I)$ ]       | $R_1 = 0.0138, wR_2 = 0.0311$                                 |
| Final R indexes [all data]                    | $R_1 = 0.0146, wR_2 = 0.0322$                                 |
| Largest diff. peak/hole / $e \text{\AA}^{-3}$ | 2.18/-1.44                                                    |

---

**Table 5.5.4** Crystal data and structure refinement for **430**.**430**

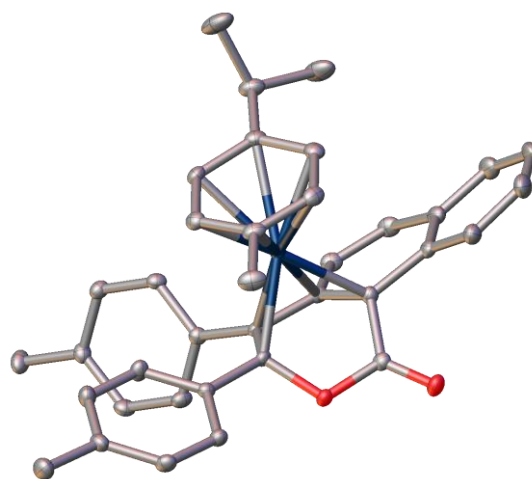
|                                    |                                                      |
|------------------------------------|------------------------------------------------------|
| Empirical formula                  | C <sub>29</sub> H <sub>38</sub> O <sub>4.5</sub> OsS |
| Formula weight                     | 680.85                                               |
| Temperature/K                      | 100                                                  |
| Crystal system                     | monoclinic                                           |
| Space group                        | C2/c                                                 |
| a/Å                                | 26.302(3)                                            |
| b/Å                                | 14.0767(14)                                          |
| c/Å                                | 15.6684(13)                                          |
| α/°                                | 90                                                   |
| β/°                                | 113.083(3)                                           |
| γ/°                                | 90                                                   |
| Volume/Å <sup>3</sup>              | 5336.6(9)                                            |
| Z                                  | 8                                                    |
| ρ <sub>calc</sub> /cm <sup>3</sup> | 1.695                                                |
| μ/mm <sup>-1</sup>                 | 4.892                                                |
| F(000)                             | 2720                                                 |
| Crystal size/mm <sup>3</sup>       | 0.121 × 0.061 × 0.029                                |
| Radiation                          | MoKα (λ = 0.71073)                                   |
| 2θ range for data collection/°     | 5.326 to 61.174                                      |

Experimental Data

|                                                |                                                               |
|------------------------------------------------|---------------------------------------------------------------|
| Index ranges                                   | $-37 \leq h \leq 37, -20 \leq k \leq 20, -22 \leq l \leq 22$  |
| Reflections collected                          | 83356                                                         |
| Independent reflections                        | 8195 [ $R_{\text{int}} = 0.0394, R_{\text{sigma}} = 0.0191$ ] |
| Data/restraints/parameters                     | 8195/0/258                                                    |
| Goodness-of-fit on $F^2$                       | 1.046                                                         |
| Final R indexes [ $I \geq 2\sigma(I)$ ]        | $R_1 = 0.0309, wR_2 = 0.0793$                                 |
| Final R indexes [all data]                     | $R_1 = 0.0356, wR_2 = 0.0824$                                 |
| Largest diff. peak/hole / $e \text{ \AA}^{-3}$ | 2.22/-0.60                                                    |

**Table 5.5.5** Crystal data and structure refinement for **431**.

**Compound**



**431**

|                   |                     |
|-------------------|---------------------|
| Empirical formula | $C_{37}H_{34}O_2Os$ |
| Formula weight    | 700.84              |
| Temperature/K     | 100                 |
| Crystal system    | monoclinic          |
| Space group       | $P2_1/n$            |
| $a/\text{\AA}$    | 16.0104(13)         |
| $b/\text{\AA}$    | 11.3652(9)          |
| $c/\text{\AA}$    | 16.2343(13)         |
| $\alpha/^\circ$   | 90                  |

Experimental Data

---

|                                               |                                                               |
|-----------------------------------------------|---------------------------------------------------------------|
| $\beta/^\circ$                                | 108.231(2)                                                    |
| $\gamma/^\circ$                               | 90                                                            |
| Volume/ $\text{\AA}^3$                        | 2805.7(4)                                                     |
| Z                                             | 4                                                             |
| $\rho_{\text{calc}}/\text{cm}^3$              | 1.659                                                         |
| $\mu/\text{mm}^{-1}$                          | 4.578                                                         |
| F(000)                                        | 1392                                                          |
| Crystal size/ $\text{mm}^3$                   | $0.123 \times 0.09 \times 0.045$                              |
| Radiation                                     | MoK $\alpha$ ( $\lambda = 0.71073$ )                          |
| $2\Theta$ range for data collection/ $^\circ$ | 4.31 to 61.158                                                |
| Index ranges                                  | $-22 \leq h \leq 22, -16 \leq k \leq 16, -23 \leq l \leq 23$  |
| Reflections collected                         | 84089                                                         |
| Independent reflections                       | 8602 [ $R_{\text{int}} = 0.0424, R_{\text{sigma}} = 0.0221$ ] |
| Data/restraints/parameters                    | 8602/0/366                                                    |
| Goodness-of-fit on $F^2$                      | 1.041                                                         |
| Final R indexes [ $I \geq 2\sigma(I)$ ]       | $R_1 = 0.0189, wR_2 = 0.0375$                                 |
| Final R indexes [all data]                    | $R_1 = 0.0248, wR_2 = 0.0395$                                 |
| Largest diff. peak/hole / $e \text{\AA}^{-3}$ | 0.75/-0.57                                                    |

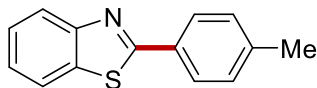
---



## 5.6 Photo-Induced C–H Arylation by Reusable Heterogeneous Copper Catalyst

### 5.6.1 Characterization Data

#### 2-(*p*-Tolyl)benzo[*d*]thiazole (405a)



1) The **General Procedure F** was followed using benzothiazole **403a** (34 mg, 0.25 mmol), 4-iodotoluene **404a** (273 mg, 1.25 mmol), **406** (30 mg, 11 mol %) and LiO*t*Bu (60 mg, 0.75 mmol) in Et<sub>2</sub>O (0.5 mL). Purification by column chromatography on silica gel (*n*-hexane/EtOAc: 70/1) yielded **405a** (52.4 mg, 93%) as a light yellow solid.

2) The **General Procedure H** was followed using benzothiazole **403a** (34 mg, 0.25 mmol), 4-bromotoluene **447a** (273 mg, 1.25 mmol), **406** (30 mg, 11 mol %) and Cs<sub>2</sub>CO<sub>3</sub> (244 mg, 0.75 mmol) in Et<sub>2</sub>O (0.5 mL). Purification by column chromatography on silica gel (*n*-hexane/EtOAc: 70/1) yielded **405a** (28.7 mg, 51%) as a light yellow solid.

**M. p.:** 86 °C.

**<sup>1</sup>H NMR** (300 MHz, CDCl<sub>3</sub>):  $\delta$  = 7.96 (dd, *J* = 8.0, 1.3 Hz, 1H), 7.92 – 7.89 (m, 1H), 7.87 (m, 1H), 7.78 (dd, *J* = 8.0, 1.3 Hz, 1H), 7.38 (ddd, *J* = 8.0, 7.2, 1.3 Hz, 1H), 7.26 (ddd, *J* = 8.0, 7.2, 1.3 Hz, 1H), 7.22 – 7.19 (m, 1H), 7.19 – 7.16 (m, 1H), 2.32 (s, 3H).

**<sup>13</sup>C NMR** (75 MHz, CDCl<sub>3</sub>):  $\delta$  = 168.0 (C<sub>q</sub>), 154.0 (C<sub>q</sub>), 141.2 (C<sub>q</sub>), 134.8 (C<sub>q</sub>), 130.8 (C<sub>q</sub>), 129.6 (CH), 127.4 (CH), 126.1 (CH), 124.9 (CH), 122.9 (CH), 121.4 (CH), 21.5 (CH<sub>3</sub>).

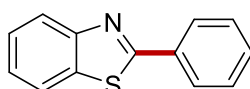
**IR** (ATR): 3024, 2918, 1611, 1445, 1074, 816, 756, 691, 485, 434 cm<sup>-1</sup>.

**MS** (ESI) *m/z* (relative intensity): 226 (100) [M+H]<sup>+</sup>, 248 (60) [M+Na]<sup>+</sup>.

**HR-MS** (ESI): *m/z* calcd for C<sub>14</sub>H<sub>12</sub>NS [M+H]<sup>+</sup>: 226.0688, found: 226.0688.

The spectral data were in accordance with those reported in the literature.<sup>[94]</sup>

#### 2-Phenylbenzo[*d*]thiazole (405b)



1) The **General Procedure F** was followed using benzothiazole **403a** (34 mg, 0.25 mmol),

iodobenzene **404b** (255 mg, 1.25 mmol), **406** (30 mg, 11 mol %) and LiOtBu (60 mg, 0.75 mmol) in Et<sub>2</sub>O (0.5 mL). Purification by column chromatography on silica gel (*n*-hexane/EtOAc: 70/1) yielded **405b** (49.7 mg, 94%) as a light yellow solid.

2) The **General Procedure H** was followed using benzothiazole **403a** (34 mg, 0.25 mmol), bromobenzene **447b** (255 mg, 1.25 mmol), **406** (30 mg, 11 mol %) and Cs<sub>2</sub>CO<sub>3</sub> (244 mg, 0.75 mmol) in Et<sub>2</sub>O (0.5 mL). Purification by column chromatography on silica gel (*n*-hexane/EtOAc: 70/1) yielded **405b** (31.2 mg, 59%) as a light yellow solid.

**M. p.:** 115 °C.

**<sup>1</sup>H NMR** (500 MHz, CDCl<sub>3</sub>): δ = 8.11 – 8.04 (m, 3H), 7.90 – 7.85 (m, 1H), 7.51 – 7.44 (m, 4H), 7.37 (ddd, *J* = 8.3, 7.2, 1.2 Hz, 1H).

**<sup>13</sup>C NMR** (125 MHz, CDCl<sub>3</sub>): δ = 168.0 (C<sub>q</sub>), 154.1 (C<sub>q</sub>), 135.0 (C<sub>q</sub>), 133.5 (C<sub>q</sub>), 130.9 (CH), 128.9 (CH), 127.5 (CH), 126.2 (CH), 125.1 (CH), 123.2 (CH), 121.5 (CH).

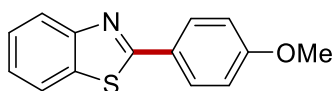
**IR** (ATR): 3016, 1510, 1478, 1433, 1313, 1252, 1215, 963, 918, 750 cm<sup>-1</sup>.

**MS** (ESI) *m/z* (relative intensity): 212 (100) [M+H]<sup>+</sup>.

**HR-MS** (ESI): *m/z* calcd for C<sub>13</sub>H<sub>10</sub>NS [M+H]<sup>+</sup>: 212.0530, found: 212.0528.

The spectral data were in accordance with those reported in the literature.<sup>[94]</sup>

### 2-(4-Methoxyphenyl)benzo[*d*]thiazole (**405c**)



1) The **General Procedure F** was followed using benzothiazole **403a** (34 mg, 0.25 mmol), 4-iodoanisole **404c** (293 mg, 1.25 mmol), **406** (30 mg, 11 mol %) and LiOtBu (60 mg, 0.75 mmol) in Et<sub>2</sub>O (0.5 mL). Purification by column chromatography on silica gel (*n*-hexane/EtOAc: 70/1) yielded **405c** (47.7 mg, 79%) as a light yellow solid.

2) The **General Procedure H** was followed using benzothiazole **403a** (34 mg, 0.25 mmol), 4-bromoanisole **447c** (293 mg, 1.25 mmol), **406** (30 mg, 11 mol %) and Cs<sub>2</sub>CO<sub>3</sub> (244 mg, 0.75 mmol) in Et<sub>2</sub>O (0.5 mL). Purification by column chromatography on silica gel (*n*-hexane/EtOAc: 70/1) yielded **405c** (25.9 mg, 43%) as a light yellow solid.

**M. p.:** 134 °C.

**<sup>1</sup>H NMR** (400 MHz, CDCl<sub>3</sub>):  $\delta$  = 8.04 – 7.98 (m, 3H), 7.86 (ddd,  $J$  = 8.0, 1.3, 0.7 Hz, 1H), 7.45 (ddd,  $J$  = 8.3, 7.2, 1.3 Hz, 1H), 7.33 (ddd,  $J$  = 8.0, 7.2, 1.3 Hz, 1H), 7.01 – 6.94 (m, 2H), 3.86 (s, 3H).

**<sup>13</sup>C NMR** (100 MHz, CDCl<sub>3</sub>):  $\delta$  = 167.8 (C<sub>q</sub>), 161.9 (C<sub>q</sub>), 154.2 (C<sub>q</sub>), 134.8 (C<sub>q</sub>), 129.1 (CH), 126.4 (C<sub>q</sub>), 126.2 (CH), 124.8 (CH), 122.8 (CH), 121.5 (CH), 114.4 (CH), 55.5 (CH<sub>3</sub>).

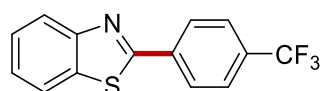
**IR** (ATR): 3061, 2994, 2836, 1604, 1483, 1434, 1256, 1225, 1171, 1027 cm<sup>-1</sup>.

**MS** (ESI)  $m/z$  (relative intensity): 242 (100) [M+H]<sup>+</sup>, 264 (30) [M+Na]<sup>+</sup>.

**HR-MS** (ESI):  $m/z$  calcd for C<sub>14</sub>H<sub>12</sub>NOS [M+H]<sup>+</sup>: 242.0635, found: 242.0634.

The spectral data were in accordance with those reported in the literature.<sup>[94]</sup>

### 2-(4-(Trifluoromethyl)phenyl)benzo[d]thiazole (**405d**)



The **General Procedure F** was followed using benzothiazole **403a** (34 mg, 0.25 mmol), 1-iodo-4-(trifluoromethyl)benzene **404d** (340 mg, 1.25 mmol), **406** (30 mg, 11 mol %) and LiOtBu (60 mg, 0.75 mmol) in Et<sub>2</sub>O (0.5 mL). Purification by column chromatography on silica gel (*n*-hexane/EtOAc: 70/1) yielded **405f** (64.9 mg, 93%) as a light yellow solid.

**M. p.:** 161 °C.

**<sup>1</sup>H NMR** (400 MHz, CDCl<sub>3</sub>):  $\delta$  = 8.22 – 8.14 (m, 2H), 8.09 (ddd,  $J$  = 8.0, 1.2, 0.7 Hz, 1H), 7.91 (ddd,  $J$  = 8.0, 1.2, 0.7 Hz, 1H), 7.76 – 7.69 (m, 2H), 7.51 (ddd,  $J$  = 8.2, 7.2, 1.2 Hz, 1H), 7.41 (ddd,  $J$  = 8.2, 7.2, 1.2 Hz, 1H).

**<sup>13</sup>C NMR** (100 MHz, CDCl<sub>3</sub>):  $\delta$  = 166.0 (C<sub>q</sub>), 154.0 (C<sub>q</sub>), 136.8 (d,  $J_{C-F}$  = 2 Hz, C<sub>q</sub>), 135.2 (C<sub>q</sub>), 132.4 (q,  $J_{C-F}$  = 33 Hz, C<sub>q</sub>), 127.8 (CH), 126.6 (CH), 126.0 (q,  $J_{C-F}$  = 4 Hz, CH), 125.8 (CH), 123.8 (d,  $J_{C-F}$  = 272 Hz, C<sub>q</sub>), 123.6 (CH), 121.7 (CH).

**<sup>19</sup>F NMR** (282 MHz, CDCl<sub>3</sub>):  $\delta$  = -62.86 (s).

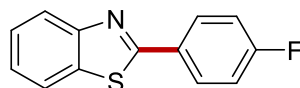
**IR** (ATR): 3072, 1324, 1214, 1132, 1067, 970, 847, 744, 668, 624 cm<sup>-1</sup>.

**MS** (ESI)  $m/z$  (relative intensity): 280 (100) [M+H]<sup>+</sup>.

**HR-MS** (ESI):  $m/z$  calcd for C<sub>14</sub>H<sub>9</sub>F<sub>3</sub>NS [M+H]<sup>+</sup>: 280.0403, found: 280.0402.

The spectral data were in accordance with those reported in the literature.<sup>[94]</sup>

### 2-(4-Fluorophenyl)benzo[d]thiazole (**405e**)



The **General Procedure F** was followed using benzothiazole **403a** (34 mg, 0.25 mmol), 1-fluoro-4-iodobenzene **404e** (278 mg, 1.25 mmol), **406** (30 mg, 11 mol %) and LiOtBu (60 mg, 0.75 mmol) in Et<sub>2</sub>O (0.5 mL). Purification by column chromatography on silica gel (*n*-hexane/EtOAc: 70/1) yielded **405e** (54.5 mg, 95%) as a light yellow solid.

**M. p.:** 101 °C.

**<sup>1</sup>H NMR** (500 MHz, CDCl<sub>3</sub>):  $\delta$  = 8.10 – 8.01 (m, 3H), 7.88 (ddd,  $J$  = 7.9, 1.2, 0.6 Hz, 1H), 7.48 (ddd,  $J$  = 8.3, 7.2, 1.2 Hz, 1H), 7.37 (ddd,  $J$  = 8.3, 7.2, 1.2 Hz, 1H), 7.20 – 7.11 (m, 2H).

**<sup>13</sup>C NMR** (125 MHz, CDCl<sub>3</sub>):  $\delta$  = 166.7 (C<sub>q</sub>), 164.4 (d,  $J_{C-F}$  = 252 Hz, C<sub>q</sub>), 154.1 (C<sub>q</sub>), 135.0 (C<sub>q</sub>), 129.9 (d,  $J_{C-F}$  = 3 Hz, C<sub>q</sub>), 129.49 (d,  $J_{C-F}$  = 9 Hz, CH), 126.39 (CH), 125.22 (CH), 123.16 (CH), 121.59 (CH), 116.13 (d,  $J_{C-F}$  = 22 Hz, CH).

**<sup>19</sup>F NMR** (282 MHz, CDCl<sub>3</sub>)  $\delta$  –108.94 (tt,  $J$  = 8.5, 5.3 Hz).

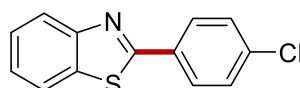
**IR** (ATR): 3063, 1602, 1519, 1481, 1434, 1314, 1250, 1097, 967, 831 cm<sup>-1</sup>.

**MS** (ESI)  $m/z$  (relative intensity): 230 (100) [M+H]<sup>+</sup>.

**HR-MS** (ESI):  $m/z$  calcd for C<sub>13</sub>H<sub>9</sub>FNS [M+H]<sup>+</sup>: 230.0436, found: 230.0434.

The spectral data were in accordance with those reported in the literature.<sup>[269]</sup>

### 2-(4-Chlorophenyl)benzo[d]thiazole (**405f**)



The **General Procedure F** was followed using benzothiazole **403a** (34 mg, 0.25 mmol), 1-chloro-4-iodobenzene **404f** (298 mg, 1.25 mmol), **406** (30 mg, 11 mol %) and LiOtBu (60 mg, 0.75 mmol) in Et<sub>2</sub>O (0.5 mL). Purification by column chromatography on silica gel (*n*-hexane/EtOAc: 70/1) yielded **405f** (56.5 mg, 92%) as a light yellow solid.

**M. p.:** 112 °C.

**<sup>1</sup>H NMR** (500 MHz, CDCl<sub>3</sub>):  $\delta$  = 8.05 (dt,  $J$  = 8.2, 0.8 Hz, 1H), 8.02 – 7.98 (m, 2H), 7.88 (ddd,  $J$  = 8.2, 0.8, 0.8 Hz, 1H), 7.48 (ddd,  $J$  = 8.2, 7.2, 1.2 Hz, 1H), 7.46 – 7.43 (m, 2H), 7.38 (ddd,  $J$  = 8.2, 7.2, 1.2 Hz, 1H).

**<sup>13</sup>C NMR** (125 MHz, CDCl<sub>3</sub>):  $\delta$  = 166.6 (C<sub>q</sub>), 154.0 (C<sub>q</sub>), 137.0 (C<sub>q</sub>), 135.0 (C<sub>q</sub>), 132.1 (C<sub>q</sub>), 129.2 (CH), 128.7 (CH), 126.5 (CH), 125.4 (CH), 123.3 (CH), 121.6 (CH).

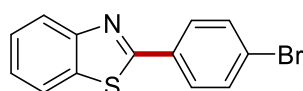
**IR** (ATR): 3062, 1590, 1474, 1433, 1399, 1314, 1287, 1225, 1091, 1015, 389 cm<sup>-1</sup>.

**MS** (ESI)  $m/z$  (relative intensity): 246 (100) [M+H]<sup>+</sup>.

**HR-MS** (ESI):  $m/z$  calcd for C<sub>13</sub>H<sub>9</sub>ClNS [M+H]<sup>+</sup>: 246.0139, found: 246.0139.

The spectral data were in accordance with those reported in the literature.<sup>[268]</sup>

### 2-(4-Bromophenyl)benzo[d]thiazole (**405g**)



The **General Procedure F** was followed using benzothiazole **403a** (34 mg, 0.25 mmol), 1-bromo-4-iodobenzene **404g** (354 mg, 1.25 mmol), **406** (30 mg, 11 mol %) and LiOtBu (60 mg, 0.75 mmol) in Et<sub>2</sub>O (0.5 mL). Purification by column chromatography on silica gel (*n*-hexane/EtOAc: 70/1) yielded **405g** (66.0 mg, 91%) as a light yellow solid.

**M. p.:** 132 °C.

**<sup>1</sup>H NMR** (500 MHz, CDCl<sub>3</sub>):  $\delta$  = 8.05 (dt,  $J$  = 8.2, 0.9 Hz, 1H), 7.94 – 7.89 (m, 2H), 7.86 (ddd,  $J$  = 8.2, 0.9, 0.9 Hz, 1H), 7.61 – 7.57 (m, 2H), 7.48 (ddd,  $J$  = 8.2, 7.2, 1.2 Hz, 1H), 7.37 (ddd,  $J$  = 8.2, 7.2, 1.2 Hz, 1H).

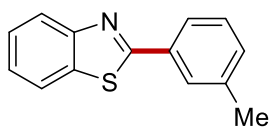
**<sup>13</sup>C NMR** (125 MHz, CDCl<sub>3</sub>):  $\delta$  = 166.6 (C<sub>q</sub>), 154.0 (C<sub>q</sub>), 135.0 (C<sub>q</sub>), 132.4(C<sub>q</sub>), 132.1 (CH), 128.8 (CH), 126.4 (CH), 125.4 (CH), 125.4 (C<sub>q</sub>), 123.2 (CH), 121.6 (CH).

**IR** (ATR): 3016, 1574, 1433, 1314, 1215, 1102, 1068, 820, 752, 683, 481 cm<sup>-1</sup>.

**MS** (ESI)  $m/z$  (relative intensity): 289 (100) (<sup>79</sup>Br) [M+H]<sup>+</sup>, 291 (100) (<sup>81</sup>Br) [M+H]<sup>+</sup>.

**HR-MS** (ESI):  $m/z$  calcd for C<sub>13</sub>H<sub>9</sub><sup>79</sup>BrNS [M+H]<sup>+</sup>: 289.9635, found: 289.9634.

The spectral data were in accordance with those reported in the literature.<sup>[269]</sup>

**2-(*m*-Tolyl)benzo[*d*]thiazole (405h)**

The **General Procedure F** was followed using benzothiazole **403a** (34 mg, 0.25 mmol), 1-iodo-3-methylbenzene **404h** (273 mg, 1.25 mmol), **406** (30 mg, 11 mol %) and LiOtBu (60 mg, 0.75 mmol) in Et<sub>2</sub>O (0.5 mL). Purification by column chromatography on silica gel (*n*-hexane/EtOAc: 70/1) yielded **405h** (52.9 mg, 94%) as a light yellow solid.

**M. p.:** 63 °C.

**<sup>1</sup>H NMR** (400 MHz, CDCl<sub>3</sub>): δ = 8.06 (dd, *J* = 8.2, 1.2 Hz, 1H), 7.96 – 7.90 (m, 1H), 7.89 (dd, *J* = 8.0, 1.2 Hz, 1H), 7.90 – 7.81 (m, 1H), 7.48 (ddd, *J* = 8.3, 7.2, 1.2 Hz, 1H), 7.37 (ddd, *J* = 7.8, 7.2, 1.2 Hz, 2H), 7.33 – 7.25 (m, 1H), 2.44 (s, 3H).

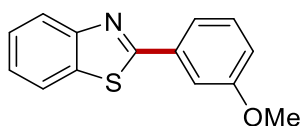
**<sup>13</sup>C NMR** (100 MHz, CDCl<sub>3</sub>): δ = 168.3 (C<sub>q</sub>), 154.1 (C<sub>q</sub>), 138.8 (C<sub>q</sub>), 135.0 (C<sub>q</sub>), 133.5 (C<sub>q</sub>), 131.8 (CH), 128.9 (CH), 128.0 (CH), 126.3 (CH), 125.1 (CH), 124.8 (CH), 123.1 (CH), 121.6 (CH), 21.3 (CH<sub>3</sub>).

**IR** (ATR): 3056, 2919, 1606, 1557, 1471, 1378, 1312, 1238, 1171, 1092, 1014 cm<sup>-1</sup>.

**MS** (ESI) *m/z* (relative intensity): 226 (100) [M+H]<sup>+</sup>, 248 (10) [M+Na]<sup>+</sup>.

**HR-MS** (ESI): *m/z* calcd for C<sub>14</sub>H<sub>12</sub>NS [M+H]<sup>+</sup>: 226.0683, found: 226.0685.

The spectral data were in accordance with those reported in the literature.<sup>[268]</sup>

**2-(3-Methoxyphenyl)benzo[*d*]thiazole (405i)**

The **General Procedure F** was followed using benzothiazole **403a** (34 mg, 0.25 mmol), 1-iodo-3-methoxybenzene **404i** (293 mg, 1.25 mmol), **406** (30 mg, 11 mol %) and LiOtBu (60 mg, 0.75 mmol) in Et<sub>2</sub>O (0.5 mL). Purification by column chromatography on silica gel (*n*-hexane/EtOAc: 70/1) yielded **405i** (45.8 mg, 76%) as a light yellow solid.

**M. p.:** 82 °C.

**<sup>1</sup>H NMR** (400 MHz, CDCl<sub>3</sub>): δ = 8.06 (ddd, *J* = 8.3, 1.3, 0.6 Hz, 1H), 7.88 (ddd, *J* = 8.0, 1.3, 0.7 Hz,

<sup>1</sup>H), 7.66 (dd,  $J = 2.6, 1.6$  Hz, 1H), 7.63 (ddd,  $J = 7.6, 1.6, 0.9$  Hz, 1H), 7.48 (ddd,  $J = 8.3, 7.2, 1.3$  Hz, 1H), 7.41 – 7.34 (m, 2H), 7.03 (ddd,  $J = 8.3, 2.6, 0.9$  Hz, 1H), 3.90 (s, 3H).

<sup>13</sup>C NMR (100 MHz, CDCl<sub>3</sub>):  $\delta = 167.9$  (C<sub>q</sub>), 160.0 (C<sub>q</sub>), 154.0 (C<sub>q</sub>), 135.1 (C<sub>q</sub>), 134.9 (C<sub>q</sub>), 130.0 (CH), 126.3 (CH), 125.2 (CH), 123.2 (CH), 121.6 (CH), 120.2 (CH), 117.3 (CH), 112.0 (CH), 55.5 (CH<sub>3</sub>).

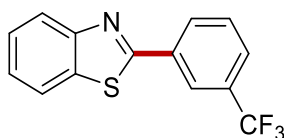
IR (ATR): 3066, 2932, 2834, 2160, 2039, 1582, 1484, 1433, 1287, 1008, 758 cm<sup>-1</sup>.

MS (ESI)  $m/z$  (relative intensity): 242 (100) [M+H]<sup>+</sup>, 264 (35) [M+Na]<sup>+</sup>.

HR-MS (ESI):  $m/z$  calcd for C<sub>14</sub>H<sub>12</sub>NOS [M+H]<sup>+</sup>: 242.0637, found: 242.0634.

The spectral data were in accordance with those reported in the literature.<sup>[268]</sup>

### 2-[3-(Trifluoromethyl)phenyl]benzo[d]thiazole (**405j**)



The **General Procedure F** was followed using benzothiazole **403a** (34 mg, 0.25 mmol), 1-iodo-3-(trifluoromethyl)benzene **404j** (340 mg, 1.25 mmol), **406** (30 mg, 11 mol %) and LiOtBu (60 mg, 0.75 mmol) in Et<sub>2</sub>O (0.5 mL). Purification by column chromatography on silica gel (*n*-hexane/EtOAc: 70/1) yielded **405j** (53.0 mg, 76%) as a light yellow solid.

**M. p.:** 87 °C.

<sup>1</sup>H NMR (400 MHz, CDCl<sub>3</sub>):  $\delta = 8.38 - 8.34$  (m, 1H), 8.23 (ddd,  $J = 7.2, 1.3, 0.7$  Hz, 1H), 8.09 (ddd,  $J = 8.2, 1.3, 0.7$  Hz, 1H), 7.91 (ddd,  $J = 8.0, 1.3, 0.7$  Hz, 1H), 7.73 (ddd,  $J = 7.8, 1.3, 0.7$  Hz, 1H), 7.61 (ddd,  $J = 7.8, 1.3, 0.7$  Hz, 1H), 7.51 (ddd,  $J = 8.2, 7.2, 1.3$  Hz, 1H), 7.41 (ddd,  $J = 8.0, 7.2, 1.3$  Hz, 1H).

<sup>13</sup>C NMR (100 MHz, CDCl<sub>3</sub>):  $\delta = 166.1$  (C<sub>q</sub>), 154.0 (C<sub>q</sub>), 135.1 (C<sub>q</sub>), 134.4 (C<sub>q</sub>), 131.6 (q,  $J_{C-F} = 32$  Hz, C<sub>q</sub>), 130.7 (CH), 129.6 (CH), 127.3 (q,  $J_{C-F} = 4$  Hz, CH), 126.6 (CH), 125.7 (CH), 124.2 (q,  $J_{C-F} = 4$  Hz, CH), 123.8 (d,  $J_{C-F} = 273$  Hz, C<sub>q</sub>), 123.5 (CH), 121.7 (CH).

<sup>19</sup>F NMR (282 MHz, CDCl<sub>3</sub>):  $\delta = -62.76$  (s).

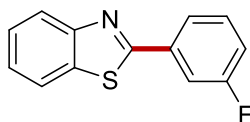
IR (ATR): 3066, 2923, 1613, 1584, 1479, 1442, 1257, 1152, 1076, 937, 880 cm<sup>-1</sup>.

MS (ESI)  $m/z$  (relative intensity): 280 (100) [M+H]<sup>+</sup>.

**HR-MS** (ESI):  $m/z$  calcd for  $C_{14}H_9F_3NS$   $[M+H]^+$ : 280.0403, found: 280.0402.

The spectral data were in accordance with those reported in the literature.<sup>[268]</sup>

### 2-(3-Fluorophenyl)benzo[d]thiazole (405k)



The **General Procedure F** was followed using benzothiazole **403a** (34 mg, 0.25 mmol), 1-fluoro-3-iodobenzene **404k** (278 mg, 1.25 mmol), **406** (30 mg, 11 mol %) and LiOtBu (60 mg, 0.75 mmol) in Et<sub>2</sub>O (0.5 mL). Purification by column chromatography on silica gel (*n*-hexane/EtOAc: 70/1) yielded **405k** (52.2 mg, 91%) as a light yellow solid.

**M. p.**: 72 °C.

**<sup>1</sup>H NMR** (500 MHz, CDCl<sub>3</sub>):  $\delta$  = 8.07 (dd,  $J$  = 8.2, 0.8 Hz, 1H), 7.89 (dd,  $J$  = 8.0, 0.8 Hz, 1H), 7.86 – 7.79 (m, 2H), 7.49 (ddd,  $J$  = 8.2, 7.2, 1.2 Hz, 1H), 7.44 (ddd,  $J$  = 8.2, 8.0, 5.7 Hz, 1H), 7.39 (ddd,  $J$  = 8.2, 7.2, 1.2 Hz, 1H), 7.17 (ddd,  $J$  = 8.2, 2.6, 1.2 Hz, 1H).

**<sup>13</sup>C NMR** (125 MHz, CDCl<sub>3</sub>):  $\delta$  = 166.4 (d,  $J_{C-F}$  = 3 Hz, C<sub>q</sub>), 163.0 (d,  $J_{C-F}$  = 247 Hz, C<sub>q</sub>), 153.9 (C<sub>q</sub>), 135.6 (d,  $J_{C-F}$  = 8 Hz, C<sub>q</sub>), 135.0 (C<sub>q</sub>), 130.6 (d,  $J_{C-F}$  = 8 Hz, CH), 126.5 (CH), 125.5 (CH), 123.4 (CH), 123.3 (d,  $J_{C-F}$  = 3 Hz, CH), 121.6 (CH), 117.8 (d,  $J_{C-F}$  = 21 Hz), 114.26 (d,  $J_{C-F}$  = 24 Hz).

**<sup>19</sup>F NMR** (282 MHz, CDCl<sub>3</sub>):  $\delta$  = -112.02 (ddd,  $J$  = 9.2, 8.5, 5.7 Hz).

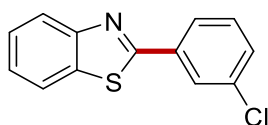
**IR** (ATR): 3053, 2162, 1590, 1457, 1423, 1312, 1230, 1160, 783, 700, 653 cm<sup>-1</sup>.

**MS** (ESI)  $m/z$  (relative intensity): 230 (100)  $[M+H]^+$ .

**HR-MS** (ESI):  $m/z$  calcd for  $C_{13}H_9FNS$   $[M+H]^+$ : 230.0437, found: 230.0435.

The spectral data were in accordance with those reported in the literature.<sup>[268]</sup>

### 2-(3-Chlorophenyl)benzo[d]thiazole (405l)



The **General Procedure F** was followed using benzothiazole **403a** (34 mg, 0.25 mmol), 1-chloro-3-iodobenzene **404l** (298 mg, 1.25 mmol), **406** (30 mg, 11 mol %) and LiOtBu (60 mg, 0.75 mmol) in



Et<sub>2</sub>O (0.5 mL). Purification by column chromatography on silica gel (*n*-hexane/EtOAc: 70/1) yielded **405l** (39.9 mg, 65%) as a light yellow solid.

**M. p.:** 96 °C.

<sup>1</sup>H NMR (500 MHz, CDCl<sub>3</sub>): δ = 8.11 – 8.09 (m, 1H), 8.07 (ddd, *J* = 8.2, 1.2, 0.7 Hz, 1H), 7.93 (ddd, *J* = 8.0, 7.2, 1.2 Hz, 1H), 7.90 (ddd, *J* = 8.0, 1.2, 0.7 Hz, 1H), 7.50 (ddd, *J* = 8.2, 7.2, 1.2 Hz, 1H), 7.46 – 7.37 (m, 3H).

<sup>13</sup>C NMR (125 MHz, CDCl<sub>3</sub>): δ = 166.3 (C<sub>q</sub>), 154.0 (C<sub>q</sub>), 135.2 (C<sub>q</sub>), 135.1 (C<sub>q</sub>), 135.1 (C<sub>q</sub>), 130.8 (CH), 130.2 (CH), 127.4 (CH), 126.5 (CH), 125.7 (CH), 125.5 (CH), 123.4 (CH), 121.7 (CH).

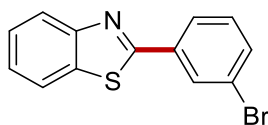
IR (ATR): 3060, 2924, 1693, 1562, 1457, 1312, 1227, 1070, 975, 862, 782 cm<sup>-1</sup>.

MS (ESI) *m/z* (relative intensity): 246 (100) [M+H]<sup>+</sup>.

HR-MS (ESI): *m/z* calcd for C<sub>13</sub>H<sub>9</sub>CINS [M+H]<sup>+</sup>: 246.0140, found: 246.0139.

The spectral data were in accordance with those reported in the literature.<sup>[268]</sup>

### 2-(3-Bromophenyl)benzo[d]thiazole (**405m**)



The **General Procedure F** was followed using benzothiazole **403a** (34 mg, 0.25 mmol), 1-bromo-3-iodobenzene **404m** (354 mg, 1.25 mmol), **406** (30 mg, 11 mol %) and LiOtBu (60 mg, 0.75 mmol) in Et<sub>2</sub>O (0.5 mL). Purification by column chromatography on silica gel (*n*-hexane/EtOAc: 70/1) yielded **405m** (42.8 mg, 59%) as a light yellow solid.

**M. p.:** 88 °C.

<sup>1</sup>H NMR (500 MHz, CDCl<sub>3</sub>): δ = 8.27 – 8.25 (m, 1H), 8.06 (ddd, *J* = 8.0, 0.9 Hz, 1H), 7.97 (ddd, *J* = 7.8, 1.7, 0.9 Hz, 1H), 7.90 (ddd, *J* = 8.0, 1.2, 0.9 Hz, 1H), 7.60 (ddd, *J* = 8.0, 2.0, 0.9 Hz, 1H), 7.50 (ddd, *J* = 8.2, 7.2, 1.2 Hz, 1H), 7.39 (ddd, *J* = 8.2, 7.2, 1.2 Hz, 1H), 7.34 (dd, *J* = 7.9 Hz, 1H).

<sup>13</sup>C NMR (125 MHz, CDCl<sub>3</sub>): δ = 166.1 (C<sub>q</sub>), 153.9 (C<sub>q</sub>), 135.4 (C<sub>q</sub>), 135.1 (C<sub>q</sub>), 133.8 (CH), 130.5 (CH), 130.2 (CH), 126.5 (CH), 126.1 (CH), 125.6 (CH), 123.4 (CH), 123.2 (C<sub>q</sub>), 121.7 (CH).

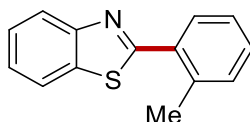
IR (ATR): 3059, 2923, 1601, 1486, 1455, 1224, 1119, 957, 726, 630, 449 cm<sup>-1</sup>.

MS (ESI) *m/z* (relative intensity): 289 (100) (<sup>79</sup>Br) [M+H]<sup>+</sup>, 291 (100) (<sup>81</sup>Br) [M+H]<sup>+</sup>.

**HR-MS** (ESI):  $m/z$  calcd for  $C_{13}H_9^{79}BrNS$   $[M+H]^+$ : 289.9634, found: 289.9634.

The spectral data were in accordance with those reported in the literature.<sup>[270]</sup>

### 2-(*o*-Tolyl)benzo[*d*]thiazole (405n)



The **General Procedure F** was followed using benzothiazole **403a** (34 mg, 0.25 mmol), 1-iodo-2-methylbenzene **404n** (273 mg, 1.25 mmol), **406** (30 mg, 11 mol %) and LiOtBu (60 mg, 0.75 mmol) in Et<sub>2</sub>O (0.5 mL). Purification by column chromatography on silica gel (*n*-hexane/EtOAc: 70/1) yielded **405n** (20.3 mg, 36%) as a yellow oil.

**<sup>1</sup>H NMR** (400 MHz, CDCl<sub>3</sub>):  $\delta$  = 8.09 (ddd,  $J$  = 8.2, 1.2, 0.6 Hz, 1H), 7.92 (ddd,  $J$  = 8.2, 1.2, 0.6 Hz, 1H), 7.74 (dd,  $J$  = 7.4, 1.4 Hz, 1H), 7.49 (ddd,  $J$  = 8.2, 7.4, 1.4 Hz, 1H), 7.42 – 7.37 (m, 1H), 7.37 – 7.27 (m, 3H), 2.64 (s, 3H).

**<sup>13</sup>C NMR** (100 MHz, CDCl<sub>3</sub>):  $\delta$  = 168.0 (C<sub>q</sub>), 153.7 (C<sub>q</sub>), 137.2 (C<sub>q</sub>), 135.6 (C<sub>q</sub>), 133.1 (C<sub>q</sub>), 131.5 (CH), 130.5 (CH), 130.0 (CH), 126.1 (CH), 126.1 (CH), 125.1 (CH), 123.4 (CH), 121.3 (CH), 21.3 (CH<sub>3</sub>).

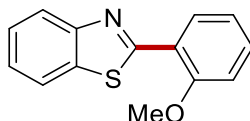
**IR** (ATR): 2924, 2838, 2612, 1977, 1571, 1500, 1115, 1021, 970, 754, 551 cm<sup>-1</sup>.

**MS** (ESI)  $m/z$  (relative intensity): 226 (100)  $[M+H]^+$ , 248 (5)  $[M+Na]^+$ .

**HR-MS** (ESI):  $m/z$  calcd for  $C_{14}H_{12}NO$   $[M+H]^+$ : 226.0686, found: 226.0685.

The spectral data were in accordance with those reported in the literature.<sup>[94]</sup>

### 2-(2-Methoxyphenyl)benzo[*d*]thiazole (405o)



The **General Procedure F** was followed using benzothiazole **403a** (34 mg, 0.25 mmol), 1-iodo-2-methoxybenzene **404o** (293 mg, 1.25 mmol), **406** (30 mg, 11 mol %) and LiOtBu (60 mg, 0.75 mmol) in Et<sub>2</sub>O (0.5 mL). Purification by column chromatography on silica gel (*n*-hexane/EtOAc: 70/1) yielded **405o** (21.7 mg, 36%) as a light yellow solid.

**M. p.:** 108 °C.

**<sup>1</sup>H NMR** (400 MHz, CDCl<sub>3</sub>):  $\delta$  = 8.51 (ddd,  $J$  = 7.9, 1.8, 0.6 Hz, 1H), 8.07 (ddd,  $J$  = 8.2, 1.1, 0.6 Hz, 1H), 7.91 (ddd,  $J$  = 7.9, 1.1, 0.6 Hz, 1H), 7.50 – 7.41 (m, 2H), 7.38 – 7.32 (m, 1H), 7.12 (ddd,  $J$  = 7.9, 7.3, 1.1 Hz, 1H), 7.06 (dd,  $J$  = 8.2, 1.1 Hz, 1H), 4.05 (s, 3H).

**<sup>13</sup>C NMR** (100 MHz, CDCl<sub>3</sub>):  $\delta$  = 163.1 (C<sub>q</sub>), 157.2 (C<sub>q</sub>), 152.2 (C<sub>q</sub>), 136.1 (C<sub>q</sub>), 131.7 (CH), 129.6 (CH), 125.9 (CH), 124.6 (CH), 124.1 (CH), 122.8 (CH), 122.3 (C<sub>q</sub>), 121.2 (CH), 111.7 (CH), 55.7 (CH<sub>3</sub>).

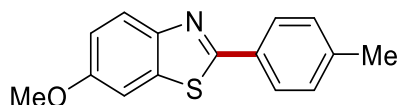
**IR** (ATR): 3007, 2971, 1893, 1519, 1181, 1122, 1054, 964, 825, 587, 416 cm<sup>-1</sup>.

**MS** (ESI)  $m/z$  (relative intensity): 242 (100) [M+H]<sup>+</sup>, 264 (30) [M+Na]<sup>+</sup>.

**HR-MS** (ESI):  $m/z$  calcd for C<sub>14</sub>H<sub>12</sub>NOS [M+H]<sup>+</sup>: 242.0637, found: 242.0635.

The spectral data were in accordance with those reported in the literature.<sup>[281]</sup>

#### 6-Methoxy-2-(*p*-tolyl)benzo[*d*]thiazole (**405p**)



The **General Procedure F** was followed using 6-methoxybenzo[*d*]thiazole **403b** (41 mg, 0.25 mmol), 4-iodotoluene **404a** (273 mg, 1.25 mmol), **406** (30 mg, 11 mol %) and LiOtBu (60 mg, 0.75 mmol) in Et<sub>2</sub>O (0.5 mL). Purification by column chromatography on silica gel (*n*-hexane/EtOAc: 70/1) yielded **405p** (35.1 mg, 55%) as a light yellow solid.

**M. p.:** 115 °C.

**<sup>1</sup>H NMR** (400 MHz, CDCl<sub>3</sub>):  $\delta$  = 7.93 – 7.88 (m, 3H), 7.33 – 7.30 (m, 1H), 7.28 – 7.23 (m, 2H), 7.06 (dd,  $J$  = 8.9, 2.6 Hz, 1H), 3.86 (s, 3H), 2.39 (s, 3H).

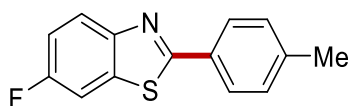
**<sup>13</sup>C NMR** (100 MHz, CDCl<sub>3</sub>):  $\delta$  = 165.7 (C<sub>q</sub>), 157.6 (C<sub>q</sub>), 148.7 (C<sub>q</sub>), 140.9 (C<sub>q</sub>), 136.2 (C<sub>q</sub>), 131.1 (C<sub>q</sub>), 129.6 (CH), 127.1 (CH), 123.5 (CH), 115.4 (CH), 104.2 (CH), 55.7 (CH<sub>3</sub>), 21.4 (CH<sub>3</sub>).

**IR** (ATR): 3020, 1606, 1488, 1411, 1321, 1119, 968, 903, 747, 667, 479 cm<sup>-1</sup>.

**MS** (ESI)  $m/z$  (relative intensity): 256 (100) [M+H]<sup>+</sup>.

**HR-MS** (ESI):  $m/z$  calcd for C<sub>15</sub>H<sub>14</sub>NOS [M+H]<sup>+</sup>: 256.0795, found: 256.0793.

The spectral data were in accordance with those reported in the literature.<sup>[281]</sup>

**6-Fluoro-2-(*p*-tolyl)benzo[*d*]thiazole (405q)**

The **General Procedure F** was followed using 6-fluorobenzo[*d*]thiazole **403c** (38 mg, 0.25 mmol), 4-iodotoluene **404a** (273 mg, 1.25 mmol), **406** (30 mg, 11 mol %) and LiOtBu (60 mg, 0.75 mmol) in Et<sub>2</sub>O (0.5 mL). Purification by column chromatography on silica gel (*n*-hexane/EtOAc: 70/1) yielded **405q** (57.8 mg, 95%) as a light yellow solid.

**M. p.:** 149 °C.

**<sup>1</sup>H NMR** (400 MHz, CDCl<sub>3</sub>): δ = 7.96 (dd, *J* = 8.9, 4.9 Hz, 2H), 7.96 – 7.87 (m, 3H), 7.53 (ddd, *J* = 8.1, 2.7, 0.5 Hz, 1H), 7.31 – 7.23 (m, 2H), 7.19 (dd, *J* = 8.9, 2.7 Hz, 1H), 2.43 – 2.37 (m, 3H).

**<sup>13</sup>C NMR** (100 MHz, CDCl<sub>3</sub>): δ = 167.9 (C<sub>q</sub>), 160.3 (d, *J*<sub>C-F</sub> = 245 Hz, C<sub>q</sub>), 150.8 (C<sub>q</sub>), 141.45 (C<sub>q</sub>), 135.87 (d, *J*<sub>C-F</sub> = 11.2 Hz, C<sub>q</sub>), 130.66 (C<sub>q</sub>), 129.71 (CH), 127.31 (CH), 123.86 (d, *J*<sub>C-F</sub> = 9.3 Hz, CH), 114.76 (d, *J*<sub>C-F</sub> = 24.6 Hz, CH), 107.74 (d, *J*<sub>C-F</sub> = 26.7 Hz, CH), 21.47 (CH<sub>3</sub>).

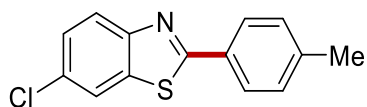
**<sup>19</sup>F NMR** (282 MHz, CDCl<sub>3</sub>): δ = -116.20 (td, *J* = 8.5, 4.8 Hz).

**IR** (ATR): 2916, 2161, 1483, 1441, 1307, 1050, 867, 816, 761, 694, 491 cm<sup>-1</sup>.

**MS** (ESI) *m/z* (relative intensity): 244 (100) [M+H]<sup>+</sup>.

**HR-MS** (ESI): *m/z* calcd for C<sub>14</sub>H<sub>11</sub>FNS [M+H]<sup>+</sup>: 244.0593, found: 244.0591.

The spectral data were in accordance with those reported in the literature.<sup>[281]</sup>

**6-Chloro-2-(*p*-tolyl)benzo[*d*]thiazole (405r)**

The **General Procedure F** was followed using 6-chlorobenzo[*d*]thiazole **403d** (42 mg, 0.25 mmol), 4-iodotoluene **404a** (273 mg, 1.25 mmol), **406** (30 mg, 11 mol %) and LiOtBu (60 mg, 0.75 mmol) in Et<sub>2</sub>O (0.5 mL). Purification by column chromatography on silica gel (*n*-hexane/EtOAc: 70/1) yielded **405r** (55.8 mg, 86%) as a light yellow solid.

**M. p.:** 160 °C.

**<sup>1</sup>H NMR** (400 MHz, CDCl<sub>3</sub>): δ = 7.95 – 7.89 (m, 3H), 7.83 (dd, *J* = 2.1, 0.5 Hz, 1H), 7.41 (dd, *J* = 8.7,

2.1 Hz, 1H), 7.30 – 7.25 (m, 2H), 2.41 (s, 3H).

<sup>13</sup>C NMR (100 MHz, CDCl<sub>3</sub>):  $\delta$  = 168.7 (C<sub>q</sub>), 152.7 (C<sub>q</sub>), 141.7 (C<sub>q</sub>), 136.1 (C<sub>q</sub>), 130.8 (C<sub>q</sub>), 130.5 (C<sub>q</sub>), 129.8 (CH), 127.4 (CH), 127.0 (CH), 123.7 (CH), 121.1 (CH), 21.5 (CH<sub>3</sub>).

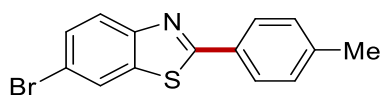
IR (ATR): 2916, 1934, 1585, 1483, 1437, 1304, 1181, 1087, 963, 816, 561 cm<sup>-1</sup>.

MS (ESI) *m/z* (relative intensity): 260 (100) [M+H]<sup>+</sup>.

HR-MS (ESI): *m/z* calcd for C<sub>14</sub>H<sub>11</sub>ClNS [M+H]<sup>+</sup>: 260.0296, found: 260.0295.

The spectral data were in accordance with those reported in the literature.<sup>[272]</sup>

### 6-Bromo-2-(*p*-tolyl)benzo[*d*]thiazole (405r)



The **General Procedure F** was followed using 6-bromobenzo[*d*]thiazole **403e** (53 mg, 0.25 mmol), 4-iodotoluene **404a** (273 mg, 1.25 mmol), **406** (30 mg, 11 mol %) and LiOtBu (60 mg, 0.75 mmol) in Et<sub>2</sub>O (0.5 mL). Purification by column chromatography on silica gel (*n*-hexane/EtOAc: 70/1) yielded **405r** (50.2 mg, 66%) as a light yellow solid.

**M. p.:** 152 °C.

<sup>1</sup>H NMR (400 MHz, CDCl<sub>3</sub>):  $\delta$  = 8.00 (dd, *J* = 2.0, 0.5 Hz, 1H), 7.96 – 7.92 (m, 2H), 7.87 (dd, *J* = 8.7, 0.5 Hz, 1H), 7.58 – 7.53 (m, 1H), 7.31 – 7.25 (m, 2H), 2.41 (s, 3H).

<sup>13</sup>C NMR (100 MHz, CDCl<sub>3</sub>):  $\delta$  = 168.7 (C<sub>q</sub>), 153.0 (C<sub>q</sub>), 141.8 (C<sub>q</sub>), 136.6 (C<sub>q</sub>), 130.5 (C<sub>q</sub>), 129.8 (CH), 129.7 (CH), 127.5 (CH), 124.1 (CH), 124.1 (CH), 118.5 (C<sub>q</sub>), 21.5 (CH<sub>3</sub>).

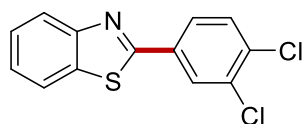
IR (ATR): 3061, 1621, 1508, 1459, 1313, 1219, 1126, 1020, 694, 877, 802 cm<sup>-1</sup>.

MS (ESI) *m/z* (relative intensity): 303 (100) (<sup>79</sup>Br) [M+H]<sup>+</sup>, 305 (100) (<sup>81</sup>Br) [M+H]<sup>+</sup>.

HR-MS (ESI): *m/z* calcd for C<sub>14</sub>H<sub>11</sub><sup>79</sup>BrNS [M+H]<sup>+</sup>: 303.9792, found: 303.9790.

The spectral data were in accordance with those reported in the literature.<sup>[273]</sup>

### 2-(3,4-Dichlorophenyl)benzo[*d*]thiazole (405t)



The **General Procedure F** was followed using benzothiazole **403a** (mg, 0.25 mmol), 1,2-dichloro-4-iodobenzene **404p** (341 mg, 1.25 mmol), **406** (30 mg, 11 mol %) and LiOtBu (60 mg, 0.75 mmol) in Et<sub>2</sub>O (0.5 mL). Purification by column chromatography on silica gel (*n*-hexane/EtOAc: 70/1) yielded **405t** (37.1 mg, 53%) as a light yellow solid.

**M. p.:** 108 °C.

**<sup>1</sup>H NMR** (500 MHz, CDCl<sub>3</sub>):  $\delta$  = 8.19 (d,  $J$  = 2.1 Hz, 1H), 8.05 (dd,  $J$  = 8.3, 0.9 Hz, 1H), 7.91 – 7.85 (m, 2H), 7.54 (d,  $J$  = 8.3 Hz, 1H), 7.50 (ddd,  $J$  = 8.3, 7.2, 1.2 Hz, 1H), 7.40 (ddd,  $J$  = 8.3, 7.2, 1.2 Hz, 1H).

**<sup>13</sup>C NMR** (125 MHz, CDCl<sub>3</sub>):  $\delta$  = 165.1 (C<sub>q</sub>), 153.9 (C<sub>q</sub>), 135.1 (C<sub>q</sub>), 135.0 (C<sub>q</sub>), 133.5 (C<sub>q</sub>), 133.4 (C<sub>q</sub>), 131.0 (CH), 129.0 (CH), 126.7 (CH), 126.5 (CH), 125.7 (CH), 123.5 (CH), 121.7 (CH).

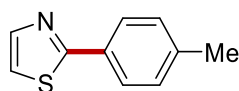
**IR** (ATR): 2919, 1621, 1555, 1500, 1451, 1215, 1109, 1054, 821, 742, 640 cm<sup>-1</sup>.

**MS** (ESI)  $m/z$  (relative intensity): 279 (100) [M+H]<sup>+</sup>.

**HR-MS** (ESI):  $m/z$  calcd for C<sub>13</sub>H<sub>8</sub>Cl<sub>2</sub>NS [M+H]<sup>+</sup>: 279.9748, found: 279.9749.

The spectral data were in accordance with those reported in the literature.<sup>[275]</sup>

### 2-(*p*-Tolyl)thiazole (**405u**)



The **General Procedure F** was followed using thiazole **403f** (21 mg, 0.25 mmol), 4-iodotoluene **404a** (273 mg, 1.25 mmol), **404a** (30 mg, 11 mol %) and LiOtBu (60 mg, 0.75 mmol) in Et<sub>2</sub>O (0.5 mL). Purification by column chromatography on silica gel (*n*-hexane/EtOAc: 70/1) yielded **405u** (37.7 mg, 86%) as a yellow oil.

**<sup>1</sup>H NMR** (500 MHz, CDCl<sub>3</sub>):  $\delta$  = 7.87 – 7.83 (m, 2H), 7.82 (d,  $J$  = 3.3 Hz, 1H), 7.26 (d,  $J$  = 3.3 Hz, 1H), 7.24 – 7.20 (m, 2H), 2.37 (s, 3H).

**<sup>13</sup>C NMR** (125 MHz, CDCl<sub>3</sub>):  $\delta$  = 168.6 (C<sub>q</sub>), 143.5 (CH), 140.2 (C<sub>q</sub>), 130.9 (C<sub>q</sub>), 129.6 (CH), 126.4 (CH), 118.3 (CH), 21.4 (CH<sub>3</sub>).

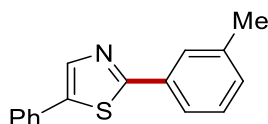
**IR** (ATR): 3067, 1613, 1473, 1328, 1162, 1068, 970, 807, 648, 546 cm<sup>-1</sup>.

**MS** (ESI)  $m/z$  (relative intensity): 176 (100) [M+H]<sup>+</sup>.

**HR-MS** (ESI):  $m/z$  calcd for  $C_{10}H_{10}NS$   $[M+H]^+$ : 176.0529, found: 176.0528.

The spectral data were in accordance with those reported in the literature.<sup>[278]</sup>

#### 5-Phenyl-2-(*m*-tolyl)thiazole (**405w**)



The **General Procedure F** was followed using 5-phenylthiazole **403g** (40 mg, 0.25 mmol), 3-iodotoluene **404h** (273 mg, 1.25 mmol), **406** (30 mg, 11 mol %) and LiOtBu (60 mg, 0.75 mmol) in Et<sub>2</sub>O (0.5 mL). Purification by column chromatography on silica gel (*n*-hexane/EtOAc: 70/1) yielded **405w** (52.2 mg, 83%) as a light yellow solid.

**M. p.:** 101 °C.

**<sup>1</sup>H NMR** (300 MHz, CDCl<sub>3</sub>):  $\delta$  = 8.00 (s, 1H), 7.82 – 7.79 (m, 1H), 7.74 (ddd,  $J$  = 7.7, 1.8, 1.2 Hz, 1H), 7.62 – 7.59 (m, 1H), 7.59 – 7.57 (m, 1H), 7.45 – 7.28 (m, 5H), 7.24 – 7.21 (m, 1H), 2.42 (s, 3H).

**<sup>13</sup>C NMR** (100 MHz, CDCl<sub>3</sub>):  $\delta$  = 167.3 (C<sub>q</sub>), 139.0 (C<sub>q</sub>), 139.0 (CH), 138.7 (C<sub>q</sub>), 133.5 (C<sub>q</sub>), 131.4 (C<sub>q</sub>), 130.8 (CH), 129.0 (CH), 128.8 (CH), 128.2 (CH), 126.8 (CH), 126.6 (CH), 123.5 (CH), 21.4 (CH<sub>3</sub>).

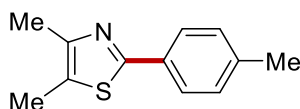
**IR** (ATR): 2918, 2855, 1547, 1515, 1453, 1237, 1109, 1001, 956, 813, 792 cm<sup>-1</sup>.

**MS** (ESI)  $m/z$  (relative intensity): 252 (100)  $[M+H]^+$ , 274 (3)  $[M+Na]^+$ .

**HR-MS** (ESI):  $m/z$  calcd for  $C_{16}H_{14}NS$   $[M+H]^+$ : 252.0843, found: 252.0841.

The spectral data were in accordance with those reported in the literature.<sup>[268]</sup>

#### 4,5-Dimethyl-2-(*p*-tolyl)thiazole (**405x**)



The **General Procedure F** was followed using 4,5-dimethylthiazole **403h** (28 mg, 0.25 mmol), 4-iodotoluene **404a** (273 mg, 1.25 mmol), **406** (30 mg, 11 mol %) and LiOtBu (60 mg, 0.75 mmol) in Et<sub>2</sub>O (0.5 mL). Purification by column chromatography on silica gel (*n*-hexane/EtOAc: 70/1) yielded **405x** (43.7 mg, 86%) as a light yellow solid.

**M. p.:** 62 °C.

**<sup>1</sup>H NMR** (500 MHz, CDCl<sub>3</sub>):  $\delta$  = 7.77 – 7.68 (m, 2H), 7.18 (d,  $J$  = 8.0 Hz, 2H), 2.36 (s, 6H), 2.35 (s, 3H).

**<sup>13</sup>C NMR** (125 MHz, CDCl<sub>3</sub>):  $\delta$  = 163.5 (C<sub>q</sub>), 149.0 (C<sub>q</sub>), 139.4 (C<sub>q</sub>), 131.3 (C<sub>q</sub>), 129.4 (CH), 126.0 (CH), 125.9 (C<sub>q</sub>), 21.3 (CH<sub>3</sub>), 14.8 (CH<sub>3</sub>), 11.4 (CH<sub>3</sub>).

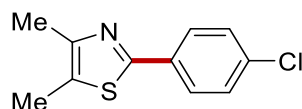
**IR** (ATR): 2955, 2923, 2854, 1810, 1480, 1448, 1143, 1082, 847, 785, 689 cm<sup>-1</sup>.

**MS** (ESI)  $m/z$  (relative intensity): 204 (100) [M+H]<sup>+</sup>.

**HR-MS** (ESI):  $m/z$  calcd for C<sub>12</sub>H<sub>14</sub>NS [M+H]<sup>+</sup>: 204.0842, found: 204.0841.

The spectral data were in accordance with those reported in the literature.<sup>[279]</sup>

### 2-(4-Chlorophenyl)-4,5-dimethylthiazole (405y)



The **General Procedure F** was followed using 4,5-dimethylthiazole **403h** (28 mg, 0.25 mmol), 1-chloro-4-iodobenzene **404f** (298 mg, 1.25 mmol), **406** (30 mg, 11 mol %) and LiOtBu (60 mg, 0.75 mmol) in Et<sub>2</sub>O (0.5 mL). Purification by column chromatography on silica gel (*n*-hexane/EtOAc: 70/1) yielded **405y** (48.7 mg, 87%) as a light yellow solid.

**M. p.:** 93 °C.

**<sup>1</sup>H NMR** (400 MHz, CDCl<sub>3</sub>):  $\delta$  = 7.78 (ddd,  $J$  = 9.1, 2.9, 2.1 Hz, 2H), 7.35 (ddd,  $J$  = 9.1, 2.9, 2.1 Hz, 2H), 2.36 (s, 6H).

**<sup>13</sup>C NMR** (100 MHz, CDCl<sub>3</sub>):  $\delta$  = 161.9 (C<sub>q</sub>), 149.5 (C<sub>q</sub>), 135.2 (C<sub>q</sub>), 132.5 (C<sub>q</sub>), 129.0 (CH), 127.2 (CH), 127.0 (C<sub>q</sub>), 14.8 (CH<sub>3</sub>), 11.5 (CH<sub>3</sub>).

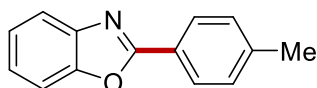
**IR** (ATR): 2922, 1724, 1679, 1611, 1494, 1364, 1257, 1076, 918, 731 cm<sup>-1</sup>.

**MS** (ESI)  $m/z$  (relative intensity): 224 (100) [M+H]<sup>+</sup>.

**HR-MS** (ESI):  $m/z$  calcd for C<sub>11</sub>H<sub>11</sub>ClNS [M+H]<sup>+</sup>: 224.0296, found: 224.0295.

The spectral data were in accordance with those reported in the literature.<sup>[268]</sup>



**2-(*p*-Tolyl)benzo[*d*]oxazole (447a)**

The **General Procedure F** was followed using benzoxazole **444a** (30 mg, 0.25 mmol), 4-iodotoluene **404a** (273 mg, 1.25 mmol), **406** (30 mg, 11 mol %) and LiOtBu (60 mg, 0.75 mmol) in Et<sub>2</sub>O (0.5 mL). Purification by column chromatography on silica gel (*n*-hexane/EtOAc: 70/1) yielded **447a** (41.3 mg, 79%) as a light yellow solid.

**M. p.:** 123 °C.

**<sup>1</sup>H NMR** (500 MHz, CDCl<sub>3</sub>): δ = 8.13 (d, *J* = 8.3 Hz, 2H), 7.79 – 7.69 (m, 1H), 7.60 – 7.50 (m, 1H), 7.32 – 7.29 (m, 3H), 2.41 (s, 3H).

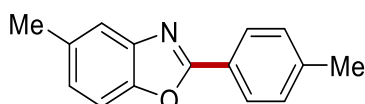
**<sup>13</sup>C NMR** (125 MHz, CDCl<sub>3</sub>): δ = 163.2 (C<sub>q</sub>), 150.6 (C<sub>q</sub>), 142.1 (C<sub>q</sub>), 142.0 (C<sub>q</sub>), 129.6 (CH), 127.5 (CH), 124.8 (CH), 124.4 (CH), 124.3 (C<sub>q</sub>), 119.8 (CH), 110.4 (CH), 21.6 (CH<sub>3</sub>).

**IR** (ATR): 3024, 2919, 1608, 1579, 1556, 1410, 1200, 1055, 926, 756, 380 cm<sup>-1</sup>.

**MS** (ESI) *m/z* (relative intensity): 210 (100) [M+H]<sup>+</sup>.

**HR-MS** (ESI): *m/z* calcd for C<sub>14</sub>H<sub>12</sub>NO [M+H]<sup>+</sup>: 210.0915, found: 210.0913.

The spectral data were in accordance with those reported in the literature.<sup>[273]</sup>

**5-Methyl-2-(*p*-tolyl)benzo[*d*]oxazole (447b)**

The **General Procedure F** was followed using 5-methylbenzo[*d*]oxazole **444b** (33 mg, 0.25 mmol), 4-iodotoluene **404a** (273 mg, 1.25 mmol), **406** (30 mg, 11 mol %) and LiOtBu (60 mg, 0.75 mmol) in Et<sub>2</sub>O (0.5 mL). Purification by column chromatography on silica gel (*n*-hexane/EtOAc: 70/1) yielded **447b** (40.7 mg, 73%) as a light yellow solid.

**M. p.:** 135 °C.

**<sup>1</sup>H NMR** (400 MHz, CDCl<sub>3</sub>): δ = 8.14 – 8.07 (m, 2H), 7.54 – 7.50 (m, 1H), 7.41 (d, *J* = 8.2 Hz, 1H), 7.33 – 7.26 (m, 2H), 7.11 (ddd, *J* = 8.2, 1.7, 0.7 Hz, 1H), 2.47 – 2.45 (m, 3H), 2.41 (s, 3H).

**<sup>13</sup>C NMR** (100 MHz, CDCl<sub>3</sub>): δ = 163.3 (C<sub>q</sub>), 148.9 (C<sub>q</sub>), 142.3 (C<sub>q</sub>), 141.8 (C<sub>q</sub>), 134.2 (C<sub>q</sub>), 129.6

(CH), 127.5 (CH), 125.9 (CH), 124.5 (C<sub>q</sub>), 119.7 (CH), 109.8 (CH), 21.6 (CH<sub>3</sub>), 21.5 (CH<sub>3</sub>).

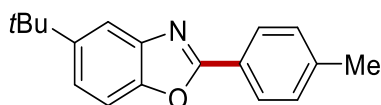
**IR** (ATR): 2958, 2866, 1616, 1581, 1268, 1018, 823, 807, 729, 650, 500 cm<sup>-1</sup>.

**MS** (ESI) *m/z* (relative intensity): 224 (100) [M+H]<sup>+</sup>, 246 (5) [M+Na]<sup>+</sup>.

**HR-MS** (ESI): *m/z* calcd for C<sub>15</sub>H<sub>14</sub>NO [M+H]<sup>+</sup>: 224.1068, found: 224.1070.

The spectral data were in accordance with those reported in the literature.<sup>[276]</sup>

#### 5-(*tert*-Butyl)-2-(*p*-tolyl)benzo[*d*]oxazole (447c)



The **General Procedure F** was followed using 5-(*tert*-butyl)benzo[*d*]oxazole **444c** (44 mg, 0.25 mmol), 4-iodotoluene **404a** (273 mg, 1.25 mmol), **406** (30 mg, 11 mol %) and LiOtBu (60 mg, 0.75 mmol) in Et<sub>2</sub>O (0.5 mL). Purification by column chromatography on silica gel (*n*-hexane/EtOAc: 70/1) yielded **447c** (49.1 mg, 74%) as a light yellow solid.

**M. p.:** 113 °C.

**<sup>1</sup>H NMR** (400 MHz, CDCl<sub>3</sub>): δ = 8.30 – 8.25 (m, 2H), 7.94 (dd, *J* = 1.9, 0.6 Hz, 1H), 7.62 (dd, *J* = 8.6, 0.6 Hz, 1H), 7.54 (dd, *J* = 8.6, 1.9 Hz, 1H), 7.49 – 7.44 (m, 2H), 2.57 (s, 3H), 1.54 (s, 9H).

**<sup>13</sup>C NMR** (100 MHz, CDCl<sub>3</sub>): δ = 163.4 (C<sub>q</sub>), 148.7 (C<sub>q</sub>), 148.0 (C<sub>q</sub>), 142.1 (C<sub>q</sub>), 141.8 (C<sub>q</sub>), 129.6 (CH), 127.5 (CH), 124.6 (C<sub>q</sub>), 122.5 (CH), 116.3 (CH), 109.6 (CH), 34.9 (C<sub>q</sub>), 31.8 (CH<sub>3</sub>), 21.6 (CH<sub>3</sub>).

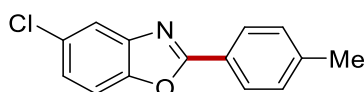
**IR** (ATR): 2920, 1616, 1556, 1497, 1462, 1215, 1166, 1118, 1049, 919, 831 cm<sup>-1</sup>.

**MS** (ESI) *m/z* (relative intensity): 266 (100) [M+H]<sup>+</sup>.

**HR-MS** (ESI): *m/z* calcd for C<sub>18</sub>H<sub>20</sub>NO [M+H]<sup>+</sup>: 266.1542, found: 266.1540.

The spectral data were in accordance with those reported in the literature.<sup>[276]</sup>

#### 5-Chloro-2-(*p*-tolyl)benzo[*d*]oxazole (447d)



The **General Procedure F** was followed using 5-chlorobenzo[*d*]oxazole **444d** (38 mg, 0.25 mmol), 4-iodotoluene **404a** (273 mg, 1.25 mmol), **406** (30 mg, 11 mol %) and LiOtBu (60 mg, 0.75 mmol) in

Et<sub>2</sub>O (0.5 mL). Purification by column chromatography on silica gel (*n*-hexane/EtOAc: 70/1) yielded **447d** (31.1 mg, 51%) as a light yellow solid.

**M. p.:** 124 °C.

**<sup>1</sup>H NMR** (400 MHz, CDCl<sub>3</sub>): δ = 8.27 – 8.22 (m, 2H), 7.79 (dd, *J* = 8.5, 0.4 Hz, 1H), 7.71 (dd, *J* = 2.1, 0.4 Hz, 1H), 7.48 – 7.44 (m, 3H), 2.58 (s, 3H).

**<sup>13</sup>C NMR** (100 MHz, CDCl<sub>3</sub>): δ = 163.9 (C<sub>q</sub>), 150.8 (C<sub>q</sub>), 142.4 (C<sub>q</sub>), 141.0 (C<sub>q</sub>), 130.4 (C<sub>q</sub>), 129.7 (CH), 127.6 (CH), 125.1 (CH), 123.9 (C<sub>q</sub>), 120.2 (CH), 111.1 (CH), 21.7 (CH<sub>3</sub>).

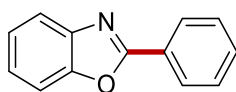
**IR** (ATR): 2956, 2851, 1737, 1461, 1377, 1190, 1121, 1082, 716, 649, 597 cm<sup>-1</sup>.

**MS** (ESI) *m/z* (relative intensity): 244 (100) [M+H]<sup>+</sup>.

**HR-MS** (ESI): *m/z* calcd for C<sub>14</sub>H<sub>11</sub>ClNO [M+H]<sup>+</sup>: 244.0524, found: 244.0524.

The spectral data were in accordance with those reported in the literature.<sup>[277]</sup>

## 2-Phenylbenzo[d]oxazole (**447e**)



The **General Procedure F** was followed using benzoxazole **444a** (30 mg, 0.25 mmol), iodobenzene **404b** (255 mg, 1.25 mmol), **406** (30 mg, 11 mol %) and LiOtBu (60 mg, 0.75 mmol) in Et<sub>2</sub>O (0.5 mL). Purification by column chromatography on silica gel (*n*-hexane/EtOAc: 70/1) yielded **447e** (39.0 mg, 80%) as a light yellow solid.

**M. p.:** 100 °C.

**<sup>1</sup>H NMR** (400 MHz, CDCl<sub>3</sub>): δ = 8.28 – 8.22 (m, 2H), 7.76 (ddd, *J* = 6.0, 3.3, 0.7 Hz, 1H), 7.57 (ddd, *J* = 6.0, 3.3, 0.7 Hz, 1H), 7.54 – 7.49 (m, 3H), 7.34 (dd, *J* = 6.0, 3.3 Hz, 2H).

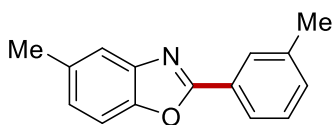
**<sup>13</sup>C NMR** (100 MHz, CDCl<sub>3</sub>): δ = 163.0 (C<sub>q</sub>), 150.8 (C<sub>q</sub>), 142.1 (C<sub>q</sub>), 131.5 (CH), 129.9 (CH), 127.6 (CH), 127.2 (C<sub>q</sub>), 125.1 (CH), 124.6 (CH), 120.0 (CH), 110.6 (CH).

**IR** (ATR): 2922, 2020, 1973, 1555, 1474, 1263, 1182, 1057, 865, 791, 719 cm<sup>-1</sup>.

**MS** (ESI) *m/z* (relative intensity): 196 (100) [M+H]<sup>+</sup>.

**HR-MS** (ESI): *m/z* calcd for C<sub>13</sub>H<sub>10</sub>NO [M+H]<sup>+</sup>: 196.0755, found: 196.0756.

The spectral data were in accordance with those reported in the literature.<sup>[275]</sup>

**5-Methyl-2-(*m*-tolyl)benzo[*d*]oxazole (447f)**

The **General Procedure F** was followed using 5-methylbenzo[*d*]oxazole **444b** (33 mg, 0.25 mmol), 3-iodotoluene **404h** (273 mg, 1.25 mmol), **406** (30 mg, 11 mol %) and LiOtBu (60 mg, 0.75 mmol) in Et<sub>2</sub>O (0.5 mL). Purification by column chromatography on silica gel (*n*-hexane/EtOAc: 70/1) yielded **447f** (43.0 mg, 77%) as a light yellow solid.

**M. p.:** 85 °C.

**<sup>1</sup>H NMR** (300 MHz, CDCl<sub>3</sub>): δ = 8.11 – 8.02 (m, 1H), 8.07 – 7.96 (m, 1H), 7.41 (ddd, *J* = 8.3, 0.3 Hz, 1H), 7.49 – 7.33 (m, 2H), 7.38 – 7.26 (m, 1H), 7.13 (ddd, *J* = 8.3, 1.7, 0.7 Hz, 1H), 2.47 (s, 3H), 2.44 (s, 3H).

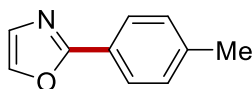
**<sup>13</sup>C NMR** (75 MHz, CDCl<sub>3</sub>): δ = 163.2 (C<sub>q</sub>), 148.9 (C<sub>q</sub>), 142.2 (C<sub>q</sub>), 138.6 (C<sub>q</sub>), 134.3 (C<sub>q</sub>), 132.1 (CH), 128.7 (CH), 128.0 (CH), 127.1 (C<sub>q</sub>), 126.0 (CH), 124.6 (CH), 119.8 (CH), 109.8 (CH), 21.6 (CH<sub>3</sub>), 21.4 (CH<sub>3</sub>).

**IR** (ATR): 2919, 1613, 1483, 1423, 1143, 1055, 971, 873, 815, 631, 478 cm<sup>-1</sup>.

**MS** (ESI) *m/z* (relative intensity): 224 (100) [M+H]<sup>+</sup>, 246 (5) [M+Na]<sup>+</sup>.

**HR-MS** (ESI): *m/z* calcd for C<sub>15</sub>H<sub>14</sub>NO [M+H]<sup>+</sup>: 224.1071, found: 224.1070.

The spectral data were in accordance with those reported in the literature.<sup>[268]</sup>

**2-(*p*-Tolyl)oxazole (447g)**

The **General Procedure F** was followed using oxazole **444e** (17 mg, 0.25 mmol), 4-iodotoluene **404a** (273 mg, 1.25 mmol), **406** (30 mg, 11 mol %) and LiOtBu (60 mg, 0.75 mmol) in Et<sub>2</sub>O (0.5 mL). Purification by column chromatography on silica gel (*n*-hexane/EtOAc: 70/1) yielded **447g** (24.3 mg, 61%) as a yellow oil.

**<sup>1</sup>H NMR** (400 MHz, CDCl<sub>3</sub>): δ = 7.93 – 7.89 (m, 2H), 7.66 (d, *J* = 0.8 Hz, 1H), 7.27 – 7.25 (m, 1H), 7.25 – 7.23 (m, 1H), 7.19 (d, *J* = 0.8 Hz, 1H), 2.38 (s, 3H).

$^{13}\text{C}$  NMR (100 MHz,  $\text{CDCl}_3$ ):  $\delta$  = 162.2 ( $\text{C}_q$ ), 140.6 ( $\text{C}_q$ ), 138.2 (CH), 129.5 (CH), 128.2 (CH), 126.3 (CH), 124.8 ( $\text{C}_q$ ), 21.5 ( $\text{CH}_3$ ).

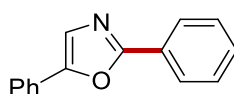
IR (ATR): 2924, 2230, 2211, 2171, 2042, 1976, 714, 686, 585, 487  $\text{cm}^{-1}$ .

MS (ESI)  $m/z$  (relative intensity): 160 (100)  $[\text{M}+\text{H}]^+$ .

HR-MS (ESI):  $m/z$  calcd for  $\text{C}_{10}\text{H}_{10}\text{NO}$   $[\text{M}+\text{H}]^+$ : 160.0759, found: 160.0758.

The spectral data were in accordance with those reported in the literature.<sup>[280]</sup>

### 2,5-Diphenyloxazole (447h)



The **General Procedure F** was followed using 5-phenyloxazole **444f** (36 mg, 0.25 mmol), iodobenzene **404b** (255 mg, 1.25 mmol), **406** (30 mg, 11 mol %) and  $\text{LiOtBu}$  (60 mg, 0.75 mmol) in  $\text{Et}_2\text{O}$  (0.5 mL). Purification by column chromatography on silica gel (*n*-hexane/ $\text{EtOAc}$ : 70/1) yielded **447h** (42.0 mg, 76%) as a light yellow solid.

M. p.: 70  $^\circ\text{C}$ .

$^1\text{H}$  NMR (300 MHz,  $\text{CDCl}_3$ ):  $\delta$  = 8.13 – 8.07 (m, 2H), 7.74 – 7.72 (m, 1H), 7.71 – 7.69 (m, 1H), 7.49 – 7.41 (m, 6H), 7.37 – 7.29 (m, 1H).

$^{13}\text{C}$  NMR (75 MHz,  $\text{CDCl}_3$ ):  $\delta$  = 161.0 ( $\text{C}_q$ ), 151.2 ( $\text{C}_q$ ), 130.2 (CH), 128.8 (CH), 128.7 (CH), 128.3 (CH), 128.0 ( $\text{C}_q$ ), 127.4 ( $\text{C}_q$ ), 126.2 (CH), 124.1 (CH), 123.4 (CH).

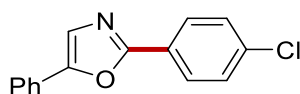
IR (ATR): 2955, 2923, 2853, 1731, 1684, 1749, 1092, 1014, 934, 685  $\text{cm}^{-1}$ .

MS (ESI)  $m/z$  (relative intensity): 222 (100)  $[\text{M}+\text{H}]^+$ .

HR-MS (ESI):  $m/z$  calcd for  $\text{C}_{15}\text{H}_{12}\text{NO}$   $[\text{M}+\text{H}]^+$ : 222.0913, found: 222.0913.

The spectral data were in accordance with those reported in the literature.<sup>[268]</sup>

### 2-(4-Chlorophenyl)-5-phenyloxazole (447i)



The **General Procedure F** was followed using 5-phenyloxazole **444f** (36 mg, 0.25 mmol), 1-chloro-

4-iodobenzene **404f** (298 mg, 1.25 mmol), **406** (30 mg, 11 mol %) and LiOtBu (60 mg, 0.75 mmol) in Et<sub>2</sub>O (0.5 mL). Purification by column chromatography on silica gel (*n*-hexane/EtOAc: 70/1) yielded **447i** (50.5 mg, 79%) as a light yellow solid.

**M. p.:** 115 °C.

<sup>1</sup>H NMR (400 MHz, CDCl<sub>3</sub>): δ = 8.05 – 7.99 (m, 2H), 7.72 – 7.67 (m, 2H), 7.47 – 7.40 (m, 5H), 7.37 – 7.30 (m, 1H).

<sup>13</sup>C NMR (100 MHz, CDCl<sub>3</sub>): δ = 160.2 (C<sub>q</sub>), 151.5 (C<sub>q</sub>), 136.4 (C<sub>q</sub>), 129.1 (CH), 129.0 (CH), 128.6 (CH), 127.8 (C<sub>q</sub>), 127.5 (CH), 126.0 (C<sub>q</sub>), 124.2 (CH), 123.5 (CH).

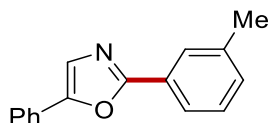
IR (ATR): 2956, 2923, 2855, 1727, 1682, 1471, 1133, 761, 725, 383 cm<sup>-1</sup>.

MS (ESI) *m/z* (relative intensity): 256 (100) [M+H]<sup>+</sup>.

HR-MS (ESI): *m/z* calcd for C<sub>15</sub>H<sub>11</sub>ClNO [M+H]<sup>+</sup>: 256.0521, found: 256.0523.

The spectral data were in accordance with those reported in the literature.<sup>[268]</sup>

### 5-Phenyl-2-(*m*-tolyl)oxazole (**447j**)



The **General Procedure F** was followed using 5-phenyloxazole **444f** (36 mg, 0.25 mmol), 3-iodotoluene **404h** (273 mg, 1.25 mmol), **406** (30 mg, 11 mol %) and LiOtBu (60 mg, 0.75 mmol) in Et<sub>2</sub>O (0.5 mL). Purification by column chromatography on silica gel (*n*-hexane/EtOAc: 70/1) yielded **447j** (43.5 mg, 74%) as a light yellow solid.

**M. p.:** 89 °C.

<sup>1</sup>H NMR (300 MHz, CDCl<sub>3</sub>): δ = 7.94 – 7.87 (m, 2H), 7.74 – 7.69 (m, 2H), 7.48 – 7.39 (m, 3H), 7.39 – 7.29 (m, 2H), 7.29 – 7.24 (m, 1H), 2.43 (s, 3H).

<sup>13</sup>C NMR (75 MHz, CDCl<sub>3</sub>): δ = 161.3 (C<sub>q</sub>), 151.1 (C<sub>q</sub>), 138.6 (C<sub>q</sub>), 131.1 (CH), 128.9 (CH), 128.7 (CH), 128.4 (CH), 128.0 (C<sub>q</sub>), 127.3 (C<sub>q</sub>), 126.8 (CH), 124.2 (CH), 123.4 (CH), 123.4 (CH), 21.4 (CH<sub>3</sub>).

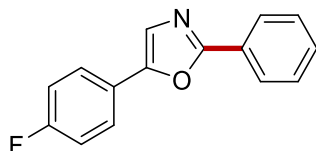
IR (ATR): 3055, 1886, 1499, 1231, 1099, 851, 823, 686, 609, 512 cm<sup>-1</sup>.

MS (ESI) *m/z* (relative intensity): 236 (100) [M+H]<sup>+</sup>, 258 (3) [M+Na]<sup>+</sup>.

**HR-MS** (ESI):  $m/z$  calcd for  $C_{16}H_{14}NO$   $[M+H]^+$ : 236.1071, found: 236.1070.

The spectral data were in accordance with those reported in the literature.<sup>[268]</sup>

#### 5-(4-Fluorophenyl)-2-phenyloxazole (447k)



The **General Procedure F** was followed using 5-(4-fluorophenyl)oxazole **444g** (41 mg, 0.25 mmol), iodobenzene **404b** (255 mg, 1.25 mmol), **406** (30 mg, 11 mol %) and LiOtBu (60 mg, 0.75 mmol) in Et<sub>2</sub>O (0.5 mL). Purification by column chromatography on silica gel (*n*-hexane/EtOAc: 70/1) yielded **447k** (48.4 mg, 81%) as a light yellow solid.

**M. p.:** 90 °C.

**<sup>1</sup>H NMR** (400 MHz, CDCl<sub>3</sub>):  $\delta$  = 8.11 – 8.06 (m, 2H), 7.71 – 7.66 (m, 2H), 7.50 – 7.43 (m, 3H), 7.37 (s, 1H), 7.16 – 7.10 (m, 2H).

**<sup>13</sup>C NMR** (100 MHz, CDCl<sub>3</sub>):  $\delta$  = 162.7 (d,  $J_{C-F}$  = 249 Hz, C<sub>q</sub>), 161.1 (C<sub>q</sub>), 150.4 (C<sub>q</sub>), 130.4 (CH), 128.8 (CH), 127.4 (C<sub>q</sub>), 126.3 (CH), 126.1 (d,  $J_{C-F}$  = 8 Hz, CH), 124.4 (d,  $J_{C-F}$  = 3 Hz, C<sub>q</sub>), 123.1 (d,  $J_{C-F}$  = 1 Hz, CH), 116.1 (d,  $J_{C-F}$  = 22 Hz, CH).

**<sup>19</sup>F NMR** (282 MHz, CDCl<sub>3</sub>):  $\delta$  = -112.21 (ddd,  $J$  = 13.8, 8.7, 5.1 Hz).

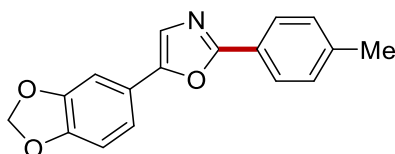
**IR** (ATR): 2917, 1724, 1608, 1497, 1362, 1323, 1260, 1106, 963, 934, 752 cm<sup>-1</sup>.

**MS** (ESI)  $m/z$  (relative intensity): 240 (100)  $[M+H]^+$ .

**HR-MS** (ESI):  $m/z$  calcd for  $C_{15}H_{11}FNO$   $[M+H]^+$ : 240.0818, found: 240.0819.

The spectral data were in accordance with those reported in the literature.<sup>[268]</sup>

#### 5-(Benzo[*d*][1,3]dioxol-5-yl)-2-(*p*-tolyl)oxazole (447l)



The **General Procedure F** was followed using 5-(benzo[*d*][1,3]dioxol-5-yl)oxazole **444h** (47 mg, 0.25 mmol), 4-iodotoluene **404a** (273 mg, 1.25 mmol), **406** (30 mg, 11 mol %) and LiOtBu (60 mg, 0.75

mmol) in Et<sub>2</sub>O (0.5 mL). Purification by column chromatography on silica gel (*n*-hexane/EtOAc: 70/1) yielded **447l** (58.7 mg, 84%) as a light yellow solid.

**M. p.:** 125 °C.

**<sup>1</sup>H NMR** (400 MHz, CDCl<sub>3</sub>):  $\delta$  = 7.98 – 7.90 (m, 2H), 7.28 – 7.26 (m, 2H), 7.25 – 7.23 (m, 1H), 7.20 (dd, *J* = 8.1, 1.7 Hz, 1H), 7.14 (dd, *J* = 1.7, 0.4 Hz, 1H), 6.85 (dd, *J* = 8.1, 0.5 Hz, 1H), 5.99 (s, 2H), 2.39 (s, 3H).

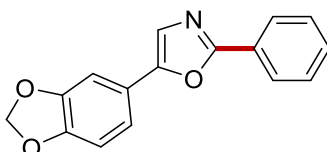
**<sup>13</sup>C NMR** (100 MHz, CDCl<sub>3</sub>):  $\delta$  = 160.9 (C<sub>q</sub>), 150.8 (C<sub>q</sub>), 148.2 (C<sub>q</sub>), 147.8 (C<sub>q</sub>), 140.5 (C<sub>q</sub>), 129.5 (CH), 126.1 (CH), 124.7 (C<sub>q</sub>), 122.3 (C<sub>q</sub>), 122.2 (CH), 118.2 (CH), 108.8 (CH), 104.8 (CH), 101.3 (CH<sub>2</sub>), 21.5 (CH<sub>3</sub>).

**IR** (ATR): 2898, 1726, 1683, 1609, 1545, 1363, 1287, 1129, 1062, 963, 776 cm<sup>-1</sup>.

**MS** (ESI) *m/z* (relative intensity): 280 (100) [M+H]<sup>+</sup>, 302 (10) [M+Na]<sup>+</sup>.

**HR-MS** (ESI): *m/z* calcd for C<sub>17</sub>H<sub>14</sub>NO<sub>3</sub> [M+H]<sup>+</sup>: 280.0967, found: 280.0968.

#### 5-(Benzo[*d*][1,3]dioxol-5-yl)-2-phenyloxazole (**447m**)



The **General Procedure F** was followed using 5-(benzo[*d*][1,3]dioxol-5-yl)oxazole **444h** (47 mg, 0.25 mmol), iodobenzene **404b** (255 mg, 1.25 mmol), **406** (30 mg, 11 mol %) and LiOtBu (60 mg, 0.75 mmol) in Et<sub>2</sub>O (0.5 mL). Purification by column chromatography on silica gel (*n*-hexane/EtOAc: 70/1) yielded **447m** (57.7 mg, 87%) as a light yellow solid.

**M. p.:** 136 °C.

**<sup>1</sup>H NMR** (400 MHz, CDCl<sub>3</sub>):  $\delta$  = 8.10 – 8.03 (m, 2H), 7.49 – 7.38 (m, 3H), 7.28 (s, 1H), 7.21 (dd, *J* = 8.1, 1.7 Hz, 1H), 7.15 (dd, *J* = 1.7, 0.4 Hz, 1H), 6.86 (dd, *J* = 8.1, 0.4 Hz, 1H), 5.99 (s, 2H).

**<sup>13</sup>C NMR** (100 MHz, CDCl<sub>3</sub>):  $\delta$  = 160.6 (C<sub>q</sub>), 151.1 (C<sub>q</sub>), 148.2 (C<sub>q</sub>), 147.9 (C<sub>q</sub>), 130.2 (CH), 128.8 (CH), 127.4 (C<sub>q</sub>), 126.1 (CH), 122.3 (CH), 122.2 (C<sub>q</sub>), 118.3 (CH), 108.8 (CH), 104.8 (CH), 101.4 (CH<sub>2</sub>).

**IR** (ATR): 2865, 1605, 1349, 1276, 1109, 1088, 964, 854, 774, 589, 422 cm<sup>-1</sup>.

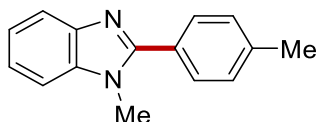
**MS** (ESI) *m/z* (relative intensity): 266 (100) [M+H]<sup>+</sup>.



**HR-MS** (ESI):  $m/z$  calcd for  $C_{16}H_{12}NO_3$   $[M+H]^+$ : 266.0817, found: 266.0815.

The spectral data were in accordance with those reported in the literature.<sup>[268]</sup>

### 1-Methyl-2-(*p*-tolyl)-1*H*-benzo[*d*]imidazole (446a)



1) The **General Procedure G** was followed using 1-methyl-1*H*-benzo[*d*]imidazole **445a** (33 mg, 0.25 mmol), 4-iodotoluene **404a** (273 mg, 1.25 mmol), **406** (30 mg, 11 mol %) and  $K_3PO_4$  (159 mg, 0.75 mmol) in THF (0.5 mL). Purification by column chromatography on silica gel (*n*-hexane/EtOAc: 4/1) yielded **446a** (35.0 mg, 63%) as a light yellow solid.

2) The **General Procedure H** was followed using 1-methyl-1*H*-benzo[*d*]imidazole **445a** (33 mg, 0.25 mmol), 4-bromotoluene **447a** (273 mg, 1.25 mmol), **406** (30 mg, 11 mol %) and  $Cs_2CO_3$  (244 mg, 0.75 mmol) in  $Et_2O$  (0.5 mL). Purification by column chromatography on silica gel (*n*-hexane/EtOAc: 4/1) yielded **446a** (41.1 mg, 74%) as a light yellow solid.

**M. p.**: 125 °C.

**$^1H$  NMR** (400 MHz,  $CDCl_3$ )  $\delta$  7.80 (ddd,  $J = 5.4, 2.4, 0.7$  Hz, 1H), 7.65 (t,  $J = 1.9$  Hz, 1H), 7.63 (t,  $J = 1.9$  Hz, 1H), 7.35 (ddd,  $J = 5.4, 2.4, 0.7$  Hz), 7.31 – 7.33 (m, 1H), 7.30 – 7.31 (m, 1H), 7.28 (m, 2H), 3.83 (s, 3H), 2.42 (s, 3H).

**$^{13}C$  NMR** (100 MHz,  $CDCl_3$ )  $\delta$  153.9 ( $C_q$ ), 142.9 ( $C_q$ ), 139.8 ( $C_q$ ), 136.5 ( $C_q$ ), 129.3 (CH), 129.3 ( $C_q$ ), 127.3 (CH), 122.6 (CH), 122.3 (CH), 119.7 (CH), 109.5 (CH), 31.6 ( $CH_3$ ), 21.4 ( $CH_3$ ).

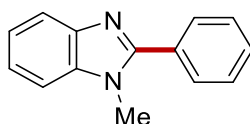
**IR** (ATR): 3419, 3402, 2919, 1936, 1613, 1459, 1381, 1276, 1005, 822, 748  $cm^{-1}$ .

**MS** (ESI)  $m/z$  (relative intensity): 223 (60)  $[M+H]^+$ , 245 (40)  $[M+Na]^+$ .

**HR-MS** (ESI):  $m/z$  calcd for  $C_{15}H_{15}N_2$   $[M+H]^+$ : 223.1237, found: 223.1235.

The spectral data were in accordance with those reported in the literature.<sup>[282]</sup>

### 1-Methyl-2-phenyl-1*H*-benzo[*d*]imidazole (446b)



1) The **General Procedure G** was followed using 1-methyl-1*H*-benzo[*d*]imidazole **445a** (33 mg, 0.25 mmol), iodobenzene **404b** (255 mg, 1.25 mmol), **406** (30 mg, 11 mol %) and K<sub>3</sub>PO<sub>4</sub> (159 mg, 0.75 mmol) in THF (0.5 mL). Purification by column chromatography on silica gel (*n*-hexane/EtOAc: 4/1) yielded **446b** (36.4 mg, 70%) as a light yellow solid.

2) The **General Procedure H** was followed using 1-methyl-1*H*-benzo[*d*]imidazole **445a** (33 mg, 0.25 mmol), bromobenzene **447b** (255 mg, 1.25 mmol), **406** (30 mg, 11 mol %) and Cs<sub>2</sub>CO<sub>3</sub> (244 mg, 0.75 mmol) in Et<sub>2</sub>O (0.5 mL). Purification by column chromatography on silica gel (*n*-hexane/EtOAc: 4/1) yielded **446b** (41.1 mg, 79%) as a light yellow solid.

**M. p.:** 96 °C.

**<sup>1</sup>H NMR** (400 MHz, CDCl<sub>3</sub>) δ 7.81 (ddd, *J* = 5.4, 2.4, 0.7 Hz, 1H), 7.76 – 7.72 (m, 2H), 7.54 – 7.47 (m, 3H), 7.36 (ddd, *J* = 5.4, 2.4, 0.7 Hz, 1H), 7.32 – 7.27 (m, 2H), 3.83 (s, 3H).

**<sup>13</sup>C NMR** (100 MHz, CDCl<sub>3</sub>) δ 153.7 (C<sub>q</sub>), 142.9 (C<sub>q</sub>), 136.5 (C<sub>q</sub>), 130.1 (C<sub>q</sub>), 129.7 (CH), 129.4 (CH), 128.6 (CH), 122.7 (CH), 122.4 (CH), 119.8 (CH), 109.6 (CH), 31.6 (CH<sub>3</sub>).

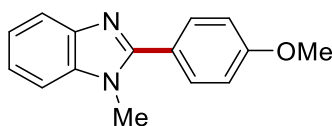
**IR** (ATR): 3059, 2924, 2159, 1469, 1442, 1382, 1328, 1006, 744, 698 cm<sup>-1</sup>.

**MS** (ESI) *m/z* (relative intensity): 210 (100) [M+H]<sup>+</sup>.

**HR-MS** (ESI): *m/z* calcd for C<sub>14</sub>H<sub>13</sub>N<sub>2</sub> [M+H]<sup>+</sup>: 210.1074, found: 210.1073.

The spectral data were in accordance with those reported in the literature.<sup>[283]</sup>

### 2-(4-Methoxyphenyl)-1-methyl-1*H*-benzo[*d*]imidazole (**446c**)



1) The **General Procedure G** was followed using 1-methyl-1*H*-benzo[*d*]imidazole **445a** (33 mg, 0.25 mmol), 4-iodoanisole **404c** (293 mg, 1.25 mmol), **406** (30 mg, 11 mol %) and K<sub>3</sub>PO<sub>4</sub> (159 mg, 0.75 mmol) in THF (0.5 mL). Purification by column chromatography on silica gel (*n*-hexane/EtOAc: 4/1) yielded **446c** (36.3 mg, 61%) as a light yellow solid.

2) The **General Procedure H** was followed using 1-methyl-1*H*-benzo[*d*]imidazole **445a** (33 mg, 0.25 mmol), 4-bromoanisole **447c** (255 mg, 1.25 mmol), **406** (30 mg, 11 mol %) and Cs<sub>2</sub>CO<sub>3</sub> (244 mg, 0.75 mmol) in Et<sub>2</sub>O (0.5 mL). Purification by column chromatography on silica gel (*n*-hexane/EtOAc:

4/1) yielded **446c** (47.1 mg, 79%) as a light yellow solid.

**M. p.:** 118 °C.

**<sup>1</sup>H NMR** (400 MHz, CDCl<sub>3</sub>)  $\delta$  7.79 (ddd,  $J = 4.9, 2.3, 0.7$  Hz, 1H), 7.70 (dd,  $J = 2.9, 2.3$  Hz, 1H), 7.68 (dd,  $J = 2.9, 2.3$  Hz, 1H), 7.35 (ddd,  $J = 4.9, 2.3, 0.7$  Hz, 1H), 7.29 (dd,  $J = 2.9, 2.3$  Hz, 1H) 7.28 (dd,  $J = 2.9, 2.3$  Hz, 1H), 7.03 (dd,  $J = 2.9, 2.3$  Hz, 1H), 7.02 (dd,  $J = 2.9, 2.3$  Hz, 1H). 3.86 (s, 3H), 3.83 (s, 3H).

**<sup>13</sup>C NMR** (100 MHz, CDCl<sub>3</sub>)  $\delta$  160.7 (C<sub>q</sub>), 142.9 (C<sub>q</sub>), 136.5 (C<sub>q</sub>), 130.8 (C<sub>q</sub>), 122.5 (CH), 122.5 (C<sub>q</sub>), 122.5 (CH), 122.3 (CH), 119.6 (CH), 114.1 (CH), 109.5 (CH), 55.4 (CH<sub>3</sub>), 31.7 (CH<sub>3</sub>).

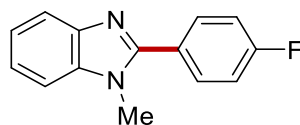
**IR** (ATR): 2938, 2837, 1706, 1611, 1461, 1250, 1177, 1025, 838, 745 cm<sup>-1</sup>.

**MS** (ESI)  $m/z$  (relative intensity): 239 (80) [M+H]<sup>+</sup>, 261 (20) [M+Na]<sup>+</sup>

**HR-MS** (ESI):  $m/z$  calcd for C<sub>15</sub>H<sub>15</sub>N<sub>2</sub>O [M+H]<sup>+</sup>: 239.1182, found: 239.1180.

The spectral data were in accordance with those reported in the literature.<sup>[282]</sup>

#### 2-(4-Fluorophenyl)-1-methyl-1H-benzo[d]imidazole (**446d**)



1) The **General Procedure G** was followed using 1-methyl-1H-benzo[d]imidazole **445a** (33 mg, 0.25 mmol), 1-fluoro-4-iodobenzene **404e** (278 mg, 1.25 mmol), **406** (30 mg, 11 mol %) and K<sub>3</sub>PO<sub>4</sub> (159 mg, 0.75 mmol) in THF (0.5 mL). Purification by column chromatography on silica gel (*n*-hexane/EtOAc: 4/1) yielded **446d** (36.7 mg, 65%) as a light yellow solid.

2) The **General Procedure H** was followed using 1-methyl-1H-benzo[d]imidazole **445a** (33 mg, 0.25 mmol), 1-bromo-4-fluorobenzene **447d** (278 mg, 1.25 mmol), **406** (30 mg, 11 mol %) and Cs<sub>2</sub>CO<sub>3</sub> (244 mg, 0.75 mmol) in Et<sub>2</sub>O (0.5 mL). Purification by column chromatography on silica gel (*n*-hexane/EtOAc: 4/1) yielded **446d** (39.6 mg, 70%) as a light yellow solid

**M. p.:** 98 °C.

**<sup>1</sup>H NMR** (400 MHz, CDCl<sub>3</sub>)  $\delta$  7.80 (ddd,  $J = 4.5, 2.0, 0.7$  Hz, 1H), 7.75 (ddd,  $J = 5.1, 3.0, 2.3$  Hz, 1H), 7.73 (ddd,  $J = 5.1, 3.0, 2.3$  Hz, 1H), 7.37 (ddd,  $J = 4.5, 2.0, 0.7$ , 1H), 7.33 – 7.28 (m, 2H), 7.25 – 7.17 (m, 2H), 3.83 (s, 3H).

$^{13}\text{C}$  NMR (100 MHz,  $\text{CDCl}_3$ )  $\delta$  163.6 (d,  $J_{\text{C-F}} = 250.5$  Hz,  $\text{C}_q$ ), 152.8 ( $\text{C}_q$ ), 142.8 ( $\text{C}_q$ ), 136.5 ( $\text{C}_q$ ), 131.4 (d,  $J_{\text{C-F}} = 8.4$  Hz, CH), 126.3 (d,  $J_{\text{C-F}} = 3.4$  Hz,  $\text{C}_q$ ), 122.9 (CH), 122.5 (CH), 119.8 (CH), 115.9 (d,  $J_{\text{C-F}} = 22.0$  Hz, CH), 109.9 (CH), 109.6 (CH), 31.6 ( $\text{CH}_3$ ).

$^{19}\text{F}$  NMR (282 MHz,  $\text{CDCl}_3$ )  $\delta$  -110.60 (ddd,  $J = 13.6, 8.5, 5.2$  Hz).

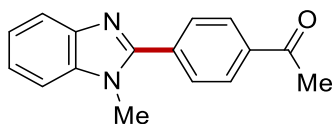
IR (ATR): 3059, 2951, 2158, 1645, 1606, 1461, 1225, 1097, 843, 744  $\text{cm}^{-1}$ .

MS (ESI)  $m/z$  (relative intensity): 227 (70)  $[\text{M}+\text{H}]^+$ , 249 (30)  $[\text{M}+\text{Na}]^+$ .

HR-MS (ESI):  $m/z$  calcd for  $\text{C}_{14}\text{H}_{12}\text{FN}_2$   $[\text{M}+\text{H}]^+$ : 227.0985, found: 227.0983.

The spectral data were in accordance with those reported in the literature.<sup>[282]</sup>

### 1-(4-(1-Methyl-1*H*-benzo[*d*]imidazol-2-yl)phenyl)ethan-1-one (446e)



The **General Procedure G** was followed using 1-methyl-1*H*-benzo[*d*]imidazole **445a** (33 mg, 0.25 mmol), 1-(4-iodophenyl)ethan-1-one **404q** (308 mg, 1.25 mmol), **406** (30 mg, 11 mol %) and  $\text{K}_3\text{PO}_4$  (159 mg, 0.75 mmol) in THF (0.5 mL). Purification by column chromatography on silica gel (*n*-hexane/EtOAc: 4/1) yielded **446e** (29.4 mg, 47%) as a light yellow solid.

**M. p.:** 153 °C.

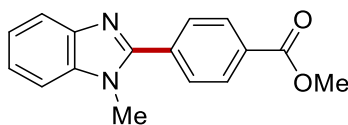
$^1\text{H}$  NMR (400 MHz,  $\text{CDCl}_3$ )  $\delta$  8.10 (dd,  $J = 2.3, 1.8$  Hz, 1H), 8.8 (dd,  $J = 2.3, 1.8$  Hz, 1H), 7.89 (dd,  $J = 2.3, 1.8$  Hz, 1H), 7.87 (dd,  $J = 2.3, 1.8$  Hz, 1H), 7.83 – 7.81 (m, 1H), 7.41 – 7.39 (m, 1H), 7.33 (ddd,  $J = 6.7, 4.1, 1.8$  Hz, 2H), 3.88 (s, 3H), 2.66 (s, 3H).

$^{13}\text{C}$  NMR (100 MHz,  $\text{CDCl}_3$ )  $\delta$  197.5 ( $\text{C}_q$ ), 152.4 ( $\text{C}_q$ ), 143.0 ( $\text{C}_q$ ), 137.6 ( $\text{C}_q$ ), 136.7 ( $\text{C}_q$ ), 134.6 ( $\text{C}_q$ ), 129.6 (CH), 128.6 (CH), 123.3 (CH), 122.8 (CH), 120.1 (CH), 109.7 (CH), 31.8 ( $\text{CH}_3$ ), 26.8 ( $\text{CH}_3$ ).

IR (ATR): 2932, 1682, 1608, 1463, 1355, 1262, 1011, 834, 744, 604  $\text{cm}^{-1}$ .

MS (ESI)  $m/z$  (relative intensity): 251 (80)  $[\text{M}+\text{H}]^+$ , 273 (20)  $[\text{M}+\text{H}]^+$ .

HR-MS (ESI):  $m/z$  calcd for  $\text{C}_{16}\text{H}_{15}\text{N}_2\text{O}$   $[\text{M}+\text{H}]^+$ : 251.1181, found: 251.1179.

**Methyl 4-(1-methyl-1*H*-benzo[*d*]imidazol-2-yl)benzoate (446f)**

The **General Procedure G** was followed using 1-methyl-1*H*-benzo[*d*]imidazole **445a** (33 mg, 0.25 mmol), methyl 4-iodobenzoate **404r** (328 mg, 1.25 mmol), **406** (30 mg, 11 mol %) and K<sub>3</sub>PO<sub>4</sub> (159 mg, 0.75 mmol) in THF (0.5 mL). Purification by column chromatography on silica gel (*n*-hexane/EtOAc: 4/1) yielded **446f** (41.9 mg, 63%) as a light yellow solid.

**M. p.:** 120 °C.

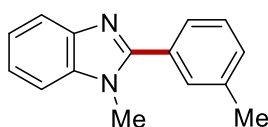
<sup>1</sup>H NMR (400 MHz, CDCl<sub>3</sub>) δ 8.20 (dd, *J* = 2.3, 1.7 Hz, 1H), 8.18 (dd, *J* = 2.3, 1.7 Hz, 1H), 7.87 (dd, *J* = 2.3, 1.7 Hz, 1H), 7.85 (dd, *J* = 2.3, 1.7 Hz, 1H), 7.82 (ddd, *J* = 4.1, 2.3, 0.8 Hz, 1H), 7.40 (ddd, *J* = 4.1, 2.3, 0.8 Hz, 1H), 7.32 (ddd, *J* = 6.6, 4.1, 1.7 Hz, 2H), 3.95 (s, 3H), 3.88 (s, 3H).

<sup>13</sup>C NMR (100 MHz, CDCl<sub>3</sub>) δ 166.5 (C<sub>q</sub>), 152.5 (C<sub>q</sub>), 143.0 (C<sub>q</sub>), 136.7 (C<sub>q</sub>), 134.5 (C<sub>q</sub>), 131.1 (C<sub>q</sub>), 129.9 (CH), 129.4 (CH), 123.2 (CH), 122.7 (CH), 120.1 (CH), 109.7 (CH), 52.4 (CH<sub>3</sub>), 31.8 (CH<sub>3</sub>).

**IR** (ATR): 2950, 1719, 1612, 1530, 1460, 1274, 1016, 964, 743 cm<sup>-1</sup>.

**MS** (ESI) *m/z* (relative intensity): 267 (90) [M+H]<sup>+</sup>, 289 (10) [M+H]<sup>+</sup>.

**HR-MS** (ESI): *m/z* calcd for C<sub>16</sub>H<sub>15</sub>N<sub>2</sub>O<sub>2</sub> [M+H]<sup>+</sup>: 267.1132, found: 267.1130.

**1-Methyl-2-(*m*-tolyl)-1*H*-benzo[*d*]imidazole (446g)**

The **General Procedure G** was followed using 1-methyl-1*H*-benzo[*d*]imidazole **445a** (33 mg, 0.25 mmol), 1-iodo-3-methylbenzene **404h** (273 mg, 1.25 mmol), **406** (30 mg, 11 mol %) and K<sub>3</sub>PO<sub>4</sub> (159 mg, 0.75 mmol) in THF (0.5 mL). Purification by column chromatography on silica gel (*n*-hexane/EtOAc: 4/1) yielded **446g** (34.5 mg, 62%) as a light yellow solid.

**M. p.:** 119 °C.

<sup>1</sup>H NMR (400 MHz, CDCl<sub>3</sub>) δ 7.80 (ddd, *J* = 5.2, 2.3, 0.9 Hz, 1H), 7.61 – 7.60 (m, 1H), 7.50 – 7.49 (m, 1H), 7.41 (t, *J* = 7.8 Hz, 1H), 7.39 – 7.37 (ddd, *J* = 5.2, 2.3, 0.9 Hz, 1H), 7.32 – 7.27 (m, 3H), 3.84 (s, 3H), 2.43 (s, 3H).

$^{13}\text{C}$  NMR (100 MHz,  $\text{CDCl}_3$ )  $\delta$  153.9 ( $\text{C}_q$ ), 142.9 ( $\text{C}_q$ ), 138.6 ( $\text{C}_q$ ), 136.5 ( $\text{C}_q$ ), 130.4 (CH), 130.2 (CH), 130.1 ( $\text{C}_q$ ), 128.4 (CH), 126.3 (CH), 122.6 (CH), 122.3 (CH), 119.8 (CH), 109.5 (CH), 31.6 ( $\text{CH}_3$ ), 21.4 ( $\text{CH}_3$ ).

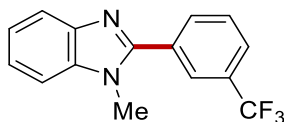
IR (ATR): 3050, 2920, 1609, 1589, 1456, 1325, 1256, 793, 742, 659  $\text{cm}^{-1}$ .

MS (ESI)  $m/z$  (relative intensity): 223 (100)  $[\text{M}+\text{H}]^+$ .

HR-MS (ESI):  $m/z$  calcd for  $\text{C}_{15}\text{H}_{14}\text{N}_2$   $[\text{M}+\text{H}]^+$ : 223.1236, found: 223.1230.

The spectral data were in accordance with those reported in the literature.<sup>[282]</sup>

### 1-Methyl-2-(*p*-tolyl)-1*H*-benzo[*d*]imidazole (446h)



The **General Procedure G** was followed using 1-methyl-1*H*-benzo[*d*]imidazole **445a** (33 mg, 0.25 mmol), 1-iodo-3-(trifluoromethyl)benzene **404j** (340 mg, 1.25 mmol), **406** (30 mg, 11 mol %) and  $\text{K}_3\text{PO}_4$  (159 mg, 0.75 mmol) in THF (0.5 mL). Purification by column chromatography on silica gel (*n*-hexane/EtOAc: 4/1) yielded **446h** (40.7 mg, 59%) as a light yellow solid.

M. p.: 141  $^\circ\text{C}$ .

$^1\text{H}$  NMR (400 MHz,  $\text{CDCl}_3$ )  $\delta$  8.06 – 8.04 (m, 1H), 7.97 – 7.93 (m, 1H), 7.82 (ddd,  $J = 3.6, 1.6, 0.8$  Hz, 1H), 7.77 – 7.73 (m, 1H), 7.68 – 7.62 (m, 1H), 7.40 (ddd,  $J = 3.6, 1.6, 0.8$  Hz, 1H), 7.34 (ddd,  $J = 6.4, 3.6, 1.6$  Hz, 2H), 3.87 (s, 3H).

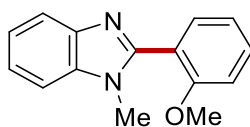
$^{13}\text{C}$  NMR (100 MHz,  $\text{CDCl}_3$ )  $\delta$  152.0 ( $\text{C}_q$ ), 142.9 ( $\text{C}_q$ ), 136.6 ( $\text{C}_q$ ), 132.5 (CH), 131.3 (d,  $J_{\text{C-F}} = 32.8$  Hz,  $\text{C}_q$ ), 131.1 ( $\text{C}_q$ ), 129.2 (CH), 126.6 (q,  $J_{\text{C-F}} = 3.8$  Hz, CH), 125.1 ( $\text{C}_q$ ), 123.7 (d,  $J_{\text{C-F}} = 273.6$  Hz, CH), 123.3 (CH), 122.8 (CH), 120.1 (CH), 109.7 (CH), 31.7 ( $\text{CH}_3$ ).

$^{19}\text{F}$  NMR (282 MHz,  $\text{CDCl}_3$ )  $\delta$  -62.73 (s).

IR (ATR): 3108, 3058, 2926, 1460, 1324, 1249, 1122, 1060, 743, 650  $\text{cm}^{-1}$ .

MS (ESI)  $m/z$  (relative intensity): 277 (100)  $[\text{M}+\text{H}]^+$ .

HR-MS (ESI):  $m/z$  calcd for  $\text{C}_{15}\text{H}_{11}\text{F}_3\text{N}_2$   $[\text{M}+\text{H}]^+$ : 277.0949, found: 277.0947.

**2-(2-Methoxyphenyl)-1-methyl-1H-benzo[d]imidazole (446i)**

The **General Procedure G** was followed using 1-methyl-1*H*-benzo[*d*]imidazole **445a** (33 mg, 0.25 mmol), 1-iodo-2-methoxybenzene **404o** (293 mg, 1.25 mmol), **406** (30 mg, 11 mol %) and K<sub>3</sub>PO<sub>4</sub> (159 mg, 0.75 mmol) in THF (0.5 mL). Purification by column chromatography on silica gel (*n*-hexane/EtOAc: 4/1) yielded **446i** (16.6 mg, 33%) as a light yellow oil.

**M. p.:** 97 °C.

<sup>1</sup>H NMR (400 MHz, CDCl<sub>3</sub>) δ 7.80 (ddd, *J* = 3.5, 1.7, 0.7 Hz, 1H), 7.56 (dd, *J* = 7.5, 1.7 Hz, 1H), 7.47 (ddd, *J* = 8.3, 7.5, 1.7 Hz, 1H), 7.37 (ddd, *J* = 3.5, 1.7, 0.7 Hz, 1H), 7.28 (ddd, *J* = 7.5, 3.5, 1.7 Hz, 2H), 7.08 (td, *J* = 7.5, 0.7 Hz, 1H), 7.00 (dd, *J* = 8.3, 0.7 Hz, 1H), 3.79 (s, 3H), 3.63 (s, 3H).

<sup>13</sup>C NMR (100 MHz, CDCl<sub>3</sub>) δ 157.4 (C<sub>q</sub>), 152.0 (C<sub>q</sub>), 143.0 (C<sub>q</sub>), 136.0 (C<sub>q</sub>), 132.2 (CH), 131.5 (CH), 122.3 (CH), 121.9 (CH), 120.9 (CH), 119.7 (CH), 119.5 (C<sub>q</sub>), 110.9 (CH), 109.3 (CH), 55.5 (CH<sub>3</sub>), 30.8 (CH<sub>3</sub>).

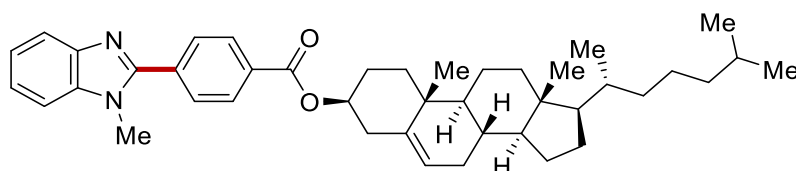
**IR** (ATR): 3059, 2941, 2837, 1458, 1437, 1251, 1117, 1201, 743, 640 cm<sup>-1</sup>.

**MS** (ESI) *m/z* (relative intensity): 239 (100) [M+H]<sup>+</sup>.

**HR-MS** (ESI): *m/z* calcd for C<sub>15</sub>H<sub>15</sub>N<sub>2</sub>O [M+H]<sup>+</sup>: 239.1184, found: 239.1182.

The spectral data were in accordance with those reported in the literature.<sup>[283]</sup>

**(3*S*,8*S*,9*S*,10*R*,13*R*,14*S*,17*R*)-10,13-Dimethyl-17-[(*R*)-6-methylheptan-2-yl]-2,3,4,7,8,9,10,11,12,13,14,15,16,17-tetradecahydro-1*H*-cyclopenta[*a*]phenanthren-3-yl 4-(1-methyl-1*H*-benzo[*d*]imidazol-2-yl)benzoate (446j)**



The **General Procedure G** was followed using 1-methyl-1*H*-benzo[*d*]imidazole **445a** (33 mg, 0.25 mmol), (3*S*,8*S*,9*S*,10*R*,13*R*,14*S*,17*R*)-10,13-dimethyl-17-[(*R*)-6-methyl heptan-2-yl]-2,3,4,7,8,9,10,11,12,13,14,15,16,17-tetradecahydro-1*H*-cyclopenta[*a*]phe nanthren-3-yl 4-iodobenzoate **404s** (770

mg, 1.25 mmol), **406** (30 mg, 11 mol %) and  $K_3PO_4$  (159 mg, 0.75 mmol) in THF (0.5 mL). Purification by column chromatography on silica gel (*n*-hexane/EtOAc: 4/1) yielded **446j** (63.6 mg, 41%) as a white solid.

**M. p.:** 192 °C.

**$^1H$  NMR** (400 MHz,  $CDCl_3$ )  $\delta$  8.20 (dd,  $J = 2.1, 1.5$  Hz, 1H), 8.17 (dd,  $J = 2.1, 1.5$  Hz, 1H), 7.86 (dd,  $J = 2.1, 1.5$  Hz, 1H), 7.84 (dd,  $J = 2.1, 1.5$  Hz, 1H), 7.83 – 7.81 (m, 1H), 7.40 (ddd,  $J = 6.3, 2.1, 0.8$  Hz, 1H), 7.30 (ddd,  $J = 6.3, 3.8, 1.5$  Hz, 2H), 5.42 (d,  $J = 4.5$  Hz, 1H), 4.90 (m, 1H), 3.88 (s, 3H), 2.49 (d,  $J = 7.7$  Hz, 2H), 2.07 – 1.92 (m, 4H), 1.88 – 1.62 (m, 3H), 1.62 – 1.42 (m, 5H), 1.34 – 1.30 (m, 3H), 1.27 – 1.16 (m, 4H), 1.12 – 1.08 (m, 3H), 1.07 – 0.95 (m, 7H), 0.91 (d,  $J = 6.5$  Hz, 3H), 0.86 (d,  $J = 1.8$  Hz, 3H), 0.84 (d,  $J = 1.8$  Hz, 3H), 0.68 (s, 3H).

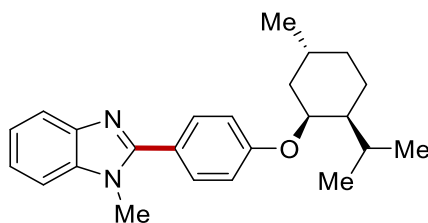
**$^{13}C$  NMR** (100 MHz,  $CDCl_3$ )  $\delta$  165.4 ( $C_q$ ), 152.6 ( $C_q$ ), 143.0 ( $C_q$ ), 139.5 ( $C_q$ ), 136.7 ( $C_q$ ), 134.3 ( $C_q$ ), 131.8 ( $C_q$ ), 129.8 (CH), 129.3 (CH), 123.2 (CH), 122.9 (CH), 122.7 (CH), 120.1 (CH), 109.7 (CH), 75.0 (CH), 56.7 (CH), 56.1 (CH), 50.0 (CH), 42.3 ( $C_q$ ), 39.7 ( $CH_2$ ), 39.5 ( $CH_2$ ), 38.2 ( $CH_2$ ), 37.0 ( $CH_3$ ), 36.7 ( $CH_2$ ), 36.2 ( $CH_2$ ), 35.8 (CH), 31.9 ( $CH_2$ ), 31.9 (CH), 31.8 ( $CH_3$ ), 28.2 ( $C_q$ ), 28.0 (CH), 27.9 ( $CH_2$ ), 24.3 ( $CH_2$ ), 23.8 ( $CH_2$ ), 22.8 ( $CH_2$ ), 22.6 ( $CH_3$ ), 21.1 ( $CH_2$ ), 19.4 ( $CH_3$ ), 18.7 ( $CH_3$ ), 11.9 ( $CH_3$ ).

**IR** (ATR): 2936, 2867, 2248, 1674, 1714, 1465, 1273, 1119, 1016, 736  $cm^{-1}$ .

**MS** (ESI)  $m/z$  (relative intensity): 621 (100)  $[M+H]^+$ .

**HR-MS** (ESI):  $m/z$  calcd for  $C_{42}H_{57}N_2O_2$   $[M+H]^+$ : 621.4412, found: 621.4415.

## 2-[4-[(1*S*,2*S*,5*R*)-2-Isopropyl-5-methylcyclohexyl]oxy]phenyl]-1-methyl-1*H*-benzo[*d*]imidazole (446k)



The **General Procedure H** was followed using 1-methyl-1*H*-benzo[*d*]imidazole **445a** (33 mg, 0.25 mmol), 1-bromo-4-[(1*S*,2*S*,5*R*)-2-isopropyl-5-methylcyclohexyl]oxy]benzene **447e** (448 mg, 1.25 mmol), **406** (30 mg, 11 mol %) and  $Cs_2CO_3$  (244 mg, 0.75 mmol) in Et<sub>2</sub>O (0.5 mL). Purification by



column chromatography on silica gel (*n*-hexane/EtOAc: 4/1) yielded **446k** (48.9 mg, 87%) as a light yellow solid.

**M. p.:** 137 °C.

**<sup>1</sup>H NMR** (400 MHz, CDCl<sub>3</sub>) δ 7.78 (ddd, *J* = 5.3, 2.3, 0.7 Hz, 1H), 7.68 (dd, *J* = 2.9, 2.3 Hz, 1H), 7.66 (dd, *J* = 2.9, 2.3 Hz, 1H), 7.36 (ddd, *J* = 5.3, 2.3, 0.7 Hz, 1H), 7.28 (ddd, *J* = 4.3, 2.3, 0.7 Hz, 2H), 7.02 (dd, *J* = 2.9, 2.3 Hz, 1H), 7.00 (dd, *J* = 2.9, 2.3 Hz, 1H), 4.71 (q, *J* = 2.6 Hz, 1H), 3.85 (s, 3H), 2.12 (dd, *J* = 14.0, 3.3 Hz, 1H), 1.83 – 1.61 (m, 4H), 1.61 – 1.51 (m, 1H), 0.97 (d, *J* = 6.7, 3H), 0.93 (d, *J* = 6.7 Hz, 3H), 0.86 (d, *J* = 6.7 Hz, 3H), 0.82 (d, *J* = 6.6 Hz, 3H).

**<sup>13</sup>C NMR** (100 MHz, CDCl<sub>3</sub>) δ 159.6 (C<sub>q</sub>), 154.0 (C<sub>q</sub>), 143.0 (C<sub>q</sub>), 136.6 (C<sub>q</sub>), 130.8 (CH), 122.4 (CH), 122.2 (CH), 121.9 (C<sub>q</sub>), 119.5 (CH), 115.7 (CH), 109.4 (CH), 73.5 (CH), 47.7 (CH), 37.6 (CH<sub>2</sub>), 34.9 (CH<sub>2</sub>), 31.7 (CH<sub>3</sub>), 29.3 (CH), 26.2 (CH), 24.8 (CH<sub>2</sub>), 22.3 (CH), 21.0 (CH), 20.8 (CH).

**IR** (ATR): 2922, 2867, 1609, 1460, 1436, 1246, 1172, 962, 836, 741 cm<sup>-1</sup>.

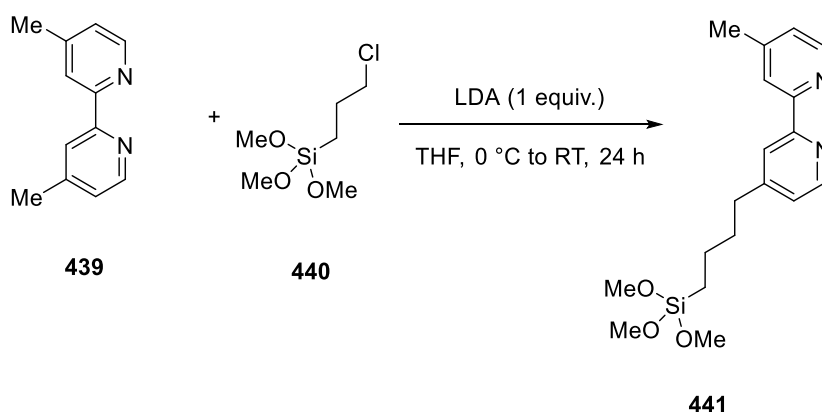
**MS** (ESI) *m/z* (relative intensity): 363 (100) [M+H]<sup>+</sup>.

**HR-MS** (ESI): *m/z* calcd for C<sub>24</sub>H<sub>31</sub>N<sub>2</sub>O [M+H]<sup>+</sup>: 363.2435, found: 363.2431.

### 5.6.2 Synthesis of Hybrid Copper Catalyst

#### 1) Linker modification:

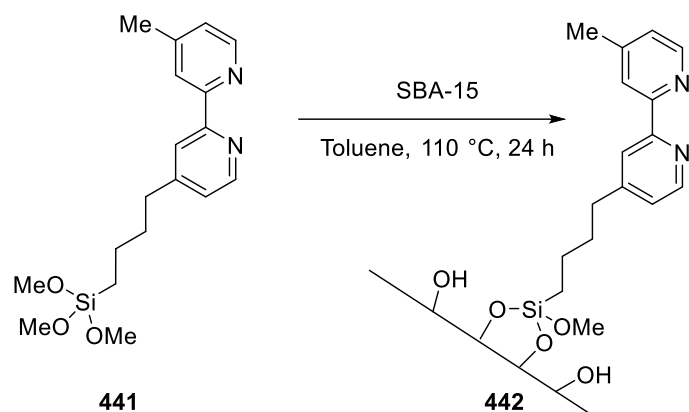
To a solution of DIPA (15 mmol, 1.1 equiv) in 40 mL of dried THF (50 mL) was added *n*-BuLi (2.1 M, 6.3 mL, 13.2 mmol, 1.0 equiv) dropwise at 0 °C under N<sub>2</sub>, *in-situ* generating LDA. After the reaction mixture was stirred for 1 h, a solution of 4,4-dimethyl-2,2'-bipyridine (**439**) (13.2 mmol, 1.0 equiv) in dried THF (100 mL) was slowly added under N<sub>2</sub>, then color was changed to dark brown. After stirring the reaction mixture for 1 h, a solution of (3-chloropropyl)trimethoxysilane (**440**) (13.2 mmol, 1.0 equiv) in 10 mL of THF was slowly added at 0 °C under N<sub>2</sub>. The solution was further stirred for an additional 2 h. The reaction mixture was warmed to room temperature and stirred for 24 h. After the reaction was quenched with two drops of acetone, the remaining solvent was removed and then dried *in vacuo* at room temperature for 24 h, affording **441**. The synthesized **441** are used for the next step without further purification (Scheme 5.6.1).



**Scheme 5.6.1** Synthesis of **441**.

#### 2) Grafting

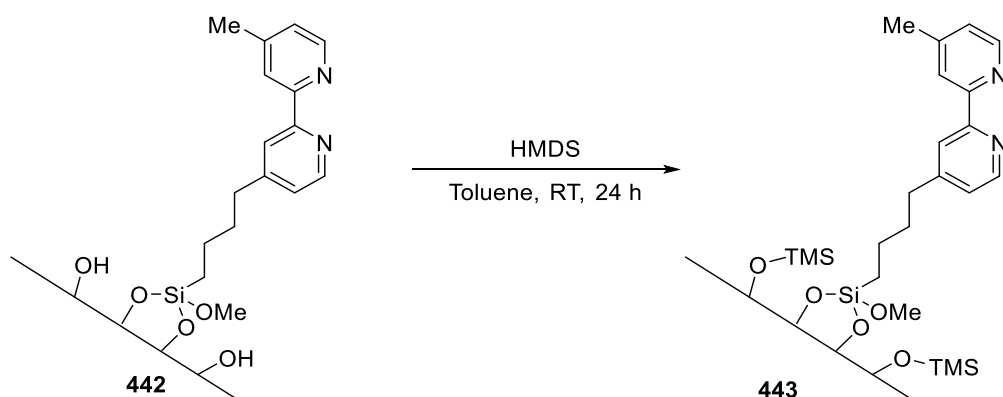
A suspension of SBA-15 (5.0 g) and the synthesized **441** were refluxed in dried toluene under N<sub>2</sub> for 24 h. The powder was filtered off, washed with toluene, *n*-hexane, and DCM (each 50 mL), and dried *in vacuo* at 100 °C for 24 h, yielding **442** (Scheme 5.6.2).



**Scheme 5.6.2** Synthesis of **442**.

### 3) End-capping

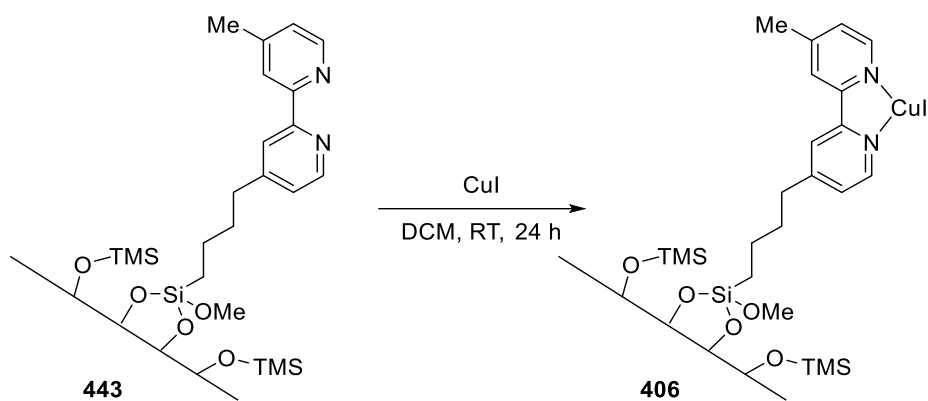
Hexamethyldisilazane (20 mL) and the isolated **442** in dried toluene (50 mL) was stirred at room temperature for 24 h. The powder was filtered off, washed with toluene, *n*-hexane, and DCM (each 50 mL), and dried *in vacuo* at 100 °C for 24 h, providing **443** (Scheme 5.6.3).



**Scheme 5.6.3** Synthesis of **443**.

### 4) Metallation

A suspension of CuI (6.0 mmol) and the isolated **443** were stirred in DCM at room temperature for 24 h. The powder filtered off, washed with DCM, MeCN, and MeOH (each 50 mL), and dried *in vacuo* at 100 °C for 24 h, finally affording **406**.



**Scheme 5.6.4** Synthesis of **406**.

### 5.6.3 Determination of Catalyst Loading

ICP-OES analysis was performed by Dr. Volker Karius for the determination of hybrid copper catalyst **406** loading (Equation 5.6.1)

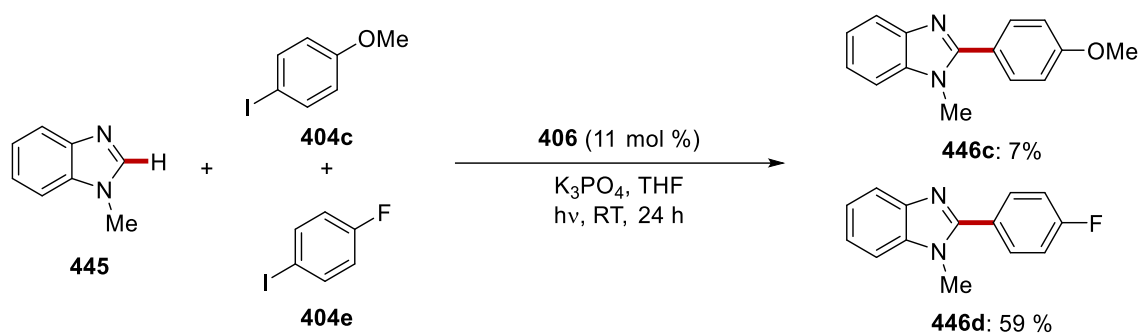
Amount of Catalyst  $\times$  ICP-OES result  $\div$  Molecular weight of copper  $\div$   
amount of substrates  $\times 100$  mol %

$$= 30 \text{ mg} \times \frac{58300 \text{ mg}}{1,000,000 \text{ mg}} \times \frac{1}{63.546 \text{ mg/mmol}} \times \frac{1}{0.25 \text{ mmol}} \times 100 \text{ mol \%} = \mathbf{11 \text{ mol \%}}$$

**Equation 5.6.1** Determination of hybrid copper catalyst loading.

### 5.6.4 Competition Experiment

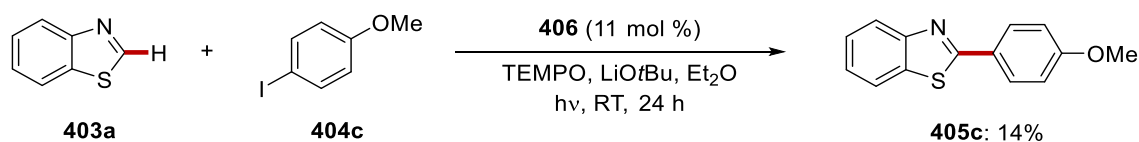
A suspension of 1-methyl-1*H*-benzo[*d*]imidazole **445a** (0.25 mmol, 1.0 equiv), 4-iodoanisole **404c** (1.25 mmol, 5.0 equiv), 1-fluoro-4-iodobenzene **404e** (278 mg, 5.0 equiv), **406** (11 mol %) and K<sub>3</sub>PO<sub>4</sub> (0.75 mmol, 3.0 equiv) in THF (1.0 mL) was stirred under photo-induced and nitrogen conditions. After 24 h the solvent was removed under reduced pressure. Purification by column chromatography on silica gel (*n*-Hexane/EtOAc = 6/1 to 1/1) afforded the desired products **446c** and **446d** respectively.



Scheme 5.6.5 Competition experiment with **445** and **404**.

### 5.6.5 Radical Experiment

A suspension of benzothiazole **403a** (0.25 mmol, 1.0 equiv), 4-iodoanisole **404c** (1.25 mmol, 5.0 equiv), **406** (11 mol %), LiOtBu (0.75 mmol, 3.0 equiv) and TEMPO (0.25 mmol, 1.0 equiv) in Et<sub>2</sub>O (0.5 mL) was stirred under photo-induced and nitrogen conditions. Purification by column chromatography on silica gel (*n*-Hexane/EtOAc: 70/1) yielded **405c**.



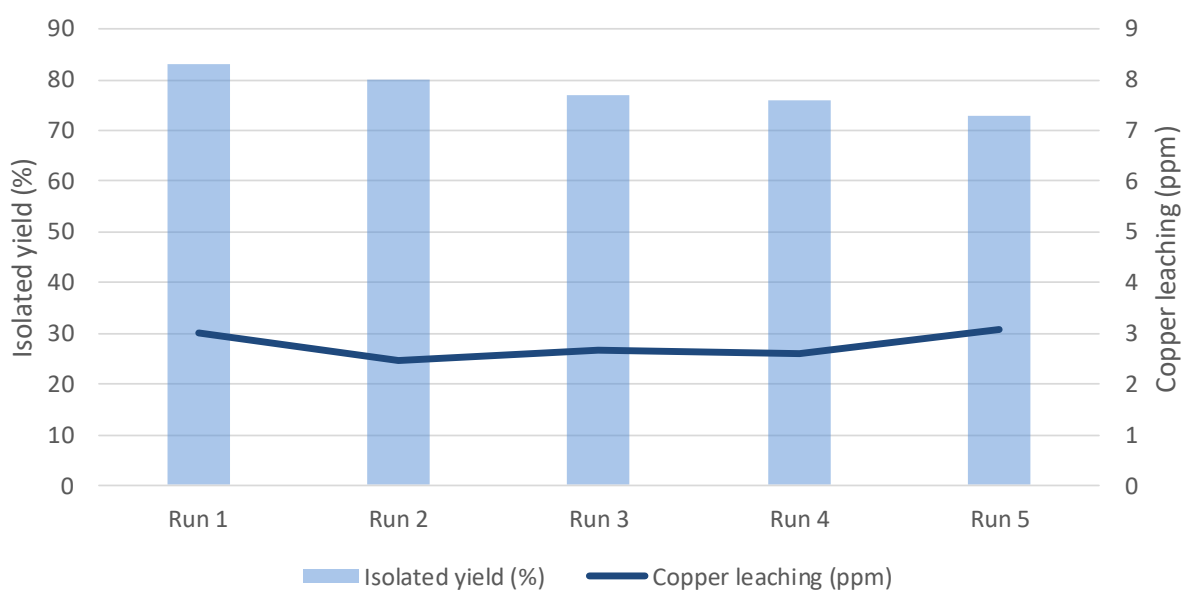
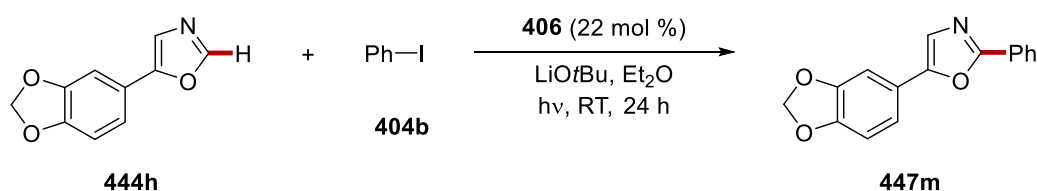
Scheme 5.6.6 Experiment with radical scavenger TEMPO.



### 5.6.8 Heterogeneity Test

#### 1) Reuse test

A suspension of 5-(benzo[*d*][1,3]dioxol-5-yl)oxazole **444h** (0.25 mmol, 1.0 equiv), iodobenzene **404b** (1.25 mmol, 5.0 equiv), **406** (22 mol %) and LiOtBu (0.75 mmol, 3.0 equiv) in Et<sub>2</sub>O (1.0 mL) was stirred under photo-induced and nitrogen conditions (Scheme 5.6.7). After 24 h the reaction tube was transferred to a glovebox. **406** was carefully filtered through branched filter (Por. 3) with Et<sub>2</sub>O and DCM (each 10 mL). Filtered **406** was dried *in vacuo* and used for next run. Filtrate was used for either obtaining desired product **447m** by column chromatography on silica or measuring metal leaching by ICP-AES.



**Scheme 5.6.7** Reuse tests and the determination of metal leaching.

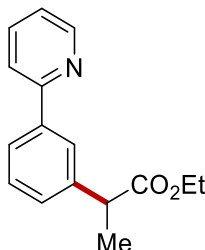




## 5.7 Distal C–H Activation by Reusable Heterogeneous Ruthenium Catalysis

### 5.7.1 Characterization Data

#### Ethyl 2-(3-(pyridin-2-yl)phenyl)propanoate (**409a**)



The **General Procedure I** was followed using 2-phenylpyridine **407a** (38.8 mg, 0.25 mmol), ethyl 2-bromopropanoate **408a** (136 mg, 0.75 mmol), **410** (30.0 mg, 10 mol %) and KOAc (49.1 mg, 0.50 mmol) in 2-MeTHF (2.0 mL). Purification by column chromatography on silica gel (*n*-hexane/EtOAc: 10/1) yielded **409a** (44.7 mg, 70%) as a colorless oil.

**<sup>1</sup>H NMR** (400 MHz, CDCl<sub>3</sub>)  $\delta$  8.62 (dd,  $J = 4.8, 1.4$  Hz, 1H), 7.92 (dd,  $J = 1.8, 0.6$  Hz, 1H), 7.82 (dd,  $J = 7.5, 1.8$  Hz, 1H), 7.65 (d,  $J = 1.4$  Hz, 1H), 7.64 (dd,  $J = 2.3, 1.4$  Hz, 1H), 7.37 (dd,  $J = 7.5, 0.6$  Hz, 1H), 7.32 (dd,  $J = 7.5, 1.8$  Hz, 1H), 7.15 – 7.11 (m, 1H), 4.14 – 3.99 (m, 2H), 3.76 (q,  $J = 7.1$  Hz, 1H), 1.50 (d,  $J = 7.1$  Hz, 3H), 1.14 (t,  $J = 7.1$  Hz, 3H).

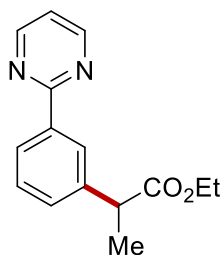
**<sup>13</sup>C NMR** (100 MHz, CDCl<sub>3</sub>)  $\delta$  174.2 (C<sub>q</sub>), 157.0 (C<sub>q</sub>), 149.4 (CH), 141.0 (C<sub>q</sub>), 139.5 (C<sub>q</sub>), 136.5 (CH), 128.8 (CH), 127.7 (CH), 126.1 (CH), 125.4 (CH), 121.9 (CH), 120.4 (CH), 60.5 (CH<sub>2</sub>), 45.4 (CH), 18.5 (CH<sub>3</sub>), 13.9 (CH<sub>3</sub>).

**IR** (ATR): 2936, 2711, 1783, 1461, 1437, 1200, 1161, 773 cm<sup>-1</sup>.

**MS** (ESI)  $m/z$  (relative intensity): 278 (20) [M+Na]<sup>+</sup>, 256 (80) [M+H]<sup>+</sup>.

**HR-MS** (ESI)  $m/z$  calcd. for C<sub>16</sub>H<sub>18</sub>NO<sub>2</sub> [M+H]<sup>+</sup>: 256.1334, found: 256.1335.

The spectral data were in accordance with those reported in the literature.<sup>[284]</sup>

**Ethyl 2-(3-(pyrimidin-2-yl)phenyl)propanoate (409b)**

The **General Procedure I** was followed using 2-phenylpyrimidine **407b** (39.0 mg, 0.25 mmol), ethyl 2-bromopropanoate **408a** (136 mg, 0.75 mmol), **410** (30.0 mg, 10 mol %) and KOAc (49.1 mg, 0.50 mmol) in 2-MeTHF (2.0 mL). Purification by column chromatography on silica gel (*n*-hexane/EtOAc: 10/1) yielded **409b** (40.4 mg, 63%) as a colorless oil.

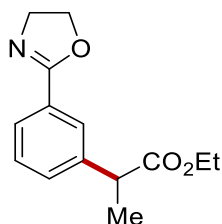
**<sup>1</sup>H NMR** (400 MHz, CDCl<sub>3</sub>)  $\delta$  8.78 (d,  $J$  = 5.0 Hz, 2H), 8.38 – 8.36 (m, 1H), 8.31 (ddd,  $J$  = 5.0, 4.2, 1.7 Hz, 1H), 7.45 – 7.42 (m, 2H), 7.16 (t,  $J$  = 4.8 Hz, 1H), 4.18 – 4.04 (m, 2H), 3.81 (q,  $J$  = 7.2 Hz, 1H), 1.54 (d,  $J$  = 7.1 Hz, 3H), 1.18 (t,  $J$  = 7.1 Hz, 3H).

**<sup>13</sup>C NMR** (100 MHz, CDCl<sub>3</sub>)  $\delta$  174.4 (C<sub>q</sub>), 164.5 (C<sub>q</sub>), 157.2 (CH), 141.1 (C<sub>q</sub>), 137.8 (C<sub>q</sub>), 129.8 (CH), 128.9 (CH), 127.5 (CH), 126.9 (CH), 119.1 (CH), 60.7 (CH<sub>2</sub>), 45.6 (CH), 18.64 (CH<sub>3</sub>), 14.1 (CH<sub>3</sub>).

**IR** (ATR): 2978, 2720, 2012, 1585, 1302, 1143, 1007, 769 cm<sup>-1</sup>.

**MS** (ESI)  $m/z$  (relative intensity): 279 (60) [M+Na]<sup>+</sup>, 257 (40) [M+H]<sup>+</sup>.

**HR-MS** (ESI)  $m/z$  calcd. for C<sub>15</sub>H<sub>17</sub>N<sub>2</sub>O<sub>2</sub> [M+H]<sup>+</sup>: 257.1286, found: 257.1285.

**Ethyl 2-(3-(4,5-dihydrooxazol-2-yl)phenyl)propanoate (409c)**

The **General Procedure I** was followed using 2-phenyl-4,5-dihydrooxazole **407c** (38.8 mg, 0.25 mmol), ethyl 2-bromopropanoate **408a** (136 mg, 0.75 mmol), **410** (30.0 mg, 10 mol %) and KOAc (49.1 mg, 0.50 mmol) in 2-MeTHF (2.0 mL). Purification by column chromatography on silica gel (*n*-hexane/EtOAc: 10/1) yielded **409c** (34.0 mg, 55%) as a colorless oil.

**<sup>1</sup>H NMR** (400 MHz, CDCl<sub>3</sub>)  $\delta$  7.89 (t,  $J$  = 1.6 Hz, 1H), 7.83 (dt,  $J$  = 7.7, 1.6 Hz, 1H), 7.43 (dt,  $J$  = 7.7, 1.6 Hz, 1H), 7.36 (t,  $J$  = 7.7 Hz, 1H), 4.43 (t,  $J$  = 9.5 Hz, 2H), 4.23 – 3.99 (m, 4H), 3.74 (q,  $J$  = 7.2 Hz, 1H), 1.51 (d,  $J$  = 7.2 Hz, 3H), 1.19 (t,  $J$  = 7.1 Hz, 3H).

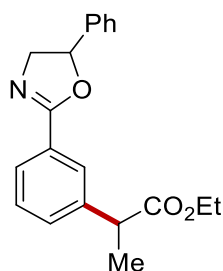
**<sup>13</sup>C NMR** (100 MHz, CDCl<sub>3</sub>)  $\delta$  174.3 (C<sub>q</sub>), 164.7 (C<sub>q</sub>), 141.1 (C<sub>q</sub>), 130.5 (CH), 128.8 (CH), 128.2 (C<sub>q</sub>), 127.6 (CH), 127.1 (CH), 67.8 (CH<sub>2</sub>), 61.0 (CH<sub>2</sub>), 55.1 (CH<sub>2</sub>), 45.6 (CH), 18.6 (CH<sub>3</sub>), 14.3 (CH<sub>3</sub>).

**IR** (ATR): 2980, 1732, 1650, 1362, 1194, 1067, 950, 711, 422 cm<sup>-1</sup>.

**MS** (EI)  $m/z$  (relative intensity): 247 (21) [M]<sup>+</sup>, 174 (100), 131 (33), 103 (26).

**HR-MS** (EI<sup>+</sup>)  $m/z$  calcd. for C<sub>14</sub>H<sub>17</sub>NO<sub>3</sub> [M]<sup>+</sup>: 247.1208, found: 247.1210.

### Ethyl 2-(3-(4-phenyl-4,5-dihydrooxazol-2-yl)phenyl)propanoate (409d)



The **General Procedure I** was followed using 2,5-diphenyl-4,5-dihydrooxazole **407d** (55.8 mg, 0.25 mmol), ethyl 2-bromopropanoate **408a** (125.2 mg, 0.75 mmol), **410** (30.0 mg, 10 mol %) and KOAc (49.1 mg, 0.50 mmol) in 2-MeTHF (2.0 mL). Purification by column chromatography on silica gel (*n*-hexane/EtOAc: 10/1) yielded **409d** (55.7 mg, 69%) as a colorless oil.

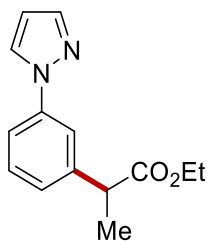
**<sup>1</sup>H NMR** (400 MHz, CDCl<sub>3</sub>)  $\delta$  7.96 (s, 1H), 7.91 (dd,  $J$  = 7.6, 1.5 Hz, 1H), 7.47 (d,  $J$  = 7.9 Hz, 1H), 7.44 – 7.31 (m, 6H), 5.66 (dd,  $J$  = 10.2, 8.0 Hz, 1H), 4.48 (dd,  $J$  = 14.9, 10.2 Hz, 1H), 4.20 – 4.05 (m, 2H), 4.00 (dd,  $J$  = 14.9, 8.0 Hz, 1H), 3.76 (q,  $J$  = 7.2 Hz, 1H), 1.52 (d,  $J$  = 7.2 Hz, 3H), 1.20 (t,  $J$  = 7.2, 3H).

**<sup>13</sup>C NMR** (100 MHz, CDCl<sub>3</sub>)  $\delta$  174.3 (C<sub>q</sub>), 164.0 (C<sub>q</sub>), 141.1 (C<sub>q</sub>), 130.7 (CH), 129.0 (CH), 129.0 (CH), 128.9 (CH), 128.5 (CH), 128.1 (C<sub>q</sub>), 127.8 (C<sub>q</sub>), 127.2 (CH), 125.9 (CH), 81.3 (CH<sub>2</sub>), 63.3 (CH), 61.0 (CH<sub>2</sub>), 45.6 (CH), 18.7 (CH<sub>3</sub>), 14.3 (CH<sub>3</sub>).

**IR** (ATR): 2979, 1731, 1651, 1337, 1193, 1064, 699 cm<sup>-1</sup>.

**MS** (EI)  $m/z$  (relative intensity): 323 (4) [M]<sup>+</sup>, 250 (10), 217 (100), 189 (12).

**HR-MS** (EI<sup>+</sup>)  $m/z$  calcd. for C<sub>20</sub>H<sub>21</sub>NO<sub>3</sub> [M]<sup>+</sup>: 323.1521, found: 323.1523.

**Ethyl 2-(3-(1*H*-pyrazol-1-yl)phenyl)propanoate (409e)**

The **General Procedure I** was followed using 1-phenyl-1*H*-pyrazole **407e** (36.0 mg, 0.25 mmol), ethyl 2-bromopropanoate **408a** (136 mg, 0.75 mmol), **410** (30.0 mg, 10 mol %) and KOAc (49.1 mg, 0.50 mmol) in 2-MeTHF (2.0 mL). Purification by column chromatography on silica gel (*n*-hexane/EtOAc: 10/1) yielded **409e** (34.2 mg, 56%) as a colorless oil.

**<sup>1</sup>H NMR** (400 MHz, CDCl<sub>3</sub>)  $\delta$  7.91 (dd,  $J = 2.5, 0.6$  Hz, 1H), 7.70 (dd,  $J = 1.7, 0.6$  Hz, 1H), 7.66 – 7.64 (m, 1H), 7.55 (ddd,  $J = 8.0, 2.2, 1.1$  Hz, 1H), 7.38 (t,  $J = 8.0$  Hz, 1H), 7.22 (dddd,  $J = 7.7, 1.7, 1.1, 0.6$  Hz, 1H), 6.44 (dd,  $J = 2.5, 1.7$  Hz, 1H), 4.17 – 4.06 (m, 2H), 3.75 (q,  $J = 7.1$  Hz, 1H), 1.52 (d,  $J = 7.1$  Hz, 3H), 1.19 (t,  $J = 7.1$  Hz, 3H).

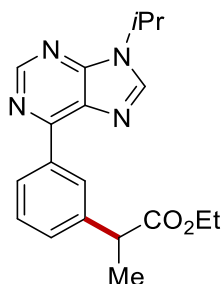
**<sup>13</sup>C NMR** (100 MHz, CDCl<sub>3</sub>)  $\delta$  174.1 (C<sub>q</sub>), 142.2 (C<sub>q</sub>), 141.1 (CH), 140.4 (C<sub>q</sub>), 129.6 (CH), 126.8 (CH), 125.5 (CH), 118.6 (CH), 117.9 (CH), 107.6 (CH), 60.9 (CH<sub>2</sub>), 45.5 (CH), 18.54 (CH<sub>3</sub>), 14.1 (CH<sub>3</sub>).

**IR** (ATR): 2853, 2749, 1987, 1582, 1461, 1203, 1170, 771 cm<sup>-1</sup>.

**MS** (ESI)  $m/z$  (relative intensity): 245 (70) [M+H]<sup>+</sup>, 267 (30) [M+Na]<sup>+</sup>.

**HR-MS** (ESI)  $m/z$  calcd. for C<sub>14</sub>H<sub>17</sub>N<sub>2</sub>O<sub>2</sub> [M+H]<sup>+</sup>: 245.1287, found: 245.1285.

The spectral data were in accordance with those reported in the literature.<sup>[284]</sup>

**Ethyl 2-(3-(9-isopropyl-9*H*-purin-6-yl)phenyl)propanoate (409f)**

The **General Procedure I** was followed using 9-isopropyl-6-phenyl-9*H*-purine **407f** (59.6 mg, 0.25 mmol), ethyl 2-bromopropanoate **408a** (136 mg, 0.75 mmol), **410** (30.0 mg, 10 mol %) and KOAc

(49.1 mg, 0.50 mmol) in 2-MeTHF (2.0 mL). Purification by column chromatography on silica gel (*n*-hexane/EtOAc: 3/1) yielded **409f** (77.8 mg, 92%) as a colorless oil.

**<sup>1</sup>H NMR** (400 MHz, CDCl<sub>3</sub>)  $\delta$  9.00 (s, 1H), 8.72 (dd,  $J = 7.4, 1.7$  Hz, 1H), 8.68 (dd,  $J = 1.7, 0.8$  Hz, 1H), 8.17 (s, 1H), 7.55 – 7.45 (m, 2H), 4.97 (sept,  $J = 6.8$  Hz, 1H), 4.12 (q,  $J = 7.2$  Hz, 2H), 3.86 (q,  $J = 7.2$  Hz, 1H), 1.66 (d,  $J = 6.8$  Hz, 6H), 1.57 (d,  $J = 7.2$  Hz, 3H), 1.19 (t,  $J = 7.2$  Hz, 3H).

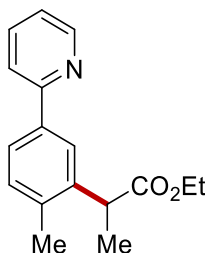
**<sup>13</sup>C NMR** (100 MHz, CDCl<sub>3</sub>)  $\delta$  174.6 (C<sub>q</sub>), 154.6 (C<sub>q</sub>), 152.2 (C<sub>q</sub>), 152.1 (CH), 142.1 (CH), 141.3 (C<sub>q</sub>), 136.2 (C<sub>q</sub>), 131.6 (C<sub>q</sub>), 129.9 (CH), 129.0 (CH), 129.0 (CH), 129.0 (CH), 60.9 (CH<sub>2</sub>), 47.4 (CH), 45.8 (CH), 22.7 (CH<sub>3</sub>), 18.8 (CH<sub>3</sub>), 14.2 (CH<sub>3</sub>).

**IR** (ATR): 2979, 1727, 1568, 1446, 1325, 1219, 1176, 1064, 797, 647 cm<sup>-1</sup>.

**MS** (EI)  $m/z$  (relative intensity): 338 (60) [M]<sup>+</sup>, 265 (81), 223 (100), 208 (52).

**HR-MS** (EI<sup>+</sup>)  $m/z$  calcd. for C<sub>19</sub>H<sub>22</sub>N<sub>4</sub>O<sub>2</sub> [M]<sup>+</sup>: 338.1743, found: 338.1735.

#### Ethyl 2-(2-methyl-5-(pyridin-2-yl)phenyl)propanoate (**409g**)



The **General Procedure I** was followed using 2-(*p*-tolyl)pyridine **407g** (42.3 mg, 0.25 mmol), ethyl 2-bromopropanoate **408a** (136 mg, 0.75 mmol), **410** (30.0 mg, 10 mol %) and KOAc (49.1 mg, 0.50 mmol) in 2-MeTHF (2.0 mL). Purification by column chromatography on silica gel (*n*-hexane/EtOAc: 10/1) yielded **409g** (48.5 mg, 72%) as a colorless oil.

**<sup>1</sup>H NMR** (400 MHz, CDCl<sub>3</sub>)  $\delta$  8.65 (ddd,  $J = 4.8, 1.8, 1.1$  Hz, 1H), 7.87 (d,  $J = 2.0$  Hz, 1H), 7.78 (dd,  $J = 7.9, 2.0$  Hz, 1H), 7.74 – 7.63 (m, 2H), 7.25 (d,  $J = 7.9$  Hz, 1H), 7.17 (ddd,  $J = 6.7, 4.8, 1.8$  Hz, 1H), 4.17 – 4.06 (m, 2H), 3.98 (q,  $J = 7.1$  Hz, 1H), 2.39 (s, 3H), 1.53 (d,  $J = 7.1$  Hz, 3H), 1.18 (t,  $J = 7.1$  Hz, 3H).

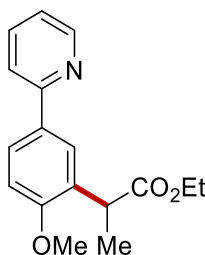
**<sup>13</sup>C NMR** (100 MHz, CDCl<sub>3</sub>)  $\delta$  174.7 (C<sub>q</sub>), 157.3 (C<sub>q</sub>), 149.6 (CH), 139.5 (C<sub>q</sub>), 137.6 (C<sub>q</sub>), 136.7 (C<sub>q</sub>), 136.6 (CH), 130.9 (CH), 125.3 (CH), 125.2 (CH), 121.8 (CH), 120.3 (CH), 60.7 (CH<sub>2</sub>), 41.6 (CH), 19.4 (CH<sub>3</sub>), 17.9 (CH<sub>3</sub>), 14.1 (CH<sub>3</sub>).

**IR** (ATR): 2971, 2732, 1739, 1460, 1436, 1232, 1159, 771  $\text{cm}^{-1}$ .

**MS** (ESI)  $m/z$  (relative intensity): 292 (20)  $[\text{M}+\text{Na}]^+$ , 270 (80)  $[\text{M}+\text{H}]^+$ .

**HR-MS** (ESI)  $m/z$  calcd. for  $\text{C}_{17}\text{H}_{20}\text{NO}_2$   $[\text{M}+\text{H}]^+$ : 270.1492, found: 270.1490.

**Ethyl 2-(2-methoxy-5-(pyridin-2-yl)phenyl)propanoate (409h)**



The **General Procedure I** was followed using 2-(4-methoxyphenyl)pyridine **407h** (46.3 mg, 0.25 mmol), ethyl 2-bromopropanoate **408a** (136 mg, 0.75 mmol), **410** (30.0 mg, 10 mol %) and KOAc (49.1 mg, 0.50 mmol) in 2-MeTHF (2.0 mL). Purification by column chromatography on silica gel (*n*-hexane/EtOAc: 10/1) yielded **409h** (62.8 mg, 88%) as a colorless oil.

**$^1\text{H}$  NMR** (400 MHz,  $\text{CDCl}_3$ )  $\delta$  8.62 (ddd,  $J = 4.8, 1.8, 1.0$  Hz, 1H), 7.87 (dd,  $J = 8.4, 2.3$  Hz, 1H), 7.86 – 7.85 (m, 1H), 7.71 – 7.62 (m, 2H), 7.14 (ddd,  $J = 7.0, 4.8, 1.8$  Hz, 1H), 6.94 (d,  $J = 8.4$  Hz, 1H), 4.12 (q,  $J = 7.2$  Hz, 2H), 4.02 (q,  $J = 7.2$  Hz, 1H), 3.85 (s, 3H), 1.50 (d,  $J = 7.2$  Hz, 3H), 1.18 (t,  $J = 7.1$  Hz, 3H).

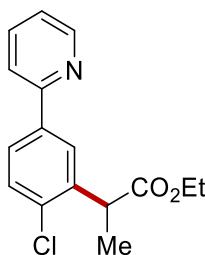
**$^{13}\text{C}$  NMR** (100 MHz,  $\text{CDCl}_3$ )  $\delta$  174.9 ( $\text{C}_q$ ), 157.6 ( $\text{C}_q$ ), 157.1 ( $\text{C}_q$ ), 149.5 (CH), 136.5 (CH), 132.0 ( $\text{C}_q$ ), 129.9 ( $\text{C}_q$ ), 126.9 (CH), 126.7 (CH), 121.4 (CH), 119.9 (CH), 110.7 (CH), 60.5 ( $\text{CH}_2$ ), 55.5 ( $\text{CH}_3$ ), 39.9 (CH), 17.2 ( $\text{CH}_3$ ), 14.2 ( $\text{CH}_3$ ).

**IR** (ATR): 2960, 2697, 1731, 1463, 1434, 1205, 1162, 770  $\text{cm}^{-1}$ .

**MS** (ESI)  $m/z$  (relative intensity): 308 (20)  $[\text{M}+\text{Na}]^+$ , 286 (80)  $[\text{M}+\text{H}]^+$ .

**HR-MS** (ESI)  $m/z$  calcd. for  $\text{C}_{17}\text{H}_{20}\text{NO}_3$   $[\text{M}+\text{H}]^+$ : 286.1441, found: 286.1439.

The spectral data were in accordance with those reported in the literature.<sup>[284]</sup>

**Ethyl 2-(2-chloro-5-(pyridin-2-yl)phenyl)propanoate (409i)**

The **General Procedure I** was followed using 2-(4-chlorophenyl)pyridine **407i** (47.4 mg, 0.25 mmol), ethyl 2-bromopropanoate **408a** (136 mg, 0.75 mmol), **410** (30.0 mg, 10 mol %) and KOAc (49.1 mg, 0.50 mmol) in 2-MeTHF (2.0 mL). Purification by column chromatography on silica gel (*n*-hexane/EtOAc: 10/1) yielded **409i** (39.1 mg, 54%) as a colorless oil.

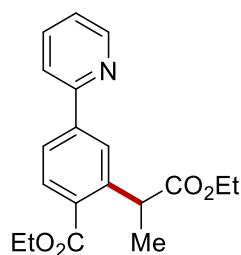
**<sup>1</sup>H NMR** (400 MHz, CDCl<sub>3</sub>) δ 8.66 (ddd, *J* = 4.8, 1.8, 1.2 Hz, 1H), 7.95 (d, *J* = 2.2 Hz, 1H), 7.82 (dd, *J* = 8.4, 2.2 Hz, 1H), 7.72 (ddd, *J* = 8.4, 7.3, 2.2 Hz, 1H), 7.67 (ddd, *J* = 7.3, 1.8, 1.2 Hz, 1H), 7.45 (d, *J* = 8.4 Hz, 1H), 7.21 (ddd, *J* = 7.3, 4.8, 1.2 Hz, 1H), 4.22 (q, *J* = 7.2 Hz, 1H), 4.18 – 4.12 (m, 2H), 1.55 (d, *J* = 7.2 Hz, 3H), 1.20 (t, *J* = 7.1 Hz, 3H).

**<sup>13</sup>C NMR** (100 MHz, CDCl<sub>3</sub>) δ 173.9 (C<sub>q</sub>), 156.1 (C<sub>q</sub>), 149.7 (CH), 138.8 (C<sub>q</sub>), 138.4 (C<sub>q</sub>), 136.8 (CH), 134.5 (C<sub>q</sub>), 129.9 (CH), 127.0 (CH), 126.6 (CH), 122.3 (CH), 120.4 (CH), 60.9 (CH<sub>2</sub>), 42.5 (CH), 17.5 (CH<sub>3</sub>), 14.1 (CH<sub>3</sub>).

**IR** (ATR): 2960, 2697, 1731, 1463, 1434, 1205, 1162, 770 cm<sup>-1</sup>.

**MS** (ESI) *m/z* (relative intensity): 312 (20) [M+Na]<sup>+</sup>, 290 (80) [M+H]<sup>+</sup>.

**HR-MS** (ESI) *m/z* calcd. for C<sub>16</sub>H<sub>17</sub><sup>35</sup>ClNO<sub>2</sub> [M+H]<sup>+</sup>: 290.0945, found: 290.0943.

**Methyl 2-(1-ethoxy-1-oxopropan-2-yl)-4-(pyridin-2-yl)benzoate (409j)**

The **General Procedure I** was followed using methyl 4-(pyridin-2-yl)benzoate **407j** (53.3 mg, 0.25 mmol), ethyl 2-bromopropanoate **408a** (136 mg, 0.75 mmol), **410** (30.0 mg, 10 mol %) and KOAc (49.1 mg, 0.50 mmol) in 2-MeTHF (2.0 mL). Purification by column chromatography on silica gel (*n*-hexane/EtOAc: 10/1) yielded **409j** (47.0 mg, 60%) as a colorless oil.

**<sup>1</sup>H NMR** (400 MHz, CDCl<sub>3</sub>) δ 8.69 (ddd, *J* = 4.8, 1.8, 1.1 Hz, 1H), 8.00 (dd, *J* = 4.8, 3.0 Hz, 2H), 7.92 (dd, *J* = 8.2, 1.8 Hz, 1H), 7.78 – 7.71 (m, 2H), 7.25 (ddd, *J* = 6.0, 4.8, 3.0 Hz, 1H), 4.67 (q, *J* = 7.1 Hz, 1H), 4.36 (q, *J* = 7.1 Hz, 2H), 4.16 – 4.05 (m, 2H), 1.60 (d, *J* = 7.1 Hz, 3H), 1.39 (t, *J* = 7.1 Hz, 3H), 1.16 (t, *J* = 7.1 Hz, 3H).

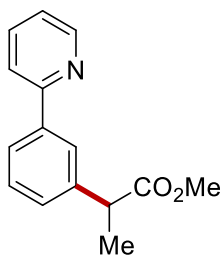
**<sup>13</sup>C NMR** (100 MHz, CDCl<sub>3</sub>) δ 174.5 (C<sub>q</sub>), 167.3 (C<sub>q</sub>), 156.1 (C<sub>q</sub>), 149.8 (CH), 142.7 (C<sub>q</sub>), 142.5 (C<sub>q</sub>), 136.8 (CH), 131.2 (CH), 129.9 (C<sub>q</sub>), 127.1 (CH), 125.1 (CH), 122.8 (CH), 120.9 (CH), 61.1 (CH<sub>2</sub>), 60.7 (CH<sub>2</sub>), 42.4 (CH), 18.3 (CH<sub>3</sub>), 14.2 (CH<sub>3</sub>), 14.1 (CH<sub>3</sub>).

**IR** (ATR): 2936, 2711, 2594, 1617, 1455, 1202, 1158, 769 cm<sup>-1</sup>.

**MS** (ESI) *m/z* (relative intensity): 350 (30) [M+Na]<sup>+</sup>, 328 (70) [M+H]<sup>+</sup>.

**HR-MS** (ESI) *m/z* calcd. for C<sub>19</sub>H<sub>22</sub>NO<sub>4</sub> [M+H]<sup>+</sup>: 328.1547, found: 328.1546.

The spectral data were in accordance with those reported in the literature.<sup>[284]</sup>

**Ethyl 2-(3-(pyridin-2-yl)phenyl)propanoate (409k)**

The **General Procedure I** was followed using 2-phenylpyridine **407a** (38.8 mg, 0.25 mmol), ethyl 2-bromopropanoate **408b** (125 mg, 0.75 mmol), **410** (30.0 mg, 10 mol %) and KOAc (49.1 mg, 0.50



mmol) in 2-MeTHF (2.0 mL). Purification by column chromatography on silica gel (*n*-hexane/EtOAc: 10/1) yielded **409k** (44.7 mg, 70%) as a colorless oil.

**<sup>1</sup>H NMR** (400 MHz, CDCl<sub>3</sub>)  $\delta$  8.69 (dt, *J* = 5.2, 1.4 Hz, 1H), 8.02 – 7.91 (m, 1H), 7.86 (dt, *J* = 7.7, 1.5 Hz, 1H), 7.80 – 7.68 (m, 2H), 7.43 (t, *J* = 7.7 Hz, 1H), 7.36 (dt, *J* = 7.7, 1.5 Hz, 1H), 7.23 (ddd, *J* = 6.6, 4.8, 2.0 Hz, 1H), 3.83 (q, *J* = 7.1 Hz, 1H), 3.66 (s, 3H), 1.56 (d, *J* = 7.2 Hz, 3H).

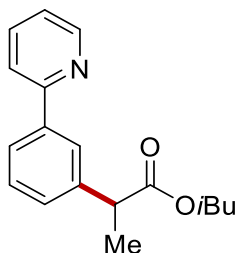
**<sup>13</sup>C NMR** (100 MHz, CDCl<sub>3</sub>)  $\delta$  175.1 (C<sub>q</sub>), 157.4 (C<sub>q</sub>), 149.8 (CH), 141.2 (C<sub>q</sub>), 139.9 (C<sub>q</sub>), 136.9 (CH), 129.2 (CH), 128.1 (CH), 126.5 (CH), 125.9 (CH), 122.3 (CH), 120.8 (CH), 52.2 (CH<sub>3</sub>), 45.6 (CH), 18.8 (CH<sub>3</sub>).

**IR** (ATR): 2980, 2951, 1733, 1585, 1462, 1435, 1202, 1165, 770 cm<sup>-1</sup>.

**MS** (EI) *m/z* (relative intensity): 241 (28) [M]<sup>+</sup>, 182 (100), 167 (55).

**HR-MS** (EI<sup>+</sup>) *m/z* calcd. for C<sub>15</sub>H<sub>15</sub>NO<sub>2</sub> [M]<sup>+</sup>: 241.1103, found: 241.1102.

#### Isobutyl 2-(3-(pyridin-2-yl)phenyl)propanoate (**409l**)



The **General Procedure I** was followed using 2-phenylpyridine **407a** (38.8 mg, 0.25 mmol), isobutyl 2-bromopropanoate **408c** (157 mg, 0.75 mmol), **410** (30.0 mg, 10 mol %) and KOAc (49.1 mg, 0.50 mmol) in 2-MeTHF (2.0 mL). Purification by column chromatography on silica gel (*n*-hexane/EtOAc: 10/1) yielded **409l** (45.3 mg, 64%) as a colorless oil.

**<sup>1</sup>H NMR** (400 MHz, CDCl<sub>3</sub>)  $\delta$  8.69 (dd, *J* = 4.9, 1.4 Hz, 1H), 7.94 (dd, *J* = 1.6, 1.4 Hz, 1H), 7.87 (dt, *J* = 7.6, 1.4 Hz, 1H), 7.81 – 7.67 (m, 2H), 7.43 (dd, *J* = 7.6, 7.5 Hz, 1H), 7.39 (dd, *J* = 7.5, 1.6 Hz, 1H), 7.23 (ddd, *J* = 6.6, 4.9, 2.0 Hz, 1H), 3.88 – 3.83 (m, 3H), 1.88 (q, *J* = 6.7 Hz, 1H), 1.57 (d, *J* = 7.1 Hz, 3H), 0.84 (d, *J* = 6.7 Hz, 6H).

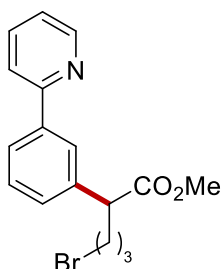
**<sup>13</sup>C NMR** (100 MHz, CDCl<sub>3</sub>)  $\delta$  174.6 (C<sub>q</sub>), 157.4 (C<sub>q</sub>), 149.8 (CH), 141.4 (C<sub>q</sub>), 139.8 (C<sub>q</sub>), 136.9 (CH), 129.1 (CH), 128.2 (CH), 126.5 (CH), 125.8 (CH), 122.3 (CH), 120.8 (CH), 71.0 (CH<sub>2</sub>), 45.9 (CH), 27.9 (CH), 19.1 (CH<sub>3</sub>), 18.7 (CH<sub>3</sub>).

**IR** (ATR): 2963, 1731, 1585, 1566, 1462, 1436, 1195, 1164, 769  $\text{cm}^{-1}$ .

**MS** (EI)  $m/z$  (relative intensity): 283 (22)  $[\text{M}]^+$ , 225 (13), 182 (100), 167 (53).

**HR-MS** (EI+)  $m/z$  calcd. for  $\text{C}_{18}\text{H}_{21}\text{NO}_2$   $[\text{M}]^+$ : 283.1572, found: 283.1574.

**Methyl 6-bromo-2-(3-(pyridin-2-yl)phenyl)hexanoate (409m)**



The **General Procedure I** was followed using 2-phenylpyridine **407a** (38.8 mg, 0.25 mmol), methyl 2,6-dibromohexanoate **408d** (216 mg, 0.75 mmol), **410** (30.0 mg, 10 mol %) and KOAc (49.1 mg, 0.50 mmol) in 2-MeTHF (2.0 mL). Purification by column chromatography on silica gel (*n*-hexane/EtOAc: 10/1) yielded **409m** (50.3 mg, 58%) as a brown oil.

**<sup>1</sup>H NMR** (400 MHz,  $\text{CDCl}_3$ ):  $\delta$  8.69 (dt,  $J = 5.0, 1.2$  Hz, 1H), 7.93 (dd,  $J = 1.8, 1.7$  Hz, 1H), 7.88 (dt,  $J = 7.7, 1.7$  Hz, 1H), 7.80 – 7.68 (m, 2H), 7.44 (dd,  $J = 7.8, 7.7$  Hz, 1H), 7.37 (dt,  $J = 7.8, 1.2$  Hz, 1H), 7.24 (ddd,  $J = 6.6, 5.0, 1.8$  Hz, 1H), 3.67 (s, 3H), 3.67 (t,  $J = 7.6$  Hz, 1H), 3.39 (t,  $J = 6.6$  Hz, 2H), 2.30 – 2.20 (m, 1H), 2.10 – 2.00 (m, 1H), 1.90 – 1.80 (m, 2H).

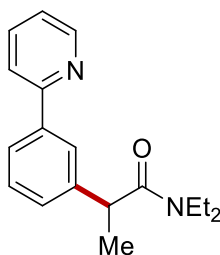
**<sup>13</sup>C NMR** (100 MHz,  $\text{CDCl}_3$ )  $\delta$  174.1 ( $\text{C}_q$ ), 157.2 ( $\text{C}_q$ ), 149.8 (CH), 140.1 ( $\text{C}_q$ ), 139.2 ( $\text{C}_q$ ), 136.9 (CH), 129.3 (CH), 128.4 (CH), 126.8 (CH), 126.2 (CH), 122.4 (CH), 120.8 (CH), 52.3 ( $\text{CH}_3$ ), 51.0 (CH), 33.2 ( $\text{CH}_2$ ), 32.1 ( $\text{CH}_2$ ), 30.8 ( $\text{CH}_2$ ).

**IR** (ATR): 2951, 1732, 1584, 1461, 1435, 1203, 1164, 771  $\text{cm}^{-1}$ .

**MS** (EI)  $m/z$  (relative intensity): 347 (14)  $[\text{M}]^+$ , 288 (18), 268 (100), 208 (61), 168 (61).

**HR-MS** (EI+)  $m/z$  calcd. for  $\text{C}_{17}\text{H}_{18}^{79}\text{BrNO}_2$   $[\text{M}]^+$ : 347.0521, found: 347.0520.

The spectral data were in accordance with those reported in the literature.<sup>[90]</sup>

***N,N*-Diethyl-2-(3-(pyridin-2-yl)phenyl)propanamide (409n)**

The **General Procedure I** was followed using 2-phenylpyridine **407a** (38.8 mg, 0.25 mmol), 2-bromo-*N,N*-diethylpropanamide **408e** (156 mg, 0.75 mmol), **410** (30.0 mg, 10 mol %) and KOAc (49.1 mg, 0.50 mmol) in 2-MeTHF (2.0 mL). Purification by column chromatography on silica gel (*n*-hexane/EtOAc: 10/1) yielded **409n** (49.4 mg, 70%) as a yellow oil.

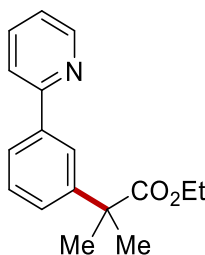
**<sup>1</sup>H NMR** (400 MHz, CDCl<sub>3</sub>)  $\delta$  8.69 (d,  $J$  = 5.0 Hz, 1H), 7.91 (s, 1H), 7.85 (dt,  $J$  = 7.6, 1.2 Hz, 1H), 7.76 – 7.70 (m, 2H), 7.42 (dd,  $J$  = 7.6, 7.5 Hz, 1H), 7.35 (dd,  $J$  = 7.6, 1.2 Hz, 1H), 7.236 – 7.22 (m, 1H), 3.94 (q,  $J$  = 7.0, 1H), 3.53 (dq,  $J$  = 7.6, 7.1 Hz, 1H), 3.36 (dq,  $J$  = 7.6, 7.1 Hz, 1H), 3.23 (dq,  $J$  = 7.6, 7.1 Hz, 1H), 3.10 (dq,  $J$  = 7.6, 7.1 Hz, 1H), 1.49 (d,  $J$  = 6.8, 3.1 Hz, 3H), 1.10 (t,  $J$  = 7.1, 3H), 1.01 (t,  $J$  = 7.1, 3H).

**<sup>13</sup>C NMR** (100 MHz, CDCl<sub>3</sub>)  $\delta$  172.8 (C<sub>q</sub>), 157.4 (C<sub>q</sub>), 149.8 (C<sub>q</sub>), 143.1 (CH), 140.0 (C<sub>q</sub>), 136.9 (CH), 129.4 (CH), 127.9 (CH), 126.1 (CH), 125.4 (CH), 122.3 (CH), 120.8 (CH), 43.3 (CH<sub>2</sub>), 41.8 (CH<sub>2</sub>), 40.4 (CH), 21.2 (CH<sub>3</sub>), 14.4 (CH<sub>3</sub>), 13.0 (CH<sub>3</sub>).

**IR** (ATR): 2973, 2932, 1636, 1584, 1461, 1433, 1264, 774, 702 cm<sup>-1</sup>.

**MS** (EI)  $m/z$  (relative intensity): 282 (18) [M]<sup>+</sup>, 225 (14), 182 (26), 167 (30), 100 (100).

**HR-MS** (EI<sup>+</sup>)  $m/z$  calcd. for C<sub>18</sub>H<sub>22</sub>N<sub>2</sub>O [M]<sup>+</sup>: 282.1732, found: 282.1730.

**Ethyl 2-methyl-2-(3-(pyridin-2-yl)phenyl)propanoate (409o)**

The **General Procedure I** was followed using 2-phenylpyridine **407a** (38.8 mg, 0.25 mmol), 2-bromo-2-methylpropanoate **408f** (146 mg, 0.75 mmol), **410** (30.0 mg, 10 mol %) and KOAc (49.1 mg, 0.50

mmol) in 2-MeTHF (2.0 mL). Purification by column chromatography on silica gel (*n*-hexane/EtOAc: 10/1) yielded **409o** (39.0 mg, 58%) as a colorless oil.

<sup>1</sup>H NMR (400 MHz, CDCl<sub>3</sub>) δ 8.70 (dt, *J* = 4.8, 1.5 Hz, 1H), 7.99 (dd, *J* = 1.9, 1.5 Hz, 1H), 7.84 (dt, *J* = 7.4, 1.6 Hz, 1H), 7.78 – 7.67 (m, 2H), 7.43 (dd, *J* = 7.5, 7.4 Hz, 2H), 7.23 (ddd, *J* = 7.5, 4.8, 1.5 Hz, 1H), 4.14 (q, *J* = 7.1 Hz, 2H), 1.65 (s, 6H), 1.19 (t, *J* = 7.1 Hz, 3H).

<sup>13</sup>C NMR (100 MHz, CDCl<sub>3</sub>) δ 176.9 (C<sub>q</sub>), 157.7 (C<sub>q</sub>), 149.8 (CH), 145.5 (C<sub>q</sub>), 139.7 (C<sub>q</sub>), 136.8 (CH), 128.9 (CH), 126.6 (CH), 125.4 (CH), 124.4 (CH), 122.2 (CH), 120.9 (CH), 61.0 (CH<sub>2</sub>), 46.8 (C<sub>q</sub>), 26.7 (CH<sub>3</sub>), 14.2 (CH<sub>3</sub>).

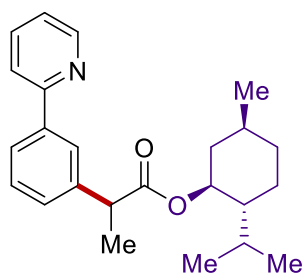
IR (ATR): 2979, 1726, 1585, 1463, 1253, 1146, 1025, 771 cm<sup>-1</sup>.

MS (EI) *m/z* (relative intensity): 269 (20) [M]<sup>+</sup>, 196 (100), 180 (21), 167 (18).

HR-MS (EI<sup>+</sup>) *m/z* calcd. for C<sub>17</sub>H<sub>19</sub>NO<sub>2</sub> [M]<sup>+</sup>: 269.1416, found: 269.1415.

The spectral data were in accordance with those reported in the literature.<sup>[84]</sup>

#### (1*R*,2*S*,5*R*)-2-Isopropyl-5-methylcyclohexyl 2-[3-(pyridin-2-yl)phenyl]propanoate (**409p**)



The **General Procedure I** was followed using 2-phenylpyridine **407a** (38.8 mg, 0.25 mmol), (1*R*,2*S*,5*R*)-2-isopropyl-5-methylcyclohexyl 2-bromopropanoate **408g** (218 mg, 0.75 mmol), **410** (30.0 mg, 10 mol %) and KOAc (49.1 mg, 0.50 mmol) in 2-MeTHF (2.0 mL). Purification by column chromatography on silica gel (*n*-hexane/EtOAc: 10/1) yielded **409p** (52.1 mg, 57%) as a colorless oil.

<sup>1</sup>H NMR (400 MHz, CDCl<sub>3</sub>) δ 8.69 (dt, *J* = 4.9, 1.4 Hz, 1H), 7.92 (dd, *J* = 3.9, 1.9 Hz, 1H), 7.87 (dd, *J* = 7.7, 1.5 Hz, 1H), 7.79 – 7.65 (m, 2H), 7.49 – 7.32 (m, 2H), 7.22 (ddd, *J* = 6.5, 4.8, 2.1 Hz, 1H), 4.69 – 4.60 (m, 1H), 3.82 – 3.76 (m, 1H), 2.06 – 1.76 (m, 2H), 1.71 – 1.58 (m, 2H), 1.56 (d, *J* = 2.7 Hz, 1H), 1.54 (d, *J* = 2.7 Hz, 1H), 1.51 – 1.39 (m, 1H), 1.38 – 1.23 (m, 2H), 1.02 – 0.93 (m, 2H), 0.95 – 0.72 (m, 7H), 0.71 (d, *J* = 6.9 Hz, 1H), 0.64 (d, *J* = 7.0 Hz, 1H), 0.49 (d, *J* = 6.9 Hz, 1H).

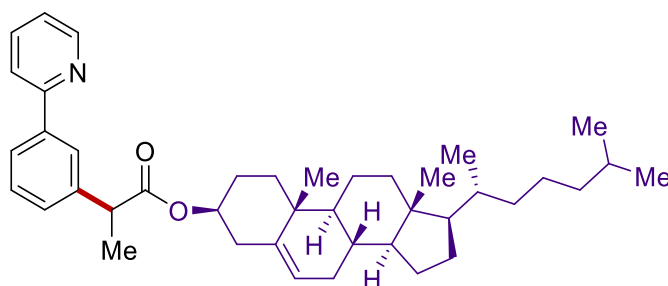
$^{13}\text{C}$  NMR (100 MHz,  $\text{CDCl}_3$ )  $\delta$  174.2 ( $\text{C}_q$ ), 157.5 ( $\text{C}_q$ ), 149.8 (CH), 141.5 ( $\text{C}_q$ ), 139.8 ( $\text{C}_q$ ), 136.8 (CH), 129.0 (CH), 128.1 (CH), 126.4 (CH), 125.7 (CH), 122.3 (CH), 120.7 (CH), 74.7 (CH), 47.1 (CH), 46.1 ( $\text{CH}_2$ ), 40.8 (CH), 34.4 ( $\text{CH}_2$ ), 31.5 ( $\text{CH}_2$ ), 26.1 (CH), 23.4 (CH), 22.1 ( $\text{CH}_3$ ), 20.8 ( $\text{CH}_3$ ), 18.7 ( $\text{CH}_3$ ), 16.2 ( $\text{CH}_3$ ).

IR (ATR): 2953, 2869, 1726, 1585, 1461, 1198, 1170, 768  $\text{cm}^{-1}$ .

MS (EI)  $m/z$  (relative intensity): 365 (18)  $[\text{M}]^+$ , 228 (28), 183 (100), 167 (42), 83 (72).

HR-MS (EI+)  $m/z$  calcd. for  $\text{C}_{24}\text{H}_{31}\text{NO}_2$   $[\text{M}]^+$ : 365.2355, found: 365.2362.

**(3*S*,8*S*,9*S*,10*R*,13*R*,14*S*,17*R*)-10,13-Dimethyl-17-((*R*)-6-methylheptan-2-yl)-2,3,4,7,8,9,10,11,12,13,14,15,16,17-tetradecahydro-1*H*-cyclopenta[*a*]phenanthren-3-yl 2-[3-(pyridin-2-yl)phenyl]propanoate (409q)**



The **General Procedure I** was followed using 2-phenylpyridine **407a** (38.8 mg, 0.25 mmol), (3*S*,8*S*,9*S*,10*R*,13*R*,14*S*,17*R*)-10,13-dimethyl-17-((*R*)-6-methylheptan-2-yl)-2,3,4,7,8,9,10,11,12,13,14,15,16,17-tetradecahydro-1*H*-cyclopenta[*a*]phenanthren-3-yl 2-bromopropanoate **408h** (391 mg, 0.75 mmol), **410** (30.0 mg, 10 mol %) and KOAc (49.1 mg, 0.50 mmol) in 2-MeTHF (2.0 mL). Purification by column chromatography on silica gel (*n*-hexane/EtOAc: 10/1) yielded **409q** (93.9 mg, 63%) as a colorless oil.

$^1\text{H}$  NMR (400 MHz,  $\text{CDCl}_3$ )  $\delta$  8.70 (dd,  $J = 5.0, 1.5$  Hz, 1H), 7.94 (t,  $J = 1.7$  Hz, 1H), 7.87 (dt,  $J = 7.6, 1.5$  Hz, 1H), 7.74 (dd,  $J = 6.6, 1.7$  Hz, 2H), 7.43 (dd,  $J = 7.6, 7.6$  Hz, 2H), 7.23 (ddd,  $J = 6.6, 5.0, 2.1$  Hz, 1H), 5.33 (ddd,  $J = 21.3, 4.3, 1.8$  Hz, 1H), 4.75 – 4.51 (m, 1H), 3.78 (q,  $J = 7.2$  Hz, 1H), 2.40 – 2.27 (m, 1H), 2.25 – 2.17 (m, 1H), 2.05 – 1.75 (m, 5H), 1.61 – 1.25 (m, 14H), 1.22 – 0.95 (m, 13H), 0.94 – 0.88 (m, 3H), 0.86 (dd,  $J = 6.6, 1.8$  Hz, 6H), 0.66 (s, 3H).

$^{13}\text{C}$  NMR (100 MHz,  $\text{CDCl}_3$ )  $\delta$  174.0 ( $\text{C}_q$ ), 157.4 ( $\text{C}_q$ ), 149.7 (CH), 141.6 ( $\text{C}_q$ ), 139.8 ( $\text{C}_q$ ), 139.7 ( $\text{C}_q$ ), 136.9 (CH), 129.1 (CH), 128.1 (CH), 126.5 (CH), 125.8 (CH), 122.7 (CH), 122.3 (CH), 120.8 (CH),

## Experimental Data

---

74.4 (CH), 56.8 (CH), 56.3 (CH), 50.1 (CH), 46.0 (CH), 42.4 (CH<sub>2</sub>), 39.9 (CH<sub>2</sub>), 39.7 (CH<sub>2</sub>), 38.1 (C<sub>q</sub>), 37.1 (CH<sub>2</sub>), 36.7 (CH<sub>2</sub>), 36.3 (CH<sub>2</sub>), 35.9 (CH), 32.0 (CH<sub>2</sub>), 32.0 (CH), 28.4 (CH<sub>2</sub>), 28.2 (CH), 27.7 (C<sub>q</sub>), 24.4 (CH<sub>2</sub>), 24.0 (CH<sub>2</sub>), 22.8 (CH<sub>3</sub>), 21.2 (CH<sub>2</sub>), 19.5 (CH<sub>3</sub>), 19.0 (CH<sub>3</sub>), 18.9 (CH<sub>3</sub>), 12.0 (CH<sub>3</sub>).

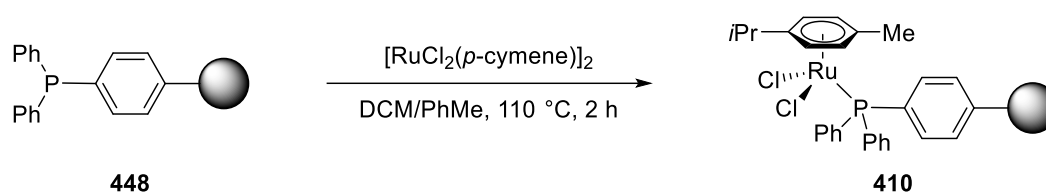
**IR** (ATR): 2935, 2867, 1731, 1585, 1462, 1195, 1165, 769 cm<sup>-1</sup>.

**MS** (ESI) *m/z* (relative intensity): 618 (100) [M+Na]<sup>+</sup>, 596 (30) [M+H]<sup>+</sup>.

**HR-MS** (ESI) *m/z* calcd for C<sub>41</sub>H<sub>58</sub>NO<sub>2</sub> [M+H]<sup>+</sup>: 596.4462, found: 596.4465.

### 5.7.2 Preparation of Hybrid Ruthenium Catalyst

A suspension of  $[\text{RuCl}_2(p\text{-cymene})]_2$  (0.30 g, 0.50 mmol) and resin **448** (triphenylphosphine, polymer supported 1.4–2.0 mmol/g on polystyrene 200–400 mesh 2% DVB loading, Fluorochem, 0.50 g) in a solvent mixture of DCM (15 mL) and PhMe (15 mL) was refluxed at 110 °C for 2 h under  $\text{N}_2$  (Scheme 5.7.1). After cooling to ambient temperature, the mixture was filtered with DCM (50 mL). **410** was dried *in vacuo* at room temperature for 24 h (Scheme 5.7.1).



**Scheme 5.7.1** Preparation of hybrid ruthenium catalyst.

### 5.7.3 Determination of Catalyst Loading

ICP-OES analysis was performed by Dr. Volker Karius for the determination of hybrid ruthenium catalyst **410** loading (Equation 5.7.1)

$$n_{\text{Cat}} = \frac{m_{\text{Cat}} \cdot \text{ICP-OES result}}{M_{\text{Ru}}}$$

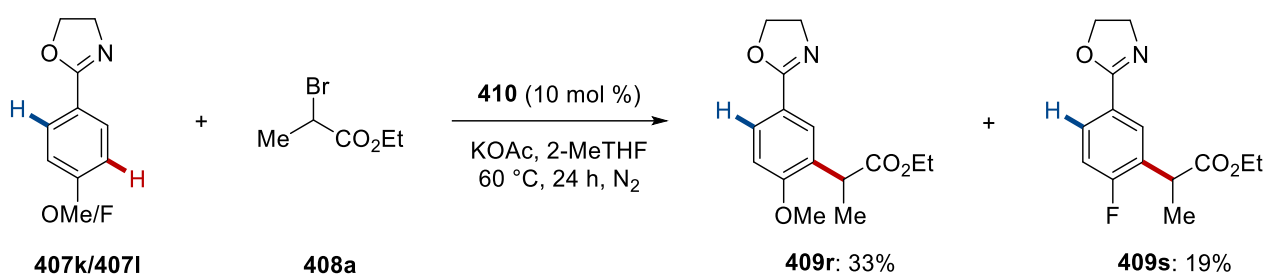
$$n_{\text{Cat}} = \frac{30 \text{ mg} \cdot 0.084}{101.07 \frac{\text{mg}}{\text{mmol}}} = 2.49 \cdot 10^{-2} \text{ mmol}$$

$$\text{Catalyst loading} = \frac{n_{\text{Cat}}}{0.25 \text{ mmol}} \cdot 100 \text{ mol \%} = 9.96 \text{ mol \%}$$

**Equation 5.7.1** Determination of hybrid ruthenium catalyst loading.

### 5.7.4 Competition Experiment

A suspension of 2-(4-fluorophenyl)-4,5-dihydrooxazole **407k** (0.25 mmol, 1.0 equiv) and 2-(4-methoxyphenyl)-4,5-dihydrooxazole **407l** (0.25 mmol, 1.0 equiv), ethyl 2-bromopropanoate **408a** (0.75 mmol, 1.0 equiv), **410** (10 mol %), KOAc (0.50 mmol, 2.0 equiv) in 2-MeTHF (2.0 mL) was stirred at 60 °C for 24 h under N<sub>2</sub>. After cooling to ambient temperature, the mixture was concentrated *in vacuo*. Purification by column chromatography on silica gel afforded the desired products **409r** and **409s** respectively (Scheme 5.7.2).

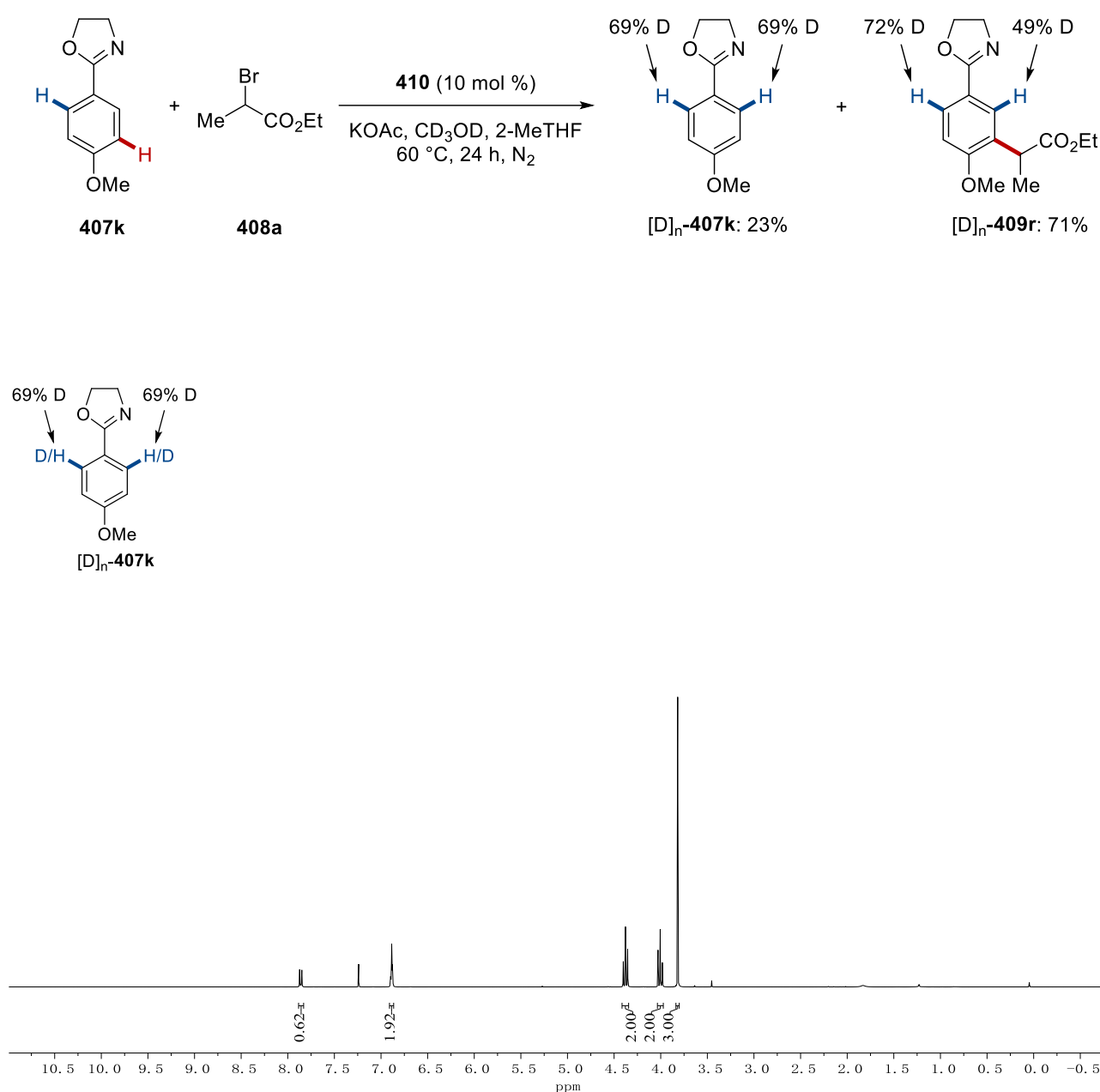


**Scheme 5.7.2** Competition experiment between **407k** and **407l**.



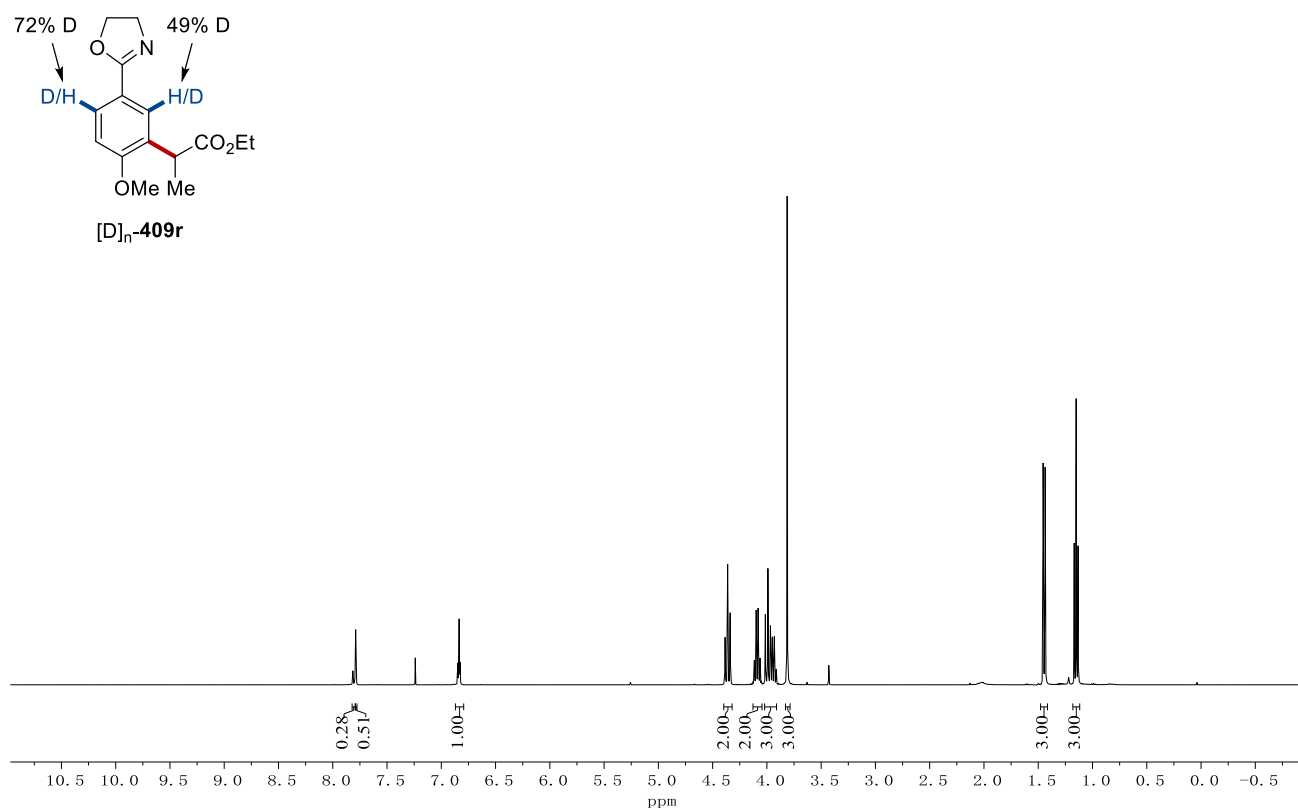
### 5.7.5 H/D Exchange Study

A suspension of 2-(4-methoxyphenyl)-4,5-dihydrooxazole **407k** (0.25 mmol, 1.0 equiv), ethyl 2-bromopropanoate **408a** (0.75 mmol, 3.0 equiv), **410** (10 mol %), KOAc (0.50 mmol, 2.0 equiv), CD<sub>3</sub>OD (0.1 mL, 10 equiv) in 2-MeTHF (2.0 mL) was stirred at 60 °C for 24 h under N<sub>2</sub>. After cooling to ambient temperature, the mixture was concentrated *in vacuo*. Purification by column chromatography on silica gel afforded the desired products [D]<sub>n</sub>-**407k** and [D]<sub>n</sub>-**409r** respectively (Scheme 5.7.3).



Scheme 5.7.3 H/D exchange study 1.

## Experimental Data

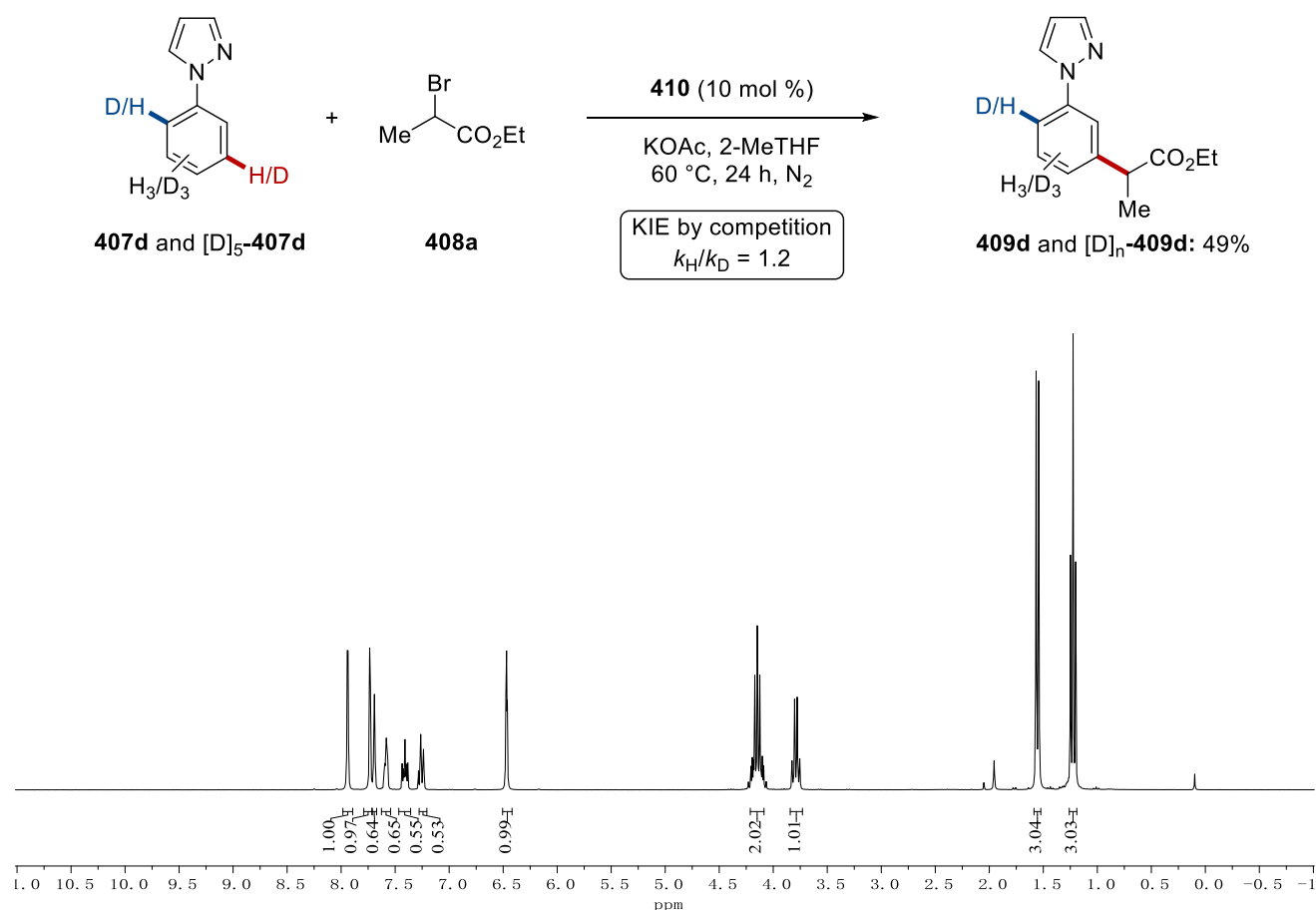


Scheme 5.7.4 H/D exchange study 2.

### 5.7.6 KIE Study

#### 1) Procedure for KIE study (intermolecular competition reaction)

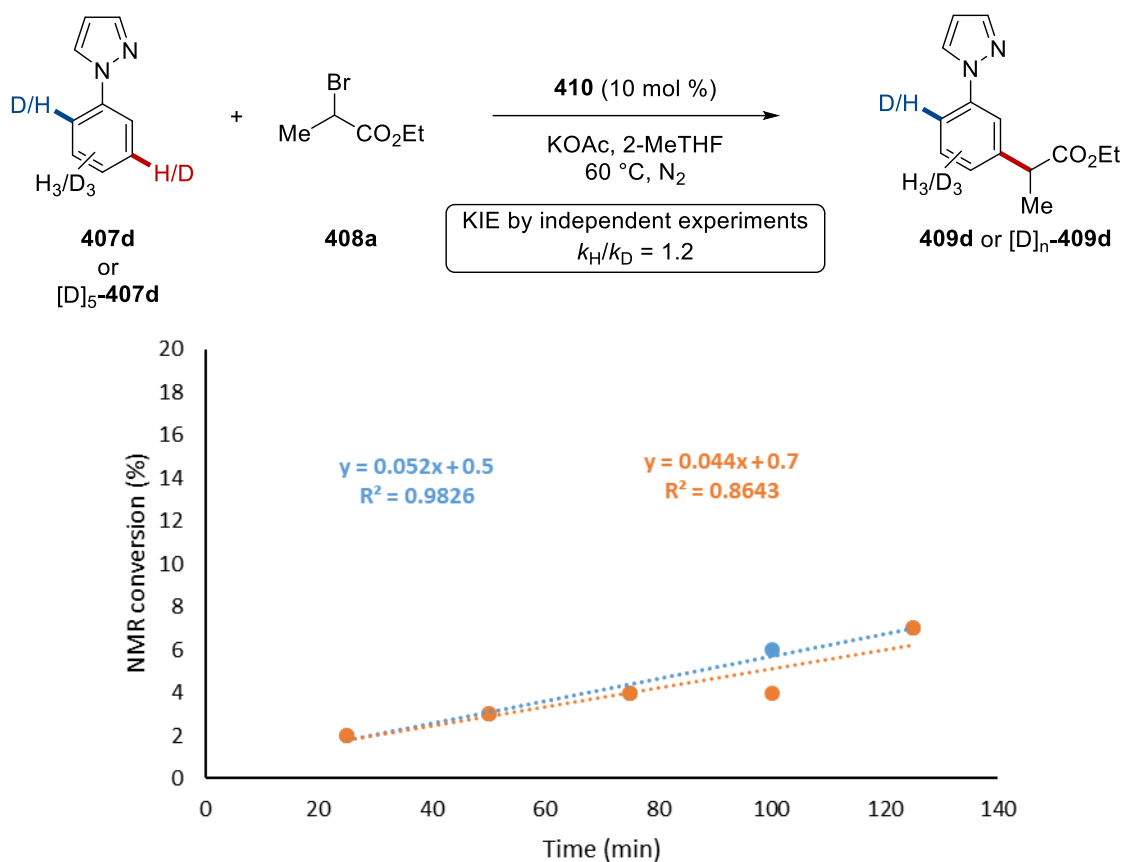
A suspension of **407d** (0.25 mmol, 1.0 equiv) and  $[D]_5$ -**407d** (0.25 mmol, 1.0 equiv), ethyl 2-bromopropanoate **408a** (0.75 mmol, 3.0 equiv), **410** (10 mol %), KOAc (0.50 mmol, 2.0 equiv), in 2-MeTHF (2.0 mL) was stirred at 60 °C for 24 h under N<sub>2</sub> to determine the KIE by intermolecular competition fashion. Purification by column chromatography on silica gel afforded the desired mixed products of **409d** and  $[D]_n$ -**409d**. The kinetic isotope effect of this reaction was determined to be  $k_H/k_D = 1.2$  as estimated by <sup>1</sup>H NMR spectroscopy (Scheme 5.7.5).



**Scheme 5.7.5** Intermolecular kinetic isotope exchange study.

## 2) Procedure for KIE study (two parallel reactions)

Two parallel reactions under the **General Procedure I** respectively using substrate **407d** (0.25 mmol, 1.0 equiv) or  $[D]_5$ -**407d** (0.25 mmol, 1.0 equiv) were performed to determine the KIE by comparison of the initial rates. Each conversion was determined after 2 h by  $^1\text{H}$  NMR measurement using 1,3,5-trimethoxybenzene as the internal standard (Scheme 5.7.6). Blue line is for **409d** and red line is for  $[D]_n$ -**409d**.

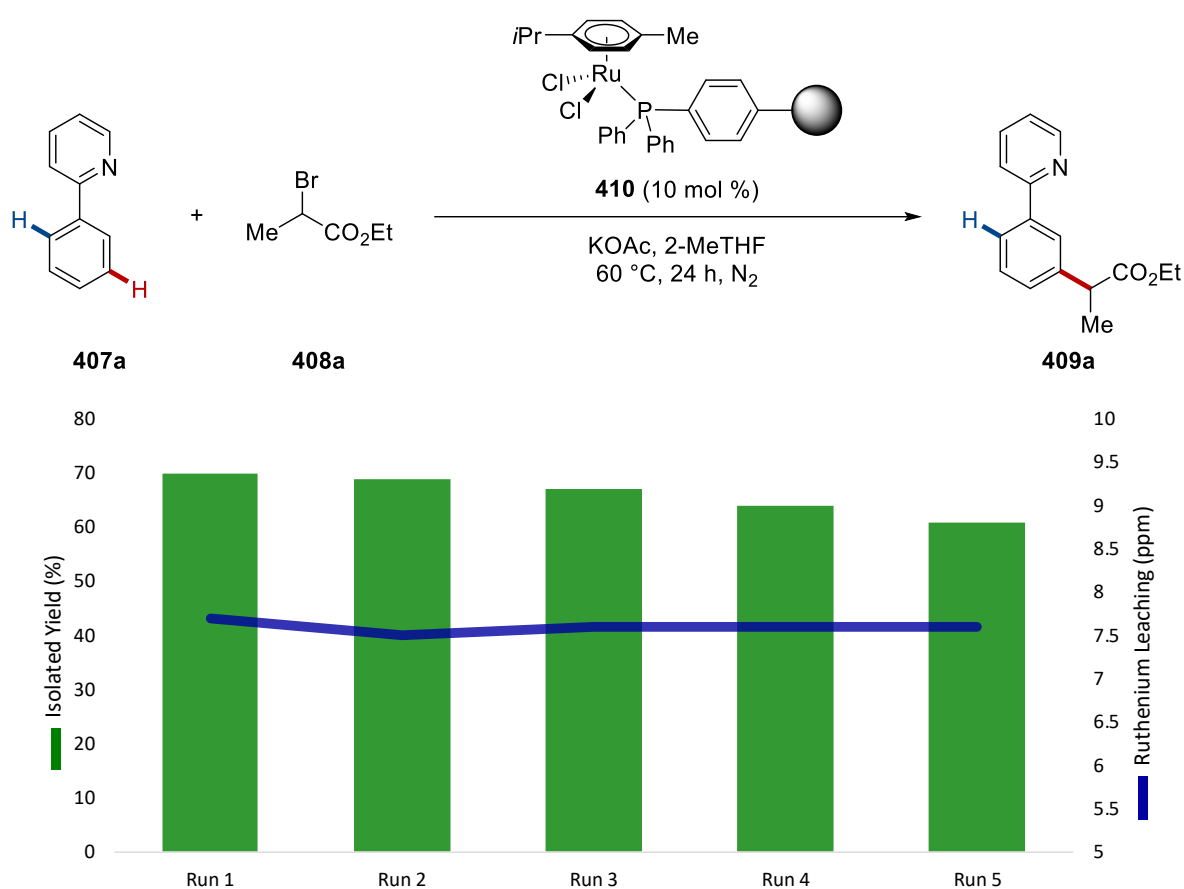


Scheme 5.7.6 Parallel kinetic isotope exchange study.

### 5.7.7 Heterogeneity test

#### 1) Reuse test

The **General Procedure I** was followed using 2-phenylpyridine **407a** (0.25 mmol, 1.0 equiv), ethyl 2-bromopropanoate **408a** (0.75 mmol, 3.0 equiv), **410** (10 mol %) and KOAc (0.50 mmol, 2.0 equiv) in 2-MeTHF (2.0 mL). After 24 h the reaction tube was transferred to a glovebox. Hybrid-Ru was carefully filtered through branched filter (Por. 3) and washed with 2-MeTHF (30 mL). Filtered hybrid ruthenium catalyst **409a** was dried *in vacuo* for 24 h and used for next run (Scheme 5.7.8).



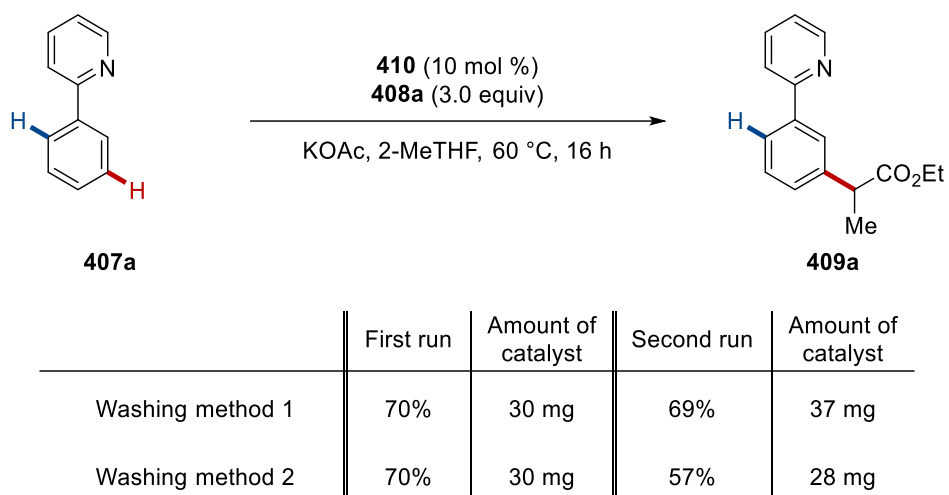
**Scheme 5.7.7** Reuse test and determination of ruthenium leaching.

## &lt;Washing method 1&gt;

After the completion of the reaction, **410** was carefully filtered through branched filter (Por. 3) and washed with DCM, 2-MeTHF, and DCM (each 30 mL). Filtered hybrid ruthenium catalyst was dried *in vacuo* for 24 h. The dried catalyst was directly used for the next run.

## &lt;Washing method 2&gt;

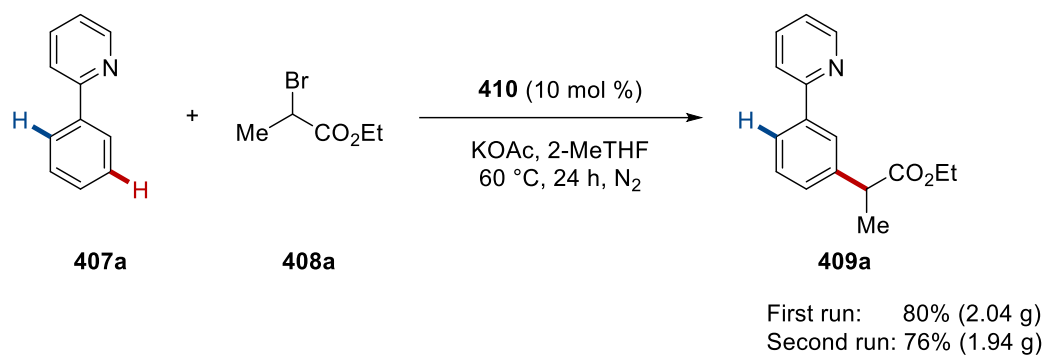
After the completion of the reaction, **410** was carefully filtered through branched filter (Por. 3) and washed with DCM, 2-MeTHF, demineralized water, EtOH, and DCM (each 30 mL). Filtered hybrid ruthenium catalyst was dried *in vacuo* for 24 h. The dried catalyst was directly used for the next run.



**Scheme 5.7.8** Reusability varying from the washing methods.

## 2) Gram-scale reuse test

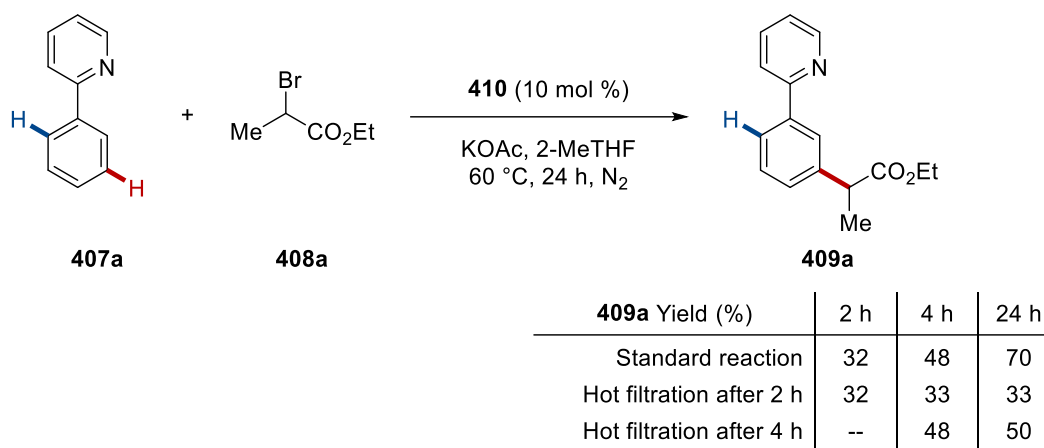
The **General Procedure I** was followed using 2-phenylpyridine **407a** (10.0 mmol, 1.0 equiv), ethyl 2-bromopropanoate **408a** (30.0 mmol, 3.0 equiv), **410** (10 mol %) and KOAc (20 mmol, 2.0 equiv) in 2-MeTHF (10.0 mL). After 24 h the reaction tube was transferred to a glovebox. Hybrid-Ru was carefully filtered through branched filter (Por. 3) with 2-MeTHF (60 mL). Filtered hybrid ruthenium catalyst was dried *in vacuo* and used for the second run. The solvent of filtrate was removed under reduced pressure. Purification by column chromatography on silica gel afforded **409a** (first run: 2.04 g, 80%; second run: 1.94 g, 76%) as a colorless oil (Scheme 5.7.10).



**Scheme 5.7.9** Scaled reuse test.

## 3) Hot filtration test

The **General Procedure I** was followed using 2-phenylpyridine **407a** (0.25 mmol, 1.0 equiv), ethyl 2-bromopropanoate **408a** (0.75 mmol, 3.0 equiv), **410** (10 mol %) and KOAc (0.50 mmol, 2.0 equiv) in 2-MeTHF (2.0 mL). After 2 or 4 hours, reaction tube was transferred to the Glove box. Hybrid-Ru was carefully filtered over pre-heated (to 60 °C) Celite<sup>®</sup> with a branched filter (Por. 3). Filtrate was directly collected to another pre-dried Schlenk tube and then sealed with septum. The sealed tube was transferred to the same reaction batch and the reaction continued for 22 or 20 h. After cooling to ambient temperature, the mixture was concentrated *in vacuo*. Purification by column chromatography on silica gel afforded the desired products **409a** (Scheme 5.7.11).



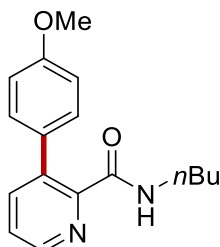
**Scheme 5.7.10** Hot filtration test.



## 5.8 C–H Arylations and Alkylations by Reusable Heterogeneous Manganese Catalyst

### 5.8.1 Characterization Data

#### *N*-Butyl-3-(4-methoxyphenyl)picolinamide (**413a**)



The **General Procedure J** was followed using *N*-butylpicolinamide **411a** (44.6 mg, 0.25 mmol), (4-methoxyphenyl)magnesium bromide **412a** (1.0 mL, 1.0 M in THF, 1.00 mmol), **416** (30 mg, 9.0 mol %), TMEDA (58.1 mg, 0.50 mmol), and 2,3-DCB (95.3 mg, 0.75 mmol). Purification by column chromatography on silica gel (*n*-hexane/EtOAc: 1/1) yielded **413a** (56.9 mg, 80%) as a white solid.

**M. p.** 97 °C.

**<sup>1</sup>H NMR** (400 MHz, CDCl<sub>3</sub>)  $\delta$  8.48 (dd,  $J = 4.6, 1.6$  Hz, 1H), 7.65 (s, 1H), 7.64 (dd,  $J = 7.8, 1.6$  Hz, 1H), 7.38 (dd,  $J = 7.8, 4.6$  Hz, 1H), 7.25 (d,  $J = 8.6$  Hz, 2H), 6.92 (d,  $J = 8.6$  Hz, 2H), 3.81 (s, 3H), 3.34 – 3.32 (m, 2H), 1.57 – 1.48 (m, 2H), 1.39 – 1.29 (m, 2H), 0.90 (t,  $J = 7.3$  Hz, 3H).

**<sup>13</sup>C NMR** (100 MHz, CDCl<sub>3</sub>)  $\delta$  165.3 (C<sub>q</sub>), 159.1 (C<sub>q</sub>), 148.3 (C<sub>q</sub>), 146.5 (CH), 140.0 (CH), 137.7 (C<sub>q</sub>), 131.6 (C<sub>q</sub>), 129.6 (CH), 124.9 (CH), 113.4 (CH), 55.1 (CH<sub>3</sub>), 39.1 (CH<sub>2</sub>), 31.6 (CH<sub>2</sub>), 20.1 (CH<sub>2</sub>), 13.7 (CH<sub>3</sub>).

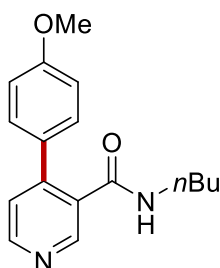
**IR** (ATR): 3398, 2928, 1652, 1510, 1245, 805, 523 cm<sup>-1</sup>.

**MS** (ESI)  $m/z$  (relative intensity): 285 (80) [M+H]<sup>+</sup>, 307 (20) [M+Na]<sup>+</sup>.

**HR-MS** (ESI) C<sub>17</sub>H<sub>21</sub>N<sub>2</sub>O<sub>2</sub> [M+H]<sup>+</sup>: 285.1599, found: 285.1598.

The spectral data were in accordance with those reported in the literature.<sup>[149]</sup>

#### *N*-Butyl-4-(4-methoxyphenyl)nicotinamide (**413b**)



The **General Procedure J** was followed using *N*-butylnicotinamide **411b** (44.6 mg, 0.25 mmol), (4-methoxyphenyl)magnesium bromide **412a** (1.0 mL, 1.0 M in THF, 1.00 mmol), **416** (30 mg, 9.0 mol %), TMEDA (58.1 mg, 0.50 mmol), and 2,3-DCB (95.3 mg, 0.75 mmol). Purification by column chromatography on silica gel (*n*-hexane/EtOAc: 1/1) yielded **413b** (24.2 mg, 34%) as a white solid.

**M. p.** 105 °C.

**<sup>1</sup>H NMR** (400 MHz, CDCl<sub>3</sub>)  $\delta$  8.71 (s, 1H), 8.52 (d, *J* = 5.2 Hz, 1H), 7.33 (d, *J* = 8.8 Hz, 2H), 7.20 (d, *J* = 5.2 Hz, 1H), 6.93 (d, *J* = 8.8 Hz, 2H), 5.66 (s, 1H), 3.80 (s, 3H), 3.21 – 3.16 (m, 2H), 1.31 – 1.19 (m, 2H), 1.12 – 0.98 (m, 2H), 0.78 (t, *J* = 7.3 Hz, 3H).

**<sup>13</sup>C NMR** (100 MHz, CDCl<sub>3</sub>)  $\delta$  167.3 (C<sub>q</sub>), 160.3 (C<sub>q</sub>), 150.5 (CH), 149.5 (CH), 146.5 (C<sub>q</sub>), 131.2 (C<sub>q</sub>), 129.6 (CH), 129.4 (C<sub>q</sub>), 123.9 (CH), 114.3 (CH), 55.3 (CH<sub>3</sub>), 39.6 (CH<sub>2</sub>), 31.0 (CH<sub>2</sub>), 19.8 (CH<sub>2</sub>), 13.6 (CH<sub>3</sub>).

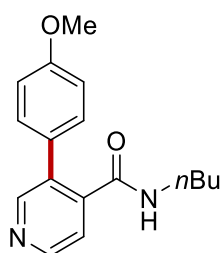
**IR** (ATR): 3274, 2929, 1638, 1516, 1251, 831, 532 cm<sup>-1</sup>.

**MS** (ESI) *m/z* (relative intensity): 285 (90) [M+H]<sup>+</sup>, 307 (10) [M+Na]<sup>+</sup>.

**HR-MS** (ESI) C<sub>17</sub>H<sub>21</sub>N<sub>2</sub>O<sub>2</sub> [M+H]<sup>+</sup>: 286.1561, found: 286.1550.

The spectral data were in accordance with those reported in the literature.<sup>[149]</sup>

#### ***N*-Butyl-3-(4-methoxyphenyl)isonicotinamide (413c)**



The **General Procedure J** was followed using *N*-butylisonicotinamide **411c** (44.6 mg, 0.25 mmol), (4-methoxyphenyl)magnesium bromide **412a** (1.0 mL, 1.0 M in THF, 1.00 mmol), **416** (30 mg, 9.0 mol %), TMEDA (58.1 mg, 0.50 mmol), and 2,3-DCB (95.3 mg, 0.75 mmol). Purification by column chromatography on silica gel (*n*-hexane/EtOAc: 1/1) yielded **413c** (21.3 mg, 30%) as a white solid.

**M. p.** 122 °C.

**<sup>1</sup>H NMR** (400 MHz, CDCl<sub>3</sub>)  $\delta$  8.61 – 8.57 (m, 2H), 7.51 (d, *J* = 5.0 Hz, 1H), 7.33 (d, *J* = 8.9 Hz, 2H), 6.96 (d, *J* = 8.9 Hz, 2H), 5.39 (s, 1H), 3.83 (s, 3H), 3.20 – 3.18 (m, 2H), 1.26 – 1.17 (m, 2H), 1.09 –

0.97 (m, 2H), 0.78 (t,  $J = 7.3$  Hz, 3H).

$^{13}\text{C}$  NMR (100 MHz,  $\text{CDCl}_3$ )  $\delta$  167.1 ( $\text{C}_q$ ), 160.0 ( $\text{C}_q$ ), 150.9 (CH), 148.7 (CH), 142.2 ( $\text{C}_q$ ), 133.5 ( $\text{C}_q$ ), 130.1 (CH), 128.5 ( $\text{C}_q$ ), 122.2 (CH), 114.4 (CH), 55.3 ( $\text{CH}_3$ ), 39.5 ( $\text{CH}_2$ ), 31.0 ( $\text{CH}_2$ ), 19.8 ( $\text{CH}_2$ ), 13.6 ( $\text{CH}_3$ ).

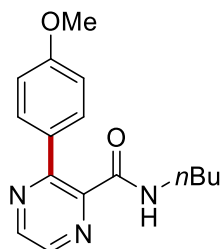
IR (ATR): 3275, 2929, 1642, 1513, 1250, 834, 548  $\text{cm}^{-1}$ .

MS (ESI)  $m/z$  (relative intensity): 285 (90)  $[\text{M}+\text{H}]^+$ , 307 (10)  $[\text{M}+\text{Na}]^+$ .

HR-MS (ESI)  $\text{C}_{17}\text{H}_{21}\text{N}_2\text{O}_2$   $[\text{M}+\text{H}]^+$ : 285.1603, found: 285.1598.

The spectral data were in accordance with those reported in the literature.<sup>[149]</sup>

### *N*-Butyl-3-(4-methoxyphenyl)pyrazine-2-carboxamide (**413d**)



The **General Procedure J** was followed using *N*-butylpyrazine-2-carboxamide **411d** (44.8 mg, 0.25 mmol), (4-methoxyphenyl)magnesium bromide **412a** (1.0 mL, 1.0 M in THF, 1.00 mmol), **416** (30 mg, 9.0 mol %), TMEDA (58.1 mg, 0.50 mmol), and 2,3-DCB (95.3 mg, 0.75 mmol). Purification by column chromatography on silica gel (*n*-hexane/EtOAc: 1/1) yielded **413d** (14.9 mg, 21%) as a white solid.

**M. p.** 67 °C.

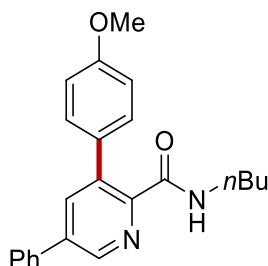
$^1\text{H}$  NMR (400 MHz,  $\text{CDCl}_3$ )  $\delta$  8.67 (d,  $J = 2.3$  Hz, 1H), 8.39 (d,  $J = 2.3$  Hz, 1H), 7.58 (d,  $J = 8.9$  Hz, 2H), 7.33 (s, 1H), 6.95 (d,  $J = 8.9$  Hz, 2H), 3.83 (s, 3H), 3.42 – 3.37 (m, 2H), 1.58 – 1.54 (m, 2H), 1.41 – 1.32 (m, 2H), 0.92 (t,  $J = 7.3$  Hz, 3H).

$^{13}\text{C}$  NMR (100 MHz,  $\text{CDCl}_3$ )  $\delta$  164.9 ( $\text{C}_q$ ), 160.6 ( $\text{C}_q$ ), 154.0 ( $\text{C}_q$ ), 144.9 (CH), 144.1 ( $\text{C}_q$ ), 139.9 (CH), 130.5 (CH), 130.1 ( $\text{C}_q$ ), 113.6 (CH), 55.3 ( $\text{CH}_3$ ), 39.4 ( $\text{CH}_2$ ), 31.5 ( $\text{CH}_2$ ), 20.1 ( $\text{CH}_2$ ), 13.7 ( $\text{CH}_3$ ).

IR (ATR): 3273, 2929, 1649, 1514, 1251, 812, 557  $\text{cm}^{-1}$ .

MS (ESI)  $m/z$  (relative intensity): 286 (55)  $[\text{M}+\text{H}]^+$ , 308 (45)  $[\text{M}+\text{Na}]^+$ .

HR-MS (ESI)  $\text{C}_{16}\text{H}_{21}\text{N}_3\text{O}_2$   $[\text{M}+\text{H}]^+$ : 286.1561, found: 286.1550.

***N*-Butyl-3-(4-methoxyphenyl)-5-phenylpicolinamide (413f)**

The **General Procedure J** was followed using *N*-butyl-5-phenylpicolinamide **411f** (63.6 mg, 0.25 mmol), (4-methoxyphenyl)magnesium bromide **412a** (1.0 mL, 1.0 M in THF, 1.00 mmol), **416** (30 mg, 9.0 mol %), TMEDA (58.1 mg, 0.50 mmol), and 2,3-DCB (95.3 mg, 0.75 mmol). Purification by column chromatography on silica gel (*n*-hexane/EtOAc: 1/1) yielded **413f** (46.0 mg, 51%) as a white solid.

**M. p.** 90 °C.

**<sup>1</sup>H NMR** (400 MHz, CDCl<sub>3</sub>) δ 8.72 (d, *J* = 2.2 Hz, 1H), 7.83 (d, *J* = 2.2 Hz, 1H), 7.77 – 7.70 (m, 1H), 7.63 – 7.60 (m, 2H), 7.53 – 7.38 (m, 3H), 7.31 (d, *J* = 8.7 Hz, 2H), 6.95 (d, *J* = 8.7 Hz, 2H), 3.83 (s, 3H), 3.39 – 3.35 (m, 2H), 1.58 – 1.53 (m, 2H), 1.44 – 1.32 (m, 2H), 0.91 (t, *J* = 7.3 Hz, 3H).

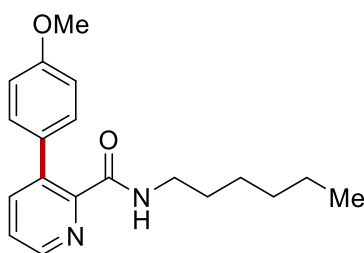
**<sup>13</sup>C NMR** (100 MHz, CDCl<sub>3</sub>) δ 165.1 (C<sub>q</sub>), 159.2 (C<sub>q</sub>), 146.6 (C<sub>q</sub>), 144.9 (CH), 138.3 (CH), 137.9 (C<sub>q</sub>), 137.8 (C<sub>q</sub>), 136.7 (C<sub>q</sub>), 131.7 (C<sub>q</sub>), 129.7 (CH), 129.2 (CH), 128.7 (CH), 127.2 (CH), 113.5 (CH), 55.2 (CH<sub>3</sub>), 39.2 (CH<sub>2</sub>), 31.7 (CH<sub>2</sub>), 20.2 (CH<sub>2</sub>), 13.8 (CH<sub>3</sub>).

**IR** (ATR): 3399, 2926, 1652, 1510, 1244, 806, 645 cm<sup>-1</sup>.

**MS** (ESI) *m/z* (relative intensity): 361 (80) [M+H]<sup>+</sup>, 383 (20) [M+Na]<sup>+</sup>.

**HR-MS** (ESI) C<sub>23</sub>H<sub>25</sub>N<sub>2</sub>O<sub>2</sub> [M+H]<sup>+</sup>: 361.1909, found: 361.1911.

The spectral data were in accordance with those reported in the literature.<sup>[149]</sup>

***N*-Hexyl-3-(4-methoxyphenyl)picolinamide (413g)**

The **General Procedure J** was followed using *N*-hexylpicolinamide **411g** (51.6 mg, 0.25 mmol), (4-

methoxyphenyl)magnesium bromide **412a** (1.0 mL, 1.0 M in THF, 1.00 mmol), **416** (30 mg, 9.0 mol %), TMEDA (58.1 mg, 0.50 mmol), and 2,3-DCB (95.3 mg, 0.75 mmol). Purification by column chromatography on silica gel (*n*-hexane/EtOAc: 1/1) yielded **413g** (66.4 mg, 85%) as a white solid.

**M. p.** 156 °C.

**<sup>1</sup>H NMR** (400 MHz, CDCl<sub>3</sub>) δ 8.50 (s, 1H), 7.65 (d, *J* = 7.8, 2H), 7.43 – 7.39 (m, 1H), 7.25 (d, *J* = 8.7 Hz, 2H), 6.92 (d, *J* = 8.7 Hz, 2H), 3.82 (s, 3H), 3.35 – 3.31 (m, 2H), 1.58 – 1.50 (m, 2H), 1.36 – 1.21 (m, 6H), 0.88 – 0.84 (t, *J* = 6.9 Hz, 3H).

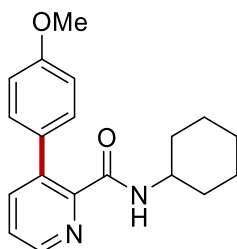
**<sup>13</sup>C NMR** (100 MHz, CDCl<sub>3</sub>) δ 165.2 (C<sub>q</sub>), 159.1 (C<sub>q</sub>), 148.3 (C<sub>q</sub>), 146.4 (CH), 140.1 (CH), 137.8 (C<sub>q</sub>), 131.6 (C<sub>q</sub>), 129.6 (CH), 125.0 (CH), 113.4 (CH), 55.2 (CH<sub>3</sub>), 39.4 (CH<sub>2</sub>), 31.5 (CH<sub>2</sub>), 29.5 (CH<sub>2</sub>), 26.6 (CH<sub>2</sub>), 22.5 (CH<sub>2</sub>), 14.0 (CH<sub>3</sub>).

**IR** (ATR): 3398, 2929, 1649, 1507, 1245, 807, 558 cm<sup>-1</sup>.

**MS** (ESI) *m/z* (relative intensity): 313 (80) [M+H]<sup>+</sup>, 335 (20) [M+Na]<sup>+</sup>.

**HR-MS** (ESI) C<sub>19</sub>H<sub>25</sub>N<sub>2</sub>O<sub>2</sub> [M+H]<sup>+</sup>: 313.1912, found: 313.1911.

#### ***N*-Cyclohexyl-3-(4-methoxyphenyl)picolinamide (413h)**



The **General Procedure J** was followed using *N*-cyclohexylpicolinamide **411h** (51.1 mg, 0.25 mmol), (4-methoxyphenyl)magnesium bromide **412a** (1.0 mL, 1.0 M in THF, 1.00 mmol), **416** (30 mg, 9.0 mol %), TMEDA (58.1 mg, 0.50 mmol), and 2,3-DCB (95.3 mg, 0.75 mmol). Purification by column chromatography on silica gel (*n*-hexane/EtOAc: 1/1) yielded **413h** (55.9 mg, 72%) as a white solid.

**M. p.** 99 °C.

**<sup>1</sup>H NMR** (400 MHz, CDCl<sub>3</sub>) δ 8.49 (dd, *J* = 4.6, 1.7 Hz, 1H), 7.63 (dd, *J* = 7.8, 1.7 Hz, 1H), 7.55 – 7.49 (m, 1H), 7.38 (dd, *J* = 7.8, 4.6 Hz, 1H), 7.25 (d, *J* = 8.8 Hz, 2H), 6.92 (d, *J* = 8.8 Hz, 2H), 3.82 (s, 3H), 1.99 – 1.86 (m, 2H), 1.74 – 1.65 (m, 2H), 1.62 – 1.56 (m, 1H), 1.40 – 1.27 (m, 2H), 1.26 – 1.10 (m, 4H).

$^{13}\text{C}$  NMR (100 MHz,  $\text{CDCl}_3$ )  $\delta$  164.4 ( $\text{C}_q$ ), 159.1 ( $\text{C}_q$ ), 148.4 ( $\text{C}_q$ ), 146.5 (CH), 140.0 (CH), 137.8 ( $\text{C}_q$ ), 131.7 ( $\text{C}_q$ ), 129.6 (CH), 124.9 (CH), 113.4 (CH), 55.2 ( $\text{CH}_3$ ), 48.0 (CH), 33.0 ( $\text{CH}_2$ ), 25.6 ( $\text{CH}_2$ ), 24.9 ( $\text{CH}_2$ ).

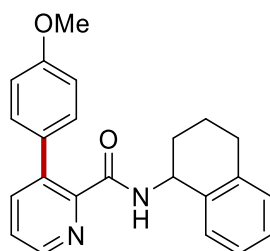
IR (ATR): 3397, 2933, 1671, 1508, 1244, 736, 557  $\text{cm}^{-1}$ .

MS (ESI)  $m/z$  (relative intensity): 311 (90)  $[\text{M}+\text{H}]^+$ , 333 (10)  $[\text{M}+\text{Na}]^+$ .

HR-MS (ESI)  $\text{C}_{19}\text{H}_{23}\text{N}_2\text{O}_2$   $[\text{M}+\text{H}]^+$ : 311.1758, found: 311.1754.

The spectral data were in accordance with those reported in the literature.<sup>[149]</sup>

### 3-(4-Methoxyphenyl)-*N*-(1,2,3,4-tetrahydronaphthalen-1-yl)picolinamide (413i)



The **General Procedure J** was followed using *N*-(1,2,3,4-tetrahydronaphthalen-1-yl)picolinamide **411i** (63.1 mg, 0.25 mmol), (4-methoxyphenyl)magnesium bromide **412a** (1.0 mL, 1.0 M in THF, 1.00 mmol), **416** (30 mg, 9.0 mol %), TMEDA (58.1 mg, 0.50 mmol), and 2,3-DCB (95.3 mg, 0.75 mmol). Purification by column chromatography on silica gel (*n*-hexane/EtOAc: 1/1) yielded **413i** (69.9 mg, 78%) as a white solid.

**M. p.** 125 °C.

$^1\text{H}$  NMR (400 MHz,  $\text{CDCl}_3$ )  $\delta$  8.47 (dd,  $J = 4.6, 1.7$  Hz, 1H), 7.82 (d,  $J = 8.8$  Hz, 1H), 7.66 (dd,  $J = 7.8, 1.7$  Hz, 1H), 7.39 (dd,  $J = 7.8, 4.6$  Hz, 1H), 7.31 (d,  $J = 8.8$  Hz, 2H), 7.25 – 7.22 (m, 1H), 7.19 – 7.11 (m, 1H), 7.11 – 7.05 (m, 1H), 6.97 (d,  $J = 8.8$  Hz, 2H), 5.28 – 5.22 (m, 1H), 3.85 (s, 3H), 2.86 – 2.70 (m, 2H), 2.12 – 1.96 (m, 2H), 1.96 – 1.76 (m, 3H).

$^{13}\text{C}$  NMR (100 MHz,  $\text{CDCl}_3$ )  $\delta$  164.7 ( $\text{C}_q$ ), 159.2 ( $\text{C}_q$ ), 148.4 ( $\text{C}_q$ ), 146.7 (CH), 139.9 (CH), 137.7 ( $\text{C}_q$ ), 137.6 ( $\text{C}_q$ ), 136.8 ( $\text{C}_q$ ), 131.6 ( $\text{C}_q$ ), 129.7 (CH), 129.0 (CH), 128.8 (CH), 127.1 (CH), 126.1 (CH), 125.0 (CH), 113.5 (CH), 55.2 ( $\text{CH}_3$ ), 47.3 (CH), 30.1 ( $\text{CH}_2$ ), 29.3 ( $\text{CH}_2$ ), 20.0 ( $\text{CH}_2$ ).

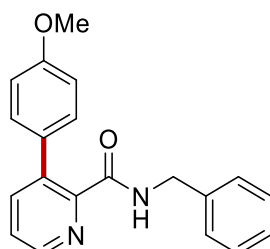
IR (ATR): 3398, 3032 1659, 1506, 1245, 698, 485  $\text{cm}^{-1}$ .

MS (ESI)  $m/z$  (relative intensity): 359 (90)  $[\text{M}+\text{H}]^+$ , 373 (10)  $[\text{M}+\text{Na}]^+$ .

**HR-MS** (ESI)  $C_{23}H_{23}N_2O_2$   $[M+H]^+$ : 359.1758, found: 359.1754.

The spectral data were in accordance with those reported in the literature.<sup>[149]</sup>

***N*-Benzyl-3-(4-methoxyphenyl)picolinamide (413j)**



The **General Procedure J** was followed using *N*-benzylpicolinamide **411j** (53.1 mg, 0.25 mmol), (4-methoxyphenyl)magnesium bromide **412a** (1.0 mL, 1.0 M in THF, 1.00 mmol), **416** (30 mg, 9.0 mol %), TMEDA (58.1 mg, 0.50 mmol), and 2,3-DCB (95.3 mg, 0.75 mmol). Purification by column chromatography on silica gel (*n*-hexane/EtOAc: 1/1) yielded **413j** (60.5 mg, 76%) as a white solid.

**M. p.** 140 °C.

**<sup>1</sup>H NMR** (400 MHz, CDCl<sub>3</sub>)  $\delta$  8.48 (dd,  $J = 4.7, 1.6$  Hz, 1H), 8.00 (s, 1H), 7.66 (dd,  $J = 7.8, 1.6$  Hz, 1H), 7.40 (dd,  $J = 7.8, 4.7$  Hz, 1H), 7.34 – 7.21 (m, 5H), 7.28 (d,  $J = 8.7$  Hz, 2H), 6.94 (d,  $J = 8.7$  Hz, 2H), 4.57 – 4.53 (m, 2H), 3.83 (s, 3H).

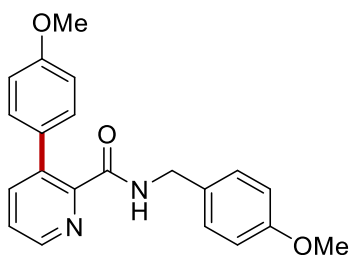
**<sup>13</sup>C NMR** (100 MHz, CDCl<sub>3</sub>)  $\delta$  165.2 (C<sub>q</sub>), 159.1 (C<sub>q</sub>), 147.9 (C<sub>q</sub>), 146.6 (CH), 140.1 (CH), 138.4 (C<sub>q</sub>), 138.0 (C<sub>q</sub>), 131.5 (C<sub>q</sub>), 129.7 (CH), 128.6 (CH), 127.8 (CH), 127.3 (CH), 125.1 (CH), 113.4 (CH), 55.2 (CH<sub>3</sub>), 43.4 (CH<sub>2</sub>).

**IR** (ATR): 3397, 2950, 1663, 1508, 1244, 728, 464 cm<sup>-1</sup>.

**MS** (ESI)  $m/z$  (relative intensity): 319 (90)  $[M+H]^+$ , 341 (10)  $[M+Na]^+$ .

**HR-MS** (ESI)  $C_{20}H_{19}N_2O_2$   $[M+H]^+$ : 319.1447, found: 319.1441.

The spectral data were in accordance with those reported in the literature.<sup>[149]</sup>

***N*-(4-Methoxybenzyl)-3-(4-methoxyphenyl)picolinamide (413k)**

The **General Procedure J** was followed using *N*-(4-methoxybenzyl)picolinamide **411k** (77.6 mg, 0.25 mmol), (4-methoxyphenyl)magnesium bromide **412a** (1.0 mL, 1.0 M in THF, 1.00 mmol), **416** (30 mg, 9.0 mol %), TMEDA (58.1 mg, 0.50 mmol), and 2,3-DCB (95.3 mg, 0.75 mmol). Purification by column chromatography on silica gel (*n*-hexane/EtOAc: 1/1) yielded **413k** (65.3 mg, 75%) as a white solid.

**M. p.** 95 °C.

**<sup>1</sup>H NMR** (400 MHz, CDCl<sub>3</sub>) δ 8.47 (dd, *J* = 4.6, 1.7 Hz, 1H), 7.90 (s, 1H), 7.65 (dd, *J* = 7.8, 1.7 Hz, 1H), 7.39 (dd, *J* = 7.8, 4.6 Hz, 1H), 7.27 (d, *J* = 8.7 Hz, 2H), 7.21 (d, *J* = 8.7 Hz, 2H), 6.93 (d, *J* = 8.8 Hz, 2H), 6.84 (d, *J* = 8.8 Hz, 2H), 4.47 (d, *J* = 5.9 Hz, 2H), 3.83 (s, 3H), 3.77 (s, 3H).

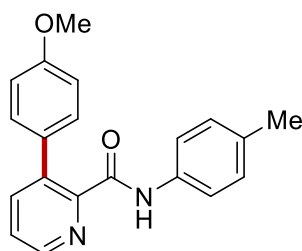
**<sup>13</sup>C NMR** (100 MHz, CDCl<sub>3</sub>) δ 165.1 (C<sub>q</sub>), 159.1 (C<sub>q</sub>), 158.9 (C<sub>q</sub>), 148.0 (C<sub>q</sub>), 146.6 (CH), 140.1 (CH), 137.9 (C<sub>q</sub>), 131.5 (C<sub>q</sub>), 130.5 (C<sub>q</sub>), 129.7 (CH), 129.2 (CH), 125.1 (CH), 114.0 (CH), 113.5 (CH), 55.3 (CH<sub>3</sub>), 55.2 (CH<sub>3</sub>), 42.9 (CH<sub>2</sub>).

**IR** (ATR): 3398, 2931, 1669, 1511, 1278, 806, 430 cm<sup>-1</sup>.

**MS** (ESI) *m/z* (relative intensity): 349 (90) [M+H]<sup>+</sup>, 391 (10) [M+Na]<sup>+</sup>.

**HR-MS** (ESI) C<sub>21</sub>H<sub>21</sub>N<sub>2</sub>O<sub>3</sub> [M+H]<sup>+</sup>: 349.1551, found: 349.1547.

The spectral data were in accordance with those reported in the literature.<sup>[149]</sup>

**3-(4-Methoxyphenyl)-*N*-(*p*-tolyl)picolinamide (413l)**

The **General Procedure J** was followed using *N*-(*p*-tolyl)picolinamide **411l** (53.1 mg, 0.25 mmol),



(4-methoxyphenyl)magnesium bromide **412a** (1.0 mL, 1.0 M in THF, 1.00 mmol), **416** (30 mg, 9.0 mol %), TMEDA (58.1 mg, 0.50 mmol), and 2,3-DCB (95.3 mg, 0.75 mmol). Purification by column chromatography on silica gel (*n*-hexane/EtOAc: 1/1) yielded **413l** (53.3 mg, 67%) as a white solid.

**M. p.** 164 °C.

**<sup>1</sup>H NMR** (400 MHz, CDCl<sub>3</sub>) δ 9.87 (s, 1H), 8.56 (dd, *J* = 4.6, 1.6 Hz, 1H), 7.69 (dd, *J* = 7.8, 1.6 Hz, 1H), 7.55 (d, *J* = 8.7 Hz, 2H), 7.45 (dd, *J* = 7.8, 4.6 Hz, 1H), 7.28 (d, *J* = 8.7 Hz, 2H), 7.10 (d, *J* = 8.7 Hz, 2H), 6.94 (d, *J* = 8.7 Hz, 2H), 3.83 (s, 3H), 2.29 (s, 3H).

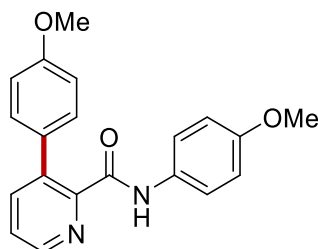
**<sup>13</sup>C NMR** (100 MHz, CDCl<sub>3</sub>) δ 162.4 (C<sub>q</sub>), 159.1 (C<sub>q</sub>), 147.2 (C<sub>q</sub>), 146.3 (CH), 140.8 (CH), 138.7 (C<sub>q</sub>), 135.5 (C<sub>q</sub>), 133.6 (C<sub>q</sub>), 131.7 (C<sub>q</sub>), 129.7 (CH), 129.4 (CH), 125.4 (CH), 119.7 (CH), 113.5 (CH), 55.2 (CH<sub>3</sub>), 20.9 (CH<sub>3</sub>).

**IR** (ATR): 3297, 2959, 1651, 1511, 839, 806, 579 cm<sup>-1</sup>.

**MS** (ESI) *m/z* (relative intensity): 319 (70) [M+H]<sup>+</sup>, 341 (30) [M+Na]<sup>+</sup>.

**HR-MS** (ESI) C<sub>20</sub>H<sub>19</sub>N<sub>2</sub>O<sub>2</sub> [M+H]<sup>+</sup>: 319.1443, found: 319.1441.

### ***N*,3-Bis(4-methoxyphenyl)picolinamide (413m)**



The **General Procedure J** was followed using *N*-(4-methoxyphenyl)picolinamide **411m** (57.1 mg, 0.25 mmol), (4-methoxyphenyl)magnesium bromide **412a** (1.0 mL, 1.0 M in THF, 1.00 mmol), **416** (30 mg, 9.0 mol %), TMEDA (58.1 mg, 0.50 mmol), and 2,3-DCB (95.3 mg, 0.75 mmol). Purification by column chromatography on silica gel (*n*-hexane/EtOAc: 1/1) yielded **413m** (49.3 mg, 59%) as a white solid.

**M. p.** 127 °C.

**<sup>1</sup>H NMR** (400 MHz, CDCl<sub>3</sub>) δ 9.80 (s, 1H), 8.55 (dd, *J* = 4.6, 1.6 Hz, 1H), 7.68 (dd, *J* = 7.8, 1.6 Hz, 1H), 7.56 (d, *J* = 9.0 Hz, 2H), 7.44 (dd, *J* = 7.8, 4.6 Hz, 1H), 7.27 (d, *J* = 8.7 Hz, 2H), 6.93 (d, *J* = 8.7 Hz, 2H), 6.82 (d, *J* = 9.0 Hz, 2H), 3.82 (s, 3H), 3.76 (s, 3H).

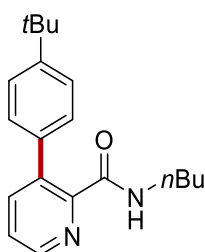
$^{13}\text{C}$  NMR (100 MHz,  $\text{CDCl}_3$ )  $\delta$  162.3 ( $\text{C}_q$ ), 159.2 ( $\text{C}_q$ ), 156.2 ( $\text{C}_q$ ), 147.3 ( $\text{C}_q$ ), 146.3 (CH), 140.8 (CH), 138.6 ( $\text{C}_q$ ), 131.7 ( $\text{C}_q$ ), 131.3 ( $\text{C}_q$ ), 129.7 (CH), 125.4 (CH), 121.3 (CH), 114.1 (CH), 113.5 (CH), 55.5 ( $\text{CH}_3$ ), 55.2 ( $\text{CH}_3$ ).

IR (ATR): 3300, 2927, 1657, 1481, 1232, 805, 490  $\text{cm}^{-1}$ .

MS (ESI)  $m/z$  (relative intensity): 335 (70)  $[\text{M}+\text{H}]^+$ , 357 (30)  $[\text{M}+\text{Na}]^+$ .

HR-MS (ESI)  $\text{C}_{20}\text{H}_{19}\text{N}_2\text{O}_3$   $[\text{M}+\text{H}]^+$ : 335.1394, found: 335.1390.

### *N*-Butyl-3-(4-(*tert*-butyl)phenyl)picolinamide (**413n**)



The **General Procedure J** was followed using *N*-butylpicolinamide **411a** (44.6 mg, 0.25 mmol), (4-methoxyphenyl)magnesium bromide **412b** (1.0 mL, 1.0 M in THF, 1.00 mmol), **416** (30 mg, 9.0 mol %), TMEDA (58.1 mg, 0.50 mmol), and 2,3-DCB (95.3 mg, 0.75 mmol). Purification by column chromatography on silica gel (*n*-hexane/EtOAc: 1/1) yielded **413n** (65.2 mg, 84%) as a white solid.

**M. p.** 110 °C.

$^1\text{H}$  NMR (400 MHz,  $\text{CDCl}_3$ )  $\delta$  8.49 (dd,  $J = 4.6, 1.6$  Hz, 1H), 7.65 (dd,  $J = 7.8, 1.6$  Hz, 1H), 7.63 (s, 1H), 7.41 (d,  $J = 8.7$  Hz, 2H), 7.39 (dd,  $J = 7.8, 4.6$  Hz, 1H), 7.27 (d,  $J = 8.7$  Hz, 2H), 3.36 – 3.31 (m, 2H), 1.57 – 1.46 (m, 2H), 1.37 – 3.31 (m, 2H), 1.34 (s, 9H), 0.90 (t,  $J = 7.3$  Hz, 3H).

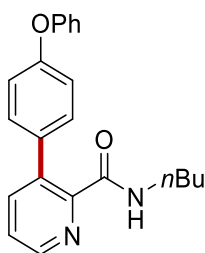
$^{13}\text{C}$  NMR (100 MHz,  $\text{CDCl}_3$ )  $\delta$  165.2 ( $\text{C}_q$ ), 150.1 ( $\text{C}_q$ ), 148.2 ( $\text{C}_q$ ), 146.6 (CH), 140.1 (CH), 137.9 ( $\text{C}_q$ ), 136.3 ( $\text{C}_q$ ), 128.1 (CH), 124.9 (CH), 124.8 (CH), 39.1 ( $\text{CH}_2$ ), 34.5 ( $\text{C}_q$ ), 31.5 ( $\text{CH}_2$ ), 31.3 ( $\text{CH}_3$ ), 20.1 ( $\text{CH}_2$ ), 13.7 ( $\text{CH}_3$ ).

IR (ATR): 3285, 3034, 1685, 1517, 1245, 809, 487  $\text{cm}^{-1}$ .

MS (ESI)  $m/z$  (relative intensity): 311 (70)  $[\text{M}+\text{H}]^+$ , 333 (30)  $[\text{M}+\text{Na}]^+$ .

HR-MS (ESI)  $\text{C}_{20}\text{H}_{27}\text{N}_2\text{O}$   $[\text{M}+\text{H}]^+$ : 311.2115, found: 311.2118.

The spectral data were in accordance with those reported in the literature.<sup>[149]</sup>

***N*-Butyl-3-(4-phenoxyphenyl)picolinamide (413o)**

The **General Procedure J** was followed using *N*-butylpicolinamide **411a** (44.6 mg, 0.25 mmol), (4-methoxyphenyl)magnesium bromide **412c** (1.0 mL, 1.0 M in THF, 1.00 mmol), **416** (30 mg, 9.0 mol %), TMEDA (58.1 mg, 0.50 mmol), and 2,3-DCB (95.3 mg, 0.75 mmol). Purification by column chromatography on silica gel (*n*-hexane/EtOAc: 1/1) yielded **413o** (82.3 mg, 95%) as a light yellow oil.

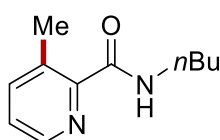
**<sup>1</sup>H NMR** (400 MHz, CDCl<sub>3</sub>) δ 8.51 (dd, *J* = 4.7, 1.6 Hz, 1H), 7.75 (s, 1H), 7.65 (dd, *J* = 7.8, 1.6 Hz, 1H), 7.39 (dd, *J* = 7.8, 4.7 Hz, 1H), 7.33 (d, *J* = 8.6 Hz, 2H), 7.28 (d, *J* = 8.6 Hz, 2H), 7.13 – 7.06 (m, 3H), 7.01 (d, *J* = 8.6 Hz, 2H), 3.38 – 3.34 (m, 2H), 1.58 – 1.51 (m, 2H), 1.41 – 1.30 (m, 2H), 0.91 (t, *J* = 7.2 Hz, 3H).

**<sup>13</sup>C NMR** (100 MHz, CDCl<sub>3</sub>) δ 165.1 (C<sub>q</sub>), 156.9 (C<sub>q</sub>), 156.6 (C<sub>q</sub>), 148.0 (C<sub>q</sub>), 146.7 (CH), 140.0 (CH), 137.5 (C<sub>q</sub>), 134.0 (C<sub>q</sub>), 129.8 (CH), 129.6 (CH), 125.0 (CH), 123.4 (CH), 119.4 (CH), 117.7 (CH), 39.1 (CH<sub>2</sub>), 31.5 (CH<sub>2</sub>), 20.1 (CH<sub>2</sub>), 13.7 (CH<sub>3</sub>).

**IR** (ATR): 3288, 2931, 1655, 1519, 1290, 811, 488 cm<sup>-1</sup>.

**MS** (ESI) *m/z* (relative intensity): 347 (80) [M+H]<sup>+</sup>, 369 (20) [M+Na]<sup>+</sup>.

**HR-MS** (ESI) C<sub>22</sub>H<sub>23</sub>N<sub>2</sub>O<sub>2</sub> [M+H]<sup>+</sup>: 347.1751, found: 347.1754.

***N*-Butyl-3-methylpicolinamide (415a)**

The **General Procedure K** was followed using *N*-butylpicolinamide **411a** (44.6 mg, 0.25 mmol), methylmagnesium bromide **414a** (0.3 mL, 3.0 M in THF, 1.00 mmol), **416** (30 mg, 9.0 mol %), TMEDA (58.1 mg, 0.50 mmol), and 2,3-DCB (95.3 mg, 0.75 mmol). Purification by column chromatography (*n*-hexane/EtOAc 8:1) yielded **415a** (38.0 mg, 79%) as a colorless oil.

**<sup>1</sup>H NMR** (400 MHz, CDCl<sub>3</sub>)  $\delta$  8.32 (dd,  $J = 4.6, 1.2$  Hz, 1H), 8.09 (brs, 1H), 7.53 (dd,  $J = 7.8, 1.2$  Hz, 1H), 7.24 (dd,  $J = 7.8, 4.6$  Hz, 1H), 3.38 (td,  $J = 7.1, 6.1$  Hz, 2H), 2.70 (s, 3H), 1.66 – 1.51 (m, 2H), 1.46 – 1.31 (m, 2H), 0.91 (t,  $J = 7.3$  Hz, 3H).

**<sup>13</sup>C NMR** (100 MHz, CDCl<sub>3</sub>)  $\delta$  165.9 (C<sub>q</sub>), 147.4 (C<sub>q</sub>), 145.3 (CH), 140.7 (CH), 135.2 (C<sub>q</sub>), 125.4 (CH), 38.9 (CH<sub>2</sub>), 31.7 (CH<sub>2</sub>), 20.5 (CH<sub>3</sub>), 20.2 (CH<sub>2</sub>), 13.7 (CH<sub>3</sub>).

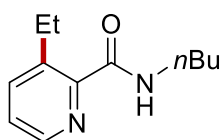
**IR** (ATR): 3384, 2927, 1574, 1465, 807, 711 cm<sup>-1</sup>.

**MS** (ESI)  $m/z$  (relative intensity) 193 (80) [M+H]<sup>+</sup>, 215 (20) [M+Na]<sup>+</sup>.

**HR-MS** (ESI)  $m/z$  calcd for C<sub>11</sub>H<sub>17</sub>N<sub>2</sub>O [M+H]<sup>+</sup> 193.1335, found 193.1337.

The spectral data were in accordance with those reported in the literature.<sup>[285]</sup>

### *N*-Butyl-3-ethylpicolinamide (**415b**)



The **General Procedure K** was followed using *N*-butylpicolinamide **411a** (44.6 mg, 0.25 mmol), ethylmagnesium bromide **414b** (0.5 mL, 2.0 M in THF, 1.00 mmol), **416** (30 mg, 9.0 mol %), TMEDA (58.1 mg, 0.50 mmol), and 2,3-DCB (95.3 mg, 0.75 mmol). Purification by column chromatography (*n*-hexane/EtOAc 8:1) yielded **415b** (35.1 mg, 68%) as a colorless oil.

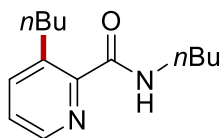
**<sup>1</sup>H NMR** (300 MHz, CDCl<sub>3</sub>)  $\delta$  8.33 (dd,  $J = 4.6, 1.7$  Hz, 1H), 8.04 (brs, 1H), 7.57 (dd,  $J = 7.8, 1.7$  Hz, 1H), 7.27 (dd,  $J = 7.8, 4.6$  Hz, 1H), 3.41 – 3.37 (m, 2H), 3.16 (q,  $J = 7.5$  Hz, 2H), 1.62 – 1.52 (m, 2H), 1.44 – 1.31 (m, 2H), 1.23 (t,  $J = 7.5$  Hz, 3H), 0.91 (t,  $J = 7.2$  Hz, 3H).

**<sup>13</sup>C NMR** (75 MHz, CDCl<sub>3</sub>)  $\delta$  165.6 (C<sub>q</sub>), 147.2 (C<sub>q</sub>), 145.1 (CH), 141.1 (C<sub>q</sub>), 139.2 (CH), 125.5 (CH), 39.0 (CH<sub>2</sub>), 31.8 (CH<sub>2</sub>), 26.3 (CH<sub>2</sub>), 20.3 (CH<sub>2</sub>), 15.6 (CH<sub>3</sub>), 13.8 (CH<sub>3</sub>).

**IR** (ATR): 3387, 2962, 1673, 1515, 803 cm<sup>-1</sup>.

**MS** (ESI)  $m/z$  (relative intensity) 207 (70) [M+H]<sup>+</sup>, 229 (30) [M+Na]<sup>+</sup>.

**HR-MS** (ESI)  $m/z$  calcd for C<sub>12</sub>H<sub>19</sub>N<sub>2</sub>O [M+H]<sup>+</sup> 207.1492, found 207.1494.

***N*,3-Dibutylpicolinamide (415c)**

The **General Procedure K** was followed using *N*-butylpicolinamide **411a** (44.6 mg, 0.25 mmol), *n*-butylmagnesium bromide **414c** (0.5 mL, 2.0 M in THF, 1.00 mmol), **416** (30 mg, 9.0 mol %), TMEDA (58.1 mg, 0.50 mmol), and 2,3-DCB (95.3 mg, 0.75 mmol). Purification by column chromatography (*n*-hexane/EtOAc 8:1) yielded **415c** (52.1 mg, 89%) as a colorless oil.

**<sup>1</sup>H NMR** (300 MHz, CDCl<sub>3</sub>) δ 8.34 (dd, *J* = 4.6, 1.7 Hz, 1H), 8.05 (brs 1H), 7.56 (dd, *J* = 7.8, 1.7 Hz, 1H), 7.27 (dd, *J* = 7.8, 4.6 Hz, 1H), 3.40 (td, *J* = 7.1, 6.0 Hz, 2H), 3.14 (t, *J* = 7.7 Hz, 2H), 1.64 – 1.54 (m, 4H), 1.45 – 1.34 (m, 4H), 0.97 – 0.86 (m, 6H).

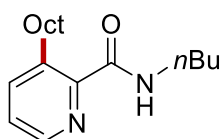
**<sup>13</sup>C NMR** (100 MHz, CDCl<sub>3</sub>) δ 165.9 (C<sub>q</sub>), 147.6 (C<sub>q</sub>), 145.4 (CH), 140.1 (C<sub>q</sub>), 140.1 (CH), 125.5 (CH), 39.1 (CH<sub>2</sub>), 33.8 (CH<sub>2</sub>), 33.0 (CH<sub>2</sub>), 31.9 (CH<sub>2</sub>), 22.9 (CH<sub>2</sub>), 20.3 (CH<sub>2</sub>), 14.1 (CH<sub>3</sub>), 13.9 (CH<sub>3</sub>).

**IR** (ATR): 2927, 2864, 1667, 1511, 1434, 807, 605 cm<sup>-1</sup>.

**MS** (ESI) *m/z* (relative intensity) 235 (40) [M+H]<sup>+</sup>, 257 (60) [M+Na]<sup>+</sup>.

**HR-MS** (ESI) *m/z* calcd for C<sub>14</sub>H<sub>22</sub>N<sub>2</sub>O [M+H]<sup>+</sup> 235.1805, found 235.1801.

The spectral data were in accordance with those reported in the literature.<sup>[286]</sup>

***N*-Butyl-3-octanoylpicolinamide (415d)**

The **General Procedure K** was followed using *N*-butylpicolinamide **411a** (44.6 mg, 0.25 mmol), octanemagnesium bromide **414d** (1.3 mL, 0.8 M in THF, 1.00 mmol), **416** (30 mg, 9.0 mol %), TMEDA (58.1 mg, 0.50 mmol), and 2,3-DCB (95.3 mg, 0.75 mmol). Purification by column chromatography (*n*-hexane/EtOAc 8:1) yielded **415d** (53.6 mg, 74%) as a colorless oil.

**<sup>1</sup>H NMR** (400 MHz, CDCl<sub>3</sub>) δ 8.35 (dd, *J* = 4.6, 1.6 Hz, 1H), 8.06 (brs, 1H), 7.57 (dd, *J* = 7.8, 1.6 Hz, 1H), 7.28 (dd, *J* = 7.8, 4.6 Hz, 1H), 3.41 (td, *J* = 7.0, 6.0 Hz, 2H), 3.18 – 3.12 (m, 2H), 1.66 – 1.56 (m, 4H), 1.46 – 1.35 (m, 3H), 1.33 – 1.22 (m, 9H), 0.94 (t, *J* = 7.3 Hz, 3H), 0.85 (t, *J* = 7.0 Hz, 3H).

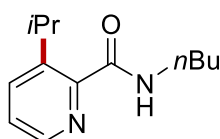
$^{13}\text{C}$  NMR (100 MHz,  $\text{CDCl}_3$ )  $\delta$  165.8 ( $\text{C}_q$ ), 147.4 ( $\text{C}_q$ ), 145.2 (CH), 140.0 ( $\text{C}_q$ ), 139.9 (CH), 125.4 (CH), 39.0 ( $\text{CH}_2$ ), 33.1 ( $\text{CH}_2$ ), 31.8 ( $\text{CH}_2$ ), 31.7 ( $\text{CH}_2$ ), 31.5 ( $\text{CH}_2$ ), 29.7 ( $\text{CH}_2$ ), 29.5 ( $\text{CH}_2$ ), 29.3 ( $\text{CH}_2$ ), 22.6 ( $\text{CH}_2$ ), 20.2 ( $\text{CH}_2$ ), 14.1 ( $\text{CH}_3$ ), 13.8 ( $\text{CH}_3$ ).

IR (ATR): 3390, 2925, 1673, 1514, 1461, 807, 613  $\text{cm}^{-1}$ .

MS (ESI)  $m/z$  (relative intensity) 291 (80)  $[\text{M}+\text{H}]^+$ , 313 (20)  $[\text{M}+\text{Na}]^+$ .

HR-MS (ESI)  $m/z$  calcd for  $\text{C}_{18}\text{H}_{31}\text{N}_2\text{O}$   $[\text{M}+\text{H}]^+$  291.2431, found 291.2432.

### *N*-Butyl-3-isopropylpicolinamide (415e)



The **General Procedure K** was followed using *N*-butylpicolinamide **411a** (44.6 mg, 0.25 mmol) and isopropylmagnesium bromide **414e** (0.33 mL, 3.0 M in THF, 1.00 mmol), **416** (30 mg, 9.0 mol %), TMEDA (58.1 mg, 0.50 mmol), and 2,3-DCB (95.3 mg, 0.75 mmol). Purification by column chromatography (*n*-hexane/EtOAc 8:1) yielded **415e** (35.8 mg, 65%) as a colorless oil.

$^1\text{H}$  NMR (400 MHz,  $\text{CDCl}_3$ )  $\delta$  8.33 (dd,  $J = 4.5, 1.5$  Hz, 1H), 7.92 (brs, 1H), 7.74 (dd,  $J = 8.1, 1.5$  Hz, 1H), 7.31 (dd,  $J = 8.1, 4.5$  Hz, 1H), 4.41 (hept,  $J = 6.9$  Hz, 1H), 3.40 (td,  $J = 7.2, 6.0$  Hz, 2H), 1.62 – 1.55 (m, 2H), 1.44 – 1.35 (m, 2H), 1.23 (d,  $J = 6.9$  Hz, 6H), 0.93 (t,  $J = 7.2$  Hz, 3H).

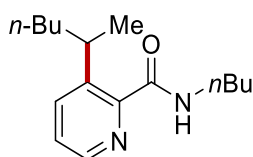
$^{13}\text{C}$  NMR (100 MHz,  $\text{CDCl}_3$ )  $\delta$  166.2 ( $\text{C}_q$ ), 147.2 ( $\text{C}_q$ ), 145.6 ( $\text{C}_q$ ), 145.0 (CH), 135.4 (CH), 125.6 (CH), 39.1 ( $\text{CH}_2$ ), 31.7 ( $\text{CH}_2$ ), 27.5 (CH), 23.6 ( $\text{CH}_3$ ), 20.2 ( $\text{CH}_2$ ), 13.7 ( $\text{CH}_3$ ).

IR (ATR): 3386, 2958, 2866, 1662, 1511, 855, 655  $\text{cm}^{-1}$ .

MS (ESI)  $m/z$  (relative intensity): 221 (20)  $[\text{M}+\text{H}]^+$ , 243 (80)  $[\text{M}+\text{Na}]^+$ .

HR-MS (ESI)  $m/z$  calcd for  $\text{C}_{13}\text{H}_{21}\text{N}_2\text{O}$   $[\text{M}+\text{H}]^+$  221.1646 found 221.1648.

### *N*-Butyl-3-(hexan-2-yl)picolinamide (415f)



The **General Procedure K** was followed using *N*-butylpicolinamide **411a** (44.6 mg, 0.25 mmol), 2-hexylmagnesium bromide **414f** (1.4 mL, 0.7 M in THF, 1.00 mmol), **416** (30 mg, 9.0 mol %), TMEDA (58.1 mg, 0.50 mmol), and 2,3-DCB (95.3 mg, 0.75 mmol). Purification by column chromatography (*n*-hexane/EtOAc 8:1) yielded **415f** (36.7 mg, 56%) as a colorless oil.

**<sup>1</sup>H NMR** (300 MHz, CDCl<sub>3</sub>)  $\delta$  8.32 (dd,  $J = 4.5, 1.5$  Hz, 1H), 7.89 (brs, 1H), 7.72 (dd,  $J = 8.1, 1.5$  Hz, 1H), 7.32 (dd,  $J = 8.1, 4.5$  Hz, 1H), 4.30 (sext,  $J = 7.2$  Hz, 1H), 3.43 – 3.39 (m, 2H), 1.63 – 1.49 (m, 4H), 1.45 – 1.34 (m, 2H), 1.30 – 1.19 (m, 3H), 1.22 (d,  $J = 6.8$  Hz, 3H), 1.16 – 1.08 (m, 1H), 0.93 (t,  $J = 7.2$  Hz, 3H), 0.81 (t,  $J = 7.2$  Hz, 3H).

**<sup>13</sup>C NMR** (100 MHz, CDCl<sub>3</sub>)  $\delta$  166.3 (C<sub>q</sub>), 147.7 (C<sub>q</sub>), 145.0 (CH), 144.9 (C<sub>q</sub>), 136.0 (CH), 125.6 (CH), 39.1 (CH<sub>2</sub>), 37.7 (CH<sub>2</sub>), 32.3 (CH), 31.7 (CH<sub>2</sub>), 29.8 (CH<sub>2</sub>), 22.8 (CH<sub>2</sub>), 22.0 (CH<sub>3</sub>), 20.2 (CH<sub>2</sub>), 14.0 (CH<sub>3</sub>), 13.8 (CH<sub>3</sub>).

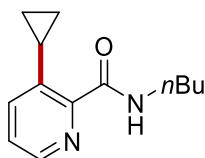
**IR** (ATR): 3387, 2955, 1665, 1511, 806, 708, 659 cm<sup>-1</sup>.

**MS** (ESI)  $m/z$  (relative intensity): 263 (70) [M+H]<sup>+</sup>, 285 (30) [M+Na]<sup>+</sup>.

**HR-MS** (ESI)  $m/z$  calcd for C<sub>17</sub>H<sub>29</sub>N<sub>2</sub>O [M+H]<sup>+</sup> 263.4050 found 263.4046.

The spectral data were in accordance with those reported in the literature.<sup>[286]</sup>

### ***N*-Butyl-3-cyclopropylpicolinamide (415g)**



The **General Procedure K** was followed using *N*-butylpicolinamide **411a** (44.6 mg, 0.25 mmol), cyclopropylmagnesium bromide **414g** (0.9 mL, 1.1 M in THF, 1.00 mmol), **416** (30 mg, 9.0 mol %), TMEDA (58.1 mg, 0.50 mmol), and 2,3-DCB (95.3 mg, 0.75 mmol). Purification by column chromatography (*n*-hexane/EtOAc 8:1) yielded **415g** (38.2 mg, 70%) as a colorless oil.

**<sup>1</sup>H NMR** (400 MHz, CDCl<sub>3</sub>)  $\delta$  8.29 (dd,  $J = 3.4, 2.8$  Hz, 1H), 8.02 (brs, 1H), 7.26 – 7.25 (m, 1H), 7.25 – 7.24 (m, 1H), 3.45 – 3.40 (m, 2H), 3.40 – 3.33 (m, 1H), 1.65 – 1.57 (m, 2H), 1.46 – 1.37 (m, 2H), 1.10 – 1.05 (m, 2H), 0.94 (t,  $J = 7.3$  Hz, 3H), 0.69 – 0.65 (m, 2H).

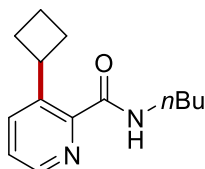
**<sup>13</sup>C NMR** (100 MHz, CDCl<sub>3</sub>)  $\delta$  166.2 (C<sub>q</sub>), 148.3 (C<sub>q</sub>), 144.3 (CH), 140.9 (C<sub>q</sub>), 133.4 (CH), 125.4 (CH), 39.0 (CH<sub>2</sub>), 31.7 (CH<sub>2</sub>), 20.2 (CH<sub>2</sub>), 13.8 (CH), 11.3 (CH<sub>3</sub>), 9.7 (CH<sub>2</sub>).

**IR** (ATR): 3379, 2960, 1670, 1514, 1465, 805, 651  $\text{cm}^{-1}$ .

**MS** (ESI)  $m/z$  (relative intensity) 219 (80)  $[\text{M}+\text{H}]^+$ , 241 (20)  $[\text{M}+\text{Na}]^+$ .

**HR-MS** (ESI)  $m/z$  calcd for  $\text{C}_{13}\text{H}_{19}\text{N}_2\text{O}$   $[\text{M}+\text{H}]^+$  219.1492, found 219.1497.

#### ***N*-Butyl-3-cyclobutylpicolinamide (415h)**



The **General Procedure K** was followed using *N*-butylpicolinamide **411a** (44.6 mg, 0.25 mmol), cyclobutylmagnesium bromide **414h** (1.3 mL, 0.8 M in THF, 1.00 mmol), **416** (30 mg, 9.0 mol %), TMEDA (58.1 mg, 0.50 mmol), and 2,3-DCB (95.3 mg, 0.75 mmol). Purification by column chromatography (*n*-hexane/EtOAc 8:1) yielded **415h** (48.8 mg, 84%) as a colorless oil.

**$^1\text{H}$  NMR** (400 MHz,  $\text{CDCl}_3$ )  $\delta$  8.32 (dd,  $J = 4.6, 1.6$  Hz, 1H), 7.88 (brs, 1H), 7.80 (dd,  $J = 8.0, 1.6$  Hz, 1H), 7.34 (dd,  $J = 8.0, 4.6$  Hz, 1H), 4.67 – 4.53 (m, 1H), 3.44 – 3.34 (m, 2H), 2.47 – 2.35 (m, 2H), 2.12 – 1.96 (m, 3H), 1.83 – 1.73 (m, 1H), 1.64 – 1.52 (m, 2H), 1.47 – 1.32 (m, 2H), 0.93 (t,  $J = 7.3$  Hz, 3H).

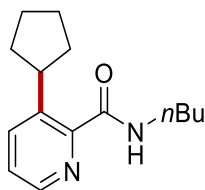
**$^{13}\text{C}$  NMR** (100 MHz,  $\text{CDCl}_3$ )  $\delta$  165.9 ( $\text{C}_q$ ), 147.4 ( $\text{C}_q$ ), 144.8 (CH), 141.7 ( $\text{C}_q$ ), 136.0 (CH), 125.4 (CH), 39.0 ( $\text{CH}_2$ ), 36.6 (CH), 31.7 ( $\text{CH}_2$ ), 29.1 ( $\text{CH}_2$ ), 20.2 ( $\text{CH}_2$ ), 18.2 ( $\text{CH}_2$ ), 13.7 ( $\text{CH}_3$ ).

**IR** (ATR): 3386, 2959, 1513, 1430, 1188, 807, 631  $\text{cm}^{-1}$ .

**MS** (ESI)  $m/z$  (relative intensity) 233 (60)  $[\text{M}+\text{H}]^+$ , 255 (40)  $[\text{M}+\text{Na}]^+$ .

**HR-MS** (ESI)  $m/z$  calcd for  $\text{C}_{14}\text{H}_{21}\text{N}_2\text{O}$   $[\text{M}+\text{H}]^+$  233.1648, found 233.1651.

#### ***N*-Butyl-3-cyclopentylpicolinamide (415i)**



The **General Procedure K** was followed using *N*-butylpicolinamide **411a** (44.6 mg, 0.25 mmol), cyclopentylmagnesium bromide **414i** (1.3 mL, 0.8 M in THF, 1.00 mmol), **416** (30 mg, 9.0 mol %),



TMEDA (58.1 mg, 0.50 mmol), and 2,3-DCB (95.3 mg, 0.75 mmol). Purification by column chromatography (*n*-hexane/EtOAc 8:1) yielded **415i** (49.4 mg, 64%) as a colorless oil.

**<sup>1</sup>H NMR** (300 MHz, CDCl<sub>3</sub>)  $\delta$  8.34 (dd, *J* = 4.5, 1.5 Hz, 1H), 7.91 (brs, 1H), 7.76 (dd, *J* = 8.1, 1.5 Hz, 1H), 7.32 (dd, *J* = 8.1, 4.5 Hz, 1H), 4.40 (tt, *J* = 9.6, 7.5 Hz, 1H), 3.42 (td, *J* = 7.1, 6.0 Hz, 2H), 2.18 – 2.11 (m, 2H), 1.77 – 1.70 (m, 4H), 1.62 – 1.36 (m, 6H), 0.93 (t, *J* = 7.2 Hz, 3H).

**<sup>13</sup>C NMR** (75 MHz, CDCl<sub>3</sub>)  $\delta$  = 166.3 (C<sub>q</sub>), 147.9 (C<sub>q</sub>), 144.8 (CH), 143.3 (C<sub>q</sub>), 136.0 (CH), 125.5 (CH), 39.7 (CH), 39.2 (CH<sub>2</sub>), 34.7 (CH<sub>2</sub>), 31.8 (CH<sub>2</sub>), 25.9 (CH<sub>2</sub>), 20.3 (CH<sub>2</sub>), 13.9 (CH<sub>3</sub>).

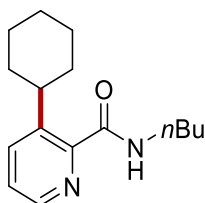
**IR** (ATR): 3385, 2947, 2859, 1660, 1508, 804, 654 cm<sup>-1</sup>.

**MS** (ESI) *m/z* (relative intensity): 247 (25) [M+H]<sup>+</sup>, 269 (75) [M+Na]<sup>+</sup>.

**HR-MS** (ESI) *m/z* calcd for C<sub>15</sub>H<sub>23</sub>N<sub>2</sub>O [M+H]<sup>+</sup> 247.1803 found 247.1805.

The spectral data were in accordance with those reported in the literature.<sup>[286]</sup>

#### ***N*-Butyl-3-cyclohexylpicolinamide (415j)**



The **General Procedure K** was followed using *N*-butylpicolinamide **411a** (44.6 mg, 0.25 mmol), cyclohexylmagnesium bromide **414j** (0.6 mL, 1.8 M in THF, 1.00 mmol), **416** (30 mg, 9.0 mol %), TMEDA (58.1 mg, 0.50 mmol), and 2,3-DCB (95.3 mg, 0.75 mmol). Purification by column chromatography (*n*-hexane/EtOAc 8:1) yielded **415j** (53.4 mg, 82%) as a colorless oil.

**<sup>1</sup>H NMR** (400 MHz, CDCl<sub>3</sub>)  $\delta$  8.33 (dd, *J* = 4.5, 1.5 Hz, 1H), 7.99 (brs, 1H), 7.75 (dd, *J* = 8.1, 1.5 Hz, 1H), 7.31 (dd, *J* = 8.1, 4.5 Hz, 1H), 4.05 (tt, *J* = 12.0, 3.2 Hz, 1H), 3.40 (td, *J* = 7.2, 6.0 Hz, 2H), 1.90 – 1.77 (m, 5H), 1.62 – 1.18 (m, 9H), 0.94 (t, *J* = 7.2 Hz, 3H).

**<sup>13</sup>C NMR** (100 MHz, CDCl<sub>3</sub>)  $\delta$  166.2 (C<sub>q</sub>), 147.2 (C<sub>q</sub>), 144.9 (CH), 144.6 (C<sub>q</sub>), 136.0 (CH), 125.5 (CH), 39.1 (CH<sub>2</sub>), 37.8 (CH), 34.1 (CH<sub>2</sub>), 31.7 (CH<sub>2</sub>), 26.7 (CH<sub>2</sub>), 26.2 (CH<sub>2</sub>), 20.2 (CH<sub>2</sub>), 13.8 (CH<sub>3</sub>).

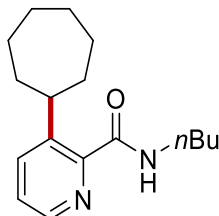
**IR** (ATR): 3382, 2922, 2850, 1663, 1504, 694, 498 cm<sup>-1</sup>.

**MS** (ESI) *m/z* (relative intensity): 261 (60) [M+H]<sup>+</sup>, 283 (40) [M+Na]<sup>+</sup>.

**HR-MS** (ESI) *m/z* calcd for C<sub>16</sub>H<sub>25</sub>N<sub>2</sub>O [M+H]<sup>+</sup> 261.1964 found 261.1962.

The spectral data were in accordance with those reported in the literature.<sup>[286]</sup>

### ***N*-Butyl-3-cycloheptylpicolinamide (415k)**



The **General Procedure K** was followed using *N*-butylpicolinamide **411a** (44.6 mg, 0.25 mmol), cycloheptylmagnesium bromide **414k** (1.7 mL, 0.6 M in THF, 1.00 mmol), **416** (30 mg, 9.0 mol %), TMEDA (58.1 mg, 0.50 mmol), and 2,3-DCB (95.3 mg, 0.75 mmol). Purification by column chromatography (*n*-hexane/EtOAc 8:1) yielded **415k** (37.0 mg, 54%) as a colorless oil.

**<sup>1</sup>H NMR** (300 MHz, CDCl<sub>3</sub>)  $\delta$  8.33 (dd,  $J = 4.5, 1.6$  Hz, 1H), 7.98 (brs, 1H), 7.74 (dd,  $J = 8.0, 1.6$  Hz, 1H), 7.32 (dd,  $J = 8.0, 4.5$  Hz, 1H), 4.32 – 4.18 (m, 1H), 3.43 (td,  $J = 7.2, 5.9$  Hz, 2H), 1.98 – 1.90 (m, 2H), 1.84 – 1.52 (m, 11H), 1.50 – 1.37 (m, 3H), 0.96 (t,  $J = 7.2$  Hz, 3H).

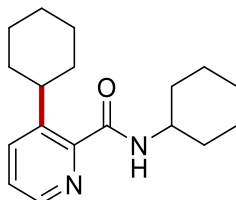
**<sup>13</sup>C NMR** (75 MHz, CDCl<sub>3</sub>)  $\delta$  166.1 (C<sub>q</sub>), 146.6 (C<sub>q</sub>), 146.2 (C<sub>q</sub>), 144.7 (CH), 136.3 (CH), 125.6 (CH), 46.4 (CH), 39.4 (CH<sub>2</sub>), 39.2 (CH<sub>2</sub>), 36.7 (CH<sub>2</sub>), 31.8 (CH<sub>2</sub>), 31.4 (CH<sub>2</sub>), 28.2 (CH<sub>2</sub>), 27.9 (CH<sub>2</sub>), 27.6 (CH<sub>2</sub>), 20.3 (CH<sub>2</sub>), 13.9 (CH<sub>3</sub>).

**IR** (ATR): 3383, 2923, 2859, 1670, 1514, 801, 624 cm<sup>-1</sup>.

**MS** (ESI)  $m/z$  (relative intensity): 275 (85) [M+H]<sup>+</sup>, 297 (15) [M+Na]<sup>+</sup>.

**HR-MS** (ESI)  $m/z$  calcd for C<sub>17</sub>H<sub>27</sub>N<sub>2</sub>O [M+H]<sup>+</sup> 275.2123 found 275.2118.

### ***N*,3-dicyclohexylpicolinamide (415l)**



The **General Procedure K** was followed using *N*-cyclohexylpicolinamide **411h** (51.1 mg, 0.25 mmol), cyclohexylmagnesium bromide **414j** (0.6 mL, 1.8 M in THF, 1.00 mmol), **416** (30 mg, 9.0 mol %), TMEDA (58.1 mg, 0.50 mmol), and 2,3-DCB (95.3 mg, 0.75 mmol). Purification by column

chromatography on silica gel (*n*-hexane/EtOAc: 1/1) yielded **415l** (49.4 mg, 69%) as a colorless oil.

**<sup>1</sup>H NMR** (400 MHz, CDCl<sub>3</sub>) δ 8.30 (dd, *J* = 4.5, 1.6 Hz, 1H), 7.89 (d, *J* = 8.8 Hz, 1H), 7.72 (dd, *J* = 8.0, 1.6 Hz, 1H), 7.29 (dd, *J* = 8.0, 4.5 Hz, 1H), 4.09 – 3.99 (m, 1H), 3.97 – 3.84 (m, 1H), 2.02 – 1.93 (m, 2H), 1.91 – 1.83 (m, 2H), 1.81 – 1.68 (m, 5H), 1.66 – 1.57 (m, 1H), 1.53 – 1.46 (m, 2H), 1.42 – 1.35 (m, 2H), 1.34 – 1.28 (m, 2H), 1.27 – 1.11 (m, 4H).

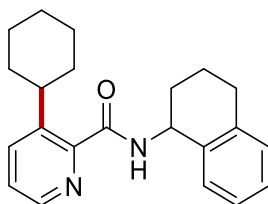
**<sup>13</sup>C NMR** (100 MHz, CDCl<sub>3</sub>) δ 165.2 (C<sub>q</sub>), 147.2 (C<sub>q</sub>), 144.8 (CH), 144.7 (C<sub>q</sub>), 136.0 (CH), 125.5 (CH), 48.0 (CH), 37.9 (CH), 34.1 (CH<sub>2</sub>), 33.1 (CH<sub>2</sub>), 26.7 (CH<sub>2</sub>), 26.2 (CH<sub>2</sub>), 25.6 (CH<sub>2</sub>), 25.0 (CH<sub>2</sub>).

**IR** (ATR): 338, 2925, 1665, 1503, 807, 593, 435 cm<sup>-1</sup>.

**MS** (ESI) *m/z* (relative intensity): 287 (90) [M+H]<sup>+</sup>, 309 (10) [M+Na]<sup>+</sup>.

**HR-MS** (ESI) C<sub>18</sub>H<sub>27</sub>N<sub>2</sub>O [M+H]<sup>+</sup>: 287.2121, found: 287.2118.

### 3-Cyclohexyl-*N*-(1,2,3,4-tetrahydronaphthalen-1-yl)picolinamide (**415m**)



The **General Procedure K** was followed using *N*-(1,2,3,4-tetrahydronaphthalen-1-yl)picolinamide **411i** (63.1 mg, 0.25 mmol), cyclohexylmagnesium bromide **414j** (0.6 mL, 1.8 M in THF, 1.00 mmol), **416** (30 mg, 9.0 mol %), TMEDA (58.1 mg, 0.50 mmol), and 2,3-DCB (95.3 mg, 0.75 mmol). Purification by column chromatography on silica gel (*n*-hexane/EtOAc: 1/1) yielded **415m** (68.6 mg, 82%) as a colorless oil.

**<sup>1</sup>H NMR** (400 MHz, CDCl<sub>3</sub>) δ 8.32 (d, *J* = 9.3 Hz, 1H), 8.28 (dd, *J* = 4.5, 1.6 Hz, 1H), 7.76 (dd, *J* = 8.1, 1.6 Hz, 1H), 7.37 – 7.33 (m, 1H), 7.31 (ddd, *J* = 8.1, 4.5 Hz, 1H), 7.17 – 7.14 (m, 2H), 7.13 – 7.09 (m, 1H), 5.38 – 5.29 (m, 1H), 4.15 (tt, *J* = 11.8, 3.1 Hz, 1H), 2.92 – 2.71 (m, 2H), 2.20 – 2.10 (m, 1H), 2.02 – 1.74 (m, 8H), 1.63 – 1.48 (m, 2H), 1.43 – 1.32 (m, 2H), 1.31 – 1.19 (m, 1H).

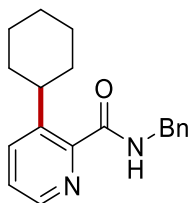
**<sup>13</sup>C NMR** (100 MHz, CDCl<sub>3</sub>) δ 165.5 (C<sub>q</sub>), 146.9 (C<sub>q</sub>), 145.0 (CH), 144.8 (C<sub>q</sub>), 137.6 (C<sub>q</sub>), 137.0 (C<sub>q</sub>), 136.0 (CH), 129.1 (CH), 128.8 (CH), 127.1 (CH), 126.1 (CH), 125.6 (CH), 47.3 (CH), 37.9 (CH), 34.2 (CH<sub>2</sub>), 30.3 (CH<sub>2</sub>), 29.3 (CH<sub>2</sub>), 26.8 (CH<sub>2</sub>), 26.3 (CH<sub>2</sub>), 20.2 (CH<sub>2</sub>).

**IR** (ATR): 3380, 2923, 1664, 1493, 735, 596, 434 cm<sup>-1</sup>.

**MS** (ESI)  $m/z$  (relative intensity): 335 (90)  $[M+H]^+$ , 357 (10)  $[M+Na]^+$ .

**HR-MS** (ESI)  $C_{22}H_{27}N_2O$   $[M+H]^+$ : 335.2120, found: 335.2118.

### ***N*-Benzyl-3-cyclohexylpicolinamide (415n)**



The **General Procedure K** was followed using *N*-benzylpicolinamide **411j** (53.1 mg, 0.25 mmol), cyclohexylmagnesium bromide **414j** (0.6 mL, 1.8 M in THF, 1.00 mmol), **416** (30 mg, 9.0 mol %), TMEDA (58.1 mg, 0.50 mmol), and 2,3-DCB (95.3 mg, 0.75 mmol). Purification by column chromatography on silica gel (*n*-hexane/EtOAc: 1/1) yielded **415n** (30.2 mg, 41%) as a colorless oil.

**<sup>1</sup>H NMR** (400 MHz,  $CDCl_3$ )  $\delta$  8.38 – 8.32 (m, 1H), 8.30 (dd,  $J = 4.5, 1.6$  Hz, 1H), 7.89 (dd,  $J = 8.8, 1.6$  Hz, 1H), 7.38 – 7.30 (m, 5H), 7.28 – 7.24 (m, 1H), 4.62 (d,  $J = 6.0$  Hz, 2H), 4.16 – 4.03 (m, 1H), 1.95 – 1.86 (m, 2H), 1.87 – 1.72 (m, 2H), 1.60 – 1.44 (m, 2H), 1.43 – 1.29 (m, 2H), 1.29 – 1.16 (m, 2H).

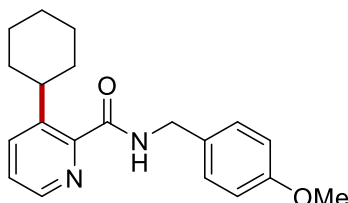
**<sup>13</sup>C NMR** (100 MHz,  $CDCl_3$ )  $\delta$  166.0 ( $C_q$ ), 146.8 ( $C_q$ ), 145.0 ( $C_q$ ), 144.9 (CH), 138.5 ( $C_q$ ), 136.1 (CH), 128.6 (CH), 127.8 (CH), 127.3 (CH), 125.8 (CH), 43.4 ( $CH_2$ ), 37.9 (CH), 34.2 ( $CH_2$ ), 26.8 ( $CH_2$ ), 26.3 ( $CH_2$ ).

**IR** (ATR): 3381, 2924, 1666, 1504, 698, 601, 480  $cm^{-1}$ .

**MS** (ESI)  $m/z$  (relative intensity): 295 (70)  $[M+H]^+$ , 317 (30)  $[M+Na]^+$ .

**HR-MS** (ESI)  $C_{19}H_{23}N_2O$   $[M+H]^+$ : 295.1801, found: 295.1805.

### **3-Cyclohexyl-*N*-(4-methoxybenzyl)picolinamide (415o)**



The **General Procedure K** was followed using *N*-(4-methoxybenzyl)picolinamide **411l** (77.6 mg, 0.25 mmol), cyclohexylmagnesium bromide **414j** (0.6 mL, 1.8 M in THF, 1.00 mmol), **416** (30 mg, 9.0 mol

%), TMEDA (58.1 mg, 0.50 mmol), and 2,3-DCB (95.3 mg, 0.75 mmol). Purification by column chromatography on silica gel (*n*-hexane/EtOAc: 1/1) yielded **415o** (42.2 mg, 52%) as a colorless oil.

**<sup>1</sup>H NMR** (400 MHz, CDCl<sub>3</sub>) δ 8.30 (dd, *J* = 4.5, 1.6 Hz, 1H), 8.28 – 8.23 (m, 1H), 7.76 (dd, *J* = 8.0, 1.6 Hz, 1H), 7.31 (dd, *J* = 8.0, 4.5 Hz, 1H), 7.28 (d, *J* = 8.6 Hz, 2H), 6.86 (d, *J* = 8.6 Hz, 2H), 4.54 (d, *J* = 5.9 Hz, 2H), 4.13 – 4.05 (m, 1H), 3.77 (s, 3H), 1.93 – 1.72 (m, 5H), 1.57 – 1.46 (m, 2H), 1.40 – 1.30 (m, 2H), 1.27 – 1.20 (m, 1H).

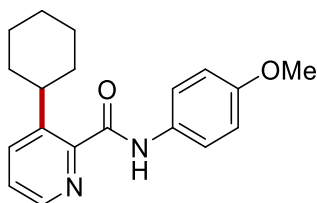
**<sup>13</sup>C NMR** (100 MHz, CDCl<sub>3</sub>) δ 166.0 (C<sub>q</sub>), 158.9 (C<sub>q</sub>), 146.9 (C<sub>q</sub>), 144.9 (CH), 144.8 (C<sub>q</sub>), 136.1 (CH), 130.6 (C<sub>q</sub>), 129.1 (CH), 125.7 (CH), 114.0 (CH), 55.3 (CH<sub>3</sub>), 42.9 (CH<sub>2</sub>), 37.9 (CH), 34.2 (CH<sub>2</sub>), 26.8 (CH<sub>2</sub>), 26.3 (CH<sub>2</sub>).

**IR** (ATR): 3387, 2925, 1666, 1508, 1247, 580, 416 cm<sup>-1</sup>.

**MS** (ESI) *m/z* (relative intensity): 325 (70) [M+H]<sup>+</sup>, 347 (30) [M+Na]<sup>+</sup>.

**HR-MS** (ESI) C<sub>20</sub>H<sub>25</sub>N<sub>2</sub>O<sub>2</sub> [M+H]<sup>+</sup>: 325.1908, found: 325.1911.

### 3-Cyclohexyl-*N*-(4-methoxyphenyl)picolinamide (**415p**)



The **General Procedure K** was followed using *N*-(4-methoxyphenyl)picolinamide **411m** (56.8 mg, 0.25 mmol), cyclohexylmagnesium bromide **414j** (0.6 mL, 1.8 M in THF, 1.00 mmol), **416** (30 mg, 9.0 mol %), TMEDA (58.1 mg, 0.50 mmol), and 2,3-DCB (95.3 mg, 0.75 mmol). Purification by column chromatography (*n*-hexane/EtOAc 8:1) yielded **415p** (32.6 mg, 42%) as a colorless oil.

**<sup>1</sup>H NMR** (300 MHz, CDCl<sub>3</sub>) δ 10.05 (brs, 1H), 8.41 (dd, *J* = 4.5, 1.5 Hz, 1H), 7.82 (dd, *J* = 8.1, 1.5 Hz, 1H), 7.64 (d, *J* = 9.0 Hz, 2H), 7.38 (dd, *J* = 8.1, 4.5 Hz, 1H), 6.91 (d, *J* = 9.0 Hz, 2H), 4.24 – 4.15 (m, 1H), 3.81 (s, 3H), 1.96 – 1.77 (m, 5H), 1.56 – 1.24 (m, 5H).

**<sup>13</sup>C NMR** (75 MHz, CDCl<sub>3</sub>) δ 163.5 (C<sub>q</sub>), 156.1 (C<sub>q</sub>), 146.3 (C<sub>q</sub>), 145.4 (C<sub>q</sub>), 144.6 (CH), 136.3 (CH), 131.2 (C<sub>q</sub>), 125.9 (CH), 121.5 (CH), 114.1 (CH), 55.5 (CH<sub>3</sub>), 37.9 (CH), 34.2 (CH<sub>2</sub>), 26.8 (CH<sub>2</sub>), 26.3 (CH<sub>2</sub>).

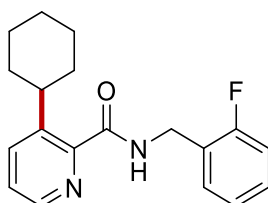
**IR** (ATR): 3319, 2922, 1673, 1240, 825, 689, 559 cm<sup>-1</sup>.

**MS** (ESI)  $m/z$  (relative intensity): 311 (65)  $[M+H]^+$ , 333 (35)  $[M+Na]^+$ .

**HR-MS** (ESI)  $m/z$  calcd for  $C_{19}H_{23}N_2O_2$   $[M+H]^+$  311.1756 found 311.1753.

The spectral data were in accordance with those reported in the literature.<sup>[286]</sup>

### 3-Cyclohexyl-*N*-(2-fluorobenzyl)picolinamide (**415q**)



The **General Procedure K** was followed using *N*-(2-fluorobenzyl)picolinamide **411n** (57.8 mg, 0.25 mmol), cyclohexylmagnesium bromide **414j** (0.6 mL, 1.8 M in THF, 1.00 mmol), **416** (30 mg, 9.0 mol %), TMEDA (58.1 mg, 0.50 mmol), and 2,3-DCB (95.3 mg, 0.75 mmol). Purification by column chromatography (*n*-hexane/EtOAc 8:1) yielded **415q** (52.3 mg, 67%) as a colorless oil.

**<sup>1</sup>H NMR** (300 MHz,  $CDCl_3$ )  $\delta$  8.39 (t,  $J = 6.3$  Hz, 1H), 8.32 (dd,  $J = 4.5, 1.5$  Hz, 1H), 7.75 (dd,  $J = 8.1, 1.5$  Hz, 1H), 7.40 (td,  $J = 7.6, 1.8$  Hz, 1H), 7.31 (dd,  $J = 8.1, 4.5$  Hz, 1H), 7.25 – 7.20 (m, 1H), 7.08 (td,  $J = 7.6, 1.2$  Hz, 1H), 7.06 – 7.00 (m, 1H), 4.67 (d,  $J = 6.3$  Hz, 2H), 4.07 (tt,  $J = 11.5, 3.0$  Hz, 1H), 1.90 – 1.73 (m, 5H), 1.56 – 1.45 (m, 2H), 1.39 – 1.21 (m, 3H).

**<sup>13</sup>C NMR** (75 MHz,  $CDCl_3$ )  $\delta$  165.9 ( $C_q$ ), 161.0 (d,  $^1J_{C-F} = 246.0$  Hz,  $C_q$ ), 146.7 ( $C_q$ ), 145.0 (CH), 144.9 ( $C_q$ ), 136.0 (CH), 130.0 (d,  $^3J_{C-F} = 4.3$  Hz, CH), 129.0 (d,  $^3J_{C-F} = 8.1$  Hz, CH), 125.8 (CH), 125.5 (d,  $^2J_{C-F} = 14.9$  Hz,  $C_q$ ), 124.2 (d,  $^4J_{C-F} = 3.6$  Hz, CH), 115.3 (d,  $^2J_{C-F} = 21.3$  Hz, CH), 37.8 (CH), 37.1 (d,  $^3J_{C-F} = 4.2$  Hz,  $CH_2$ ), 34.1 ( $CH_2$ ), 26.7 ( $CH_2$ ), 26.2 ( $CH_2$ ).

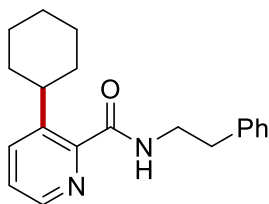
**<sup>19</sup>F NMR** (282 MHz,  $CDCl_3$ )  $\delta$  -118.7 – -118.8 (m).

**IR** (ATR): 3381, 2922, 1501, 1227, 805, 625  $cm^{-1}$ .

**MS** (ESI)  $m/z$  (relative intensity): 313 (20)  $[M+H]^+$ , 335 (100)  $[M+Na]^+$ .

**HR-MS** (ESI)  $m/z$  calcd for  $C_{19}H_{22}FN_2O$   $[M+H]^+$  313.1708 found 313.1707.

The spectral data were in accordance with those reported in the literature.<sup>[286]</sup>

**3-Cyclohexyl-*N*-phenethylpicolinamide (415r)**

The **General Procedure K** was followed using *N*-phenethylpicolinamide **411o** (56.3 mg, 0.25 mmol), cyclohexylmagnesium bromide **414j** (0.6 mL, 1.8 M in THF, 1.00 mmol), **416** (30 mg, 9.0 mol %), TMEDA (58.1 mg, 0.50 mmol), and 2,3-DCB (95.3 mg, 0.75 mmol). Purification by column chromatography (*n*-hexane/EtOAc 8:1) yielded **415r** (66.3 mg, 86%) as a colorless oil.

**<sup>1</sup>H NMR** (300 MHz, CDCl<sub>3</sub>)  $\delta$  8.22 (dd,  $J = 4.5, 1.5$  Hz, 1H), 8.01 (brs, 1H), 7.67 (dd,  $J = 8.1, 1.5$  Hz, 1H), 7.25 – 7.10 (m, 6H), 3.97 (tt,  $J = 11.8, 3.0$  Hz, 1H), 3.69–3.53 (m, 2H), 2.86 (t,  $J = 7.2$  Hz, 2H), 1.79 – 1.67 (m, 5H), 1.55–1.08 (m, 5H).

**<sup>13</sup>C NMR** (75 MHz, CDCl<sub>3</sub>)  $\delta$  166.0 (C<sub>q</sub>), 146.9 (C<sub>q</sub>), 144.7 (CH), 144.4 (C<sub>q</sub>), 138.9 (C<sub>q</sub>), 135.7 (CH), 128.6 (CH), 128.3 (CH), 126.1 (CH), 125.4 (CH), 40.6 (CH<sub>2</sub>), 37.8 (CH), 35.9 (CH<sub>2</sub>), 34.1 (CH<sub>2</sub>), 26.7 (CH<sub>2</sub>), 26.2 (CH<sub>2</sub>).

**IR** (ATR): 3385, 2923, 1665, 1000, 806, 697, 497 cm<sup>-1</sup>.

**MS** (ESI)  $m/z$  (relative intensity): 309 (100) [M+H]<sup>+</sup>, 331 (40) [M+Na]<sup>+</sup>.

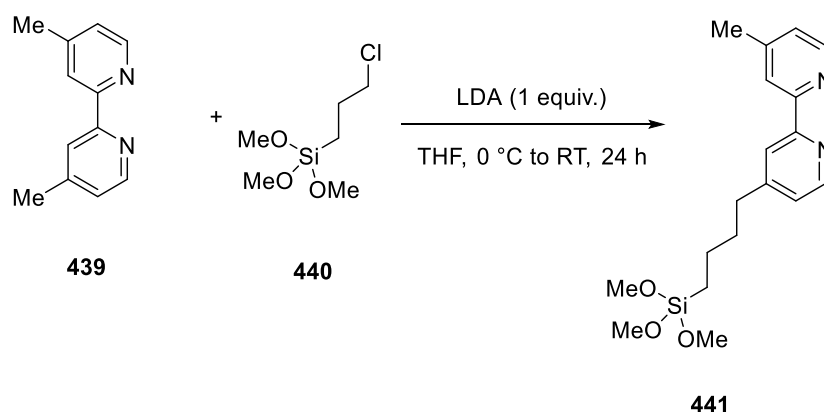
**HR-MS** (ESI)  $m/z$  calcd for C<sub>20</sub>H<sub>25</sub>N<sub>2</sub>O [M+H]<sup>+</sup> 309.1965 found 309.1961.

The spectral data were in accordance with those reported in the literature.<sup>[286]</sup>

## 5.8.2 Synthesis of Hybrid Manganese Catalyst

### 1) Linker modification

To a solution of DIPA (15 mmol, 1.1 mmol) in 40 mL of dried THF (50 mL) was added *n*-BuLi (2.1 M, 6.3 mL, 13.2 mmol, 1.0 equiv) dropwise at 0 °C under N<sub>2</sub>, *in-situ* generating LDA. After the reaction mixture was stirred for 1 h, a solution of 4,4-dimethyl-2,2'-bipyridine (**439**) (13.2 mmol, 1.0 equiv) in dried THF (100 mL) was slowly added under N<sub>2</sub>, then color was changed to dark brown. After stirring the reaction mixture for 1 h, a solution of (3-chloropropyl)trimethoxysilane (**440**) (13.2 mmol, 1.0 equiv) in 10 mL of THF was slowly added at 0 °C under N<sub>2</sub>. The solution was further stirred for an additional 2 h. The reaction mixture was warmed to room temperature and stirred for 24 h. After the reaction was quenched with two drops of acetone, the remaining solvent was removed and then dried *in vacuo* at room temperature for 24 h, affording **441**. The synthesized **441** are used for the next step without further purification (Scheme 5.8.1).

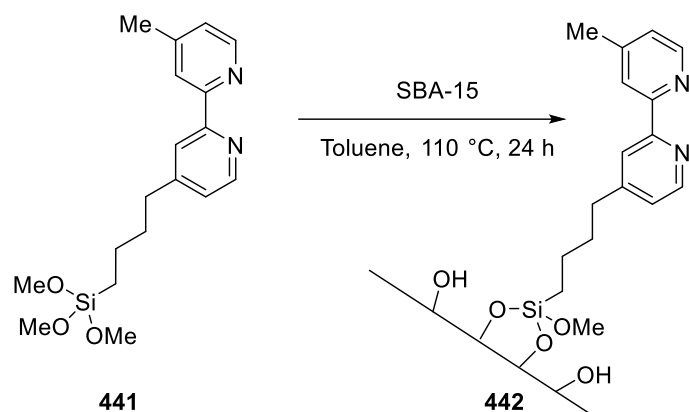


**Scheme 5.8.1** Synthesis of **441**.

### 2) Grafting

A suspension of SBA-15 (5.0 g) and the synthesized **441** in dried toluene were refluxed under N<sub>2</sub> for 24 h. The powder was filtered off, washed with toluene, *n*-hexane, and DCM (each 50 mL), and dried *in vacuo* at 100 °C for 24 h, yielding **442** (Scheme 5.8.2).

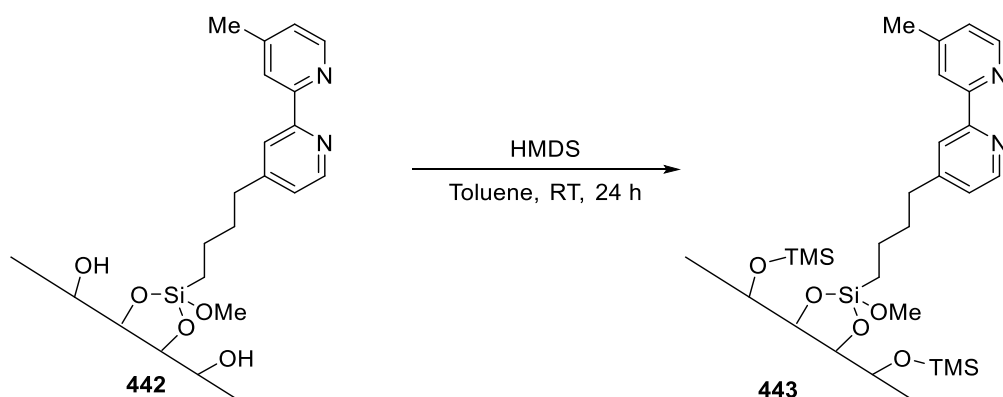




**Scheme 5.8.2** Synthesis of **442**.

### 3) End-capping

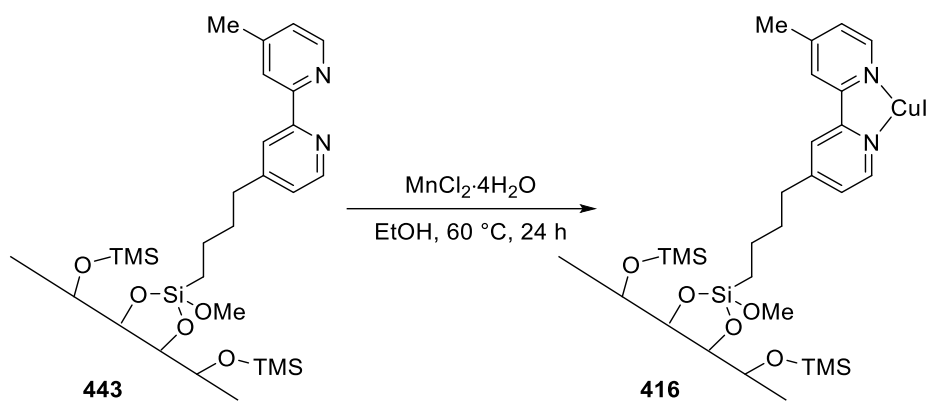
Hexamethyldisilazane (20 mL) and the isolated **442** in dried toluene (50 mL) was stirred at room temperature for 24 h. The powder was filtered off, washed with toluene, *n*-hexane, and DCM (each 50 mL), and dried *in vacuo* at 100 °C for 24 h, providing **443** (Scheme 5.8.3).



**Scheme 5.8.3** Synthesis of **443**.

### 4) Metallation

A suspension of  $\text{MnCl}_2 \cdot 4\text{H}_2\text{O}$  (1.2 g, 6.0 mmol) and the isolated **443** (1.9 g) was stirred in EtOH (50 mL) at 60 °C for 24 h under  $\text{N}_2$ . The powder was filtered off, washed with excess EtOH ( $3 \times 50$  mL), and dried *in vacuo* at 100 °C for 24 h, affording **416** (Scheme 5.8.4).



**Scheme 5.8.4** Synthesis of **416**.

### 5.8.3 Determination of Catalyst Loading

ICP-OES analysis was performed by Dr. Volker Karius for the determination of hybrid manganese catalyst **416** loading (Equation 5.8.1).

Amount of Catalyst  $\times$  ICP-OES result  $\div$  Molecular weight of manganese  $\div$   
 amount of substrates  $\times 100$  mol %

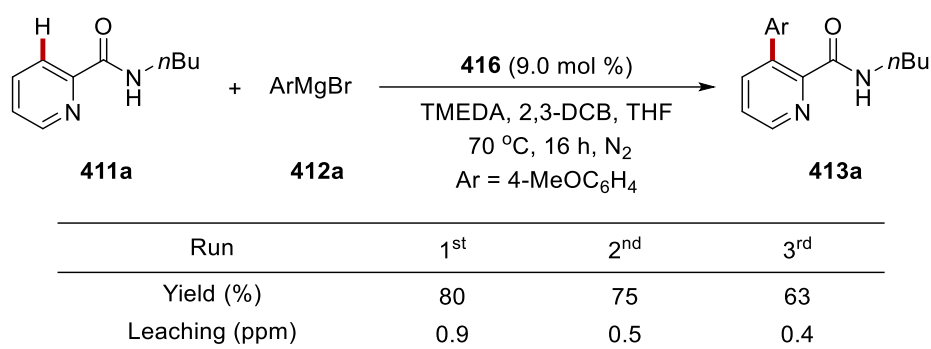
$$= 30\text{ mg} \times \frac{40930\text{ mg}}{1,000,000\text{ mg}} \times \frac{1}{54.938\text{ mg/mmol}} \times \frac{1}{0.25\text{ mmol}} \times 100\text{ mol \%} = \mathbf{9\text{ mol \%}}$$

**Equation 5.8.1** Determination of hybrid manganese catalyst loading.

### 5.8.4 Heterogeneity Test

#### 1) Reuse test for hybrid-manganese-catalyzed C–H arylations

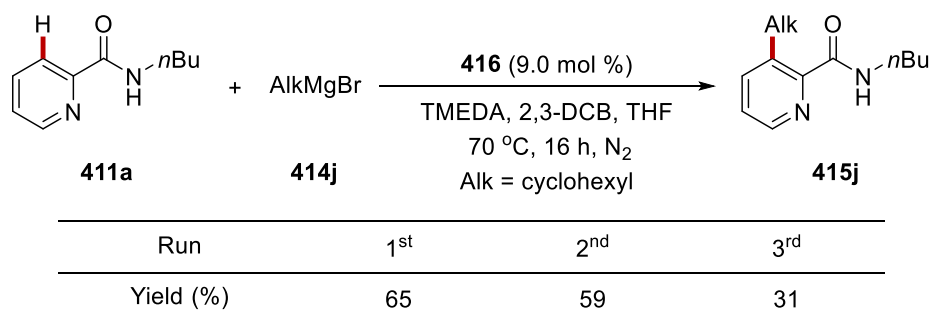
The **General Procedure J** was followed using *N*-butylpicolinamide **411a** (0.25 mmol, 1.0 equiv), (4-methoxyphenyl)magnesium bromide **412a** (1.00 mmol, 4.0 equiv, 1.0 mL, 1.0 M in THF), **416** (9.0 mol %), TMEDA (0.50 mmol, 2.0 equiv), and 2,3-DCB (0.75 mmol, 3.0 equiv). After 16 h the reaction tube was transferred to a glovebox. **416** was carefully filtered through branched filter (Por. 3) with Et<sub>2</sub>O (3 × 10 mL). Filtered **416** was dried *in vacuo* for 12 h and used for next run (Scheme 5.8.5).



**Scheme 5.8.5** Reuse test of hybrid manganese-catalyzed C–H arylation.

#### 2) Reuse test for hybrid-manganese-catalyzed C–H alkylations

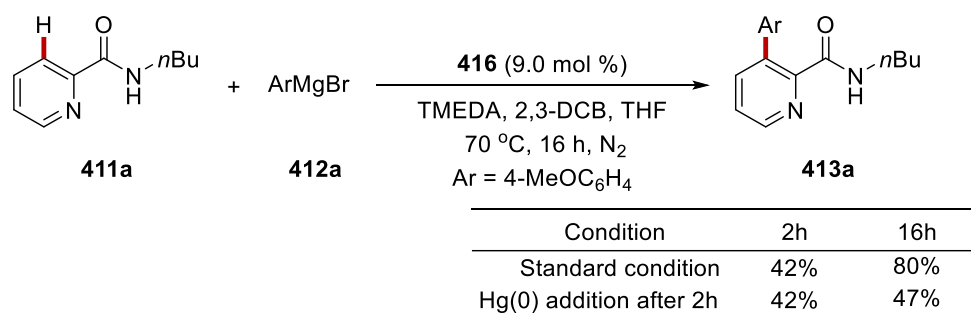
The **General Procedure K** was followed using *N*-butylpicolinamide **411a** (0.25 mmol, 1.0 equiv), cyclohexylmagnesium bromide **414j** (1.00 mmol, 4.0 equiv, 1.0 mL, 1.0 M in THF), **416** (9.0 mol %), TMEDA (0.50 mmol, 2.0 equiv), and 2,3-DCB (0.75 mmol, 3.0 equiv). Reuse procedure is same as described above (Scheme 5.8.6).



**Scheme 5.8.6** Reuse test of hybrid manganese-catalyzed C–H alkylation.

## 3) Mercury test

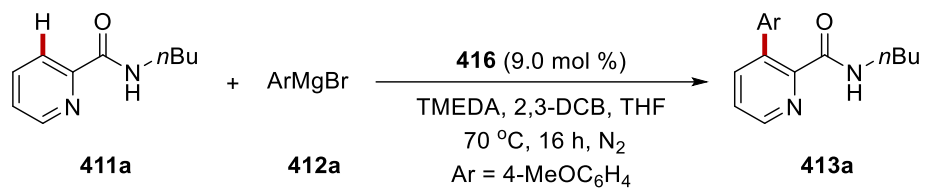
The **General Procedure J** was followed using *N*-butylpicolinamide **414a** (0.25 mmol, 1.0 equiv), (4-methoxyphenyl)magnesium bromide **412a** (1.00 mmol, 4.0 equiv, 1.0 mL, 1.0 M in THF), **416** (9.0 mol %), TMEDA (0.50 mmol, 2.0 equiv), and 2,3-DCB (0.75 mmol, 3.0 equiv). After 2 hours, Hg(0) (0.12 mL, 400 equiv to catalyst loading) was added to the Schlenk tube and then the reaction continued for 14 h. Afterwards, a saturated aqueous NH<sub>4</sub>Cl (15 mL) was added and the reaction mixture was extracted with EtOAc (3 × 15 mL). The combined organic layers were dried over Na<sub>2</sub>SO<sub>4</sub>, filtered, and concentrated *in vacuo*. Purification by column chromatography on silica gel afforded the desired product **413a**.



Scheme 5.8.7 Mercury test.

## 4) Hot-filtration test

The **General Procedure J** was followed using *N*-butylpicolinamide **414a** (0.25 mmol, 1.0 equiv), (4-methoxyphenyl)magnesium bromide **412a** (1.00 mmol, 4.0 equiv, 1.0 mL, 1.0 M in THF), **416** (9.0 mol %), TMEDA (0.50 mmol, 2.0 equiv), and 2,3-DCB (0.75 mmol, 3.0 equiv). After 2 hours, Schlenk tube was transferred to a glovebox. **416** was carefully filtered over pre-heated Celite<sup>®</sup> with a branched filter (Por. 3). Filtrate was directly collected to another pre-dried Schlenk tube and then sealed with septum. The sealed Schlenk tube was directly transferred to pre-heated oil-bath and the reaction continued for 14 h. Afterwards, saturated aqueous NH<sub>4</sub>Cl (15 mL) was added and the reaction mixture was extracted with EtOAc (3 × 15 mL). The combined organic layers were dried over Na<sub>2</sub>SO<sub>4</sub>, filtered, and concentrated *in vacuo*. Purification by column chromatography on silica gel afforded the desired product **413a** (Scheme 5.8.8).



| Condition               | 2h  | 16h |
|-------------------------|-----|-----|
| Standard condition      | 42% | 80% |
| Hot filtration after 2h | 42% | 49% |

Scheme 5.8.8 Hot-filtration test.

## 6. References

- [1] a) P. Gandeepan, L. H. Finger, T. H. Meyer, L. Ackermann, *Chem. Soc. Rev.* **2020**, *49*, 4254-4272; b) T. H. Meyer, L. H. Finger, P. Gandeepan, L. Ackermann, *Trends Chem.* **2019**, *1*, 63-76.
- [2] B. Trost, *Science* **1991**, *254*, 1471-1477.
- [3] a) P. T. Anastas, M. M. Kirchhoff, *Acc. Chem. Res.* **2002**, *35*, 686-694; b) P. T. Anastas, J. C. Warner, Oxford University Press, New York, **1998**.
- [4] U. Dhawa, N. Kaplaneris, L. Ackermann, *Org. Chem. Front.* **2021**.
- [5] C. C. C. Johansson Seechurn, M. O. Kitching, T. J. Colacot, V. Snieckus, *Angew. Chem. Int. Ed.* **2012**, *51*, 5062-5085.
- [6] a) N. Miyaura, A. Suzuki, *Chem. Rev.* **1995**, *95*, 2457-2483; b) A. Suzuki, *Acc. Chem. Res.* **1982**, *15*, 178-184; c) N. Miyaura, A. Suzuki, *J. Chem. Soc., Chem. Commun.* **1979**, 866-867; d) N. Miyaura, K. Yamada, A. Suzuki, *Tetrahedron Lett.* **1979**, *20*, 3437-3440.
- [7] a) E.-i. Negishi, T. Takahashi, S. Baba, D. E. Van Horn, N. Okukado, *J. Am. Chem. Soc.* **1987**, *109*, 2393-2401; b) E.-i. Negishi, *Acc. Chem. Res.* **1982**, *15*, 340-348; c) A. O. King, N. Okukado, E.-i. Negishi, *J. Chem. Soc., Chem. Commun.* **1977**, 683-684; d) E.-i. Negishi, A. O. King, N. Okukado, *J. Org. Chem.* **1977**, *42*, 1821-1823.
- [8] a) H. A. Dieck, R. F. Heck, *J. Org. Chem.* **1975**, *40*, 1083-1090; b) H. A. Dieck, R. F. Heck, *J. Am. Chem. Soc.* **1974**, *96*, 1133-1136; c) R. F. Heck, J. P. Nolley, *J. Org. Chem.* **1972**, *37*, 2320-2322; d) T. Mizoroki, K. Mori, A. Ozaki, *Bull. Chem. Soc. Jpn.* **1971**, *44*, 581-581.
- [9] a) R. J. P. Corriu, J. P. Masse, *J. Chem. Soc., Chem. Commun.* **1972**, 144a-144a; b) K. Tamao, K. Sumitani, M. Kumada, *J. Am. Chem. Soc.* **1972**, *94*, 4374-4376.
- [10] a) T. Hiyama, *J. Organomet. Chem.* **2002**, *653*, 58-61; b) Y. Hatanaka, T. Hiyama, *J. Org. Chem.* **1988**, *53*, 918-920.
- [11] a) J. K. Stille, *Angew. Chem. Int. Ed.* **1986**, *25*, 508-524; b) D. Milstein, J. K. Stille, *J. Am. Chem. Soc.* **1979**, *101*, 4992-4998; c) D. Milstein, J. K. Stille, *J. Am. Chem. Soc.* **1978**, *100*, 3636-3638.

- [12] a) K. Sonogashira, *J. Organomet. Chem.* **2002**, *653*, 46-49; b) K. Sonogashira, Y. Tohda, N. Hagihara, *Tetrahedron Lett.* **1975**, *16*, 4467-4470.
- [13] a) J. Tsuji, *Tetrahedron* **1986**, *42*, 4361-4401; b) B. M. Trost, *Acc. Chem. Res.* **1980**, *13*, 385-393; c) B. M. Trost, T. J. Fullerton, *J. Am. Chem. Soc.* **1973**, *95*, 292-294; d) J. Tsuji, H. Takahashi, M. Morikawa, *Tetrahedron Lett.* **1965**, *6*, 4387-4388.
- [14] a) I. Goldberg, *Ber. Dtsch. Chem. Ges.* **1906**, *39*, 1691-1692; b) F. Ullmann, *Ber. Dtsch. Chem. Ges.* **1903**, *36*, 2382-2384.
- [15] a) A. S. Guram, S. L. Buchwald, *J. Am. Chem. Soc.* **1994**, *116*, 7901-7902; b) F. Paul, J. Patt, J. F. Hartwig, *J. Am. Chem. Soc.* **1994**, *116*, 5969-5970.
- [16]
- [17] T. Rogge, N. Kaplaneris, N. Chatani, J. Kim, S. Chang, B. Punji, L. L. Schafer, D. G. Musaev, J. Wencel-Delord, C. A. Roberts, R. Sarpong, Z. E. Wilson, M. A. Brimble, M. J. Johansson, L. Ackermann, *Nature Reviews Methods Primers* **2021**, *1*, 43.
- [18] a) P. Gandeepan, T. Muller, D. Zell, G. Cera, S. Warratz, L. Ackermann, *Chem. Rev.* **2019**, *119*, 2192-2452; b) Z. Dong, Z. Ren, S. J. Thompson, Y. Xu, G. Dong, *Chem. Rev.* **2017**, *117*, 9333-9403; c) D.-S. Kim, W.-J. Park, C.-H. Jun, *Chem. Rev.* **2017**, *117*, 8977-9015; d) T. Gensch, M. N. Hopkinson, F. Glorius, J. Wencel-Delord, *Chem. Soc. Rev.* **2016**, *45*, 2900-2936; e) Q.-Z. Zheng, N. Jiao, *Chem. Soc. Rev.* **2016**, *45*, 4590-4627; f) O. Daugulis, J. Roane, L. D. Tran, *Acc. Chem. Res.* **2015**, *48*, 1053-1064; g) F. Kakiuchi, T. Kochi, S. Murai, *Synlett* **2014**, *25*, 2390-2414; h) G. Rouquet, N. Chatani, *Angew. Chem. Int. Ed.* **2013**, *52*, 11726-11743; i) L. Ackermann, R. Vicente, A. R. Kapdi, *Angew. Chem. Int. Ed.* **2009**, *48*, 9792-9826; j) R. Giri, B.-F. Shi, K. M. Engle, N. Maugel, J.-Q. Yu, *Chem. Soc. Rev.* **2009**, *38*, 3242-3272.
- [19] a) A. M. Faisca Phillips, M. d. F. C. Guedes da Silva, A. J. L. Pombeiro, *Catalysts* **2020**, *10*, 529; b) A. K. Bagdi, M. Rahman, D. Bhattacharjee, G. V. Zyryanov, S. Ghosh, O. N. Chupakhin, A. Hajra, *Green Chem.* **2020**, *22*, 6632-6681; c) A. M. Faisca Phillips, A. J. L. Pombeiro, *ChemCatChem* **2018**, *10*, 3354-3383; d) S. A. Girard, T. Knauber, C.-J. Li, *Angew. Chem. Int. Ed.* **2014**, *53*, 74-100; e) W.-J. Yoo, C.-J. Li, in *C-H Activation* (Eds.: J.-Q. Yu, Z. Shi), Springer

- Berlin Heidelberg, Berlin, Heidelberg, **2010**, pp. 281-302; f) C. J. Scheuermann, *Chem. Asian J.* **2010**, *5*, 436-451; g) C.-J. Li, Z. Li, *Pure Appl. Chem.* **2006**, *78*, 935-945.
- [20] a) L. Ackermann, *Chem. Rev.* **2011**, *111*, 1315-1345; b) D. Balcells, E. Clot, O. Eisenstein, *Chem. Rev.* **2010**, *110*, 749-823.
- [21] a) D. Lapointe, K. Fagnou, *Chem. Lett.* **2010**, *39*, 1118-1126; b) S. I. Gorelsky, D. Lapointe, K. Fagnou, *J. Am. Chem. Soc.* **2008**, *130*, 10848-10849.
- [22] Y. Boutadla, D. L. Davies, S. A. Macgregor, A. I. Poblador-Bahamonde, *Dalton Trans.* **2009**, 5820-5831.
- [23] T. Rogge, J. C. A. Oliveira, R. Kuniyil, L. Hu, L. Ackermann, *ACS Catal.* **2020**, *10*, 10551-10558.
- [24] D. Zell, M. Bursch, V. Müller, S. Grimme, L. Ackermann, *Angew. Chem. Int. Ed.* **2017**, *56*, 10378-10382.
- [25] a) T. Piou, T. Rovis, *Acc. Chem. Res.* **2018**, *51*, 170-180; b) S.-S. Li, L. Qin, L. Dong, *Org. Biomol. Chem.* **2016**, *14*, 4554-4570; c) J. Wencel-Delord, F. W. Patureau, F. Glorius, in *C-H Bond Activation and Catalytic Functionalization I* (Eds.: P. H. Dixneuf, H. Doucet), Springer International Publishing, Cham, **2016**, pp. 1-27; d) B. Ye, N. Cramer, *Acc. Chem. Res.* **2015**, *48*, 1308-1318; e) D. A. Colby, A. S. Tsai, R. G. Bergman, J. A. Ellman, *Acc. Chem. Res.* **2012**, *45*, 814-825; f) G. Song, F. Wang, X. Li, *Chem. Soc. Rev.* **2012**, *41*, 3651-3678; g) J. Du Bois, *Org. Process Res. Dev.* **2011**, *15*, 758-762; h) D. A. Colby, R. G. Bergman, J. A. Ellman, *Chem. Rev.* **2010**, *110*, 624-655.
- [26] a) P. Y. Choy, S. M. Wong, A. Kapdi, F. Y. Kwong, *Org. Chem. Front.* **2018**, *5*, 288-321; b) J. Le Bras, J. Muzart, *Eur. J. Org. Chem.* **2018**, *2018*, 1176-1203; c) O. Baudoïn, *Acc. Chem. Res.* **2017**, *50*, 1114-1123; d) F. Kakiuchi, T. Kochi, *Isr. J. Chem.* **2017**, *57*, 953-963; e) N. Della Ca', M. Fontana, E. Motti, M. Catellani, *Acc. Chem. Res.* **2016**, *49*, 1389-1400; f) J. Ye, M. Lautens, *Nat. Chem.* **2015**, *7*, 863-870; g) C.-L. Sun, B.-J. Li, Z.-J. Shi, *Chem. Commun.* **2010**, *46*, 677-685; h) X. Chen, K. M. Engle, D.-H. Wang, J.-Q. Yu, *Angew. Chem. Int. Ed.* **2009**, *48*, 5094-5115; i) M. Catellani, E. Motti, N. Della Ca', *Acc. Chem. Res.* **2008**, *41*, 1512-1522.



- [27] a) C. Haldar, M. Emdadul Hoque, R. Bisht, B. Chattopadhyay, *Tetrahedron Lett.* **2018**, *59*, 1269-1277; b) J. Kim, S. Chang, *Angew. Chem. Int. Ed.* **2014**, *53*, 2203-2207; c) S. Pan, T. Shibata, *ACS Catal.* **2013**, *3*, 704-712.
- [28] a) O. M. Ogba, N. C. Warner, D. J. O'Leary, R. H. Grubbs, *Chem. Soc. Rev.* **2018**, *47*, 4510-4544; b) B. M. Trost, F. D. Toste, A. B. Pinkerton, *Chem. Rev.* **2001**, *101*, 2067-2096.
- [29] J. Chatt, J. M. Davidson, *J. Chem. Soc.* **1965**, 843-855.
- [30] L. N. Lewis, J. F. Smith, *J. Am. Chem. Soc.* **1986**, *108*, 2728-2735.
- [31] S. Murai, F. Kakiuchi, S. Sekine, Y. Tanaka, A. Kamatani, M. Sonoda, N. Chatani, *Nature* **1993**, *366*, 529-531.
- [32] T. Matsubara, N. Koga, D. G. Musaev, K. Morokuma, *J. Am. Chem. Soc.* **1998**, *120*, 12692-12693.
- [33] a) J. C. Gaunt, B. L. Shaw, *J. Organomet. Chem.* **1975**, *102*, 511-516; b) J. M. Duff, B. E. Mann, B. L. Shaw, B. Turtle, *J. Chem. Soc., Dalton Trans.* **1974**, 139-145; c) J. M. Duff, B. L. Shaw, *J. Chem. Soc., Dalton Trans.* **1972**, 2219-2225.
- [34] D. L. Davies, O. Al-Duaij, J. Fawcett, M. Giardiello, S. T. Hilton, D. R. Russell, *Dalton Trans.* **2003**, 4132-4138.
- [35] a) L. Ackermann, *Org. Process Res. Dev.* **2015**, *19*, 260-269; b) J. Hubrich, T. Himmler, L. Rodefeld, L. Ackermann, *ACS Catal.* **2015**, *5*, 4089-4093; c) J. Li, L. Ackermann, *Org. Chem. Front.* **2015**, *2*, 1035-1039; d) M. Schinkel, I. Marek, L. Ackermann, *Angew. Chem. Int. Ed.* **2013**, *52*, 3977-3980; e) L. Ackermann, N. Hofmann, R. Vicente, *Org. Lett.* **2011**, *13*, 1875-1877.
- [36] a) L. David, F. Keith, *Chem. Lett.* **2010**, *39*, 1118-1126; b) M. Lafrance, K. Fagnou, *J. Am. Chem. Soc.* **2006**, *128*, 16496-16497.
- [37] A. Ricci, *Amino group chemistry: from synthesis to the life sciences*, John Wiley & Sons, **2008**.
- [38] a) F. Ullmann, P. Sponagel, *Ber. Dtsch. Chem. Ges.* **1905**, *38*, 2211-2212; b) F. Ullmann, J. Bielecki, *Ber. Dtsch. Chem. Ges.* **1901**, *34*, 2174-2185.
- [39] a) J. F. Hartwig, *Acc. Chem. Res.* **2008**, *41*, 1534-1544; b) J. F. Hartwig, *Nature* **2008**, *455*, 314-322; c) D. S. Surry, S. L. Buchwald, *Angew. Chem. Int. Ed.* **2008**, *47*, 6338-6361; d) J. F.

- Hartwig, *Inorg. Chem.* **2007**, *46*, 1936-1947; e) B. H. Yang, S. L. Buchwald, *J. Organomet. Chem.* **1999**, *576*, 125-146; f) J. F. Hartwig, *Angew. Chem. Int. Ed.* **1998**, *37*, 2046-2067; g) J. P. Wolfe, S. Wagaw, J.-F. Marcoux, S. L. Buchwald, *Acc. Chem. Res.* **1998**, *31*, 805-818.
- [40] a) M. A. Ali, X. Yao, G. Li, H. Lu, *Org. Lett.* **2016**, *18*, 1386-1389; b) X.-H. Hu, X.-F. Yang, T.-P. Loh, *ACS Catal.* **2016**, *6*, 5930-5934; c) J. Wippich, N. Truchan, T. Bach, *Adv. Synth. Catal.* **2016**, *358*, 2083-2087; d) S. Yu, Y. Li, X. Zhou, H. Wang, L. Kong, X. Li, *Org. Lett.* **2016**, *18*, 2812-2815; e) C. Zhang, Y. Zhou, Z. Deng, X. Chen, Y. Peng, *Eur. J. Org. Chem.* **2015**, *2015*, 1735-1744; f) T. Ryu, J. Min, W. Choi, W. H. Jeon, P. H. Lee, *Org. Lett.* **2014**, *16*, 2810-2813; g) J. Shi, G. Zhao, X. Wang, H. E. Xu, W. Yi, *Org. Biomol. Chem.* **2014**, *12*, 6831-6836; h) N. Wang, R. Li, L. Li, S. Xu, H. Song, B. Wang, *J. Org. Chem.* **2014**, *79*, 5379-5385; i) R. J. Tang, C. P. Luo, L. Yang, C. J. Li, *Adv. Synth. Catal.* **2013**, *355*, 869-873; j) S. Yu, B. Wan, X. Li, *Org. Lett.* **2013**, *15*, 3706-3709; k) H. Zhao, Y. Shang, W. Su, *Org. Lett.* **2013**, *15*, 5106-5109; l) B. Zhou, J. Du, Y. Yang, H. Feng, Y. Li, *Org. Lett.* **2013**, *15*, 6302-6305; m) B. Zhou, J. Du, Y. Yang, Y. Li, *Org. Lett.* **2013**, *15*, 2934-2937; n) B. Zhou, Y. Yang, J. Shi, H. Feng, Y. Li, *Chem. Eur. J.* **2013**, *19*, 10511-10515; o) T. Cochet, V. Bellosta, D. Roche, J.-Y. Ortholand, A. Greiner, J. Cossy, *Chem. Commun.* **2012**, *48*, 10745-10747; p) J. Y. Kim, S. H. Park, J. Ryu, S. H. Cho, S. H. Kim, S. Chang, *J. Am. Chem. Soc.* **2012**, *134*, 9110-9113; q) K.-H. Ng, Z. Zhou, W.-Y. Yu, *Org. Lett.* **2012**, *14*, 272-275; r) K. P. Kornecki, J. F. Berry, *Chem. Eur. J.* **2011**, *17*, 5827-5832; s) M. Shen, B. E. Leslie, T. G. Driver, *Angew. Chem. Int. Ed.* **2008**, *47*, 5056-5059; t) R. P. Reddy, H. M. L. Davies, *Org. Lett.* **2006**, *8*, 5013-5016.
- [41] a) K. Clagg, H. Hou, A. B. Weinstein, D. Russell, S. S. Stahl, S. G. Koenig, *Org. Lett.* **2016**, *18*, 3586-3589; b) S. Choi, T. Chatterjee, W. J. Choi, Y. You, E. J. Cho, *ACS Catal.* **2015**, *5*, 4796-4802; c) J. He, T. Shigenari, J.-Q. Yu, *Angew. Chem. Int. Ed.* **2015**, *54*, 6545-6549; d) W. A. Nack, G. Chen, *Synlett* **2015**, *26*, 2505-2511; e) M. Anand, R. B. Sunoj, H. F. Schaefer, *J. Am. Chem. Soc.* **2014**, *136*, 5535-5538; f) A. McNally, B. Haffemayer, B. S. L. Collins, M. J. Gaunt, *Nature* **2014**, *510*, 129-133; g) A. B. Weinstein, S. S. Stahl, *Catal. Sci. Technol.* **2014**, *4*, 4301-4307; h) R. Shrestha, P. Mukherjee, Y. Tan, Z. C. Litman, J. F. Hartwig, *J. Am. Chem. Soc.* **2013**, *135*, 8480-8483; i) G. He, Y. Zhao, S. Zhang, C. Lu, G. Chen, *J. Am. Chem. Soc.*

- 2012, 134, 3-6; j) Á. Iglesias, R. Álvarez, Á. R. de Lera, K. Muñiz, *Angew. Chem. Int. Ed.* **2012**, 51, 2225-2228; k) K. Sun, Y. Li, T. Xiong, J. Zhang, Q. Zhang, *J. Am. Chem. Soc.* **2011**, 133, 1694-1697; l) B. Xiao, T.-J. Gong, J. Xu, Z.-J. Liu, L. Liu, *J. Am. Chem. Soc.* **2011**, 133, 1466-1474; m) Z. Ke, T. R. Cundari, *Organometallics* **2010**, 29, 821-834; n) Y. Tan, J. F. Hartwig, *J. Am. Chem. Soc.* **2010**, 132, 3676-3677; o) W. C. P. Tsang, R. H. Munday, G. Brasche, N. Zheng, S. L. Buchwald, *J. Org. Chem.* **2008**, 73, 7603-7610; p) K. Inamoto, T. Saito, M. Katsuno, T. Sakamoto, K. Hiroya, *Org. Lett.* **2007**, 9, 2931-2934; q) H.-Y. Thu, W.-Y. Yu, C.-M. Che, *J. Am. Chem. Soc.* **2006**, 128, 9048-9049.
- [42] a) X. Dong, P. Ma, T. Zhang, H. B. Jalani, G. Li, H. Lu, *J. Org. Chem.* **2020**, 85, 13096-13107; b) T. Zhang, X. Dong, H. B. Jalani, J. Zou, G. Li, H. Lu, *Org. Lett.* **2019**, 21, 3706-3710; c) C. Pan, Y. Wang, C. Wu, J.-T. Yu, *Org. Biomol. Chem.* **2018**, 16, 3711-3715; d) M. Yu, T. Zhang, H. B. Jalani, X. Dong, H. Lu, G. Li, *Org. Lett.* **2018**, 20, 4828-4832; e) T. Zhang, X. Hu, X. Dong, G. Li, H. Lu, *Org. Lett.* **2018**, 20, 6260-6264; f) D. Mu, X. Wang, G. Chen, G. He, *J. Org. Chem.* **2017**, 82, 4497-4503; g) Y. Kim, J. Park, S. Chang, *Org. Lett.* **2016**, 18, 1892-1895; h) T. Zhang, X. Hu, Z. Wang, T. Yang, H. Sun, G. Li, H. Lu, *Chem. Eur. J.* **2016**, 22, 2920-2924; i) H. Kim, S. Chang, *ACS Catal.* **2015**, 5, 6665-6669; j) C. Suzuki, K. Hirano, T. Satoh, M. Miura, *Org. Lett.* **2015**, 17, 1597-1600; k) T. Kang, Y. Kim, D. Lee, Z. Wang, S. Chang, *J. Am. Chem. Soc.* **2014**, 136, 4141-4144; l) H. Kim, K. Shin, S. Chang, *J. Am. Chem. Soc.* **2014**, 136, 5904-5907.
- [43] a) M. Ju, J. M. Schomaker, *Nat. Rev. Chem.* **2021**, 5, 580-594; b) H. Hayashi, T. Uchida, *Eur. J. Org. Chem.* **2020**, 2020, 909-916; c) T. Shimbayashi, K. Sasakura, A. Eguchi, K. Okamoto, K. Ohe, *Chem. Eur. J.* **2019**, 25, 3156-3180; d) J. C. K. Chu, T. Rovis, *Angew. Chem. Int. Ed.* **2018**, 57, 62-101; e) P. F. Kuijpers, J. I. van der Vlugt, S. Schneider, B. de Bruin, *Chem. Eur. J.* **2017**, 23, 13819-13829; f) J. M. Alderson, J. R. Corbin, J. M. Schomaker, *Acc. Chem. Res.* **2017**, 50, 2147-2158; g) A. I. O. Suarez, V. Lyaskovskyy, J. N. H. Reek, J. I. van der Vlugt, B. de Bruin, *Angew. Chem. Int. Ed.* **2013**, 52, 12510-12529; h) D. N. Zalatan, J. D. Bois, in *C-H Activation* (Eds.: J.-Q. Yu, Z. Shi), Springer Berlin Heidelberg, Berlin, Heidelberg, **2010**, pp. 347-378; i) H. M. L. Davies, J. R. Manning, *Nature* **2008**, 451, 417-424.

- [44] a) S. J. Blanksby, G. B. Ellison, *Acc. Chem. Res.* **2003**, *36*, 255-263; b) Y.-R. Luo, *Handbook of bond dissociation energies in organic compounds*, CRC press, **2002**.
- [45] V. S. Thirunavukkarasu, K. Raghuvanshi, L. Ackermann, *Org. Lett.* **2013**, *15*, 3286-3289.
- [46] X. Zhou, P. Luo, L. Long, M. Ouyang, X. Sang, Q. Ding, *Tetrahedron* **2014**, *70*, 6742-6748.
- [47] X. Wang, C. Zhang, J. Li, C. Jiang, F. Su, Z. Zhan, L. Hai, Z. Chen, Y. Wu, *RSC Adv.* **2016**, *6*, 68929-68933.
- [48] J. Kim, J. Kim, S. Chang, *Chem. Eur. J.* **2013**, *19*, 7328-7333.
- [49] Q.-Z. Zheng, Y.-F. Liang, C. Qin, N. Jiao, *Chem. Commun.* **2013**, *49*, 5654-5656.
- [50] Y. Shin, S. Han, U. De, J. Park, S. Sharma, N. K. Mishra, E.-K. Lee, Y. Lee, H. S. Kim, I. S. Kim, *J. Org. Chem.* **2014**, *79*, 9262-9271.
- [51] C. Pan, A. Abdukader, J. Han, Y. Cheng, C. Zhu, *Chem. Eur. J.* **2014**, *20*, 3606-3609.
- [52] M. R. Yadav, R. K. Rit, A. K. Sahoo, *Org. Lett.* **2013**, *15*, 1638-1641.
- [53] M. van Eickels, S. Wassmann, A. Schäfer, J. Bauersachs, H. Strobel, H. Rütten, *BMC Pharmacology* **2007**, *7*, S4.
- [54] K. Shin, J. Ryu, S. Chang, *Org. Lett.* **2014**, *16*, 2022-2025.
- [55] M. Shang, S.-H. Zeng, S.-Z. Sun, H.-X. Dai, J.-Q. Yu, *Org. Lett.* **2013**, *15*, 5286-5289.
- [56] K. Raghuvanshi, D. Zell, K. Rauch, L. Ackermann, *ACS Catal.* **2016**, *6*, 3172-3175.
- [57] S.-M. Au, W.-H. Fung, M.-C. Cheng, C.-M. Che, S.-M. Peng, *Chem. Commun.* **1997**, 1655-1656.
- [58] a) J. Wei, W. Xiao, C.-Y. Zhou, C.-M. Che, *Chem. Commun.* **2014**, *50*, 3373-3376; b) S. K.-Y. Leung, W.-M. Tsui, J.-S. Huang, C.-M. Che, J.-L. Liang, N. Zhu, *J. Am. Chem. Soc.* **2005**, *127*, 16629-16640; c) L. He, P. W. H. Chan, W.-M. Tsui, W.-Y. Yu, C.-M. Che, *Org. Lett.* **2004**, *6*, 2405-2408; d) S.-M. Au, J.-S. Huang, W.-Y. Yu, W.-H. Fung, C.-M. Che, *J. Am. Chem. Soc.* **1999**, *121*, 9120-9132.
- [59] X.-Q. Yu, J.-S. Huang, X.-G. Zhou, C.-M. Che, *Org. Lett.* **2000**, *2*, 2233-2236.
- [60] X.-G. Zhou, X.-Q. Yu, J.-S. Huang, C.-M. Che, *Chem. Commun.* **1999**, 2377-2378.
- [61] E. Milczek, N. Boudet, S. Blakey, *Angew. Chem. Int. Ed.* **2008**, *47*, 6825-6828.

- [62] S. Fantauzzi, E. Gallo, A. Caselli, F. Ragaini, N. Casati, P. Macchi, S. Cenini, *Chem. Commun.* **2009**, 3952-3954.
- [63] G. Manca, E. Gallo, D. Intrieri, C. Mealli, *ACS Catal.* **2014**, *4*, 823-832.
- [64] M. E. Harvey, D. G. Musaev, J. Du Bois, *J. Am. Chem. Soc.* **2011**, *133*, 17207-17216.
- [65] Y. Nishioka, T. Uchida, T. Katsuki, *Angew. Chem. Int. Ed.* **2013**, *52*, 1739-1742.
- [66] Z. Zhou, S. Chen, J. Qin, X. Nie, X. Zheng, K. Harms, R. Riedel, K. N. Houk, E. Meggers, *Angew. Chem. Int. Ed.* **2019**, *58*, 1088-1093.
- [67] Q. Xing, C.-M. Chan, Y.-W. Yeung, W.-Y. Yu, *J. Am. Chem. Soc.* **2019**, *141*, 3849-3853.
- [68] T. W. Greulich, C. G. Daniliuc, A. Studer, *Org. Lett.* **2015**, *17*, 254-257.
- [69] E. Ito, T. Fukushima, T. Kawakami, K. Murakami, K. Itami, *Chem* **2017**, *2*, 383-392.
- [70] a) J.-i. Yoshida, A. Shimizu, R. Hayashi, *Chem. Rev.* **2018**, *118*, 4702-4730; b) J.-i. Yoshida, Y. Ashikari, K. Matsumoto, T. Nokami, *J. Synth. Org. Chem Jpn.* **2013**, *71*, 1136-1144; c) J.-i. Yoshida, S. Suga, *Chem. Eur. J.* **2002**, *8*, 2650-2658.
- [71] T. Morofuji, G. Ikarashi, N. Kano, *Org. Lett.* **2020**, *22*, 2822-2827.
- [72] a) A. Dey, S. K. Sinha, T. K. Achar, D. Maiti, *Angew. Chem. Int. Ed.* **2019**, *58*, 10820-10843; b) M. T. Mihai, G. R. Genov, R. J. Phipps, *Chem. Soc. Rev.* **2018**, *47*, 149-171; c) J. A. Leitch, C. G. Frost, *Chem. Soc. Rev.* **2017**, *46*, 7145-7153; d) J. Li, S. De Sarkar, L. Ackermann, *Top. Organomet. Chem.* **2016**, *55*, 217-257; e) A. Dey, S. Agasti, D. Maiti, *Org. Biomol. Chem.* **2016**, *14*, 5440-5453; f) C. G. Frost, A. J. Paterson, *ACS Cent. Sci.* **2015**, *1*, 418-419.
- [73] a) P. Wang, P. Verma, G. Xia, J. Shi, J. X. Qiao, S. Tao, P. T. W. Cheng, M. A. Poss, M. E. Farmer, K.-S. Yeung, J.-Q. Yu, *Nature* **2017**, *551*, 489-493; b) C. Cheng, J. F. Hartwig, *Science* **2014**, *343*, 853-857; c) R. J. Phipps, M. J. Gaunt, *Science* **2009**, *323*, 1593-1597; d) J.-Y. Cho, M. K. Tse, D. Holmes, R. E. Maleczka, M. R. Smith, *Science* **2002**, *295*, 305-308.
- [74] a) S. Porey, X. Zhang, S. Bhowmick, V. Kumar Singh, S. Guin, R. S. Paton, D. Maiti, *J. Am. Chem. Soc.* **2020**, *142*, 3762-3774; b) R. Bisht, M. E. Hoque, B. Chattopadhyay, *Angew. Chem. Int. Ed.* **2018**, *57*, 15762-15766; c) R. Jayarajan, J. Das, S. Bag, R. Chowdhury, D. Maiti, *Angew. Chem. Int. Ed.* **2018**, *57*, 7659-7663; d) S. Bag, R. Jayarajan, U. Dutta, R. Chowdhury, R. Mondal, D. Maiti, *Angew. Chem. Int. Ed.* **2017**, *56*, 12538-12542; e) G. Cheng, P. Wang, J.-Q.

- Yu, *Angew. Chem. Int. Ed.* **2017**, *56*, 8183-8186; f) H. J. Davis, G. R. Genov, R. J. Phipps, *Angew. Chem. Int. Ed.* **2017**, *56*, 13351-13355; g) H. J. Davis, R. J. Phipps, *Chem. Sci.* **2017**, *8*, 864-877; h) M. E. Hoque, R. Bisht, C. Halder, B. Chattopadhyay, *J. Am. Chem. Soc.* **2017**, *139*, 7745-7748; i) A. J. Neel, M. J. Hilton, M. S. Sigman, F. D. Toste, *Nature* **2017**, *543*, 637-646; j) Z. Zhang, K. Tanaka, J.-Q. Yu, *Nature* **2017**, *543*, 538-542; k) H. J. Davis, M. T. Mihai, R. J. Phipps, *J. Am. Chem. Soc.* **2016**, *138*, 12759-12762; l) S. Li, L. Cai, H. Ji, L. Yang, G. Li, *Nat. Commun.* **2016**, *7*, 10443; m) A. Maji, B. Bhaskararao, S. Singha, R. B. Sunoj, D. Maiti, *Chem. Sci.* **2016**, *7*, 3147-3153; n) Y. Kuninobu, H. Ida, M. Nishi, M. Kanai, *Nat. Chem.* **2015**, *7*, 712-717; o) D. Leow, G. Li, T.-S. Mei, J.-Q. Yu, *Nature* **2012**, *486*, 518-522; p) R. Breslow, *Acc. Chem. Res.* **1980**, *13*, 170-177.
- [75] a) M. E. Farmer, P. Wang, H. Shi, J.-Q. Yu, *ACS Catal.* **2018**, *8*, 7362-7367; b) R. Li, G. Dong, *Angew. Chem. Int. Ed.* **2018**, *57*, 1697-1701; c) H. Shi, A. N. Herron, Y. Shao, Q. Shao, J.-Q. Yu, *Nature* **2018**, *558*, 581-585; d) K.-Y. Yoon, G. Dong, *Angew. Chem. Int. Ed.* **2018**, *57*, 8592-8596; e) Z. Dong, J. Wang, G. Dong, *J. Am. Chem. Soc.* **2015**, *137*, 5887-5890; f) P.-X. Shen, X.-C. Wang, P. Wang, R.-Y. Zhu, J.-Q. Yu, *J. Am. Chem. Soc.* **2015**, *137*, 11574-11577; g) X.-C. Wang, W. Gong, L.-Z. Fang, R.-Y. Zhu, S. Li, K. M. Engle, J.-Q. Yu, *Nature* **2015**, *519*, 334-338.
- [76] a) K. Korvorapun, R. C. Samanta, T. Rogge, L. Ackermann, *Synthesis* **2021**; b) K. Korvorapun, R. C. Samanta, T. Rogge, L. Ackermann, in *Remote C-H Bond Functionalizations*, **2021**, pp. 137-167.
- [77] G. R. Clark, C. E. L. Headford, W. R. Roper, L. J. Wright, V. P. D. Yap, *Inorganica Chim. Acta* **1994**, *220*, 261-272.
- [78] J.-P. Sutter, D. M. Grove, M. Beley, J.-P. Collin, N. Veldman, A. L. Spek, J.-P. Sauvage, G. van Koten, *Angew. Chem. Int. Ed.* **1994**, *33*, 1282-1285.
- [79] C. Coudret, S. Fraysse, *Chem. Commun.* **1998**, 663-664.
- [80] a) A. M. Clark, C. E. F. Rickard, W. R. Roper, L. J. Wright, *J. Organomet. Chem.* **2000**, *598*, 262-275; b) A. M. Clark, C. E. F. Rickard, W. R. Roper, L. J. Wright, *Organometallics* **1999**, *18*, 2813-2820.

- [81] X. Guo, C.-J. Li, *Org. Lett.* **2011**, *13*, 4977-4979.
- [82] N. Hofmann, L. Ackermann, *J. Am. Chem. Soc.* **2013**, *135*, 5877-5884.
- [83] J. Li, S. Warratz, D. Zell, S. De Sarkar, E. E. Ishikawa, L. Ackermann, *J. Am. Chem. Soc.* **2015**, *137*, 13894-13901.
- [84] A. J. Paterson, S. St John-Campbell, M. F. Mahon, N. J. Press, C. G. Frost, *Chem. Commun.* **2015**, *51*, 12807-12810.
- [85] J. Li, K. Korvorapun, S. De Sarkar, T. Rogge, D. J. Burns, S. Warratz, L. Ackermann, *Nat. Commun.* **2017**, *8*, 15430.
- [86] G. Li, X. Ma, C. Jia, Q. Han, Y. Wang, J. Wang, L. Yu, S. Yang, *Chem. Commun.* **2017**, *53*, 1261-1264.
- [87] G. Li, P. Gao, X. Lv, C. Qu, Q. Yan, Y. Wang, S. Yang, J. Wang, *Org. Lett.* **2017**, *19*, 2682-2685.
- [88] Z. Ruan, S.-K. Zhang, C. Zhu, P. N. Ruth, D. Stalke, L. Ackermann, *Angew. Chem. Int. Ed.* **2017**, *56*, 2045-2049.
- [89] Z.-Y. Li, L. Li, Q.-L. Li, K. Jing, H. Xu, G.-W. Wang, *Chem. Eur. J.* **2017**, *23*, 3285-3290.
- [90] K. Korvorapun, N. Kaplaneris, T. Rogge, S. Warratz, A. C. Stückl, L. Ackermann, *ACS Catal.* **2018**, *8*, 886-892.
- [91] X.-G. Wang, Y. Li, H.-C. Liu, B.-S. Zhang, X.-Y. Gou, Q. Wang, J.-W. Ma, Y.-M. Liang, *J. Am. Chem. Soc.* **2019**, *141*, 13914-13922.
- [92] F. Fumagalli, S. Warratz, S.-K. Zhang, T. Rogge, C. Zhu, A. C. Stückl, L. Ackermann, *Chem. Eur. J.* **2018**, *24*, 3984-3988.
- [93] K. Jing, Z.-Y. Li, G.-W. Wang, *ACS Catal.* **2018**, *8*, 11875-11881.
- [94] P. Gandeepan, J. Koeller, K. Korvorapun, J. Mohr, L. Ackermann, *Angew. Chem. Int. Ed.* **2019**, *58*, 9820-9825.
- [95] A. Sagadevan, M. F. Greaney, *Angew. Chem. Int. Ed.* **2019**, *58*, 9826-9830.
- [96] a) G. Li, X. Lv, K. Guo, Y. Wang, S. Yang, L. Yu, Y. Yu, J. Wang, *Org. Chem. Front.* **2017**, *4*, 1145-1148; b) G. Li, B. Zhu, X. Ma, C. Jia, X. Lv, J. Wang, F. Zhao, Y. Lv, S. Yang, *Org. Lett.* **2017**, *19*, 5166-5169; c) P. Marcé, A. J. Paterson, M. F. Mahon, C. G. Frost, *Catal. Sci. Technol.*

- 2016**, *6*, 7068-7076; d) O. Saidi, J. Marafie, A. E. W. Ledger, P. M. Liu, M. F. Mahon, G. Kociok-Köhn, M. K. Whittlesey, C. G. Frost, *J. Am. Chem. Soc.* **2011**, *133*, 19298-19301.
- [97] a) Z. Fan, H. Lu, Z. Cheng, A. Zhang, *Chem. Commun.* **2018**, *54*, 6008-6011; b) G. M. Reddy, N. S. Rao, H. Maheswaran, *Org. Chem. Front.* **2018**, *5*, 1118-1123; c) C. J. Teskey, A. Y. Lui, M. F. Greaney, *Angew. Chem. Int. Ed.* **2015**, *54*, 11677-11680; d) Q. Yu, L. a. Hu, Y. Wang, S. Zheng, J. Huang, *Angew. Chem. Int. Ed.* **2015**, *54*, 15284-15288.
- [98] a) Z. Fan, H. Lu, A. Zhang, *J. Org. Chem.* **2018**, *83*, 3245-3251; b) Z. Fan, J. Li, H. Lu, D.-Y. Wang, C. Wang, M. Uchiyama, A. Zhang, *Org. Lett.* **2017**, *19*, 3199-3202; c) S. Warratz, D. J. Burns, C. Zhu, K. Korvorapun, T. Rogge, J. Scholz, C. Jooss, D. Gelman, L. Ackermann, *Angew. Chem. Int. Ed.* **2017**, *56*, 1557-1560; d) Z. Fan, J. Ni, A. Zhang, *J. Am. Chem. Soc.* **2016**, *138*, 8470-8475.
- [99] J. A. Leitch, C. L. McMullin, A. J. Paterson, M. F. Mahon, Y. Bhonoah, C. G. Frost, *Angew. Chem. Int. Ed.* **2017**, *56*, 15131-15135.
- [100] a) C. Yuan, L. Zhu, C. Chen, X. Chen, Y. Yang, Y. Lan, Y. Zhao, *Nat. Commun.* **2018**, *9*, 1189; b) C. Yuan, L. Zhu, R. Zeng, Y. Lan, Y. Zhao, *Angew. Chem. Int. Ed.* **2018**, *57*, 1277-1281.
- [101]
- [102] a) G. B. Shul'pin, M. M. Vinogradov, L. S. Shul'pina, *Catal. Sci. Technol.* **2018**, *8*, 4287-4313; b) G. Chelucci, S. Baldino, W. Baratta, *Acc. Chem. Res.* **2015**, *48*, 363-379; c) S. D. R. Christie, A. D. Warrington, *Synthesis* **2008**, *2008*, 1325-1341; d) J. Gonzalez, W. D. Harman, in *Category 1, Organometallics, Vol. Volume 1*, Georg Thieme Verlag, Stuttgart, **2001**; e) R. A. Sánchez-Delgado, M. Rosales, M. A. Esteruelas, L. A. Oro, *J. Mol. Catal. A Chem.* **1995**, *96*, 231-243; f) P. A. Shapley, in *Encyclopedia of Inorganic and Bioinorganic Chemistry*.
- [103] a) M. L. Buil, M. A. Esteruelas, J. Herrero, S. Izquierdo, I. M. Pastor, M. Yus, *ACS Catal.* **2013**, *3*, 2072-2075; b) Y. Zhu, H. Yan, L. Lu, D. Liu, G. Rong, J. Mao, *J. Org. Chem.* **2013**, *78*, 9898-9905; c) Masruri, A. C. Willis, M. D. McLeod, *J. Org. Chem.* **2012**, *77*, 8480-8491; d) G. R. Morello, T. R. Cundari, T. B. Gunnoe, *J. Organomet. Chem.* **2012**, *697*, 15-22; e) W. Baratta, G. Bossi, E. Putignano, P. Rigo, *Chem. Eur. J.* **2011**, *17*, 3474-3481; f) M. Bertoli, A. Choualeb, A. J. Lough, B. Moore, D. Spasyuk, D. G. Gusev, *Organometallics* **2011**, *30*, 3479-3482; g) S.



- R. Hart, D. C. Whitehead, B. R. Travis, B. Borhan, *Org. Biomol. Chem.* **2011**, *9*, 4741-4744; h) T. J. Donohoe, K. M. P. Wheelhouse, P. J. Lindsay-Scott, G. H. Churchill, M. J. Connolly, S. Butterworth, P. A. Glossop, *Chem. Asian J.* **2009**, *4*, 1237-1247; i) W. Baratta, M. Ballico, A. Del Zotto, K. Siega, S. Magnolia, P. Rigo, *Chem. Eur. J.* **2008**, *14*, 2557-2563; j) W. A. Braunecker, Y. Itami, K. Matyjaszewski, *Macromolecules* **2005**, *38*, 9402-9404; k) G. Süss-Fink, S. Haak, V. Ferrand, H. Stoeckli-Evans, *J. Mol. Catal. A Chem.* **1999**, *143*, 163-170.
- [104] a) R. Criegee, B. Marchand, H. Wannowius, *Justus Liebigs Ann. Chem.* **1942**, *550*, 99-133; b) R. Criegee, *Justus Liebigs Ann. Chem.* **1936**, *522*, 75-96.
- [105] T. Katsuki, K. B. Sharpless, *J. Am. Chem. Soc.* **1980**, *102*, 5974-5976.
- [106] a. M. I. Bruce, B. L. Goodall, F. Gordon, A. Stone, *J. Organomet. Chem.* **1973**, *60*, 343-349.
- [107] a) R. Cerón-Camacho, M. A. Roque-Ramires, A. D. Ryabov, R. Le Lagadec, *Molecules* **2021**, *26*, 1563; b) P. W. Wanandi, T. D. Tilley, *Organometallics* **1997**, *16*, 4299-4313; c) M. Beley, S. Chodorowski, J.-P. Collin, J.-P. Sauvage, L. Flamigni, F. Barigelletti, *Inorg. Chem.* **1994**, *33*, 2543-2547; d) J. M. Kisenyi, G. J. Sunley, J. A. Cabeza, A. J. Smith, H. Adams, N. J. Salt, P. M. Maitlis, *J. Chem. Soc., Dalton Trans.* **1987**, 2459-2466.
- [108] a) T. Iida, S. Ogawa, K. Hosoi, M. Makino, Y. Fujimoto, T. Goto, N. Mano, J. Goto, A. F. Hofmann, *J. Org. Chem.* **2007**, *72*, 823-830; b) S. Ogawa, K. Hosoi, T. Iida, Y. Wakatsuki, M. Makino, Y. Fujimoto, A. F. Hofmann, *Eur. J. Org. Chem.* **2007**, *2007*, 3555-3563.
- [109] S. Ogawa, Y. Wakatsuki, M. Makino, Y. Fujimoto, K. Yasukawa, T. Kikuchi, M. Ukiya, T. Akihisa, T. Iida, *Chem. Phys. Lipids* **2010**, *163*, 165-171.
- [110] G. Wang, Z. Zhou, X. Shen, S. Ivlev, E. Meggers, *Chem. Commun.* **2020**, *56*, 7714-7717.
- [111] B. D. Ravetz, N. E. S. Tay, C. L. Joe, M. Sezen-Edmonds, M. A. Schmidt, Y. Tan, J. M. Janey, M. D. Eastgate, T. Rovis, *ACS Cent. Sci.* **2020**, *6*, 2053-2059.
- [112] J. Yang, L. Wu, H. Xu, H. Gao, Z. Zhou, W. Yi, *Org. Lett.* **2019**, *21*, 9904-9908.
- [113] a) Y. Nishii, M. Miura, *ACS Catal.* **2020**, *10*, 9747-9757; b) L. Ackermann, *Acc. Chem. Res.* **2014**, *47*, 281-295.
- [114] a) A. Sigel, H. Sigel, R. K. O. Sigel, *Interrelations between essential metal ions and human diseases, Vol. 13*, Springer, **2013**; b) P. B. Tchounwou, C. G. Yedjou, A. K. Patlolla, D. J. Sutton,

- in *Molecular, Clinical and Environmental Toxicology: Volume 3: Environmental Toxicology* (Ed.: A. Luch), Springer Basel, Basel, **2012**, pp. 133-164; c) S. H. Gilani, Y. Alibhai, *Journal of Toxicology and Environmental Health* **1990**, *30*, 23-31.
- [115] F. A. Cotton, G. Wilkinson, C. A. Murillo, M. Bochmann, R. Grimes, *Advanced inorganic chemistry, Vol. 6*, Wiley New York, **1988**.
- [116] a) E. M. McGarrigle, D. G. Gilheany, *Chem. Rev.* **2005**, *105*, 1563-1602; b) T. Katsuki, *Synlett* **2003**, *2003*, 0281-0297; c) R. Irie, K. Noda, Y. Ito, N. Matsumoto, T. Katsuki, *Tetrahedron Lett.* **1990**, *31*, 7345-7348; d) W. Zhang, J. L. Loebach, S. R. Wilson, E. N. Jacobsen, *J. Am. Chem. Soc.* **1990**, *112*, 2801-2803.
- [117] a) X. Huang, T. Zhuang, P. A. Kates, H. Gao, X. Chen, J. T. Groves, *J. Am. Chem. Soc.* **2017**, *139*, 15407-15413; b) M. Milan, M. Bietti, M. Costas, *ACS Cent. Sci.* **2017**, *3*, 196-204; c) X. Huang, T. M. Bergsten, J. T. Groves, *J. Am. Chem. Soc.* **2015**, *137*, 5300-5303; d) S. M. Paradine, J. R. Griffin, J. Zhao, A. L. Petronico, S. M. Miller, M. Christina White, *Nat. Chem.* **2015**, *7*, 987-994; e) X. Huang, W. Liu, H. Ren, R. Neelamegam, J. M. Hooker, J. T. Groves, *J. Am. Chem. Soc.* **2014**, *136*, 6842-6845; f) D. Shen, C. Miao, S. Wang, C. Xia, W. Sun, *Org. Lett.* **2014**, *16*, 1108-1111; g) W. Liu, J. T. Groves, *Angew. Chem. Int. Ed.* **2013**, *52*, 6024-6027; h) W. Liu, X. Huang, M.-J. Cheng, R. J. Nielsen, W. A. Goddard, J. T. Groves, *Science* **2012**, *337*, 1322-1325; i) W. Liu, J. T. Groves, *J. Am. Chem. Soc.* **2010**, *132*, 12847-12849.
- [118] a) G. Cahiez, O. Gager, F. Lecomte, *Org. Lett.* **2008**, *10*, 5255-5256; b) G. Cahiez, A. Moyeux, J. Buendia, C. Duplais, *J. Am. Chem. Soc.* **2007**, *129*, 13788-13789; c) M. Rueping, W. Ieawsuwan, *Synlett* **2007**, *2007*, 0247-0250.
- [119] M. I. Bruce, M. Z. Iqbal, F. G. A. Stone, *J. Chem. Soc. A* **1970**, 3204-3209.
- [120] a) G. J. Depree, L. Main, B. K. Nicholson, N. P. Robinson, G. B. Jameson, *J. Organomet. Chem.* **2006**, *691*, 667-679; b) G. J. Depree, L. Main, B. K. Nicholson, *J. Organomet. Chem.* **1998**, *551*, 281-291; c) C. Morton, D. J. Duncalf, J. P. Rourke, *J. Organomet. Chem.* **1997**, *530*, 19-25; d) W. Tully, L. Main, B. K. Nicholson, *J. Organomet. Chem.* **1995**, *503*, 75-92; e) R. C. Cambie, L. C. Mui Mui, P. S. Rutledge, P. D. Woodgate, *J. Organomet. Chem.* **1994**, *464*, 171-182; f) R. C. Cambie, M. R. Metzler, P. S. Rutledge, P. D. Woodgate, *J. Organomet. Chem.*

- 1992, 429, 41-57; g) R. C. Cambie, M. R. Metzler, P. S. Rutledge, P. D. Woodgate, *J. Organomet. Chem.* **1990**, 381, C26-C30; h) R. C. Cambie, M. R. Metzler, P. S. Rutledge, P. D. Woodgate, *J. Organomet. Chem.* **1990**, 398, C22-C24; i) J. M. Cooney, L. H. P. Gommans, L. Main, B. K. Nicholson, *J. Organomet. Chem.* **1988**, 349, 197-207; j) J. M. Ressler, P. C. Wernett, C. S. Kraihanzel, A. L. Rheingold, *Organometallics* **1988**, 7, 1661-1663; k) N. P. Robinson, L. Main, B. K. Nicholson, *J. Organomet. Chem.* **1988**, 349, 209-218; l) L. H. P. Gommans, L. Main, B. K. Nicholson, *J. Chem. Soc., Chem. Commun.* **1987**, 761-762; m) A. Suárez, J. Manuel Vila, M. Teresa Pereira, E. Gayoso, M. Gayoso, *J. Organomet. Chem.* **1987**, 335, 359-363; n) M. I. Bruce, B. L. Goodall, M. Z. Iqbal, F. G. A. Stone, R. J. Doedens, R. G. Little, *Journal of the Chemical Society D: Chemical Communications* **1971**, 1595-1596.
- [121] Y. Kuninobu, Y. Nishina, T. Takeuchi, K. Takai, *Angew. Chem. Int. Ed.* **2007**, 46, 6518-6520.
- [122] B. Zhou, H. Chen, C. Wang, *J. Am. Chem. Soc.* **2013**, 135, 1264-1267.
- [123] a) L. A. Hammarback, I. P. Clark, I. V. Sazanovich, M. Towrie, A. Robinson, F. Clarke, S. Meyer, I. J. S. Fairlamb, J. M. Lynam, *Nat. Catal.* **2018**, 1, 830-840; b) N. P. Yahaya, K. M. Appleby, M. Teh, C. Wagner, E. Troschke, J. T. W. Bray, S. B. Duckett, L. A. Hammarback, J. S. Ward, J. Milani, N. E. Pridmore, A. C. Whitwood, J. M. Lynam, I. J. S. Fairlamb, *Angew. Chem. Int. Ed.* **2016**, 55, 12455-12459.
- [124] C. Zhu, R. Kuniyil, L. Ackermann, *Angew. Chem. Int. Ed.* **2019**, 58, 5338-5342.
- [125] R. He, Z.-T. Huang, Q.-Y. Zheng, C. Wang, *Angew. Chem. Int. Ed.* **2014**, 53, 4950-4953.
- [126] a) B. Liu, Y. Yuan, P. Hu, G. Zheng, D. Bai, J. Chang, X. Li, *Chem. Commun.* **2019**, 55, 10764-10767; b) G. Zheng, J. Sun, Y. Xu, S. Zhai, X. Li, *Angew. Chem. Int. Ed.* **2019**, 58, 5090-5094.
- [127] Q. Lu, S. Greßies, F. J. R. Klauck, F. Glorius, *Angew. Chem. Int. Ed.* **2017**, 56, 6660-6664.
- [128] Z. Ruan, N. Sauermann, E. Manoni, L. Ackermann, *Angew. Chem. Int. Ed.* **2017**, 56, 3172-3176.
- [129] B. Zhou, P. Ma, H. Chen, C. Wang, *Chem. Commun.* **2014**, 50, 14558-14561.
- [130] S. L. Liu, Y. Li, J. R. Guo, G. C. Yang, X. H. Li, J. F. Gong, M. P. Song, *Org. Lett.* **2017**, 19, 4042-4045.
- [131] Q. Lu, S. Mondal, S. Cembellín, F. Glorius, *Angew. Chem. Int. Ed.* **2018**, 57, 10732-10736.

- [132] W. Liu, S. C. Richter, Y. Zhang, L. Ackermann, *Angew. Chem. Int. Ed.* **2016**, *55*, 7747-7750.
- [133] H. Wang, M. M. Lorion, L. Ackermann, *Angew. Chem. Int. Ed.* **2017**, *56*, 6339-6342.
- [134] T. H. Meyer, W. Liu, M. Feldt, A. Wuttke, R. A. Mata, L. Ackermann, *Chem. Eur. J.* **2017**, *23*, 5443-5447.
- [135] Q. Lu, F. J. R. Klauck, F. Glorius, *Chem. Sci.* **2017**, *8*, 3379-3383.
- [136] S.-Y. Chen, Q. Li, H. Wang, *J. Org. Chem.* **2017**, *82*, 11173-11181.
- [137] J. Ni, H. Zhao, A. Zhang, *Org. Lett.* **2017**, *19*, 3159-3162.
- [138] Y.-F. Liang, V. Müller, W. Liu, A. Münch, D. Stalke, L. Ackermann, *Angew. Chem. Int. Ed.* **2017**, *56*, 9415-9419.
- [139] W. Liu, D. Zell, M. John, L. Ackermann, *Angew. Chem. Int. Ed.* **2015**, *54*, 4092-4096.
- [140] C. Zhu, J. L. Schwarz, S. Cembellín, S. Greßies, F. Glorius, *Angew. Chem. Int. Ed.* **2018**, *57*, 437-441.
- [141] a) S.-Y. Chen, X.-L. Han, J.-Q. Wu, Q. Li, Y. Chen, H. Wang, *Angew. Chem. Int. Ed.* **2017**, *56*, 9939-9943; b) S.-Y. Chen, Q. Li, X.-G. Liu, J.-Q. Wu, S.-S. Zhang, H. Wang, *ChemSusChem* **2017**, *10*, 2360-2364.
- [142] C. Wang, A. Wang, M. Rueping, *Angew. Chem. Int. Ed.* **2017**, *56*, 9935-9938.
- [143] C. Lei, L. Peng, K. Ding, *Adv. Synth. Catal.* **2018**, *360*, 2952-2958.
- [144] J. R. Hummel, J. A. Boerth, J. A. Ellman, *Chem. Rev.* **2017**, *117*, 9163-9227.
- [145] W. Liu, J. Bang, Y. Zhang, L. Ackermann, *Angew. Chem. Int. Ed.* **2015**, *54*, 14137-14140.
- [146] B. Zhou, Y. Hu, C. Wang, *Angew. Chem. Int. Ed.* **2015**, *54*, 13659-13663.
- [147] a) Y.-F. Liang, L. Massignan, L. Ackermann, *ChemCatChem* **2018**, *10*, 2768-2772; b) Y.-F. Liang, L. Massignan, W. Liu, L. Ackermann, *Chem. Eur. J.* **2016**, *22*, 14856-14859.
- [148] a) C. Zhu, T. Pinkert, S. Greßies, F. Glorius, *ACS Catal.* **2018**, *8*, 10036-10042; b) B. Zhou, Y. Hu, T. Liu, C. Wang, *Nat. Commun.* **2017**, *8*, 1169.
- [149] C. Zhu, J. C. A. Oliveira, Z. Shen, H. Huang, L. Ackermann, *ACS Catal.* **2018**, *8*, 4402-4407.
- [150] C. Zhu, M. Stangier, J. C. A. Oliveira, L. Massignan, L. Ackermann, *Chem. Eur. J.* **2019**, *25*, 16382-16389.

- [151] Y.-F. Liang, R. Steinbock, L. Yang, L. Ackermann, *Angew. Chem. Int. Ed.* **2018**, *57*, 10625-10629.
- [152] a) W.-H. Rao, B.-F. Shi, *Org. Chem. Front.* **2016**, *3*, 1028-1047; b) X.-X. Guo, D.-W. Gu, Z. Wu, W. Zhang, *Chem. Rev.* **2015**, *115*, 1622-1651; c) J.-P. Wan, Y. Jing, *Beilstein Journal of Organic Chemistry* **2015**, *11*, 2209-2222; d) C. Sambigiato, S. P. Marsden, A. J. Blacker, P. C. McGowan, *Chem. Soc. Rev.* **2014**, *43*, 3525-3550; e) S. E. Allen, R. R. Walvoord, R. Padilla-Salinas, M. C. Kozlowski, *Chem. Rev.* **2013**, *113*, 6234-6458; f) I. P. Beletskaya, A. V. Cheprakov, *Coord. Chem. Rev.* **2004**, *248*, 2337-2364.
- [153] C. Glaser, *Ber. Dtsch. Chem. Ges.* **1869**, *2*, 422-424.
- [154] a) J. Hassan, M. Sévignon, C. Gozzi, E. Schulz, M. Lemaire, *Chem. Rev.* **2002**, *102*, 1359-1470; b) P. E. Fanta, *Chem. Rev.* **1964**, *64*, 613-632.
- [155] a) B. Maciá, in *Progress in Enantioselective Cu(I)-catalyzed Formation of Stereogenic Centers* (Ed.: S. R. Harutyunyan), Springer International Publishing, Cham, **2016**, pp. 41-98; b) M. T. Pirnot, Y.-M. Wang, S. L. Buchwald, *Angew. Chem. Int. Ed.* **2016**, *55*, 48-57; c) X. Zhu, S. Chiba, *Chem. Soc. Rev.* **2016**, *45*, 4504-4523; d) S. D. McCann, S. S. Stahl, *Acc. Chem. Res.* **2015**, *48*, 1756-1766; e) B. L. Ryland, S. S. Stahl, *Angew. Chem. Int. Ed.* **2014**, *53*, 8824-8838; f) N. Yoshikai, E. Nakamura, *Chem. Rev.* **2012**, *112*, 2339-2372; g) C. Zhang, C. Tang, N. Jiao, *Chem. Soc. Rev.* **2012**, *41*, 3464-3484; h) T. Jerphagnon, M. G. Pizzuti, A. J. Minnaard, B. L. Feringa, *Chem. Soc. Rev.* **2009**, *38*, 1039-1075; i) A. Alexakis, J. E. Bäckvall, N. Krause, O. Pàmies, M. Diéguez, *Chem. Rev.* **2008**, *108*, 2796-2823; j) G. Evano, N. Blanchard, M. Toumi, *Chem. Rev.* **2008**, *108*, 3054-3131; k) S. Reymond, J. Cossy, *Chem. Rev.* **2008**, *108*, 5359-5406; l) N. Armaroli, G. Accorsi, F. Cardinali, A. Listorti, in *Photochemistry and Photophysics of Coordination Compounds I* (Eds.: V. Balzani, S. Campagna), Springer Berlin Heidelberg, Berlin, Heidelberg, **2007**, pp. 69-115; m) S. V. Ley, A. W. Thomas, *Angew. Chem. Int. Ed.* **2003**, *42*, 5400-5449.
- [156] C. Björklund, M. Nilsson, T. Olson, T. Norin, *Acta Chem. Scand.* **1968**, *22*.
- [157] H. Ljusberg, R. Wahren, *Acta Chem. Scand.* **1973**, *27*, 2712-2721.

- [158] a) P.-A. Sommai, S. Tetsuya, K. Yoshiki, M. Masahiro, N. Masakatsu, *Bull. Chem. Soc. Jpn.* **1998**, *71*, 467-473; b) P.-A. Sommai, F. Yuka, M. Masahiro, N. Masakatsu, *Bull. Chem. Soc. Jpn.* **1996**, *69*, 2039-2042.
- [159] J. Lindley, *Tetrahedron* **1984**, *40*, 1433-1456.
- [160] H.-Q. Do, O. Daugulis, *J. Am. Chem. Soc.* **2007**, *129*, 12404-12405.
- [161] H.-Q. Do, O. Daugulis, *J. Am. Chem. Soc.* **2008**, *130*, 1128-1129.
- [162] H.-Q. Do, R. M. K. Khan, O. Daugulis, *J. Am. Chem. Soc.* **2008**, *130*, 15185-15192.
- [163] L. Ackermann, H. K. Potukuchi, D. Landsberg, R. Vicente, *Org. Lett.* **2008**, *10*, 3081-3084.
- [164] a) N.-N. Jia, X.-C. Tian, X.-X. Qu, X.-X. Chen, Y.-N. Cao, Y.-X. Yao, F. Gao, X.-L. Zhou, *Scientific Reports* **2017**, *7*, 43758; b) D. Kim, K. Yoo, S. E. Kim, H. J. Cho, J. Lee, Y. Kim, M. Kim, *J. Org. Chem.* **2015**, *80*, 3670-3676; c) R. Kadu, H. Roy, V. K. Singh, *Appl. Organomet. Chem.* **2015**, *29*, 746-755; d) T. Kawano, T. Yoshizumi, K. Hirano, T. Satoh, M. Miura, *Org. Lett.* **2009**, *11*, 3072-3075.
- [165] C. Yang, H. M. Lee, S. P. Nolan, *Org. Lett.* **2001**, *3*, 1511-1514.
- [166] D. Zhao, W. Wang, F. Yang, J. Lan, L. Yang, G. Gao, J. You, *Angew. Chem. Int. Ed.* **2009**, *48*, 3296-3300.
- [167] C. Cheng, Y.-C. Shih, H.-T. Chen, T.-C. Chien, *Tetrahedron* **2013**, *69*, 1387-1396.
- [168] a) S. Li, J. Tang, Y. Zhao, R. Jiang, T. Wang, G. Gao, J. You, *Chem. Commun.* **2017**, *53*, 3489-3492; b) D. P. Khambhati, K. A. N. Sachinthani, A. L. Rheingold, T. L. Nelson, *Chem. Commun.* **2017**, *53*, 5107-5109; c) Y. Cheng, G. Li, Y. Liu, Y. Shi, G. Gao, D. Wu, J. Lan, J. You, *J. Am. Chem. Soc.* **2016**, *138*, 4730-4738; d) J. Wu, Q. You, J. Lan, Q. Guo, X. Li, Y. Xue, J. You, *Org. Biomol. Chem.* **2015**, *13*, 5372-5375; e) Y.-T. Song, P.-H. Lin, C.-Y. Liu, *Adv. Synth. Catal.* **2014**, *356*, 3761-3768.
- [169] a) F. Yang, J. Koeller, L. Ackermann, *Angew. Chem. Int. Ed.* **2016**, *55*, 4759-4762; b) P. Gandeepan, J. Mo, L. Ackermann, *Chem. Commun.* **2017**, *53*, 5906-5909.
- [170] R. Jeyachandran, H. K. Potukuchi, L. Ackermann, *Beilstein Journal of Organic Chemistry* **2012**, *8*, 1771-1777.
- [171] R. J. Phipps, N. P. Grimster, M. J. Gaunt, *J. Am. Chem. Soc.* **2008**, *130*, 8172-8174.

- [172] A. K. Pitts, F. O'Hara, R. H. Snell, M. J. Gaunt, *Angew. Chem. Int. Ed.* **2015**, *54*, 5451-5455.
- [173] H. A. Duong, R. E. Gilligan, M. L. Cooke, R. J. Phipps, M. J. Gaunt, *Angew. Chem. Int. Ed.* **2011**, *50*, 463-466.
- [174] B. Chen, X.-L. Hou, Y.-X. Li, Y.-D. Wu, *J. Am. Chem. Soc.* **2011**, *133*, 7668-7671.
- [175] C.-L. Ciana, R. J. Phipps, J. R. Brandt, F.-M. Meyer, M. J. Gaunt, *Angew. Chem. Int. Ed.* **2011**, *50*, 458-462.
- [176] I. Ban, T. Sudo, T. Taniguchi, K. Itami, *Org. Lett.* **2008**, *10*, 3607-3609.
- [177] a) B. Musio, F. Mariani, E. P. Śliwiński, M. A. Kabeshov, H. Odajima, S. V. Ley, *Synthesis* **2016**, *48*, 3515-3526; b) Y. Shen, J. Chen, M. Liu, J. Ding, W. Gao, X. Huang, H. Wu, *Chem. Commun.* **2014**, *50*, 4292-4295; c) F. Yang, Z. Xu, Z. Wang, Z. Yu, R. Wang, *Chem. Eur. J.* **2011**, *17*, 6321-6325.
- [178] M. Shang, S.-Z. Sun, H.-X. Dai, J.-Q. Yu, *Org. Lett.* **2014**, *16*, 5666-5669.
- [179] a) Q. Zhang, Y. Liu, T. Wang, X. Zhang, C. Long, Y.-D. Wu, M.-X. Wang, *J. Am. Chem. Soc.* **2018**, *140*, 5579-5587; b) Y. Liu, C. Long, L. Zhao, M.-X. Wang, *Org. Lett.* **2016**, *18*, 5078-5081.
- [180] W. I. Dzik, P. P. Lange, L. J. Gooßen, *Chem. Sci.* **2012**, *3*, 2671-2678.
- [181] L. Chen, L. Ju, K. A. Bustin, J. M. Hoover, *Chem. Commun.* **2015**, *51*, 15059-15062.
- [182] T. Patra, S. Nandi, S. K. Sahoo, D. Maiti, *Chem. Commun.* **2016**, *52*, 1432-1435.
- [183] S. Zhao, Y.-J. Liu, S.-Y. Yan, F.-J. Chen, Z.-Z. Zhang, B.-F. Shi, *Org. Lett.* **2015**, *17*, 3338-3341.
- [184] K. Takamatsu, K. Hirano, M. Miura, *Angew. Chem. Int. Ed.* **2017**, *56*, 5353-5357.
- [185] J. A. Ashenhurst, *Chem. Soc. Rev.* **2010**, *39*, 540-548.
- [186] a) S. Paul, R. Shrestha, T. N. J. I. Edison, Y. R. Lee, S. H. Kim, *Adv. Synth. Catal.* **2016**, *358*, 3050-3056; b) S. Lei, H. Cao, L. Chen, J. Liu, H. Cai, J. Tan, *Adv. Synth. Catal.* **2015**, *357*, 3109-3114; c) M. Zhu, K.-i. Fujita, R. Yamaguchi, *Chem. Commun.* **2011**, *47*, 12876-12878; d) Y. Li, J. Jin, W. Qian, W. Bao, *Org. Biomol. Chem.* **2010**, *8*, 326-330; e) D. Monguchi, A. Yamamura, T. Fujiwara, T. Somete, A. Mori, *Tetrahedron Lett.* **2010**, *51*, 850-852; f) H.-Q. Do, O. Daugulis, *J. Am. Chem. Soc.* **2009**, *131*, 17052-17053.

- [187] a) R. P. Pandit, J.-J. Shim, S. H. Kim, Y. R. Lee, *RSC Adv.* **2017**, *7*, 55288-55295; b) L.-H. Zou, J. Mottweiler, D. L. Priebbenow, J. Wang, J. A. Stubenrauch, C. Bolm, *Chem. Eur. J.* **2013**, *19*, 3302-3305; c) S. Fan, Z. Chen, X. Zhang, *Org. Lett.* **2012**, *14*, 4950-4953; d) X. Qin, B. Feng, J. Dong, X. Li, Y. Xue, J. Lan, J. You, *J. Org. Chem.* **2012**, *77*, 7677-7683; e) M. S. Reddy, Y. K. Kumar, N. Thirupathi, *Org. Lett.* **2012**, *14*, 824-827; f) H.-Q. Do, O. Daugulis, *J. Am. Chem. Soc.* **2011**, *133*, 13577-13586.
- [188] a) K. N. Tripathi, D. Ray, R. P. Singh, *Eur. J. Org. Chem.* **2017**, *2017*, 5809-5813; b) D. Ray, T. Manikandan, A. Roy, K. N. Tripathi, R. P. Singh, *Chem. Commun.* **2015**, *51*, 7065-7068.
- [189] a) A. K. Jha, N. Jain, *Eur. J. Org. Chem.* **2017**, *2017*, 4765-4772; b) J. Le, Y. Gao, Y. Ding, C. Jiang, *Tetrahedron Lett.* **2016**, *57*, 1728-1731; c) R. Odani, K. Hirano, T. Satoh, M. Miura, *Angew. Chem. Int. Ed.* **2014**, *53*, 10784-10788; d) M. Nishino, K. Hirano, T. Satoh, M. Miura, *Angew. Chem. Int. Ed.* **2012**, *51*, 6993-6997; e) M. Kitahara, N. Umeda, K. Hirano, T. Satoh, M. Miura, *J. Am. Chem. Soc.* **2011**, *133*, 2160-2162; f) X. Chen, G. Dobereiner, X.-S. Hao, R. Giri, N. Mangel, J.-Q. Yu, *Tetrahedron* **2009**, *65*, 3085-3089; g) X. Chen, X.-S. Hao, C. E. Goodhue, J.-Q. Yu, *J. Am. Chem. Soc.* **2006**, *128*, 6790-6791.
- [190] a) A. Mandal, J. Selvakumar, S. Dana, U. Mukherjee, M. Baidya, *Chem. Eur. J.* **2018**, *24*, 3448-3454; b) B. K. Singh, R. Jana, *J. Org. Chem.* **2016**, *81*, 831-841; c) M. Wang, Y. Hu, Z. Jiang, H. C. Shen, X. Sun, *Org. Biomol. Chem.* **2016**, *14*, 4239-4246; d) R. Odani, K. Hirano, T. Satoh, M. Miura, *J. Org. Chem.* **2015**, *80*, 2384-2391; e) S. Zhao, J. Yuan, Y.-C. Li, B.-F. Shi, *Chem. Commun.* **2015**, *51*, 12823-12826; f) M. Nishino, K. Hirano, T. Satoh, M. Miura, *Angew. Chem. Int. Ed.* **2013**, *52*, 4457-4461; g) R. Odani, K. Hirano, T. Satoh, M. Miura, *J. Org. Chem.* **2013**, *78*, 11045-11052.
- [191] S. Hübner, J. G. de Vries, V. Farina, *Adv. Synth. Catal.* **2016**, *358*, 3-25.
- [192] a) M. Safaei, M. M. Foroughi, N. Ebrahimpoor, S. Jahani, A. Omidi, M. Khatami, *Trends Anal. Chem.* **2019**, *118*, 401-425; b) M. Liu, J. Wu, H. Hou, *Chem. Eur. J.* **2019**, *25*, 2935-2948; c) N. J. O'Connor, A. S. M. Jonayat, M. J. Janik, T. P. Senftle, *Nat. Catal.* **2018**, *1*, 531-539; d) L. Liu, A. Corma, *Chem. Rev.* **2018**, *118*, 4981-5079; e) N. Yang, S. F. Bent, *J. Catal.* **2017**, *351*, 49-58; f) D. Pla, M. Gomez, *ACS Catal.* **2016**, *6*, 3537-3552; g) E. Lam, J. H. Luong, *ACS*



- Catal.* **2014**, *4*, 3393-3410; h) U. Díaz, D. Brunel, A. Corma, *Chem. Soc. Rev.* **2013**, *42*, 4083-4097; i) N. Kann, *Molecules* **2010**, *15*, 6306-6331; j) J. Lu, P. H. Toy, *Chem. Rev.* **2009**, *109*, 815-838; k) M. R. Buchmeiser, *Chem. Rev.* **2009**, *109*, 303-321; l) N. Madhavan, C. W. Jones, M. Weck, *Acc. Chem. Res.* **2008**, *41*, 1153-1165; m) F. Rodriguez-Reinoso, *Carbon* **1998**, *36*, 159-175.
- [193] a) J.-i. Yoshida, K. Itami, *Chem. Rev.* **2002**, *102*, 3693-3716; b) A. P. Wight, M. E. Davis, *Chem. Rev.* **2002**, *102*, 3589-3614; c) I. F. J. Vankelecom, *Chem. Rev.* **2002**, *102*, 3779-3810; d) R. van Heerbeek, P. C. J. Kamer, P. W. N. M. van Leeuwen, J. N. H. Reek, *Chem. Rev.* **2002**, *102*, 3717-3756; e) C. E. Song, S.-g. Lee, *Chem. Rev.* **2002**, *102*, 3495-3524; f) A. Roucoux, J. Schulz, H. Patin, *Chem. Rev.* **2002**, *102*, 3757-3778; g) D. Rechavi, M. Lemaire, *Chem. Rev.* **2002**, *102*, 3467-3494; h) T. Okuhara, *Chem. Rev.* **2002**, *102*, 3641-3666; i) C. A. McNamara, M. J. Dixon, M. Bradley, *Chem. Rev.* **2002**, *102*, 3275-3300; j) Z.-l. Lu, E. Lindner, H. A. Mayer, *Chem. Rev.* **2002**, *102*, 3543-3578; k) N. E. Leadbeater, M. Marco, *Chem. Rev.* **2002**, *102*, 3217-3274; l) A. K. Kakkar, *Chem. Rev.* **2002**, *102*, 3579-3588; m) Q.-H. Fan, Y.-M. Li, A. S. C. Chan, *Chem. Rev.* **2002**, *102*, 3385-3466; n) J. Dupont, R. F. de Souza, P. A. Z. Suarez, *Chem. Rev.* **2002**, *102*, 3667-3692; o) R. Duchateau, *Chem. Rev.* **2002**, *102*, 3525-3542; p) T. J. Dickerson, N. N. Reed, K. D. Janda, *Chem. Rev.* **2002**, *102*, 3325-3344; q) D. E. De Vos, M. Dams, B. F. Sels, P. A. Jacobs, *Chem. Rev.* **2002**, *102*, 3615-3640; r) D. E. Bergbreiter, *Chem. Rev.* **2002**, *102*, 3345-3384; s) A. G. M. Barrett, B. T. Hopkins, J. Köbberling, *Chem. Rev.* **2002**, *102*, 3301-3324.
- [194] I. Fechete, Y. Wang, J. C. Védrine, *Catal. Today* **2012**, *189*, 2-27.
- [195] H. Davy, *Phil. Trans. Roy. Soc.* **1817**, *107*, 45-76.
- [196] J. W. Döbereiner, *Annl. Chim. Phys.* **1823**, *24*, 91.
- [197] M. W. M. Hisham, S. W. Benson, *J. Phys. Chem.* **1995**, *99*, 6194-6198.
- [198] F. Haber, G. Van Oordt, *Zeitschrift für anorganische Chemie* **1905**, *43*, 111-115.
- [199] S. Santoro, S. I. Kozhushkov, L. Ackermann, L. Vaccaro, *Green Chem.* **2016**, *18*, 3471-3493.
- [200] N. Nakamura, Y. Tajima, K. Sakai, *Heterocycles* **1982**, *17*, 235-245.
- [201] M. Parisien, D. Valette, K. Fagnou, *J. Org. Chem.* **2005**, *70*, 7578-7584.

- [202] H. Miura, K. Wada, S. Hosokawa, M. Inoue, *Chem. Eur. J.* **2010**, *16*, 4186-4189.
- [203] H. Miura, K. Wada, S. Hosokawa, M. Inoue, *ChemCatChem* **2010**, *2*, 1223-1225.
- [204] a) R. Ye, J. Zhao, B. B. Wickemeyer, F. D. Toste, G. A. Somorjai, *Nat. Catal.* **2018**, *1*, 318-325;  
b) J. M. Notestein, A. Katz, *Chem. Eur. J.* **2006**, *12*, 3954-3965.
- [205] H. M. L. Davies, A. M. Walji, *Org. Lett.* **2005**, *7*, 2941-2944.
- [206] K. M. Chepiga, Y. Feng, N. A. Brunelli, C. W. Jones, H. M. L. Davies, *Org. Lett.* **2013**, *15*, 6136-6139.
- [207] N. R. Candeias, C. A. M. Afonso, P. M. P. Gois, *Org. Biomol. Chem.* **2012**, *10*, 3357-3378.
- [208] C.-J. Yoo, D. Rackl, W. Liu, C. B. Hoyt, B. Pimentel, R. P. Lively, H. M. L. Davies, C. W. Jones, *Angew. Chem. Int. Ed.* **2018**, *57*, 10923-10927.
- [209] L.-C. Lee, J. He, J.-Q. Yu, C. W. Jones, *ACS Catal.* **2016**, *6*, 5245-5250.
- [210] a) P. Gandeepan, L. Ackermann, *Chem* **2018**, *4*, 199-222; b) L. Ackermann, R. Vicente, *Top. Curr. Chem.* **2010**, *292*, 211-229; c) L. Ackermann, *Synlett* **2007**, 507-526.
- [211] I. Choi, A. M. Messinis, L. Ackermann, *Angew. Chem. Int. Ed.* **2020**, *59*, 12534-12540.
- [212] I. Choi, V. Müller, L. Ackermann, *Tetrahedron Lett.* **2021**, *72*, 153064.
- [213] I. Choi, V. Müller, G. Lole, R. Köhler, V. Karius, W. Viöl, C. Jooss, L. Ackermann, *Chem. Eur. J.* **2020**, *26*, 3509-3514.
- [214] I. Choi, V. Müller, Y. Wang, K. Xue, R. Kuniyil, L. B. Andreas, V. Karius, J. G. Alauzun, L. Ackermann, *Chem. Eur. J.* **2020**, *26*, 15290-15297.
- [215] a) Y. Park, S. Chang, *Nat. Catal.* **2019**, *2*, 219-227; b) D. A. Petrone, J. Ye, M. Lautens, *Chem. Rev.* **2016**, *116*, 8003-8104; c) P. B. Arockiam, C. Bruneau, P. H. Dixneuf, *Chem. Rev.* **2012**, *112*, 5879-5918; d) T. Satoh, M. Miura, *Chem. Eur. J.* **2010**, *16*, 11212-11222.
- [216] P. Gandeepan, T. Müller, D. Zell, G. Cera, S. Warratz, L. Ackermann, *Chem. Rev.* **2019**, *119*, 2192-2452.
- [217] J. Alvarez-Builla, J. J. Vaquero, J. Barluenga, *Modern heterocyclic chemistry, 4 volume set, Vol. 2*, John Wiley & Sons, **2011**.
- [218] a) A. Srivastava, S. Pandeya, *Int. J. Curr. Pharm. Rev. Res* **2011**, *4*, 5-8; b) A. J. Kochanowska-Karamyan, M. T. Hamann, *Chem. Rev.* **2010**, *110*, 4489-4497; c) F. R. de Sa Alves, E. J.

- Barreiro, C. A. Manssour Fraga, *Mini-Rev. Med. Chem.* **2009**, *9*, 782-793; d) G. W. Gribble, *J. Chem. Soc., Perkin Trans. 1* **2000**, 1045-1075.
- [219] J. A. Leitch, Y. Bhonoah, C. G. Frost, *ACS Catal.* **2017**, *7*, 5618-5627.
- [220] T. A. Shah, P. B. De, S. Pradhan, T. Punniyamurthy, *Chem. Commun.* **2019**, *55*, 572-587.
- [221] S. Santoro, F. Ferlin, L. Ackermann, L. Vaccaro, *Chem. Soc. Rev.* **2019**, *48*, 2767-2782.
- [222] J. Kalepu, P. Gandeepan, L. Ackermann, L. T. Pilarski, *Chem. Sci.* **2018**, *9*, 4203-4216.
- [223] a) W.-L. Wang, Z.-Y. Lu, H.-W. Tao, T.-J. Zhu, Y.-C. Fang, Q.-Q. Gu, W.-M. Zhu, *J. Nat. Prod.* **2007**, *70*, 1558-1564; b) J. G. Ondeyka, G. L. Helms, O. D. Hensens, M. A. Goetz, D. L. Zink, A. Tsipouras, W. L. Shoop, L. Slayton, A. W. Dombrowski, J. D. Polishook, D. A. Ostlind, N. N. Tsou, R. G. Ball, S. B. Singh, *J. Am. Chem. Soc.* **1997**, *119*, 8809-8816; c) R. J. Capon, J. K. Macleod, P. J. Scammells, *Tetrahedron* **1986**, *42*, 6545-6550; d) H. W. Dudley, C. Moir, *Br. Med. J.* **1935**, *1*, 520-523.
- [224] a) V. Lanke, K. R. Prabhu, *Chem. Commun.* **2017**, *53*, 5117-5120; b) V. Lanke, K. Ramaiah Prabhu, *Org. Lett.* **2013**, *15*, 6262-6265.
- [225] a) A. J. Borah, Z. Shi, *Chem. Commun.* **2017**, *53*, 3945-3948; b) Y. Yang, P. Gao, Y. Zhao, Z. Shi, *Angew. Chem. Int. Ed.* **2017**, *56*, 3966-3971; c) Y. Yang, R. Li, Y. Zhao, D. Zhao, Z. Shi, *J. Am. Chem. Soc.* **2016**, *138*, 8734-8737.
- [226] G. Yang, P. Lindovska, D. Zhu, J. Kim, P. Wang, R.-Y. Tang, M. Movassaghi, J.-Q. Yu, *J. Am. Chem. Soc.* **2014**, *136*, 10807-10813.
- [227] Y. Feng, D. Holte, J. Zoller, S. Umemiya, L. R. Simke, P. S. Baran, *J. Am. Chem. Soc.* **2015**, *137*, 10160-10163.
- [228] a) H. Chen, C. Lin, C. Xiong, Z. Liu, Y. Zhang, *Org. Chem. Front.* **2017**, *4*, 455-459; b) J. A. Leitch, C. L. McMullin, M. F. Mahon, Y. Bhonoah, C. G. Frost, *ACS Catal.* **2017**, *7*, 2616-2623; c) L. Legnani, G. Prina Cerai, B. Morandi, *ACS Catal.* **2016**, *6*, 8162-8165; d) H. Liu, C. Zheng, S.-L. You, *J. Org. Chem.* **2014**, *79*, 1047-1054.
- [229] a) G. Mihara, K. Ghosh, Y. Nishii, M. Miura, *Org. Lett.* **2020**, *22*, 5706-5711; b) K. Ueura, T. Satoh, M. Miura, *Org. Lett.* **2007**, *9*, 1407-1409.

- [230] a) S. Warratz, C. Kornhaaß, A. Cajaraville, B. Niepötter, D. Stalke, L. Ackermann, *Angew. Chem. Int. Ed.* **2015**, *54*, 5513-5517; b) M. Deponti, S. I. Kozhushkov, D. S. Yufit, L. Ackermann, *Org. Biomol. Chem.* **2013**, *11*, 142-148; c) L. Ackermann, J. Pospech, K. Graczyk, K. Rauch, *Org. Lett.* **2012**, *14*, 930-933.
- [231] D. A. Frasco, C. P. Lilly, P. D. Boyle, E. A. Ison, *ACS Catal.* **2013**, *3*, 2421-2429.
- [232] a) P. Sihag, M. Jeganmohan, *J. Org. Chem.* **2019**, *84*, 2699-2712; b) Q. Lu, S. Mondal, S. Cembellín, S. Greßies, F. Glorius, *Chem. Sci.* **2019**, *10*, 6560-6564; c) G. Liu, G. Kuang, X. Zhang, N. Lu, Y. Fu, Y. Peng, Y. Zhou, *Org. Lett.* **2019**, *21*, 3043-3047; d) X.-G. Liu, H. Gao, S.-S. Zhang, Q. Li, H. Wang, *ACS Catal.* **2017**, *7*, 5078-5086; e) S. L. Yedage, B. M. Bhanage, *Green Chem.* **2016**, *18*, 5635-5642; f) R. K. Chinnagolla, M. Jeganmohan, *Chem. Commun.* **2012**, *48*, 2030-2032.
- [233] a) R. Santhoshkumar, C.-H. Cheng, *Chem. Eur. J.* **2019**, *25*, 9366-9384; b) V. P. Boyarskiy, D. S. Ryabukhin, N. A. Bokach, A. V. Vasilyev, *Chem. Rev.* **2016**, *116*, 5894-5986.
- [234] a) L. F. T. Novaes, J. Liu, Y. Shen, L. Lu, J. M. Meinhardt, S. Lin, *Chem. Soc. Rev.* **2021**; b) K. Yamamoto, M. Kuriyama, O. Onomura, *Acc. Chem. Res.* **2020**, *53*, 105-120; c) Q. Jing, K. D. Moeller, *Acc. Chem. Res.* **2020**, *53*, 135-143; d) K.-J. Jiao, Y.-K. Xing, Q.-L. Yang, H. Qiu, T.-S. Mei, *Acc. Chem. Res.* **2020**, *53*, 300-310; e) T. Fuchigami, S. Inagi, *Acc. Chem. Res.* **2020**, *53*, 322-334; f) P. Xiong, H.-C. Xu, *Acc. Chem. Res.* **2019**, *52*, 3339-3350; g) M. Elsherbini, T. Wirth, *Acc. Chem. Res.* **2019**, *52*, 3287-3296; h) S. R. Waldvogel, S. Lips, M. Selt, B. Riehl, C. J. Kampf, *Chem. Rev.* **2018**, *118*, 6706-6765; i) S. Tang, Y. Liu, A. Lei, *Chem* **2018**, *4*, 27-45; j) G. S. Sauer, S. Lin, *ACS Catal.* **2018**, *8*, 5175-5187; k) J. E. Nutting, M. Rafiee, S. S. Stahl, *Chem. Rev.* **2018**, *118*, 4834-4885; l) M. Yan, Y. Kawamata, P. S. Baran, *Chem. Rev.* **2017**, *117*, 13230-13319; m) R. Francke, R. D. Little, *Chem. Soc. Rev.* **2014**, *43*, 2492-2521; n) A. Jutand, *Chem. Rev.* **2008**, *108*, 2300-2347.
- [235] a) Y. Qiu, C. Zhu, M. Stangier, J. Struwe, L. Ackermann, *CCS Chem.* **2021**, *3*, 1529-1552; b) R. C. Samanta, T. H. Meyer, I. Siewert, L. Ackermann, *Chem. Sci.* **2020**, *11*, 8657-8670; c) T. H. Meyer, L. H. Finger, P. Gandeepan, L. Ackermann, *Trends Chem.* **2019**, *1*, 63-76; d) Q.-L. Yang, P. Fang, T.-S. Mei, *Chin. J. Chem.* **2018**, *36*, 338-352; e) C. Ma, P. Fang, T.-S. Mei, *ACS*

- Catal.* **2018**, *8*, 7179-7189; f) N. Sauermann, T. H. Meyer, Y. Qiu, L. Ackermann, *ACS Catal.* **2018**, *8*, 7086-7103.
- [236] a) Y. Wang, J. C. A. Oliveira, Z. Lin, L. Ackermann, *Angew. Chem. Int. Ed.* **2021**, *60*, 6419-6424; b) X. Tan, X. Hou, T. Rogge, L. Ackermann, *Angew. Chem. Int. Ed.* **2021**, *60*, 4619-4624; c) L. Yang, R. Steinbock, A. Scheremetjew, R. Kuniyil, L. H. Finger, A. M. Messinis, L. Ackermann, *Angew. Chem. Int. Ed.* **2020**, *59*, 11130-11135; d) W.-J. Kong, L. H. Finger, J. C. A. Oliveira, L. Ackermann, *Angew. Chem. Int. Ed.* **2019**, *58*, 6342-6346; e) W.-J. Kong, L. H. Finger, A. M. Messinis, R. Kuniyil, J. C. A. Oliveira, L. Ackermann, *J. Am. Chem. Soc.* **2019**, *141*, 17198-17206; f) Y. Qiu, C. Tian, L. Massignan, T. Rogge, L. Ackermann, *Angew. Chem. Int. Ed.* **2018**, *57*, 5818-5822; g) Y. Qiu, M. Stangier, T. H. Meyer, J. C. A. Oliveira, L. Ackermann, *Angew. Chem. Int. Ed.* **2018**, *57*, 14179-14183; h) Y. Qiu, W.-J. Kong, J. Struwe, N. Sauermann, T. Rogge, A. Scheremetjew, L. Ackermann, *Angew. Chem. Int. Ed.* **2018**, *57*, 5828-5832; i) R. Mei, J. Koeller, L. Ackermann, *Chem. Commun.* **2018**, *54*, 12879-12882.
- [237] a) Q.-L. Yang, H.-W. Jia, Y. Liu, Y.-K. Xing, R.-C. Ma, M.-M. Wang, G.-R. Qu, T.-S. Mei, H.-M. Guo, *Org. Lett.* **2021**, *23*, 1209-1215; b) Y.-K. Xing, X.-R. Chen, Q.-L. Yang, S.-Q. Zhang, H.-M. Guo, X. Hong, T.-S. Mei, *Nat. Commun.* **2021**, *12*, 930; c) Q.-L. Yang, Y.-K. Xing, X.-Y. Wang, H.-X. Ma, X.-J. Weng, X. Yang, H.-M. Guo, T.-S. Mei, *J. Am. Chem. Soc.* **2019**, *141*, 18970-18976; d) Z.-Q. Wang, C. Hou, Y.-F. Zhong, Y.-X. Lu, Z.-Y. Mo, Y.-M. Pan, H.-T. Tang, *Org. Lett.* **2019**, *21*, 9841-9845; e) M.-J. Luo, T.-T. Zhang, F.-J. Cai, J.-H. Li, D.-L. He, *Chem. Commun.* **2019**, *55*, 7251-7254; f) M.-J. Luo, M. Hu, R.-J. Song, D.-L. He, J.-H. Li, *Chem. Commun.* **2019**, *55*, 1124-1127; g) F. Xu, Y.-J. Li, C. Huang, H.-C. Xu, *ACS Catal.* **2018**, *8*, 3820-3824.
- [238] a) K. Naksomboon, J. Poater, F. M. Bickelhaupt, M. Á. Fernández-Ibáñez, *J. Am. Chem. Soc.* **2019**, *141*, 6719-6725; b) E. Tan, O. Quinonero, M. Elena de Orbe, A. M. Echavarren, *ACS Catal.* **2018**, *8*, 2166-2172; c) W. Ma, R. Mei, G. Tenti, L. Ackermann, *Chem. Eur. J.* **2014**, *20*, 15248-15251.
- [239] a) K. Hirano, M. Miura, *Chem. Lett.* **2015**, *44*, 868-873; b) A. E. Wendlandt, A. M. Suess, S. S. Stahl, *Angew. Chem. Int. Ed.* **2011**, *50*, 11062-11087.

- [240] T. Yoshizumi, H. Tsurugi, T. Satoh, M. Miura, *Tetrahedron Lett.* **2008**, *49*, 1598-1600.
- [241] a) L. Marzo, S. K. Pagire, O. Reiser, B. König, *Angew. Chem. Int. Ed.* **2018**, *57*, 10034-10072; b) K. L. Skubi, T. R. Blum, T. P. Yoon, *Chem. Rev.* **2016**, *116*, 10035-10074; c) O. Reiser, *Acc. Chem. Res.* **2016**, *49*, 1990-1996; d) D. C. Miller, K. T. Tarantino, R. R. Knowles, *Top. Curr. Chem.* **2016**, *374*, 30; e) M. D. Kärkäs, J. A. Porco, C. R. J. Stephenson, *Chem. Rev.* **2016**, *116*, 9683-9747; f) I. Ghosh, L. Marzo, A. Das, R. Shaikh, B. König, *Acc. Chem. Res.* **2016**, *49*, 1566-1577; g) D. C. Fabry, M. Rueping, *Acc. Chem. Res.* **2016**, *49*, 1969-1979; h) R. Brimiouille, D. Lenhart, M. M. Maturi, T. Bach, *Angew. Chem. Int. Ed.* **2015**, *54*, 3872-3890; i) S. Paria, O. Reiser, *ChemCatChem* **2014**, *6*, 2477-2483; j) D. Ravelli, M. Fagnoni, A. Albini, *Chem. Soc. Rev.* **2013**, *42*, 97-113; k) C. K. Prier, D. A. Rankic, D. W. C. MacMillan, *Chem. Rev.* **2013**, *113*, 5322-5363.
- [242] a) J. He, C. Chen, G. C. Fu, J. C. Peters, *ACS Catal.* **2018**, *8*, 11741-11748; b) G. J. Choi, Q. Zhu, D. C. Miller, C. J. Gu, R. R. Knowles, *Nature* **2016**, *539*, 268-271; c) T. R. Blum, Z. D. Miller, D. M. Bates, I. A. Guzei, T. P. Yoon, *Science* **2016**, *354*, 1391-1395; d) T. S. Ratani, S. Bachman, G. C. Fu, J. C. Peters, *J. Am. Chem. Soc.* **2015**, *137*, 13902-13907; e) D. B. Bagal, G. Kachkovskiy, M. Knorn, T. Rawner, B. M. Bhanage, O. Reiser, *Angew. Chem. Int. Ed.* **2015**, *54*, 6999-7002; f) J. Du, K. L. Skubi, D. M. Schultz, T. P. Yoon, *Science* **2014**, *344*, 392-396; g) D. P. Hari, B. König, *Angew. Chem. Int. Ed.* **2013**, *52*, 4734-4743; h) J. D. Nguyen, E. M. D'Amato, J. M. R. Narayanam, C. R. J. Stephenson, *Nat. Chem.* **2012**, *4*, 854; i) D. P. Hari, P. Schroll, B. König, *J. Am. Chem. Soc.* **2012**, *134*, 2958-2961.
- [243] a) W. Zhao, R. P. Wurz, J. C. Peters, G. C. Fu, *J. Am. Chem. Soc.* **2017**, *139*, 12153-12156; b) C. D. Matier, J. Schwaben, J. C. Peters, G. C. Fu, *J. Am. Chem. Soc.* **2017**, *139*, 17707-17710; c) J. M. Ahn, T. S. Ratani, K. I. Hannoun, G. C. Fu, J. C. Peters, *J. Am. Chem. Soc.* **2017**, *139*, 12716-12723; d) Q. M. Kainz, C. D. Matier, A. Bartoszewicz, S. L. Zultanski, J. C. Peters, G. C. Fu, *Science* **2016**, *351*, 681-684; e) S. E. Creutz, K. J. Lotito, G. C. Fu, J. C. Peters, *Science* **2012**, *338*, 647-651.
- [244] Y. Liang, X. Zhang, D. W. C. MacMillan, *Nature* **2018**, *559*, 83-88.
- [245] W.-J. Yoo, T. Tsukamoto, S. Kobayashi, *Org. Lett.* **2015**, *17*, 3640-3642.

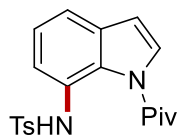
- [246] a) D. C. Fabry, M. A. Ronge, J. Zoller, M. Rueping, *Angew. Chem. Int. Ed.* **2015**, *54*, 2801-2805; b) J. Zoller, D. C. Fabry, M. A. Ronge, M. Rueping, *Angew. Chem. Int. Ed.* **2014**, *53*, 13264-13268; c) D. C. Fabry, J. Zoller, S. Raja, M. Rueping, *Angew. Chem. Int. Ed.* **2014**, *53*, 10228-10231; d) D. Kalyani, K. B. McMurtrey, S. R. Neufeldt, M. S. Sanford, *J. Am. Chem. Soc.* **2011**, *133*, 18566-18569.
- [247] P. Gandeepan, J. Mo, L. Ackermann, *Chem. Commun.* **2017**, *53*, 5906-5909.
- [248] a) C. Xie, W. Sun, H. Lu, A. Kretzschmann, J. Liu, M. Wagner, H.-J. Butt, X. Deng, S. Wu, *Nat. Commun.* **2018**, *9*, 3842; b) D. Rackl, C.-J. Yoo, C. W. Jones, H. M. L. Davies, *Org. Lett.* **2017**, *19*, 3055-3058; c) M. Opanasenko, P. Štěpnička, J. Čejka, *RSC Adv.* **2014**, *4*, 65137-65162; d) S. Shylesh, W. R. Thiel, *ChemCatChem* **2011**, *3*, 278-287; e) E. L. Margelefsky, R. K. Zeidan, M. E. Davis, *Chem. Soc. Rev.* **2008**, *37*, 1118-1126; f) F.-X. Felpin, E. Fouquet, *ChemSusChem* **2008**, *1*, 718-724; g) C. T. Kresge, M. E. Leonowicz, W. J. Roth, J. C. Vartuli, J. S. Beck, *Nature* **1992**, *359*, 710-712; h) J. S. Beck, J. C. Vartuli, W. J. Roth, M. E. Leonowicz, C. T. Kresge, K. D. Schmitt, C. T. W. Chu, D. H. Olson, E. W. Sheppard, S. B. McCullen, J. B. Higgins, J. L. Schlenker, *J. Am. Chem. Soc.* **1992**, *114*, 10834-10843.
- [249] a) F. Wu, Y. Feng, C. W. Jones, *ACS Catal.* **2014**, *4*, 1365-1375; b) Y. Feng, E. G. Moschetta, C. W. Jones, *Chem. Asian J.* **2014**, *9*, 3142-3152.
- [250] a) S. Kawamorita, R. Murakami, T. Iwai, M. Sawamura, *J. Am. Chem. Soc.* **2013**, *135*, 2947-2950; b) S. Kawamorita, T. Miyazaki, T. Iwai, H. Ohmiya, M. Sawamura, *J. Am. Chem. Soc.* **2012**, *134*, 12924-12927; c) S. Kawamorita, H. Ohmiya, T. Iwai, M. Sawamura, *Angew. Chem. Int. Ed.* **2011**, *50*, 8363-8366; d) S. Kawamorita, H. Ohmiya, M. Sawamura, *J. Org. Chem.* **2010**, *75*, 3855-3858; e) S. Kawamorita, H. Ohmiya, K. Hara, A. Fukuoka, M. Sawamura, *J. Am. Chem. Soc.* **2009**, *131*, 5058-5059.
- [251] K. Korvorapun, R. Kuniyil, L. Ackermann, *ACS Catal.* **2020**, *10*, 435-440.
- [252] C. J. Teskey, A. Y. W. Lui, M. F. Greaney, *Angew. Chem. Int. Ed.* **2015**, *54*, 11677-11680.
- [253] a) G. Li, C. Jia, X. Cai, L. Zhong, L. Zou, X. Cui, *Chem. Commun.* **2020**, *56*, 293-296; b) B. Li, S.-L. Fang, D.-Y. Huang, B.-F. Shi, *Org. Lett.* **2017**, *19*, 3950-3953; c) Z. Fan, J. Li, H. Lu, D.-Y. Wang, C. Wang, M. Uchiyama, A. Zhang, *Org. Lett.* **2017**, *19*, 3199-3202.

- [254] P. Gandeepan, N. Kaplaneris, S. Santoro, L. Vaccaro, L. Ackermann, *ACS Sustain. Chem. Eng.* **2019**, *7*, 8023-8040.
- [255] M. D. Hill, *Chem. Eur. J.* **2010**, *16*, 12052-12062.
- [256] a) R. Alam, M. A. Alam, A. K. Panda, Rahisuddin, *J. Heterocycl. Chem.* **2017**, *54*, 1812-1821; b) N. C. Desai, D. D. Pandya, V. V. Joshi, K. M. Rajpara, H. V. Vaghani, H. M. Satodiya, *Med. Chem. Res.* **2012**, *21*, 4463-4472; c) Y. Xia, C.-D. Fan, B.-X. Zhao, J. Zhao, D.-S. Shin, J.-Y. Miao, *Eur. J. Med. Chem.* **2008**, *43*, 2347-2353.
- [257] Y. Nakao, *Synthesis* **2011**, *2011*, 3209-3219.
- [258] a) Y. Hu, B. Zhou, C. Wang, *Acc. Chem. Res.* **2018**, *51*, 816-827; b) R. Cano, K. Mackey, G. P. McGlacken, *Catal. Sci. Technol.* **2018**, *8*, 1251-1266.
- [259] a) S. Sueki, Z. Wang, Y. Kuninobu, *Org. Lett.* **2016**, *18*, 304-307; b) Y. Kuninobu, Y. Nishina, T. Takeuchi, K. Takai, *Angew. Chem. Int. Ed.* **2007**, *46*, 6518-6520.
- [260] a) B. Zhou, Y. Hu, T. Liu, C. Wang, *Nat. Commun.* **2017**, *8*, 1169; b) B. Zhou, Y. Hu, C. Wang, *Angew. Chem. Int. Ed.* **2015**, *54*, 13659-13663.
- [261] a) N. Kaplaneris, J. Son, L. Mendive-Tapia, A. Kopp, N. D. Barth, I. Maksso, M. Vendrell, L. Ackermann, *Nat. Commun.* **2021**, *12*, 3389; b) N. Kaplaneris, F. Kaltenhäuser, G. Sirvinskaite, S. Fan, T. De Oliveira, L.-C. Conradi, L. Ackermann, *Sci. Adv.* **2021**, *7*, eabe6202; c) H. Wang, N. Kaplaneris, L. Ackermann, *Cell Rep. Phys. Sci.* **2020**, *1*, 100178; d) N. Kaplaneris, T. Rogge, R. Yin, H. Wang, G. Sirvinskaite, L. Ackermann, *Angew. Chem. Int. Ed.* **2019**, *58*, 3476-3480; e) H. Wang, I. Choi, T. Rogge, N. Kaplaneris, L. Ackermann, *Nat. Catal.* **2018**, *1*, 993-1001.
- [262] C. Wang, B. Maity, L. Cavallo, M. Rueping, *Org. Lett.* **2018**, *20*, 3105-3108.
- [263] a) D. Aynedinova, M. C. Callens, H. B. Hicks, C. Y. X. Poh, B. D. A. Shennan, A. M. Boyd, Z. H. Lim, J. A. Leitch, D. J. Dixon, *Chem. Soc. Rev.* **2021**; b) S. D. Friis, M. J. Johansson, L. Ackermann, *Nat. Chem.* **2020**, *12*, 511-519.
- [264] H. E. Gottlieb, V. Kotlyar, A. Nudelman, *J. Org. Chem.* **1997**, *62*, 7512-7515.
- [265] L. Xu, C. Zhang, Y. He, L. Tan, D. Ma, *Angew. Chem. Int. Ed.* **2016**, *55*, 321-325.
- [266] A. Bechtoldt, M. E. Baumert, L. Vaccaro, L. Ackermann, *Green Chem.* **2018**, *20*, 398-402.
- [267] S. W. Youn, H. J. Yoo, *Adv. Synth. Catal.* **2017**, *359*, 2176-2183.

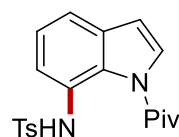
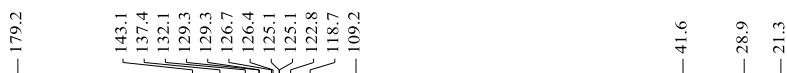
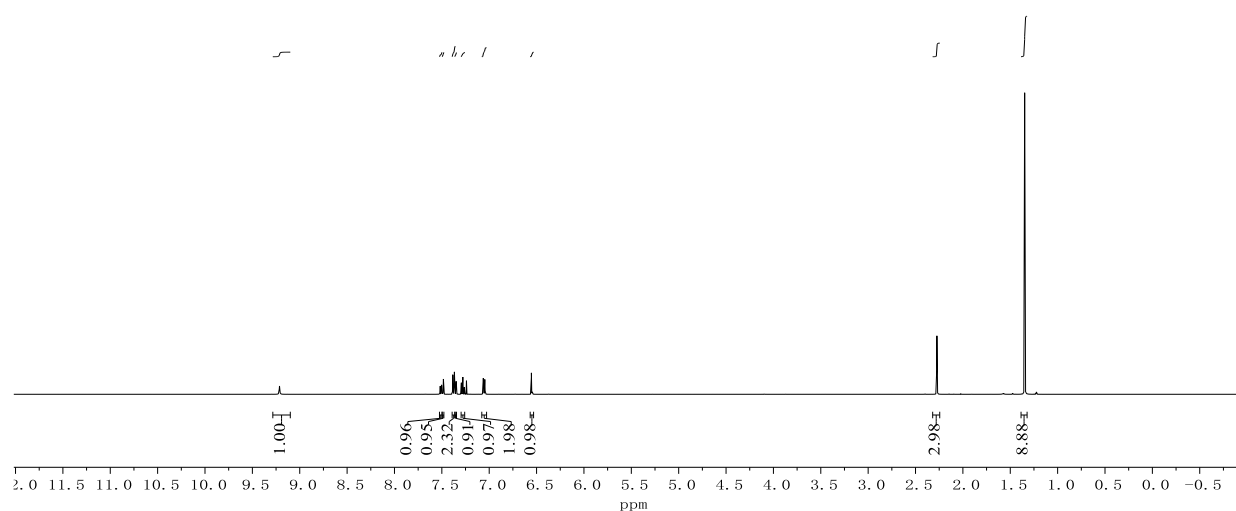


- [268] J. R. Bolton, M. I. Stefan, P.-S. Shaw, K. R. Lykke, *J. Photochem. Photobiol. A* **2011**, *222*, 166-169.
- [269] M. C. Biesinger, L. W. M. Lau, A. R. Gerson, R. S. C. Smart, *Appl. Surf. Sci.* **2010**, *257*, 887-898.
- [270] J. Cr epelli ere, P. L. Popa, N. Bahlawane, R. Leturcq, F. Werner, S. Siebentritt, D. Lenoble, J. *Mater. Chem. C* **2016**, *4*, 4278-4287
- [271] J. Liu, Q. Gui, Z. Yang, Z. Tan, R. Guo, J.-C. Shi, *Synthesis*, **2013**, *45*, 943-951.
- [272] S. K. Alla, P. Sadhu, T. Punniyamurthy, *J. Org. Chem.* **2014**, *79*, 7502-7511.
- [273] D. Yang, K. Yan, W. Wei, L. Tian, Y. Shuai, R. Li, J. You, H. Wang, *Asian J. Org. Chem.* **2014**, *3*, 969-973.
- [274] K. Gopalaiah, S. N. Chandrudua, *RSC Adv.* **2015**, *5*, 5015-5023.
- [275] G. Naresh, R. Kant, T. Narender, *J. Org. Chem.* **2014**, *79*, 3821-3829.
- [276] L. Yang, J. Yuan, P. Mao, Q. Guoa, *RSC Adv.* **2015**, *5*, 107601-107607.
- [277] P. H. Tran, A.-H. T. Hanga, *RSC Adv.* **2018**, *8*, 11127-11133.
- [278] M. J. Iglesias, A. Prieto, M. C. Nicasio, *Org. Lett.* **2012**, *14*, 4318-4321.
- [279] B. Liu, Z. Wang, N. Wu, M. Li, J. You, J. Lan, *Chem, Eur. J.* **2012**, *18*, 1599-1603.
- [280] X. Li, C. Li, B. Yin, C. Li, P. Liu, J. Li, Z. Shi, *Chem. Asian J.* **2013**, *8*, 1408-1411.
- [281] S. Ray, P. Das, B. Banerjee, A. Bhaumikb, C. Mukhopadhyay, *RSC Adv.* **2015**, *5*, 72745-72754.
- [282] Z.-S. Gu, W.-W. Chen, L.-X. Shao, *J. Org. Chem.* **2014**, *79*, 5806-5811.
- [283] W. Zhang, Q. Zeng, X. Zhang, Y. Tian, Y. Yue, Y. Guo, Z. Wang, *J. Org. Chem.* **2011**, *76*, 4741-4745.
- [284] A. J. Paterson, C. J. Heron, C. L. McMullin, M. F. Mahon, N. J. Press, C. G. Frost, *Org. Biomol. Chem.* **2017**, *15*, 5993-6000.
- [285] H. Xie, Z. Ye, Z. Ke, J. Lan, H. Jiang, W. Zeng, *Chem. Sci.* **2018**, *9*, 985-989.
- [286] Z. Shen, H. Huang, C. Zhu, S. Warratz, L. Ackermann, *Org. Lett.* **2019**, *21*, 571-574.
- [287] G. Sheldrick, *Acta Crystallographica Section A* **2015**, *71*, 3-8.

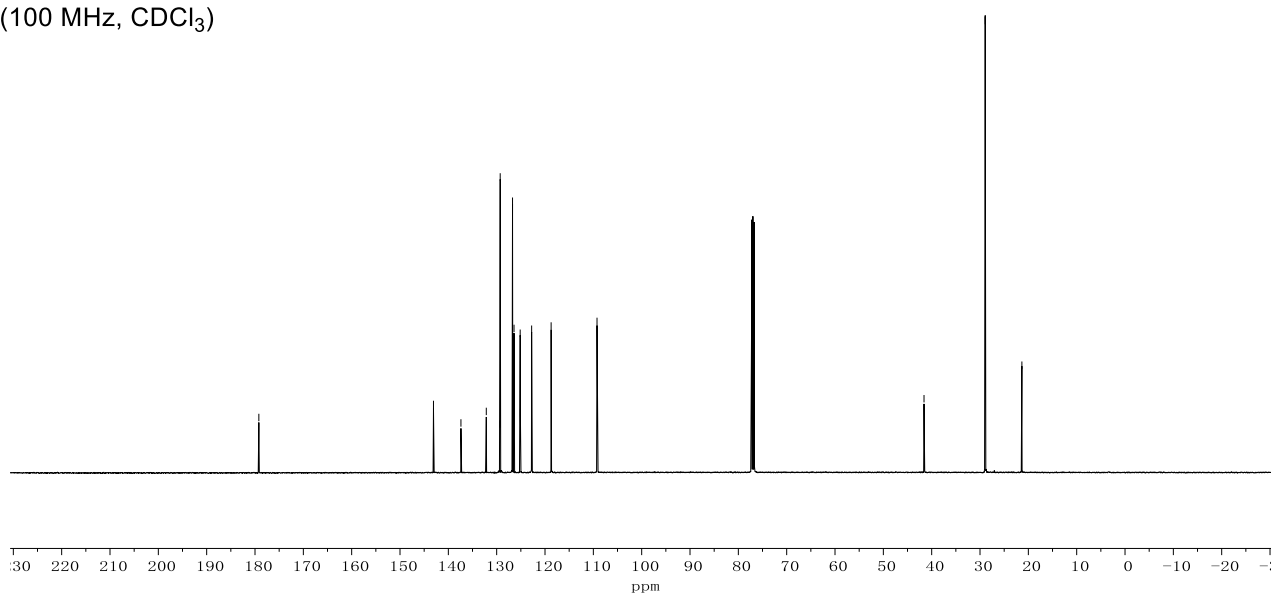
## 7. Appendix: NMR Spectra



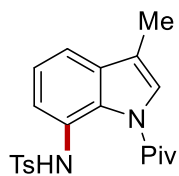
**392a**  
(400 MHz, CDCl<sub>3</sub>)



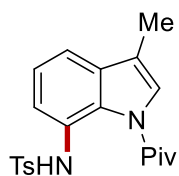
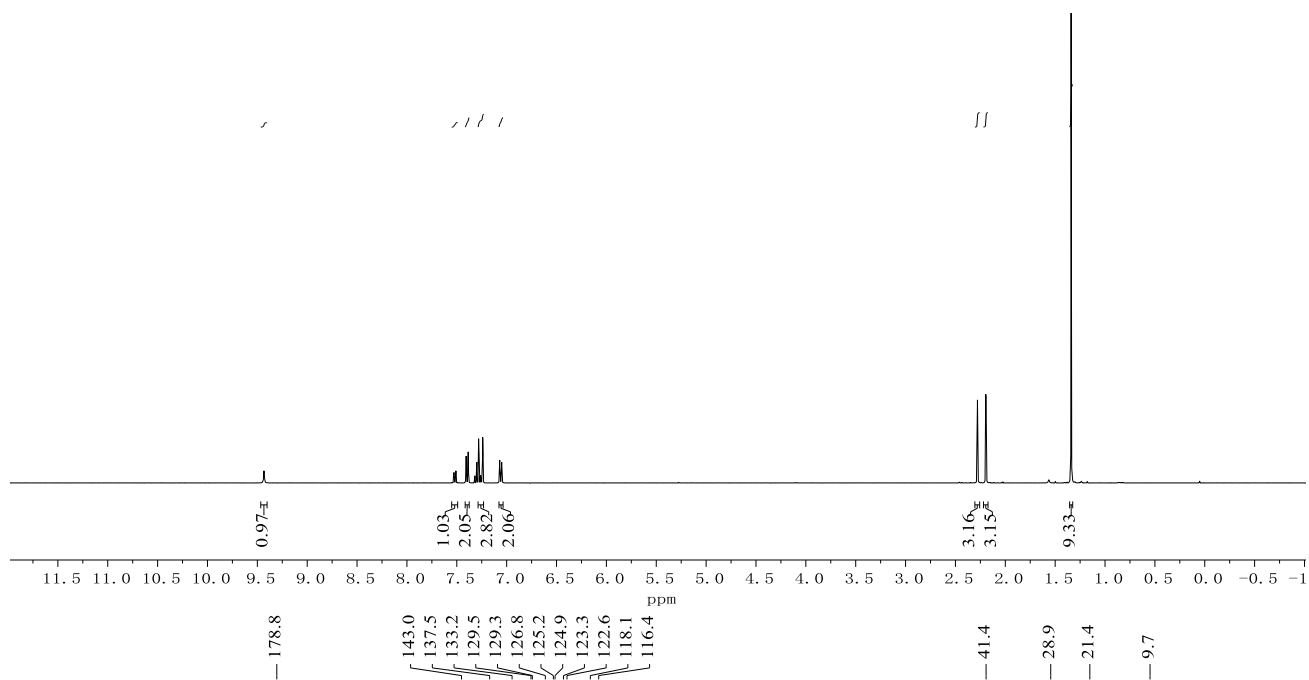
**392a**  
(100 MHz, CDCl<sub>3</sub>)



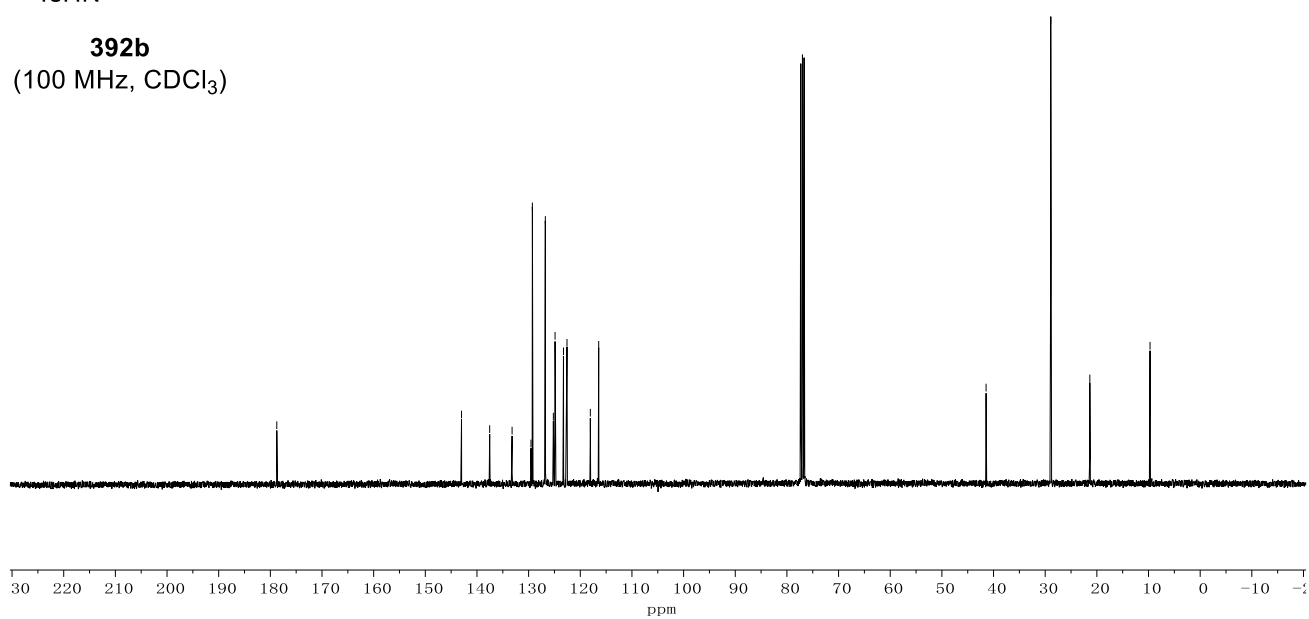
Appendix: NMR Spectra



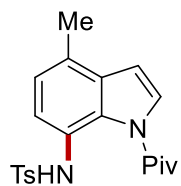
**392b**  
(400 MHz, CDCl<sub>3</sub>)



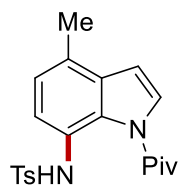
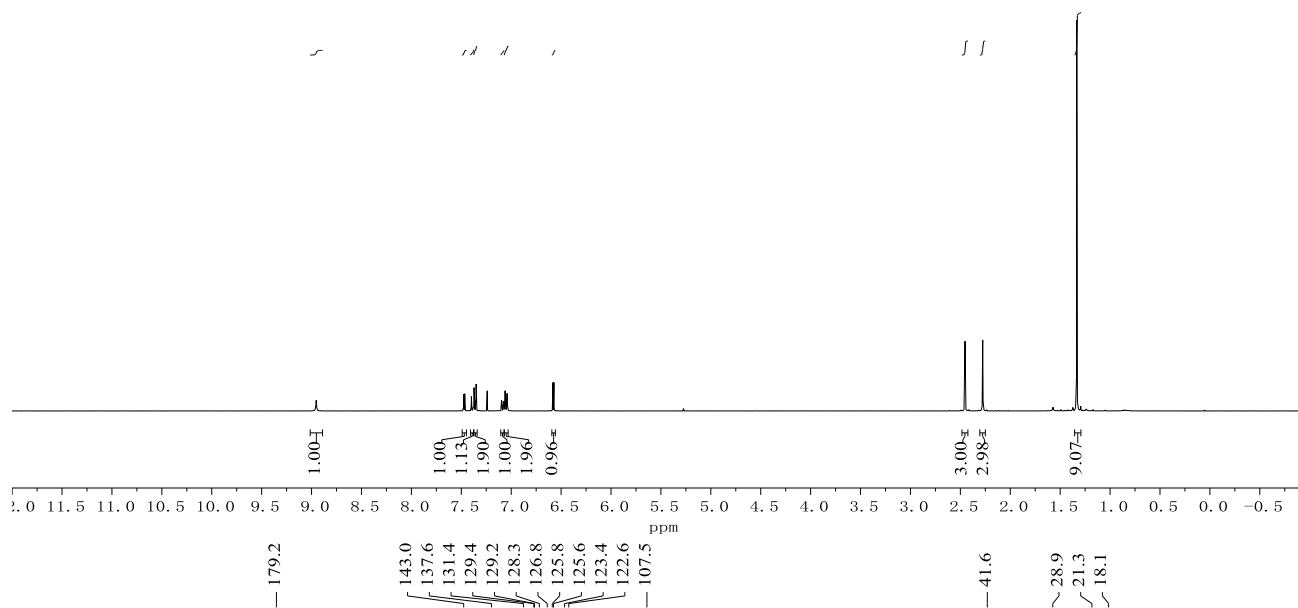
**392b**  
(100 MHz, CDCl<sub>3</sub>)



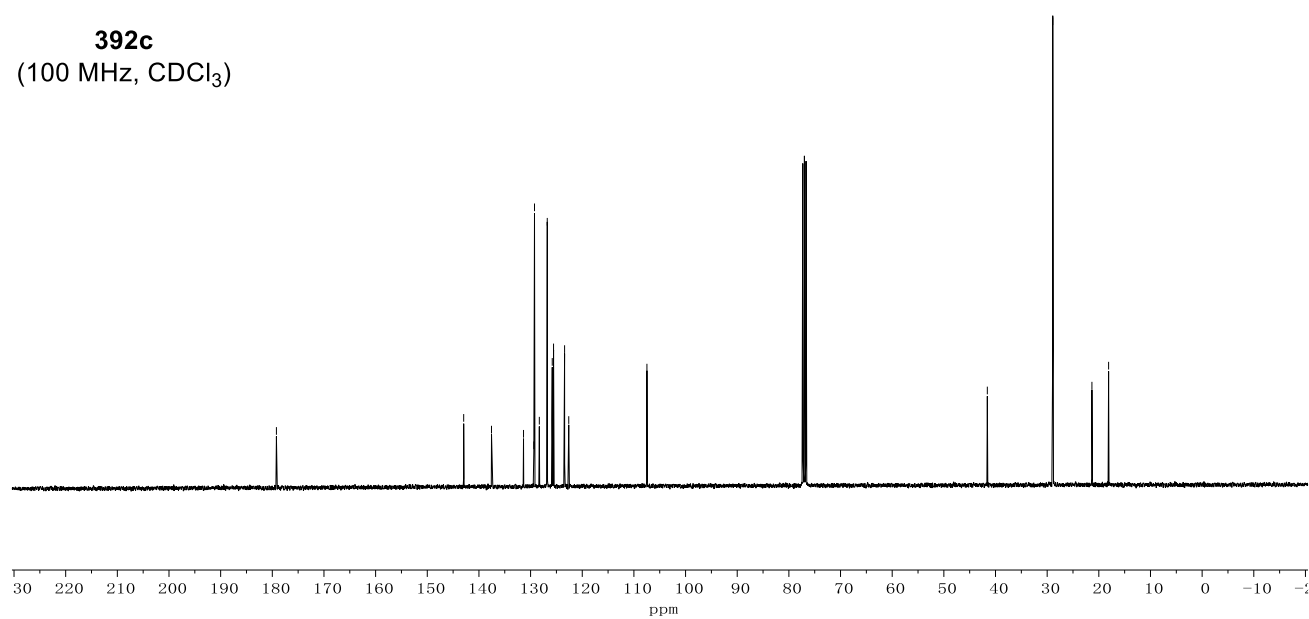
Appendix: NMR Spectra



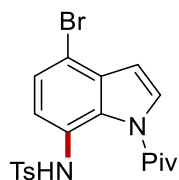
**392c**  
(400 MHz, CDCl<sub>3</sub>)



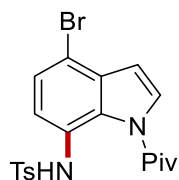
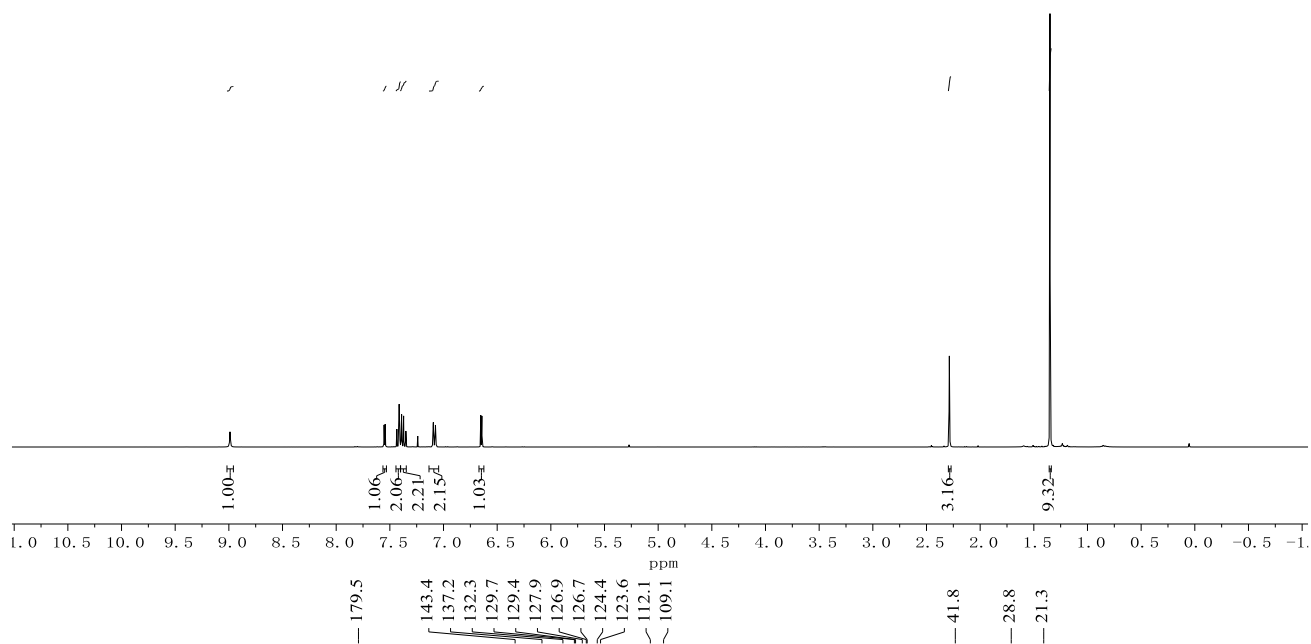
**392c**  
(100 MHz, CDCl<sub>3</sub>)



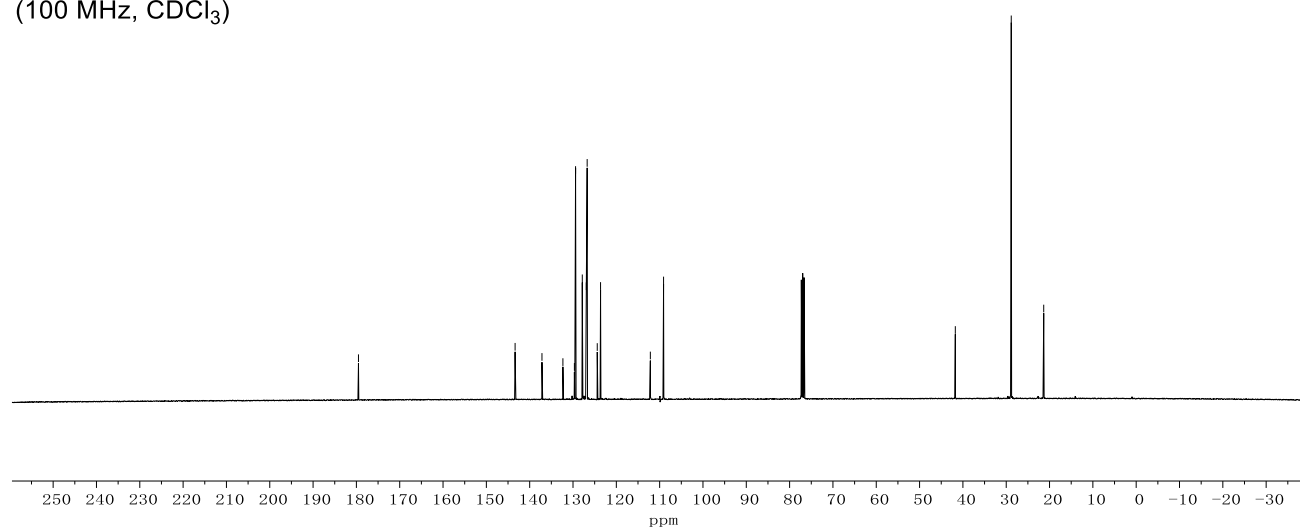
Appendix: NMR Spectra



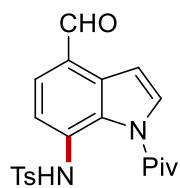
**392d**  
(400 MHz, CDCl<sub>3</sub>)



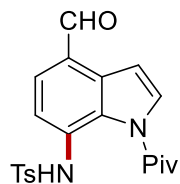
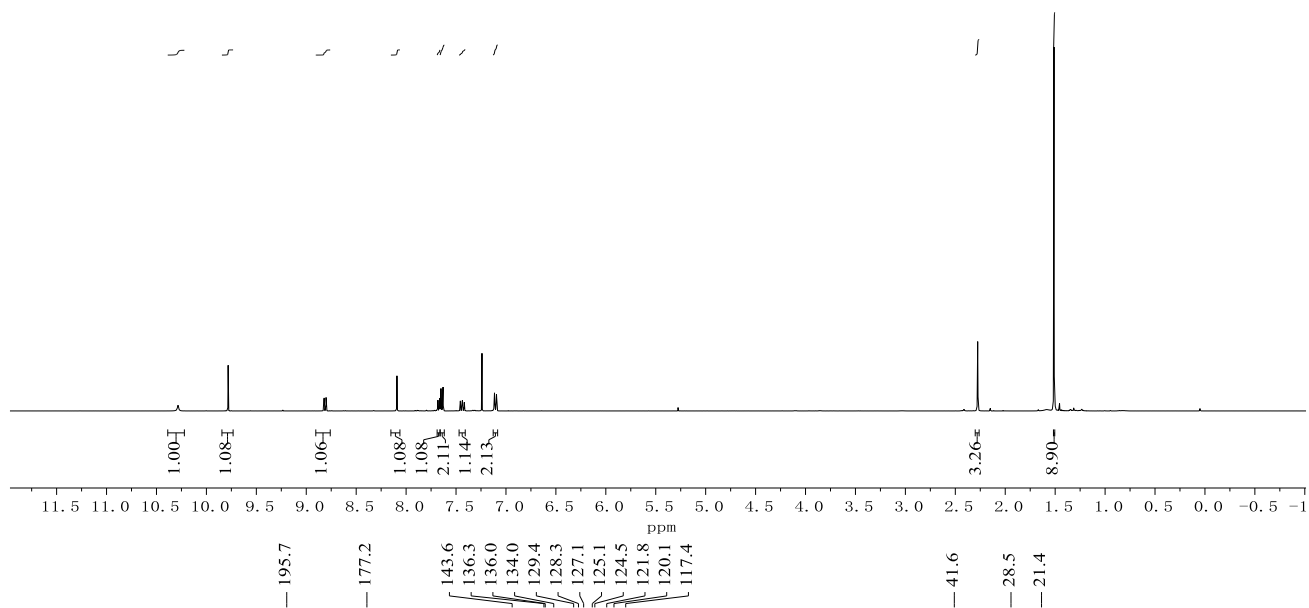
**392d**  
(100 MHz, CDCl<sub>3</sub>)



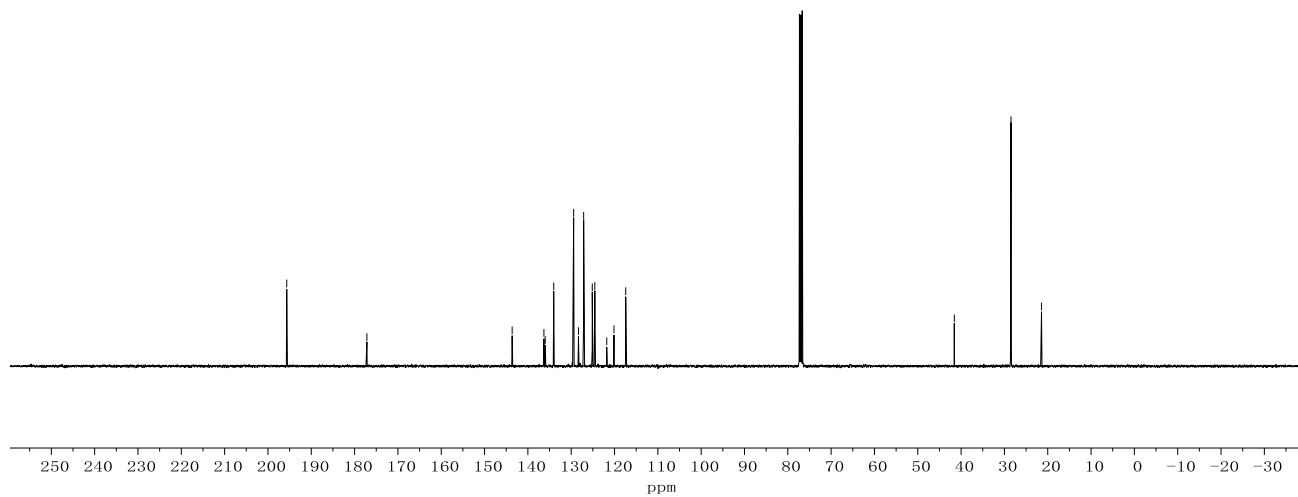
Appendix: NMR Spectra



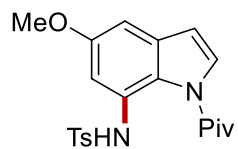
**392e**  
(400 MHz, CDCl<sub>3</sub>)



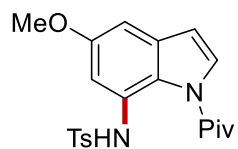
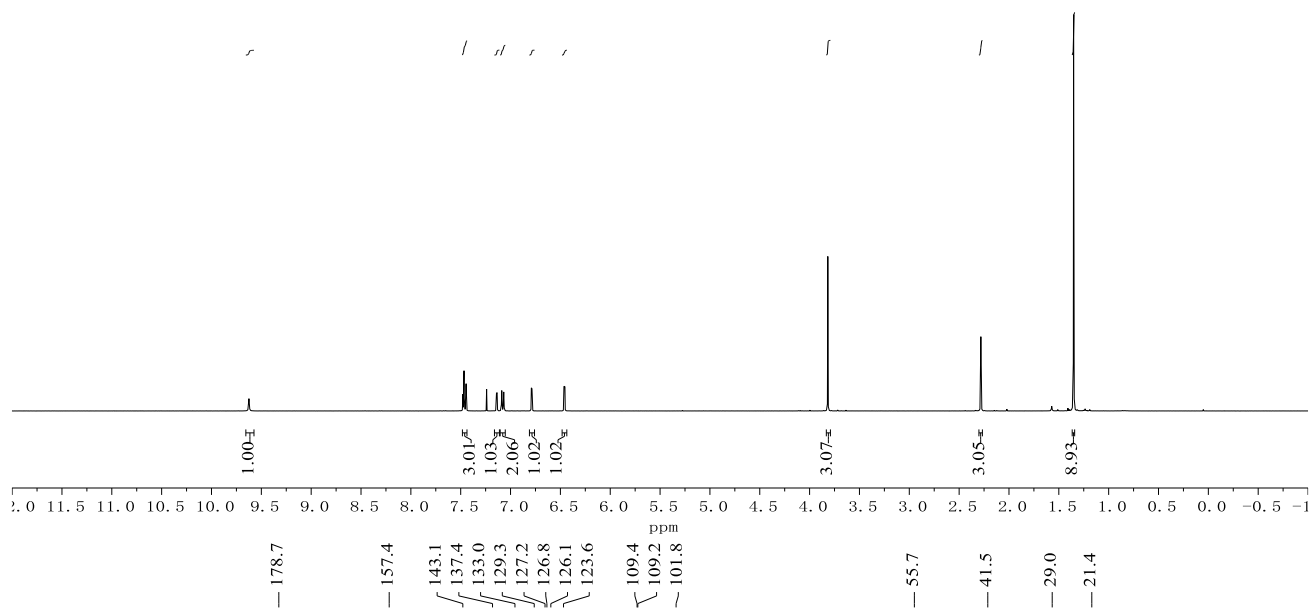
**392e**  
(100 MHz, CDCl<sub>3</sub>)



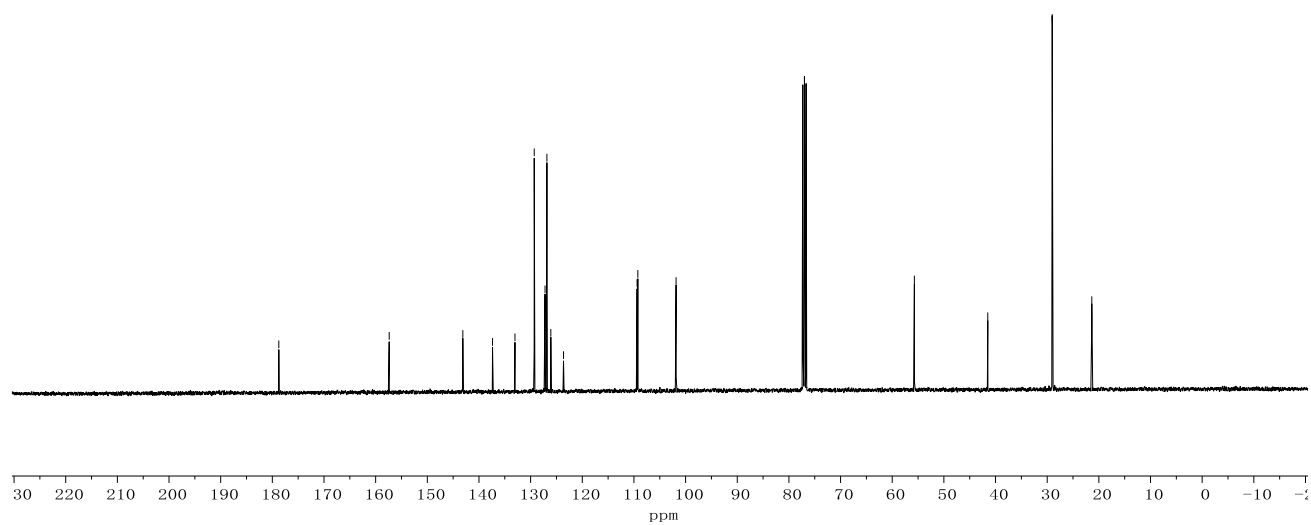
Appendix: NMR Spectra



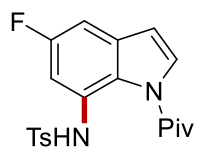
**392f**  
(400 MHz, CDCl<sub>3</sub>)



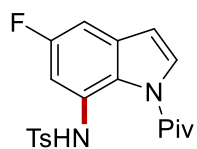
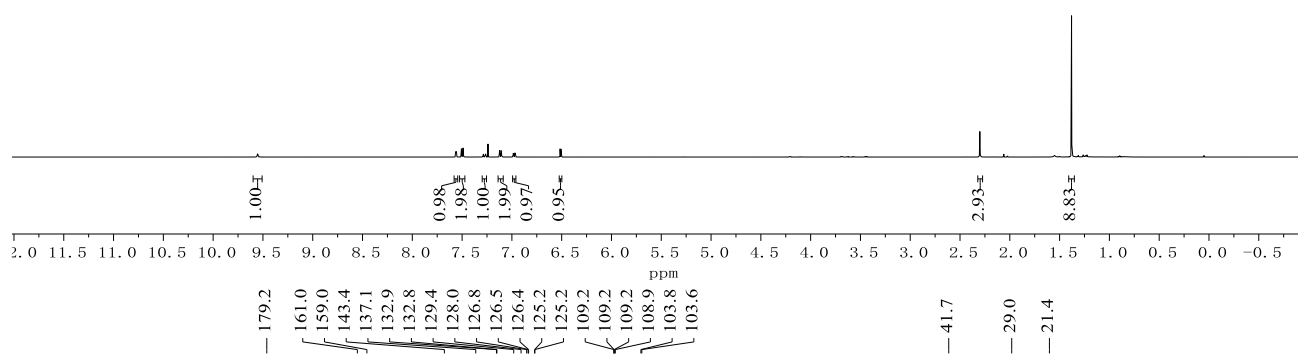
**392f**  
(100 MHz, CDCl<sub>3</sub>)



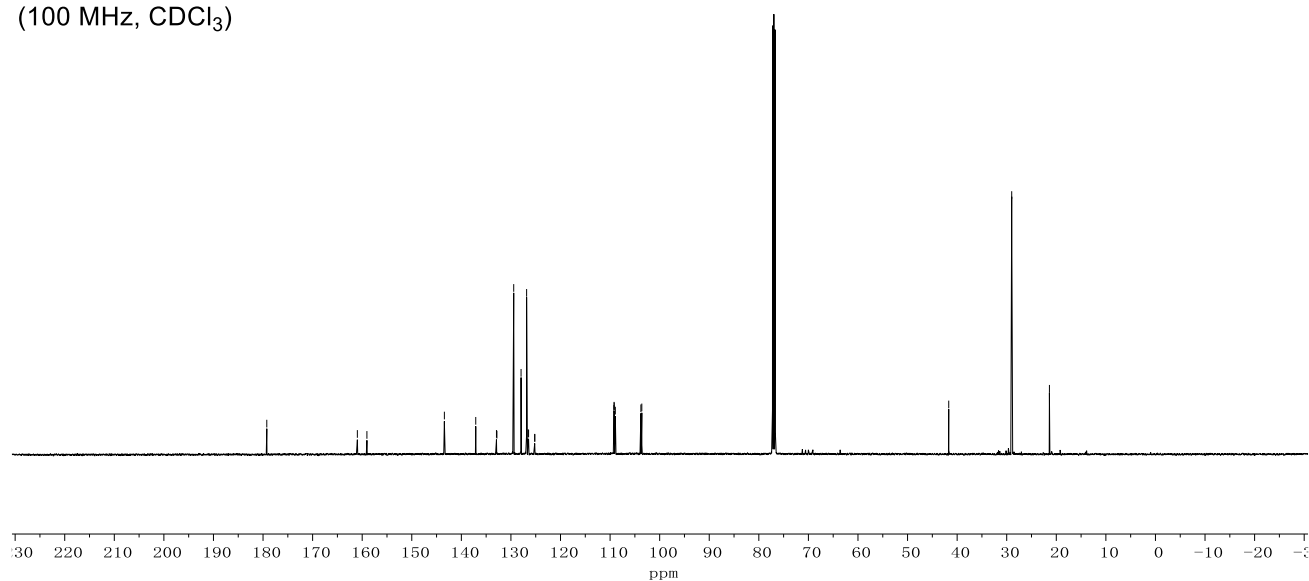
Appendix: NMR Spectra



**392g**  
(400 MHz, CDCl<sub>3</sub>)

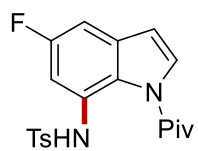


**392g**  
(100 MHz, CDCl<sub>3</sub>)



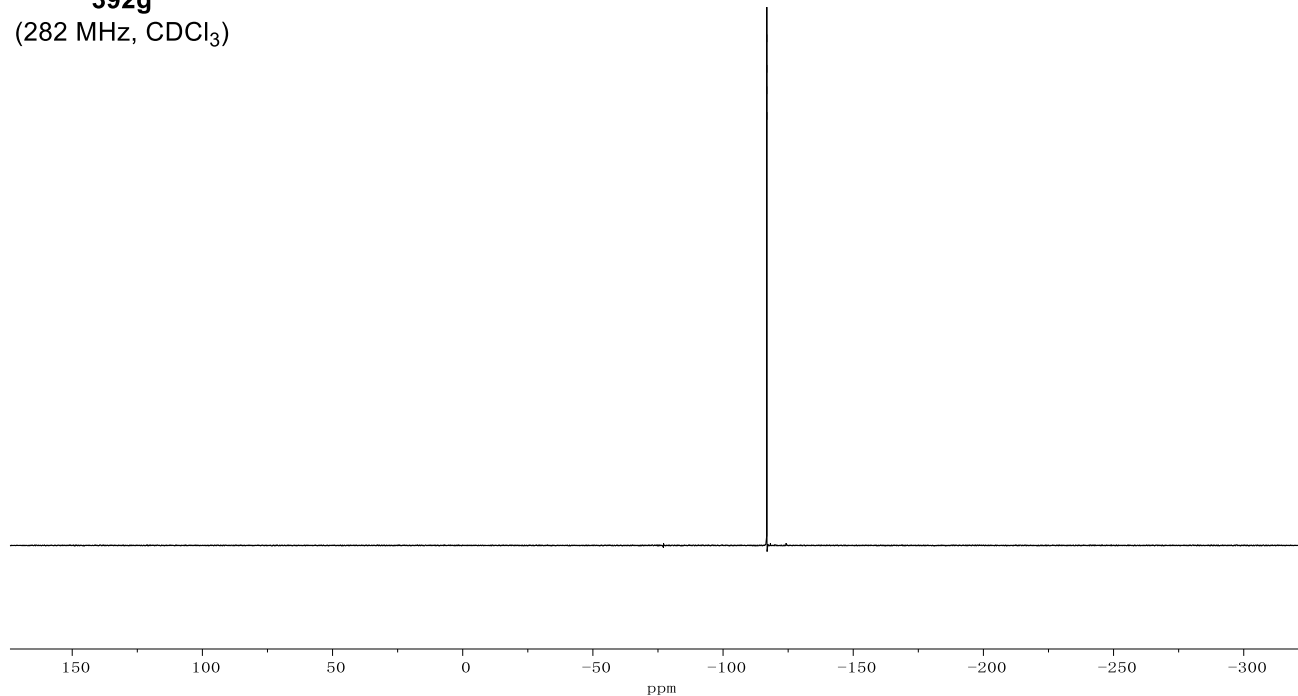


Appendix: NMR Sepctra

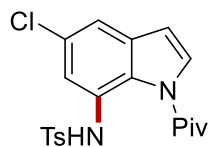


-116.8  
-116.8  
-116.8  
-116.8

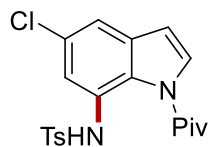
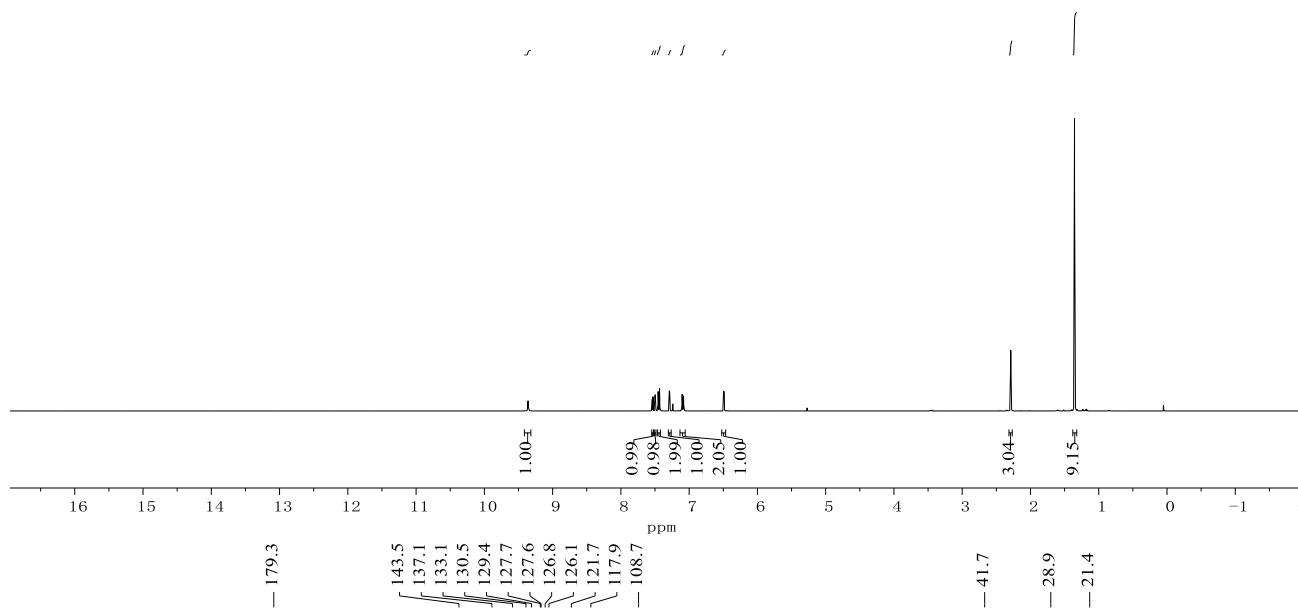
**392g**  
(282 MHz, CDCl<sub>3</sub>)



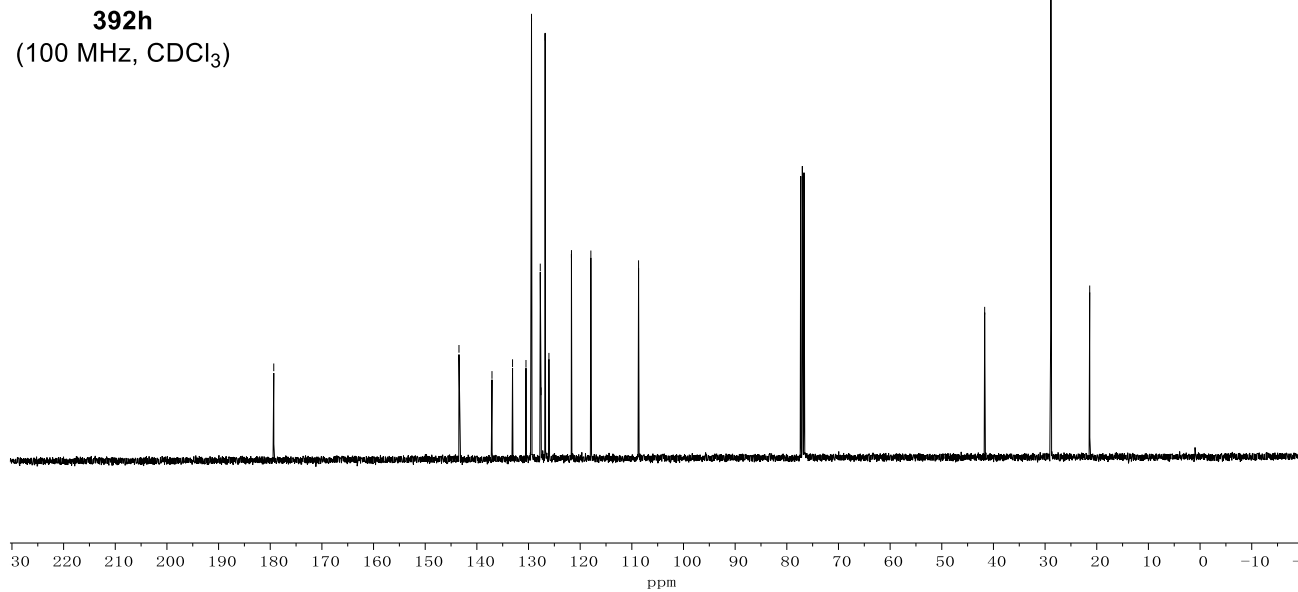
Appendix: NMR Spectra



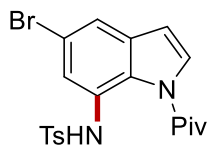
**392h**  
(400 MHz, CDCl<sub>3</sub>)



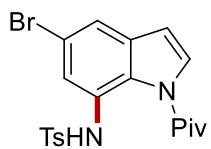
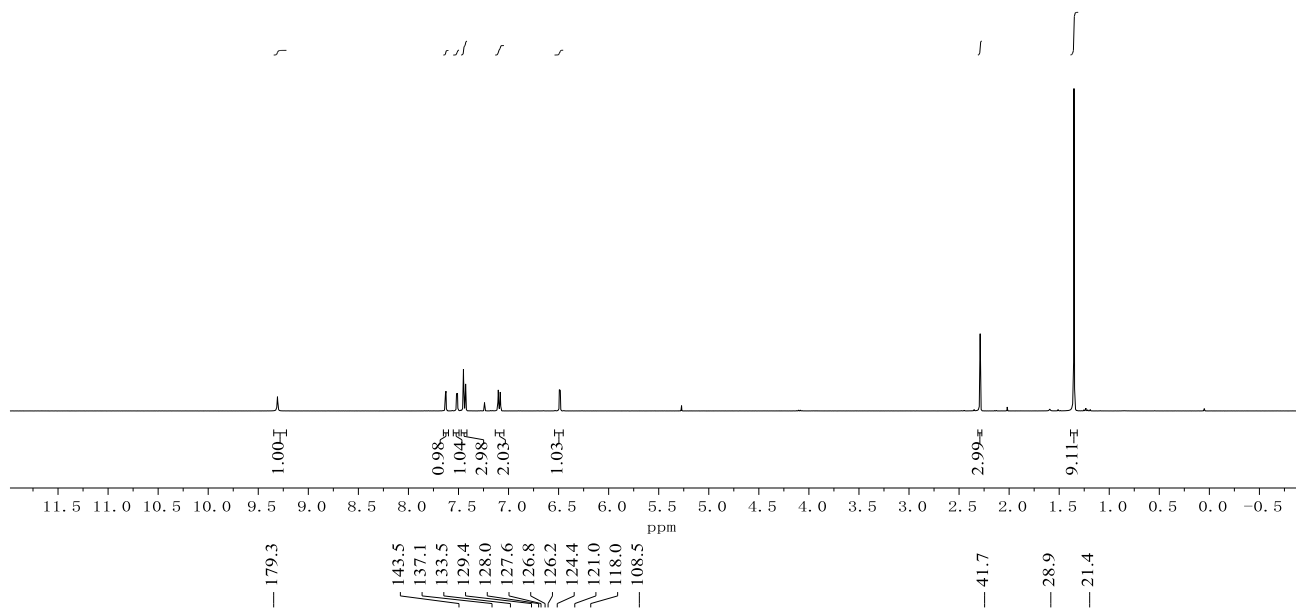
**392h**  
(100 MHz, CDCl<sub>3</sub>)



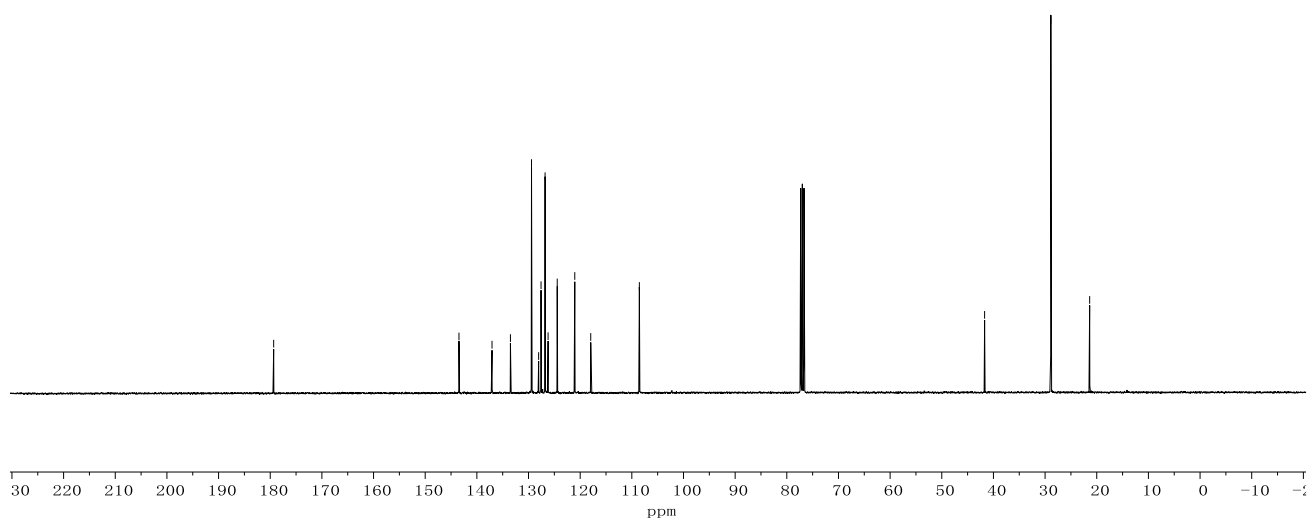
Appendix: NMR Spectra



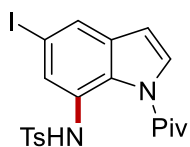
**392i**  
(400 MHz, CDCl<sub>3</sub>)



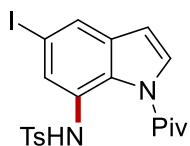
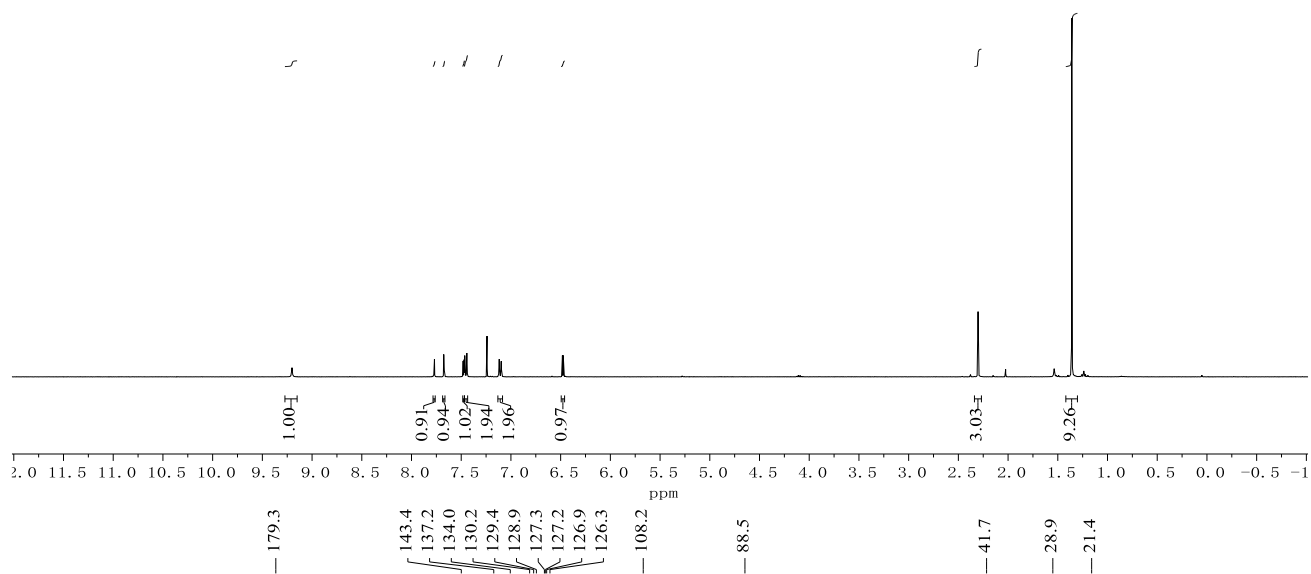
**392i**  
(100 MHz, CDCl<sub>3</sub>)



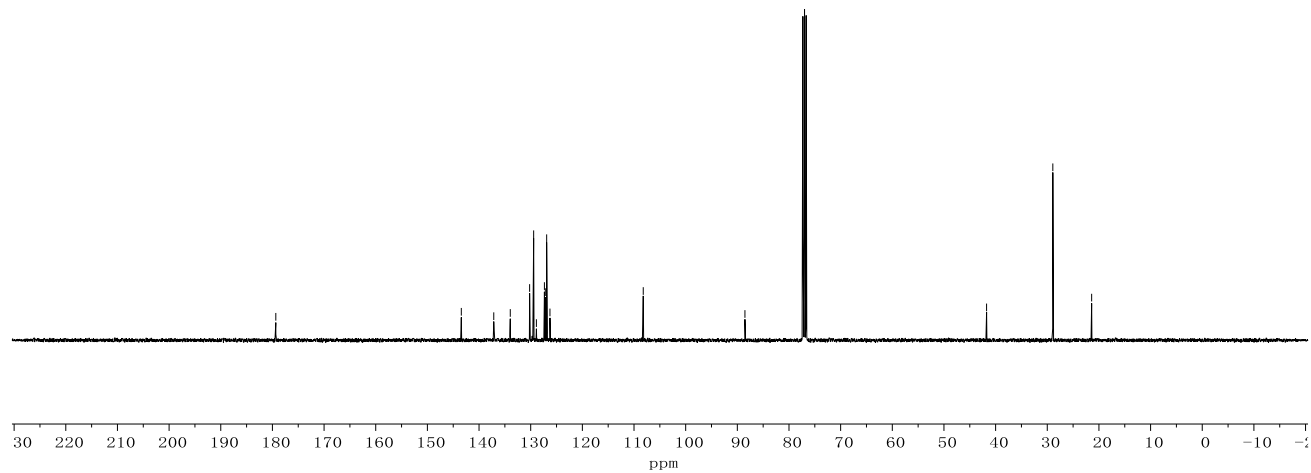
Appendix: NMR Spectra



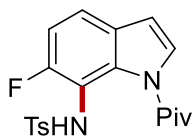
**392j**  
(400 MHz, CDCl<sub>3</sub>)



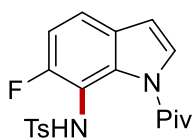
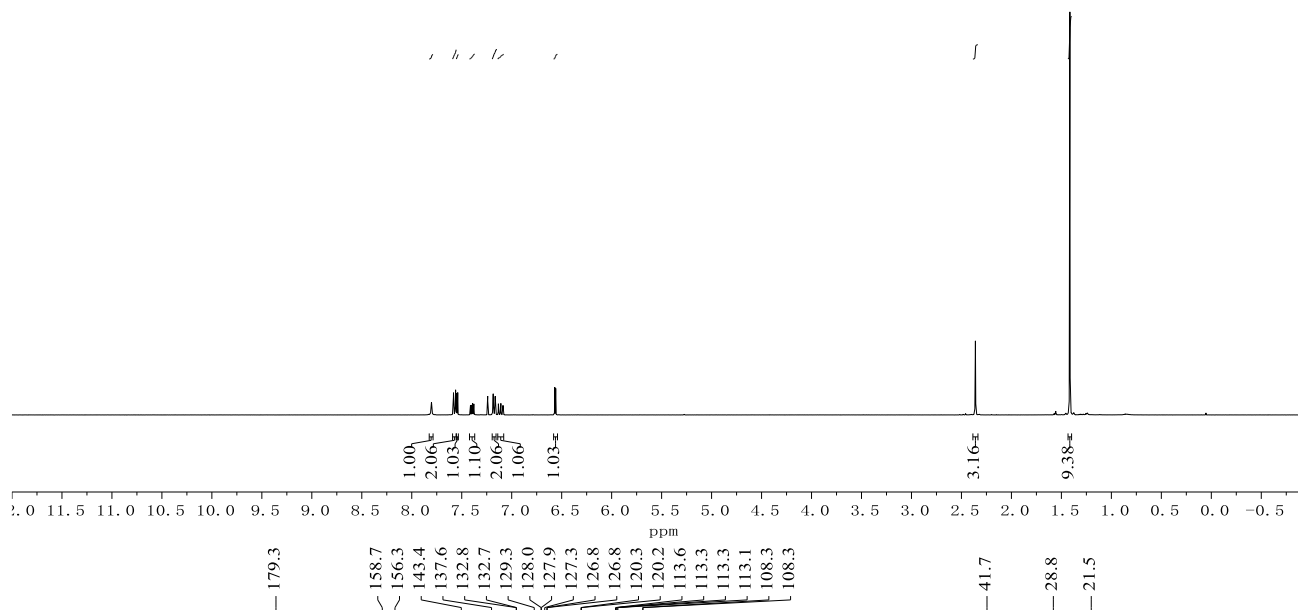
**392j**  
(100 MHz, CDCl<sub>3</sub>)



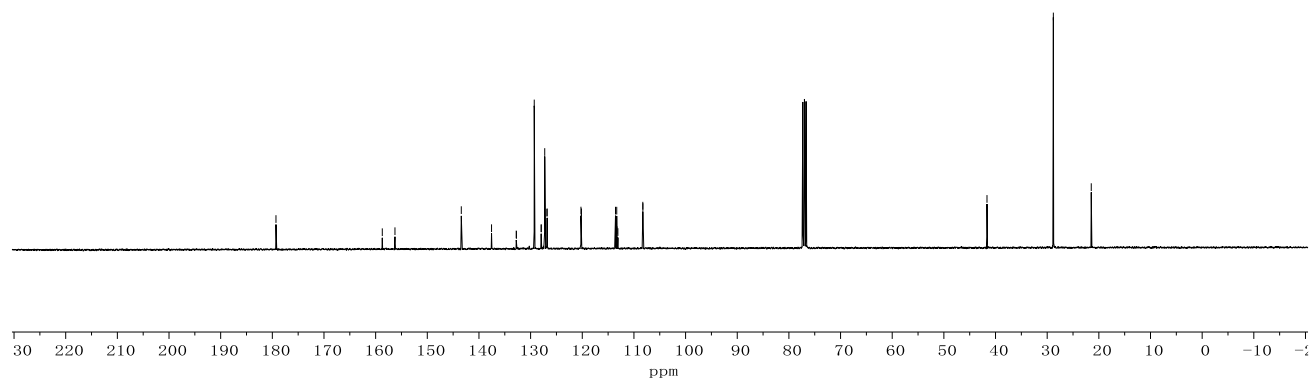
Appendix: NMR Spectra



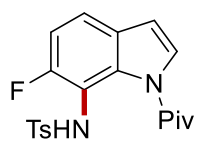
**392k**  
(400 MHz, CDCl<sub>3</sub>)



**392k**  
(100 MHz, CDCl<sub>3</sub>)

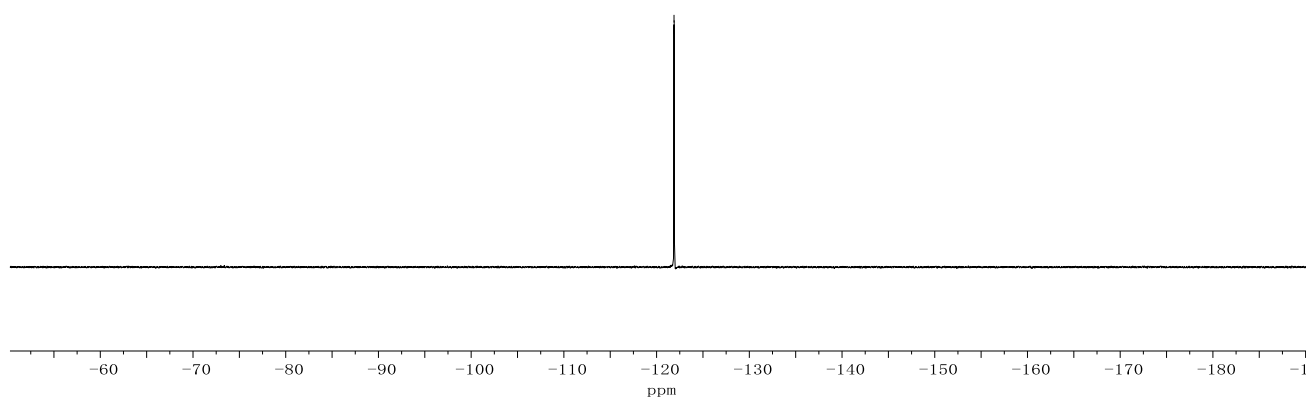


Appendix: NMR Spectra

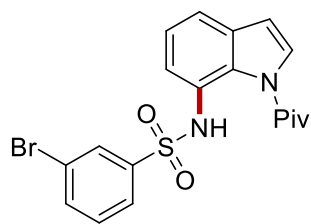


-121.9  
-121.9  
-121.9  
-121.9

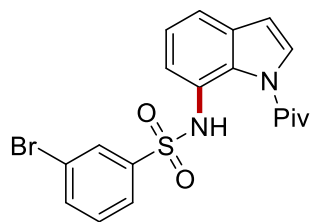
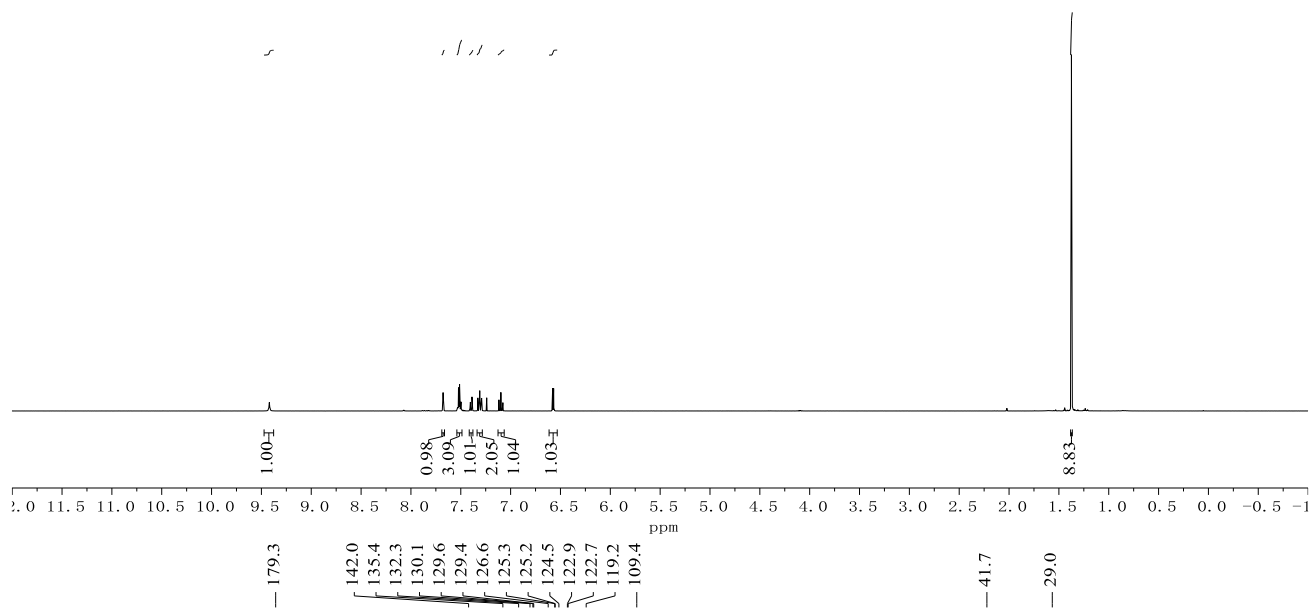
**392k**  
(282 MHz, CDCl<sub>3</sub>)



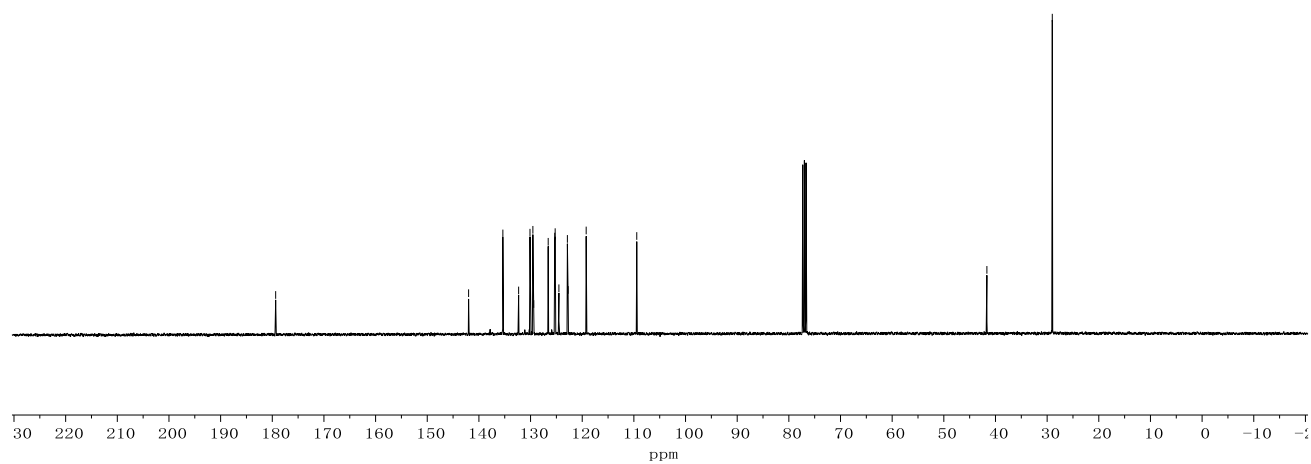
Appendix: NMR Spectra



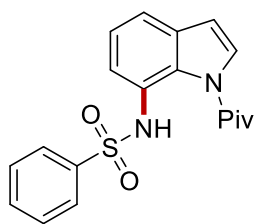
**392I**  
(400 MHz, CDCl<sub>3</sub>)



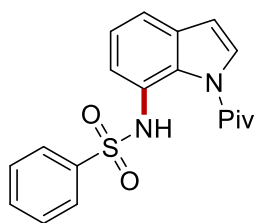
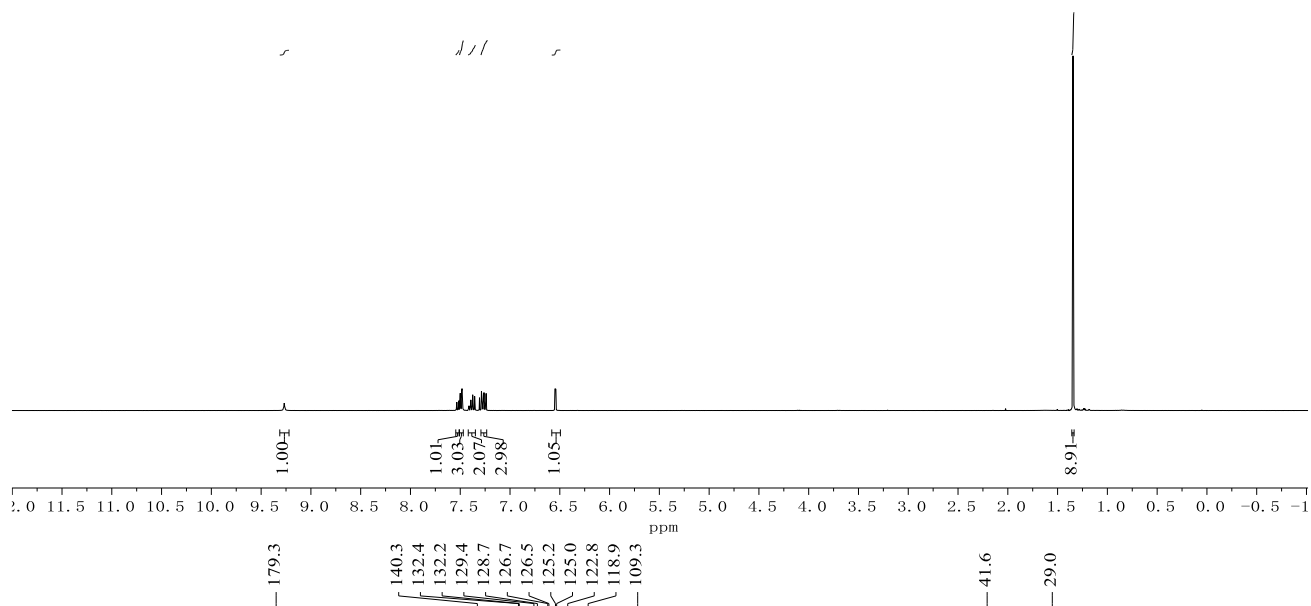
**392I**  
(100 MHz, CDCl<sub>3</sub>)



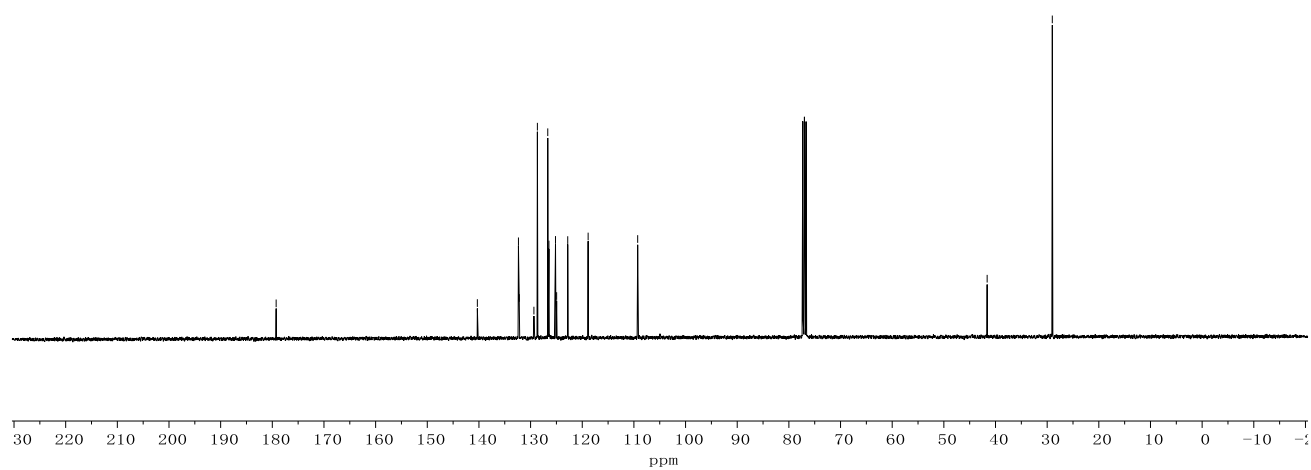
Appendix: NMR Spectra



**392m**  
(400 MHz, CDCl<sub>3</sub>)

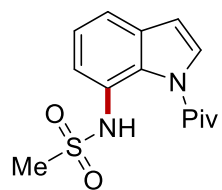


**392m**  
(100 MHz, CDCl<sub>3</sub>)

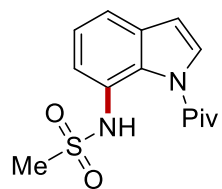
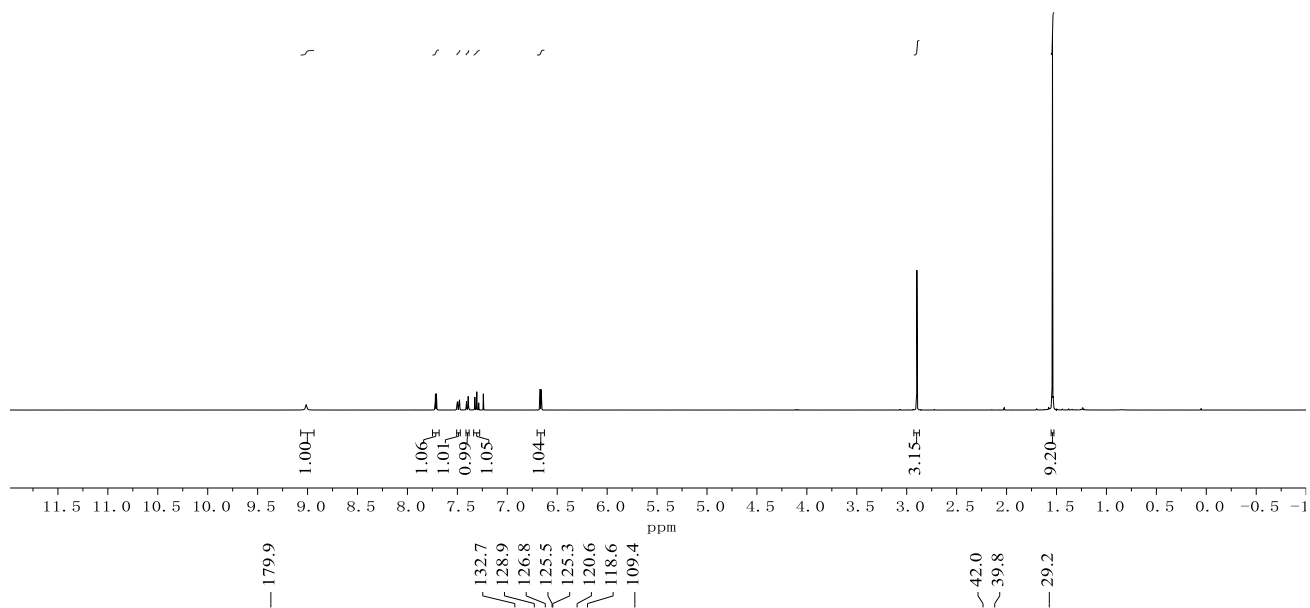




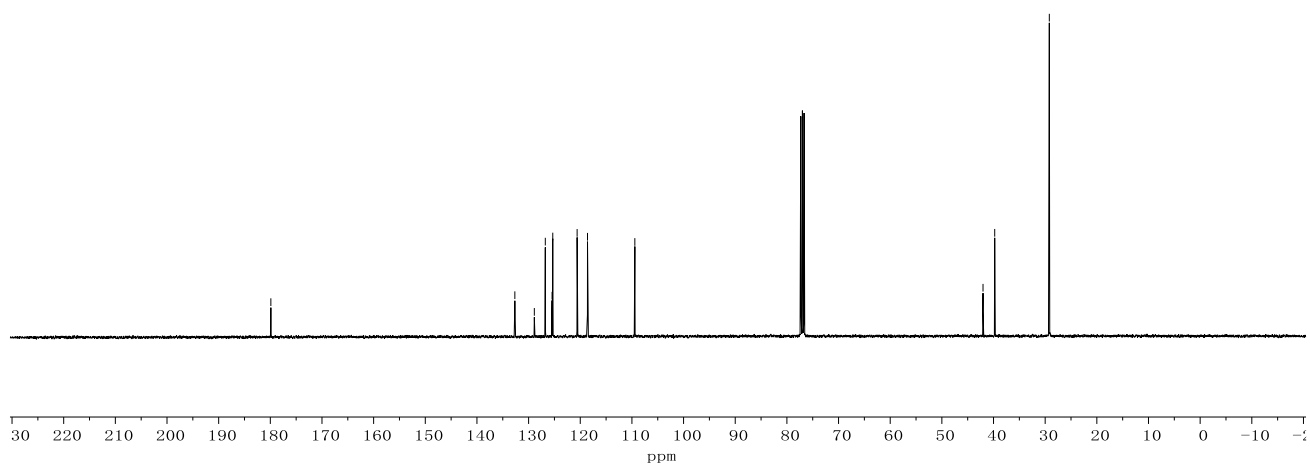
Appendix: NMR Spectra



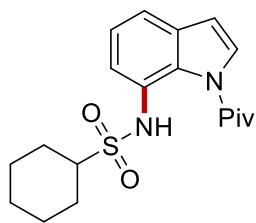
**392n**  
(400 MHz, CDCl<sub>3</sub>)



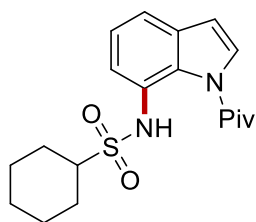
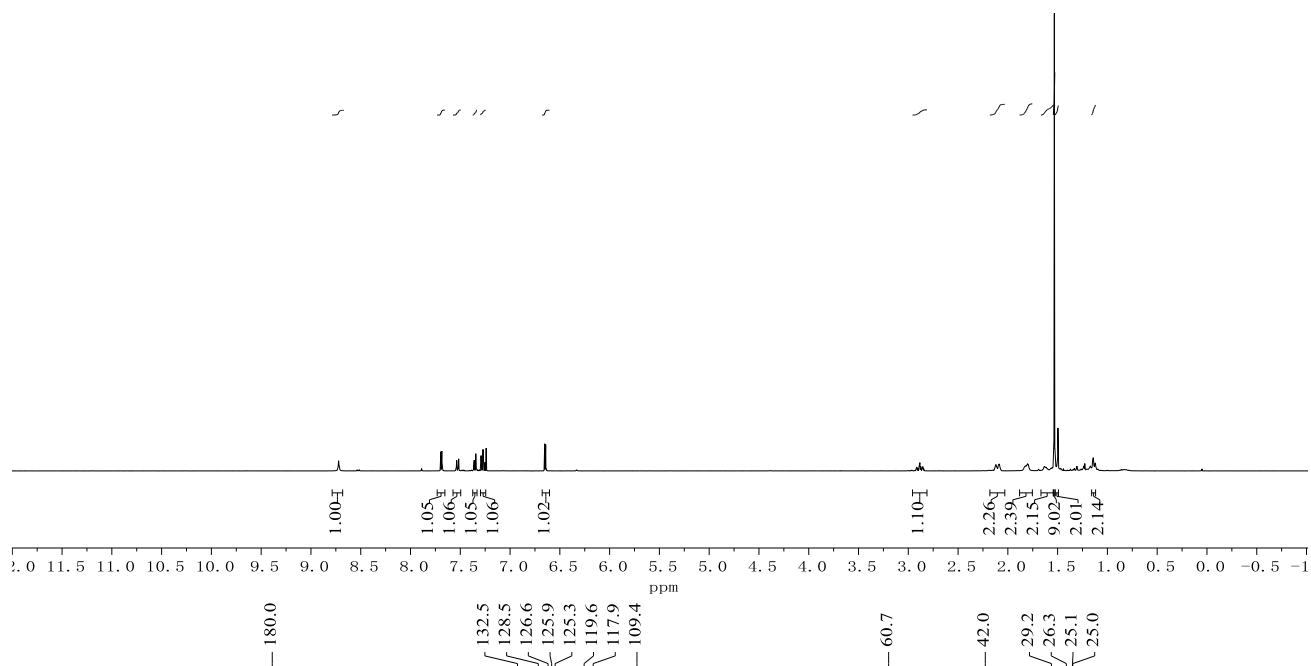
**392n**  
(100 MHz, CDCl<sub>3</sub>)



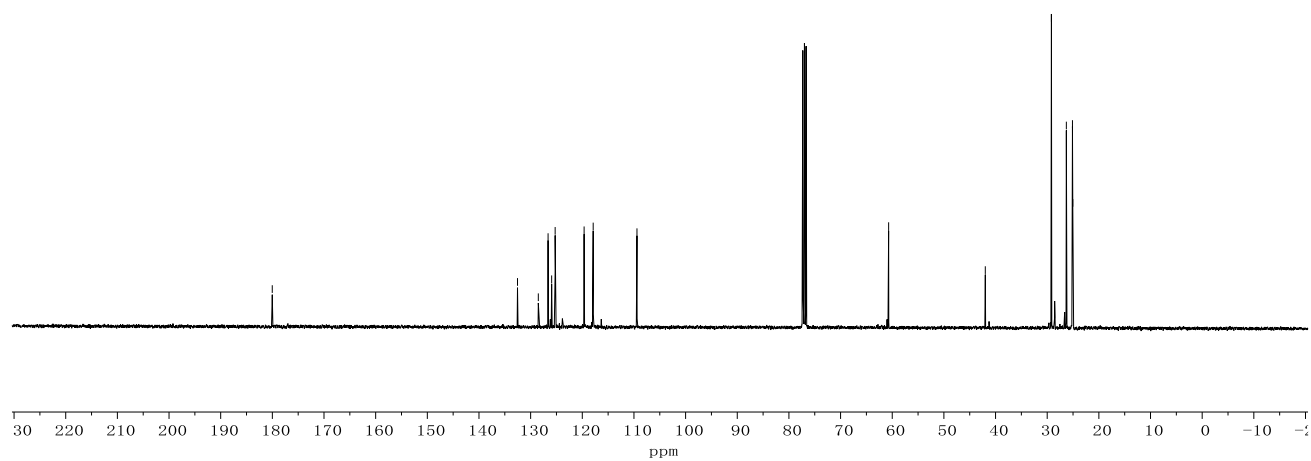
Appendix: NMR Spectra



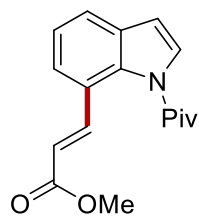
**392o**  
(400 MHz, CDCl<sub>3</sub>)



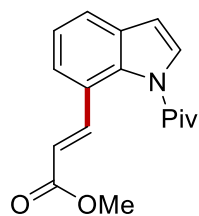
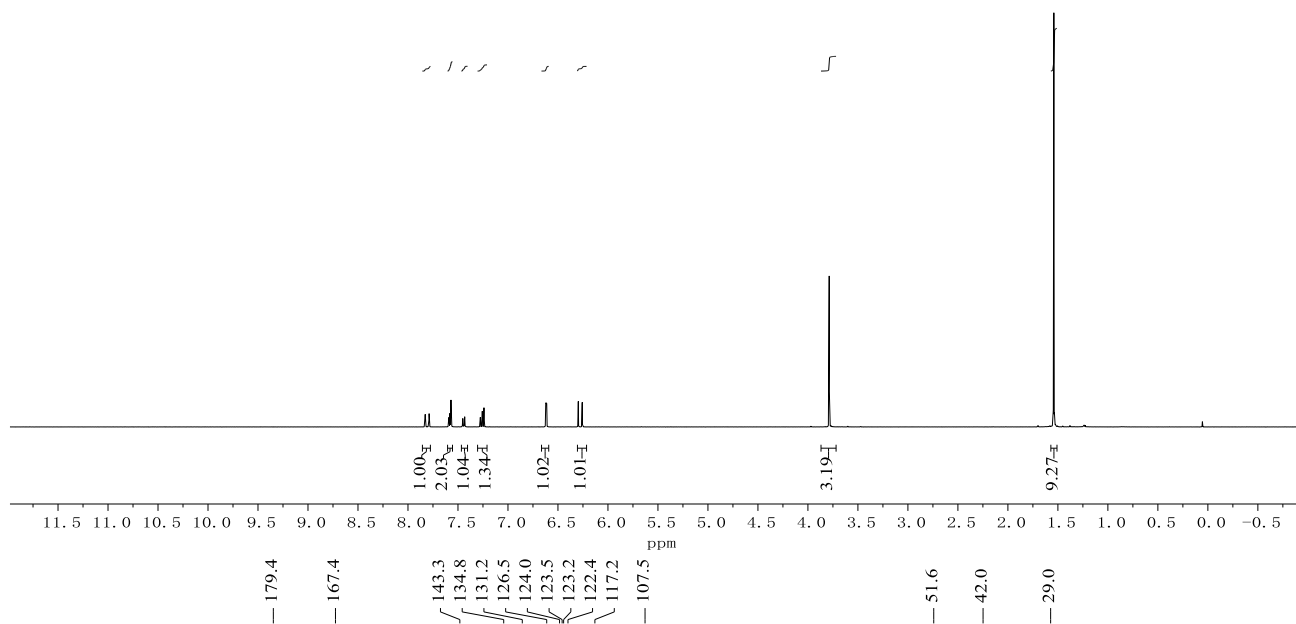
**392o**  
(100 MHz, CDCl<sub>3</sub>)



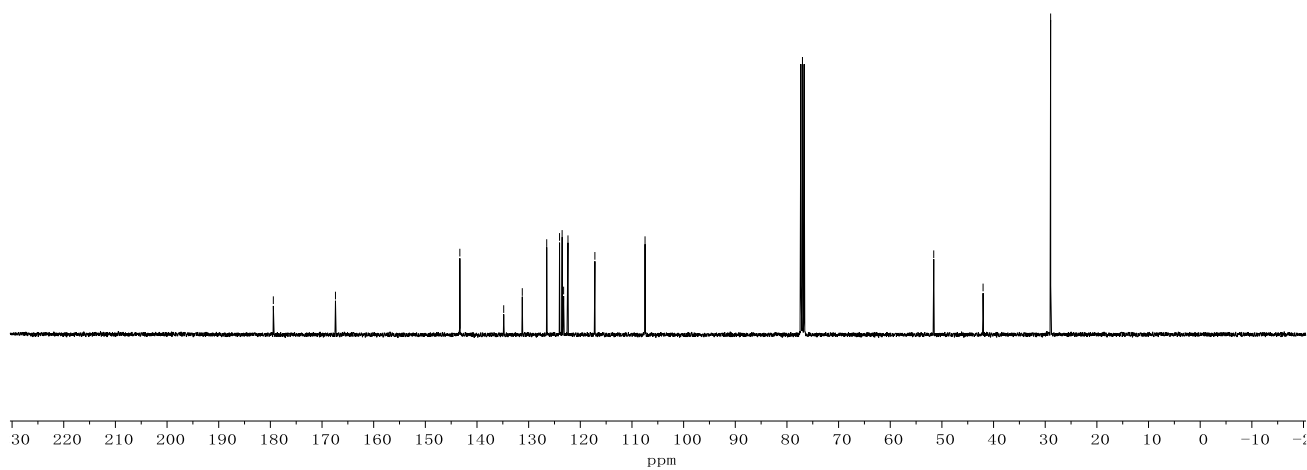
Appendix: NMR Spectra



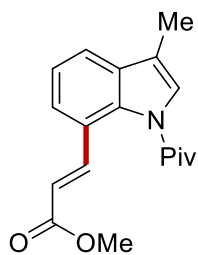
**394a**  
(400 MHz, CDCl<sub>3</sub>)



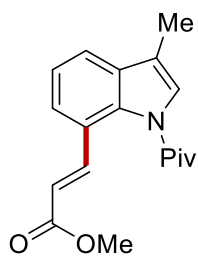
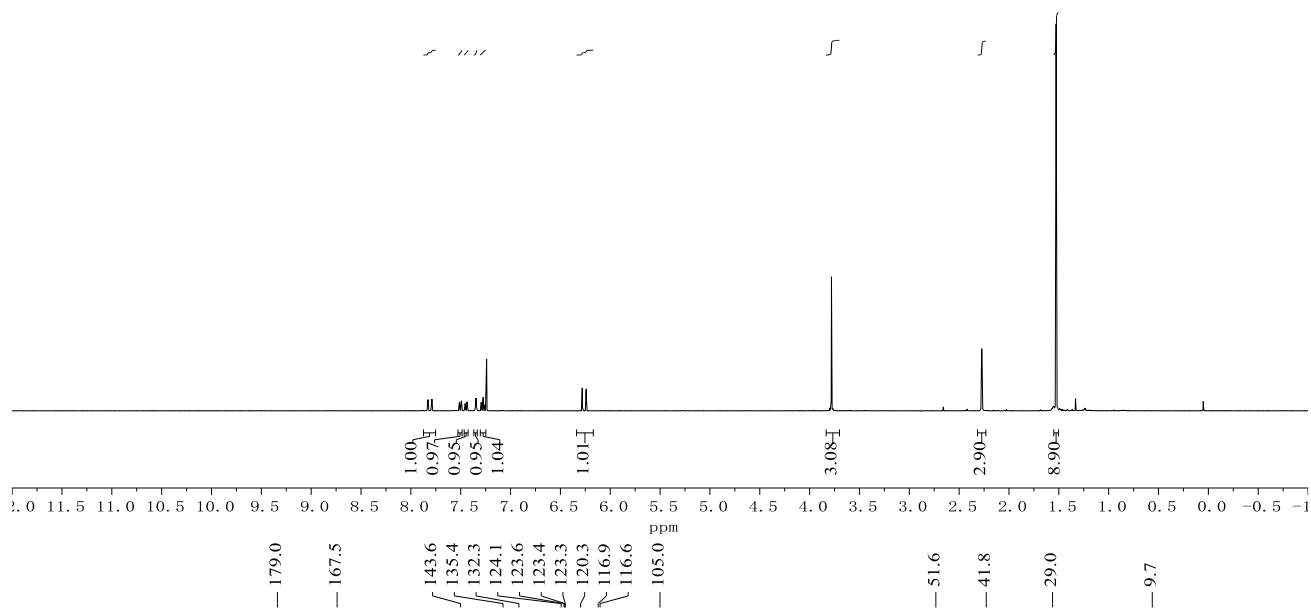
**394a**  
(100 MHz, CDCl<sub>3</sub>)



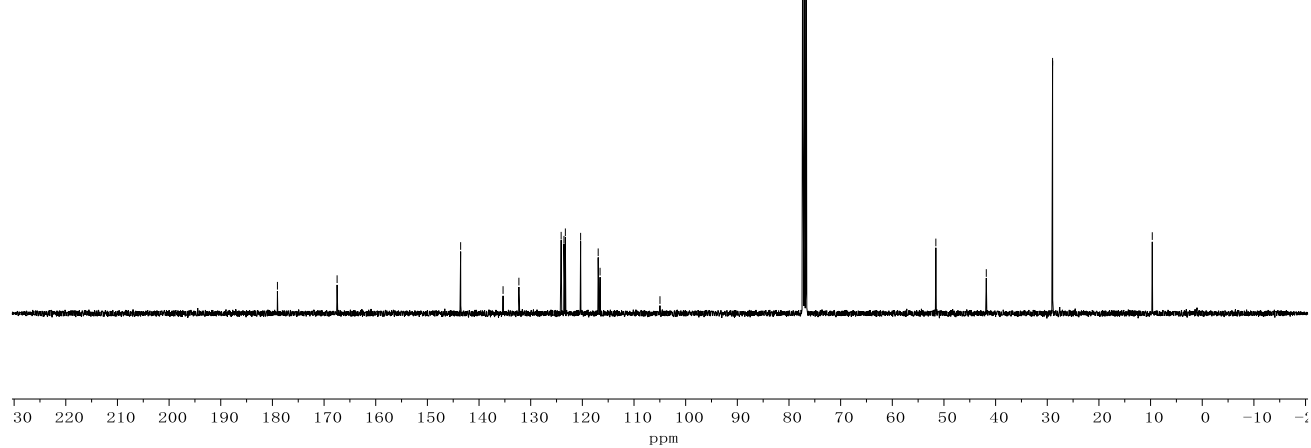
Appendix: NMR Spectra



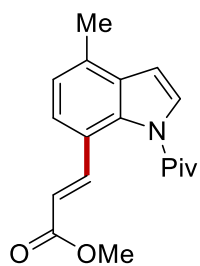
**394b**  
(400 MHz, CDCl<sub>3</sub>)



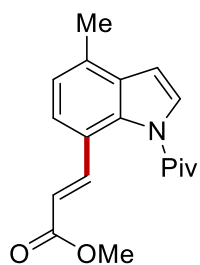
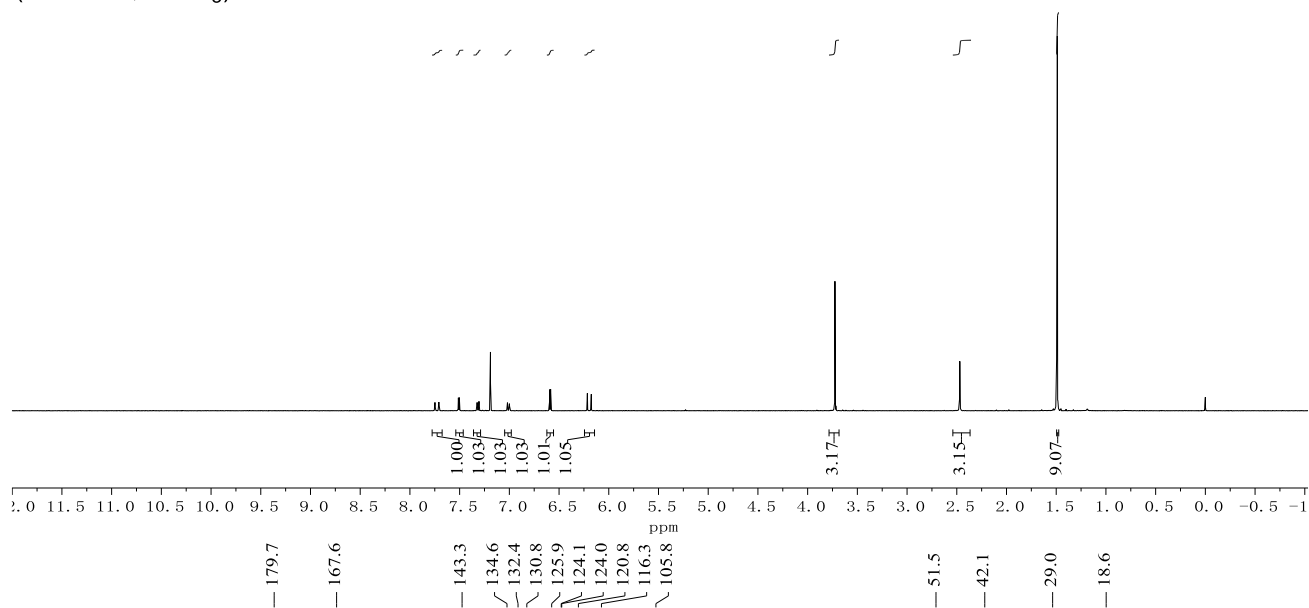
**394b**  
(100 MHz, CDCl<sub>3</sub>)



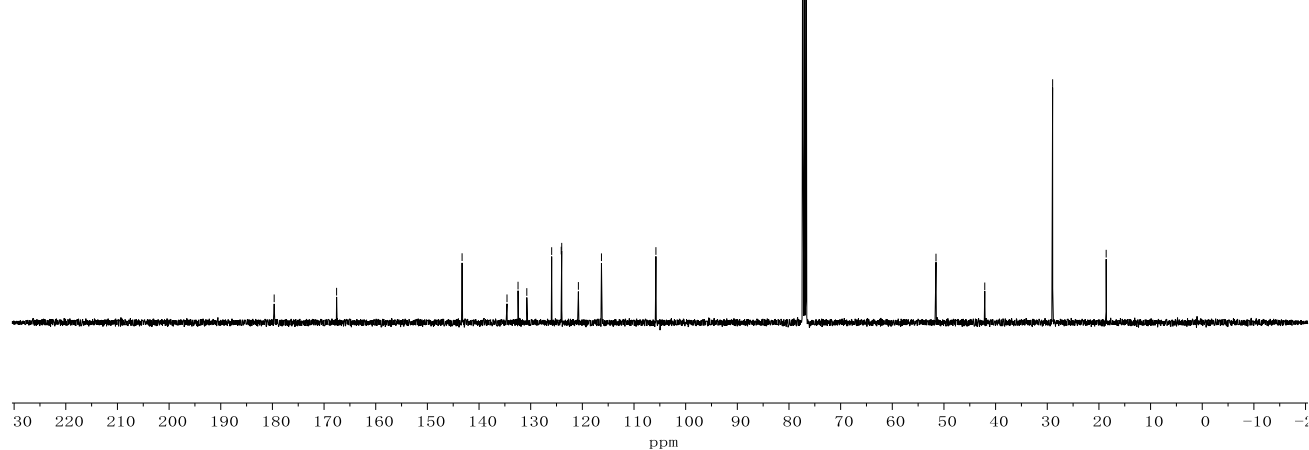
Appendix: NMR Spectra



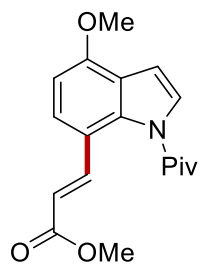
**394c**  
(400 MHz, CDCl<sub>3</sub>)



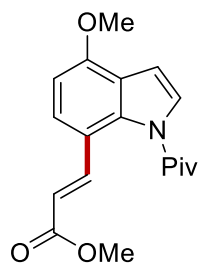
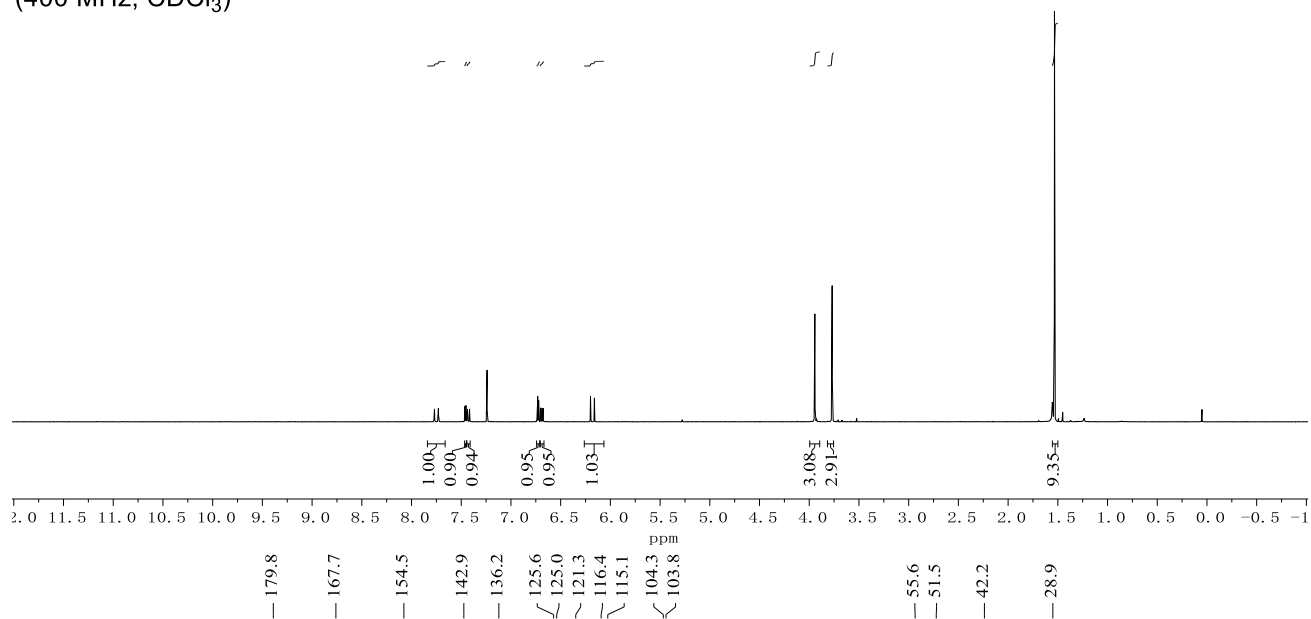
**394c**  
(100 MHz, CDCl<sub>3</sub>)



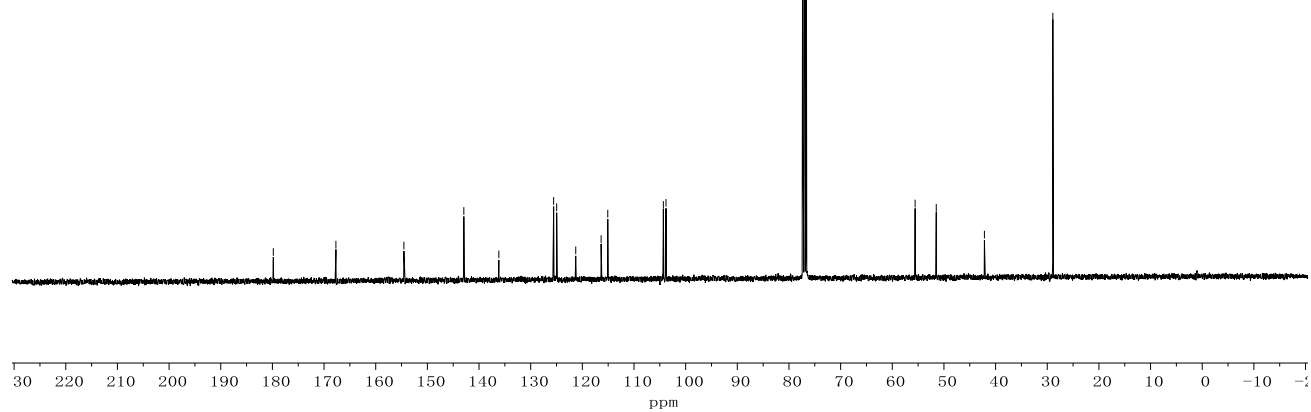
Appendix: NMR Spectra



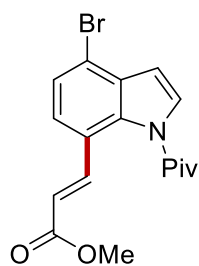
**394d**  
(400 MHz, CDCl<sub>3</sub>)



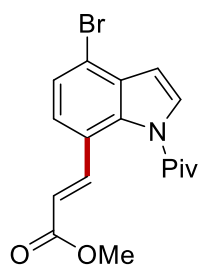
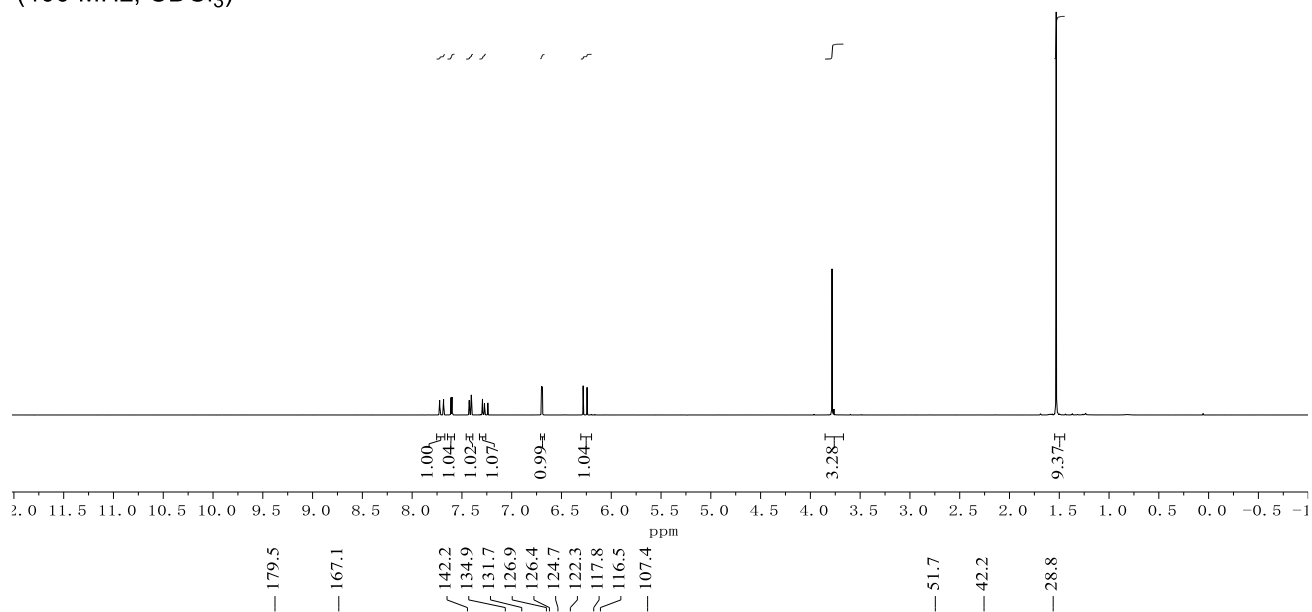
**394d**  
(100 MHz, CDCl<sub>3</sub>)



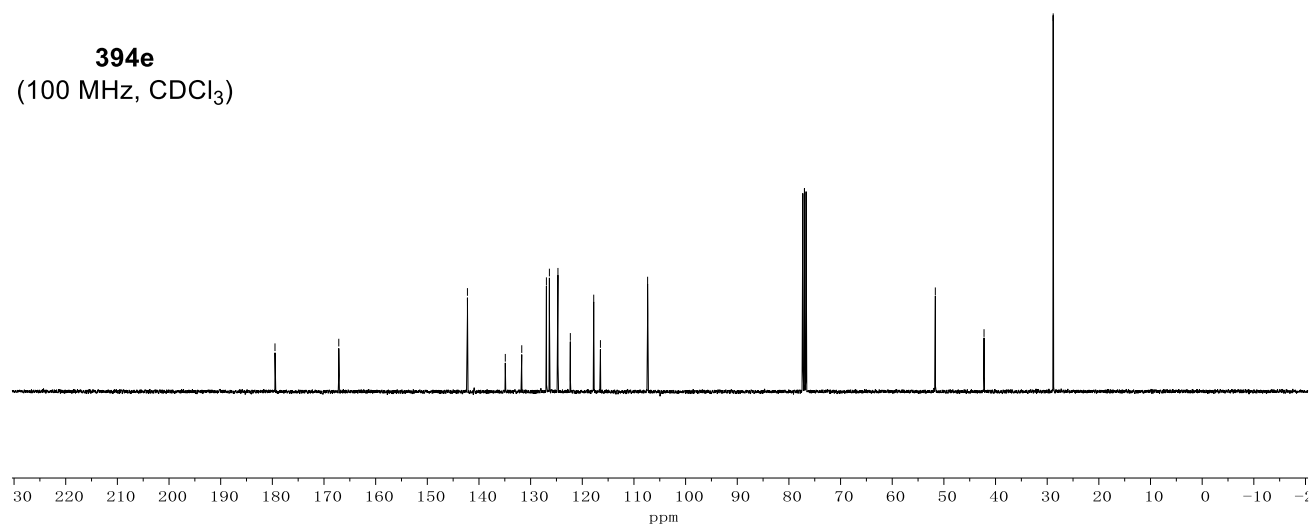
Appendix: NMR Spectra



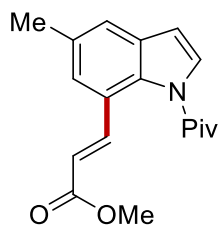
**394e**  
(400 MHz, CDCl<sub>3</sub>)



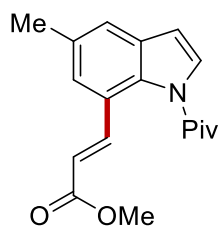
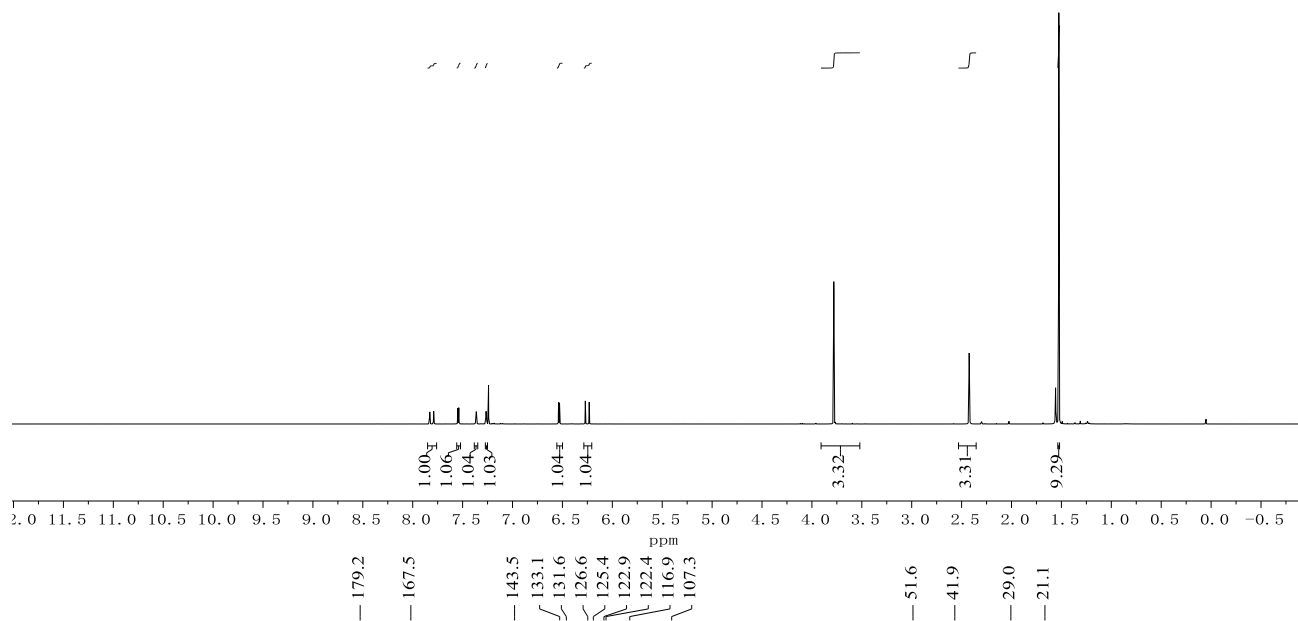
**394e**  
(100 MHz, CDCl<sub>3</sub>)



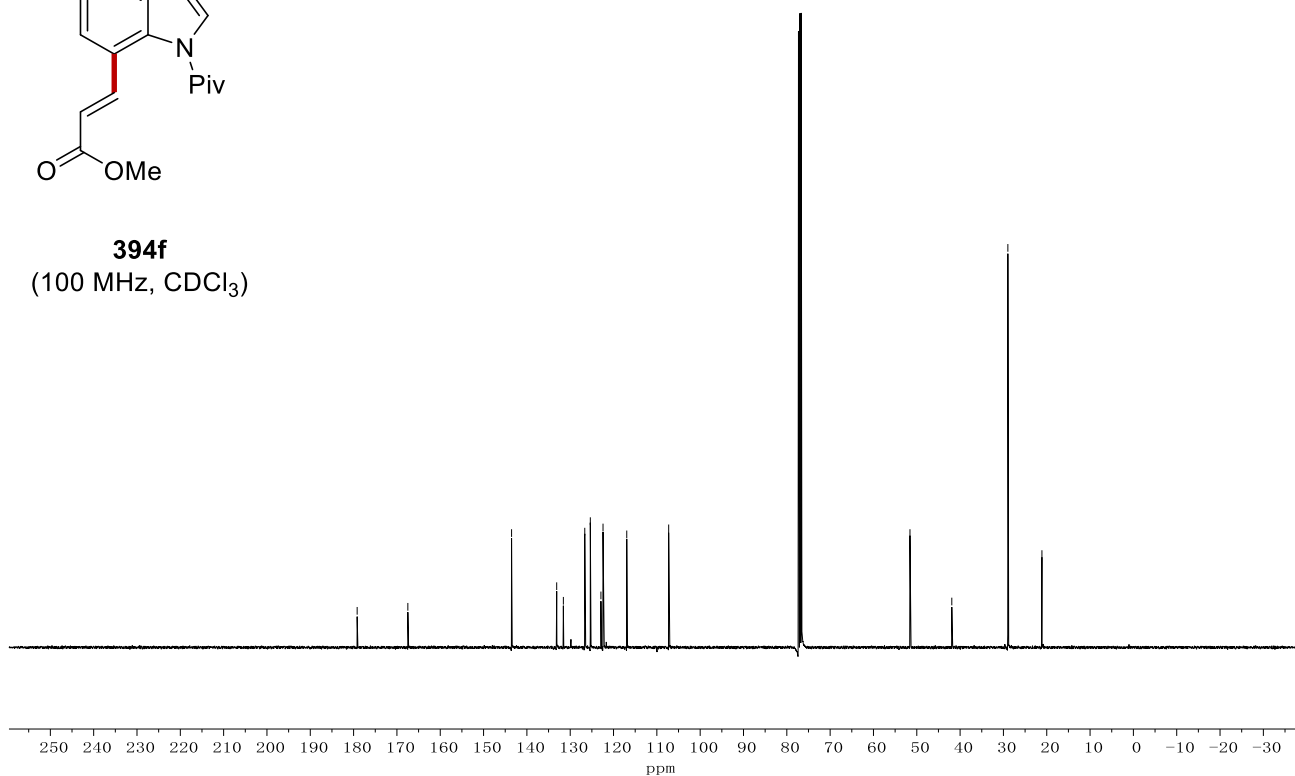
Appendix: NMR Spectra



**394f**  
(400 MHz, CDCl<sub>3</sub>)

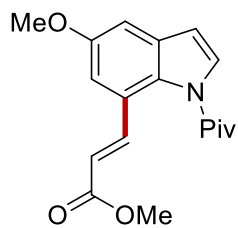


**394f**  
(100 MHz, CDCl<sub>3</sub>)

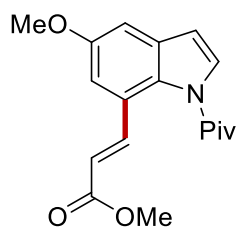
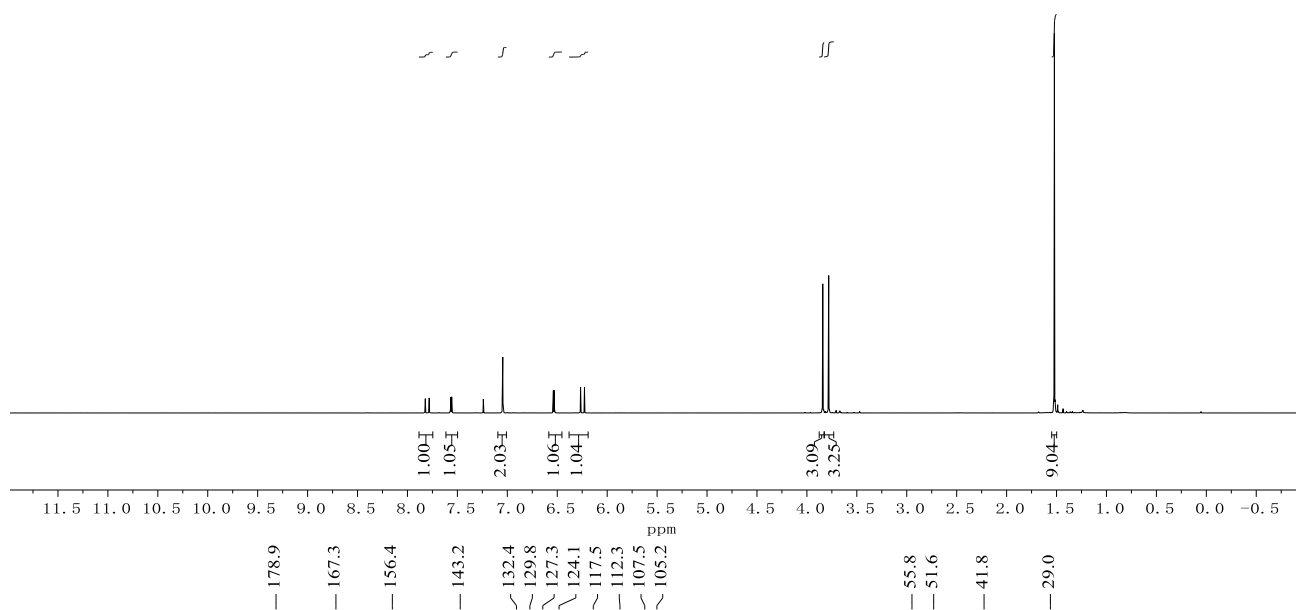




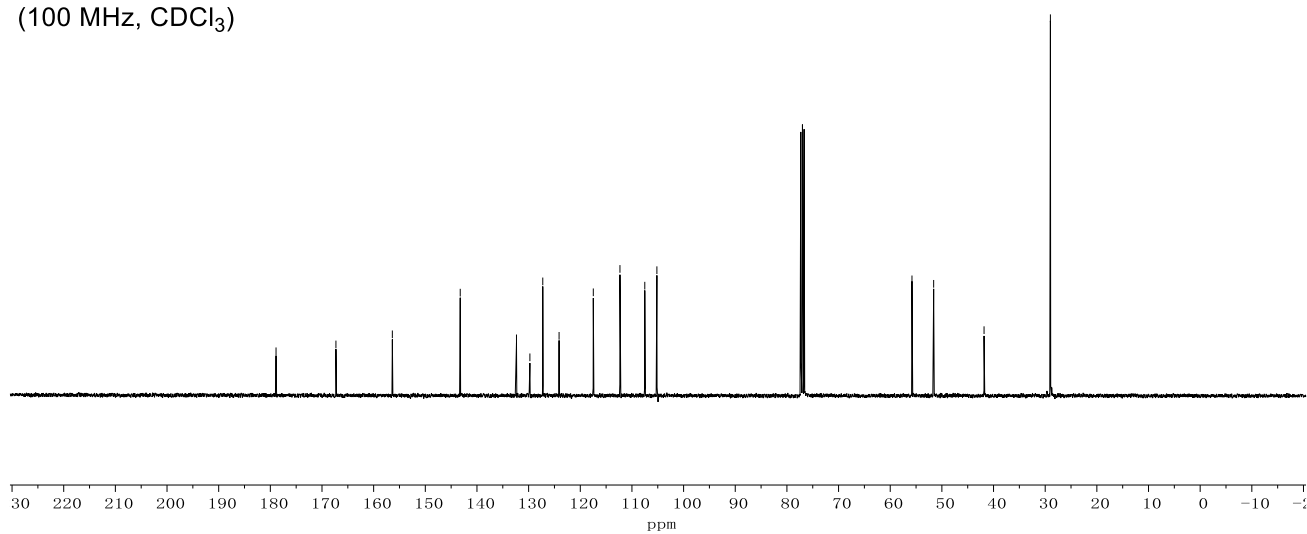
Appendix: NMR Spectra



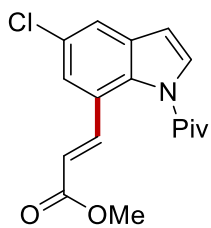
**394g**  
(400 MHz, CDCl<sub>3</sub>)



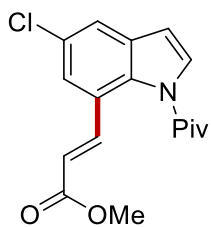
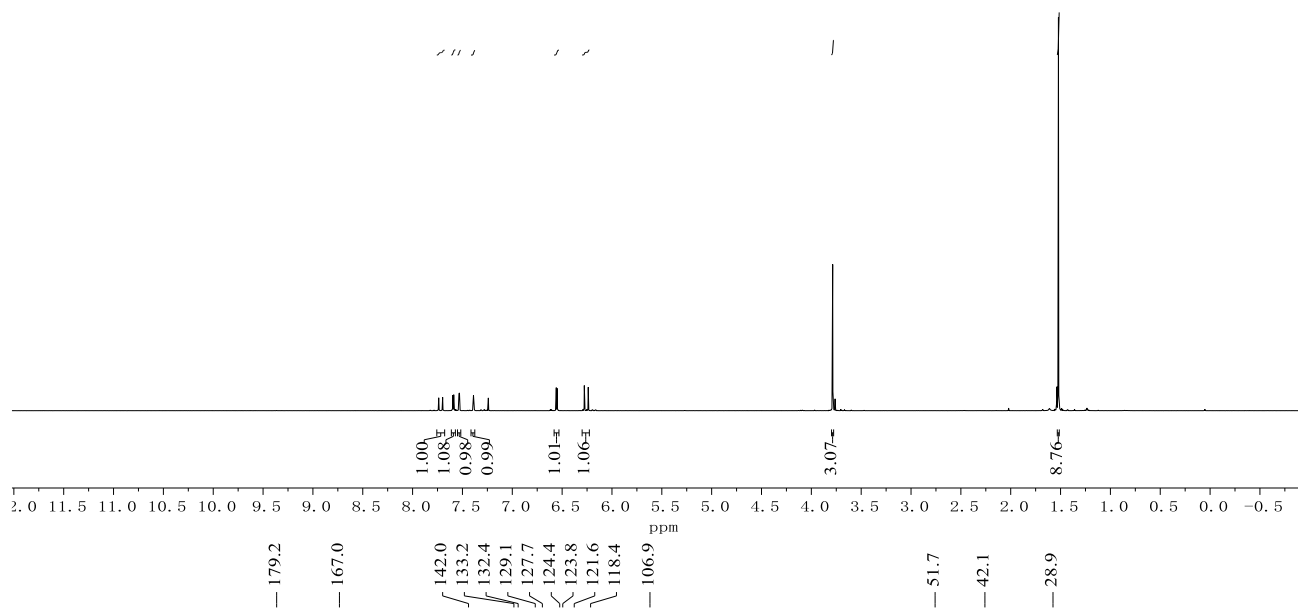
**394g**  
(100 MHz, CDCl<sub>3</sub>)



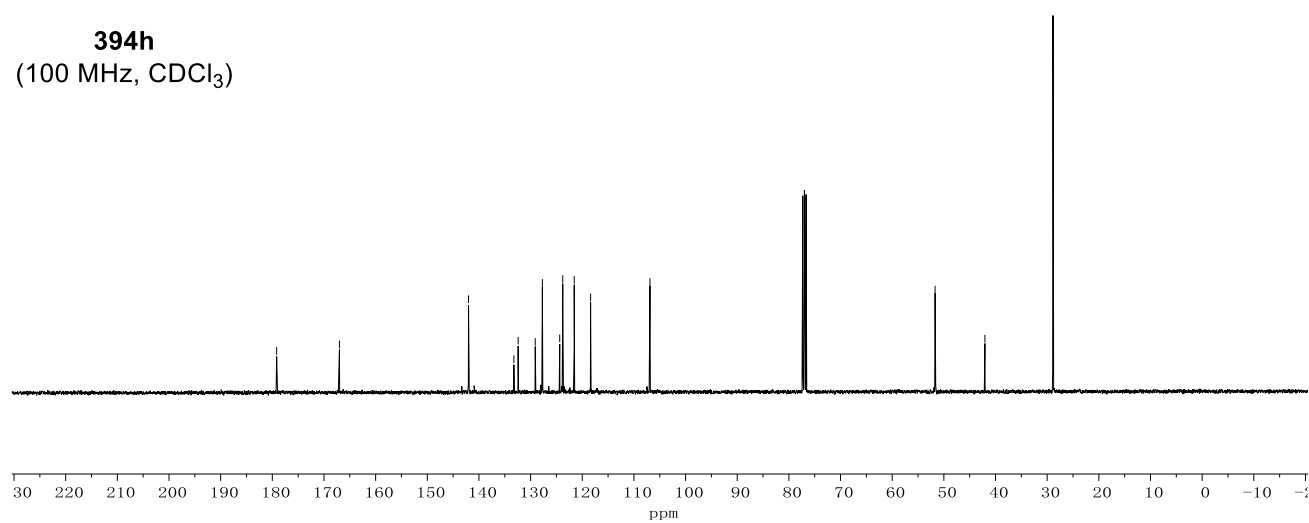
Appendix: NMR Spectra



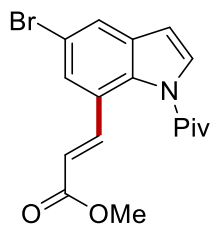
**394h**  
(400 MHz, CDCl<sub>3</sub>)



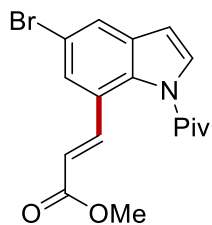
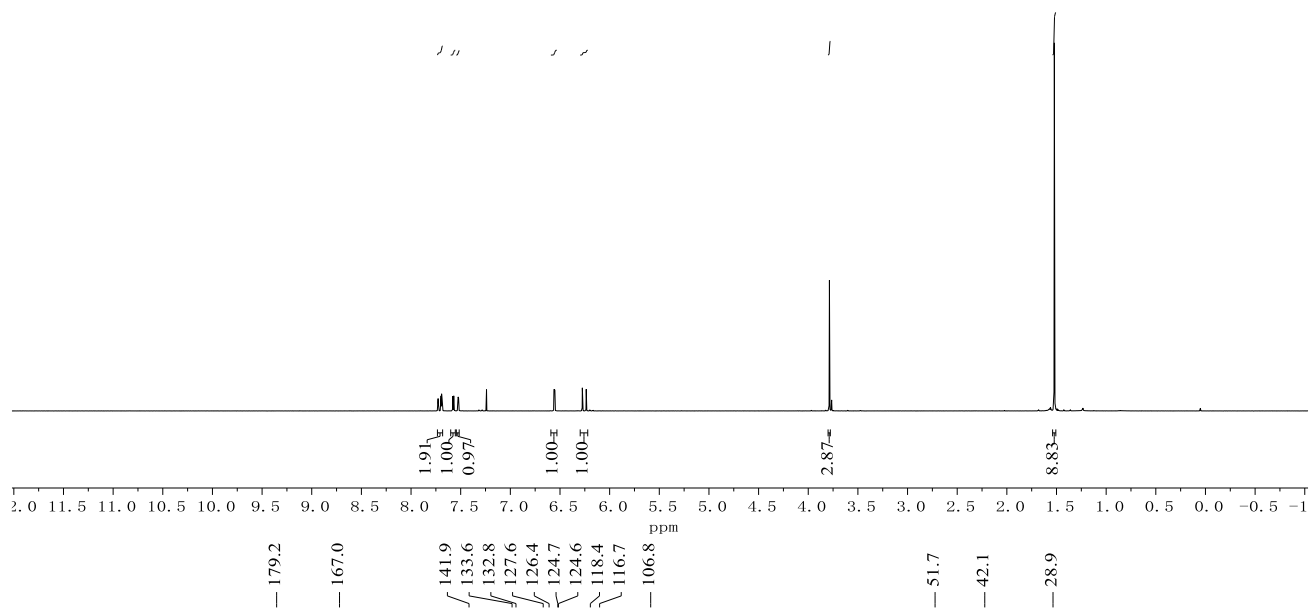
**394h**  
(100 MHz, CDCl<sub>3</sub>)



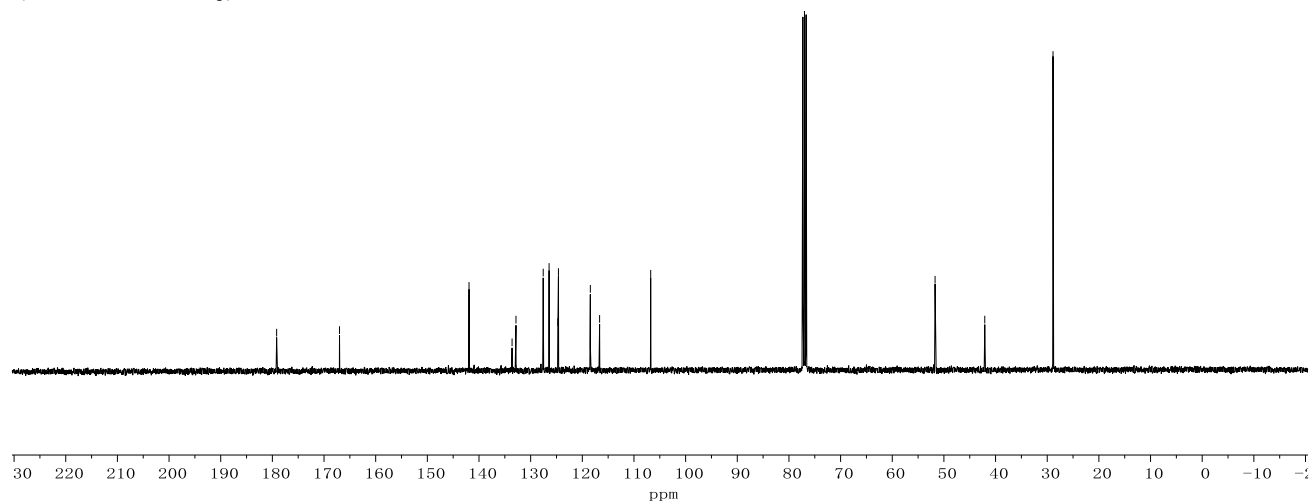
Appendix: NMR Spectra



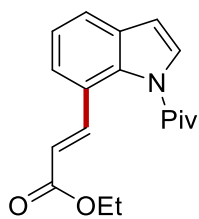
**394i**  
(400 MHz, CDCl<sub>3</sub>)



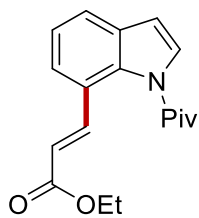
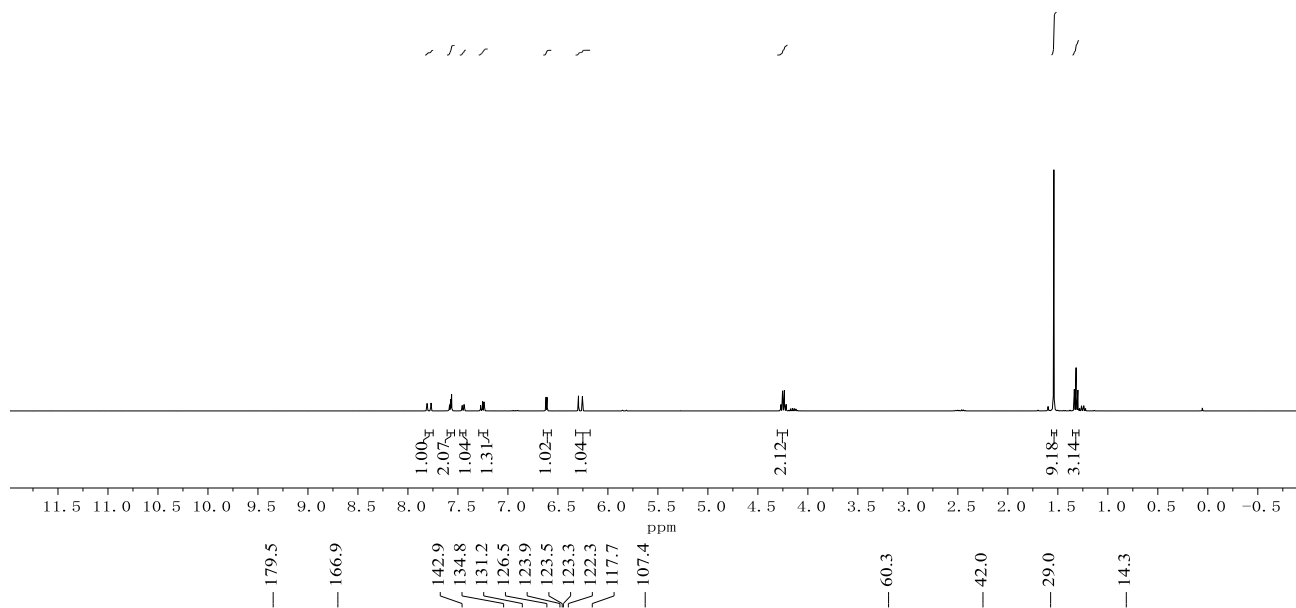
**394i**  
(100 MHz, CDCl<sub>3</sub>)



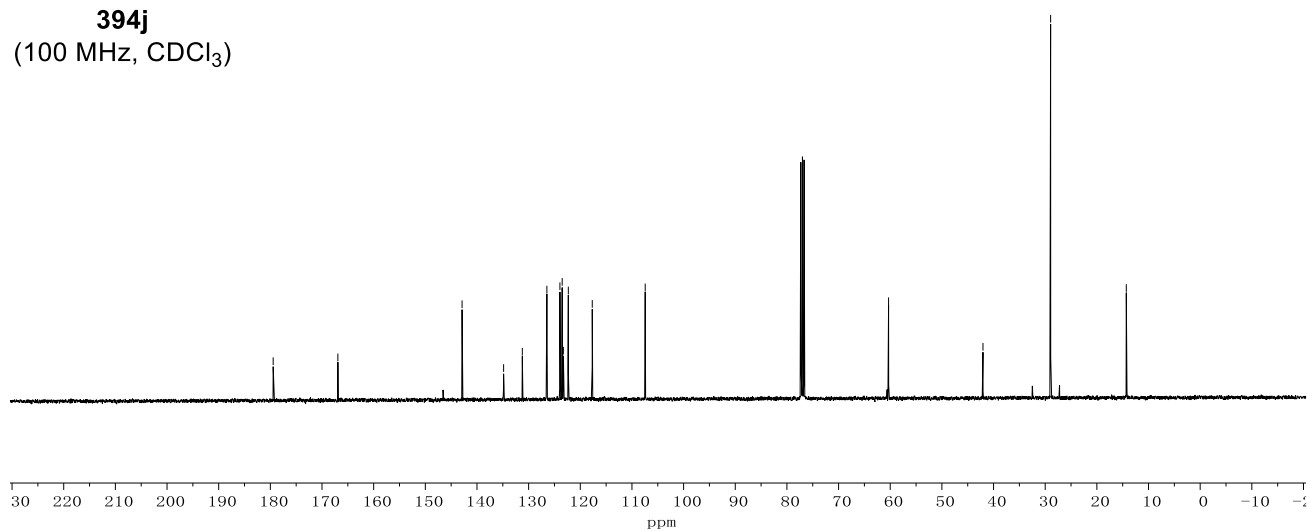
Appendix: NMR Spectra



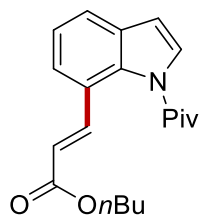
**394j**  
(400 MHz, CDCl<sub>3</sub>)



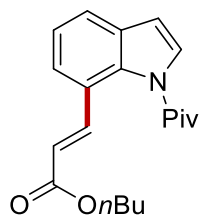
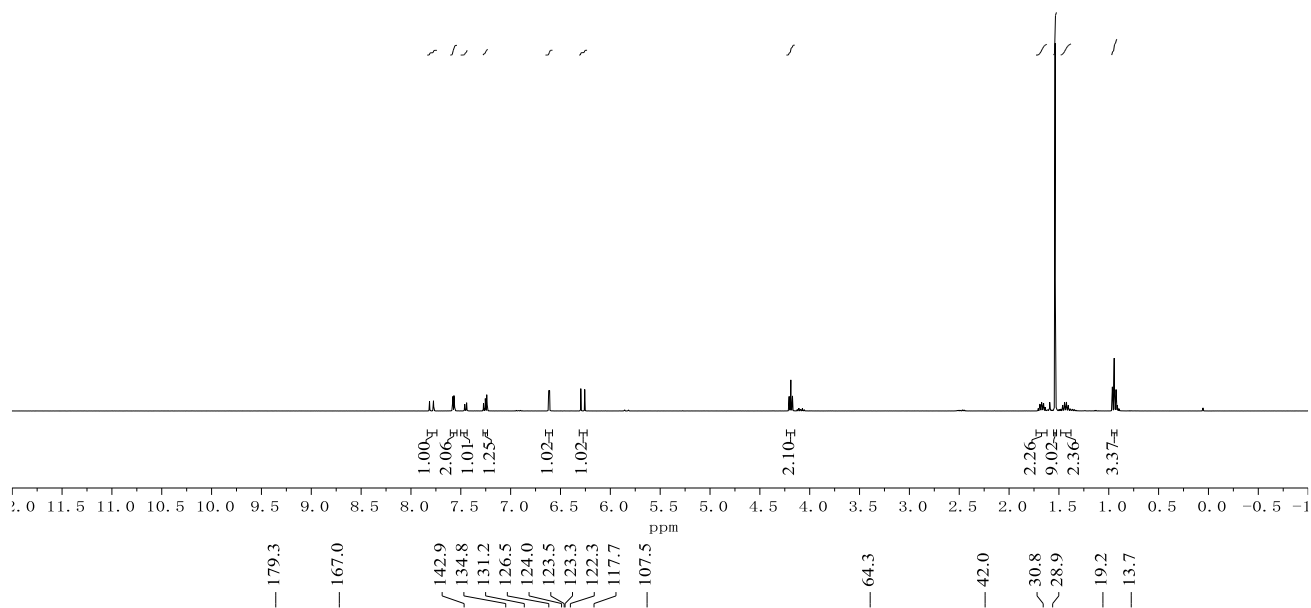
**394j**  
(100 MHz, CDCl<sub>3</sub>)



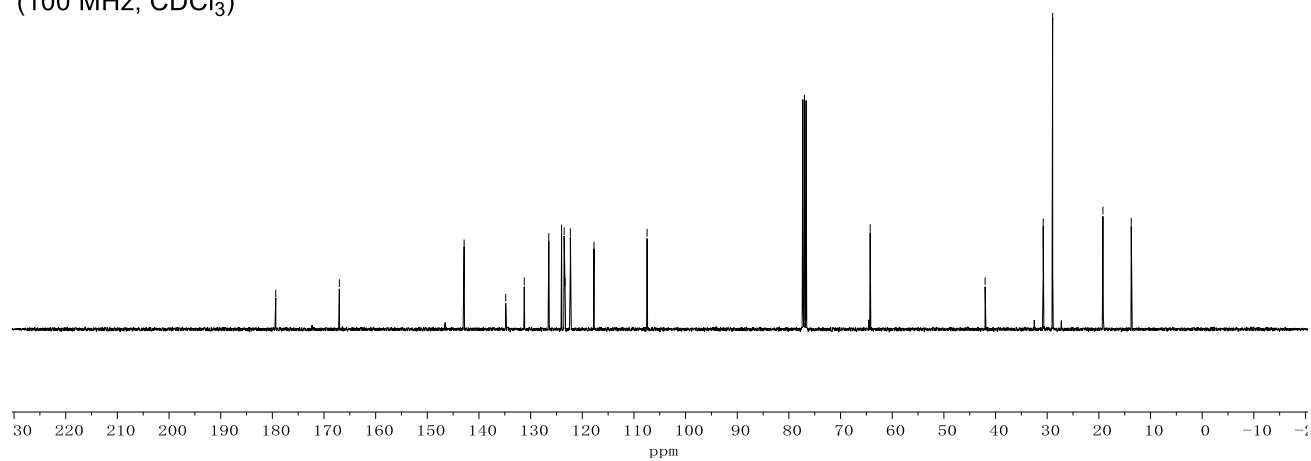
Appendix: NMR Spectra



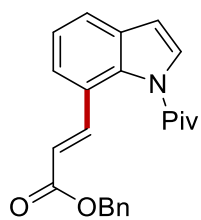
**394k**  
(400 MHz, CDCl<sub>3</sub>)



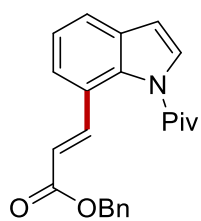
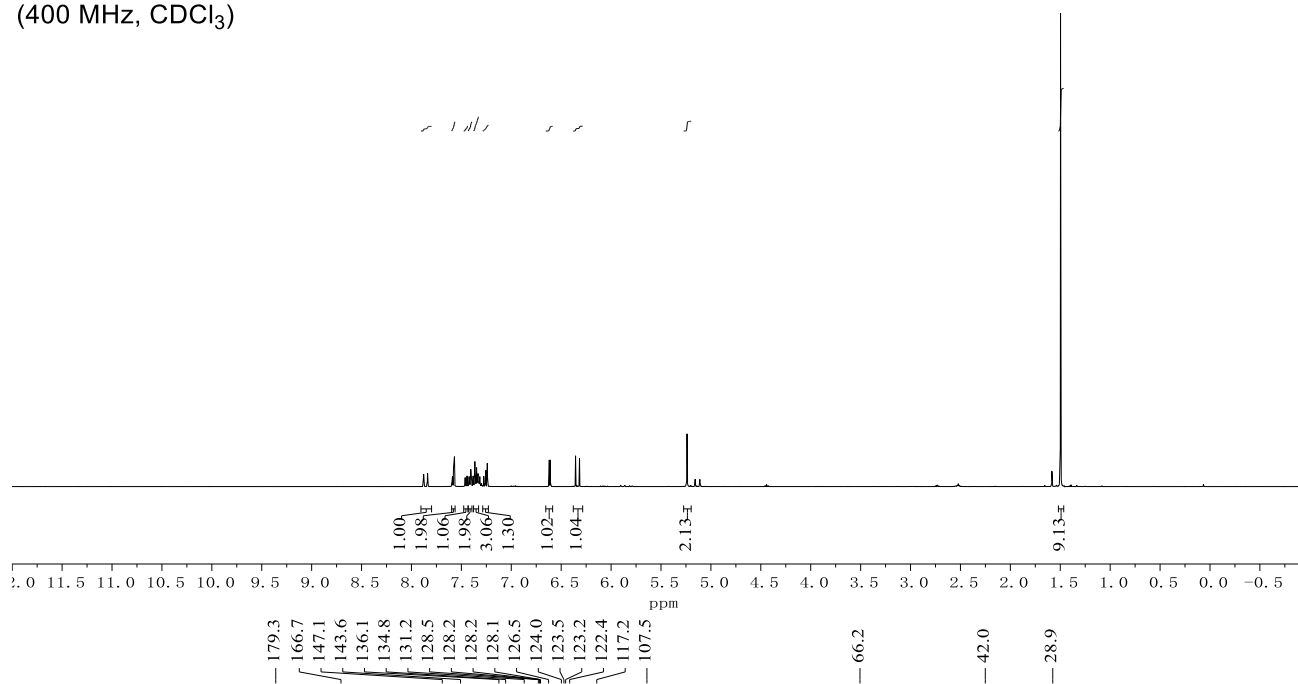
**394k**  
(100 MHz, CDCl<sub>3</sub>)



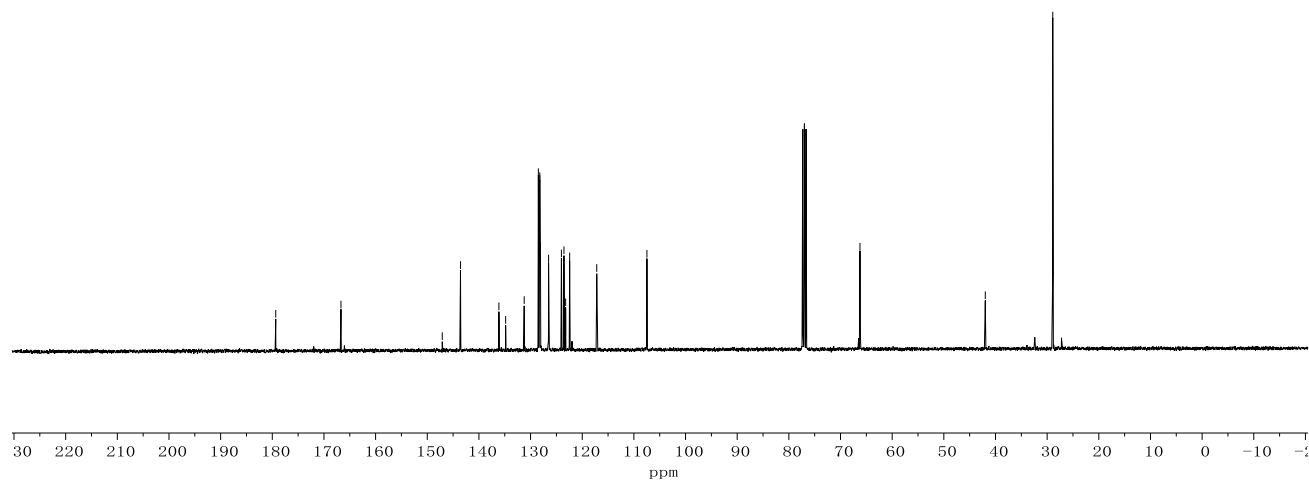
Appendix: NMR Spectra



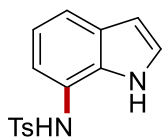
**3941**  
(400 MHz, CDCl<sub>3</sub>)



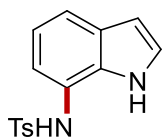
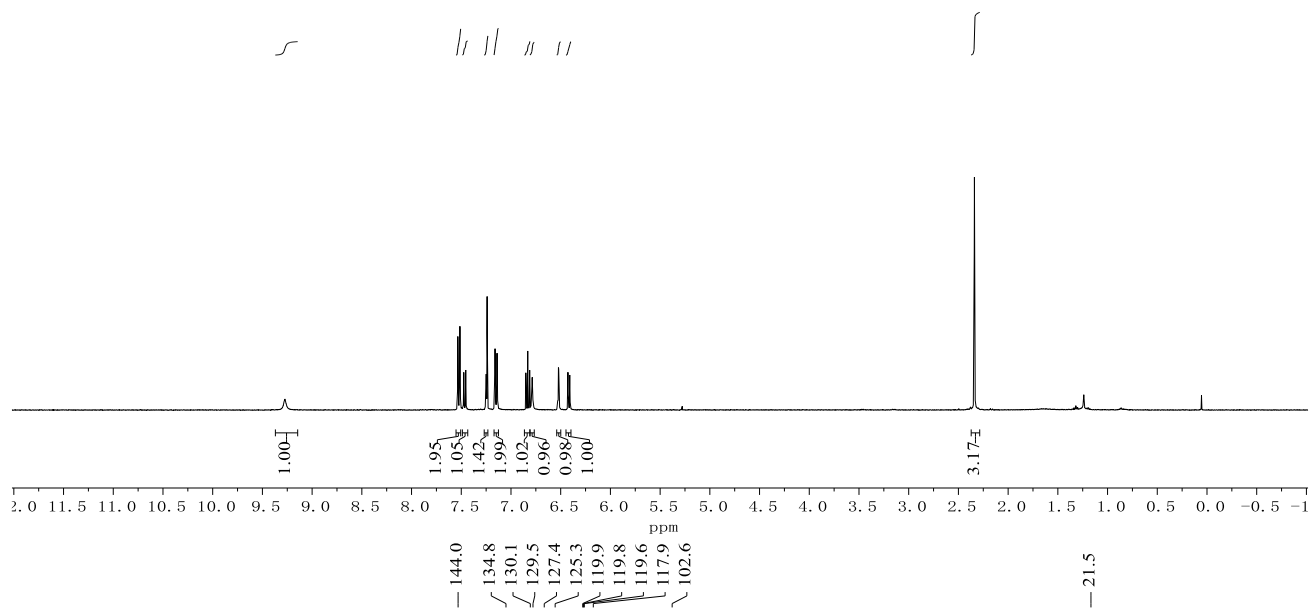
**3941**  
(100 MHz, CDCl<sub>3</sub>)



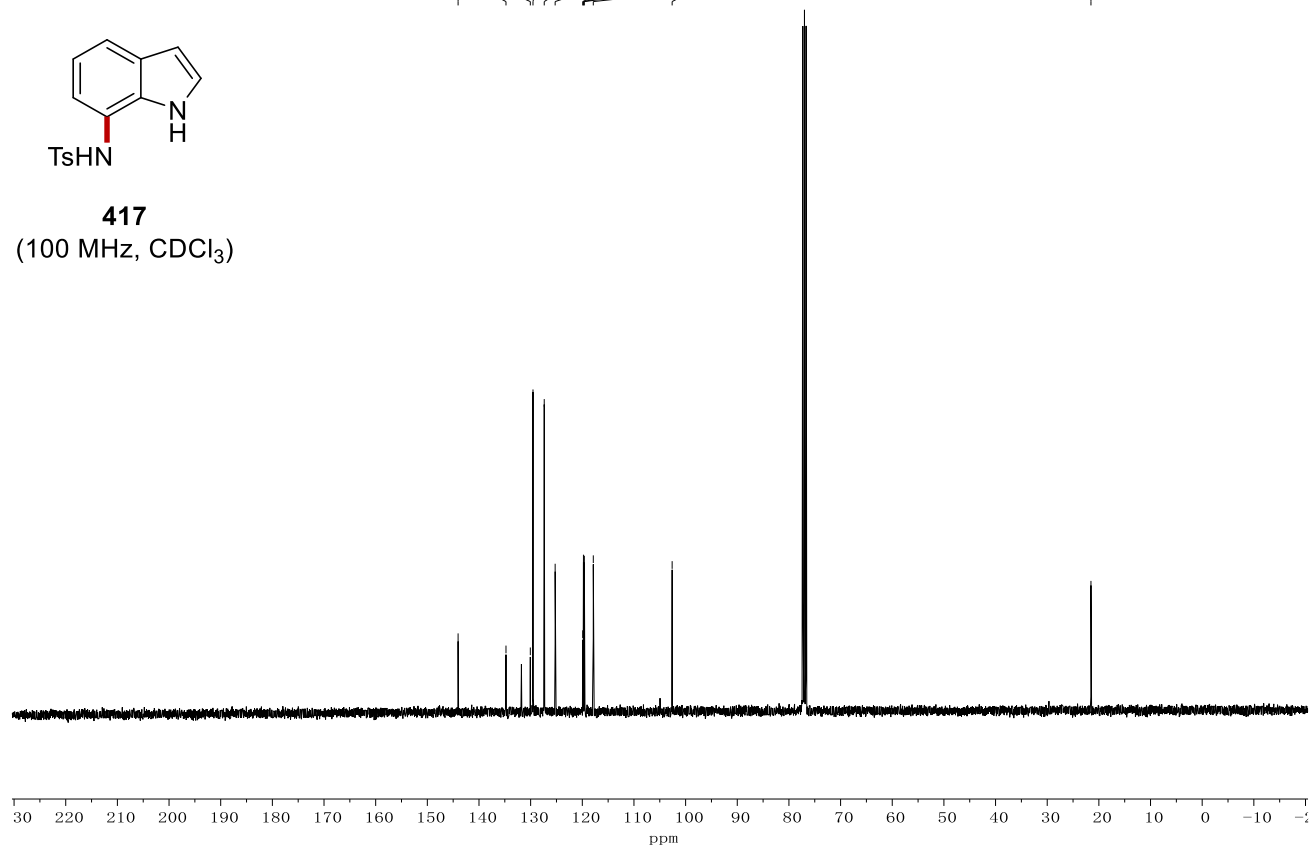
Appendix: NMR Spectra



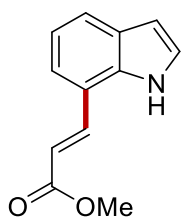
**417**  
(400 MHz, CDCl<sub>3</sub>)



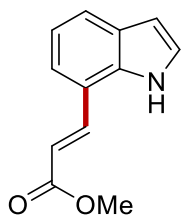
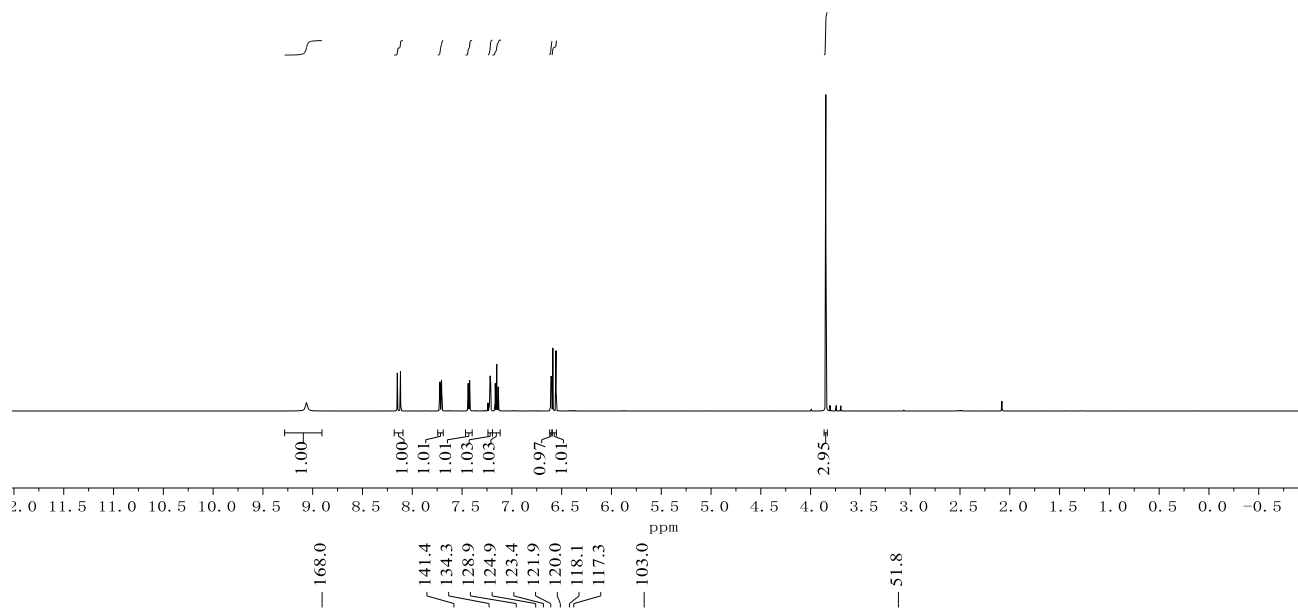
**417**  
(100 MHz, CDCl<sub>3</sub>)



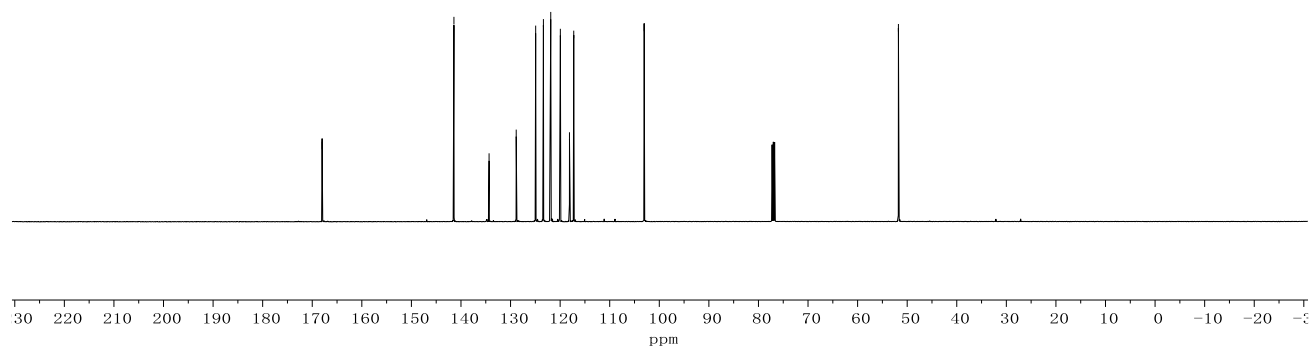
Appendix: NMR Spectra



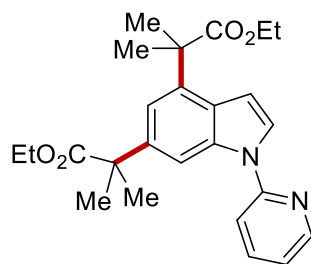
**418**  
(400 MHz, CDCl<sub>3</sub>)



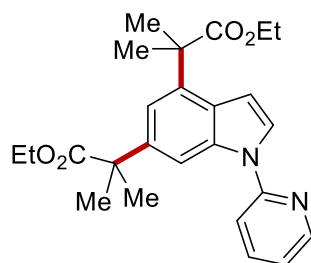
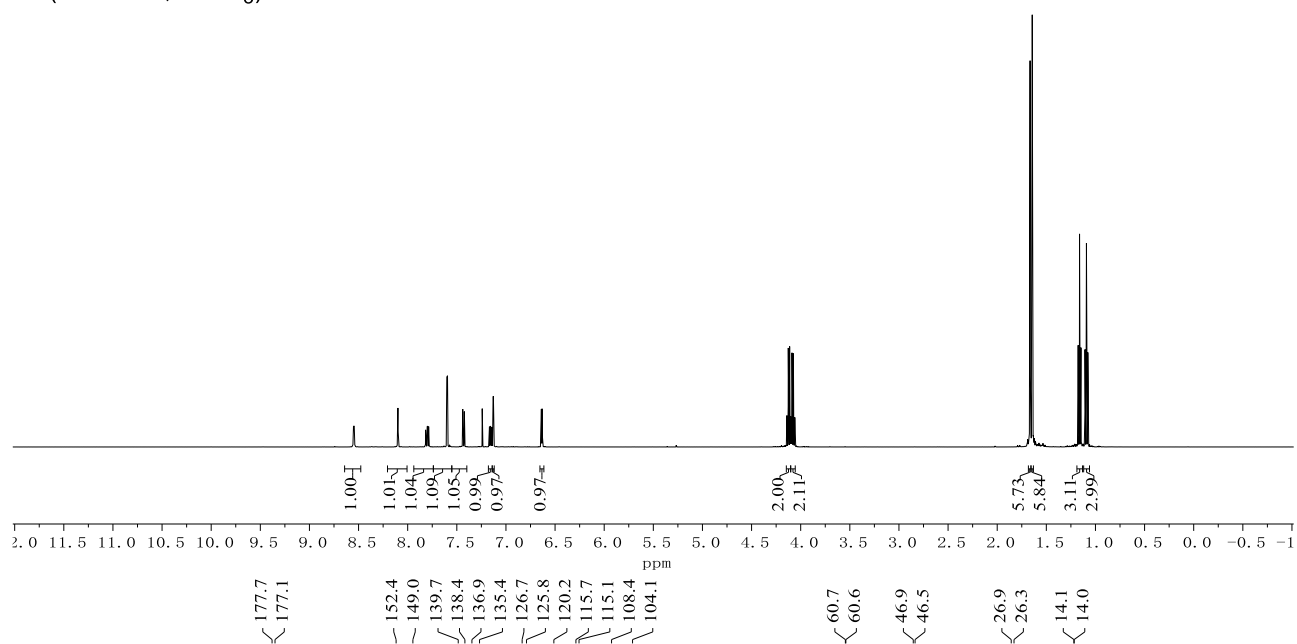
**418**  
(100 MHz, CDCl<sub>3</sub>)



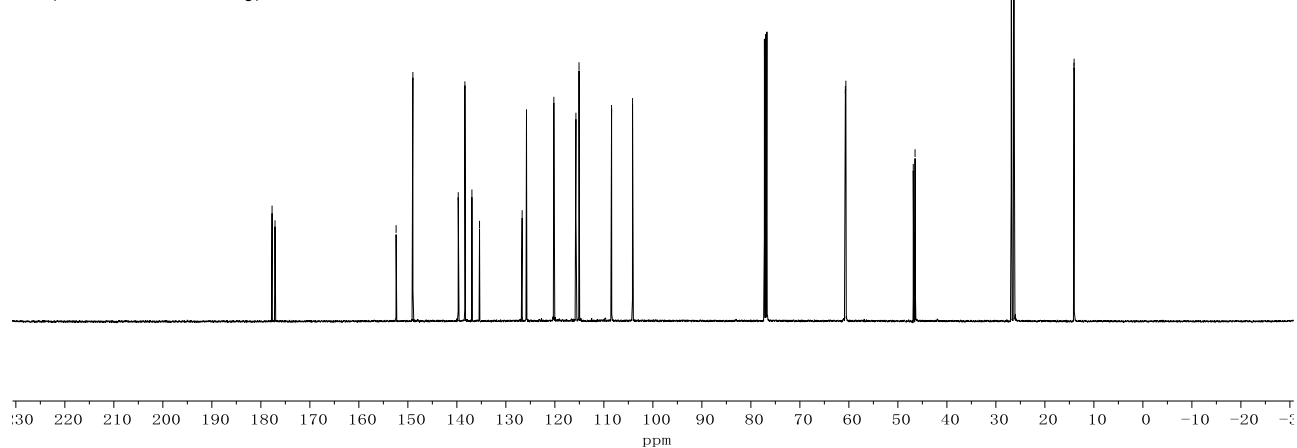




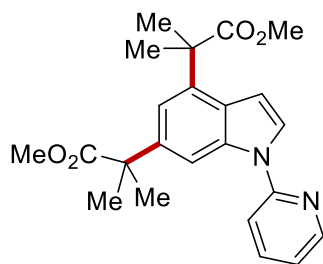
**397a**  
(400 MHz, CDCl<sub>3</sub>)



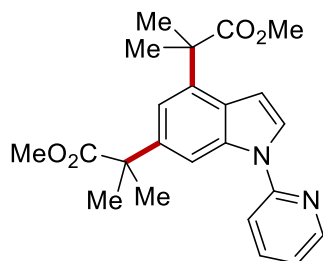
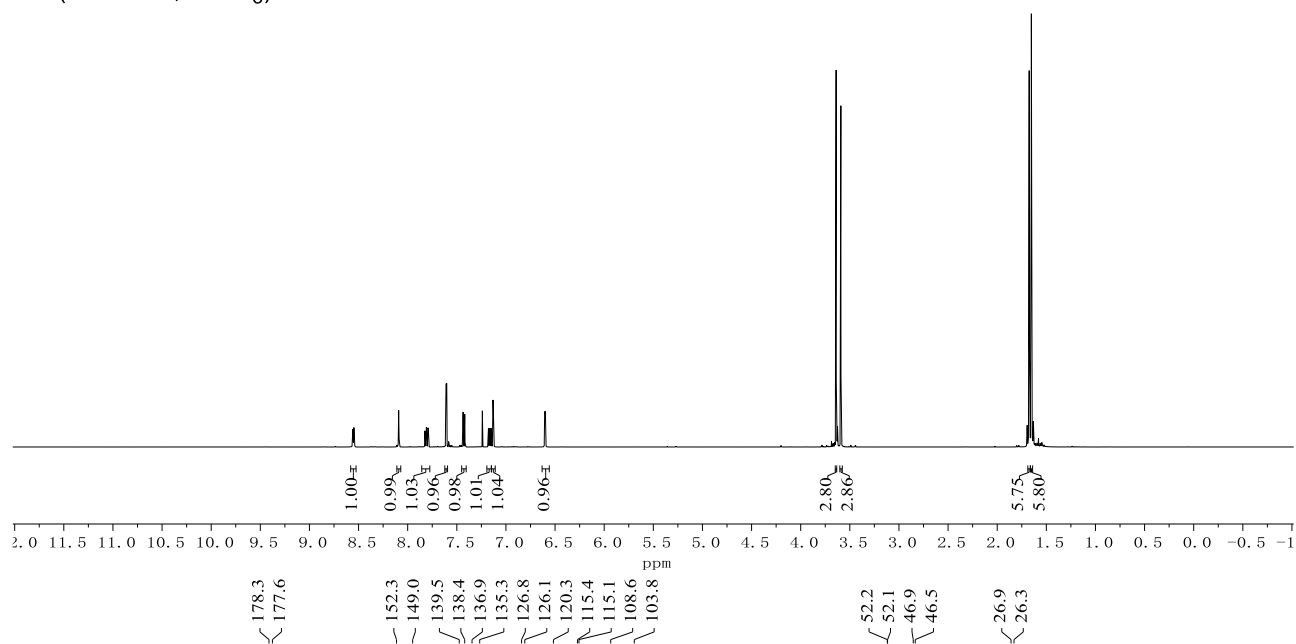
**397a**  
(100 MHz, CDCl<sub>3</sub>)



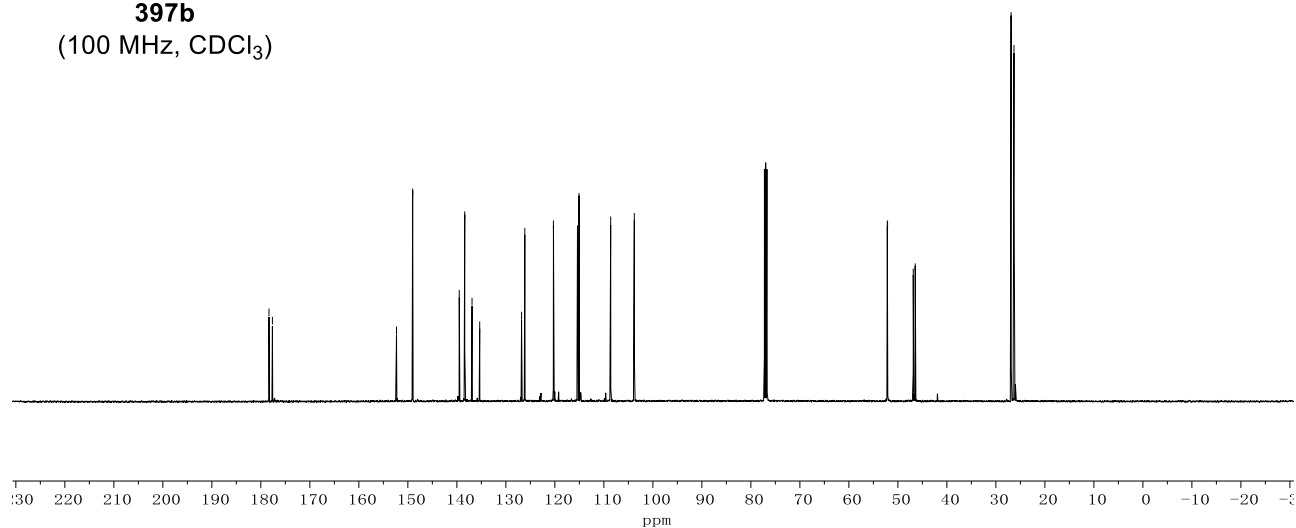
Appendix: NMR Spectra



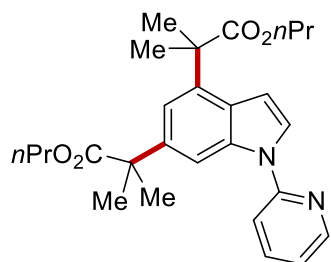
**397b**  
(400 MHz, CDCl<sub>3</sub>)



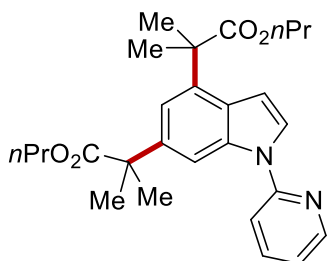
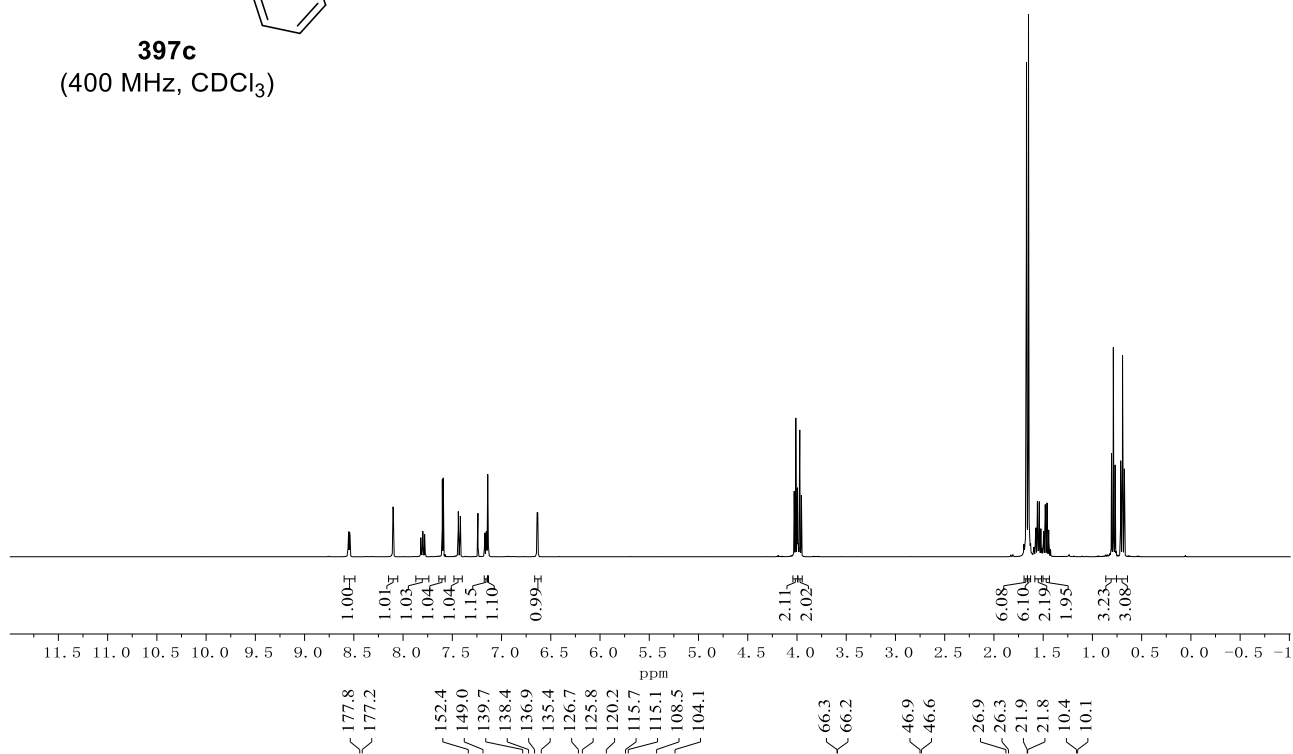
**397b**  
(100 MHz, CDCl<sub>3</sub>)



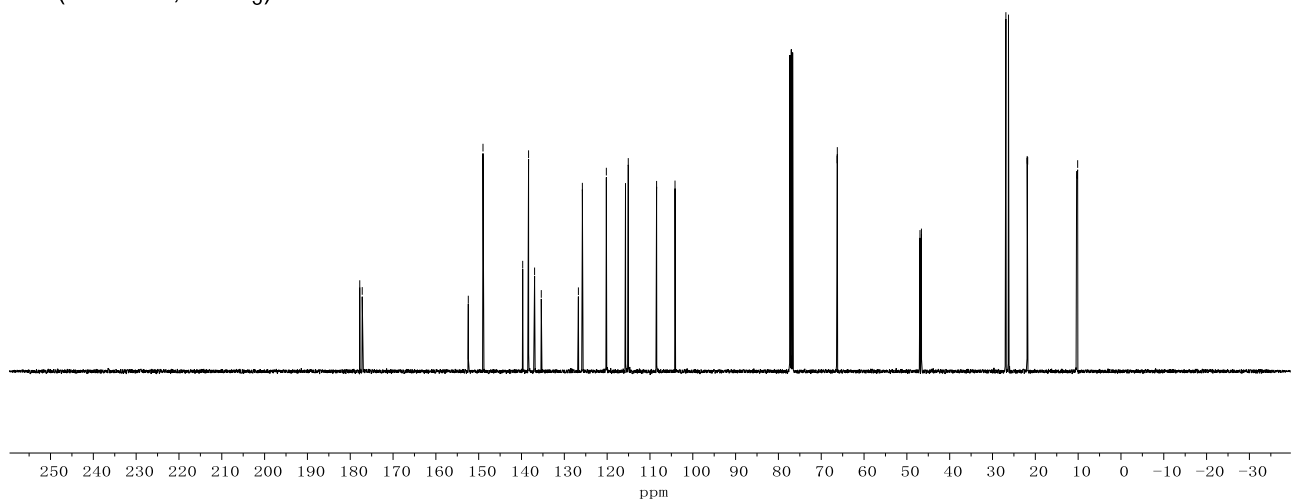
Appendix: NMR Spectra

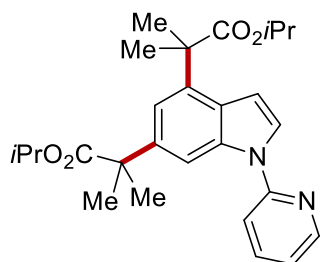


**397c**  
(400 MHz, CDCl<sub>3</sub>)

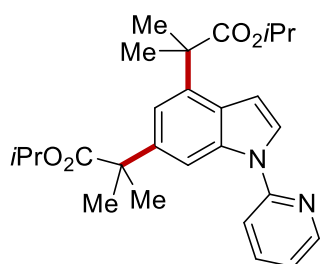
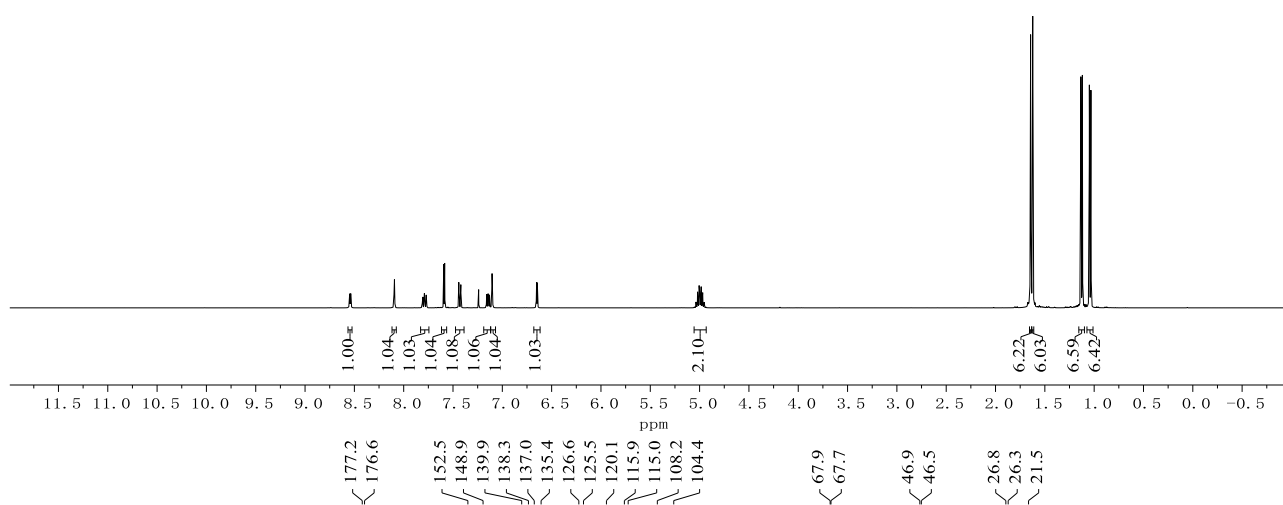


**397c**  
(100 MHz, CDCl<sub>3</sub>)

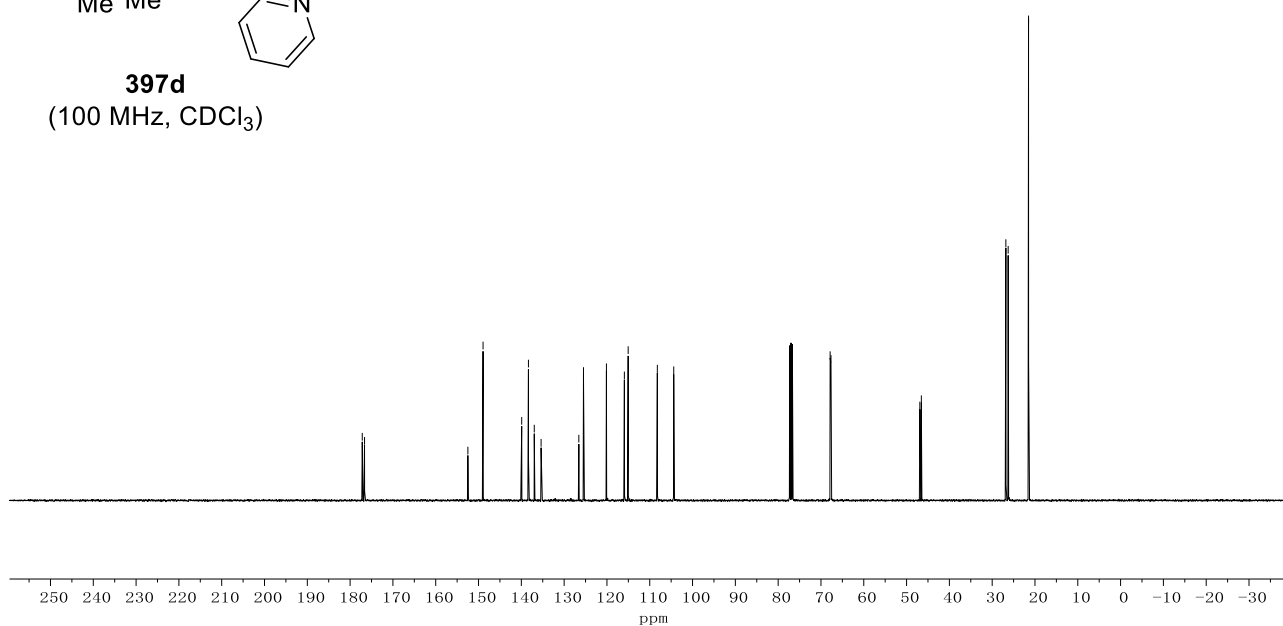


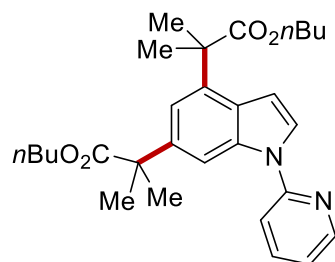


**397d**  
(400 MHz, CDCl<sub>3</sub>)

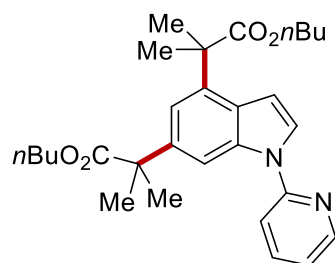
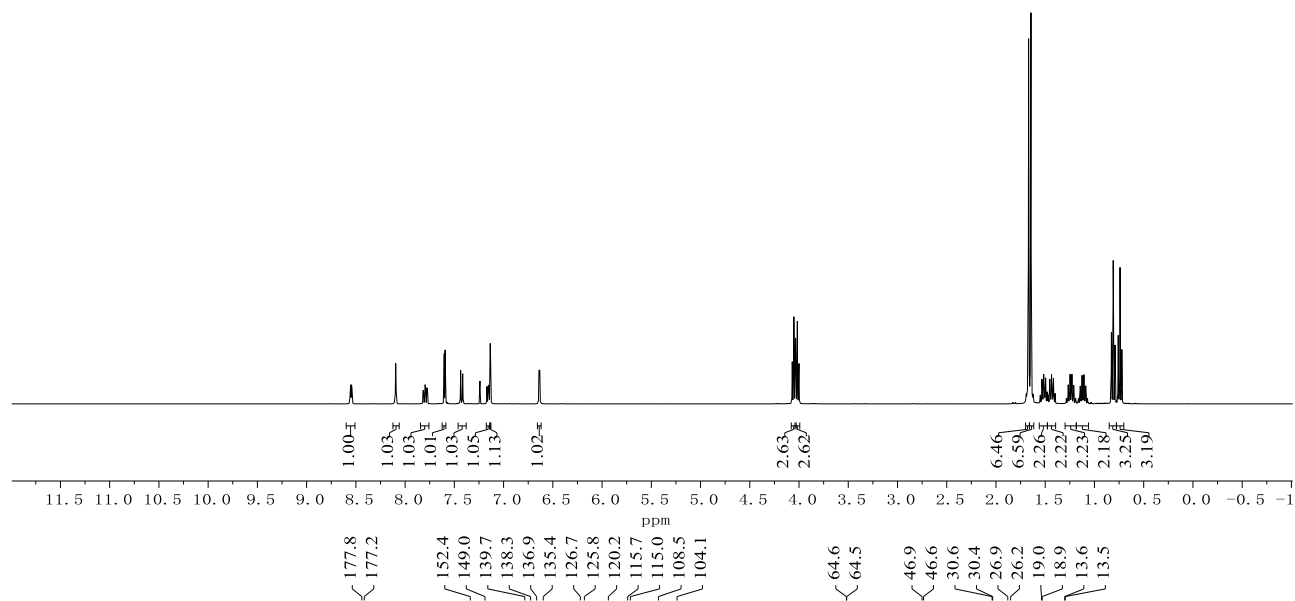


**397d**  
(100 MHz, CDCl<sub>3</sub>)

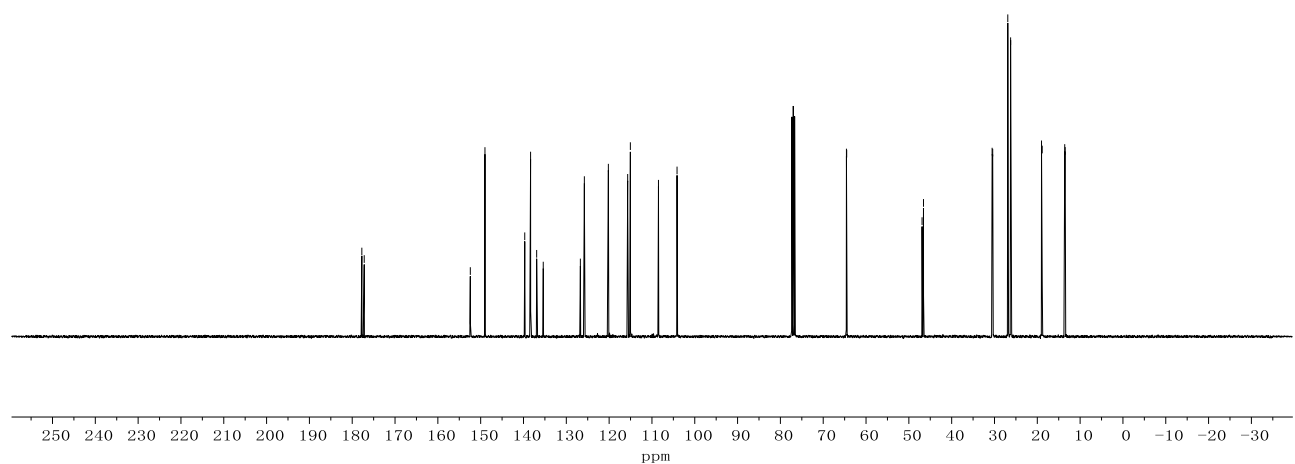


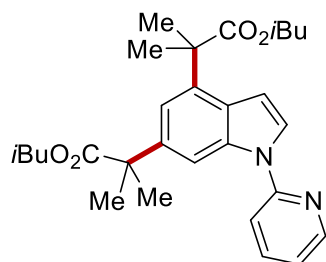


**397e**  
(400 MHz, CDCl<sub>3</sub>)

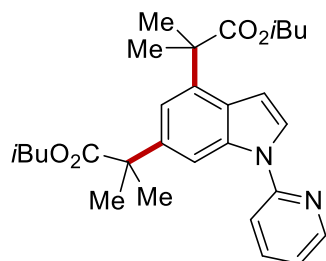
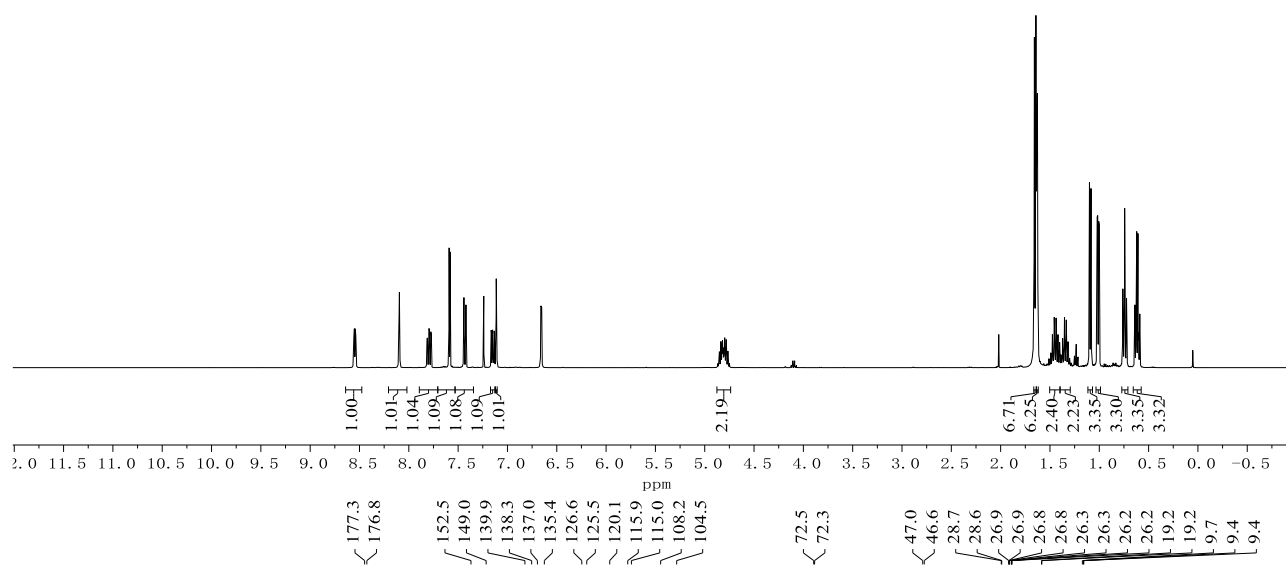


**397e**  
(100 MHz, CDCl<sub>3</sub>)

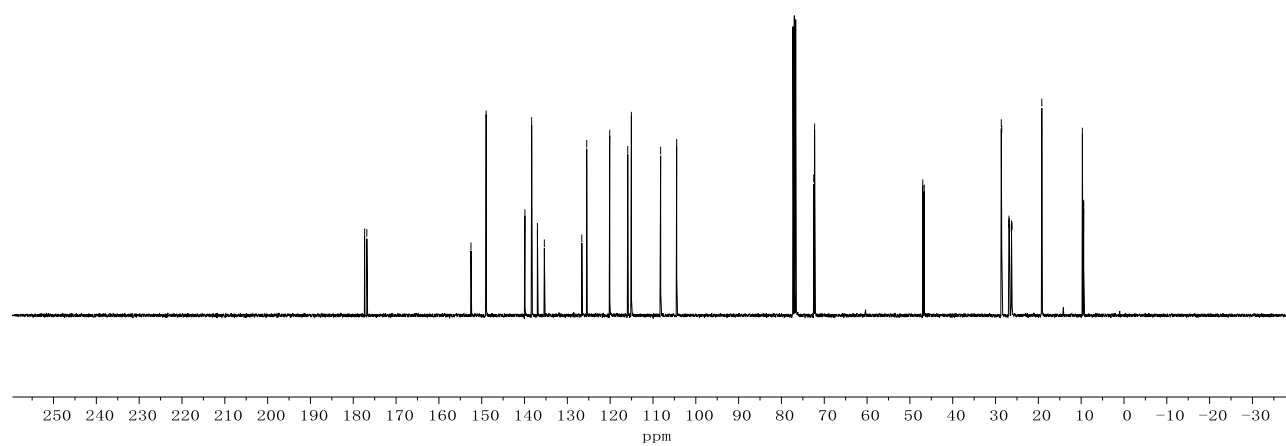


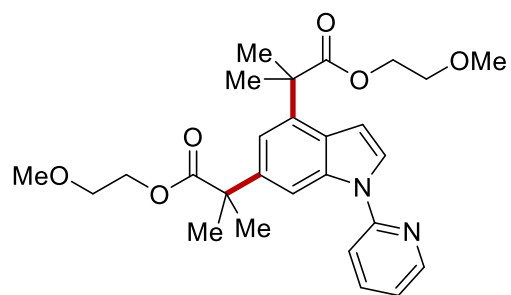


**397f**  
(400 MHz, CDCl<sub>3</sub>)

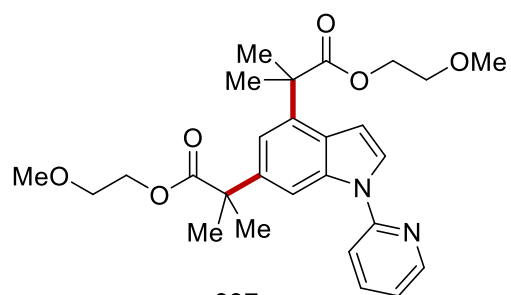
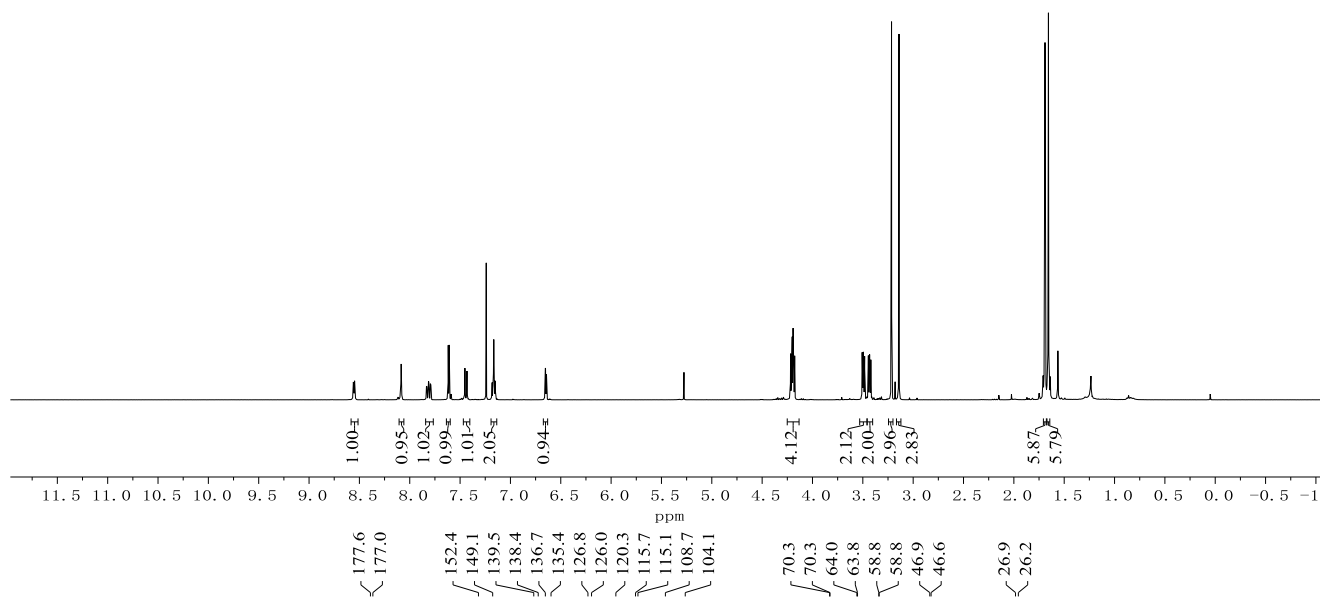


**397f**  
(100 MHz, CDCl<sub>3</sub>)

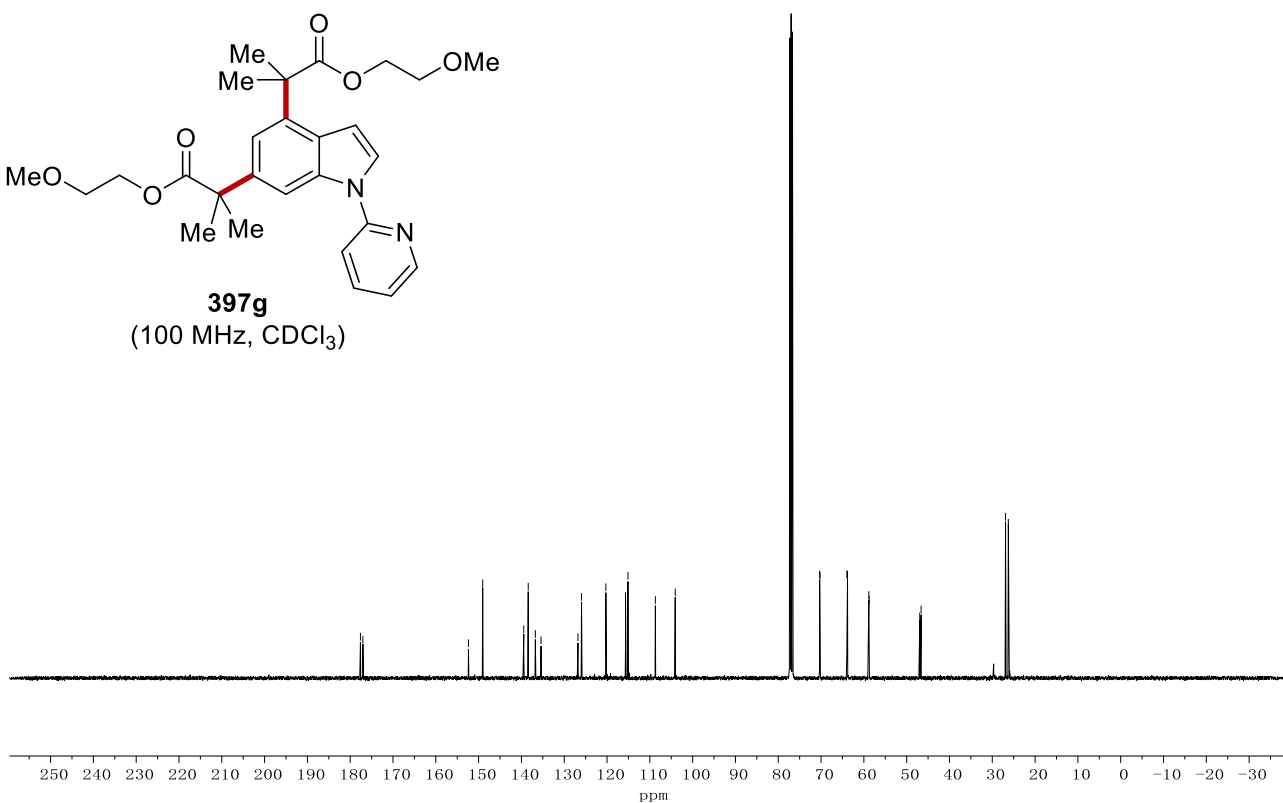


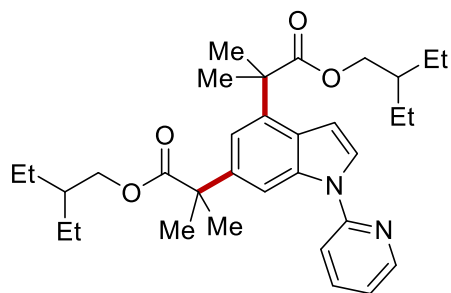


**397g**  
(400 MHz, CDCl<sub>3</sub>)

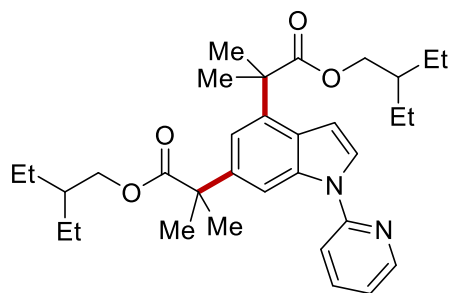
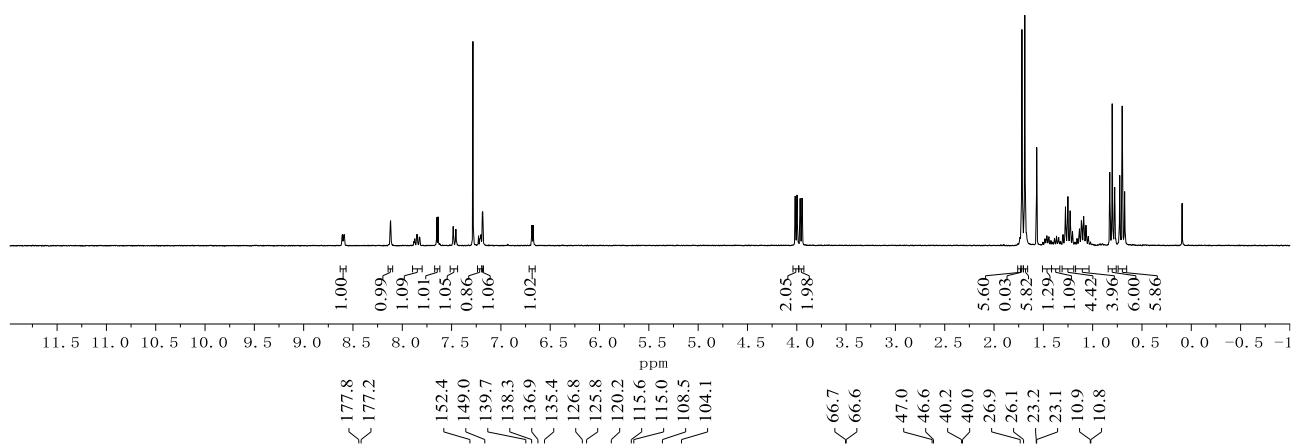


**397g**  
(100 MHz, CDCl<sub>3</sub>)

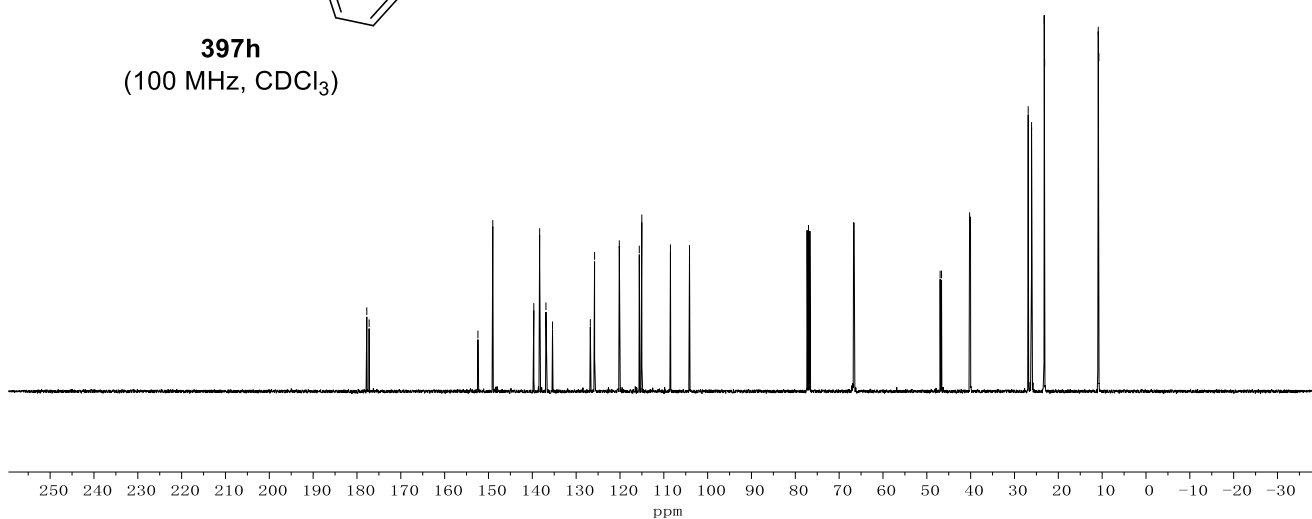




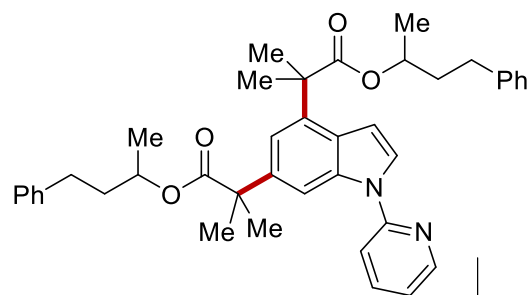
**397h**  
(400 MHz, CDCl<sub>3</sub>)



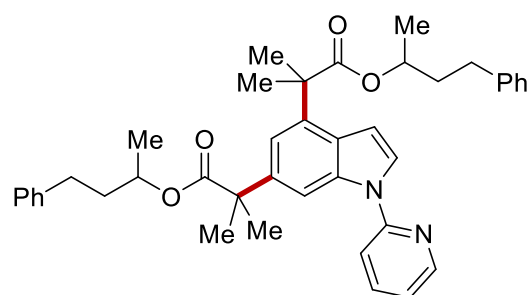
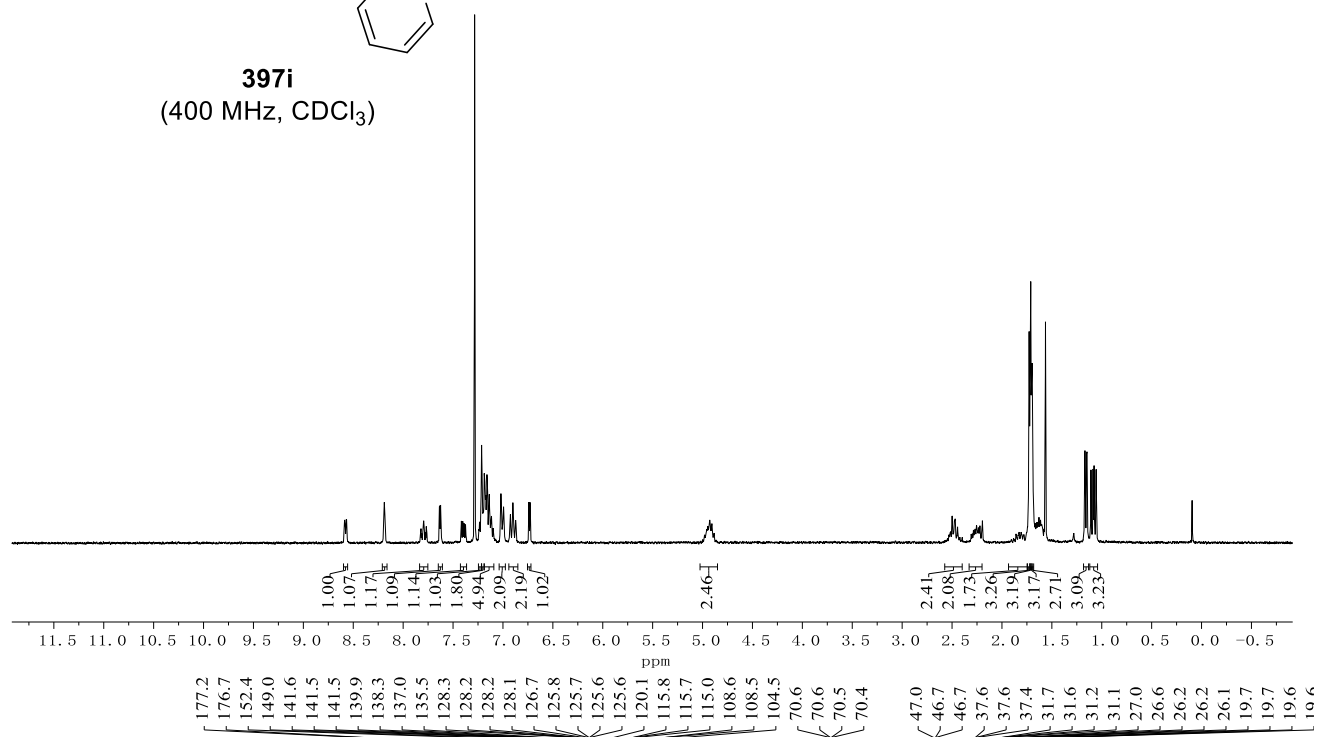
**397h**  
(100 MHz, CDCl<sub>3</sub>)



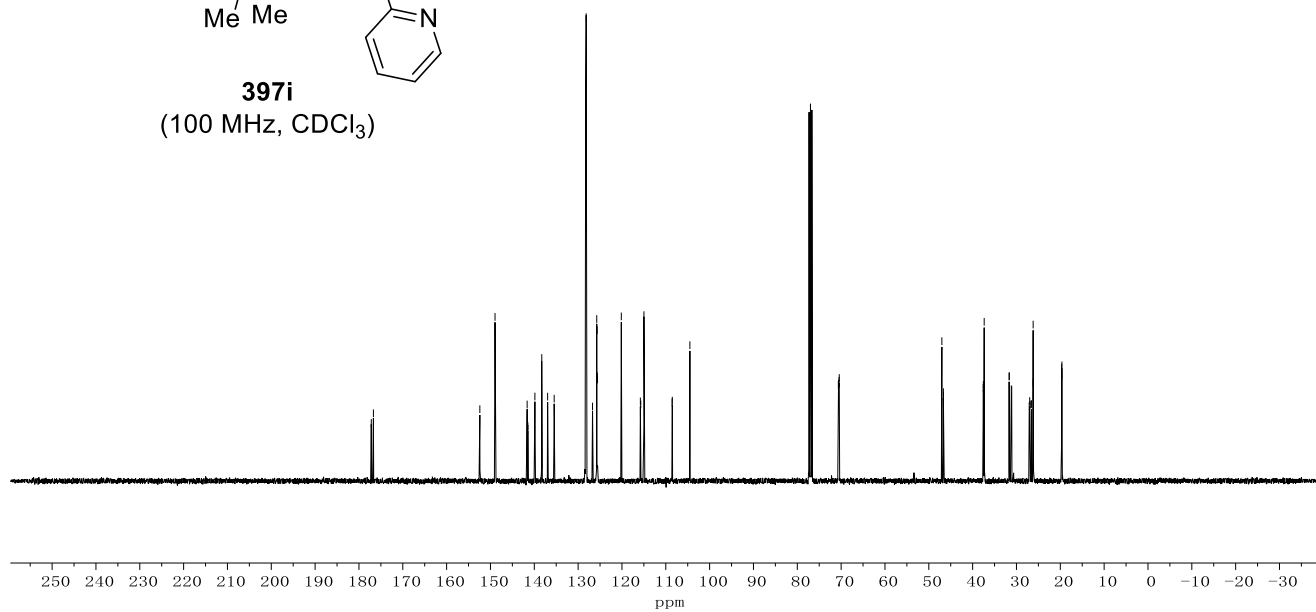


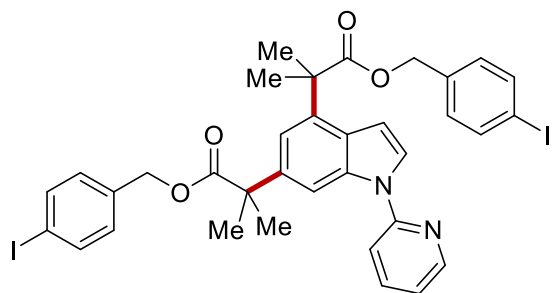


**397i**  
(400 MHz, CDCl<sub>3</sub>)

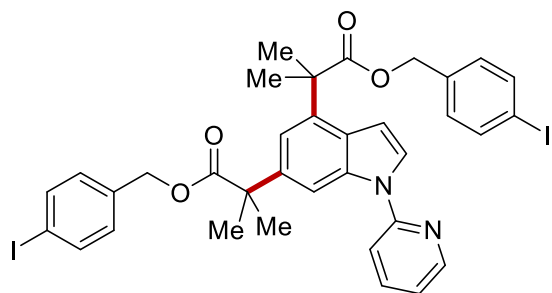
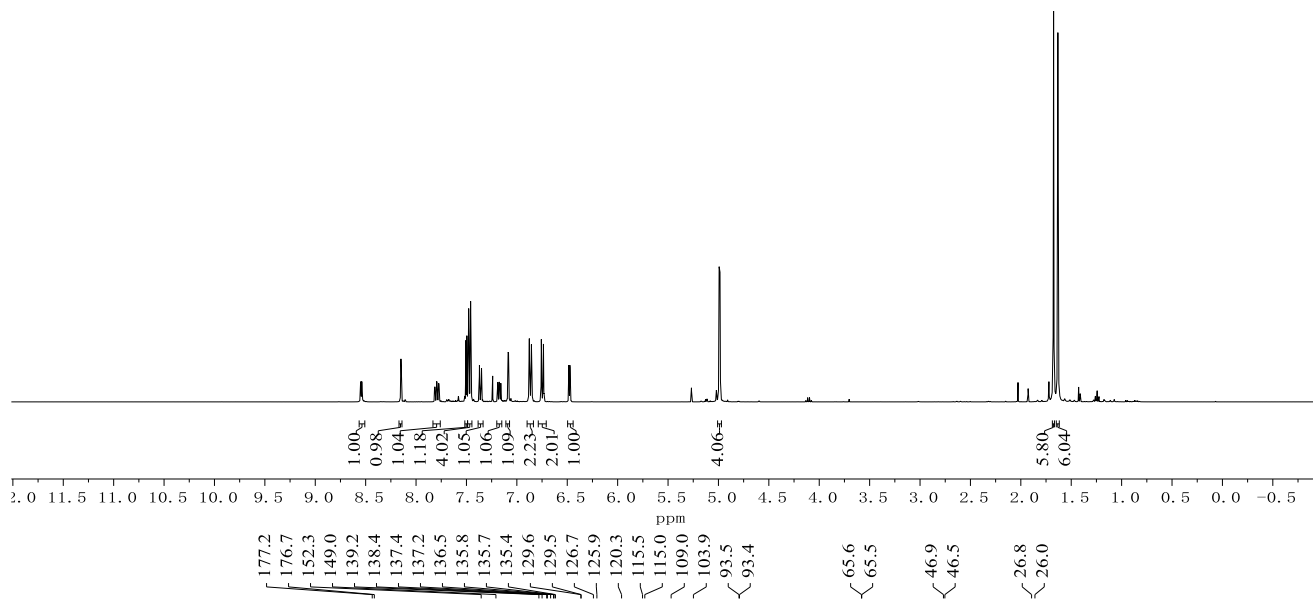


**397i**  
(100 MHz, CDCl<sub>3</sub>)

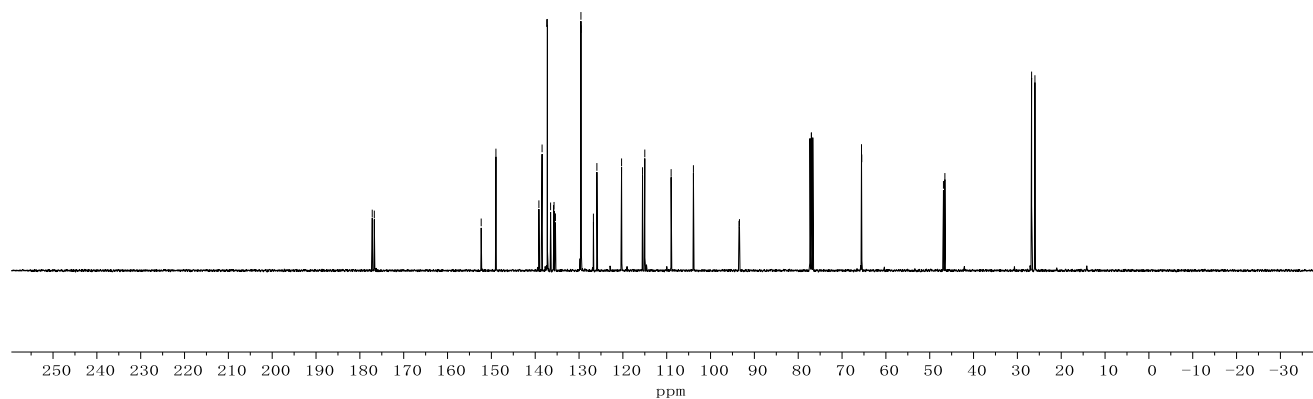


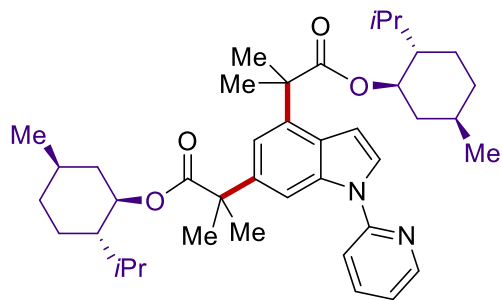


**397j**  
(400 MHz, CDCl<sub>3</sub>)

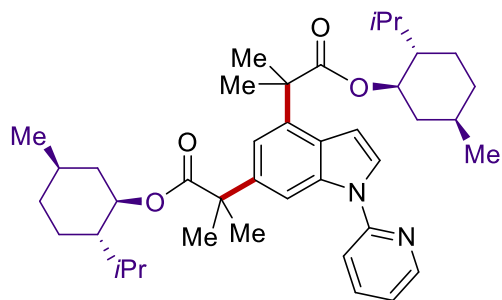
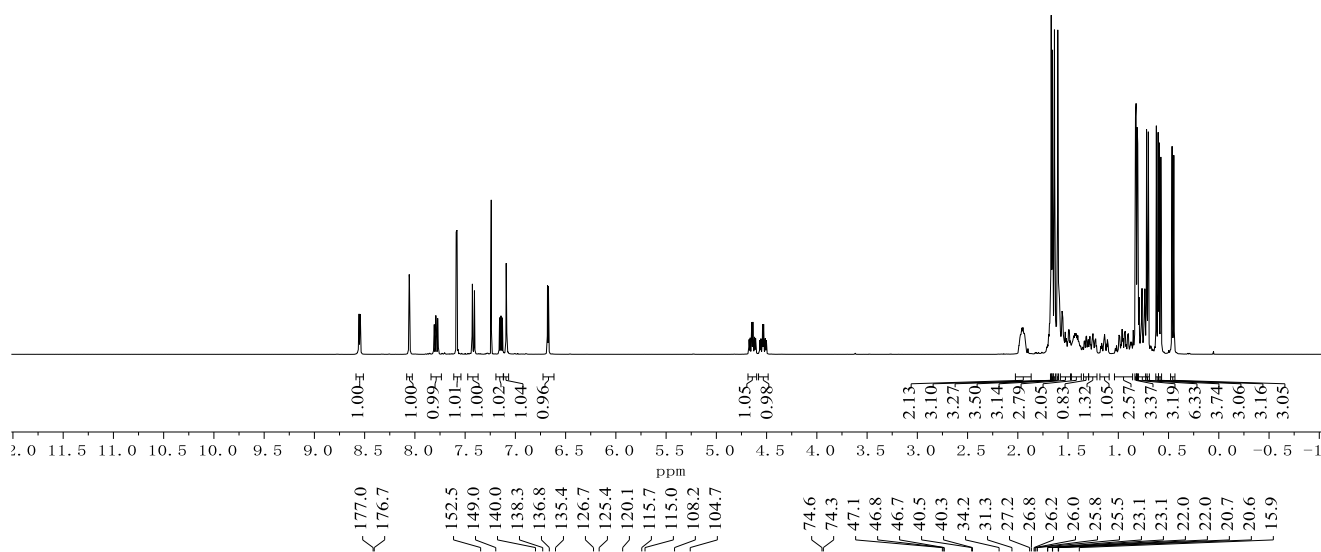


**397j**  
(100 MHz, CDCl<sub>3</sub>)

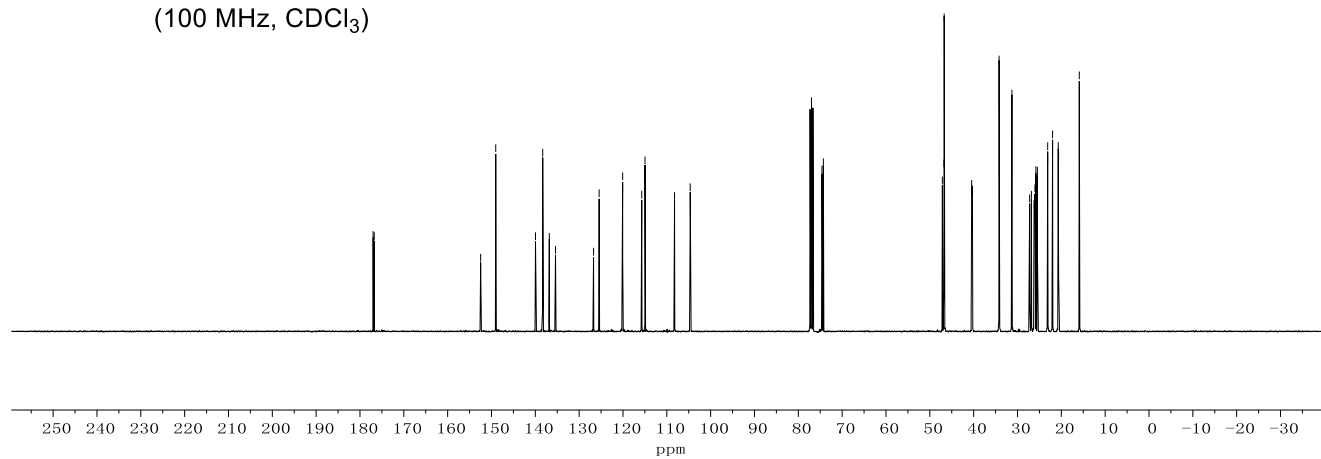




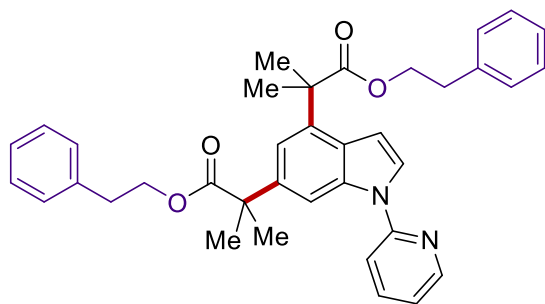
**397k**  
(400 MHz, CDCl<sub>3</sub>)



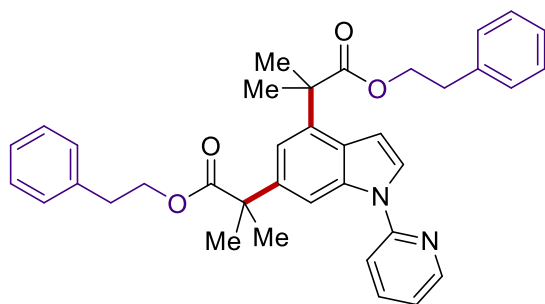
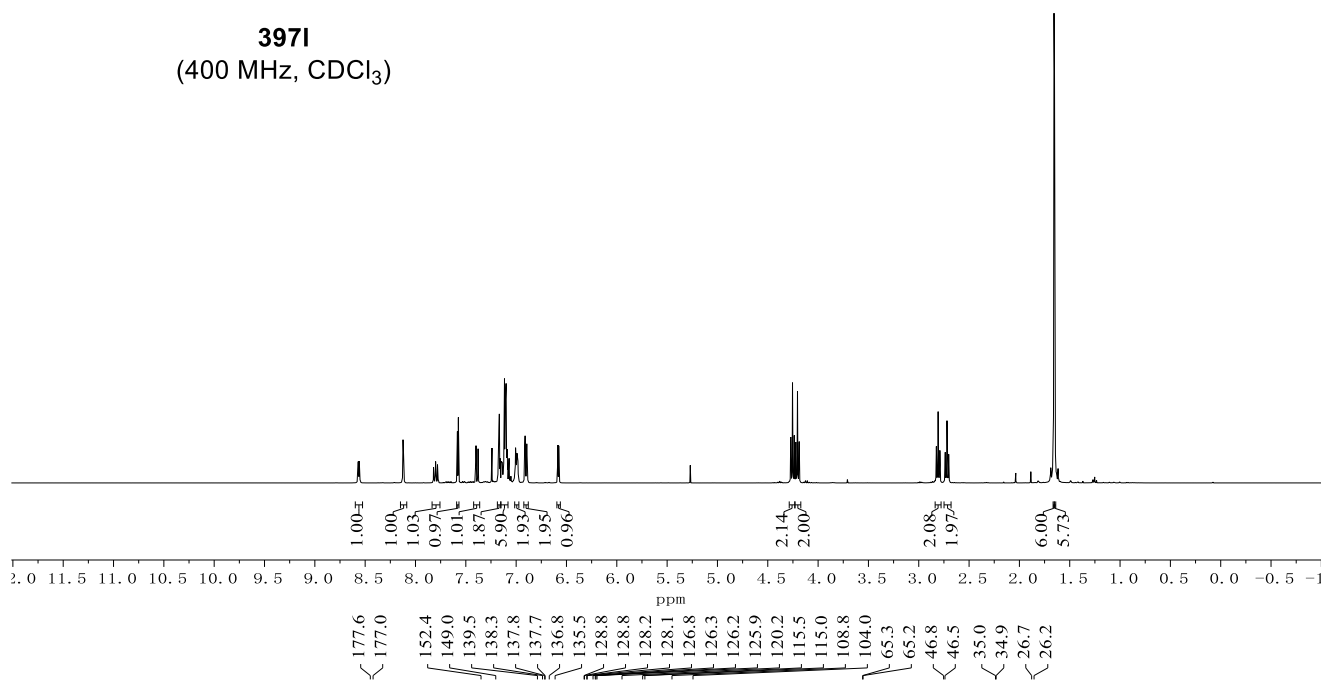
**397k**  
(100 MHz, CDCl<sub>3</sub>)



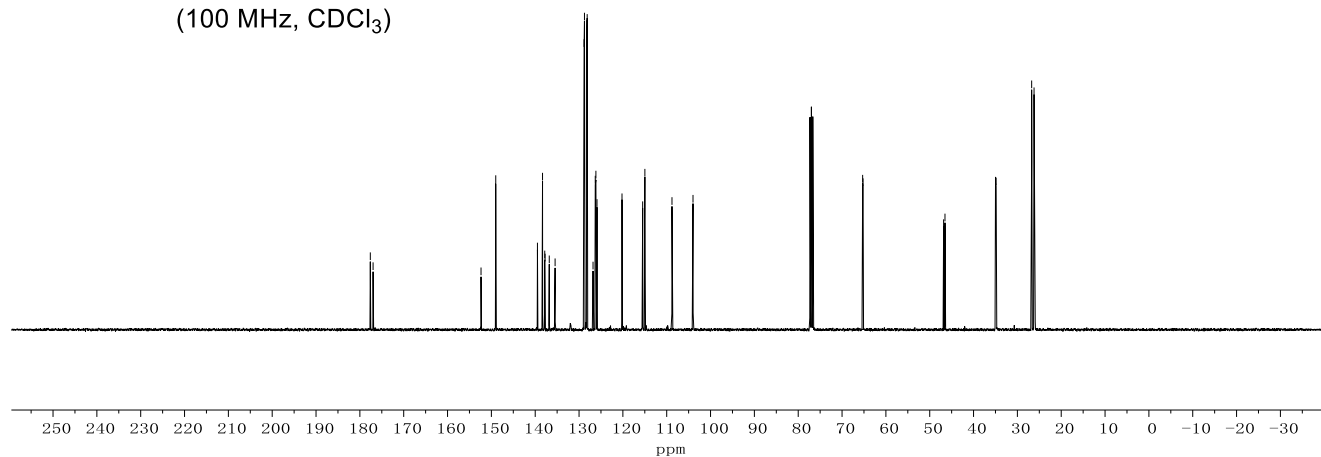
Appendix: NMR Spectra



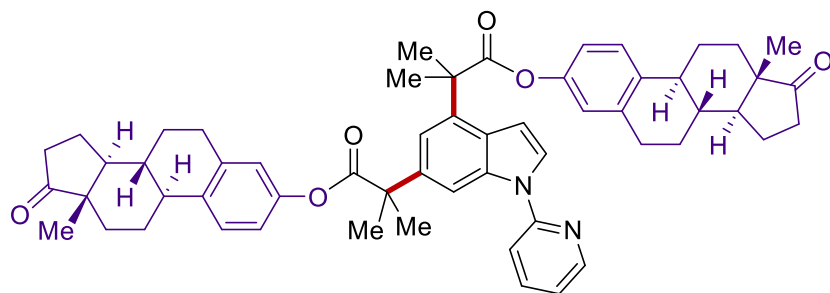
**3971**  
(400 MHz, CDCl<sub>3</sub>)



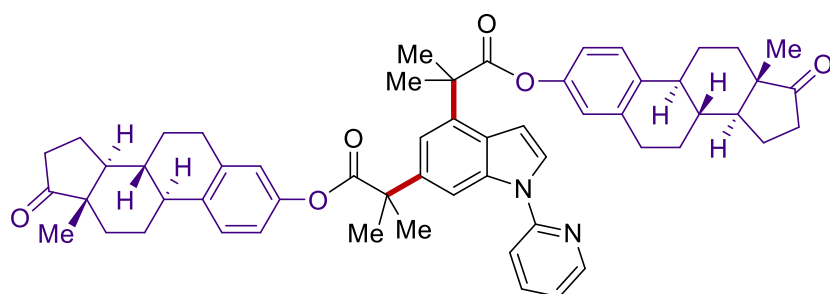
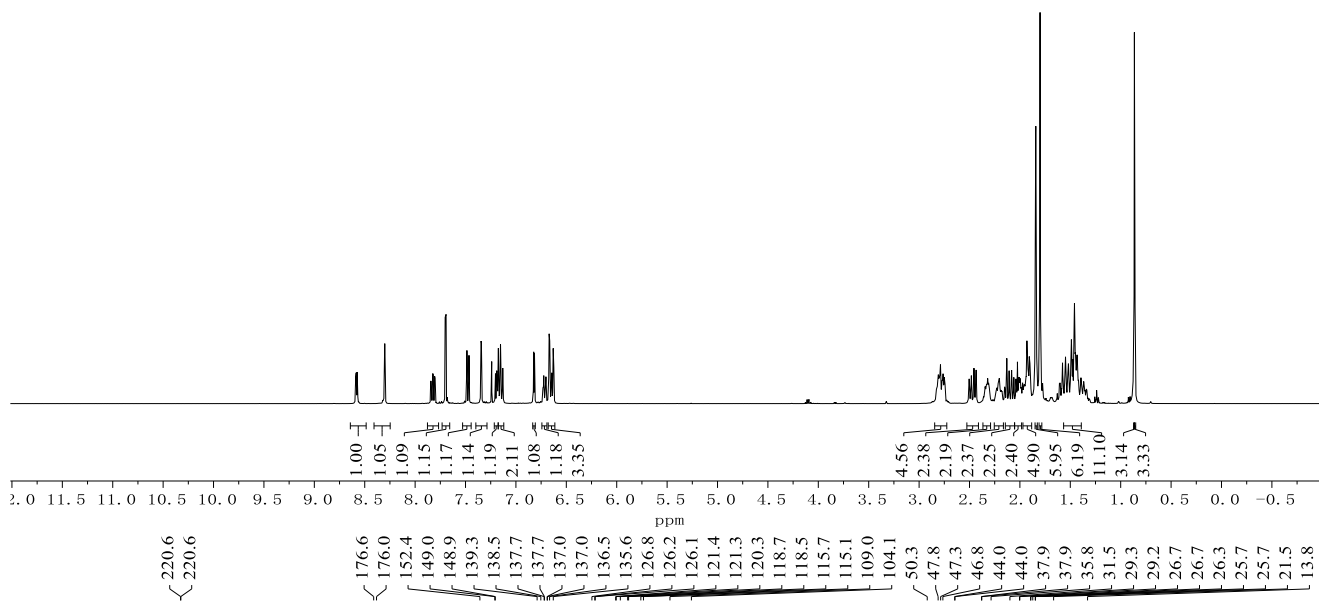
**3971**  
(100 MHz, CDCl<sub>3</sub>)



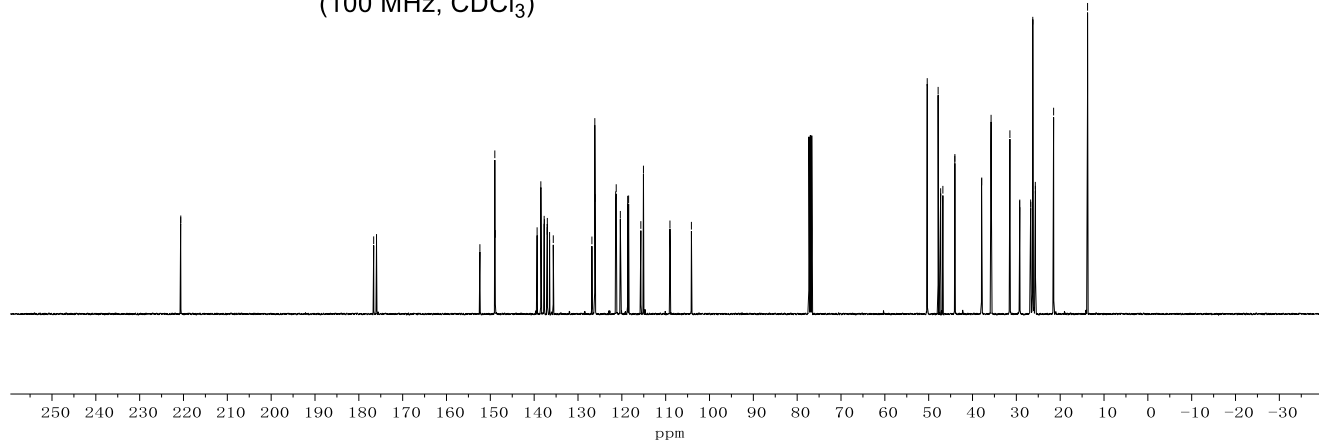
Appendix: NMR Spectra



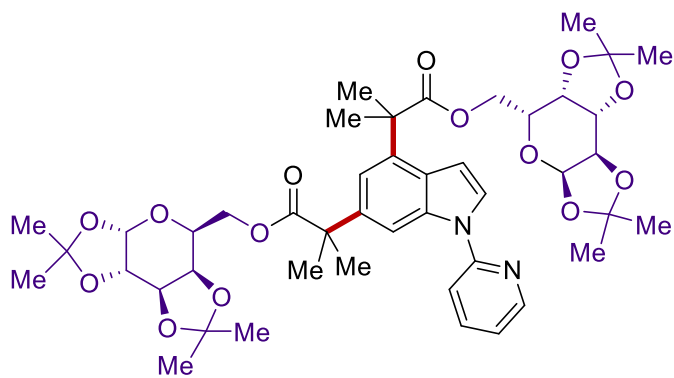
**397m**  
(400 MHz, CDCl<sub>3</sub>)



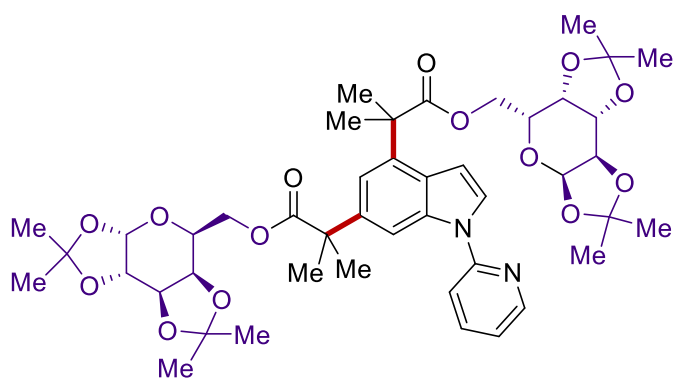
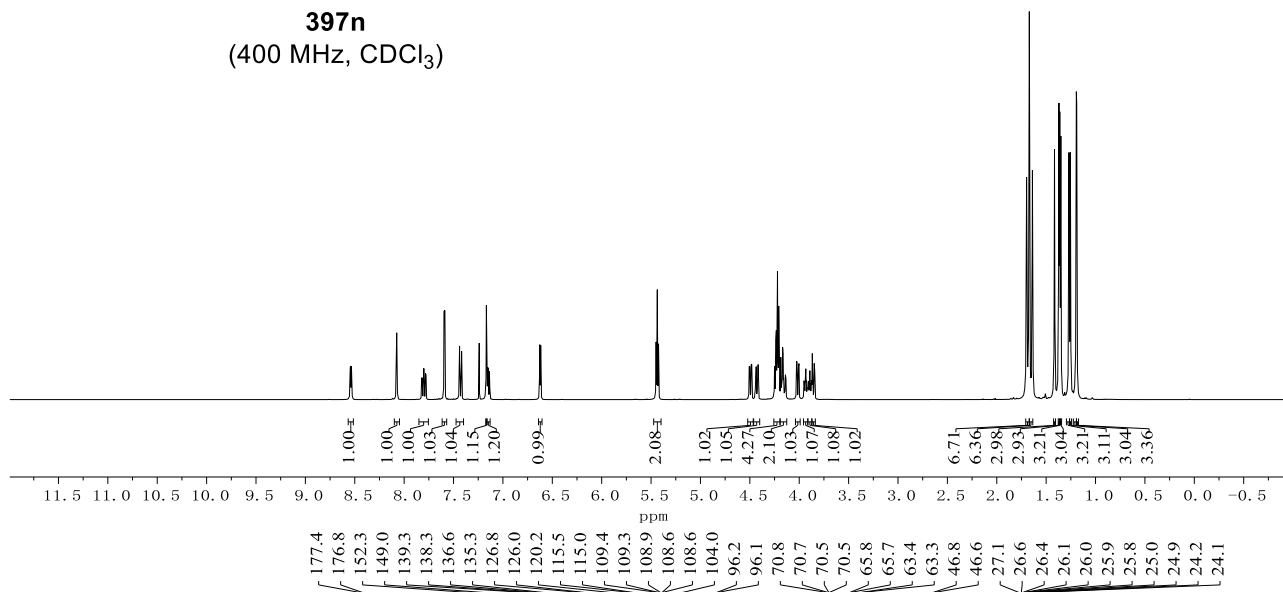
**397m**  
(100 MHz, CDCl<sub>3</sub>)



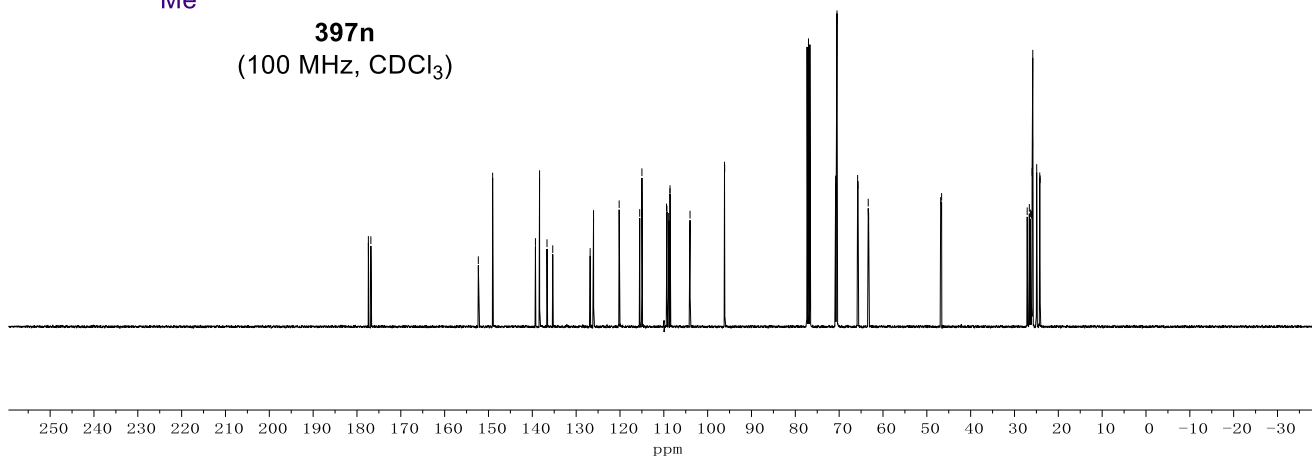
Appendix: NMR Spectra

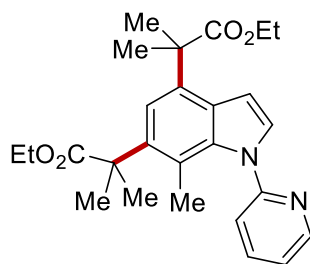


**397n**  
(400 MHz, CDCl<sub>3</sub>)

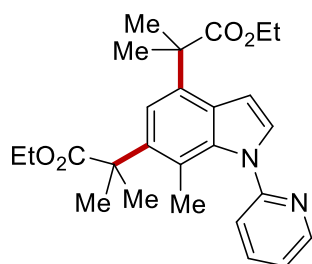
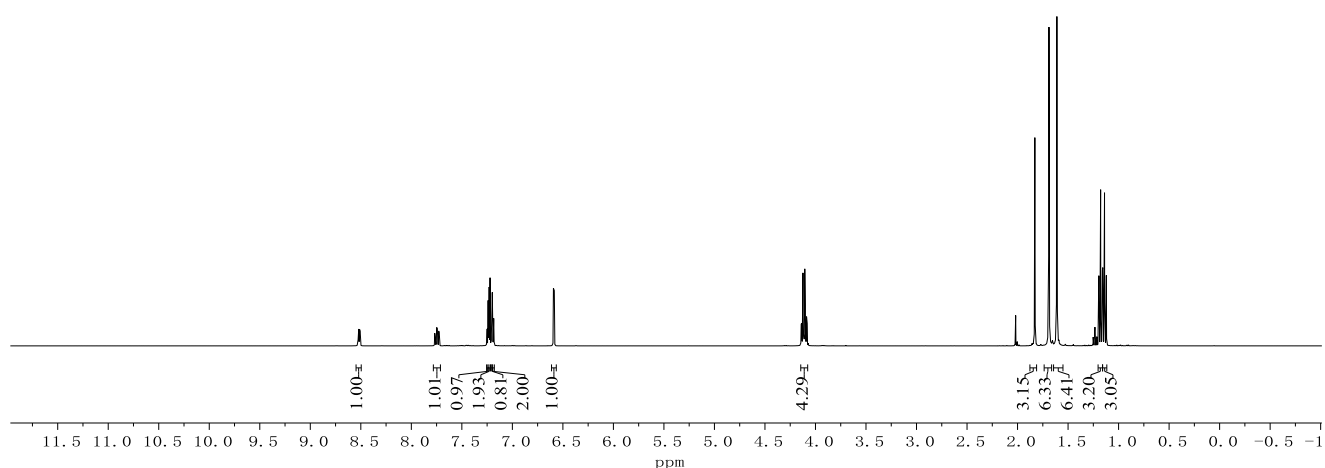


**397n**  
(100 MHz, CDCl<sub>3</sub>)

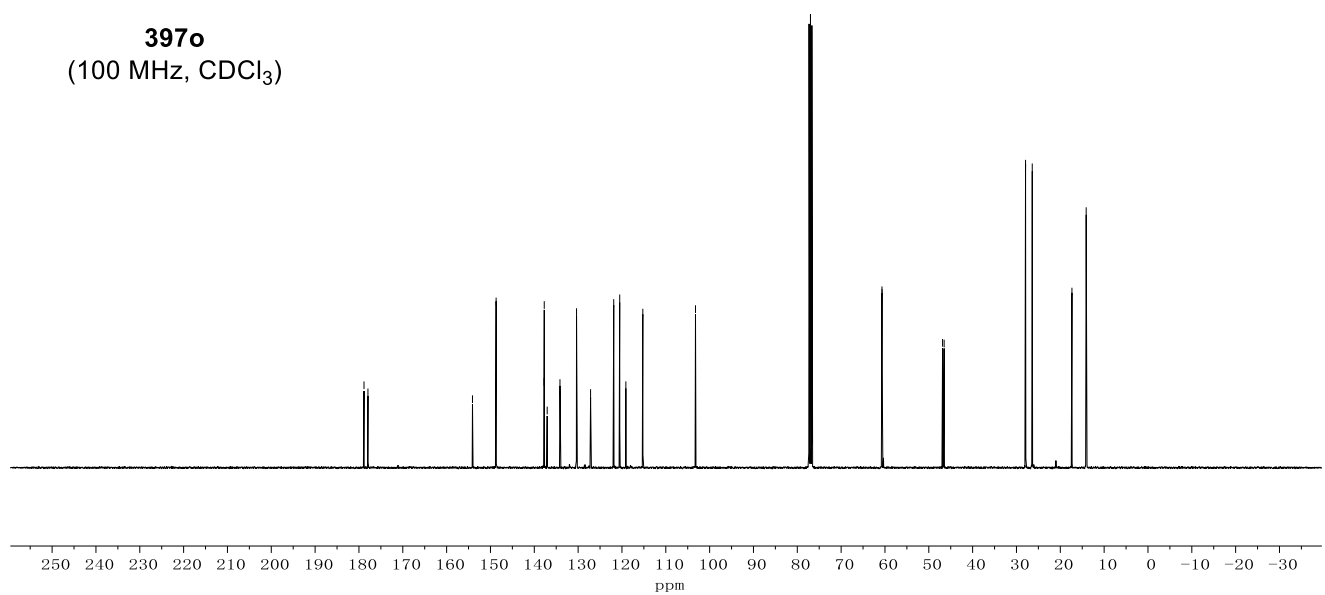


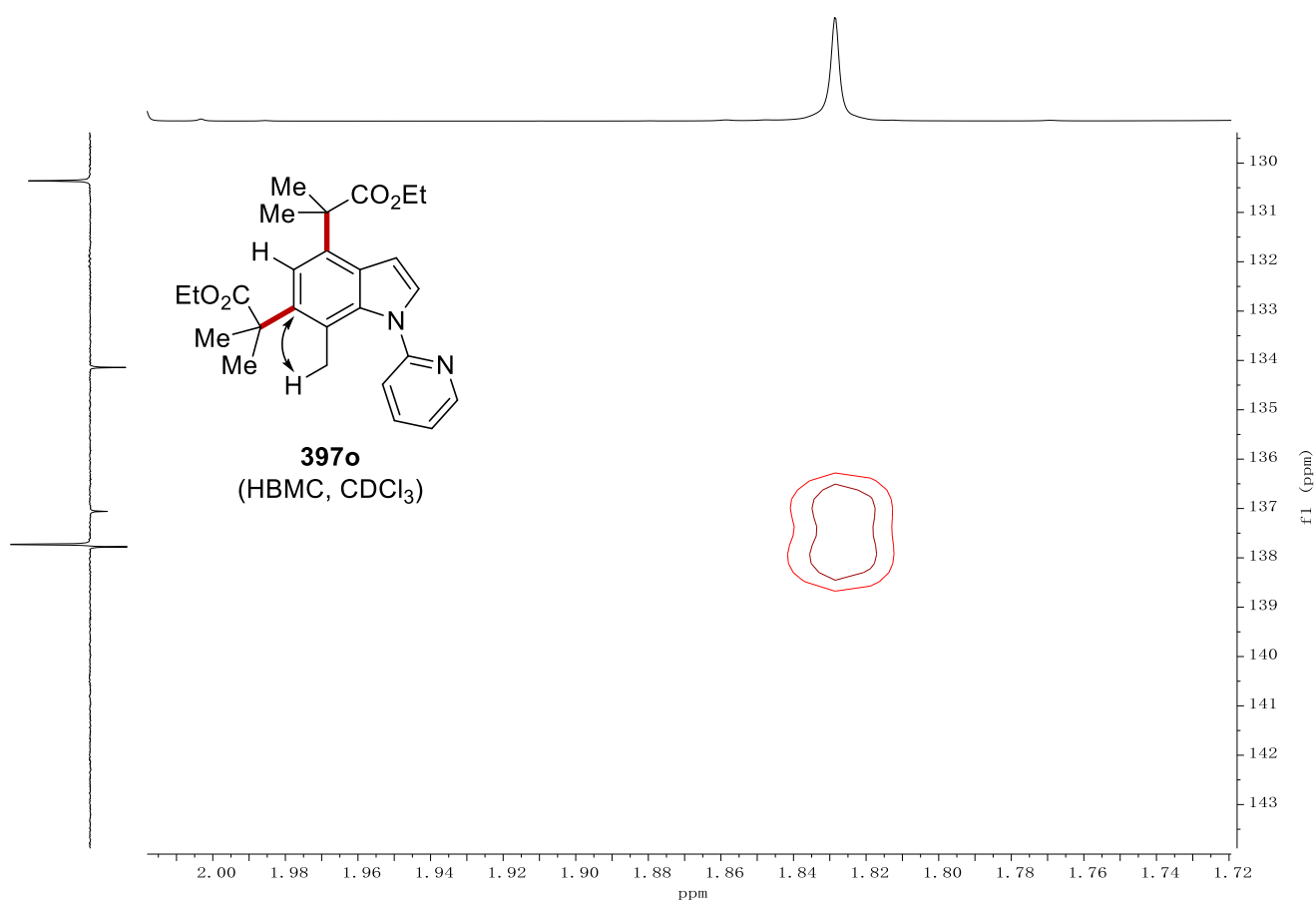
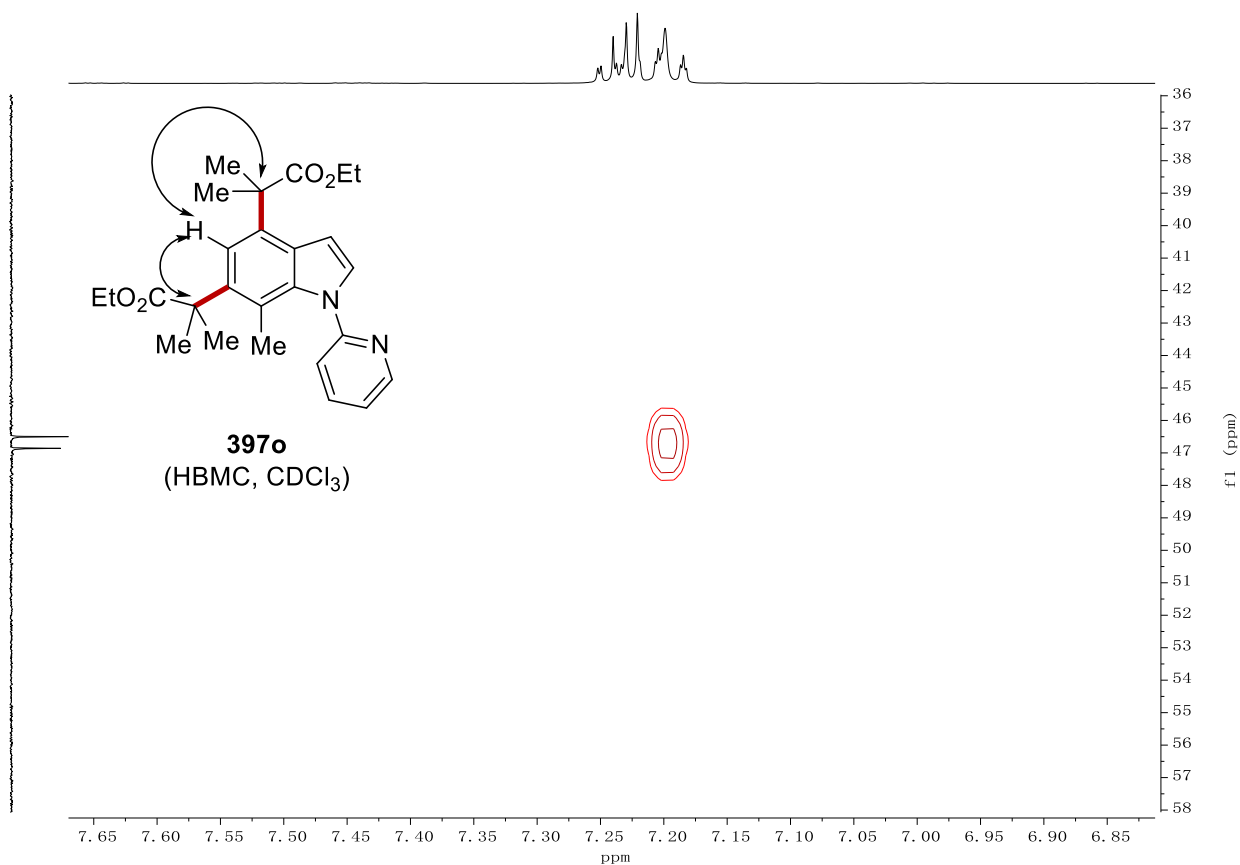


**397o**  
(400 MHz, CDCl<sub>3</sub>)



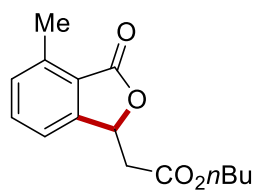
**397o**  
(100 MHz, CDCl<sub>3</sub>)



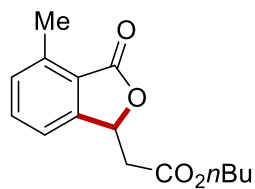
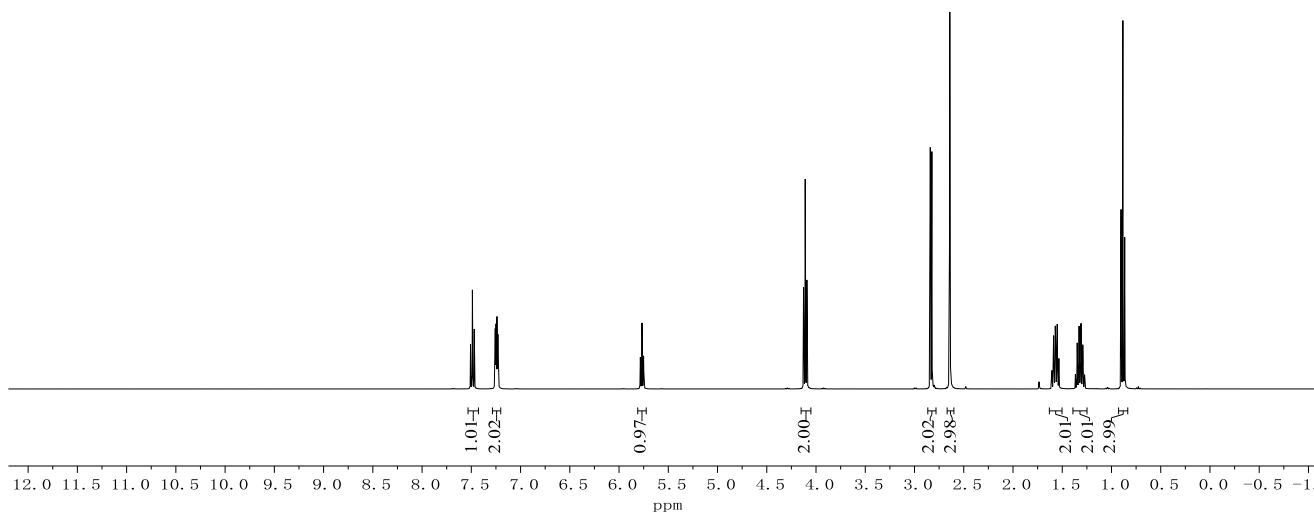




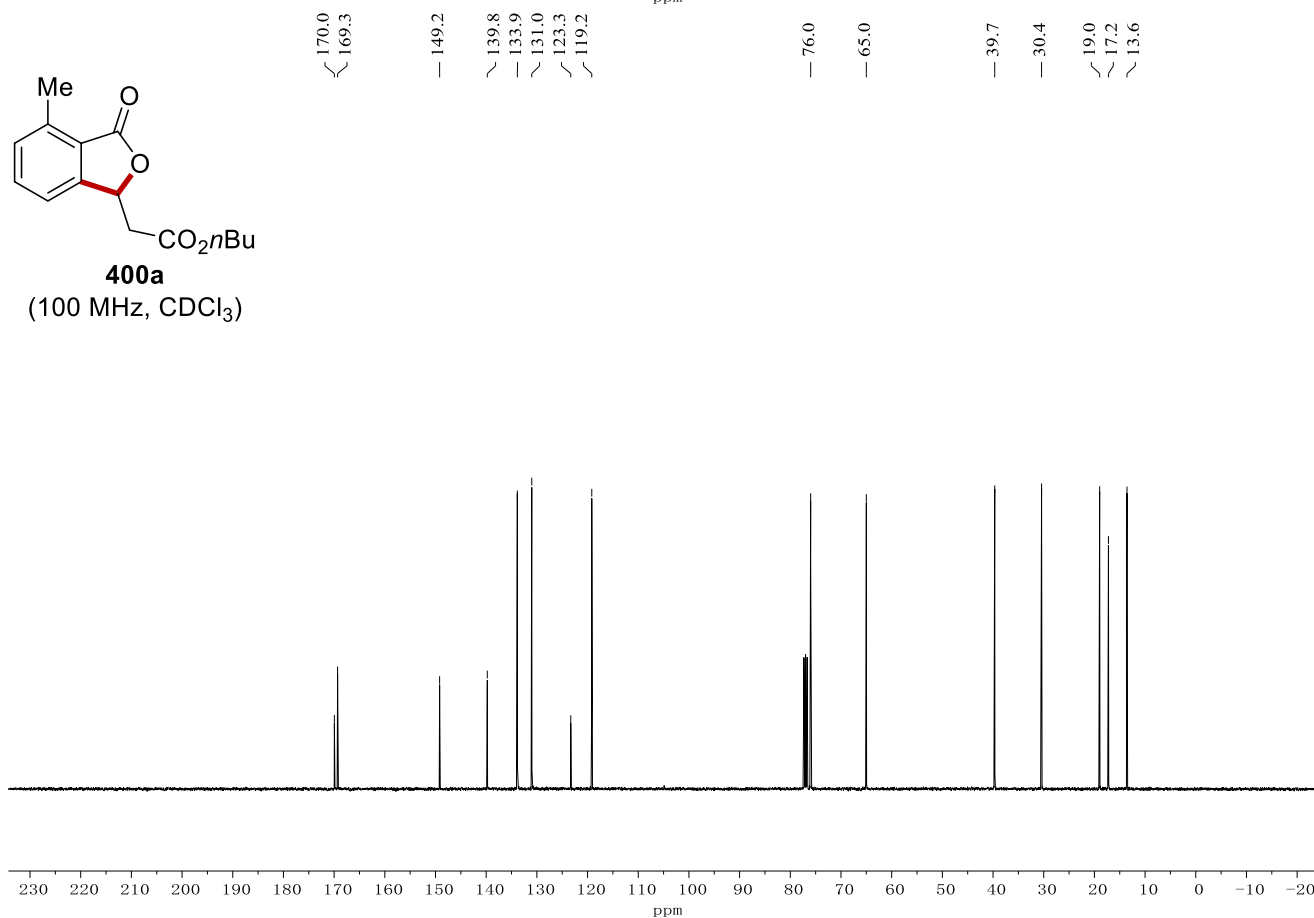
Appendix: NMR Spectra



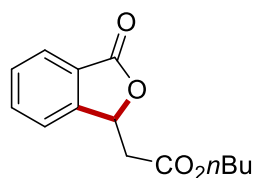
**400a**  
(400 MHz, CDCl<sub>3</sub>)



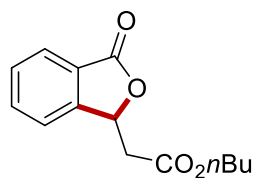
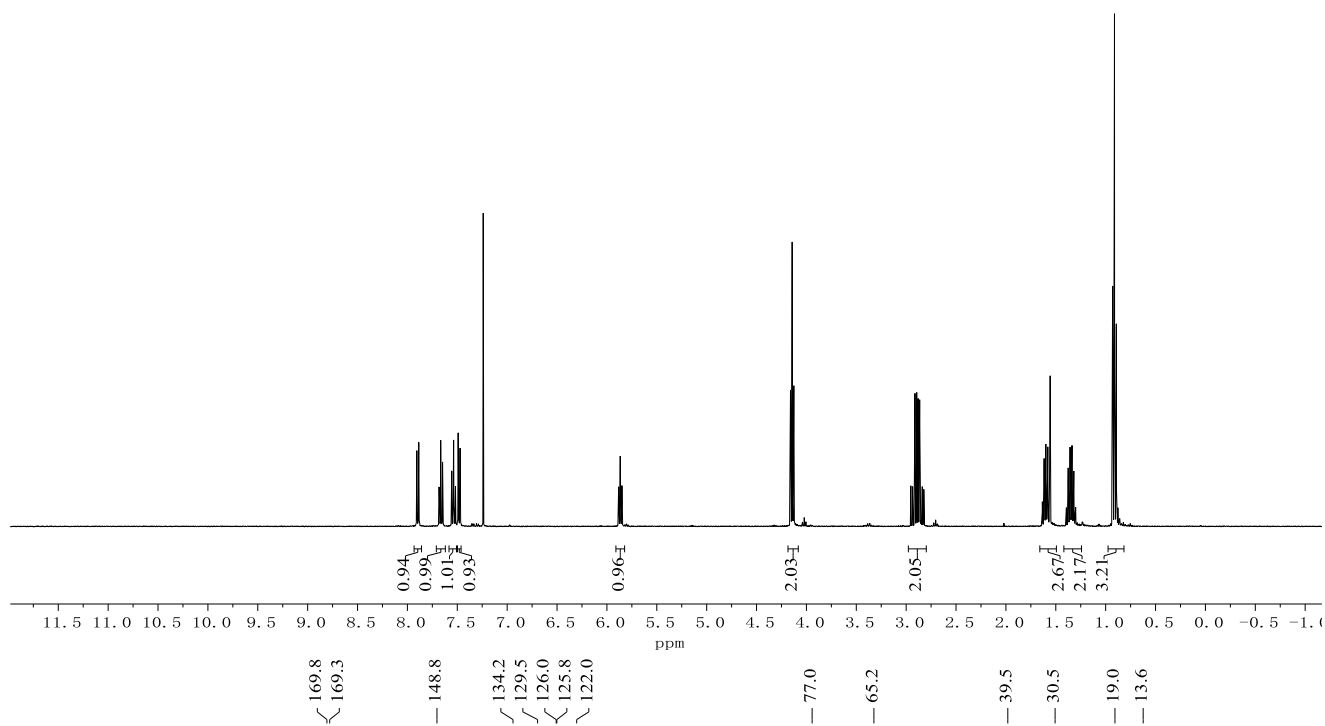
**400a**  
(100 MHz, CDCl<sub>3</sub>)



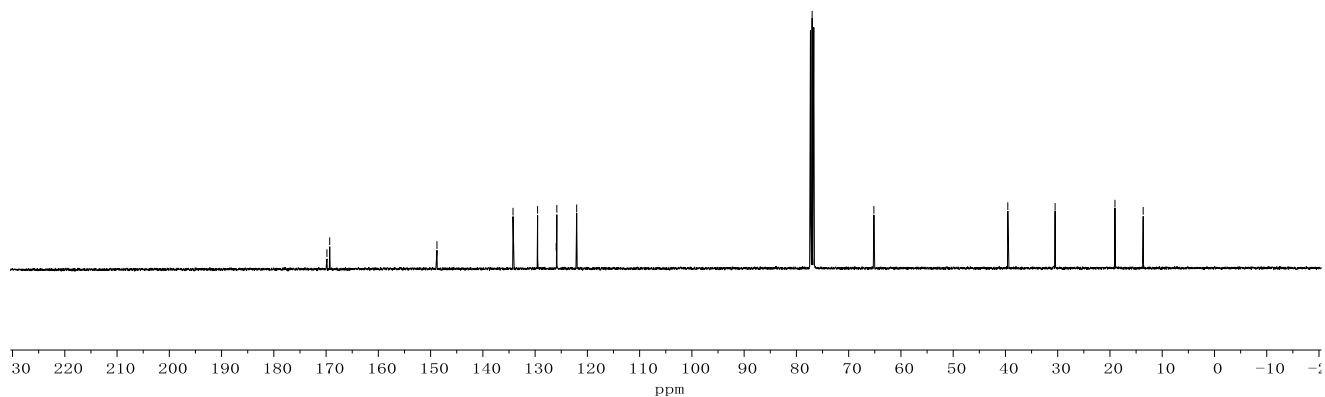
Appendix: NMR Spectra



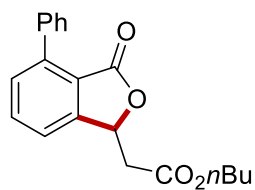
**400b**  
(400 MHz, CDCl<sub>3</sub>)



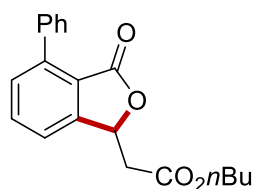
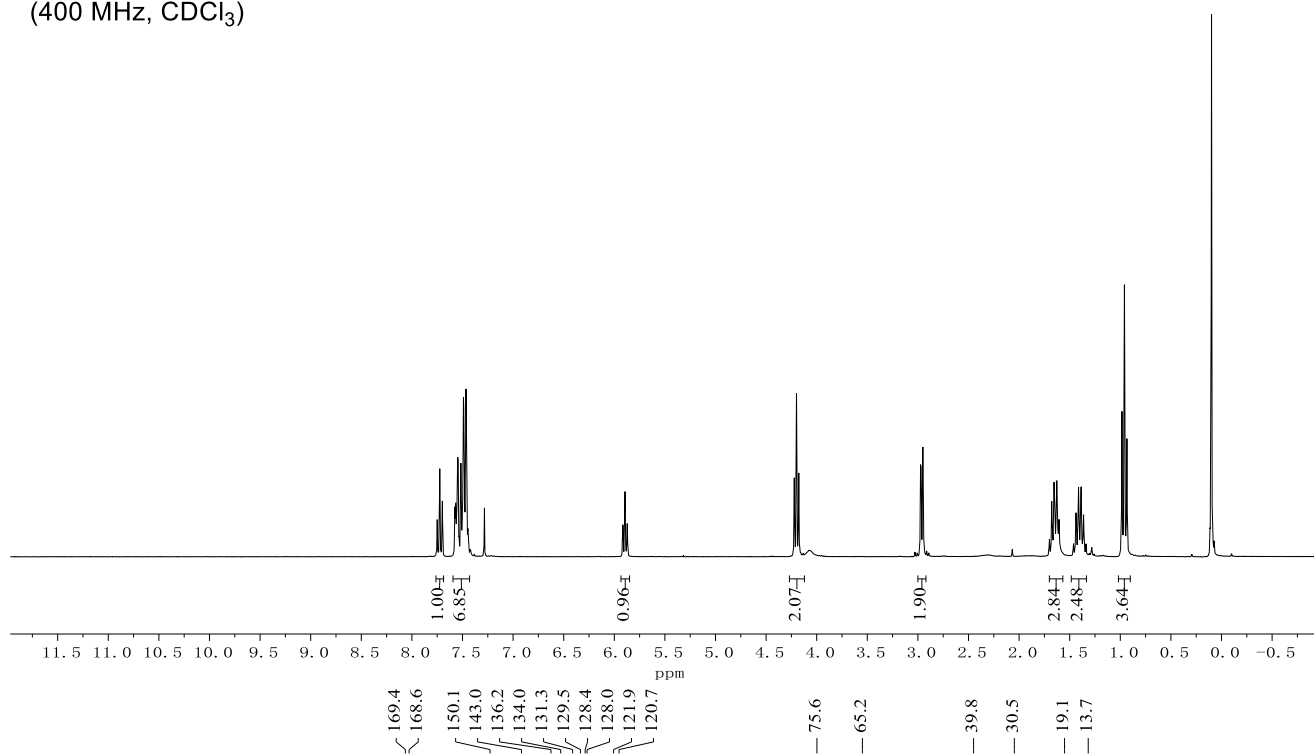
**400b**  
(100 MHz, CDCl<sub>3</sub>)



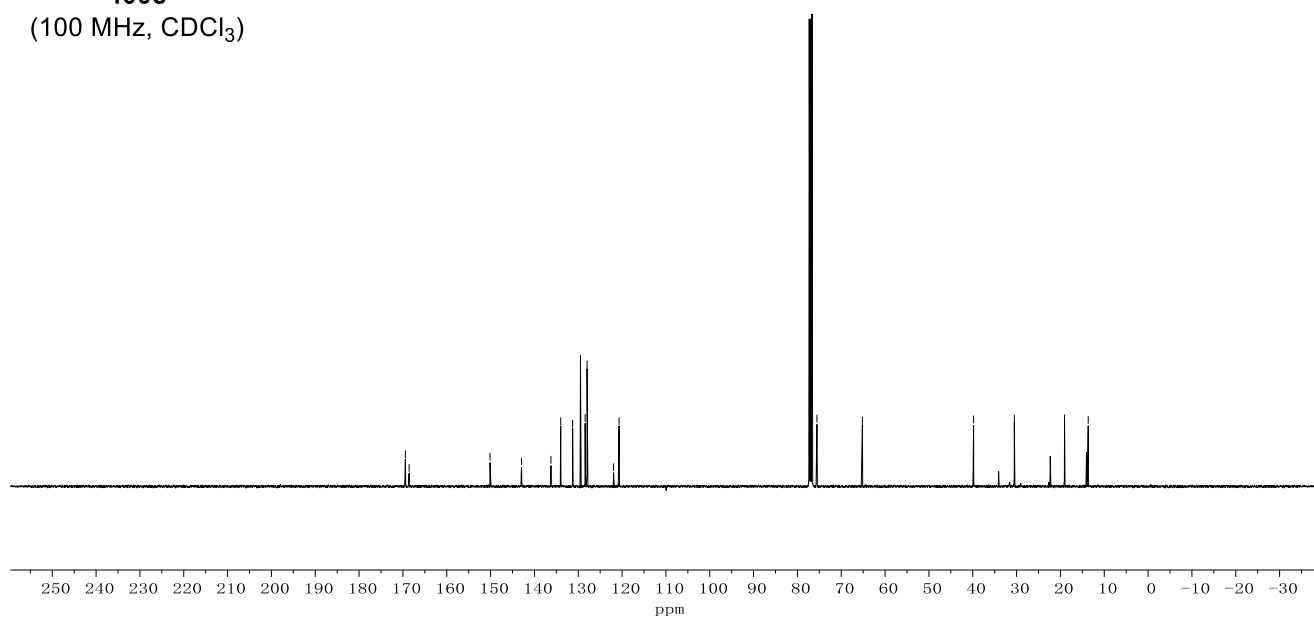
Appendix: NMR Spectra



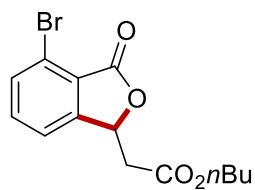
**400c**  
(400 MHz, CDCl<sub>3</sub>)



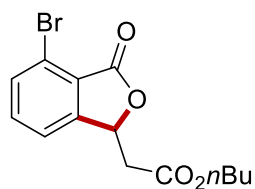
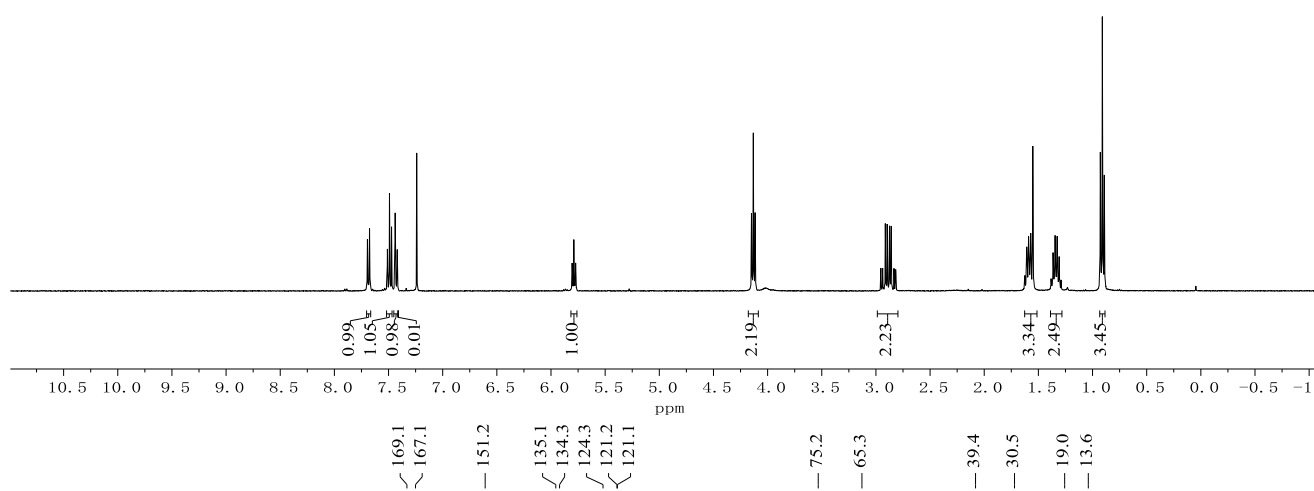
**400c**  
(100 MHz, CDCl<sub>3</sub>)



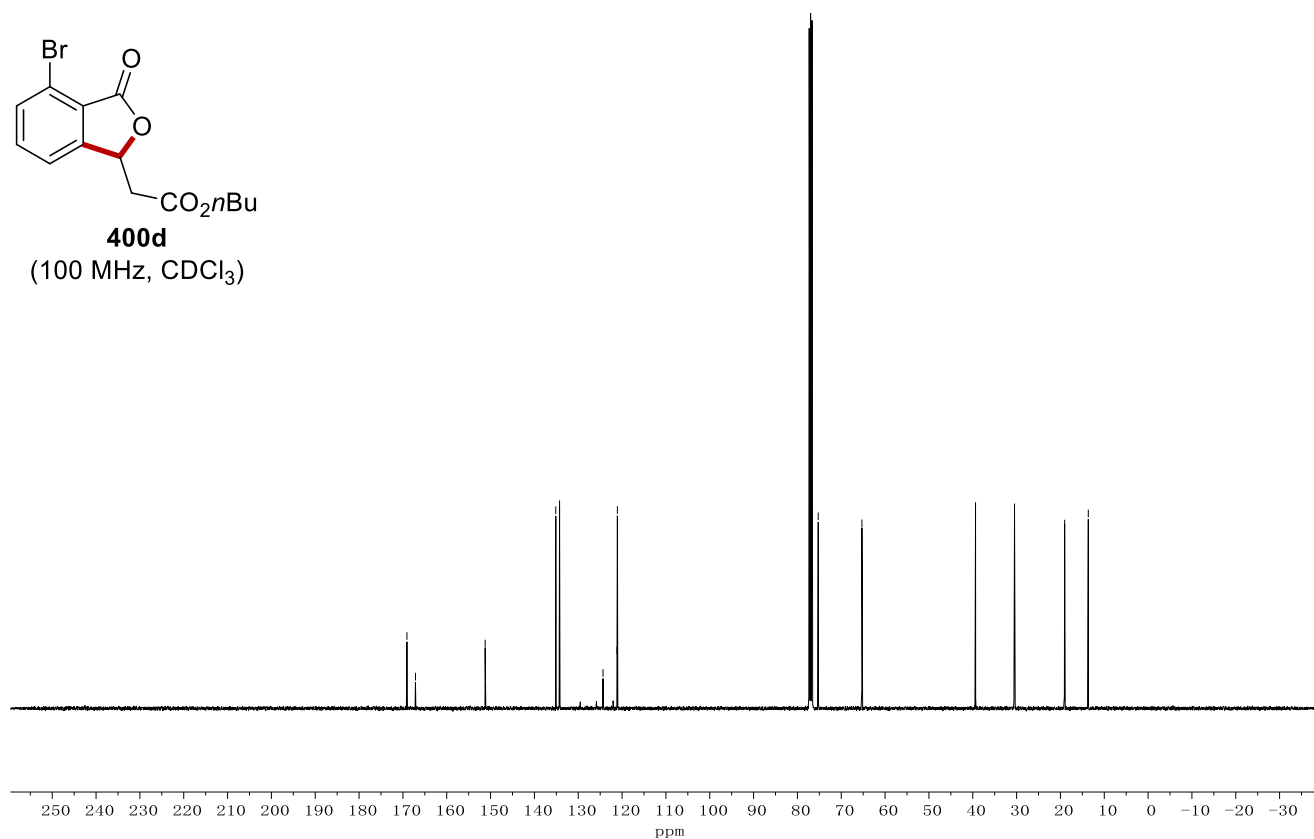
Appendix: NMR Spectra



**400d**  
(400 MHz, CDCl<sub>3</sub>)

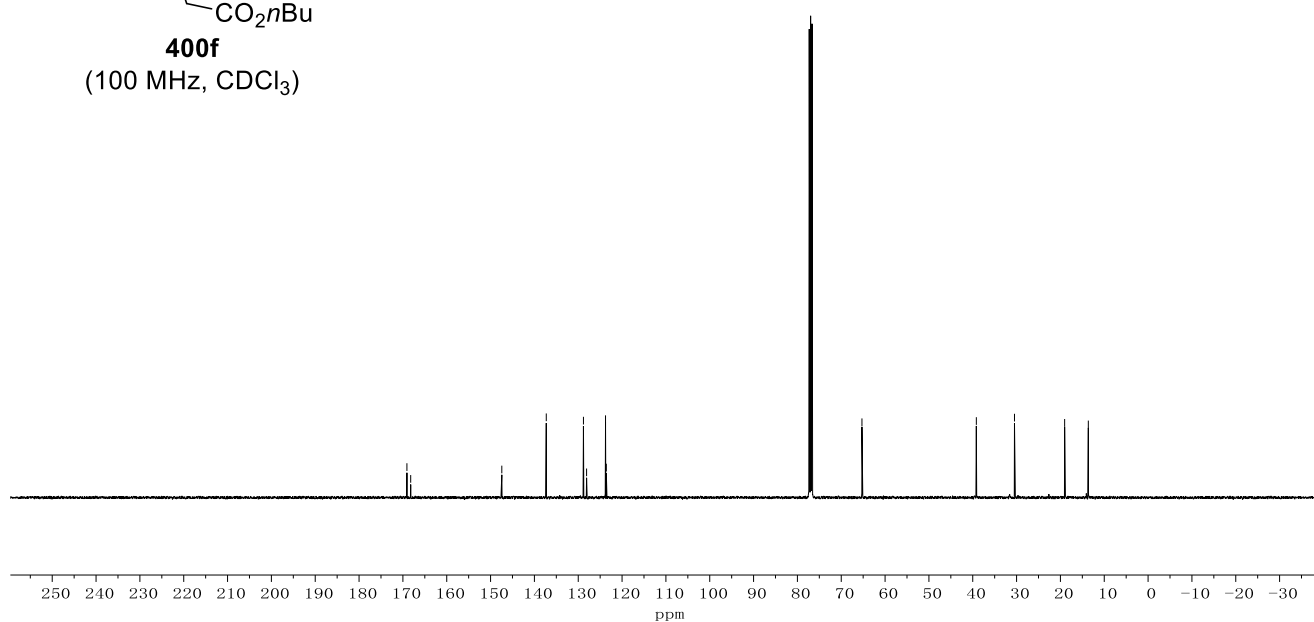
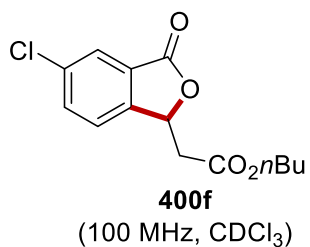
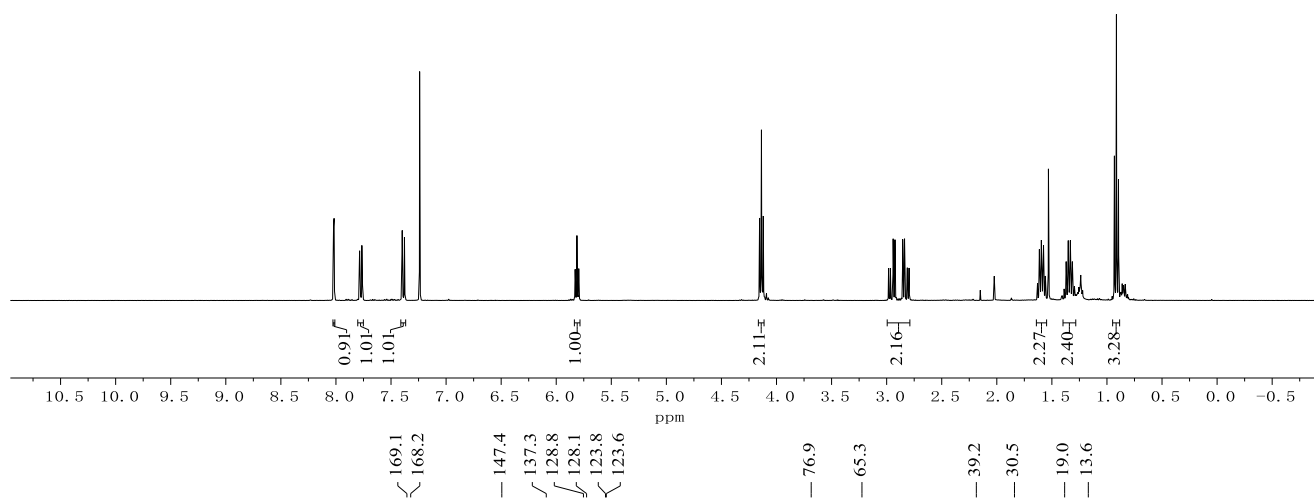
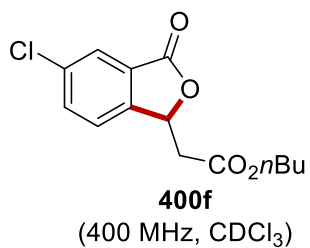


**400d**  
(100 MHz, CDCl<sub>3</sub>)

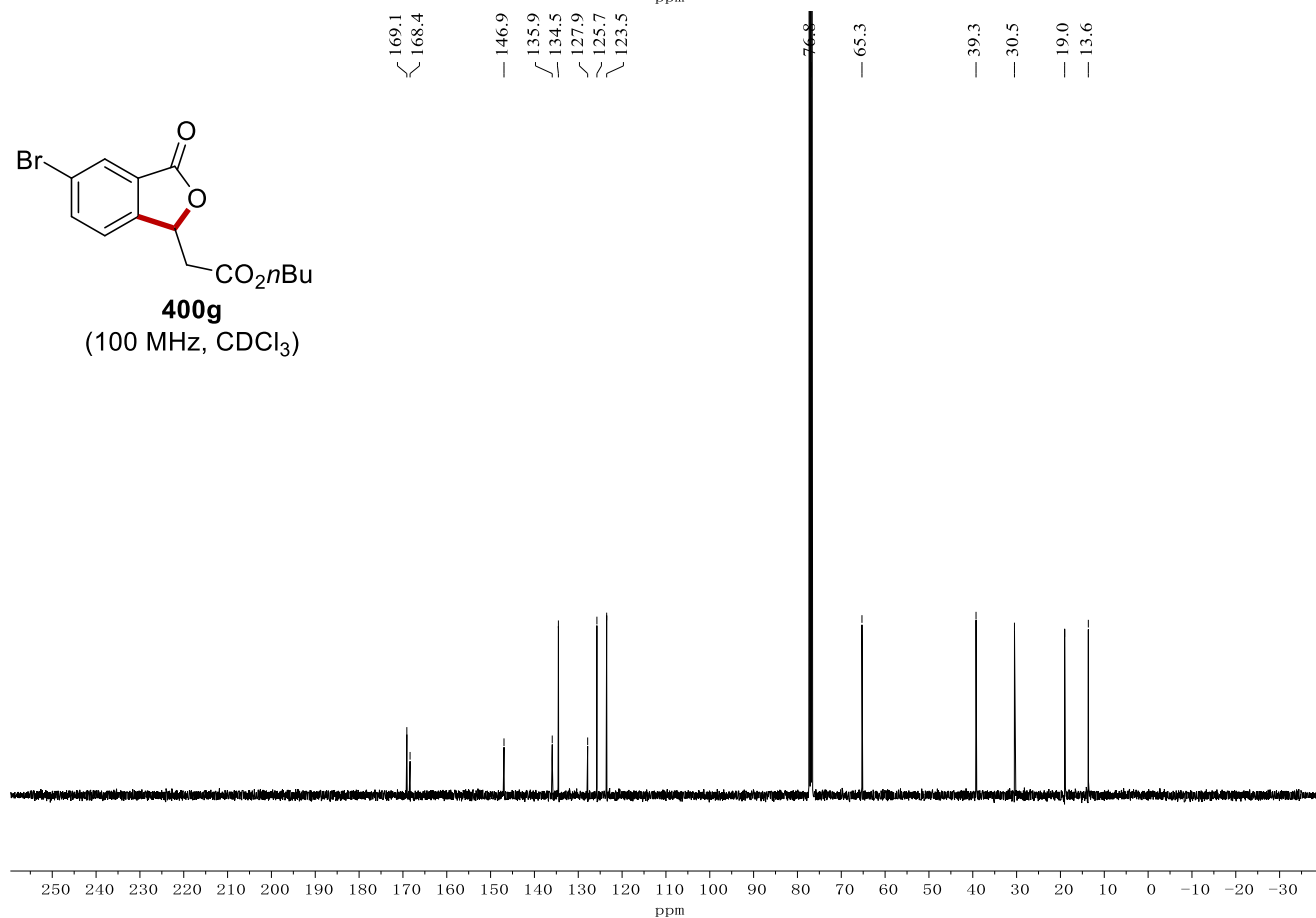
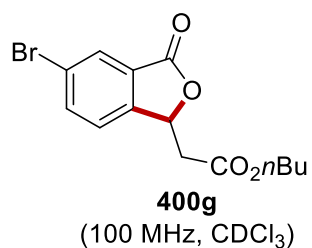
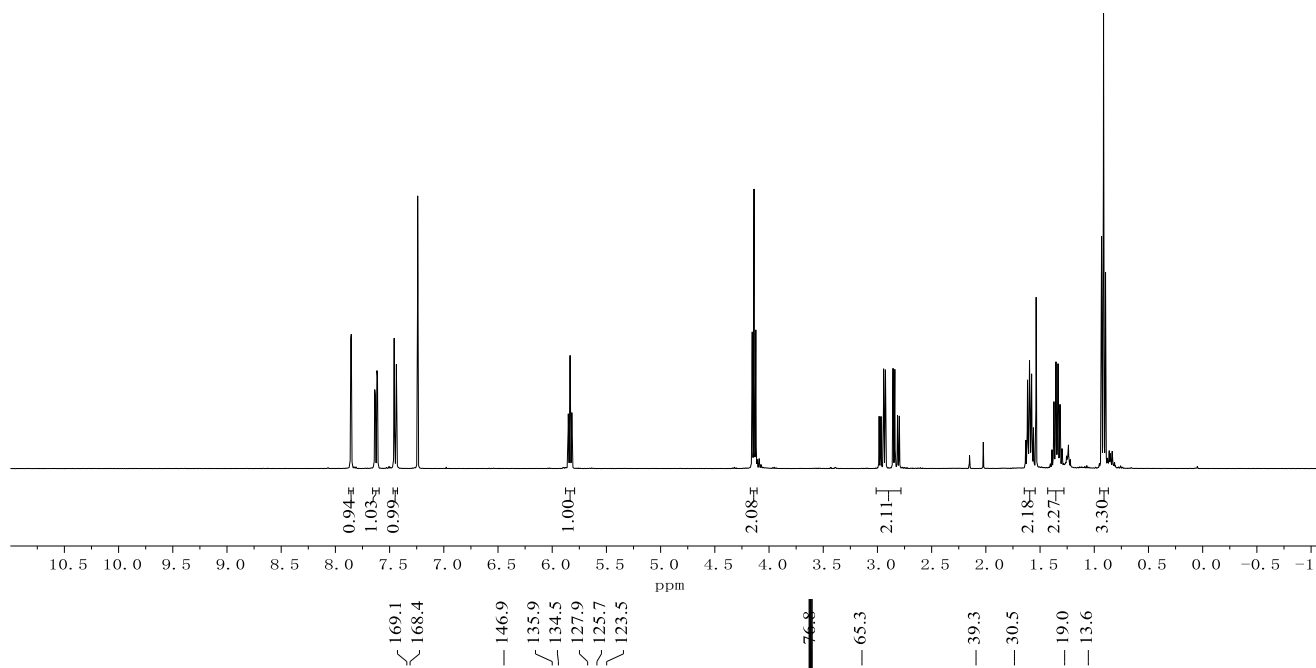
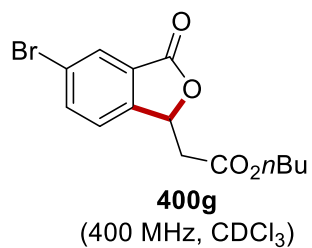




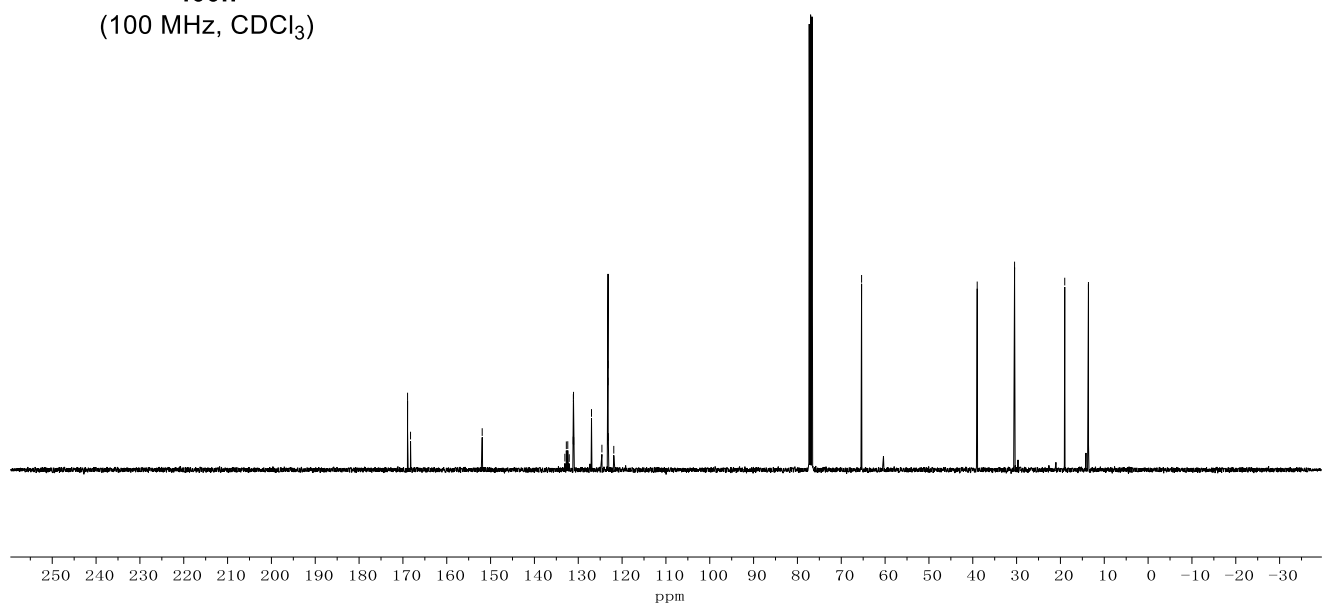
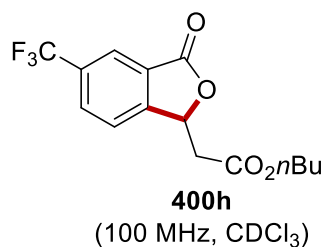
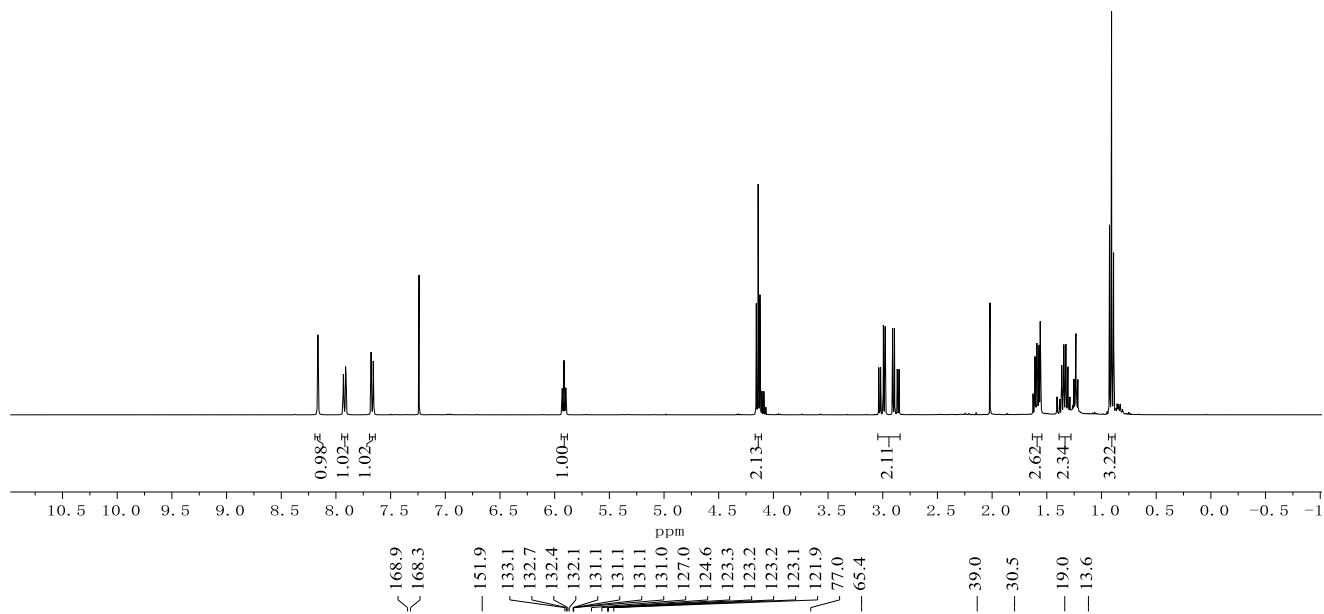
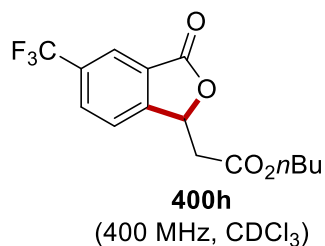
Appendix: NMR Spectra



Appendix: NMR Spectra

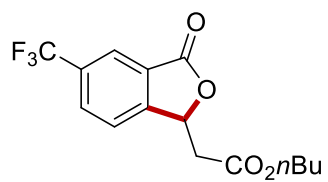


Appendix: NMR Spectra



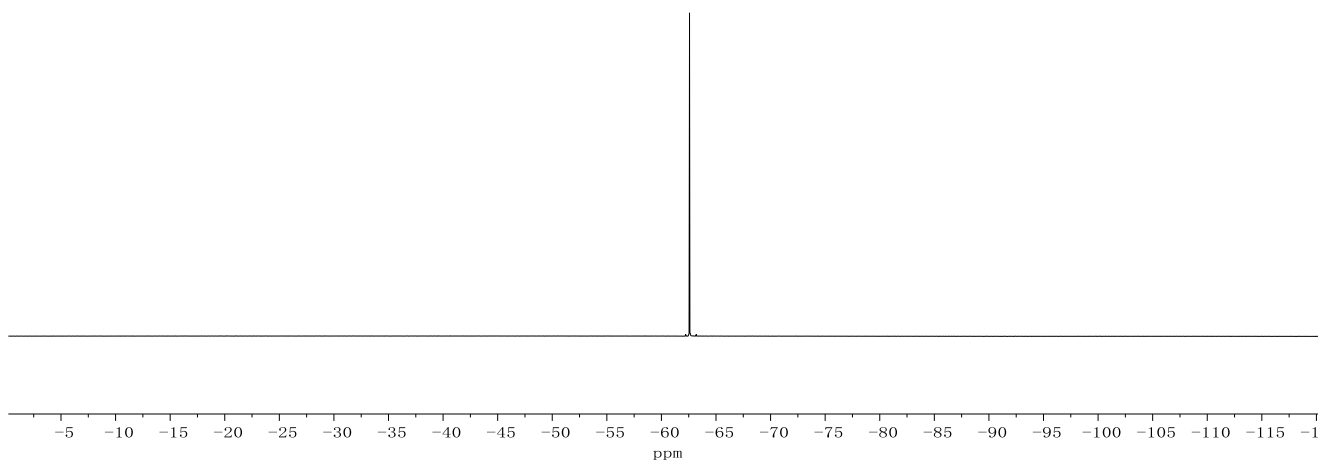


Appendix: NMR Spectra

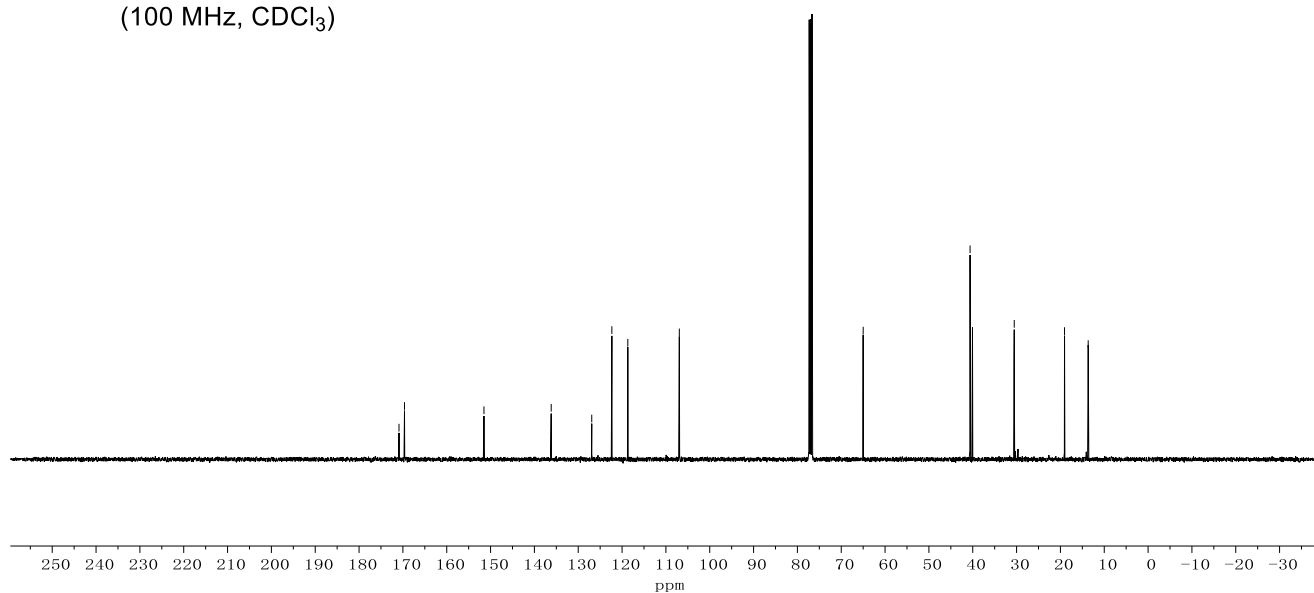
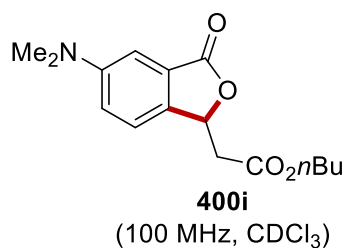
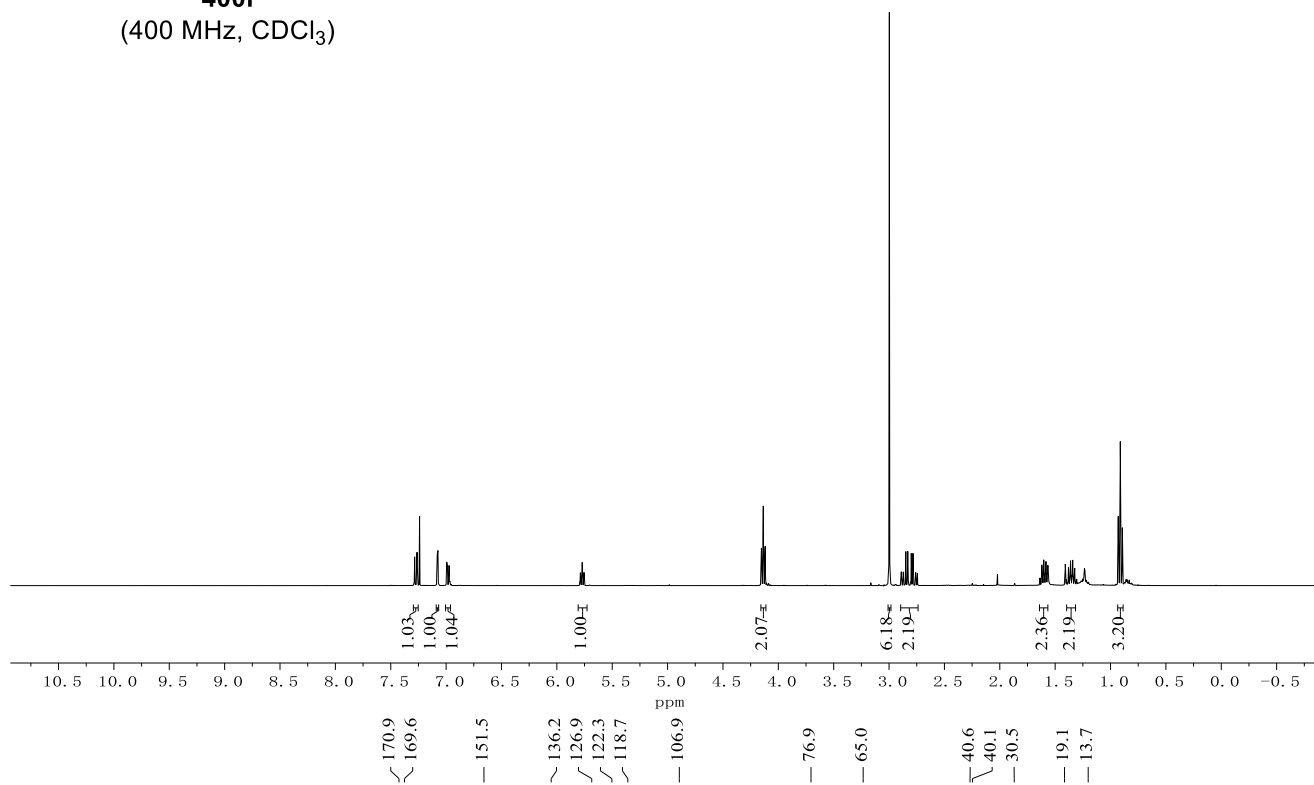
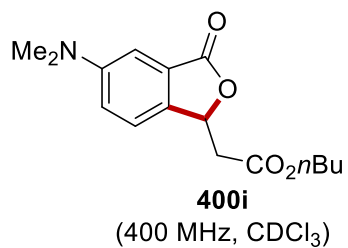


**400h**  
(282 MHz, CDCl<sub>3</sub>)

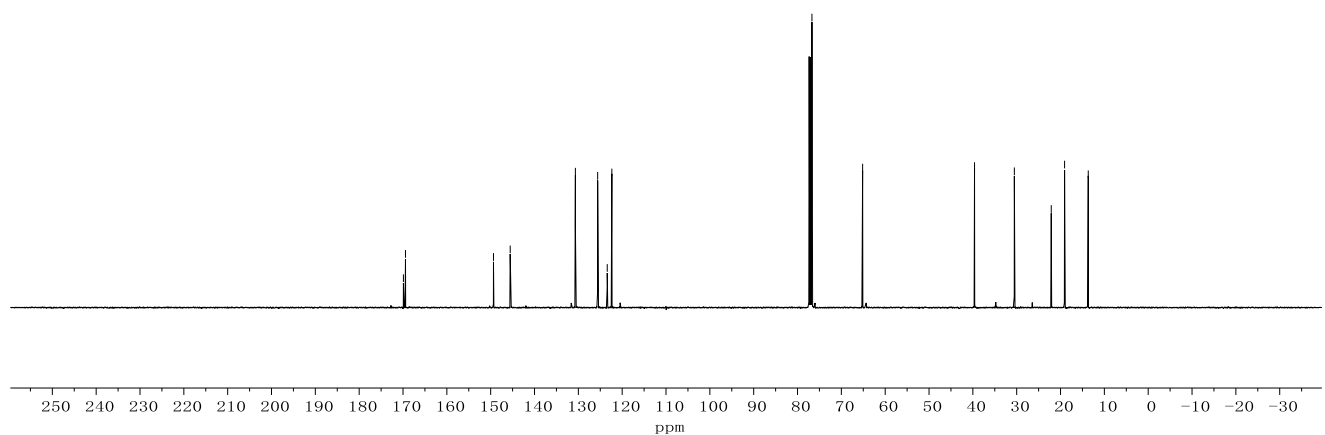
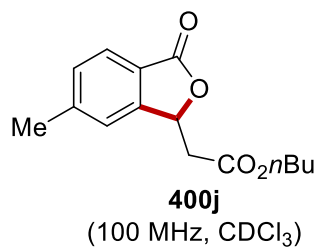
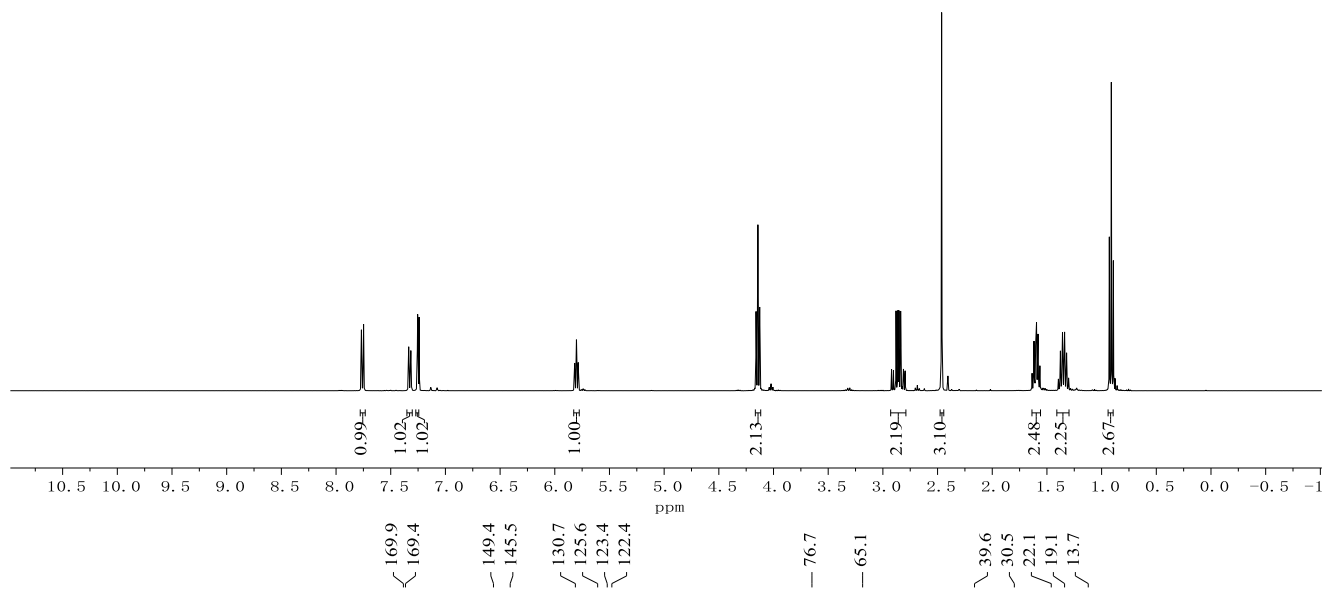
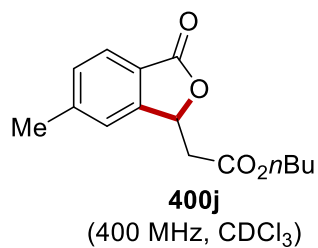
---62.6



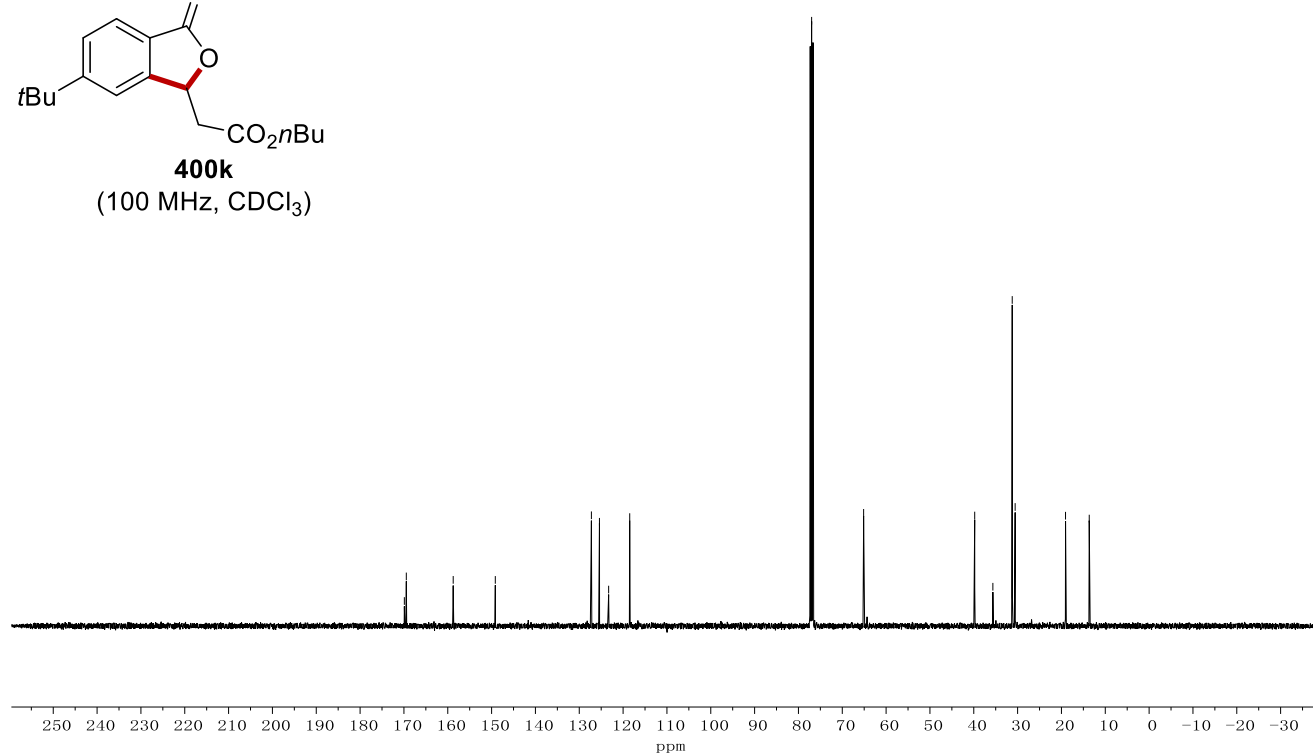
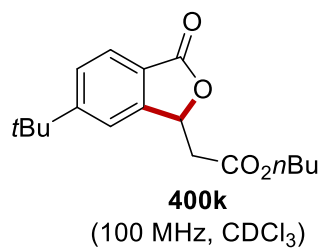
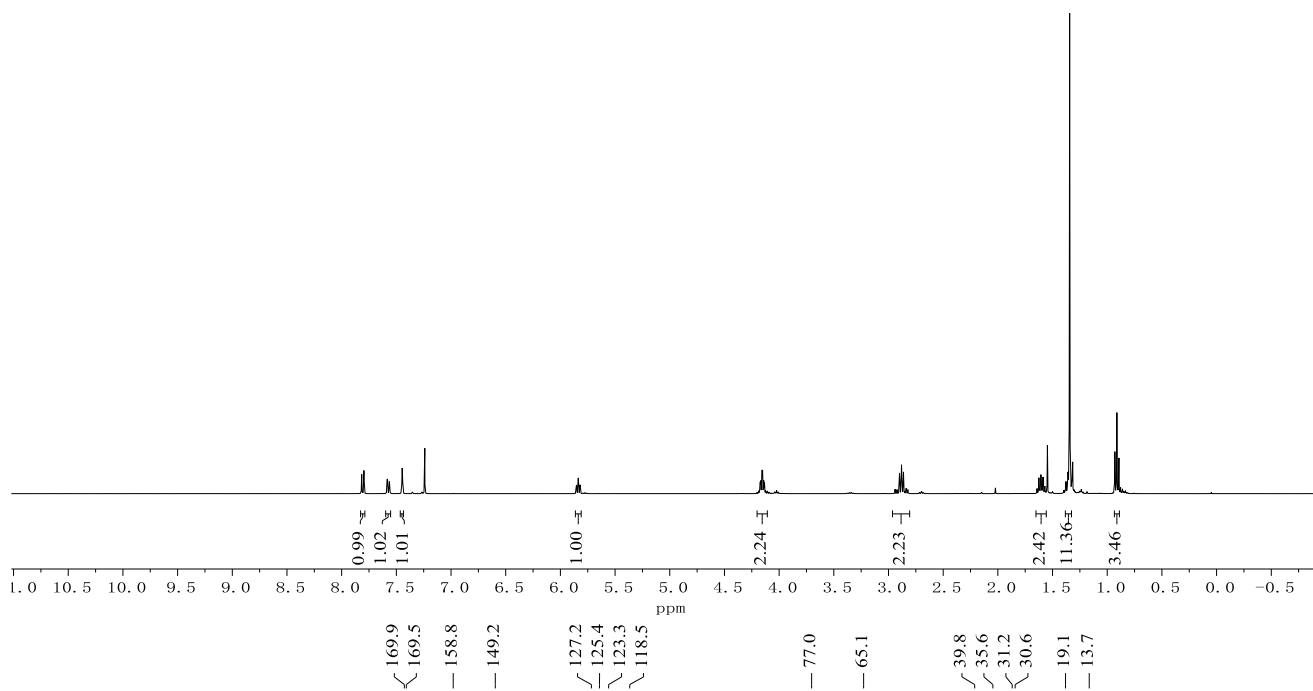
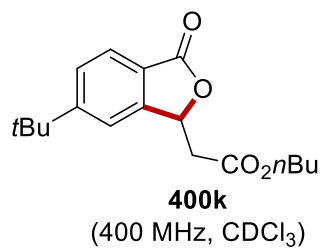
Appendix: NMR Spectra



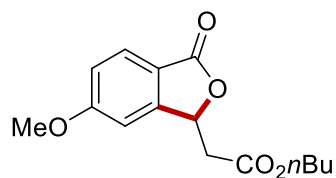
Appendix: NMR Spectra



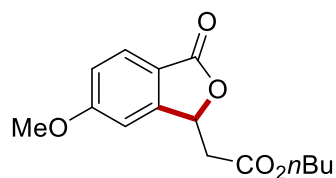
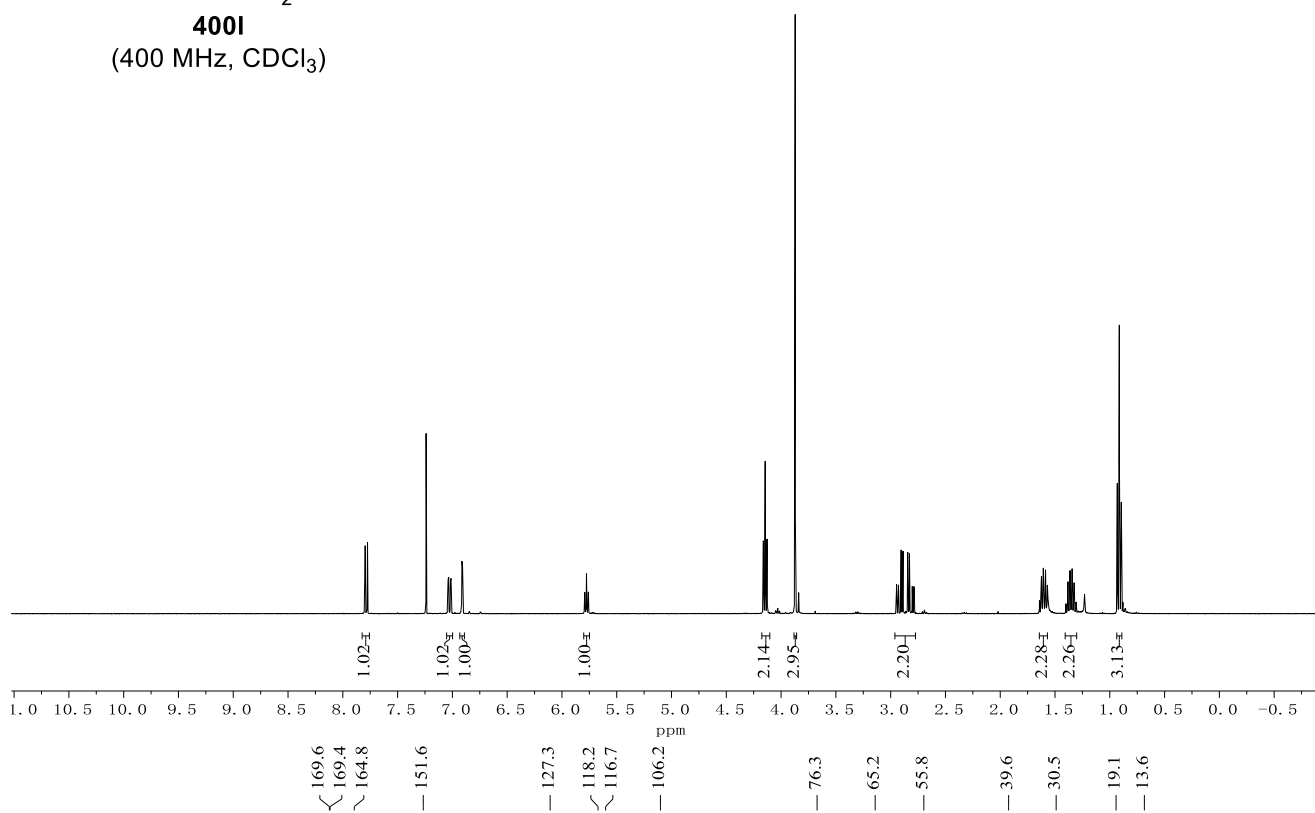
Appendix: NMR Spectra



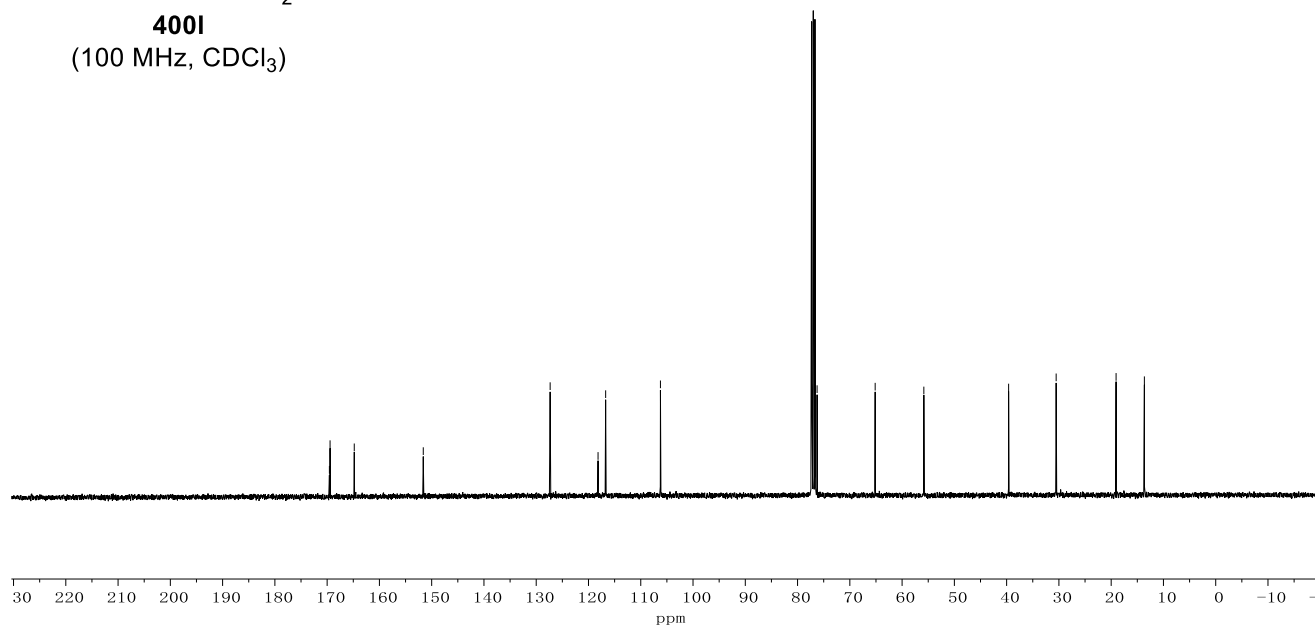
Appendix: NMR Spectra



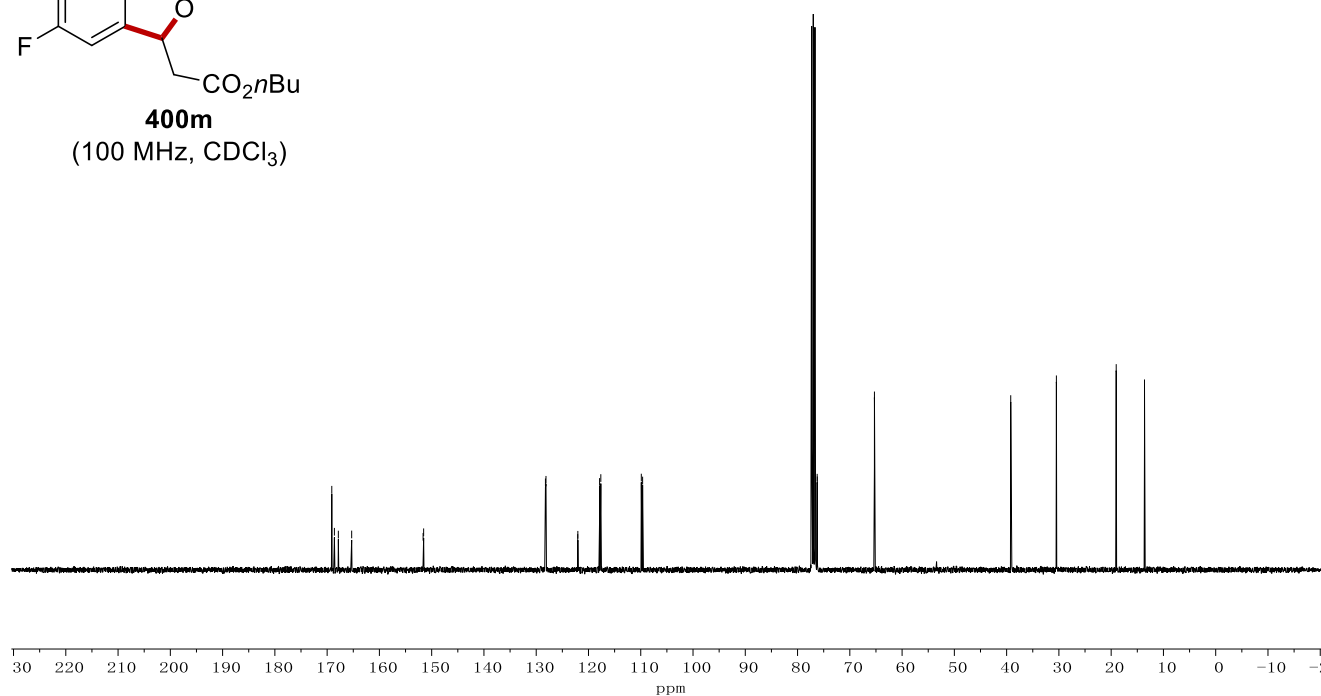
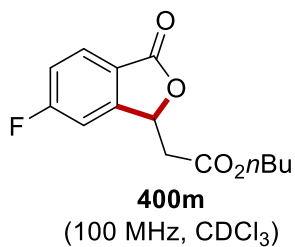
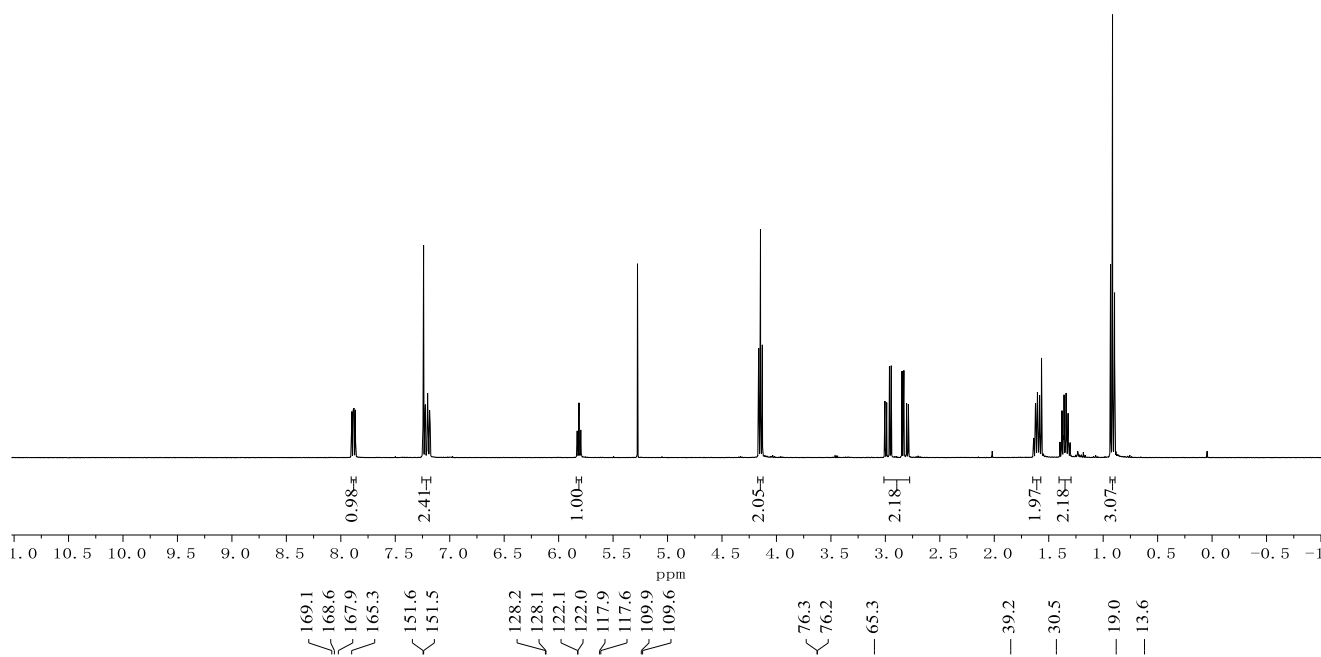
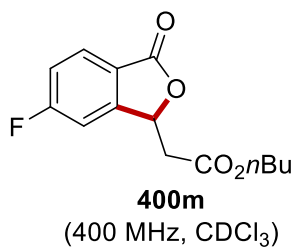
**400I**  
(400 MHz, CDCl<sub>3</sub>)



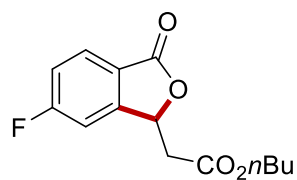
**400I**  
(100 MHz, CDCl<sub>3</sub>)



Appendix: NMR Spectra

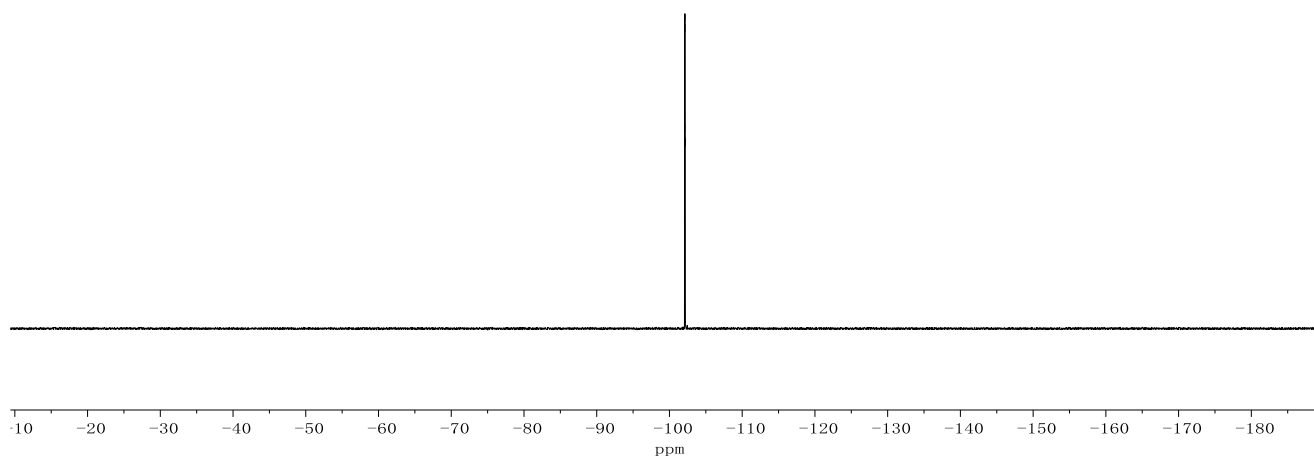


Appendix: NMR Spectra

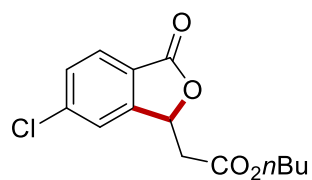


**400m**  
(282 MHz, CDCl<sub>3</sub>)

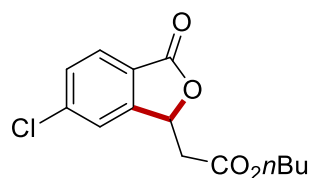
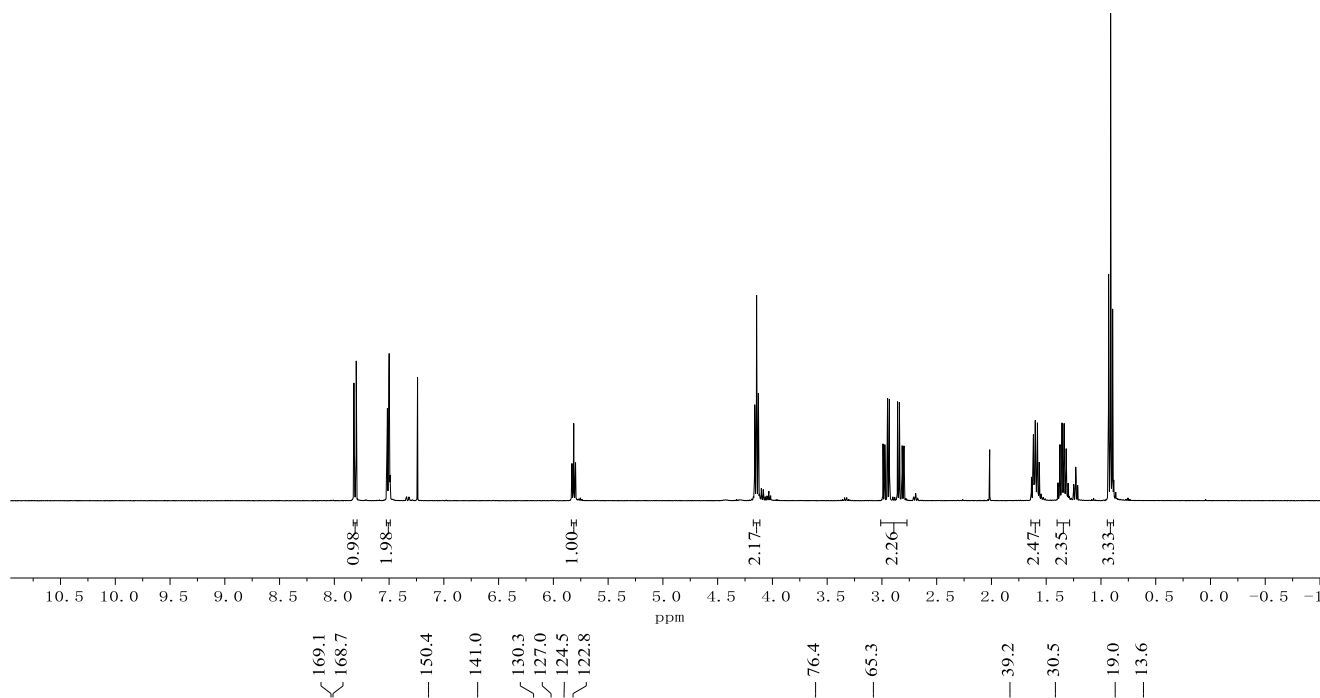
-102.1  
-102.1  
-102.1  
-102.1  
-102.2



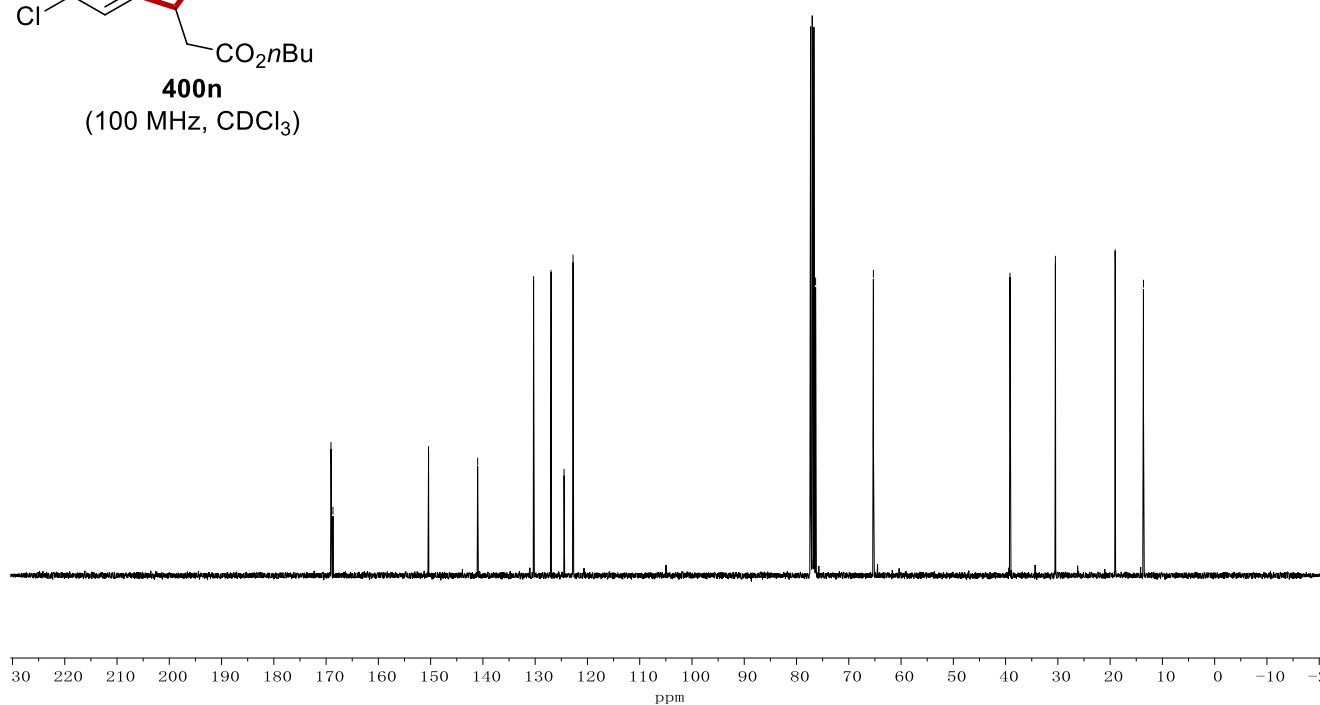
Appendix: NMR Spectra



**400n**  
(400 MHz, CDCl<sub>3</sub>)

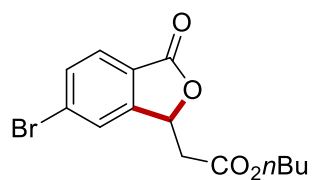


**400n**  
(100 MHz, CDCl<sub>3</sub>)

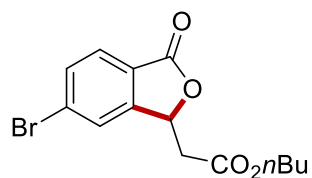
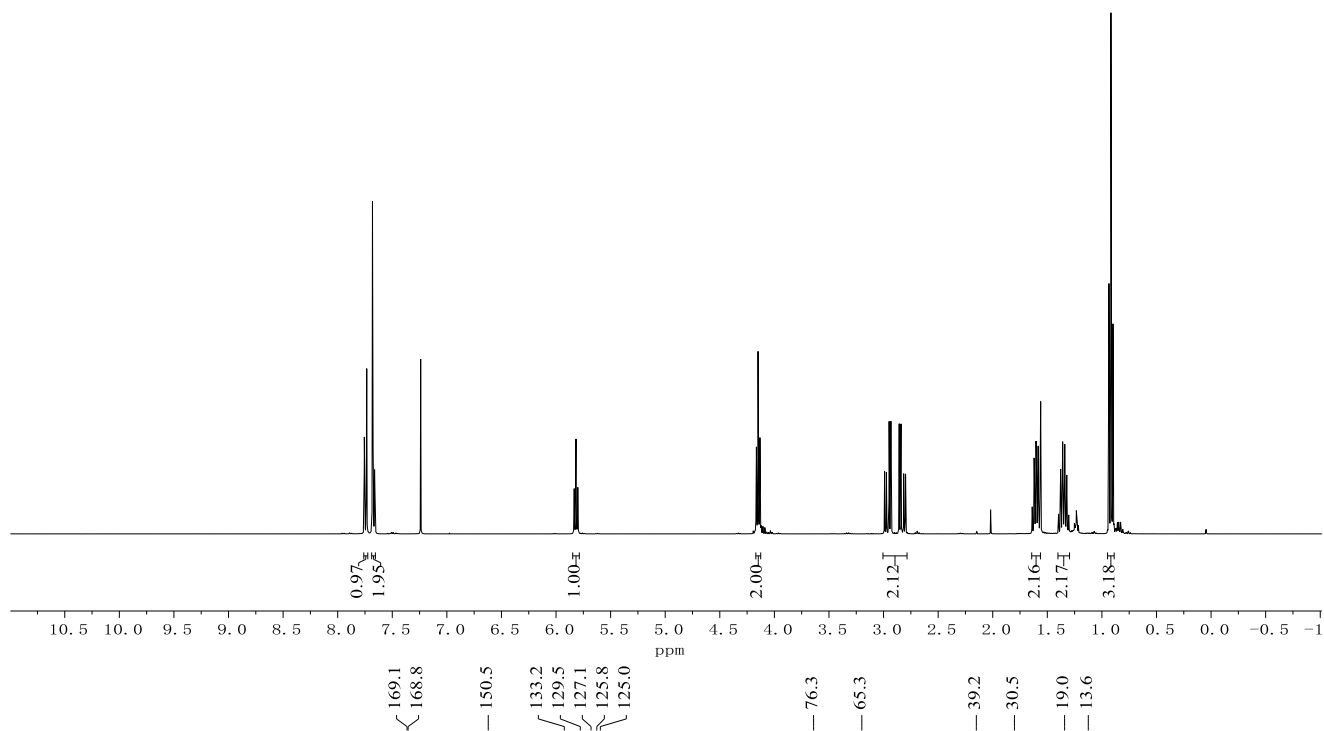




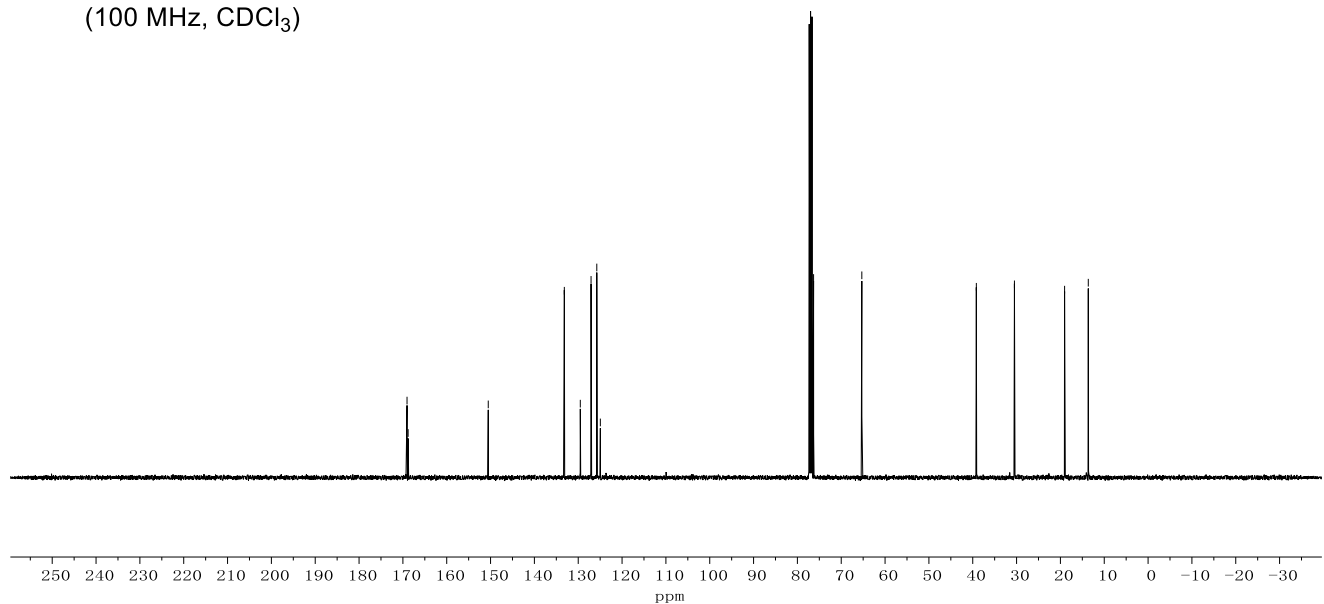
Appendix: NMR Spectra



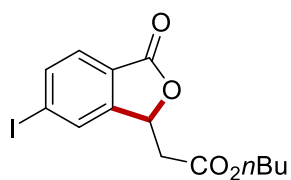
**400o**  
(400 MHz, CDCl<sub>3</sub>)



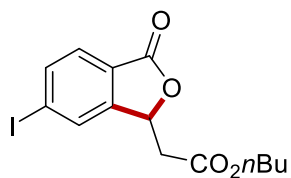
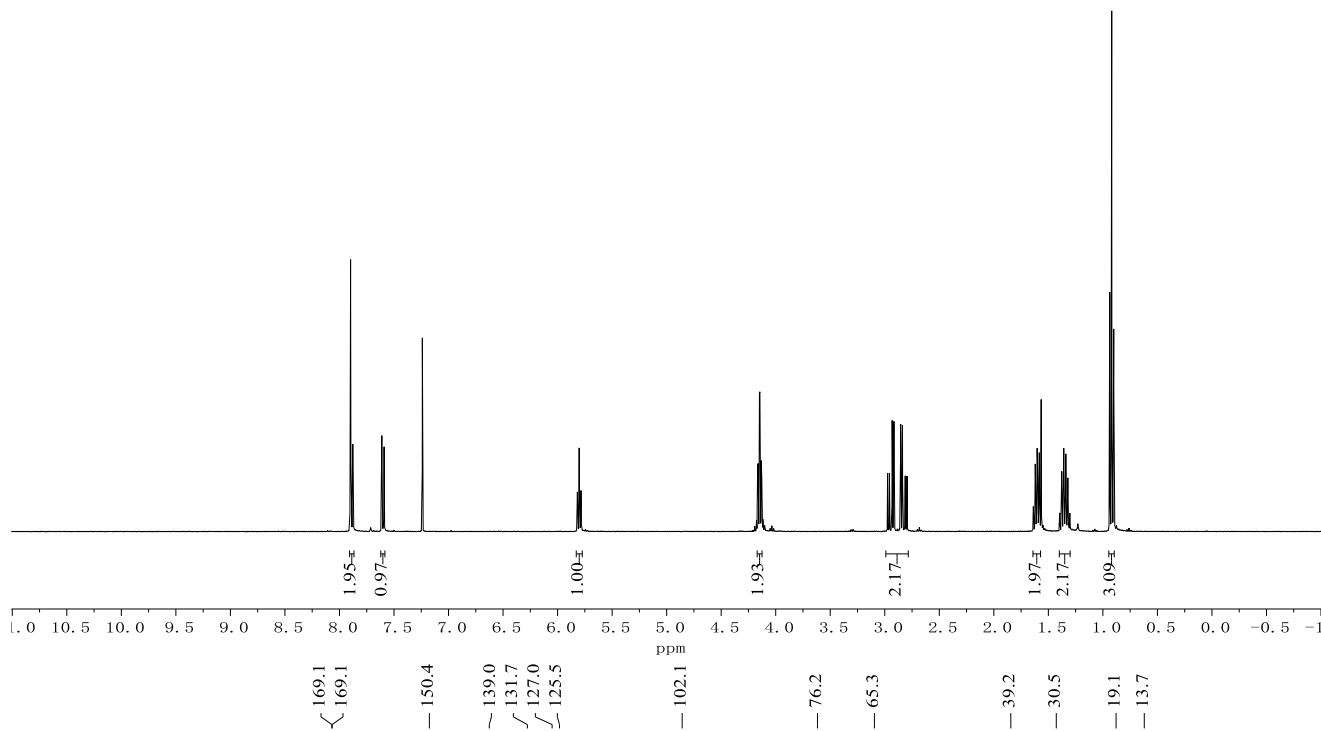
**400o**  
(100 MHz, CDCl<sub>3</sub>)



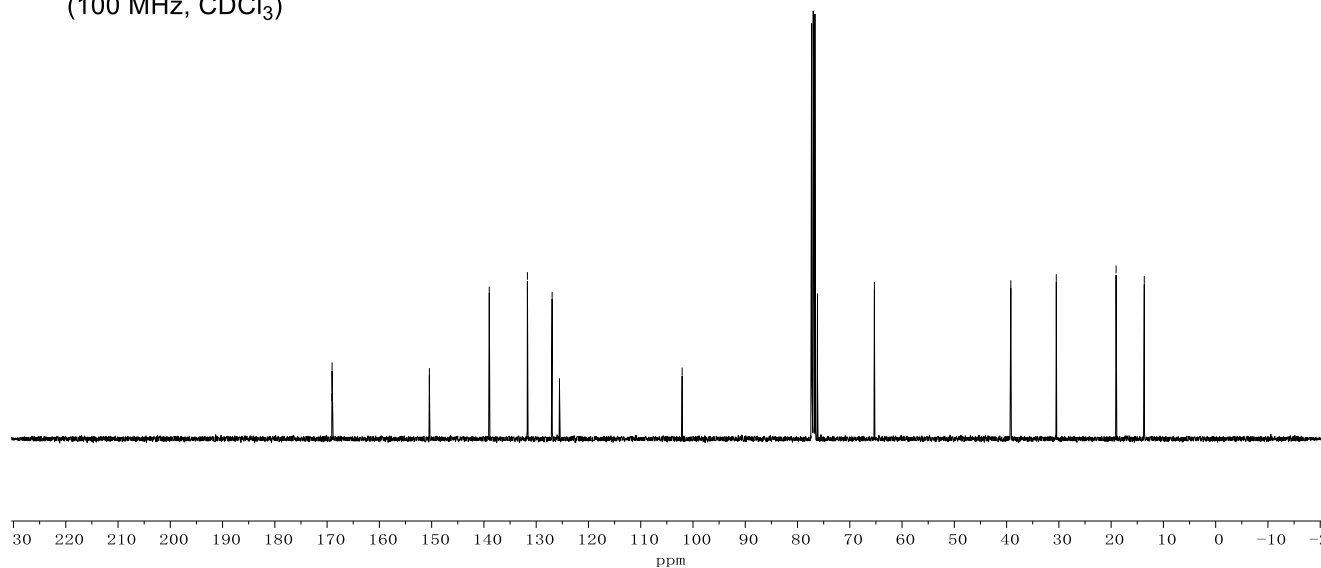
Appendix: NMR Spectra



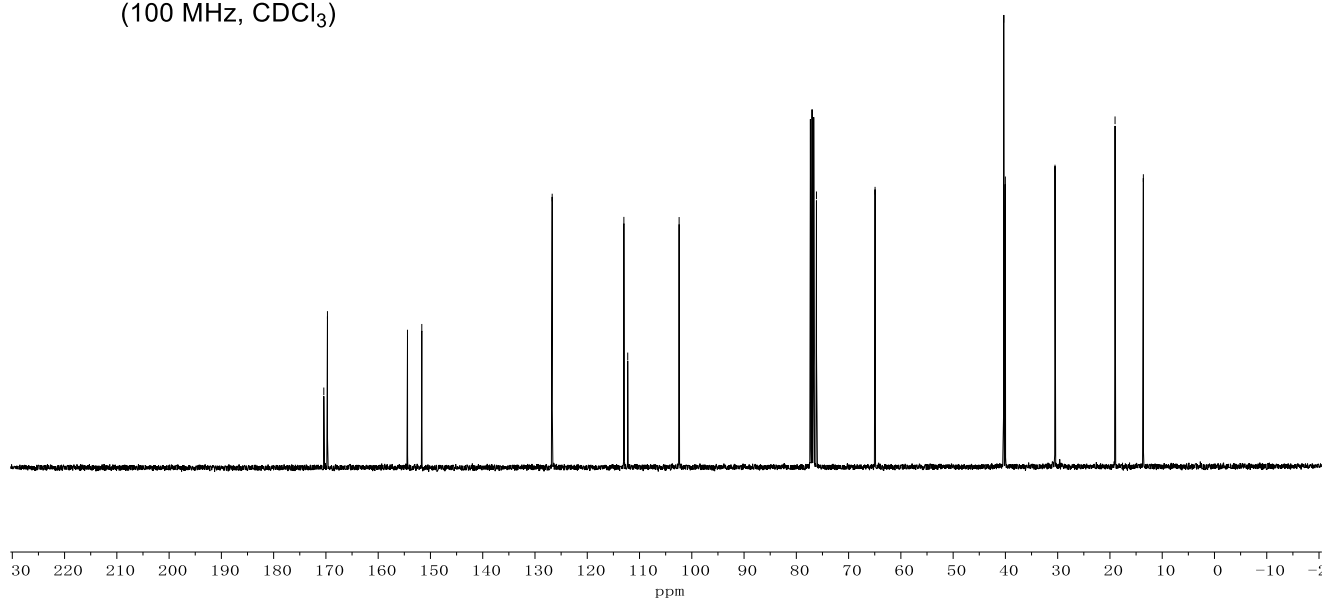
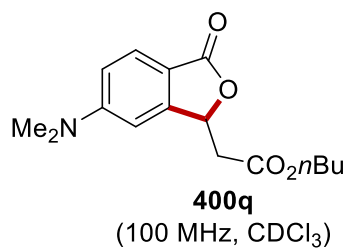
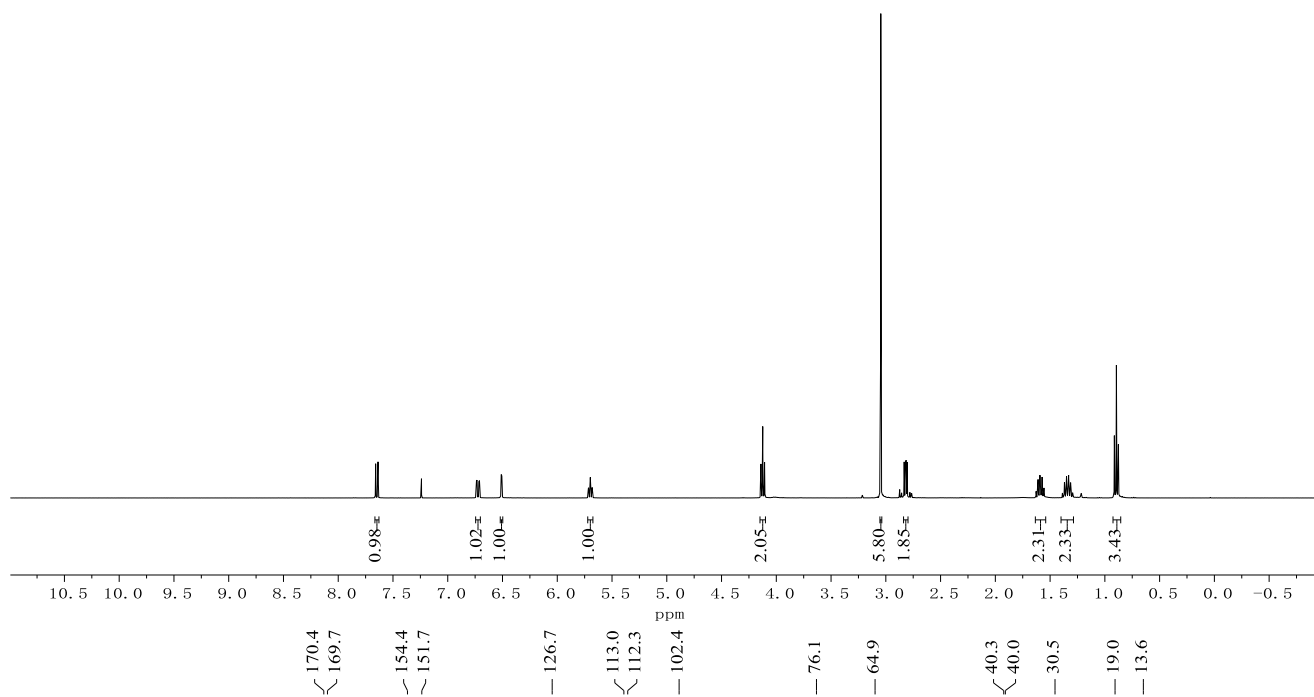
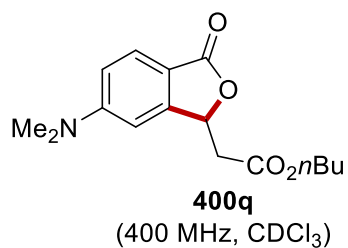
**400p**  
(400 MHz, CDCl<sub>3</sub>)



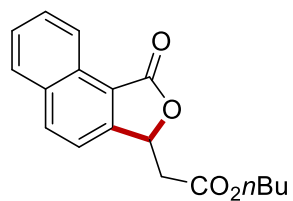
**400p**  
(100 MHz, CDCl<sub>3</sub>)



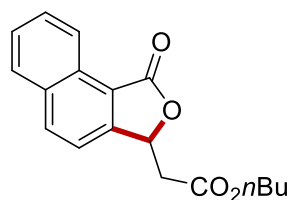
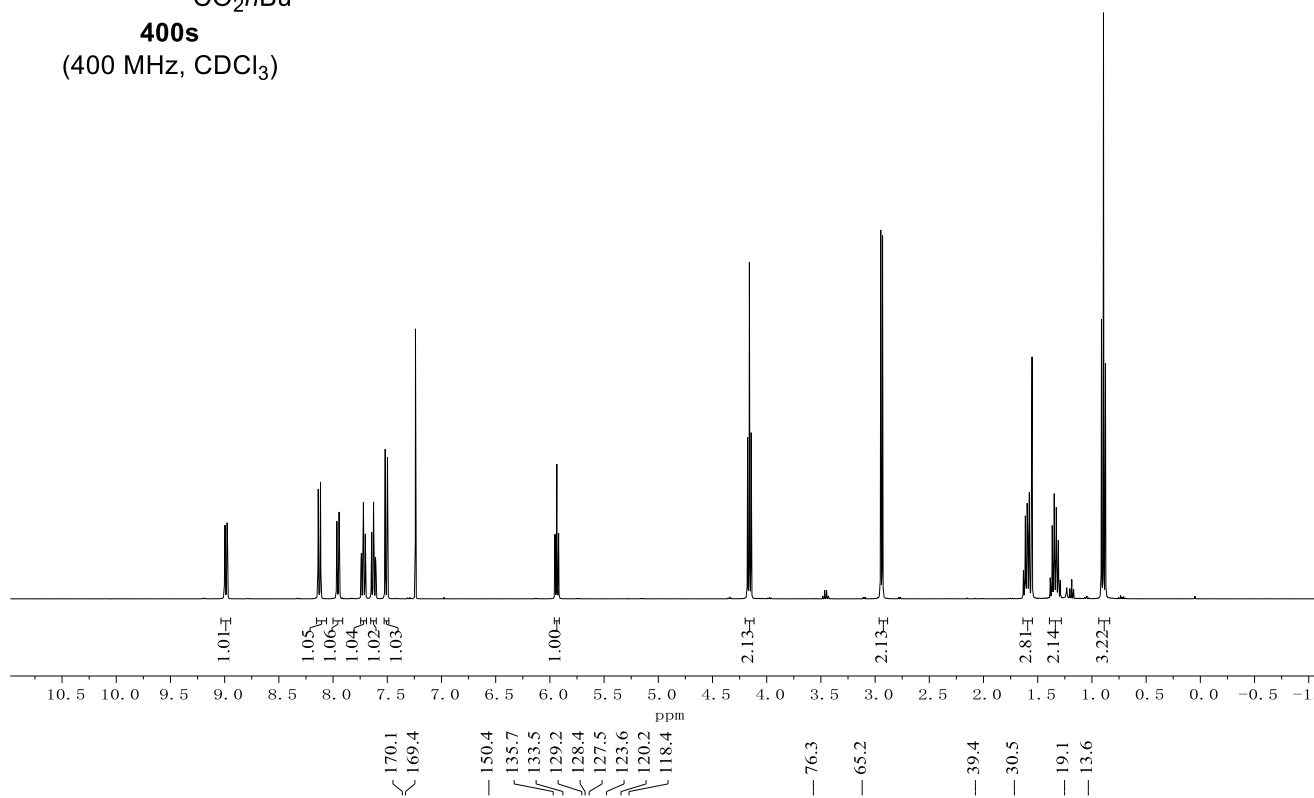
Appendix: NMR Spectra



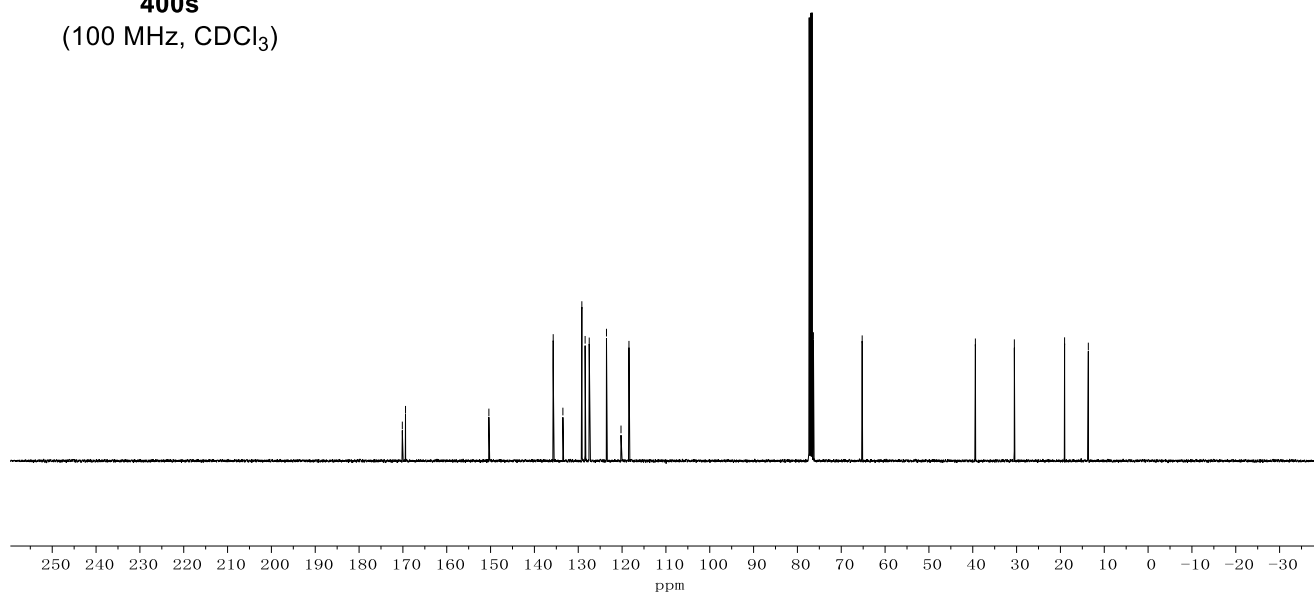
Appendix: NMR Spectra



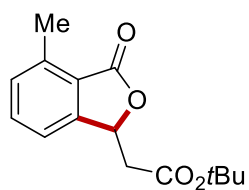
**400s**  
(400 MHz, CDCl<sub>3</sub>)



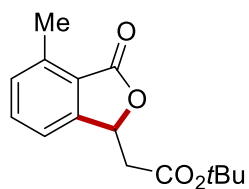
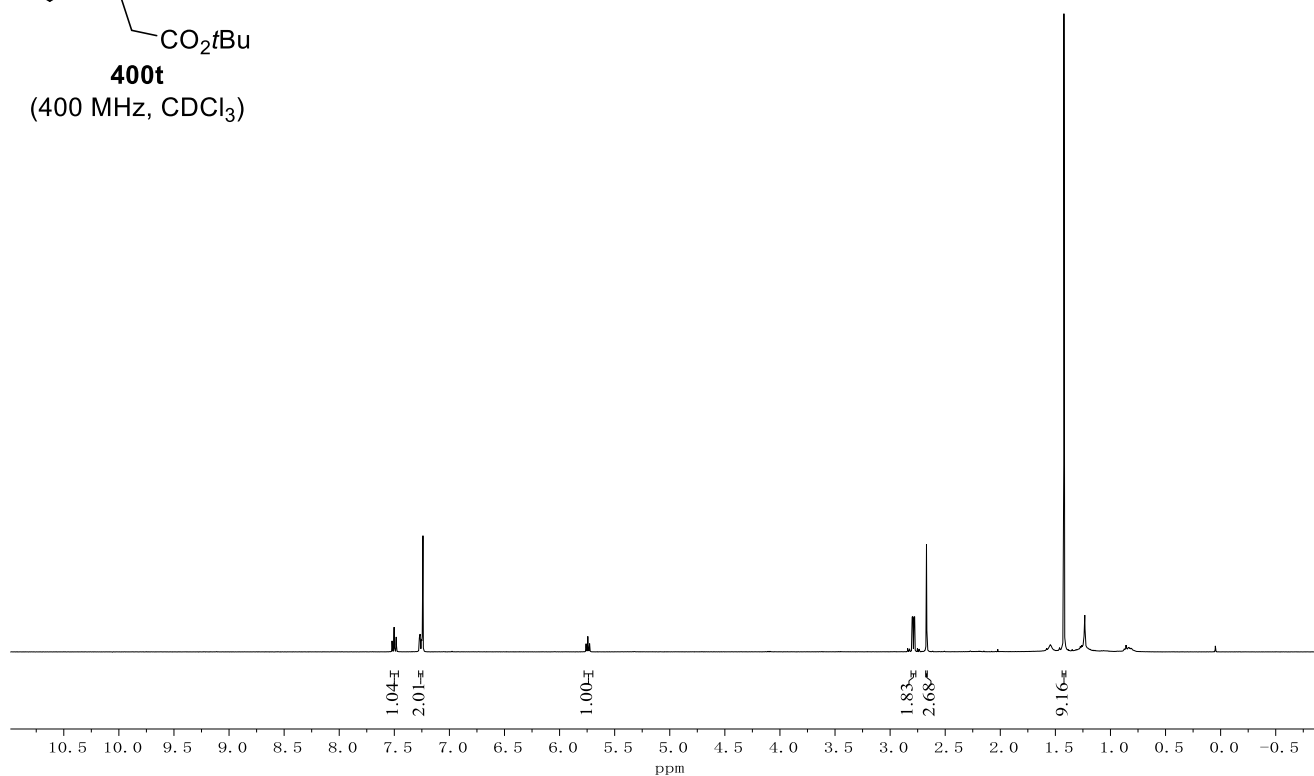
**400s**  
(100 MHz, CDCl<sub>3</sub>)



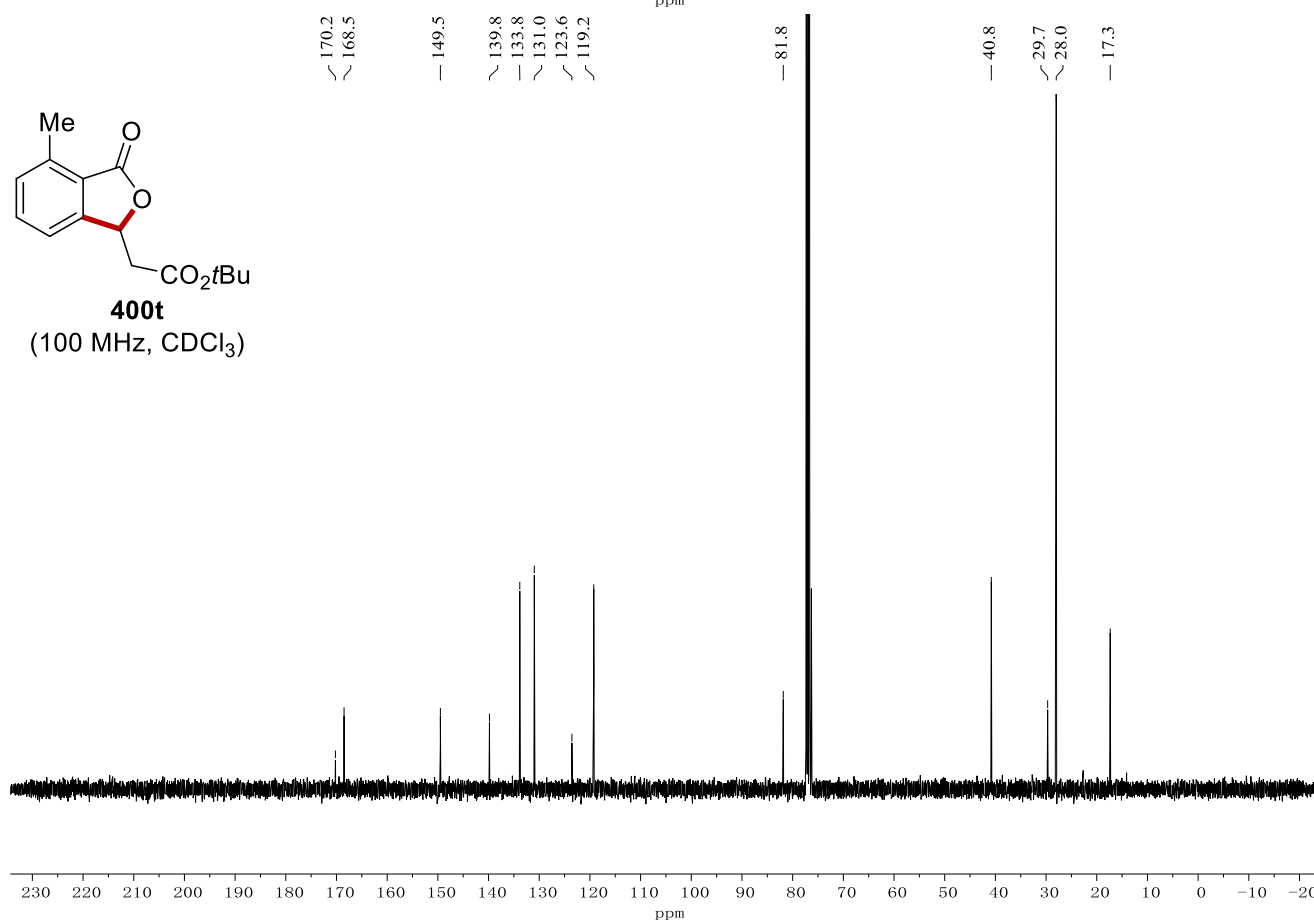
Appendix: NMR Spectra



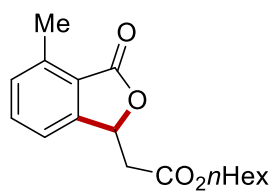
**400t**  
(400 MHz, CDCl<sub>3</sub>)



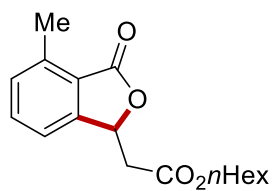
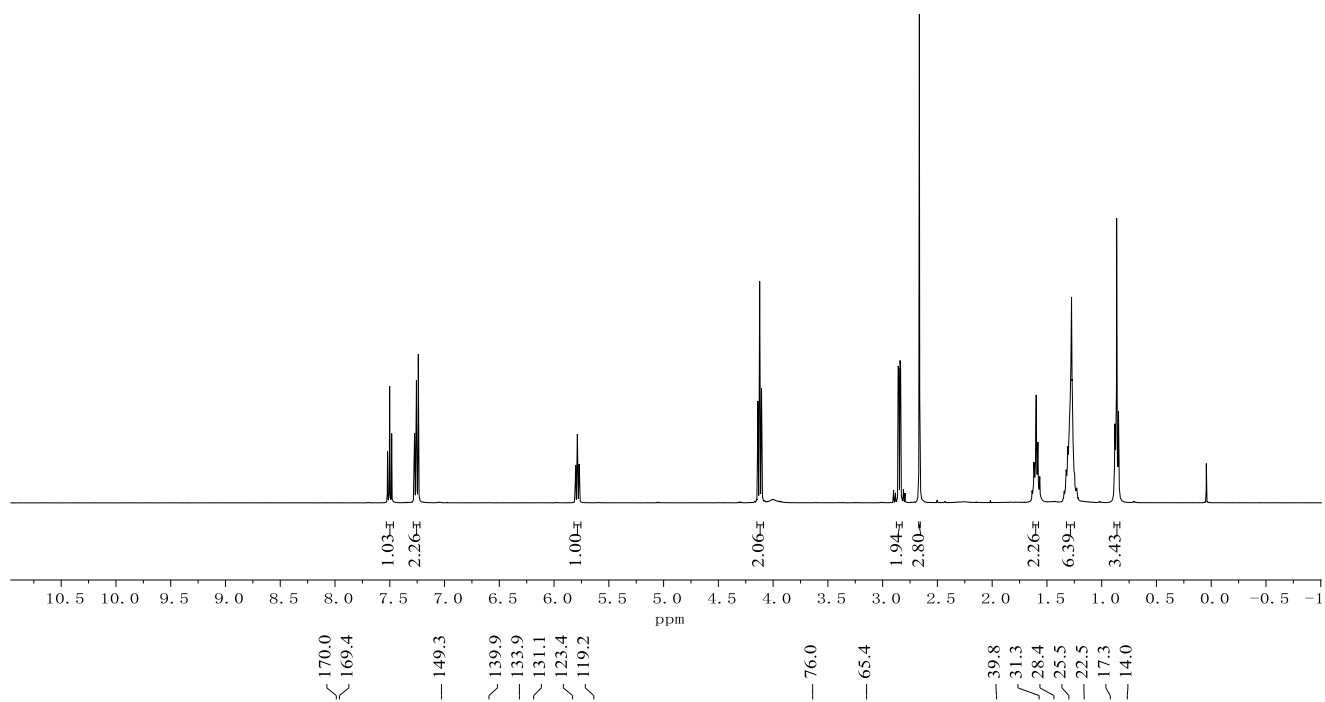
**400t**  
(100 MHz, CDCl<sub>3</sub>)



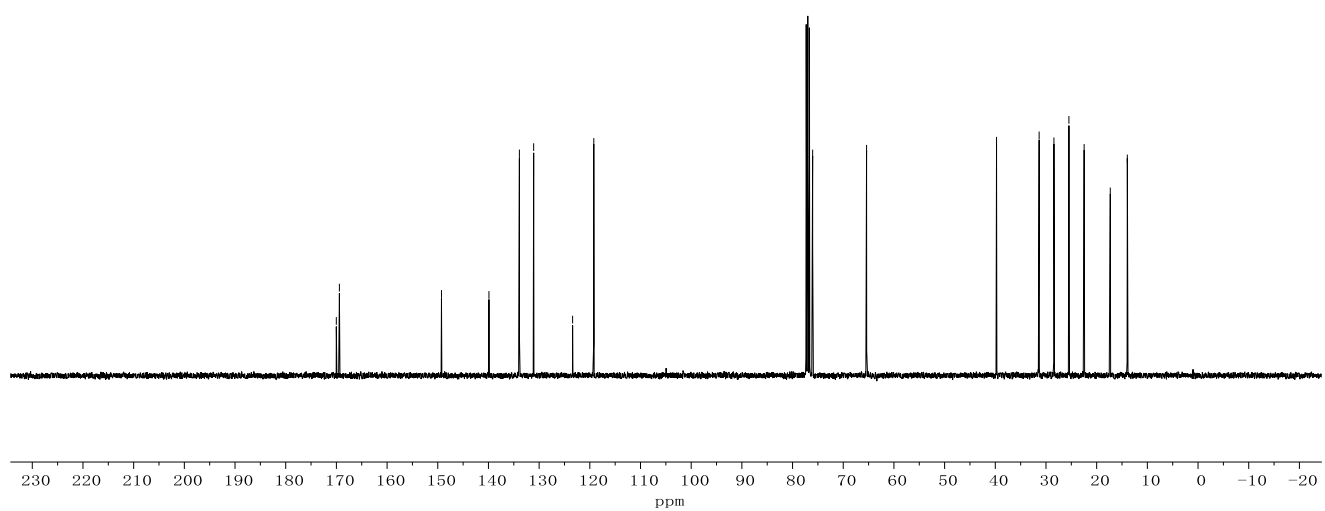
Appendix: NMR Spectra



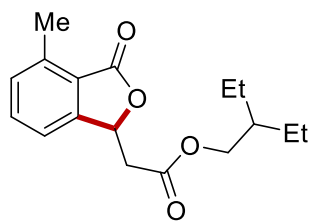
**400u**  
(400 MHz, CDCl<sub>3</sub>)



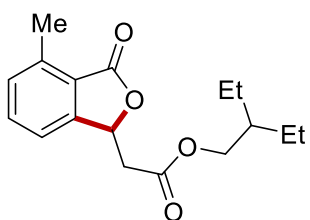
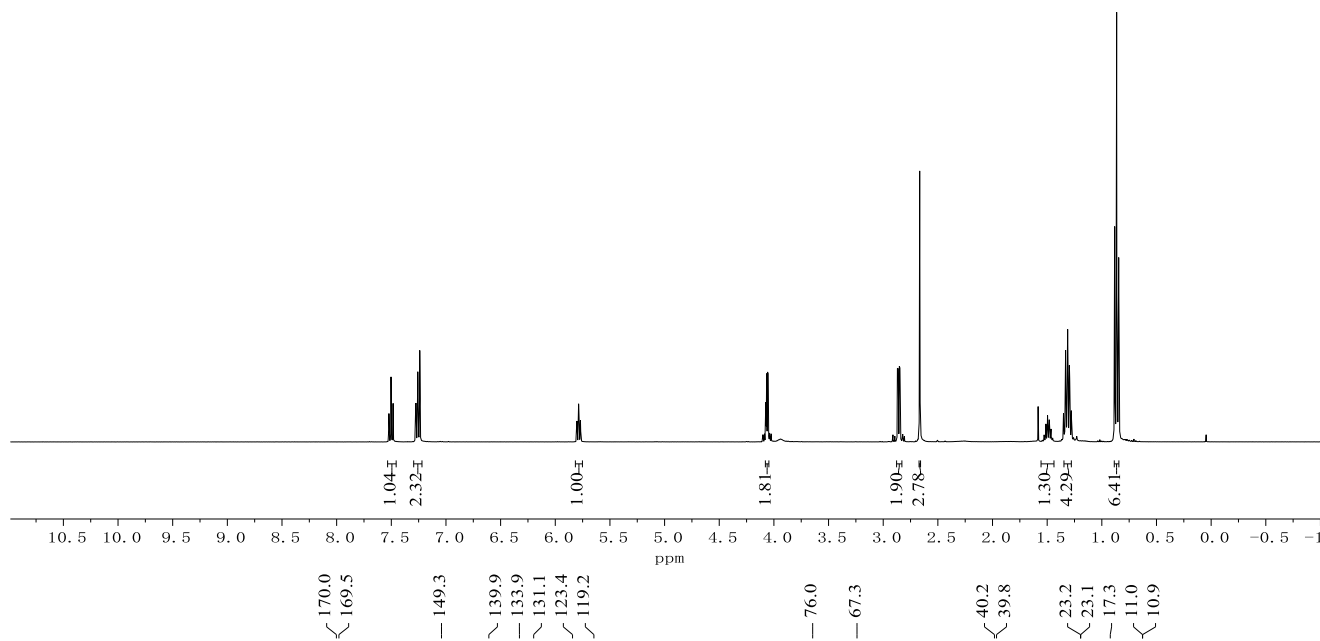
**400u**  
(100 MHz, CDCl<sub>3</sub>)



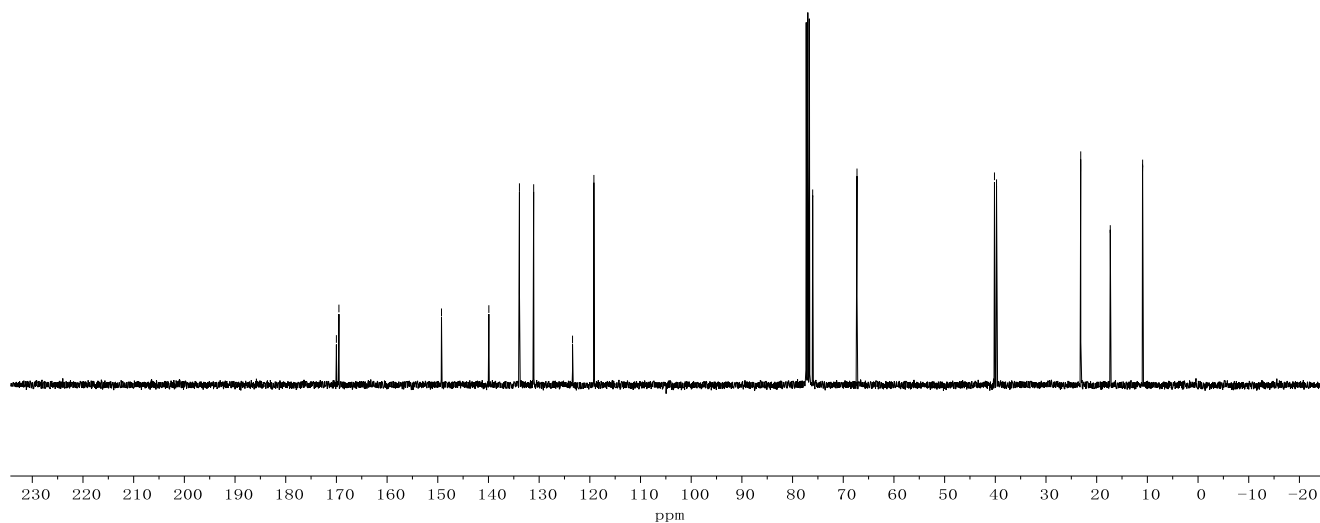
Appendix: NMR Spectra



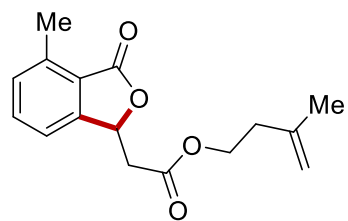
**400w**  
(400 MHz, CDCl<sub>3</sub>)



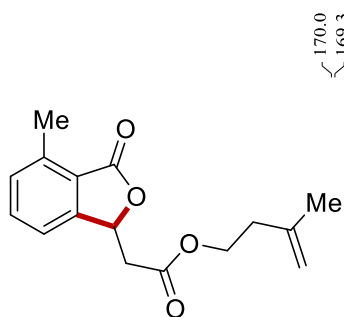
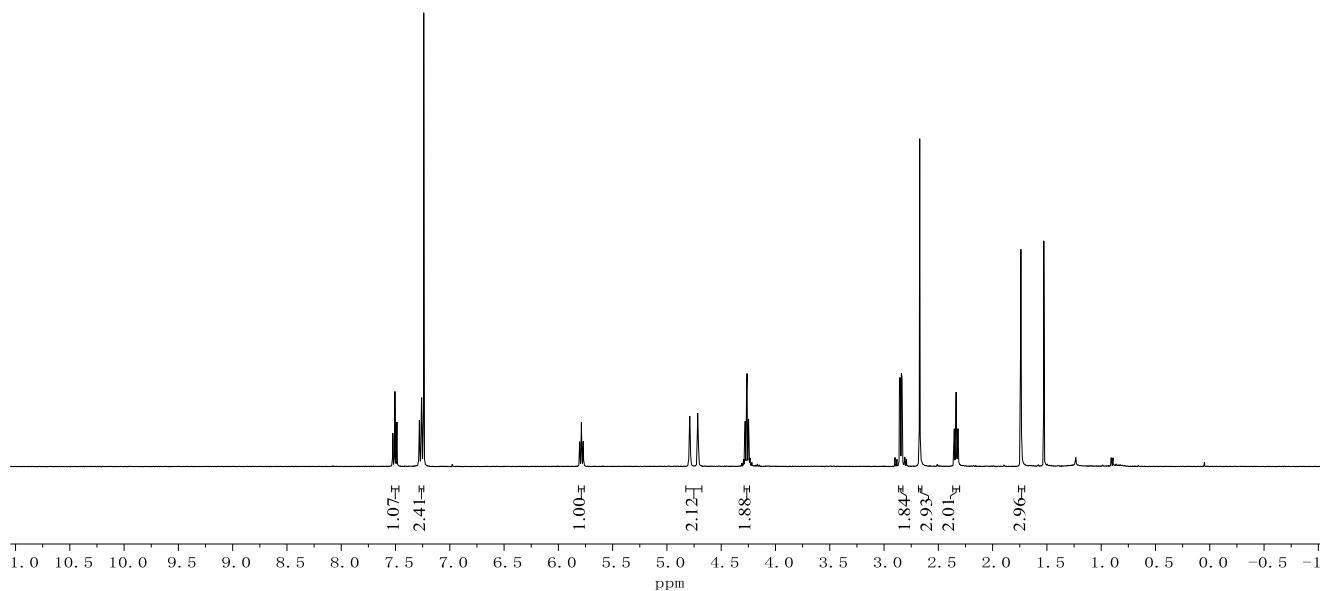
**400w**  
(100 MHz, CDCl<sub>3</sub>)



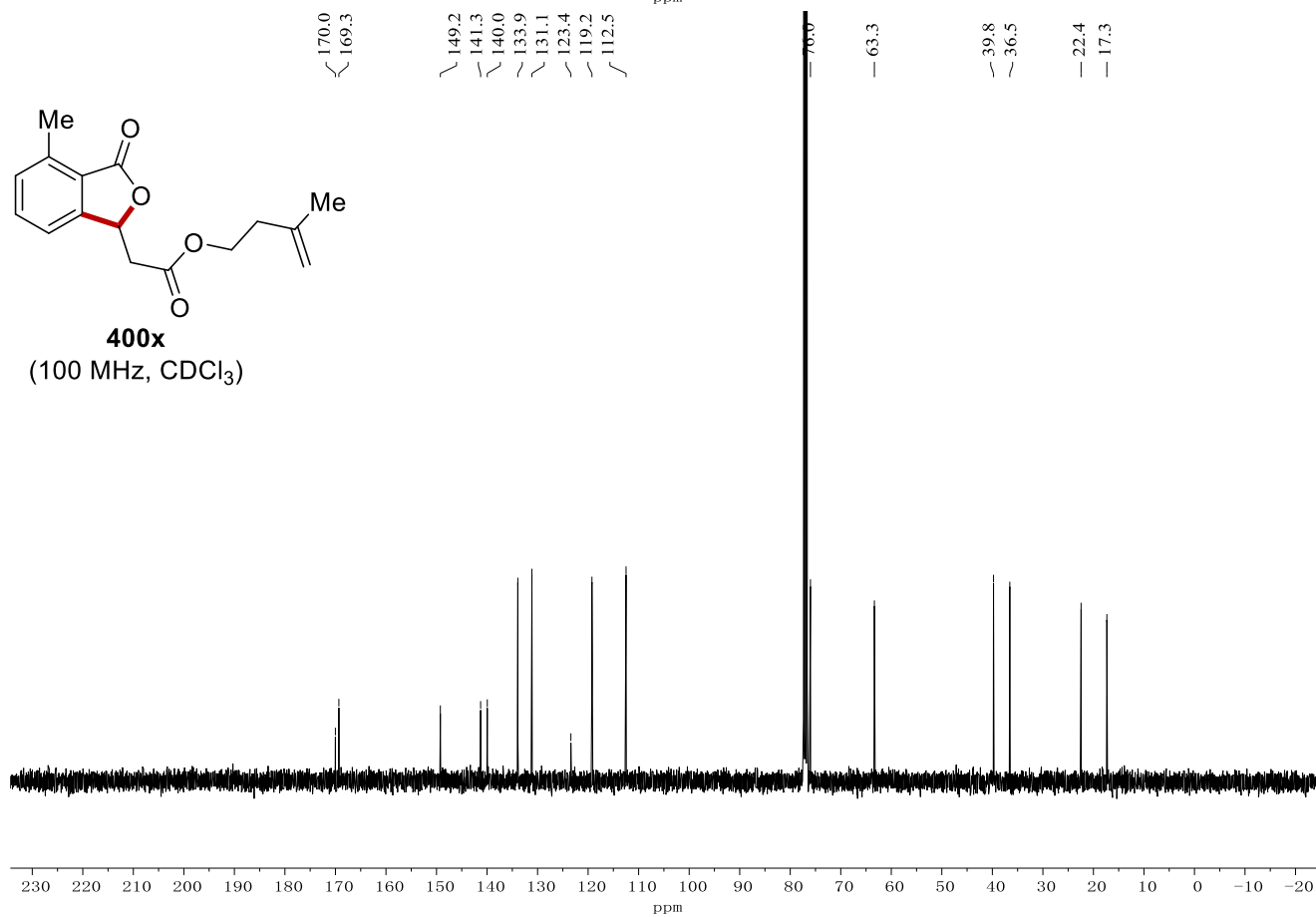
Appendix: NMR Spectra



**400x**  
(400 MHz, CDCl<sub>3</sub>)

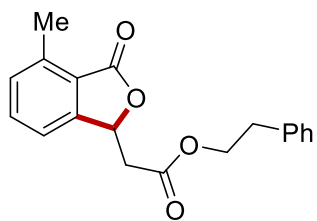


**400x**  
(100 MHz, CDCl<sub>3</sub>)

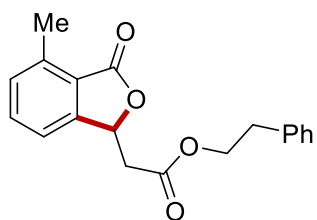
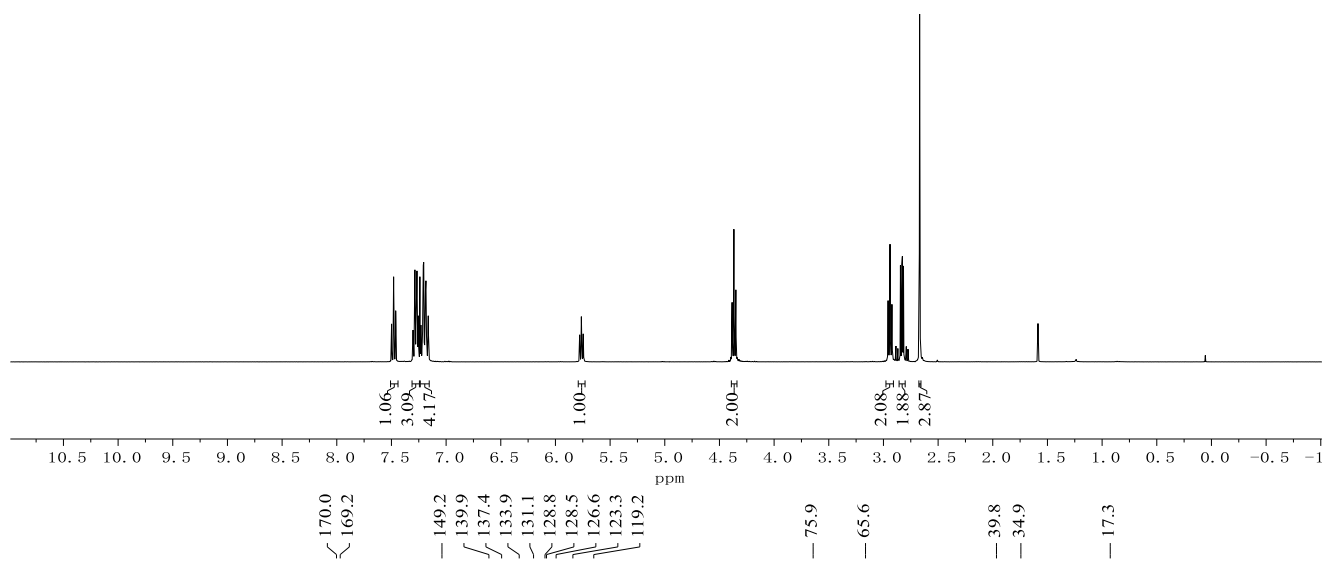




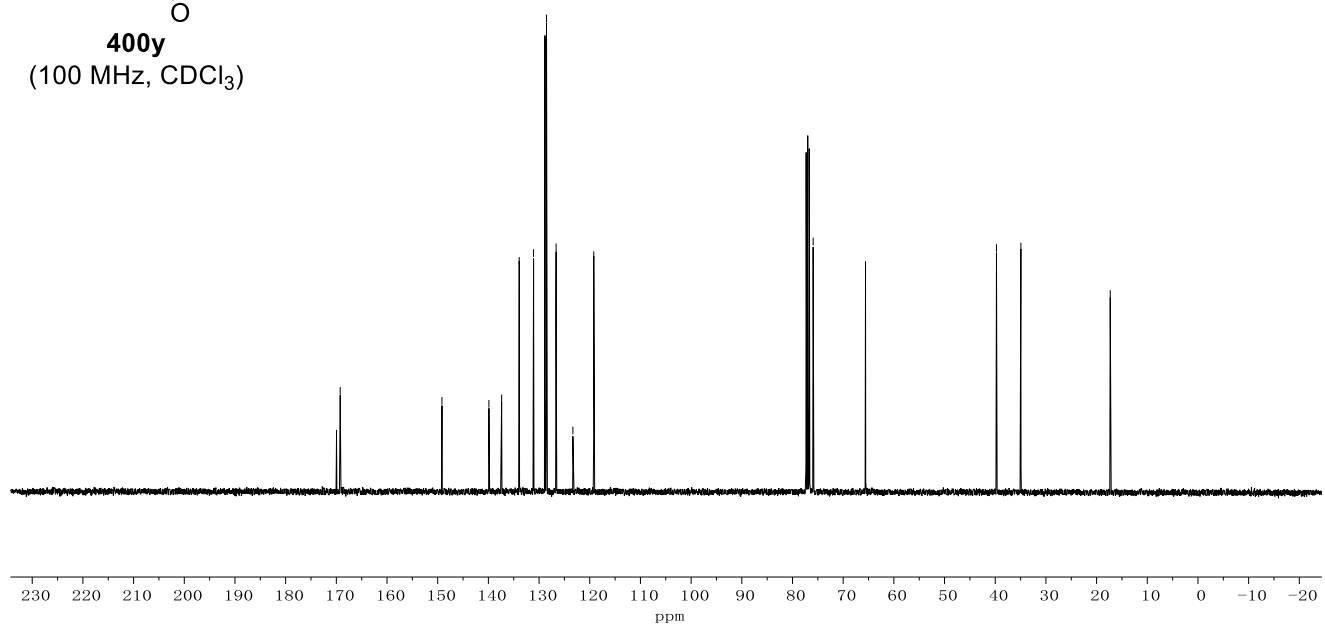
Appendix: NMR Spectra



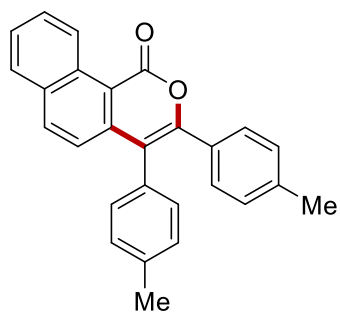
**400y**  
(400 MHz, CDCl<sub>3</sub>)



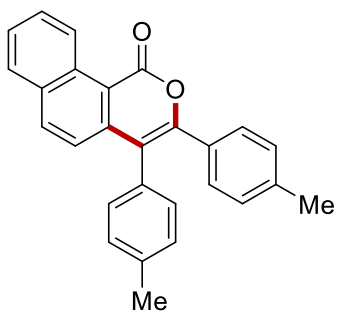
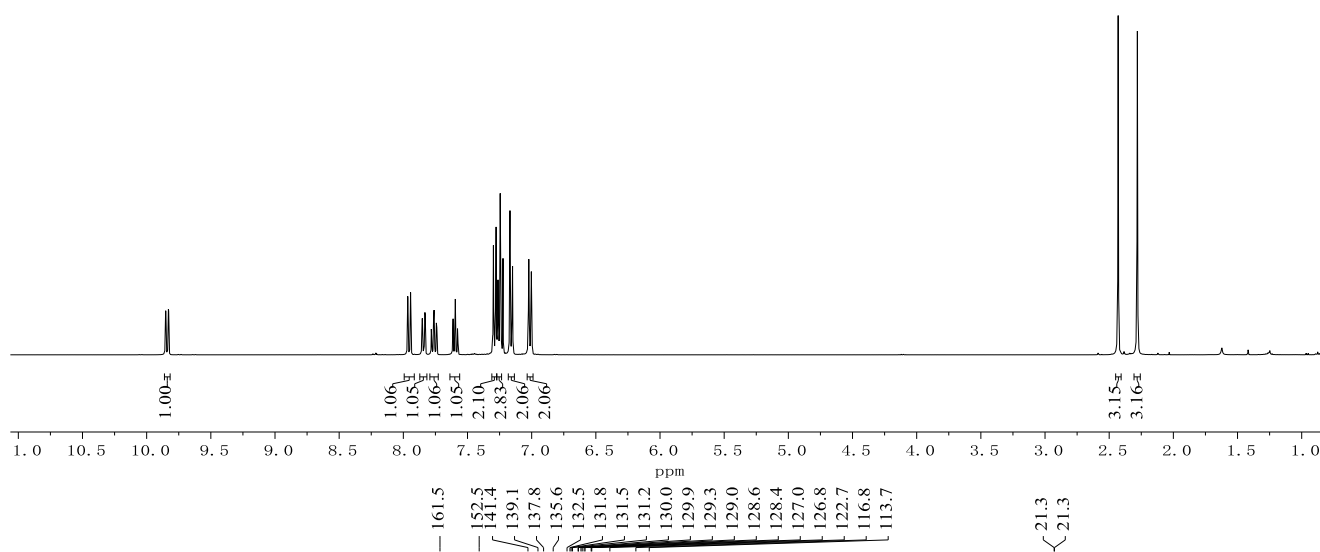
**400y**  
(100 MHz, CDCl<sub>3</sub>)



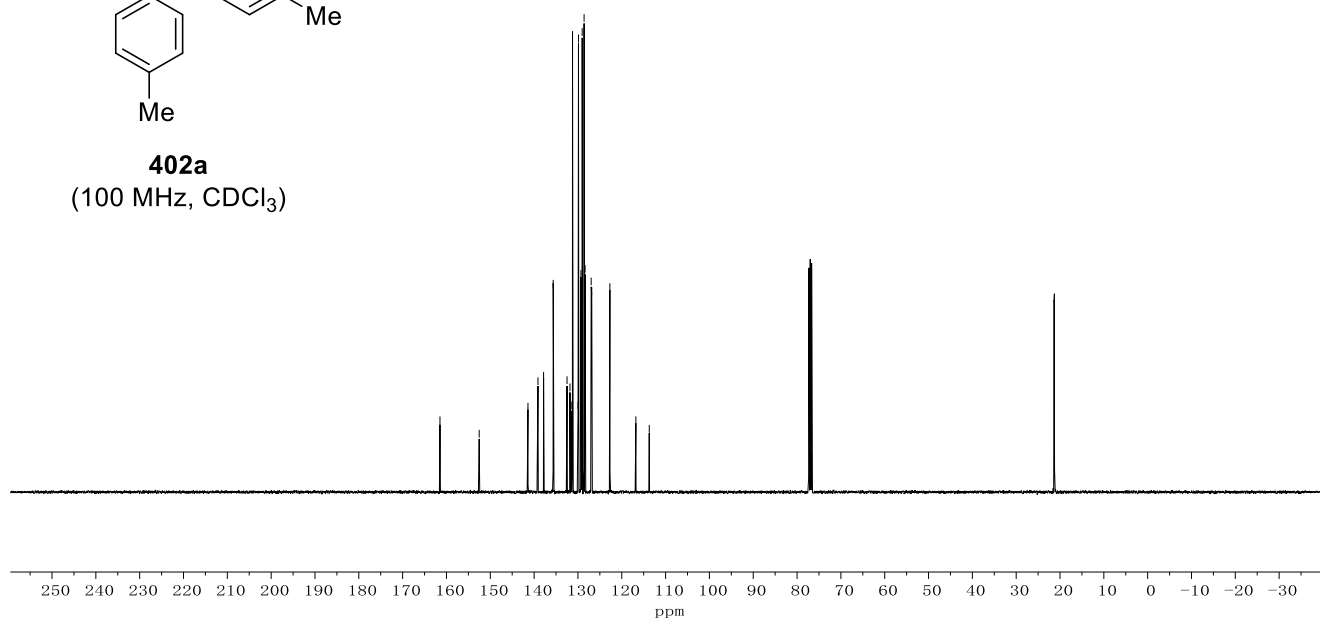
Appendix: NMR Spectra



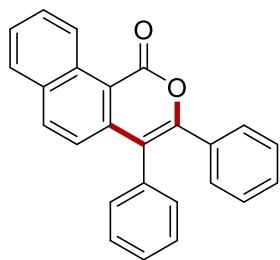
**402a**  
(400 MHz, CDCl<sub>3</sub>)



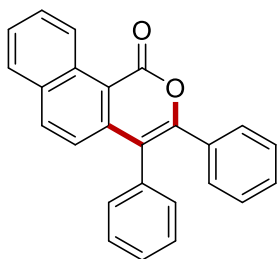
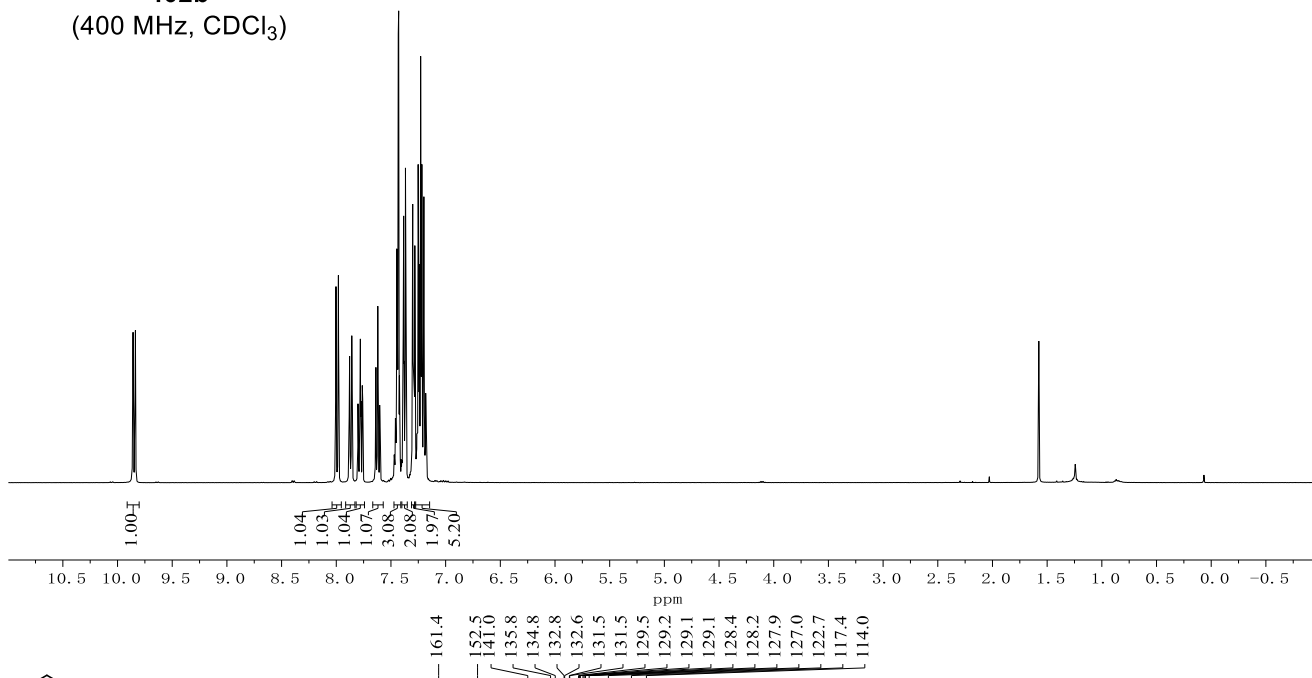
**402a**  
(100 MHz, CDCl<sub>3</sub>)



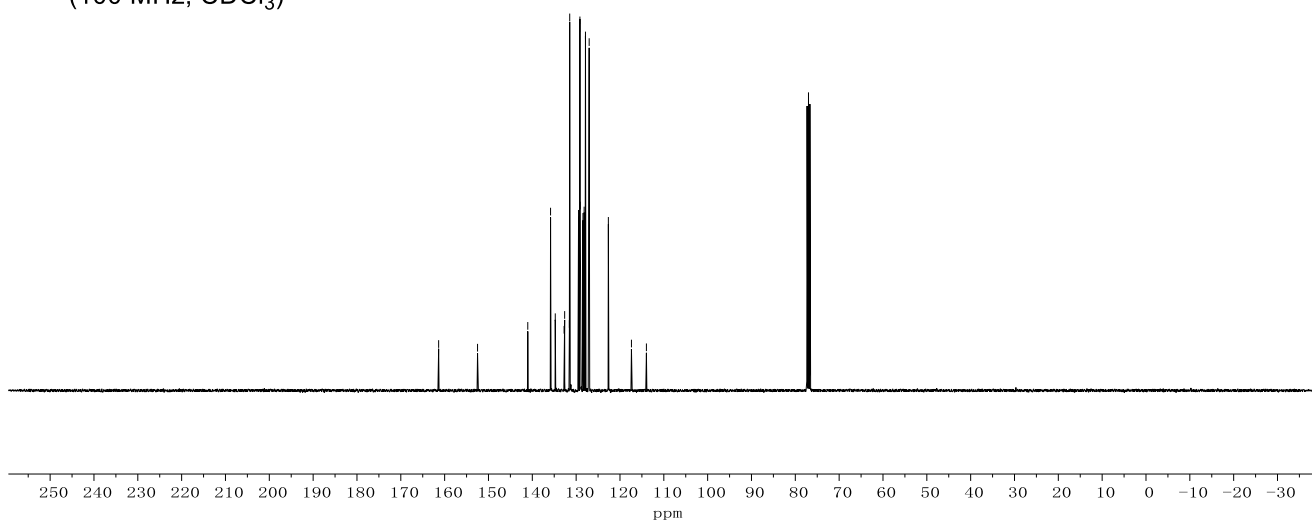
Appendix: NMR Spectra

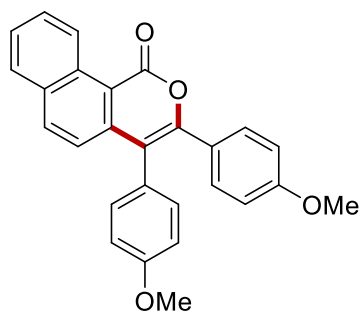


**402b**  
(400 MHz, CDCl<sub>3</sub>)

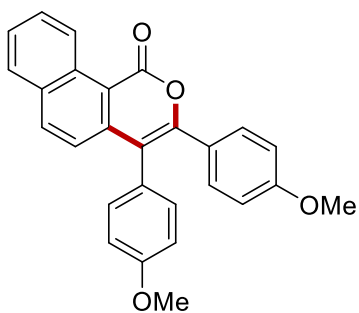
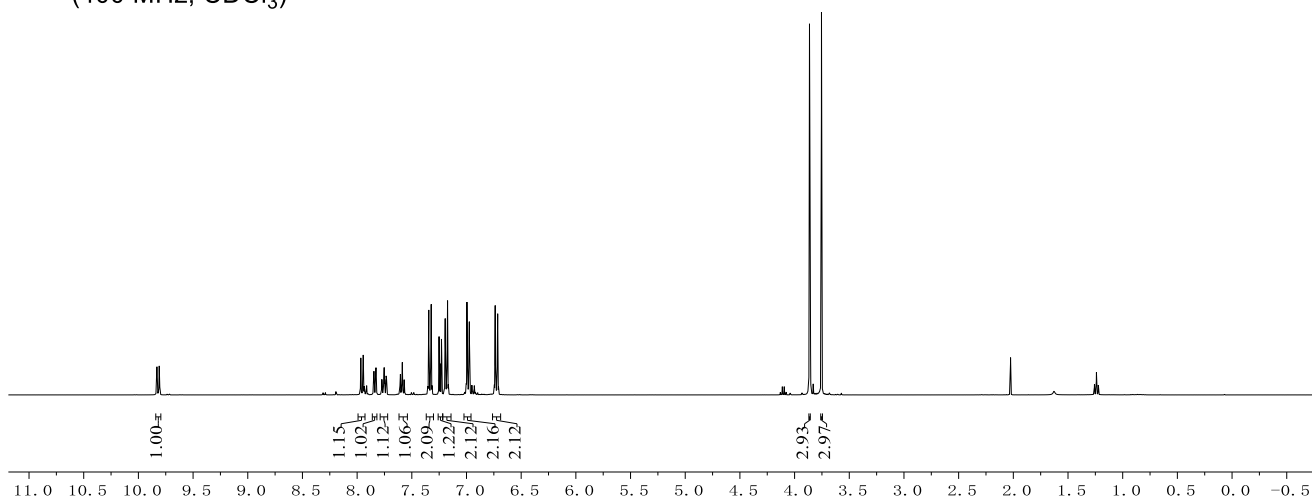


**402b**  
(100 MHz, CDCl<sub>3</sub>)

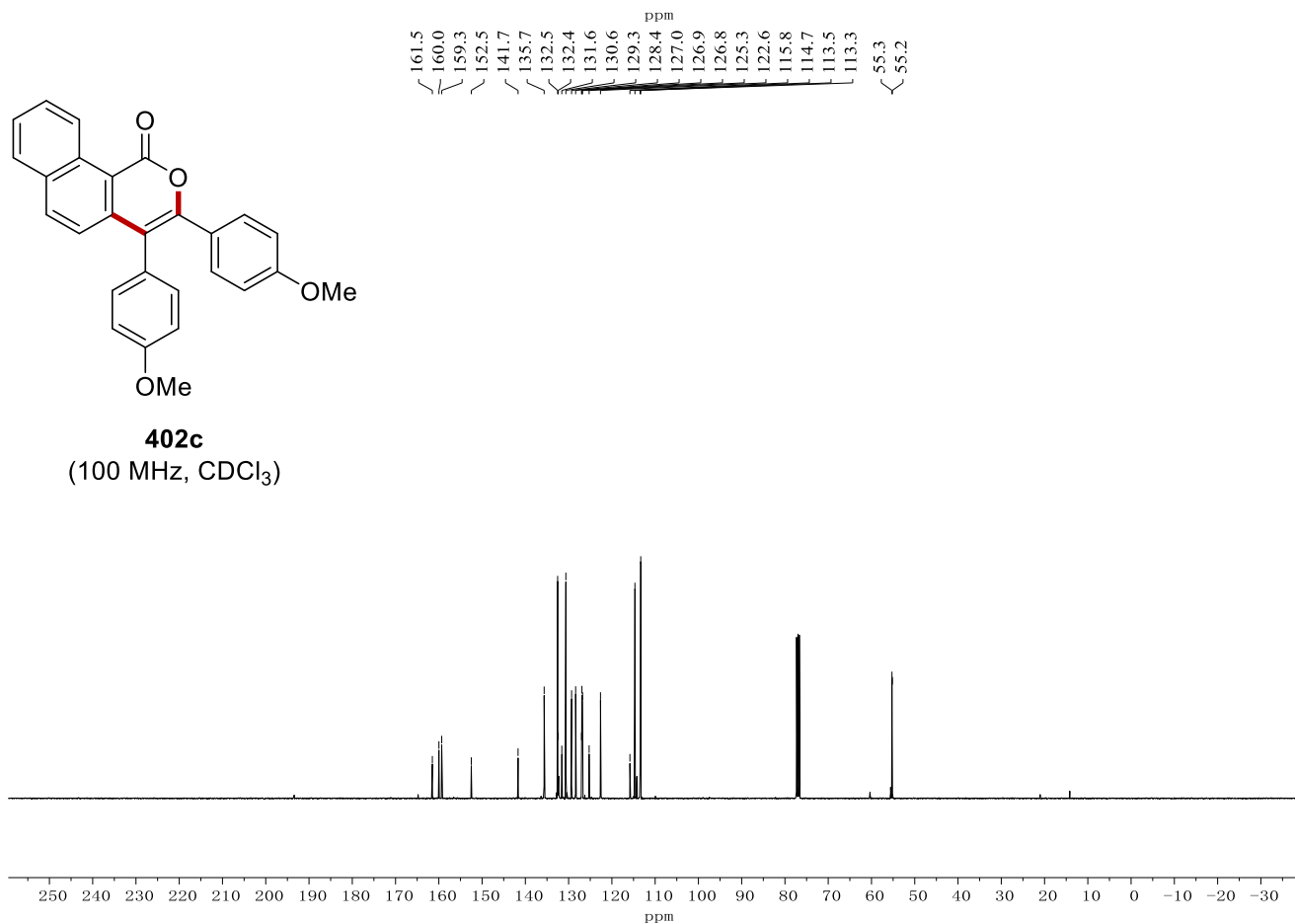




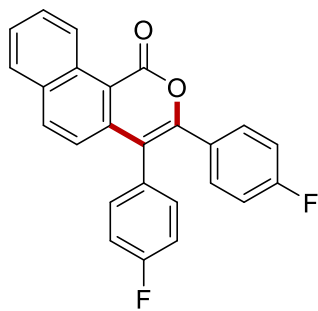
**402c**  
(400 MHz, CDCl<sub>3</sub>)



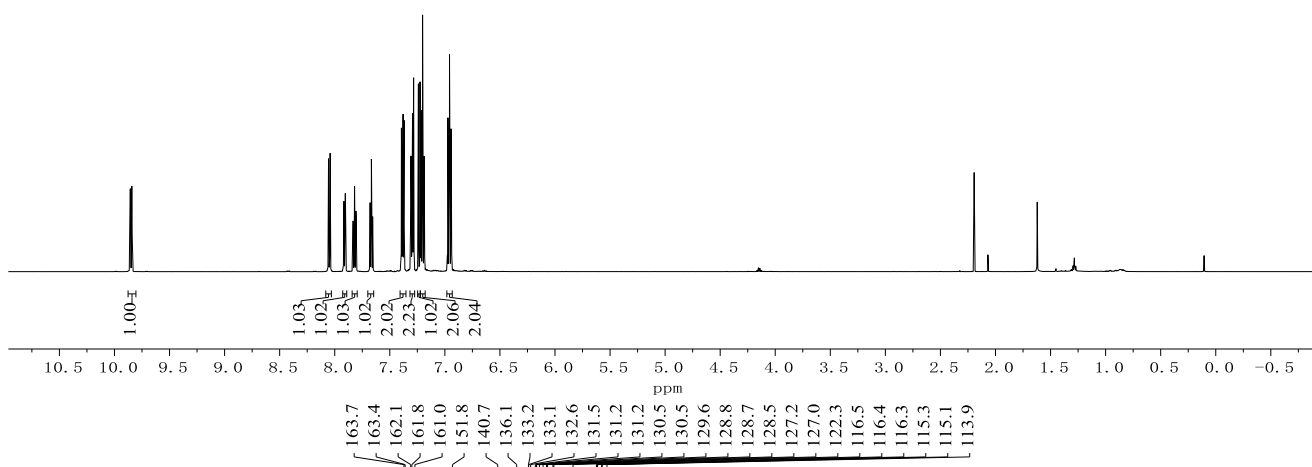
**402c**  
(100 MHz, CDCl<sub>3</sub>)



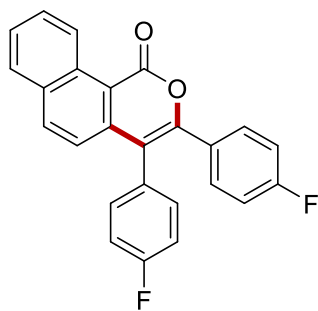
Appendix: NMR Spectra



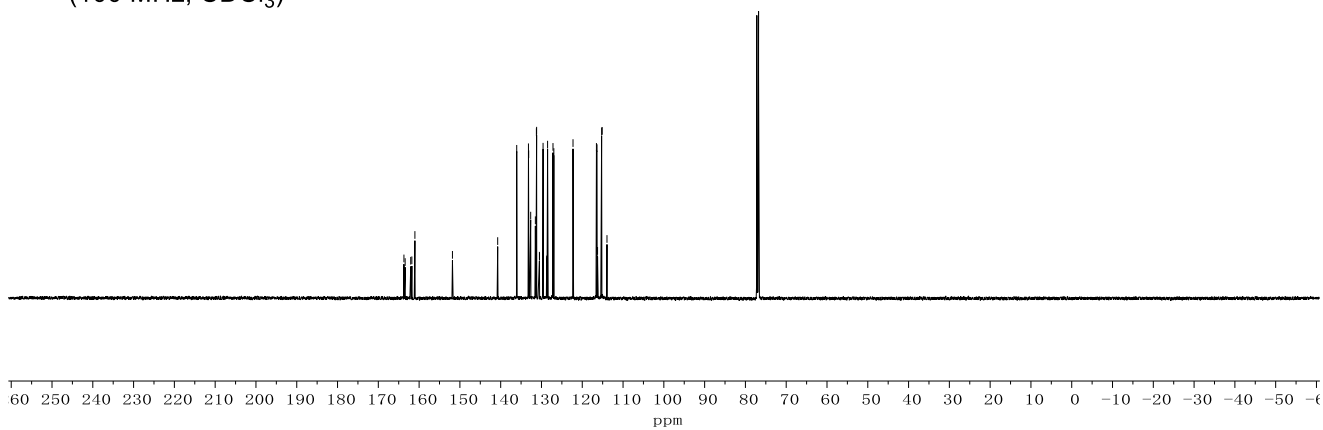
**402d**  
(400 MHz, CDCl<sub>3</sub>)



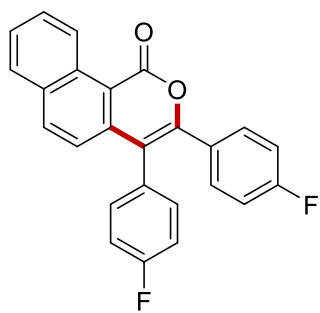
163.7  
163.4  
162.1  
161.8  
161.0  
151.8  
140.7  
136.1  
133.2  
133.1  
132.6  
131.5  
131.2  
131.2  
130.5  
130.5  
129.6  
128.8  
128.7  
128.5  
127.2  
127.0  
122.3  
116.5  
116.4  
116.3  
115.3  
115.1  
113.9



**402d**  
(100 MHz, CDCl<sub>3</sub>)

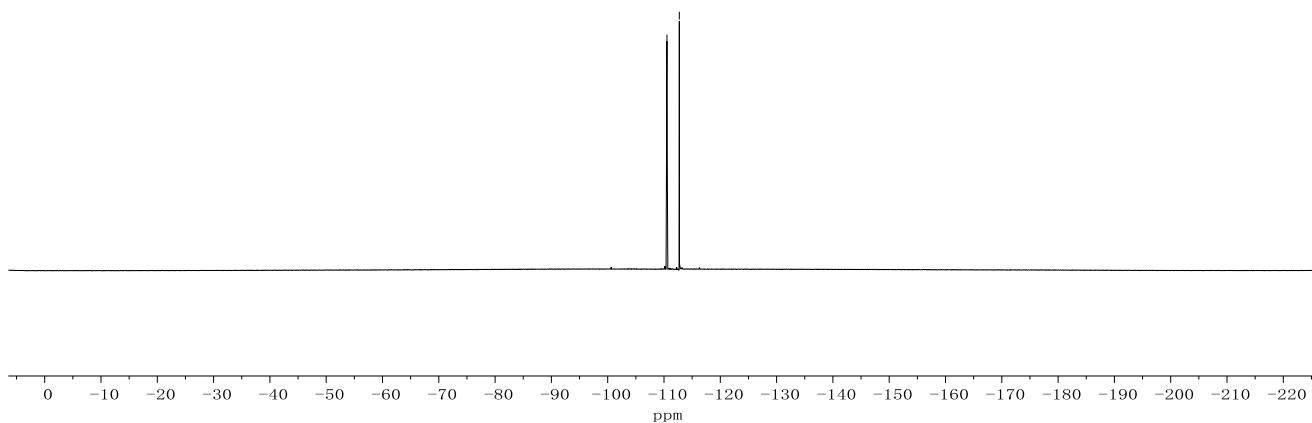


Appendix: NMR Spectra

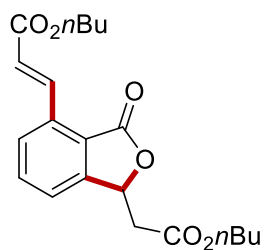


**402d**  
(282 MHz, CDCl<sub>3</sub>)

~ -110.5  
~ -112.7

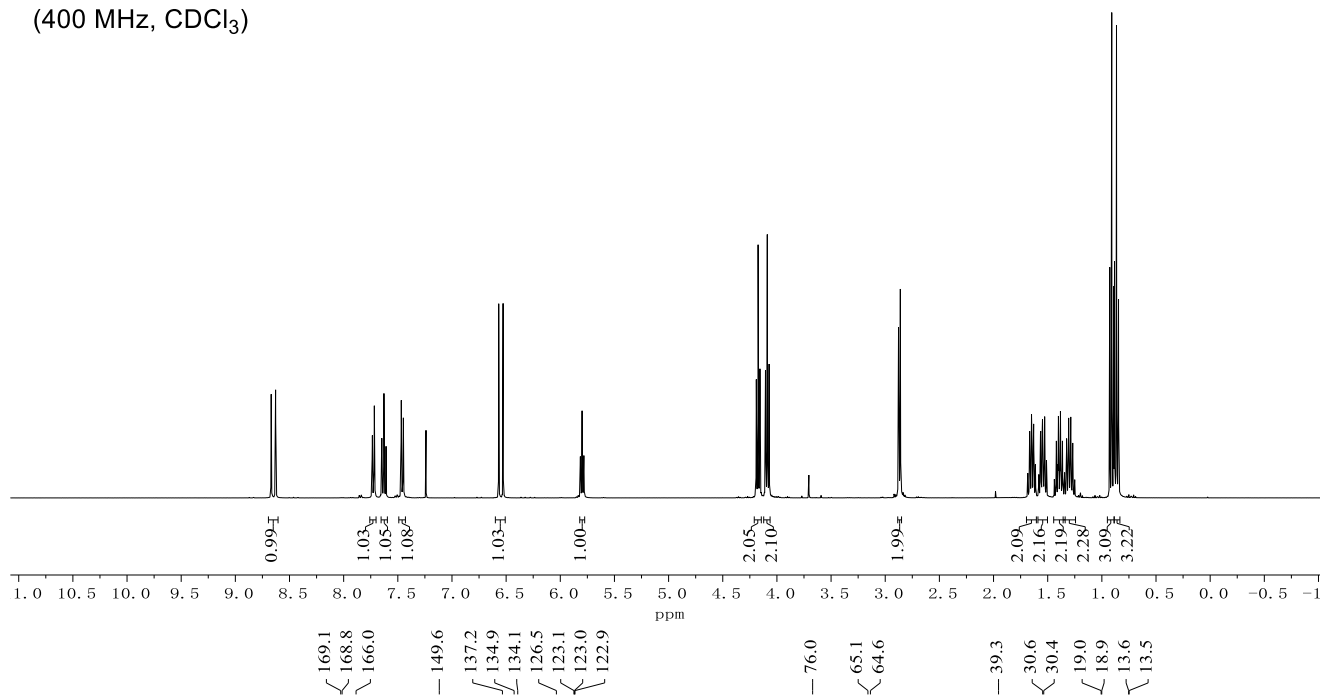


Appendix: NMR Spectra

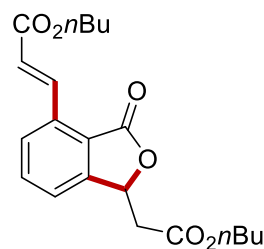


**426**

(400 MHz, CDCl<sub>3</sub>)

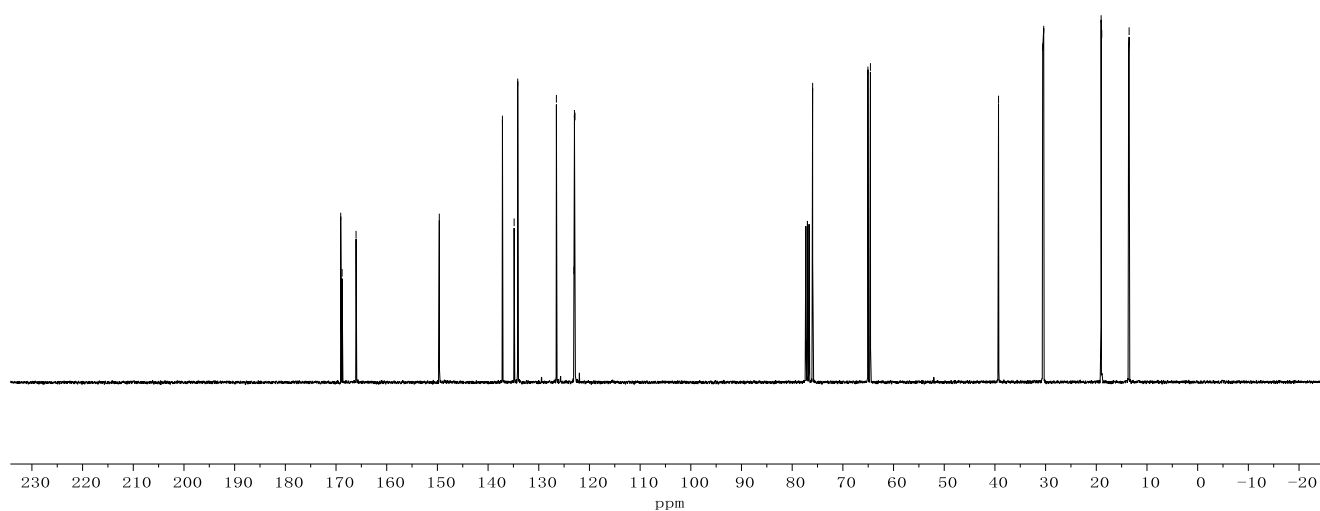


169.1  
168.8  
166.0  
149.6  
137.2  
134.9  
134.1  
126.5  
123.1  
123.0  
122.9  
76.0  
65.1  
64.6  
39.3  
30.6  
30.4  
19.0  
18.9  
13.6  
13.5



**426**

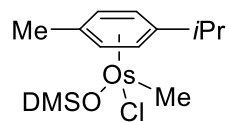
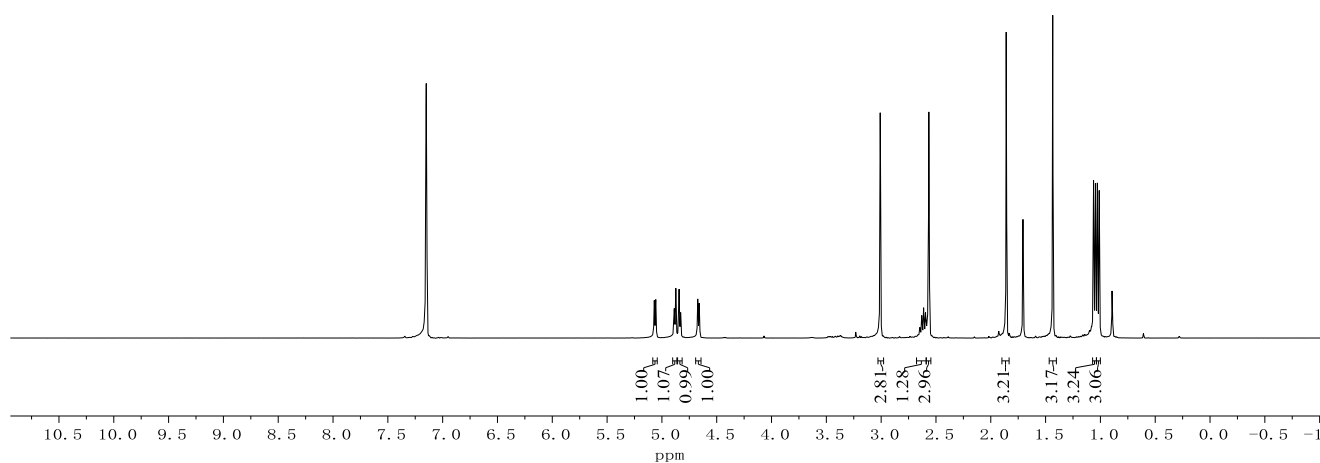
(100 MHz, CDCl<sub>3</sub>)



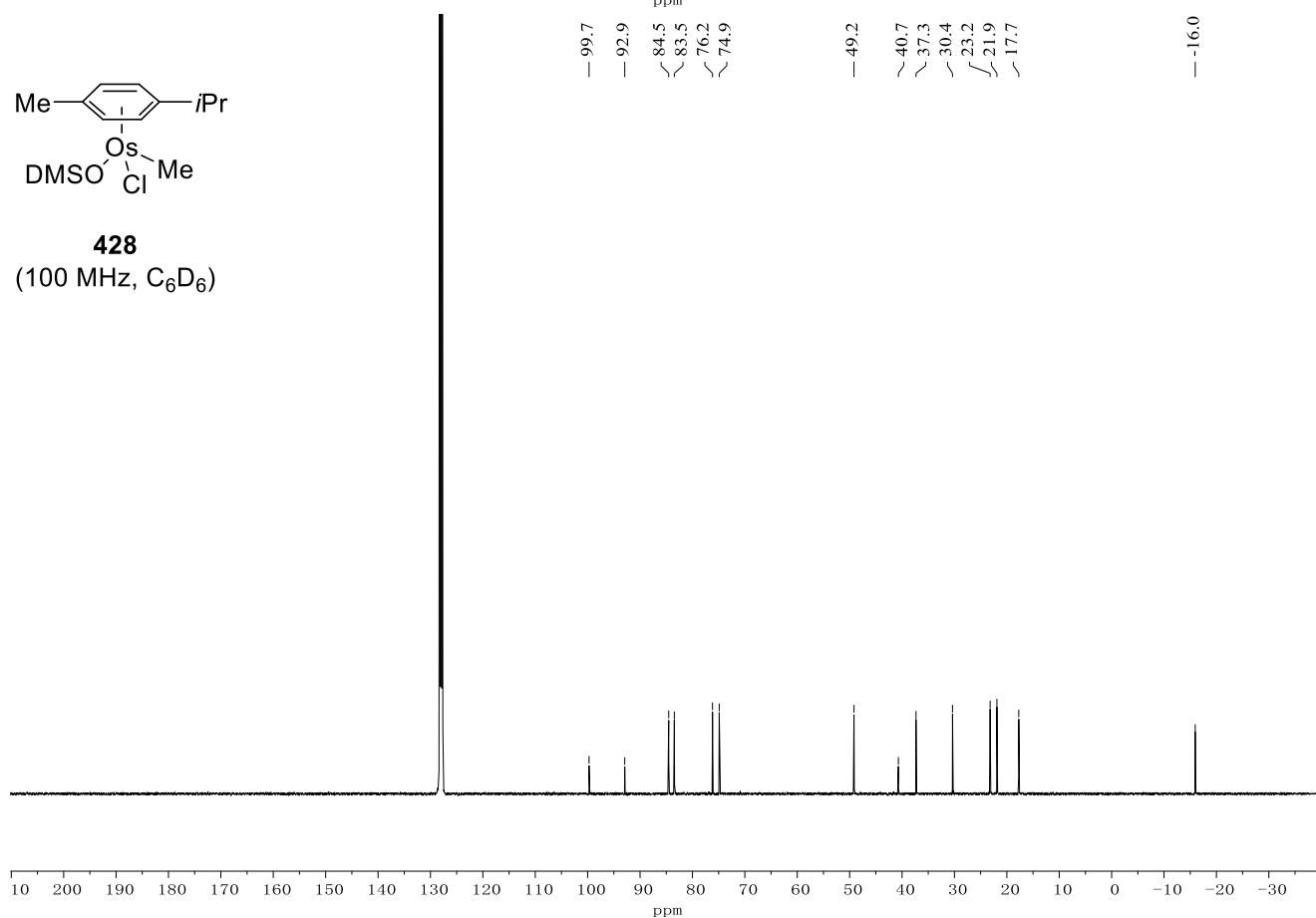
Appendix: NMR Spectra



**428**  
(400 MHz, C<sub>6</sub>D<sub>6</sub>)

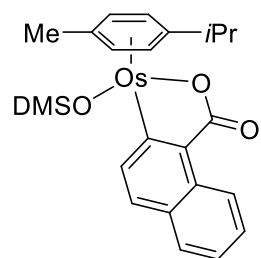


**428**  
(100 MHz, C<sub>6</sub>D<sub>6</sub>)

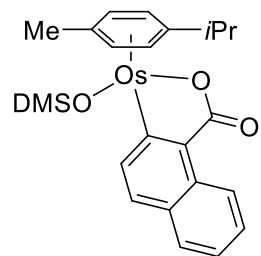
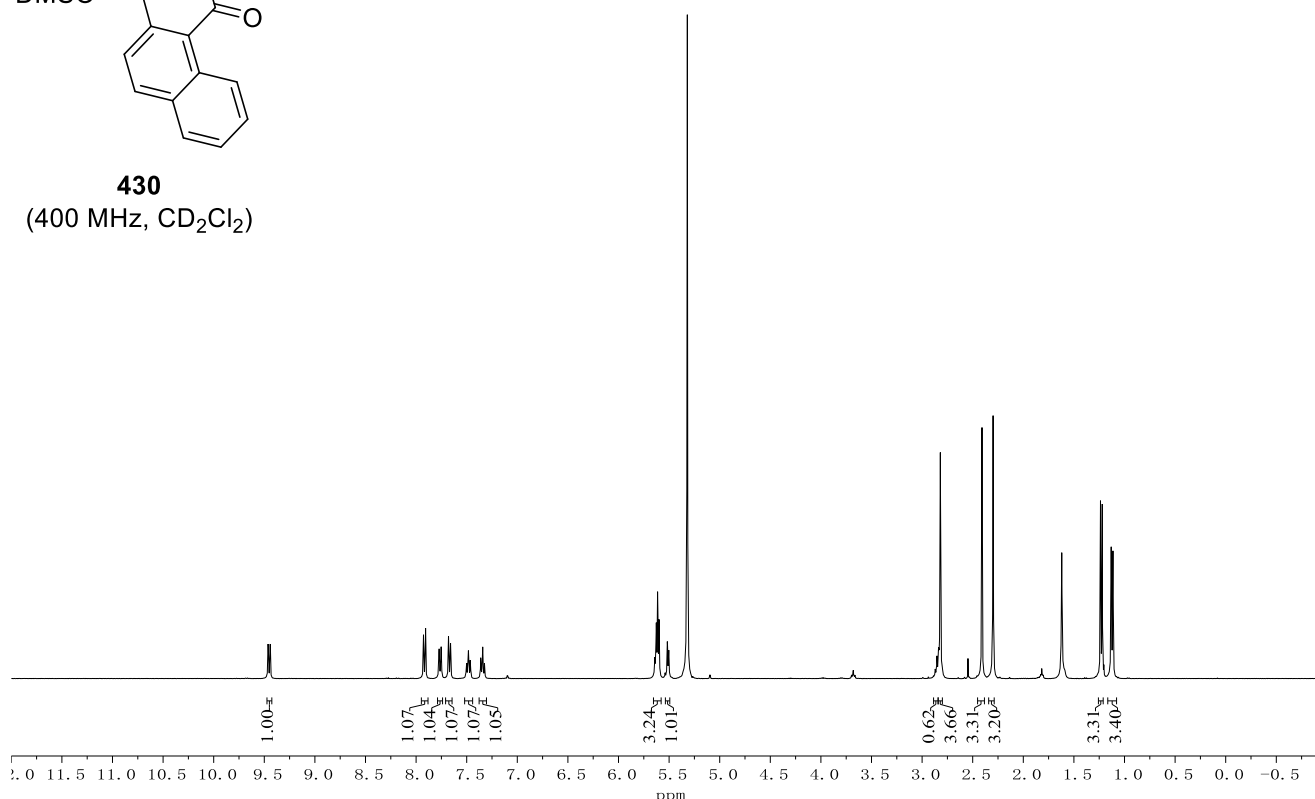




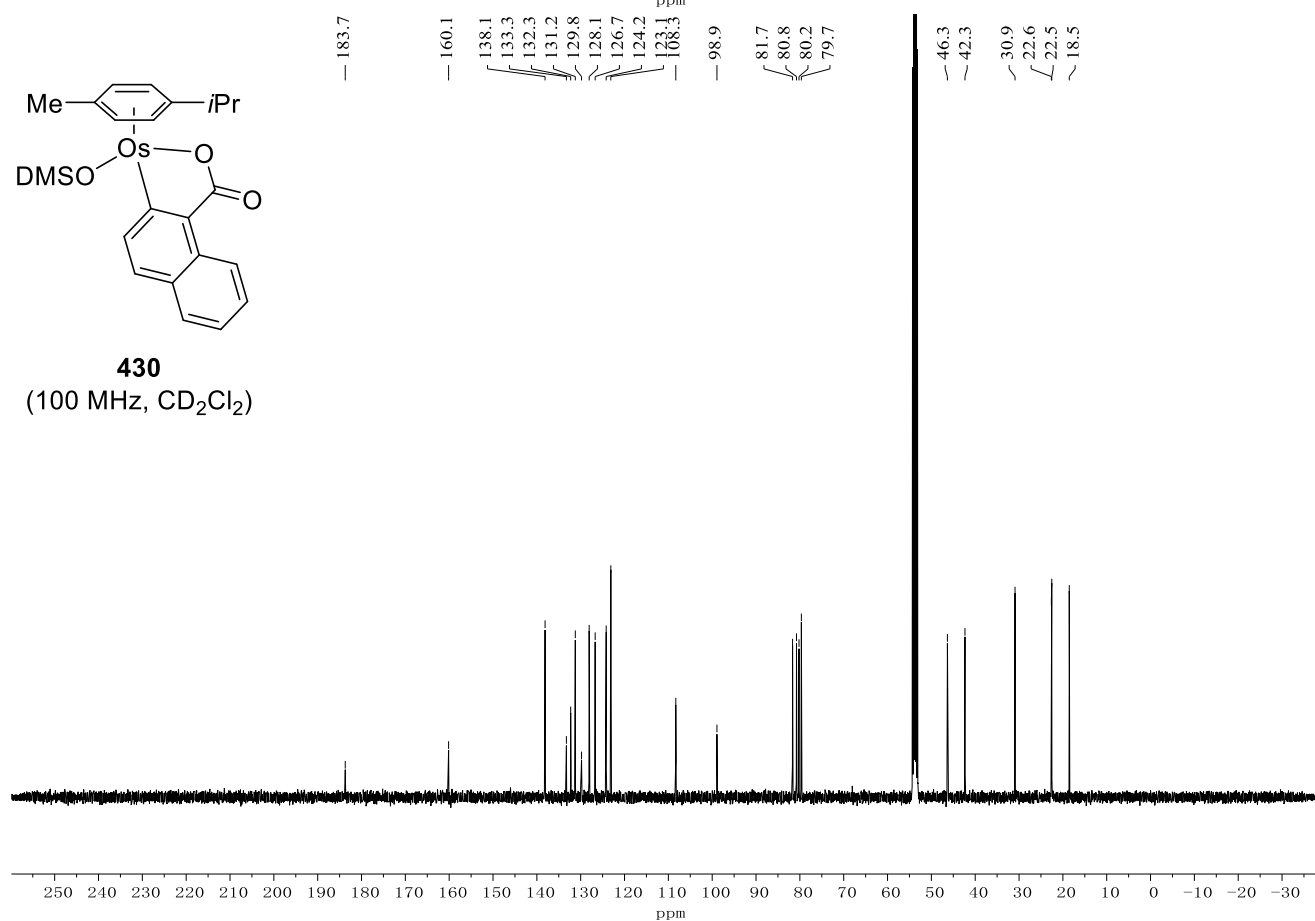
Appendix: NMR Spectra



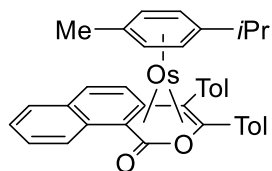
**430**  
(400 MHz, CD<sub>2</sub>Cl<sub>2</sub>)



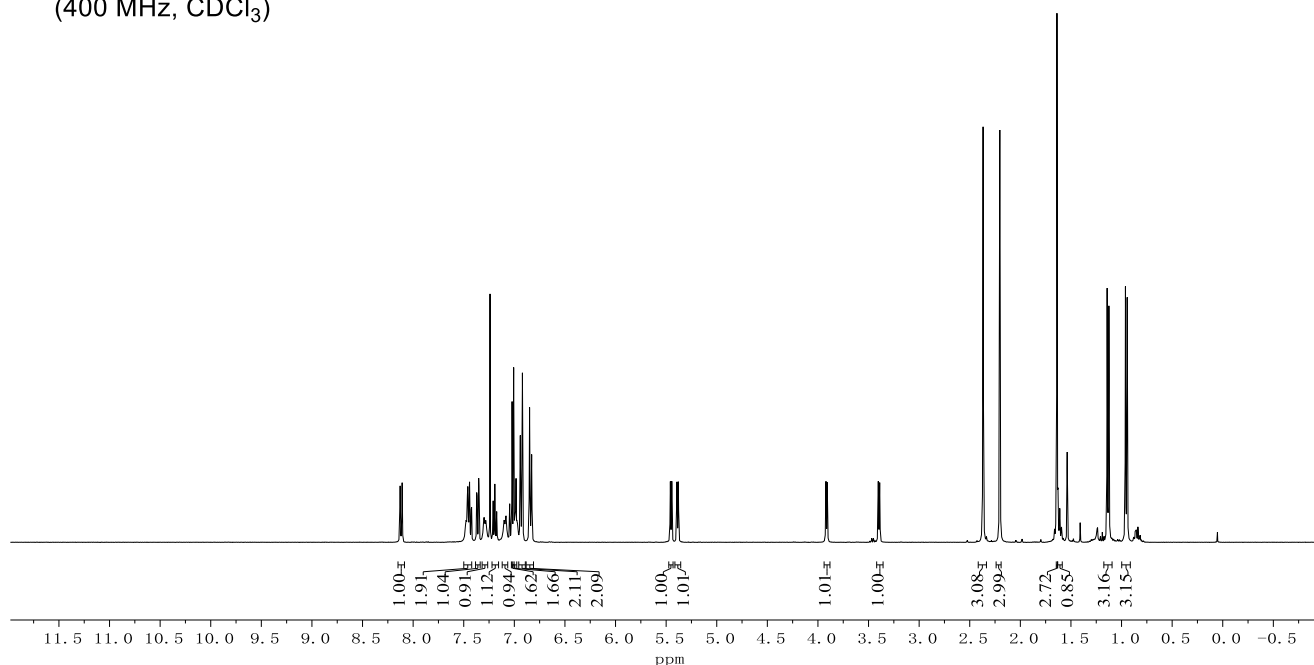
**430**  
(100 MHz, CD<sub>2</sub>Cl<sub>2</sub>)



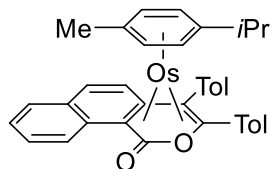
Appendix: NMR Spectra



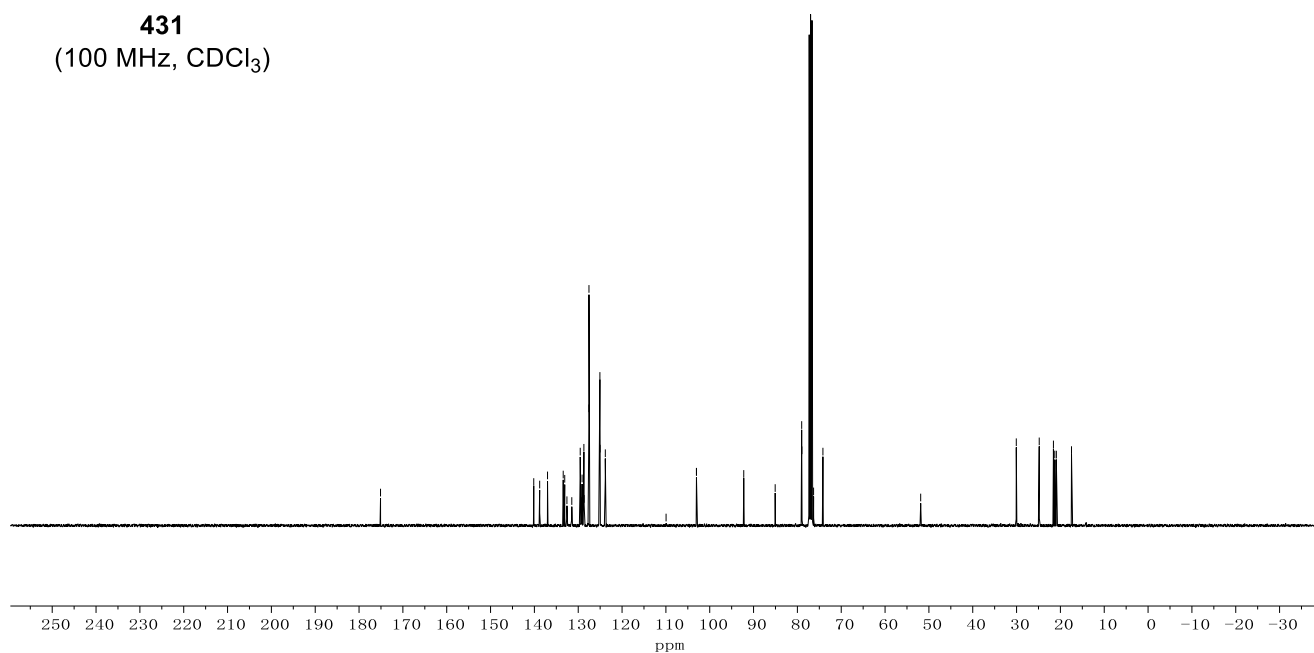
**431**  
(400 MHz, CDCl<sub>3</sub>)



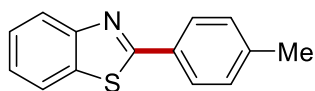
175.1  
140.1  
138.8  
137.0  
133.4  
133.1  
132.6  
131.5  
129.5  
129.3  
129.1  
128.7  
127.6  
127.5  
125.1  
125.0  
123.8  
110.0  
103.0  
103.0  
92.2  
85.1  
79.0  
79.0  
76.3  
74.2  
— 51.9  
30.1  
24.8  
21.6  
21.3  
20.9  
17.5



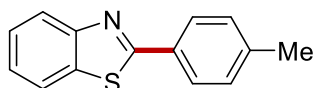
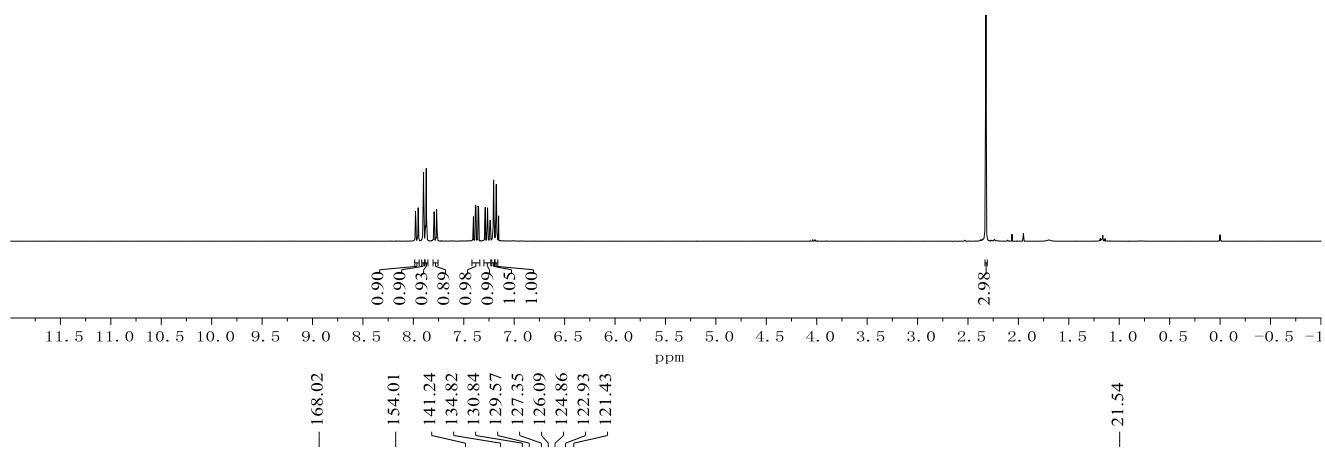
**431**  
(100 MHz, CDCl<sub>3</sub>)



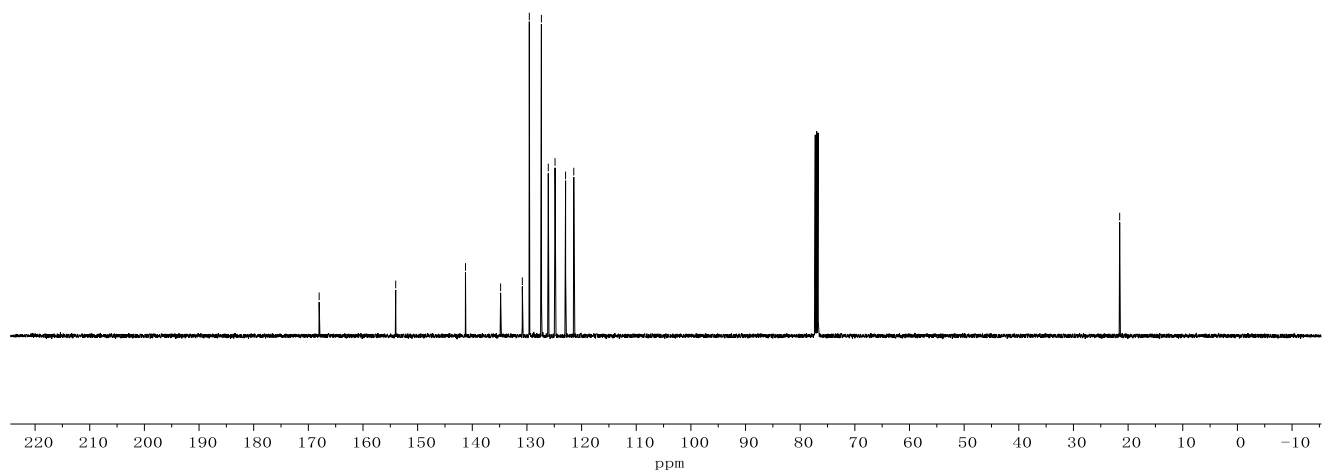
Appendix: NMR Spectra



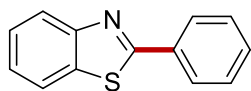
**405a**  
(300 MHz, CDCl<sub>3</sub>)



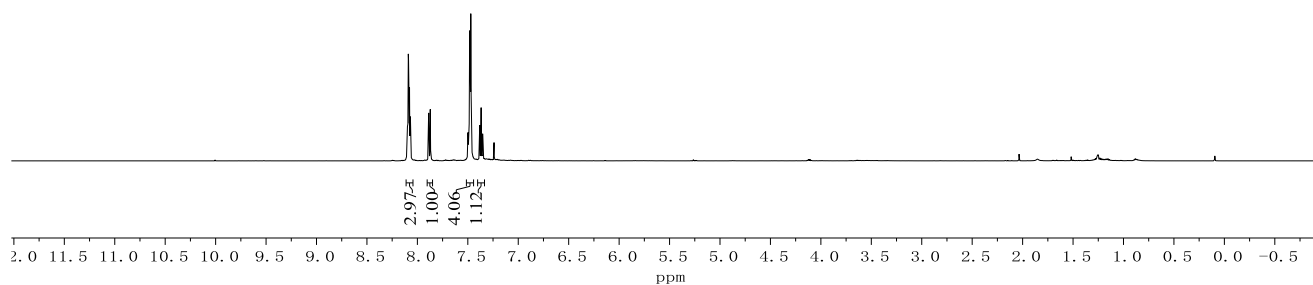
**405a**  
(75 MHz, CDCl<sub>3</sub>)



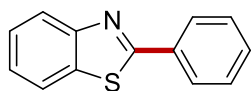
Appendix: NMR Spectra



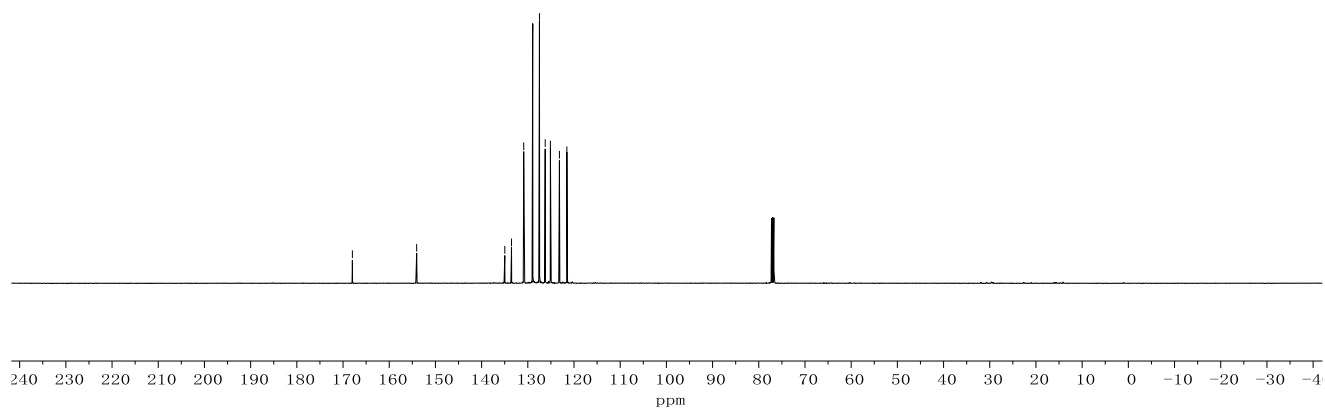
**405b**  
(500 MHz, CDCl<sub>3</sub>)



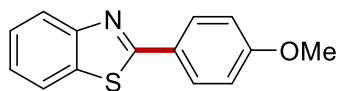
167.97  
154.06  
134.98  
133.53  
130.89  
128.94  
127.48  
126.24  
125.11  
123.15  
121.54



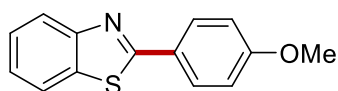
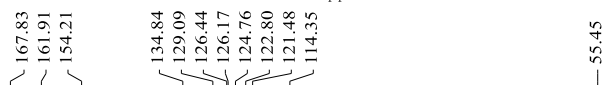
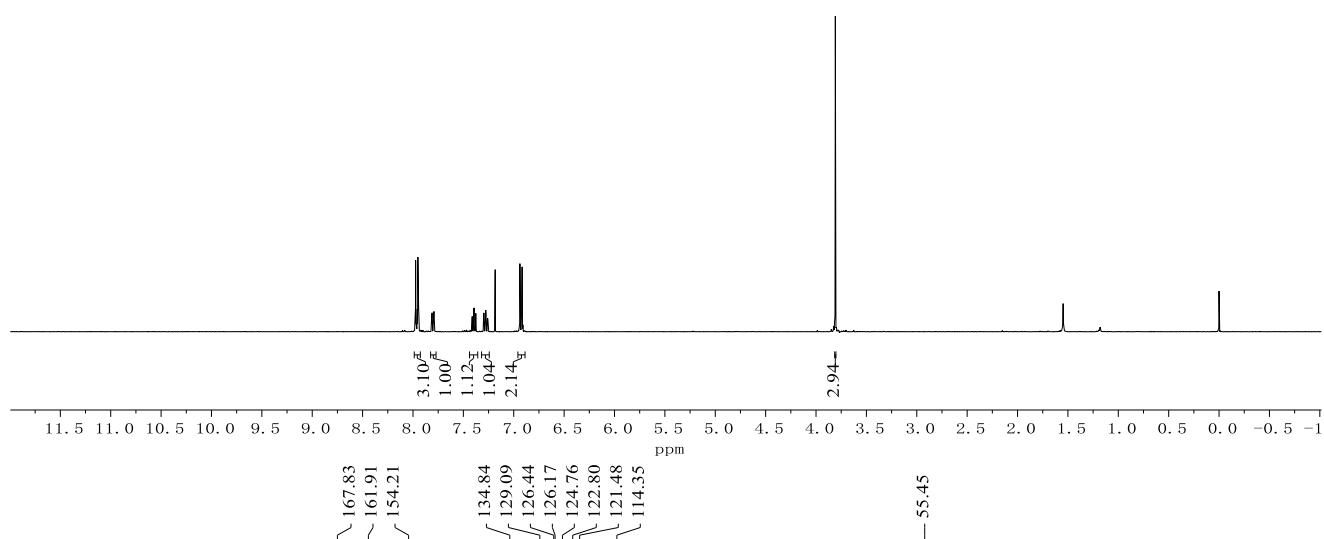
**405b**  
(125 MHz, CDCl<sub>3</sub>)



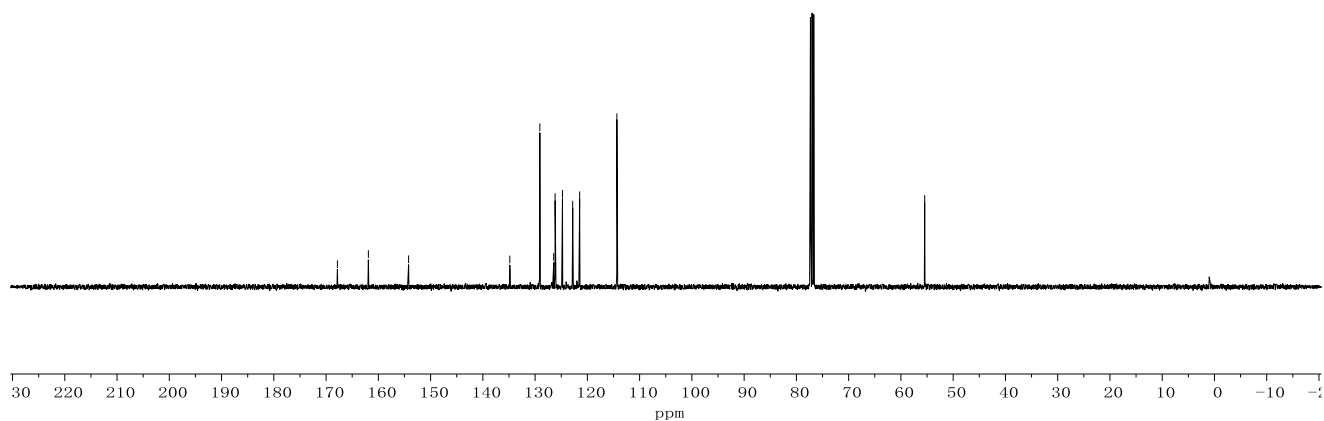
Appendix: NMR Spectra



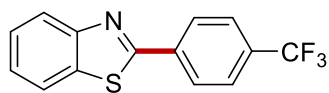
**405c**  
(400 MHz, CDCl<sub>3</sub>)



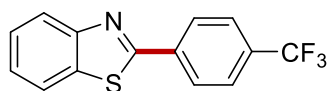
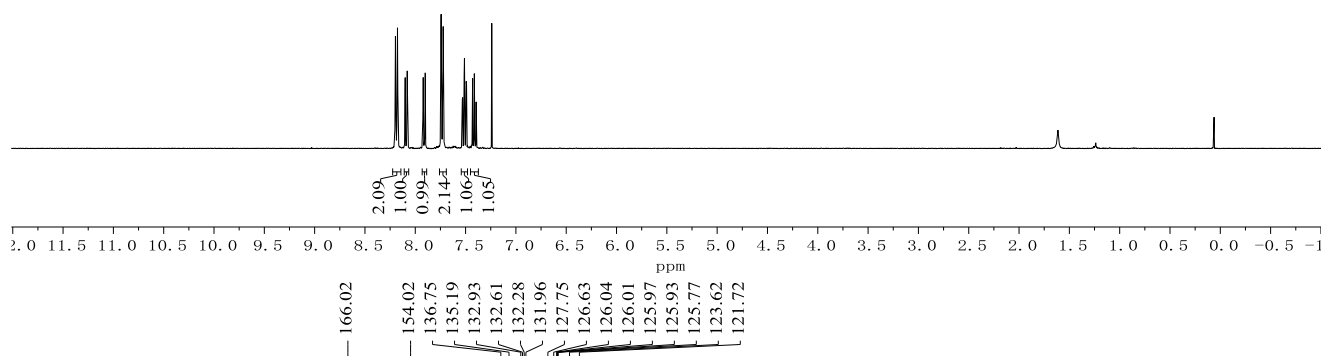
**405c**  
(100 MHz, CDCl<sub>3</sub>)



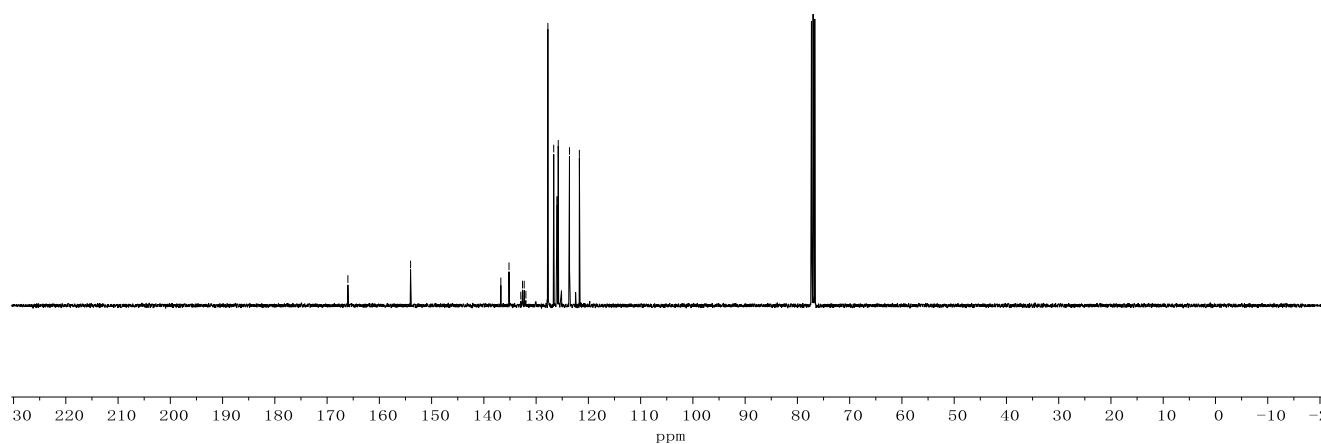
Appendix: NMR Spectra



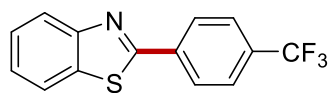
**405d**  
(400 MHz, CDCl<sub>3</sub>)



**405d**  
(100 MHz, CDCl<sub>3</sub>)

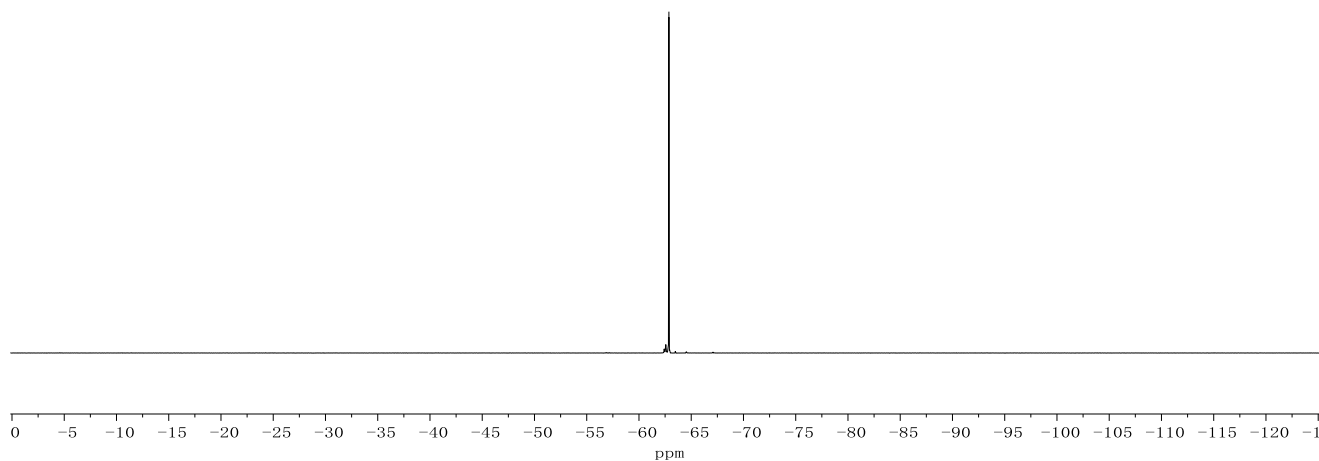


Appendix: NMR Spectra

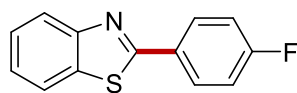


**405d**  
(282 MHz, CDCl<sub>3</sub>)

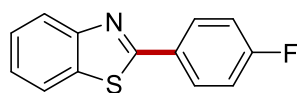
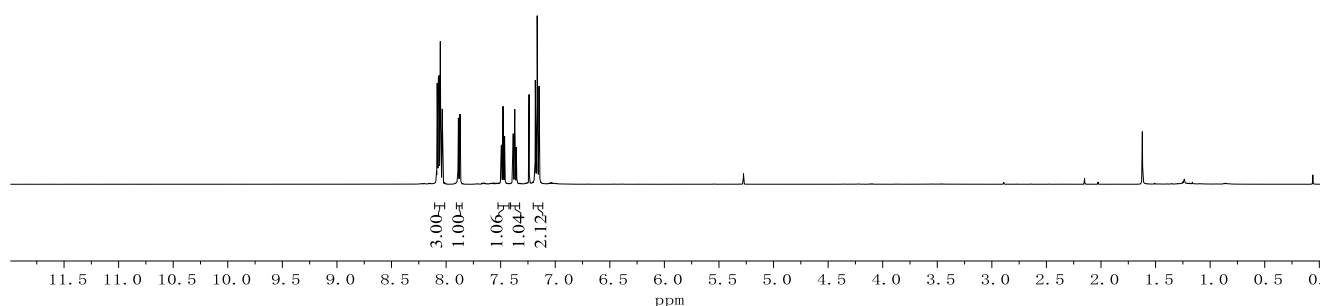
-62.9



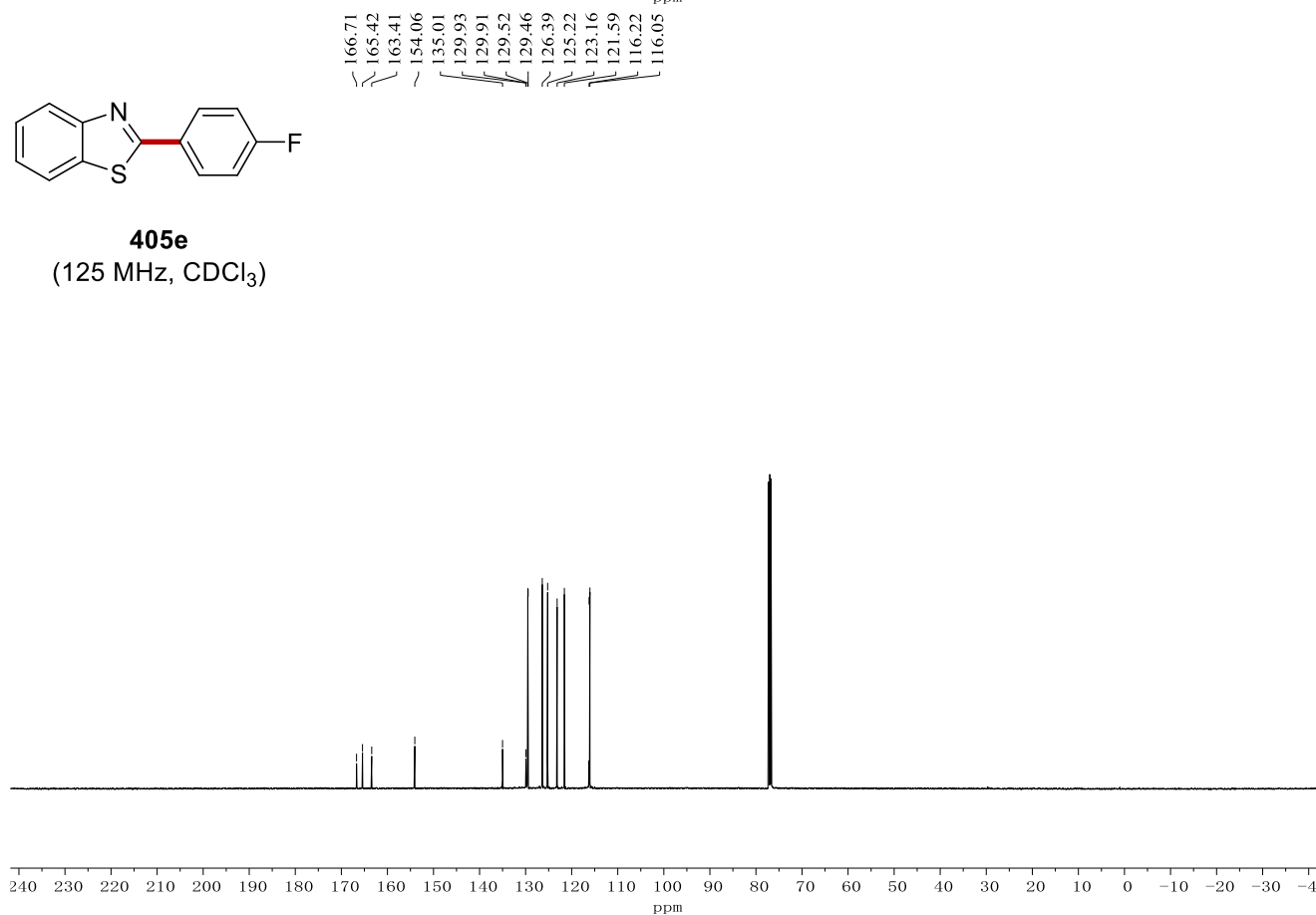
Appendix: NMR Septra



**405e**  
(500 MHz, CDCl<sub>3</sub>)

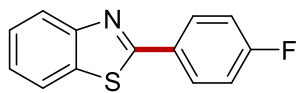


**405e**  
(125 MHz, CDCl<sub>3</sub>)



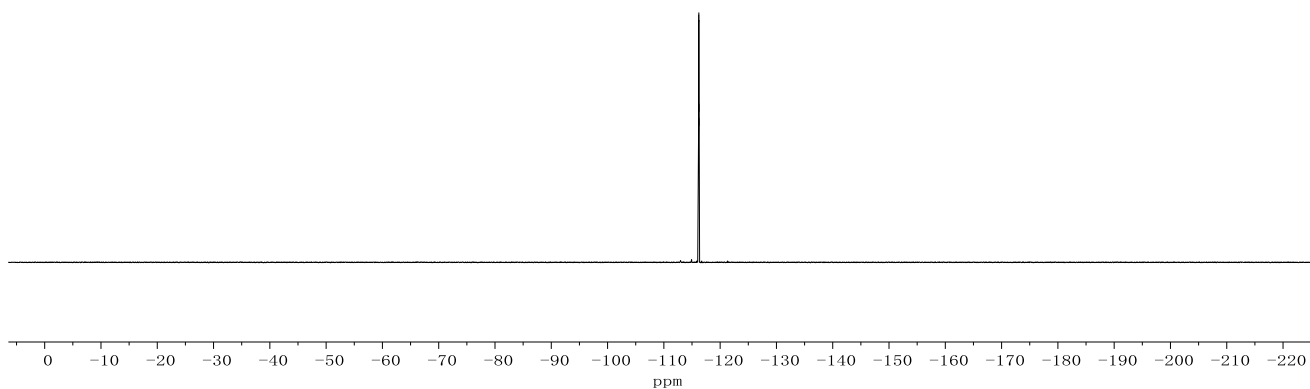


Appendix: NMR Spectra

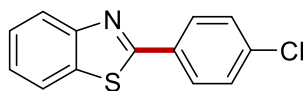


**405e**  
(282 MHz, CDCl<sub>3</sub>)

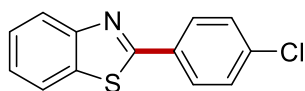
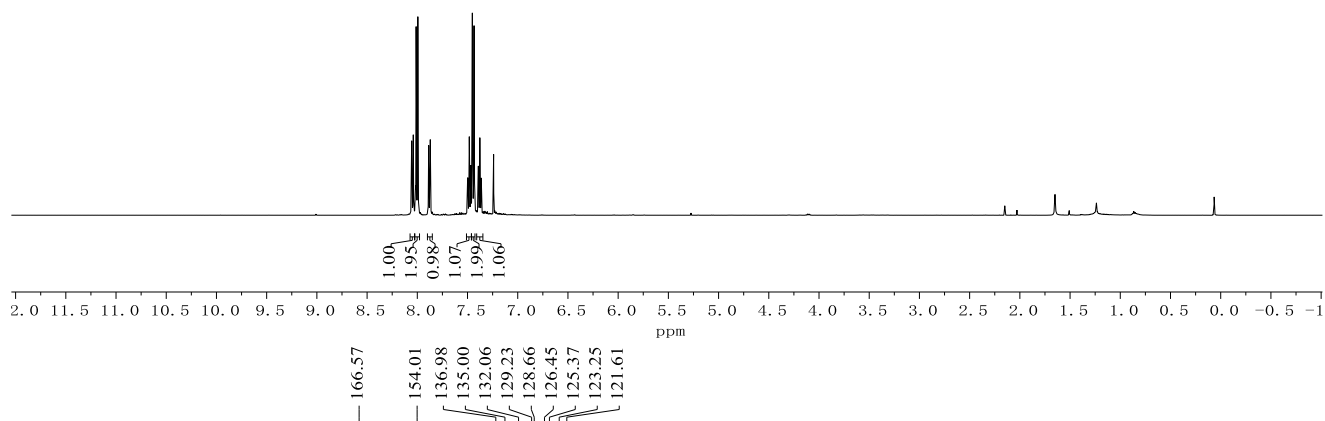
-116.2  
-116.2  
-116.2  
-116.2  
-116.2



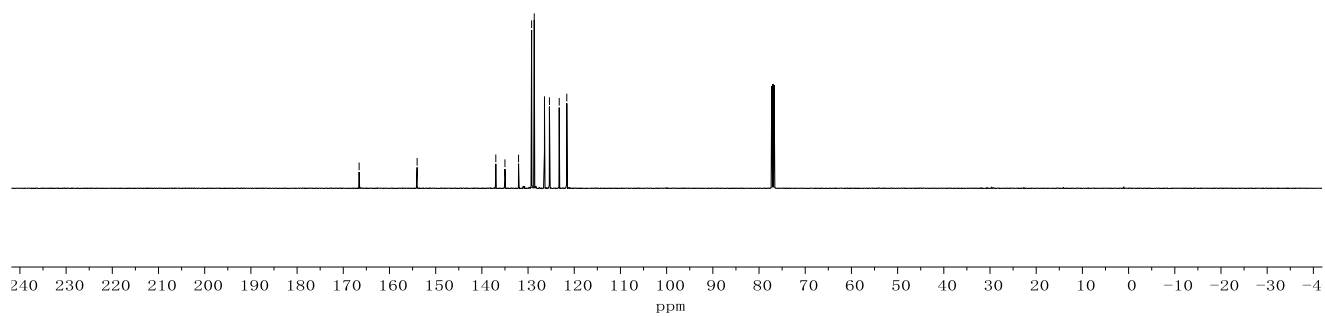
Appendix: NMR Sepctra



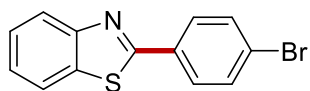
**405f**  
(500 MHz, CDCl<sub>3</sub>)



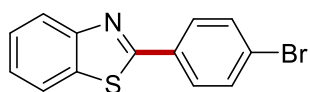
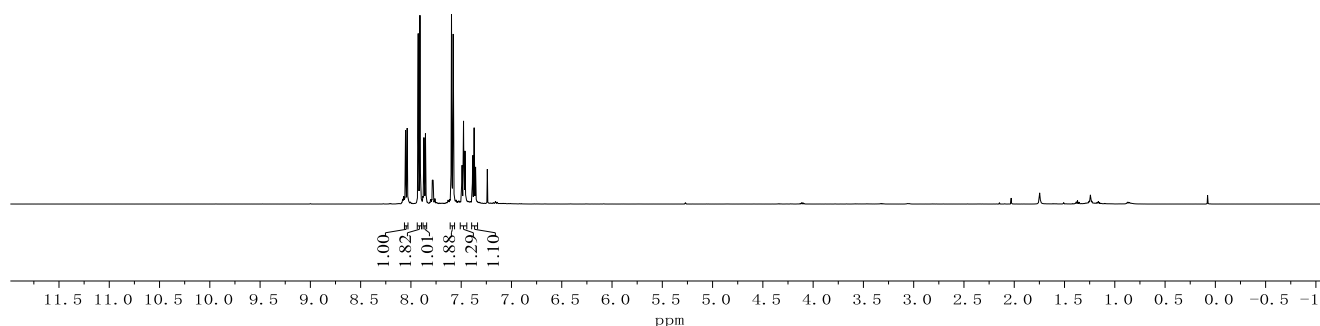
**405f**  
(125 MHz, CDCl<sub>3</sub>)



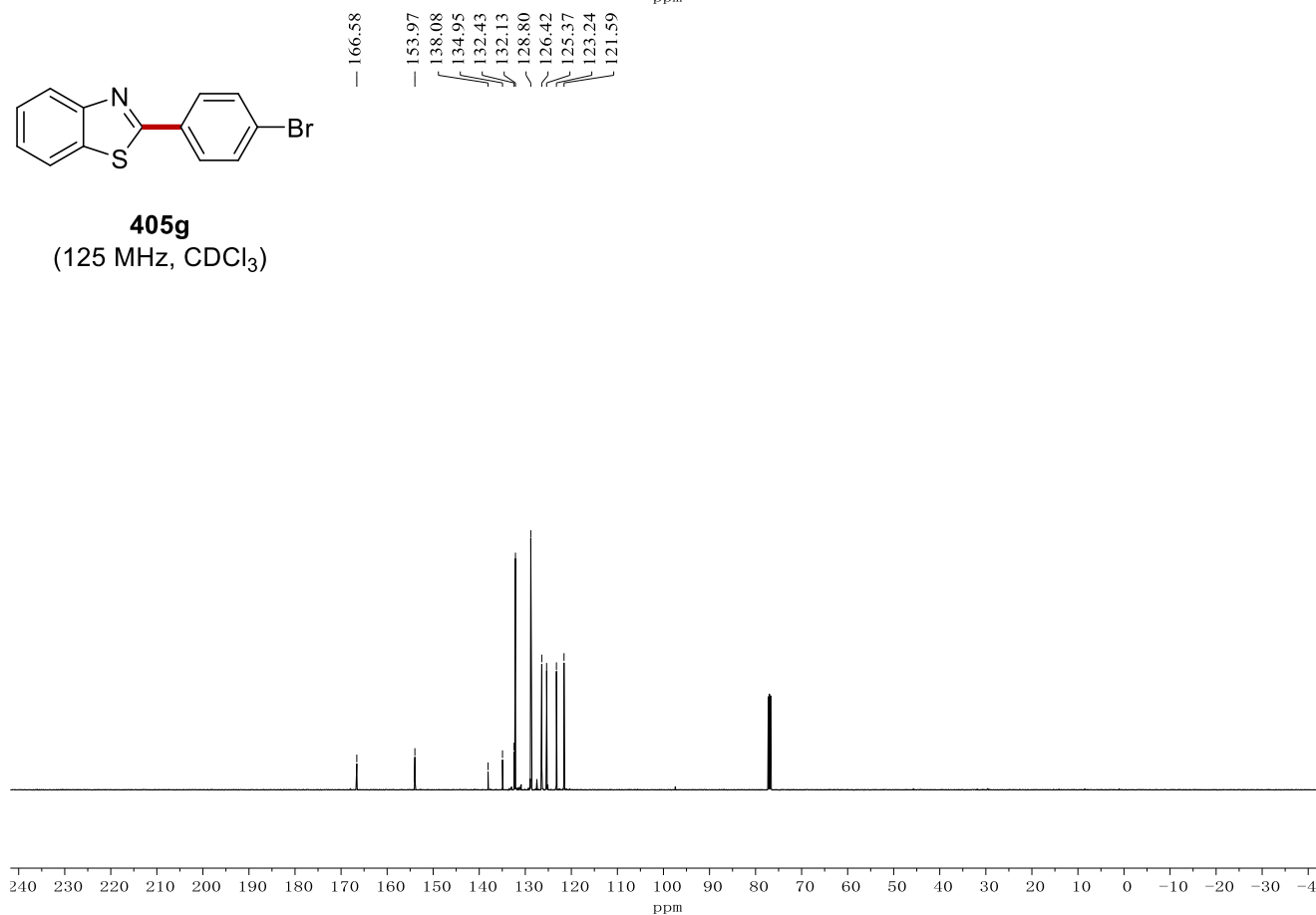
Appendix: NMR Spectra



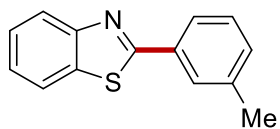
**405g**  
(500 MHz, CDCl<sub>3</sub>)



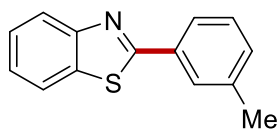
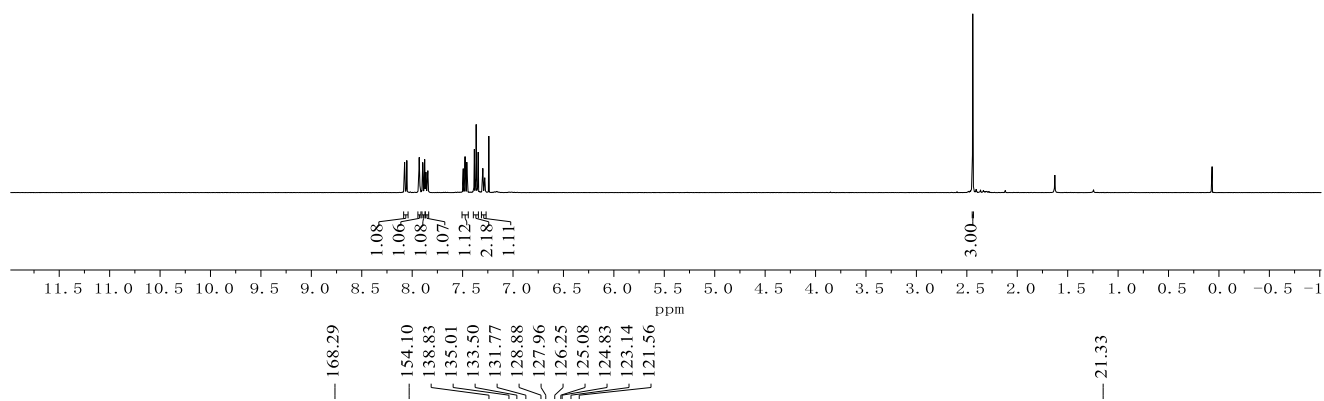
**405g**  
(125 MHz, CDCl<sub>3</sub>)



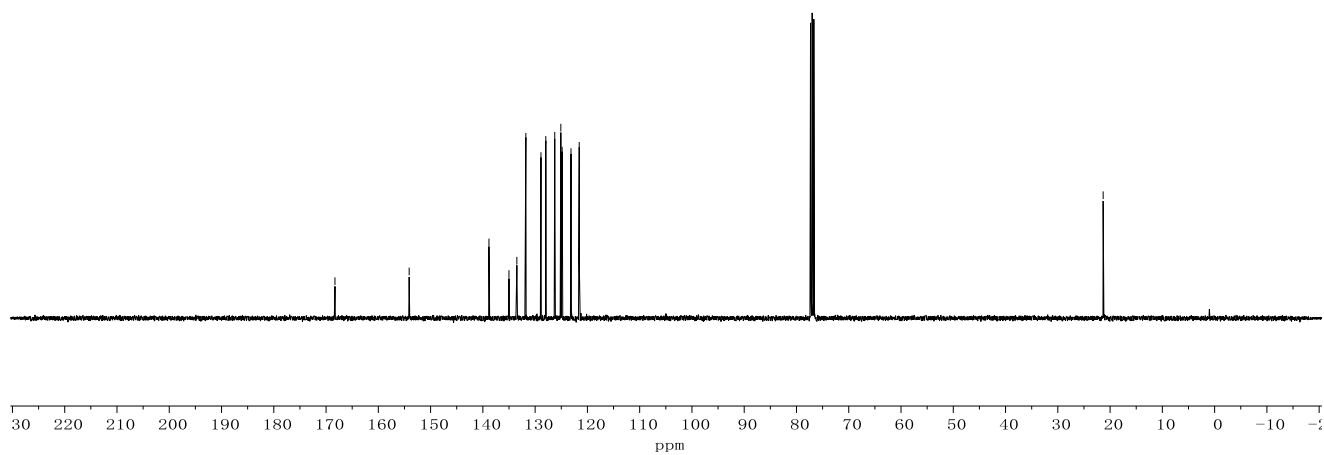
Appendix: NMR Spectra



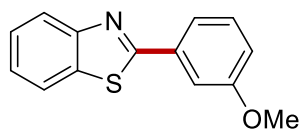
**405h**  
(400 MHz, CDCl<sub>3</sub>)



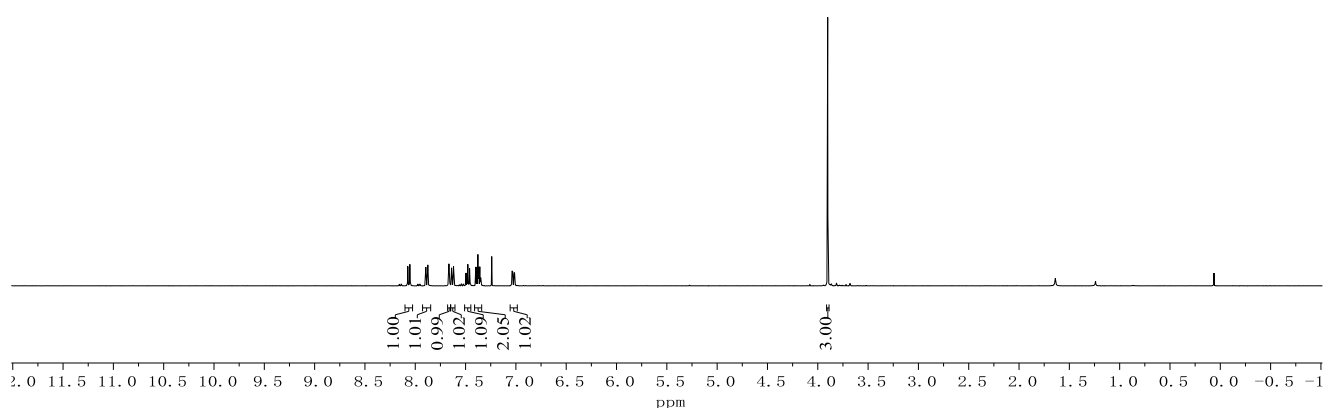
**405h**  
(100 MHz, CDCl<sub>3</sub>)



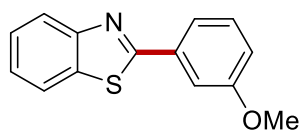
Appendix: NMR Spectra



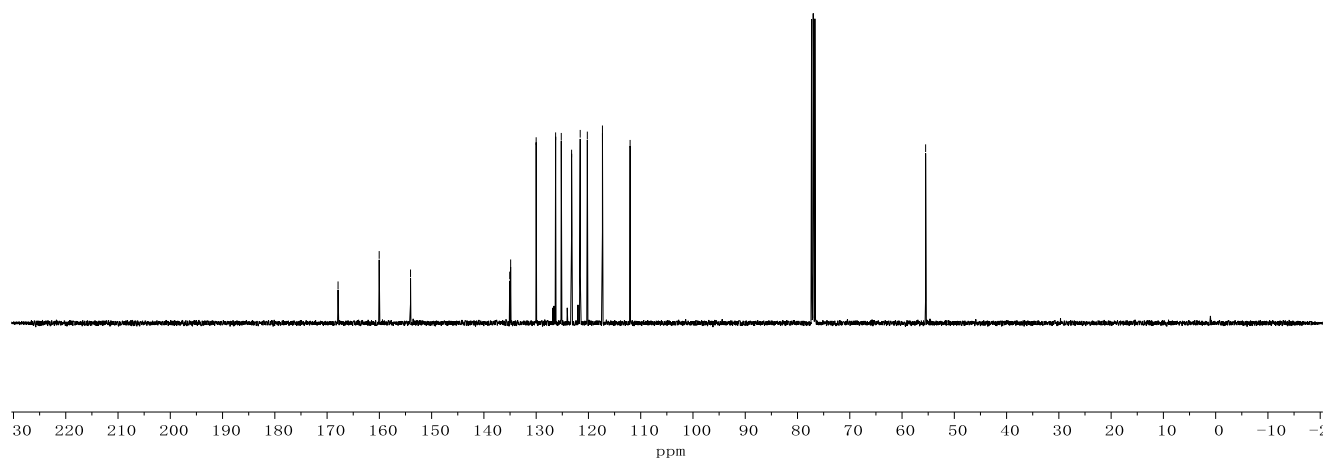
**405i**  
(400 MHz, CDCl<sub>3</sub>)



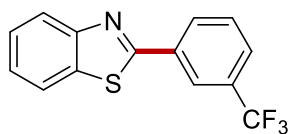
167.90  
160.03  
154.04  
135.07  
134.88  
130.00  
126.28  
125.20  
123.22  
121.58  
120.21  
117.32  
112.03  
55.49



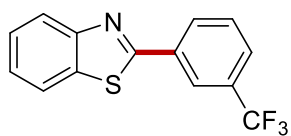
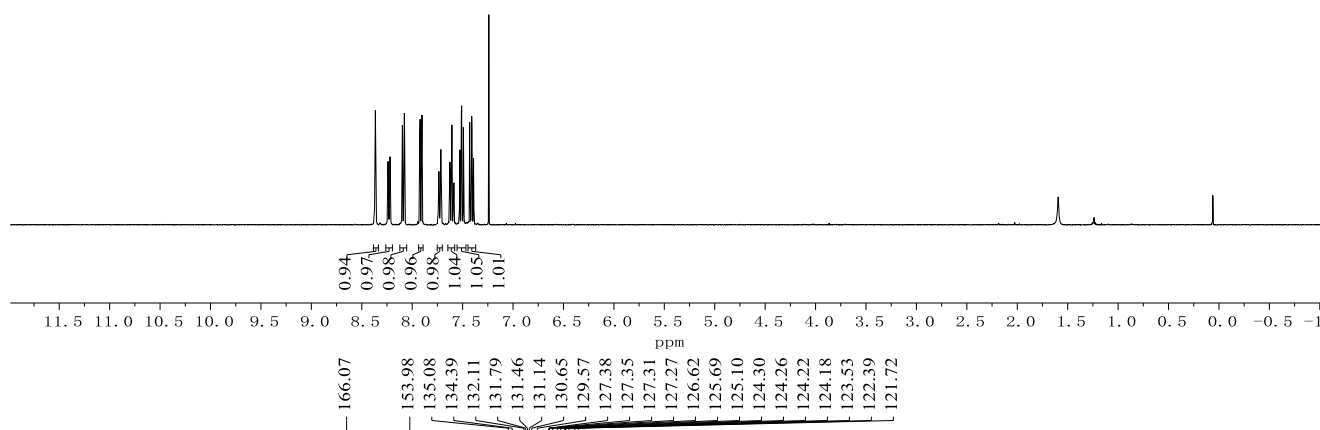
**405i**  
(100 MHz, CDCl<sub>3</sub>)



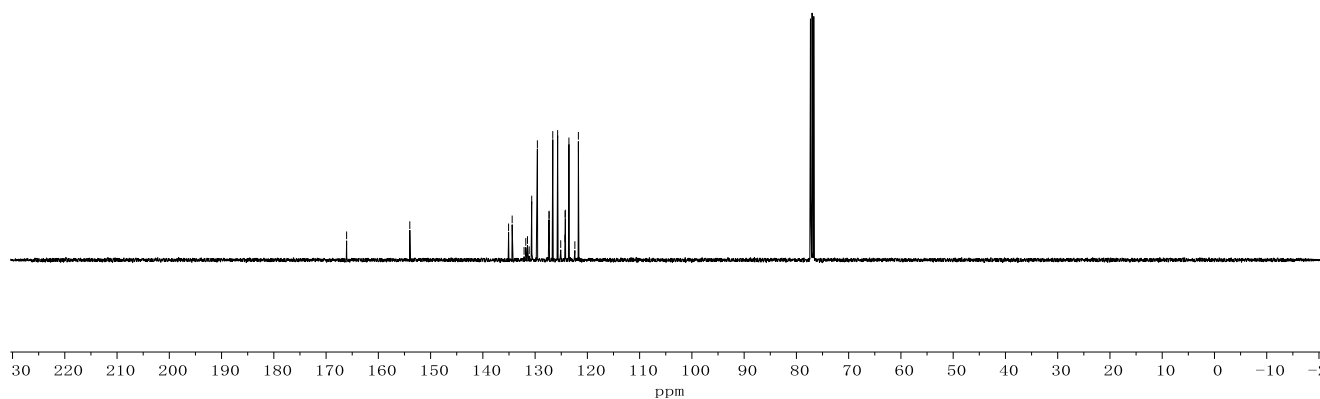
Appendix: NMR Spectra



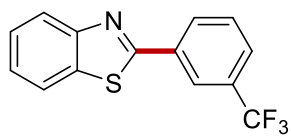
**405j**  
(400 MHz, CDCl<sub>3</sub>)



**405j**  
(100 MHz, CDCl<sub>3</sub>)

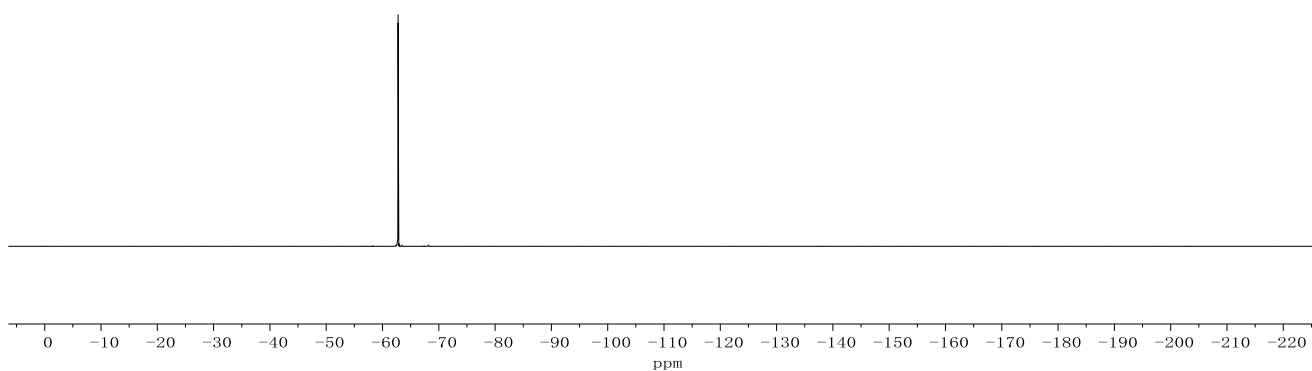


Appendix: NMR Spectra

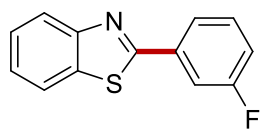


**405j**  
(282 MHz, CDCl<sub>3</sub>)

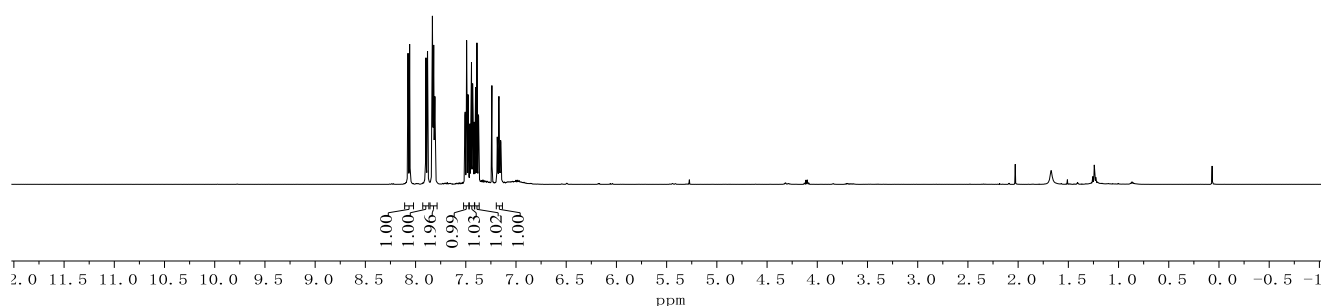
-62.8



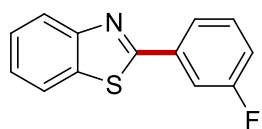
Appendix: NMR Spectra



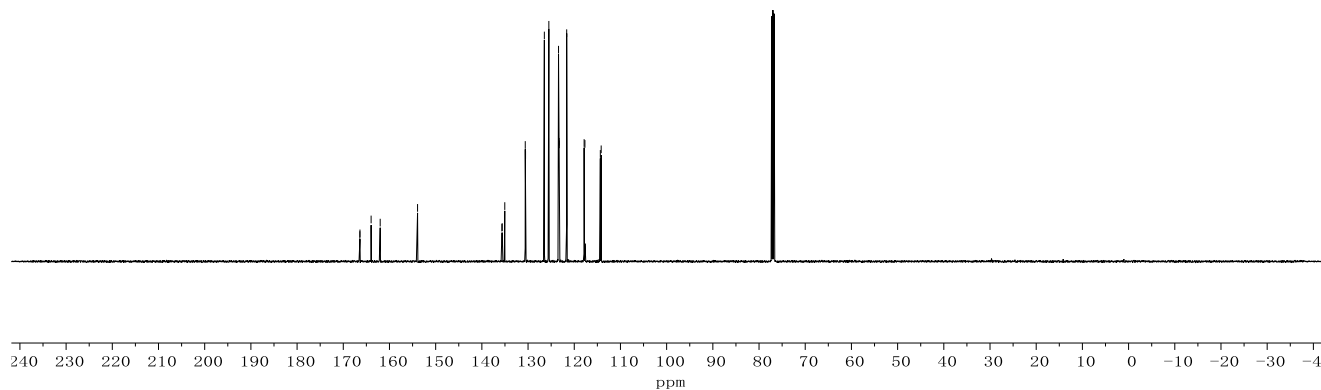
**405k**  
(500 MHz, CDCl<sub>3</sub>)



166.41  
166.39  
163.98  
162.01  
153.92  
135.66  
135.60  
135.04  
130.61  
130.54  
126.47  
125.50  
123.41  
123.28  
123.26  
121.64  
117.86  
117.69  
114.36  
114.17

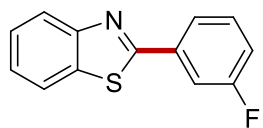


**405k**  
(125 MHz, CDCl<sub>3</sub>)



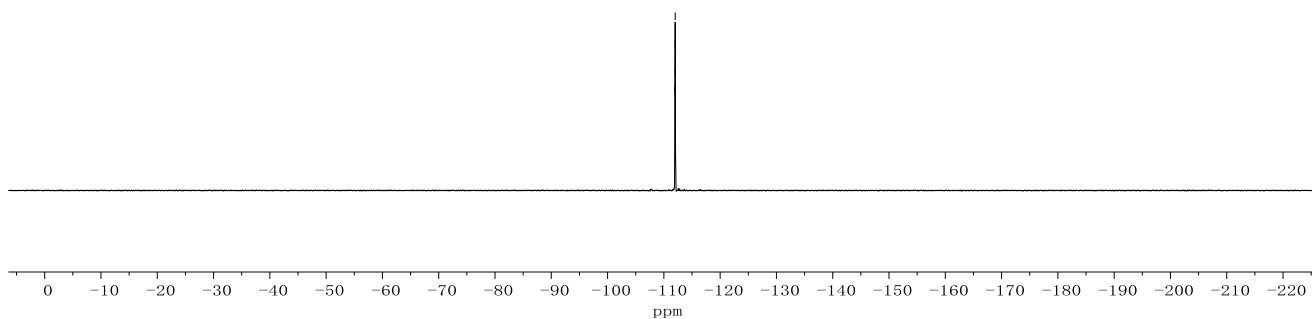


# Appendix: NMR Sepctra

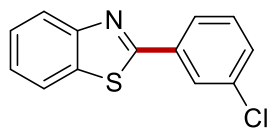


**405k**  
(282 MHz, CDCl<sub>3</sub>)

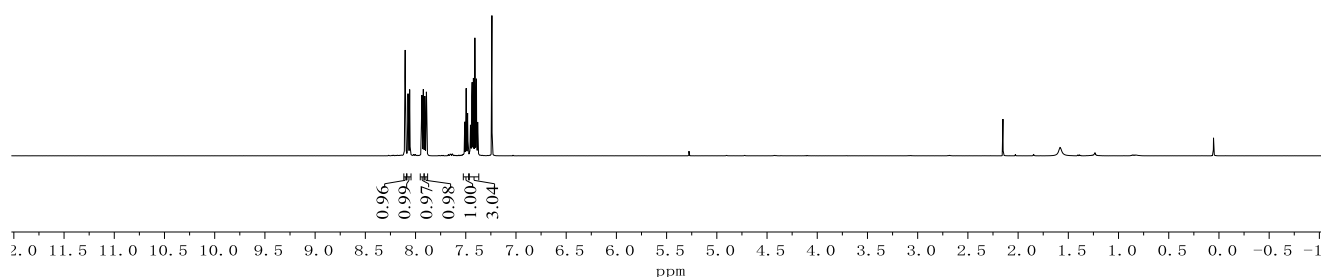
-111.98  
-112.00  
-112.00  
-112.01  
-112.03  
-112.03  
-112.04  
-112.05  
-112.06



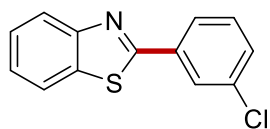
Appendix: NMR Spectra



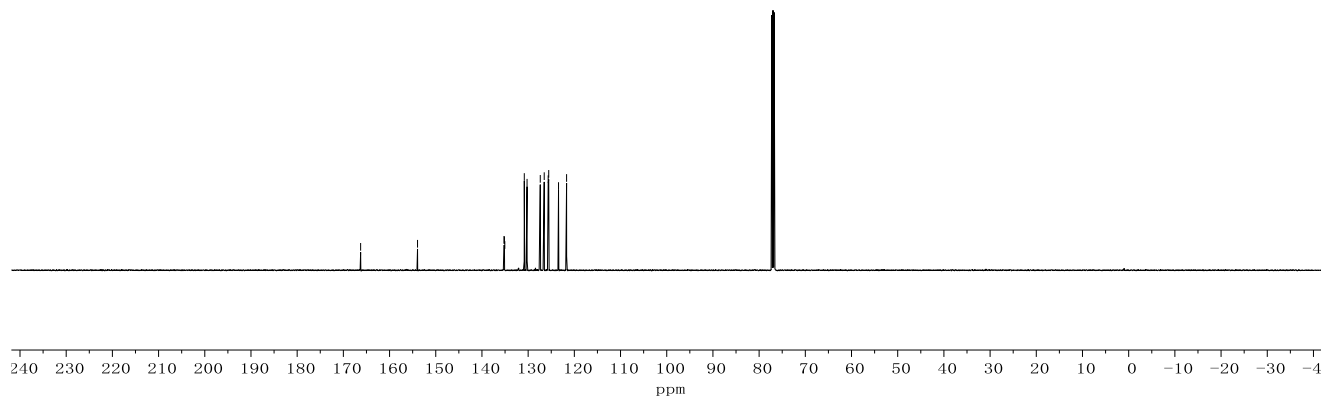
**4051**  
(500 MHz, CDCl<sub>3</sub>)



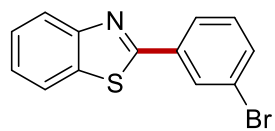
166.26  
153.95  
135.24  
135.13  
135.05  
130.84  
130.24  
127.38  
126.52  
125.66  
125.54  
123.42  
121.68



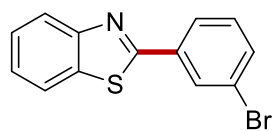
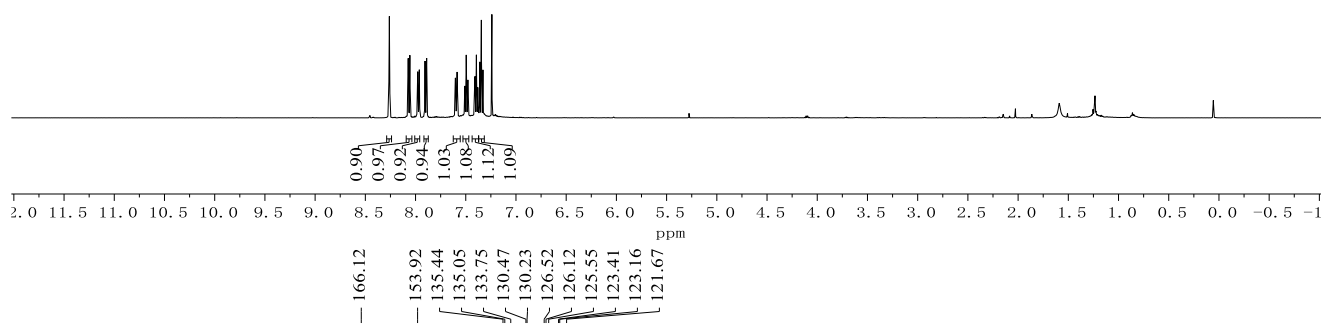
**4051**  
(125 MHz, CDCl<sub>3</sub>)



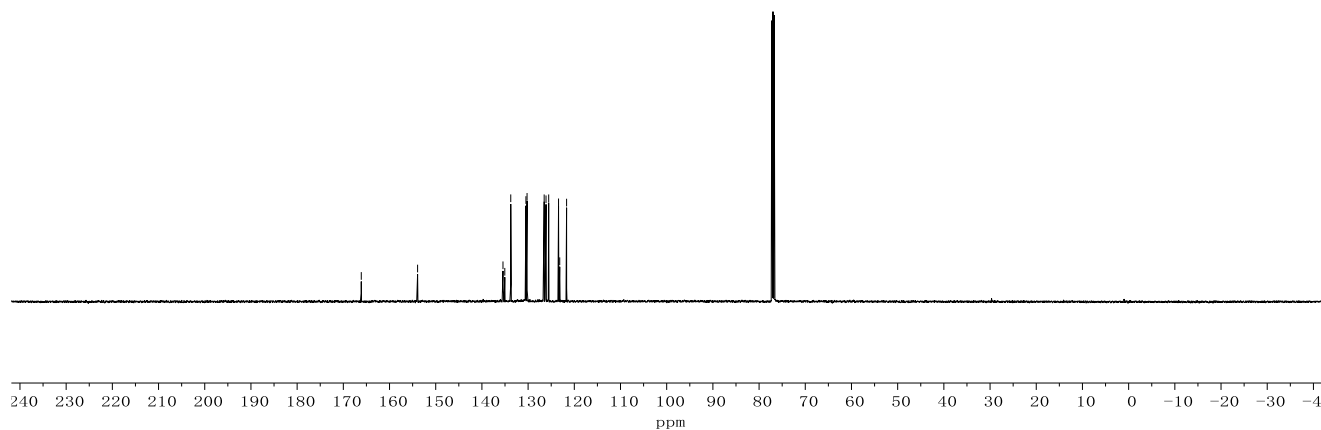
Appendix: NMR Spectra



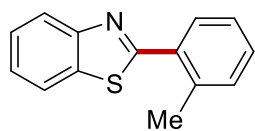
**405m**  
(500 MHz, CDCl<sub>3</sub>)



**405m**  
(125 MHz, CDCl<sub>3</sub>)

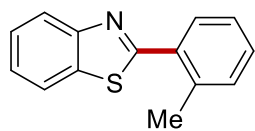
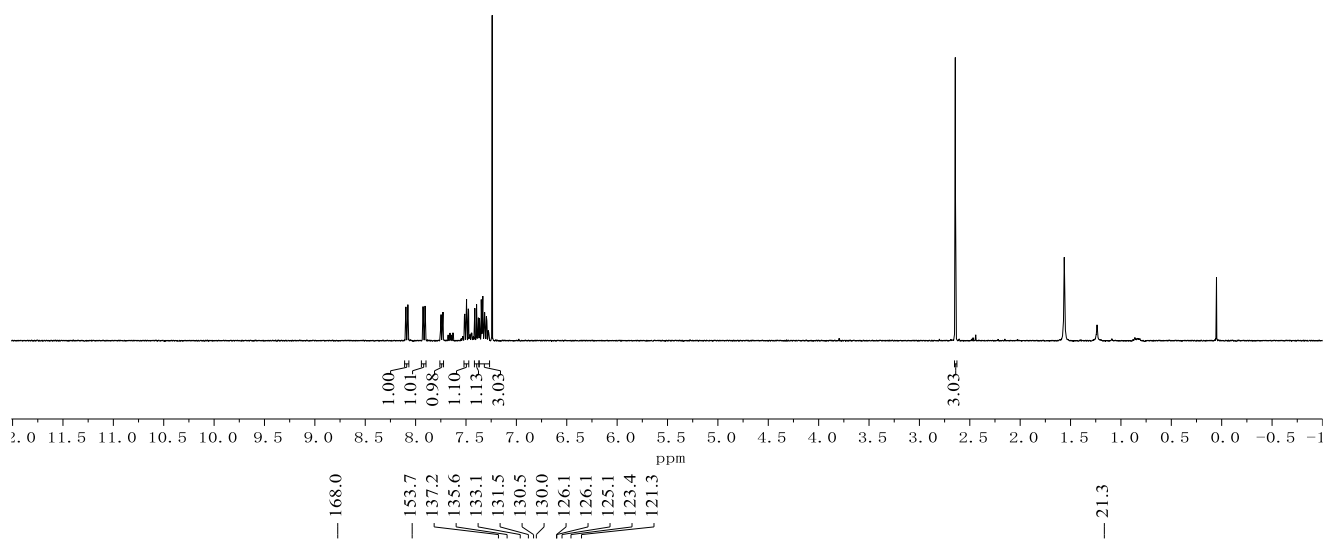


Appendix: NMR Spectra



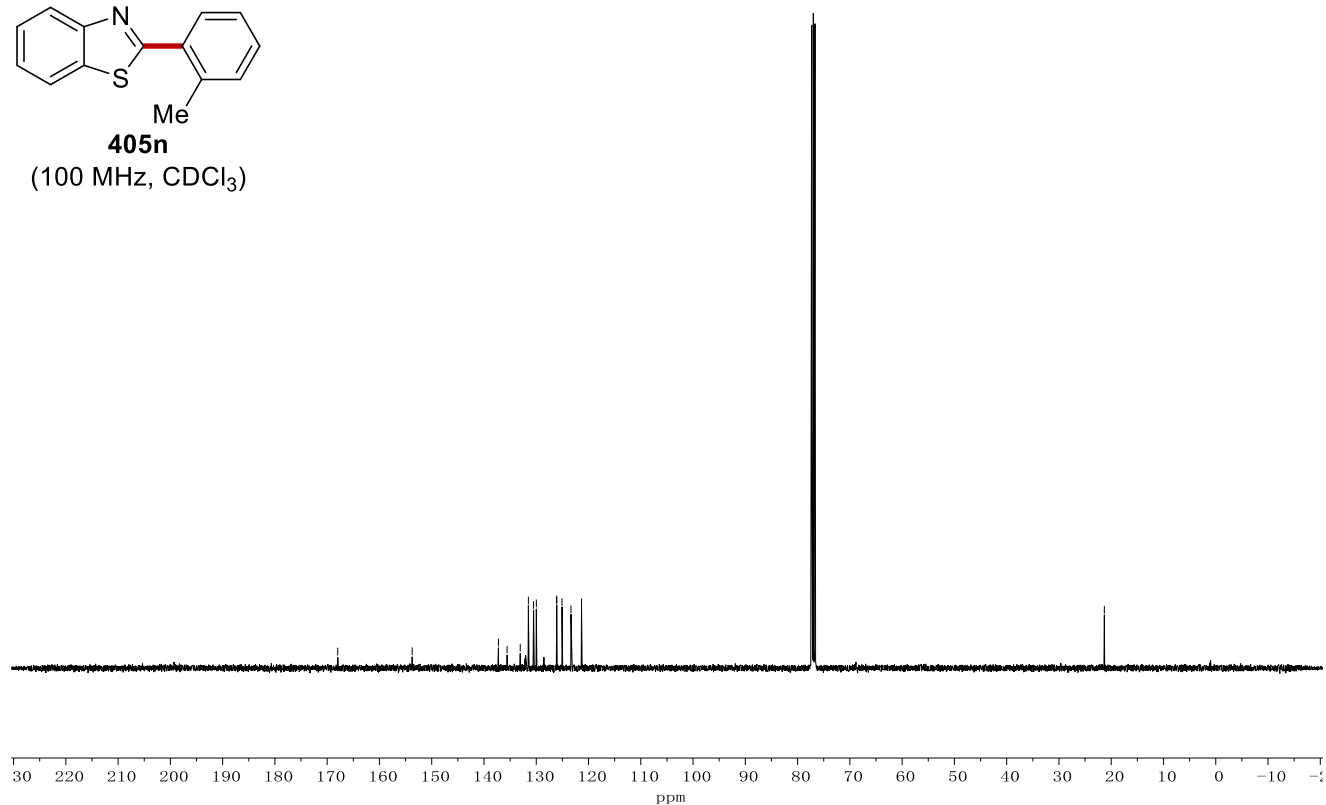
**405n**

(400 MHz, CDCl<sub>3</sub>)

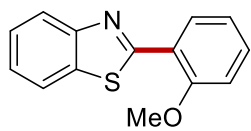


**405n**

(100 MHz, CDCl<sub>3</sub>)

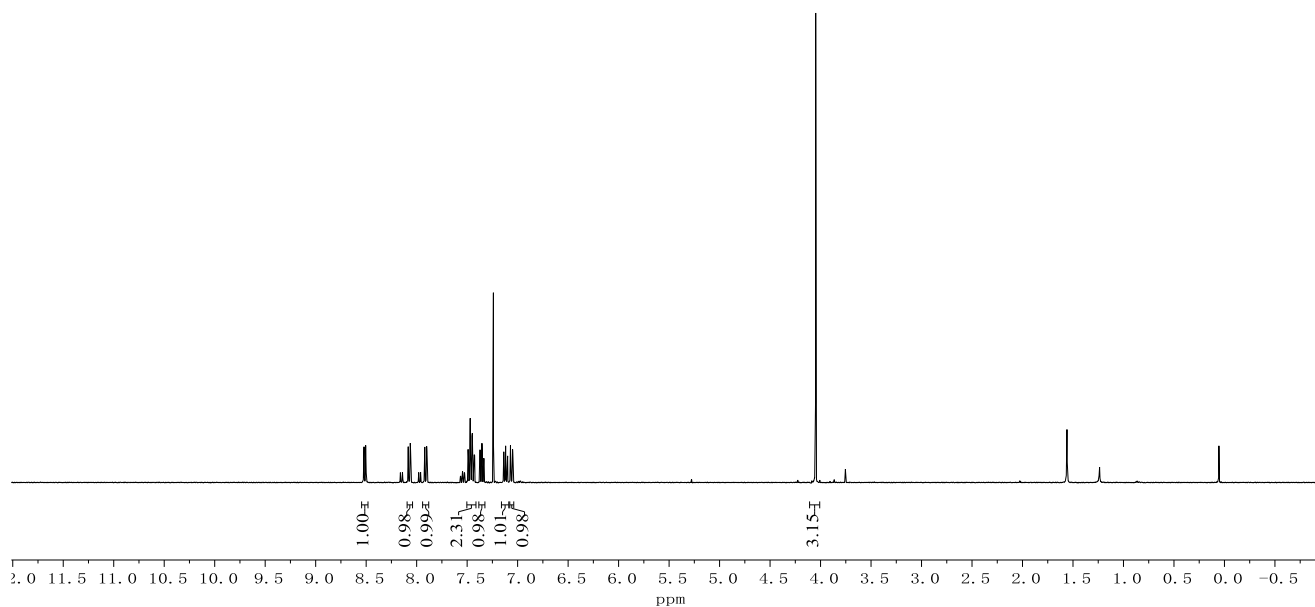


Appendix: NMR Spectra

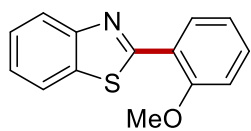


**405o**

(400 MHz, CDCl<sub>3</sub>)

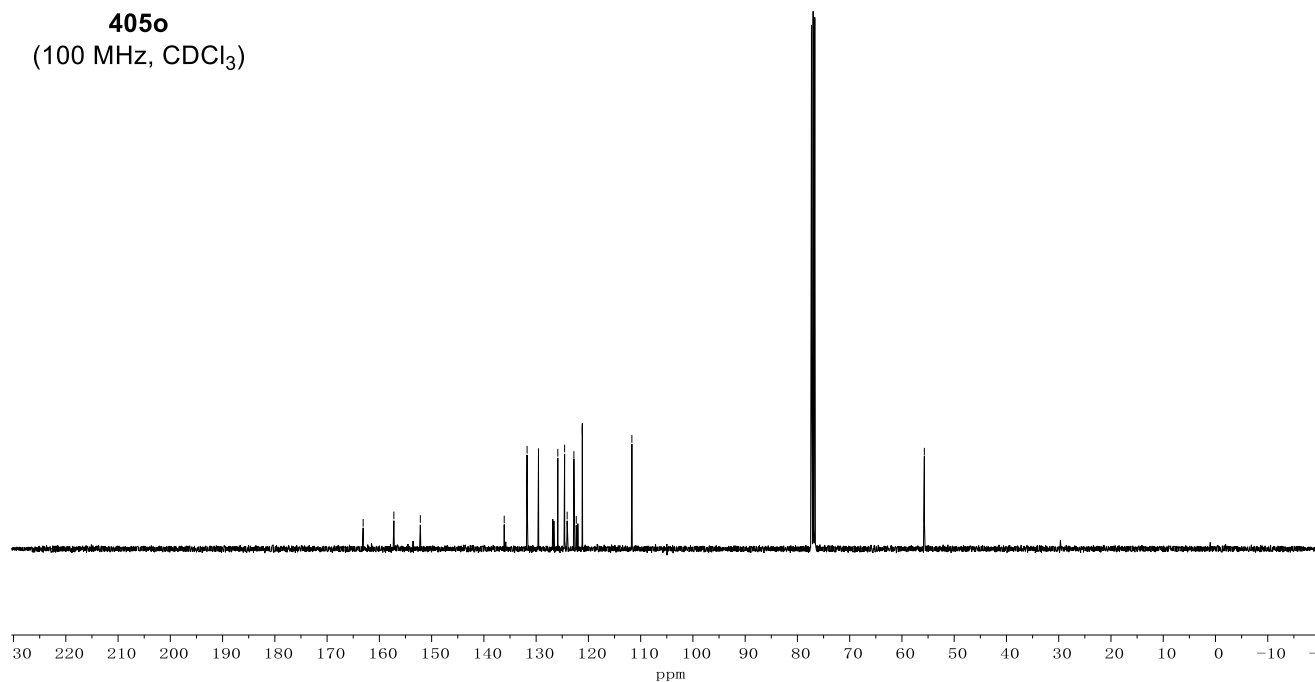


163.11  
157.23  
152.16  
136.11  
131.73  
129.55  
125.86  
124.55  
124.07  
122.78  
122.52  
121.17  
111.68  
55.71

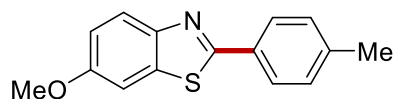


**405o**

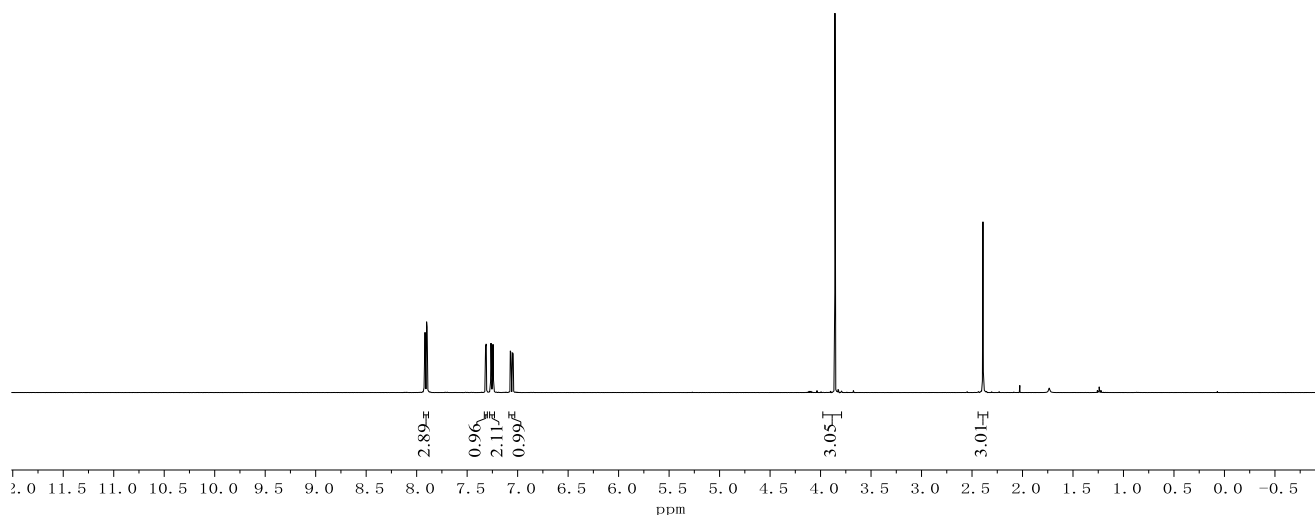
(100 MHz, CDCl<sub>3</sub>)



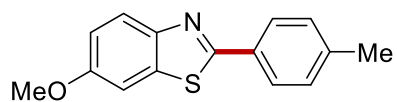
Appendix: NMR Spectra



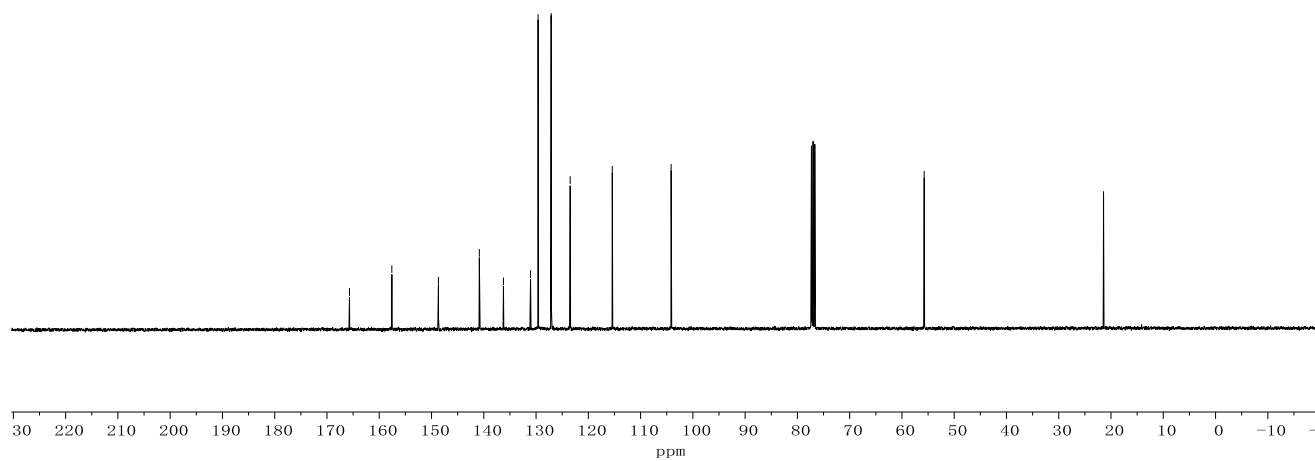
**405p**  
(400 MHz, CDCl<sub>3</sub>)



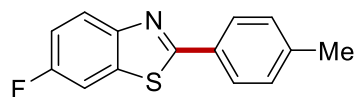
165.70  
157.59  
148.68  
140.85  
136.24  
131.05  
129.61  
127.11  
123.47  
115.42  
104.16  
55.74  
21.43



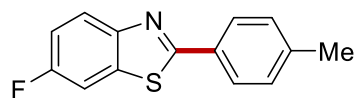
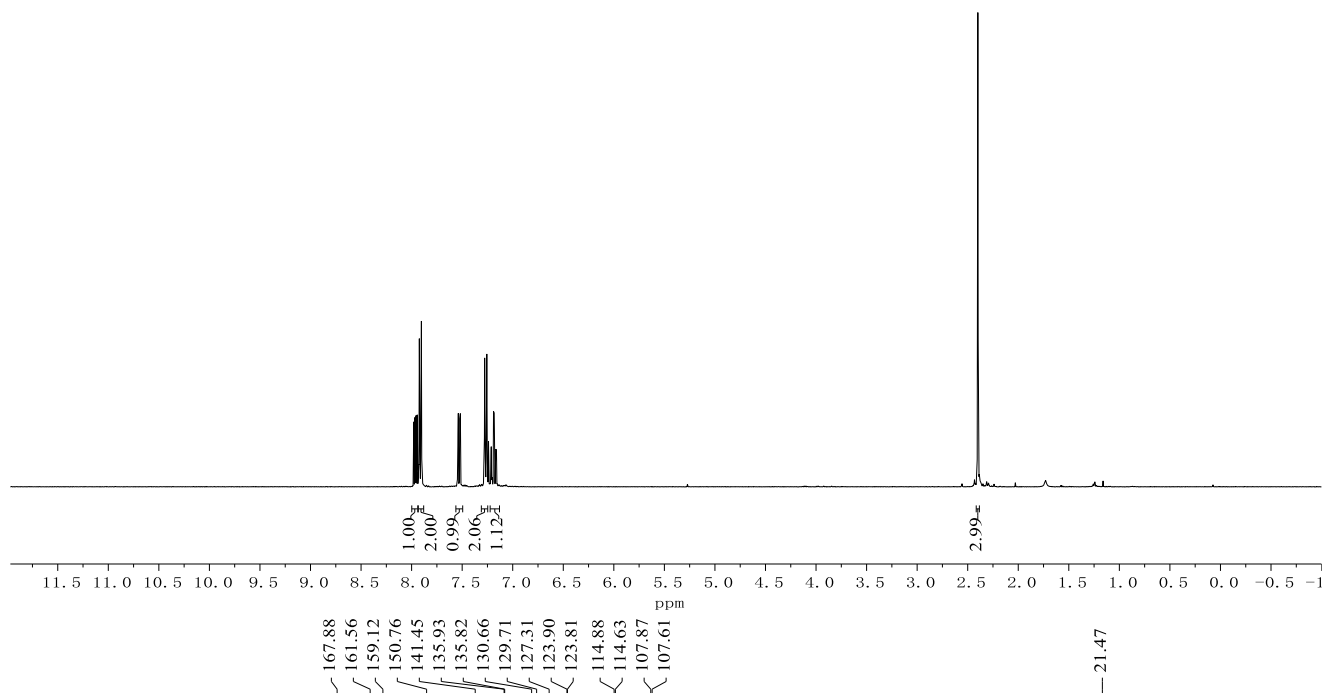
**405p**  
(100 MHz, CDCl<sub>3</sub>)



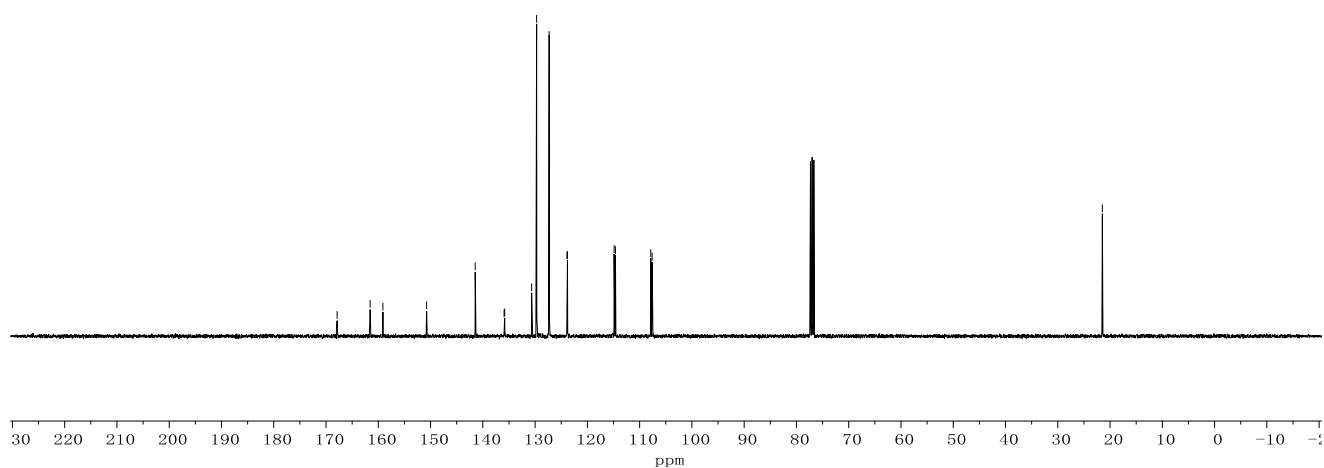
Appendix: NMR Spectra



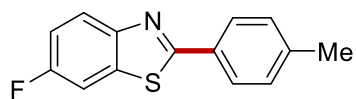
**405q**  
(400 MHz, CDCl<sub>3</sub>)



**405q**  
(100 MHz, CDCl<sub>3</sub>)

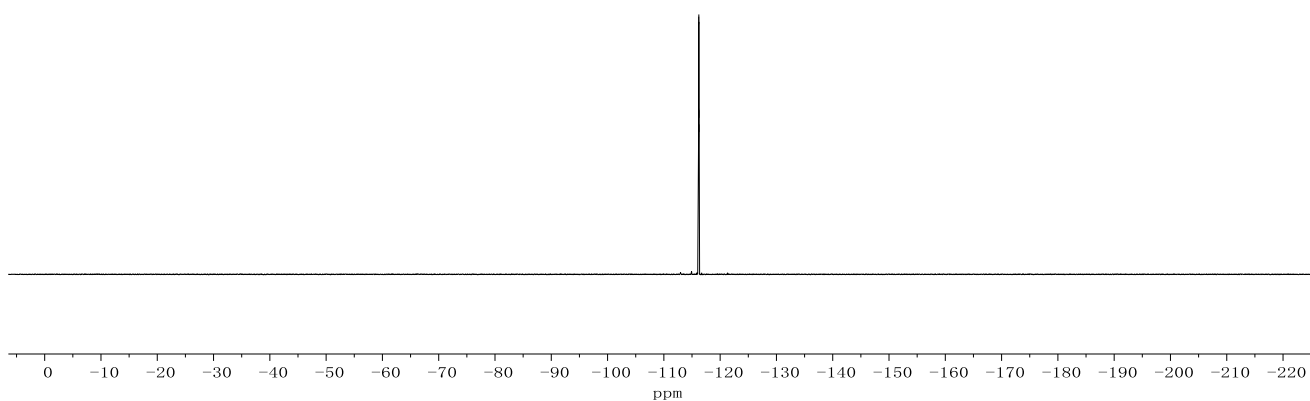


Appendix: NMR Spectra



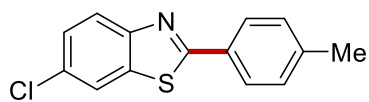
-116.2  
-116.2  
-116.2  
-116.2  
-116.2

**405q**  
(282 MHz, CDCl<sub>3</sub>)

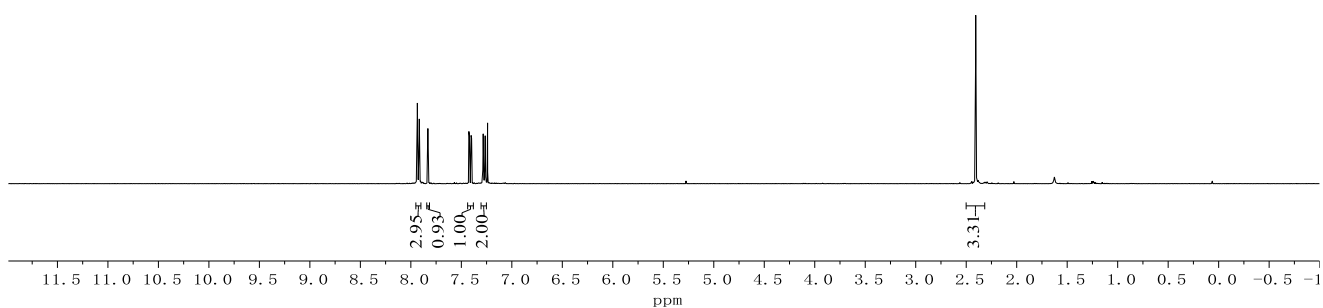




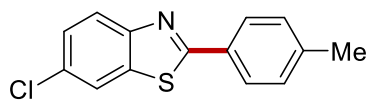
Appendix: NMR Spectra



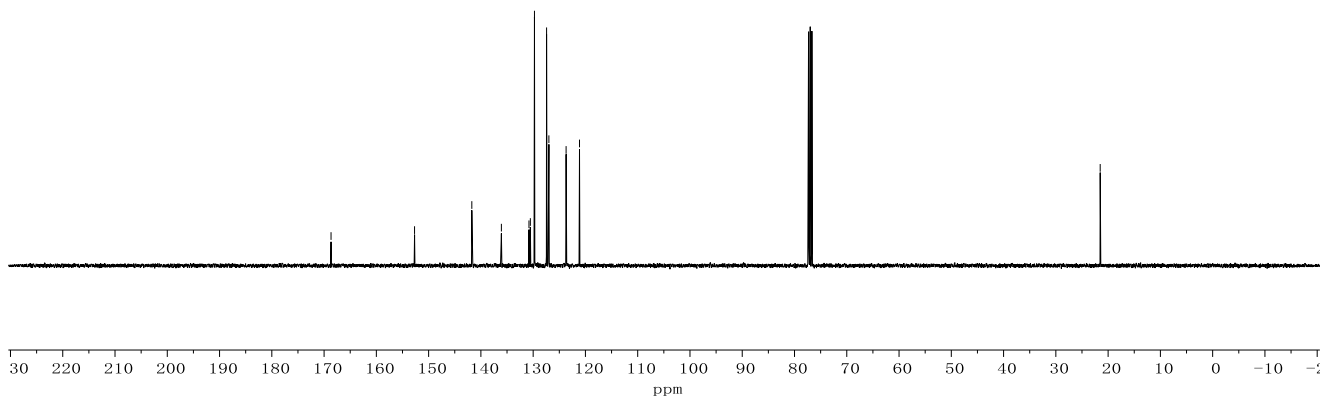
**405r**  
(400 MHz, CDCl<sub>3</sub>)



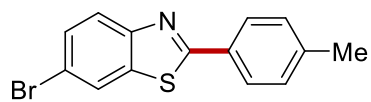
168.67  
152.69  
141.74  
136.08  
130.80  
130.54  
129.75  
127.43  
126.99  
123.70  
121.13  
21.52



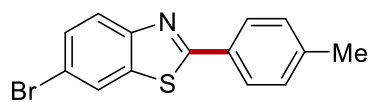
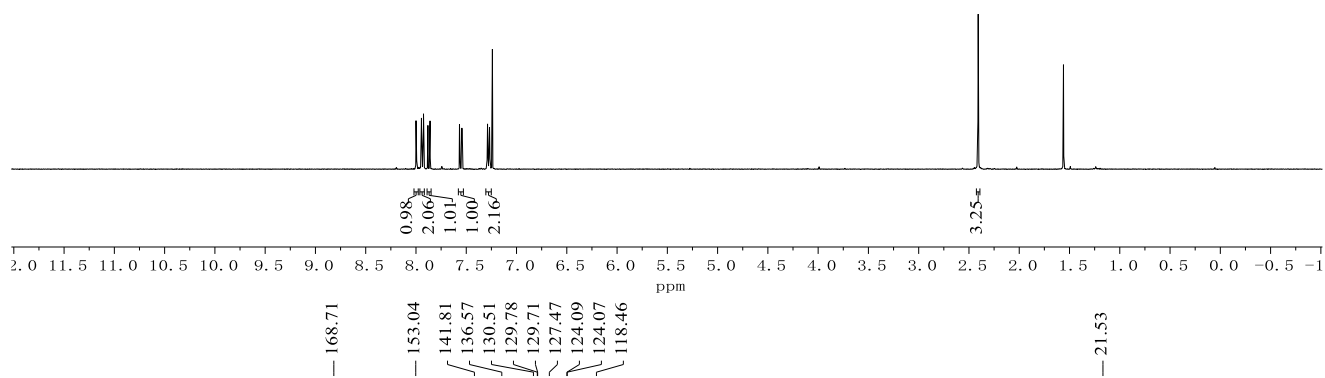
**405r**  
(100 MHz, CDCl<sub>3</sub>)



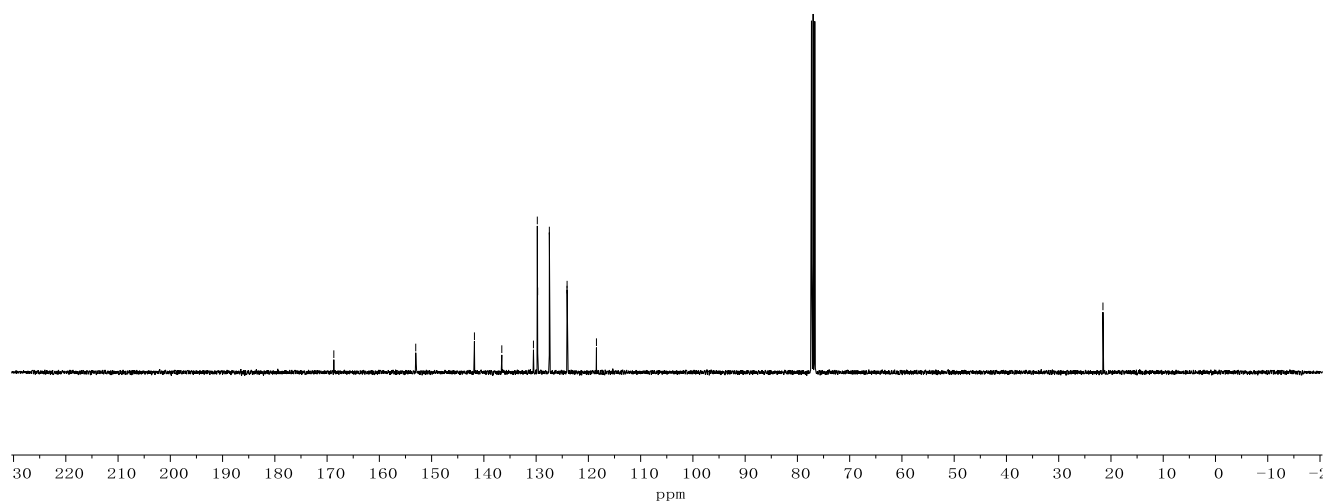
Appendix: NMR Spectra



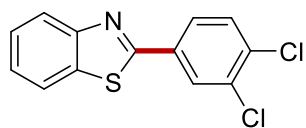
**405s**  
(400 MHz, CDCl<sub>3</sub>)



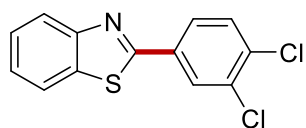
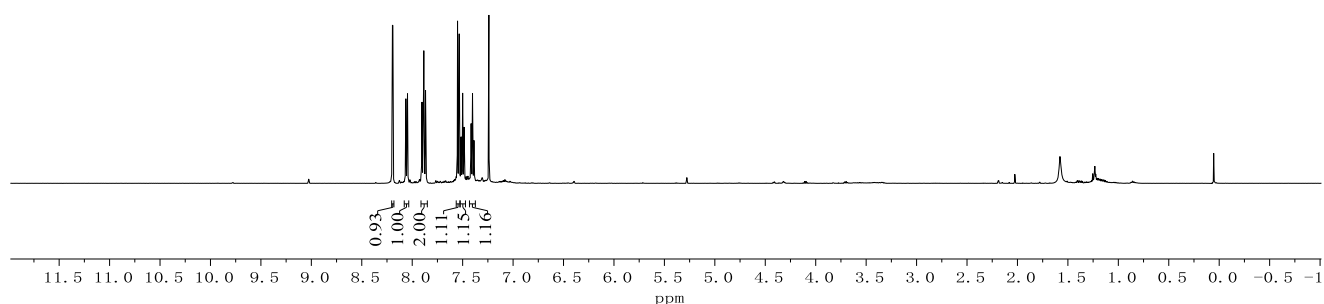
**405s**  
(100 MHz, CDCl<sub>3</sub>)



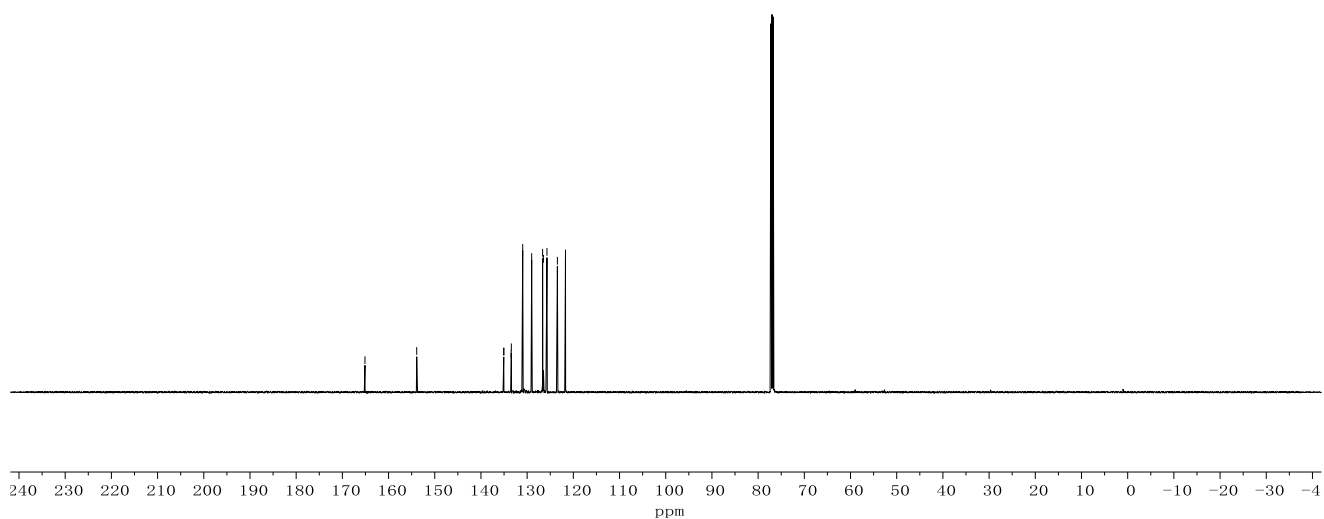
Appendix: NMR Spectra



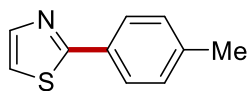
**405t**  
(500 MHz, CDCl<sub>3</sub>)



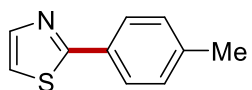
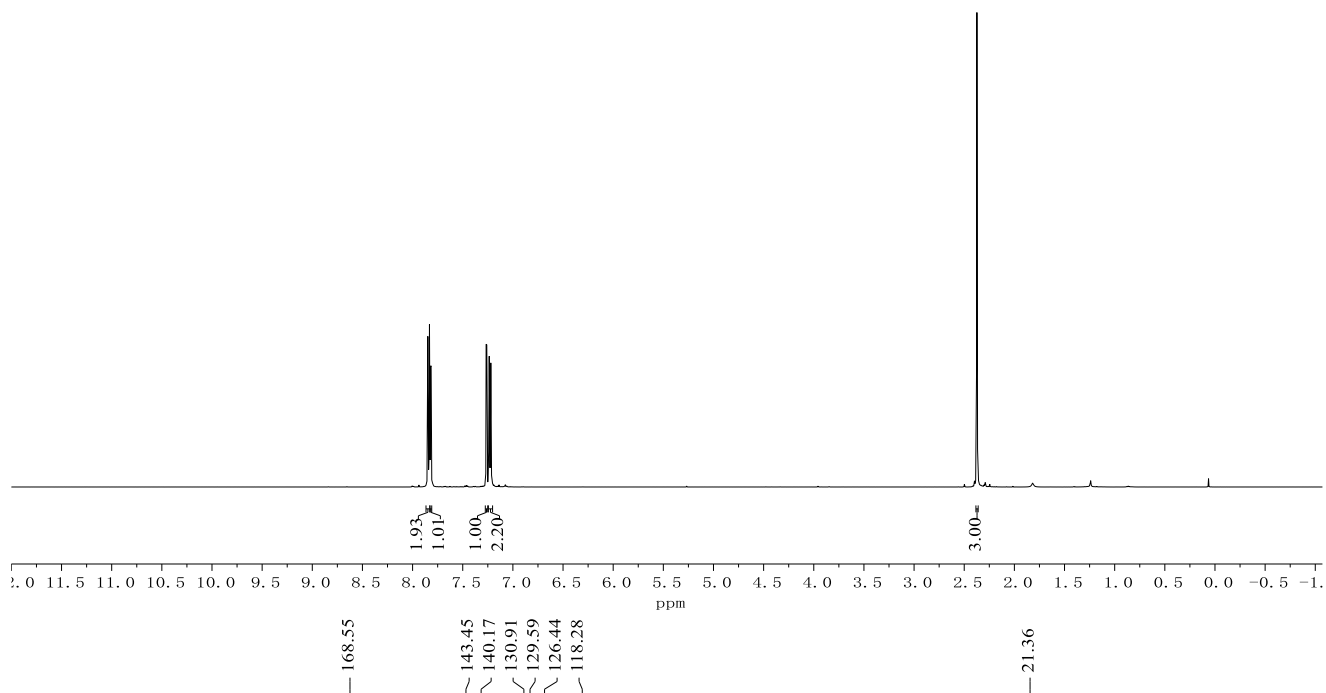
**405t**  
(125 MHz, CDCl<sub>3</sub>)



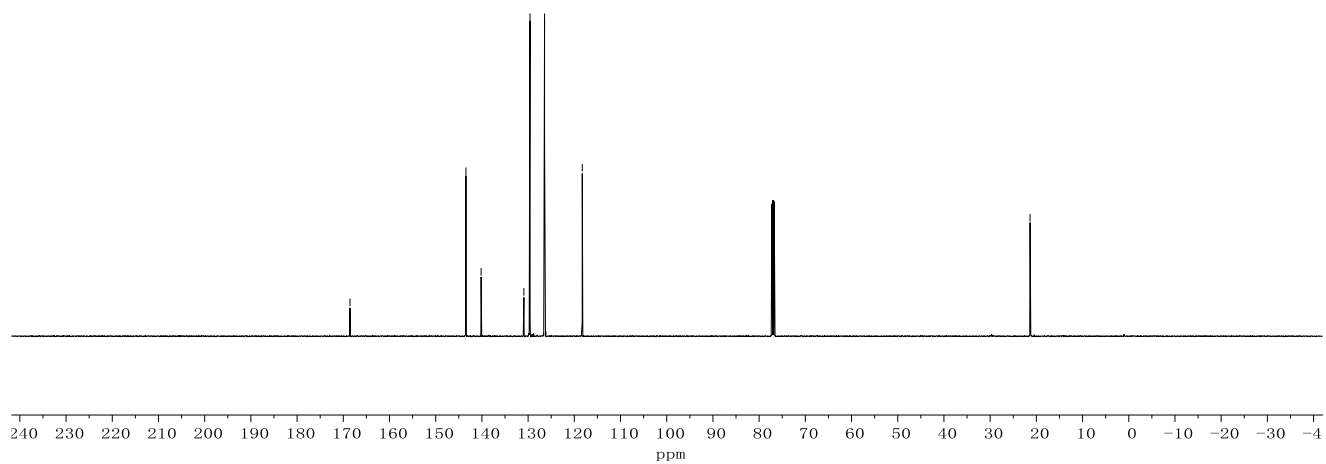
Appendix: NMR Spectra



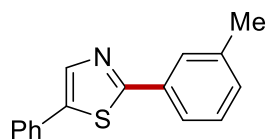
**405u**  
(500 MHz, CDCl<sub>3</sub>)



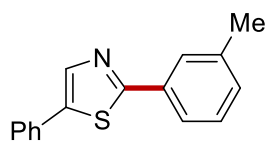
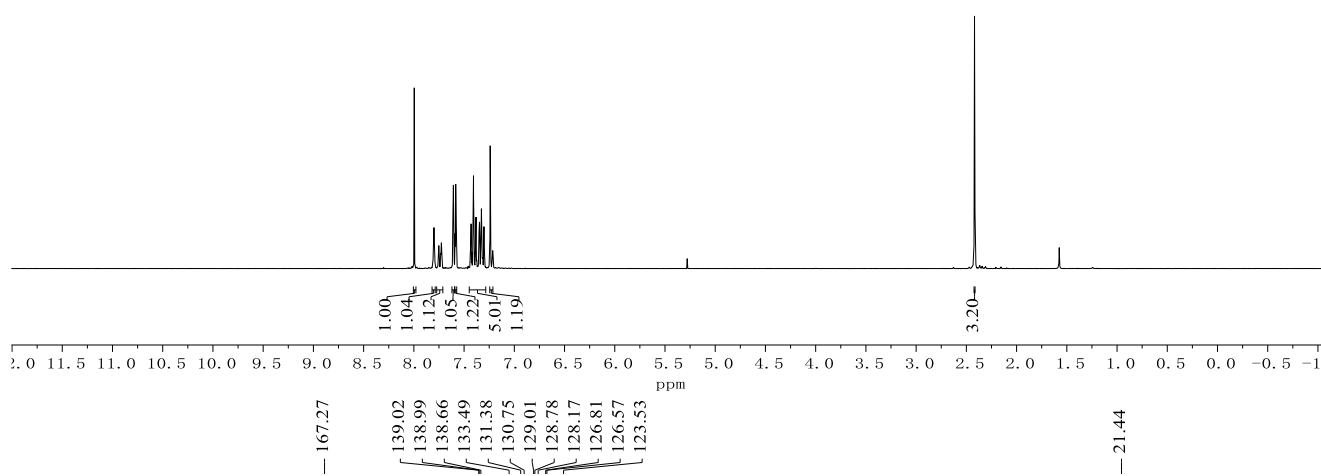
**405u**  
(125 MHz, CDCl<sub>3</sub>)



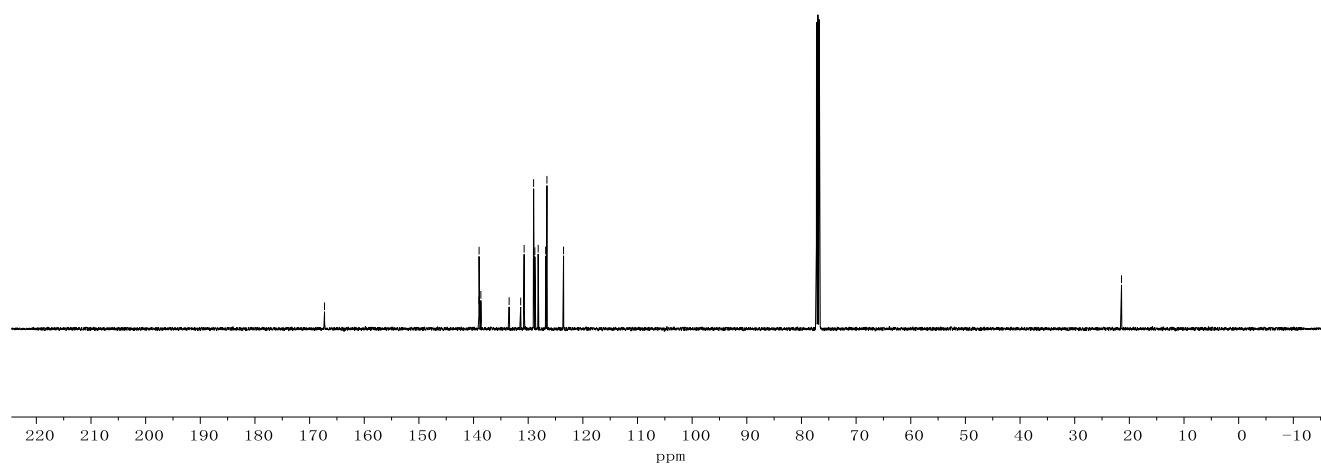
Appendix: NMR Spectra



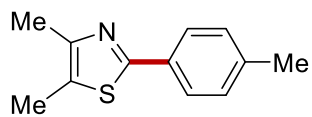
**405w**  
(300 MHz, CDCl<sub>3</sub>)



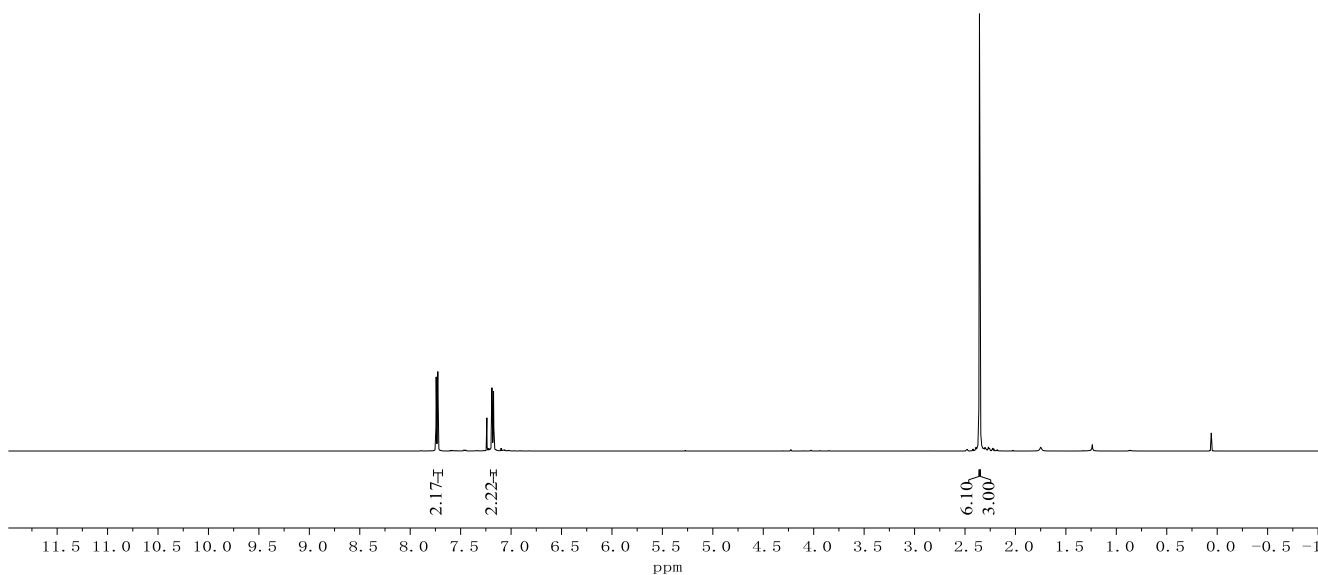
**405w**  
(75 MHz, CDCl<sub>3</sub>)



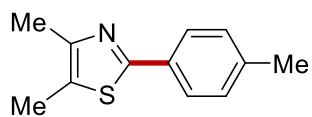
Appendix: NMR Spectra



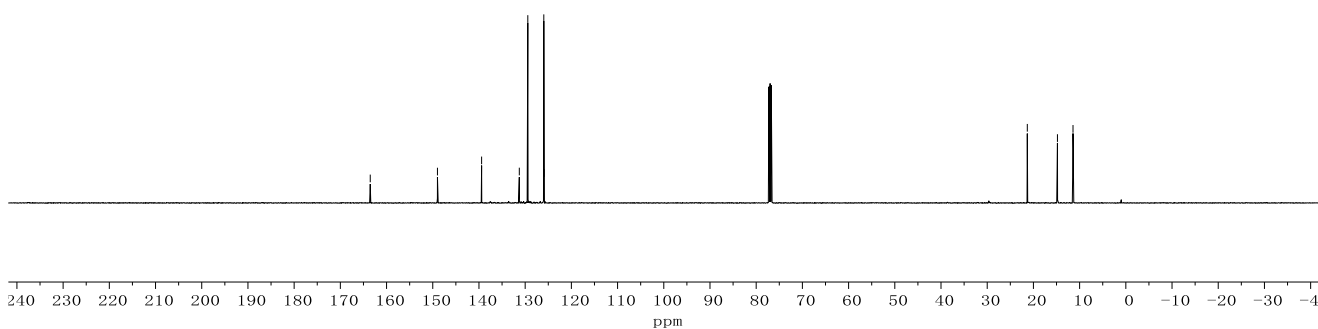
**405x**  
(500 MHz, CDCl<sub>3</sub>)



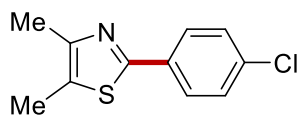
163.53  
148.98  
139.43  
131.27  
129.43  
125.96  
125.90  
21.32  
14.80  
11.43



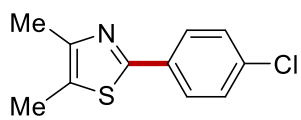
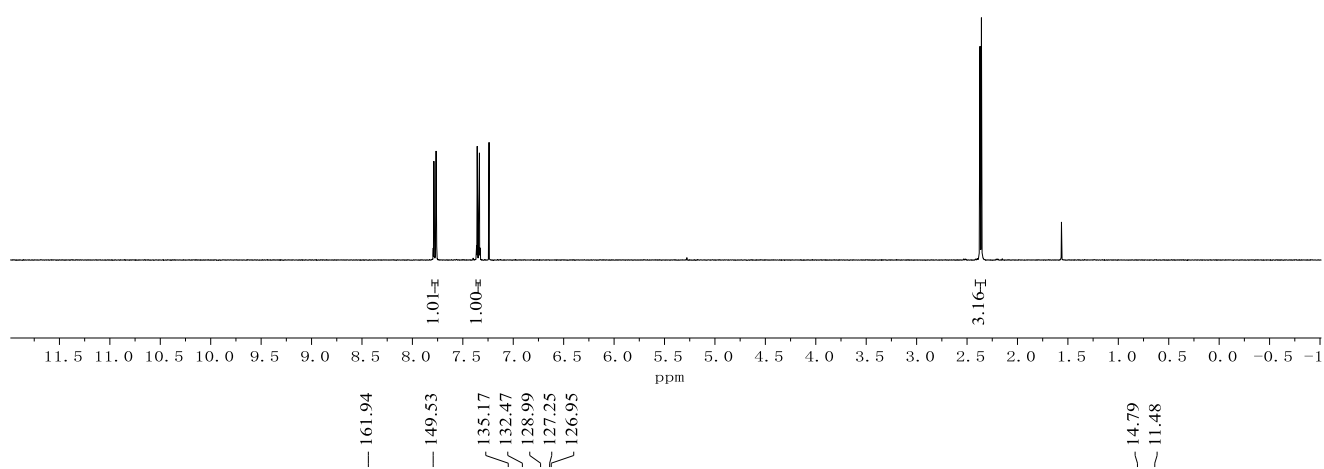
**405x**  
(125 MHz, CDCl<sub>3</sub>)



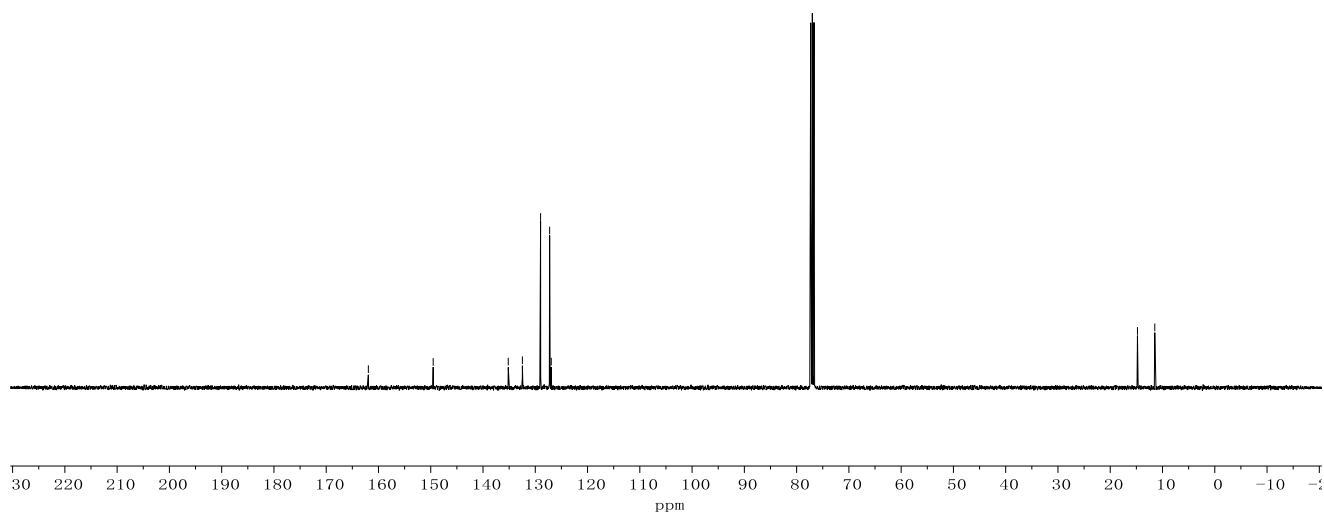
Appendix: NMR Spectra



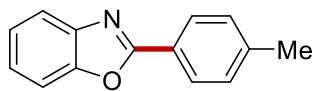
**405y**  
(400 MHz, CDCl<sub>3</sub>)



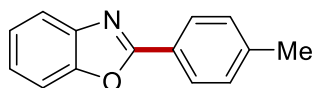
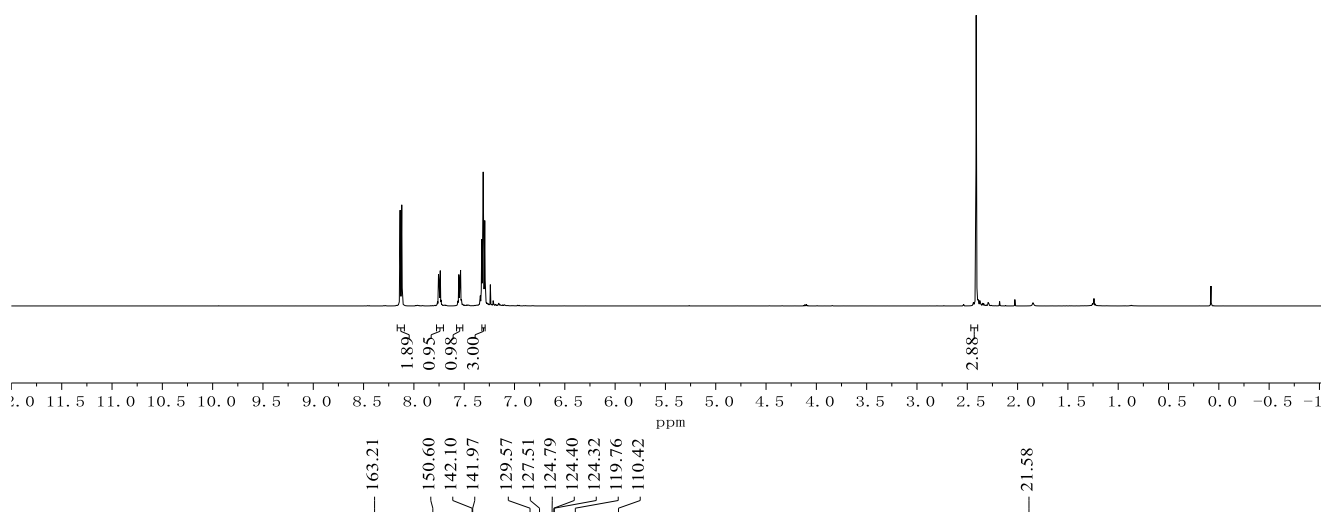
**405y**  
(100 MHz, CDCl<sub>3</sub>)



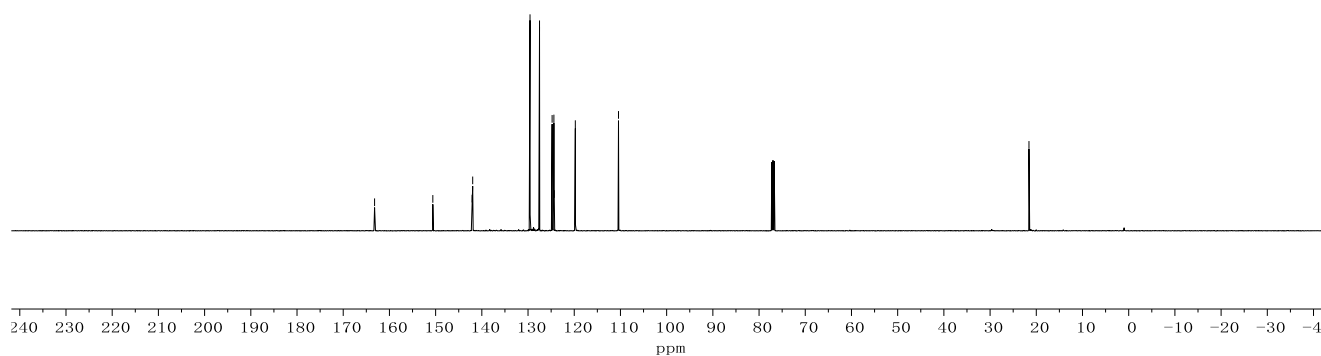
Appendix: NMR Spectra



**447a**  
(500 MHz, CDCl<sub>3</sub>)

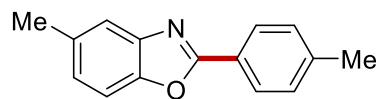


**447a**  
(125 MHz, CDCl<sub>3</sub>)

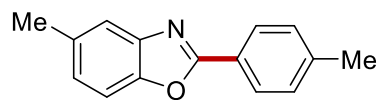
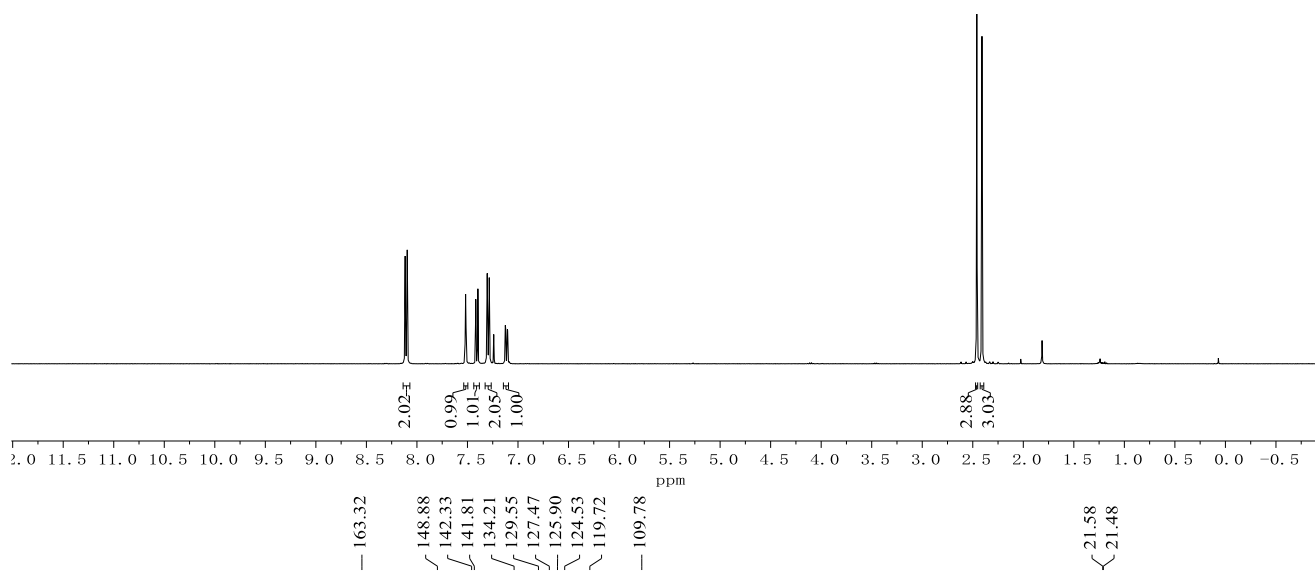




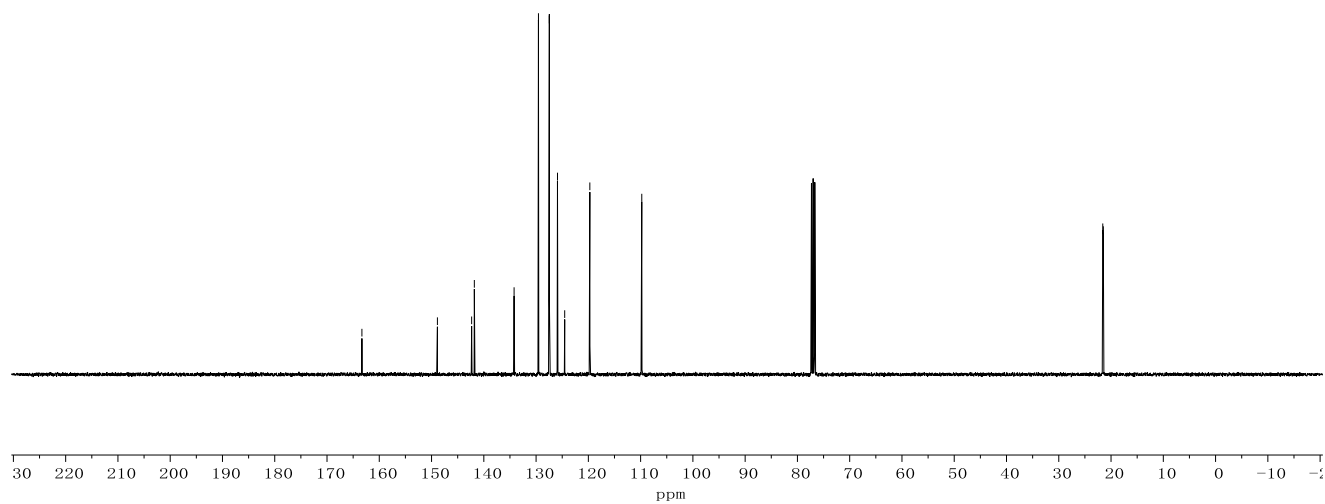
Appendix: NMR Spectra



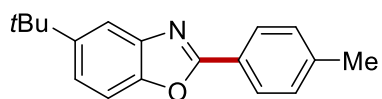
**447b**  
(400 MHz, CDCl<sub>3</sub>)



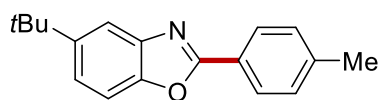
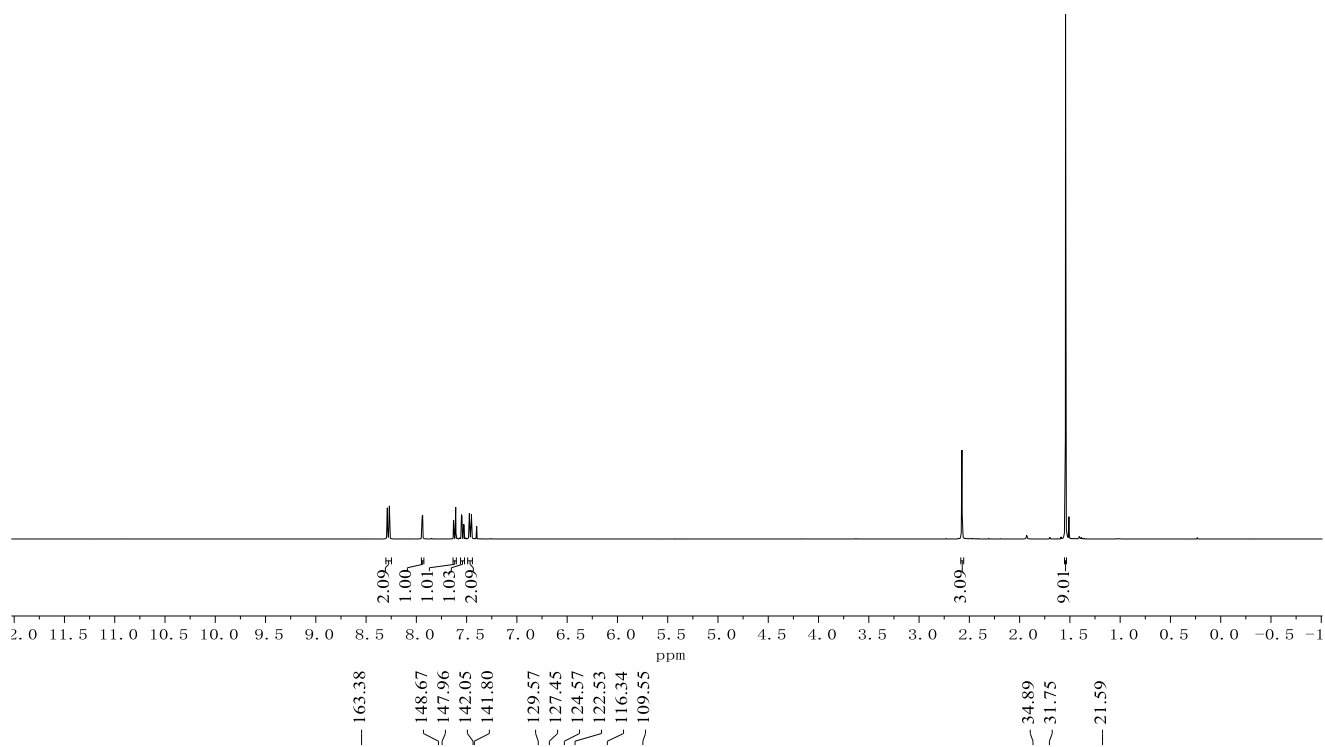
**447b**  
(100 MHz, CDCl<sub>3</sub>)



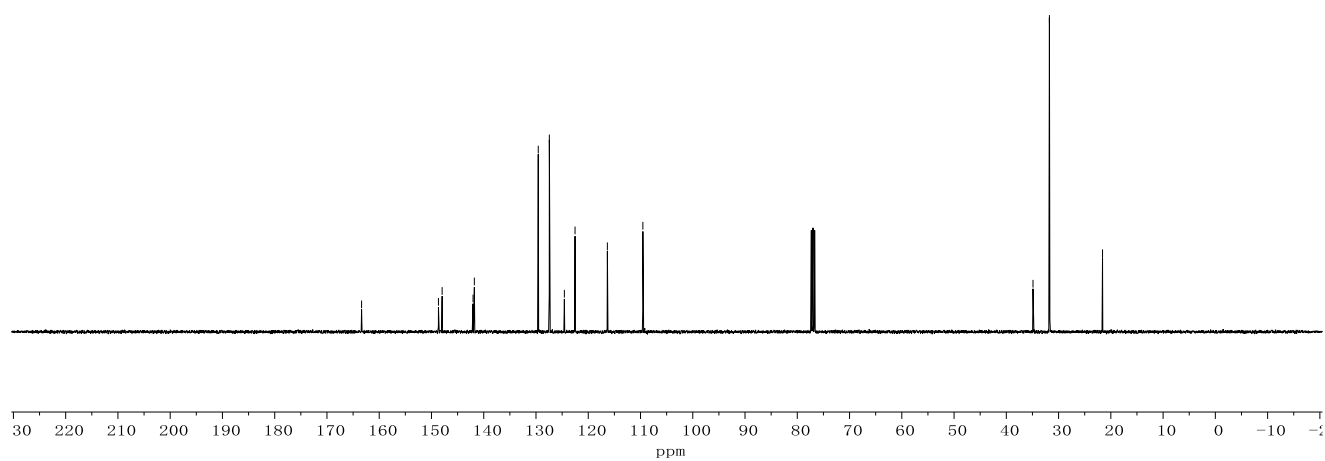
Appendix: NMR Spectra



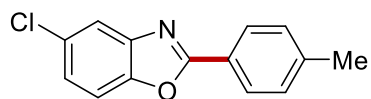
**447c**  
(400 MHz, CDCl<sub>3</sub>)



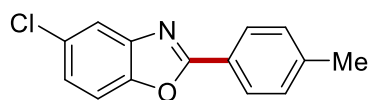
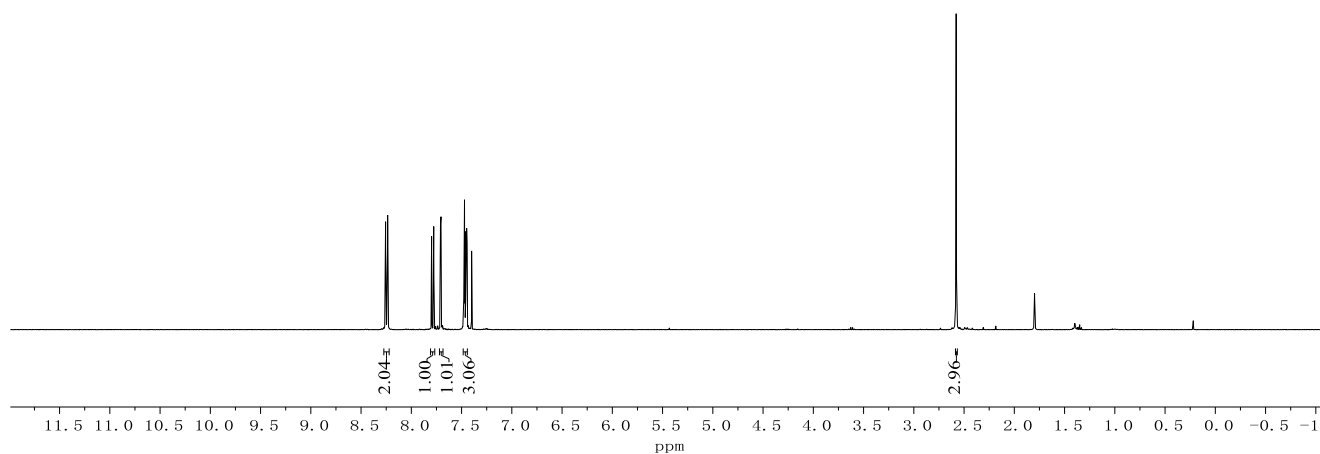
**447c**  
(100 MHz, CDCl<sub>3</sub>)



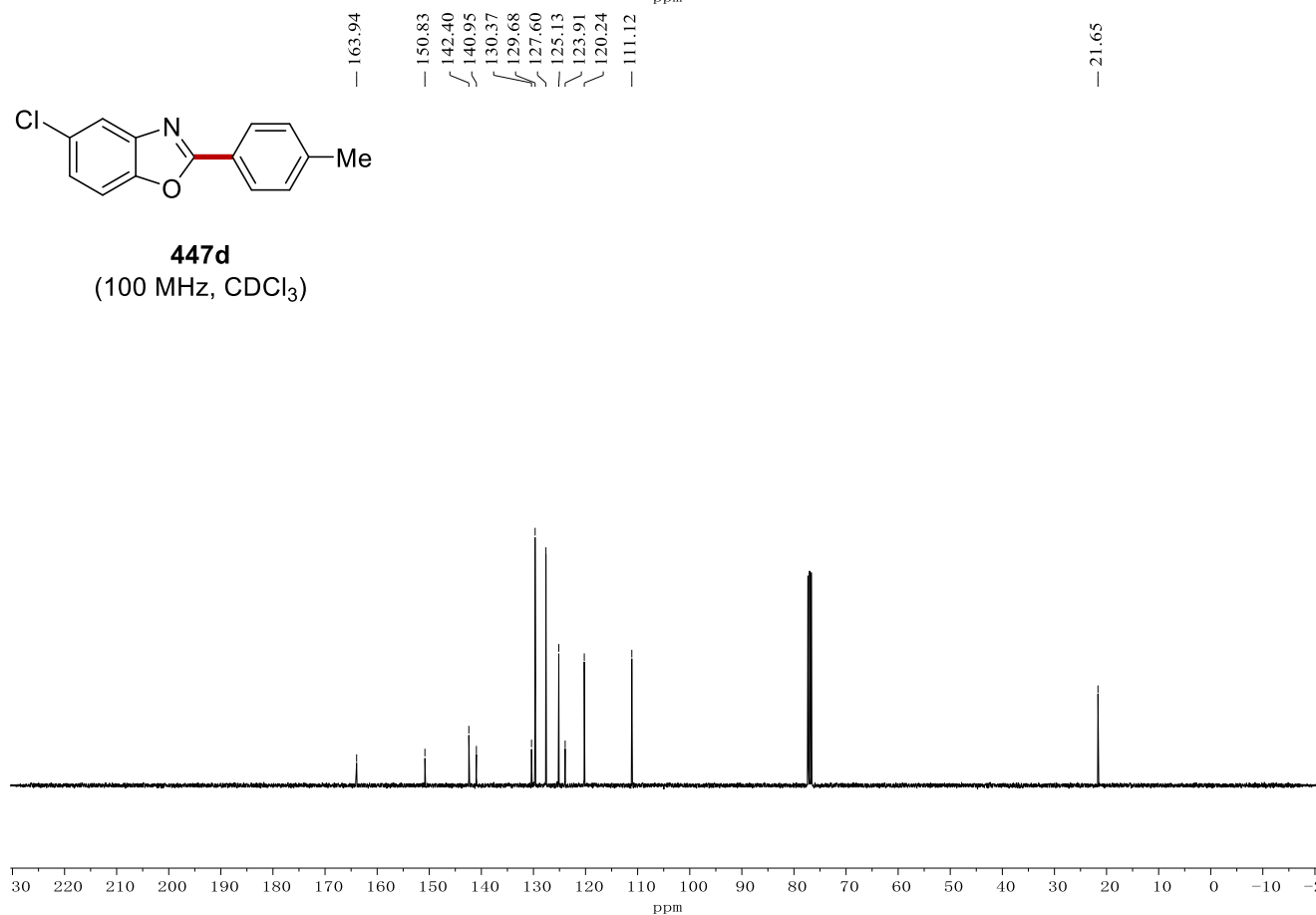
Appendix: NMR Spectra



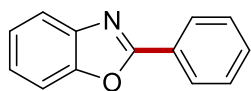
**447d**  
(400 MHz, CDCl<sub>3</sub>)



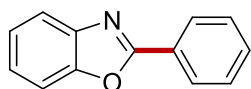
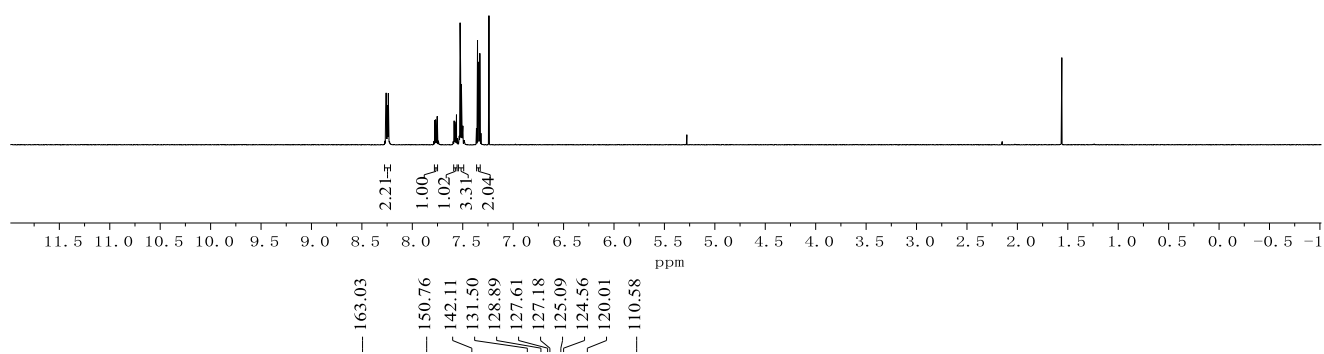
**447d**  
(100 MHz, CDCl<sub>3</sub>)



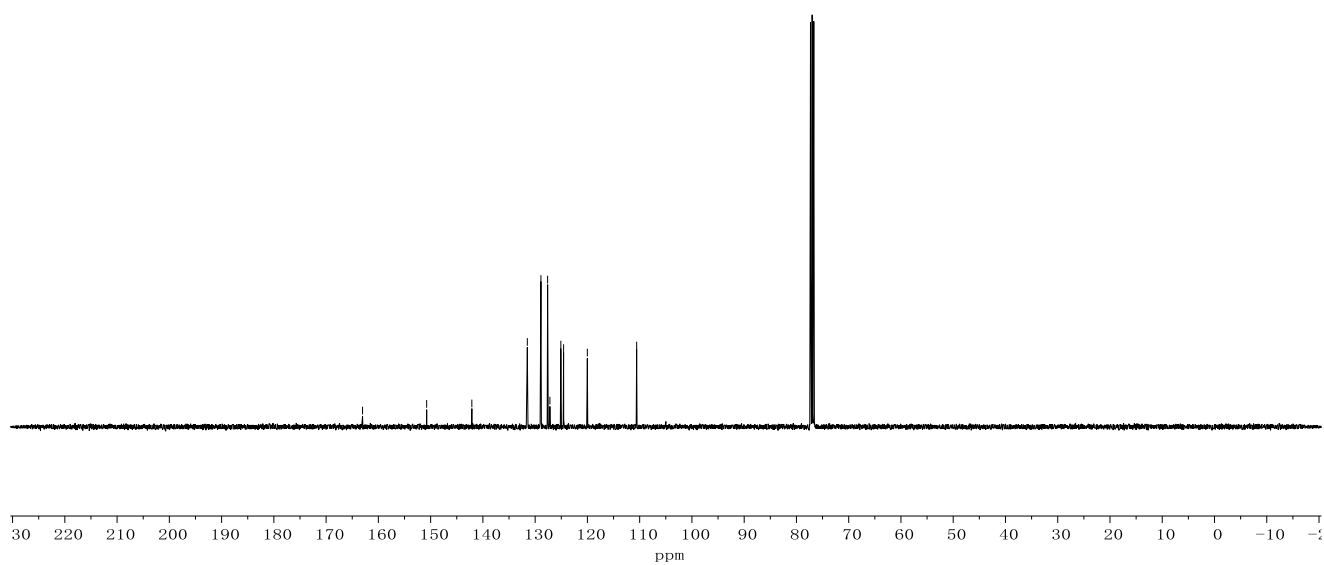
Appendix: NMR Spectra



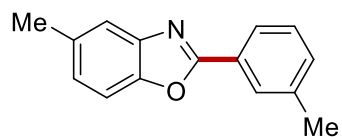
**447e**  
(400 MHz, CDCl<sub>3</sub>)



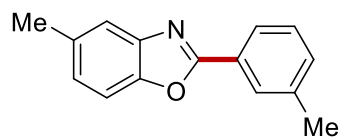
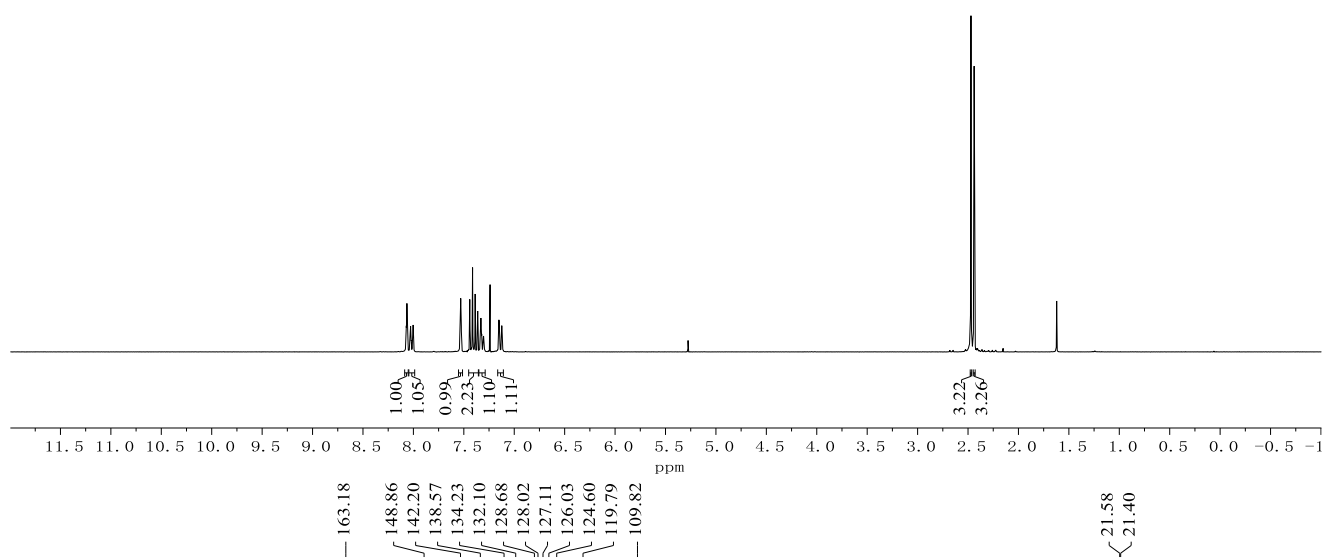
**447e**  
(100 MHz, CDCl<sub>3</sub>)



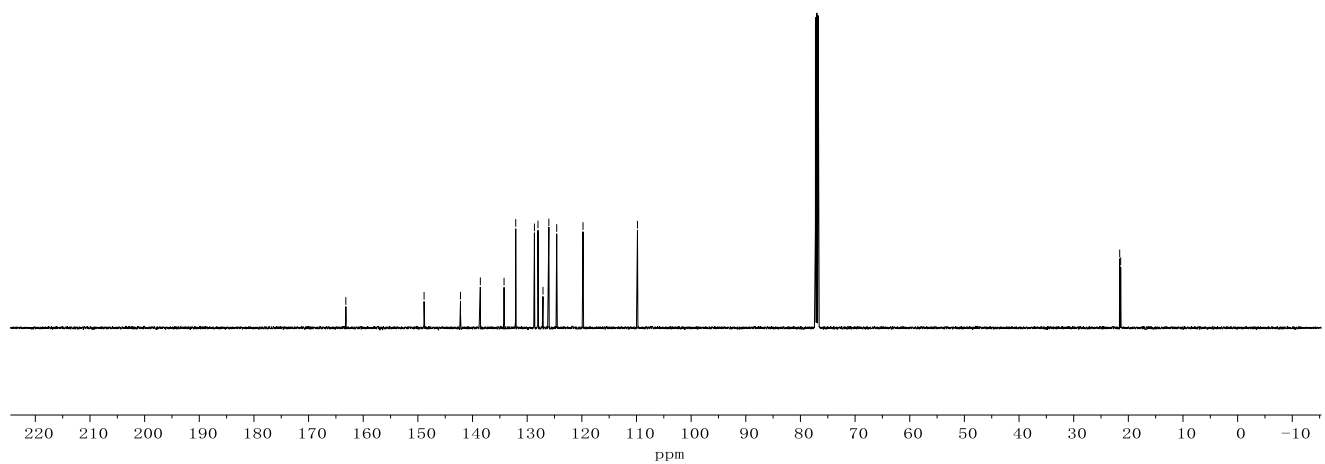
Appendix: NMR Spectra



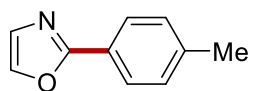
**447f**  
(300 MHz, CDCl<sub>3</sub>)



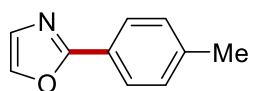
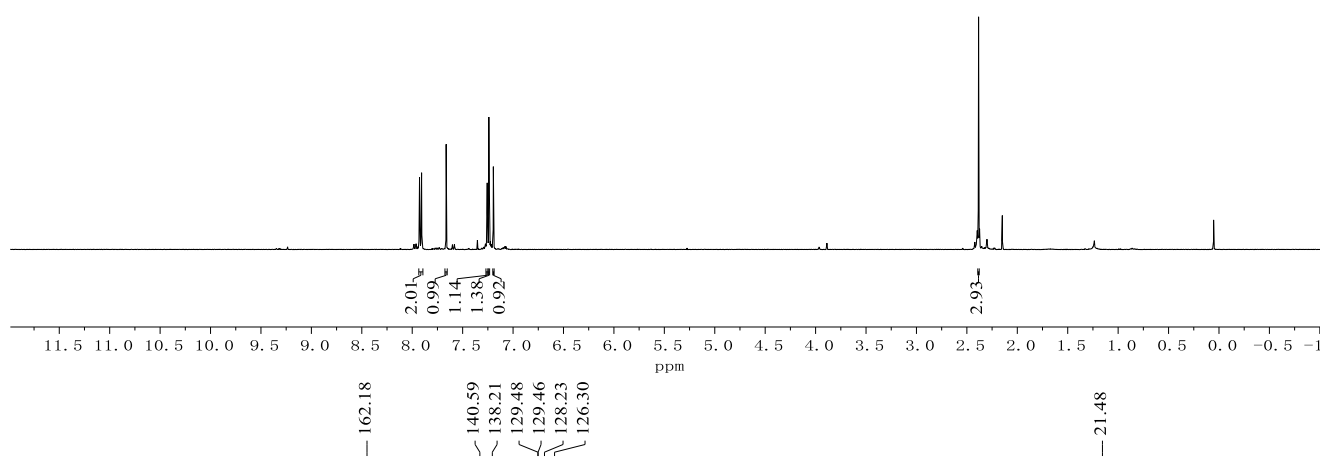
**447f**  
(75 MHz, CDCl<sub>3</sub>)



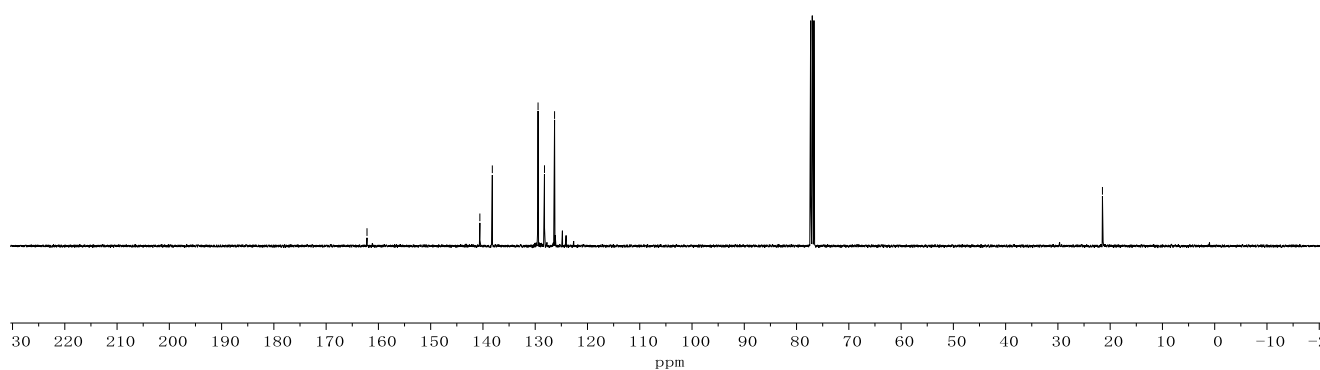
Appendix: NMR Spectra



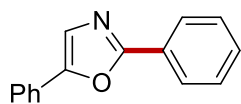
**447g**  
(400 MHz, CDCl<sub>3</sub>)



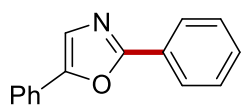
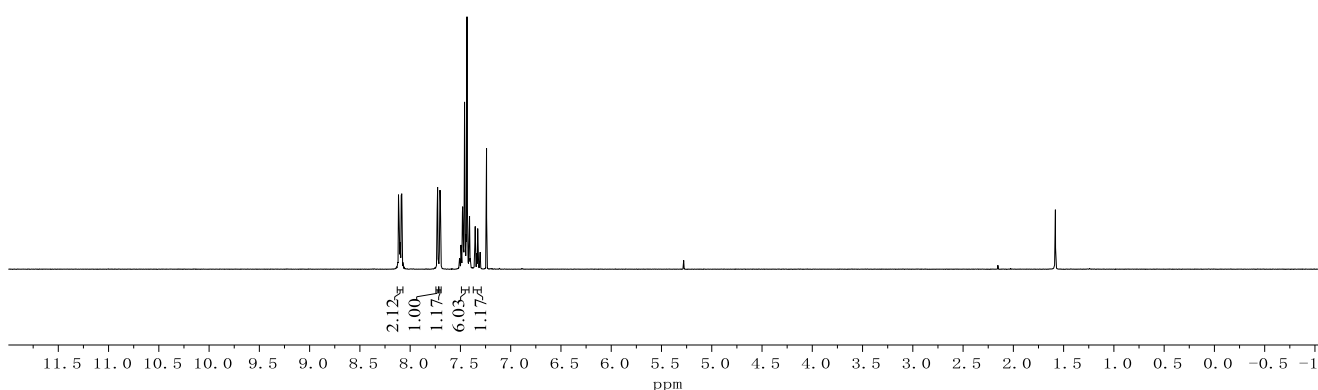
**447g**  
(100 MHz, CDCl<sub>3</sub>)



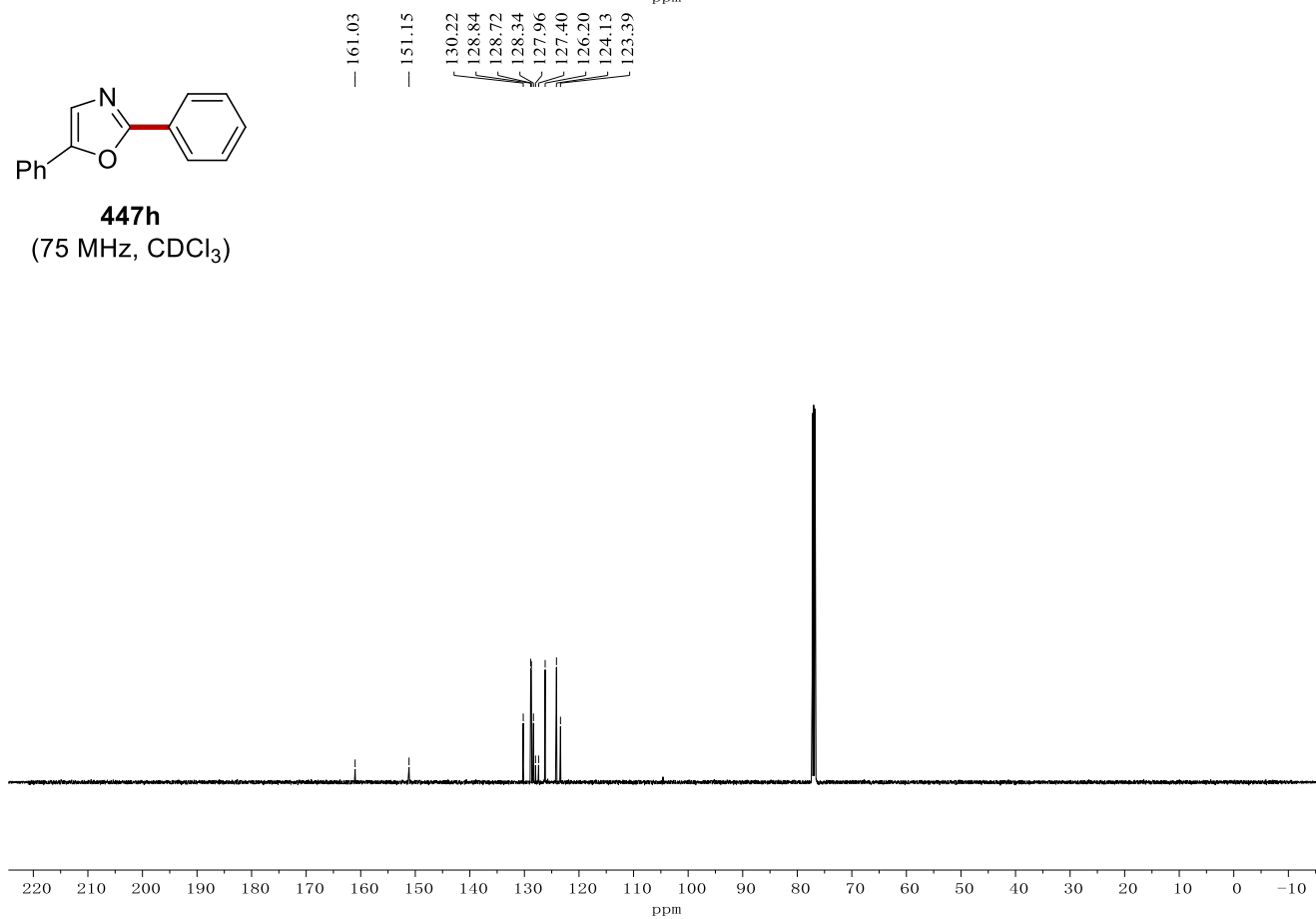
Appendix: NMR Spectra



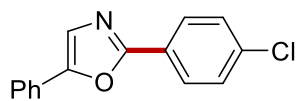
**447h**  
(300 MHz, CDCl<sub>3</sub>)



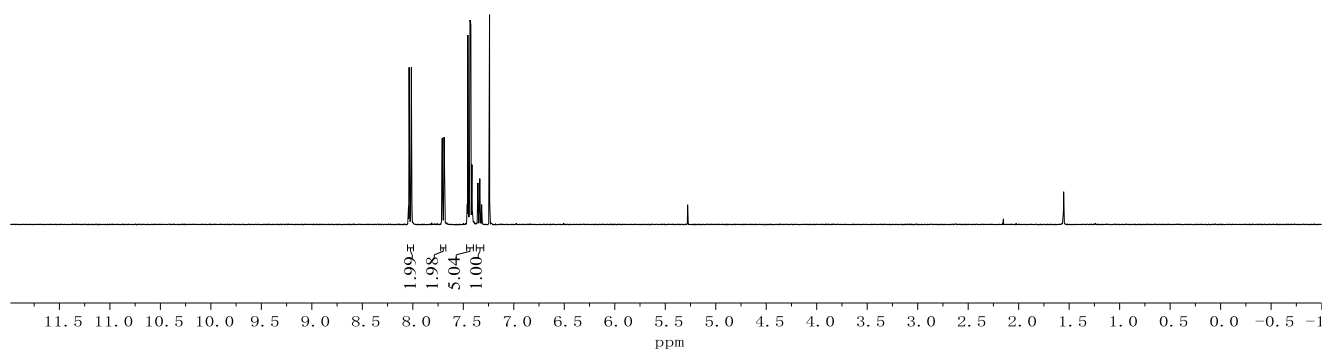
**447h**  
(75 MHz, CDCl<sub>3</sub>)



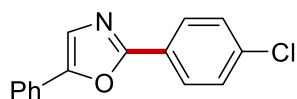
Appendix: NMR Spectra



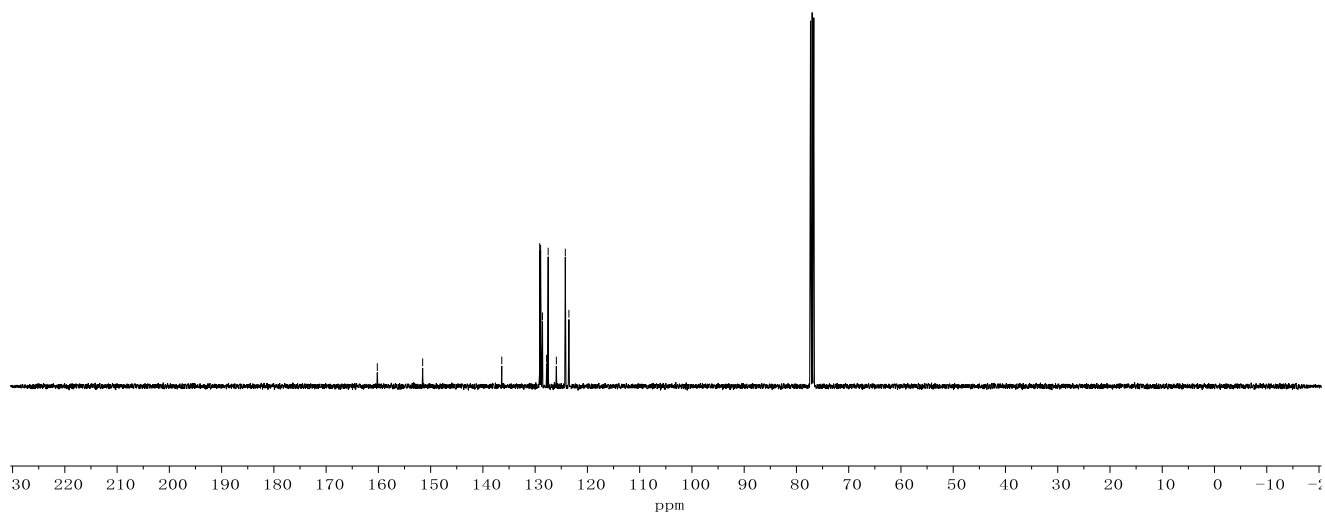
**447i**  
(400 MHz, CDCl<sub>3</sub>)



160.21  
151.53  
136.39  
129.13  
128.96  
128.59  
127.82  
127.51  
125.95  
124.23  
123.54

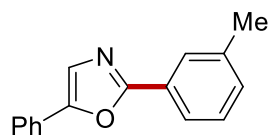


**447i**  
(100 MHz, CDCl<sub>3</sub>)

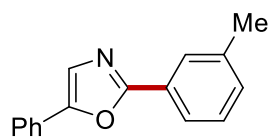
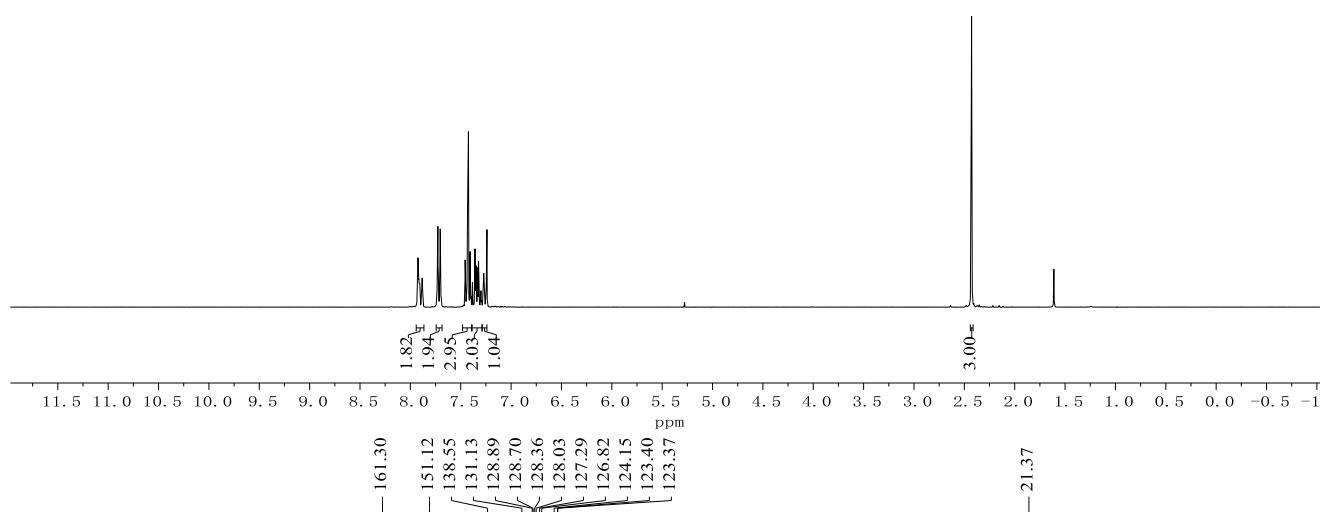




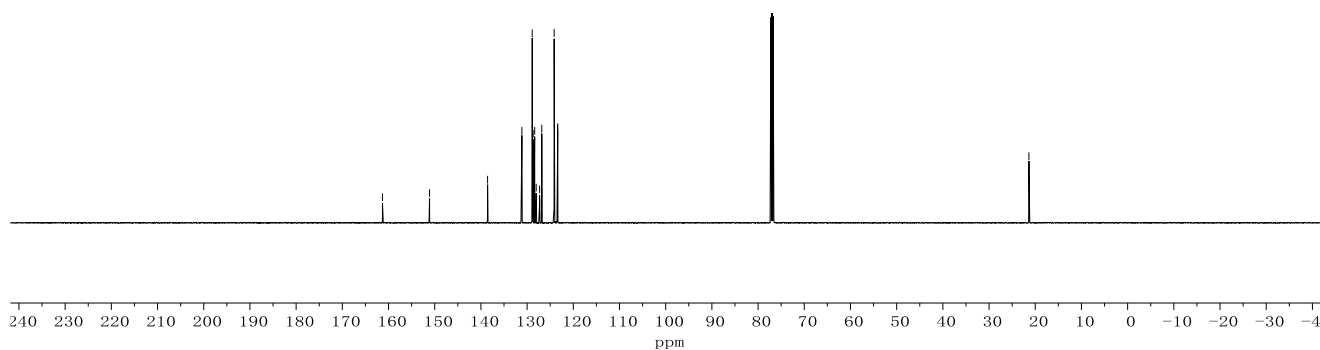
Appendix: NMR Spectra



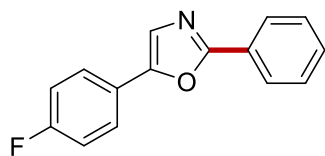
**447j**  
(300 MHz, CDCl<sub>3</sub>)



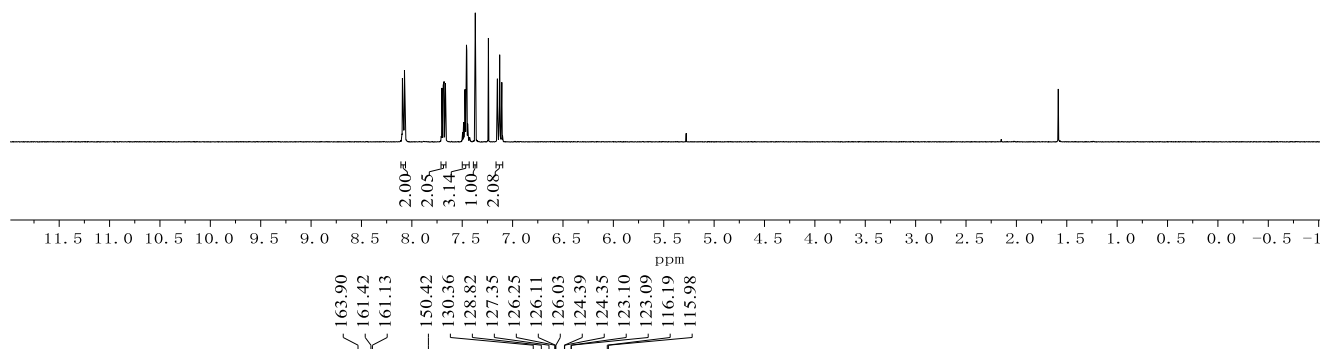
**447j**  
(75 MHz, CDCl<sub>3</sub>)



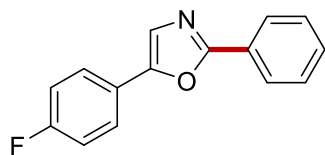
Appendix: NMR Spectra



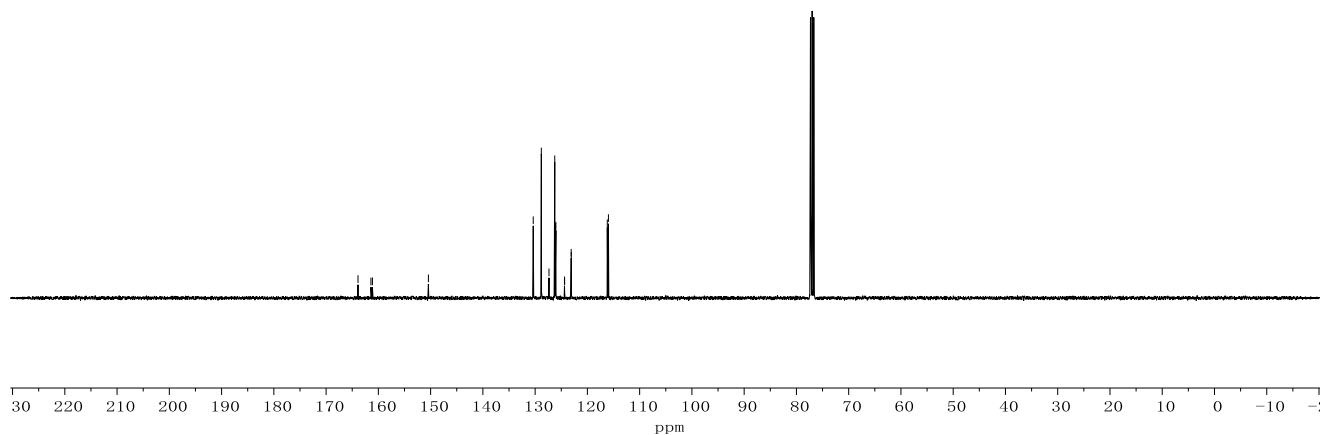
**447k**  
(400 MHz, CDCl<sub>3</sub>)



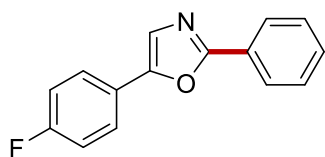
163.90  
161.42  
161.13  
150.42  
130.36  
128.82  
127.35  
126.25  
126.11  
126.03  
124.39  
124.35  
123.10  
123.09  
116.19  
115.98



**447k**  
(100 MHz, CDCl<sub>3</sub>)

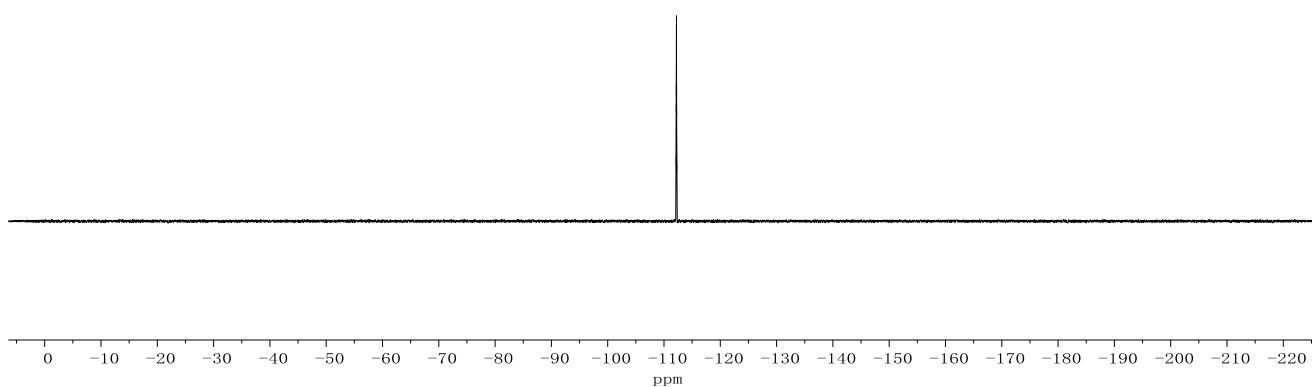


Appendix: NMR Spectra

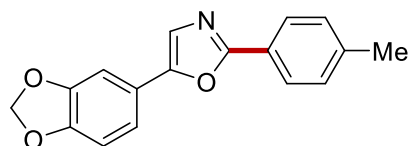


**447k**  
(282 MHz, CDCl<sub>3</sub>)

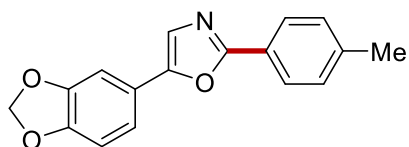
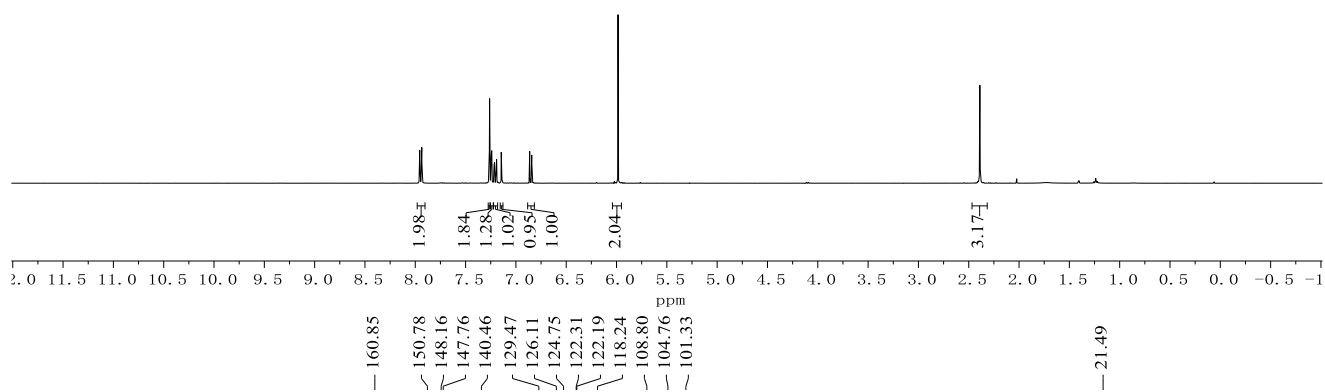
-112.2  
-112.2  
-112.2  
-112.2  
-112.2  
-112.3



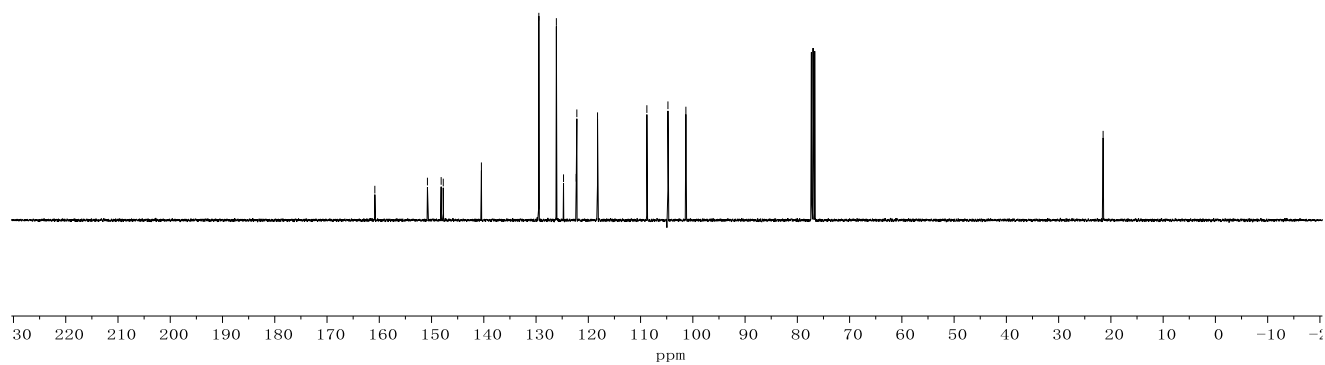
Appendix: NMR Spectra



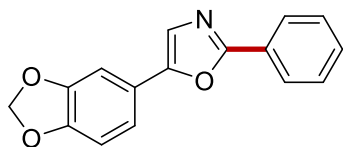
**4471**  
(400 MHz, CDCl<sub>3</sub>)



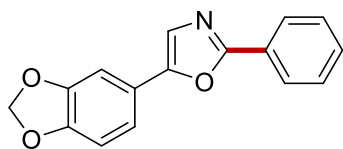
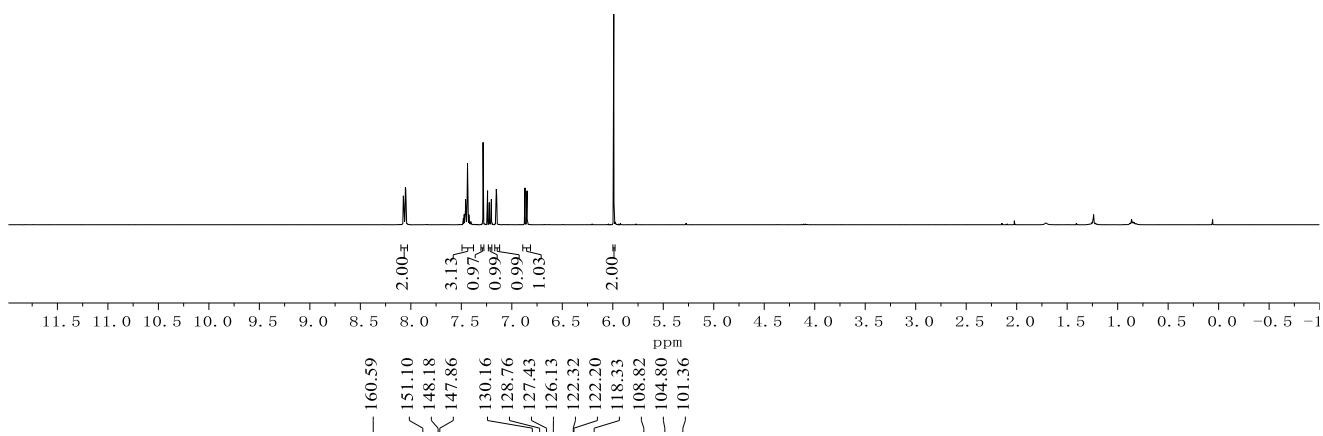
**4471**  
(100 MHz, CDCl<sub>3</sub>)



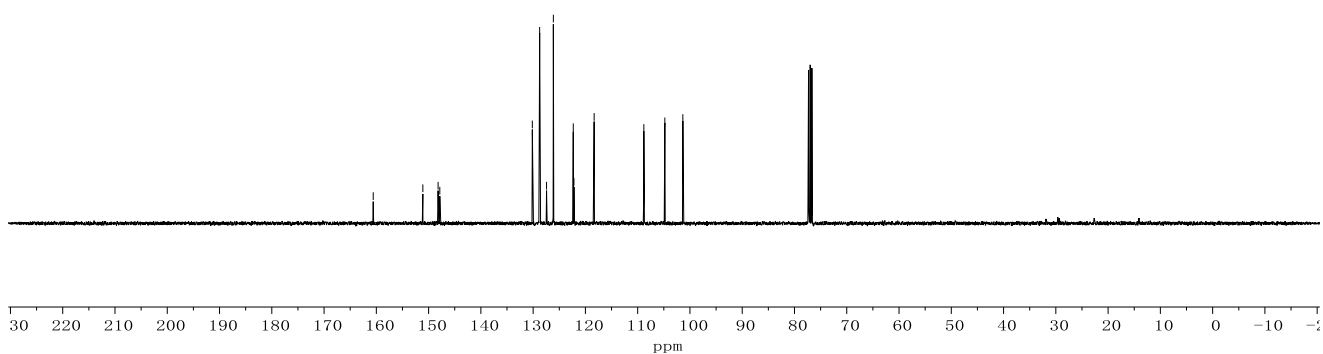
Appendix: NMR Spectra



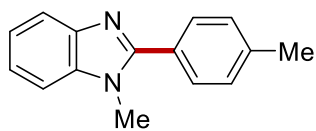
**447m**  
(400 MHz, CDCl<sub>3</sub>)



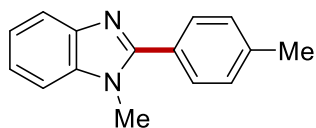
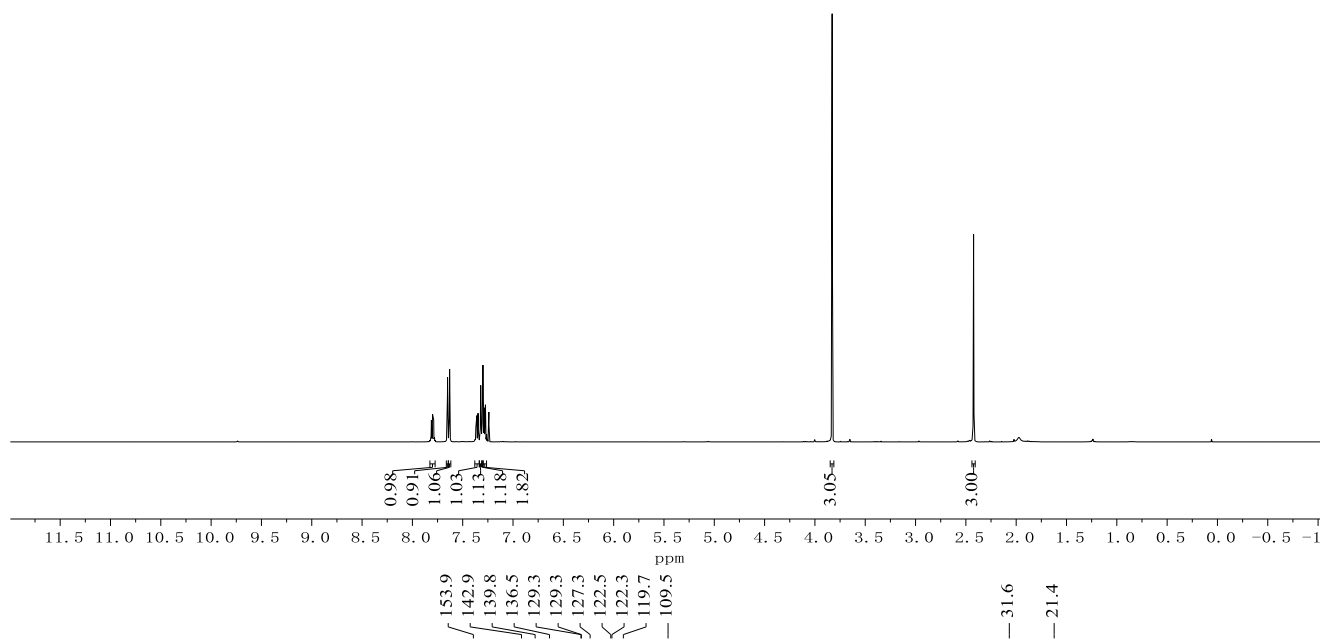
**447m**  
(100 MHz, CDCl<sub>3</sub>)



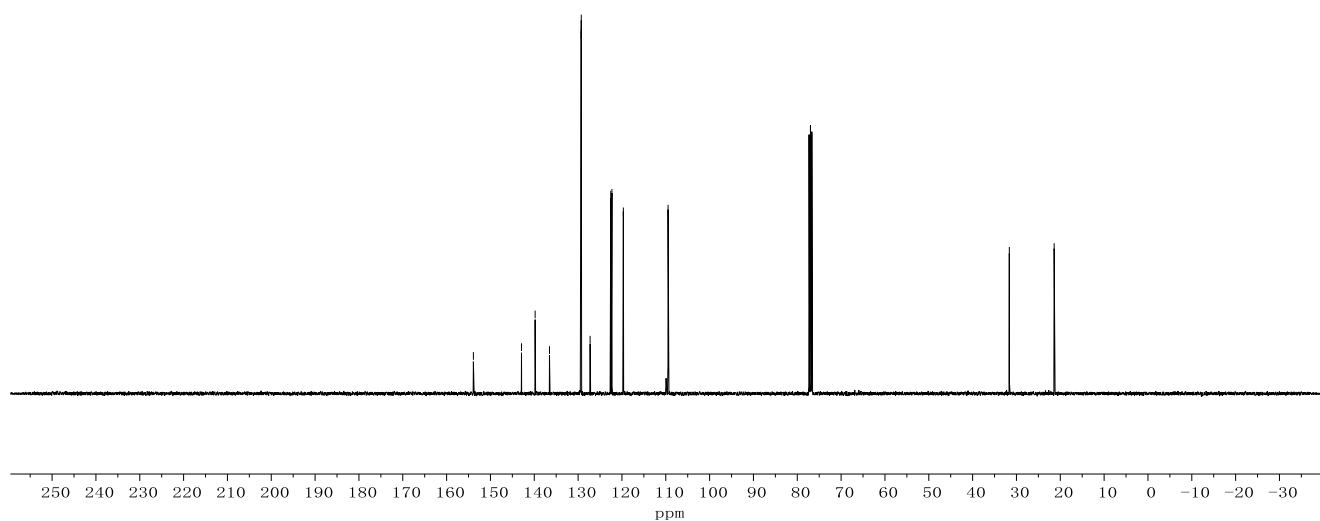
Appendix: NMR Spectra



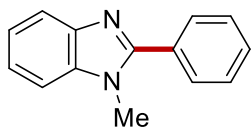
**446a**  
(400 MHz, CDCl<sub>3</sub>)



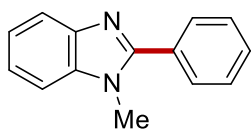
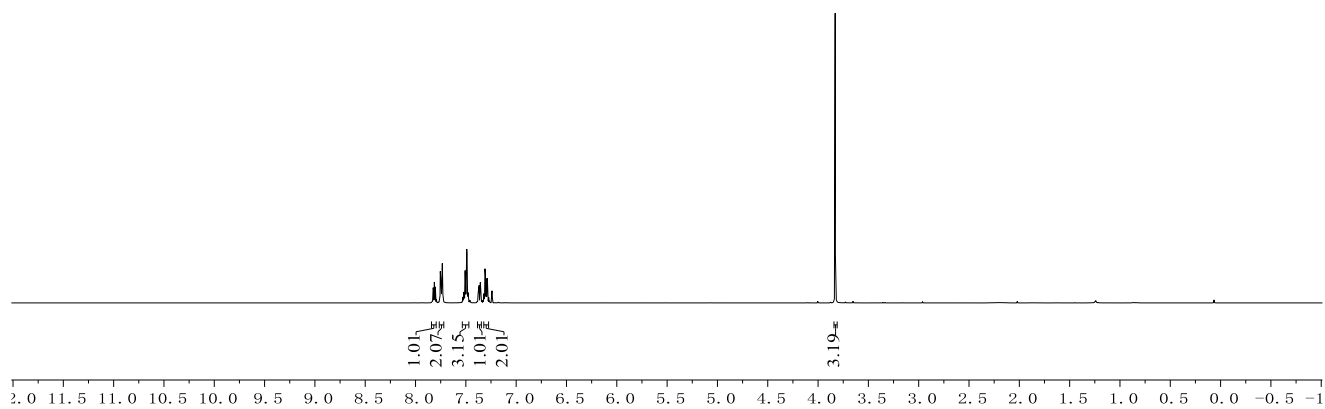
**446a**  
(100 MHz, CDCl<sub>3</sub>)



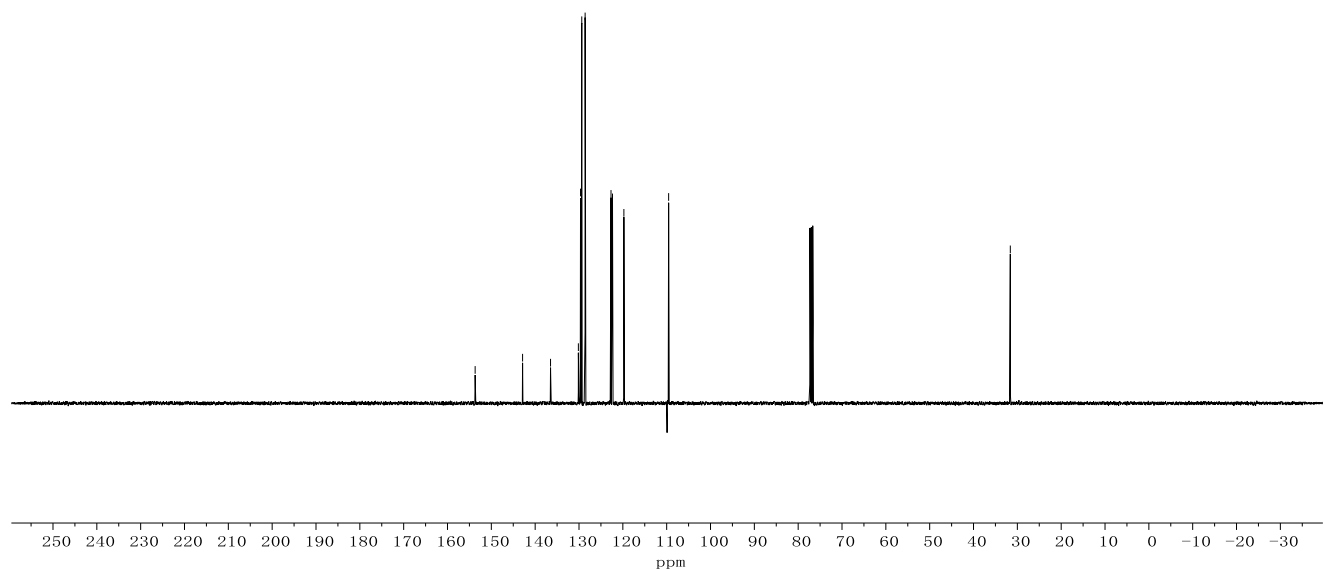
Appendix: NMR Spectra



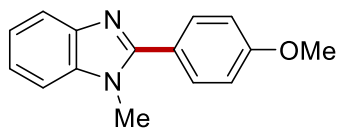
**446b**  
(400 MHz, CDCl<sub>3</sub>)



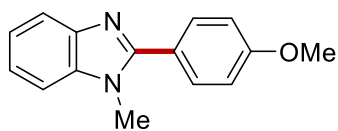
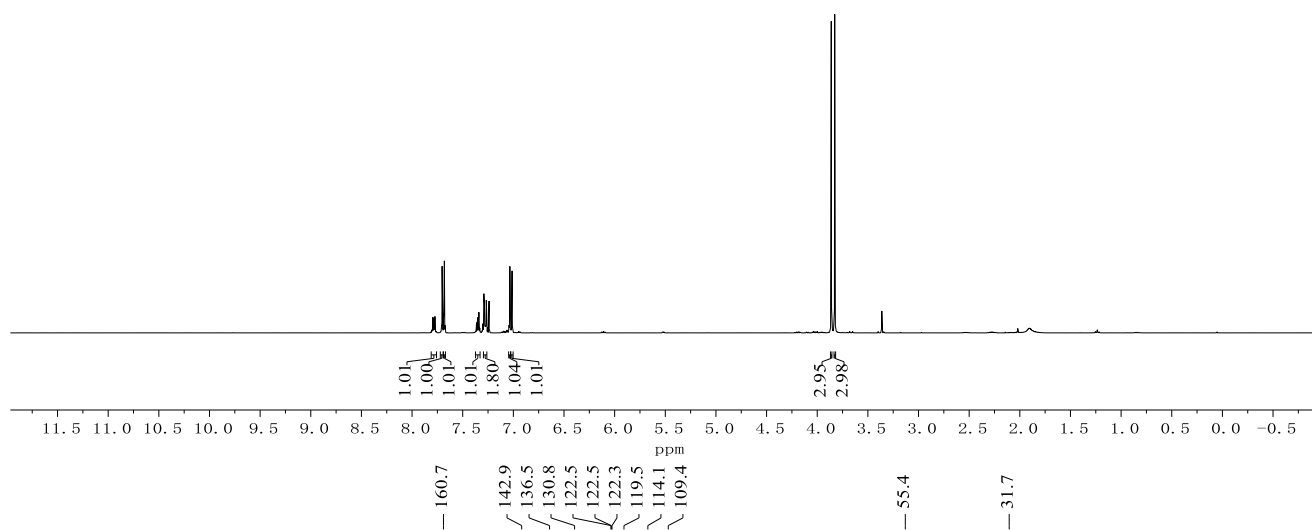
**446b**  
(100 MHz, CDCl<sub>3</sub>)



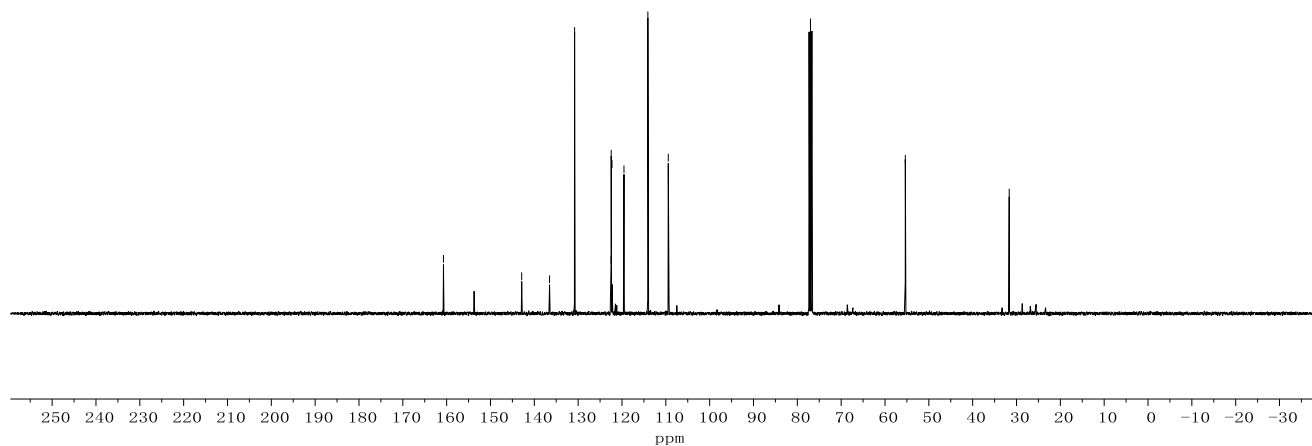
Appendix: NMR Spectra



**446c**  
(400 MHz, CDCl<sub>3</sub>)

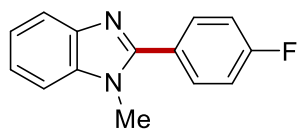


**446c**  
(100 MHz, CDCl<sub>3</sub>)

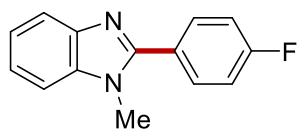
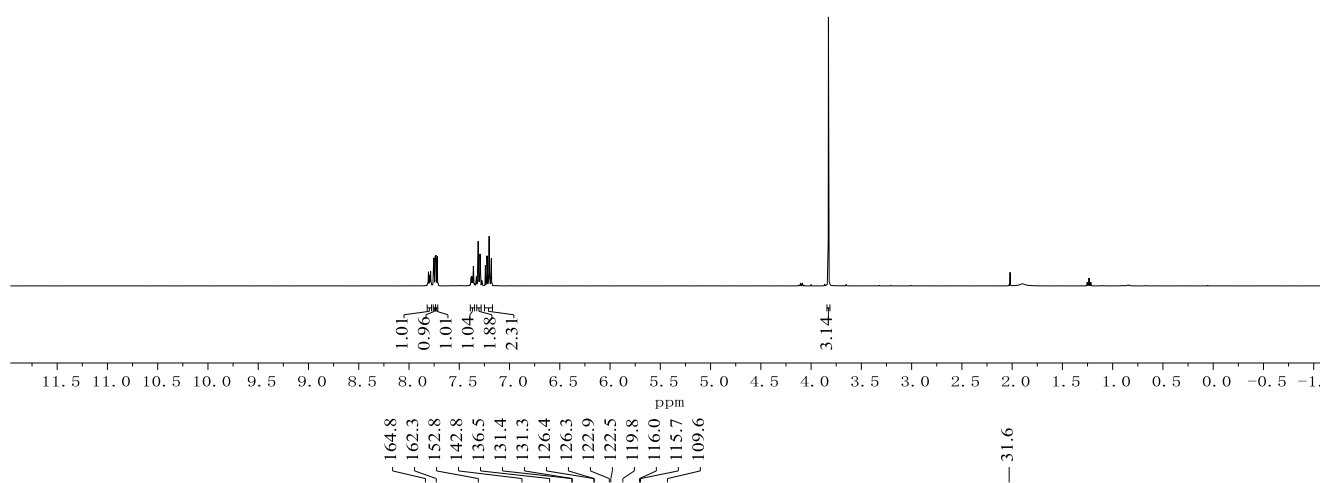




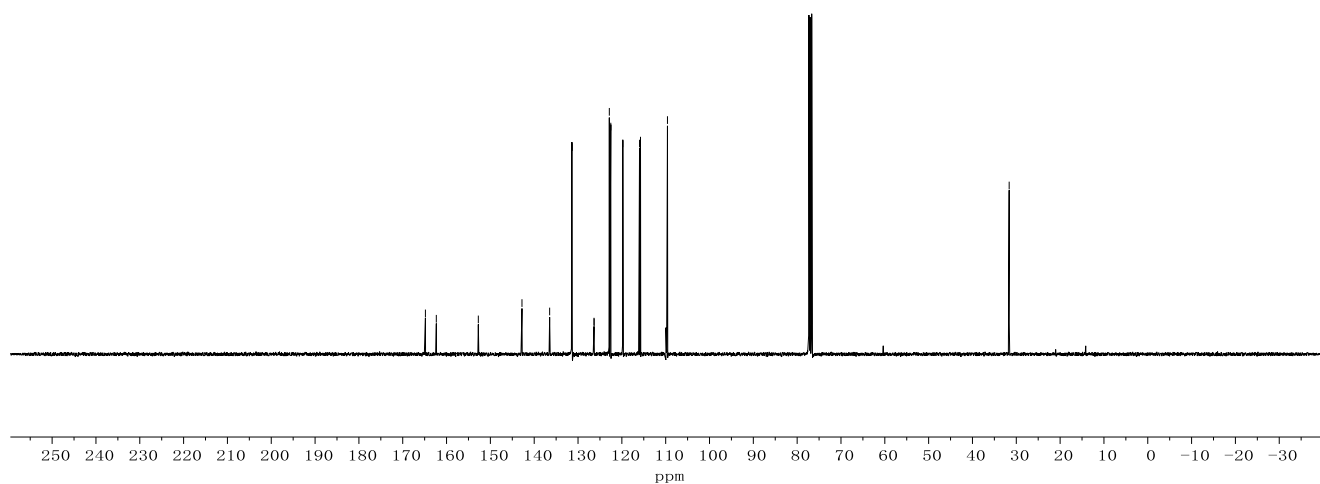
Appendix: NMR Spectra



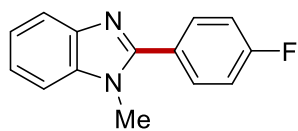
**446d**  
(400 MHz, CDCl<sub>3</sub>)



**446d**  
(100 MHz, CDCl<sub>3</sub>)

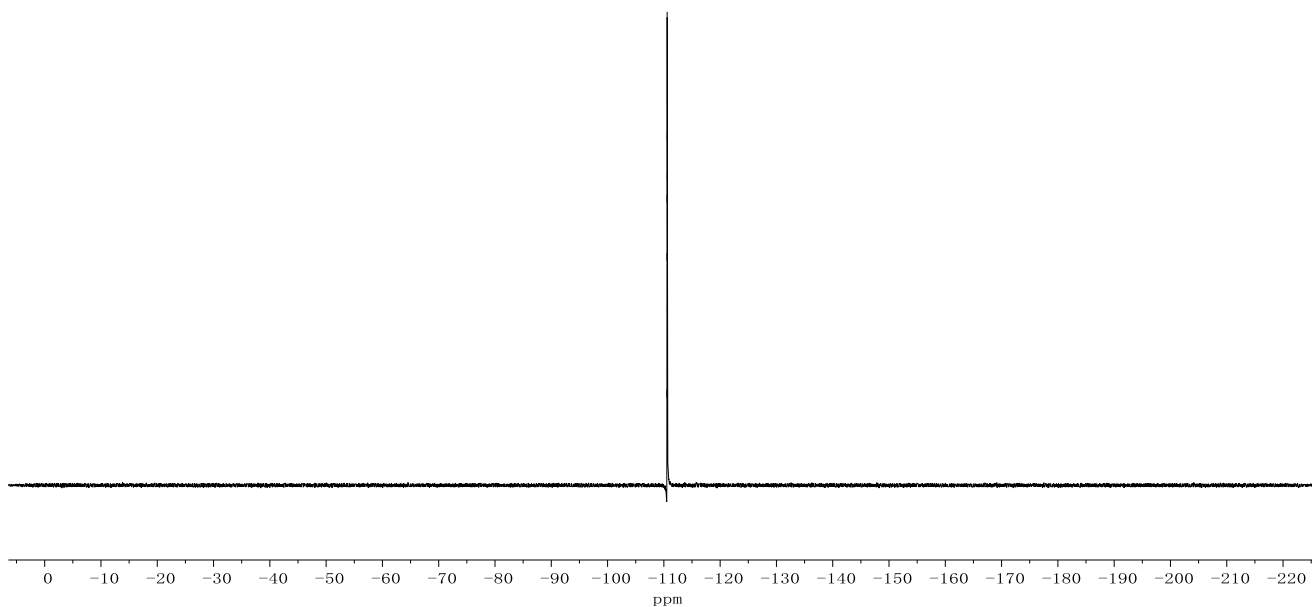


Appendix: NMR Sepctra

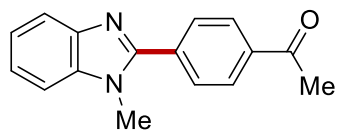


**446d**  
(282 MHz, CDCl<sub>3</sub>)

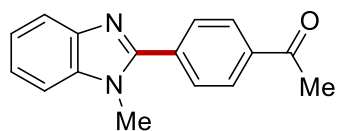
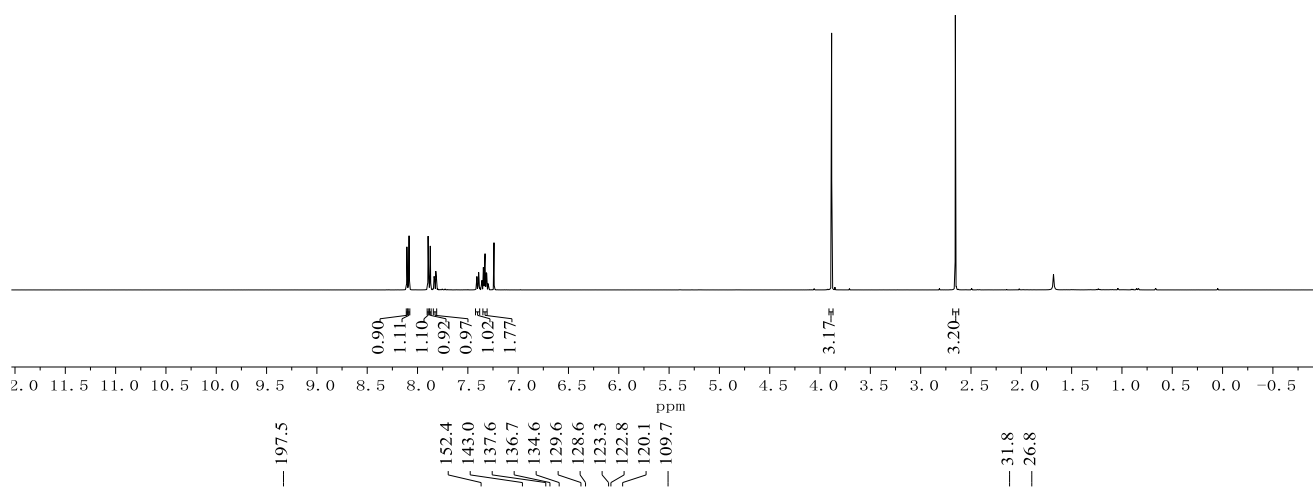
-110.5  
-110.6  
-110.6  
-110.6  
-110.6  
-110.6



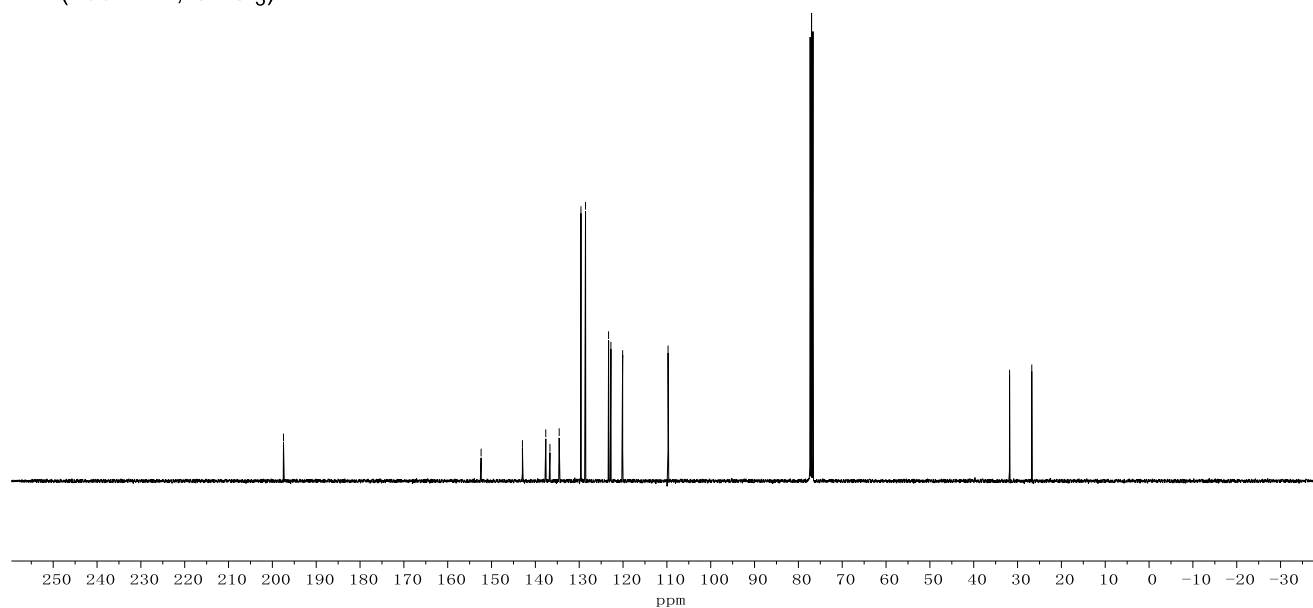
Appendix: NMR Spectra



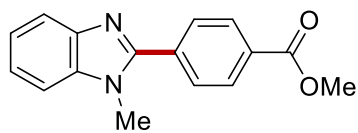
**446e**  
(400 MHz, CDCl<sub>3</sub>)



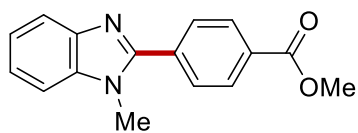
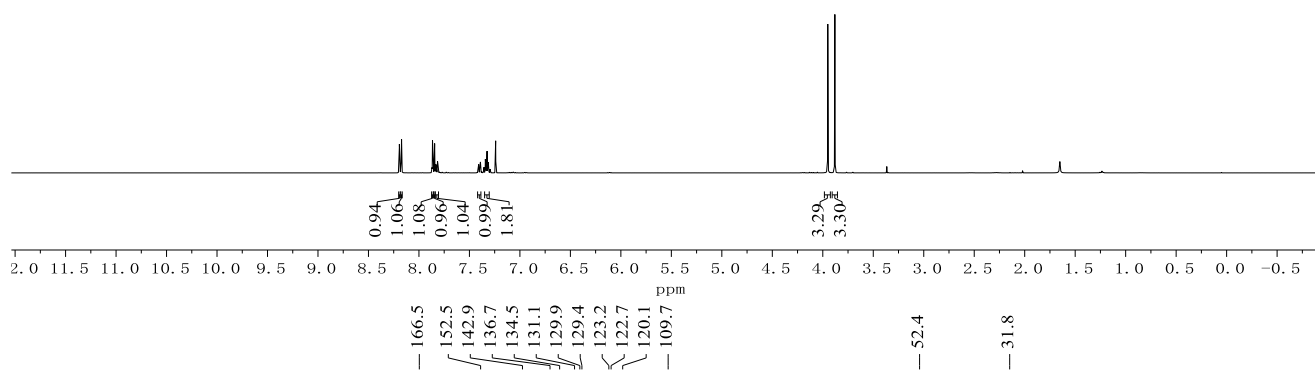
**446e**  
(100 MHz, CDCl<sub>3</sub>)



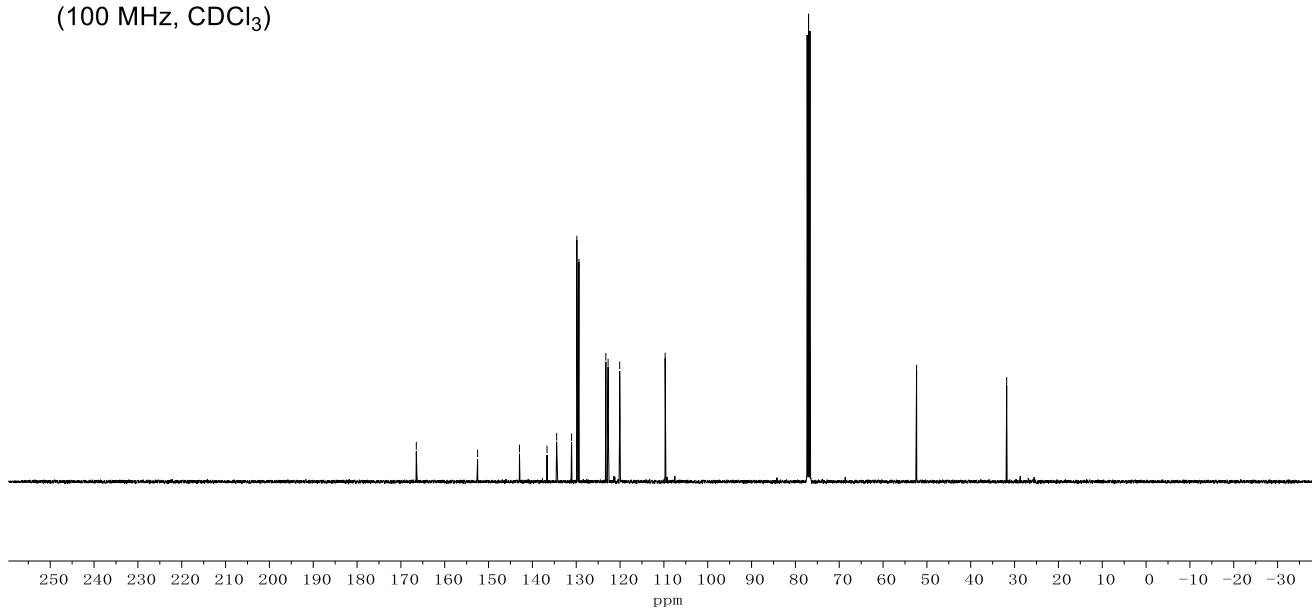
Appendix: NMR Spectra



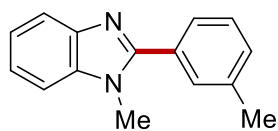
**446f**  
(400 MHz, CDCl<sub>3</sub>)



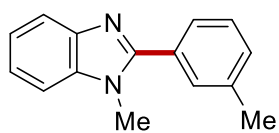
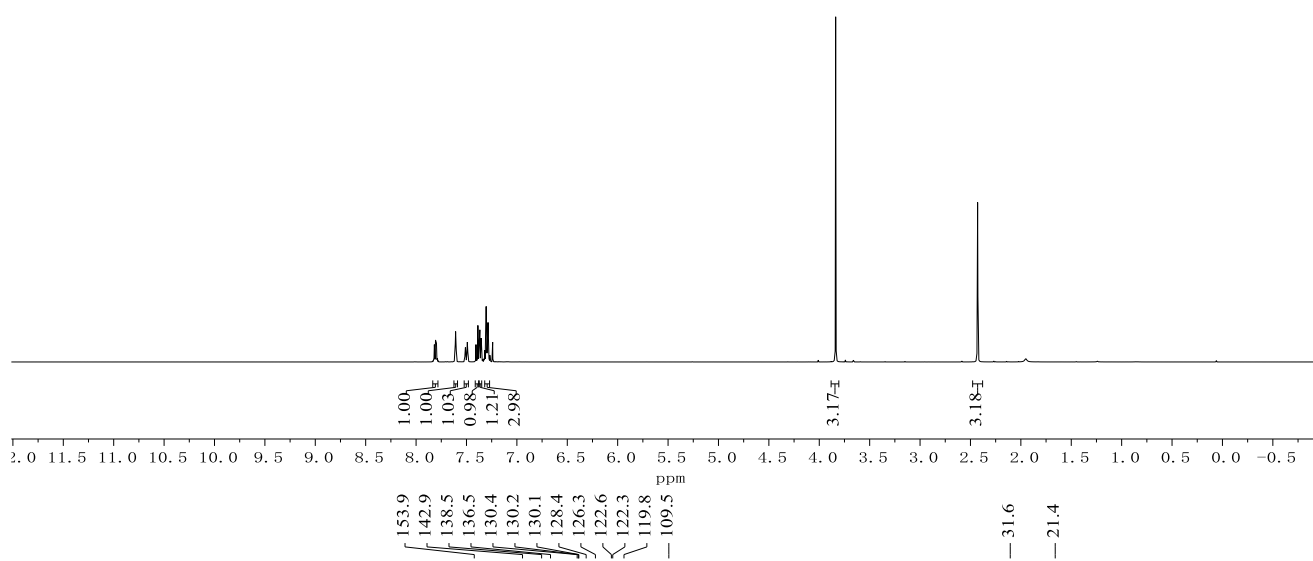
**446f**  
(100 MHz, CDCl<sub>3</sub>)



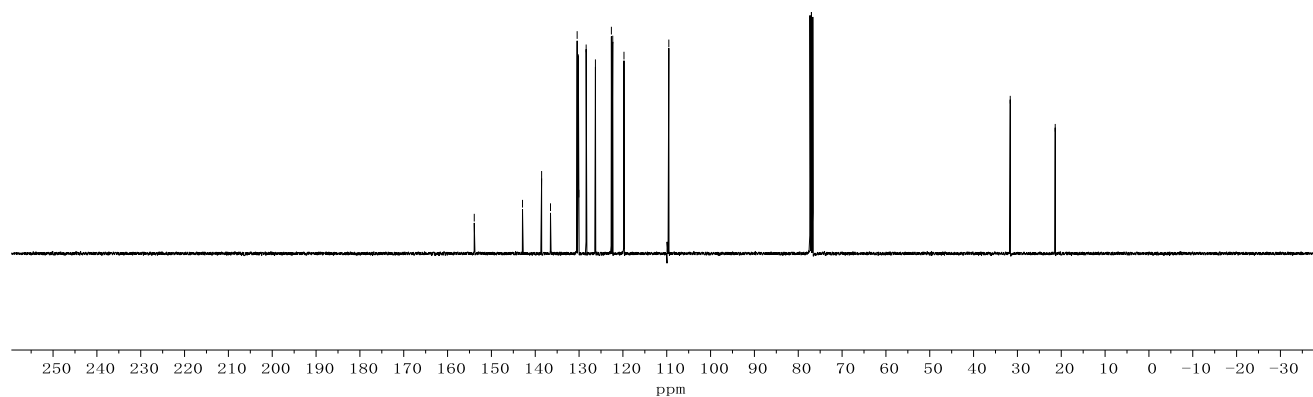
Appendix: NMR Spectra



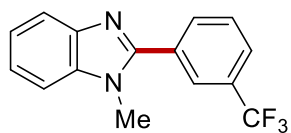
**446g**  
(400 MHz, CDCl<sub>3</sub>)



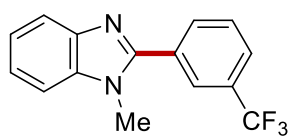
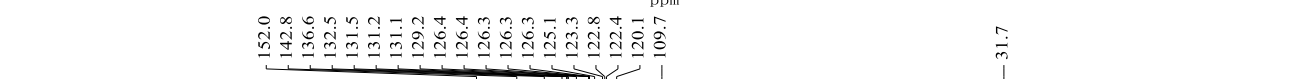
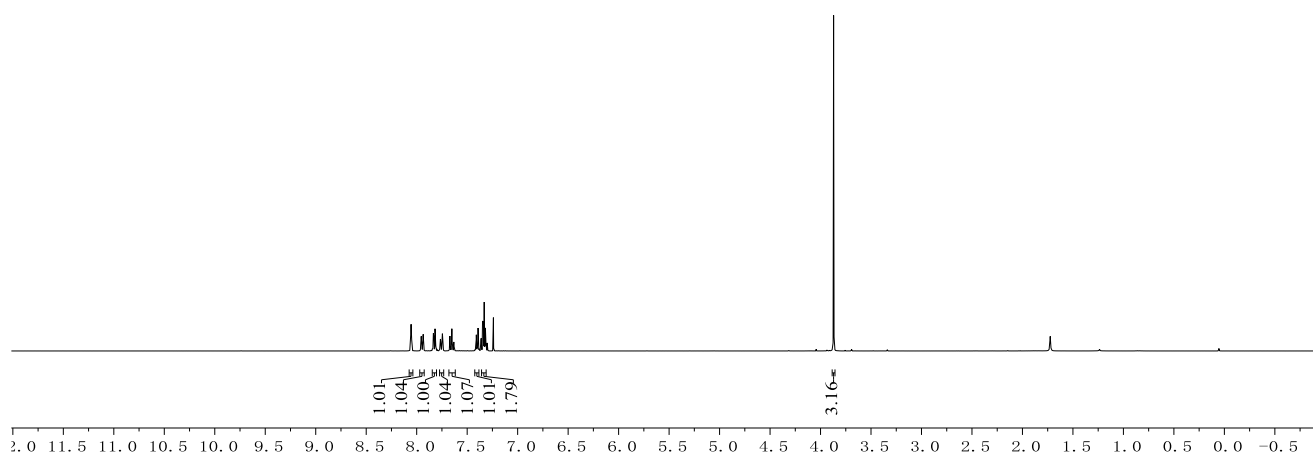
**446g**  
(100 MHz, CDCl<sub>3</sub>)



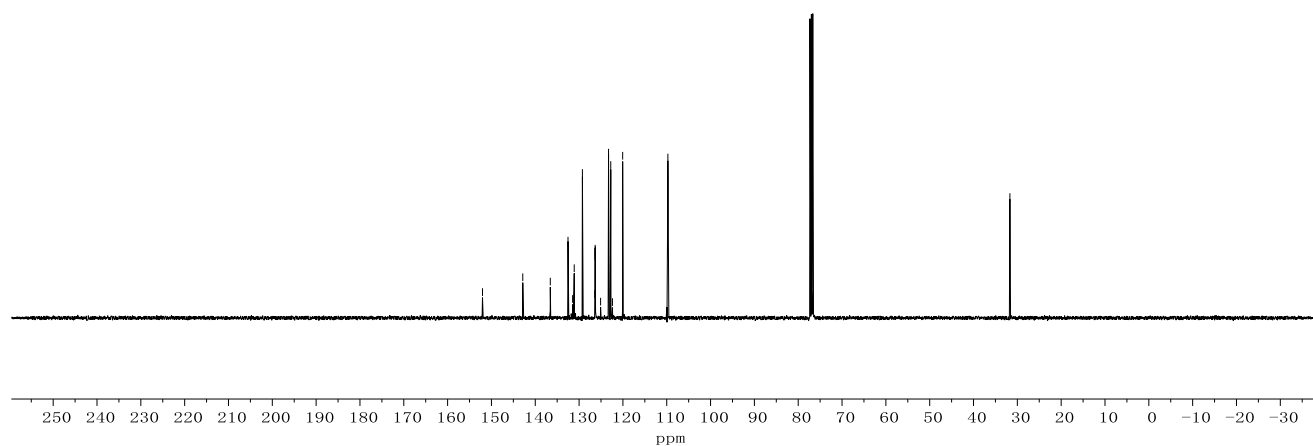
Appendix: NMR Spectra



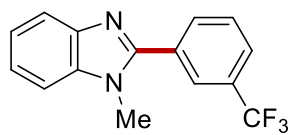
**446h**  
(500 MHz, CDCl<sub>3</sub>)



**446h**  
(125 MHz, CDCl<sub>3</sub>)

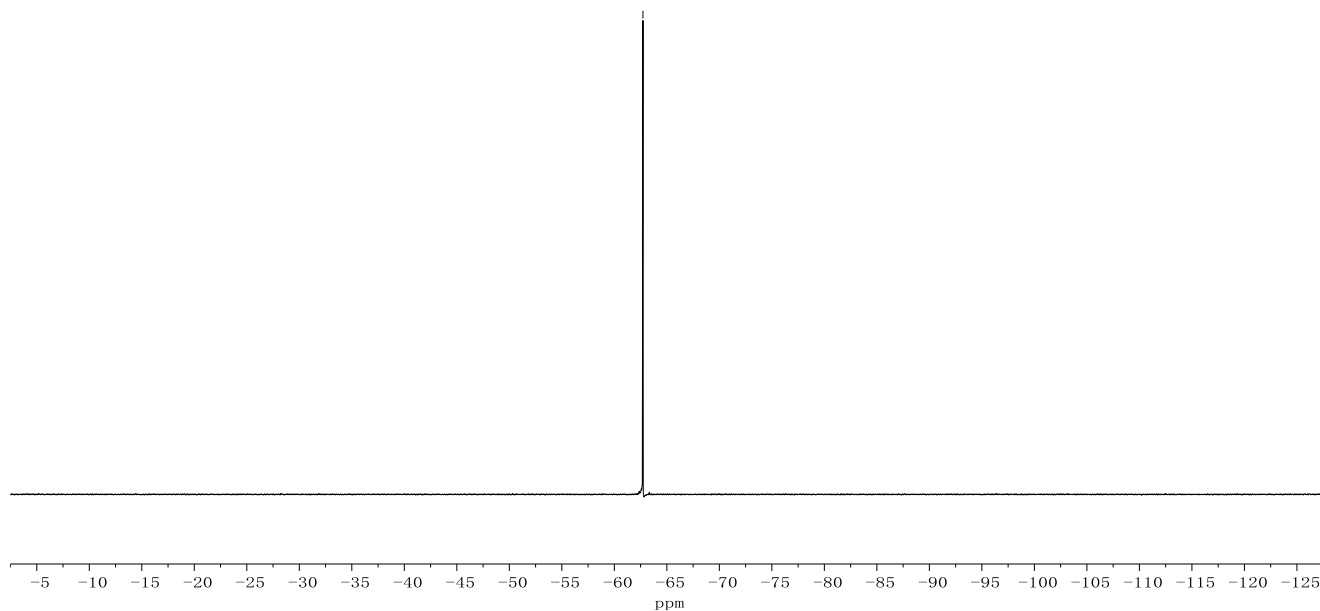


Appendix: NMR Spectra

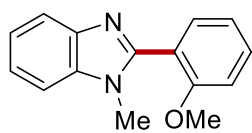


**446h**  
(282 MHz, CDCl<sub>3</sub>)

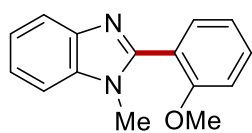
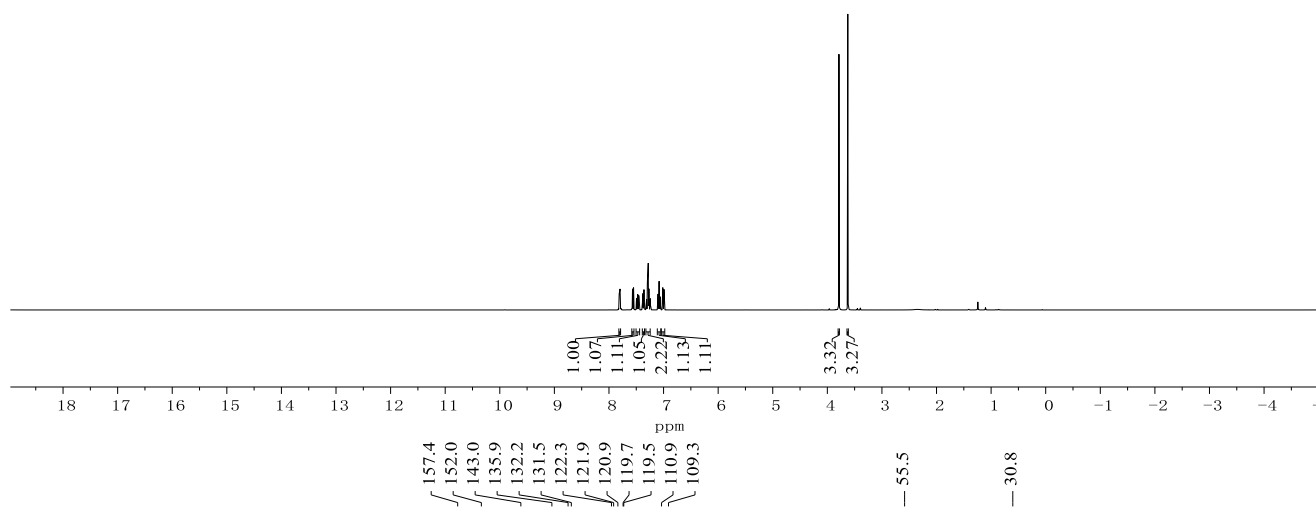
--62.7



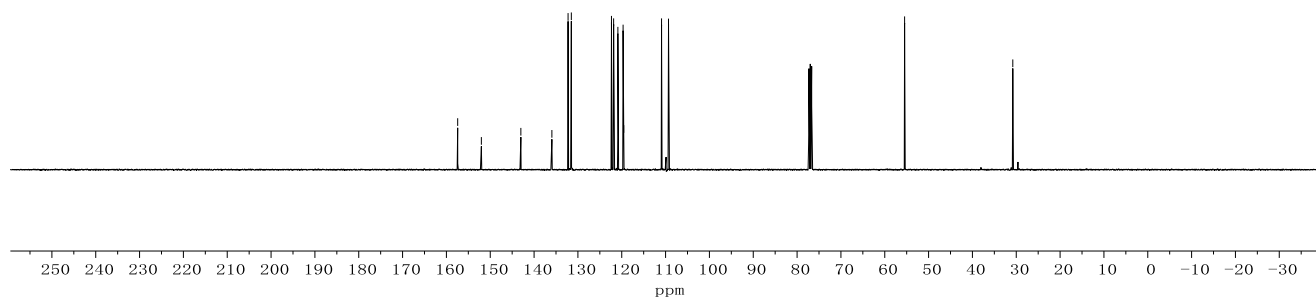
Appendix: NMR Spectra



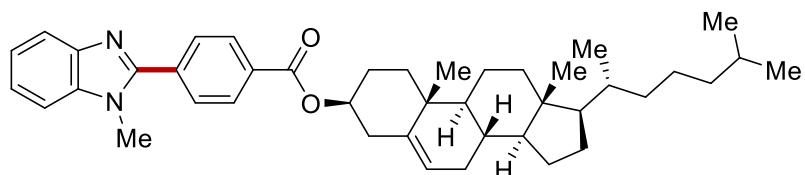
**446i**  
(400 MHz, CDCl<sub>3</sub>)



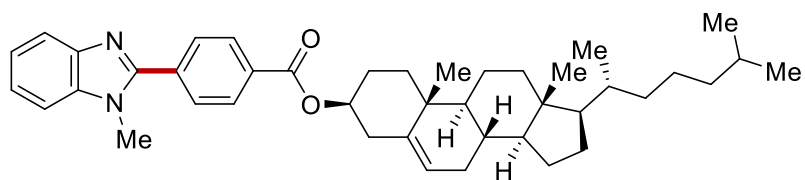
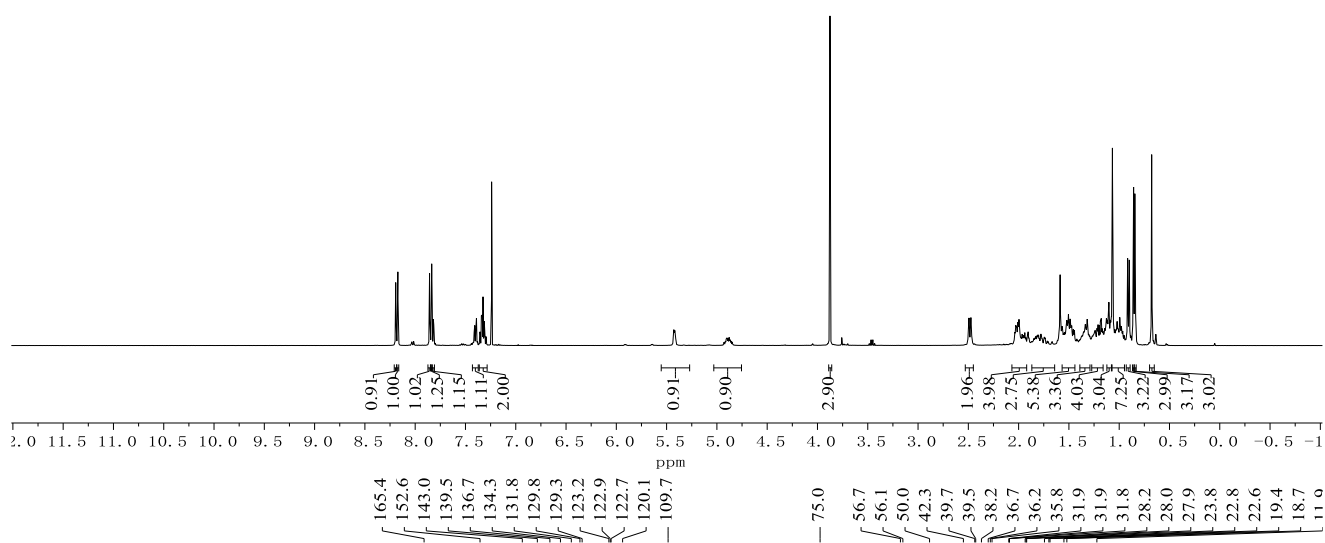
**446i**  
(100 MHz, CDCl<sub>3</sub>)



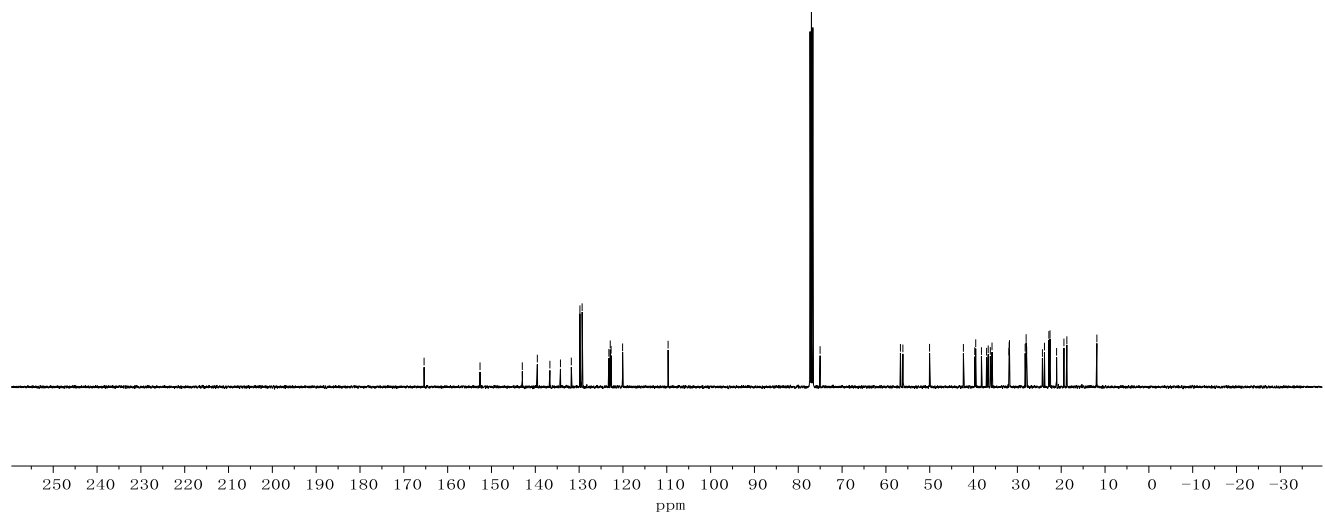




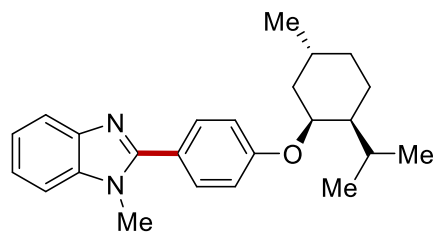
**446j**  
(400 MHz, CDCl<sub>3</sub>)



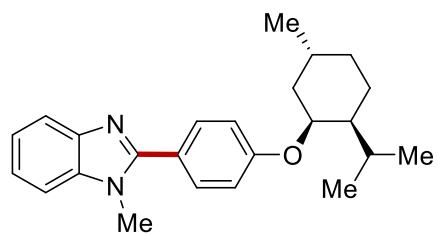
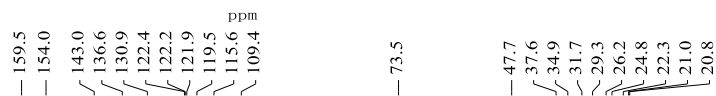
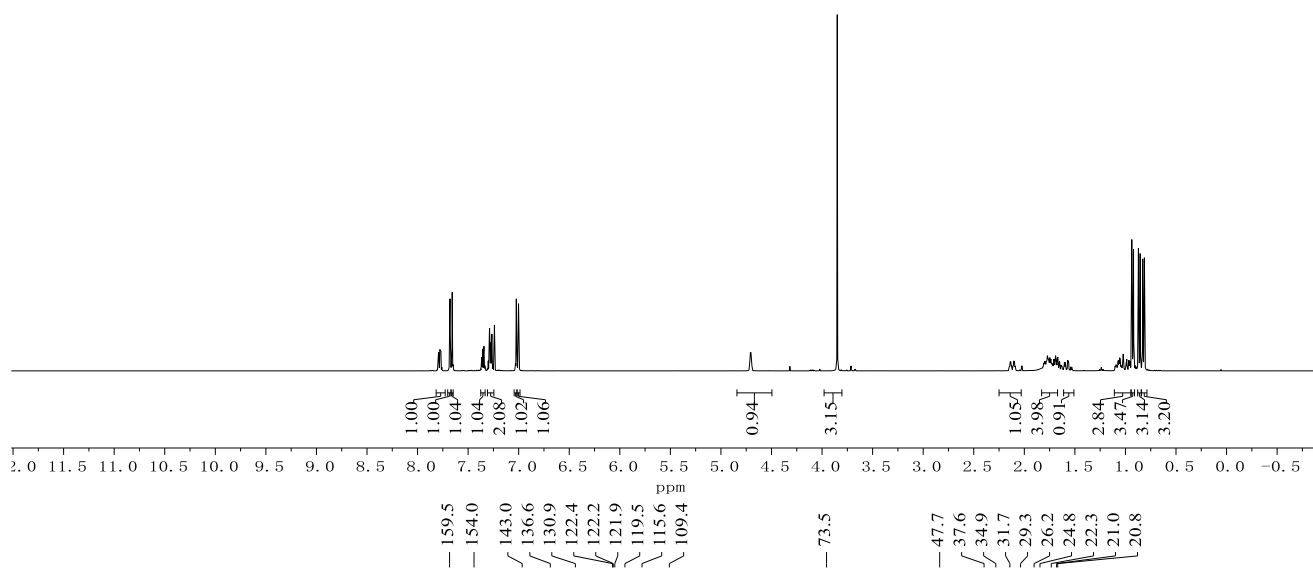
**446j**  
(100 MHz, CDCl<sub>3</sub>)



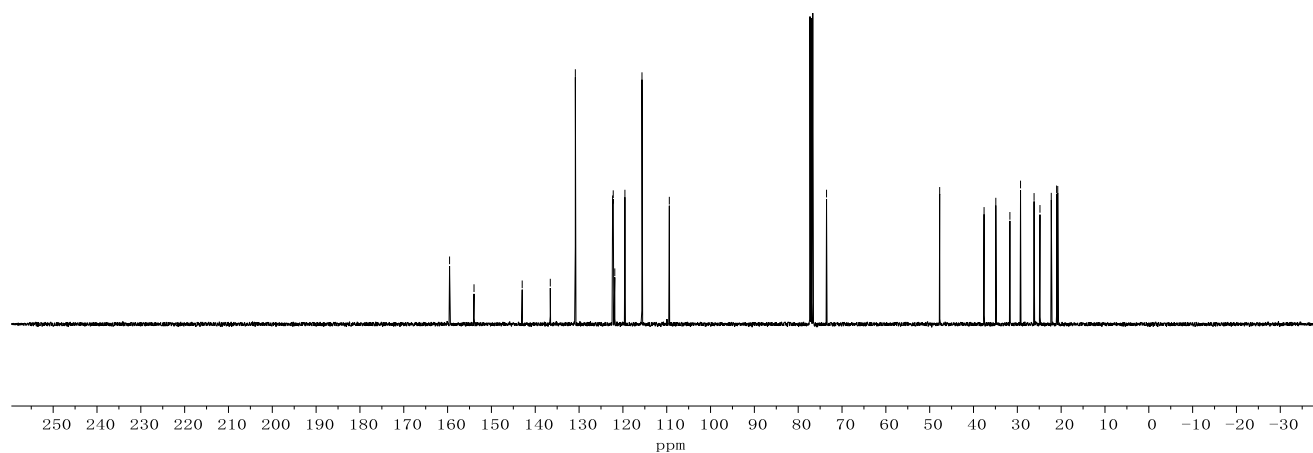
Appendix: NMR Spectra



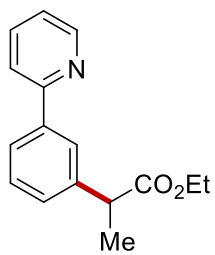
**446k**  
(400 MHz, CDCl<sub>3</sub>)



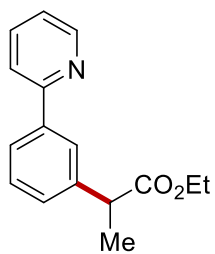
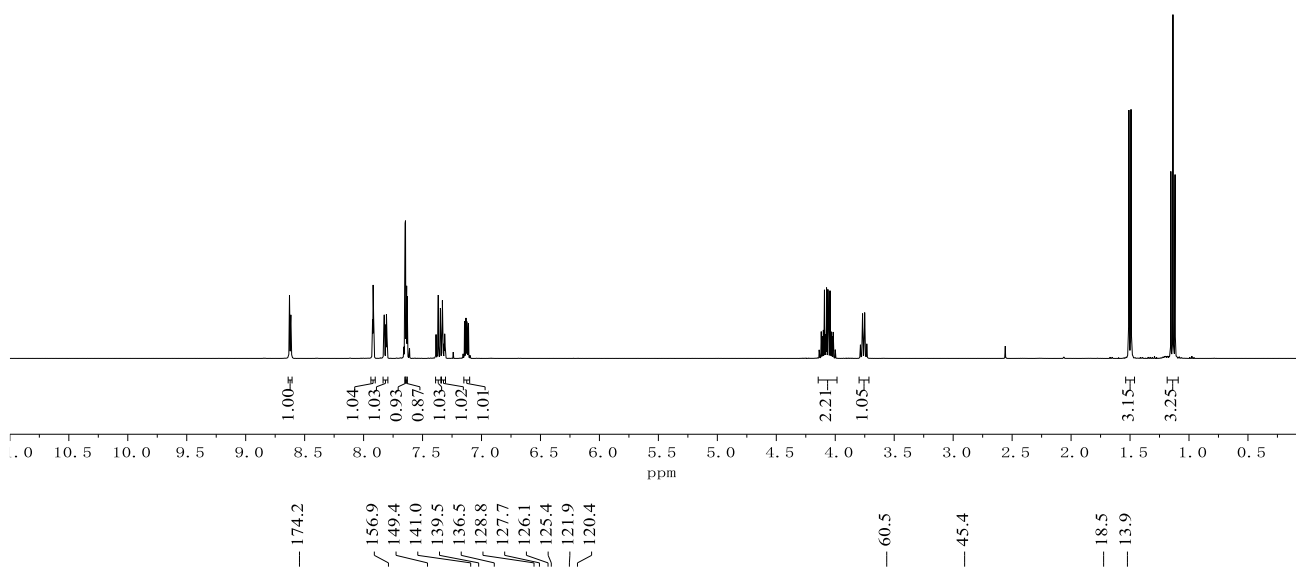
**446k**  
(100 MHz, CDCl<sub>3</sub>)



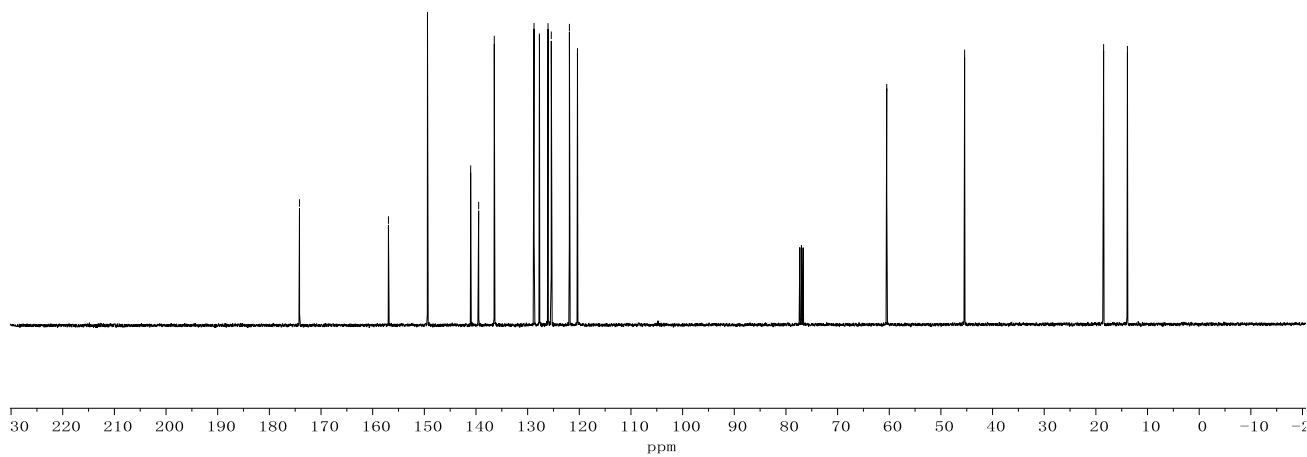
Appendix: NMR Spectra

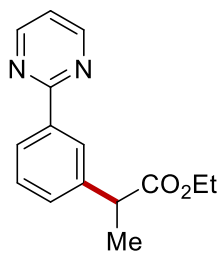


**409a**  
(400 MHz, CDCl<sub>3</sub>)

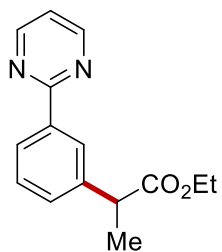
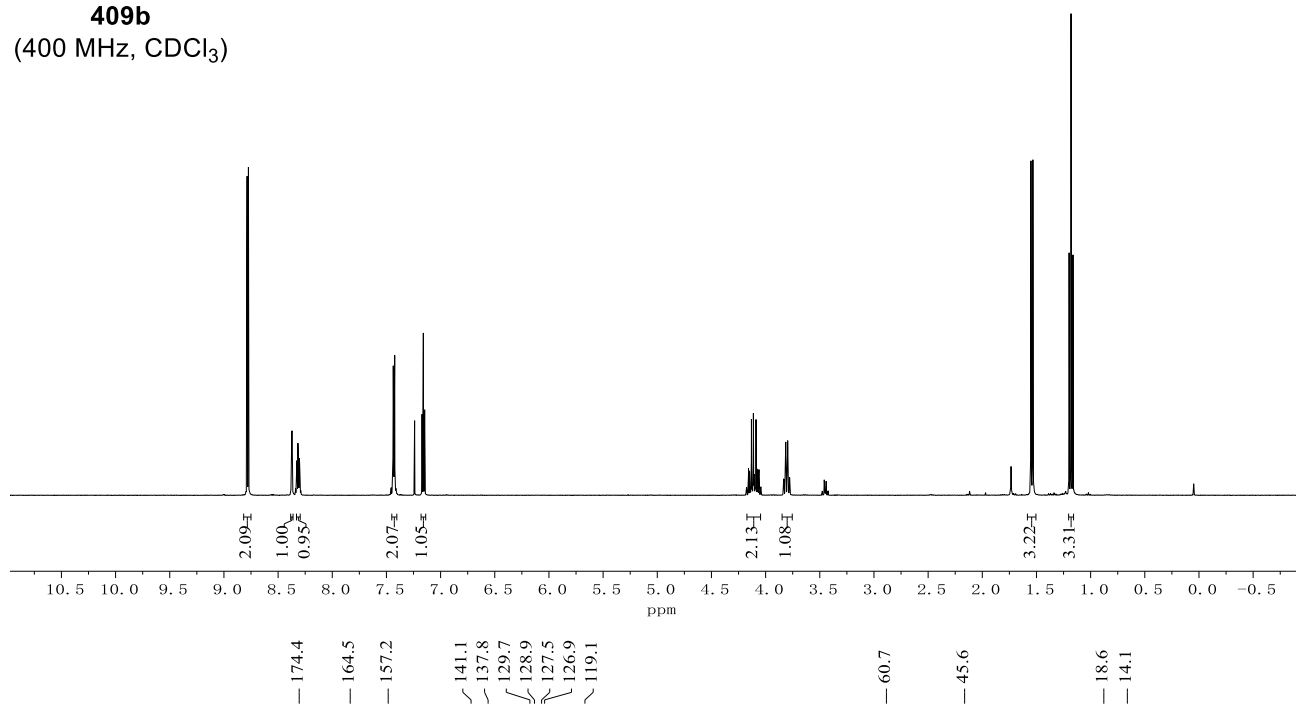


**409a**  
(100 MHz, CDCl<sub>3</sub>)

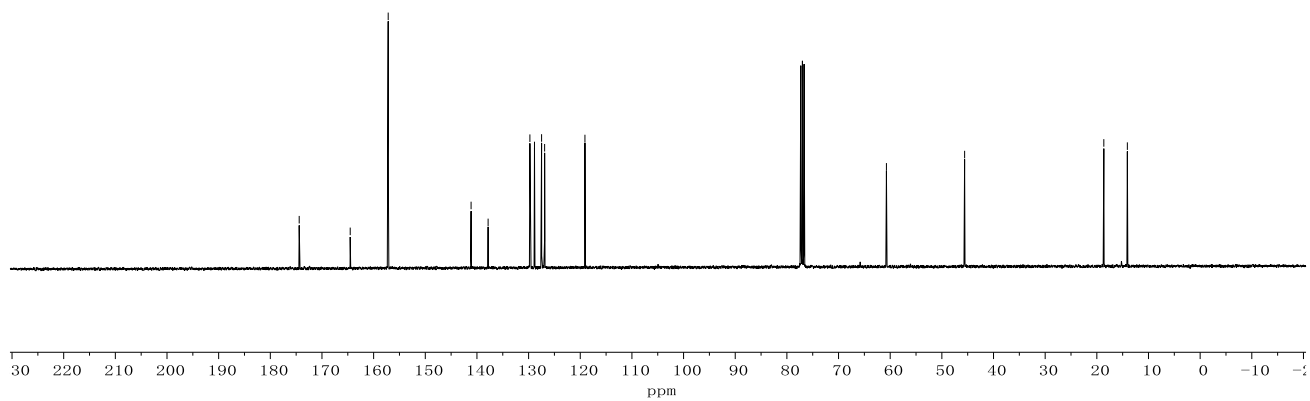




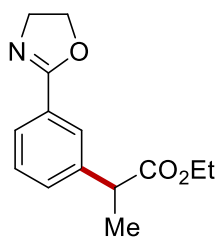
**409b**  
(400 MHz, CDCl<sub>3</sub>)



**409b**  
(100 MHz, CDCl<sub>3</sub>)

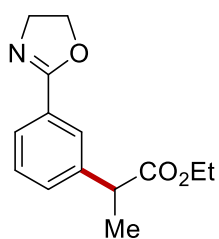
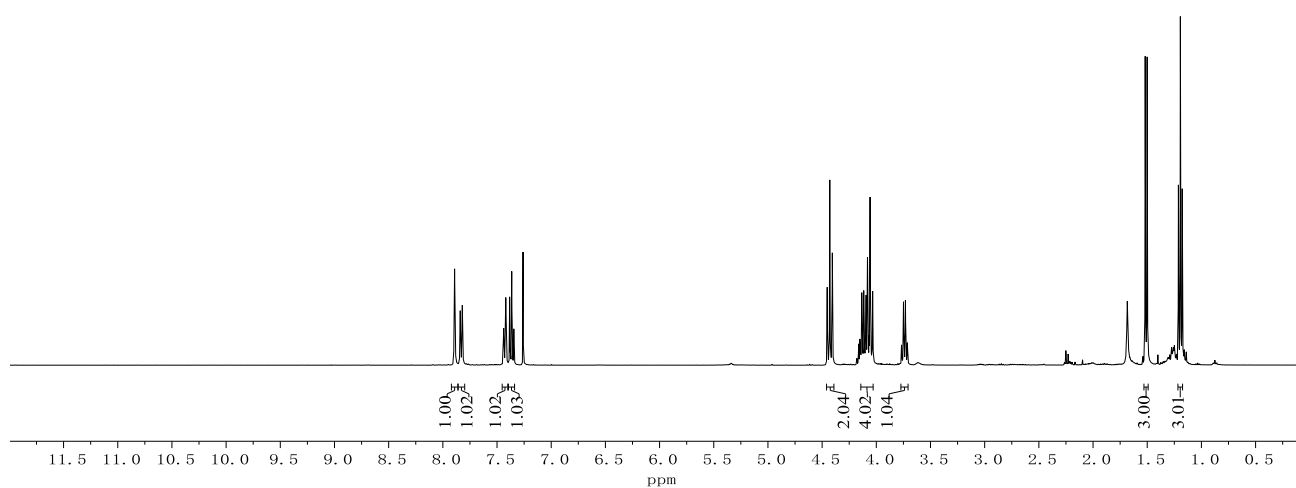


Appendix: NMR Spectra



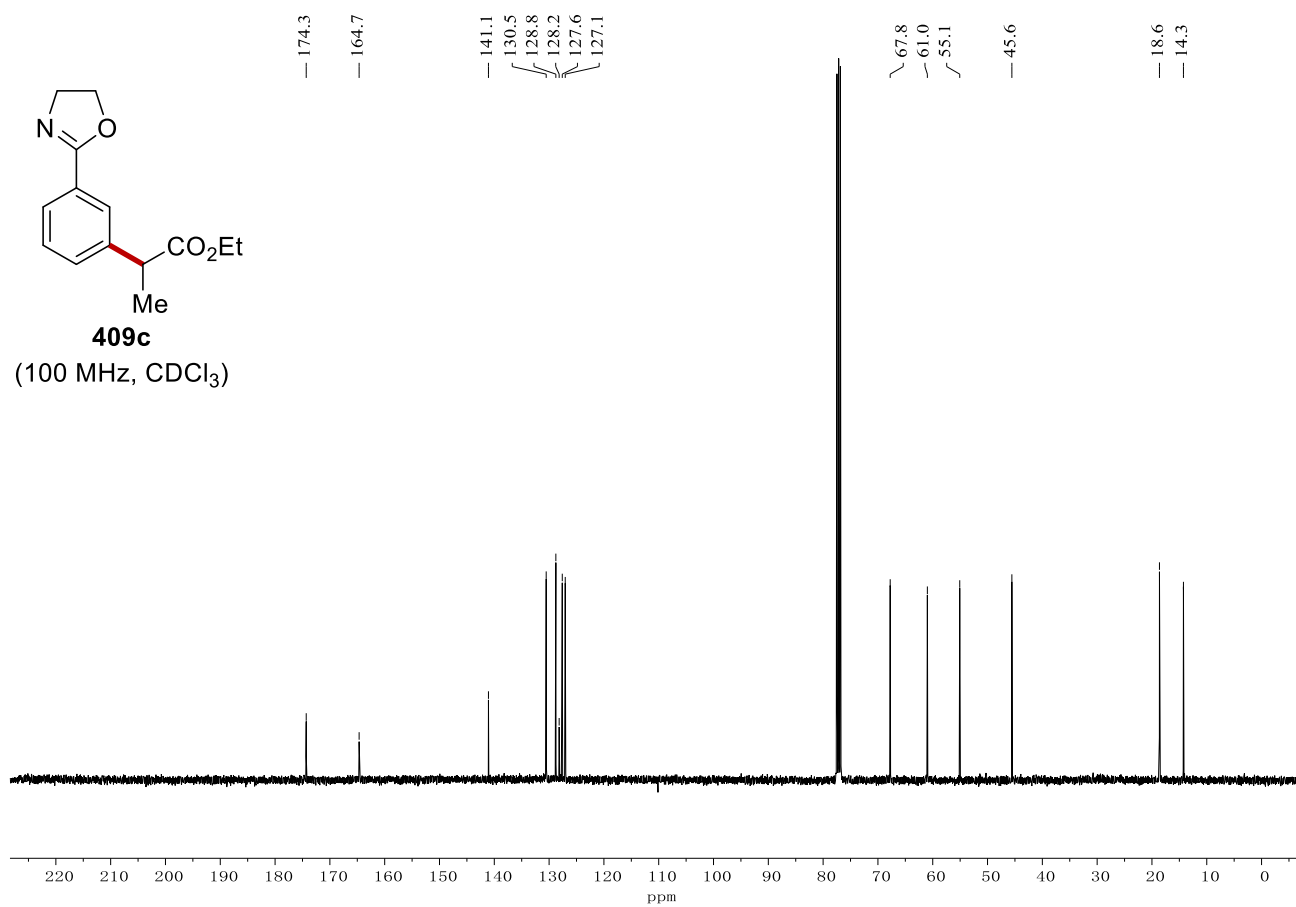
**409c**

(400 MHz, CDCl<sub>3</sub>)

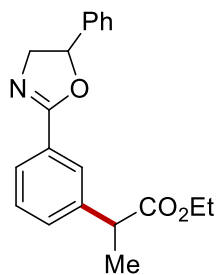


**409c**

(100 MHz, CDCl<sub>3</sub>)

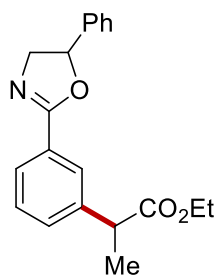
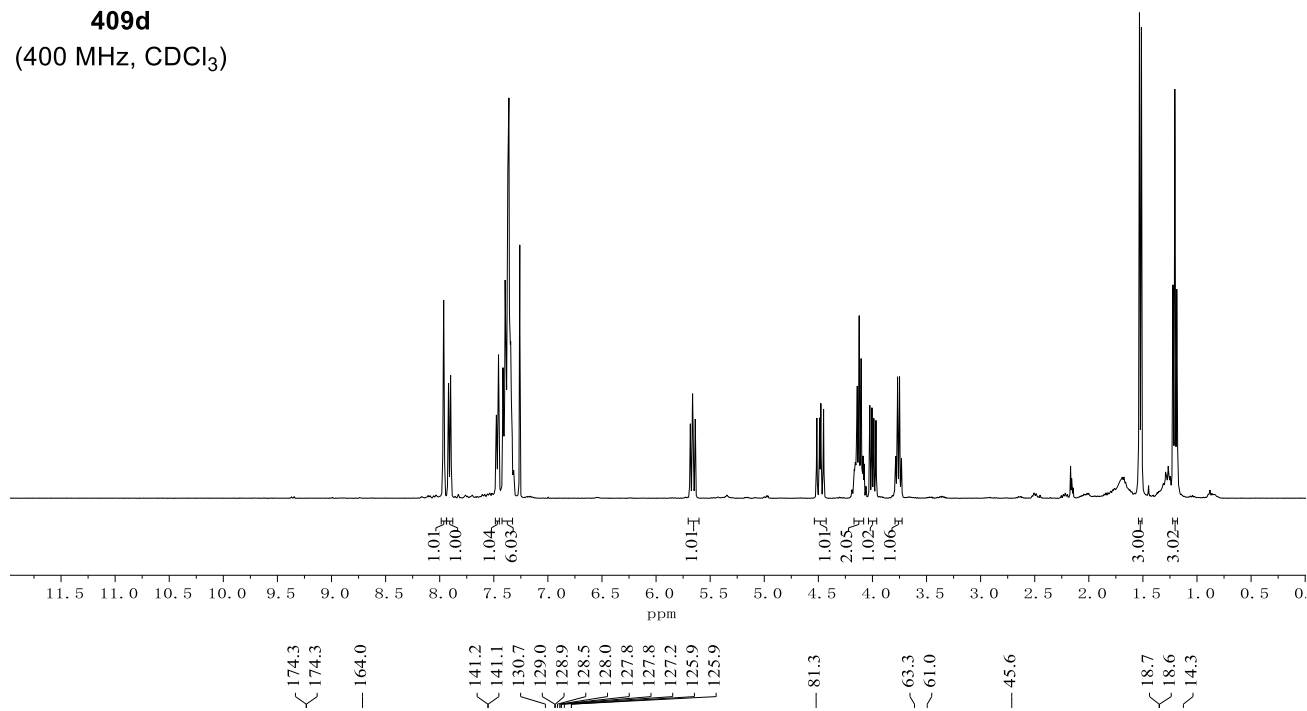


Appendix: NMR Spectra



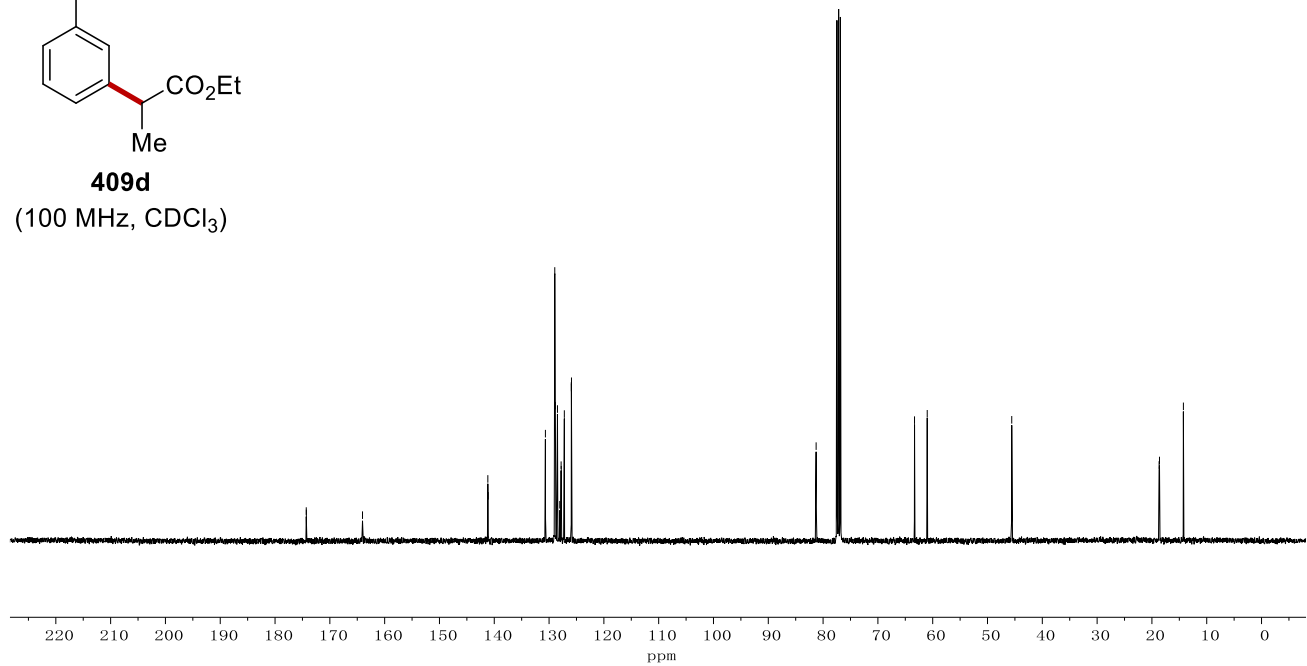
**409d**

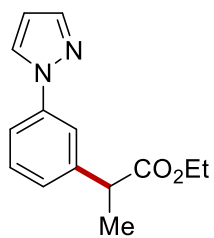
(400 MHz, CDCl<sub>3</sub>)



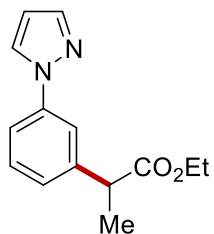
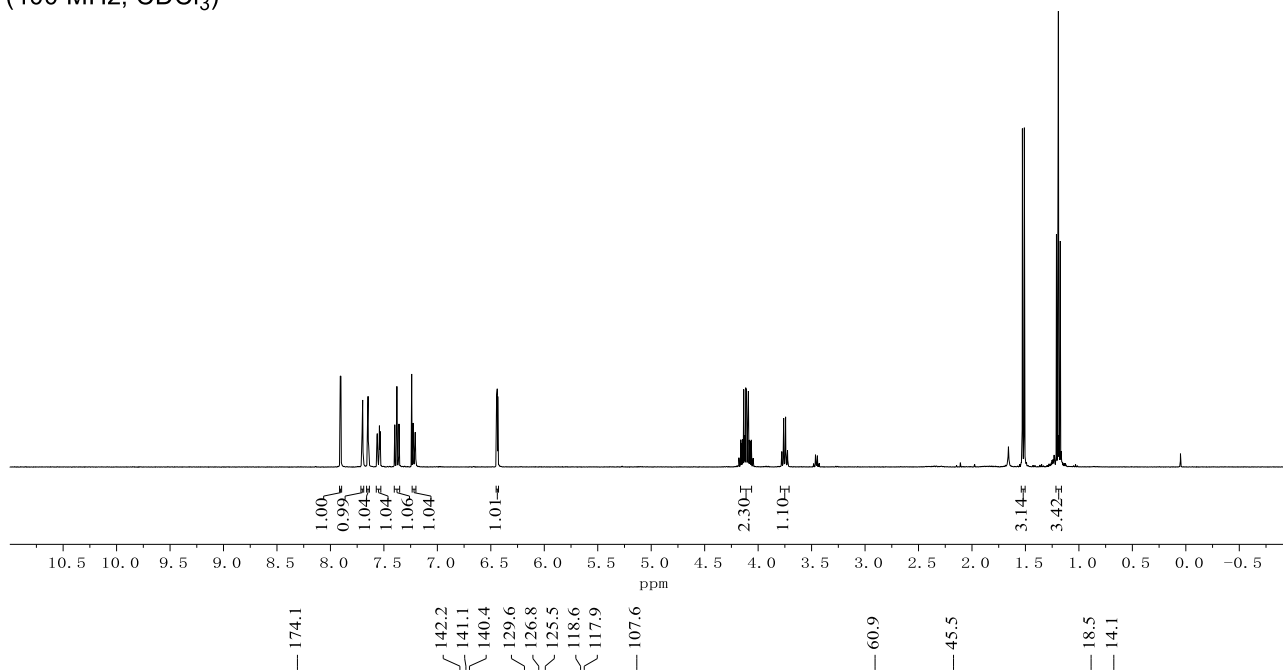
**409d**

(100 MHz, CDCl<sub>3</sub>)

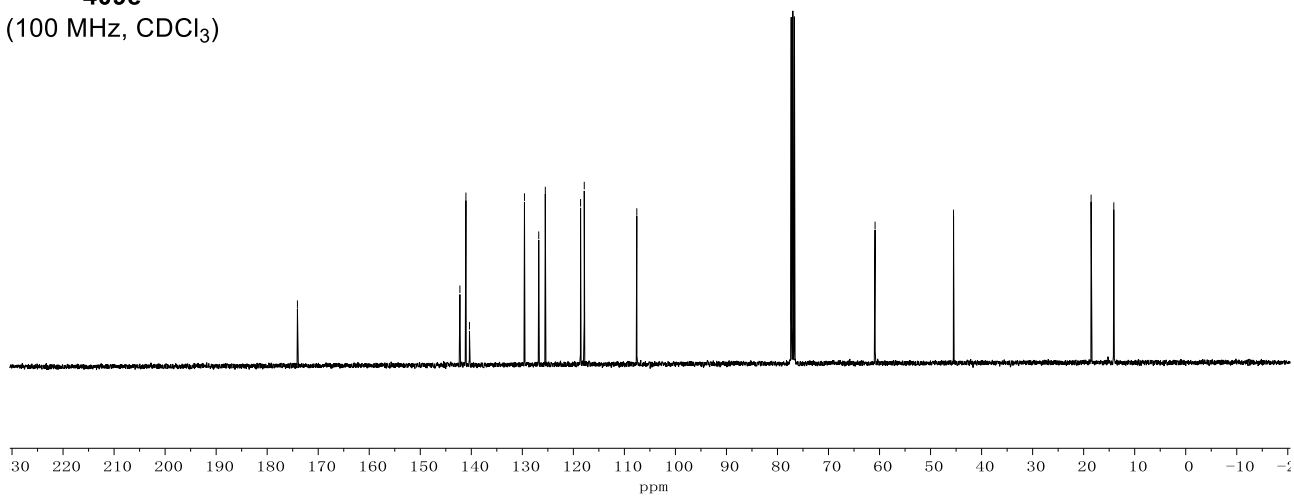




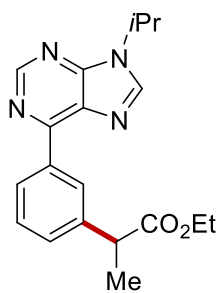
**409e**  
(400 MHz, CDCl<sub>3</sub>)



**409e**  
(100 MHz, CDCl<sub>3</sub>)

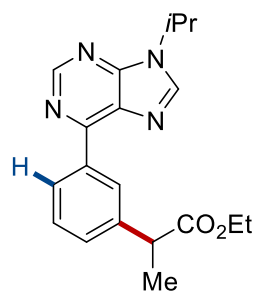
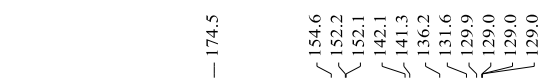
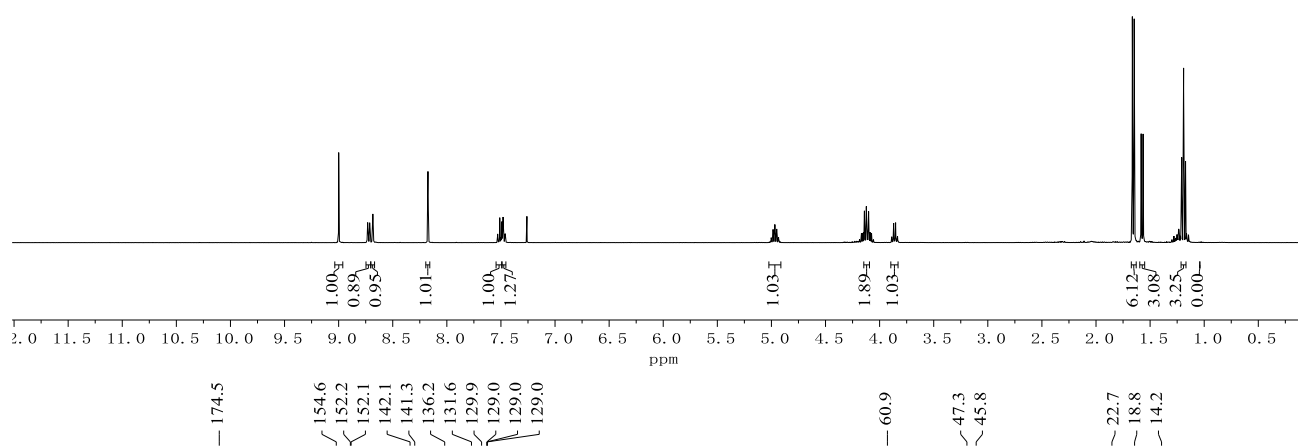


Appendix: NMR Spectra



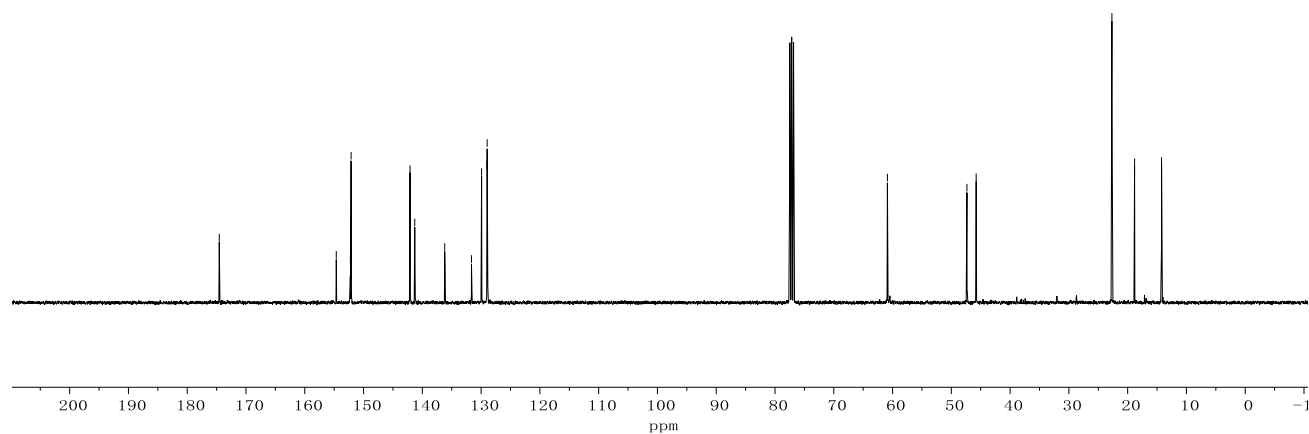
**409f**

(400 MHz, CDCl<sub>3</sub>)



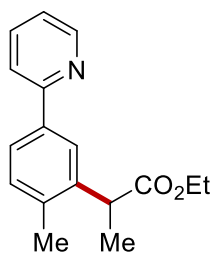
**409f**

(100 MHz, CDCl<sub>3</sub>)

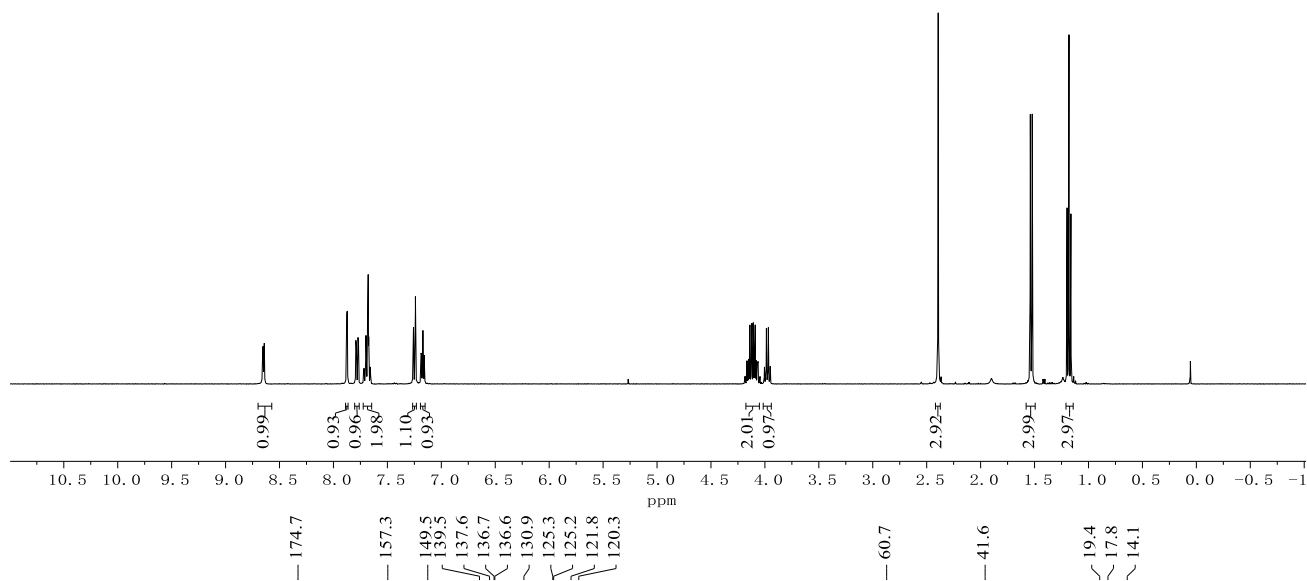




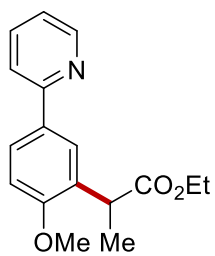
Appendix: NMR Spectra



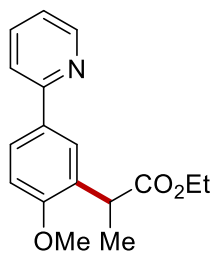
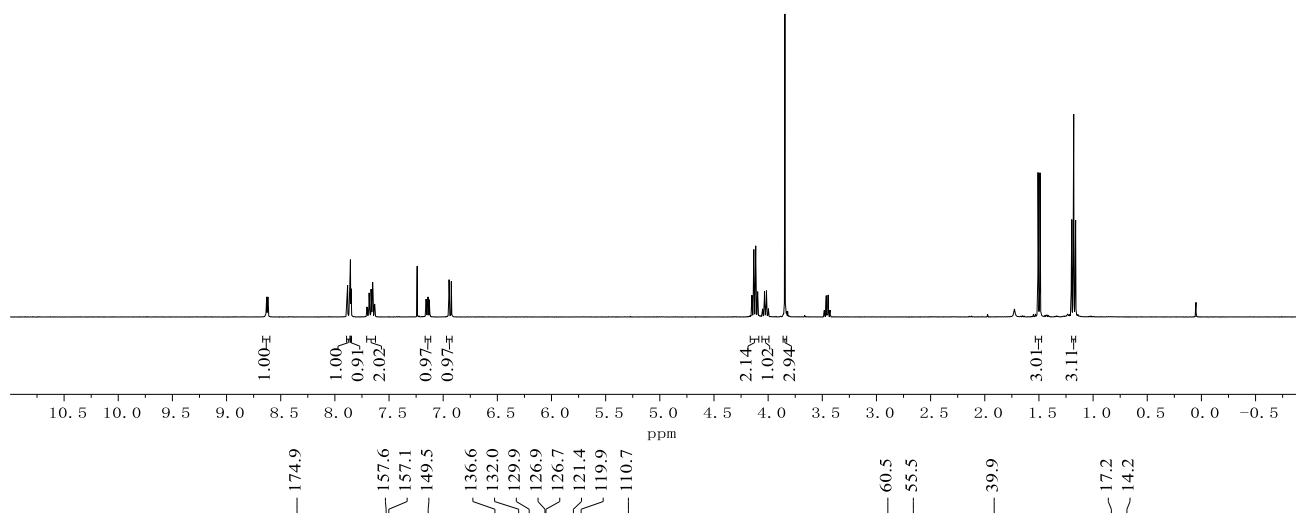
**409g**  
(400 MHz, CDCl<sub>3</sub>)



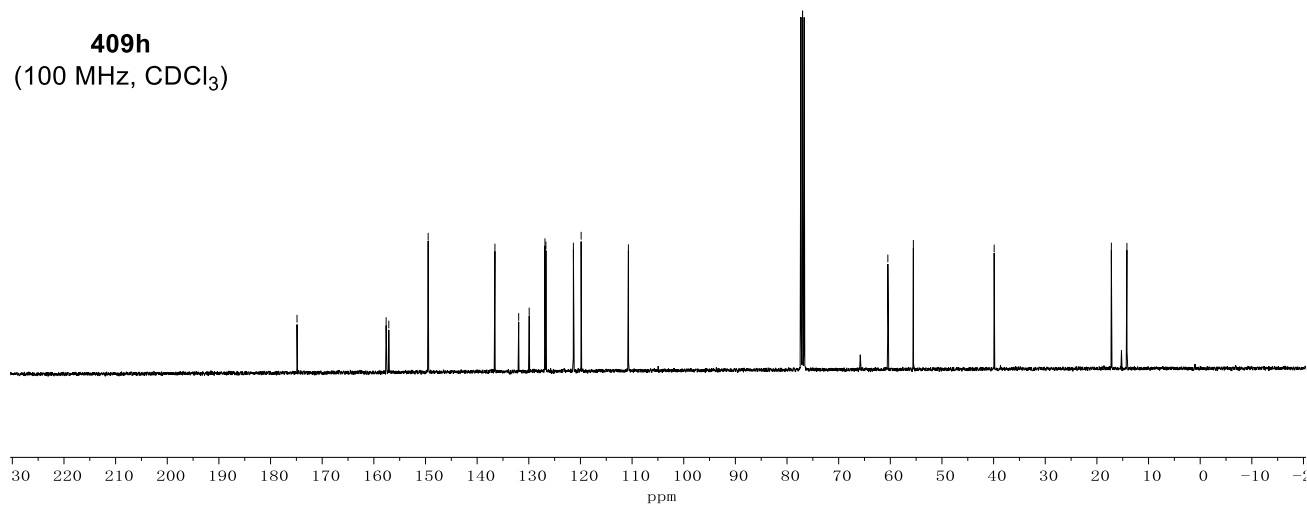
Appendix: NMR Spectra



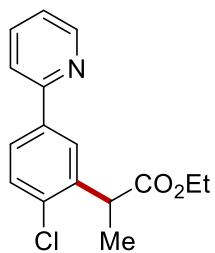
**409h**  
(400 MHz, CDCl<sub>3</sub>)



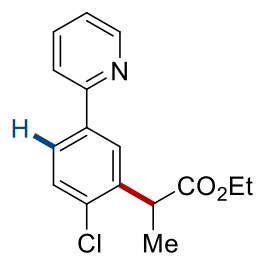
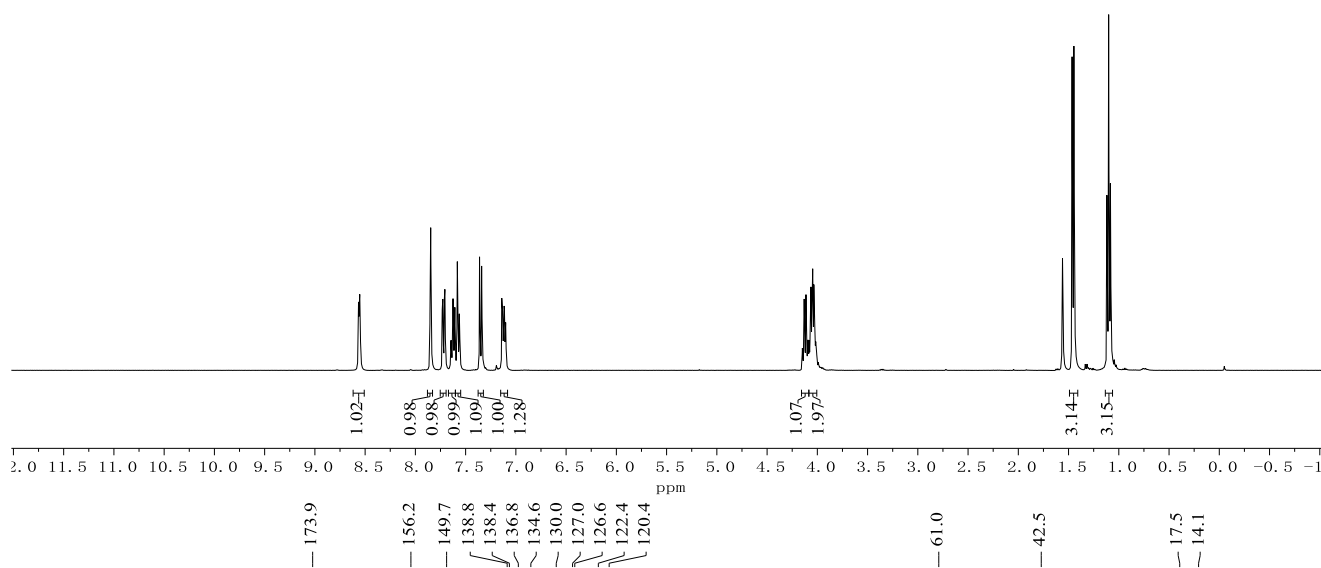
**409h**  
(100 MHz, CDCl<sub>3</sub>)



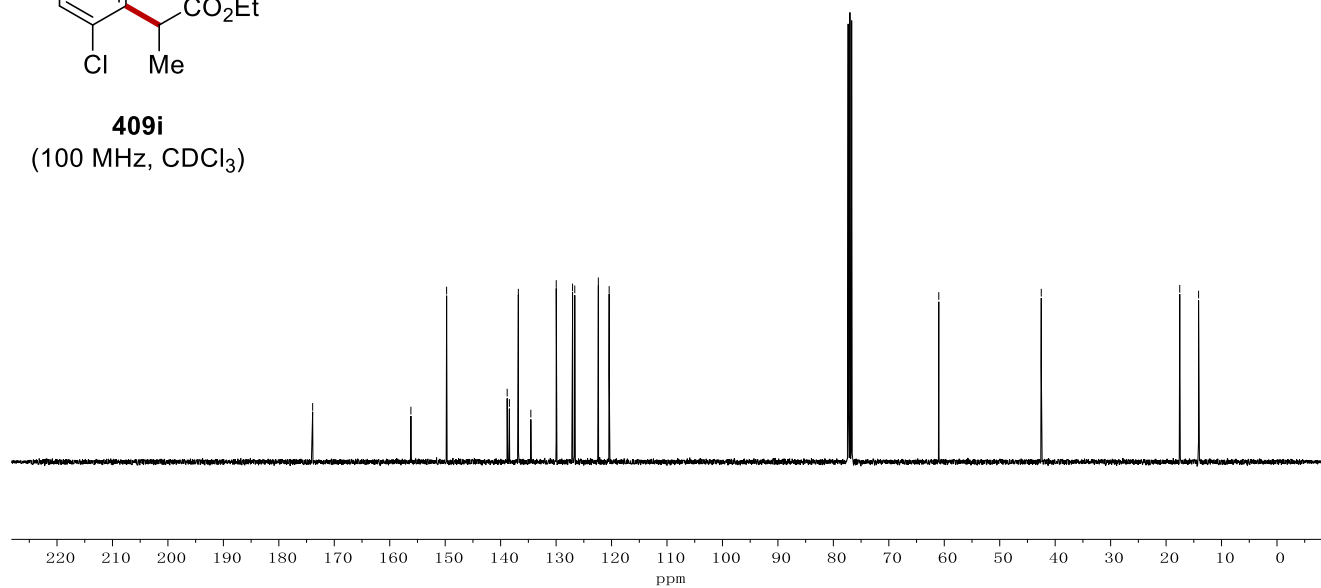
Appendix: NMR Spectra

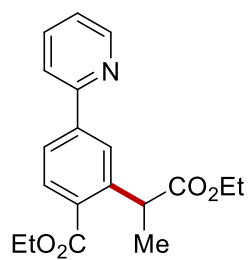


**409i**  
(400 MHz, CDCl<sub>3</sub>)

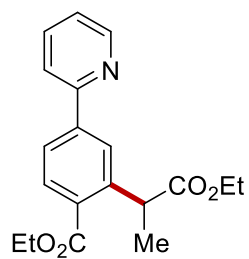
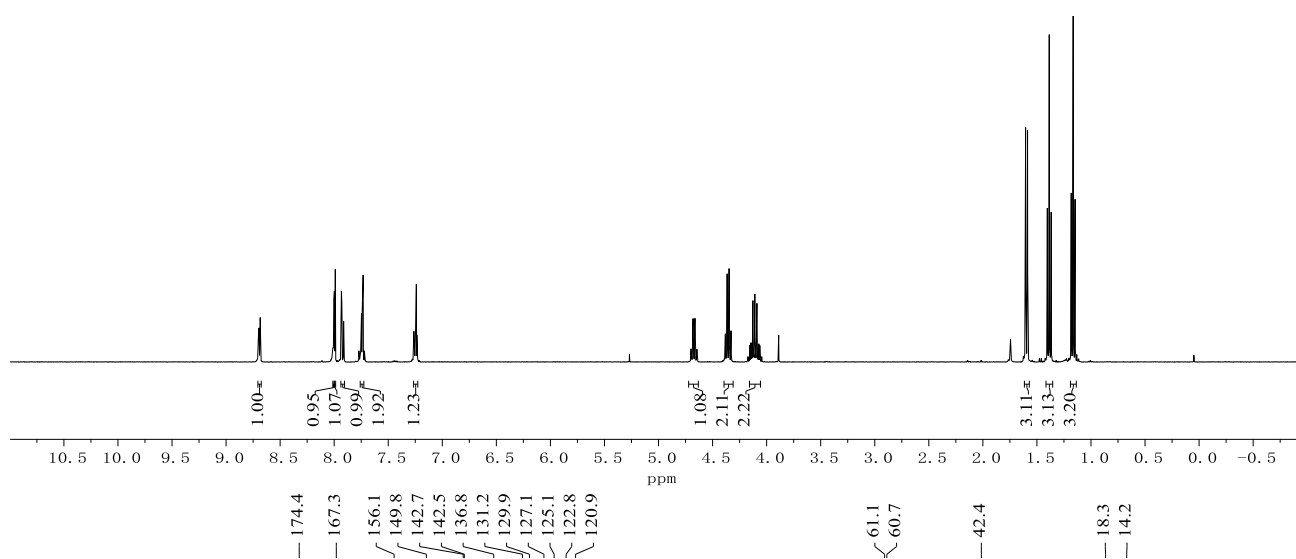


**409i**  
(100 MHz, CDCl<sub>3</sub>)

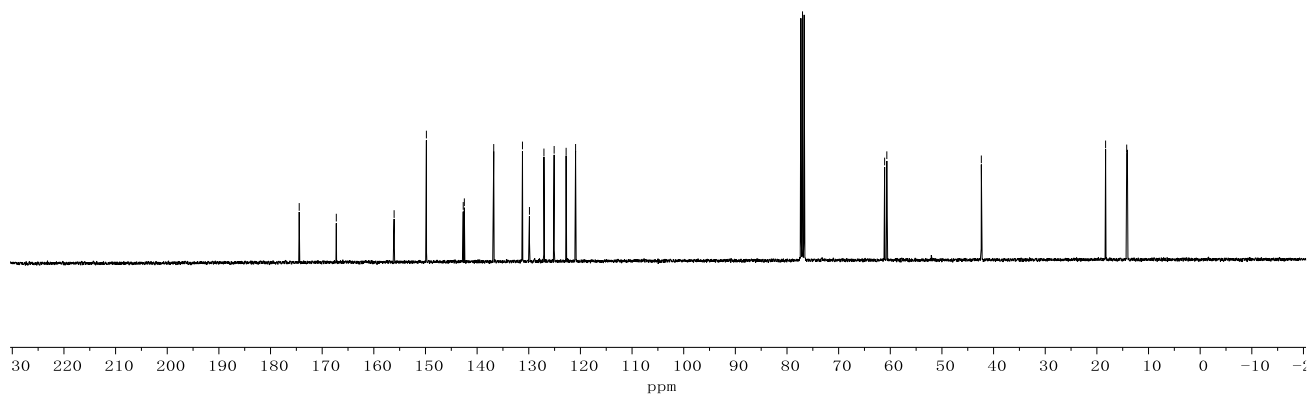




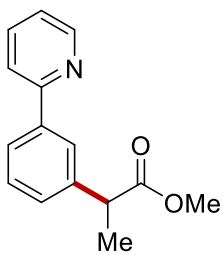
**409j**  
(400 MHz, CDCl<sub>3</sub>)



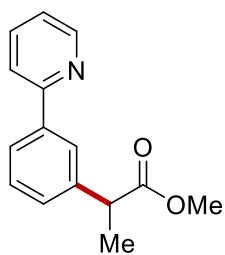
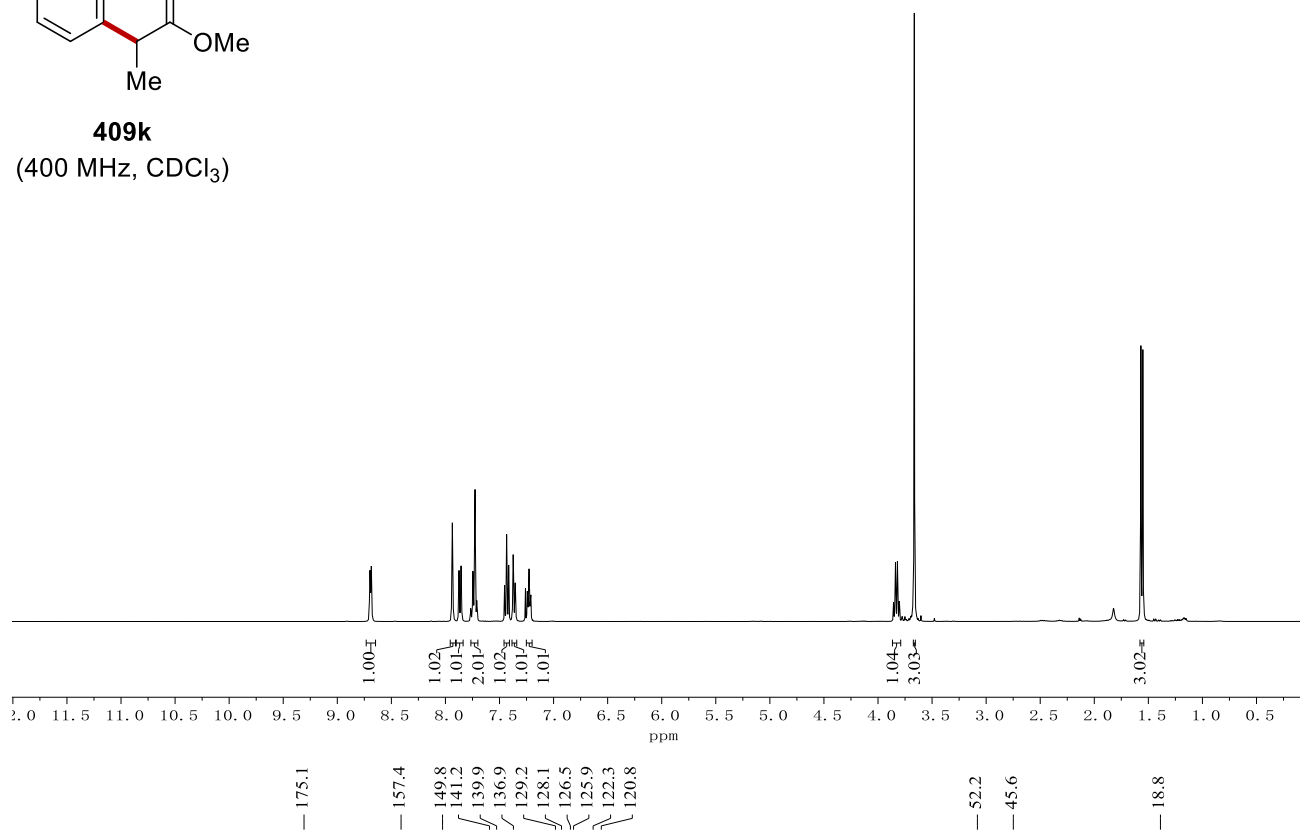
**409j**  
(100 MHz, CDCl<sub>3</sub>)



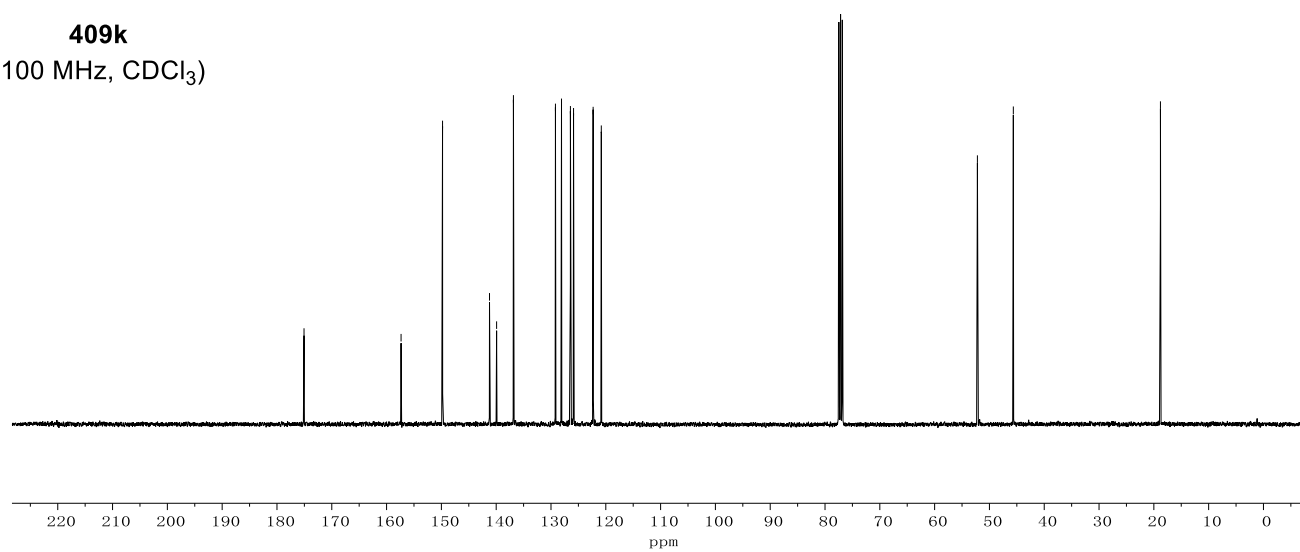
Appendix: NMR Spectra



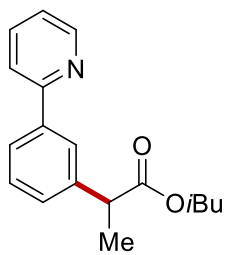
**409k**  
(400 MHz, CDCl<sub>3</sub>)



**409k**  
(100 MHz, CDCl<sub>3</sub>)

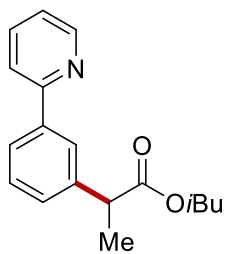
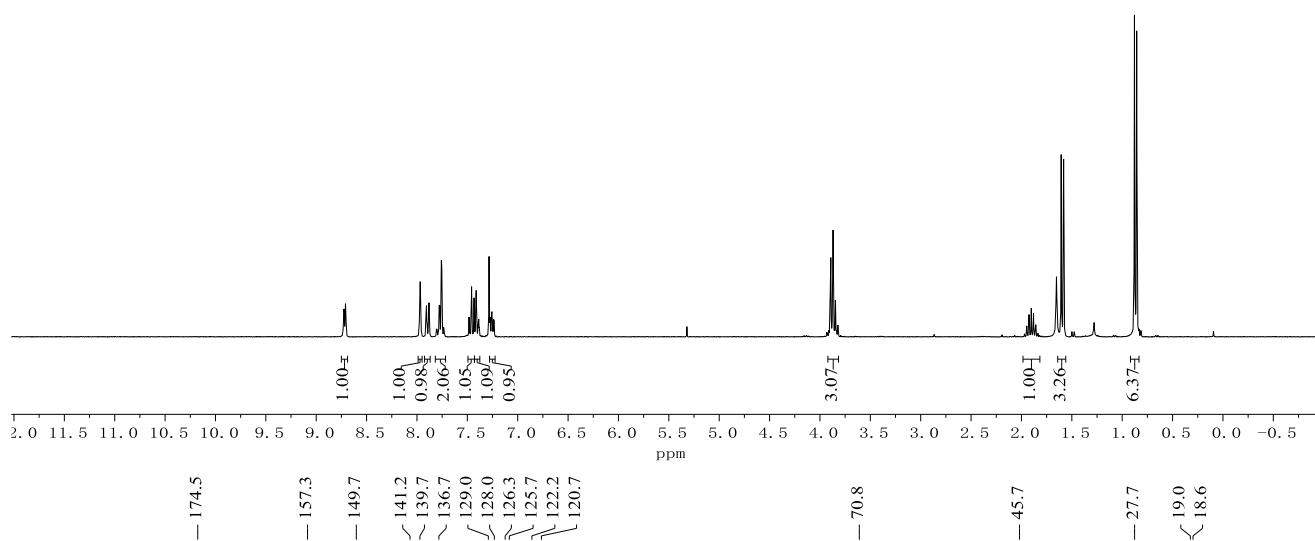


Appendix: NMR Spectra



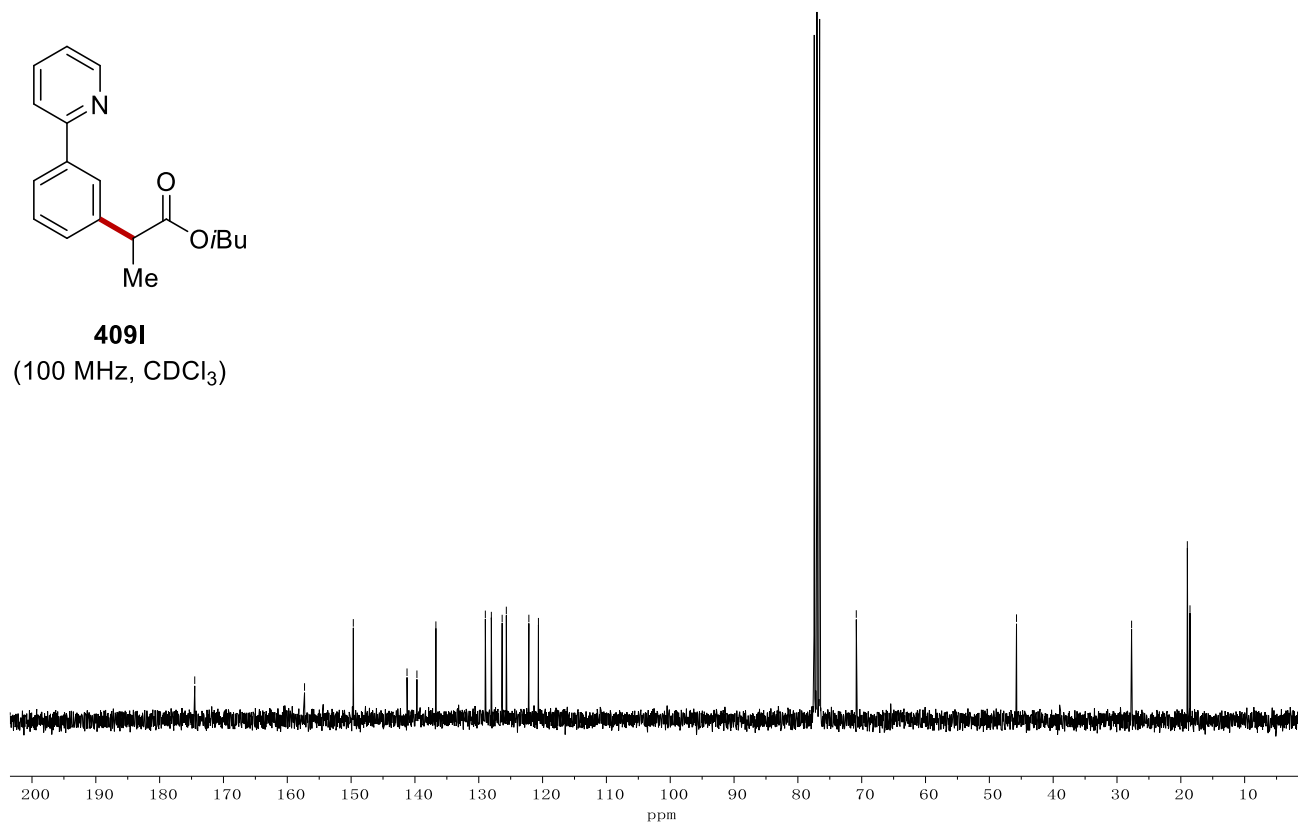
**409I**

(400 MHz, CDCl<sub>3</sub>)

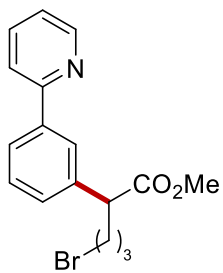


**409I**

(100 MHz, CDCl<sub>3</sub>)

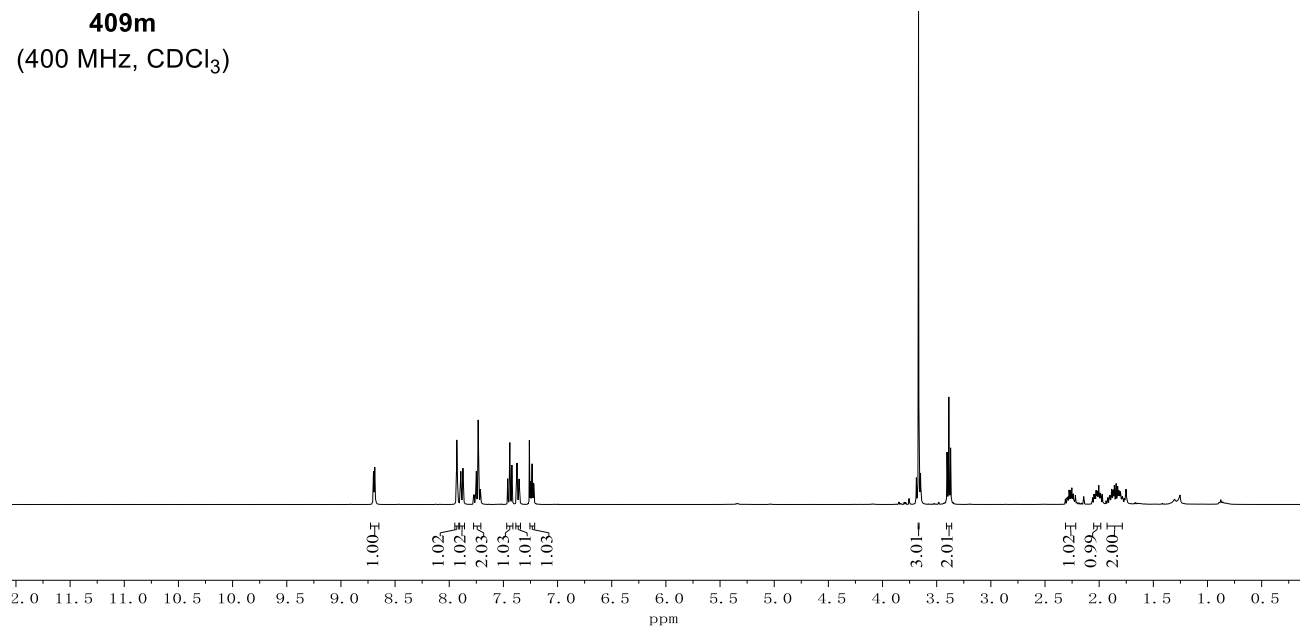


Appendix: NMR Spectra



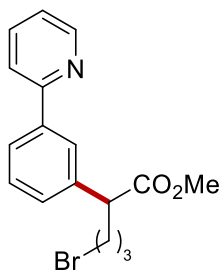
**409m**

(400 MHz, CDCl<sub>3</sub>)



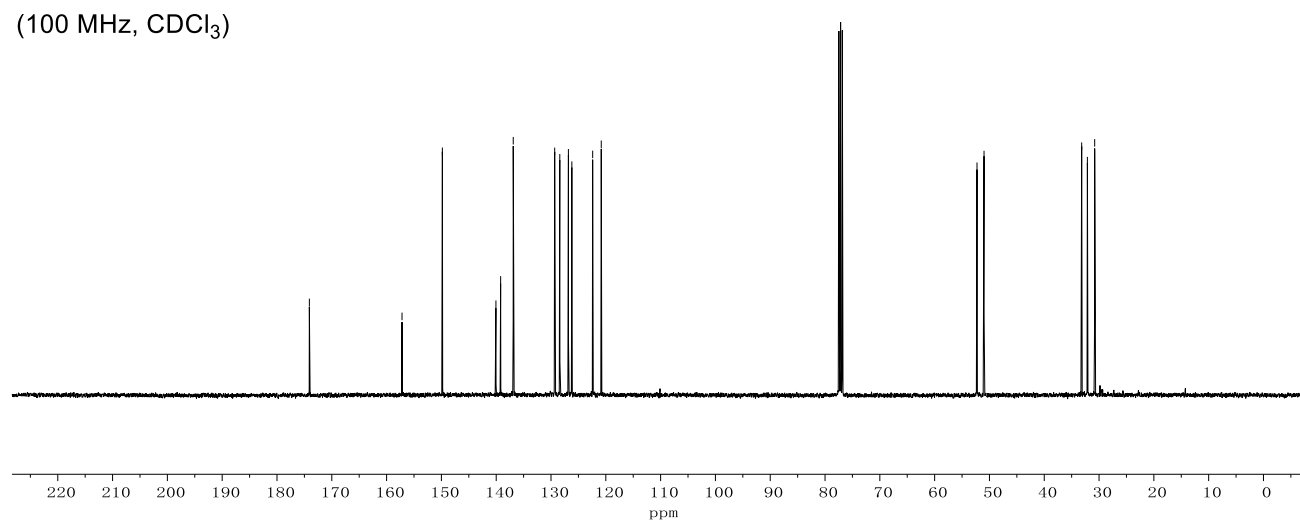
174.1  
157.2  
149.8  
140.1  
139.2  
136.9  
129.3  
128.4  
126.8  
126.2  
122.4  
120.8

52.3  
51.0  
33.2  
32.1  
30.8

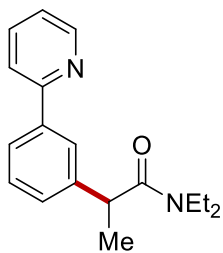


**409m**

(100 MHz, CDCl<sub>3</sub>)

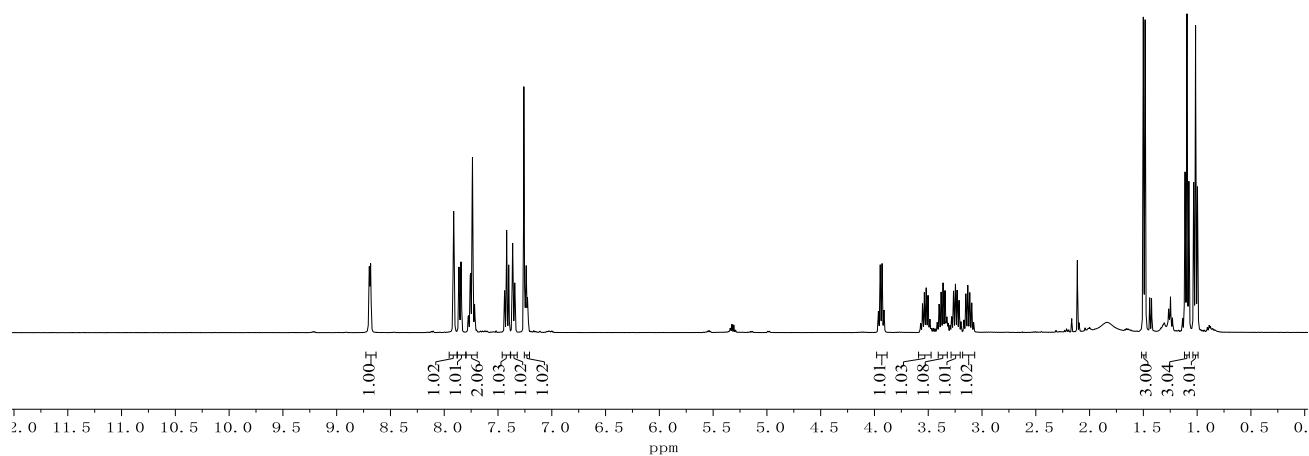


Appendix: NMR Spectra

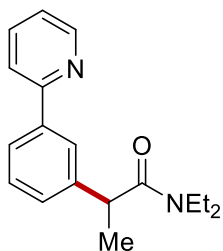


**409n**

(400 MHz, CDCl<sub>3</sub>)

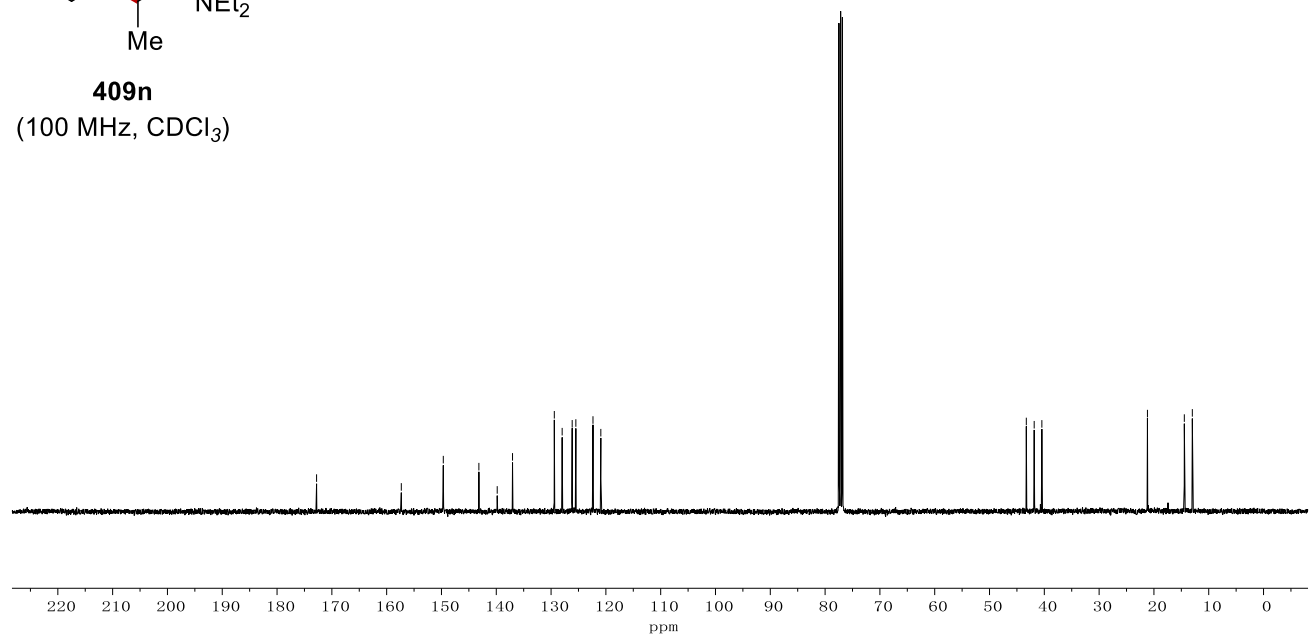


172.8, 157.3, 149.7, 143.2, 139.8, 137.0, 129.4, 128.0, 126.1, 125.5, 122.4, 120.9, 43.3, 41.8, 40.4, 21.2, 14.5, 13.0



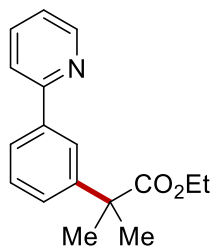
**409n**

(100 MHz, CDCl<sub>3</sub>)



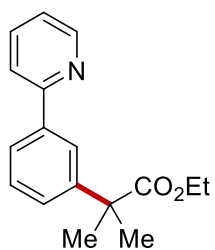
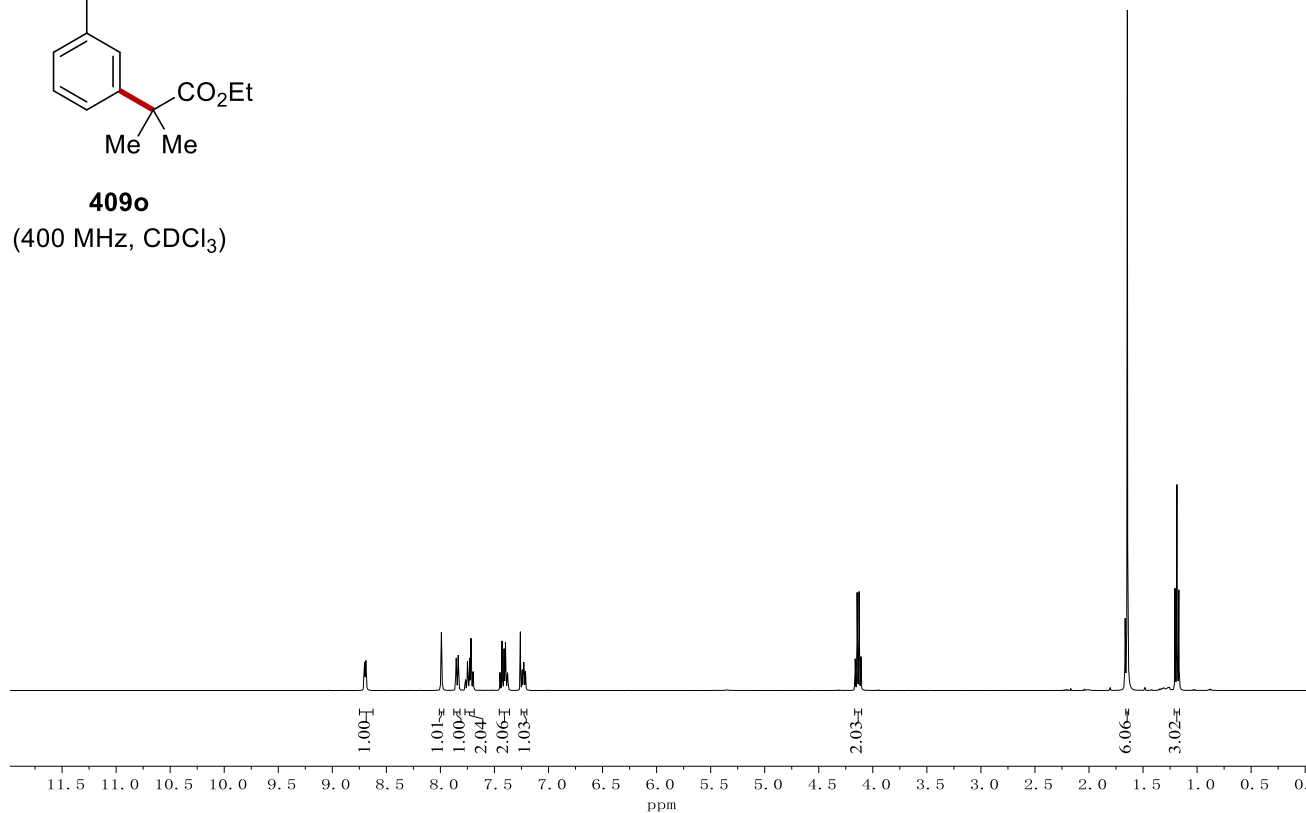


Appendix: NMR Spectra



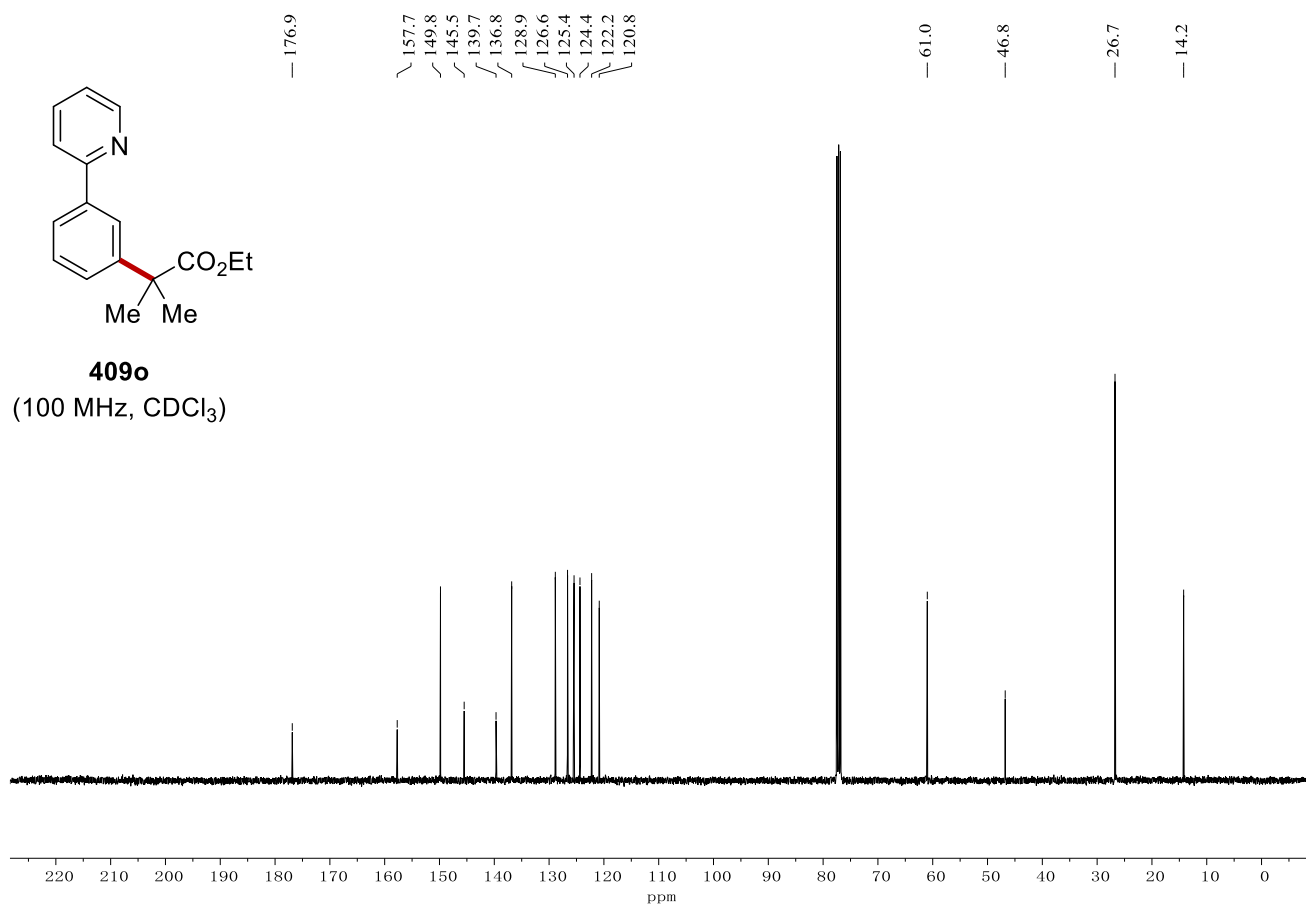
**409o**

(400 MHz, CDCl<sub>3</sub>)

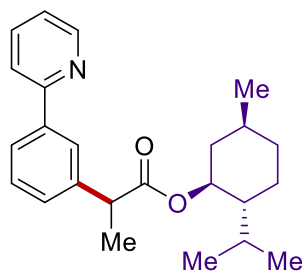


**409o**

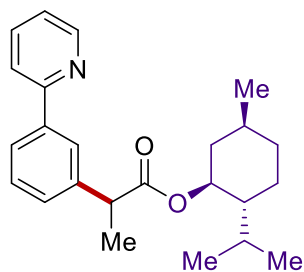
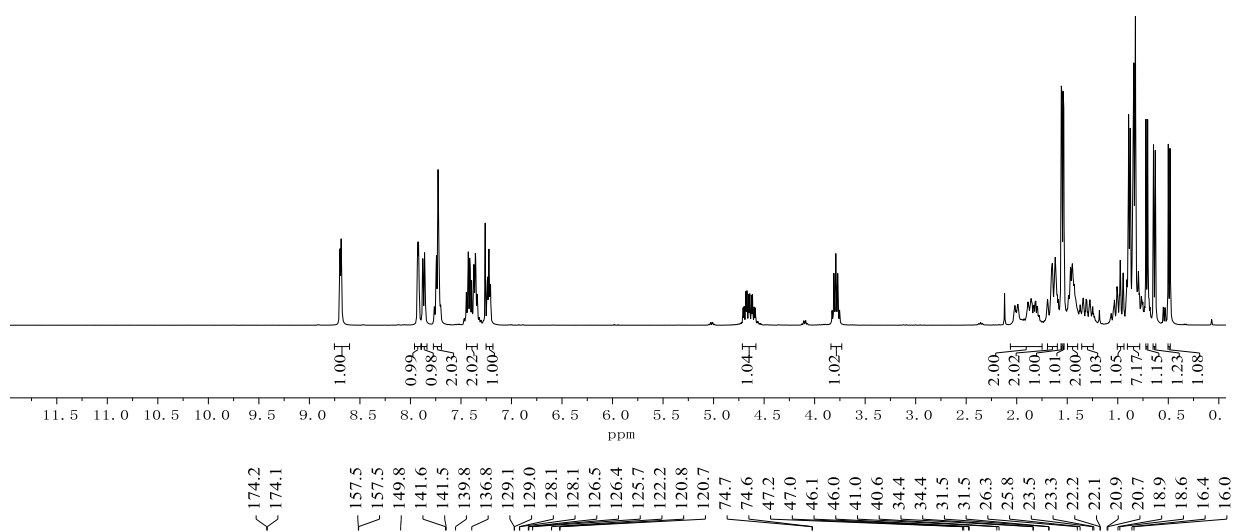
(100 MHz, CDCl<sub>3</sub>)



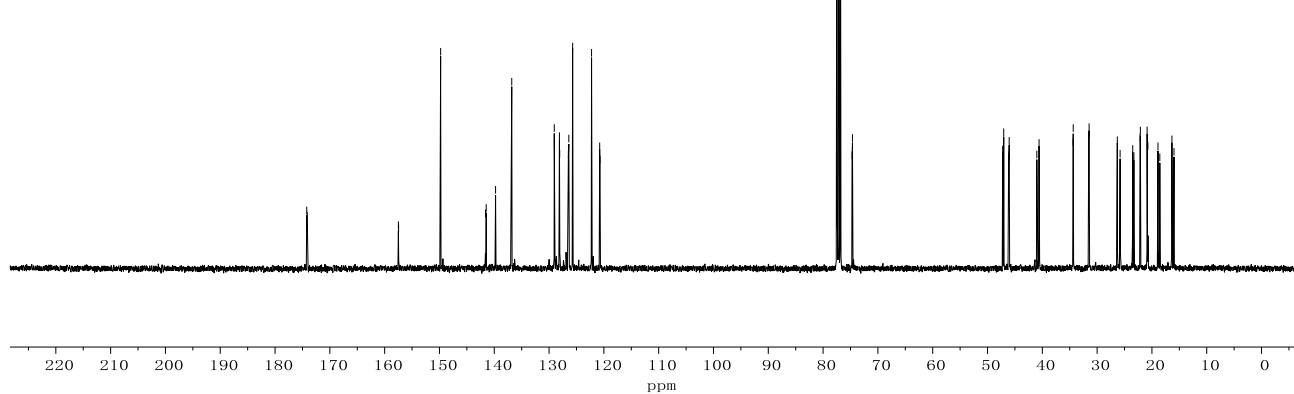
Appendix: NMR Spectra



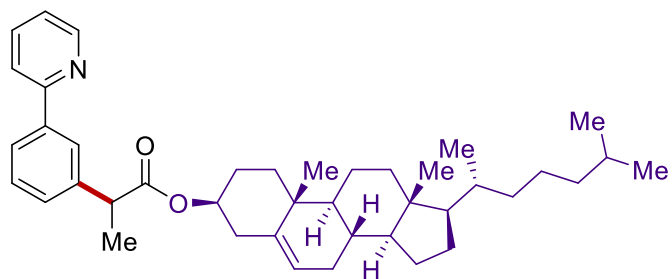
**409p**  
(400 MHz, CDCl<sub>3</sub>)



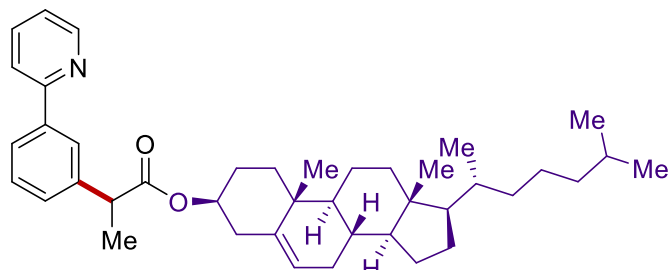
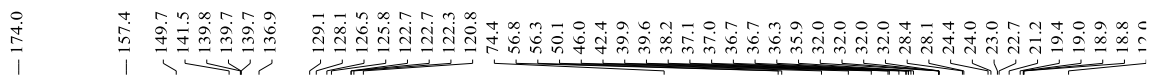
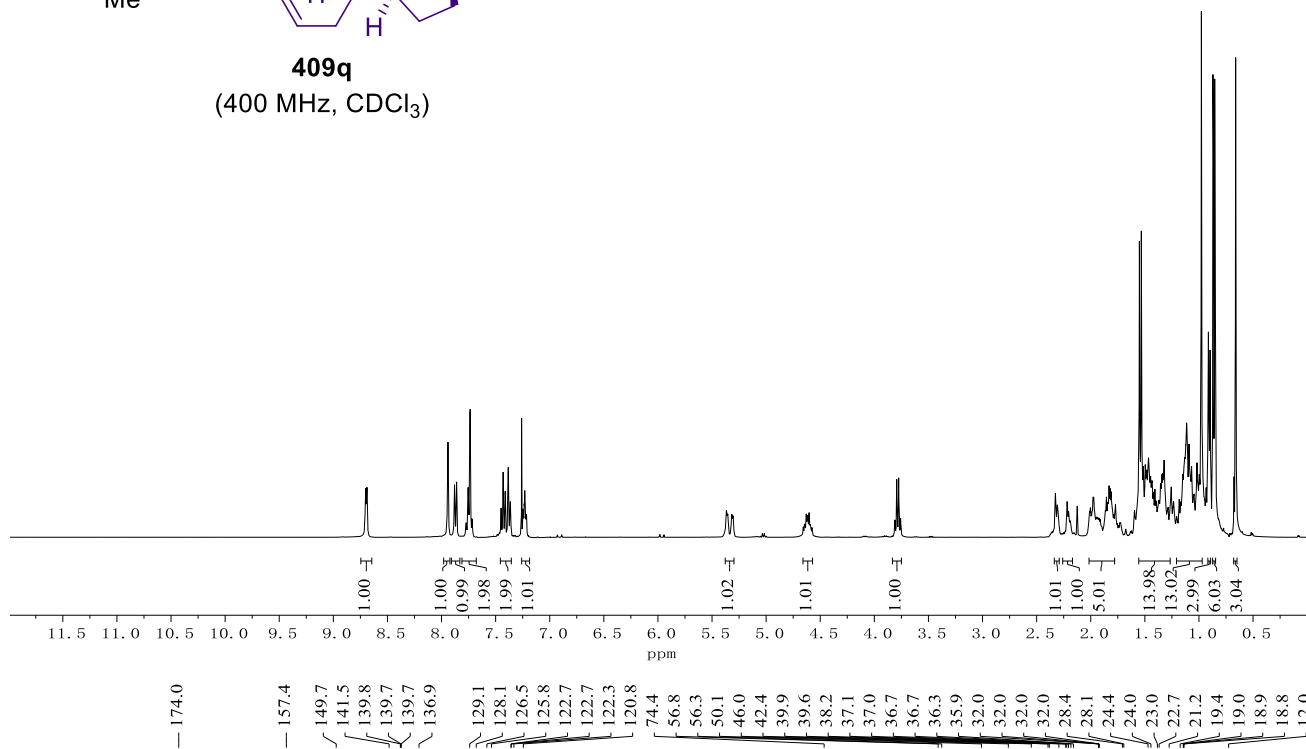
**409p**  
(100 MHz, CDCl<sub>3</sub>)



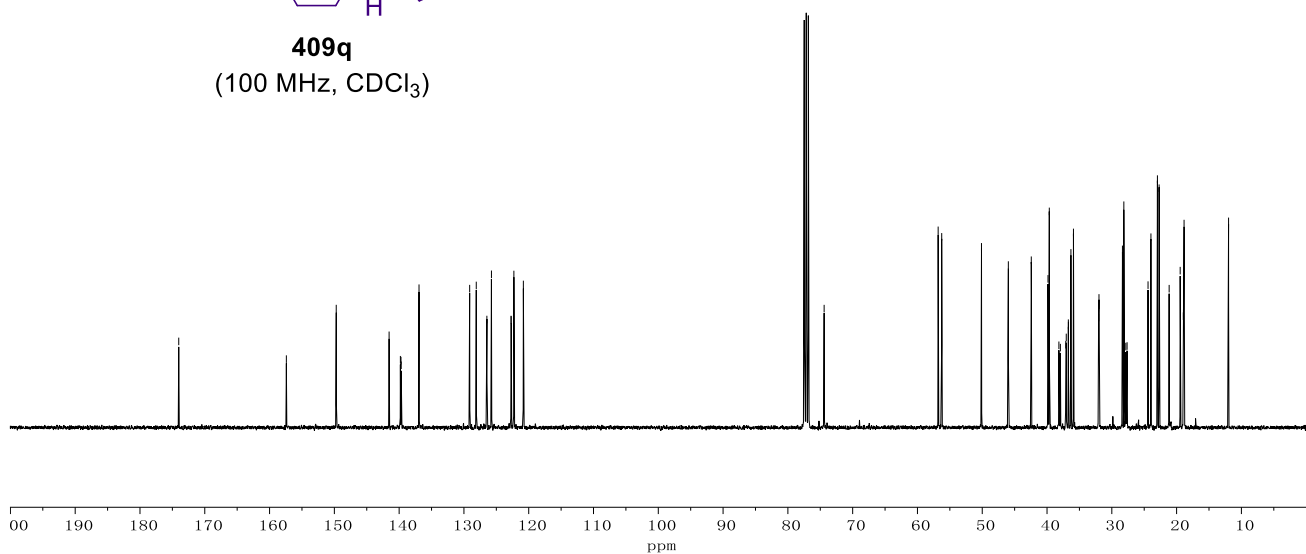
Appendix: NMR Spectra



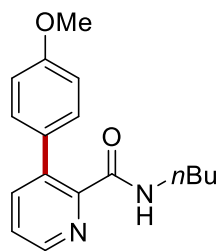
**409q**  
(400 MHz, CDCl<sub>3</sub>)



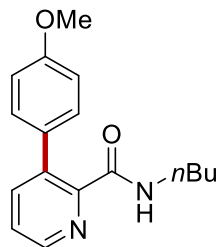
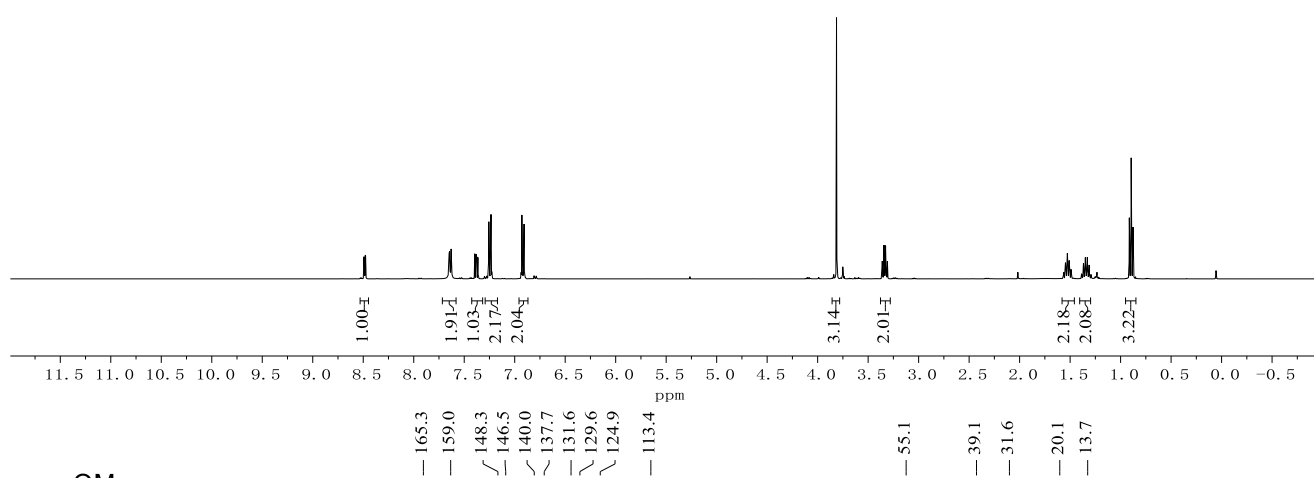
**409q**  
(100 MHz, CDCl<sub>3</sub>)



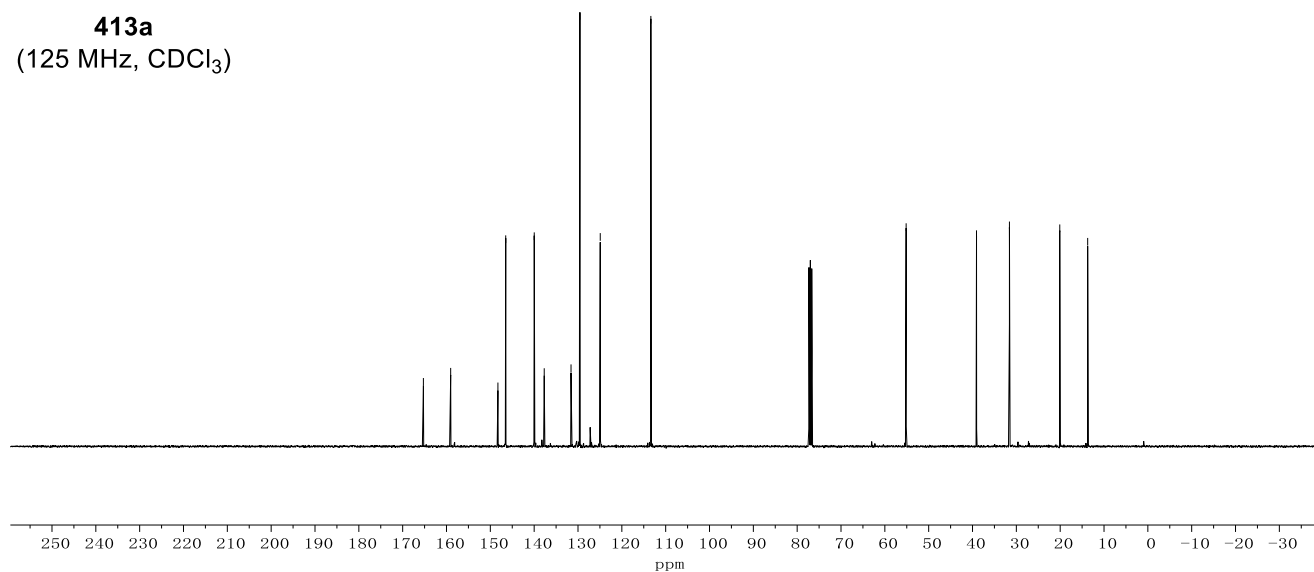
Appendix: NMR Spectra



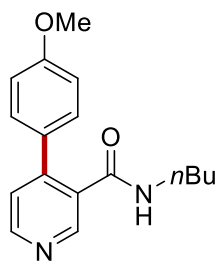
**413a**  
(400 MHz, CDCl<sub>3</sub>)



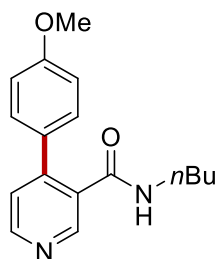
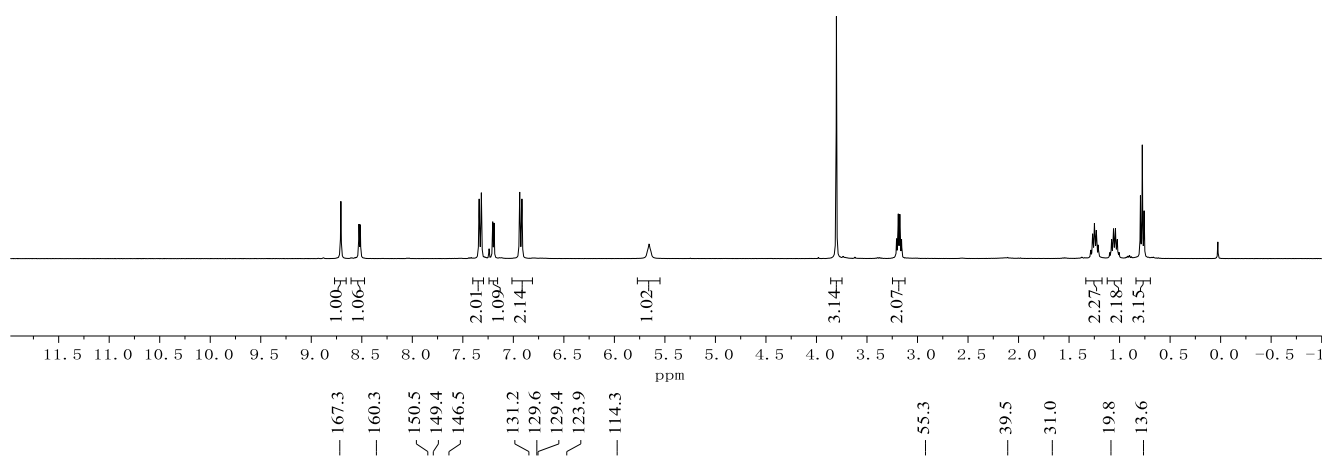
**413a**  
(125 MHz, CDCl<sub>3</sub>)



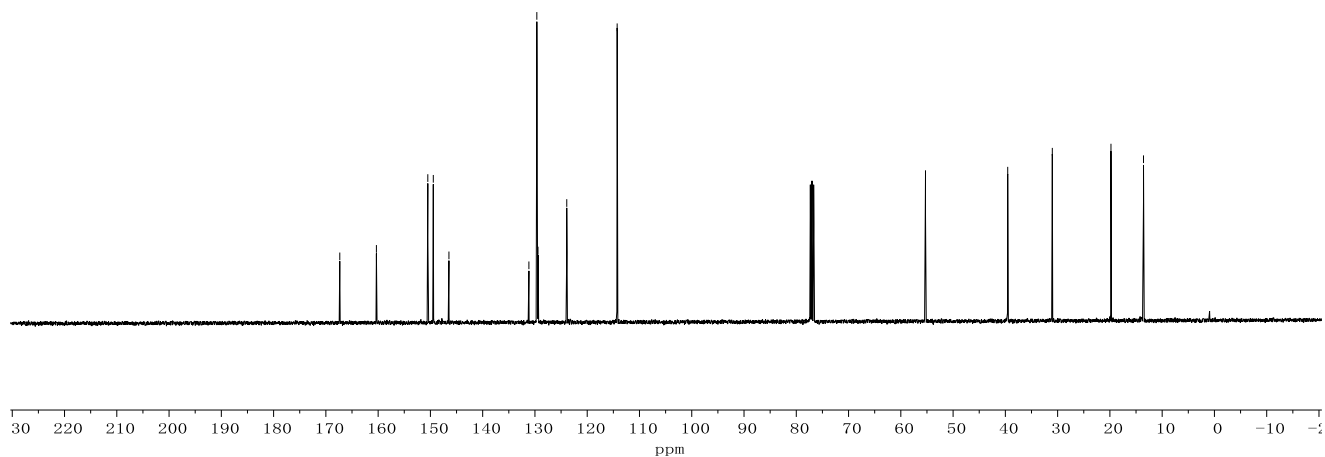
Appendix: NMR Spectra



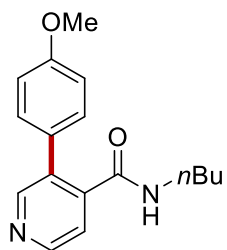
**413b**  
(400 MHz, CDCl<sub>3</sub>)



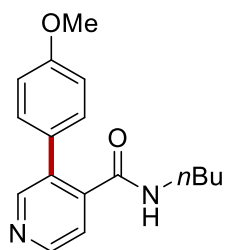
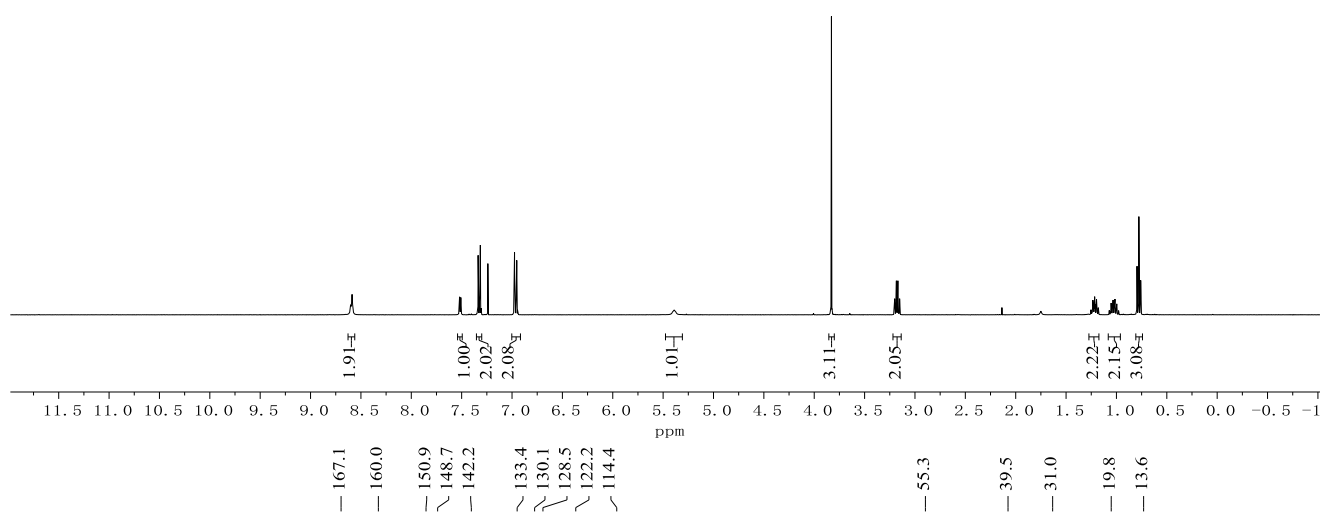
**413b**  
(100 MHz, CDCl<sub>3</sub>)



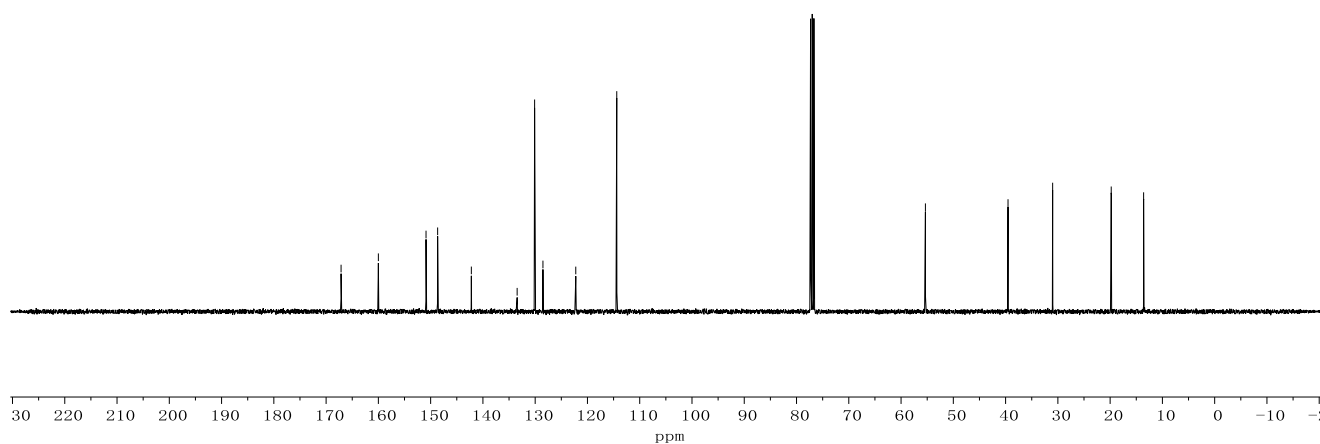
Appendix: NMR Spectra



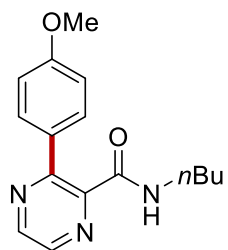
**413c**  
(400 MHz, CDCl<sub>3</sub>)



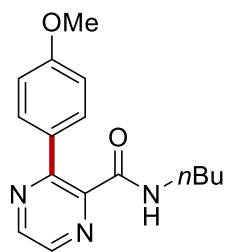
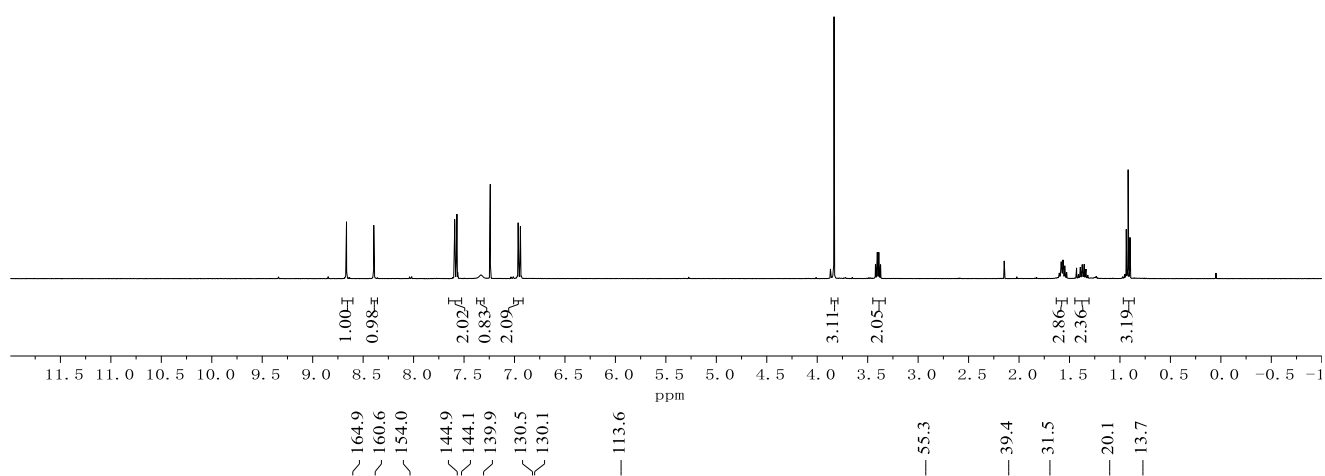
**413c**  
(100 MHz, CDCl<sub>3</sub>)



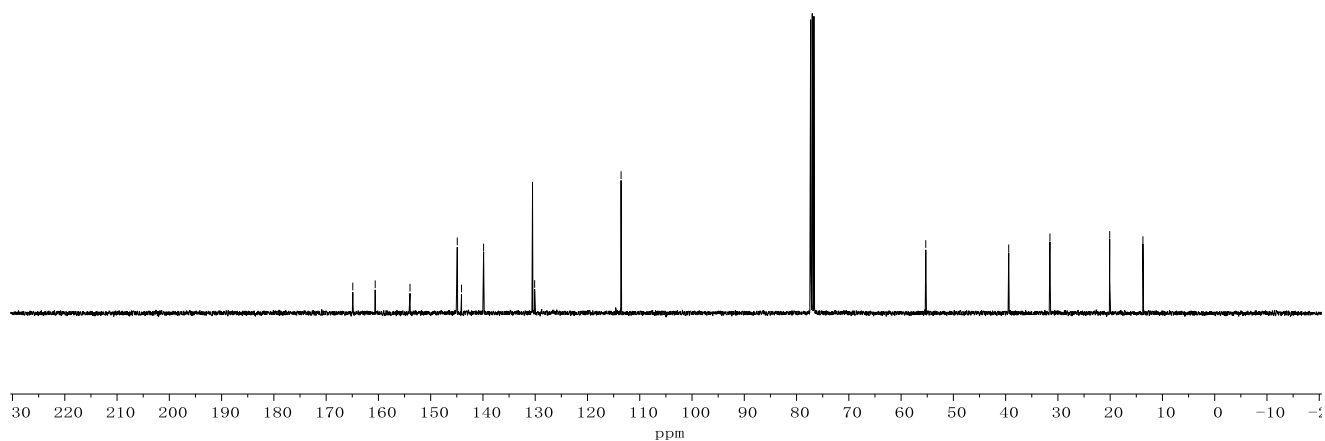
Appendix: NMR Spectra



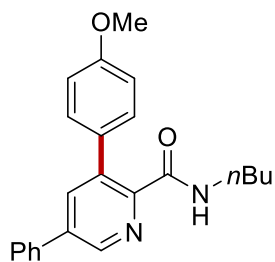
**413d**  
(400 MHz, CDCl<sub>3</sub>)



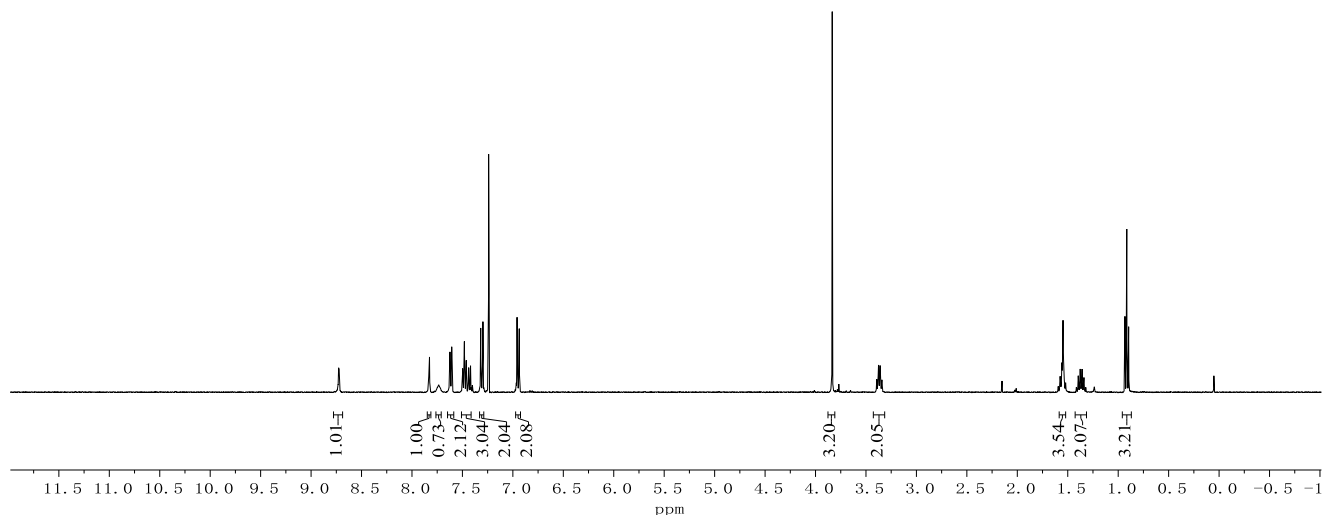
**413d**  
(100 MHz, CDCl<sub>3</sub>)



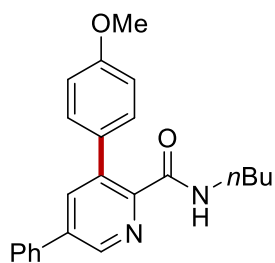
Appendix: NMR Spectra



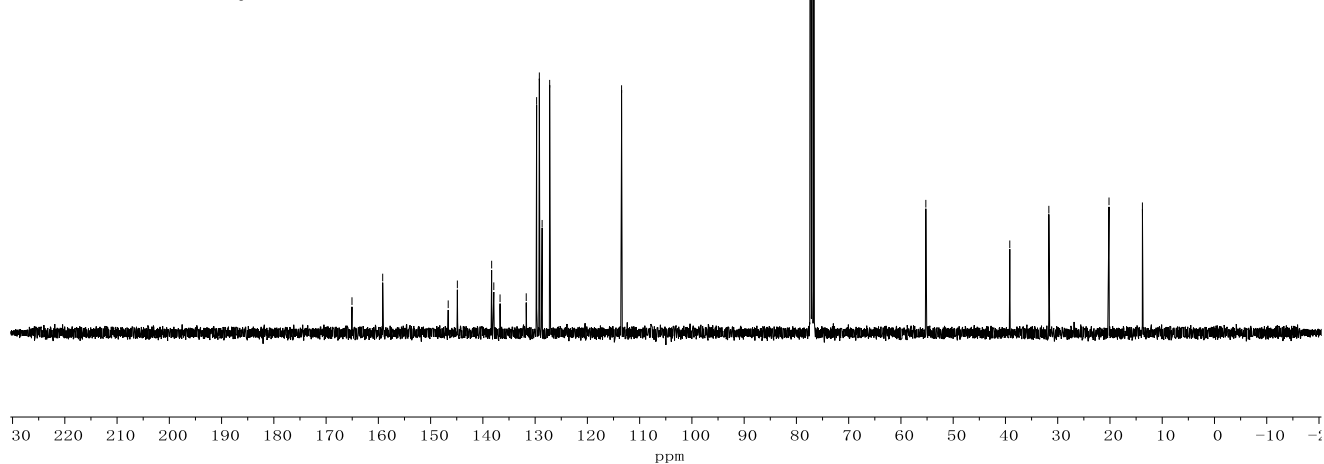
**413f**  
(400 MHz, CDCl<sub>3</sub>)



165.0  
159.2  
146.6  
144.9  
138.3  
137.9  
136.7  
131.7  
129.7  
129.2  
128.7  
127.2  
113.5



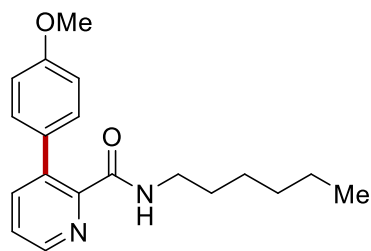
**413f**  
(100 MHz, CDCl<sub>3</sub>)



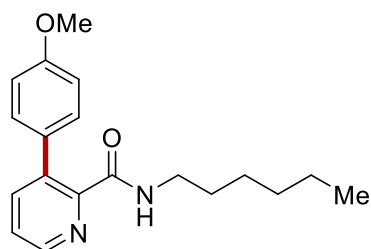
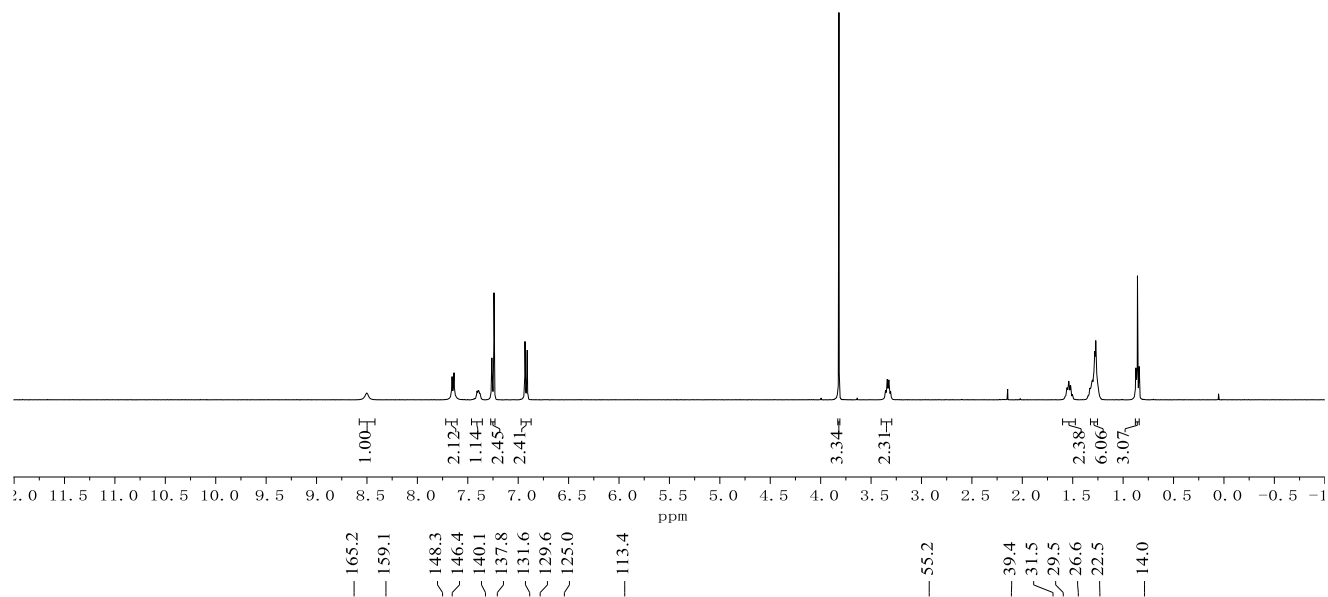
55.2  
39.2  
31.7  
20.2  
13.8



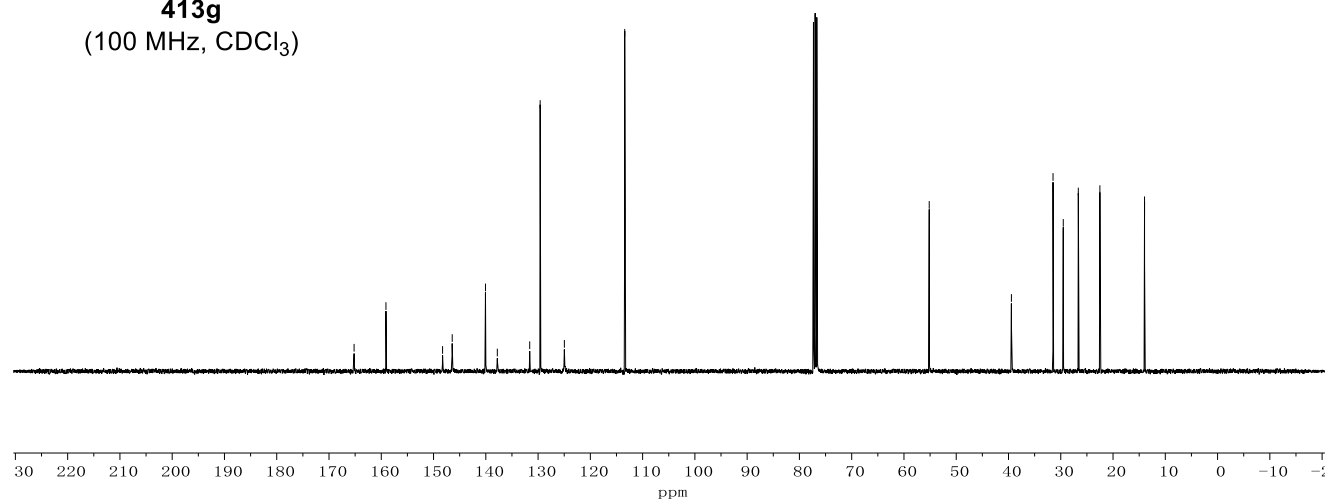
Appendix: NMR Spectra



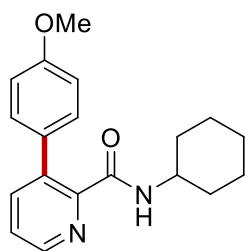
**413g**  
(400 MHz, CDCl<sub>3</sub>)



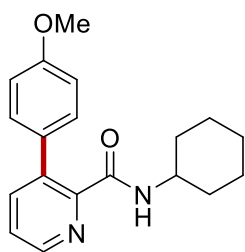
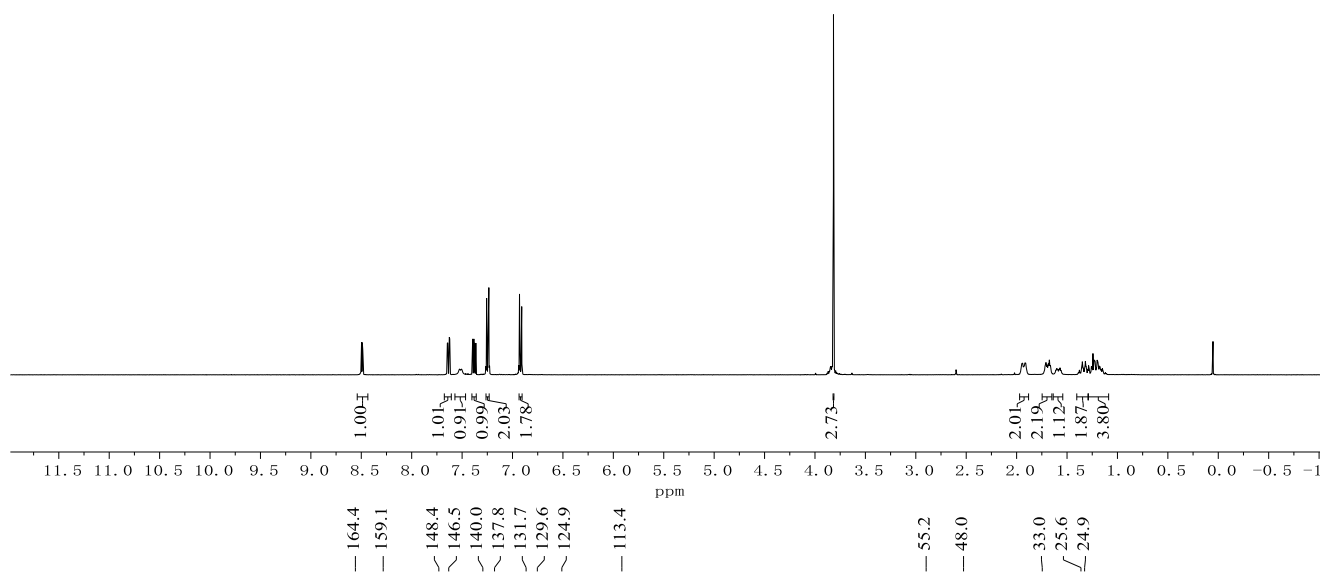
**413g**  
(100 MHz, CDCl<sub>3</sub>)



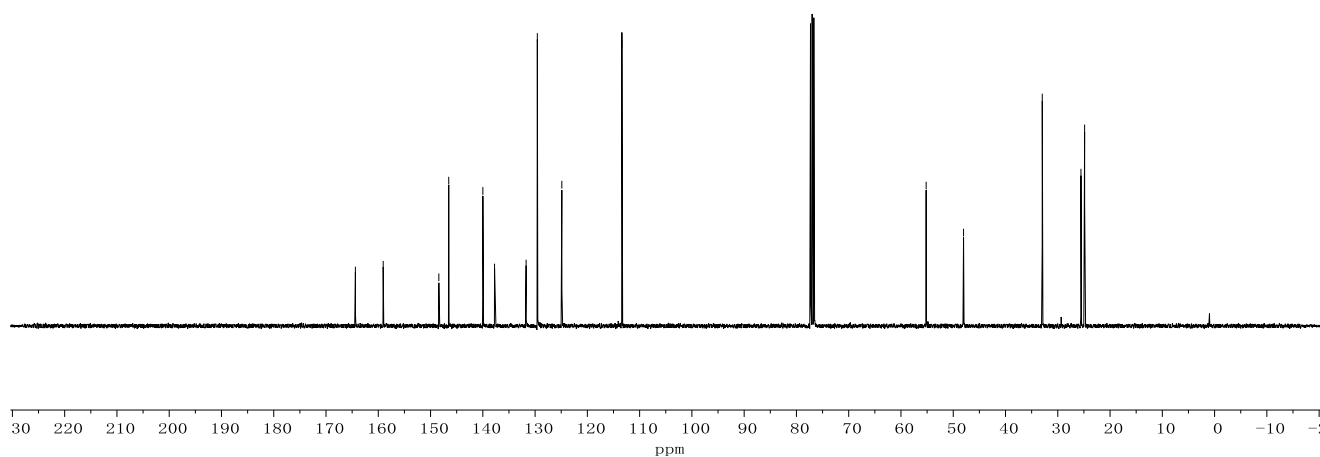
Appendix: NMR Spectra

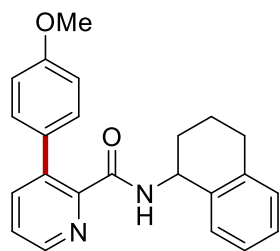


**413h**  
(400 MHz, CDCl<sub>3</sub>)

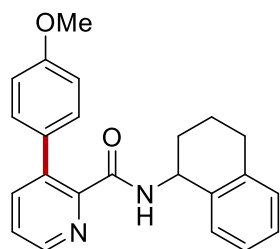
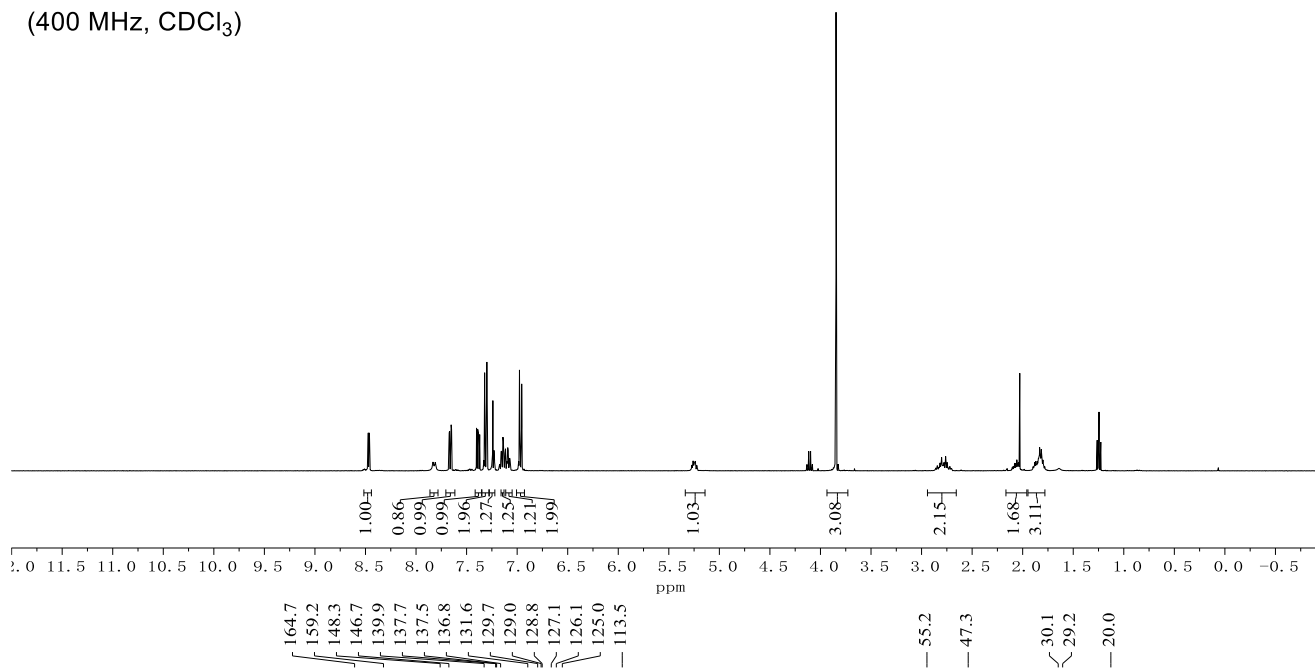


**413h**  
(100 MHz, CDCl<sub>3</sub>)

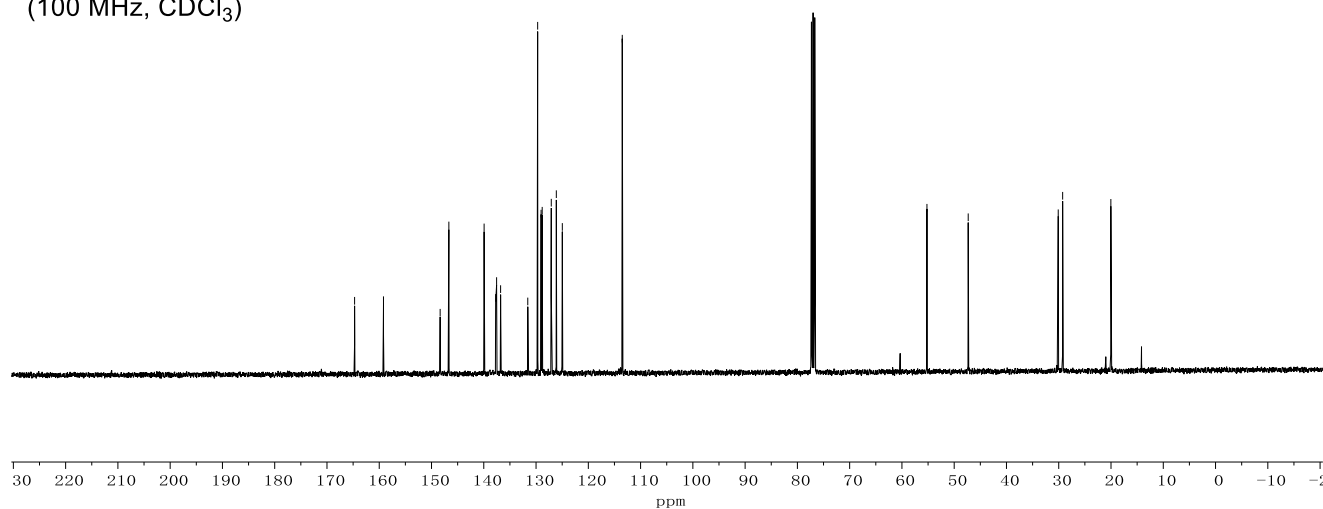




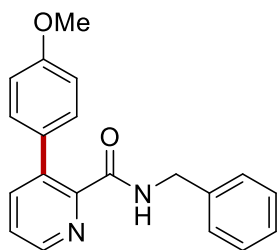
**413i**  
(400 MHz, CDCl<sub>3</sub>)



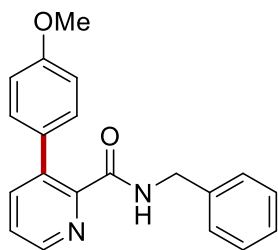
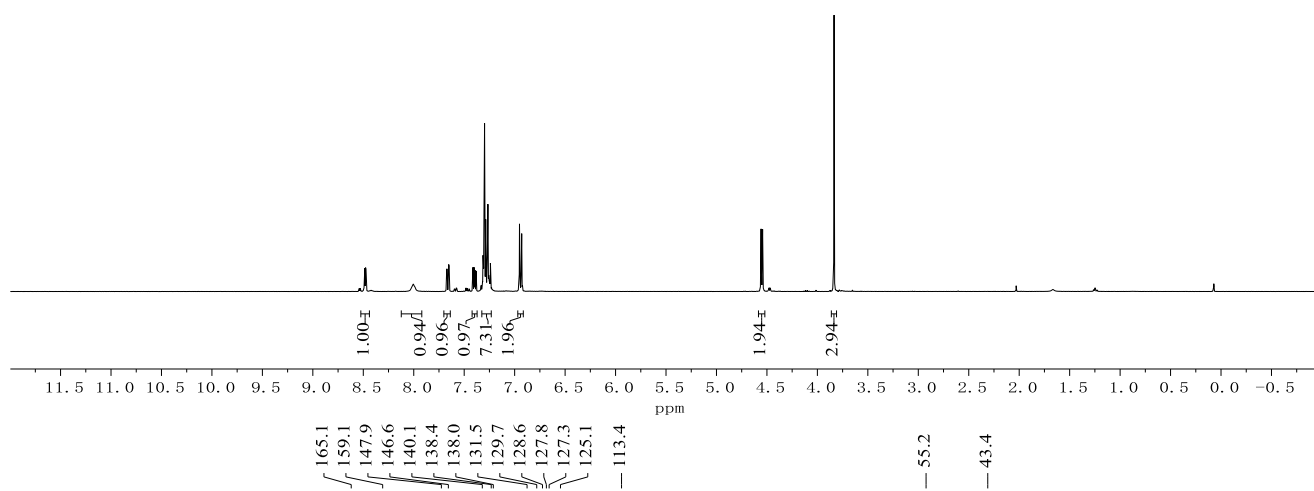
**413i**  
(100 MHz, CDCl<sub>3</sub>)



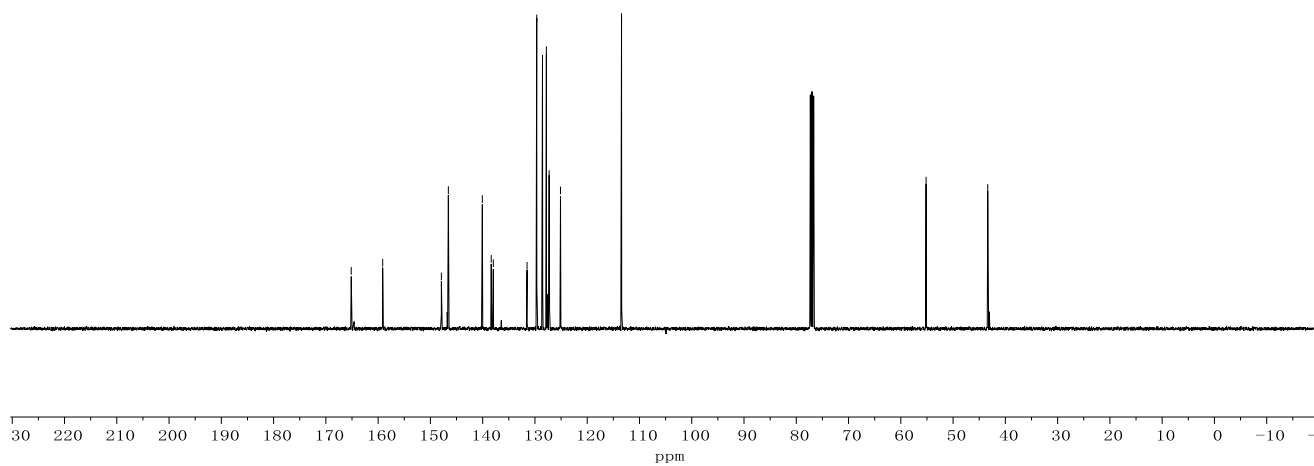
Appendix: NMR Spectra



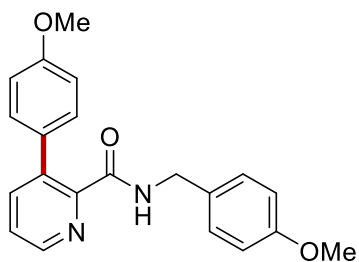
**413j**  
(400 MHz, CDCl<sub>3</sub>)



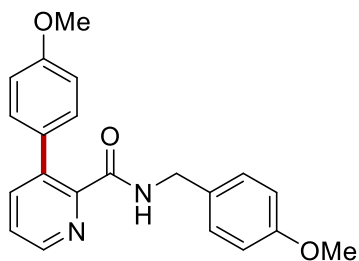
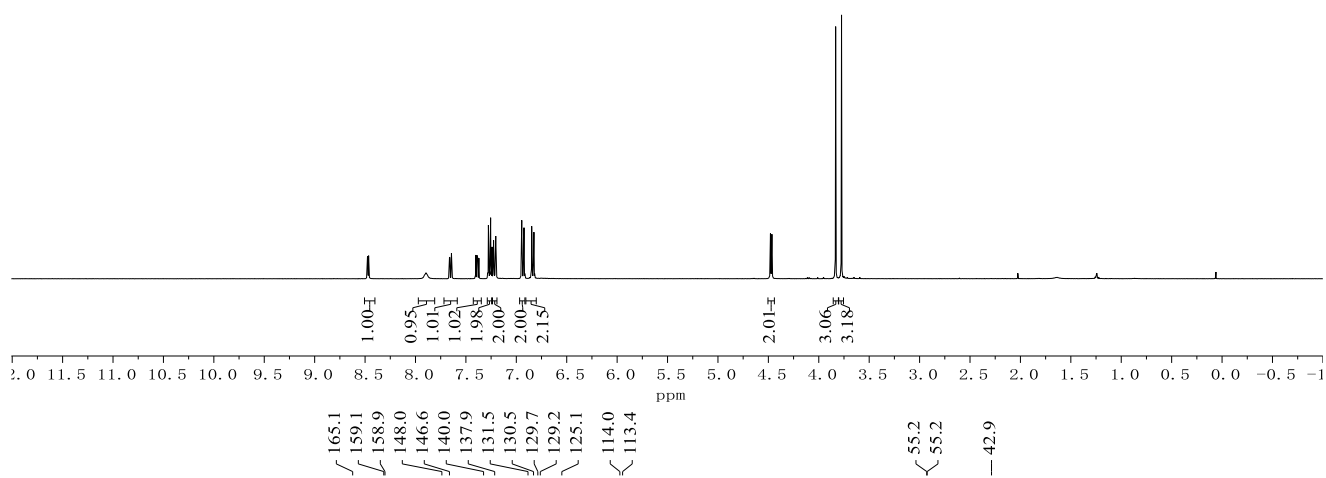
**413j**  
(100 MHz, CDCl<sub>3</sub>)



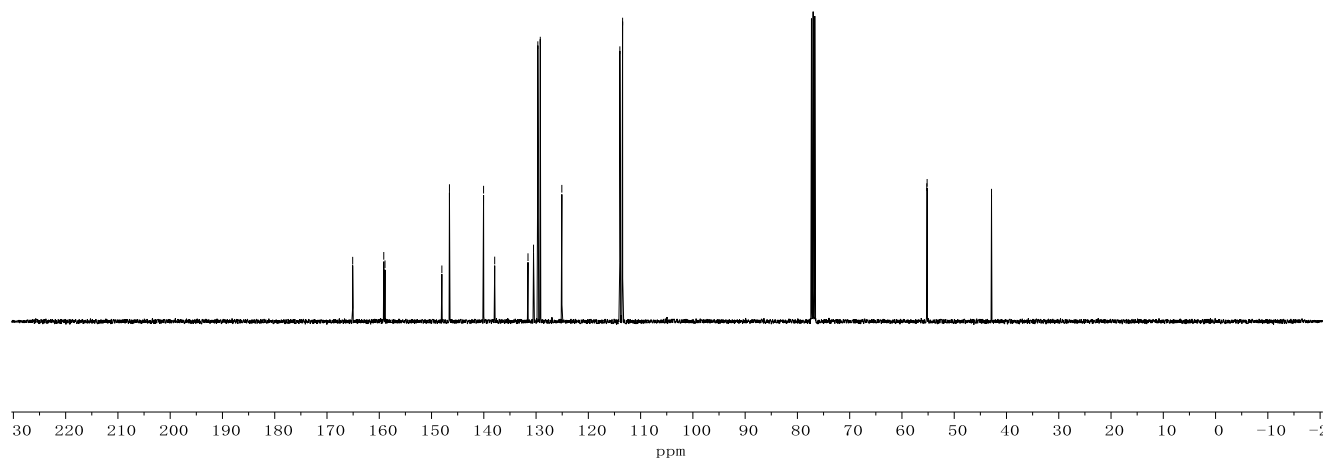
Appendix: NMR Spectra



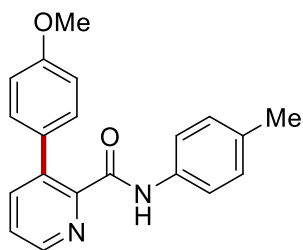
**413k**  
(400 MHz, CDCl<sub>3</sub>)



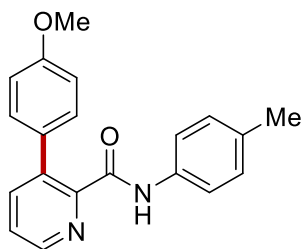
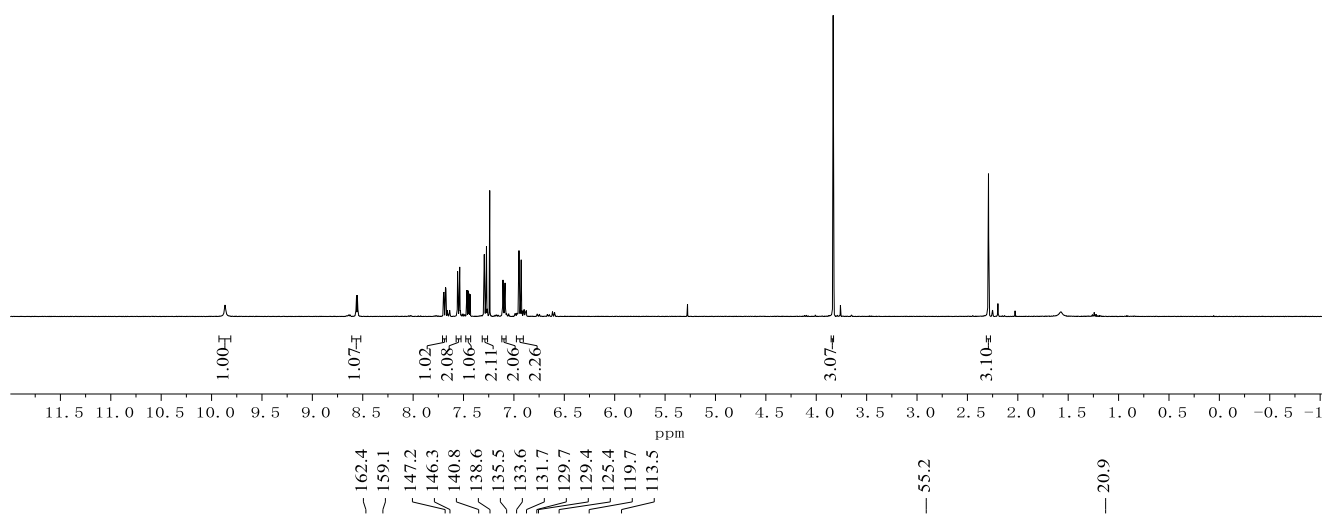
**413k**  
(100 MHz, CDCl<sub>3</sub>)



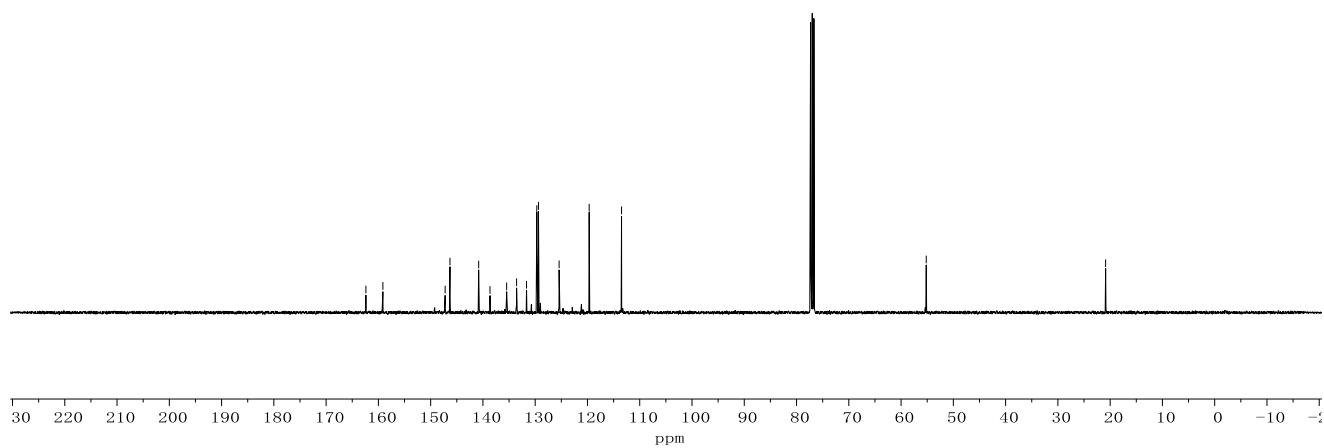
Appendix: NMR Spectra



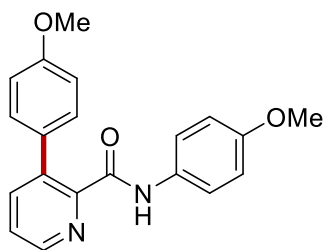
**413I**  
(400 MHz, CDCl<sub>3</sub>)



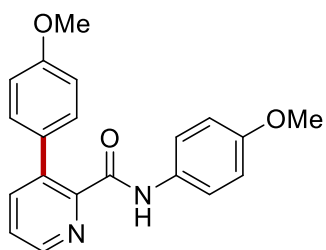
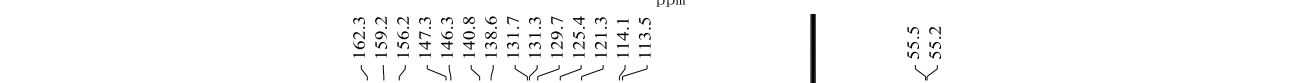
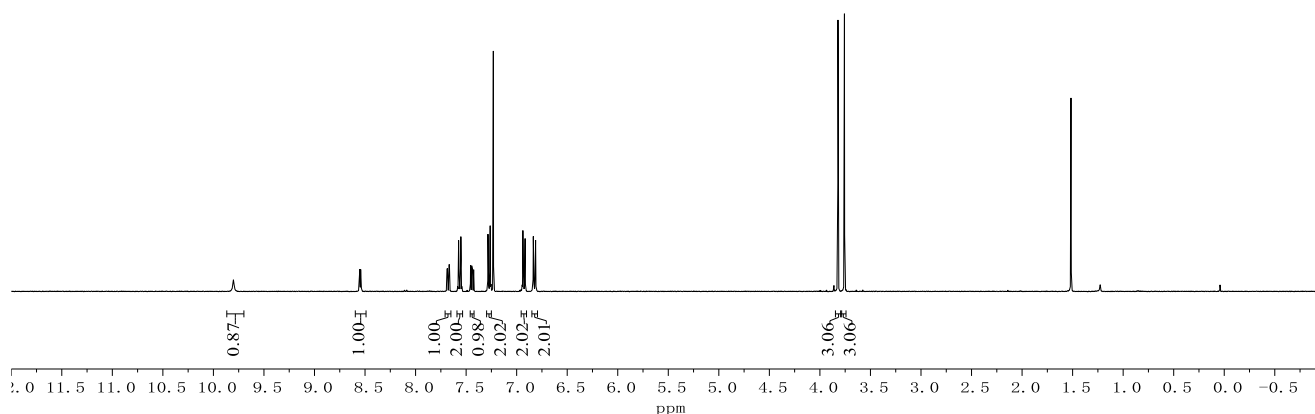
**413I**  
(100 MHz, CDCl<sub>3</sub>)



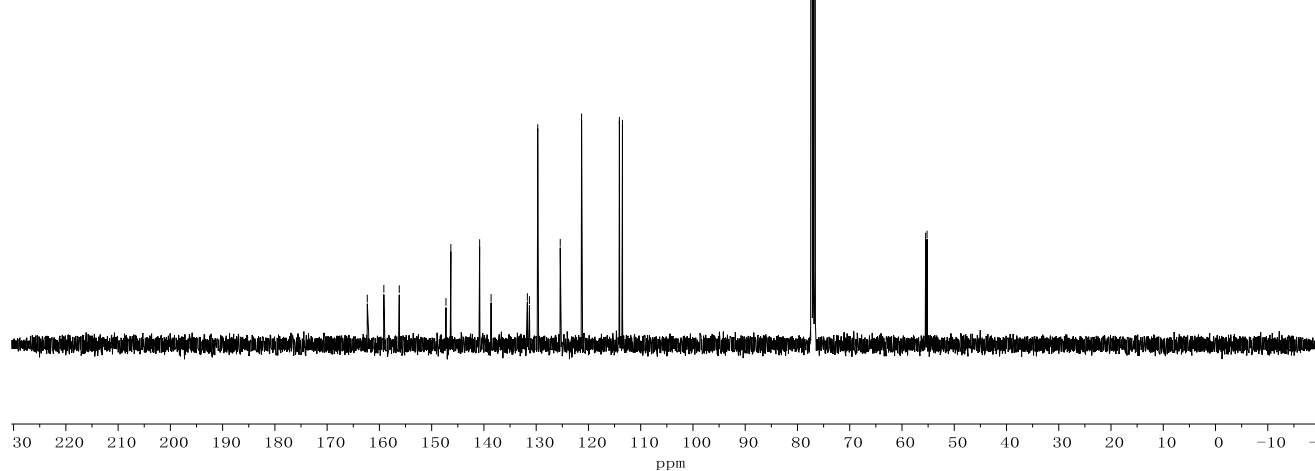
Appendix: NMR Spectra



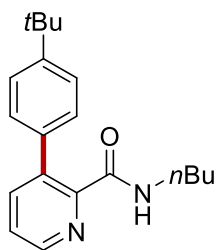
**413m**  
(400 MHz, CDCl<sub>3</sub>)



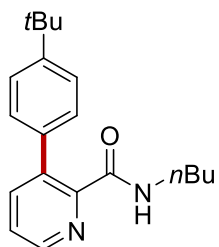
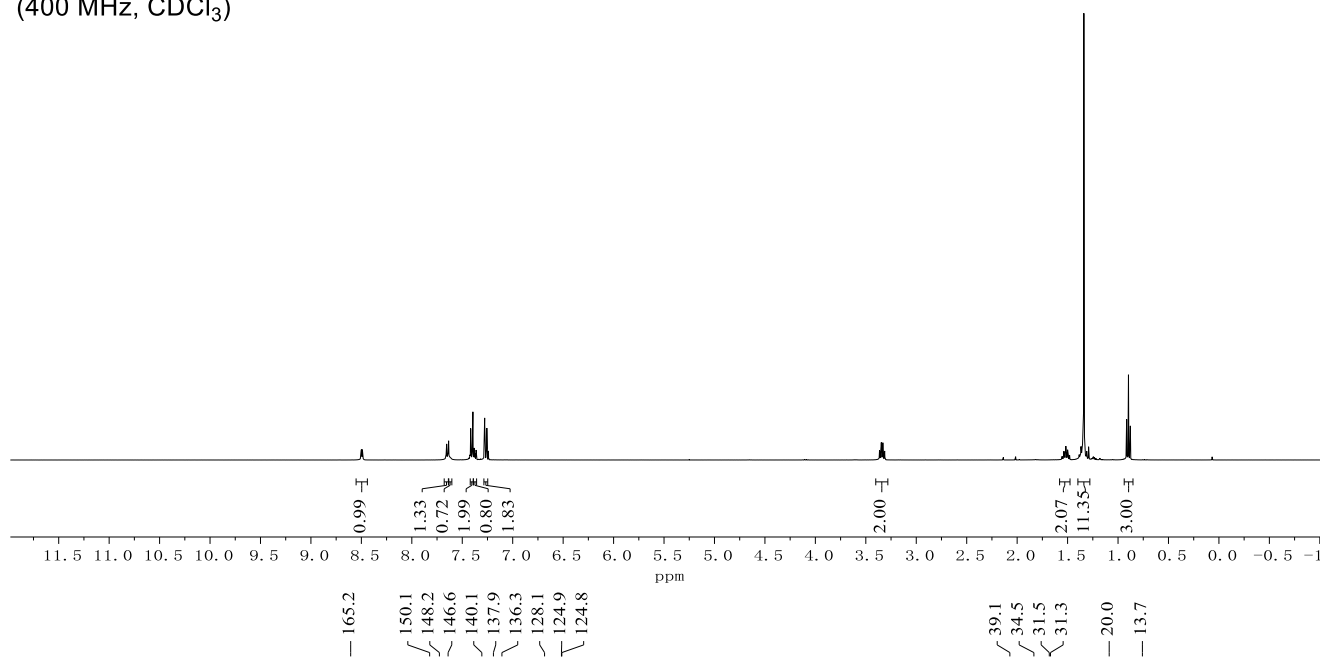
**413m**  
(100 MHz, CDCl<sub>3</sub>)



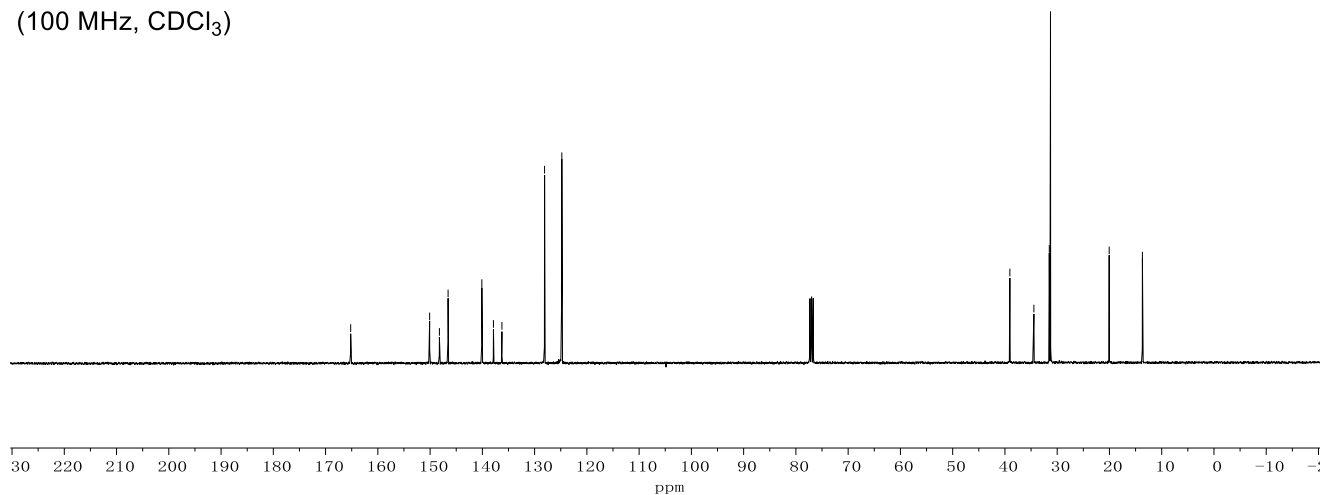
Appendix: NMR Spectra



**413n**  
(400 MHz, CDCl<sub>3</sub>)

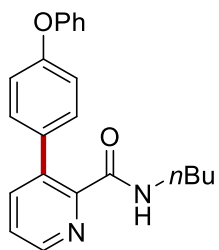


**413n**  
(100 MHz, CDCl<sub>3</sub>)

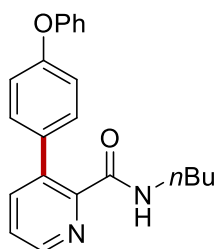
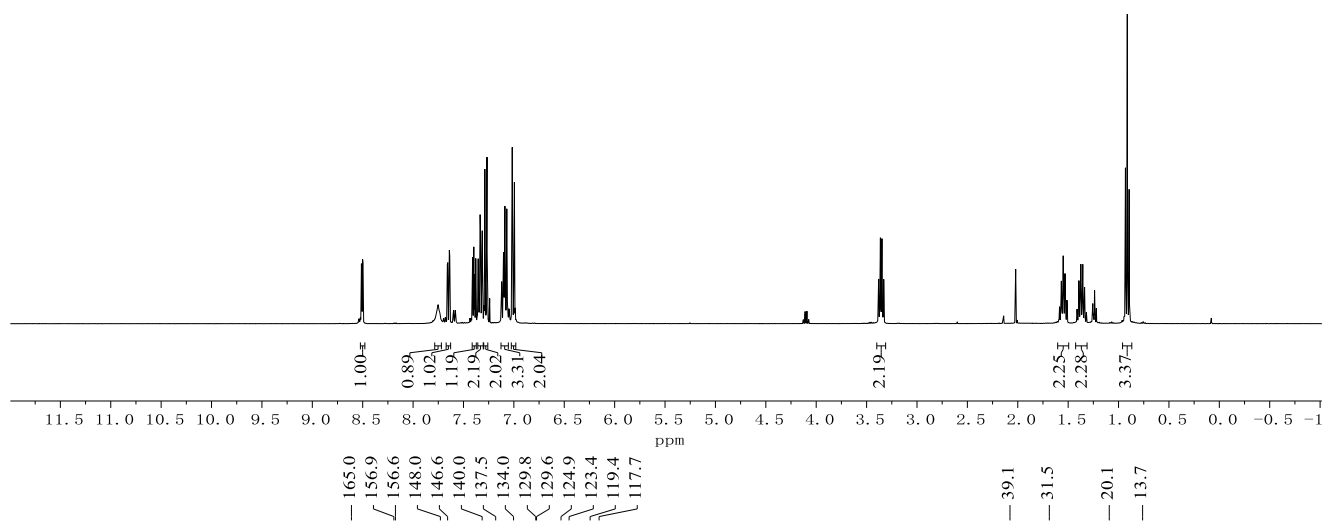




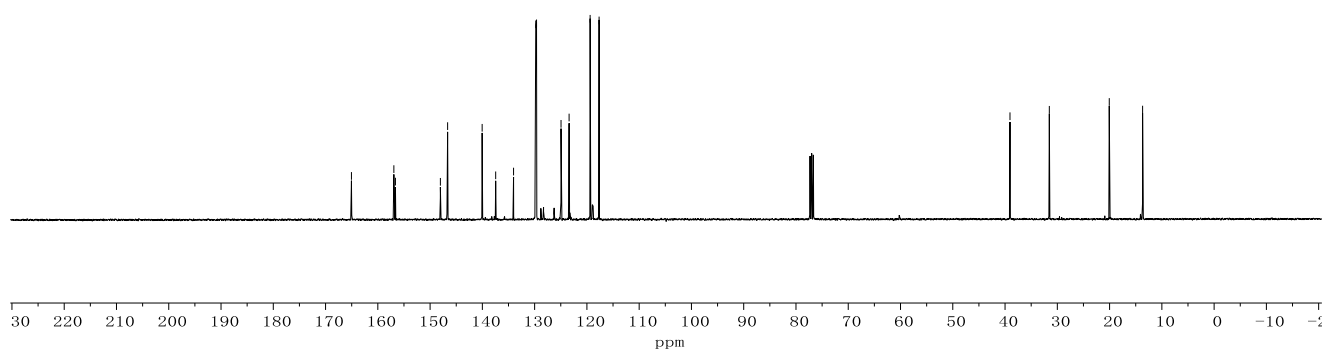
Appendix: NMR Spectra



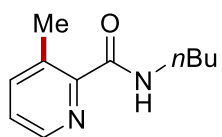
**413o**  
(400 MHz, CDCl<sub>3</sub>)



**413o**  
(100 MHz, CDCl<sub>3</sub>)

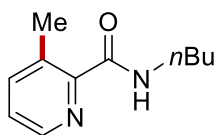
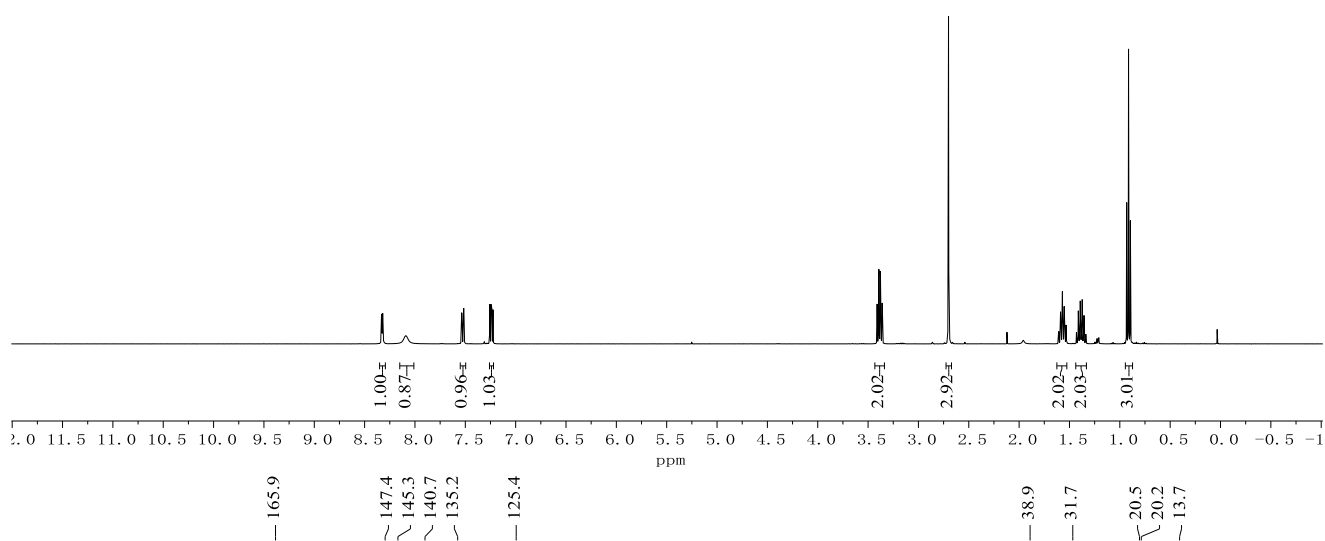


Appendix: NMR Spectra



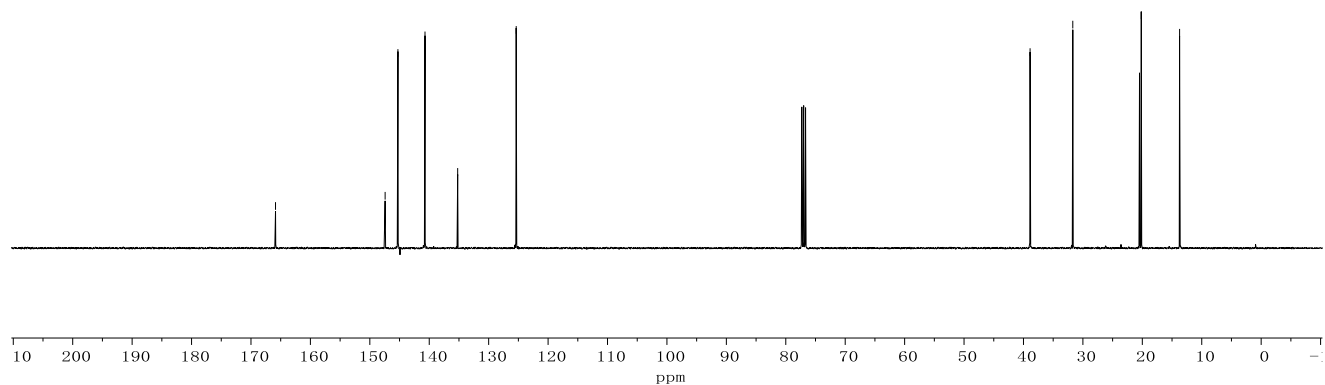
**415a**

(300 MHz, CDCl<sub>3</sub>)

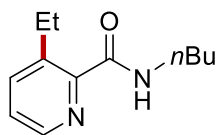


**415a**

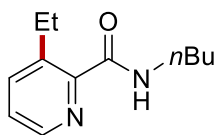
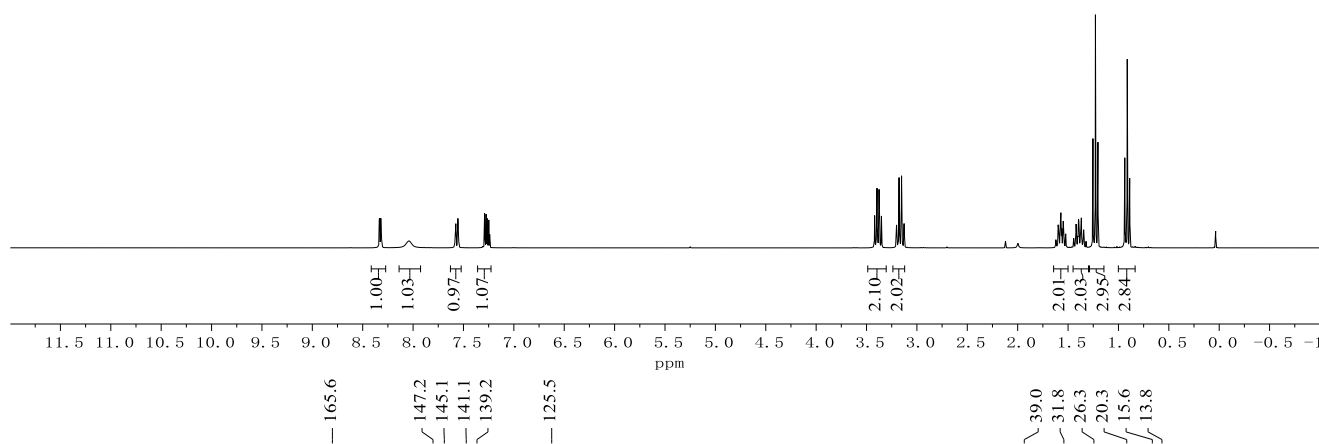
(75 MHz, CDCl<sub>3</sub>)



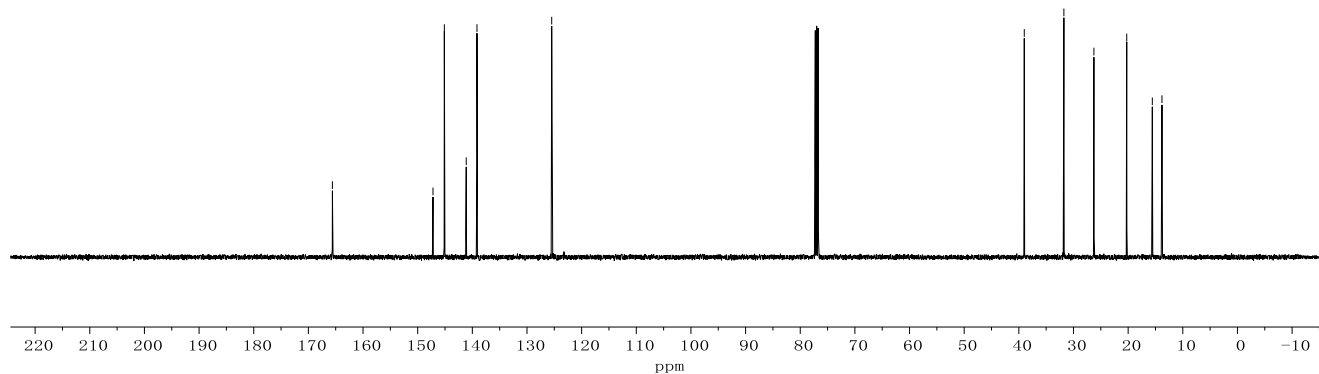
Appendix: NMR Spectra



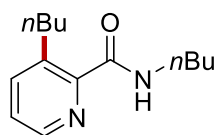
**415b**  
(300 MHz, CDCl<sub>3</sub>)



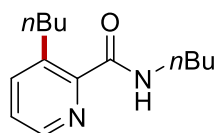
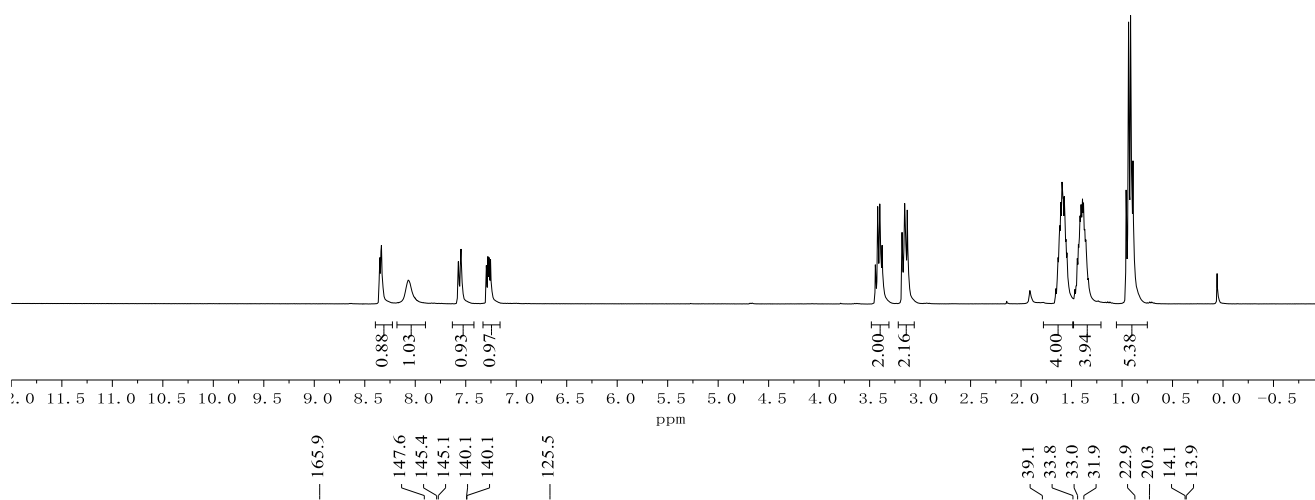
**415b**  
(75 MHz, CDCl<sub>3</sub>)



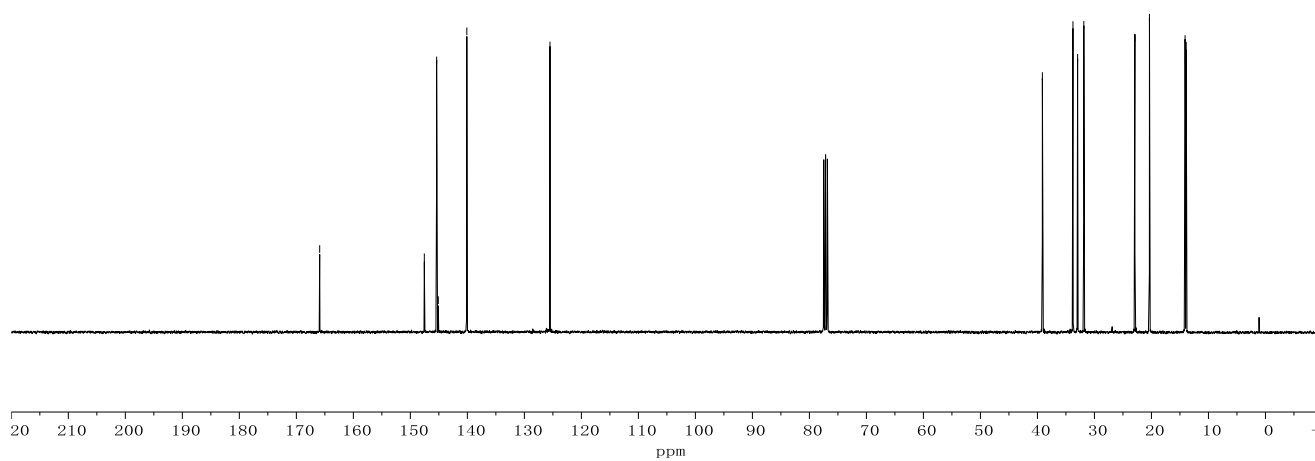
Appendix: NMR Spectra



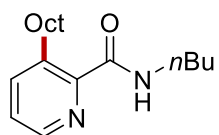
**415c**  
(300 MHz, CDCl<sub>3</sub>)



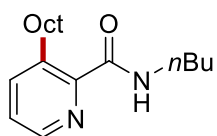
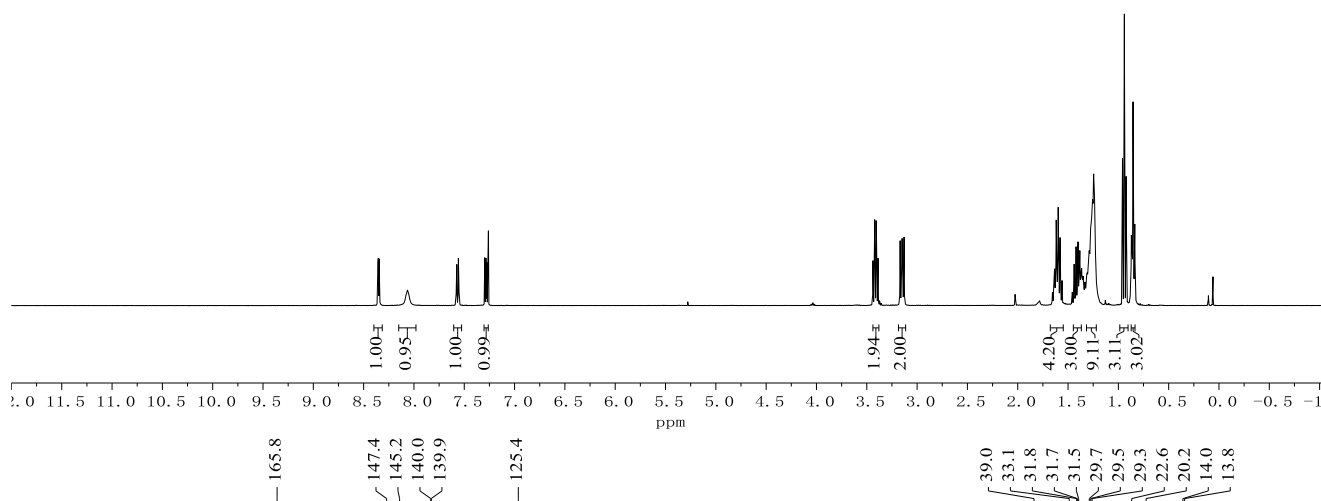
**415c**  
(75 MHz, CDCl<sub>3</sub>)



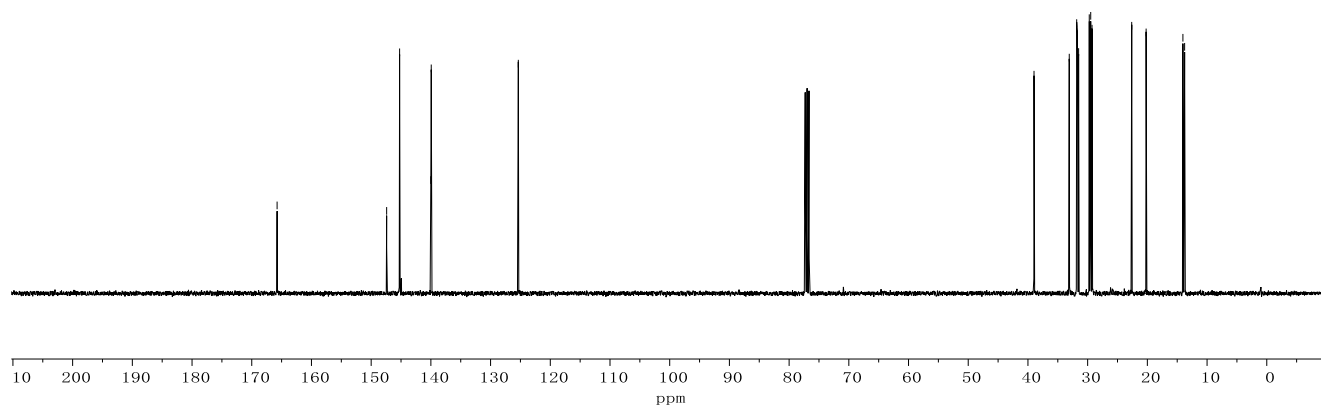
Appendix: NMR Spectra



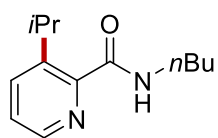
**415d**  
(400 MHz, CDCl<sub>3</sub>)



**415d**  
(100 MHz, CDCl<sub>3</sub>)

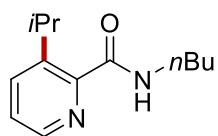
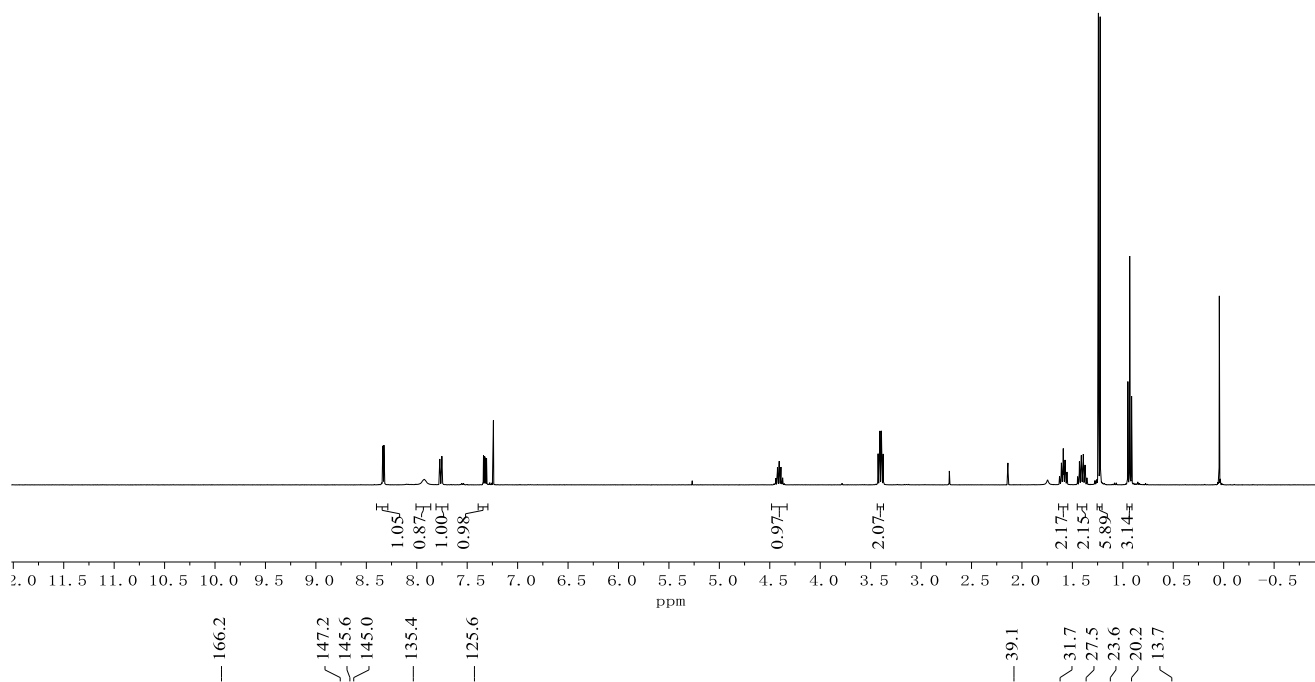


Appendix: NMR Spectra



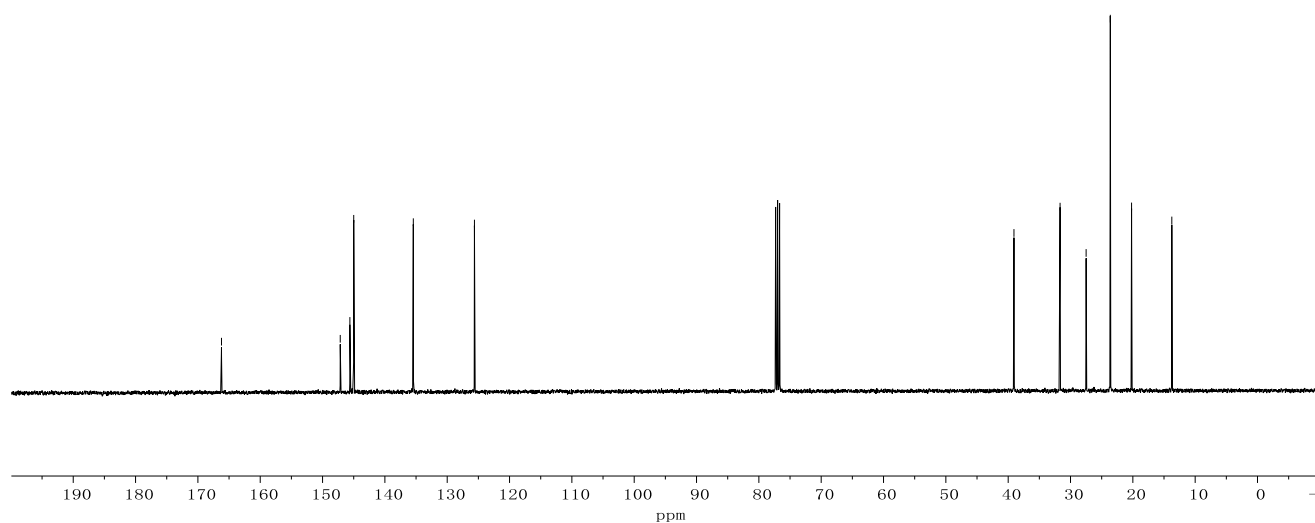
**415e**

(400 MHz, CDCl<sub>3</sub>)

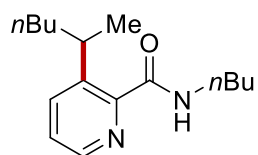


**415e**

(100 MHz, CDCl<sub>3</sub>)

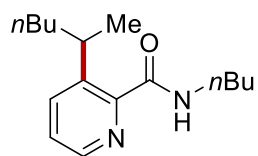
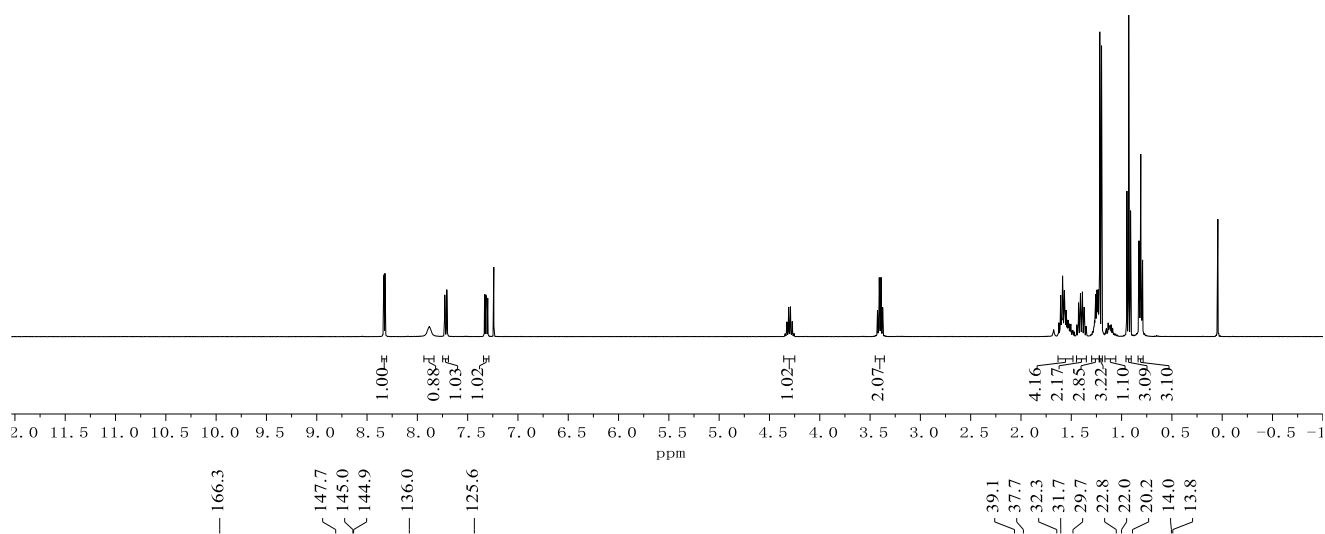


Appendix: NMR Spectra



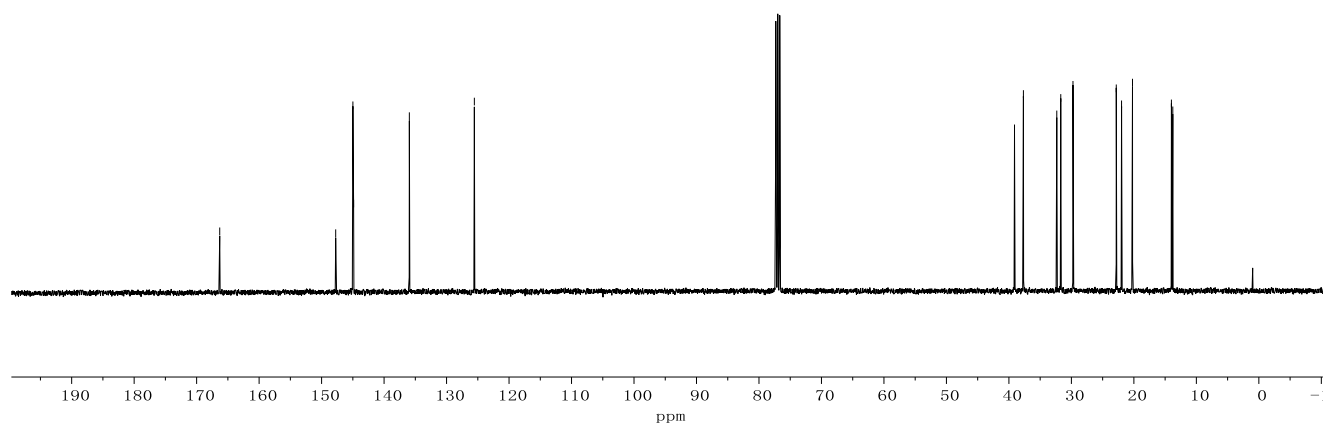
**415f**

(300 MHz, CDCl<sub>3</sub>)

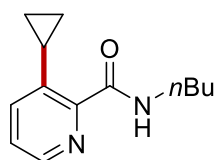


**415f**

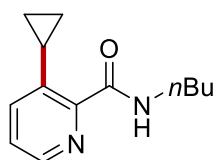
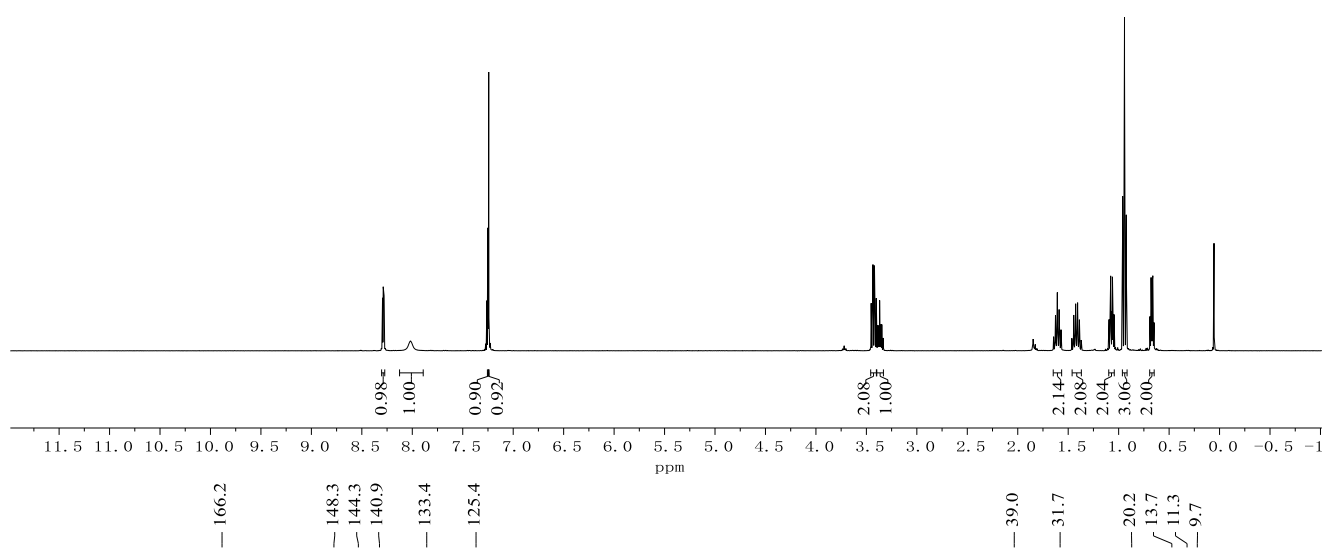
(75 MHz, CDCl<sub>3</sub>)



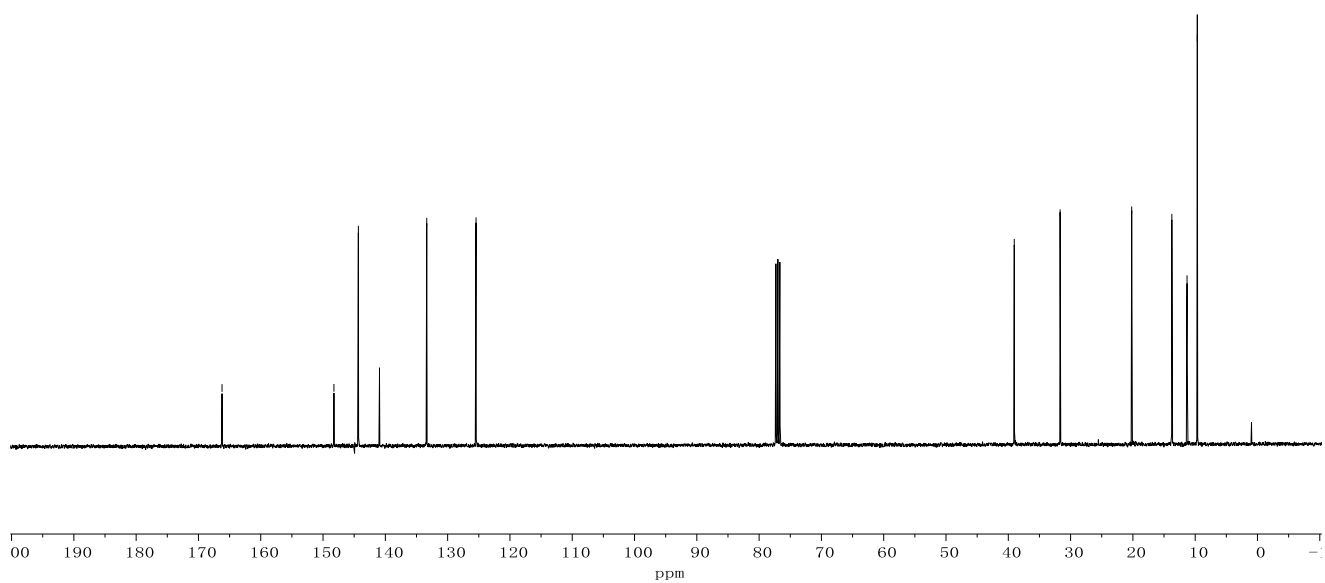
Appendix: NMR Spectra



**415g**  
(400 MHz, CDCl<sub>3</sub>)

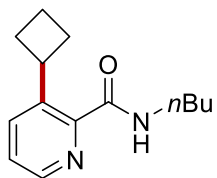


**415g**  
(100 MHz, CDCl<sub>3</sub>)



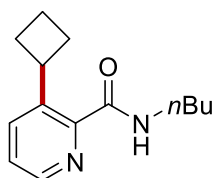
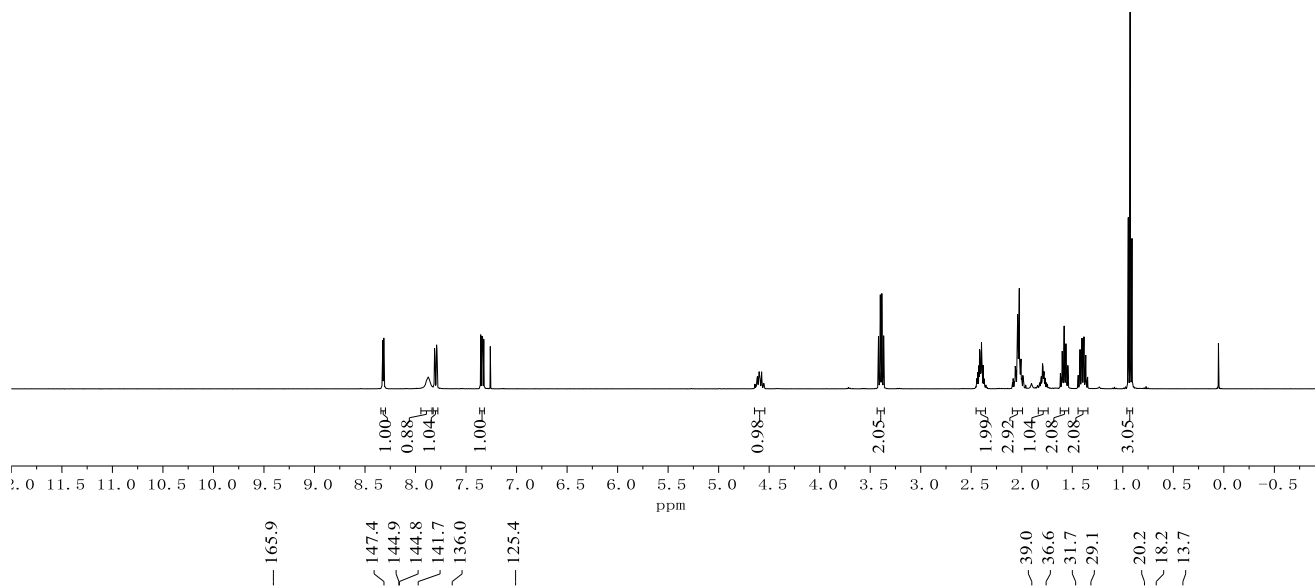


Appendix: NMR Spectra



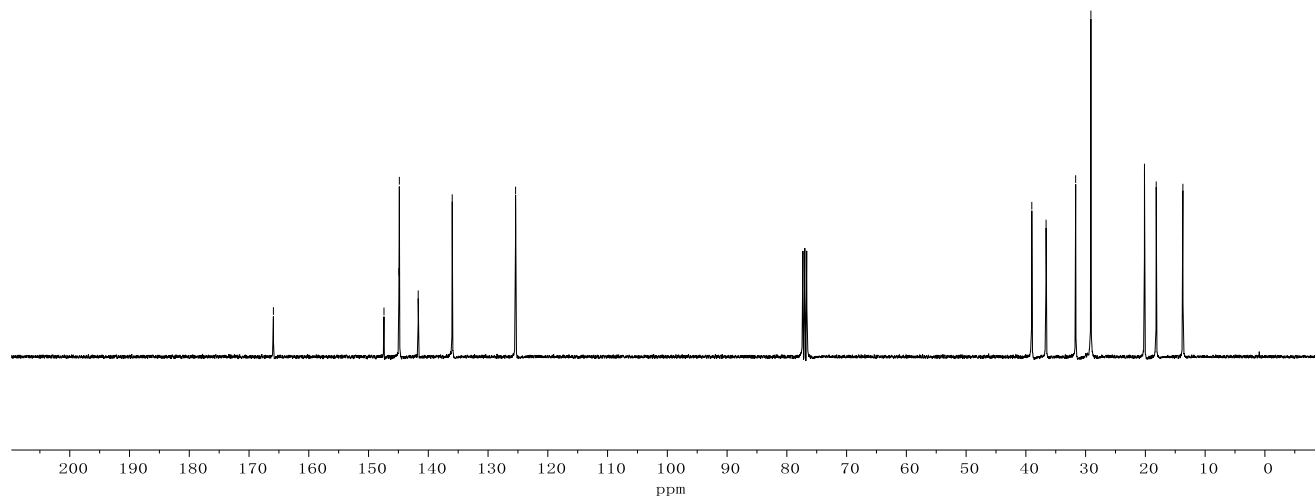
**415h**

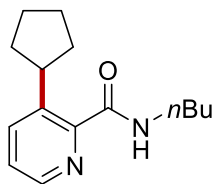
(400 MHz, CDCl<sub>3</sub>)



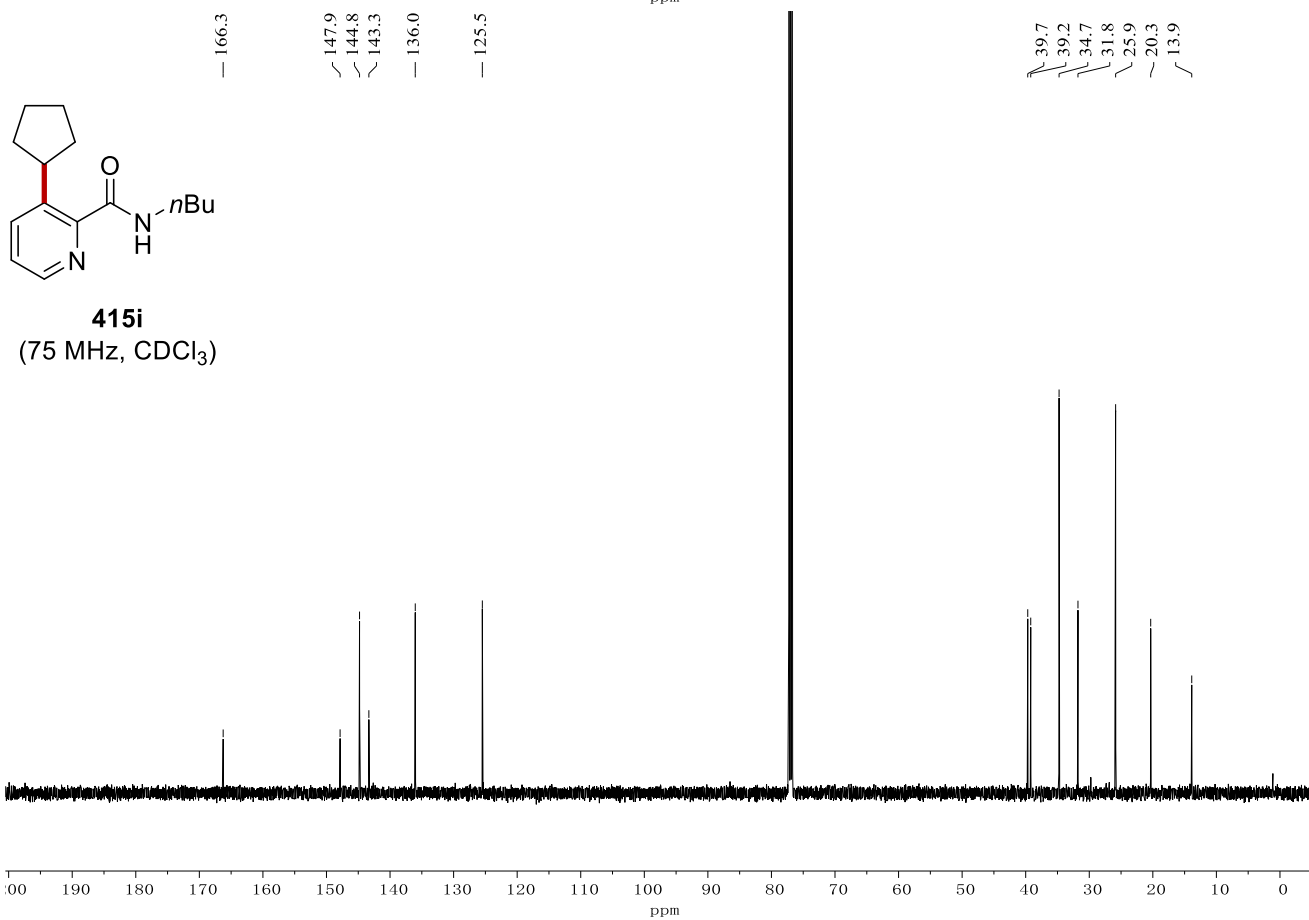
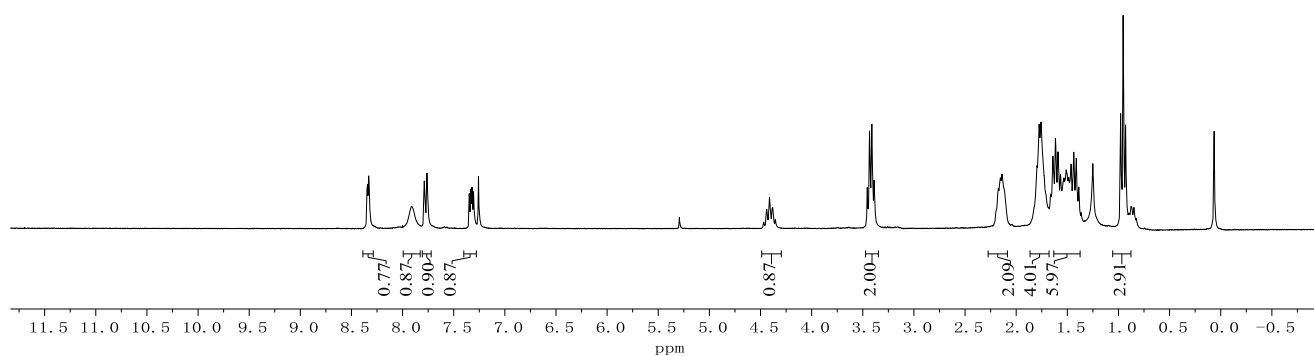
**415h**

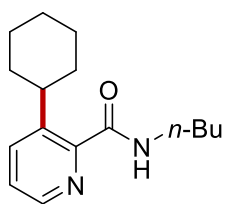
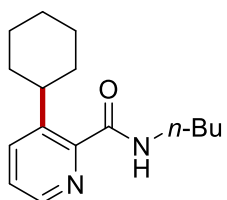
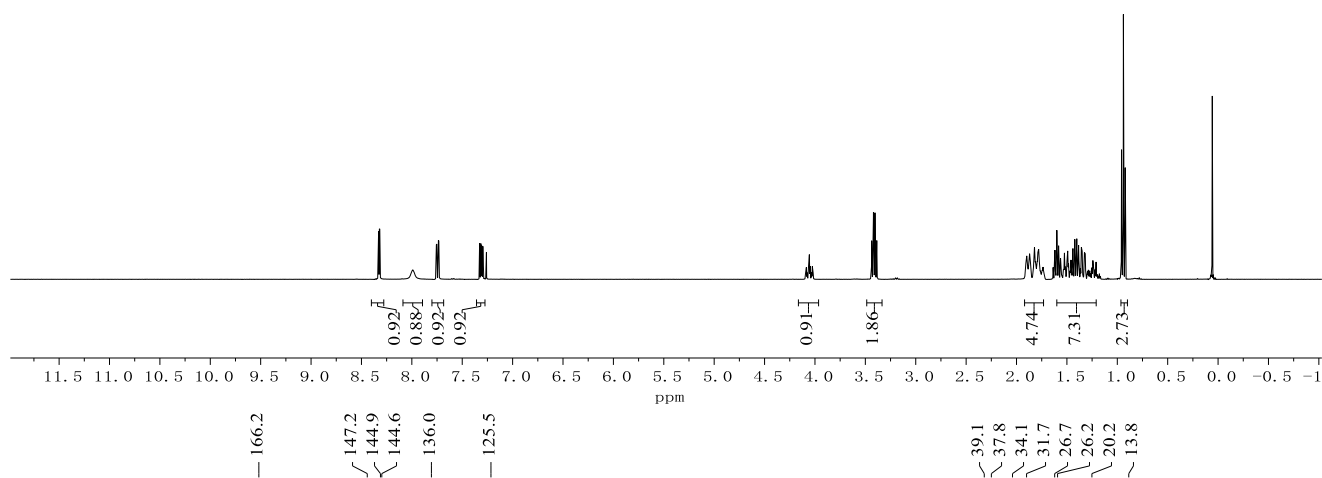
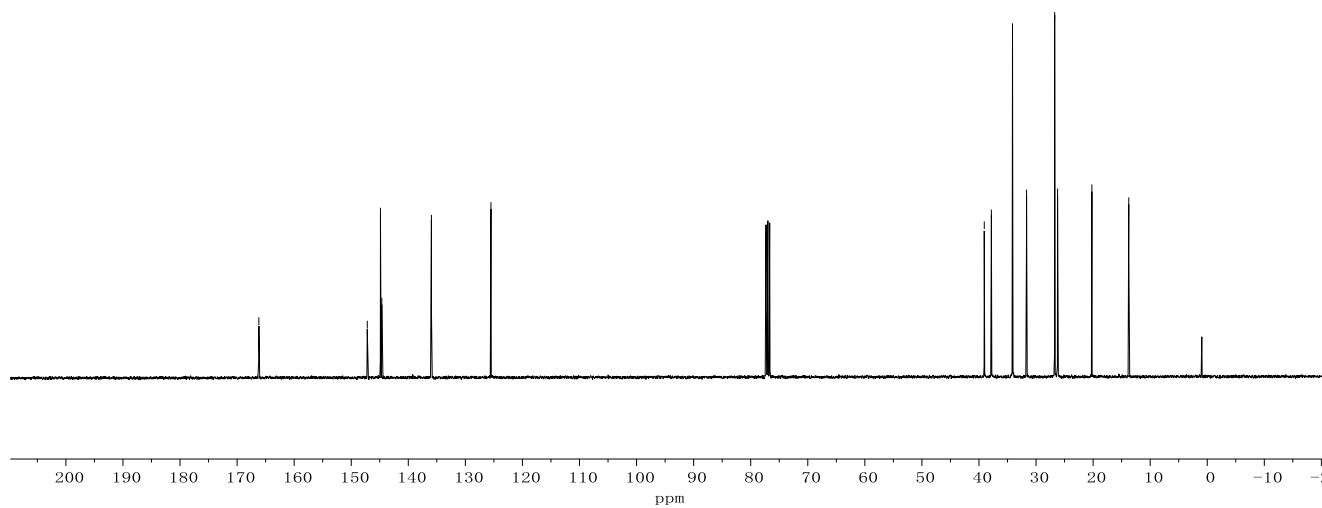
(100 MHz, CDCl<sub>3</sub>)



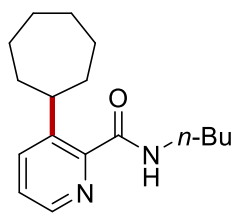


**415i**  
(300 MHz, CDCl<sub>3</sub>)

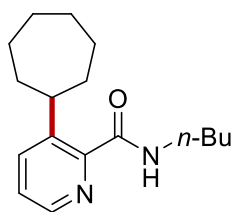
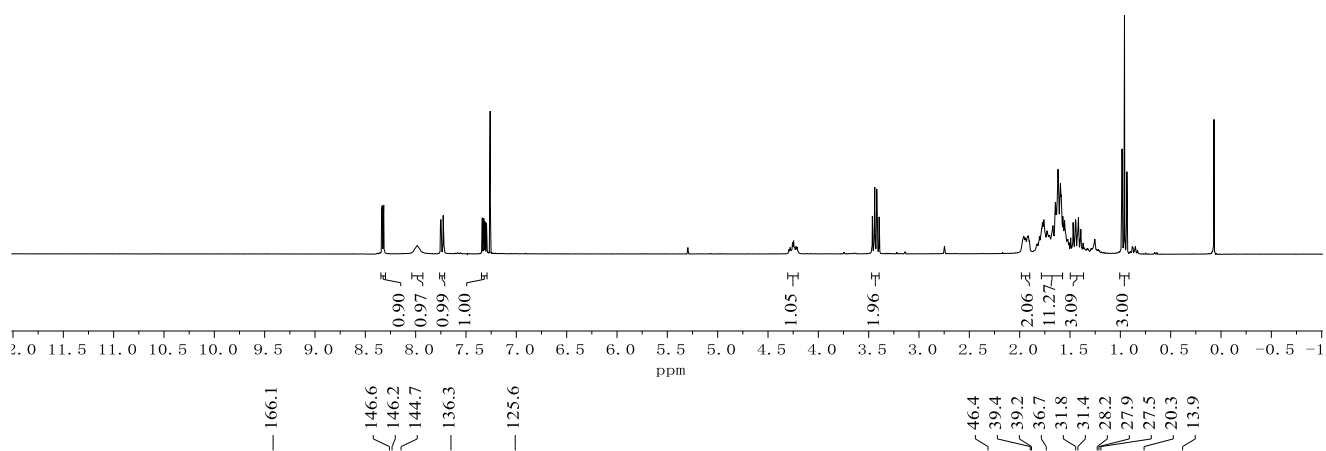


**415j**(400 MHz, CDCl<sub>3</sub>)**415j**(100 MHz, CDCl<sub>3</sub>)

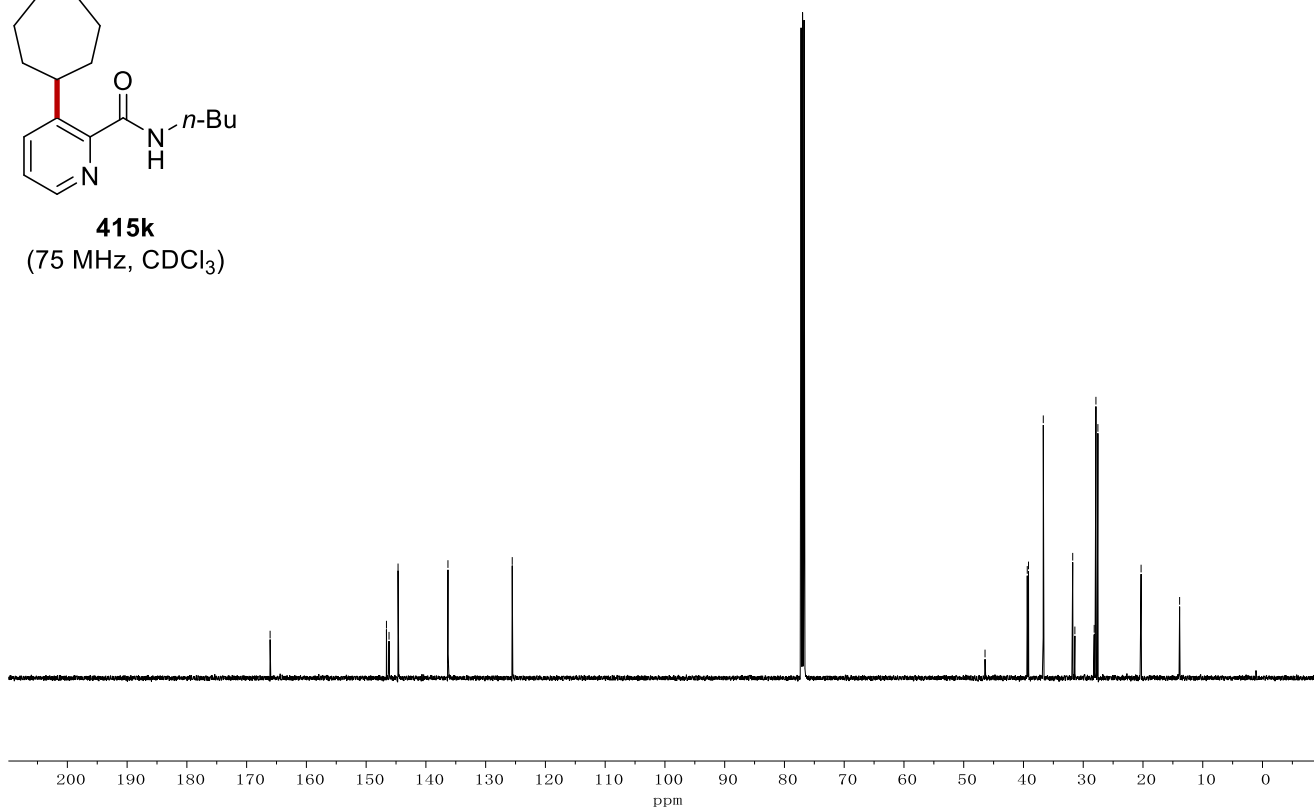
Appendix: NMR Spectra



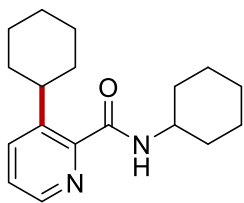
**415k**  
(300 MHz, CDCl<sub>3</sub>)



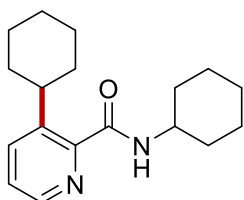
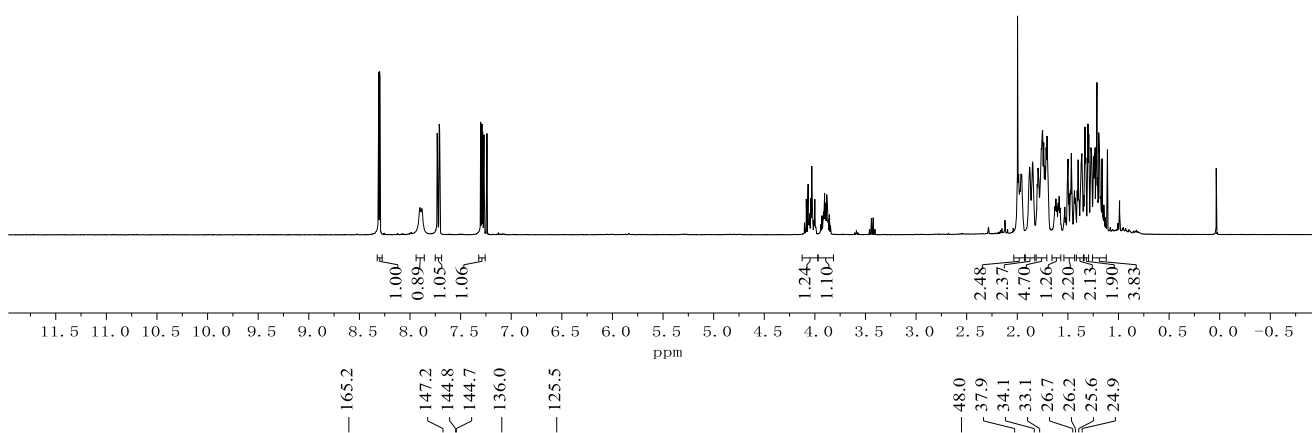
**415k**  
(75 MHz, CDCl<sub>3</sub>)



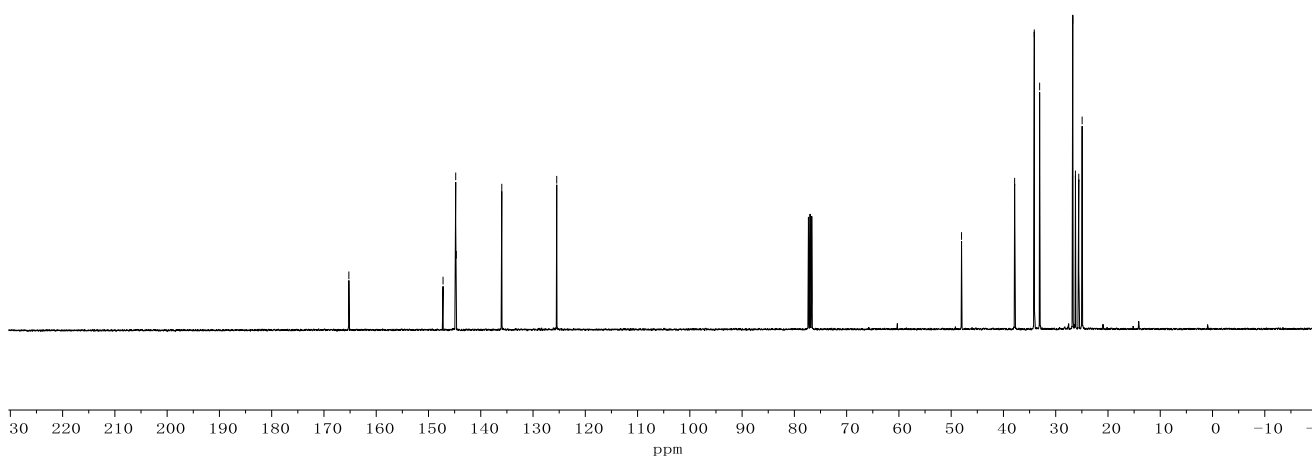
Appendix: NMR Spectra



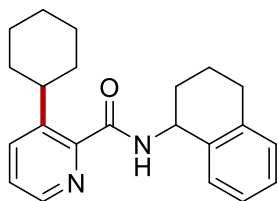
**415I**  
(400 MHz, CDCl<sub>3</sub>)



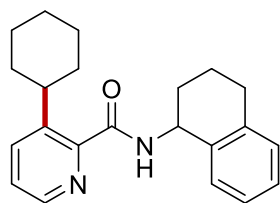
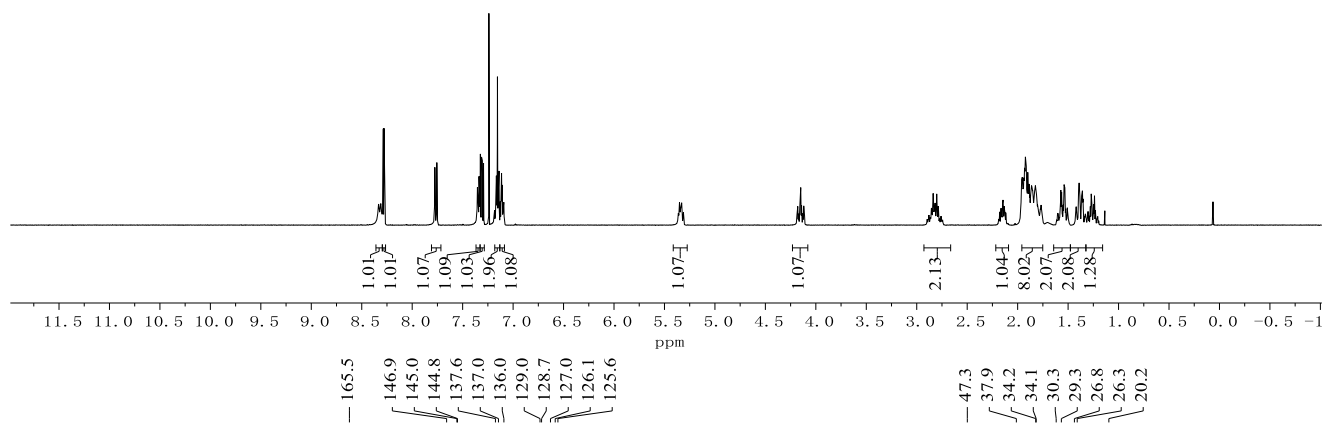
**415I**  
(100 MHz, CDCl<sub>3</sub>)



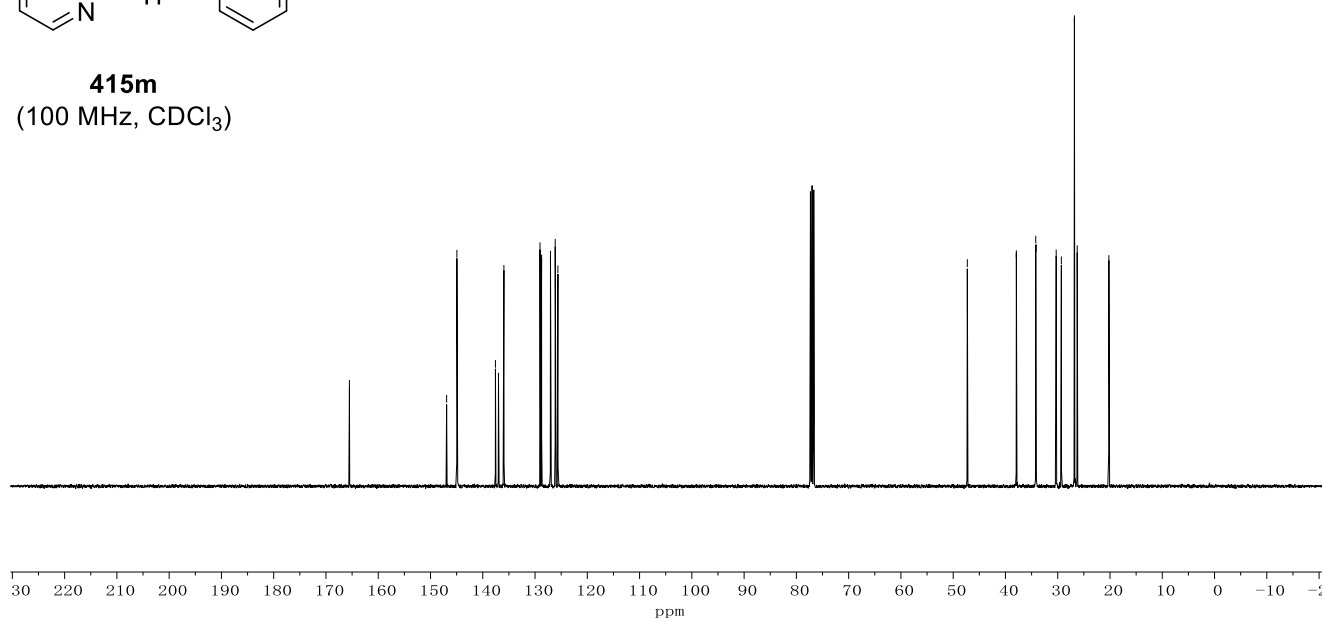
Appendix: NMR Spectra

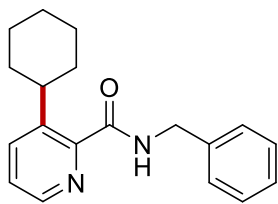


**415m**  
(400 MHz, CDCl<sub>3</sub>)

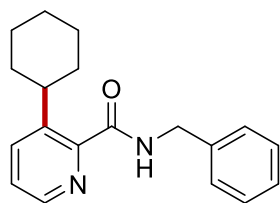
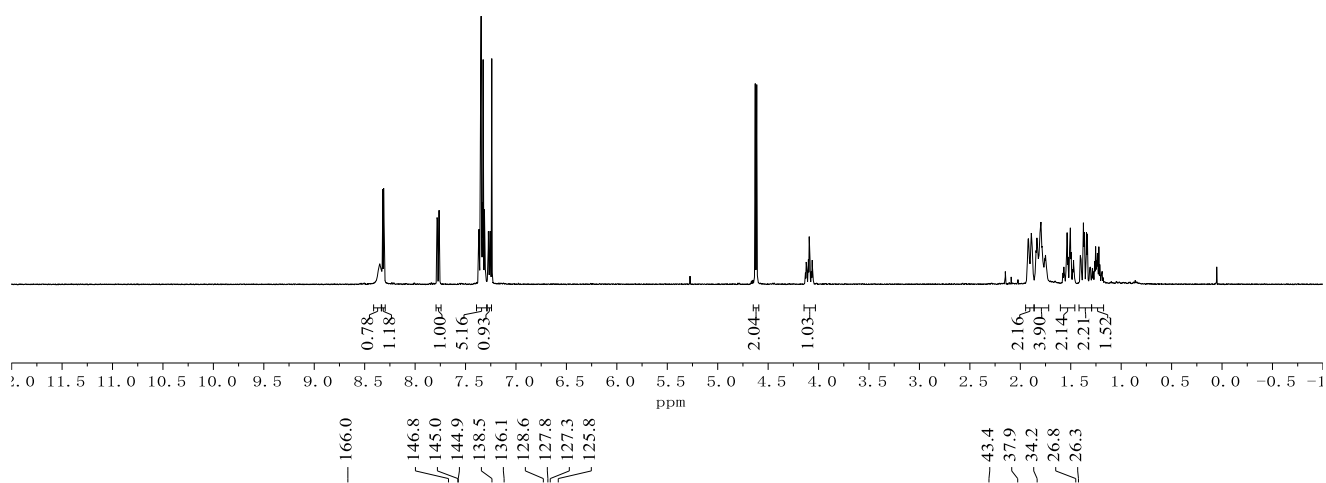


**415m**  
(100 MHz, CDCl<sub>3</sub>)

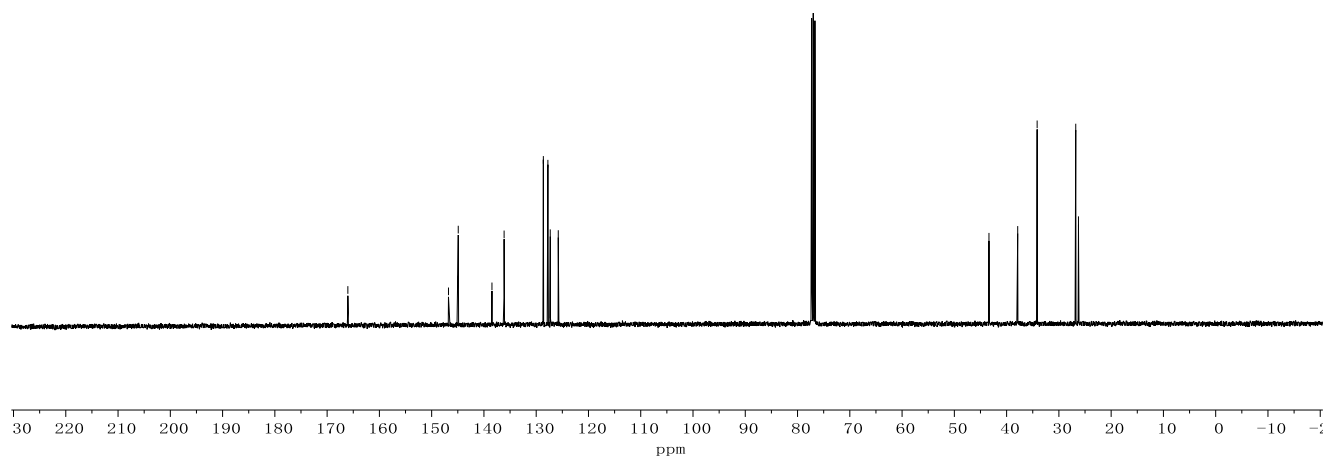




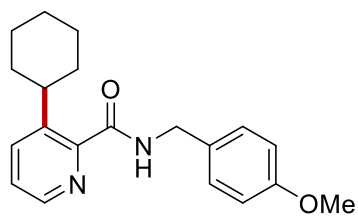
**415n**  
(400 MHz, CDCl<sub>3</sub>)



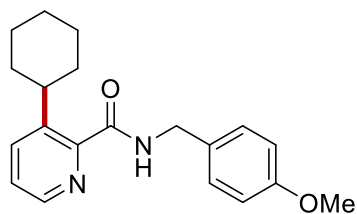
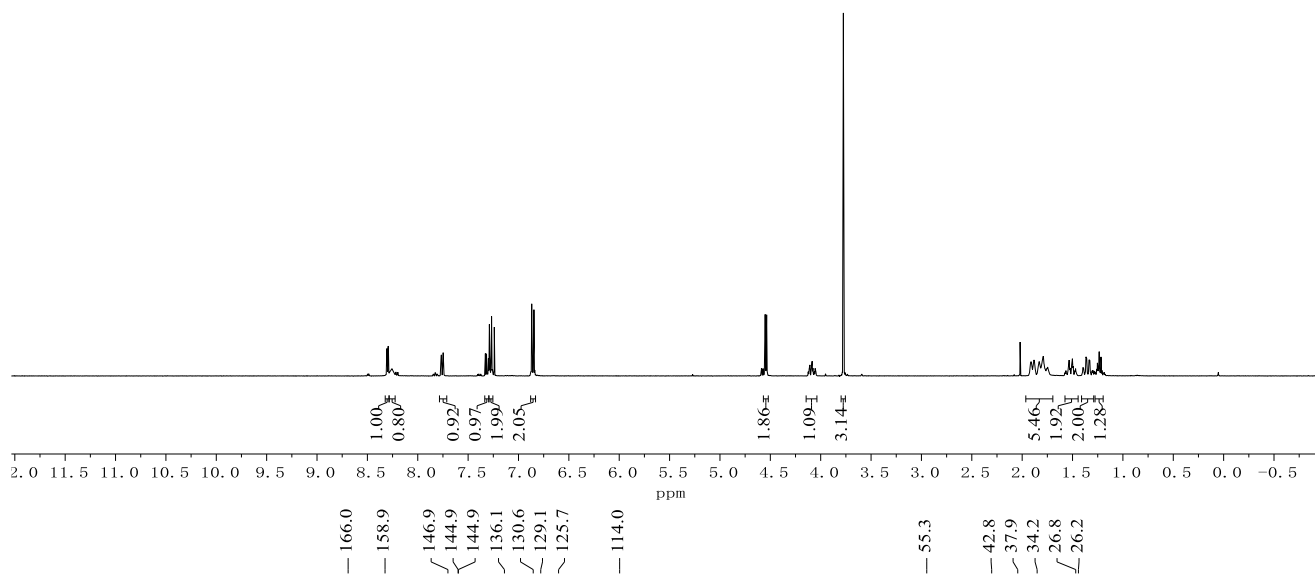
**415n**  
(100 MHz, CDCl<sub>3</sub>)



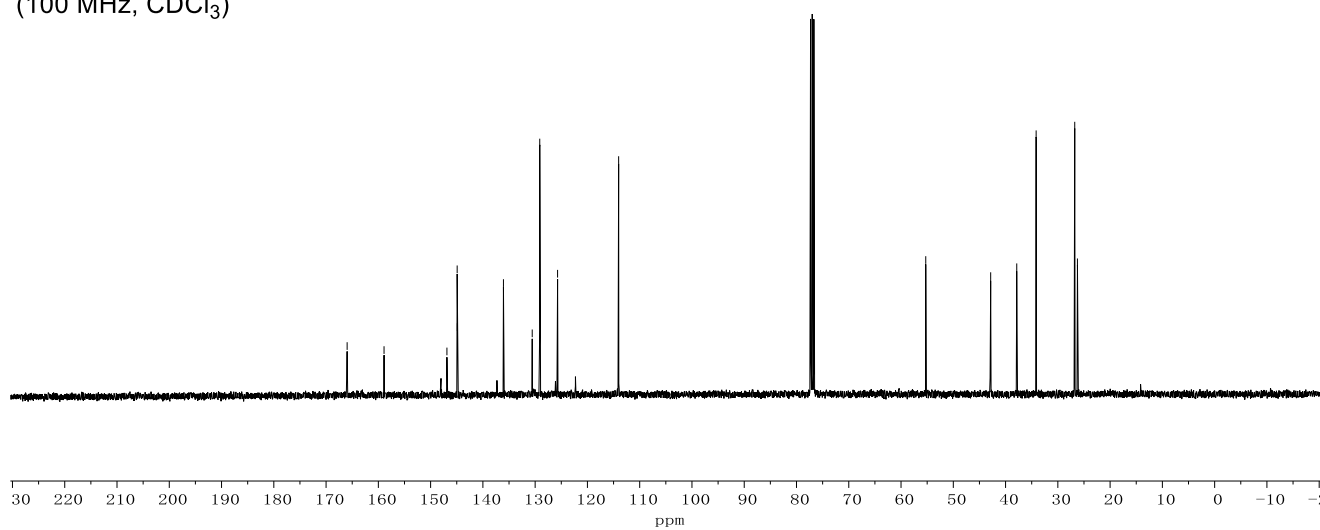
Appendix: NMR Spectra



**415o**  
(400 MHz, CDCl<sub>3</sub>)

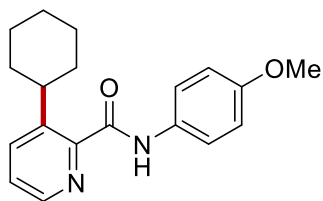


**415o**  
(100 MHz, CDCl<sub>3</sub>)

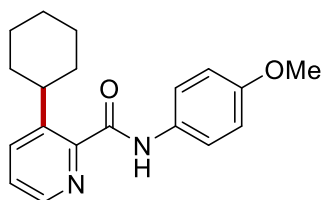
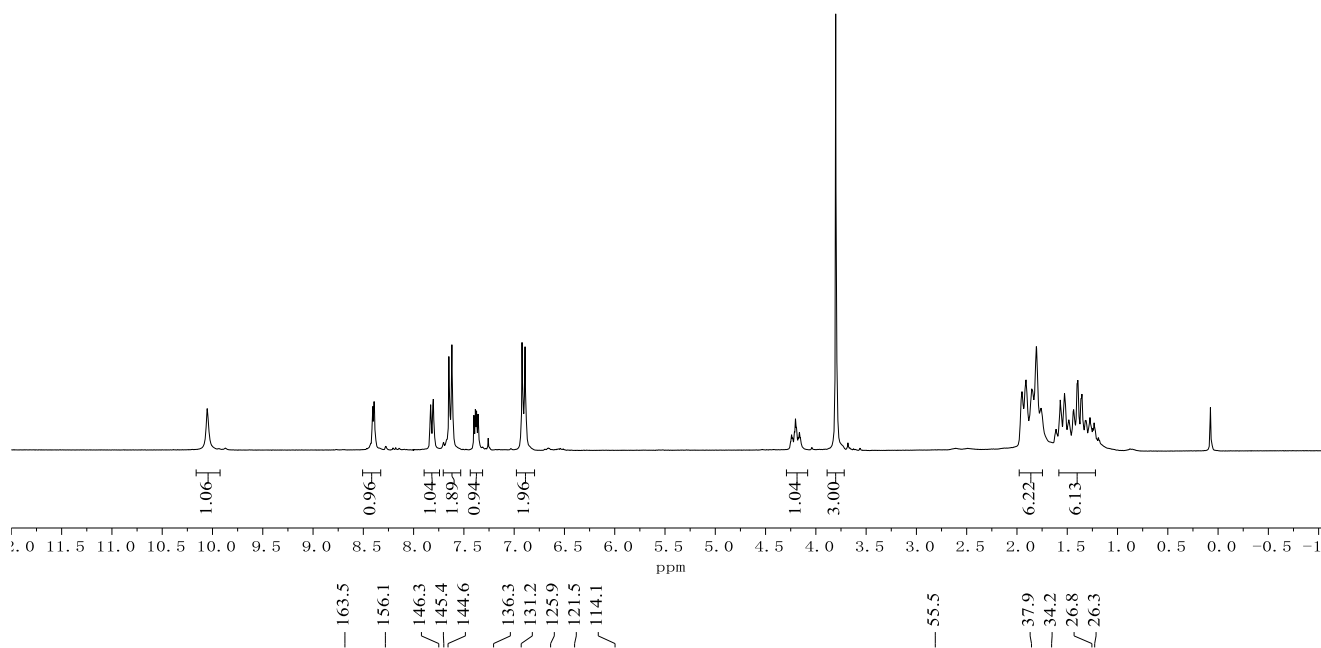




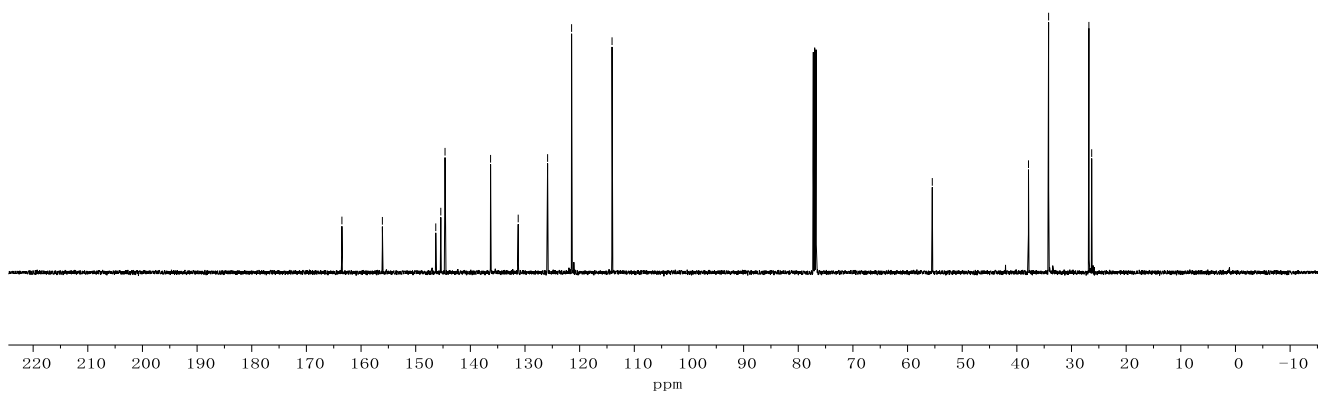
Appendix: NMR Spectra



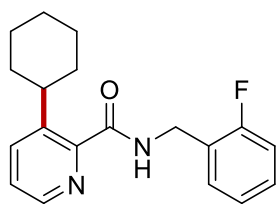
**415p**  
(300 MHz, CDCl<sub>3</sub>)



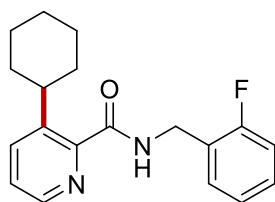
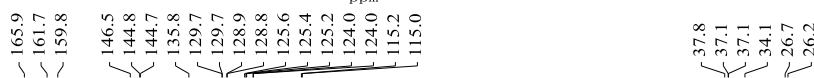
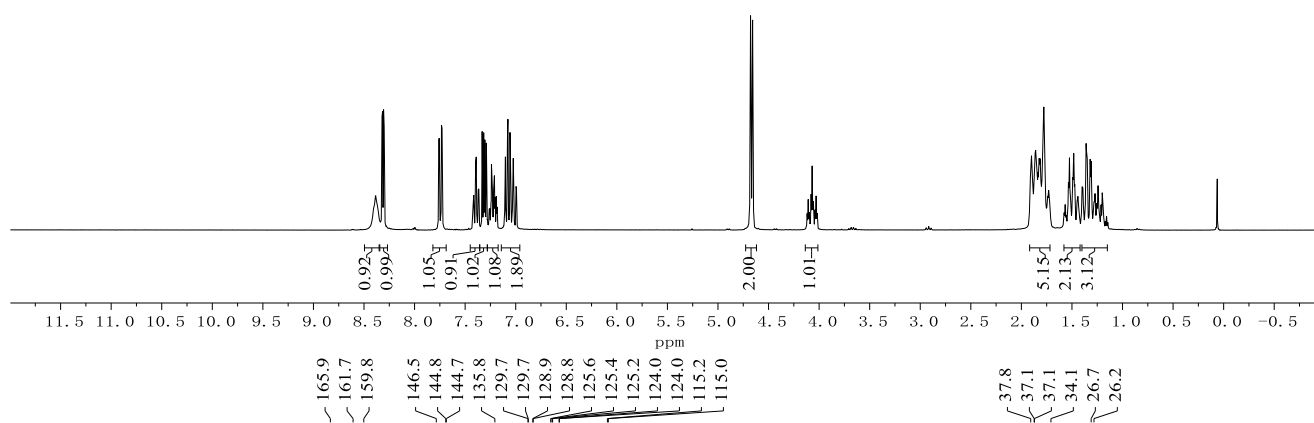
**415p**  
(75 MHz, CDCl<sub>3</sub>)



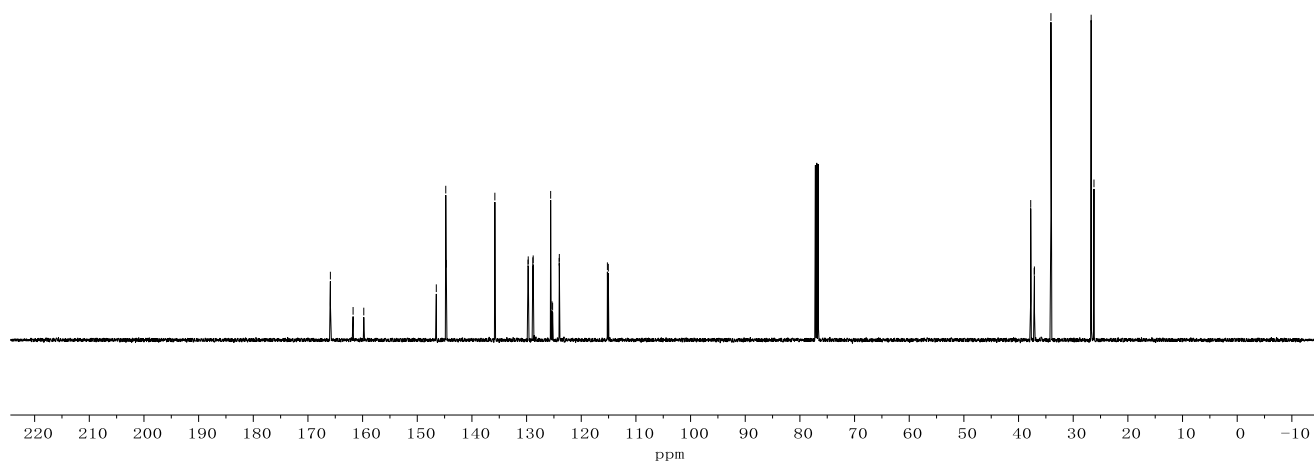
Appendix: NMR Spectra



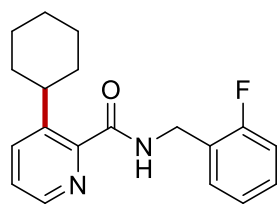
**415q**  
(300 MHz, CDCl<sub>3</sub>)



**415q**  
(75 MHz, CDCl<sub>3</sub>)

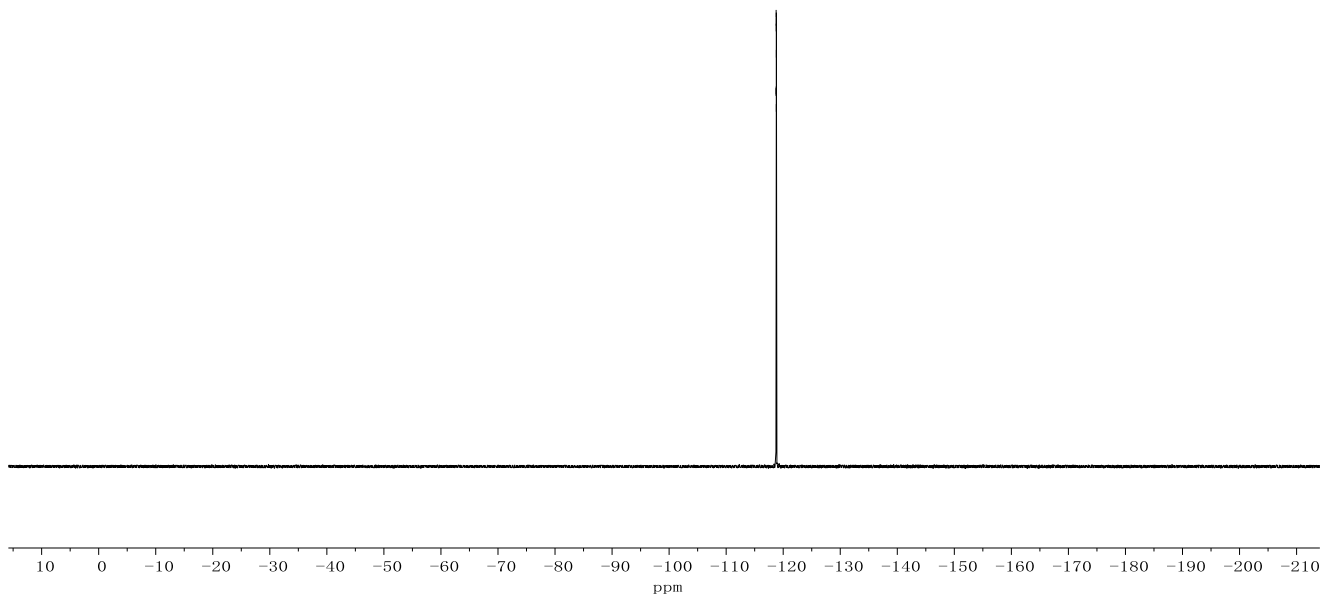


Appendix: NMR Spectra

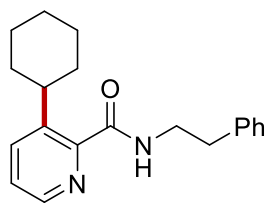


**415q**  
(282 MHz, CDCl<sub>3</sub>)

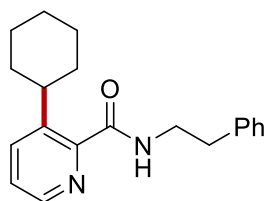
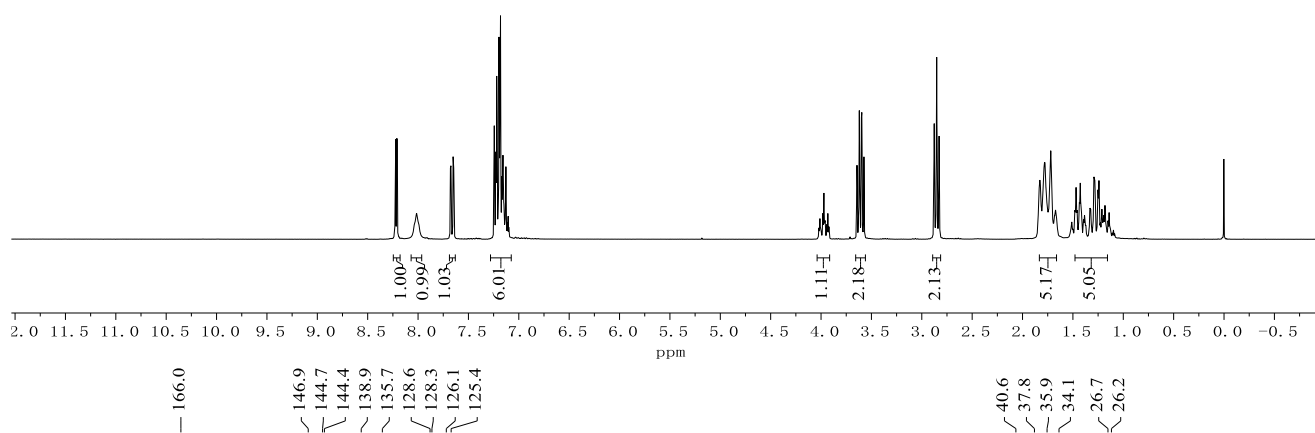
-118.7  
-118.8  
-118.8  
-118.8  
-118.8  
-118.8  
-118.8



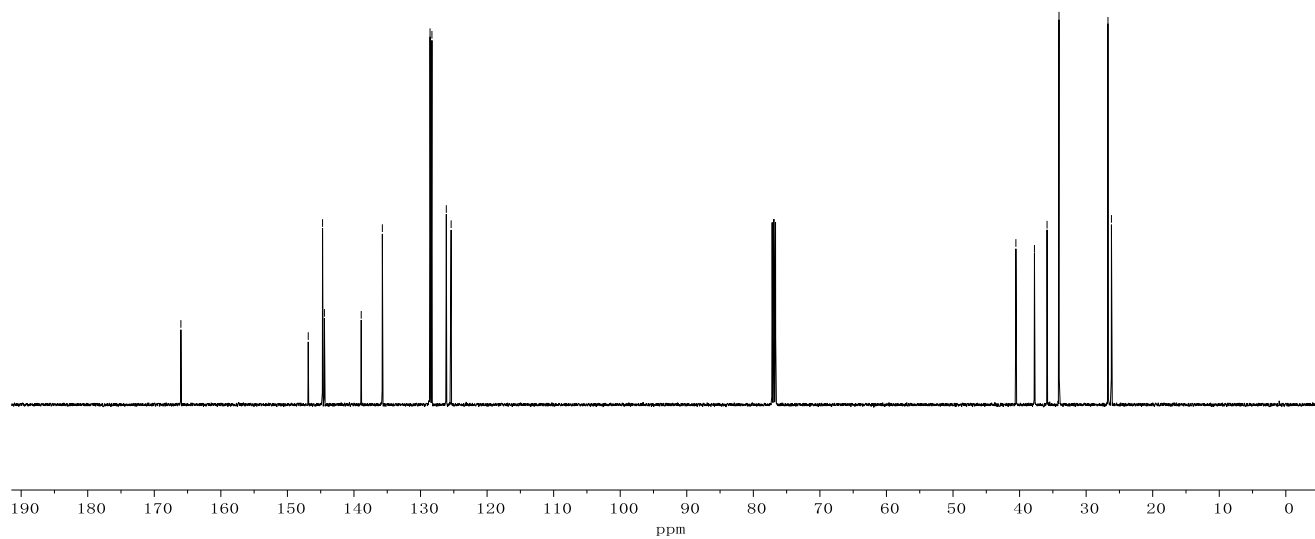
Appendix: NMR Spectra



**415r**  
(300 MHz, CDCl<sub>3</sub>)



**415r**  
(75 MHz, CDCl<sub>3</sub>)



## **Erklärung**

Ich versichere, dass ich die vorliegende Dissertation im Zeitraum von Mai 2017 bis September 2021

am Institut für Organische und Biomolekulare Chemie der

Georg-August-Universität Göttingen

auf Anregung und unter Anleitung von

**Professor Dr. Lutz Ackermann**

selbstständig durchgeführt und keine weiteren als die angegebenen Hilfsmittel und

Quellen verwendet habe.

Göttingen, den 12.08.2021

---

Isaac Choi